DEVELOPMENT OF ALKYL-PYRAZOLE-BASED PHOSPHINE LIGANDS AND THEIR APPLICATIONS IN PALLADIUM-CATALYZED CHEMOSELECTIVE CROSS-COUPLING REACTIONS

GU CHANGXUE

PhD

The Hong Kong Polytechnic University

2025

The Hong Kong Polytechnic University

Department of Applied Biology and Chemical Technology

Development of Alkyl-Pyrazole-Based Phosphine Ligands and Their Applications in Palladium-Catalyzed Chemoselective Cross-Coupling Reactions

Gu Changxue

A thesis submitted in partial fulfillment of the requirements for the degree of Doctor of Philosophy

August, 2024

CERTIFICATE OF ORIGINALITY

I hereby declare that this thesis is my own work and that, to the best of my knowledge and belief, it reproduces no material previously published or written, nor material that has been accepted for the award of any other degree or diploma, except where due acknowledgement has been made in the text.

Gu Changxue

Abstract

Abstract of thesis entitled “Development of Alkyl-Pyrazole-Based Phosphine Ligands and Their Applications in Palladium-Catalyzed Chemoselective Cross-Coupling Reactions”

Submitted by Gu Changxue
for the Degree of Doctor of Philosophy
at The Hong Kong Polytechnic University
in August 2024

Palladium catalysts represent one of the most widely utilized classes of catalysts for cross-coupling reactions in contemporary organic synthesis. Rational design of the ligands can lead to the development of high-performance palladium catalysts, enabling the utilization of more challenging substrates, the enhancement of reactivity, as well as the implementation of milder and more environmentally benign reaction conditions. However, the challenging chemoselectivity of cross-coupling reactions, which utilize electrophiles featuring two or more potentially competitive reaction sites, have only seen a resurgence in recent years. Over the past few years, our group has been actively exploring palladium-catalyzed chemoselective cross-coupling reactions via a ligand control strategy, especially for electrophiles bearing Cl and OTf. Based on this, our group developed a novel alkyl-indole-based phosphine ligand and then achieved a

series of Pd-catalyzed chemoselective cross-coupling reactions such as chemoselective Suzuki–Miyaura coupling, Sonogashira reaction, and α-arylation of carbonyl compounds, with the reactivity order of C–Cl > C–OTf. Nevertheless, the design of new ligands for chemoselectivity control, particularly for inverting traditional reactivity order (e.g., C–Cl > C–OTf), is still limited.

This thesis focuses on the exploration of novel phosphine ligands and their subsequent application in underexplored palladium-catalyzed chemoselective cross-coupling reactions. In **Chapter 1**, a brief introduction of some palladium-catalyzed reaction including C–N bond formation via Buchwald-Hartwig amination, redox-neutral decarboxylative cross-coupling reaction and direct C–H bond arylation of heterocycles as well as corresponding chemoselective investigations. Then, we will discuss the chemoselective reactions with unconventional C–Cl > C–OTf reactivity order. Our investigation on exploring new skeleton phosphine ligands to finish Pd-catalyzed chemoselective cross-coupling reactions is depicted in the subsequent sections of this thesis (Chapters 2-5).

In **Chapter 2**, the successful preparation of pyrazole-based phosphine ligands bearing two Cy groups at C3 and C5 positions of pyrazole enabled inter-, and intramolecular chemoselective amination with excellent chemoselectivity in a C–Cl > C–OTf reactivity order. The high-performance catalytic system showed good reactivity and good functional group tolerance toward a wide range of chloro(hetero)aryl triflates as well as various amines including aromatic, aliphatic, and heterocyclic amines. Late-

stage functionalization of some drugs and the gram-scale reaction were also feasible.

In **Chapter 3**, further modification on the alkyl groups attached to the pyrazole scaffold resulted in the achievement of regio-, and chemoselective C–H arylation of heterocyclic compounds with excellent α-regioselectivity and chemoselectivity at C–Cl bond. This approach enabled a series of heterocycles to be feasible substrates including benzo[*b*]thiophene, thiophene, furan, benzofuran, and thiazole. Gram-scale synthesis and synthetic application for the synthesis of optical materials were also demonstrated. Density functional theory (DFT) results revealed that the modification of the cycloalkyl ring size influences the angle and length of the Pd···H–C interaction, thereby inducing differential stabilizing effects on the critical intermediates of the reaction. Mechanistic investigations supported by both experimental and DFT results suggest that the alkyl-pyrazole-based phosphine ligands bearing optimal ring sizes (five-membered cycloalkyl ring) enable the reaction to proceed with a lower energy barrier through a concerted metalation–deprotonation (CMD) pathway.

In **Chapter 4**, the further investigation of the alkyl-pyrazole phosphine ligand showed that it could lower the reaction temperature of the redox-neutral decarboxylative cross-coupling reaction. Compared to Buchwald-type ligands such as SPhos, pyrazole-based phosphine ligand bearing *i*-Pr group could lower the reaction temperature by 60–80 ºC and enable a wide range of aryl chlorides couple well with a series of benzoates under relatively mild conditions. Moreover, we utilized the Hammett plot and Eyring plot to explore the mechanism of the reaction and determine

the rate-determining step might be the decarboxylative step.

In **Chapter 5**, considering that the Pd···H–C interaction provided by the newly developed pyrazole-based phosphine ligand bearing *i*-Pr group may also effectively control the chemoselectivity towards the C–Cl bond under mild conditions, we subsequently leveraged this ligand to achieve chemoselective decarboxylative cross-coupling reaction. Various chloroaryl triflates coupled well with 2,6-difluoro benzoates affording corresponding diaryl compounds remaining OTf group under mild conditions, which demonstrated the high-performance of our developed catalytic system.

In summary, our research focuses on developing novel phosphine ligands for palladium-catalyzed chemoselective cross-coupling reactions. We successfully achieved various reactions, including amination, C–H arylation, and decarboxylative coupling, demonstrating improved chemoselectivity, reactivity, and functional group tolerance, highlighting the potential for milder and environmentally friendly conditions.

Publications

Parts of this thesis have been adapted from the following published articles co-written by the authors:

1. Chen, Z.; Gu, C.; Yuen, O. Y.; So, C. M.* Palladium-catalyzed chemoselective direct α-arylation of carbonyl compounds with chloroaryl triflates at the C–Cl site, *Chem. Sci.* **2022**, *13*, 4762–4769.
2. Gu, C.; Yuen, O. Y.; Ng, S. S.; So, C. M.* Palladium-Catalyzed Chemoselective Amination of Chloro(hetero)aryl Triflates Enabled by Alkyl-Pyrazole-Based Phosphine Ligands, *Adv. Synth. Catal*. **2024**, *366*, 1565-1574.
3. Gu, C.; So, C. M.* Regio- and Chemoselective Palladium-Catalyzed Additive-Free Direct C–H Functionalization of Heterocycles with Chloroaryl Triflates Using Pyrazole-Alkyl Phosphine Ligands, *Adv. Sci*. **2024**, 2309192.
4. Gu, C.; So, C. M.* Alkyl-Pyrazole-Phosphine Ligands Featuring Pd···H–C Interaction Enabled Pd-Catalyzed Decarboxylative Cross-Coupling at Moderate Temperature and Late-Stage Functionalization of Drugs. *ACS Catal. Manuscript under preparation*.
5. Gu, C.; So, C. M.* Palladium-Catalyzed Chemoselective Decarboxylative Cross-Coupling of Polyfluoroarenes with Chloroaryl Triflates at C–Cl Site under Mild Conditions. *Org. Lett, Manuscript under preparation*.

Acknowledgements

I am very grateful to the many people. Without their support and guidance, my research cannot go on smoothly. First, I would like to express my deepest gratitude to my research supervisor Dr. So Chau Ming for his expert and patient guidance. He supervised the progress of the work in a timely manner, explained the problems in the project carefully, pushed the project in a good direction, and I also gained a lot of knowledge from it. More importantly, he led me to see a different world of chemistry and let me touch upon areas I had never touched before, such as DFT calculations. At the same time, with his help, I was fortunate to get my first high-scoring article in my life.

I wish to thank all the members in our team. I am also grateful to Dr. Yuen On Ying and Ms. Ng Shan Shan for maintaining laboratory routines, and being supportive all the time. I wish to thank Dr. Zicong Chen, Mr. Wai Hang Pang, and Chuan Han for their company during my study period. Additionally, I would like to thank all the technical staff and administrative staff in ABCT department for their kind support and consideration.

Lastly, I am thankful to my family, my girlfriend OuYang Lingli, and friends for their love and full support in various ways of my study and life.

Gu Chang Xue

August, 2024

Table of contents

Abbreviation

Full Name	Abbreviation
Adamantyl	Ad
Aryl	Ar
3-(*t*-Butyl)-4-(2,6-dimethoxyphenyl)-2,3-dihydrobenzo[*d*][1,3]oxaphosphole	BI-DIME
2,2’-Bis(diphenylphosphino)-1,1’-binaphthyl	BINAP
Boronic acid pinacol	Bpin
Cyclopentyl methyl ether	CPME
Cyclohexyl	Cy
Dibenzylideneacetone	Dba
Dimethylacetamide	DMAc
1,1’-Bis(di-*tert*-butylphosphino)ferrocene	Dtbpf
1,1’-Bis-(diphenylphosphino)ferrocene	Dppf
Ethyl acetate	EA
Ethyl	Et
Equivalent	equiv.
Gas chromatography	GC
Isopropyl	*i*-Pr
Generalized ligand	L
Methyl	Me
2-(Diphenylphosphino)-2’-methoxy-1,1’-binaphthyl	Meo-mop
N-methylimidodiacetic	MIDA
Mass spectrometry	MS
n-Butyl	*n*-Bu
N-Heterocyclic Carbene	NHC
Acetate	OAc
Trifluoromethanesulfonate (triflate)	OTf
Tricyclohexylphosphine	PCy_3

Tetrakis(triphenylphosine)palladium(0)	$Pd(PPh_3)_4$
Tri-*ortho*-tolylphosphine	$P(o\text{-tol})_3$
Phenyl	Ph
Triphenylphosphine	PPh_3
Generalized group	R
1,3-bis(2,4,6-trimethylphenyl)-4,5-dihydroimidazol-2-ylidene]	SIMes
1,3-bis(2,6-diisopropylphenyl)-4,5-dihydroimidazol-2-ylidene]	SIPr
Room temperature	r.t.
tert-Butyl	*t*-Bu
Tetrahydrofuran	THF

Chapter 1 Introduction

1.1 Background

Transition-metal-catalyzed cross-coupling reactions have evolved into one of the most effective synthetic tools for the construction of C–C bond and C–X bond.[1] Among the transition metals that have been applied to cross-coupling reactions, palladium as a promising metal is widely harnessed in cross-coupling reactions due to its versatility, reliability, and high reactivity in many cross-coupling reactions.[2] These advancements have brought about a revolutionary impact across diverse industries, encompassing pharmaceuticals, agrochemicals, and bulk chemicals.[3] Generally, the development of high-performance palladium catalysts relies on the exploration of new ligands[4] to improve reaction protocols, thereby enabling higher reactivity,[5] a wider substrate scope incorporating challenging coupling reagents, or milder reaction conditions.

For instance, Kwong group utilized 2-phenylbenzimidazole as the main ligand scaffold to develop a new class of P, N-type ligands, which effectively lowered the palladium catalyst loading to 1 ppm in the Suzuki cross-coupling reaction (Scheme 1.1 A).[5c] Another example is the modification of oxaphosphole-containing ligands in the BI-DIME family, which allows the Suzuki coupling of a wide range of functionalized aryl bromides, as well as various boron sources including boronic acids, Bpin or B(MIDA) derivatives, and BF_3K salts. Moreover, Pd/HandaPhos catalytic system also enabled the use of water as the solvent rather than organic solvents at room temperature, utilizing only ppm levels palladium as the catalyst (Scheme 1.1 B).[5a]

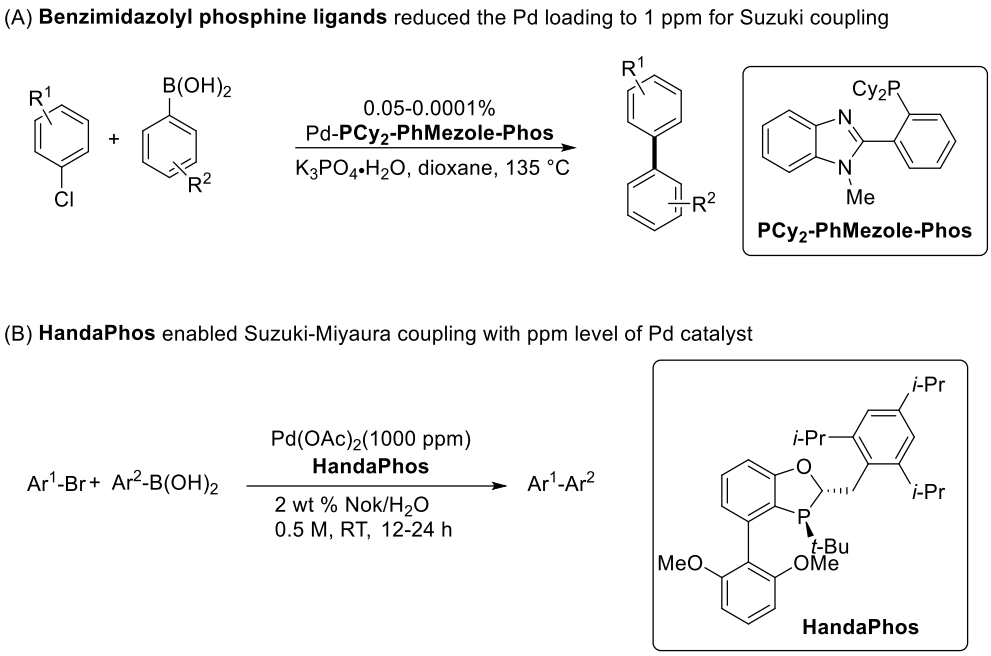

Scheme 1.1 Examples of ligand design to improve catalyst efficiency

Although the ligand design strategy has significant contributed to the development of the field of palladium catalysis, relatively few studies have applied this strategy to solve the problem of chemoselectivity when electrophiles with two or more active reaction sites. In this and the following chapters, we will discuss some investigations about Pd-promoted chemoselective cross-coupling reaction as well as the related research progress in our group.

1.2. The Development of Palladium-Catalyzed Chemoselective Amination

Aryl amines are pivotal structural scaffolds in a series of natural compounds, pharmaceutical agents, and functional organic materials.[3d] Therefore, developing the efficient and versatile methodology to access these important and useful compounds is highly alluring for chemists. In addition to traditional methods for obtaining such structures, such as aromatic nucleophilic substitution,[6] addition of liquid ammonia to

benzyne,[7] electrophilic nitration,[8] and reductive amination,[9] the emergence of transition metal-catalyzed (TM-catalyzed) cross-coupling reactions[10] has attracted much attention because they can forge C–N bonds more directly and efficiently. The developed protocols include oxidative methodology typified by the Chan-Lam reaction[11] and the classical method (electrophile-nucleophile) represented by the Ullmann-Goldberg[12] and Buchwald-Hartwig reactions[13] (Scheme 1.2).

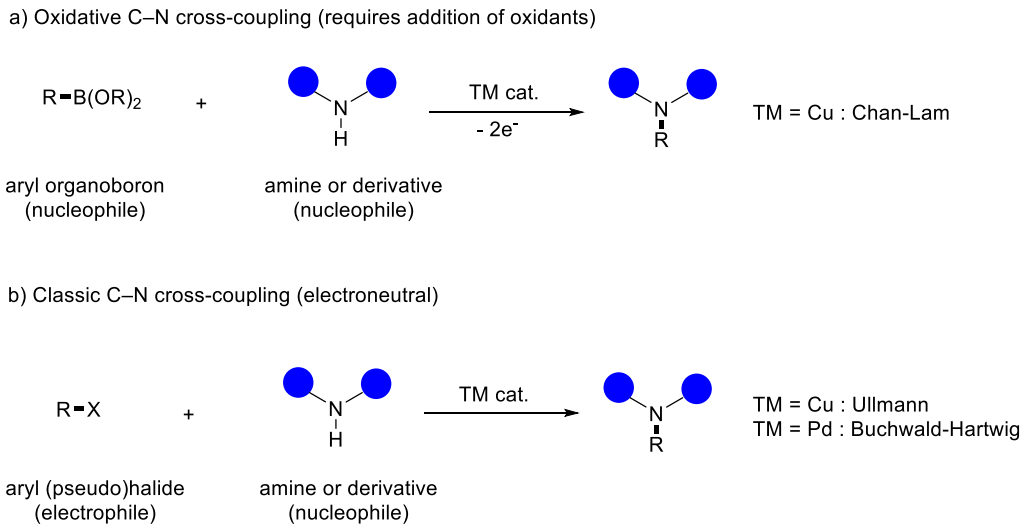

Scheme 1.2 General approaches to TM-catalyzed C−N cross-coupling

1.2.1. Brief Introduction of Ligand Development Used in Buchwald-Hartwig Amination

Compared to the Cu-catalyzed Ullmann-Goldberg reaction, the palladium-catalyzed Buchwald-Hartwig amination could afford broaden substrate scope under relatively mild reaction conditions. In early investigations of this type of reaction, PPh_3 and P(*o*-tolyl)$_3$ were utilized as ligands in so-called "first generation" Buchwald-Hartwig catalyst systems (Scheme 1.3).[13a, 14] However, using PPh_3 as ligand required

more than an equivalent of $Pd(PPh_3)_4$ to complete the reaction,[14] while only a catalytic amount of palladium catalyst was needed using P(*o*-tolyl)$_3$ as ligand. Though modified conditions reduced the loading of the catalyst and increased the reaction rate, the substrate scope was limited almost entirely to secondary amines due to competitive hydrodehalogenation of the bromoarenes.[13a]

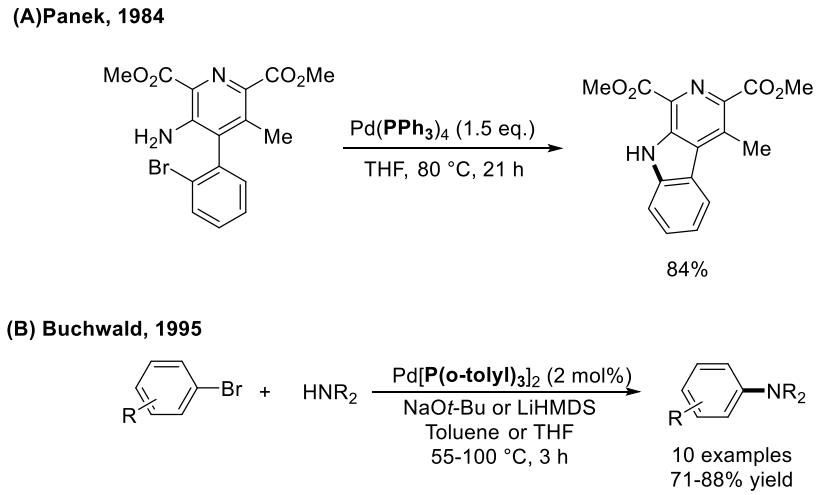

Scheme 1.3 Early research of Pd-catalyzed amination

The employment of so-called "second generation" biphosphine ligands such as BINAP and DPPF for the Buchwald–Hartwig amination not only expanded the scope of amine from secondary amines to primary amines at that time, but also allowed the amines to react efficiently with aryl iodides and triflates (Scheme 1.4).[15] Additionally, these ligands usually afford the amination products at higher rates and better yields than the first generation of catalysts.

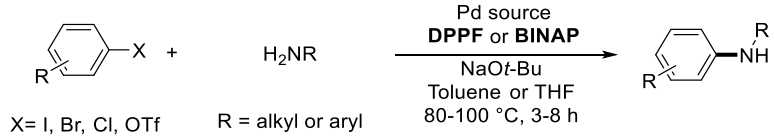

Scheme 1.4 Early application of biphosphine ligands in Buchwald-Hartwig amination

Further investigations on modifying ligands gained the following benefits: (i) reduce the reaction temperature; (ii) enable the reaction system to use weaker bases (even organic base) and then broaden the scope of the substrate; (iii) decrease loading of catalyst; and (iv) activate more inert carbon halides bond such as C−Cl or carbon pseudohalogen bond like C−OTs more efficiently. In this regard, the Buchwald group has rationally designed a series of dialkylbiaryl phosphine ligands[16] achieving mentioned benefits, while the Hartwig group has developed ferrocene-derived phosphine ligands[17] (Table 1.1). Other types of ligands such as BippyPhos,[18] MorDalPhos,[19] and IPr·HCl[20] have also been shown to be effective ligands for the Pd-catalyzed amination reactions.

Table 1.1 Examples of developed phosphine ligands

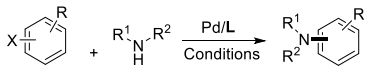

Reference	Eletrophiles	Amines	Pd/**L**	Reaction Conditions
Hartwig, 1998[17]	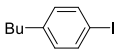	NH_2Ph	$Pd(dba)_2$ (1 mol%)/(**DBt-PF**)	NaO*t*-Bu, **r.t.**, 24 h
Buchwald, 1999[16c]	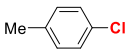	MeNHPh	$Pd_2(dba)_3$ (**0.005** mol%)/**JohnPhos**	NaO*t*-Bu, 100 °C, 19 h
Buchwald, 2003[16b]	 X = **OSO_2Ph** or **OTs**	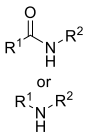	$Pd(dba)_2$ (1-2 mol%)/**XPhos**	K_2CO_3, 80-110 °C 11-24 h
Buchwald, 2018[16a]	 X = **OTf, Br or Cl**		COD(**Pd-AlPhos**)$_2$	**DBU**, 60 °C, 16 h
Stradiotto, 2013[18]		**NH_3** or **$N_2H_4•H_2O$**	[Pd(cinnamyl)Cl]$_2$ (1 mol%) **BippyPhos**	NaO*t*-Bu, 110 °C, 1-6 h
Stradiotto, 2012[19]	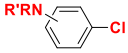	NH_2R'' or 	[Pd(cinnamyl)Cl]$_2$ (1-4 mol%) **MorDalPhos**	NaO*t*-Bu or LiHMDS 65-110 °C, 12-48 h
Nolan, 2006[20]	 X = **Br or Cl**		(**IPr**)Pd(acac)Cl (1 mol%)	KO*t*-Bu, 50 °C, **0.2**-6 h

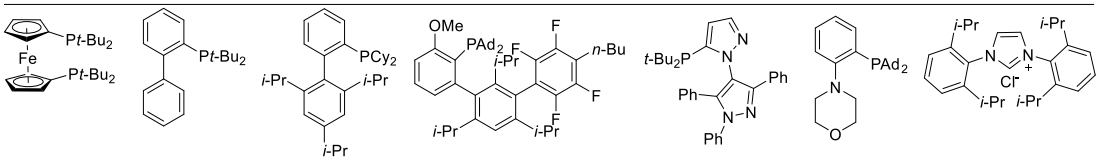

(DBt-PF) **JohnPhos** **XPhos** **AlPhos** **BippyPhos** **MorDalPhos** **IPr•HCl**

1.2.2 Chemoselective Aminations Followed the Traditional Reactivity Order

Systematic investigations of Pd-catalyzed chemoselective amination reactions are relatively rare, with many works reporting only one or two examples in the entire article.[16a, 21] As depicted in Table 1.2, Schoenebeck only reported one example of chemoselective amination utilizing Pd (I) dimer with P*t*-Bu_3 as ligand, and the reactivity order was C−Br > C−Cl,[21d] which is consistent with the general occurring reactivity order: C−I > C−Br ≈ C−OTf > C−Cl.[22] The use of bidentate phosphine ligand 1,3-Bis(diphenylphosphino)propane (dppp) preferred to activate C−OTf bond over C−Br bond,[21b] whereas utilizing Buchwald-type phosphine ligand like XPhos resulted in a

reversed reactivity order (C−Br over C−OTf).[21g] Buchwald,[16a, 21j] and Kakiuchi[21f] successively achieved one or two examples of chemoselective amination of chloroaryl triflates utilizing Buchwald-type phosphine ligands, and the reactivity order was C−OTf > C−Cl, which also follow the traditional reactivity order. While these reports provide some valuable insights into the control of chemoselectivity, the limited number of examples of amination in the studies inevitably restricts the generalizability.

Table 1.2 Examples of Pd-catalyzed chemoselective amination

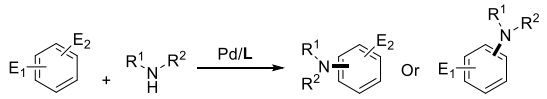

Reference	Eletrophiles	Amines	Pd/**L**	Examples	Reactivity Order
Schoenebeck, 2020[15e]	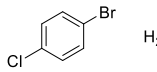	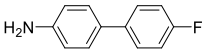	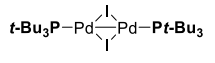 **Pd$^{(I)}$ dimer**	**1**	C−Br > C−Cl
Brown, 2007[15c]	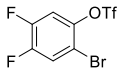		$Pd_2(dba)_3$/**dppp**	**1**	C−OTf > C−Br
Pospech, 2020[15h]	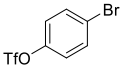	Me_2NH	$Pd_2(dba)_3$/**XPhos**	**1**	C−Br > C−OTf
Buchwald, 2016[15k]	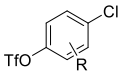	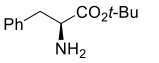	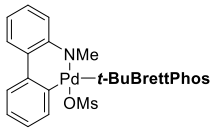 **Pd G4**	**2**	C−OTf > C−Cl
Buchwald, 2018[15a]	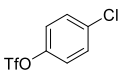	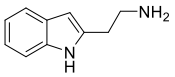	COD(**Pd-AlPhos**)$_2$	**1**	C−OTf > C−Cl
Kakiuchi, 2019[15g]	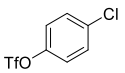		$Pd(dba)_2$/***t*-BuBrettPhos**	**1**	C−OTf > C−Cl

Verkade group's investigation shows that bicyclic triaminophosphine ligands tend to preferentially activate C−I or C−Br bonds over C−Cl bond in the chemoselective aminations, but they only exhibited 7 examples (Scheme 1.5).[21h]

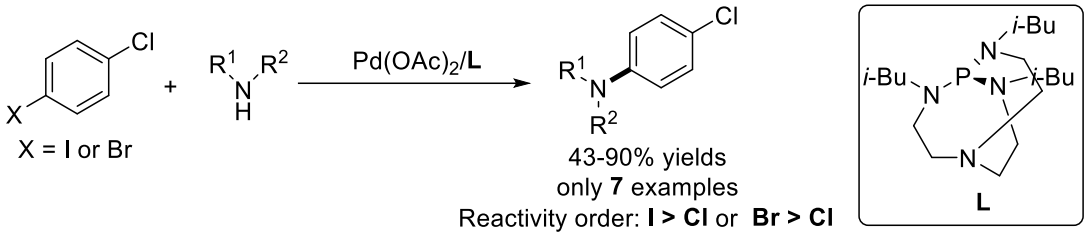

Scheme 1.5 Reports with examples in chemoselective aminations

Bunnelle group systematic investigated the effect of a series of ligands on the chemoselective aminations of pyridine substrates bearing bromide and chloride, and found that $Pd_2(dba)_3$/**XantPhos** catalytic system could finish the reaction well and provide a C−Br > C−Cl reactivity order (Scheme 1.6 A).[21c] However, limited substrate scope was shown.

Nolan *et al.* utilized NHC as ligand such as IPr·HCl to investigate the chemoselective amination. Leveraging the developed catalytic system, the reactions still preferentially activate the more reactive C–I or C–Br bonds, ultimately furnishing the aminated products that retain the inert –Cl group (Scheme 1.6 B).[21e] Despite the remarkably low 0.4 mol% loading of the palladium catalyst employed, the scope of the demonstrated examples remains limited, and the reaction temperatures are relatively high.

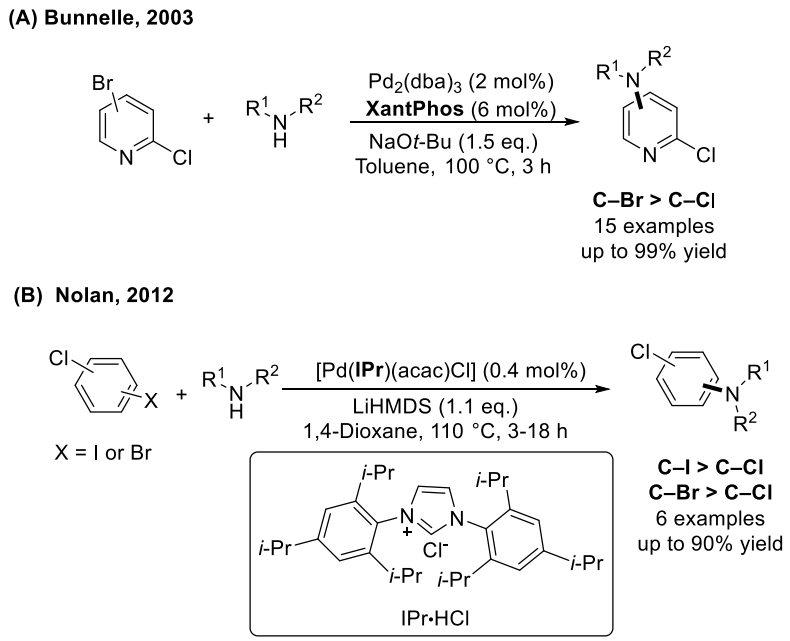

Scheme 1.6 Chemoselective aminations with conventional reactivity order

1.2.3 Chemoselective Aminations Exhibited Uncommon Reactivity Order

In the chemoselective amination reactions described above, the developed catalytic systems, whether employing mono-phosphine, bis-phosphine, or NHC ligands, have all demonstrated a preferential reactivity towards the more activated carbon–halide (or pseudo-halide) bonds, ultimately preserving the more inert C–Cl bonds. On the contrary, developing suitable catalytic systems that would react more inert C–Cl bonds first, thereby preserving the more reactive sites for subsequent functionalization, would be of considerable value in the synthesis of complex molecules.

Serrano-Wu reported a single example in the Buchwald-Hartwig amination of *p*-anisidine with substituted pyridine using NHC as the ligand to control the selectivity, which provided uncommon C–Cl > C–Br reactivity order, albeit a low yield was obtained (Scheme 1.7 A).[23] Further investigations by Sigman and Tan demonstrated that

utilizing the ferrocene "DMAPF" ligand accomplished the chemoselective amination reaction with high efficiency and high reversal chemoselectivity (C–Cl > C–Br) (Scheme 1.7B).[24] This work demonstrates the importance of manipulating chemoselectivity in such transformations via ligand strategy. However, the substrate scope of Sigman and Tan's valuable finding was presently limited to pyridine derivatives bearing Cl and Br, wherein the inert –Cl group is situated at the inherently activated 2-position of pyridine.

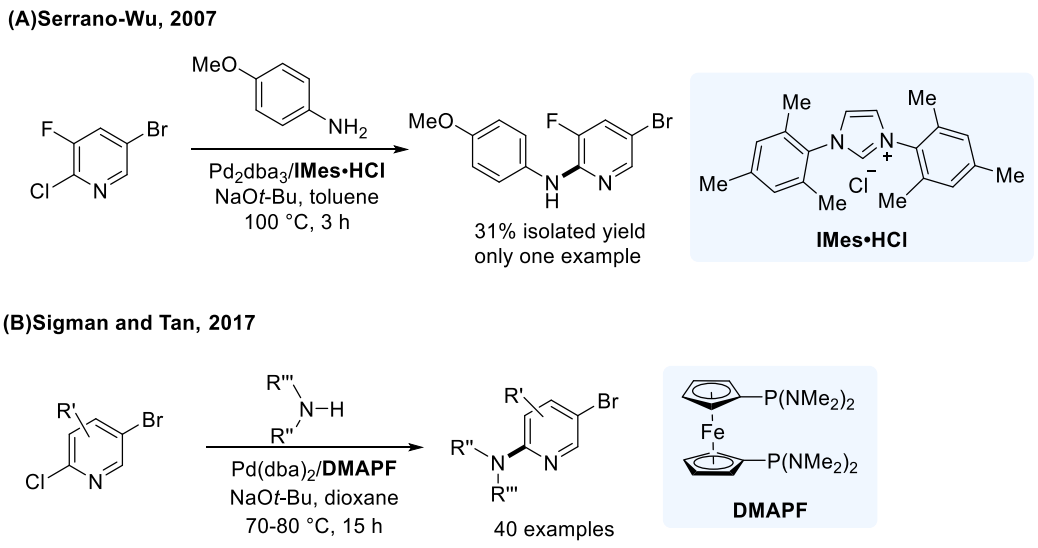

Scheme 1.7 Inversion of chemoselectivity in palladium-catalyzed amination between C–Br and C–Cl

To the best of our knowledge, before our investigations into the chemoselective amination between C–OTf and C–Cl, no successful examples have been reported. Until recently, Qiu group utilized $PdCl_2$/P*t*-Bu_3 catalytic system finished chemoselective amination of chloro(hetero)aryl triflates with C–Cl > C–OTf reactivity order (Scheme 1.8).[25] However, this protocol used large amounts of P*t*-Bu_3 and catalytic amounts of

additives to improve the yield but still furnished products with only moderate yields. The inherent catalytic activity of P*t*-Bu$_3$ in promoting this transformation may not entirely satisfactory albeit with excellent chemoselectivity at C–Cl.

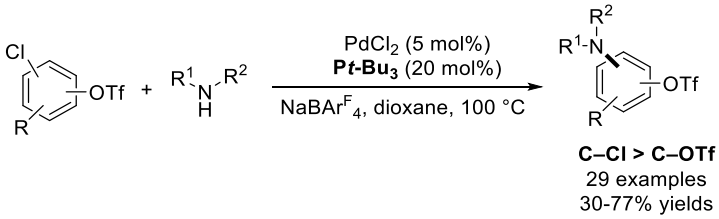

Scheme 1.8 Inversion of chemoselectivity in palladium-catalyzed amination between C–Cl and C–OTf

1.3 Palladium-Promoted Redox-Neutral Decarboxylative Cross-Coupling Reaction

Carboxylic acids, renowned for their remarkable structural diversity and inherent stability, are widely available either through commercial sources or synthetic means,[26] and are generally straightforward to handle.[27] The decarboxylative cross-coupling reaction, which leverages carboxylic acids as surrogates for more costly and less robust nucleophilic coupling partners such as organozinc reagents or organotin reagents, has thus emerged as a captivating synthetic strategy.[28] Currently developed methodologies for decarboxylation cross-coupling reactions involving palladium generally have two catalytic systems, including bimetallic catalytic systems which incorporate Pd/Cu bimetallic system or Pd/Ag bimetallic system and monometallic systems catalyzed by palladium alone.

1.3.1 Development of Bimetallic Catalytic System Enabled Redox-Neutral

Decarboxylative Cross-Coupling Reaction

As for the bimetallic catalytic system, the proposed reaction mechanism is shown in Scheme 1.9. In the copper/silver system, salt exchange between potassium carboxylate and copper/silver salt **A** generates a metal carboxylate **B**, which then extrudes the CO_2 to form aryl copper/silver species **C**. Such a species undergoes transmetallation step with an arylpalladium(II) complex **E** affording a biarylpalladium species **F**, followed by reductive elimination step to give rise to biaryl products. Then the entire palladium catalytic cycle is completed and the palladium (0) species **D** is regenerated to start the next cycle.

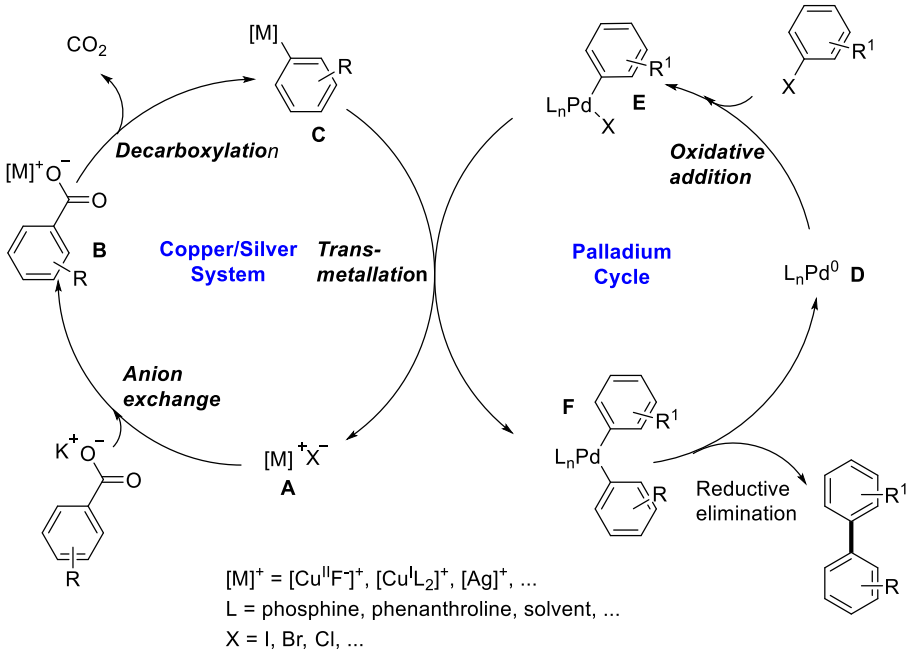

Scheme 1.9 Proposed mechanism for bimetallic catalytic system

Such operating mode typically relies on the copper or silver to facilitate the decarboxylation step and the palladium to promote the oxidative addition, transmetalation, and reductive elimination steps, thereby expanding both the substrate

scope of the arene carboxylic acids and electrophiles. Therefore, expansion of the use of inert electrophiles relies on the use or development of phosphine ligands that are compatible with the entire catalytic cycle. The used electrophiles in some developed methodologies were limited to aryl iodides and bromides.[28b, 29] The selection of electron-rich and sterically hindered phosphine ligands has been proofed to expand the scope of electrophilic coupling partners to aryl chlorides (Scheme 1.10 A).[30] Goossen *et al*. subsequently improved both palladium and copper catalysts by using suitable ligand or type of catalyst to allow *meta*- or *para*-substituted non-*ortho*-substituted benzoates react with various aryl chlorides bearing electron-withdraw or electron-donating groups in moderate to good yields (Scheme 1.10 B).[31]

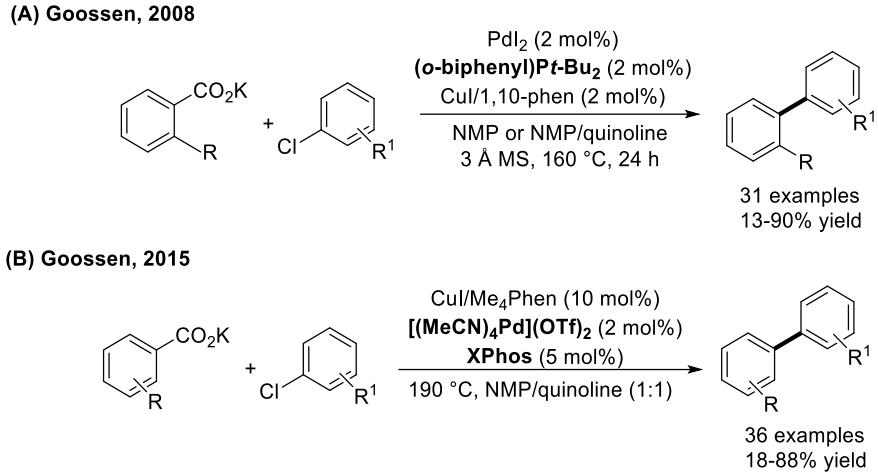

Scheme 1.10 Expansion of the types of electrophiles to aryl chlorides

Furthermore, Goossen group has expanded the scope of electrophiles to include aryl pseudohalides as competitive substrates by exploring suitable coordinate ligands for palladium center. They then successfully used aryl triflates[32] (Scheme 1.11 A), the relatively inert aryl tosylates[33] (Scheme 1.11 B), and even the more sluggish yet

structurally diverse aryl and alkenyl mesylates[34] as coupling partners (Scheme 1.11 C). It is noteworthy that the employment of customized imidazolyl phosphines has, for the first time, enabled the utilization of aryl and alkenyl mesylates as electrophilic coupling partners in decarboxylative cross-coupling reactions, further underscoring the pivotal role of phosphine ligands in expanding the scope of viable electrophiles. (Scheme 1.11 C).

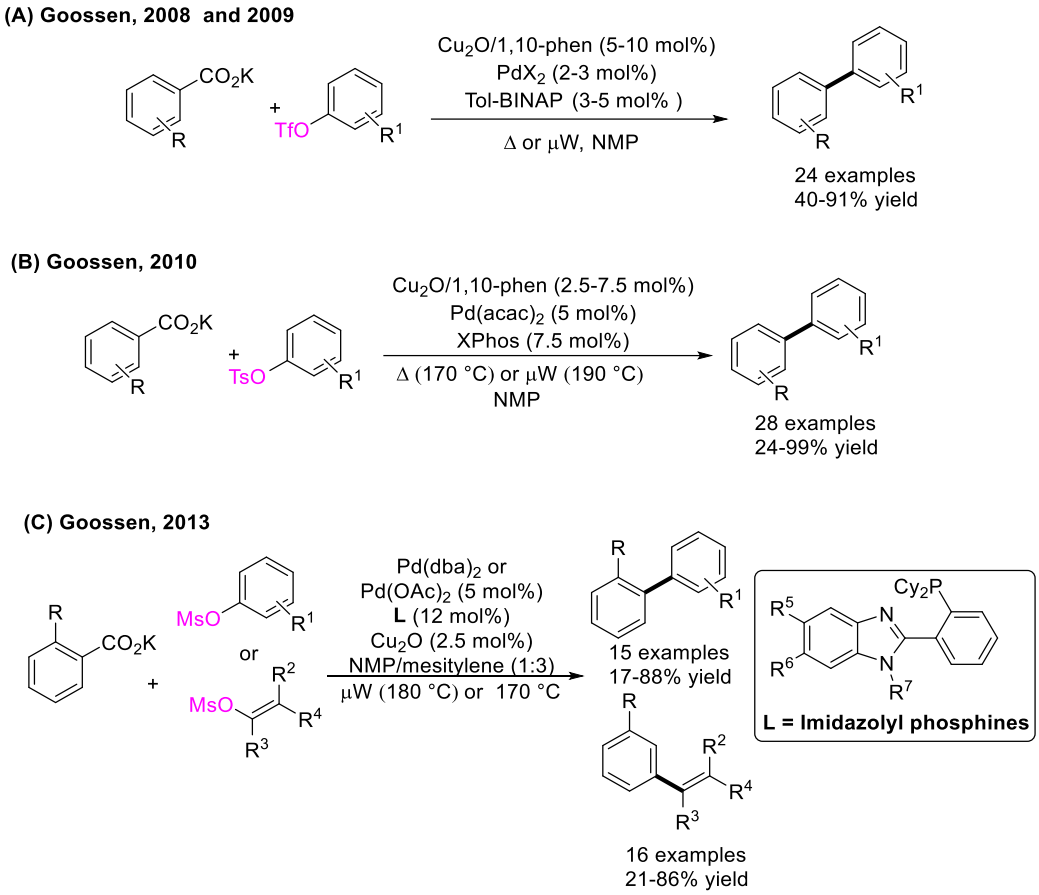

Scheme 1.11 Expansion of the types of electrophiles to aryl pseudohalides

1.3.2 Development of Palladium-Catalyzed Decarboxylative Cross-Coupling Reaction

Although the bimetallic catalytic system has successfully expanded both the

substrate scope of electrophiles and carboxylic acids, the tedious optimization process of the reaction conditions remains less than ideal. Therefore, monometallic catalytic systems demonstrate some complementary advantages compared to bimetallic catalytic system. However, reports on palladium-catalyzed decarboxylative cross-coupling reactions are relatively limited,[35] especially for the reaction involving easily available and structurally diverse aryl chlorides (Scheme 1.12). Limitations were obviously included (i) the narrow substrate scope, (ii) the requirement for additives, and (iii) especially the need for high reaction temperatures, which remains a persistent and significant scientific challenge hindering the broader applicability of decarboxylative cross-coupling transformations.

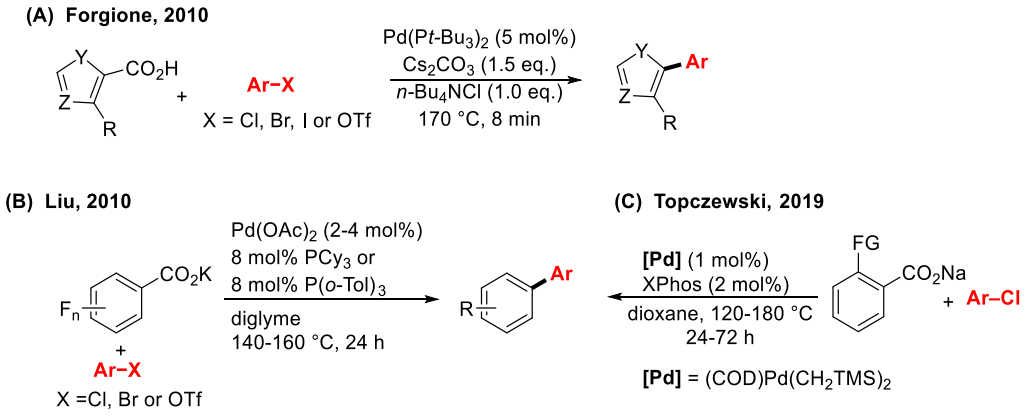

Scheme 1.12 Pd-catalyzed decarboxylative cross-coupling reactions involving Ar–Cl

1.3.3 Examples of Chemoselective Decarboxylative Cross-Coupling Reaction

There are also few studies involving chemoselectivity in decarboxylative cross-coupling reactions, summarized in Table 1.3.[29c, 36] In 2009, Wu achieved chemoselective decarboxylative cross-coupling reaction in C–I > C–Cl or C–Br > C–

Cl order utilizing palladium as catalyst and silver salt as additive. However, merely two examples have been shown, and there are limitations such as the requirement for high reaction temperatures and low efficiency.[29c] Subsequent mechanistic investigations[37] conducted by Gooßen facilitated the development of efficient Pd/Ag[36a] and Pd/Cu[36b] bimetallic catalytic systems, enabling the realization of chemoselective C–C bond formation preferentially at C–OTf over C–Cl sites under comparatively mild reaction temperatures. Particularly noteworthy is the fact that improving the efficiency of the rate-determining step of the reaction through rational ligand design is of great significance in reducing the reaction temperature. The rational designed P, N-bidentate phosphine ligand as shown in Table 1.3 was able to bridge the Pd and Cu centers well, thus promoting the rate-determining transmetalation step and reducing the reaction temperature to 100 °C.

Table 1.3 Examples of chemoselective decarboxylative cross-coupling reaction

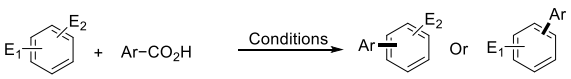

Reference	Eletrophiles	Conditions	Examples	Reactivity Order
Wu, 2009[21c]	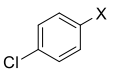 X = I or Br	$PdCl_2$ (10 mol%)/**BINAP** (10 mol%) Ag_2CO_3 (3.0 eq.), 150 °C	**3**	C–I > C–Cl C–Br > C–Cl
Gooßen, 2010[28a]	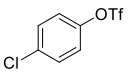	[Ag] (10 mol%), $PdCl_2$ (10 mol%) **PPh_3** (9 mol%) 2,6-lutidine (20 mol%), 130 °C	**12**	C–OTf > C–Cl
Gooßen, 2015[28b]	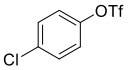	Cu_2O (10 mol%)/**1,10-Phen** (10 mol%) **P, N-ligand** (6 mol%), 100 °C 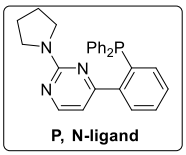 **P, N-ligand**	**5**	C–OTf > C–Cl

According to the literature review above, the unresolved issues in the redox-neutral decarboxylative cross-coupling reaction are: (1) how to harness palladium-based monometallic system to lower the reaction temperature while still allow to utilize more inert aryl chlorides; and (2) how to achieve chemoselectivity favoring C–Cl over C–OTf.

1.4 Pd-Catalyzed C–H Arylation of Heterocycles

Transition metal-catalyzed C–H bond functionalization has long been an effective method for the concise building of carbon-carbon or carbon-heteroatom bonds in the field of chemistry.[38] Five-membered heteroaromatics (such as thiophene) or their derivatives are useful building blocks for the conjugated polymers which are innovative materials.[39] Methods that utilizing such heteroaromatics without pre-functionalization to react aryl (peuso)halides could become useful surrogate to Suzuki coupling or Stille coupling in terms of environmental friendliness and atom economy.

Since the first report of the direct arylation of isoxazoles by Nakamura, Tajima, and Sakai in 1982,[40] the palladium-catalyzed direct arylation of five-membered heterocyclic compounds with aryl (pseudo)halides through C–H activation has become one of the most efficient methods to access arylated heterocyclic derivatives in a simple and straightforward manner. Among the used electrophiles[41] in direct arylation of heteroaromatics, aryl iodides[42] and bromides[43] were frequently utilized coupling reagents. Other types of electrophiles were summarized in Table 1.4 including aryl chlorides,[44] triflates[45], tosylates[46] and mesylates.[47] A series of monophosphines were

prove to facilitate the activation of aryl chlorides including *n*-BuPAd$_2$,[44b] PCy$_3$,[44a] P*t*-Bu$_3$,[44e] P(*o*-tol)$_3$, JohnPhos[44f] and Cy$_2$P-*o*-biphenyl.[44e] However, the catalysts formed by these ligands and palladium typically require high temperatures (above 110 °C) or the use of coordinating polar solvents to achieve their high performance. NHC ligand also exhibited its exclusive reactivity for direct arylation of heterocycles, which achieved a broad substrate scope including a series of aryl chlorides featuring both electron-donating and electron-withdrawing groups as well as a range of heterocycles (including furan, thiophene, pyrrole and benzo[*b*]thiophene).[44c] Nevertheless, such an effective Pd/NHC catalytic system required the addition of additives and coordinating polar solvents to achieve optimal reactivity. As for aryl sulfonates, the use of PPh$_3$ was able to activate reactive aryl triflates, albeit with narrow substrate scope and high reaction temperature.[45] Fener *et al.* utilized a catalyst derived from XPhos which allowed a broadly applicable C–H bond functionalization of an array of heterocycles harnessing aryl tosylates, and also explored the possibility of direct arylation of mesylates.[46a] The mesylates were subsequently widely explored by Kalyani group via the Pd/ bisphosphine (dcype) catalytic system.[47]

Table 1.4 Electrophiles (excluding aryl iodides or bromides) for arylation of heterocycles were selectively displayed

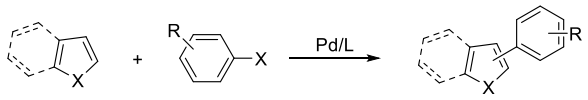

Reference	Electrophiles	Pd/L	Other reaction conditions	Subtrate Scope
Daugulis, 2007[43b]	Ar–**Cl**	$Pd(OAc)_2$ (5 mol%)/***n*-BuPAd$_2$**	K_3PO_4, **NMP** **125 °C**, 24 h	17 examples 52-84% yields
Born, 2008[43a]		$Pd(OAc)_2$ (4 mol%)/**PCy_3**	K_2CO_3, Toluene **120 °C**, 18-24 h	29 examples 47-95% yields
Marsais, 2008[43f]		$Pd(OAc)_2$ (5 mol%) **P(*o*-tol)$_3$** or **JohnPhos**	Cs_2CO_3, Toluene 110 °C, 18 h	8 examples 29-95% yields
Mori, 2010[43e]		Pd(**P*t*-Bu$_3$**)$_2$ (2 mol%)	**LiO*t*-Bu**, DMF 100 °C, 15 h	6 examples 58-92% yields
Daugulis, 2011[43d]		$Pd(OAc)_2$ (5 mol%)/**Cy_2P-*o*-biphenyl**	Na_2CO_3, **DMA** **125 °C**, 24 h	30 examples 42-92% yields
Lee, 2012[43c]		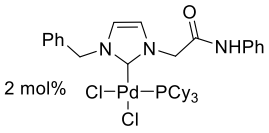 2 mol%	**PivOH** (30 mol%) K_2CO_3, **DMAc** 110 °C, 12-15 h	34 examples 41-91% yields
Doucet, 2008[44]	Ar–**OTf**	$Pd(OAc)_2$ (5 mol%)/**PPh_3**	KOAc, **DMF** **150** °C, 20 h	15 examples **28**-86% yields
Fenner, 2009[45a]	Ar–**OTs**	$Pd(OAc)_2$ (5 mol%)/**XPhos**	K_2CO_3, **DMF/tBuOH** *t*-$BuCO_2H$ (15 mol%) 100 °C, 18-22 h	33 examples **58**-95% yields
Kalyani, 2014[46]	Ar–**OMs**	$Pd(OAc)_2$ (5-10 mol%)/**dcype** 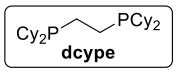	Cs_2CO_3, CsOPiv Toluene, **120 °C**	7 examples 86-98% yields

In exploring suitable catalysis to achieve satisfactory regioselectivity, Doucet *et al.* found that controlling the regioselectivity of benzofuran was particularly difficult. After a series of base screenings, no satisfactory results were obtained (Scheme 1.13).[43j] Similar results were obtained by Mihovilovic group, who utilized Pd/SPhos as catalyst, CsOPiv as base and DMA as solvent to couple benzo[*b*]furan and aryl bromides at 140 ^{o}C to obtain a series of mixtures of α- and β-arylated products as well as dimers.[43k] These results indicated the difficulty in exploring suitable catalytic system to achieve excellent regioselectivity.

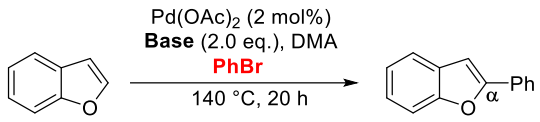

Base	Conv. (%)	Ratio α: β: Dimer
KOAc	71	50: 17: 33
CsOAc	15	67: 22: 11
NaOAc	0	-
K_2CO_3	45	58: 21: 21
K_3PO_4	50	58: 23: 19

Scheme 1.13 Exploration of regioselectivity

As for chemoselective direct arylation of heterocycles, only one study has reported this aspect by Born *et al.* (Scheme 1.14).[44a] With Pd/PCy_3 as catalyst, the coupling of 1-bromo-4-chlorobenzene or 4-chlorophenyl tosylate with heterocycles provided C−Br > C−Cl and C−Cl > C−OTs reactivity order, respectively, following the common reactivity order.[22, 48]

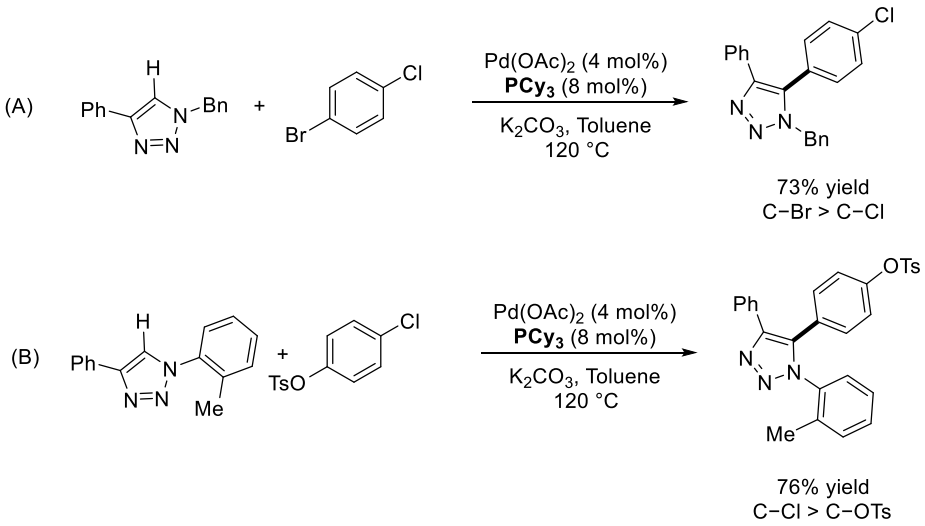

Scheme 1.14 Chemoselective direct C−H arylation of heterocycles

The examples illustrated that direct C−H arylation of heterocycles typically requires elevated reaction temperatures and the use of various additives. Given

considerations of energy efficiency and atom economy, further exploration of new catalyst remains desirable. Moreover, the development of dual selective reactions that achieve both regio- and chemoselectivity with nucleophilic and electrophilic coupling partners has been relatively unexplored.

1.5 Palladium-Catalyzed Chemoselective Cross-Coupling with Ar–Cl over Ar–OTf Reactivity order

Precisely controlling the chemoselectivity of cross-coupling reactions when electrophiles bearing two or more potential competitive reaction sites is challenging (Scheme 1.15). As depicted in the typical catalytic cycle (Scheme 1.16), the oxidative addition of electrophiles typically serves as the critical and chemoselective-determining step in cross-coupling reactions, prompting recent investigations into the chemoselective functionalization of electrophiles.[49]

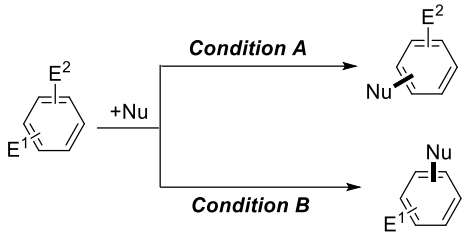

Scheme 1.15 Chemodivergent cross-coupling reaction

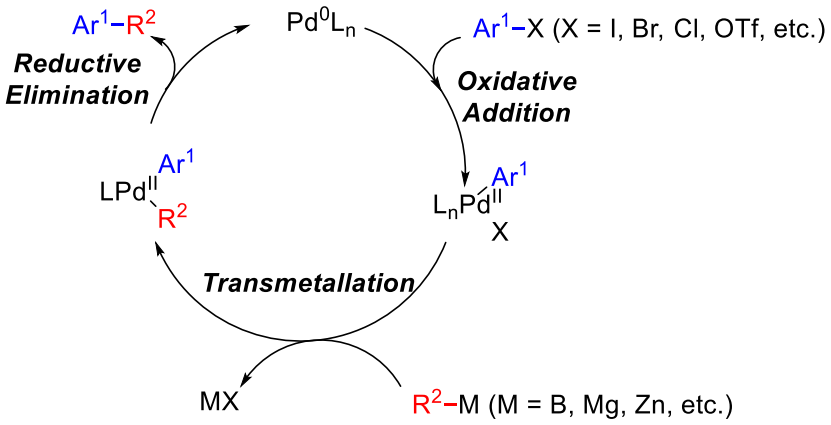

Scheme 1.16 Typical catalytic cycle for Pd-catalyzed cross-coupling reactions

It was not until 2000 that chemodivergent cross-coupling reactions of chloroaryl triflates were reported by Fu *et al*. They found that utilizing Pd/P*t*-Bu_3 system provided the coupling product exclusively via Ar–Cl bond cleavage whereas Pd/PCy_3 system inverted the selectivity result (Scheme 1.17).[50] The critical role of the catalytic system in controlling chemoselectivity was further demonstrated by the same group via intra-, and intermolecular chemoselective Stille cross-coupling reaction (Scheme 1.18).[51] These encouraging results suggest that phosphine ligands undoubtedly exert a critical influence on the chemoselectivity regardless of the type of nucleophile utilized, thus providing a viable framework for future investigations. However, the origination of chemoselectivity requires further detailed mechanistic investigations.

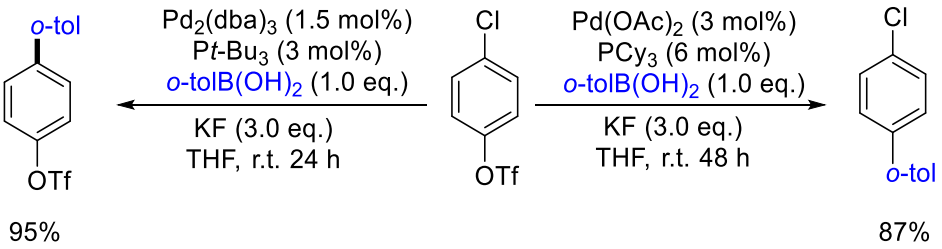

Scheme 1.17 First chemoselective cross-coupling of chloroaryl triflate

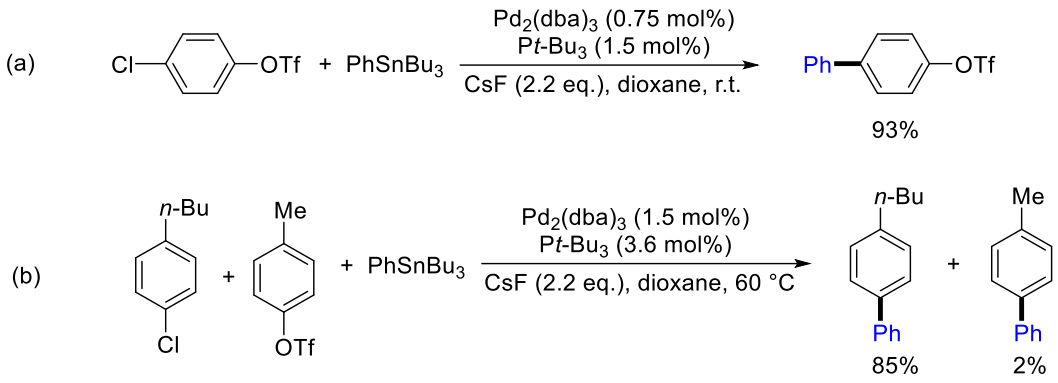

Scheme 1.18 Chemoselective Stille coupling with C–Cl > C–OTf reactivity order

Regarding mechanism researches, Schoenebeck and Houk performed DFT studies to provide insights into the origination of the chemoselectivity.[52] As oxidative addition step can be the crucial step to manipulate the reaction direction, they calculated the free energies of each transition state during the oxidative addition step. According to the calculation results (Scheme 1.19), although the transition state of substrate/Pd(P*t*-Bu$_3$)$_2$ coordination complex was not located, a general trend can still be discerned that transition states involving monoligated [Pd(**L**)] (**L** = PCy$_3$, P*t*-Bu$_3$ or PMe$_3$) complexes preferentially favored C–Cl activation, whereas bisligated Pd complexes were more likely to insert into the C−OTf bond. However, Fu's work showed that the Pd/PCy$_3$ catalytic system preferentially activated the C–OTf bond,[50] which was inconsistent with the DFT results. This contradictory result might stem from the fact that Pd(PCy$_3$)$_2$ is the active palladium species under the actual reaction conditions. Consequently, a ligation state hypothesis was proposed, wherein a monoligated palladium complex (PdL) reacts at the C–Cl bond, while a bisligated palladium complex (PdL$_2$) reacts at C–OTf bond.

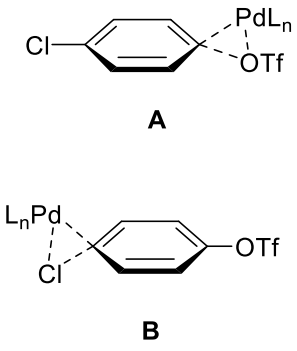

PdL_n	$\Delta\Delta G^{\ddagger}_{(B\text{-}A)}$
$PdPCy_3$	-3.6
$Pd(PCy_3)_2$	+4.7
$PdPt\text{-}Bu_3$	-5.8
$Pd(Pt\text{-}Bu_3)$	n.d.
$PdPMe_3$	-6.4
$Pd(PMe_3)_2$	+3.3

Scheme 1.19 DFT investigations on the monoligated or bisligated Pd species

In addition, in 2016, Sigman *et al.* attempted to reveal mechanistic pathways and predict chemoselectivity results via parameterization of phosphine ligands.[53] They used Suzuki cross-coupling as model reaction to measure an array of monodentate phosphines (Table 1.5). The results showed that the product ratios were good consistent with those predicted by a parameterized model. Among the phosphine ligands evaluated, six ligands containing *tert*-butyl (*t*-Bu) or 1-adamantly (1-Ad) groups were found to preferentially activate the C–Cl bond. This may be due to the sufficient steric hindrance provided by *t*-Bu or 1-Ad groups, preventing the formation of PdL_2, which favors the oxidative addition of Ar–Cl bond. Other phosphines are deemed to generate bisligated active palladium species tending to react at triflate. JohnPhos which is regarded as a monophosphine also bearing *t*-Bu groups, exhibited preference for the C–OTf bond. This outcome can be rationalized by the hemilabile Pd–arene interaction[4d] between the biaryl moiety and the Pd center, which facilitates the formation of P and π bisligated complex.

Table 1.5 Comparison of measured chemoselectivities utilizing different phosphines

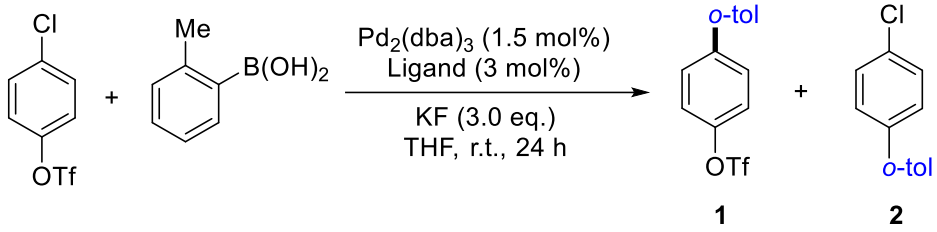

Ligand	$\Delta\Delta G^{\ddagger}_{(2\text{-}1)}$ (kcal/mol)	Ligand	$\Delta\Delta G^{\ddagger}_{(2\text{-}1)}$ (kcal/mol)	Ligand	$\Delta\Delta G^{\ddagger}_{(2\text{-}1)}$ (kcal/mol)
P(*o*-Tol)$_3$	1.42	P*t*-Bu$_2$(*p*-CF$_3$Ph)	-1.46	P*n*-Bu$_3$	2.40
P(*m*-Tol)$_3$	3.12	P*t*-Bu$_2$Ph	-0.26	PEt$_3$	3.75
PPh$_3$	2.64	P*t*-Bu$_3$	-2.72	P*c*-Pent$_3$	0.59
PEtPh$_2$	3.57	P*n*-Bu(1-Ad)$_2$	-1.43	P*c*-Hex$_3$	1.94
PMePh$_2$	3.70	PBn(1-Ad)$_2$	-1.35	P*c*-Hex$_2$Ph	2.08
PMe$_2$Ph	4.00	P*i*-Pr$_2$*t*-Bu	-0.30	CyJohnPhos	3.32
P*t*-BuPh$_2$	2.36	P*i*-Pr$_3$	1.02	JohnPhos	2.91

Other type of phosphines such as ylide-functionalized phosphines (YPhos), developed by Gessner's group and proved to exhibit C−Cl selectivity.[54] The Pd/**keYPhos** or Pd/**prYPhos** catalytic system was found to activate aryl chlorides well, especially for sterically hindered substrates, affording corresponding coupling products in good to excellent yields as well as satisfactory chemoselectivity to Cl (Scheme 20).

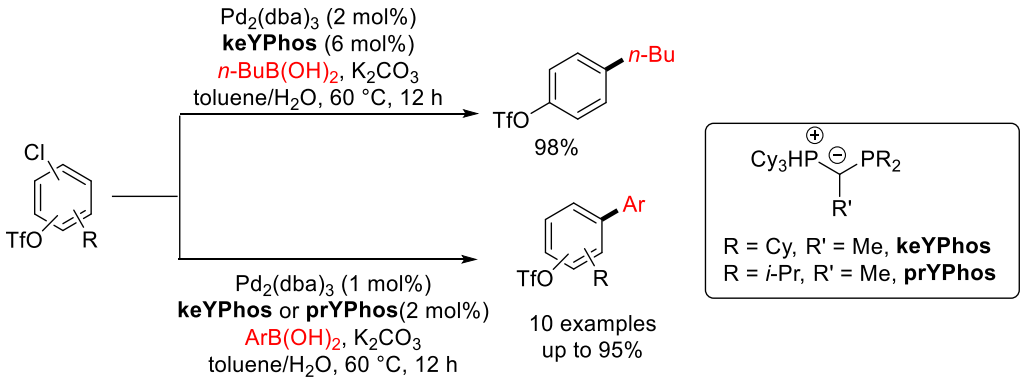

Scheme 1.20 Ylide-functionalized phosphines controlled chemoselective Suzuki coupling

In addition to the above-mentioned phosphine ligands that can be utilized to control chemoselectivity of cross-coupling reactions, *N*-heterocyclic carbenes (NHC)[55] have also been proven by Neufeldt group to be effective ligands in this type of reaction. The use of SIMes as ligand resulted in C–OTf bond activation, whereas utilizing SIPr as ligand exhibited preference for C–Cl bond (Scheme 1.21). DFT calculations were consistent with prior reports on Pd/phosphine catalytic systems to some extent. The calculation indicated that monoligated Pd^0(NHC) complexes favored reactivity at the Ar−Cl bond, regardless of the NHC ligand. These results help elucidate the chemoselectivity of the active Pd/SIPr catalyst, which may function as a monoligated species. As previously hypothesized, bisligated catalysts preferentially react at the Ar−OTf bond. DFT results indicated that Ar−OTf selectivity with SIMes may be due to the formation bisligated $Pd(SIMes)_2$ or $[Pd(SIMes)(OH)]^-$ active species.

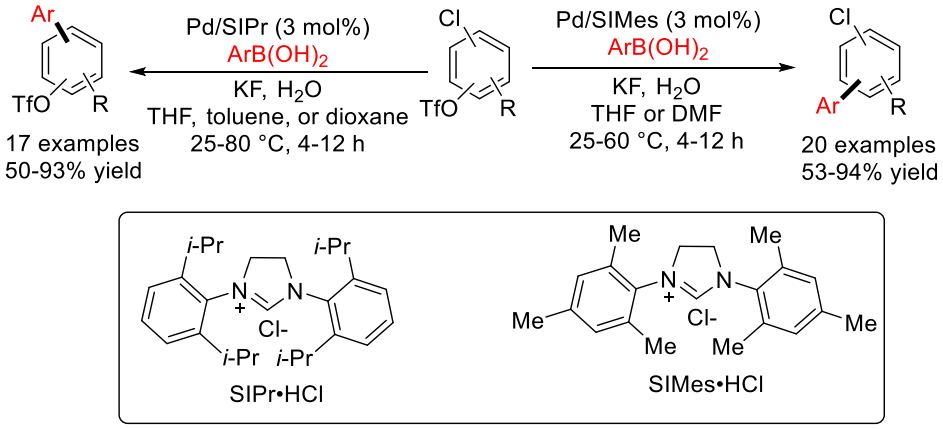

Scheme 1.21 NHC-controlled chemoselective Suzuki coupling

Mechanistic investigations and experimental results suggest that the ligand plays a pivotal role in determining the chemoselectivity of the cross-coupling reaction.

In 2011, Schoenebeck group discussed the contradictory selectivity observed in chemoselective Suzuki–Miyaura coupling using Pd/P*t*-Bu_3 as catalyst in polar coordinating solvents (Table 1.6 and Table 1.7).[56] They investigated the coordination patterns of the active palladium centers by DFT calculations and verified the hypothesis experimentally, finding that in polar solvents, the catalytically active species change in the presence of coordination cross-coupling partner or additives, resulting a reversal of regioselectivity. Further investigations by Neufeldt *et al.* combined DFT calculations and experiments to provide new insights into solvent/additive effects that.[57] In coordinating solvents, the preferential activation of triflate may be mediated by Pd(L)(Solvent) active species, whereas in non-coordinating solvents, the reaction of chloride may proceed through a monoligated Pd(L) active species.

Table 1.6 Effect of solvent and base on chemoselective Suzuki coupling

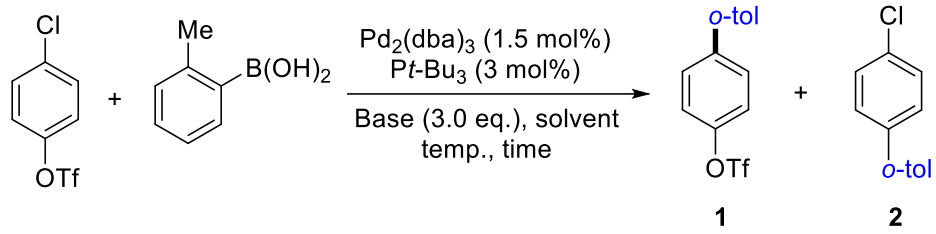

1 **2**

Entry	Solvent	Base	Temp.	Time	**1**	**2**
1	Toluene	KF	70 °C	48 h	70%	0
2	MeCN	KF	r.t.	48 h	3%	74%
3	DMF	KF	r.t.	48 h	3%	22%
4	THF	DIPA	r.t.	24 h	14%	7%
5	MeCN	DIPA	r.t.	48 h	2%	27%
6	MeCN	lutidine	r.t.	48 h	<1%	25%

Table 1.7 Effect of additive on chemoselective Stille coupling

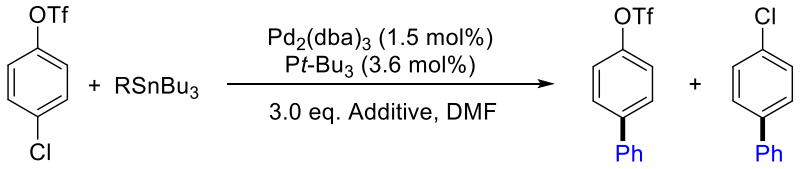

3 **4** **5**

Entry	Additive	Temp.	Time	Coupling partner	Ratio of compounds **3**	**4**	**5**
1	KPF_6	r.t.	38 h	$PhSnBu_3$	45	47	8
2[a]	KPF_6	100 °C	7 d	$PhSnBu_3$	3	88	9
3	KF	r.t.	38 h	$PhSnBu_3$	18	30	51
4	CsF	r.t.	38 h	$PhSnMe_3$	-	21	79

[a]1.5% [$Pd(Pt\text{-}Bu_3)_2$]/0.75% [$Pd_2(dba)_3$]

The mechanistic investigation outlined above suggests that altering the solvent to coordinating polar solvent, introducing additives, or even utilizing coordinating coupling partners can lead to an inversion of the chemoselectivity towards the C−OTf

bond. This observation highlights the inherent challenge in achieving C−Cl > C−OTf reactivity order. These mechanistic insights provide valuable guidance for the future exploration of chemoselective cross-coupling reaction with C−Cl selectivity. The aforementioned work demonstrates that the C−Cl bond can be selectively activated using suitable ancillary ligands. Therefore, the rational design of ligands is the key to achieving such chemoselctive cross-coupling reaction.

Based on this concept, our group designed and developed a novel class of indole-based phosphine ligands featuring an alkyl group as the bottom ring (Scheme 1.22, **SelectPhos**). With developed high-performance catalyst, a broad range of polyhalogenated (hetero)aryl triflates, reacted smoothly with (hetero)aryl, alkenyl, and alkylboronic acids to provide the corresponding products with good chemoselectivity and yields.[58] Importantly, the reported chemoselective transformations have been readily scaled up to the gram scale, and have also been found to proceed effectively at remarkably low palladium catalyst loadings (as low as 10 ppm Pd). Crystallographic analysis of the palladium oxidative addition complex **C1** reveals that it was a chloride-bridged dimeric Pd(II) complex with a Pd−L ratio of 1:1 (Scheme 1.23). The distances (2.698 Å) and angles (138.7°) of the atoms, which lie within a standard range of 2.3−2.9 Å and 110−170° with a downfield shift (5.73 ppm) of the methine hydrogen, indicate this C−H···Pd interaction as anagostic/preagostic interactions,[59] which might be the key factor to control the chemoselectivity. Later on, a series of chemoselective cross-coupling including Songashira reaction, deuterohalogenation, α-arylation of carbonyl compounds, phosphorylation, borylation, and desulfinative cross-coupling reaction

were achieved utilizing newly developed ligands (Scheme 1.24),[60] demonstrating the importance of exploring new type of ligands for realizing such reaction.

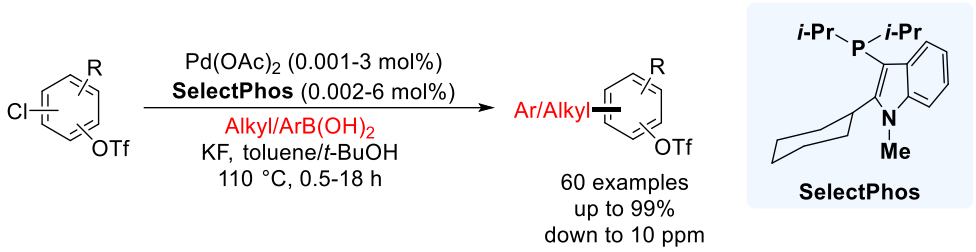

Scheme 1.22 Indole-Alkyl-Based phosphine ligands enabled chemoselective Suzuki coupling

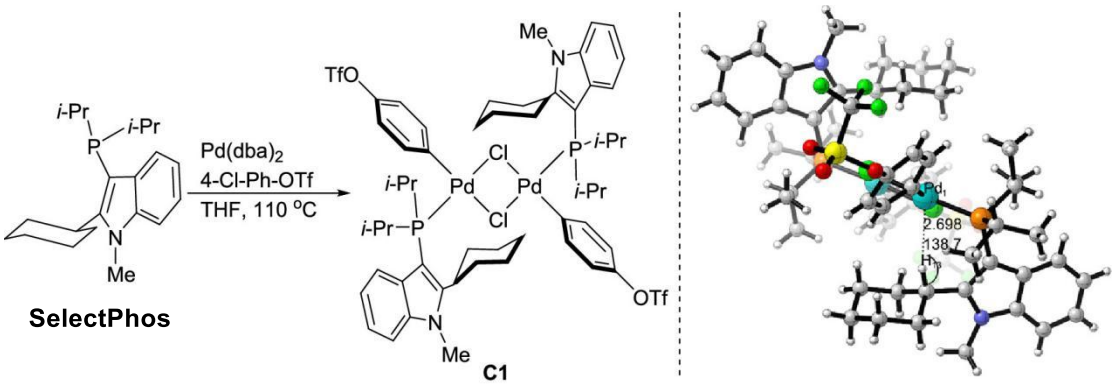

Scheme 1.23 Preparation and C−H···Pd interaction of **C1**

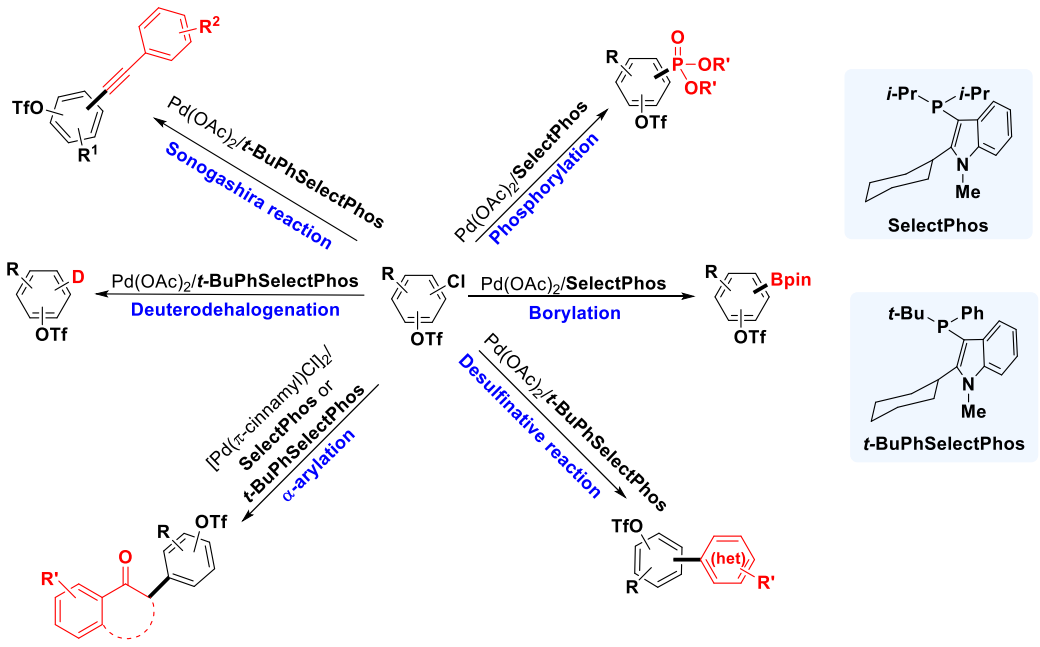

Scheme 1.24 Indole-Alkyl-Based phosphine ligands enabled a series of chemoselective cross-coupling reactions

1.6 Purpose of Research

Precise control of chemical selectivity is a challenging but important topic in organic synthesis. By manipulating chemical selectivity, target fragments can be introduced sequentially at specific positions to construct structurally complex compounds. Although our research group has successfully achieved a series of chemoselective cross-coupling reactions via rational ligand design strategies, where the ligands manipulate the selectivity at Cl, limitations are still exist in expanding the scope of these coupling reactions. Since the use of alkyl as bottom ring in place of aryl groups are the key to control reactivity order, we envision that selecting alternative ligand scaffolds and strategically introducing alkyl groups at suitable positions could provide Pd···H–C interactions to control the chemoselectivity. Modifying the ligand backbone

offers new avenues for tuning both the electronic and steric properties, thereby generating more active catalysts to enable new reactions.

1.7 References

(1) (a) Hassan, J. *Chem. Rev.* **2002**, *102 (5)*, 1359-1470; For selective book chapters: (b) King, A. O.; Yasuda, N. In *Organometallics in Process Chemistry*; Larsen, R. D. Ed.; Springer: Berlin, **2004**, pp 205-246; (c) Miyaura, N. In *Cross-Coupling Reactions*; Miyaura, N. Ed.; Springer: Berlin/Heidelberg, **2002**, *Vol. 219*, pp 11-59; (d) Suzuki, A. In *Modern Arene Chemistry*; Astruc, D. Ed.; Wiley-VCH: Weinheim, **2002**, pp 53-106.

(2) (a) Miyaura, N.; Buchwald, S. L. *Cross-coupling reactions: a practical guide*; Springer, **2002**; (b) King, A. O.; Yasuda, N. Palladium-Catalyzed Cross-Coupling Reactions in the Synthesis of Pharmaceuticals. In *Organometallics in Process Chemistry*, Springer Berlin Heidelberg, **2004**; pp 205-245; (c) Johansson Seechurn, C. C.; Kitching, M. O.; Colacot, T. J.; Snieckus, V. *Angew. Chem. Int. Ed.* **2012**, *51 (21)*, 5062-5085; (d) Devendar, P.; Qu, R.-Y.; Kang, W.-M.; He, B.; Yang, G.-F. *J. Agric. Food. Chem.* **2018**, *66 (34)*, 8914-8934.

(3) (a) Yin, L.; Liebscher, J. *Chem. Rev.* **2007**, *107 (1)*, 133-173; (b) Gardner, B. M.; Seechurn, C. C. J.; Colacot, T. J. *Organomet. Chem. Ind.* **2020**, 1-22; (c) Schlummer, B.; Scholz, U. *Adv. Synth, Catal.* **2004**, *346 (13-15)*, 1599-1626; (d) Ruiz-Castillo, P.; Buchwald, S. L. *Chem. Rev.* **2016**, *116 (19)*, 12564-12649.

(4) (a) Lundgren, R. J.; Stradiotto, M. *Chem, Eur. J.* **2012**, *18 (32)*, 9758-9769; (b) Biscoe, M. R.; Fors, B. P.; Buchwald, S. L. *J. Am. Chem. Soc.* **2008**, *130 (21)*, 6686-6687; (c) Fu, G. C. *Acc. Chem. Res.* **2008**, *41 (11)*, 1555-1564; (d) Martin, R.; Buchwald, S. L. *Acc. Chem. Res.* **2008**, *41 (11)*, 1461-1473.

(5) (a) Handa, S.; Andersson, M. P.; Gallou, F.; Reilly, J.; Lipshutz, B. H. *Angew. Chem.*

Int. Ed. **2016**, *55 (16)*, 4914-4918; (b) Patel, N. D.; Rivalti, D.; Buono, F. G.; Chatterjee, A.; Qu, B.; Braith, S.; Desrosiers, J. N.; Rodriguez, S.; Sieber, J. D.; Haddad, N. *Asian J. Org. Chem.* **2017**, *6 (9)*, 1285-1291; (c) Wong, S. M.; So, C. M.; Chung, K. H.; Lau, C. P.; Kwong, F. Y. *Eur. J. Org. Chem.* **2012**, *2012 (22)*, 4172-4177; (d) Yan, M.-Q.; Yuan, J.; Lan, F.; Zeng, S.-H.; Gao, M.-Y.; Liu, S.-H.; Chen, J.; Yu, G.-A. *Org. Biomol. Chem.* **2017**, *15 (18)*, 3924-3929; (e) Choy, P. Y.; Yuen, O. Y.; Leung, M. P.; Chow, W. K.; Kwong, F. Y. *Eur. J. Org. Chem.* **2020**, *2020 (19)*, 2846-2853; (f) Li, C. L.; Tse, M. H.; Choy, P. Y.; Kwong, F. Y. *J. Organomet. Chem.* **2024**, *1011* 123124; (g) Akporji, N.; Thakore, R. R.; Cortes-Clerget, M.; Andersen, J.; Landstrom, E.; Aue, D. H.; Gallou, F.; Lipshutz, B. H. *Chem. Sci.* **2020**, *11 (20)*, 5205-5212.

(6) Bunnett, J. F.; Zahler, R. E. *Chem. Rev.* **1951**, *49 (2)*, 273-412.

(7) Heaney, H. *Chem. Rev.* **1962**, *62 (2)*, 81-97.

(8) Olah, G. A.; Narang, S. C.; Olah, J. A.; Lammertsma, K. *Proc. Natl. Acad. Sci. U.S.A.* **1982**, *79 (14)*, 4487-4494.

(9) (a) Abdel-Magid, A. F.; Carson, K. G.; Harris, B. D.; Maryanoff, C. A.; Shah, R. D. *J. Org. Chem.* **1996**, *61 (11)*, 3849-3862; (b) Alinezhad, H.; Yavari, H.; Salehian, F. *Curr. Org. Chem.* **2015**, *19 (11)*, 1021-1049; (c) Raoufmoghaddam, S. *Org. Biomol. Chem.* **2014**, *12 (37)*, 7179-7193.

(10) Jiang, L.; Buchwald, S. L. *Metal-Catalyzed Cross-Coupling Reactions*, **2004**, 699-760.

(11) (a) Chan, D. M.; Monaco, K. L.; Wang, R.-P.; Winters, M. P. *Tetrahedron Lett.* **1998**, *39 (19)*, 2933-2936; (b) Evans, D. A.; Katz, J. L.; West, T. R. *Tetrahedron Lett.*

1998, *39 (19)*, 2937-2940; (c) Lam, P. Y.; Clark, C. G.; Saubern, S.; Adams, J.; Winters, M. P.; Chan, D. M.; Combs, A. *Tetrahedron Lett.* **1998**, *39 (19)*, 2941-2944.

(12) (a) Goldberg, I. *Ber. Dtsch. Chem. Ges.* **1906**, *39 (2)*, 1691-1692; (b) Ullmann, F. *Ber. Dtsch. Chem. Ges.* **1903**, *36 (2)*, 2382-2384.

(13) (a) Guram, A. S.; Rennels, R. A.; Buchwald, S. L. *Angew. Chem, Int. Ed. Engl.* **1995**, *34 (12)*, 1348-1350; (b) Paul, F.; Patt, J.; Hartwig, J. F. *J. Am. Chem. Soc.* **1994**, *116 (13)*, 5969-5970.

(14) Boger, L. D.; Panek, J. S. *Tetrahedron Lett.* **1984**, *25 (30)*, 3175-3178.

(15) (a) Driver, M. S.; Hartwig, J. F. *J. Am. Chem. Soc.* **1996**, *118 (30)*, 7217-7218; (b) Wolfe, J. P.; Wagaw, S.; Buchwald, S. L. *J. Am. Chem. Soc.* **1996**, *118 (30)*, 7215-7216; (c) Louie, J.; Driver, M. S.; Hamann, B. C.; Hartwig, J. F. *J. Org. Chem.* **1997**, *62 (5)*, 1268-1273.

(16) (a) Dennis, J. M.; White, N. A.; Liu, R. Y.; Buchwald, S. L. *J. Am. Chem. Soc.* **2018**, *140 (13)*, 4721-4725; (b) Huang, X.; Anderson, K. W.; Zim, D.; Jiang, L.; Klapars, A.; Buchwald, S. L. *J. Am. Chem. Soc.* **2003**, *125 (22)*, 6653-6655; (c) Old, D. W.; Wolfe, J. P.; Buchwald, S. L. *J. Am. Chem. Soc.* **1998**, *120 (37)*, 9722-9723; (d) Wolfe, J. P.; Buchwald, S. L. *Angew. Chem. Int. Ed.* **1999**, *38 (16)*, 2413-2416.

(17) Hamann, B. C.; Hartwig, J. F. *J. Am. Chem. Soc.* **1998**, *120 (48)*, 12706-12706.

(18) Crawford, S. M.; Lavery, C. B.; Stradiotto, M. *Chem, Eur. J.* **2013**, *19 (49)*, 16760-16771.

(19) Tardiff, B. J.; McDonald, R.; Ferguson, M. J.; Stradiotto, M. *J. Org. Chem.* **2012**, *77 (2)*, 1056-1071.

(20) Marion, N.; Ecarnot, E. C.; Navarro, O.; Amoroso, D.; Bell, A.; Nolan, S. P. *J. Org. Chem.* **2006**, *71 (10)*, 3816-3821.

(21) (a) Dennis, J. M.; White, N. A.; Liu, R. Y.; Buchwald, S. L. *Acs Catal.* **2019**, *9 (5)*, 3822-3830; (b) Espino, G.; Kurbangalieva, A.; Brown, J. M. *Chem. Commun.* **2007**, *(17)*, 1742-1744; (c) Ji, J.; Li, T.; Bunnelle, W. H. *Org. Lett.* **2003**, *5 (24)*, 4611-4614; (d) Kreisel, T.; Mendel, M.; Queen, A. E.; Deckers, K.; Hupperich, D.; Riegger, J.; Fricke, C.; Schoenebeck, F. *Angew. Chem. Int. Ed.* **2022**, *61 (20)*, e202201475; (e) Meiries, S.; Chartoire, A.; Slawin, A. M.; Nolan, S. P. *Organometallics* **2012**, *31 (8)*, 3402-3409. (f) Onodera, S.; Kochi, T.; Kakiuchi, F. *J. Org. Chem.* **2019**, *84 (10)*, 6508-6515; (g) Taeufer, T.; Pospech, J. *J. Org. Chem.* **2020**, *85 (11)*, 7097-7111; (h) Urgaonkar, S.; Nagarajan, M.; Verkade, J. *J. Org. Chem.* **2003**, *68 (2)*, 452-459; (i) Wolfe, J. P.; Buchwald, S. L. *Org. Synth.* **2003**, *78* 23-23. (j) King, S. M.; Buchwald, S. L. *Org. Lett.* **2016**, *18 (16)*, 4128-4131.

(22) (a) Fitton, P.; Rick, E. A., *J. Organomet. Chem.* **1971,** *28* (2), 287-291; (b) Echavarren, A. M.; Stille, J. K., *J. Am. Chem. Soc.* **1987,** *109* (18), 5478-5486.

(23) Stroup, B. W.; Szklennik, P. V.; Forster, C. J.; Serrano-Wu, M. H. *Org. Lett.* **2007**, *9 (10)*, 2039-2042.

(24) Keylor, M. H.; Niemeyer, Z. L.; Sigman, M. S.; Tan, K. L. *J. Am. Chem. Soc.* **2017**, *139 (31)*, 10613-10616.

(25) Pu, X.; Zhang, Y.; Su, M.; He, X.; Qiu, L. *Tetrahedron Lett.* **2024**, *142* 155096.

(26) Hegedus, L.; Wade, L. *Preparation of carboxylic acids, acid halides and anhydrides.* John Wiley & Sons Hoboken, NJ: **1977**; *Vol. 3*, pp 8-32.

(27) (a) March, J. *Advanced Organic Chemistry*, 4th edn., Wiley, New York, **1992**, pp. 1183-1184; (b) Hudlick, M. *Oxidation in Organic Chemistry*, American Chemical Society, Washington, **1990**, pp. 105–109, 127–132; (c) Vollhardt, K. P. C. and Schore, N. E. *Organische Chemie,* 3. Aufl., Wiley-VCH, Weinheim, **2000**, pp. 1081-1087; (d) Beyer, H. and Walter, W. *Lehrbuch der Organischen Chemie*, 24. Aufl., Hirzel Verlag, Stuttgart, **2004**.

(28) (a) Rodríguez, N.; Goossen, L. J. *Chem. Soc. Rev.* **2011**, *40 (10)*, 5030-5048; (b) Goossen, L. J.; Deng, G.; Levy, L. M. *Science* **2006**, *313 (5787)*, 662-664; (c) Wei, Y.; Hu, P.; Zhang, M.; Su, W. *Chem. Rev.* **2017**, *117 (13)*, 8864-8907.

(29) (a) Goossen, L. J.; Rodríguez, N.; Melzer, B.; Linder, C.; Deng, G.; Levy, L. M. *J. Am. Chem. Soc.* **2007**, *129 (15)*, 4824-4833; (b) Wang, S.; Lu, H.; Li, J.; Zou, D.; Wu, Y.; Wu, Y. *Tetrahedron Lett.* **2017**, *58 (12)*, 1107-1111; (c) Wang, Z.; Ding, Q.; He, X.; Wu, J. *Tetrahedron* **2009**, *65 (24)*, 4635-4638; (d) Wang, S.; Lu, H.; Li, J.; Zou, D.; Wu, Y.; Wu, Y. *Tetrahedron Lett.* **2017**, *58 (28)*, 2723-2726; (e) Le Pham, N. S.; Lee, J.; Shin, H.; Sohn, J.-H. *Tetrahedron* **2018**, *74 (28)*, 3843-3851; (f) Vardhan Reddy, K. H.; Brion, J.-D.; Messaoudi, S.; Alami, M. *J. Org. Chem.* **2016**, *81 (2)*, 424-432; (g) Messaoudi, S.; Brion, J.-D.; Alami, M. *Org. Lett.* **2012**, *14 (6)*, 1496-1499; (h) Becht, J.-M.; Catala, C.; Le Drian, C.; Wagner, A. *Org. Lett.* **2007**, *9 (9)*, 1781-1783.

(30) Gooßen, L. J.; Zimmermann, B.; Knauber, T. *Angew. Chem. Int. Ed.* **2008**, *47 (37)*, 7103-7106.

(31) Tang, J.; Biafora, A.; Goossen, L. J. *Angew. Chem. Int. Ed.* **2015**, *54 (44)*, 13130-13133.

(32) (a) Goossen, L. J.; Linder, C.; Rodríguez, N.; Lange, P. P. *Chem, Eur. J.* **2009**, *15 (37)*, 9336-9349; (b) Goossen, L. J.; Rodriguez, N.; Linder, C. *J. Am. Chem. Soc.* **2008**, *130 (46)*, 15248-15249.

(33) Gooßen, L. J.; Rodríguez, N.; Lange, P. P.; Linder, C. *Angew. Chem. Int. Ed.* **2010**, *6 (49)*, 1111-1114.

(34) Song, B.; Knauber, T.; Gooßen, L. J. *Angew. Chem. Int. Ed.* **2013**, *52 (10)*.

(35) (a) Daley, R. A.; Liu, E.-C.; Topczewski, J. J. *Org. Lett.* **2019**, *21 (12)*, 4734-4738; (b) Forgione, P.; Brochu, M.-C.; St-Onge, M.; Thesen, K. H.; Bailey, M. D.; Bilodeau, F. *J. Am. Chem. Soc.* **2006**, *128 (35)*, 11350-11351; (c) Shang, R.; Xu, Q.; Jiang, Y.-Y.; Wang, Y.; Liu, L. *Org. Lett.* **2010**, *12 (5)*, 1000-1003; (d) Wang, J.; Cui, Y.; Xie, S.; Zhang, J.-Q.; Hu, D.; Shuai, S.; Zhang, C.; Ren, H. *Org. Lett.* **2023**, *26 (1)*, 137-141.

(36) (a) Gooßen, L. J.; Lange, P. P.; Rodríguez, N.; Linder, C. *Chem, Eur. J.* **2010**, *13 (16)*, 3906-3909; (b) Hackenberger, D.; Song, B.; Grünberg, M. F.; Farsadpour, S.; Menges, F.; Kelm, H.; Groß, C.; Wolff, T.; Niedner-Schatteburg, G.; Thiel, W. R. *ChemCatChem* **2015**, *7 (21)*, 3579-3588.

(37) (a) Fromm, A.; van Wüllen, C.; Hackenberger, D.; Goossen, L. J. *J. Am. Chem. Soc.* **2014**, *136 (28)*, 10007-10023; (b) Gooßen, L. J.; Rodríguez, N.; Linder, C.; Lange, P. P.; Fromm, A. *ChemCatChem* **2010**, *2 (4)*, 430-442.

(38) (a) Lyons, T. W.; Sanford, M. S. *Chem. Rev.* **2010**, *110 (2)*, 1147-1169; (b) Ackermann, L. *Chem. Rev.* **2011**, *111 (3)*, 1315-1345.

(39) (a) Bura, T.; Blaskovits, J. T.; Leclerc, M. *J. Am. Chem. Soc.* **2016**, *138 (32)*, 10056-10071; (b) Morin, P.-O.; Bura, T.; Leclerc, M. *Mater. Horiz.* **2016**, *3 (1)*, 11-20;

(c) Okamoto, K.; Zhang, J.; Housekeeper, J. B.; Marder, S. R.; Luscombe, C. K. *Macromolecules* **2013**, *46 (20)*, 8059-8078; (d) Pouliot, J.-R.; Grenier, F.; Blaskovits, J. T.; Beaupré, S.; Leclerc, M. *Chem. Rev.* **2016**, *116 (22)*, 14225-14274.

(40) Nakamura, N.; Tajima, Y.; Sakai, K. *Heterocycles* **1982**, *17*.

(41) (a) Seregin, I. V.; Gevorgyan, V. *Chem. Soc. Rev.* **2007**, *36 (7)*, 1173-1193; (b) Bheeter, C. B.; Chen, L.; Soulé, J.-F.; Doucet, H. *Catalysis Science & Technology* **2016**, *6 (7)*, 2005-2049.

(42) (a) Bellina, F.; Calandri, C.; Cauteruccio, S.; Rossi, R. *Tetrahedron* **2007**, *63 (9)*, 1970-1980; (b) Colletto, C.; Islam, S.; Juliá-Hernández, F.; Larrosa, I. *J. Am. Chem. Soc.* **2016**, *138 (5)*, 1677-1683; (c) Kobayashi, K.; Sugie, A.; Takahashi, M.; Masui, K.; Mori, A. *Org. Lett.* **2005**, *7 (22)*, 5083-5085; (d) Lane, B. S.; Sames, D. *Org. Lett.* **2004**, *6 (17)*, 2897-2900; (e) Lebrasseur, N.; Larrosa, I. *J. Am. Chem. Soc.* **2008**, *130 (10)*, 2926-2927; (f) Matsuda, S.; Takahashi, M.; Monguchi, D.; Mori, A. *Synlett* **2009**, *2009 (12)*, 1941-1944; (g) Rene, O.; Fagnou, K. *Adv. Synth, Catal.* **2010**, *352 (13)*, 2116-2120. (h) Touré, B. B.; Lane, B. S.; Sames, D. *Org. Lett.* **2006**, *8 (10)*, 1979-1982; (i) Wang, L.; Yi, W.-b.; Cai, C. *Chem. Commun.* **2011**, *47 (2)*, 806-808. (j) Xu, Z.; Xu, Y.; Lu, H.; Yang, T.; Lin, X.; Shao, L.; Ren, F. *Tetrahedron* **2015**, *71 (18)*, 2616-2621.

(43) (a) Fu, H. Y.; Doucet, H. *Methyl 2-Furoate: An Alternative Reagent to Furan for Palladium-Catalysed Direct Arylation.* Wiley Online Library: **2011**; (b) Lapointe, D.; Markiewicz, T.; Whipp, C. J.; Toderian, A.; Fagnou, K. *J. Org. Chem.* **2011**, *76 (3)*, 749-759; (c) Liegault, B.; Lapointe, D.; Caron, L.; Vlassova, A.; Fagnou, K. *J. Org. Chem.* **2009**, *74 (5)*, 1826-1834; (d) Ohta, A.; Akita, Y.; Ohkuwa, T.; Chiba, M.;

Fukunaga, R.; Miyafuji, A.; Nakata, T.; Tani, N.; Aoyagi, Y. *Heterocycles* **1990**, *31 (11)*, 1951; (e) Ouyang, J.-S.; Li, Y.-F.; Shen, D.-S.; Ke, Z.; Liu, F.-S. *Dalton Trans.* **2016**, *45 (38)*, 14919-14927; (f) Piou, T.; Slutskyy, Y.; Kevin, N. J.; Sun, Z.; Xiao, D.; Kong, J. *Org. Lett.* **2021**, *23 (6)*, 1996-2001; (g) Roger, J.; Požgan, F.; Doucet, H. *Adv. Synth, Catal.* **2010**, *352 (4)*, 696-710; (h) Satoh, T.; Miura, M. *Chem. Lett.* **2007**, *36 (2)*, 200-205; (i) Zheng, D.-Z.; Li, D.-H.; Liu, H.; Shao, Y.; Ke, Z.; Liu, F.-S. *Organometallics* **2022**, *41 (8)*, 948-961; (j) Loukotova, L.; Yuan, K.; Doucet, H. *ChemCatChem* **2014**, *6 (5)*, 1303-1309; (k) Dao-Huy, T.; Haider, M.; Glatz, F.; Schnürch, M.; Mihovilovic, M. D. *Eur. J. Org. Chem.* **2014**, *2014 (36)*, 8119-8125.

(44) (a) Ackermann, L.; Vicente, R.; Born, R. *Adv. Synth, Catal.* **2008**, *350 (5)*, 741-748; (b) Chiong, H. A.; Daugulis, O. *Org. Lett.* **2007**, *9 (8)*, 1449-1451; (c) Ghosh, D.; Lee, H. M. *Org. Lett.* **2012**, *14 (21)*, 5534-5537; (d) Nadres, E. T.; Lazareva, A.; Daugulis, O. *J. Org. Chem.* **2011**, *76 (2)*, 471-483; (e) Tamba, S.; Okubo, Y.; Tanaka, S.; Monguchi, D.; Mori, A. *J. Org. Chem.* **2010**, *75 (20)*, 6998-7001. (f) Verrier, C.; Martin, T.; Hoarau, C.; Marsais, F. *J. Org. Chem.* **2008**, *73 (18)*, 7383-7386.

(45) Roger, J.; Doucet, H. *Org. Biomol. Chem.* **2008**, *6 (1)*, 169-174.

(46) (a) Ackermann, L.; Althammer, A.; Fenner, S. *Angew. Chem. Int. Ed.* **2009**, *48 (1)*, 201-204; (b) Fan, S.; Yang, J.; Zhang, X. *Org. Lett.* **2011**, *13 (16)*, 4374-4377.

(47) Ferguson, D. M.; Rudolph, S. R.; Kalyani, D. *Acs Catal.* **2014**, *4 (7)*, 2395-2401.

(48) (a) Jui, N. T.; Buchwald, S. L. *Angew. Chem. Int. Ed.* **2013**, *52 (44)*, 11624-11627; (b) Mendel, M.; Kalvet, I.; Hupperich, D.; Magnin, G.; Schoenebeck, F. *Angew. Chem. Int. Ed.* **2020**, *59 (5)*, 2115-2119; (c) Ogata, T.; Hartwig, J. F. *J. Am. Chem. Soc.* **2008**,

130 (42), 13848-13849; (d) Wu, X.-F. *RSC Adv.* **2016**, *6 (87)*, 83831-83837.

(49) Reeves, E. K.; Entz, E. D.; Neufeldt, S. R. *Chem, Eur. J.* **2021**, *27 (20)*, 6161-6177.

(50) Littke, A. F.; Dai, C.; Fu, G. C. *J. Am. Chem. Soc.* **2000**, *122 (17)*, 4020-4028.

(51) Littke, A. F.; Schwarz, L.; Fu, G. C. *J. Am. Chem. Soc.* **2002**, *124 (22)*, 6343-6348.

(52) Schoenebeck, F.; Houk, K. *J. Am. Chem. Soc.* **2010**, *132 (8)*, 2496-2497.

(53) Niemeyer, Z. L.; Milo, A.; Hickey, D. P.; Sigman, M. S. *Nat. Chem.* **2016**, *8 (6)*, 610-617.

(54) Wei, X. J.; Xue, B.; Handelmann, J.; Hu, Z.; Darmandeh, H.; Gessner, V. H.; Gooßen, L. J. *Adv. Synth, Catal.* **2022**, *364 (19)*, 3336-3341.

(55) Reeves, E. K.; Humke, J. N.; Neufeldt, S. R. *J. Org. Chem.* **2019**, *84 (18)*, 11799-11812.

(56) Proutiere, F.; Schoenebeck, F. *Angew. Chem. Int. Ed.* **2011**, *50 (35)*, 8192-8195.

(57) (a) Reeves, E. K.; Bauman, O. R.; Mitchem, G. B.; Neufeldt, S. R. *Isr. J. Chem.* **2020**, *60 (3-4)*, 406-409; (b) Elias, E. K.; Rehbein, S. M.; Neufeldt, S. R. *Chem. Sci.* **2022**, *13 (6)*, 1618-1628.

(58) So, C. M.; Yuen, O. Y.; Ng, S. S.; Chen, Z. *Acs Catal.* **2021**, *11 (13)*, 7820-7827.

(59) (a) Brookhart, M.; Green, M. L. H.; Parkin, G. *Proc. Natl. Acad. Sci. U.S.A* **2007**, *104 (17)*, 6908-6914; (b) Scherer, W.; Dunbar, A. C.; Barquera-Lozada, J. E.; Schmitz, D.; Eickerling, G.; Kratzert, D.; Stalke, D.; Lanza, A.; Macchi, P.; Casati, N. P. M.; Ebad-Allah, J.; Kuntscher, C. *Angew. Chem., Int. Ed.* **2015**, *54 (8)*, 2505-2509. (c) Lepetit, C.; Poater, J.; Alikhani, M. E.; Silvi, B.; Canac, Y.; Contreras-García, J.; Solà, M.; Chauvin, R. *Inorg. Chem.* **2015**, *54 (6)*, 2960-2969. (d) Sundquist, W. I.; Bancroft,

D. P.; Lippard, S. J. *J. Am. Chem. Soc.* **1990**, *112 (4)*, 1590-1596. (e) Taubmann, C.; Öfele, K.; Herdtweck, E.; Herrmann, W. A. *Organometallics* **2009**, *28 (15)*, 4254-4257. (60) (a) Chen, Z.; Gu, C.; Yuen, O. Y.; So, C. M. *Chem. Sci.* **2022**, *13 (17)*, 4762-4769; (b) Chen, Z.; Pang, W. H.; Yuen, O. Y.; Ng, S. S.; So, C. M. *J. Org. Chem.* **2024**, Article ASAP; (c) Ng, S. S.; Chen, Z.; Yuen, O. Y.; So, C. M. *Adv. Synth, Catal.* **2022**, *364 (9)*, 1596-1601; (d) Wang, M.; Pang, W. H.; Yuen, O. Y.; Ng, S. S.; So, C. M. *Org. Lett.* **2023**, *25 (47)*, 8429-8433. (e) Wang, M.; So, C. M. *Org. Lett.* **2022**, *24 (2)*, 681-685; (f) Wang, M.; Yuen, O. Y.; So, C. M. *Chin. J. Chem.* **2023**, *41 (8)*, 909-914.

Chapter 2 Palladium-Catalyzed Chemoselective Amination of Chloro(hetero)aryl Triflates Enabled by Alkyl-Pyrazole-Based Phosphine Ligands

2.1 Introduction

Palladium-catalyzed *N*-arylation of amines represents a potent strategy for the synthesis of aromatic amines, which are essential for applications in pharmaceuticals, functional materials and catalysts.[1] There has been a great advancement of catalysts in the past decades which allow for expanding the scope of electrophiles to include more inert electrophiles, such as aryl chlorides and even aryl sulfonates, for the amination reaction.[2] These studies mainly focused on enhancing the catalytic activity of the catalysts to activate the single inert electrophile within the substrates. However, the study of the chemoselectivity of those highly active catalysts toward molecules bearing several active electrophilic sites (i.e., Br, OTf, Cl) is rather limited (Scheme 2.1A).[3] Moreover, a narrow substrate scope and poor functional group compatibility are common encountered problems in currently reported chemoselective amination protocols. For instance, chemoselective amination of sterically hindered electrophiles and those with electron-deficient groups has not been realized. The OTf group is highly reactive and frequently undergoes reactions preferentially in the presence of multiple electrophilic groups. Retaining the OTf group, which is an excellent leaving group, could facilitate the synthesis of complex molecular structures, particularly in cases involving challenging reaction partners. When substrates have multiple reactive

electrophilic sites,[4] tuning reaction conditions is essential to avoid product mixtures. This requirement becomes an obstacle when using coupling reactions in the late-stage modifications of many drug-like molecules, natural products, and materials. Hence, controlling chemoselectivity not only introduces precise functional groups but also aids in assembling complex molecular structures efficiently.[5] The use of catalysts with suitable ligands is a promising strategy to manipulate chemoselectivity and tackle issues in coupling reactions. Despite some advancements, the design of new ligands for chemoselectivity control, particularly for inverting traditional reactivity order (e.g., C−Cl > C−OTf), is still limited. The role of the Pd complex's ligation state in chemoselectivity has been explored theoretically.[6] While some effective ligands for such chemoselectivity have been discovered, they are used in C−C bond formations.[6a, 7] Our group recently developed a new class of 2-alkyl indole-based phosphine ligands and then achieved several chemoselective cross-coupling reactions,[8] highlighting the significance of rationally design appropriate ligands to enable chemoselective coupling reactions.

The construction of C–N bond in a chemoselective manner, especially inverting reactivity order, is underexplored.[9] Serrano-Wu utilized NHC ligand for selectivity control in a Buchwald-Hartwig amination investigation, albeit resulting in poor yield (Scheme 2.1B).[9a] Sigman and Tan's investigations leveraged the ferrocene "DMAPF" ligand, resulting in high efficiency and chemoselectivity. However, the substrates only limited to heteroarenes bearing Br and Cl (Scheme 1B).[9b] To the best of our knowledge, there has been no chemoselective amination example in a C−Cl > C−OTf order to date.

Therefore, we aim to explore new phosphine ligands to control reactivity order with excellent chemoselectivity in amination reactions, expanding the ligand library for chemoselectivity challenges in synthetic pathways.

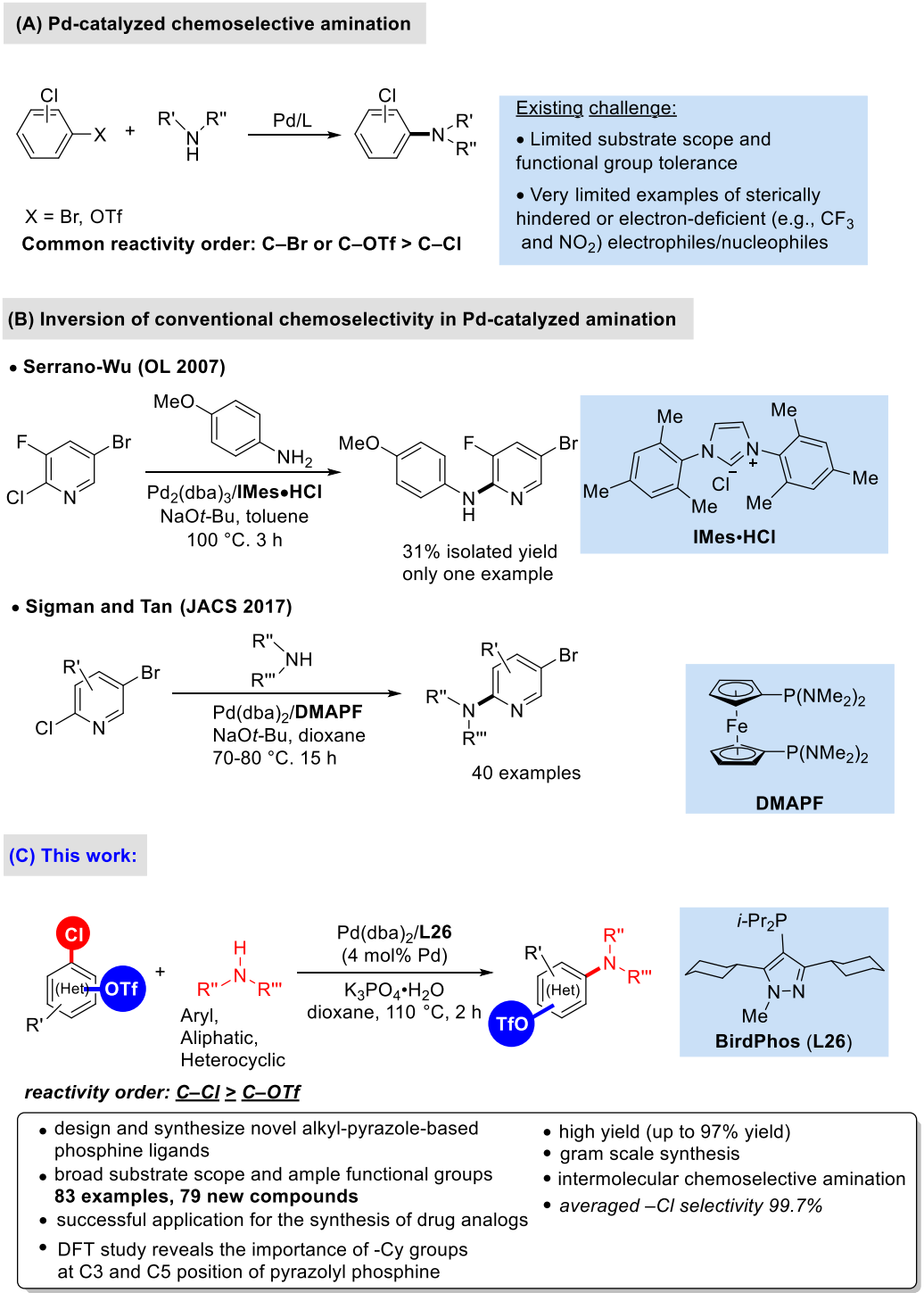

Scheme 2.1 Palladium-catalyzed chemoselective amination

2.2 Results and Discussion

2.2.1 Design and Synthesis of Alkyl-Pyrazole-Based Phosphine Ligands

The reactivity of cross-coupling reactions can be enhanced by the implementation of utilizing appropriate phosphine ligands. It is well established that the use of electron-rich ligands enhance the rates of oxidative addition step, while sterically hindered ones facilitate reductive elimination processes and stimulate the formation of active monoligated Pd(0) complexes.[10] Ligands such as BrettPhos, HandaPhos, and Zheda-Phos, which feature two bulky substituents at the *ortho* positions of the phosphorus atom, exhibit exceptional efficacy (Scheme 2.2). For instance, BrettPhos was demonstrated to facilitate the Pd-catalyzed monoarylation of methylamine with aryl chlorides,[11] while Suzuki-Miyaura coupling reaction in water at room temperature can be achieved with HandaPhos using only ppm level of palladium.[12] At the same time, Zheda-Phos considerably promoted Pd-catalyzed monoarylation of acetone with a series of aryl chlorides.[13]

Besides the reactivity, the selectivity is also important for cross-coupling reactions in terms of efficiency, atom economy, and environmental friendliness. Regarding the chemoselectivity for the activation of C−OTf and C−Cl bonds, previous investigations indicated that phosphine ligands with aryl bottom rings prefer to offer C−OTf > C−Cl reactivity order due to the existence of Pd-π interaction,[6c, 14] while our recent investigations revealed that a reversed reactivity order can be obtained by introducing a secondary alkyl group in the *ortho* position of phosphine ligands. The explanation for achieving this reversed chemoselectivity lies in the preagostic C–H···Pd interaction and

sufficient steric hindrance provided by ligands.[8] Building on these principles, we designed novel pyrazole-based phosphine ligands featuring two bulky alkyl groups at the *ortho*-positions of the phosphine moiety. (Scheme 2.2).

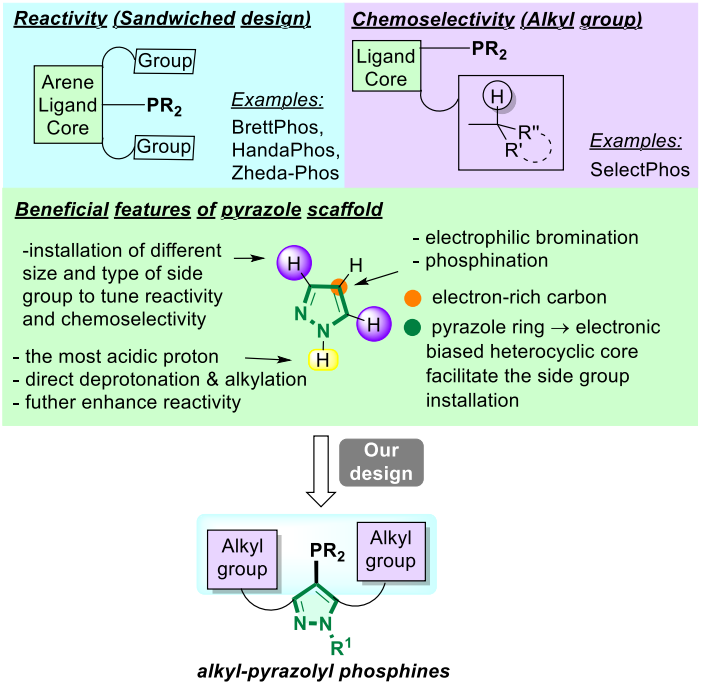

Scheme 2.2 Rational design of pyrazolyl phosphine ligands

Pyrazoles serve as important core structures of many pharmaceuticals and pharmaceutical leads, with a wide range of biological activities.[15] We chose pyrazole as the heterocyclic moiety for the ligand skeleton, as it provides several benefits (Scheme 2.2): (1) Easy installation of different sizes and types of side groups at the C3 and C5 positions, (2) The electronic-biased C4 position allows rapid regioselective bromination and phosphination, (3) The first and second advantages allow the easy modification of substituents on pyrazole, which allows tuning electronic and steric properties easily for specific reactions,[16] and (4) The synthetic pathway involves Knorr pyrazole synthesis, alkylation, bromination, and phosphination, which is simple and

straightforward, starting from inexpensive and readily available diketones and hydrazine (Scheme 2.3).[17]

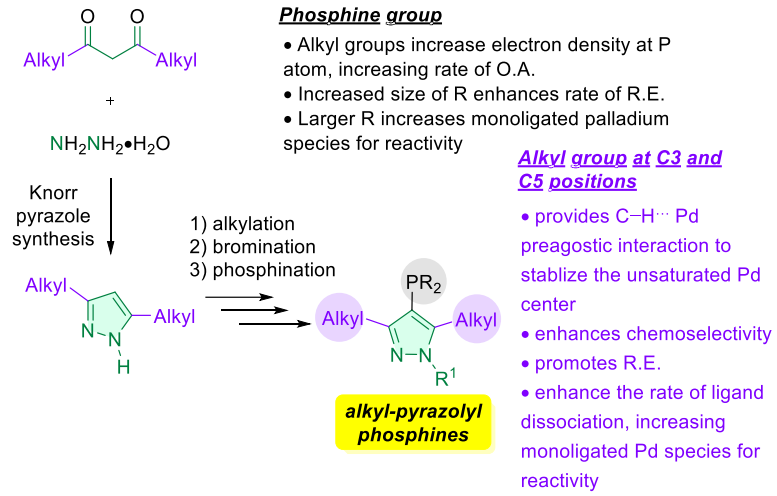

Scheme 2.3 Synthetic pathway and features of alkyl-pyrazole-based phosphine ligands

We first synthesized pyrazole-based phosphine ligands bearing cyclohexyl group at C-3 and C-5 positions of the pyrazole skeleton (Scheme 2.4). The synthesis route began with the condensation of 1-cyclohexylethan-1-one and methyl cyclohexanecarboxylate to provide di-ketone compound **A**, which then reacted with hydrazine hydrate via Knorr pyrazole synthesis to give nitrogen atom unprotected pyrazole **B**, followed by alkylation and bromination to generate compound **D**. Treating **D** with *n*-butyllithium followed by addition of different substituted phosphorus chlorides, phosphine ligands with different groups on the P atom can be obtained. The overall yields of **L25**, **L26,** and **L27** synthesized by the 5-step synthetic route were 49%, 37%, and 54%, respectively. Moreover, the successful implementation of the same or similar strategy has led to the successful synthesis of **L28**, **L29**, **L30,** and **L31** (Figure 2.1). Due to the varying number of synthetic steps for each ligand and the different types of ligand precursors used for ligand synthesis, only the yields of the final

phosphination step were reported here.

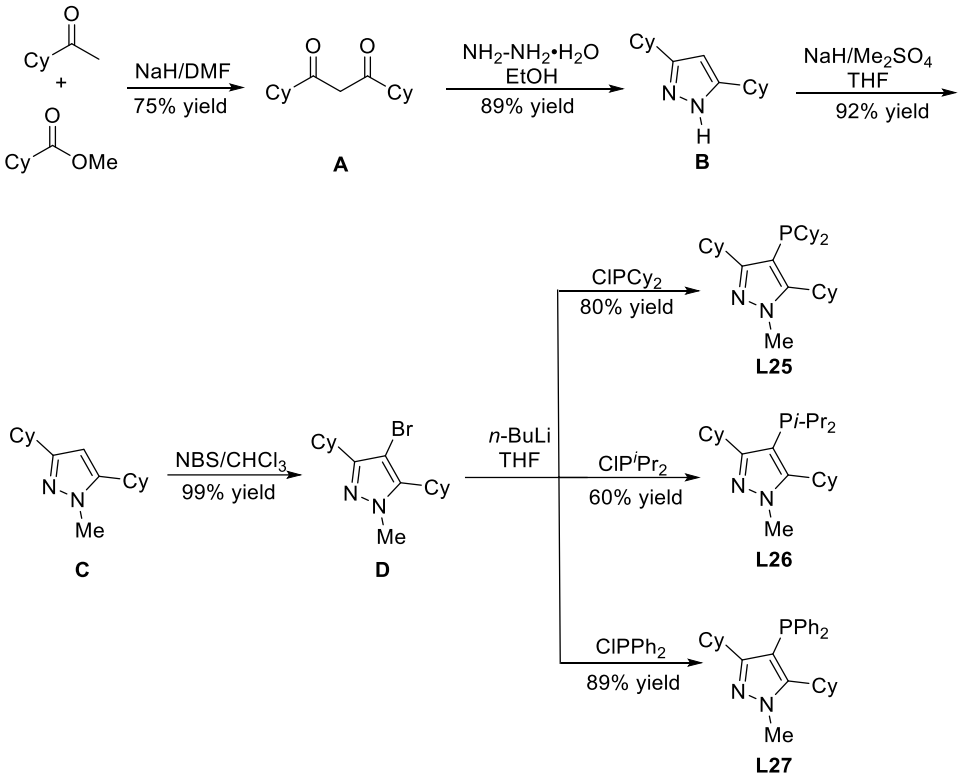

Scheme 2.4 Newly synthesized alkyl-pyrazole-based phosphine ligands

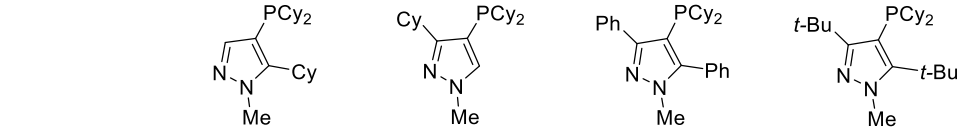

Figure 2.1 Other newly synthesized pyrazole-based phosphine ligands

2.2.2 Evaluation of Ligand Effect in the Chemoselective Amination

After synthesizing a series of pyrazole-based phosphine ligands, we then investigated the feasibility of chemoselective amination reaction with a C−Cl > C−OTf order using 4-chlorophenyl triflate **1a** and *N*-methylaniline **2a** as our model substrates (Table 2.1). We first tested some commercially available ligands (Table 2.1, **L1**−**L23**).

PPh_3 (Table 2.1, **L1**) and PCy_3 (Table 2.1, **L2**) exhibited no reactivity. Only P^tBu_3 (Table 2.1, **L3**), $[Pd(\mu\text{-}I)P\textit{t}\text{-}Bu_3]_2$ (Table 2.1, **L4**) and $P\textit{t}\text{-}Bu_3 \cdot HBF_4$ (Table 2.1, **L5**) showed C−Cl selectivity, but poor yields were provided. The employment of Buchwald-type ligands (Table 2.1, **L8**−**L13**) and CM-Phos (Table 2.1, **L14**) resulted in C−OTf activation, consistent with the typical reactivity trend of C−OTf > C−Cl. P, N-type ligands (Table 2.1, **L15** and **L16**) have also exhibited chemoselectivity toward the C−OTf bond. In contrast, most of the diphosphine ligands (Table 2.1, **L17**−**L19**) proved ineffective in this catalytic transformation. BINAP (Table 2.1, **L20**) and XantPhos (Table 2.1, **L21**) preferentially reacted with the C−OTf bond. NHC ligands (Table 2.1, **L22** and **L23**) displayed poor chemoselectivity and reactivity. Intriguingly, SelectPhos (**L24**) demonstrated excellent chemoselectivity and reactivity toward the C−Cl bond in a series of coupling reactions,[8] but with suboptimal catalytic activity in this reaction. Remarkably, the newly developed pyrazole-based phosphine ligands featuring a cyclohexyl group at C3 and C5 positions (**L25**−**L27**) reversed the chemoselectivity (C−Cl > C−OTf), and **L26** (BirdPhos) bearing $-P\textit{i}\text{-}Pr_2$ provided the highest yield of **3a** with excellent chemoselectivity. Replacing the phosphine group with less electron-rich and sterically hindered $-PPh_2$ (**L27**) led to a considerably reduced yield of **3a**, yet the chemoselectivity toward the C−Cl bond was retained. We deemed that the cyclohexyl groups at the C3 and C5 positions may prevent the rotation of $-PPh_2$ group, thereby inhibiting the formation of the active bis-coordinated species preferred to activate the C−OTf bond.[8b] In contrast, the pyrazolyl phosphine ligand containing the phenyl group (**L30**) at the C3 and C5 positions afforded a mixture of products, **3a** and **4a**, exhibiting

a preference for the C−OTf over C−Cl. To further elucidate the significance of cyclohexyl groups at the C3 and C5 positions of the *N*-methyl pyrazole ring, the pyrazolyl phosphine ligands bearing −PCy_2 group with the cyclohexyl group at the C5 (**L28**) and C3 position (**L29**) on the pyrazole core were synthesized, respectively. When the cyclohexyl group was installed only at the C3 or C5 position of *N*-methyl pyrazole, results of low yields of the product were obtained, but chemoselectivity at the C–Cl bond remained unchanged, in stark contrast to the observations for **L25**. These outcomes suggest that the coexistence of cyclohexyl groups at the C3 and C5 positions might play a crucial role in catalyst reactivity. Notably, changing the cyclohexyl group at the C3 and C5 positions to a more sterically hindered tertiary alkyl group of *t*-Bu (**L31**), resulted in an inactive ligand in this reaction due to the lack of methine hydrogen.

Table 2.1 Ligand screening of palladium-catalyzed chemoselective C−Cl (over C−OTf) amination[a]

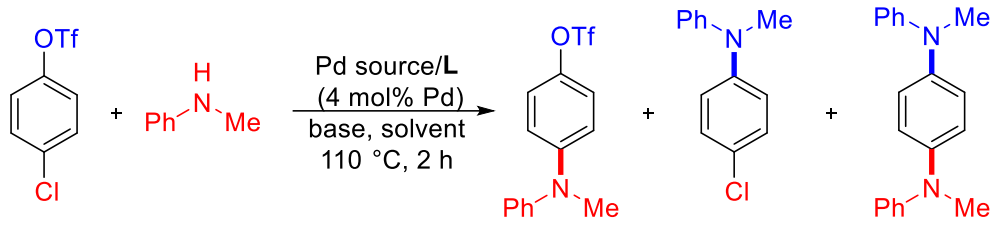

1a **2a** **3a** **4a** **5a**

L1: PPh_3
L2: PCy_3
L3: P*t*-Bu_3
L4[b]: [Pd(μ-I)P*t*-Bu_3]$_2$
L5: P*t*-Bu_3•HBF_4
L6: P(p-*tolyl*)$_3$
L7: P(o-*tolyl*)$_3$
L8: CyJohnPhos
L9: DavePhos
L10: SPhos
L11: RuPhos
L12: XPhos
L13: BrettPhos
L14: CMPhos
L15: PhMezole-Phos
L16: MorDalPhos
L17: dppe
L18: dppf
L19: dippf
L20: BINAP
L21: XantPhos
L22: IMes•HCl
L23: IPr•HCl
L24: SelectPhos

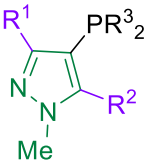

L25: R^1=R^2=R^3=Cy
L26: R^1=R^2=Cy, R^3=*i*-Pr (BirdPhos)
L27: R^1=R^2=Cy, R^3=Ph
L28: R^1=H, R^2=Cy, R^3=Cy
L29: R^1=Cy,R^2=H, R^3=Cy
L30: R^1=Ph, R^2=Ph, R^3=Cy
L31: R^1=R^2=*t*-Bu, R^3=Cy

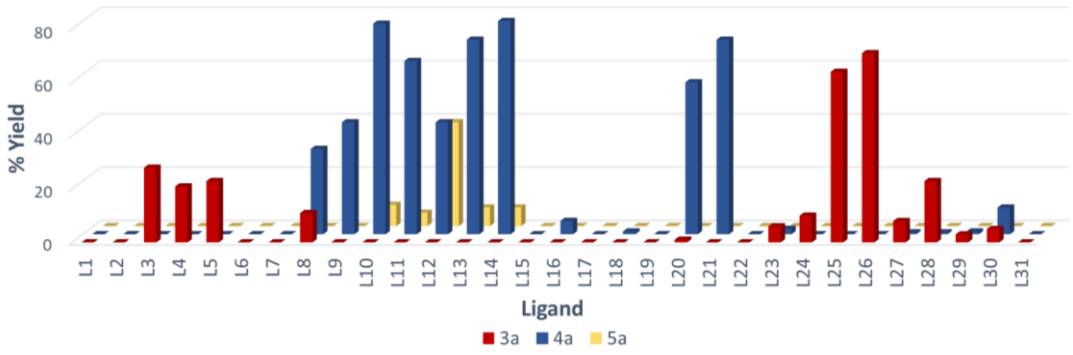

[a]Reaction condition: 4-chlorophenyltriflate **1a** (0.20 mmol), *N*-methylaniline **2a** (0.30 mmol), $Pd(OAc)_2$ (4.0 mol%), **L** (4.0 mol%), $K_3PO_4·H_2O$ (0.40 mmol) and dioxane (1.0 mL) were stirred at 110 °C for 2 h. Calibrated GC yields were reported by using dodecane as an internal standard. [b][Pd(μ-I)P*t*-Bu_3]$_2$ (2 mol%) was used without $Pd(OAc)_2$.

2.2.3 Optimization of Condition Parameters

We next chose the alkyl-pyrazole-based phosphine ligand **L26** to further optimize the other condition parameters (Table 2.2). The evaluation of the effect of palladium source on the chemoselective amination revealed that $Pd(dba)_2$ was the most effective catalyst among the $Pd(OAc)_2$, $PdCl_2$, $[Pd(\pi\text{-cinnamyl})Cl]_2$, $[Pd(2\text{-butenyl})Cl]_2$, and Pd_2dba_3 (Table 2.2, entries **1**−**6**). $K_3PO_4 \cdot H_2O$ was still the best base among the inorganic bases screened including K_3PO_4, $K_3PO_4 \cdot 3H_2O$, Cs_2CO_3, K_2CO_3 and Na_3PO_4 (Table 2.2, entries **7**−**11**). In terms of solvent screening, other solvents such as THF, Toluene, CPME, Hexane, and *t*-BuOH all provided inferior yields than dioxane, but also with excellent chemoselectivity at C–Cl bond (Table 2.2, entries **12**−**16**). Upon increasing the ligand-to-palladium ratio to 1:2, we were able to further improve the isolated yield of product **3a** to 89% (Table 2.2, entry **17**). However, a further increase in the ligand loading to 1:3 or 1:4 led to a slight reduction in reactivity, though the performance remained superior to the 1:1 ligand-to-palladium ratio (Table 2.2, entries **18** and **19**). Lowering the reaction temperature to 100 °C, a slight attenuation in the reactivity of the chemoselective amination was observed, while further decreasing the temperature to 90 °C resulted in a significant reduction in the yield of product **3a**, albeit with the excellent chemoselectivity (Table 2.2, entries **20** and **21**). We then utilized a combination of $Pd(dba)_2$/**L26** (1:2) as a catalyst with $K_3PO_4 \cdot H_2O$ as the base and dioxane as the solvent to broaden the substrate scope.

Table 2.2 Screening of reaction conditions[a]

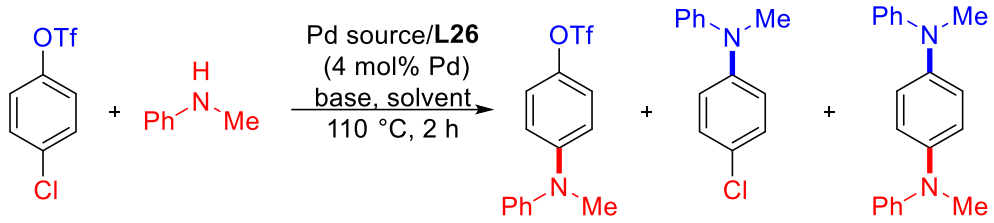

1a **2a** **3a** **4a** **5a**

Entry	Pd source	Pd:L	Base	Solvent	**3a** (%)[b]	**4a** (%)[b]	**5a** (%)[b]
1	$Pd(OAc)_2$	1:1	$K_3PO_4·H_2O$	Dioxane	71	0	0
2	$Pd(dba)_2$	1:1	$K_3PO_4·H_2O$	Dioxane	74	0	1
3	$PdCl_2$	1:1	$K_3PO_4·H_2O$	Dioxane	69	0	0
4	[Pd(π-cinnamyl)Cl]$_2$	1:1	$K_3PO_4·H_2O$	Dioxane	64	0	0
5	[Pd(2-butenyl)Cl]$_2$	1:1	$K_3PO_4·H_2O$	Dioxane	59	0	0
6	Pd_2dba_3	1:1	$K_3PO_4·H_2O$	Dioxane	73	0	0
7	$Pd(dba)_2$	1:1	K_3PO_4	Dioxane	55	0	0
8	$Pd(dba)_2$	1:1	$K_3PO_4·3H_2O$	Dioxane	55	0	0
9	$Pd(dba)_2$	1:1	Cs_2CO_3	Dioxane	60	0	8
10	$Pd(dba)_2$	1:1	K_2CO_3	Dioxane	50	0	0
11	$Pd(dba)_2$	1:1	Na_3PO_4	Dioxane	3	0	0
12	$Pd(dba)_2$	1:1	$K_3PO_4·H_2O$	THF	67	0	6
13	$Pd(dba)_2$	1:1	$K_3PO_4·H_2O$	Toluene	34	0	0
14	$Pd(dba)_2$	1:1	$K_3PO_4·H_2O$	CPME	42	0	0
15	$Pd(dba)_2$	1:1	$K_3PO_4·H_2O$	Hexane	37	0	0

16	$Pd(dba)_2$	1:1	$K_3PO_4·H_2O$	*t*-BuOH	30	0	0
17	$Pd(dba)_2$	1:2	$K_3PO_4·H_2O$	Dioxane	76 (89[c])	0	0
18	$Pd(dba)_2$	1:3	$K_3PO_4·H_2O$	Dioxane	75	0	0
19	$Pd(dba)_2$	1:4	$K_3PO_4·H_2O$	Dioxane	72	0	0
20[d]	$Pd(dba)_2$	1:2	$K_3PO_4·H_2O$	Dioxane	50	0	0
21[e]	$Pd(dba)_2$	1:2	$K_3PO_4·H_2O$	Dioxane	13	0	0

[a] Reaction condition: 4-chlorophenyltriflate (0.20 mmol), *N*-methylaniline (0.30 mmol), palladium source (4.0 mol% Pd), **L26**, base (0.40 mmol) and solvent (1.0 mL) were stirred at 110 °C for 2 h. [b] Calibrated GC yields were reported by using dodecane as an internal standard. [c]Isolated yield was reported. [d]100 °C was conducted. [e]90 °C was conducted.

2.2.4 Scope of Chloroaryl Triflates and Amines

We subsequently explored the scope of the chemoselective amination of chloroaryl triflates. A wide range of aryl amines were initially tested (Table 2.3). A range of *N*-methylaniline (Table 2.3, **3a**−**3g**) and aniline derivatives (Table 2.3, **3h**−**3af**) were identified as feasible substrates. An array of anilines containing electron-donating groups (−OMe, −OPh, and −Me) and electron-withdrawing groups (−F, $-CF_3$, −Ph, and $-NO_2$), underwent smooth coupling with chloroaryl triflates, furnishing the corresponding products in excellent-to-good yields. Ketone (Table 2.3, **3g**), methoxyl (Table 2.3, **3j**), and trifluoromethyl (Table 2.3, **3k**) were well tolerated. Notably, sterically hindered anilines also proved to be effective cross-coupling reagents (Table 2.3, **3u**, **3x**, **3y**, **3ae**, and **3af**). The excellent chemoselectivity of the Pd/**L26** catalyst enables the preparation of reactive secondary arylamines while maintaining the

electrophilic triflate group within the same molecules, thus facilitating for further diversification.

Table 2.3 Pd-catalyzed amination of aryl amines with chloroaryl triflates[a]

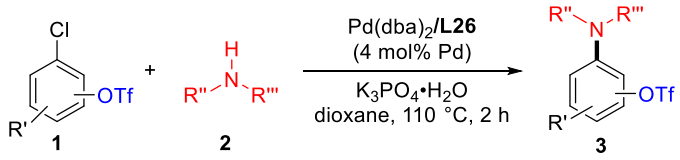

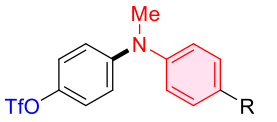

3a, R = H, 89% (100:0:0)
3b, R = Me, 94% (100:0:0)

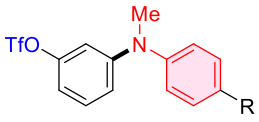

3c, R = H, 82% (100:0:0)
3d, R = Me, 86% (93:0:7)

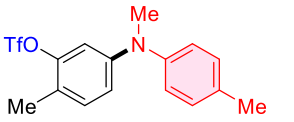

3e, 85% (99.4:0.6:0)

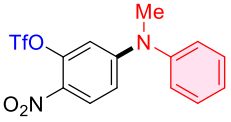

3f, 65%[c,l] (98.5:1.5:0)

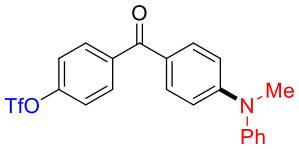

3g, 95% (100:0:0)

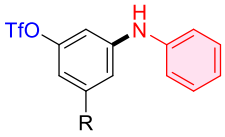

3h, R = H, 82%[c] (90:0:10)
3i, R = Me, 87%[b] (100:0:0)
3j, R = OMe, 77%[d] (100:0:0)
3k, R = CF_3, 71%[e] (100:0:0)

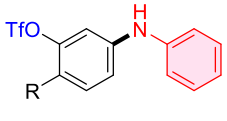

3l, R = Me, 90% (99.7:0.3:0)
3m, R = F, 70%[h,j] (94.3:2.8:2.9)

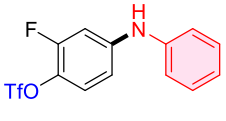

3n, 76%[i] (99:1:0)

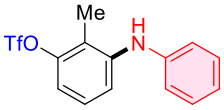

3o, 93% (100:0:0)

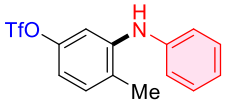

3p, 90% (100:0:0)

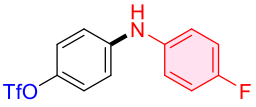

3q, 90% (100:0:0)

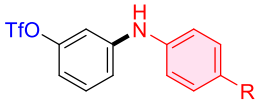

3r, R = F, 90%[c] (100:0:0)
3s, R = Ph, 91% (100:0:0)
3t, R = OMe, 78% (100:0:0)

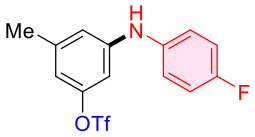

3u, 85%[b,f] (100:0:0)

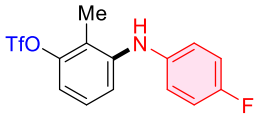

3v, 81% (100:0:0)

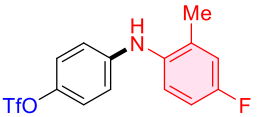

3w, 92% (100:0:0)

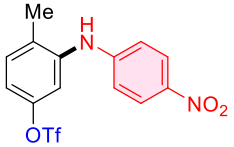

3x 78% (100:0:0)

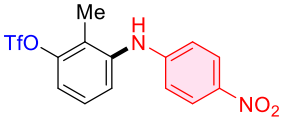

3y, 84% (100:0:0)

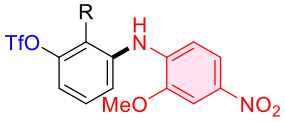

3z, R = H, 78% (100:0:0)
3aa, R = Me, 72% (100:0:0)

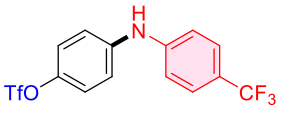

3ab, 91% (99.7:0.3:0)

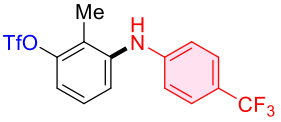

3ac, 90% (99:0:1)

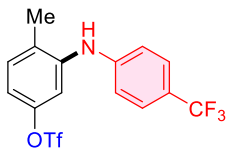

3ad, 90% (97:0:3)

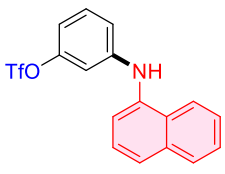

3ae, 82% (100:0:0)

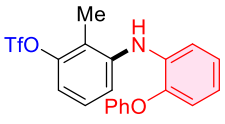

3af, 81% (100:0:0)

[a]Reaction conditions: Cl−Ar−OTf (0.20 mmol), amines (0.30 mmol), $K_3PO_4 \cdot H_2O$ (0.40 mmol), $Pd(dba)_2$ (4.0 mol%), **L26** (8.0 mol%), and dioxane (1.0 mL) were stirred at 110 °C for 2 h under a nitrogen atmosphere. Isolated yields were reported. The ratio in the blanket represents the chemoselectivity ratio in a crude reaction mixture (products from reacting on the C−Cl site: C−OTf site: both sites). [b]100 °C was conducted. [c]1.5 h

was conducted. [d]1 h was conducted. [e]30 min was conducted. [f]2.5 h was conducted. [g]3 h was conducted. [h]12 h was conducted. [i]Toluene as solvent. [j]3.0 eq. K_2CO_3 as base.

Except aryl amines, we also investigated the tolerance of heterocyclic aryl amines in this reaction (Table 2.4, **3ag**−**3as**). These transformations afforded good-to-excellent product yields. An indole core bearing diverse substituents was smoothly *N*-arylated. Other NH-containing heterocyclic scaffolds, including 1,2,3,4-tetrahydrocyclopenta[*b*]indole, 10-phenoxazine, carbazole, and iminostilbene, were also applicable substrates (Table 2.4, **3ap**−**3as**). Aliphatic cyclic amines, such as morpholine, 1-methylpiperazine, and 4-methylpiperidine, were successfully converted to the corresponding products (Table 2.4, **3at**−**3av**). Notably, we were able to achieve chemoselective amination at the C−Cl bond, regardless of whether the C−Cl and C−OTf bonds were positioned *para* (Table 2.3, **3a**, **3b**, **3n**, **3q**, **3u**, **3z**, and Table 2.4 **3aj**, **3ak**, and **3am**−**3av**) or *meta* (Table 2.3, **3c**−**3e**, **3g**−**3m**, **3o**, **3p**, **3r**−**3t**, **3v**−**3y**, **3aa**−**3af**, and Table 2.4, **3ag**−**3ai**, and **3al**) to each other. More importantly, when we utilizing chloroaryl triflates containing steric group (−Me) *ortho* to −Cl and electron-withdraw groups (−F, $-CF_3$ and $-NO_2$) *ortho* to −OTf which increase the reactivity of −OTf in the reactions, we still obtained satisfied yield and chemoselectivity to −Cl (Table 2.3, **3g**, **3m**−**3o**, **3p**, **3t**, **3v**, **3w**, **3y**, **3aa**, **3ab**, **3af**, and Table 2.4, **3aj**).

Table 2.4 Pd-catalyzed amination of aryl amines with chloroaryl triflates[a]

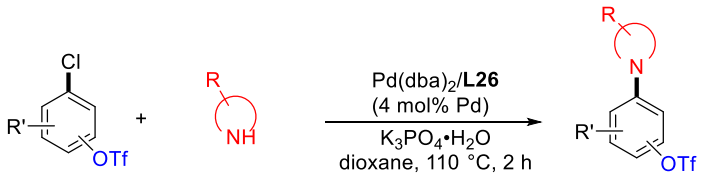

Heterocyclic aryl amines

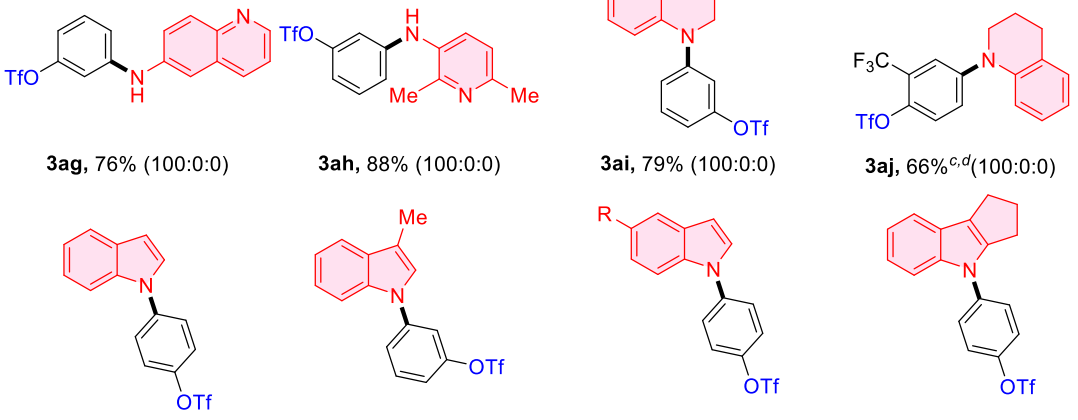

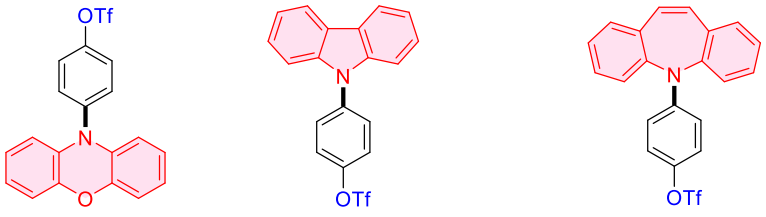

Heterocyclic aliphatic amines

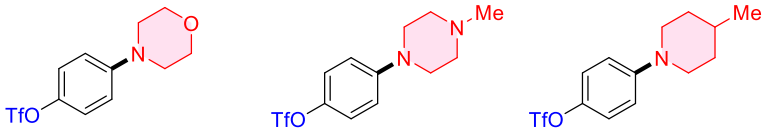

[a]Reaction conditions: Cl−Ar−OTf (0.20 mmol), amines (0.30 mmol), $K_3PO_4 \cdot H_2O$ (0.40 mmol), $Pd(dba)_2$ (4.0 mol%), **L26** (8.0 mol%), and dioxane (1.0 mL) were stirred at 110 °C for 2 h under a nitrogen atmosphere. Isolated yields were reported. The ratio in the blanket represents the chemoselectivity ratio in a crude reaction mixture (products from reacting on the C−Cl site: C−OTf site: both sites). [b]4 mol% **L25** was used. [c]3 h was conducted. [d]3.0 eq. K_2CO_3 as base.

We also evaluated the feasibility of heterocycle substrates containing −Cl and −OTf for this transformation. Such reactants were found to undergo amination with a

wide range of amines, including aryl amines, heterocyclic aryl amines and aliphatic amines and the corresponding products were obtained with excellent chemoselectivity in yields ranging from 59% to 90% (Table 2.5, **3aw**−**3be**).

Table 2.5 Palladium-catalyzed chemoselective C−Cl (over C−OTf) cross-coupling of chloroheteroaryl triflates with various amines[a]

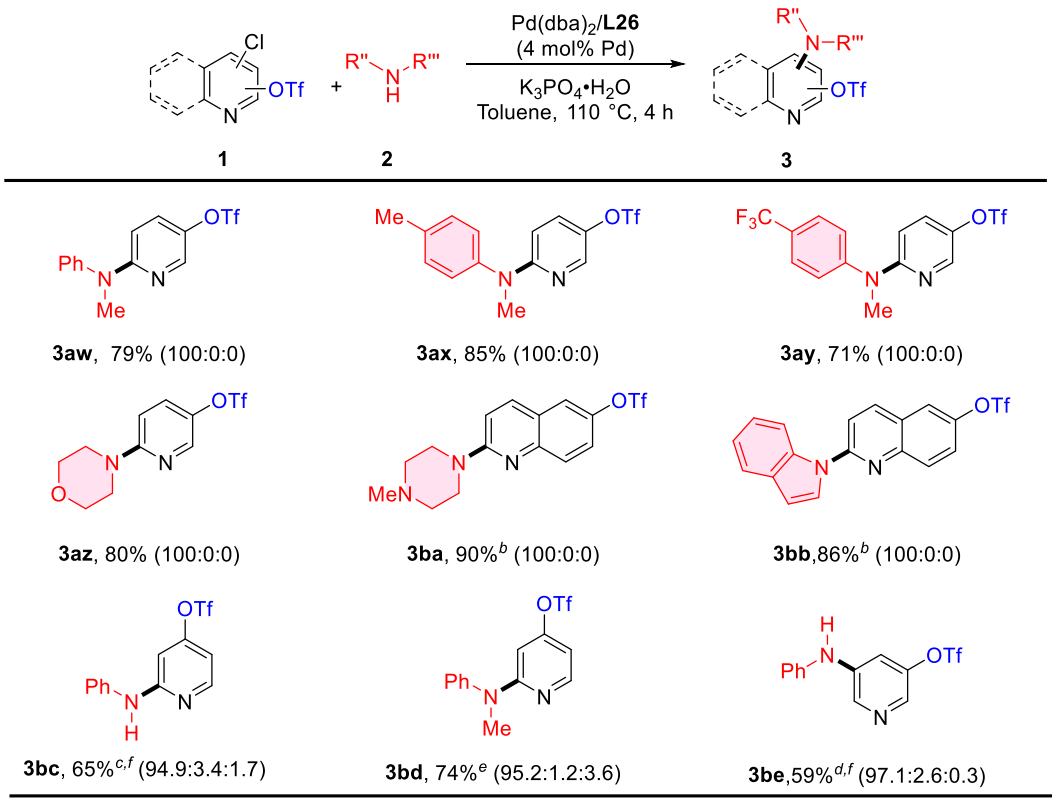

[a]Reaction conditions: Cl−HetAr−OTf (0.20 mmol), amines (0.30 mmol), $K_3PO_4 \cdot H_2O$ (0.40 mmol), $Pd(dba)_2$ (4.0 mol%), **L26** (8.0 mol%), and toluene (1.0 mL) were stirred at 110 °C for 4 h under a nitrogen atmosphere. Isolated yields were reported. The ratio in the blanket represents the chemoselectivity ratio in a crude reaction mixture (products from reacting on the C−Cl site: C−OTf site: both sites). [b]30 min was conducted. [c]8 h was conducted. [d]12 h was conducted. [e]18 h was conducted. [f]120 °C was conducted.

The chemoselective amination of sterically hindered aryl amines with chloroaryl triflates in the order of C−Cl > C−OTf also proceeded smoothly, and target products were obtained in excellent-to-good yields. (Table 2.6). It is particularly noteworthy that

extremely sterically bulky 2,6-diethylaniline and 2,6-diisopropylaniline also proved to be applicable substrates for this transformation (Table 2.6, **3bj**–**3bn**).

Table 2.6 Palladium-catalyzed chemoselective C–Cl (over C–OTf) *N*-arylation of sterically congested aryl amines[a]

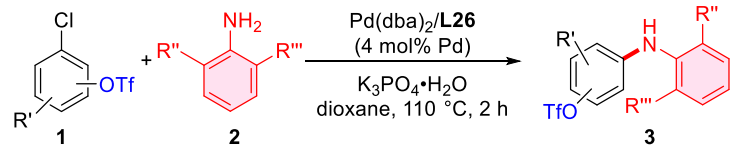

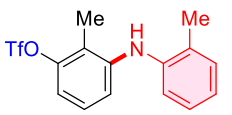

3bf, 92% (100:0:0)

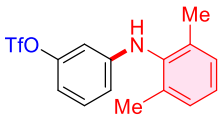

3bg, 79% (98.3:0.4:1.3)

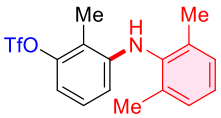

3bh, 78% (100:0:0)

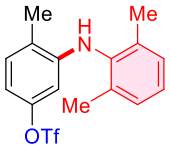

3bi, 94%[b] (98:0:2)

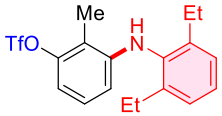

3bj, 74% (100:0:0)

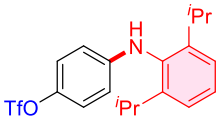

3bk, 90%[b] (100:0:0)

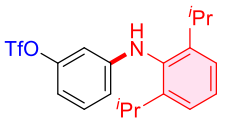

3bl, 62% (99.5:0.5:0.5)

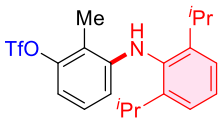

3bm, 65% (100:0:0)

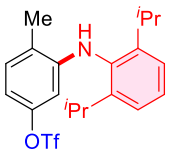

3bn, 79% (100:0:0)

[a]Reaction conditions: Cl–Ar–OTf (0.20 mmol), amines (0.30 mmol), $K_3PO_4 \cdot H_2O$ (0.40 mmol), $Pd(dba)_2$ (4.0 mol%), **L26** (8.0 mol%), and dioxane (1.0 mL) were stirred at 110 °C for 2 h under a nitrogen atmosphere. Isolated yields were reported. The ratio in the blanket represents the chemoselectivity ratio in a crude reaction mixture (products from reacting on the C–Cl site: C–OTf site: both sites). [b]2.5 h was conducted.

In addition to the intramolecular reaction, we also explored an intermolecular cross-coupling reaction of 3-aminophenyl triflate or 4-aminophenyl triflate with a series of aryl chlorides (Table 2.7). These transformations showed excellent chemoselectivity at the C–Cl bond under this developed catalyst system and gave target products in fair-to-good yields. A range of commonly encountered functional groups including electron-

withdraw groups such as −CF_3, ketone, and nitrile, as well as electron-donating groups like −*t*-Bu, −Me and −OMe were well tolerated (Table 2.7, **3bo**−3**bw** and **3by**−**3cb**). 2-Chloroquinoline was also a suitable substrate (Table 2.7, **3bx**). Excitingly, we were able to successfully couple certain chlorine-containing drugs with 3-aminophenyl triflate to provide the corresponding modified pharmaceuticals (Table 2.7, entries **3cc**−**3ce**). These derivatives keep the −OTf functional group, providing the opportunity for subsequent elaboration into more sophisticated drug analogs. This achievement in late-stage functionalization highlights the efficiency and practical utility of the catalyst we have developed.

It is worth noting that the 76 out of 80 compounds synthesized in Tables 2.3 to 2.7 are new compounds, which may suggest that this newly developed catalytic system can fill the blanks of general synthetic methodologies in producing the synthetically important amino aryl triflates building blocks. Report ways to prepare the aminoaryl triflates (**3t**, **3ar**, and **3at**) required multiple steps and synthetic approaches,[18] which can now be obatained in a single step utilizing our developed method.

Table 2.7 Palladium-catalyzed chemoselective C−Cl (over C−OTf) intermolecular cross-coupling reaction of 3- or 4-aminophenyl triflate with aryl chlorides[a]

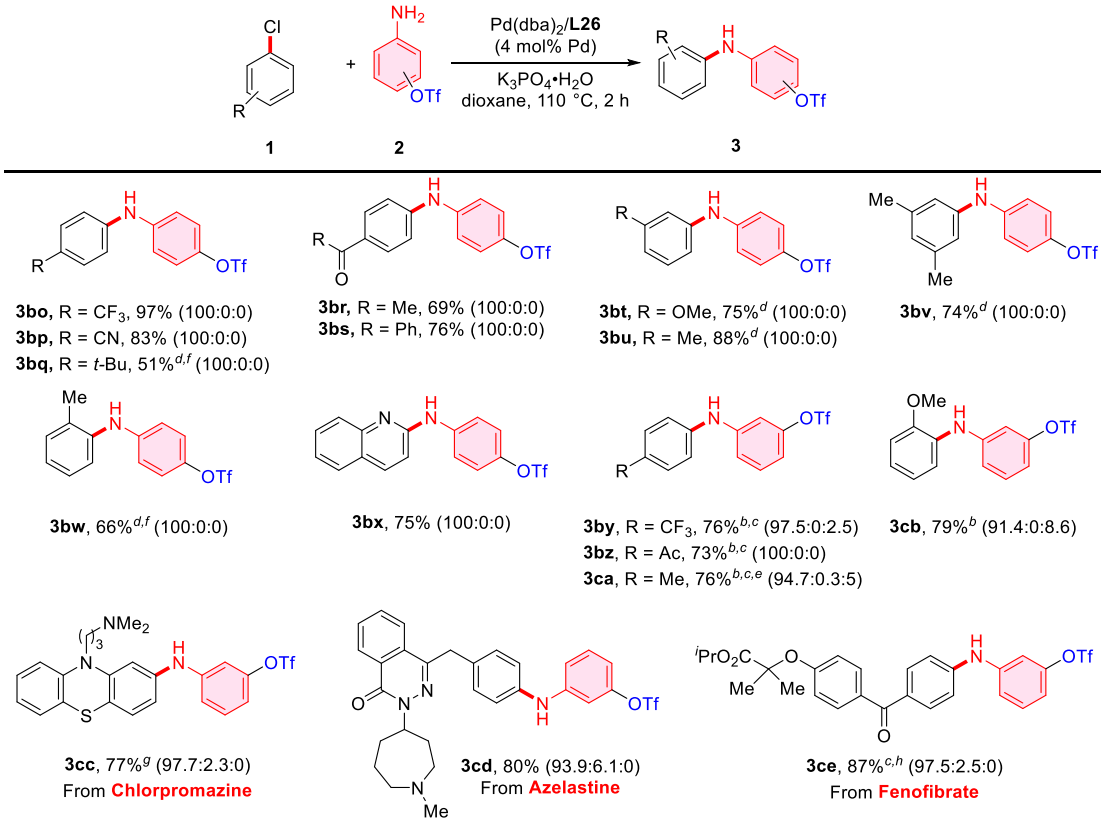

[a]Reaction conditions: Ar–Cl (0.20 mmol), amine–OTf (0.30 mmol), $K_3PO_4 \cdot H_2O$ (0.40 mmol), $Pd(dba)_2$ (4.0 mol%), **L26** (8.0 mol%), and dioxane (1.0 mL) were stirred at 110 °C for 2 h under a nitrogen atmosphere. Isolated yields were reported. The reaction on the triflate site was not observed. [b]1.2 eq. amine–OTf was used. [c]100 °C was conducted. [d]120 °C was conducted. [e]3 h was conducted. [f]18 h was conducted. [g]1 h was conducted. [h]3.0 eq K_2CO_3 as the base.

2.2.5 Gram-Scale Chemoselective Amination and Stability Testing of L26

To explore the feasibility of scaling up the current reaction condition, we performed a gram-scale reaction of 4-chlorophenyl triflate **1a** with *N*-methylaniline **2a** (Scheme 2.5). It yielded the desired coupling product **3a** in 82% yield, with no erosion of the previously observed chemoselectivity. Additionally, we conducted the air stability evaluation on this new class of pyrazole ligand. No detectable level of phosphine oxide of **L26** when the ligand was exposed to ambient air for 3 days in solution form or 14 days in solid form. In contrast, P*t*-Bu_3 has been shown to be rapidly destroyed in the air within 2 h.[19] These results collectively underscore the practical

scalability and robustness of the developed ligand, which will be advantageous for potential synthetic applications.

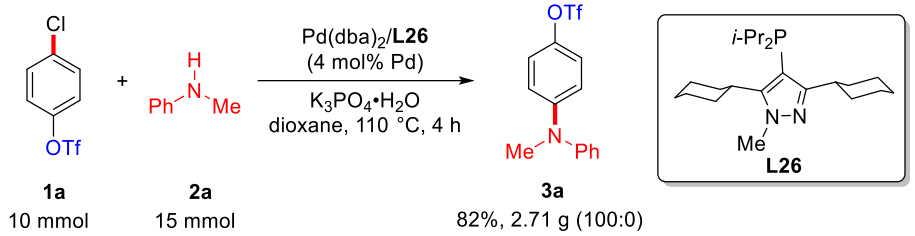

Scheme 2.5 Gram-Scale chemoselective C−Cl (over C−OTf) amination.

2.2.6 Mechanism Investigations

To better elucidate the role of the cyclohexyl substituents at the C3 and C5 positions of the *N*-methyl pyrazole framework, a single crystal of the Pd–**L25** complex from $[Pd(\eta^3\text{-}C_3H_5)Cl]_2$ and **L25** was grown at room temperature utilizing a liquid-liquid diffusion of hexane into dichloromethane of the complex solution. Crystallographic analysis of the Pd–**L25** complex shows that the cyclohexyl group at the C5 position is closer to the Pd center, which may be a preferred reaction-occurring center (Figure 2.5). Additionally, the Pd–**L25** complex shows the C−H···Pd separation between the methine hydrogen of the cyclohexyl group at the C5 position and in close proximity to the vacant axial position around the Pd center. The observed distances (2.436 Å) and angles (164.5°) of the atoms, which lie within a standard range of 2.3-2.9 Å and 110-170°, respectively, along with the downfield shift (4.05 ppm) of the methine hydrogen, suggest the existence of anagostic/preagostic interactions of the C−H···Pd separation in this new class of phosphine ligand.[20] We also tried to use the same method to obtain a single crystal of the Pd–**L26** complex, but we were unable to obtain it.

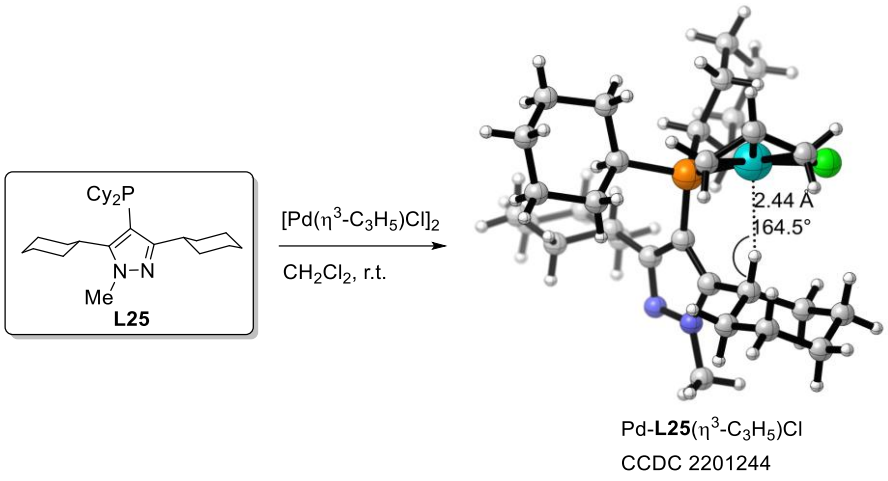

Figure 2.5 X-ray structure of Pd-**L25**(η^3-C_3H_5)Cl complex.

To gain better insight into the ligand effect on reactivity and chemoselectivity originating from this new class of alkyl-pyrazole-based phosphine ligand, we carried out a density functional theory (DFT) study to investigate the amination process for the Pd/**L25** catalytic systems. The calculations were conducted at the SMD (1,4-Dioxane) B3PW91-D3(BJ)/6-31G*//PBE0-D3(BJ)/Def2-TZVP level of theory. We utilized 4-chlorophenyl triflate and *N*-methylaniline as model substrates in this study. The investigation began with the calculation of the oxidative addition step of the amination reaction, which is deemed to be the key step in determining chemoselectivity.[6c, 8, 21] The calculated results show that the oxidative addition of C–Cl bond (6D-TS, 11.4 kcal mol^{-1}) is 10.8 kcal mol^{-1} less than that of C–OTf bond (6M-TS, 22.2 kcal mol^{-1}), which explains the excellent chemoselectivity of Pd/**L26** catalytic system toward C–Cl bond and is consistent with the experimental results. In addition, we utilized distortion-interaction model [6b] to elucidated the selectivity-determining step, which is associated with the correlation between the ligation state and selectivity. Following the oxidative addition step, the reaction is generally a downhill process up to the reductive

elimination step. The calculated results indicate that the reductive elimination step has the highest energy barrier (**6J-TS**, 32.5 kcal mol^{-1}) in the reaction pathway, suggesting that this is the rate-determining step in the reaction. We also investigated the possibility of the reaction occurring with a palladium center, located at the C3 position (**L26-3**'). The results show that the reaction energy barrier for the key steps at the C3 reactive center is generally higher, which is consistent with the observed crystal structure, whereas the palladium center at the C5 position is more favored (Figure 2.6). To elucidate the structure-activity relationship of this new class of pyrazole-based phosphine ligands, we have attempted to computationally model and compare the key reaction steps across the ligand series (**L24**−**L30**). The calculated results suggest the critical role of the alkyl substituent design in governing the preference for activation of the C–Cl bond versus the C–OTf bond. The phosphine ligands (**L24**−**L29**) with the cyclohexyl alkyl group design clearly demonstrate the preference for reacting the C−Cl bond rather than the C−OTf bond. In the contrary, **L30** containing the phenyl ring at the 3, 5 positions of the pyrazole skeleton, demonstrated the preference towards the C−OTf bond (**6M-TS**$_{L30}$, 11.3 kcal mol^{-1}) over C−Cl (**6J-TS**$_{L30}$, 12.6 kcal mol^{-1}), which was consistent with the experimental results and followed the common reactivity order (C−OTf > C−Cl) (Figure 2.6).

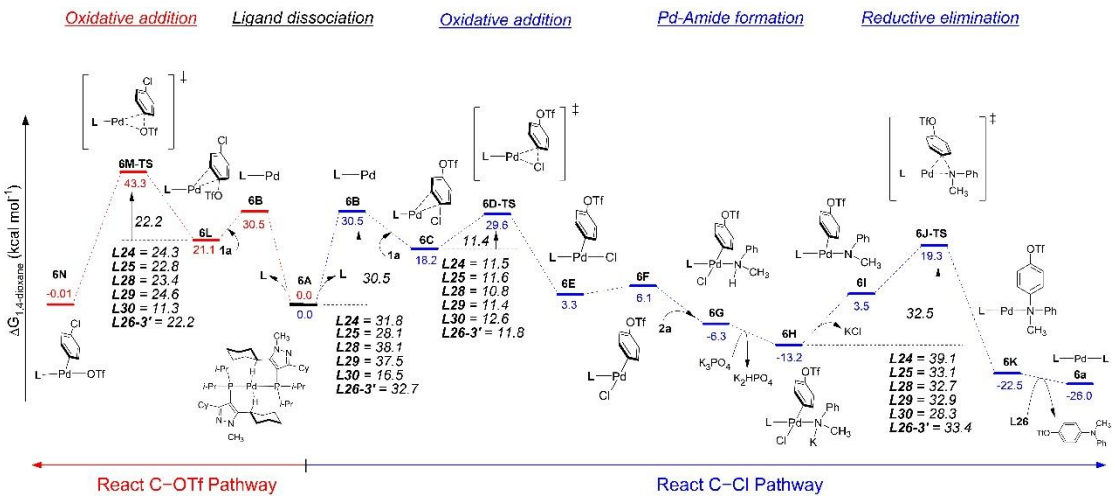

Figure 2.6 Free energy profiles were calculated for the chemoselective Pd/(**L24**−**L30**) cross-coupling reaction of 4-chlorophenyl triflate with *N*-methylaniline.

The properties of C−H···Pd separation in this new class of phosphine ligands were further investigated, and the bond path and an associated bond critical point (BCP) for the Pd···H separation were revealed by the quantum theory of atoms in molecules (QTAIM) analysis of the **6D-TS** in the Pd-**L26** catalyst system. The electron density's Laplacian at the BCP was positive [$\nabla 2\varrho$-(BCP) = 0.0740 e/bohr^5], and the energy density was negative [H(BCP)=-0.0056 e/bohr^3], suggesting a preagostic interaction.[20, 22] The Pd to antibonding sp^3 C−H back donation with 5.52 kcal mol^{-1} of the second-order perturbation energy in the natural bond orbital (NBO) analysis indicates a significant interaction with an attractive nature. In addition, the NCl isosurface plot for the region between the Pd···H shows a light-blue region, which indicates a weak attraction in the Pd···H separation (Figure 2.7).[23]

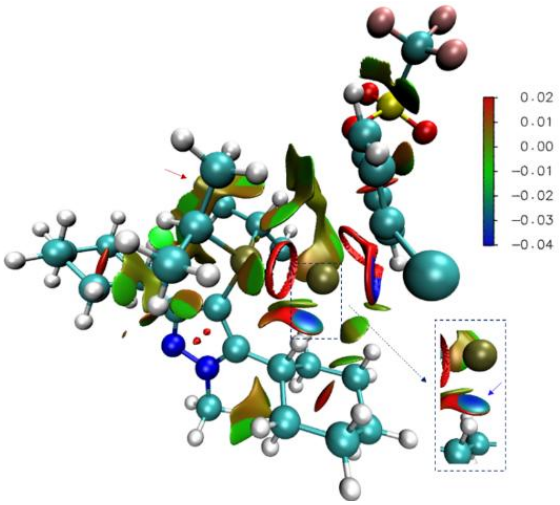

Figure 2.7 NCI isosurface plot of **6D-TS**. The enlarged part is the C–H interaction with the palladium center. The sign of the second-density Hessian eigenvalue (λ2) times the electron density is shown by the color map.

The computational analysis suggests that the interaction that exists between C−H···Pd separation in the Pd/**L26** complexes is not a typical anagostic interaction, which is solely based on repulsive electrostatics. Rather, the data indicates the presence of a preagostic interaction, which involves in stabilizing and affecting the activity of the unsaturated Pd intermediate during the catalytic cycle.[24] Importantly, the stabilizing effect offered by the preagostic interaction from the methine hydrogen of the alkyl group appears to be distinct from the Pd-π-arene interaction with the arene group that the mono-phosphine ligated palladium complex with preagostic interaction offered in which the chemoselectivity preference was towards the C–Cl bond over the C–OTf bond.

Despite the high chemoselectivity observed, the Pd/**SelectPhos** system exhibited relatively low activity in the amination reaction, which raised questions. Consistent

with our previous works, the Pd/**SelectPhos** system preferentially activated the C−Cl bond.[8] Nevertheless, the DFT calculated result indicates that the Pd/**SelectPhos** system exhibits a high energy barrier in the reductive elimination step (39.1 kcal mol^{-1}) compared with the Pd/**L25** system (32.5 kcal mol^{-1}), which may explain the higher reactivity of this new class of pyrazole phosphine ligands over the indolyl phosphine ligand. This underscores the importance of diverse ligand designs in addressing various chemoselective cross-coupling reactions. To further rationalize the influence of the design of the 3, 5-disubstituted alkyl groups, investigated the performance of ligands bearing cyclohexyl substituents at the 3 or 5 positions of the pyrazole core (**L28** and **L29**). The calculated results reveal that the presence of the cyclohexyl group in either the 3 or 5 position leads to a preference for C–Cl bond cleavage by approximately 12 kcal/mol, while the reductive elimination barrier is similar to that of the Pd/L**25** system. The advantage of the 3, 5-disubstituted alkyl design was found in the ligand dissociation step, which generates the active mono-coordinated Pd/**L25** catalyst. Notably, the lack of alkyl substitution at the 3 or 5 positions in **L28** and **L29** results in significantly higher ligand dissociation energies (~38 kcal/mol) compared to Pd/**L25** (30.5 kcal/mol), making this step the turnover-limiting step, which may account for the lower experimental yields observed with Pd/**L28-L29**. The extra steric effect offered by the alkyl group on the backside of the −P*i*-Pr_2 group of **L26**, as indicated by the brown region in the NCI plot (Figure 2.7), may provide advantages in accelerating the generation of the unsaturated Pd complex to commence the catalytic cycle.

2.3 Conclusion

In conclusion, we have successfully designed a series of new types of alkyl-pyrazole-based phosphine ligands, enabling the first palladium-catalyzed chemoselective amination of chloro(hetero)aryl triflates, wherein the C–Cl bond is preferentially activated over the C–OTf bond. The Pd/**L26** catalytic system facilitated the coupling of a diverse array of chloro(hetero)aryl triflates with a wide range of amines, giving the desired amino aryl triflate products in excellent yields and chemoselectivity. This methodology provides a practical synthetic pathway for the preparation of valuable amino aryl triflate building blocks. Importantly, our developed catalytic system also allows intermolecular chemoselective amination reactions. The pyrazole core combined with the strategically placed alkyl substituents at the C3 and C5 positions contribute to the observed unconventional reactivity trend. The computational studies suggest that the preagostic C−H···Pd interactions help stabilize the Pd complex during the catalytic cycle, while the alkyl groups accelerate the formation of the active Pd species. These structural and mechanistic insights are crucial for understanding the factors governing the unique chemoselectivity of this ligand system. We anticipate that these findings will open up new possibilities for the synthesis of complex molecules and provide valuable design principles for developing chemoselective cross-coupling catalysts.

2.4 Experimental Section

2.4.1 General Consideration

Unless otherwise noted, all reagents were purchased from commercial suppliers

and used without purification. All amination were performed in a resealable screw cap Schlenk tube (approx. 20 mL volume) in the presence of a Teflon-coated magnetic stirrer bar (5 mm x 10 mm). Dioxane, cyclopentyl methyl ether (CPME) and toluene were freshly distilled from sodium under nitrogen. Tetrahydrofuran (THF) was freshly distilled from sodium benzophenone ketyl under nitrogen. *tert*-Butanol (*t*-BuOH) and *n*-hexane was freshly distilled from anhydrous CaH_2 under nitrogen.[25] Ligands **L1**–**L13**, and **L16**–**L23** were purchased from commercial suppliers. CM-Phos **L14** and PhMezole-Phos **L15** was prepared according to the reported literature.[2e, 26] SelectPhos **L24** were prepared according to the reported literature.[8a] A new bottle of *n*-butyllithium was used. Thin-layer chromatography was performed on pre-coated silica gel 60 F254 plates. Silica gel (Grace, 60Å, 40-63 mm) was used for column chromatography. Melting points were recorded on an uncorrected Stuart Melting Point SMP30 instrument. NMR spectra were recorded on a Brüker spectrometer (400 MHz for ^{1}H, 100 MHz for ^{13}C, 376 MHz for ^{19}F and 162 MHz for ^{31}P) and Jeol JMN-ECZ500R/S1 spectrometer (465.89 MHz for ^{19}F and 200.43 MHz for ^{31}P). Spectra were referenced internally to the residual proton resonance in $CDCl_3$ (δ 7.26 ppm) as the internal standard. ^{13}C NMR spectra were referenced to $CDCl_3$ (δ 77.0 ppm, the middle peak). ^{19}F NMR chemical shifts were determined relative to $CFCl_3$ as the external standard and low field is positive. ^{31}P NMR spectra were referenced to 85% H_3PO_4 externally. Coupling constants (J) were reported in Hertz (Hz). Mass spectra (EI-MS) were recorded on an HP 5977A MSD Mass Spectrometer. High-resolution mass spectra (HRMS) were obtained on the Agilent 6540 ESI-QTof-MS or APPI-QTof-MS and a

Waters GCT Premier EI-ToF-MS. GC-MS analysis was conducted on a HP 7890B GC system using a HP5MS column (30 m x 0.25 mm). The products described in GC yield were accorded to the authentic samples/dodecane calibration standard from HP 7890B GC-FID system. All yields reported referring to the isolated yield of compounds estimated to be greater than 95% purity as determined by capillary gas chromatography (GC) or ^{1}H NMR. Compounds described in the literature were characterized by a comparison of their ^{1}H, ^{13}C, ^{19}F and/or ^{31}P NMR spectra to the previously reported data. The procedures in this section are representative, and thus the yields may differ from those reported in tables.

2.4.2 General Procedure for Initial Ligand Screening

$Pd(OAc)_2$ (0.0080 mmol), ligand (0.0080 mmol), and $K_3PO_4 \cdot H_2O$ (0.40 mmol) were added to the Schlenk tube that was charged with Teflon-coated magnetic stir bar (5 mm x 10 mm) and equipped with screw cap. The tube was carefully evacuated and flushed with nitrogen (3 cycles). 4-Chlorophenyltriflate (0.20 mmol), *N*-methylaniline (0.30 mmol) and the freshly distilled dioxane (1.00 mL) were added via syringes. The tube was sealed and magnetically stirred at a preheated 110 ºC oil bath for 2 h. The reaction was then allowed to reach room temperature. Ethyl acetate (~4 mL), dodecane (45.2 mL, internal standard), and water (~2 mL) were added. The organic layer was subjected to GC analysis. The GC yield was previously calibrated by an authentic sample/dodecane calibration curve.

2.4.3 General Procedure for Reaction Condition Screening

Pd source (0.0080 mmol), **L26** (0.0080-0.032 mmol), and base (0.40 mmol) were added to the Schlenk tube that was charged with Teflon-coated magnetic stir bar (5 mm x 10 mm) and equipped with screw cap. The tube was carefully evacuated and flushed with nitrogen (3 cycles). 4-Chlorophenyltriflate (0.20 mmol), *N*-methylaniline (0.30 mmol) and the freshly distilled solvent (1.00 mL) were added via syringes. The tube was sealed and magnetically stirred at a preheated 110 ^{o}C oil bath for 2 h. The reaction was then allowed to reach room temperature. Ethyl acetate (~4 mL), dodecane (45.2 mL, internal standard), and water (~2 mL) were added. The organic layer was subjected to GC analysis. The GC yield was previously calibrated by an authentic sample/dodecane calibration curve.

2.4.4 General Procedure for Palladium-Catalyzed Chemoselective Amination of Chloro(hetero)aryl Triflates

$Pd(dba)_2$ (0.0080 mmol), **L26** (0.0080-0.016 mmol), amine (0.30 mmol, if solid) and $K_3PO_4 \cdot H_2O$ (0.40 mmol) or K_2CO_3 (0.6 mmol) were added to the Schlenk tube that was charged with Teflon-coated magnetic stir bar (5 mm x 10 mm) and equipped with screw cap. The tube was carefully evacuated and flushed with nitrogen (3 cycles). Chloro(hetero)aryl triflates (0.20 mmol), amines (0.30 mmol, if liquid), and freshly distillated dioxane/toluene (1.00 mL) were added to the tube via syringe. The tube was resealed and magnetically stirred in a preheated 100-120 ^{o}C oil bath for the time indicated in Table 2-4. The reaction was allowed to reach room temperature. Ethyl acetate (~4 mL) and water (~2 mL) were added. The organic layer was subjected to GC

analysis. The aqueous layer was washed with ethyl acetate. The organic layers were combined and concentrated. The crude products were purified by column chromatography on silica gel (230-400 mesh) to afford the desired product.

2.4.5 General Procedure for Palladium-Catalyzed Chemoselective Intermolecular Cross-Coupling Reaction of 4-Aminophenyl triflate or 3-Aminophenyl Triflate with Aryl Chlorides

$Pd(dba)_2$ (0.0080 mmol), **L26** (0.016 mmol), and $K_3PO_4 \cdot H_2O$ (0.40 mmol) were added to the Schlenk tube that was charged with Teflon-coated magnetic stir bar (5 mm x 10 mm) and equipped with screw cap. The tube was carefully evacuated and flushed with nitrogen (3 cycles). Aryl chlorides (0.20 mmol), 4-aminophenyl triflate or 3-aminophenyl triflate (0.24-0.30 mmol), and freshly distillated dioxane (1.00 mL) were added to the tube via syringe. The tube was resealed and magnetically stirred in a preheated 100-120 ^oC oil bath for 2-18 h. The reaction was allowed to reach room temperature. Ethyl acetate (~4 mL) and water (~2 mL) were added. The organic layer was subjected to GC analysis. The aqueous layer was washed with ethyl acetate. The organic layers were combined and concentrated. The crude products were purified by column chromatography on silica gel (230-400 mesh) to afford the desired product.

2.4.6 General Procedure for Gram-Scale Chemoselective Amination of Chloroaryl Triflates

$Pd(dba)_2$ (0.40 mmol), **L26** (0.80 mmol) and $K_3PO_4 \cdot H_2O$ (20.0 mmol) were added into 250 mL Schlenk flask that was charged with a Teflon-coated magnetic stirrer bar

(6 mm x 30 mm) and equipped with screw cap. The flask was carefully evacuated and flushed with nitrogen (3 cycles). 4-Chlorophenyltriflate (10.0 mmol), *N*-methylaniline (15.0 mmol), and freshly distillated dioxane (50.0 mL) were added to the flask by syringe. The flask was resealed and magnetically stirred in a preheated 110 ºC oil bath for 4 h. Ethyl acetate and water were added to the flask and the mixture was transferred to separating funnel and subjected to extraction. The organic layers were combined and concentrated. The crude product was purified by column chromatography on silica gel (230-400 mesh) to afford the desired product.

2.4.7 Synthesis and Characterization Data

All polyhalogenated aryl triflates were prepared from their corresponding phenols with triflyl chloride in the presence of triethylamine in dry dichloromethane according to the literature method.[6d]

General Procedure: The corresponding phenol (10 mmol) was dissolved in freshly distilled DCM (25 mL) at room temperature under a nitrogen atmosphere, followed by the addition of triethylamine (14 mmol). The solution was cooled to -78 ºC in dry ice/acetone bath. Triflyl chloride (10 mmol) was added dropwise by syringe. The reaction was allowed to warm to room temperature and stirred for 1 h. Ethyl acetate and water were then added to the mixture, and the organic phase was separated. The organic layer was washed with water several times. The combined organic mixture was dried over Na_2SO_4 and then concentrated. The concentrated solution was subjected to column chromatography and eluted with ethyl acetate/hexane. The corresponding

fractions were collected, and the solvent was evaporated to give the product.

5-Chloro-2-fluorophenyl trifluoromethanesulfonate

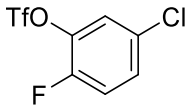

Yield: 81% (2.25 g). Colorless liquid. Eluents (R_f = 0.8, Hexane: EA = 10:1) was used for flash column chromatography. **^{1}H NMR** (400 MHz, $CDCl_3$) δ 7.38- 7.33 (m, 2H), 7.25-7.19 (m, 1H); **^{13}C NMR** (100 MHz, $CDCl_3$) δ 152.5 (d, *J* = 252.2 Hz, 1C), 136.8 (d, *J* = 14.5 Hz, 1C), 129.9 (d, *J* = 3.9 Hz, 1C), 129.8 (d, *J* = 6.9 Hz, 1C), 124.0, 118.6 (q, *J* = 318.9 Hz, 1C), 118.4 (d, *J* = 19.7 Hz, 1C); **^{19}F NMR** (565 MHz, $CDCl_3$) δ -73.1, -129.2; HRMS (EI): calcd for $C_7H_3F_4O_3ClS^+$: 277.9422, found 277.9420.

4-Chloro-2-(trifluoromethyl)phenyl trifluoromethanesulfonate

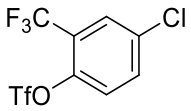

Yield: 91% (3.00 g). Yellow liquid. Eluents (R_f = 0.6, Hexane = 100) was used for flash column chromatography. **^{1}H NMR** (400 MHz, $CDCl_3$) δ 7.74 (d, *J* = 2.5 Hz, 1H), 7.63 (dd, *J* = 8.9, 2.5 Hz, 1H), 7.47 (d, *J* = 8.9 Hz, 1H); **^{13}C NMR** (100 MHz, $CDCl_3$) δ 144.4 (q, *J* = 1.8 Hz, 1C), 134.3, 133.9, 128.3 (q, *J* = 5.0 Hz, 1C), 124.7 (q, *J* = 33.3 Hz, 1C), 123.8, 121.3 (q, *J* = 271.9 Hz, 1C), 118.4 (q, *J* = 318.3 Hz, 1C); **^{19}F NMR** (565 MHz, $CDCl_3$) δ -61.5, -73.8; **HRMS** (EI): calcd for $C_8H_3F_6O_3ClS^+$: 327.9390, found 327.9386.

2-Chloroquinolin-6-yl trifluoromethanesulfonate

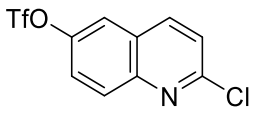

Yield: 61% (1.90 g). White solid, m.p. = 82.4–84.0 °C. Eluents (R_f = 0.3, Hexane: EA = 20:1) was used for flash column chromatography. **^{1}H NMR** (400 MHz, $CDCl_3$) δ 8.14 (dd, *J* = 12.0, 9.0 Hz, 2H), 7.76 (d, *J* = 2.7 Hz, 1H), 7.63 (dd, *J* = 9.2, 2.7 Hz, 1H), 7.50 (d, *J* = 8.6 Hz, 1H); **^{13}C NMR** (100 MHz, $CDCl_3$) δ 152.2, 147.2, 146.5, 138.7, 131.4, 126.9, 124.2, 124.0, 119.2, 118.7 (q, *J* = 318.9 Hz, 1C); **^{19}F NMR** (565 MHz, $CDCl_3$) δ -72.6; **HRMS** (EI): calcd for $C_{10}H_5F_3O_3NClS^+$: 310.9625, found 310.9618.

1,3-Dicyclohexylpropane-1,3-dione

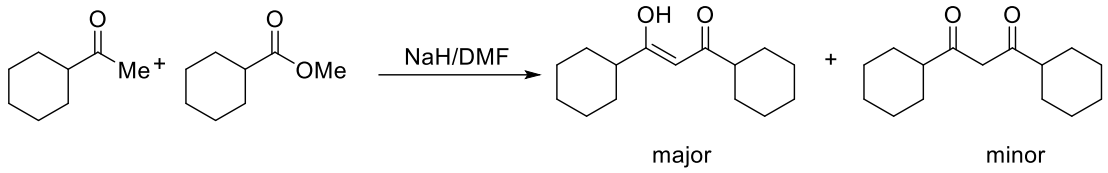

A 500 mL flask was equipped with a magnetic stir bar, which was dried under vacuum with a heat gun and refilled with nitrogen. Sodium hydride (60% in mineral oil, 3.00 g, 75.0 mmol) and DMF (80.0 mL) were added to the flask, and the mixture was stirred. Cyclohexyl methyl ketone (6.90 mL, 50.0 mmol) and methyl cyclohexanecarboxylate (7.90 mL, 55.0 mmol) was added dropwise to the mixture for 30 min, and the resulting mixture was stirred overnight at room temperature. The solution was quenched by 1 M HCl solution and extracted three times with Et_2O. The combined organic layer was washed with water and brine, and dried over Na_2SO_4. The organic layer was then concentrated. The residue was subjected to recrystallization with EtOH: water = 1:1.

Yield: 75% (5.30 g). White solid. **^{1}H NMR** (400 MHz, $CDCl_3$) δ 15.76 (s, 1H), 5.47 (s,

1H), 2.16 (tt, *J* = 11.5, 3.2 Hz, 2H), 1.86-1.77 (m, 10H), 1.41-1.23 (m, 10H); **^{13}C NMR** (100 MHz, $CDCl_3$) δ 198.2, 95.6, 46.7, 29.6, 25.80, 25.76. The data are in agreement with those previously reported in the literature.[27]

3,5-Dicyclohexyl-1*H*-pyrazole

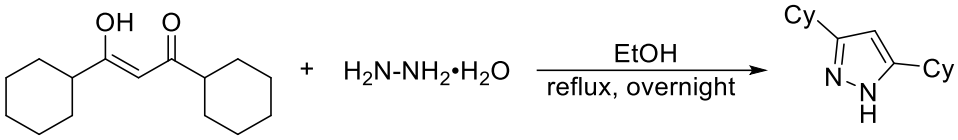

1,3-Dicyclohexylpropane-1,3-dione (2.36 g, 10.0 mmol) was dissolved in ethanol (10.0 mL), and hydrazine monohydrate (0.600 mL, 12.4 mmol) was then added to the solution. The mixture was refluxed overnight and was allowed to reach room temperature. The solvent was then removed under reduced pressure. DCM and water were added to the residue. And the aqueous layer was extracted with DCM three times. The combined organic layer was then concentrated, and the residue was purified by column chromatography and eluted with Hexane: Ethyl acetate = 4:1. The combined solution was evaporated to give the product.

Yield: 89% (2.09 g). White solid, m.p.= 54.0–54.6 ºC. **^{1}H NMR** (400 MHz, $CDCl_3$) δ 5.83 (s, 1H), 2.64-2.58 (m, 2H), 1.99-1.93 (m, 4H), 1.83-1.78 (m, 4H), 1.72-1.69 (m, 2H), 1.45-1.19 (m, 10H); **^{13}C NMR** (100 MHz, $CDCl_3$) δ 98.5, 36.5, 33.0, 26.3, 26.0; **HRMS** (ESI): calcd. for $C_{15}H_{25}N_2^+$: 233.2012, found 233.2015.

3,5-Dicyclohexyl-1-methyl-1*H*-pyrazole

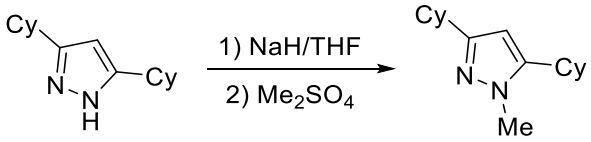

3,5-Dicyclohexyl-1*H*-pyrazole (2.45 g, 10.5 mmol) and sodium hydride (0.546 g, 13.7 mmol, 60% dispersion in mineral oil) was dissolved in freshly distilled THF (50.0 mL) at -78 °C under nitrogen atmosphere. The reaction was allowed to warm to room temperature. Dimethyl sulfate (1.00 mL, 10.5 mmol) was added to the reaction mixture and the reaction mixture was allowed to stir for 45 min. After the completion of the reaction monitored by GC-MS, ethyl acetate and water were added to the mixture. The organic layer was then concentrated. The concentrated mixture was purified by column chromatography and eluted with Hexane: Ethyl acetate = 4: 1 to afford the product.

Yield: 92% (2.61 g). White solid, m.p.= 42.6–45.9 °C. **^{1}H NMR** (400 MHz, $CDCl_3$) δ 5.78 (s, 1H), 3.72 (s, 3H), 2.58-2.47 (m, 2H), 1.96-1.68 (m, 10H), 1.43-1.22 (m, 10H); **^{13}C NMR** (100 MHz, $CDCl_3$) δ 157.0, 148.5, 98.7, 37.7, 35.7, 35.4, 33.5, 32.8, 26.5, 26.4, 26.2, 25.9; **HRMS** (ESI): calcd. for $C_{16}H_{27}N_2^+$: 247.2169, found 247.2171.

4-Bromo-3,5-dicyclohexyl-1-methyl-1*H*-pyrazole

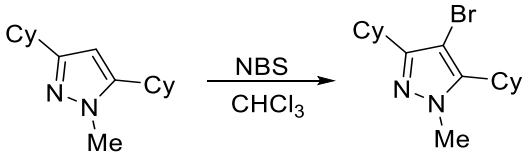

N-Bromosuccinimide (1.93 g, 10.8 mmol) was added to a solution of 3,5-dicyclohexyl-1-methyl-1*H*-pyrazole (2.54 g, 10.3 mmol) in anhydrous chloroform (40.0 mL) in portion at room temperature. After stirring for 50 min, solvent was removed by vacuum. DCM and water were added to the mixture and the organic phase was separated. The organic layer was washed with water for three times. The combined organic layer was then concentrated to the product.

Yield: 99% (3.32 g). White solid, m.p. = 86.6–89.6 °C. **^{1}H NMR** (400 MHz, $CDCl_3$) δ

3.78 (s, 3H), 2.76-2.58 (m, 2H), 1.98-1.68 (m, 12H), 1.56-1.20 (m, 8H); **^{13}C NMR** (100 MHz, $CDCl_3$) δ 153.8, 143.4, 90.6, 37.7, 36.5, 36.4, 31.8, 29.9, 26.7, 26.6, 26.0, 25.7; **HRMS** (ESI): calcd. for $C_{16}H_{26}BrN_2^+$: 325.1274, found 325.1274.

3,5-Dicyclohexyl-4-(dicyclohexylphosphaneyl)-1-methyl-1*H*-pyrazole (L25)

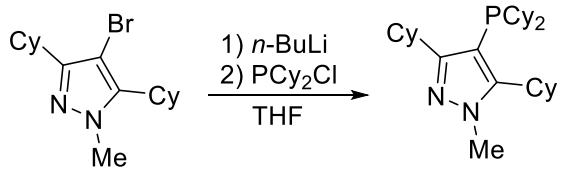

4-Bromo-3,5-dicyclohexyl-1-methyl-1*H*-pyrazole (0.970 g, 3.00 mmol) was dissolved in freshly distilled THF (15.0 mL) at room temperature under nitrogen atmosphere. The solution was cooled to -78 °C in a dry ice/acetone bath. Titrated *n*-BuLi (3.15 mmol) was added dropwise with a syringe. After the reaction mixture was stirred for 45 min at -78 °C, chlorodicyclohexylphosphine (0.700 mL, 3.15 mmol) was added. The reaction was allowed to warm to room temperature and stirred for 70 min. The solvent was removed under reduced pressure. After the solvent was removed under vacuum, the solid product was washed with methanol (10.0 mL), 90% methanol/water mixture (10.0 mL x 2) and methanol (10.0 mL). The white solid was collected by filtration and dried over vacuum to afford **L25**.

Yield: 80% (1.06 g). White solid, m.p. = 195.5–198.9 °C. **^{1}H NMR** (400 MHz, C_6D_6) δ 3.44 (s, 3H), 3.26 (bs, 1H), 2.84 (bs, 1H), 2.14-1.11 (m, 42H); **^{13}C NMR** (100 MHz, C_6D_6) δ 104.9, 104.7, 39.1, 37.4, 35.8, 35.7, 34.3, 33.1, 32.8, 31.7, 31.2, 31.1, 29.7, 27.3, 27.2, 27.1, 27.0, 26.5, 26.4, 25.9, 25.4; **^{31}P NMR** (200 MHz, C_6D_6) δ -26.1; **HRMS** (ESI): calcd. for $C_{28}H_{48}N_2P^+$: 443.3550, found 443.3558.

3,5-Dicyclohexyl-4-(diisopropylphosphaneyl)-1-methyl-1*H*-pyrazole (L26)

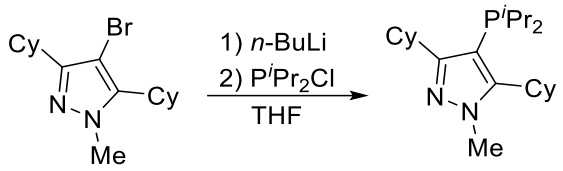

4-Bromo-3,5-dicyclohexyl-1-methyl-1*H*-pyrazole (3.24 g, 10.0 mmol) was dissolved in freshly distilled THF (25.0 mL) at room temperature under nitrogen atmosphere. The solution was cooled to -78 °C in a dry ice/acetone bath. Titrated *n*-BuLi (10.5 mmol) was added dropwise with a syringe. After the reaction mixture was stirred for 45 min at -78 °C, chlorodiisopropylphosphine (1.67 mL, 10.5 mmol) was added. The reaction was allowed to warm to room temperature and stirred for 70 min. The solvent was removed under reduced pressure. After the solvent was removed under vacuum, the solid product was washed with methanol (10.0 mL), 90% methanol/water mixture (10.0 mL x 2) and methanol (10.0 mL). The white solid was collected by filtration and dried over vacuum to afford **L26**.

Yield: 60% (2.10 g).White solid, m.p. = 117.4–118.9 °C. **^{1}H NMR** (400 MHz, C_6D_6) δ 3.41 (s, 3H), 3.31-3.10 (m, 1H), 2.99-2.71 (m, 1H), 2.34-2.25 (m, 2H), 2.09-1.99 (m, 4H), 1.83-1.80 (m, 3H), 1.68-1.52 (m, 7H), 1.40-1.28 (m, 3H), 1.24-1.07 (m, 9H), 1.05-0.98 (m, 6H); **^{13}C NMR** (100 MHz, C_6D_6) δ 106.1, 106.0, 38.6, 37.5, 36.6, 34.2, 31.5, 27.2, 27.0, 26.4, 25.9, 25.1, 25.0, 22.4, 22.1, 21.6, 21.4; **^{31}P NMR** (200 MHz, C_6D_6) δ -13.3; **HRMS** (ESI): calcd. for $C_{22}H_{40}N_2P^+$: 363.2924, found 363.2933.

3,5-Dicyclohexyl-4-(diphenylphosphaneyl)-1-methyl-1*H*-pyrazole (L27)

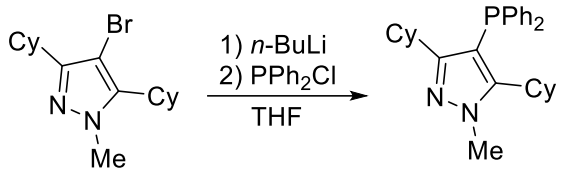

4-Bromo-3,5-dicyclohexyl-1-methyl-1*H*-pyrazole (0.970 g, 3.00 mmol) was dissolved in freshly distilled THF (15.0 mL) at room temperature under nitrogen atmosphere. The solution was cooled to -78 ºC in a dry ice/acetone bath. Titrated *n*-BuLi (3.15 mmol) was added dropwise with a syringe. After the reaction mixture was stirred for 45 min at -78 ºC, chlorodiphenylphosphine (0.564 mL, 3.15 mmol) was added. The reaction was allowed to warm to room temperature and stirred for 70 min. The solvent was removed under reduced pressure. After the solvent was removed under vacuum, the solid product was washed with methanol (10.0 mL x 3). The white solid was collected by filtration and dried over vacuum to afford **L27**.

Yield: 89% (1.15 g). White solid, m.p. = 168.5–170.0 °C. **^{1}H NMR** (400 MHz, $CDCl_3$) δ 7.41-7.26 (m, 10H), 3.91 (s, 3H), 2.96-2.90 (m, 1H), 2.38-2.37 (m, 1H), 1.93-1.84 (m, 2H), 1.76-1.10 (m, 16H), 0.94-0.91(m, 2H); **^{13}C NMR** (100 MHz, $CDCl_3$) δ 161.6, 161.5, 152.9, 152.6, 137.4, 137.3, 131.9, 131.7, 128.1, 128.0, 127.5, 104.6, 104.5, 38.0, 36.92, 36.88, 36.74, 36.70. 33.0, 31.12. 31.07, 26.8, 26.7, 25.9, 25.8; **^{31}P NMR** (162 MHz, $CDCl_3$) δ -36.3; **HRMS** (ESI): calcd. for $C_{28}H_{36}N_2P^+$: 431.2611, found 431.2620.

Mixture of 3-cyclohexyl-1-methyl-1*H*-pyrazole and 5-cyclohexyl-1-methyl-1*H*-pyrazole

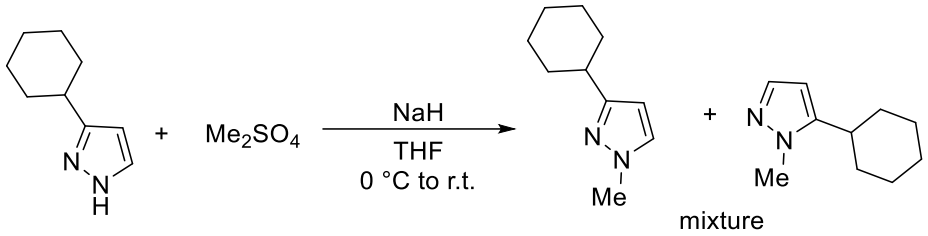

3-Cyclohexyl-1*H*-pyrazole (4.79 g, 31.6 mmol) and sodium hydride (1.64 g, 41.1 mmol, 60% dispersion in mineral oil) was dissolved in freshly distilled THF (80.0 mL) at 0 °C under nitrogen atmosphere. The reaction was allowed to warm to room temperature. Dimethyl sulfate (2.98 mL, 31.6 mmol) was added to the reaction mixture and the reaction mixture was allowed to stir for 45 min. After the completion of the reaction monitored by GC-MS, ethyl acetate and water were added to the mixture. The organic layer was then concentrated. The concentrated mixture was purified by column chromatography and eluted with Hexane: Ethyl acetate = 4:1. The solution was evaporated to give a mixture product as a light-yellow liquid (4.10 g, 79%).

5-Cyclohexyl-1-methyl-1*H*-pyrazole

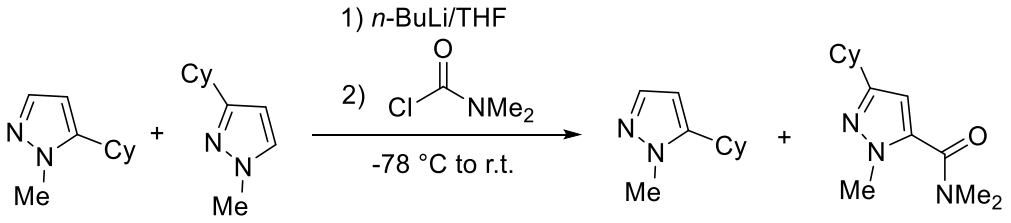

A mixture of 5-cyclohexyl-1-methyl-1*H*-pyrazole and 3-cyclohexyl-1-methyl-1*H*-pyrazole (3.72 mmol) was in freshly distilled THF (10.0 mL) at room temperature under nitrogen atmosphere. The solution was cooled to -78 °C in a dry ice/acetone bath. Titrated *n*-BuLi (3.90 mmol) was added dropwise with a syringe. After the reaction mixture was stirred for 30 min at -78 °C, dimethylcarbamoyl chloride (0.340 mL, 3.72

mmol) was added dropwise. The reaction was allowed to warm to room temperature and stirred for 12 h. Then ethyl acetate and water were added to the mixture, organic layer was extracted by ethyl acetate, washed by brine and dried by anhydrous sodium sulfate and concentrated under reduced pressure. Purification by column chromatography (Hexane: Ethyl acetate = 10: 1) to afford the major product 5-cyclohexyl-1-methyl-1*H*-pyrazole as light-yellow liquid (0.390 g).

^{1}H NMR (400 MHz, $CDCl_3$) δ 7.36 (d, *J* = 1.5 Hz, 1H), 5.98 (d, *J* = 1.7 Hz, 1H), 3.79 (s, 3H), 2.58-2.51 (m, 1H), 1.92-1.89 (m, 2H), 1.85-1.80 (m, 2H), 1.75 (d, *J* = 13.4 Hz, 1H), 1.39-1.32 (m, 4H), 1.27-1.22 (m, 1H); **^{13}C NMR** (100 MHz, $CDCl_3$) δ 148.1, 138.0, 101.9, 36.0, 35.2, 32.7, 26.3, 25.8; **HRMS** (ESI): calcd. for $C_{10}H_{17}N_2^+$: 165.1386, found 165.1390.

4-Bromo-5-cyclohexyl-1-methyl-1*H*-pyrazole

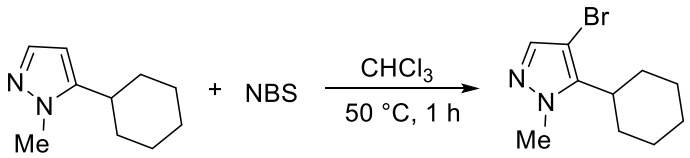

N-Bromosuccinimide (0.420 g, 2.36 mmol) was added to a solution of 5-cyclohexyl-1-methyl-1*H*-pyrazole (0.368 g, 2.20 mmol) in anhydrous chloroform (8.00 mL) in portion at room temperature. After stirring for 60 min under 50 ºC, the reaction system was cooling to room temperature, anhydrous chloroform was removed under vacuum, and residue was washed by water and extracted by DCM (20.0 mL x 3). The combined organic layers were washed with brine, dried by anhydrous sodium sulfate and concentrated under reduced pressure to afford the desired product without further purification.

Yield: 84% (0.446 g). White solid, m.p. = 50.9–54.6 °C. **^{1}H NMR** (400 MHz, $CDCl_3$) δ 7.32 (s, 1H), 3.85 (s, 3H), 2.80-2.72 (m, 1H), 1.96-1.93 (m, 1H), 1.90-1.85 (m, 3H), 1.77-1.70 (m, 3H), 1.39-1.36 (m, 1H), 1.36-1.29 (m, 2H); **^{13}C NMR** (100 MHz, $CDCl_3$) δ 143.4, 139.3 91.2, 38.0, 36.3, 30.0, 26.6, 25.7; **HRMS** (ESI): calcd. for $C_{10}H_{16}N_2Br^+$: 243.0491, found 243.0490.

5-Cyclohexyl-4-(dicyclohexylphosphaneyl)-1-methyl-1*H*-pyrazole (L28)

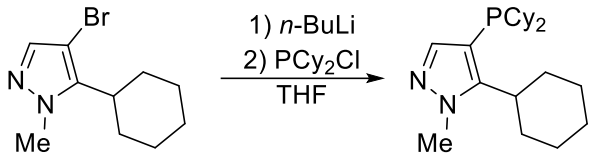

4-Bromo-5-cyclohexyl-1-methyl-1*H*-pyrazole (0.416 g, 1.72 mmol) was dissolved in freshly distilled THF (8.00 mL) at room temperature under nitrogen atmosphere. The solution was cooled to -78 ºC in a dry ice/acetone bath. Titrated *n*-BuLi (1.80 mmol) was added dropwise with a syringe. After the reaction mixture was stirred for 60 min at -78 ºC, dicyclohexylchlorophosphine (0.400 mL, 1.82 mmol) was added. The reaction was allowed to warm to room temperature and stirred for 70 min. The solvent was removed under reduced pressure to afford light-yellow foam solid. The solid was washed with degassed methanol (5.00 mL x 3) to give **L28**.

Yield: 59% (0.363 g). White solid, m.p. = 135.3–137.8 °C. **^{1}H NMR** (400 MHz, $CDCl_3$) δ 7.35 (s, 1H), 3.87 (s, 3H), 3.00 (td, *J* = 12.4, 2.9 Hz, 1H), 1.96-1.87 (m, 2H), 1.85-1.70 (m, 10H), 1.69-1.57 (m, 8H), 1.41-1.24 (m, 5H), 1.13 (dt, *J* = 15.5, 7.6 Hz, 4H), 1.07-1.02 (m, 3H); **^{13}C NMR** (100 MHz, $CDCl_3$) δ 153.2 (d, *J* = 31.6 Hz, 1C), 141.8 (d, *J* = 5.6 Hz, 1C), 107.5 (d, *J* = 12.8 Hz, 1C), 37.8, 36.6 (d, *J* = 5.9 Hz, 1C), 33.4 (d, *J* = 7.8 Hz, 1C), 31.8 (d, *J* = 4.7 Hz, 1C), 30.5 (d, *J* = 16.5 Hz, 1C), 29.0 (d, *J* = 6.8 Hz,

1C), 27.3, 27.1 (d, J = 7.0 Hz, 1C), 27.0, 26.9, 26.4, 25.8; **^{31}P NMR** (100 MHz, $CDCl_3$) δ -30.0; **HRMS** (ESI): calcd. for $C_{22}H_{38}N_2P^+$: 361.2767, found 361.2775.

4-Bromo-3-cyclohexyl-1-methyl-1*H*-pyrazole

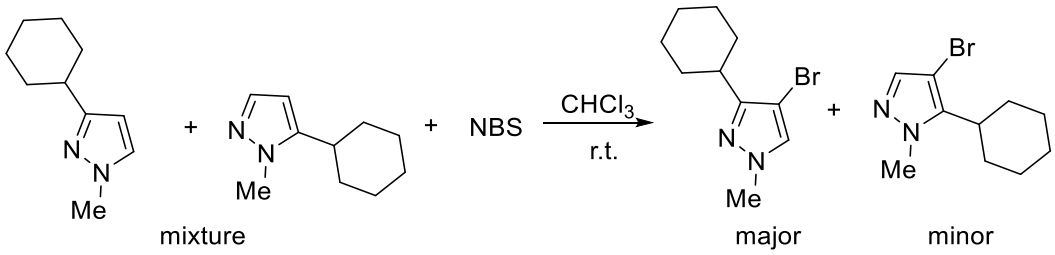

N-Bromosuccinimide (1.90 g, 10.7 mmol) was added to a solution of mixture of 3-cyclohexyl-1-methyl-1*H*-pyrazole and 5-cyclohexyl-1-methyl-1*H*-pyrazole (1.69 g, 10.2 mmol) in anhydrous chloroform (30.0 mL) in portion at room temperature. After stirring for 40 min, anhydrous chloroform was removed under vacuum, and residue was washed by water and extracted by DCM (20.0 mL x 3). The combined organic layers were washed with brine, dried by anhydrous sodium sulfate and concentrated under reduced pressure. Purification by column chromatography (ethyl acetate/hexane = 1:5 to 1:4) to afford the major product 4-bromo-3-cyclohexyl-1-methyl-1*H*-pyrazole as light-yellow liquid.

Yield: 56% (0.760 g). **^{1}H NMR** (400 MHz, $CDCl_3$) δ 7.28 (s, 1H), 3.82 (s, 3H), 2.69-2.62 (m, 1H), 1.91-1.70 (m, 4H), 1.71 (dd, J = 10.0, 3.4 Hz, 1H), 1.54 (qd, J = 12.4, 2.7 Hz, 2H), 1.42-1.33 (m, 2H), 1.30-1.23 (m, 1H); **^{13}C NMR** (100 MHz, $CDCl_3$) δ 155.1, 130.3, 91.7, 39.2, 36.3, 31.9, 26.5, 26.0; **HRMS** (ESI): calcd. for $C_{10}H_{16}N_2Br^+$: 243.0491, found 243.0495.

3-Cyclohexyl-4-(dicyclohexylphosphaneyl)-1-methyl-1*H*-pyrazole (L29)

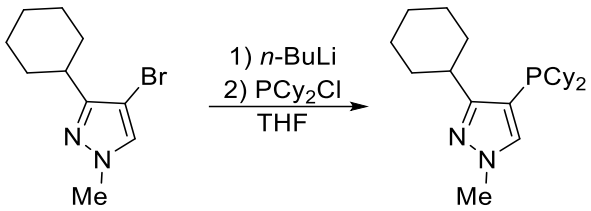

4-Bromo-3-cyclohexyl-1-methyl-1*H*-pyrazole (0.850 g, 3.50 mmol) was dissolved in freshly distilled THF (10.0 mL) at room temperature under nitrogen atmosphere. The solution was cooled to -78 °C in a dry ice/acetone bath. Titrated *n*-BuLi (4.20 mmol) was added dropwise with a syringe. After the reaction mixture was stirred for 45 min at -78 °C, dicyclohexylchlorophosphine (0.810 mL, 3.68 mmol) was added. The reaction was allowed to warm to room temperature and stirred for 60 min. The solvent was removed under reduced pressure, After the solvent was removed under vacuum, the solid product was washed with 90% methanol/water mixture (10.0 mL x 3). The white solid was collected by filtration and dried over vacuum to afford the desired product.

Yield: 37% (0.400 g). White solid, m.p. = 127.4–130.4 °C. **^{1}H NMR** (400 MHz, $CDCl_3$) δ 7.17 (s, 1H), 3.86 (s, 3H), 2.88 (t, *J* = 11.9 Hz, 1H), 1.84-1.76 (m, 9H), 1.68 (d, *J* = 11.9 Hz, 5H), 1.60-1.55 (m, 5H), 1.39-1.33 (m, 3H), 1.28-1.21 (m, 3H), 1.16-1.13 (m, 3H), 1.07-0.97 (m, 4H); **^{13}C NMR** (100 MHz, $CDCl_3$) δ 164.3 (d, *J* = 24.3 Hz, 1C), 133.3 (d, *J* = 3.0 Hz, 1C), 106.9 (d, *J* = 14.7 Hz, 1C), 38.8, 36.6 (d, *J* = 6.8 Hz, 1C), 33.5, 33.4 (d, *J* = 8.2 Hz, 1C), 30.3 (d, *J* = 16.2 Hz, 1C), 28.8 (d, *J* = 6.7 Hz, 1C), 27.3, 27.1 (d, *J* = 8.3 Hz, 1C), 26.7, 26.4, 26.1; **^{31}P NMR** (100 MHz, $CDCl_3$) δ -31.6; **HRMS** (ESI): calcd. for $C_{22}H_{38}N_2P^+$: 361.2767, found 361.2774.

1-Methyl-3,5-diphenyl-1*H*-pyrazole[28]

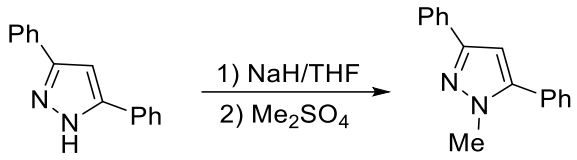

3,5-Diphenyl-1*H*-pyrazole (3.30 g, 15.0 mmol) was placed in the dropping funnel and dissolved with 20.0 mL tetrahydrofuran. The solution was added dropwise to the 1.5 equivalent sodium hydride (0.900 g, 22.5 mmol, 60% dispersion in mineral oil) which suspended in 60.0 mL tetrahydrofuran at room temperature. Sodium hydride was washed with anhydrous hexane (5.00 mL x 3) to remove mineral oil prior to usage. The reaction mixture was stirred at room temperature for 15 min. Dimethyl sulfate (1.60 mL, 16.5 mmol) was added to the reaction mixture and additional 30.0 mL tetrahydrofuran was added. After the reaction mixture was allowed to stir overnight, solvent was removed by vacuum. Ethyl acetate and water were added to the mixture and the organic phase was separated. The organic phase was washed with water and brine several times and concentrated. The concentrated mixture was purified by column chromatography on silica gel and eluted with ethyl acetate/hexane (1:4). The solution was evaporated in vacuum to give the desired product.

Yield: 97% (3.40 g). Yellow solid. **^{1}H NMR** (400 MHz, $CDCl_3$) δ 3.94 (s, 3H), 6.63 (s, 1H), 7.30-7.34 (m, 1H), 7.41-7.46 (m, 3H), 7.47-7.51 (m, 4H), 7.85-7.87 (m, 2H); **^{13}C NMR** (100 MHz, $CDCl_3$) δ 37.5, 103.2, 125.5, 127.5, 128.5, 128.6, 128.6, 128.7,130.6, 133.4, 145.0, 150.4.

4-Bromo-1-methyl-3,5-diphenyl-1*H*-pyrazole

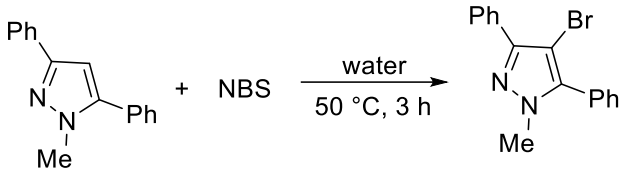

A mixture of 1-methyl-3,5-diphenyl-1*H*-pyrazole (3.28 g, 14.0 mmol) and *N*-bromosuccinimide (2.50 g, 14.0 mmol) in water (30.0 mL) was stirred at 50 °C for 3 h. The white solid was filtered and then washed with water. The solid was dissolved in DCM and dried with Na_2SO_4. The solution was evaporated to give the desired product. **Yield**: 98% (4.28 g). White solid. **^{1}H NMR** (400 MHz, $CDCl_3$) δ 3.94 (s, 3H), 6.63 (s, 1H), 7.30-7.34 (m, 1H), 7.41-7.46 (m, 3H), 7.47-7.51 (m, 4H), 7.85-7.87 (m, 2H); **^{13}C NMR** (100 MHz, $CDCl_3$) δ 37.5, 103.2, 125.5, 127.5, 128.5, 128.6, 128.6, 128.7, 130.6, 133.4, 145.0, 150.4; **HRMS** (ESI): calcd. for $C_{16}H_{14}N_2Br^+$: 313.0335, found 313.0340.

4-(Dicyclohexylphosphaneyl)-1-methyl-3,5-diphenyl-1*H*-pyrazole (L30)

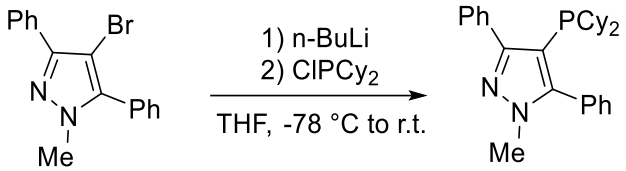

4-Bromo-1-methyl-3,5-diphenyl-1*H*-pyrazole (0.940 g, 3.00 mmol) was dissolved in freshly distilled THF (15.0 mL) at room temperature under nitrogen atmosphere. The solution was cooled to -78 °C in a dry ice/acetone bath. Titrated *n*-BuLi (3.30 mmol) was added dropwise with a syringe. After the reaction mixture was stirred for 30 min at -78 °C, chlorodicyclohexylphosphine (0.780 mL, 3.54 mmol) dissolving in freshly distilled THF (5.00 mL) was added. The reaction was allowed to warm to room temperature and stirred overnight. The solvent was removed under reduced pressure. After the solvent was removed under vacuum, the solid product was subjected to

recrystallization from hot degassed ethanol/water (10:1). The solid was generated and washed by a mixture solvent of Ethanol: Water = 5:1 for 2 times. The white solid was collected by filtration and dried over vacuum to afford the product.

Yield: 39% (0.500 g). White solid. m.p.= 121.3–122.4 °C. **^{1}H NMR** (400 MHz, $CDCl_3$) δ 0.89-1.25 (m, 10H), 1.58-1.75 (m, 12H), 3.71 (s, 3H), 7.28-7.64 (m, 10H); **^{13}C NMR** (100 MHz, $CDCl_3$) δ 26.2, 26.8, 26.9, 30.7, 30.8, 32.0, 32.3, 34.8, 34.9, 37.1, 127.7, 127.8, 128.3, 129.0, 129.6, 129.7, 130.4; **^{31}P NMR** (162 MHz, $CDCl_3$) δ -22.93; **HRMS** (ESI): calcd. for $C_{28}H_{36}N_2P^+$: 431.2611, found 431.2612.

3,5-Di-*tert*-butyl-1*H*-pyrazole[29]

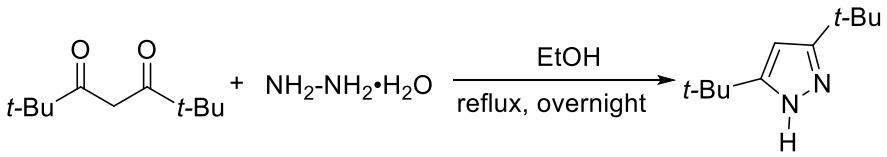

2,2,6,6-Tetramethylheptane-3,5-dione (10.4 mL, 50.0 mmol) was dissolved in ethanol (50.0 mL). Hydrazine monohydrate (2.90 mL, 60.0 mmol) was then added. The mixture was refluxed for overnight and cooled down to room temperature. After the completion of the reaction monitored by GC-MS, the solvent was removed under reduced pressure. DCM and water were added to the mixture, the organic phase was separated and dried by Na_2SO_4. The solution was evaporated to give solid and the solid was subjected to recrystallization from hot ethanol/water (3:2) mixture (25.0 mL) and washed by ethanol/water (1:1) mixture for two times. The white solid was filtered and dried under vacuum to yield 3,5-di-*tert*-butyl-1*H*-pyrazole.

Yield: 90% (8.07 g); **^{1}H NMR** (400 MHz, $CDCl_3$) δ 5.93 (s 1H), 1.37 (s, 18H); **^{13}C NMR** (100 MHz, $CDCl_3$) δ 97.3, 31.4, 30.5.

4-Bromo-3,5-di-*tert*-butyl-1*H*-pyrazole[29]

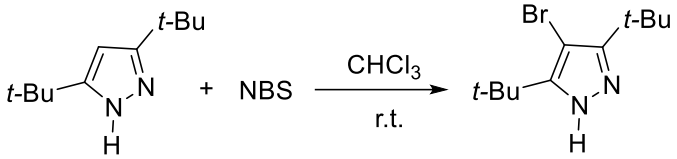

N-Bromosuccinimide (4.45 g, 25.0 mmol) was added to a solution of 3,5-di-tert-butyl-1*H*-pyrazole (4.50 g, 25.0 mmol) in anhydrous chloroform (125 mL) in portion. After stirring for 15 min, the solvent was removed by vacuum. DCM and water were added to the mixture and the organic phase was separated. The organic layer was washed with water for three times. The organic layer was washed by brine and dried by Na_2SO_4. The solution was evaporated to give the product.

Yield: 84% (5.44 g). White solid. **^{1}H NMR** (400 MHz, $CDCl_3$) δ 1.44 (s, 18H); **^{13}C NMR** (100 MHz, $CDCl_3$) δ 88.9, 32.6, 29.7, 28.6.

4-Bromo-3,5-di-*tert*-butyl-1-methyl-1*H*-pyrazole

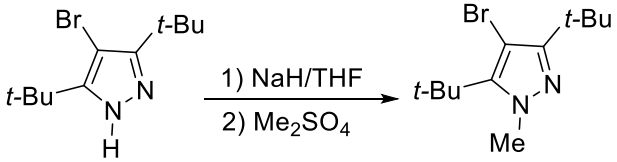

4-Bromo-3,5-di-*tert*-butyl-1*H*-pyrazole (2.60 g, 10.1 mmol) was dissolved in freshly distilled THF (30.0 mL) at room temperature under nitrogen atmosphere. The reaction was cooled down to 0 ºC in ice bath. Sodium hydride (0.524 g, 13.1 mmol) was then added. Dimethyl sulfate (1.00 mL, 10.6 mmol) was then added dropwisely and the reaction mixture was stirred for 50 min. After the completion of the reaction monitored by GC-MS, ethyl acetate and water were added to the mixture. The organic layer was then concentrated. The concentrated mixture was purified by column

chromatography and eluted with Hexane: Ethyl acetate = 4:1. The solution was evaporated to give the desired product.

Yield: 93% (2.56 g). White solid, m.p.= 75.6–77.1 ºC. **^{1}H NMR** (400 MHz, $CDCl_3$) δ 3.96 (s, 3H), 1.52 (s, 9H), 1.40 (s, 9H); **^{13}C NMR** (100 MHz, $CDCl_3$) δ 155.2, 146.0, 90.0, 42.4, 33.6, 33.0, 30.5, 28.9, 28.4; **HRMS** (ESI): calcd. for $C_{12}H_{22}BrN_2^+$: 273.0961, found 273.0964.

3,5-Di-*tert*-butyl-4-(dicyclohexylphosphaneyl)-1-methyl-1*H*-pyrazole (L31)

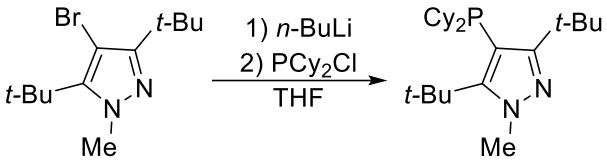

Bromo-3,5-di-*tert*-butyl-1-methyl-1*H*-pyrazole (1.37 g, 5.00 mmol) was dissolved in freshly distilled THF (25.0 mL) at room temperature under nitrogen atmosphere. The solution was cooled to -78 ºC in a dry ice/acetone bath. Titrated *n*-BuLi (5.25 mmol) was added dropwise with a syringe. After the reaction mixture was stirred for 45 min at -78 ºC, chlorodicyclohexylphosphine (1.16 mL, 5.25 mmol) was added. The reaction was allowed to warm to room temperature and stirred for 60 min. The solvent was removed under reduced pressure. After the solvent was removed under vacuum, the solid product was washed with 90% methanol/water mixture (10.0 mL x 3). The white solid was collected by filtration and dried over vacuum to afford **L30**.

Yield: (0.900 g, 46%). White solid, m.p.= 134.2–136.6 ºC. **^{1}H NMR** (400 MHz, $CDCl_3$) δ 3.97 (s, 3H), 2.25-1.64 (m, 11H), 1.50 (s, 9H), 1.45 (s, 9H), 1.35-1.01 (m, 11H); **^{13}C NMR** (100 MHz, $CDCl_3$) δ 41.8, 37.3 (d, J = 16.1 Hz, 1C), 34.4, 33.8, 33.6, 33.5 (d, J = 4.6 Hz, 1C), 32.6, 32.0, 31.8, 31.6, 31.3 (d, J = 9.8 Hz, 1C), 30.9, 27.4, 27.3, 27.2,

26.3; **^{31}P NMR** (200 MHz, C_6D_6) δ -21.4; **HRMS** (ESI): calcd. for $C_{24}H_{44}N_2P^+$: 391.3237, found 391.3244.

Palladium complex: Pd-L25(η^3-C_3H_5)Cl

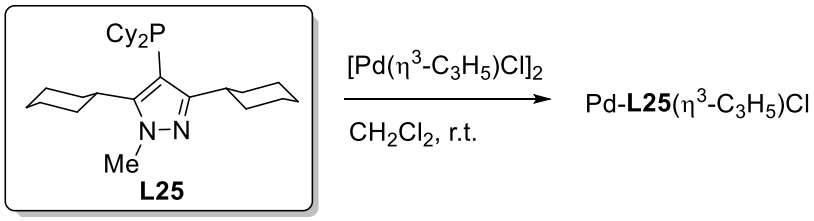

A solution of [Pd(η^3-C_3H_5)Cl]$_2$ (0.0370 g, 0.100 mmol, and **L25** (0.0890 g, 0.200 mmol, 1.0 equiv.) in CH_2Cl_2 (1.00 mL) was stirred at room temperature for 30 min. A single crystal of the complex suitable for X-ray diffraction was obtained by vapor diffusion of hexane (5.00 mL) into a dichloromethane solution.

NMR data: **^{1}H NMR** (400 MHz, $CDCl_3$) δ 1.10-1.50 (m, 14H), 1.55-1.95 (m, 26H), 2.20-2.35 (m, 2H), 2.69-2.84 (m, 2H), 3.71-3.78 (m, 2H), 3.90 (s, 3H), 4.05 (s, 1H), 4.65 (t, *J* = 7.1 Hz, 1H), 5.47 (sept, *J* = 7.1 Hz, 1H); **^{13}C NMR** (100 MHz, $CDCl_3$) δ 25.91, 25.96, 26.0, 26.91, 26.96, 27.0, 27.1, 28.1, 30.2, 30.3, 30.7, 31.1, 34.3, 34.4, 36.6, 36.7, 37.0, 37.2, 38.5, 39.4, 52.6, 53.3, 79.5, 79.8, 99.0, 99.8, 114.9, 115.0, 151.8, 152.0, 158.7; **^{31}P NMR** (162 MHz, $CDCl_3$) δ 10.4.

Palladium complex: Pd-L26(η^3-C_3H_5)Cl

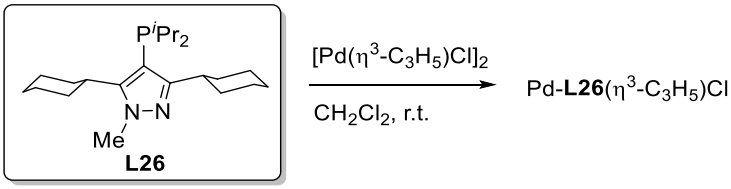

A solution of [Pd(η^3-C_3H_5)Cl]$_2$ (0.0370 g, 0.100 mmol, and **L26** (0.0890 g, 0.200

mmol, 1.0 equiv.) in CH_2Cl_2 (1.00 mL) was stirred at room temperature for 30 min. The DCM was removed under vacuum. The resulting complex was washed with hexane and dried under vacuum to afford Pd-**L26**(η^3-C_3H_5)Cl.

NMR data: **^{1}H NMR** (400 MHz, $CDCl_3$) δ 1.10–1.45 (m, 17H), 1.55-1.90 (m, 15H), 2.55-2.70 (m, 3H), 2.75-2.85 (m, 1H), 3.74-3.78 (m, 2H), 3.93 (s, 3H), 4.04 (s, 1H), 4.69 (t, *J* = 6.7 Hz, 1H), 5.45 (sept, *J* = 7.1 Hz, 1H); **^{13}C NMR** (100 MHz, $CDCl_3$) δ 20.8, 20.9, 21.0, 21.1, 25.92, 25.98, 26.7, 26.92, 26.97, 27.0, 27.11, 27.17, 30.3, 30.4, 34.4, 34.5, 36.71, 36.78, 38.6, 39.5, 52.1, 80.1, 80.4, 99.5, 99.9, 115.1, 115.2, 151.8, 152.0, 158.8; **^{31}P NMR** (162 MHz, $CDCl_3$) δ 22.9.

4-(Methyl(phenyl)amino)phenyl trifluoromethanesulfonate (Table 2.3, compound 3a)

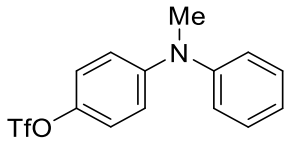

Yield: 89% (58.7 mg). Yellow liquid. Eluents (R_f = 0.6, Hexane: Ethyl acetate = 10:1) was used for flash column chromatography. The % conversion of starting material = 100%. The % of minor product (reacting C–OTf site): major product (reacting C–Cl site): diarylated product (reacting both C–OTf & C–Cl site) = 0: 100: 0. **^{1}H NMR** (400 MHz, $CDCl_3$) δ 7.40-7.36 (m, 2H), 7.17-7.09 (m, 5H), 6.90-6.87 (m, 2H), 3.33 (s, 3H); **^{13}C NMR** (100 MHz, $CDCl_3$) δ 148.9, 148.0, 142.0, 129.7, 124.1, 124.0, 121.8, 118.8 (q, *J* = 319.0 Hz, 1C), 117.3, 40.3; ^{19}F NMR (376 MHz, $CDCl_3$) δ -72.7; **HRMS** (APPI): calcd for $C_{14}H_{13}F_3NO_3S^+$: 332.0563, found 332.0566.

4-(Methyl(*p*-tolyl)amino)phenyl trifluoromethanesulfonate (Table 2.3, compound 3b)

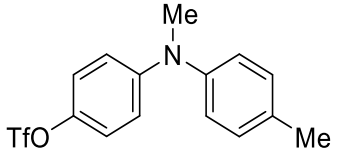

Yield: 94% (64.9 mg). Yellow liquid. Eluents (R_f = 0.7, Hexane: Ethyl acetate = 10:1) was used for flash column chromatography. The % conversion of starting material = 100%. The % of minor product (reacting C–OTf site): major product (reacting C–Cl site): diarylated product (reacting both C–OTf & C–Cl site) = 0: 100: 0. **^{1}H NMR** (400 MHz, $CDCl_3$) δ 7.21 (d, *J* = 8.2 Hz, 2H), 7.10-7.08 (m, 4H), 6.82-6.77 (m, 2H), 3.30 (s, 3H), 2.38 (s, 3H); **^{13}C NMR** (100 MHz, $CDCl_3$) δ 149.1, 145.5, 141.4, 134.6, 130.4, 125.1, 123.8, 121.7, 118.8 (q, *J* = 319.2 Hz, 1C), 115.8, 40.4, 20.8; **^{19}F NMR** (376 MHz, $CDCl_3$) δ -72.7; **HRMS** (APPI): calcd for $C_{15}H_{15}F_3NO_3S^+$: 346.0719, found 346.0724.

3-(Methyl(phenyl)amino)phenyl trifluoromethanesulfonate (Table 2.3, compound 3c)

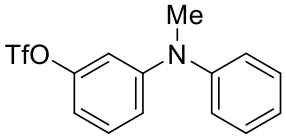

Yield: 82% (54.3 mg). Yellow liquid. Eluents (R_f = 0.5, Hexane: Ethyl acetate = 10:1) was used for flash column chromatography. The % conversion of starting material = 100%. The % of minor product (reacting C–OTf site): major product (reacting C–Cl site): diarylated product (reacting both C–OTf & C–Cl site) = 0: 100: 0. **^{1}H NMR** (400 MHz, $CDCl_3$) δ 7.40 (t, *J* = 7.8 Hz, 2H), 7.26-7.18 (m, 4H), 6.83-6.81 (m, 1H), 6.70-6.68 (m, 2H), 3.33 (s, 3H); **^{13}C NMR** (100 MHz, $CDCl_3$) δ 150.7, 150.5, 147.5, 130.1,

129.8, 124.8, 118.7 (q, J = 318.7 Hz, 1C), 115.4, 110.5, 108.3, 40.2; **^{19}F NMR** (376 MHz, $CDCl_3$) δ -72.9; **HRMS** (APPI): calcd for $C_{14}H_{13}F_3NO_3S^+$: 332.0563, found 332.0567.

3-(Methyl(*p*-tolyl)amino)phenyl trifluoromethanesulfonate (Table 2.3, compound 3d)

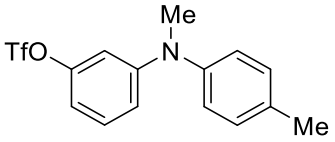

Yield: 94% (64.9 mg). Yellow liquid. Eluents (R_f = 0.5, Hexane: Ethyl acetate = 10:1) was used for flash column chromatography. The % conversion of starting material = 100%. The % of minor product (reacting C–OTf site): major product (reacting C–Cl site): diarylated product (reacting both C–OTf & C–Cl site) = 0: 93: 7. **^{1}H NMR** (400 MHz, $CDCl_3$) δ 7.23-7.19 (m, 3H), 7.10 (d, J = 8.2 Hz, 2H), 6.77-6.75 (m, 1H), 6.66-6.64 (m, 2H), 3.30 (s, 3H), 2.39 (s, 3H); **^{13}C NMR** (100 MHz, $CDCl_3$) δ 151.0, 150.5, 144.9, 135.1, 130.4, 130.0, 125.5, 118.7 (q, J = 318.9 Hz, 1C), 114.4, 109.7, 107.3, 40.3, 20.9; **^{19}F NMR** (376 MHz, $CDCl_3$) δ -72.9; **HRMS** (APPI): calcd for $C_{15}H_{15}F_3NO_3S^+$: 346.0719, found 346.0728.

2-Methyl-5-(methyl(*p*-tolyl)amino)phenyl trifluoromethanesulfonate (Table 2.3, compound 3e)

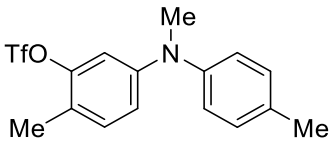

Yield: 85% (60.8 mg). Yellow liquid. Eluents (R_f = 0.7, Hexane: Ethyl acetate = 10:1) was used for flash column chromatography. The % conversion of starting material = 100%. The % of minor product (reacting C–OTf site): major product (reacting C–Cl site): diarylated product (reacting both C–OTf & C–Cl site) = 0.6: 99.4: 0. **^{1}H NMR** (400 MHz, $CDCl_3$) δ 7.19 (d, *J* = 8.2 Hz, 2H), 7.10-7.05 (m, 3H), 6.75 (dd, *J* = 8.4, 2.3 Hz, 1H), 6.71 (d, *J* = 2.2 Hz, 1H), 3.28 (s, 3H), 2.37 (s, 3H), 2.29 (s, 3H); **^{13}C NMR** (100 MHz, $CDCl_3$) δ 148.9, 148.9, 145.4, 134.0, 130.2, 124.3, 119.6, 118.6 (q, *J* = 318.2 Hz, 1C), 115.9, 108.6, 40.3, 20.8, 15.3; **^{19}F NMR** (376 MHz, $CDCl_3$) δ -73.8; **HRMS** (APPI): calcd for $C_{16}H_{17}F_3NO_3S^+$: 360.0876, found 360.0879.

5-(Methyl(phenyl)amino)-2-nitrophenyl trifluoromethanesulfonate (Table 2, compound 3f)

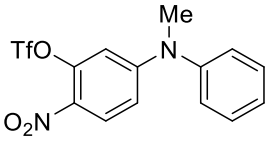

Yield: 65% (48.9 mg). Light-yellow solid, m.p.= 102.2–105.2 ºC. Eluents (R_f = 0.5, Hexane: Ethyl acetate = 5:1) was used for flash column chromatography. The % conversion of starting material = 95%. The % of minor product (reacting C–OTf site): major product (reacting C–Cl site): diarylated product (reacting both C–OTf & C–Cl site) = 98.5: 1.5: 0. **^{1}H NMR** (400 MHz, $CDCl_3$) δ 8.07 (d, *J* = 9.4 Hz, 1H), 7.50 (t, *J* = 7.7 Hz, 2H), 7.38 (t, *J* = 7.4 Hz, 1H), 7.23 (d, *J* = 7.8 Hz, 2H), 6.64 (dd, *J* = 9.4, 2.4 Hz, 1H), 6.44 (d, *J* = 2.3 Hz, 1H), 3.42 (s, 3H); **^{13}C NMR** (100 MHz, $CDCl_3$) δ 154.2, 145.0, 143.8, 130.5, 130.1, 128.7, 127.8, 126.6, 118.5 (q, *J* = 319.1 Hz, 1C), 111.3, 106.7, 40.5; **^{19}F NMR** (565 MHz, $CDCl_3$) δ -73.4; **HRMS** (EI): calcd for $C_{14}H_{11}F_3N_2O_5S^+$:

376.0335, found 376.0331.

4-(4-(Methyl(phenyl)amino)benzoyl)phenyl trifluoromethanesulfonate (Table 2.3, compound 3g)

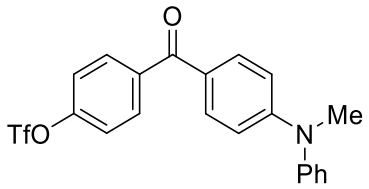

Yield: 95% (82.6 mg). Light-yellow solid, m.p.= 75.6–78.6 ºC. Eluents (R_f = 0.4, Hexane: Ethyl acetate = 10:1) was used for flash column chromatography. The % conversion of starting material = 100%. The % of minor product (reacting C–OTf site): major product (reacting C–Cl site): diarylated product (reacting both C–OTf & C–Cl site) = 0: 100: 0. **^{1}H NMR** (400 MHz, $CDCl_3$) δ 7.82 (d, *J* = 8.3 Hz, 2H), 7.71 (d, *J* = 8.5 Hz, 2H), 7.43 (t, *J* = 7.4 Hz, 2H), 7.36 (d, *J* = 8.3 Hz, 2H), 7.26 (t, *J* = 8.9 Hz, 3H), 6.77 (d, *J* = 8.6 Hz, 2H), 3.40 (s, 3H); **^{13}C NMR** (100 MHz, $CDCl_3$) δ 193.0, 152.9, 151.2, 146.9, 139.1, 132.4, 131.5, 129.9, 126.4, 126.0, 125.6, 121.1, 118.7 (q, *J* = 318.8 Hz, 1C), 113.1, 40.2; **^{19}F NMR** (376 MHz, $CDCl_3$) δ -72.6; **HRMS** (APPI): calcd for $C_{21}H_{17}F_3NO_4S^+$: 436.0825, found 436.0832.

3-(Phenylamino)phenyl trifluoromethanesulfonate (Table 2.3, compound 3h)

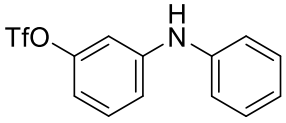

Yield: 82% (52.3 mg). Light-yellow liquid. Eluents (R_f = 0.4, Hexane: Ethyl acetate = 10:1) was used for flash column chromatography. The % conversion of starting material = 100%. The % of minor product (reacting C–OTf site): major product (reacting C–Cl

site): diarylated product (reacting both C–OTf & C–Cl site) = 0: 90: 10. **^{1}H NMR** (400 MHz, $CDCl_3$) δ 7.35 (t, *J* = 7.8 Hz, 2H), 7.28 (t, *J* = 8.2 Hz, 1H), 7.13 (d, *J* = 7.8 Hz, 2H), 7.08 (t, *J* = 7.4 Hz, 1H), 6.99 (dd, *J* = 8.2, 1.5 Hz, 1H), 6.94 (d, *J* = 2.0 Hz, 1H), 6.77 (dd, *J* = 8.1, 1.8 Hz, 1H), 5.89 (s, 1H); **^{13}C NMR** (100 MHz, $CDCl_3$) δ 150.4, 145.7, 141.1, 130.7, 129.6, 123.5, 119.5, 118.7 (q, *J* = 318.8 Hz, 1C), 116.0, 112.2, 108.7; **^{19}F NMR** (376 MHz, $CDCl_3$) δ -72.9; **HRMS** (EI): calcd for $C_{13}H_{10}F_3NO_3S^+$: 317.0328, found 317.0332.

3-Methyl-5-(phenylamino)phenyl trifluoromethanesulfonate (Table 2.3, compound 3i)

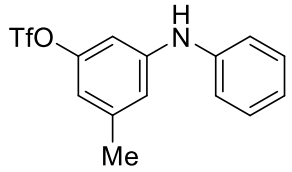

Yield: 87% (57.5 mg). Light-yellow liquid. Eluents (R_f = 0.4, Hexane: Ethyl acetate = 10:1) was used for flash column chromatography. The % conversion of starting material = 100%. The % of minor product (reacting C–OTf site): major product (reacting C–Cl site): diarylated product (reacting both C–OTf & C–Cl site) = 0: 100: 0. **^{1}H NMR** (400 MHz, $CDCl_3$) δ 7.34 (t, *J* = 7.9 Hz, 2H), 7.11 (d, *J* = 7.6 Hz, 2H), 7.06 (t, *J* = 7.4 Hz, 1H), 6.80 (s, 1H), 6.76 (s, 1H), 6.60 (s, 1H), 5.81 (s, 1H), 2.33 (s, 3H); **^{13}C NMR** (100 MHz, $CDCl_3$) δ 150.3, 145.3, 141.4, 141.3, 129.5, 122.6, 119.5, 118.7 (q, *J* = 318.8 Hz, 1C), 116.7, 113.1, 106.0, 21.5; **^{19}F NMR** (376 MHz, $CDCl_3$) δ -73.0; **HRMS** (EI): calcd for $C_{14}H_{12}F_3NO_3S^+$: 331.0485, found 331.0494.

3-Methoxy-5-(phenylamino)phenyl trifluoromethanesulfonate (Table 2.3, compound 3j)

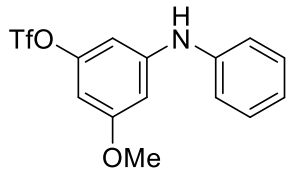

Yield: 77% (53.4 mg). Light-yellow liquid. Eluents (R_f = 0.4, Hexane: Ethyl acetate = 5:1) was used for flash column chromatography. The % conversion of starting material = 97%. The % of minor product (reacting C–OTf site): major product (reacting C–Cl site): diarylated product (reacting both C–OTf & C–Cl site) = 0: 100: 0. **^{1}H NMR** (400 MHz, $CDCl_3$) δ 7.34 (t, *J* = 7.8 Hz, 2H), 7.12 (d, *J* = 7.7 Hz, 2H), 7.07 (t, *J* = 7.4 Hz, 1H), 6.53 (s, 2H), 6.34 (s, 1H), 5.87 (s, 1H), 3.78 (s, 3H); **^{13}C NMR** (100 MHz, $CDCl_3$) δ 161.5, 151.0, 146.1, 141.0, 129.5, 122.9, 119.9, 118.7 (q, *J* = 318.8 Hz, 1C), 101.5, 101.3, 98.8, 55.6; **^{19}F NMR** (376 MHz, $CDCl_3$) δ -72.9; **HRMS** (EI): calcd for $C_{14}H_{12}F_3NO_4S^+$: 347.0434, found 347.0427.

3-(Phenylamino)-5-(trifluoromethyl)phenyl trifluoromethanesulfonate (Table 2.3, compound 3k)

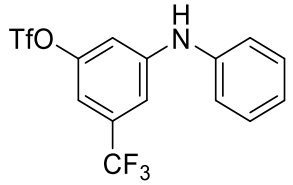

Yield: 71% (55.0 mg). Yellow liquid. Eluents (R_f = 0.4, Hexane: Ethyl acetate = 10:1) was used for flash column chromatography. The % conversion of starting material = 100%. The % of minor product (reacting C–OTf site): major product (reacting C–Cl site): diarylated product (reacting both C–OTf & C–Cl site) = 0: 100: 0. **^{1}H NMR** (400

MHz, $CDCl_3$) δ 7.40 (t, *J* = 7.7 Hz, 2H), 7.17 (m, 4H), 7.04 (s, 1H), 6.96 (s, 1H), 6.08 (s, 1H); **^{13}C NMR** (100 MHz, $CDCl_3$) δ 150.3, 146.7, 139.8, 133.5 (q, *J* = 33.8 Hz, 1C), 129.9, 124.2, 122.9 (q, *J* = 217.1 Hz, 1C), 120.8, 111.9 (q, *J* = 3.8 Hz, 1C), 118.7 (q, *J* = 318.8 Hz, 1C), 110.7, 108.6 (q, *J* = 4.0 Hz, 1C); **^{19}F NMR** (376 MHz, $CDCl_3$) δ -72.8, -63.3; **HRMS** (EI): calcd for $C_{14}H_9F_6NO_3S^+$: 385.0202, found 385.0214.

2-Methyl-5-(phenylamino)phenyl trifluoromethanesulfonate (Table 2.3, compound 3l)

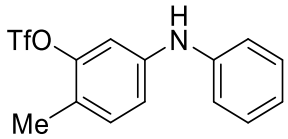

Yield: 90% (59.6 mg). Yellow liquid. Eluents (R_f = 0.4, Hexane: Ethyl acetate = 10:1) was used for flash column chromatography. The % conversion of starting material = 100%. The % of minor product (reacting C–OTf site): major product (reacting C–Cl site): diarylated product (reacting both C–OTf & C–Cl site) = 0.3: 99.7: 0. **^{1}H NMR** (400 MHz, $CDCl_3$) δ 7.34-7.30 (m, 2H), 7.16 (d, *J* = 8.2 Hz, 1H), 7.08 (d, *J* = 7.7 Hz, 2H), 7.02 (t, *J* = 7.4 Hz, 1H), 6.97-6.93 (m, 2H), 5.76 (s, 1H), 2.32 (s, 3H); **^{13}C NMR** (100 MHz, $CDCl_3$) δ 148.8, 143.0, 141.9, 132.5, 129.5, 122.0, 121.9, 120.2, 118.4, 117.03 (q, *J* = 317.6 Hz, 1C), 117.00, 109.7, 15.5; **^{19}F NMR** (376 MHz, $CDCl_3$) δ -73.9; **HRMS** (APPI): calcd for $C_{14}H_{13}F_3NO_3S^+$: 332.0563, found 332.0564.

2-Fluoro-5-(phenylamino)phenyl trifluoromethanesulfonate (Table 2.3, compound 3m)

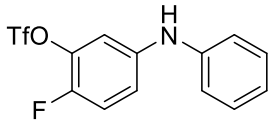

Yield: 70% (47.1 mg). Red liquid. Eluents (R_f = 0.5, Hexane: Toluene = 2:1) was used for flash column chromatography. The % conversion of starting material = 97%. The % of minor product (reacting C–OTf site): major product (reacting C–Cl site): diarylated product (reacting both C–OTf & C–Cl site) = 94.3: 2.8: 2.9. **^{1}H NMR** (400 MHz, $CDCl_3$) δ 7.33 (t, *J* = 7.9 Hz, 2H), 7.13 (t, *J* = 9.1 Hz, 1H), 7.08-6.94 (m, 5H), 5.74 (s, 1H); **^{13}C NMR** (100 MHz, $CDCl_3$) δ 147.7 (d, *J* = 244.7 Hz, 1C), 147.8, 140.7 (d, *J* = 2.8 Hz, 1C), 136.9 (d, *J* = 14.4 Hz, 1C), 129.6, 122.4, 118.62 (q, *J* = 318.8 Hz, 1C), 118.58, 117.9 (d, *J* = 26.8 Hz, 1C), 117.8 (d, *J* = 1.4 Hz, 1C), 111.6; **^{19}F NMR** (376 MHz, $CDCl_3$) δ -73.2, -138.3; **HRMS** (EI): calcd for $C_{13}H_9F_4NO_3S^+$: 335.0234, found 335.0237.

2-Fluoro-4-(phenylamino)phenyl trifluoromethanesulfonate (Table 2.3, compound 3n)

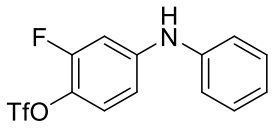

Yield: 76% (51.0 mg). Light-yellow liquid. Eluents (R_f = 0.5, Hexane: Toluene = 2:1) was used for flash column chromatography. The % conversion of starting material = 100%. The % of minor product (reacting C–OTf site): major product (reacting C–Cl site): diarylated product (reacting both C–OTf & C–Cl site) = 100: 0: 0. **^{1}H NMR** (400 MHz, $CDCl_3$) δ 7.35 (t, *J* = 7.8 Hz, 2H), 7.18-7.10 (m, 4H), 6.85 (dd, *J* = 12.1, 2.7 Hz, 1H), 6.73-6.70 (m, 1H), 5.89 (s, 1H); **^{13}C NMR** (100 MHz, $CDCl_3$) δ 154.4 (d, *J* = 249.1 Hz, 1C), 145.5 (d, *J* = 9.5 Hz, 1C), 140.6, 129.7, 129.1 (d, *J* = 13.9 Hz, 1C), 124.0, 123.5, 120.5, 118.7 (q, *J* = 318.8 Hz, 1C), 111.4 (d, *J* = 2.9 Hz, 1C), 103.6 (d, *J* = 21.9

Hz, 1C); **^{19}F NMR** (565 MHz, $CDCl_3$) δ -73.5, -126.5; **HRMS** (EI): calcd for $C_{13}H_9F_4NO_3S^+$: 335.0234, found 335.0235.

2-Methyl-3-(phenylamino)phenyl trifluoromethanesulfonate (Table 2.3, compound 3o)

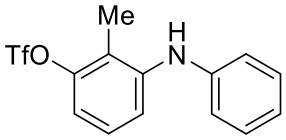

Yield: 93% (61.8 mg). Yellow liquid. Eluents (R_f = 0.4, Hexane: Ethyl acetate = 10:1) was used for flash column chromatography. The % conversion of starting material = 100%. The % of minor product (reacting C–OTf site): major product (reacting C–Cl site): diarylated product (reacting both C–OTf & C–Cl site) = 0: 97: 3. **^{1}H NMR** (400 MHz, $CDCl_3$) δ 7.33 (t, *J* = 7.7 Hz, 2H), 7.23 (d, *J* = 8.1 Hz, 1H), 7.16 (t, *J* = 8.1 Hz, 1H), 7.09-7.00 (m, 3H), 6.91 (d, *J* = 8.0 Hz, 1H), 5.51 (s, 1H), 2.28 (s, 3H); **^{13}C NMR** (100 MHz, $CDCl_3$) δ 149.0, 144.1, 142.4, 129.5, 127.2, 122.1, 120.1, 119.2, 118.6 (q, *J* = 318.3 Hz, 1C), 116.7, 113.7, 11.1; **^{19}F NMR** (376 MHz, $CDCl_3$) δ -73.7; **HRMS** (APPI): calcd for $C_{14}H_{13}F_3NO_3S^+$: 332.0563, found 332.0564.

4-Methyl-3-(phenylamino)phenyl trifluoromethanesulfonate (Table 2.3, compound 3p)

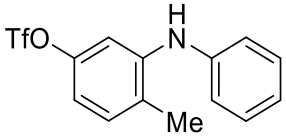

Yield: 90% (59.5 mg). Light-yellow liquid. Eluents (R_f = 0.4, Hexane: Ethyl acetate = 10:1) was used for flash column chromatography. The % conversion of starting material

= 100%. The % of minor product (reacting C–OTf site): major product (reacting C–Cl site): diarylated product (reacting both C–OTf & C–Cl site) = 0: 100: 0. **^{1}H NMR** (400 MHz, $CDCl_3$) δ 7.36 (t, *J* = 7.9 Hz, 2H), 7.21 (d, *J* = 8.3 Hz, 1H), 7.12-7.04 (m, 4H), 6.76 (dd, *J* = 8.3, 2.5 Hz, 1H), 5.53 (s, 1H), 2.28 (s, 3H); **^{13}C NMR** (100 MHz, $CDCl_3$) δ 148.5, 143.5, 141.6, 131.7, 129.6, 125.8, 122.6, 119.6, 118.7 (q, *J* = 318.8 Hz, 1C), 112.4, 108.2, 17.3; **^{19}F NMR** (376 MHz, $CDCl_3$) δ -72.9; **HRMS** (EI): calcd for $C_{14}H_{12}F_3NO_3S^+$: 331.0485, found 331.0483.

4-((4-Fluorophenyl)amino)phenyl trifluoromethanesulfonate (Table 2.3, compound 3q)

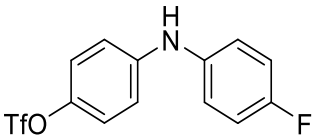

Yield: 90% (60.3 mg). Yellow liquid. Eluents (R_f = 0.4, Hexane: Ethyl acetate = 10:1) was used for flash column chromatography. The % conversion of starting material = 100%. The % of minor product (reacting C–OTf site): major product (reacting C–Cl site): diarylated product (reacting both C–OTf & C–Cl site) = 0: 100: 0. **^{1}H NMR** (400 MHz, $CDCl_3$) δ 7.13-7.00 (m, 6H), 6.92 (d, *J* = 9.0 Hz, 2H), 5.67 (bs, 1H); **^{13}C NMR** (100 MHz, $CDCl_3$) δ 158.9 (d, *J* = 240.6 Hz, 1C), 144.6, 142.4, 137.5 (d, *J* = 2.7 Hz, 1C), 122.4, 122.3 (d, *J* = 7.9 Hz, 1C), 118.8 (q, *J* = 319.0 Hz, 1C), 116.3, 116.2 (d, *J* = 22.4 Hz, 1C); **^{19}F NMR** (376 MHz, $CDCl_3$) δ -72.8, -119.8; **HRMS** (EI): calcd for $C_{13}H_9F_4NO_3S^+$: 335.0234, found 335.0239.

3-((4-Fluorophenyl) amino)phenyl trifluoromethanesulfonate (Table 2.3, compound 3r)

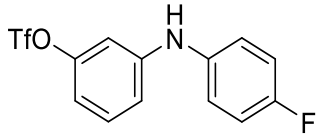

Yield: 90% (60.3 mg). Yellow liquid. Eluents (R_f = 0.4, Hexane: Ethyl acetate = 10:1) was used for flash column chromatography. The % conversion of starting material = 100%. The % of minor product (reacting C–OTf site): major product (reacting C–Cl site): diarylated product (reacting both C–OTf & C–Cl site) = 0: 100: 0. **^{1}H NMR** (400 MHz, $CDCl_3$) δ 7.26 (t, *J* = 8.2 Hz, 1H), 7.12-7.02 (m, 4H), 6.89 (d, *J*= 8.2 Hz, 1H), 6.80 (s, 1H), 6.73 (d, *J*= 8.2 Hz, 1H); 5.77 (s, 1H); **^{13}C NMR** (100 MHz, $CDCl_3$) δ 159.0 (d, *J* = 241.2 Hz, 1C), 150.5, 146.5, 136.9, 130.8, 122.6 (d, *J* = 8.0 Hz, 1C), 118.8 (q, *J* = 318.9 Hz, 1C), 116.3 (d, *J* = 22.5 Hz, 1C), 115.2, 111.9, 107.9; **^{19}F NMR** (376 MHz, $CDCl_3$) δ -119.2, -72.9; **HRMS** (EI): calcd for $C_{13}H_9F_4NO_3S^+$: 335.0234, found 335.0231.

3-([1,1'-Biphenyl]-4-ylamino)phenyl trifluoromethanesulfonate (Table 2.3, compound 3s)

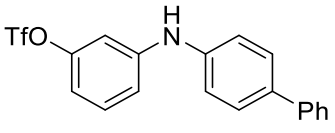

Yield: 91% (71.9 mg). Light-yellow liquid. Eluents (R_f = 0.2, Hexane: Ethyl acetate = 10:1) was used for flash column chromatography. The % conversion of starting material = 100%. The % of minor product (reacting C–OTf site): major product (reacting C–Cl site): diarylated product (reacting both C–OTf & C–Cl site) = 0: 100: 0. **^{1}H NMR** (400

MHz, $CDCl_3$) δ 7.50-7.35 (m, 8H), 7.28 (t, *J* = 8.6 Hz, 1H), 7.17 (t, *J* = 7.5, 1H), 6.95-6.93 (m, 2H), 6.79 (d, *J* = 8.2 Hz, 1H), 5.74 (s, 1H); **^{13}C NMR** (100 MHz, $CDCl_3$) δ 150.5, 146.0, 138.5, 138.2, 133.3, 131.2, 130.7, 129.2, 128.9, 128.4, 127.7, 123.1, 119.6, 118.7 (q, *J* = 318.8 Hz, 1C), 116.3, 112.3, 108.9; **^{19}F NMR** (376 MHz, $CDCl_3$) δ -72.9; **HRMS** (EI): calcd for $C_{19}H_{14}F_3NO_3S^+$: 393.0641, found 393.0648.

3-((4-Methoxyphenyl)amino)phenyl trifluoromethanesulfonate (Table 2.3, compound 3t)

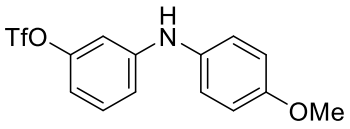

Yield: 78% (54.1 mg). Light-yellow liquid. Eluents (R_f = 0.4, Hexane: Ethyl acetate = 5:1) was used for flash column chromatography. The % conversion of starting material = 100%. The % of minor product (reacting C–OTf site): major product (reacting C–Cl site): diarylated product (reacting both C–OTf & C–Cl site) = 0: 100: 0. **^{1}H NMR** (400 MHz, $CDCl_3$) δ 7.22 (t, *J* = 8.2 Hz, 1H), 7.10 (d, *J* = 8.8 Hz, 2H), 6.92 (d, *J* = 8.9 Hz, 2H), 6.81 (dd, *J* = 8.3, 1.6 Hz, 1H), 6.73 (s, 1H), 6.67 (dd, *J* = 8.1, 1.9 Hz, 1H), 5.72 (s, 1H), 3.83 (s, 3H); **^{13}C NMR** (100 MHz, $CDCl_3$) δ 156.3, 150.6, 147.6, 133.6, 130.6, 123.7, 118.7 (q, *J* = 318.7 Hz, 1C), 114.8, 114.4, 110.8, 106.9, 55.5; **^{19}F NMR** (376 MHz, $CDCl_3$) δ -73.0; **HRMS** (APPI): calcd for $C_{14}H_{13}F_3NO_4S^+$: 348.0512, found 348.0519.

3-((4-Fluorophenyl)amino)-5-methylphenyl trifluoromethanesulfonate (Table 2.3, compound 3u)

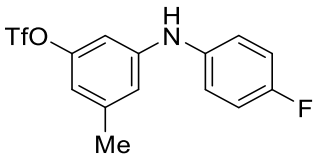

Yield: 85% (59.0 mg). Light-yellow liquid. Eluents (R_f = 0.6, Hexane: Ethyl acetate = 10:1) was used for flash column chromatography. The % conversion of starting material = 91%. The % of minor product (reacting C–OTf site): major product (reacting C–Cl site): diarylated product (reacting both C–OTf & C–Cl site) = 0: 100: 0. **^{1}H NMR** (400 MHz, $CDCl_3$) δ 7.10-7.01 (m, 4H), 6.70 (s, 1H), 6.62 (s, 1H), 6.57 (s, 1H), 5.70 (s, 1H), 2.31 (s, 3H); **^{13}C NMR** (100 MHz, $CDCl_3$) δ 158.9 (d, *J* = 240.9 Hz, 1C), 150.4, 146.1, 141.5, 137.1 (d, *J* = 2.6 Hz, 1C), 122.4 (d, *J* = 8.0 Hz, 1C), 118.7 (q, *J* = 318.6 Hz, 1C), 116.2 (d, *J* = 22.5 Hz, 1C), 115.9, 112.7, 105.2, 21.5; **^{19}F NMR** (376 MHz, $CDCl_3$) δ -119.5, -73.0; **HRMS** (EI): calcd for $C_{14}H_{11}F_4NO_4S^+$: 349.0390, found 349.0398.

3-((4-Fluorophenyl)amino)-2-methylphenyl trifluoromethanesulfonate (Table 2.3, compound 3v)

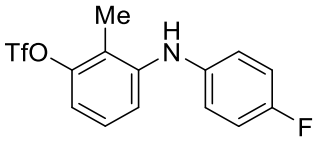

Yield: 81% (56.7 mg). Pale-yellow solid, m.p.= 45.0–46.2 °C. Eluents (R_f = 0.4, Hexane: Ethyl acetate = 10:1) was used for flash column chromatography. The % conversion of starting material = 100%. The % of minor product (reacting C–OTf site): major product (reacting C–Cl site): diarylated product (reacting both C–OTf & C–Cl site) = 0.03: 99.97: 0. **^{1}H NMR** (400 MHz, $CDCl_3$) δ 7.13 (t, *J* = 8.2 Hz, 1H), 7.03-7.02 (m, 5H), 6.84 (d, *J* = 8.2 Hz, 1H), 5.43 (s, 1H), 2.26 (s, 3H); **^{13}C NMR** (100 MHz, $CDCl_3$) δ 158.8 (d, *J* = 240.4 Hz, 1C), 149.0, 145.0, 138.03 (d, *J* = 2.6 Hz, 1C), 127.3,

122.3 (d, *J* = 7.9 Hz, 1C), 118.8, 118.6 (q, *J* = 318.2 Hz, 1C), 116.2 (d, *J* = 22.5 Hz, 1C), 115.1, 113.0, 10.9; **^{19}F NMR** (376 MHz, $CDCl_3$) δ -120.2, -73.7; **HRMS** (EI): calcd for $C_{14}H_{11}F_4NO_3S^+$: 349.0390, found 349.0394.

4-((4-Fluoro-2-methylphenyl)amino)phenyl trifluoromethanesulfonate (Table 2.3, compound 3w)

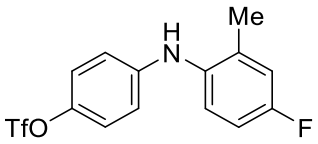

Yield: 92% (64.1 mg). Yellow liquid. Eluents (R_f = 0.5, Hexane: Ethyl acetate = 10:1) was used for flash column chromatography. The % conversion of starting material = 100%. The % of minor product (reacting C–OTf site): major product (reacting C–Cl site): diarylated product (reacting both C–OTf & C–Cl site) = 1.6: 98.4: 0. **^{1}H NMR** (400 MHz, $CDCl_3$) δ 7.18-7.15 (m, 1H), 7.09 (d, *J* = 9.0 Hz, 2H), 6.98 (dd, *J* = 9.2, 2.7 Hz, 1H), 6.90 (td, *J* = 8.4, 2.8 Hz, 1H), 6.72 (d, *J* = 9.0 Hz, 2H), 5.39 (s, 1H), 2.23 (s, 3H); **^{13}C NMR** (100 MHz, $CDCl_3$) δ 159.8 (d, *J* = 242.0 Hz, 1C), 145.6, 141.9, 135.3 (d, *J* = 2.7 Hz, 1C), 134.89 (d, *J* = 8.1 Hz, 1C), 125.25 (d, *J* = 8.6 Hz, 1C), 122.2, 118.7 (q, *J* = 319.1 Hz, 1C), 117.6 (d, *J* = 22.0 Hz, 1C), 115.3, 113.6 (d, *J* = 22.2 Hz, 1C), 18.0; **^{19}F NMR** (376 MHz, $CDCl_3$) δ -118.0, -72.7; **HRMS** (EI): calcd for $C_{14}H_{11}F_4NO_3S^+$: 349.0390, found 349.0394.

4-Methyl-3-((4-nitrophenyl)amino)phenyl trifluoromethanesulfonate (Table 2.3, compound 3x)

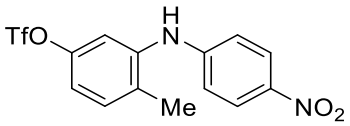

Yield: 78% (58.6 mg). Yellow liquid. Eluents (R_f = 0.4, Hexane: Ethyl acetate = 5:1) was used for flash column chromatography. The % conversion of starting material = 100%. The % of minor product (reacting C–OTf site): major product (reacting C–Cl site): diarylated product (reacting both C–OTf & C–Cl site) = 0: 100: 0. **^{1}H NMR** (400 MHz, $CDCl_3$) δ 8.13 (d, *J* = 9.1 Hz, 2H), 7.34 (d, *J* = 8.5 Hz, 1H), 7.23 (s, 1H), 7.02 (dd, *J* = 8.4, 2.3 Hz, 1H), 6.88 (d, *J* = 9.1 Hz, 2H), 6.22 (s, 1H), 2.29 (s, 3H); **^{13}C NMR** (100 MHz, $CDCl_3$) δ 149.5, 147.9, 140.4, 139.5, 132.6, 131.9, 126.2, 118.7 (q, *J* = 318.9 Hz, 1C), 117.4, 115.4, 114.3, 17.4; **^{19}F NMR** (376 MHz, $CDCl_3$) δ -72.8; **HRMS** (EI): calcd for $C_{14}H_{11}F_3N_2O_5S^+$: 376.0335, found 376.0325.

2-Methyl-3-((4-nitrophenyl)amino)phenyl trifluoromethanesulfonate (Table 2.3, compound 3y)

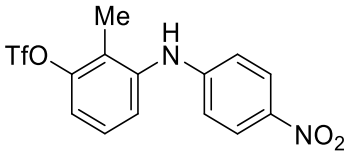

Yield: 84% (63.3 mg). Yellow solid, m.p.= 97.5–98.1 ^{o}C. Eluents (R_f = 0.4, Hexane: Ethyl acetate = 5:1) was used for flash column chromatography. The % conversion of starting material = 100%. The % of minor product (reacting C–OTf site): major product (reacting C–Cl site): diarylated product (reacting both C–OTf & C–Cl site) = 0: 100: 0. **^{1}H NMR** (400 MHz, $CDCl_3$) δ 8.11 (d, *J* = 9.2 Hz, 2H), 7.36-7.29 (m, 2H), 7.16 (d, *J* = 7.8 Hz, 1H), 6.80 (d, *J* = 9.2 Hz, 2H), 6.31 (s, 1H), 2.27 (s, 3H); **^{13}C NMR** (100 MHz, $CDCl_3$) δ 150.2, 149.1, 140.3, 140.1, 127.7, 126.23, 126.16, 123.6, 118.6 (q, *J* = 318.3

Hz, 1C), 118.4, 114.0, 11.6; **^{19}F NMR** (376 MHz, $CDCl_3$) δ -73.6; **HRMS** (EI): calcd for $C_{14}H_{11}F_3N_2O_5S^+$: 376.0335, found 376.0342.

3-((2-Methoxy-4-nitrophenyl)amino)phenyl trifluoromethanesulfonate (Table 2.3, compound 3z)

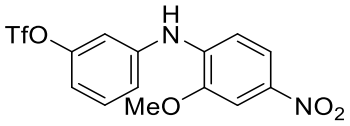

Yield: 78% (61.4 mg). Light-yellow solid, m.p.= 88.5–90.3 ºC. Eluents (R_f = 0.6, Hexane: Toluene = 10:1) was used for flash column chromatography. The % conversion of starting material = 100%. The % of minor product (reacting C–OTf site): major product (reacting C–Cl site): diarylated product (reacting both C–OTf & C–Cl site) = 0: 100: 0. **^{1}H NMR** (400 MHz, $CDCl_3$) δ 7.88 (dd, *J* = 8.9, 2.0 Hz, 1H), 7.76 (s, 1H), 7.45 (t, *J* = 8.2 Hz, 1H), 7.27-7.17 (m, 3H), 7.01 (d, *J* = 8.1 Hz, 1H), 6.84 (s, 1H), 4.02 (s, 3H); **^{13}C NMR** (100 MHz, $CDCl_3$) δ 150.2, 146.6, 141.7, 140.2, 138.6, 131.1, 120.4, 118.7 (q, *J* = 319.0 Hz, 1C), 118.5, 116.0, 113.5, 110.4, 105.8, 56.2; **^{19}F NMR** (376 MHz, $CDCl_3$) δ -72.8; **HRMS** (EI): calcd for $C_{14}H_{11}F_3N_2O_6S^+$: 392.0284, found 392.0295.

3-((2-Methoxy-4-nitrophenyl)amino)-2-methylphenyl trifluoromethanesulfonate (Table 2.3, compound 3aa)

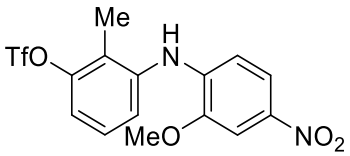

Yield: 72% (58.8 mg). Yellow solid, m.p.= 88.3–84.3 °C. Eluents (R_f = 0.8, Toluene = 100) was used for flash column chromatography. The % conversion of starting material = 100%. The % of minor product (reacting C–OTf site): major product (reacting C–Cl site): diarylated product (reacting both C–OTf & C–Cl site) = 0: 100: 0. **^{1}H NMR** (400 MHz, $CDCl_3$) δ 7.81 (dd, *J* = 8.9, 2.4 Hz, 1H), 7.75 (s, 1H), 7.38 (d, *J* = 7.8 Hz, 1H), 7.31 (t, *J* = 8.1 Hz, 1H), 7.14 (d, *J* = 8.1 Hz, 1H), 6.74 (d, *J* = 8.9 Hz, 1H), 6.53 (s, 1H), 4.03 (s, 3H), 2.28 (s, 3H); **^{13}C NMR** (100 MHz, $CDCl_3$) δ 149.1, 146.0, 140.2, 140.1, 139.5, 127.6, 126.1, 123.3, 118.7, 118.6 (q, *J* = 318.2 Hz, 1C), 118.1, 109.9, 105.6, 56.2, 11.6; **^{19}F NMR** (376 MHz, $CDCl_3$) δ -73.6; **HRMS** (EI): calcd for $C_{15}H_{11}F_6NO_3S^+$: 406.0441, found 406.0444.

4-((4-(Trifluoromethyl)phenyl)amino)phenyl trifluoromethanesulfonate (Table 2.3, compound 3ab and Table 2.7, compound 3bo)

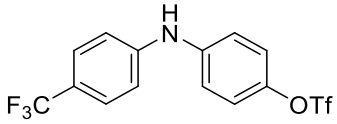

Yield (In Table 2.3, compound **3ab**): 91% (70.4 mg). Light-yellow solid, m.p.= 70.3–72.1 °C. **Yield** (In Table 2.7, compound **3bo**): 97% (74.7 mg). Eluents (R_f = 0.3, Hexane: Ethyl acetate = 10:1) was used for flash column chromatography. The % conversion of starting material = 92%. The % of minor product (reacting C–OTf site): major product (reacting C–Cl site): diarylated product (reacting both C–OTf & C–Cl site) = 0.26: 99.74: 0. **^{1}H NMR** (400 MHz, $CDCl_3$) δ 7.52 (d, *J* = 8.5 Hz, 2H), 7.21 (d, *J* = 9.1 Hz, 2H), 7.15 (d, *J* = 9.1 Hz, 2H), 7.10 (d, *J* = 8.5 Hz, 2H), 6.04 (s, 1H); **^{13}C NMR** (100 MHz, $CDCl_3$) δ 145.4, 143.9, 141.7, 126.8 (q, *J* = 3.8 Hz), 124.4 (q, *J* = 270.1 Hz, 1C),

123.1 (q, J = 32.1 Hz, 1C), 122.5, 119.7, 118.7 (q, J = 318.9 Hz, 1C), 116.6; **^{19}F NMR** (376 MHz, $CDCl_3$) δ -72.8, -61.7; **HRMS** (EI): calcd for $C_{14}H_9F_6NO_3S^+$: 385.0202, found 385.0203.

2-Methyl-3-((4-(trifluoromethyl)phenyl)amino)phenyl trifluoromethanesulfonate (Table 2.3, compound 3ac)

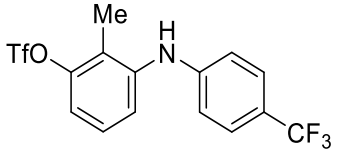

Yield: 90% (72.1 mg). Light-yellow liquid. Eluents (R_f = 0.7, Hexane: DCM = 2:1) was used for flash column chromatography. The % conversion of starting material = 100%. The % of minor product (reacting C–OTf site): major product (reacting C–Cl site): diarylated product (reacting both C–OTf & C–Cl site) = 0: 99: 1. **^{1}H NMR** (400 MHz, $CDCl_3$) δ 7.51 (d, J = 8.5 Hz, 2H), 7.31 (d, J = 8.0 Hz, 1H), 7.25 (t, J = 8.1 Hz, 1H), 7.05 (d, J = 8.1 Hz, 1H), 6.95 (d, J = 8.5 Hz, 2H), 5.72 (s, 1H), 2.28 (s, 3H); **^{13}C NMR** (100 MHz, $CDCl_3$) δ 149.2, 146.4, 142.0, 127.5, 126.78 (q, J = 3.8 Hz, 1C), 124.5 (q, J = 269.3 Hz, 1C), 123.6, 122.5 (q, J = 32.5 Hz, 1C), 120.5, 118.6 (q, J = 318.3 Hz, 1C), 116.3, 116.0, 11.4; **^{19}F NMR** (376 MHz, $CDCl_3$) δ -73.7, -61.6; **HRMS** (EI): calcd for $C_{15}H_{11}F_6NO_3S^+$: 399.0358, found 399.0352.

2-Methyl-3-((4-(trifluoromethyl)phenyl)amino)phenyl trifluoromethanesulfonate (Table 2.3, compound 3ad)

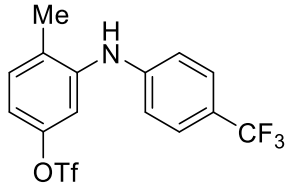

Yield: 90% (71.8 mg). White solid, m.p.= 96.1–98.3 °C. Eluents (R_f = 0.7, Hexane: DCM = 2:1) was used for flash column chromatography. The % conversion of starting material = 100%. The % of minor product (reacting C–OTf site): major product (reacting C–Cl site): diarylated product (reacting both C–OTf & C–Cl site) = 0: 97: 3. **^{1}H NMR** (400 MHz, $CDCl_3$) δ 7.54 (d, *J* = 8.5 Hz, 2H), 7.29 (d, *J* = 8.4 Hz, 1H), 7.20 (s, 1H), 7.03 (d, *J* = 8.5 Hz, 2H), 6.90 (dd, *J* = 8.4, 2.5 Hz, 1H), 5.72 (s, 1H), 2.29 (s, 3H); **^{13}C NMR** (100 MHz, $CDCl_3$) δ 148.2, 145.6, 141.3, 132.2, 129.0, 126.9 (q, *J* = 3.8 Hz, 1C), 124.4 (q, *J* = 269.3 Hz, 1C), 123.0 (q, *J* = 32.7 Hz, 1C), 118.7 (q, *J* = 318.9 Hz, 1C), 116.5, 115.0, 111.8, 17.4; **^{19}F NMR** (376 MHz, $CDCl_3$) δ -72.9, -61.6; **HRMS** (EI): calcd for $C_{15}H_{11}F_6NO_3S^+$: 399.0358, found 399.0362.

3-(Naphthalen-1-ylamino)phenyl trifluoromethanesulfonate (Table 2.3, compound 3ae)

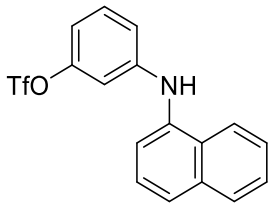

Yield: 82% (64.4 mg). Light-yellow liquid. Eluents (R_f = 0.2, Hexane: Ethyl acetate = 10:1) was used for flash column chromatography. The % conversion of starting material = 100%. The % of minor product (reacting C–OTf site): major product (reacting C–Cl site): diarylated product (reacting both C–OTf & C–Cl site) = 0: 100: 0. **^{1}H NMR** (400 MHz, $CDCl_3$) δ 7.98 (d, *J* = 8.2 Hz, 1H), 7.93 (d, *J* = 7.6 Hz, 1H), 7.72 (d, *J* = 8.0 Hz, 1H), 7.58-7.41 (m, 4H), 7.25 (t, *J* = 8.2 Hz, 1H), 6.85 (dd, *J* = 8.2, 1.8 Hz, 1H), 6.79-6.74 (m, 2H), 6.02 (s, 1H); **^{13}C NMR** (100 MHz, $CDCl_3$) δ 150.5, 147.5, 136.7, 134.7,

130.6, 128.6, 126.4, 126.2, 125.9, 125.0, 121.9, 118.9, 118.7 (q, *J* = 318.9 Hz, 1C), 115.4, 111.6, 108.2; **^{19}F NMR** (376 MHz, $CDCl_3$) δ -72.9; **HRMS** (APPI): calcd for $C_{17}H_{13}F_3NO_3S^+$: 368.0563, found 368.0566.

2-Methyl-3-((2-phenoxyphenyl)amino)phenyl trifluoromethanesulfonate (Table 2.3, compound 3af)

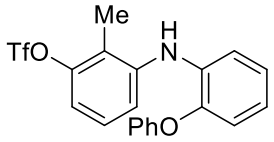

Yield: 81% (68.5 mg). White solid, m.p.= 60.5–63.2 °C. Eluents (R_f = 0.6, Hexane: Ethyl acetate = 10:1) was used for flash column chromatography. The % conversion of starting material = 92%. The % of minor product (reacting C–OTf site): major product (reacting C–Cl site): diarylated product (reacting both C–OTf & C–Cl site) = 0: 100: 0. **^{1}H NMR** (400 MHz, $CDCl_3$) δ 7.38-7.32 (m, 3H), 7.23-7.08 (m, 4H), 7.04-7.00 (m, 3H), 6.96-6.91 (m, 2H), 5.87 (s, 1H), 2.18 (s, 3H); **^{13}C NMR** (100 MHz, $CDCl_3$) δ 157.0, 149.0, 145.5, 143.0, 134.8, 129.8, 127.1, 124.4, 123.3, 121.8, 121.4, 120.0, 118.6 (q, *J* = 318.3 Hz, 1C), 118.2, 117.6, 117.4, 114.6, 11.0; **^{19}F NMR** (376 MHz, $CDCl_3$) δ -73.7; **HRMS** (EI): calcd for $C_{20}H_{16}F_3NO_4S^+$: 423.0747, found 423.0753.

3-(Quinolin-6-ylamino)phenyl trifluoromethanesulfonate (Table 2.4, compound 3ag)

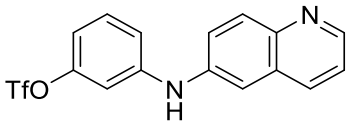

Yield: 76% (56.0 mg). Light-yellow solid, m.p.= 136.7–137.9 °C. Eluents (R_f = 0.2, Hexane: Ethyl acetate = 4:1) was used for flash column chromatography. The %

conversion of starting material = 100%. The % of minor product (reacting C–OTf site): major product (reacting C–Cl site): diarylated product (reacting both C–OTf & C–Cl site) = 0: 100: 0. **^{1}H NMR** (400 MHz, $CDCl_3$) δ 8.76 (s, 1H), 8.02-7.97 (m, 2H), 7.45-7.30 (m, 4H), 7.16-7.09 (m, 2H), 6.93 (s, 1H), 6.83 (d, *J* = 7.8 Hz, 1H); **^{13}C NMR** (100 MHz, $CDCl_3$) δ 150.4, 148.3, 144.74, 144.66, 139.9, 134.8, 130.9, 130.7, 129.3, 123.7, 121.7, 118.7 (q, *J* = 318.7 Hz, 1C), 117.1, 113.1, 111.7, 110.0; **^{19}F NMR** (376 MHz, $CDCl_3$) δ -72.8; **HRMS** (APPI): calcd for $C_{16}H_{12}F_3N_2O_3S^+$: 369.0515, found 369.0512.

3-((2,6-Dimethylpyridin-3-yl)amino)phenyl trifluoromethanesulfonate (Table 2.4, compound 3ah)

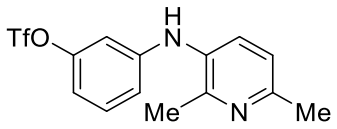

Yield: 88% (60.8 mg). Yellow liquid. Eluents (R_f = 0.3, Hexane: Ethyl acetate = 5:1) was used for flash column chromatography. The % conversion of starting material = 100%. The % of minor product (reacting C–OTf site): major product (reacting C–Cl site): diarylated product (reacting both C–OTf & C–Cl site) = 0: 100: 0. **^{1}H NMR** (400 MHz, $CDCl_3$) δ 7.41 (d, *J* = 8.1 Hz, 1H), 7.22 (t, *J* = 8.2 Hz, 1H), 6.99 (d, *J* = 8.1 Hz, 1H), 6.74 (dd, *J* = 8.2, 2.0 Hz, 1H), 6.69 (dd, *J* = 8.2, 2.2 Hz, 1H), 6.63 (s, 1H), 5.83 (s, 1H), 2.50 (s, 3H), 2.43 (s, 3H); **^{13}C NMR** (100 MHz, $CDCl_3$) δ 153.6, 151.7, 150.5, 146.6, 132.7, 130.7, 130.4, 121.4, 118.6 (q, *J* = 318.7 Hz, 1C), 115.0, 111.6, 107.8, 23.7, 20.6; **^{19}F NMR** (376 MHz, $CDCl_3$) δ -73.0; **HRMS** (APPI): calcd for $C_{14}H_{14}F_3N_2O_3S^+$: 347.0672, found 347.0678.

3-(3,4-Dihydroquinolin-1(2H)-yl)phenyl trifluoromethanesulfonate (Table 2.4, compound 3ai)

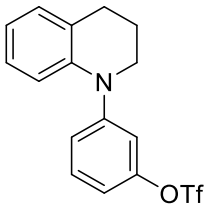

Yield: 79% (56.7 mg). Yellow liquid. Eluents (R_f = 0.5, Hexane: DCM = 10:1) was used for flash column chromatography. The % conversion of starting material = 100%. The % of minor product (reacting C–OTf site): major product (reacting C–Cl site): diarylated product (reacting both C–OTf & C–Cl site) = 0: 100: 0. **^{1}H NMR** (400 MHz, $CDCl_3$) δ 7.35 (t, *J* = 8.2 Hz, 1H), 7.23 (d, *J* = 8.3 Hz, 1H), 7.12-7.11 (m, 2H), 7.06-6.99 (m, 2H), 6.90-6.84 (m, 2H), 3.65 (t, *J* = 5.9 Hz, 2H), 2.83 (t, *J* = 6.4 Hz, 2H), 2.08-2.02 (m, 2H); **^{13}C NMR** (100 MHz, $CDCl_3$) δ 150.2, 150.1, 142.4, 130.4, 129.4, 127.3, 126.4, 121.5, 120.6, 118.7 (q, *J* = 319.1 Hz, 1C), 117.6, 114.6, 114.2, 49.9, 27.4, 23.1; **^{19}F NMR** (466 MHz, $CDCl_3$) δ -72.8; **HRMS** (APPI): calcd for $C_{16}H_{15}F_3NO_3S^+$: 358.0719, found 358.0712.

4-(3,4-dihydroquinolin-1(2H)-yl)-2-(trifluoromethyl)phenyl trifluoromethanesulfonate (Table 2.4, compound 3aj)

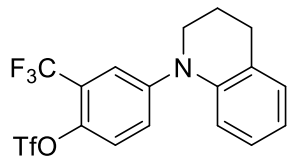

Yield: 66% (56.0 mg). Red liquid. Eluents (R_f= 0.6, Hexane: Ethyl acetate = 10:1) was used for flash column chromatography. The % conversion of starting material = 95%. The % of minor product (reacting C–OTf site): major product (reacting C–Cl site):

diarylated product (reacting both C–OTf & C–Cl site) = 100: 0: 0. **^{1}H NMR** (400 MHz, $CDCl_3$) δ 7.51 (d, *J* = 2.7 Hz, 1H), 7.41 (dd, *J* = 9.1, 2.7 Hz, 1H), 7.35 (d, *J* = 9.1 Hz, 1H), 7.14 (d, *J* = 7.5 Hz, 1H), 7.07 (t, *J* = 7.6 Hz, 1H), 7.01 (d, *J* = 7.5 Hz, 1H), 6.91 (t, *J* = 7.2 Hz, 1H), 3.66 (t, *J* = 6.0 Hz, 2H), 2.82 (t, *J* = 6.4 Hz, 2H), 2.10- 2.01 (m, 2H); **^{13}C NMR** (100 MHz, $CDCl_3$) δ 148.1, 141.7, 139.1, 129.6, 128.4, 126.6, 124.9, 123.9 (q, *J* = 32.2 Hz, 1C), 123.3, 122.0 (q, *J* = 271.5 Hz, 1C), 121.5, 119.5 (q, *J* = 4.8 Hz, 1C), 118.4 (q, *J* = 318.4 Hz, 1C), 118.0, 49.8, 27.3, 23.3; **^{19}F NMR** (565 MHz, $CDCl_3$) δ -60.9, -73.7; **HRMS** (EI): calcd for $C_{17}H_{13}F_6NO_3S^+$: 425.0515, found 425.0525.

4-(1*H*-Indol-1-yl)phenyl trifluoromethanesulfonate (Table 2.4, compound 3ak)

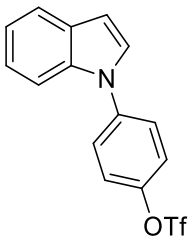

Yield: 75% (51.2 mg). White liquid. Eluents (R_f = 0.4, Hexane: Ethyl acetate = 20:1) was used for flash column chromatography. The % conversion of starting material = 95%. The % of minor product (reacting C–OTf site): major product (reacting C–Cl site): diarylated product (reacting both C–OTf & C–Cl site) = 0: 100: 0. **^{1}H NMR** (400 MHz, $CDCl_3$) δ 7.74 (d, *J* = 7.6 Hz, 1H), 7.61-7.56 (m, 3H), 7.45 (d, *J* = 8.8 Hz, 2H), 7.32-7.23 (m, 3H), 6.76 (d, *J* = 3.3 Hz, 1H); **^{13}C NMR** (100 MHz, $CDCl_3$) δ 147.1, 139.8, 135.6, 129.5, 127.5, 125.5, 122.9, 122.7, 121.4, 120.9, 118.8 (q, *J* = 318.9 Hz, 1C), 110.1, 104.7; **^{19}F NMR** (466 MHz, $CDCl_3$) δ -72.5; **HRMS** (APPI): calcd for $C_{15}H_{11}F_3NO_3S^+$: 342.0406, found 342.0410.

3-(3-Methyl-1*H*-indol-1-yl)phenyl trifluoromethanesulfonate (Table 2.4, compound 3al)

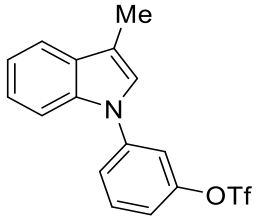

Yield: 90% (63.9 mg). White liquid. Eluents (R_f = 0.4, Hexane: Ethyl acetate = 20:1) was used for flash column chromatography. The % conversion of starting material = 100%. The % of minor product (reacting C–OTf site): major product (reacting C–Cl site): diarylated product (reacting both C–OTf & C–Cl site) = 0: 100: 0. **^{1}H NMR** (400 MHz, $CDCl_3$) δ 7.70 (d, *J* = 7.7 Hz, 1H), 7.63-7.54 (m, 3H), 7.49 (s, 1H), 7.35-7.23 (m, 3H), 7.16 (s, 1H), 2.44 (s, 3H); **^{13}C NMR** (100 MHz, $CDCl_3$) δ 150.0, 141.7, 135.6, 131.1, 130.2, 124.7, 123.2, 123.1, 120.6, 119.5, 118.8 (q, *J* = 317.6 Hz, 1C), 118.1, 116.6, 114.4, 110.0, 9.5; **^{19}F NMR** (466 MHz, $CDCl_3$) δ -72.5; **HRMS** (APPI): calcd for $C_{16}H_{13}F_3NO_3S^+$: 356.0563, found 365.0556.

4-(5-Methyl-1*H*-indol-1-yl)phenyl trifluoromethanesulfonate (Table 2.4, compound 3am)

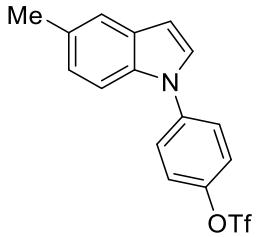

Yield: 89% (63.4 mg). Light-yellow liquid. Eluents (R_f = 0.6, Hexane: Ethyl acetate = 10:1) was used for flash column chromatography. The % conversion of starting material = 94%. The % of minor product (reacting C–OTf site): major product (reacting C–Cl

site): diarylated product (reacting both C–OTf & C–Cl site) = 0: 100: 0. **^{1}H NMR** (400 MHz, $CDCl_3$) δ 7.59-7.42 (m, 6H), 7.28 (d, *J* = 3.3 Hz, 1H), 7.13 (d, *J* = 8.5, 1H), 6.67 (d, *J* = 3.2 Hz, 1H), 2.52 (s, 3H); **^{13}C NMR** (100 MHz, $CDCl_3$) δ 146.9, 139.9, 133.9, 130.3, 129.83, 127.4, 125.2, 124.4, 122.7, 121.0, 118.8 (q, *J* = 318.8 Hz, 1C), 109.8, 104.3, 21.3; **^{19}F NMR** (376 MHz, $CDCl_3$) δ -72.7; **HRMS** (APPI): calcd for $C_{16}H_{13}F_3NO_3S^+$: 356.0563, found 356.0557.

4-(5-Methoxy-1*H*-indol-1-yl)phenyl trifluoromethanesulfonate (Table 2.4, compound 3an)

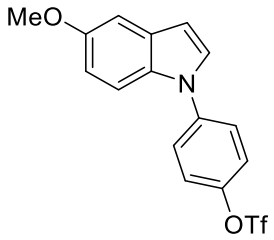

Yield: 81% (60.4 mg). Light-yellow solid, m.p.= 62.2–64.8 °C. Eluents (R_f = 0.6, Hexane: Ethyl acetate = 5:1) was used for flash column chromatography. The % conversion of starting material = 95%. The % of minor product (reacting C–OTf site): major product (reacting C–Cl site): diarylated product (reacting both C–OTf & C–Cl site) = 0.3: 99.7: 0. **^{1}H NMR** (400 MHz, $CDCl_3$) δ 7.57-7.53 (m, 2H), 7.45 (d, *J* = 8.9 Hz, 1H), 7.44-7.40 (m, 2H), 7.28 (d, *J* = 3.3 Hz, 1H), 7.16 (d, *J* = 2.4 Hz, 1H), 6.93 (dd, *J* = 9.0, 2.5 Hz, 1H), 6.66 (d, *J* = 3.2 Hz, 1H), 3.89 (s, 3H); **^{13}C NMR** (100 MHz, $CDCl_3$) δ 154.8, 146.9, 139.9, 130.7, 130.2, 127.9, 125.1, 122.7, 118.7 (q, *J* = 318.9 Hz, 1C), 112.9, 110.9, 104.4, 102.9, 55.7; **^{19}F NMR** (376 MHz, $CDCl_3$) δ -72.7; **HRMS** (APPI): calcd for $C_{16}H_{13}F_3NO_4S^+$: 372.0512, found 372.0513.

4-(5-Fluoro-1*H*-indol-1-yl)phenyl trifluoromethanesulfonate (Table 2.4, compound 3ao)

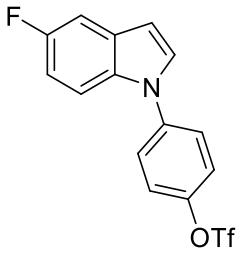

Yield: 84% (60.0 mg). Light-yellow solid, m.p.= 69.8–71.6 ºC. Eluents (R_f = 0.6, Hexane: Ethyl acetate = 10:1) was used for flash column chromatography. The % conversion of starting material = 97%. The % of minor product (reacting C–OTf site): major product (reacting C–Cl site): diarylated product (reacting both C–OTf & C–Cl site) = 0.2: 99.8: 0. **^{1}H NMR** (400 MHz, $CDCl_3$) δ 7.58-7.54 (m, 2H), 7.47-7.43 (m, 3H), 7.36-7.33 (m, 2H), 7.00 (td, *J* = 9.0, 2.5 Hz, 1H), 6.69 (d, *J* = 3.2 Hz, 1H); **^{13}C NMR** (100 MHz, $CDCl_3$) δ 158.3 (d, *J* = 234.9 Hz, 1C), 147.3, 139.6, 132.2, 130.0 (d, *J* = 10.2 Hz, 1C), 129.0, 125.5, 122.8, 118.7 (q, *J* = 318.9 Hz, 1C), 111.2 (d, *J* = 26.1 Hz, 1C), 110.9 (d, *J* = 9.5 Hz, 1C), 106.2 (d, *J* = 23.3 Hz, 1C), 104.5 (d, *J* = 4.5 Hz, 1C); **^{19}F NMR** (376 MHz, $CDCl_3$) δ-123.3, -72.7; **HRMS** (EI): calcd for $C_{15}H_9F_4NO_3S^+$: 359.0234, found 359.0233.

4-(2,3-Dihydrocyclopenta[*b*]indol-4(1*H*)-yl)phenyl trifluoromethanesulfonate (Table 2.4, compound 3ap)

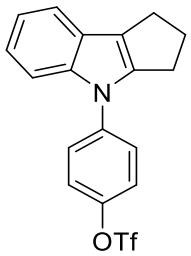

Yield: 79% (60.0 mg). White solid, m.p.= 89.3–90.2 ^{o}C. Eluents (R_f = 0.7, Hexane: Ethyl acetate = 10:1) was used for flash column chromatography. The % conversion of starting material = 87%. The % of minor product (reacting C–OTf site): major product (reacting C–Cl site): diarylated product (reacting both C–OTf & C–Cl site) = 0.8: 99.2: 0. **^{1}H NMR** (400 MHz, $CDCl_3$) δ 7.56-7.51 (m, 3H), 7.47-7.41 (m, 3H), 7.23-7.17 (m, 2H), 2.97-2.90 (m, 4H), 2.64-2.57 (m, 2H); **^{13}C NMR** (100 MHz, $CDCl_3$) δ 146.8, 145.1, 140.6, 139.0, 125.8, 125.3, 122.5, 121.6, 121.4, 120.7, 118.9, 118.7 (q, *J* = 318.8 Hz, 1C), 110.4, 28.2, 26.3, 24.5; **^{19}F NMR** (376 MHz, $CDCl_3$) δ -72.7; **HRMS** (APPI): calcd for $C_{18}H_{15}F_3NO_3S^+$: 382.0719, found 382.0724.

4-(10*H*-Phenoxazin-10-yl)phenyl trifluoromethanesulfonate (Table 2.4, compound 3aq)

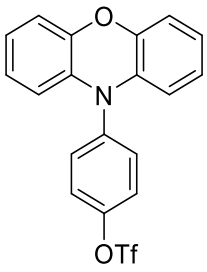

Yield: 91% (74.1 mg). Light-yellow solid, m.p.= 126.5–128.7 ^{o}C. Eluents (R_f = 0.7, Hexane: Ethyl acetate = 10:1) was used for flash column chromatography. The % conversion of starting material = 100%. The % of minor product (reacting C–OTf site): major product (reacting C–Cl site): diarylated product (reacting both C–OTf & C–Cl site) = 0: 100: 0. **^{1}H NMR** (400 MHz, $CDCl_3$) δ 7.54-7.46 (m, 4H), 6.74-6.61 (m, 6H), 5.88 (d, *J* = 7.8 Hz, 2H); **^{13}C NMR** (100 MHz, $CDCl_3$) δ148.8, 143.9, 139.2, 133.7, 133.2, 124.2, 123.3, 121.9, 118.7 (q, *J* = 318.9 Hz, 1C), 115.7, 113.1; **^{19}F NMR** (376

MHz, $CDCl_3$) δ -72.7; **HRMS** (EI): calcd for $C_{19}H_{12}F_3NO_4S^+$: 407.0434, found 407.0431.

4-(Quinolin-2-ylamino)phenyl trifluoromethanesulfonate (Table 2.4, compound 3ar)

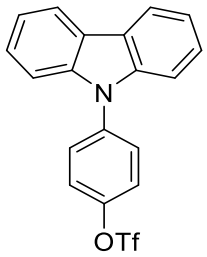

Yield: 73% (57.0 mg). Yellow solid, m.p.= 112.3–114.8 ^oC. Eluents (R_f = 0.7, Hexane: Ethyl acetate = 10:1) was used for flash column chromatography. The % conversion of starting material = 90%. The % of minor product (reacting C–OTf site): major product (reacting C–Cl site): diarylated product (reacting both C–OTf & C–Cl site) = 0.2: 99.8: 0. **^{1}H NMR** (400 MHz, $CDCl_3$) δ 8.18 (d, *J* = 7.8 Hz, 2H), 7.68 (d, *J* = 9.0 Hz, 2H), 7.54 (d, *J* = 8.9 Hz, 2H), 7.49-7.42 (m, 4H), 7.36 (t, *J* = 7.3 Hz, 2H); **^{13}C NMR** (100 MHz, $CDCl_3$) δ 147.8, 140.4, 137.9, 128.6, 126.2, 123.6, 123.0, 120.53, 120.45, 118.8 (q, *J* = 318.9 Hz, 1C), 109.4; **^{19}F NMR** (376 MHz, $CDCl_3$) δ -72.6; **HRMS** (EI): calcd for $C_{19}H_{12}F_3NO_3S^+$: 391.0485, found 391.0485.

4-(5*H*-Dibenzo[*b*,*f*]azepin-5-yl)phenyl trifluoromethanesulfonate (Table 2.4, compound 3as)

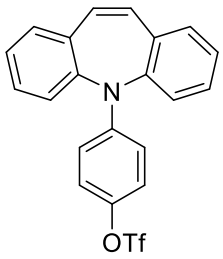

Yield: 81% (67.3 mg). White solid, m.p.= 112.8–115.0 ^{o}C. Eluents (R_f = 0.6, Hexane: Ethyl acetate = 10:1) was used for flash column chromatography. The % conversion of starting material = 94%. The % of minor product (reacting C–OTf site): major product (reacting C–Cl site): diarylated product (reacting both C–OTf & C–Cl site) = 2.3: 97.7: 0. **^{1}H NMR** (400 MHz, $CDCl_3$) δ 7.56-7.48 (m, 6H), 7.42-7.39 (m, 2H), 6.93-6.87 (m, 4H), 6.30 (d, *J* = 9.2 Hz, 2H); **^{13}C NMR** (100 MHz, $CDCl_3$) δ 148.6, 142.2, 141.4, 136.0, 130.55, 130.45, 129.98, 129.95, 127.5, 121.2, 118.7 (q, *J* = 319.0 Hz, 1C), 112.4; **^{19}F NMR** (376 MHz, $CDCl_3$) δ -72.8; **HRMS** (EI): calcd for $C_{21}H_{14}F_3NO_3S^+$: 417.0641, found 417.0648.

4-Morpholinophenyl trifluoromethanesulfonate (Table 2.4, compound 3at)

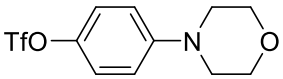

Yield: 85% (53.0 mg). Light-yellow liquid. Eluents (R_f = 0.2, Hexane: Ethyl acetate = 10:1) was used for flash column chromatography. The % conversion of starting material = 100%. The % of minor product (reacting C–OTf site): major product (reacting C–Cl site): diarylated product (reacting both C–OTf & C–Cl site) = 0: 100: 0. **^{1}H NMR** (400 MHz, $CDCl_3$) δ 7.16 (d, *J* = 9.2 Hz, 2H), 6.89 (d, *J* = 9.2 Hz, 2H), 3.85 (t, *J* = 4.8 Hz, 4H), 3.16 (t, *J* = 4.8 Hz, 4H); **^{13}C NMR** (100 MHz, $CDCl_3$) δ 150.9, 142.3, 121.9, 118.7

(q, *J* = 319.1 Hz, 1C), 116.0, 66.6, 48.8; **^{19}F NMR** (376 MHz, $CDCl_3$) δ -72.8; **HRMS** (APPI): calcd for $C_{11}H_{13}F_3NO_4S^+$: 312.0512, found 312.0517.

4-(4-Methylpiperazin-1-yl)phenyl trifluoromethanesulfonate (Table 2.4, compound 3au)

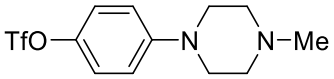

Yield: 88% (57.2 mg). Light-yellow liquid. Eluents (R_f = 0.2, DCM: MeOH = 10:1) was used for flash column chromatography. The % conversion of starting material = 100%. The % of minor product (reacting C–OTf site): major product (reacting C–Cl site): diarylated product (reacting both C–OTf & C–Cl site) = 2.0: 98.0: 0. **^{1}H NMR** (400 MHz, $CDCl_3$) δ 7.12 (d, *J* = 9.0 Hz, 2H), 6.88 (d, *J* = 9.0 Hz, 2H), 3.20 (dd, *J* = 4.3, 4.2 Hz, 4H), 2.55 (dd, *J* = 4.3, 4.2 Hz, 4H), 2.33 (s, 3H); **^{13}C NMR** (100 MHz, $CDCl_3$) δ 150.8, 142.0, 121.8, 118.7 (q, *J* = 318.8 Hz, 1C), 116.3, 54.8, 48.6, 46.0; **^{19}F NMR** (376 MHz, $CDCl_3$) δ -72.9; **HRMS** (APPI): calcd for $C_{12}H_{16}F_3N_2O_3S^+$: 325.0828, found 325.0821.

4-(4-Methylpiperidin-1-yl)phenyl trifluoromethanesulfonate (Table 2.4, compound 3av)

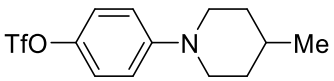

Yield: 74% (47.8 mg). Light-yellow liquid. Eluents (R_f = 0.6, Hexane: Ethyl acetate = 10:1) was used for flash column chromatography. The % conversion of starting material = 96%. The % of minor product (reacting C–OTf site): major product (reacting C–Cl site): diarylated product (reacting both C–OTf & C–Cl site) = 5.6: 94.4: 0. **^{1}H NMR**

(400 MHz, $CDCl_3$) δ 7.11 (d, *J* = 9.2 Hz, 2H), 6.89 (d, *J* = 9.3 Hz, 2H), 3.70-3.60 (m, 2H), 2.73 (td, *J* = 12.3, 2.5 Hz, 2H), 1.80-1.70 (m, 2H), 1.61-1.48 (m, 1H), 1.37-1.27 (m, 2H), 0.98 (d, *J* = 6.5 Hz, 3H); **^{13}C NMR** (100 MHz, $CDCl_3$) δ 151.4, 141.6, 121.7, 118.8 (q, *J* = 319.0 Hz, 1C), 116.5, 49.4, 33.8, 30.5, 21.7; **^{19}F NMR** (376 MHz, $CDCl_3$) δ -72.9; **HRMS** (EI): calcd for $C_{13}H_{16}F_3NO_4S^+$: 323.0798, found 323.0793.

6-(Methyl(phenyl)amino)pyridin-3-yl trifluoromethanesulfonate (Table 2.5, compound 3aw)

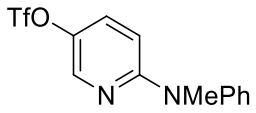

Yield: 79% (52.3 mg). Light-yellow solid. Eluents (R_f = 0.5, Hexane: Toluene = 1:1) was used for flash column chromatography. The % conversion of starting material = 100%. The % of minor product (reacting C–OTf site): major product (reacting C–Cl site): diarylated product (reacting both C–OTf & C–Cl site) = 100: 0: 0. **^{1}H NMR** (400 MHz, $CDCl_3$) δ 8.13 (d, *J* = 2.9 Hz, 1H), 7.42 (t, *J* = 7.8 Hz, 2H), 7.28- 7.23 (m, 3H), 7.17 (dd, *J* = 9.4, 3.0 Hz, 1H), 6.43 (d, *J* = 9.4 Hz, 1H), 3.45 (s, 3H); **^{13}C NMR** (100 MHz, $CDCl_3$) δ 157.9, 145.9, 140.2, 138.9, 130.1, 129.9, 126.7, 126.6, 118.7 (q, *J* = 319.2 Hz, 1C), 108.9, 38.8; **^{19}F NMR** (565 MHz, $CDCl_3$) δ -72.5; **HRMS** (EI): calcd for $C_{13}H_{11}F_3N_2O_3S^+$: 332.0437, found 332.0440.

6-(Methyl(p-tolyl)amino)pyridin-3-yl trifluoromethanesulfonate (Table 2.5, compound 3ax)

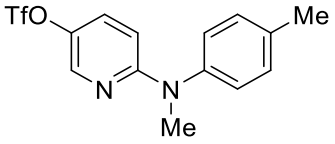

Yield: 85% (58.6 mg). Light-yellow liquid. Eluents (R_f = 0.5, Hexane: Ethyl acetate = 10:1) was used for flash column chromatography. The % conversion of starting material = 100%. The % of minor product (reacting C–OTf site): major product (reacting C–Cl site): diarylated product (reacting both C–OTf & C–Cl site) = 100: 0: 0. **^{1}H NMR** (400 MHz, $CDCl_3$) δ 8.14 (d, *J* = 2.9 Hz, 1H), 7.24 (d, *J* = 8.2 Hz, 2H), 7.17 (dd, *J* = 9.4, 3.0 Hz, 1H), 7.13 (d, *J* = 8.2 Hz, 2H), 6.41 (d, *J* = 9.4 Hz, 1H), 3.44 (s, 3H), 2.38 (s, 3H); **^{13}C NMR** (100 MHz, $CDCl_3$) δ 158.0, 143.2, 140.2, 138.7, 136.5, 130.7, 129.8, 126.6, 118.7 (q, *J* = 319.2 Hz, 1C), 108.7, 38.8, 21.0; **^{19}F NMR** (565 MHz, $CDCl_3$) δ -72.8; HRMS (EI): calcd for $C_{14}H_{13}F_3N_2O_3S^+$: 346.0593, found 346.0599.

6-(Methyl(4-(trifluoromethyl)phenyl)amino)pyridin-3-yl trifluoromethanesulfonate (Table 2.5, compound 3ay)

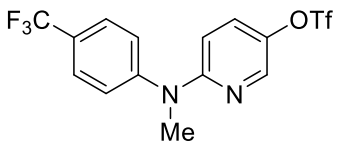

Yield: 71% (56.8 mg). Light-yellow liquid. Eluents (R_f = 0.3, Hexane: Ethyl acetate = 10:1) was used for flash column chromatography. The % conversion of starting material = 91%. The % of minor product (reacting C–OTf site): major product (reacting C–Cl site): diarylated product (reacting both C–OTf & C–Cl site) = 100: 0: 0. **^{1}H NMR** (400 MHz, $CDCl_3$) δ 8.19 (d, *J* = 2.9 Hz, 1H), 7.67 (d, *J* = 8.4 Hz, 2H), 7.39 (d, *J* = 8.4 Hz, 2H), 7.30 (dd, *J* = 9.3, 3.0 Hz, 1H), 6.66 (d, *J* = 9.3 Hz, 1H), 3.51 (s, 3H); **^{13}C NMR** (100 MHz, $CDCl_3$) δ 157.2, 149.1, 140.6, 139.6, 130.4, 127.6 (q, *J* = 33.1 Hz, 1C), 127.0 (q, *J* = 3.7 Hz, 1C), 125.7, 123.9 (q, *J* = 270.0 Hz, 1C), 118.7 (q, *J* = 319.q Hz, 1C), 109.6, 38.7; **^{19}F NMR** (565 MHz, $CDCl_3$) δ -62.3, -72.5; **HRMS** (EI): calcd for

$C_{14}H_{10}F_6N_2O_3S^+$: 400.0311, found 400.0319.

6-Morpholinopyridin-3-yl trifluoromethanesulfonate (Table 2.5, compound 3az)

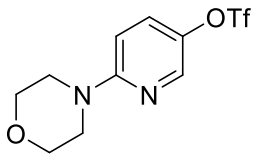

Yield: 80% (49.6 mg). Light-yellow solid, m.p.= 45.0–47.2 ºC. Eluents (R_f = 0.4, Hexane: Ethyl acetate = 5:1) was used for flash column chromatography. The % conversion of starting material = 100%. The % of minor product (reacting C–OTf site): major product (reacting C–Cl site): diarylated product (reacting both C–OTf & C–Cl site) = 100: 0: 0. **^{1}H NMR** (600 MHz, $CDCl_3$) δ 8.12 (d, *J* = 3.5 Hz, 1H), 7.40 (dd, *J* = 9.7, 3.3 Hz, 1H), 6.61 (d, *J* = 9.7 Hz, 1H), 3.81-3.79 (m, 4H), 3.53-3.51 (m, 4H); **^{13}C NMR** (150 MHz, $CDCl_3$) δ 158.3, 140.5, 139.0, 130.7, 118.7 (q, *J* = 319.1 Hz, 1C), 106.7, 66.5, 45.3; **^{19}F NMR** (565 MHz, $CDCl_3$) δ -72.8; **HRMS** (EI): calcd for $C_{10}H_{11}F_2N_2O_4S^+$: 312.0386, found 312.0387.

2-(4-Methylpiperazin-1-yl)quinolin-6-yl trifluoromethanesulfonate (Table 2.5, compound 3ba)

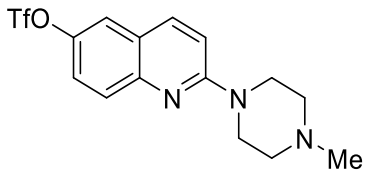

Yield: 90% (67.7 mg). Light-yellow solid, m.p.= 132.3–134.4 ºC. Eluents (R_f = 0.5, DCM: MeOH = 10:1) was used for flash column chromatography. The % conversion of starting material = 98%. The % of minor product (reacting C–OTf site): major product (reacting C–Cl site): diarylated product (reacting both C–OTf & C–Cl site) =

100: 0: 0. **^{1}H NMR** (400 MHz, $CDCl_3$) δ 7.83 (d, *J* = 9.2 Hz, 1H), 7.69 (d, *J* = 9.2 Hz, 1H), 7.47 (d, *J* = 2.3 Hz, 1H), 7.37 (dd, *J* = 9.1, 2.4 Hz, 1H), 7.01 (d, *J* = 9.2 Hz, 1H), 3.77-3.75 (m, 4H), 2.53-2.51 (m, 4H), 2.34 (s, 3H); **^{13}C NMR** (100 MHz, $CDCl_3$) δ 157.7, 147.0, 143.9, 137.0, 128.6, 122.6, 122.5, 118.72 (q, *J* = 319.1 Hz, 1C), 118.65, 110.8, 54.8, 46.1, 44.8; **^{19}F NMR** (565 MHz, $CDCl_3$) δ -73.3; **HRMS** (EI): calcd for $C_{15}H_{16}F_3N_3O_3S^+$: 375.0864, found 375.0865.

2-(1H-indol-1-yl)quinolin-6-yl trifluoromethanesulfonate (Table 2.5, compound 3ba)

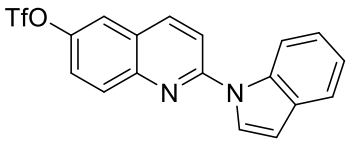

Yield: 86% (67.7 mg). Light-yellow solid, m.p.= 148.6–150.4 ºC. Eluents (R_f = 0.5, Hexane: Toluene = 2:1) was used for flash column chromatography. The % conversion of starting material = 100%. The % of minor product (reacting C–OTf site): major product (reacting C–Cl site): diarylated product (reacting both C–OTf & C–Cl site) = 100: 0: 0. **^{1}H NMR** (400 MHz, $CDCl_3$) δ 8.65 (d, *J* = 8.3 Hz, 1H), 8.10 (t, *J* = 8.6 Hz, 2H), 7.74 (d, *J* = 3.5 Hz, 1H), 7.70-7.67 (m, 2H), 7.60-7.57 (m, 2H), 7.39 (t, *J* = 7.5 Hz, 1H), 7.30 (t, *J* = 7.5 Hz, 1H), 6.76 (d, *J* = 3.5 Hz, 1H); **^{13}C NMR** (100 MHz, $CDCl_3$) δ 152.0, 146.1, 146.0, 138.4, 135.3, 130.8, 130.7, 125.4, 125.2, 123.7, 123.6, 122.1, 121.1, 119.0, 118.8 (q, *J* = 319.1 Hz, 1C), 114.8, 114.6, 107.0; **^{19}F NMR** (565 MHz, $CDCl_3$) δ -73.3; **HRMS** (EI): calcd for $C_{18}H_{11}F_3N_2O_3S^+$: 392.0437, found 392.0438.

2-(Phenylamino)pyridin-4-yl trifluoromethanesulfonate (Table 2.5, compound

3bc)

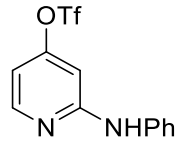

Yield: 65% (41.1 mg). Light-yellow solid, m.p.= 77.5–79.6 ºC. Eluents (R_f = 0.3, Hexane: Ethyl acetate = 10:1) was used for flash column chromatography. The % conversion of starting material = 100%. The % of minor product (reacting C–OTf site): major product (reacting C–Cl site): diarylated product (reacting both C–OTf & C–Cl site) = 94.9: 3.4: 1.7. **^{1}H NMR** (400 MHz, $CDCl_3$) δ 8.24 (d, *J* = 5.7 Hz, 1H), 7.54 (s, 1H), 7.40 (t, *J* = 7.8 Hz, 2H), 7.31 (d, *J* = 7.8 Hz, 2H), 7.16 (t, *J* = 7.3 Hz, 1H), 6.72 (d, *J* = 1.8 Hz, 1H), 6.64 (dd, *J* = 5.7, 1.8 Hz, 1H); **^{13}C NMR** (100 MHz, $CDCl_3$) δ 158.6, 157.6, 151.0, 139.0, 129.6, 124.5, 121.5, 118.6 (q, *J* = 318.8 Hz, 1C), 107.0, 99.5; **^{19}F NMR** (565 MHz, $CDCl_3$) δ -73.1; **HRMS** (EI): calcd for $C_{12}H_9F_3N_2O_3S^+$: 318.0280, found 318.0292.

2-(Methyl(phenyl)amino)pyridin-4-yl trifluoromethanesulfonate (Table 2.5, compound 3bd)

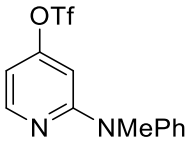

Yield: 74% (48.8 mg). Light-yellow solid, m.p.= 61.4–62.5 ºC. Eluents (R_f = 0.5, Hexane: Ethyl acetate = 10:1) was used for flash column chromatography. The % conversion of starting material = 100%. The % of minor product (reacting C–OTf site): major product (reacting C–Cl site): diarylated product (reacting both C–OTf & C–Cl site) = 95.2: 1.2: 3.6. **^{1}H NMR** (400 MHz, $CDCl_3$) δ 8.26 (d, *J* = 5.7 Hz, 1H), 7.46 (t, *J*

= 7.8 Hz, 2H), 7.30 (t, *J* = 7.5 Hz, 1H), 7.26 (d, *J* = 7.5 Hz, 2H), 6.52 (dd, *J* = 5.7, 2.0 Hz, 1H), 6.29 (d, *J* = 2.0 Hz, 1H), 3.49 (s, 3H); **^{13}C NMR** (100 MHz, $CDCl_3$) δ 160.6, 156.9, 150.3, 145.3, 130.1, 126.8, 126.5, 118.5 (q, *J* = 318.8 Hz, 1C), 105.1, 100.2, 38.7; **^{19}F NMR** (565 MHz, $CDCl_3$) δ -73.6; **HRMS** (EI): calcd for $C_{13}H_{11}F_3N_2O_3S^+$: 332.0437, found 332.0449.

5-(Phenylamino)pyridin-3-yl trifluoromethanesulfonate (Table 2.5, compound 3be)

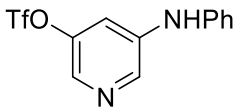

Yield: 66% (42.0 mg). Light-yellow solid, m.p.= 152.3–155.5 ºC. Eluents (R_f = 0.3, Hexane: Ethyl acetate = 4:1) was used for flash column chromatography. The % conversion of starting material = 99%. The % of minor product (reacting C–OTf site): major product (reacting C–Cl site): diarylated product (reacting both C–OTf & C–Cl site) = 97.1: 2.6: 0.3. **^{1}H NMR** (400 MHz, $CDCl_3$) δ 8.32 (s, 1H), 8.05 (s, 1H), 7.39-7.36 (m, 2H), 7.14 (d, *J* = 7.3 Hz, 3H), 6.08 (s, 1H); **^{13}C NMR** (100 MHz, $CDCl_3$) δ 147.2, 142.0, 139.8, 138.4, 132.8, 129.9, 124.1, 120.2, 118.7 (q, *J* = 319.3 Hz, 1C), 114.0; **^{19}F NMR** (565 MHz, $CDCl_3$) δ -72.6; **HRMS** (EI): calcd for $C_{12}H_9F_3N_2O_3S^+$: 318.0280, found 318.0279.

2-Methyl-3-(*o*-tolylamino)phenyl trifluoromethanesulfonate (Table 2.6, compound 3bf)

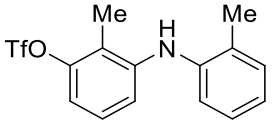

Yield: 92% (63.8 mg). Yellow liquid. Eluents (R_f = 0.5, Hexane: Ethyl acetate = 10:1) was used for flash column chromatography. The % conversion of starting material = 95%. The % of minor product (reacting C–OTf site): major product (reacting C–Cl site): diarylated product (reacting both C–OTf & C–Cl site) = 0: 100: 0. **^{1}H NMR** (400 MHz, $CDCl_3$) δ 7.29 (d, *J* = 7.3 Hz, 1H), 7.21 (t, *J* = 7.5 Hz, 1H), 7.13 (t, *J* = 8.2 Hz, 1H), 7.11-7.05 (m, 2H), 6.87 (d, *J* = 8.2 Hz, 2H), 5.30 (s, 1H), 2.31 (s, 3H), 2.28 (s, 3H); **^{13}C NMR** (100 MHz, $CDCl_3$) δ 149.0, 145.0, 140.3, 131.1, 130.0, 127.2, 127.0, 123.5, 121.2, 118.8, 118.7 (q, *J* = 318.2 Hz, 1C), 115.8, 112.8, 17.7, 10.9; **^{19}F NMR** (376 MHz, $CDCl_3$) δ -73.6; **HRMS** (APPI): calcd for $C_{15}H_{15}F_3NO_3S^+$: 346.0719, found 346.0721.

3-((2,6-Dimethylphenyl)amino)phenyl trifluoromethanesulfonate (Table 2.6, compound 3bg)

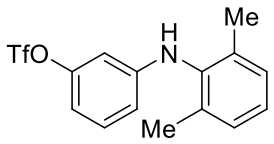

Yield: 79% (54.4 mg). Light-yellow liquid. Eluents (R_f = 0.4, Hexane: Ethyl acetate = 10:1) was used for flash column chromatography. The % conversion of starting material = 95%. The % of minor product (reacting C–OTf site): major product (reacting C–Cl site): diarylated product (reacting both C–OTf & C–Cl site) = 0.4: 98.3: 1.3. **^{1}H NMR** (400 MHz, $CDCl_3$) δ 7.22-7.15 (m, 4H), 6.63 (dd, *J* = 8.1, 2.3 Hz, 1H), 6.54 (dd, *J* = 8.2, 2.1 Hz, 1H), 6.32 (t, *J* = 2.2 Hz, 1H), 5.39 (s, 1H), 2.23 (s, 6H); **^{13}C NMR** (100 MHz, $CDCl_3$) δ 150.9, 148.4, 136.7, 136.3, 130.6, 128.8, 126.8, 118.7 (q, *J* = 318.7 Hz, 1C), 113.0, 109.9, 105.4, 18.1; **^{19}F NMR** (466 MHz, $CDCl_3$) δ -73.0; **HRMS** (APPI): calcd for $C_{15}H_{15}F_3NO_3S^+$: 346.0719, found 346.0722.

3-((2,6-Dimethylphenyl)amino)-2-methylphenyl trifluoromethanesulfonate (Table 2.6, compound 3bh)

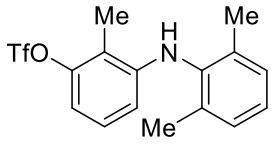

Yield: 78% (56.2 mg). Yellow solid, m.p.= 73.8–74.6 ºC. Eluents (R_f = 0.6, Hexane: Ethyl acetate = 10:1) was used for flash column chromatography. The % conversion of starting material = 88%. The % of minor product (reacting C–OTf site): major product (reacting C–Cl site): diarylated product (reacting both C–OTf & C–Cl site) = 0: 100: 0. **^{1}H NMR** (400 MHz, $CDCl_3$) δ 7.21-7.12 (m, 3H), 7.00 (t, *J* = 8.2 Hz, 1H), 6.71 (d, *J* = 8.2 Hz, 1H), 6.16 (d, *J* = 8.2 Hz, 1H), 5.10 (s, 1H), 2.35 (s, 3H), 2.20 (s, 6H); **^{13}C NMR** (100 MHz, $CDCl_3$) δ 148.8, 146.3, 137.6, 135.9, 128.7, 127.4, 126.4, 114.9, 118.7 (q, *J* = 318.1 Hz, 1C), 111.1, 110.5, 18.1, 10.5; **^{19}F NMR** (466 MHz, $CDCl_3$) δ -73.7; **HRMS** (APPI): calcd for $C_{16}H_{17}F_3NO_3S^+$: 360.0876, found 360.0877.

3-((2,6-Dimethylphenyl)amino)-4-methylphenyl trifluoromethanesulfonate (Table 2.6, compound 3bi)

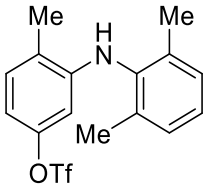

Yield: 94% (67.3 mg). Light-yellow solid, m.p.= 83.8–86.5 ºC. Eluents (R_f = 0.4, Hexane: Ethyl acetate = 10:1) was used for flash column chromatography. The % conversion of starting material = 100%. The % of minor product (reacting C–OTf site): major product (reacting C–Cl site): diarylated product (reacting both C–OTf & C–Cl

site) = 0: 98: 2. **^{1}H NMR** (400 MHz, $CDCl_3$) δ 7.22-7.16 (m, 4H), 6.60 (s, 1H), 6.00 (s, 1H), 5.13 (s, 1H), 2.35 (s, 3H), 2.21 (s, 6H); **^{13}C NMR** (100 MHz, $CDCl_3$) δ 149.3, 145.9, 137.0, 135.9, 131.1, 128.8, 126.7, 122.0, 118.6 (q, *J* = 318.9 Hz, 1C), 109.5, 103.8, 17.9, 17.1; **^{19}F NMR** (376 MHz, $CDCl_3$) δ -73.0; **HRMS** (EI): calcd for $C_{16}H_{16}F_3NO_3S^+$: 359.0798, found 359.0802.

3-((2,6-Diethylphenyl)amino)-2-methylphenyl trifluoromethanesulfonate (Table 2.6, compound 3bj)

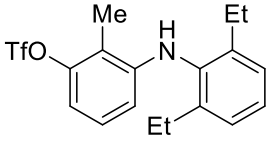

Yield: 74% (57.2 mg). Yellow liquid. Eluents (R_f = 0.4, Hexane: Ethyl acetate = 10:1) was used for flash column chromatography. The % conversion of starting material = 88%. The % of minor product (reacting C–OTf site): major product (reacting C–Cl site): diarylated product (reacting both C–OTf & C–Cl site) = 0.04: 99.96: 0. **^{1}H NMR** (400 MHz, $CDCl_3$) δ 7.29-7.20 (m, 3H), 6.97 (t, *J* = 8.2 Hz, 1H), 6.68 (d, *J* = 8.2 Hz, 1H), 6.15 (d, *J* = 8.2 Hz, 1H), 5.12 (s, 1H), 2.62-2.45 (m, 4H), 2.35 (s, 3H), 1.17 (t, *J* = 7.6 Hz, 6H); **^{13}C NMR** (100 MHz, $CDCl_3$) δ 148.8, 147.2, 142.2, 136.3, 127.3, 127.2, 126.9, 118.7 (q, *J* = 318.2 Hz, 1C), 114.4, 111.1, 110.2, 24.6, 14.6, 10.5; **^{19}F NMR** (466 MHz, $CDCl_3$) δ -73.7; HRMS (APPI): calcd for $C_{18}H_{21}F_3NO_3S^+$: 388.1189, found 388.1188.

4-((2,6-Diisopropylphenyl)amino)phenyl trifluoromethanesulfonate (Table 2.6, compound 3bk)

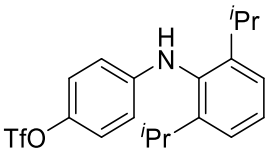

Yield: 90% (72.2 mg). Pink solid, m.p.= 49.6–51.3 °C. Eluents (R_f = 0.4, Hexane: Ethyl acetate = 10:1) was used for flash column chromatography. The % conversion of starting material = 92%. The % of minor product (reacting C–OTf site): major product (reacting C–Cl site): diarylated product (reacting both C–OTf & C–Cl site) = 0: 100: 0. **^{1}H NMR** (400 MHz, $CDCl_3$) δ 7.39-7.27 (m, 3H), 7.07 (d, *J* = 9.1 Hz, 2H), 6.49 (d, *J* = 8.6 Hz, 2H), 5.32 (s, 1H), 3.22-3.15 (m, 2H), 1.19 (d, *J* = 6.9 Hz, 12H); **^{13}C NMR** (100 MHz, $CDCl_3$) δ 148.0, 147.6, 141.0, 134.2, 127.9, 124.1, 122.1, 118.8 (q, *J* = 319.0 Hz, 1C), 113.2, 28.2, 23.8; **^{19}F NMR** (376 MHz, $CDCl_3$) δ -72.9; **HRMS** (EI): calcd for $C_{19}H_{22}F_3NO_3S^+$: 401.1267, found 401.1271.

3-((2,6-Diisopropylphenyl)amino)phenyl trifluoromethanesulfonate (Table 2.6, compound 3bl)

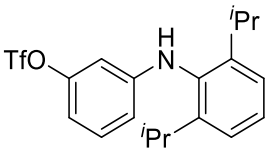

Yield: 62% (49.6 mg). Yellow liquid. Eluents (R_f = 0.4, Hexane: Ethyl acetate = 10:1) was used for flash column chromatography. The % conversion of starting material = 90%. The % of minor product (reacting C–OTf site): major product (reacting C–Cl site): diarylated product (reacting both C–OTf & C–Cl site) = 0.5: 99.5: 0. **^{1}H NMR** (400 MHz, $CDCl_3$) δ 7.38-7.16 (m, 4H), 6.61-6.53 (m, 2H), 6.28 (s, 1H), 5.34 (s, 1H), 3.19-3.12 (m, 2H), 1.17 (d, *J* = 6.9 Hz, 12H); **^{13}C NMR** (100 MHz, $CDCl_3$) δ 150.9, 150.1, 147.7, 133.6, 130.5, 128.2, 124.1, 118.7 (q, *J* = 318.7 Hz, 1C), 112.8, 109.6, 105.0, 28.3,

23.7; **^{19}F NMR** (466 MHz, $CDCl_3$) δ -73.0; **HRMS** (APPI): calcd for $C_{19}H_{23}F_3NO_3S^+$: 402.1345, found 402.1345.

3-((2,6-Diisopropylphenyl)amino)-2-methylphenyl trifluoromethanesulfonate (Table 2.6, compound 3bm)

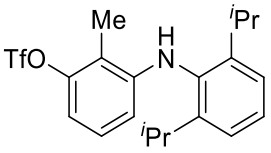

Yield: 65% (54.2 mg). Light-yellow solid, m.p.= 83.8–86.1 °C. Eluents (R_f = 0.4, Hexane: Ethyl acetate = 10:1) was used for flash column chromatography. The % conversion of starting material = 93%. The % of minor product (reacting C–OTf site): major product (reacting C–Cl site): diarylated product (reacting both C–OTf & C–Cl site) = 0: 100: 0. **^{1}H NMR** (400 MHz, $CDCl_3$) δ 7.40-7.32 (m, 1H), 7.27 (d, *J* = 7.6 Hz, 2H), 6.98 (t, *J* = 8.2 Hz, 1H), 6.67 (d, *J* = 8.2 Hz, 1H), 6.14 (d, *J* = 8.2 Hz, 1H), 5.09 (s, 1H), 3.10-3.04 (m, 2H), 2.36 (s, 3H), 1.21 (d, *J* = 6.8 Hz, 6H), 1.14 (d, *J* = 6.8 Hz, 6H); **^{13}C NMR** (100 MHz, $CDCl_3$) δ 148.8, 148.0, 147.3, 134.6, 127.8, 127.3, 124.0, 118.7 (q, *J* = 318.2 Hz, 1C), 113.9, 111.0, 110.0, 28.3, 24.6, 23.0, 10.5; **^{19}F NMR** (376 MHz, $CDCl_3$) δ -73.8; **HRMS** (APPI): calcd for $C_{20}H_{25}F_3NO_3S^+$: 416.1502, found 416.1494.

3-((2,6-Diisopropylphenyl)amino)-4-methylphenyl trifluoromethanesulfonate (Table 2.6, compound 3bn)

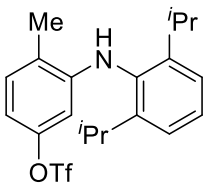

Yield: 79% (65.6 mg). Light-yellow liquid. Eluents (R_f = 0.4, Hexane: Ethyl acetate = 10:1) was used for flash column chromatography. The % conversion of starting material = 93%. The % of minor product (reacting C–OTf site): major product (reacting C–Cl site): diarylated product (reacting both C–OTf & C–Cl site) = 0: 100: 0. **^{1}H NMR** (400 MHz, $CDCl_3$) δ 7.40-7.35 (m, 1H), 7.28 (d, *J* = 7.6 Hz, 2H), 7.16 (d, *J* = 8.2 Hz, 1H), 6.57 (dd, *J* = 8.2, 2.4 Hz, 1H), 5.96 (s, 1H), 5.10 (s, 1H), 3.11-3.04 (m, 2H), 2.36 (s, 3H), 1.20 (d, *J* = 6.9 Hz, 6H), 1.16 (d, *J* = 6.9 Hz, 6H); **^{13}C NMR** (100 MHz, $CDCl_3$) δ 149.3, 147.7, 147.3, 134.0, 131.0, 128.1, 124.1, 121.2, 118.6 (q, *J* = 318.8 Hz, 1C), 109.1, 103.6, 28.3, 24.6, 22.8, 17.1; **^{19}F NMR** (466 MHz, $CDCl_3$) δ -73.0; **HRMS** (APPI): calcd for $C_{20}H_{25}F_3NO_3S^+$: 416.1502, found 416.1503.

4-((4-Cyanophenyl)amino)phenyl trifluoromethanesulfonate (Table 2.7, compound 3bp)

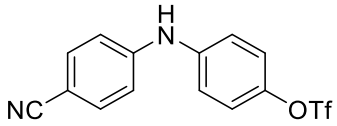

Yield: 83% (56.8 mg). Yellow solid, m.p.= 124.2–125.3 °C. Eluents (R_f = 0.4, Toluene = 100) was used for flash column chromatography. The % conversion of starting material = 100%. The % of minor product (reacting C–OTf site): major product (reacting C–Cl site): diarylated product (reacting both C–OTf & C–Cl site) = 0: 100: 0. **^{1}H NMR** (400 MHz, $CDCl_3$) δ 7.52 (d, *J* = 8.7 Hz, 2H), 7.26-7.19 (m, 4H), 7.04 (d, *J* = 8.8 Hz, 2H), 6.32 (s, 1H); **^{13}C NMR** (100 MHz, $CDCl_3$) δ 146.8, 144.6, 140.6, 133.8, 122.6, 121.2, 119.5, 118.7 (q, *J* = 319.1 Hz, 1C), 115.8, 102.9; **^{19}F NMR** (376 MHz, $CDCl_3$) δ -72.7; **HRMS** (EI): calcd for $C_{14}H_9F_3N_2O_3S^+$: 342.0280, found 342.0278.

4-((4-(Tert-butyl)phenyl)amino)phenyl trifluoromethanesulfonate (Table 2.7, compound 3bq)

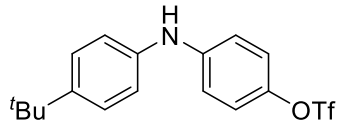

Yield: 51% (38.3 mg). Red liquid. Eluents (R_f= 0.5, Hexane: Toluene = 2:1) was used for flash column chromatography. The % conversion of starting material = 95%. The % of minor product (reacting C–OTf site): major product (reacting C–Cl site): diarylated product (reacting both C–OTf & C–Cl site) = 100: 0: 0. **^{1}H NMR** (400 MHz, $CDCl_3$) δ 7.35 (d, *J* = 8.5 Hz, 2H), 7.12 (d, *J* = 9.0 Hz, 2H), 7.07 (d, *J* = 8.5 Hz, 2H), 7.02-6.96 (m, 2H), 5.76 (s, 1H), 1.34 (s, 9H); **^{13}C NMR** (100 MHz, $CDCl_3$) δ 145.8, 144.3, 142.2, 138.8, 126.3, 122.2, 119.6, 118.8 (q, *J* = 318.9 Hz, 1C), 116.6, 34.3, 31.4; **^{19}F NMR** (565 MHz, $CDCl_3$) δ -73.4; **HRMS** (EI): calcd for $C_{17}H_{18}F_3NO_3S^+$: 373.0954, found 373.0952.

4-((4-Acetylphenyl)amino)phenyl trifluoromethanesulfonate (Table 2.7, compound 3br)

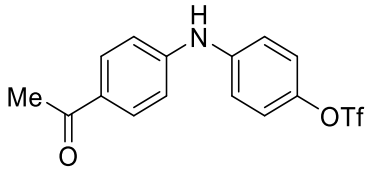

Yield: 69% (49.1 mg). Light brown solid, m.p.= 98.4–99.7 ºC. Eluents (R_f= 0.3, Hexane: Ethyl acetate = 3:1) was used for flash column chromatography. The % conversion of starting material = 100%. The % of minor product (reacting C–OTf site): major product (reacting C–Cl site): diarylated product (reacting both C–OTf & C–Cl site) = 0: 100: 0.

^{1}H NMR (400 MHz, $CDCl_3$) δ 7.89 (d, *J* = 8.7 Hz, 2H), 7.23-7.18 (m, 4H), 7.04 (d, *J* = 8.7 Hz, 2H), 6.56 (s, 1H), 2.54 (s, 3H); **^{13}C NMR** (100 MHz, $CDCl_3$) δ 196.7, 147.1, 144.1, 141.3, 130.6, 129.9, 122.5, 120.4, 118.7 (q, *J* = 319.0 Hz, 1C), 115.4, 26.2; **^{19}F NMR** (376 MHz, $CDCl_3$) δ -72.7; **HRMS** (APPI): calcd for $C_{15}H_{13}F_3NO_4S^+$ 360.0512, found 360.0516.

4-((4-Benzoylphenyl)amino)phenyl trifluoromethanesulfonate (Table 5, compound 3bs)

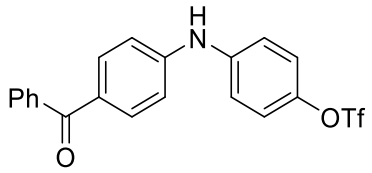

Yield: 76% (64.3 mg). Yellow solid, m.p.= 150.6–151.2 ºC. Eluents (R_f = 0.2, Hexane: Ethyl acetate = 3:1) was used for flash column chromatography. The % conversion of starting material = 100%. The % of minor product (reacting C–OTf site): major product (reacting C–Cl site): diarylated product (reacting both C–OTf & C–Cl site) = 0: 100: 0. **^{1}H NMR** (400 MHz, $CDCl_3$) δ 7.80-7.75 (m, 4H), 7.56 (t, *J* = 7.3 Hz, 1H), 7.49-7.45 (m, 2H), 7.25-7.17 (m, 4H), 7.06 (d, *J* = 7.5 Hz, 2H), 6.50 (s, 1H); **^{13}C NMR** (100 MHz, $CDCl_3$) δ 195.4, 146.8, 144.1, 141.2, 138.3, 132.6, 131.9, 129.7, 129.6, 128.2, 122.5, 120.4, 118.7 (q, *J* = 318.8 Hz, 1C), 115.3; **^{19}F NMR** (376 MHz, $CDCl_3$) δ -72.7; **HRMS** (APPI): calcd for $C_{20}H_{15}F_3NO_4S^+$: 422.0668, found 422.0676.

4-((3-Methoxyphenyl)amino)phenyl trifluoromethanesulfonate (Table 2.7, compound 3bt)

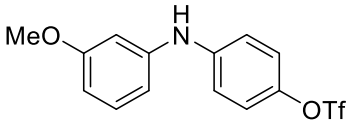

Yield: 75% (52.0 mg). Light-yellow liquid. Eluents (R_f = 0.4, Hexane: Toluene = 2:1) was used for flash column chromatography. The % conversion of starting material = 98%. The % of minor product (reacting C–OTf site): major product (reacting C–Cl site): diarylated product (reacting both C–OTf & C–Cl site) = 100: 0: 0. **^{1}H NMR** (400 MHz, $CDCl_3$) δ 7.22 (t, *J* = 8.1 Hz, 1H), 7.17-7.11 (m, 2H), 7.09-7.02 (m, 2H), 6.70-6.67 (m, 1H), 6.65 (t, *J* = 2.1 Hz, 1H), 6.58 (dd, *J* = 8.2, 2.2 Hz, 1H), 5.83 (s, 1H), 3.80 (s, 3H); **^{13}C NMR** (100 MHz, $CDCl_3$) δ 160.7, 143.4, 143.1, 142.7, 130.3, 122.3, 118.7 (q, *J* = 318.9 Hz, 1C), 117.8, 111.4, 107.4, 104.9, 55.2; **^{19}F NMR** (565 MHz, $CDCl_3$) δ -73.0; **HRMS** (EI): calcd for $C_{14}H_{12}F_3NO_4S^+$: 347.0434, found 347.0445.

4-(*m*-Tolylamino)phenyl trifluoromethanesulfonate (Table 2.7, compound 3bu)

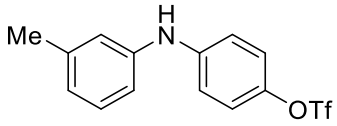

Yield: 88% (58.5 mg). Light-yellow liquid. Eluents (R_f = 0.5, Hexane: Toluene = 2:1) was used for flash column chromatography. The % conversion of starting material = 99%. The % of minor product (reacting C–OTf site): major product (reacting C–Cl site): diarylated product (reacting both C–OTf & C–Cl site) = 100: 0: 0. **^{1}H NMR** (400 MHz, $CDCl_3$) δ 7.24-7.20 (m, 1H), 7.16-7.12 (m, 2H), 7.04-7.01 (m, 2H), 6.92 (d, *J* = 6.7 Hz, 2H), 6.87 (d, *J* = 7.5 Hz, 1H), 5.78 (s, 1H), 2.35 (s, 3H); **^{13}C NMR** (100 MHz, $CDCl_3$) δ 143.9, 142.5, 141.6, 139.5, 129.3, 123.4, 122.2, 120.0, 118.8 (q, *J* = 319.1 Hz, 1C), 117.2, 116.3, 21.4; **^{19}F NMR** (565 MHz, $CDCl_3$) δ -73.0; **HRMS** (EI): calcd for

$C_{14}H_{12}F_3NO_3S^+$: 331.0485, found 331.0488.

4-((3,5-Dimethylphenyl)amino)phenyl trifluoromethanesulfonate (Table 2.7, compound 3bv)

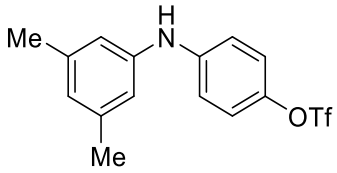

Yield: 74% (51.5 mg). Light-yellow liquid. Eluents (R_f = 0.5, Hexane: Toluene = 2:1) was used for flash column chromatography. The % conversion of starting material = 95%. The % of minor product (reacting C–OTf site): major product (reacting C–Cl site): diarylated product (reacting both C–OTf & C–Cl site) = 100: 0: 0. **^{1}H NMR** (600 MHz, $CDCl_3$) δ 7.14 (d, *J* = 8.7 Hz, 2H), 7.02 (d, *J* = 8.6 Hz, 2H), 6.75 (s, 2H), 6.70 (s, 1H), 5.74 (s, 1H), 2.31 (s, 6H); **^{13}C NMR** (150 MHz, $CDCl_3$) δ 143.9, 142.4, 141.5, 139.3, 124.3, 122.2, 118.8 (q, *J* = 319.2 Hz, 1C), 117.2, 117.0, 21.3; **^{19}F NMR** (565 MHz, $CDCl_3$) δ -73.1; **HRMS** (EI): calcd for $C_{15}H_{14}F_3NO_3S^+$: 345.0641, found 345.0649.

4-(*o*-Tolylamino)phenyl trifluoromethanesulfonate (Table 2.7, compound 3bw)

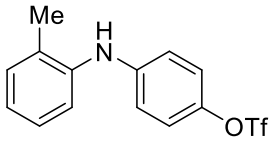

Yield: 66% (44.0 mg). Red liquid. Eluents (R_f = 0.5, Hexane: Toluene = 2:1) was used for flash column chromatography. The % conversion of starting material = 99%. The % of minor product (reacting C–OTf site): major product (reacting C–Cl site): diarylated product (reacting both C–OTf & C–Cl site) = 100: 0: 0. **^{1}H NMR** (400 MHz, $CDCl_3$) δ 7.27-7.23 (m, 2H), 7.20 (t, *J* = 7.5 Hz, 1H), 7.14-7.10 (m, 2H), 7.06 (td, *J* = 7.3, 1.1 Hz,

1H), 6.89-6.85 (m, 2H), 5.51 (s, 1H), 2.26 (s, 3H); **^{13}C NMR** (100 MHz, $CDCl_3$) δ 144.7, 142.2, 139.7, 131.2, 130.4, 126.9, 123.8, 122.2, 121.2, 118.8 (q, *J* = 318.9 Hz, 1C), 116.5, 17.8; **^{19}F NMR** (565 MHz, $CDCl_3$) δ -73.4; **HRMS** (EI): calcd for $C_{14}H_{12}F_3NO_3S^+$: 331.0485, found 331.0491.

4-(Quinolin-2-ylamino)phenyl trifluoromethanesulfonate (Table 2.7, compound 3bx)

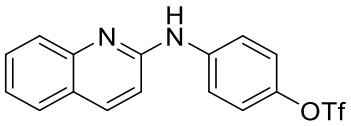

Yield: 75% (55.4 mg). Yellow solid, m.p.= 89.5–90.1 ^{o}C. Eluents (R_f = 0.2, Hexane: Ethyl acetate = 4:1) was used for flash column chromatography. The % conversion of starting material = 94%. The % of minor product (reacting C–OTf site): major product (reacting C–Cl site): diarylated product (reacting both C–OTf & C–Cl site) = 0: 100: 0. **^{1}H NMR** (400 MHz, $CDCl_3$) δ 7.92 (d, *J* = 8.8 Hz, 1H), 7.84 (d, *J* = 8.4 Hz, 1H), 7.78 (d, *J* = 9.1 Hz, 2H), 7.67-7.60 (m, 2H), 7.34 (t, *J* = 7.4 Hz, 1H), 7.23 (d, *J* = 9.0 Hz, 2H), 7.04 (s, 1H), 6.83 (d, *J* = 8.8 Hz, 1H); **^{13}C NMR** (100 MHz, $CDCl_3$) δ 153.2, 147.1, 143.8, 140.5, 137.9, 129.9, 127.4, 126.9, 124.2, 123.7, 121.8, 120.1, 118.7 (q, *J* = 318.9 Hz, 1C), 112.4; **^{19}F NMR** (376 MHz, $CDCl_3$) δ -72.7; **HRMS** (APPI): calcd for $C_{16}H_{11}F_3N_2O_3S^+$: 369.0515, found 369.0510.

3-((4-(Trifluoromethyl)phenyl)amino)phenyl trifluoromethanesulfonate (Table 2.7, compound 3by)

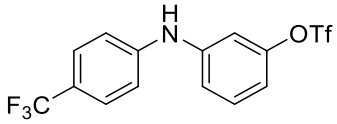

Yield: 76% (58.4 mg). Light-yellow solid, m.p.= 75.5–76.7 °C. Eluents (Hexane: Toluene = 2:1, R_f = 0.5) was used for flash column chromatography. The % conversion of starting material = 100%. The % of minor product (reacting C–OTf site): major product (reacting C–Cl site): diarylated product (reacting both C–OTf & C–Cl site) = 97.5: 0: 2.5. **^{1}H NMR** (400 MHz, $CDCl_3$) δ 7.54 (d, *J* = 8.5 Hz, 2H), 7.36 (t, *J* = 8.2 Hz, 1H), 7.13-7.09 (m, 3H), 7.04 (t, *J* = 2.0 Hz, 1H), 6.89 (dd, *J* = 8.2, 2.1 Hz, 1H), 6.09 (s, 1H); **^{13}C NMR** (100 MHz, $CDCl_3$) δ 150.3, 144.8, 143.6, 131.0, 126.9 (q, *J* = 15.0 Hz, 1C), 124.3 (q, *J* = 269.4 Hz, 1C), 123.5 (q, *J* = 32.5 Hz, 1C), 118.7 (q, *J* = 318.9 Hz, 1C), 118.1, 116.9, 114.3, 111.0; **^{19}F NMR** (565 MHz, $CDCl_3$) δ -62.3, -73.5; **HRMS** (EI): calcd for $C_{14}H_9F_6NO_3S^+$: 385.0202, found 385.0205.

3-((4-Acetylphenyl)amino)phenyl trifluoromethanesulfonate (Table 2.7, compound 3bz)

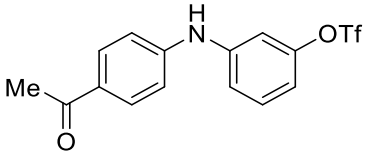

Yield: 73% (52.3 mg). Light-yellow solid, m.p.= 139.4–142.3 °C. Eluents (Hexane: EA = 4:1, R_f = 0.3) was used for flash column chromatography. The % conversion of starting material = 100%. The % of minor product (reacting C–OTf site): major product (reacting C–Cl site): diarylated product (reacting both C–OTf & C–Cl site) = 100: 0: 0. **^{1}H NMR** (400 MHz, $CDCl_3$) δ 7.92 (d, *J* = 7.9 Hz, 2H), 7.37 (t, *J* = 7.9 Hz, 1H), 7.11 (dd, *J* = 29.5, 7.6 Hz, 4H), 6.91 (d, *J* = 7.4 Hz, 1H), 6.42 (s, 1H), 2.56 (s, 3H); **^{13}C NMR**

(100 MHz, $CDCl_3$) δ 196.6, 150.3, 146.5, 143.1, 131.0, 130.6, 130.4, 118.8, 118.7 (q, *J* = 319.4 Hz, 1C), 115.8, 114.7, 111.8, 26.2; **^{19}F NMR** (565 MHz, $CDCl_3$) δ -72.8; **HRMS** (EI): calcd for $C_{14}H_{12}F_3NO_3S^+$: 359.0434, found 359.0443.

3-(*p*-Tolylamino)phenyl trifluoromethanesulfonate (Table 2.7, compound 3ca)

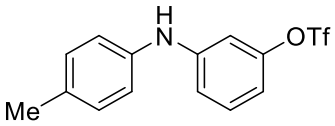

Yield: 76% (50.0 mg). Light-yellow liquid. Eluents (R_f = 0.5, Hexane: Toluene = 2:1) was used for flash column chromatography. The % conversion of starting material = 96%. The % of minor product (reacting C–OTf site): major product (reacting C–Cl site): diarylated product (reacting both C–OTf & C–Cl site) = 94.7: 0.3: 5.0. **^{1}H NMR** (400 MHz, $CDCl_3$) δ 7.25 (t, *J* = 8.2 Hz, 1H), 7.16 (d, *J* = 8.2 Hz, 2H), 7.04 (d, *J* = 8.3 Hz, 2H), 6.92 (dd, *J* = 8.2, 1.9 Hz, 1H), 6.86 (t, *J* = 2.1 Hz, 1H), 6.72 (dd, *J* = 8.2, 2.2 Hz, 1H), 5.79 (s, 1H), 2.35 (s, 3H); **^{13}C NMR** (100 MHz, $CDCl_3$) δ 150.5, 146.5, 138.3, 132.9, 130.6, 130.1, 120.5, 118.7 (q, *J* = 318.7 Hz, 1C), 115.3, 111.5, 107.9, 20.7; **^{19}F NMR** (565 MHz, $CDCl_3$) δ -73.3; **HRMS** (EI): calcd for $C_{14}H_{12}F_3NO_3S^+$: 331.0485, found 331.0475.

3-((2-Methoxyphenyl)amino)phenyl trifluoromethanesulfonate (Table 2.7, compound 3cb)

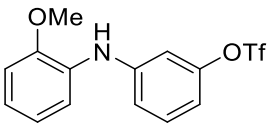

Yield: 79% (54.8 mg). Light-yellow liquid. Eluents (R_f = 0.5, Hexane: Toluene = 2:1)

was used for flash column chromatography. The % conversion of starting material = 99%. The % of minor product (reacting C–OTf site): major product (reacting C–Cl site): diarylated product (reacting both C–OTf & C–Cl site) = 91.4: 0: 8.6. **^{1}H NMR** (400 MHz, $CDCl_3$) δ 7.34-7.26 (m, 2H), 7.08 (dd, *J* = 8.2, 1.8 Hz, 1H), 7.02 (t, *J* = 2.2 Hz, 1H), 7.00-6.93 (m, 3H), 6.78 (dd, *J* = 8.2, 2.1 Hz, 1H), 6.28 (s, 1H), 3.90 (s, 3H); **^{13}C NMR** (100 MHz, $CDCl_3$) δ 150.4, 149.1, 145.2, 130.8, 130.6, 121.9, 120.8, 118.7 (q, *J* = 318.9 Hz, 1C), 116.8, 116.6, 112.3, 110.8, 109.3, 55.5; **^{19}F NMR** (565 MHz, $CDCl_3$) δ -73.3; **HRMS** (EI): calcd for $C_{14}H_{12}F_3NO_4S^+$: 347.0434, found 347.0430.

3-((10-(3-(Dimethylamino)propyl)-10H-phenothiazin-2-yl)amino)phenyl trifluoromethanesulfonate (Table 2.7, compound 3cc)

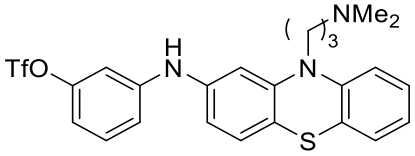

Yield: 77% (80.4 mg). Light-yellow solid, m.p.= 56.0–57.4 ºC. Eluents (R_f = 0.3, Hexane: Ethyl acetate: Et_3N = 10: 10: 1) was used for flash column chromatography. The % conversion of starting material = 100%. The % of minor product (reacting C–OTf site): major product (reacting C–Cl site): diarylated product (reacting both C–OTf & C–Cl site) = 97.7: 0: 2.3: 0. **^{1}H NMR** (600 MHz, $CDCl_3$) δ 7.22 (t, *J* = 8.2 Hz, 1H), 7.14-7.11 (m, 2H), 7.01 (d, *J* = 8.2 Hz, 1H), 6.98-6.97 (m, 1H), 6.94-6.93 (m, 1H), 6.91 (t, *J* = 7.4 Hz, 1H), 6.83 (d, *J* = 8.7 Hz, 2H), 6.74-6.68 (m, 3H), 3.84 (t, *J* = 6.6 Hz, 2H), 2.66 (m, t, *J* = 7.3 Hz, 2H), 2.36 (s, 6H), 2.11-2.03 (m, 2H); **^{13}C NMR** (150 MHz, $CDCl_3$) δ 150.3, 146.2, 145.7, 144.6, 141.3, 130.7, 127.9, 127.5, 127.3, 125.4, 122.7, 118.6 (q, *J* = 319.3 Hz, 1C), 117.7, 116.3, 115.6, 113.1, 111.8, 108.6, 107.6, 56.3, 44.9,

44.4, 23.8; **^{19}F NMR** (565 MHz, $CDCl_3$) δ -72.9; **HRMS** (ESI): calcd for $C_{24}H_{25}F_3N_3O_3S_2^+$: 524.1284, found 524.1292.

3-((4-((3-(1-Methylazepan-4-yl)-4-oxo-3,4-dihydrophthalazin-1-yl)methyl)phenyl)amino)phenyl trifluoromethanesulfonate (Table 2.7, compound 3cd)

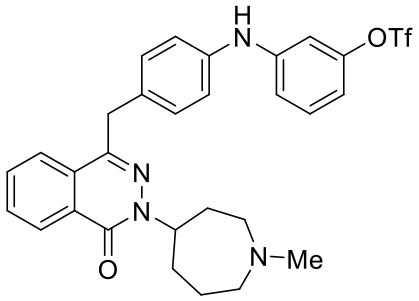

Yield: 80% (93.9 mg). White solid, m.p.= 45.0–47.5 ºC. Eluents (R_f = 0.6, Toluene: MeOH: Et_3N = 10:1:1) was used for flash column chromatography. The % conversion of starting material = 100%. The % of minor product (reacting C–OTf site): major product (reacting C–Cl site): diarylated product (reacting both C–OTf & C–Cl site) = 93.9: 6.1: 0. **^{1}H NMR** (600 MHz, $CDCl_3$) δ 8.44 (d, *J* = 8.4 Hz, 1H), 7.78-7.69 (m, 3H), 7.23-7.19 (m, 3H), 7.11 (d, *J* = 7.8 Hz, 2H), 7.02 (d, *J* = 7.7 Hz, 2H), 6.94 (s, 1H), 6.80 (s, 1H), 6.68 (d, *J* = 7.3 Hz, 1H), 5.38-5.33 (m, 1H), 4.26 (s, 2H), 2.98-2.92 (m, 1H), 2.85-2.72 (m, 3H), 2.51 (s, 3H), 2.30-2.24 (m, 1H), 2.22-2.18 (m, 1H), 2.11-2.05 (m, 2H), 2.00-1.94 (m, 1H), 1.85-1.79 (m, 1H); **^{13}C NMR** (150 MHz, $CDCl_3$) δ 158.3, 150.3, 145.8, 145.5, 140.1, 132.8, 131.5, 131.1, 130.5, 129.8, 128.7, 127.8, 127.3, 124.6, 119.5, 118.6 (q, *J* = 318.6 Hz, 1C), 117.5, 115.9, 111.6, 108.4, 58.5, 55.2, 53.8, 45.8, 38.1, 31.8, 31.4, 23.2; **^{19}F NMR** (565 MHz, $CDCl_3$) δ -73.0; **HRMS** (ESI): calcd for $C_{29}H_{30}F_3N_4O_4S^+$: 587.1934, found 587.1941.

(Isopropylpthyl)sulfonyl)oxy)phenyl)amino)benzoyl)phenoxy)propanoate (Table 2.7, compound 3ce)

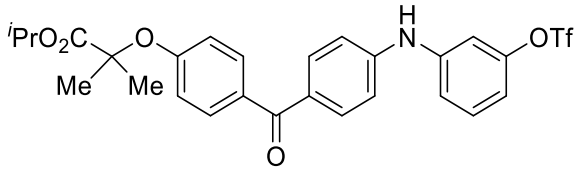

Yield: 87% (98.6 mg). Light-yellow liquid. Eluents (R_f = 0.3, Hexane: Ethyl acetate = 4:1) was used for flash column chromatography. The % conversion of starting material = 100%. The % of minor product (reacting C–OTf site): major product (reacting C–Cl site): diarylated product (reacting both C–OTf & C–Cl site) = 97.5: 2.5: 0. **^{1}H NMR** (600 MHz, $CDCl_3$) δ 7.73 (dd, *J* = 11.1, 8.7 Hz, 4H), 7.34 (t, *J* = 8.2 Hz, 1H), 7.14 (dd, *J* = 8.2, 1.2 Hz, 1H), 7.09-7.08 (m, 3H), 6.88-6.85 (m, 3H), 6.68 (s, 1H), 5.12-5.06 (m, 1H), 1.65 (s, 6H), 1.21 (s, 3H), 1.20 (s, 3H); **^{13}C NMR** (150 MHz, $CDCl_3$) δ 194.2, 173.2, 159.1, 150.2, 145.9, 143.4, 132.2, 131.6, 131.1, 130.9, 130.6, 118.6 (q, *J* = 318.6 Hz, 1C), 118.4, 117.2, 115.8, 114.2, 111.4, 79.3, 69.3, 25.3, 21.4; **^{19}F NMR** (565 MHz, $CDCl_3$) δ -72.9; **HRMS** (ESI): calcd for $C_{27}H_{26}F_3NO_7SNa^+$: 588.1274, found 588.1280.

2.4.8 X-Ray Crystallography Data of L25 and Pd-L25

Table 2.8 Crystal data and structure refinement for **L25**.

Identification code	exp_8889
Empirical formula	$C_{28}H_{47}N_2P$
Formula weight	442.64
Temperature/K	293(2)
Crystal system	monoclinic
Space group	I2/a
a/Å	20.943(2)
b/Å	10.4945(14)
c/Å	26.517(4)
α/°	90

β/°	112.950(14)
γ/°	90
Volume/Å^3	5366.6(13)
Z	8
ρ_{calc}g/cm^3	1.096
μ/mm^{-1}	0.119
F(000)	1952.0
Crystal size/mm^3	0.25 × 0.19 × 0.18
Radiation	Mo Kα (λ = 0.71073)
2Θ range for data collection/°	4.224 to 48.998
Index ranges	-24 ≤ h ≤ 22, 0 ≤ k ≤ 12, 0 ≤ l ≤ 30
Reflections collected	4364
Independent reflections	4364 [R_{int} = ?, R_{sigma} = 0.0836]
Data/restraints/parameters	4364/0/282
Goodness-of-fit on F^2	1.105
Final R indexes [I>=2σ (I)]	R_1 = 0.1063, wR_2 = 0.2347
Final R indexes [all data]	R_1 = 0.1328, wR_2 = 0.2505
Largest diff. peak/hole / e Å^{-3}	0.37/-0.39

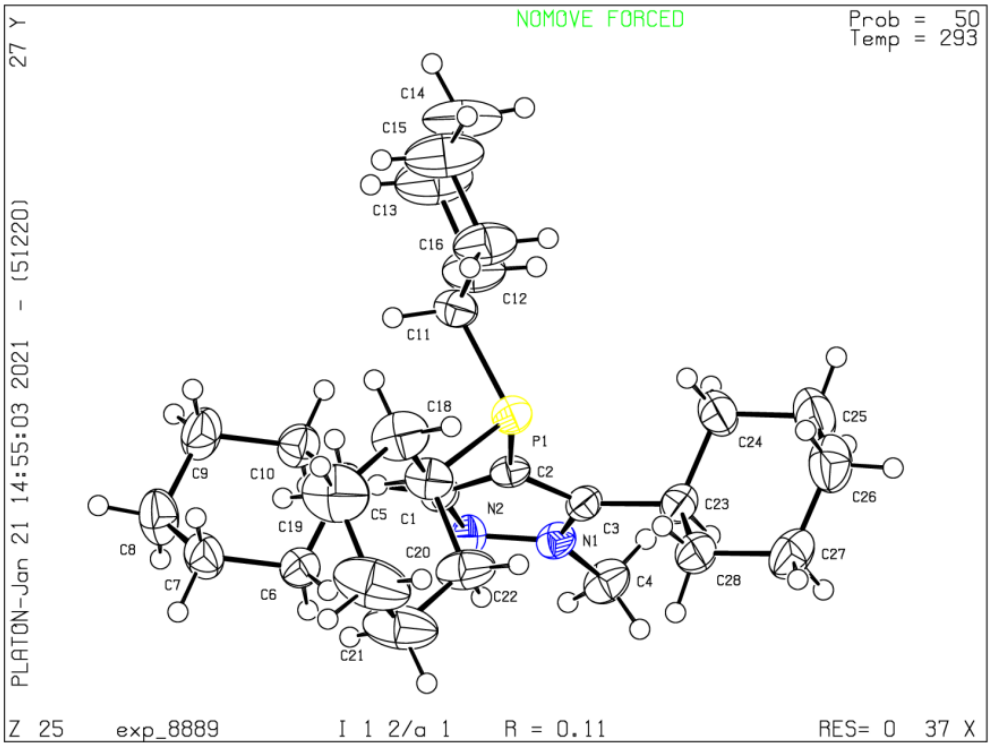

Table 2.9 Fractional Atomic Coordinates (×10^4) and Equivalent Isotropic

Displacement Parameters ($Å^2×10^3$) for exp_8889. U_{eq} is defined as 1/3 of of the trace of the orthogonalised U_{IJ} tensor.

Atom	*x*	*y*	*z*	U(eq)
P1	6333.8(7)	7449.4(14)	6599.1(5)	36.1(4)
N1	5440(2)	8459(4)	5041.5(15)	34.3(10)
N2	4880(2)	7850(4)	5053.9(17)	33.8(10)
C5	4588(2)	6609(5)	5709.3(19)	32.2(11)
C2	5778(2)	7762(5)	5882.4(19)	30.0(11)
C6	4536(3)	5262(5)	5465(2)	40.3(13)
C3	5986(2)	8443(5)	5524(2)	33.0(11)
C1	5083(3)	7405(5)	5569(2)	34.6(11)
C11	5839(3)	8066(5)	7001(2)	41.2(13)
C17	6240(3)	5697(5)	6628(2)	43.9(13)
C23	6672(3)	9044(5)	5599(2)	40.0(13)
C10	3862(3)	7167(5)	5524(2)	44.6(14)
C28	7262(3)	8096(6)	5751(3)	47.5(14)
C8	3362(3)	4986(6)	5473(3)	58.8(17)
C7	4078(3)	4408(5)	5635(3)	49.8(15)
C24	6850(3)	10161(6)	5989(3)	53.6(16)
C4	5368(3)	9081(6)	4529(2)	46.1(14)
C18	6524(4)	5157(6)	7209(3)	60.0(17)
C12	5426(4)	9257(7)	6763(2)	63.2(18)
C27	7945(3)	8715(7)	5816(3)	55.8(16)
C22	6603(4)	5071(6)	6291(2)	58.4(17)
C26	8114(3)	9841(7)	6198(3)	64.6(19)
C25	7529(4)	10780(7)	6039(3)	69(2)
C16	6354(4)	8333(7)	7585(2)	66(2)
C9	3390(3)	6315(6)	5689(3)	55.9(16)
C21	6531(5)	3626(7)	6281(3)	83(2)
C14	5596(5)	10029(8)	7701(3)	89(3)
C13	5081(4)	9800(9)	7128(3)	91(3)
C19	6452(5)	3724(7)	7196(3)	81(2)
C20	6806(5)	3110(7)	6858(3)	91(3)
C15	6010(5)	8844(9)	7947(3)	91(3)

Table 2.10 Anisotropic Displacement Parameters ($Å^2×10^3$) for exp_8889. The Anisotropic displacement factor exponent takes the form: -

$2\pi^2[h^2a^{*2}U_{11}+2hka^*b^*U_{12}+\ldots]$.

Atom	U_{11}	U_{22}	U_{33}	U_{23}	U_{13}	U_{12}
P1	37.3(7)	39.0(8)	30.8(7)	2.0(6)	11.9(5)	1.8(6)
N1	42(2)	35(2)	28(2)	5.2(19)	16.3(19)	3(2)
N2	34(2)	31(2)	37(2)	4.0(19)	14.2(18)	-2.1(18)
C5	33(3)	35(3)	30(3)	2(2)	13(2)	1(2)
C2	34(3)	29(3)	30(2)	0(2)	14(2)	8(2)
C6	40(3)	40(3)	43(3)	-1(2)	18(2)	0(2)
C3	36(3)	32(3)	36(3)	1(2)	20(2)	2(2)
C1	40(3)	33(3)	32(3)	3(2)	16(2)	2(2)
C11	51(3)	35(3)	37(3)	-2(2)	17(2)	1(3)
C17	49(3)	40(3)	38(3)	4(3)	12(2)	9(3)
C23	43(3)	41(3)	44(3)	1(3)	25(2)	-1(2)
C10	44(3)	40(3)	54(3)	4(3)	24(3)	6(3)
C28	41(3)	45(3)	64(4)	-7(3)	29(3)	1(3)
C8	41(3)	54(4)	81(5)	4(4)	23(3)	-7(3)
C7	52(3)	34(3)	69(4)	-1(3)	29(3)	-4(3)
C24	49(3)	41(3)	75(4)	-12(3)	29(3)	-10(3)
C4	58(4)	47(3)	38(3)	15(3)	24(3)	9(3)
C18	74(4)	55(4)	48(4)	17(3)	22(3)	21(3)
C12	76(4)	65(4)	42(3)	1(3)	16(3)	22(4)
C27	38(3)	78(5)	56(4)	3(3)	23(3)	3(3)
C22	84(5)	55(4)	40(3)	4(3)	28(3)	19(4)
C26	50(4)	78(5)	61(4)	4(4)	16(3)	-16(4)
C25	70(5)	51(4)	89(5)	-4(4)	33(4)	-20(4)
C16	68(4)	85(5)	39(3)	-7(3)	14(3)	18(4)
C9	39(3)	57(4)	81(4)	4(4)	33(3)	2(3)
C21	126(7)	53(4)	62(4)	-1(4)	29(5)	33(4)
C14	115(7)	89(6)	61(5)	-21(4)	32(4)	38(5)
C13	85(5)	109(7)	72(5)	-9(5)	22(4)	45(5)
C19	119(7)	54(4)	68(5)	26(4)	32(5)	25(4)
C20	131(7)	50(4)	72(5)	3(4)	17(5)	30(5)
C15	114(7)	111(7)	42(4)	-9(4)	23(4)	35(6)

Table 2.11 Bond Lengths for exp_8889.

Atom	Atom	Length/Å	Atom	Atom	Length/Å
P1	C2	1.830(5)	C23	C28	1.513(7)
P1	C11	1.868(6)	C23	C24	1.511(8)
P1	C17	1.854(6)	C10	C9	1.519(8)

N1	N2	1.349(6)	C28	C27	1.518(8)
N1	C3	1.343(6)	C8	C7	1.516(8)
N1	C4	1.460(6)	C8	C9	1.500(9)
N2	C1	1.345(6)	C24	C25	1.522(8)
C5	C6	1.541(7)	C18	C19	1.510(10)
C5	C1	1.488(7)	C12	C13	1.528(9)
C5	C10	1.521(7)	C27	C26	1.505(9)
C2	C3	1.388(7)	C22	C21	1.523(9)
C2	C1	1.418(7)	C26	C25	1.498(9)
C6	C7	1.505(7)	C16	C15	1.506(9)
C3	C23	1.509(7)	C21	C20	1.510(10)
C11	C12	1.511(8)	C14	C13	1.500(10)
C11	C16	1.529(8)	C14	C15	1.511(11)
C17	C18	1.527(8)	C19	C20	1.512(11)
C17	C22	1.529(8)			

Table 2.12 Bond Angles for exp_8889.

Atom	Atom	Atom	Angle/°	Atom	Atom	Atom	Angle/°
C2	P1	C11	105.1(2)	C18	C17	C22	110.0(5)
C2	P1	C17	100.7(2)	C22	C17	P1	108.5(4)
C17	P1	C11	103.2(3)	C3	C23	C28	113.4(4)
N2	N1	C4	117.3(4)	C3	C23	C24	112.5(4)
C3	N1	N2	113.3(4)	C24	C23	C28	111.7(5)
C3	N1	C4	129.3(4)	C9	C10	C5	111.2(5)
C1	N2	N1	104.8(4)	C23	C28	C27	112.6(5)
C1	C5	C6	110.6(4)	C9	C8	C7	112.2(5)
C1	C5	C10	114.2(4)	C6	C7	C8	110.6(5)
C10	C5	C6	108.7(4)	C23	C24	C25	111.3(5)
C3	C2	P1	124.2(4)	C19	C18	C17	110.6(6)
C3	C2	C1	105.0(4)	C11	C12	C13	112.3(6)
C1	C2	P1	130.8(4)	C26	C27	C28	112.2(5)
C7	C6	C5	111.6(4)	C21	C22	C17	111.6(6)
N1	C3	C2	106.4(4)	C25	C26	C27	111.9(5)
N1	C3	C23	122.2(4)	C26	C25	C24	112.2(6)
C2	C3	C23	131.4(5)	C15	C16	C11	112.8(6)
N2	C1	C5	118.3(4)	C8	C9	C10	111.7(5)
N2	C1	C2	110.5(4)	C20	C21	C22	110.1(6)
C2	C1	C5	131.2(4)	C13	C14	C15	111.8(7)
C12	C11	P1	113.8(4)	C14	C13	C12	111.7(6)

C12	C11	C16	109.5(5)		C18	C19	C20	111.7(7)	
C16	C11	P1	108.2(4)		C21	C20	C19	111.5(6)	
C18	C17	P1	113.8(4)		C16	C15	C14	110.7(6)	

Table 2.13 Torsion Angles for exp_8889.

A	B	C	D	Angle/°	A	B	C	D	Angle/°
P1	C2	C3	N1	179.7(3)	C11	P1	C2	C3	125.0(4)
P1	C2	C3	C23	2.0(8)	C11	P1	C2	C1	-55.3(5)
P1	C2	C1	N2	179.8(4)	C11	P1	C17	C18	-59.3(5)
P1	C2	C1	C5	-3.5(8)	C11	P1	C17	C22	177.8(4)
P1	C11	C12	C13	-174.9(5)	C11	C12	C13	C14	54.5(10)
P1	C11	C16	C15	179.7(6)	C11	C16	C15	C14	-55.9(10)
P1	C17	C18	C19	-177.9(5)	C17	P1	C2	C3	-128.0(4)
P1	C17	C22	C21	-178.3(5)	C17	P1	C2	C1	51.7(5)
N1	N2	C1	C5	-176.4(4)	C17	P1	C11	C12	-141.1(5)
N1	N2	C1	C2	0.8(5)	C17	P1	C11	C16	97.0(5)
N1	C3	C23	C28	-117.1(6)	C17	C18	C19	C20	56.4(9)
N1	C3	C23	C24	115.0(6)	C17	C22	C21	C20	-56.3(9)
N2	N1	C3	C2	0.7(6)	C23	C28	C27	C26	51.9(7)
N2	N1	C3	C23	178.6(4)	C23	C24	C25	C26	-54.8(8)
C5	C6	C7	C8	56.6(7)	C10	C5	C6	C7	-58.1(6)
C5	C10	C9	C8	-56.1(7)	C10	C5	C1	N2	-48.2(6)
C2	P1	C11	C12	-35.9(5)	C10	C5	C1	C2	135.2(6)
C2	P1	C11	C16	-157.8(4)	C28	C23	C24	C25	53.5(7)
C2	P1	C17	C18	-167.8(4)	C28	C27	C26	C25	-52.5(8)
C2	P1	C17	C22	69.3(4)	C7	C8	C9	C10	54.0(7)
C2	C3	C23	C28	60.2(7)	C24	C23	C28	C27	-52.5(7)
C2	C3	C23	C24	-67.7(7)	C4	N1	N2	C1	-178.3(4)
C6	C5	C1	N2	74.7(6)	C4	N1	C3	C2	177.7(5)
C6	C5	C1	C2	-101.9(6)	C4	N1	C3	C23	-4.4(8)
C6	C5	C10	C9	57.0(6)	C18	C17	C22	C21	56.5(8)
C3	N1	N2	C1	-1.0(5)	C18	C19	C20	C21	-56.6(10)
C3	C2	C1	N2	-0.4(6)	C12	C11	C16	C15	55.2(8)
C3	C2	C1	C5	176.4(5)	C27	C26	C25	C24	54.3(8)
C3	C23	C28	C27	179.2(5)	C22	C17	C18	C19	-55.9(8)
C3	C23	C24	C25	-177.7(5)	C22	C21	C20	C19	55.7(10)
C1	C5	C6	C7	175.9(4)	C16	C11	C12	C13	-53.7(8)
C1	C5	C10	C9	-179.1(5)	C9	C8	C7	C6	-54.2(7)
C1	C2	C3	N1	-0.2(5)	C13	C14	C15	C16	55.0(11)

C1	C2	C3	C23	-177.8(5)
C15	C14	C13	C12	-54.3(11)

Table 2.14 Hydrogen Atom Coordinates (Å×10^4) and Isotropic Displacement Parameters (Å^2×10^3) for exp_8889.

Atom	*x*	*y*	*z*	U(eq)
H5	4771	6524	6109	39
H6A	4351	5320	5069	48
H6B	4996	4892	5586	48
H11	5518	7400	7015	49
H17	5745	5490	6457	53
H23	6616	9391	5241	48
H10A	3886	8003	5687	54
H10B	3670	7267	5129	54
H28A	7148	7447	5469	57
H28B	7314	7681	6091	57
H8A	3134	5000	5077	71
H8B	3088	4456	5613	71
H7A	4284	4283	6028	60
H7B	4040	3582	5461	60
H24A	6888	9872	6347	64
H24B	6481	10787	5859	64
H4A	5714	8759	4409	69
H4B	5427	9984	4587	69
H4C	4915	8910	4256	69
H18A	7009	5386	7393	72
H18B	6273	5522	7413	72
H12A	5072	9062	6406	76
H12B	5731	9895	6714	76
H27A	8313	8091	5957	67
H27B	7921	8992	5461	67
H22A	6405	5394	5919	70
H22B	7091	5295	6446	70
H26A	8216	9545	6568	78
H26B	8525	10262	6195	78
H25A	7471	11164	5691	83
H25B	7645	11452	6311	83
H16A	6596	7551	7743	79
H16B	6695	8945	7573	79
H9A	3556	6287	6085	67

H9B	2926	6672	5550	67
H21A	6047	3394	6095	99
H21B	6787	3256	6081	99
H14A	5354	10308	7927	107
H14B	5910	10705	7696	107
H13A	4853	10597	6974	109
H13B	4729	9210	7138	109
H19A	5964	3500	7044	98
H19B	6654	3396	7567	98
H20A	7301	3265	7030	109
H20B	6732	2196	6847	109
H15A	6360	9043	8305	109
H15B	5705	8200	7993	109

Table 2.15 Crystal data and structure refinement for Pd-**L25**(η^3-C_3H_5)Cl complex.

Identification code	exp_9180
Empirical formula	$C_{32}H_{54}Cl_3N_2PPd$
Formula weight	710.49
Temperature/K	293(2)
Crystal system	triclinic
Space group	P-1
a/Å	10.3981(5)
b/Å	13.0129(6)
c/Å	14.2206(7)
α/°	111.933(4)
β/°	93.039(4)
γ/°	96.714(4)
Volume/Å^3	1762.88(15)
Z	2
ρ_{calc}g/cm^3	1.338
μ/mm^{-1}	0.822
F(000)	744.0
Crystal size/mm^3	0.31 × 0.15 × 0.1
Radiation	Mo Kα (λ = 0.71073)
2Θ range for data collection/°	3.966 to 49
Index ranges	$-9 \leq h \leq 12$, $-15 \leq k \leq 15$, $-16 \leq l \leq 16$
Reflections collected	12705
Independent reflections	5805 [R_{int} = 0.0263, R_{sigma} = 0.0402]

Data/restraints/parameters	5805/0/353
Goodness-of-fit on F^2	1.049
Final R indexes [I>=2σ (I)]	$R_1 = 0.0420$, $wR_2 = 0.1029$
Final R indexes [all data]	$R_1 = 0.0491$, $wR_2 = 0.1085$
Largest diff. peak/hole / e Å^{-3}	1.19/-0.99

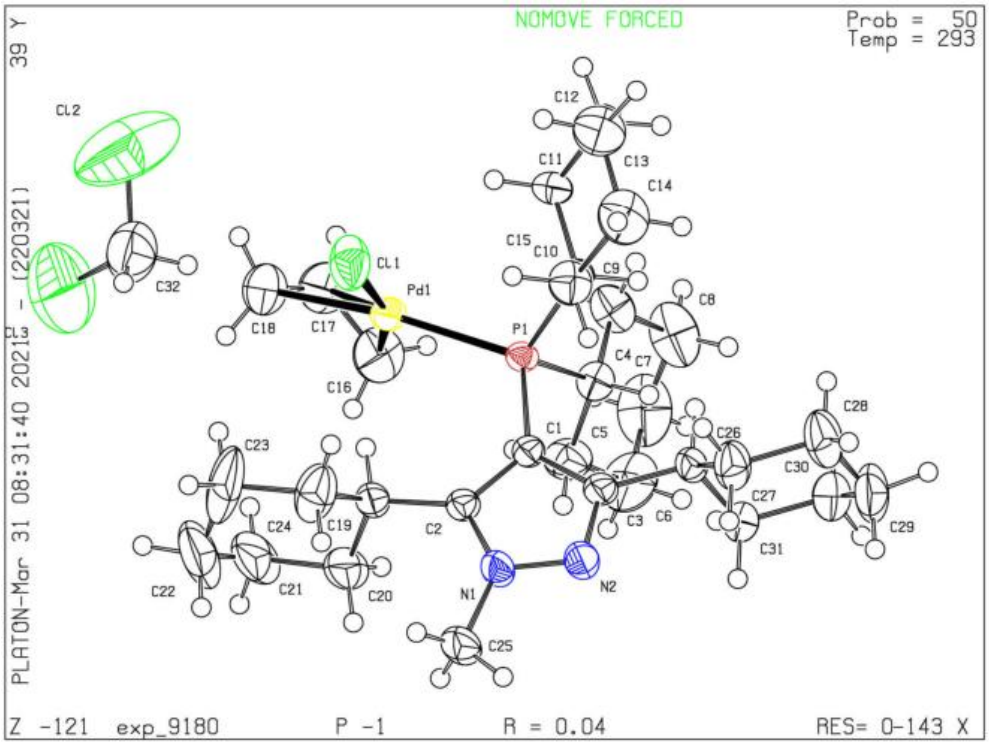

Table 2.16 Fractional Atomic Coordinates (×10^4) and Equivalent Isotropic Displacement Parameters (Å^2×10^3) for exp_9180. U_{eq} is defined as 1/3 of of the trace of the orthogonalised U_{IJ} tensor.

Atom	*x*	*y*	*z*	U(eq)
Pd1	3981.5(3)	5004.1(2)	8326.1(2)	35.83(12)
P1	3285.0(8)	6542.8(7)	8091.3(6)	26.81(19)
Cl1	5989.7(11)	5133.5(9)	7655.1(10)	66.5(3)
Cl2	8859(3)	3120(3)	7469(3)	203.6(16)
Cl3	6600(4)	1391(2)	6706(3)	194.8(13)
N1	2066(3)	5564(2)	5163(2)	38.3(7)
N2	1908(3)	6660(2)	5442(2)	42.2(7)
C1	2730(3)	6336(3)	6794(2)	29.8(7)
C10	4576(3)	7786(3)	8562(2)	31.9(7)
C4	1884(3)	7095(3)	8767(3)	37.7(8)

C2	2555(3)	5329(3)	5947(2)	30.1(7)
C26	2197(4)	8354(3)	6967(3)	35.7(8)
C3	2314(3)	7134(3)	6429(2)	33.2(8)
C19	2788(4)	4185(3)	5850(3)	35.8(8)
C31	772(4)	8532(3)	7059(3)	48.4(10)
C11	5455(4)	7812(3)	9472(3)	45.1(9)
C9	2110(4)	7496(4)	9922(3)	51.1(10)
C25	1617(5)	4833(3)	4105(3)	51.6(11)
C15	5410(4)	7902(3)	7743(3)	46.2(9)
C27	2836(5)	9089(3)	6444(3)	51.2(10)
C5	636(4)	6256(4)	8333(3)	53.6(11)
C20	1523(5)	3368(3)	5607(4)	61.1(12)
C28	2724(5)	10320(3)	7023(4)	64.3(13)
C12	6441(5)	8875(4)	9900(4)	68.0(14)
C30	646(5)	9751(4)	7631(4)	59.7(12)
C8	909(5)	7946(4)	10406(4)	73.5(15)
C16	2359(5)	4349(4)	8875(4)	67.8(13)
C17	3463(6)	4037(4)	9225(4)	70.5(14)
C18	4275(6)	3461(4)	8545(4)	72.5(15)
C24	3820(5)	3724(4)	5154(4)	68.0(14)
C13	7231(5)	9032(4)	9094(5)	83.9(17)
C14	6368(5)	8989(4)	8193(4)	70.8(14)
C7	-298(6)	7090(5)	9983(5)	86.6(18)
C29	1321(6)	10488(4)	7146(4)	76.0(15)
C23	4008(8)	2573(6)	5155(5)	107(3)
C21	1778(7)	2239(4)	5598(4)	88.6(19)
C6	-533(5)	6715(5)	8847(5)	83.3(17)
C22	2739(10)	1763(5)	4888(5)	120(3)
C32	7413(7)	2623(5)	6712(5)	94.4(19)

Table 2.17 Anisotropic Displacement Parameters ($Å^2 \times 10^3$) for exp_9180. The Anisotropic displacement factor exponent takes the form: $-2\pi^2[h^2a^{*2}U_{11}+2hka^*b^*U_{12}+\ldots]$.

Atom	U_{11}	U_{22}	U_{33}	U_{23}	U_{13}	U_{12}
Pd1	41.17(19)	30.35(17)	37.73(18)	18.15(12)	-6.33(12)	-0.72(11)
P1	29.4(5)	26.5(4)	24.5(4)	11.2(3)	-0.5(3)	0.6(3)
Cl1	45.5(6)	47.1(6)	102.8(9)	21.0(6)	18.8(6)	12.6(5)
Cl2	111.9(18)	297(4)	287(4)	232(3)	-34(2)	-24(2)

Cl3	229(3)	91.4(16)	263(4)	79.6(19)	-3(3)	-5.9(18)
N1	55(2)	29.6(16)	27.3(15)	8.3(12)	-2.4(13)	8.1(14)
N2	65(2)	32.5(16)	29.4(16)	12.1(13)	-4.9(14)	10.1(15)
C1	33.8(19)	27.9(17)	28.1(17)	12.0(14)	-1.3(13)	3.3(14)
C10	30.6(18)	24.9(17)	37.3(19)	10.5(14)	-3.3(14)	0.4(14)
C4	36(2)	40(2)	40(2)	17.7(16)	8.0(15)	6.0(16)
C2	32.3(18)	30.4(18)	27.6(17)	12.0(14)	0.4(13)	3.3(14)
C26	52(2)	25.6(17)	29.0(18)	10.8(14)	-3.9(15)	5.8(15)
C3	40(2)	30.2(18)	29.0(18)	12.9(14)	-4.0(14)	2.8(15)
C19	48(2)	30.5(18)	27.9(17)	10.9(14)	-1.9(15)	6.9(15)
C31	54(3)	37(2)	52(2)	14.9(18)	-5.2(18)	11.7(18)
C11	47(2)	40(2)	40(2)	10.2(17)	-12.7(16)	1.3(17)
C9	64(3)	49(2)	39(2)	15.5(18)	16.4(19)	4(2)
C25	78(3)	41(2)	28.9(19)	7.1(16)	-9.6(18)	9(2)
C15	41(2)	45(2)	55(2)	23.1(19)	10.5(17)	-0.7(17)
C27	74(3)	38(2)	50(2)	23.3(18)	12(2)	14(2)
C5	35(2)	61(3)	61(3)	21(2)	3.2(18)	0.8(19)
C20	74(3)	39(2)	69(3)	28(2)	-19(2)	-10(2)
C28	98(4)	35(2)	67(3)	26(2)	18(3)	10(2)
C12	56(3)	45(3)	78(3)	3(2)	-28(2)	0(2)
C30	64(3)	48(3)	65(3)	14(2)	7(2)	21(2)
C8	86(4)	65(3)	70(3)	22(3)	48(3)	11(3)
C16	72(3)	59(3)	85(3)	46(3)	14(3)	-6(2)
C17	95(4)	62(3)	71(3)	51(3)	-6(3)	-5(3)
C18	96(4)	45(3)	87(4)	43(3)	-13(3)	1(3)
C24	92(4)	73(3)	56(3)	32(2)	29(3)	46(3)
C13	44(3)	59(3)	135(5)	31(3)	-15(3)	-16(2)
C14	54(3)	58(3)	106(4)	42(3)	14(3)	-10(2)
C7	79(4)	87(4)	111(5)	48(4)	62(3)	21(3)
C29	111(5)	37(2)	82(4)	21(2)	8(3)	28(3)
C23	183(7)	102(5)	70(4)	39(4)	52(4)	113(6)
C21	142(6)	35(3)	80(4)	25(3)	-30(4)	-13(3)
C6	41(3)	96(4)	124(5)	52(4)	25(3)	12(3)
C22	240(10)	34(3)	73(4)	10(3)	-21(5)	29(5)
C32	119(5)	80(4)	92(4)	36(3)	7(4)	34(4)

Table 2.18 Bond Lengths for exp_9180.

Atom	Atom	Length/Å	Atom	Atom	Length/Å
Pd1	P1	2.3363(9)	C26	C31	1.531(5)

Pd1	Cl1	2.3555(11)	C26	C27	1.531(5)
Pd1	C16	2.117(4)	C19	C20	1.526(6)
Pd1	C17	2.151(4)	C19	C24	1.520(6)
Pd1	C18	2.197(4)	C31	C30	1.513(5)
P1	C1	1.813(3)	C11	C12	1.519(6)
P1	C10	1.859(3)	C9	C8	1.529(6)
P1	C4	1.854(3)	C15	C14	1.527(6)
Cl2	C32	1.709(7)	C27	C28	1.525(6)
Cl3	C32	1.719(7)	C5	C6	1.518(6)
N1	N2	1.363(4)	C20	C21	1.520(6)
N1	C2	1.351(4)	C28	C29	1.510(7)
N1	C25	1.462(4)	C12	C13	1.506(8)
N2	C3	1.326(4)	C30	C29	1.509(7)
C1	C2	1.394(4)	C8	C7	1.506(8)
C1	C3	1.421(5)	C16	C17	1.390(7)
C10	C11	1.532(5)	C17	C18	1.379(7)
C10	C15	1.529(5)	C24	C23	1.533(7)
C4	C9	1.523(5)	C13	C14	1.505(8)
C4	C5	1.529(5)	C7	C6	1.500(8)
C2	C19	1.493(5)	C23	C22	1.522(11)
C26	C3	1.507(5)	C21	C22	1.480(10)

Table 2.19 Bond Angles for exp_9180.

Atom	Atom	Atom	Angle/°	Atom	Atom	Atom	Angle/°
P1	Pd1	Cl1	96.22(4)	C31	C26	C27	108.8(3)
C16	Pd1	P1	102.99(14)	N2	C3	C1	110.9(3)
C16	Pd1	Cl1	160.29(15)	N2	C3	C26	117.3(3)
C16	Pd1	C17	38.0(2)	C1	C3	C26	131.7(3)
C16	Pd1	C18	67.6(2)	C2	C19	C20	112.2(3)
C17	Pd1	P1	135.94(17)	C2	C19	C24	114.2(3)
C17	Pd1	Cl1	125.44(17)	C24	C19	C20	113.1(4)
C17	Pd1	C18	36.97(19)	C30	C31	C26	111.9(3)
C18	Pd1	P1	170.04(16)	C12	C11	C10	111.3(3)
C18	Pd1	Cl1	92.97(16)	C4	C9	C8	110.3(4)
C1	P1	Pd1	116.21(11)	C14	C15	C10	109.7(3)
C1	P1	C10	106.55(15)	C28	C27	C26	111.3(3)
C1	P1	C4	101.03(16)	C6	C5	C4	111.7(4)
C10	P1	Pd1	111.84(11)	C21	C20	C19	111.1(4)
C4	P1	Pd1	116.88(12)	C29	C28	C27	111.2(4)

C4	P1	C10	102.81(16)	C13	C12	C11	111.9(4)
N2	N1	C25	116.1(3)	C29	C30	C31	111.4(4)
C2	N1	N2	112.9(3)	C7	C8	C9	111.6(4)
C2	N1	C25	130.8(3)	C17	C16	Pd1	72.3(3)
C3	N2	N1	105.2(3)	C16	C17	Pd1	69.7(2)
C2	C1	P1	126.7(3)	C18	C17	Pd1	73.3(3)
C2	C1	C3	105.2(3)	C18	C17	C16	120.2(5)
C3	C1	P1	128.1(2)	C17	C18	Pd1	69.7(3)
C11	C10	P1	111.7(2)	C19	C24	C23	109.2(4)
C15	C10	P1	114.1(2)	C14	C13	C12	111.3(4)
C15	C10	C11	109.7(3)	C13	C14	C15	111.7(4)
C9	C4	P1	114.4(3)	C6	C7	C8	111.3(4)
C9	C4	C5	111.9(3)	C30	C29	C28	112.0(4)
C5	C4	P1	110.9(3)	C22	C23	C24	112.8(5)
N1	C2	C1	105.8(3)	C22	C21	C20	111.8(5)
N1	C2	C19	123.6(3)	C7	C6	C5	111.3(5)
C1	C2	C19	130.6(3)	C21	C22	C23	110.6(4)
C3	C26	C31	111.4(3)	Cl2	C32	Cl3	115.7(4)
C3	C26	C27	112.8(3)				

Table 2.20 Torsion Angles for exp_9180.

A	B	C	D	Angle/°	A	B	C	D	Angle/°
Pd1	P1	C1	C2	6.9(3)	C4	C5	C6	C7	-54.3(6)
Pd1	P1	C1	C3	-176.9(3)	C2	N1	N2	C3	0.3(4)
Pd1	P1	C10	C11	-31.6(3)	C2	C1	C3	N2	0.4(4)
Pd1	P1	C10	C15	93.6(3)	C2	C1	C3	C26	176.7(4)
Pd1	P1	C4	C9	59.9(3)	C2	C19	C20	C21	-175.3(4)
Pd1	P1	C4	C5	-67.7(3)	C2	C19	C24	C23	177.6(4)
Pd1	C16	C17	C18	-55.3(4)	C26	C31	C30	C29	55.9(5)
P1	C1	C2	N1	176.7(3)	C26	C27	C28	C29	-56.4(5)
P1	C1	C2	C19	-1.5(5)	C3	C1	C2	N1	-0.2(4)
P1	C1	C3	N2	-176.4(3)	C3	C1	C2	C19	-178.4(3)
P1	C1	C3	C26	-0.1(6)	C3	C26	C31	C30	178.0(3)
P1	C10	C11	C12	-175.7(3)	C3	C26	C27	C28	-178.8(4)
P1	C10	C15	C14	175.9(3)	C19	C20	C21	C22	-55.3(6)
P1	C4	C9	C8	179.4(3)	C19	C24	C23	C22	54.0(6)
P1	C4	C5	C6	-177.6(3)	C31	C26	C3	N2	69.5(4)
N1	N2	C3	C1	-0.4(4)	C31	C26	C3	C1	-106.7(4)
N1	N2	C3	C26	-177.3(3)	C31	C26	C27	C28	57.0(5)

N1	C2	C19	C20	-65.7(5)	C31	C30	C29	C28	-54.0(6)
N1	C2	C19	C24	64.7(5)	C11	C10	C15	C14	-57.8(4)
N2	N1	C2	C1	0.0(4)	C11	C12	C13	C14	54.0(6)
N2	N1	C2	C19	178.3(3)	C9	C4	C5	C6	53.4(5)
C1	P1	C10	C11	-159.6(3)	C9	C8	C7	C6	-57.3(6)
C1	P1	C10	C15	-34.4(3)	C25	N1	N2	C3	176.7(3)
C1	P1	C4	C9	-172.9(3)	C25	N1	C2	C1	-175.8(4)
C1	P1	C4	C5	59.4(3)	C25	N1	C2	C19	2.6(6)
C1	C2	C19	C20	112.2(4)	C15	C10	C11	C12	56.7(4)
C1	C2	C19	C24	-117.4(4)	C27	C26	C3	N2	-53.3(5)
C10	P1	C1	C2	132.3(3)	C27	C26	C3	C1	130.5(4)
C10	P1	C1	C3	-51.5(3)	C27	C26	C31	C30	-57.0(4)
C10	P1	C4	C9	-63.0(3)	C27	C28	C29	C30	54.3(6)
C10	P1	C4	C5	169.4(3)	C5	C4	C9	C8	-53.4(5)
C10	C11	C12	C13	-54.8(5)	C20	C19	C24	C23	-52.5(6)
C10	C15	C14	C13	58.1(5)	C20	C21	C22	C23	56.7(7)
C4	P1	C1	C2	-120.7(3)	C12	C13	C14	C15	-55.9(6)
C4	P1	C1	C3	55.6(3)	C8	C7	C6	C5	56.3(6)
C4	P1	C10	C11	94.6(3)	C16	C17	C18	Pd1	53.6(4)
C4	P1	C10	C15	-140.2(3)	C24	C19	C20	C21	53.7(5)
C4	C9	C8	C7	55.5(6)	C24	C23	C22	C21	-57.1(7)

Table 2.21 Hydrogen Atom Coordinates (Å×10^4) and Isotropic Displacement Parameters (Å^2×10^3) for exp_9180.

Atom	*x*	*y*	*z*	U(eq)
H10	4136	8449	8805	38
H4	1752	7755	8617	45
H26	2640	8609	7658	43
H19	3142	4268	6531	43
H31A	311	8275	6382	58
H31B	369	8089	7410	58
H11A	4923	7769	10001	54
H11B	5910	7166	9260	54
H9A	2858	8082	10176	61
H9B	2294	6880	10110	61
H25A	1353	5276	3739	77
H25B	891	4296	4089	77
H25C	2311	4449	3792	77
H15A	5883	7270	7493	55

H15B	4855	7907	7175	55
H27A	3748	9002	6405	61
H27B	2420	8846	5754	61
H5A	482	6079	7607	64
H5B	742	5569	8427	64
H20A	935	3676	6112	73
H20B	1108	3270	4945	73
H28A	3212	10583	7690	77
H28B	3100	10759	6658	77
H12A	5988	9514	10191	82
H12B	7021	8842	10442	82
H30A	-268	9835	7641	72
H30B	1025	9988	8331	72
H8A	1048	8155	11138	88
H8B	785	8613	10281	88
H16A	1937	4891	9386	81
H16B	1750	3752	8369	81
H17	3751	4348	9957	85
H18A	3882	2760	8008	87
H18B	5136	3437	8828	87
H24A	4635	4231	5391	82
H24B	3550	3654	4467	82
H13A	7793	9749	9382	101
H13B	7780	8450	8871	101
H14A	6904	9053	7673	85
H14B	5888	9620	8402	85
H7A	-204	6448	10158	104
H7B	-1043	7411	10291	104
H29A	1287	11266	7563	91
H29B	862	10321	6482	91
H23A	4612	2253	4667	128
H23B	4391	2667	5824	128
H21A	2097	2324	6281	106
H21B	967	1724	5399	106
H6A	-713	7343	8676	100
H6B	-1291	6140	8595	100
H22A	2389	1613	4196	143
H22B	2906	1060	4924	143
H32A	7576	2513	6018	113
H32B	6846	3191	6931	113

2.4.9 Computational Details

All density functional theory (DFT) calculations were performed using the Gaussian 16 software.[30] The B3PW91[31] functional has been used in this study. This hybrid functional has been shown to perform well in modelling a range of reactions involving transition metals.[32] Geometry optimizations of all the minima and transition states were fully optimized at the B3PW91-D3(BJ) level of theory, with the SDD[33] pseudopotential for Pd and the 6-31G(d) for other atoms in dioxane solvent employing the Solvation Model Based on Density (SMD).[34] Dispersion corrections according to Grimmes's DFT-D3 scheme[35] including Becke–Johnson damping was utilized.[36] Vibrational frequencies were computed at the same level of theory to check whether each optimized structure is an energy minimum or a transition state. Intrinsic reaction coordinates (IRC) calculations were performed to confirm whether the located transition state connects the correct reactant and product.[37] On the basis of the optimized structures, the single point energies were calculated at the PBE0-D3(BJ)/Def2-TZVP[38] level and solvation energy corrections were calculated using the SMD model with dioxane as the solvent. The reported Gibbs free energies were corrected using the quasi-harmonic mode[39] with a cut-off frequency of 100 cm^{-1}. The Gibbs free energies were further corrected to standard state from 1 atm to 1 mol/L, a correction of $RTLn(c_s/c_g)$ (1.89 kcal/mol) is added to energies of all species. c_s is the standard molar concentration in solution (1 mol/L), c_g is the standard molar concentration in the gas phase (0.0446 mol/L), and R is the gas constant. Conformational searches are conducted to ensure that the most stable conformers are located The NBO calculations were performed with the NBO7.0

package.[40] For the QTAIM calculations, electron density map, and NCI scatter plots were performed with the Multiwfn 3.7 software package.[41] The NCI isosurface plot was produced with VMD software.[42] The images of computed species were generated using CYLView.[43]

Table 2.22 Table of energies of minimum energy structures[a]

Structure	*ZPE*	*tcH*	*E caled*	*H*	*G*	*qh-G*	*Imaginary frequency (cm^{-1})*
6A	1.176975	1.235682	-2751.71632910	-2750.48064710	-2750.63025910	-2750.6194471	
6B	0.58733	0.617604	-1439.79093910	-1439.17333510	-1439.26373210	-1439.25862810	
6C	0.6979	0.743602	-3091.81518210	-3091.07158010	-3091.20014510	-3091.18849110	
6D-TS	0.697705	0.742761	-3091.79757110	-3091.05481010	-3091.18108210	-3091.17025110	-65.21
6E	0.699589	0.745206	-3091.84063510	-3091.09542910	-3091.22358310	-3091.21229010	
6F	0.700731	0.745836	-3091.83843010	-3091.09259410	-3091.21787110	-3091.20775910	
6G	0.850658	0.903780	-3418.53838610	-3417.63460610	-3417.77652510	-3417.76452910	
6H	0.836792	0.891790	-4017.74323710	-4016.85144710	-4016.99804110	-4016.98537610	
6I	0.833467	0.885113	-2957.78889010	-2956.90377710	-2957.04684410	-2957.03265810	
6J-TS	0.832273	0.883424	-2957.76420710	-2956.88078310	-2957.02014110	-2957.00749910	-411.51
6K	0.835114	0.886583	-2957.80059810	-2956.91401510	-2957.05548010	-2957.04190510	
6L	0.697291	0.743141	-3091.81026210	-3091.06712110	-3091.19547010	-3091.18389110	
6M-TS	0.700288	0.745094	-3091.77952910	-3091.03443510	-3091.15812610	-3091.14847110	-383.25
6N	0.700332	0.745420	-3091.84845510	-3091.10303510	-3091.22663410	-3091.21750110	
$6A_{L24}$	0.989098	1.04221	-2557.72270210	-2556.68049210	-2556.82065310	-2556.80975210	
$6B_{L24}$	0.494203	0.521415	-1342.79478810	-1342.27337310	-1342.35713610	-1342.35260110	
$6C_{L24}$	0.604679	0.647309	-2994.82015310	-2994.17284410	-2994.29389910	-2994.28328510	
$6D\text{-}TS_{L24}$	0.604235	0.646332	-2994.80151810	-2994.15518610	-2994.27530710	-2994.26492510	-60.94
$6H_{L24}$	0.743312	0.795304	-3920.74222910	-3919.94692510	-3920.08640310	-3920.07483210	
$6I_{L24}$	0.740152	0.788649	-2860.77706510	-2859.98841610	-2860.12224610	-2860.11014410	
$6J\text{-}TS_{L24}$	0.739188	0.787222	-2860.75287310	-2859.96565110	-2860.09823110	-2860.08635110	-407.66
$6L_{L24}$	0.604689	0.647172	-2994.82280510	-2994.17563310	-2994.29596010	-2994.28556410	
$6M\text{-}TS_{L24}$	0.603922	0.645885	-2994.78431710	-2994.13843210	-2994.25556410	-2994.24683210	-382.78
$6A_{L25}$	1.443354	1.509649	-3218.3246440	-3218.32163210	-3216.81198310	-3216.98216810	
$6B_{L25}$	0.720525	0.754492	-1673.0992790	-1673.09626710	-1672.34177510	-1672.44239210	
$6C_{L25}$	0.83124	0.880609	-3325.1242270	-3325.12121510	-3324.24060610	-3324.37859310	
$6D\text{-}TS_{L25}$	0.831424	0.880083	-3325.1069960	-3325.10398410	-3324.22390110	-3324.35918810	-105.27
$6H_{L25}$	0.970087	1.028745	-4251.0508180	-4251.04780610	-4250.01906110	-4250.17539410	
$6I_{L25}$	0.967041	1.022236	-3191.0926810	-3191.08966910	-3190.06743310	-3190.21766110	
$6J\text{-}TS_{L25}$	0.966291	1.020840	-3191.0721850	-3191.06917310	-3190.04833310	-3190.19613810	-409.79
$6L_{L25}$	0.832318	0.881213	-3325.11999110	-3324.23877810	-3324.37297310	-3324.36058510	
$6M\text{-}TS_{L25}$	0.829946	0.878808	-3325.08134110	-3324.20253310	-3324.33607810	-3324.32422210	-372.07
$6A_{L28}$	1.138420	1.192718	-2749.33024010	-2748.13752210	-2748.28119410	-2748.26861910	
$6B_{L28}$	0.568521	0.596451	-1438.59385310	-1437.99740210	-1438.08503710	-1438.07885610	
$6C_{L28}$	0.679124	0.722597	-3090.61735310	-3089.89475610	-3090.02049810	-3090.00781010	
$6D\text{-}TS_{L28}$	0.678822	0.721633	-3090.60074110	-3089.87910810	-3090.00242010	-3089.99062810	-104.31

$6H_{L28}$	0.817858	0.870575	-4016.54464020	-4015.67406520	-4015.81727620	-4015.80402220	
$6I_{L28}$	0.814818	0.863226	-2956.58636410	-2955.72313810	-2955.85693510	-2955.84446210	
$6J\text{-}TS_{L28}$	0.813894	0.86257	-2956.56612110	-2955.70355110	-2955.83906310	-2955.82576710	-409.52
$6L_{L28}$	0.680497	0.723191	-3090.621037	-3090.61802510	-3089.89483410	-3090.01520110	
$6M\text{-}TS_{L28}$	0.678057	0.720832	-3090.581286	-3090.57827410	-3089.85744210	-3089.97781010	-378.02
$6A_{L29}$	1.137594	1.192241	-2749.33138110	-2748.13914010	-2748.28403010	-2748.27098710	
$6B_{L29}$	0.5679650	0.596120	-1438.59418410	-1437.99806410	-1438.08632510	-1438.07987910	
$6C_{L29}$	0.6788550	0.722379	-3090.61916710	-3089.89678810	-3090.02316310	-3090.00999710	
$6D\text{-}TS_{L29}$	0.6783520	0.721358	-3090.60119810	-3089.87984010	-3090.00405310	-3089.99180710	-97.49
$6H_{L29}$	0.8170540	0.870095	-4016.54564810	-4015.67555310	-4015.82029510	-4015.80626410	
$6I_{L29}$	0.8142380	0.863633	-2956.58970310	-2955.72607010	-2955.86382010	-2955.84996910	
$6J\text{-}TS_{L29}$	0.8133900	0.862229	-2956.56752710	-2955.70529810	-2955.84144410	-2955.82781110	-410.32
$6L_{L29}$	0.679475	0.722682	-3090.62061710	-3089.89793510	-3090.02049710	-3090.00923510	
$6M\text{-}TS_{L29}$	0.677112	0.720242	-3090.57900510	-3089.85876310	-3089.98108810	-3089.97002870	-367.25
$6A_{L32}$	1.161624	1.222449	-3203.82127710	-3202.59882810	-3202.75722310	-3202.74269710	
$6B_{L32}$	0.578847	0.609952	-1665.86136910	-1665.25141710	-1665.34460410	-1665.33853010	
$6C_{L32}$	0.690673	0.737106	-3317.87852010	-3317.14141410	-3317.27135910	-3317.25926210	
$6D\text{-}TS_{L32}$	0.689684	0.735974	-3317.85711110	-3317.12113710	-3317.25166810	-3317.23913510	-145.92
$6H_{L32}$	0.82897	0.885003	-4243.79907210	-4242.91406910	-4243.06426110	-4243.05025410	
$6I_{L32}$	0.82591	0.878525	-3183.85164310	-3182.97311810	-3183.11657810	-3183.10274410	
$6J\text{-}TS_{L32}$	0.825317	0.877293	-3183.82815410	-3182.95086110	-3183.09244210	-3183.07898510	-407.57
$6L_{L32}$	0.690369	0.606857	-3317.87587810	-3317.13895810	-3317.26902110	-3317.25680510	
$6M\text{-}TS_{L32}$	0.689360	0.606299	-3317.85702210	-3317.12145310	-3317.25072310	-3317.23883010	-115.27
$6A_{L26\text{-}3'}$	1.176975	1.08607	-2751.71632910	-2750.48064710	-2750.63025910	-2750.61944710	
$6B_{L26\text{-}3'}$	0.587467	0.527413	-1439.78799010	-1439.17033010	-1439.26057710	-1439.25551210	
$6C_{L26\text{-}3'}$	0.697874	0.615115	-3091.81307310	-3091.06954110	-3091.19795810	-3091.18627110	
$6D\text{-}TS_{L26\text{-}3'}$	0.697891	0.616580	-3091.79505110	-3091.05218310	-3091.17847110	-3091.16749010	-69.13
$6H_{L26\text{-}3'}$	0.836086	0.742897	-4017.74085110	-4016.84946110	-4016.99795410	-4016.98443910	
$6I_{L26\text{-}3'}$	0.833498	0.744088	-2957.78704910	-2956.90198710	-2957.04296110	-2957.02984310	
$6J\text{-}TS_{L26\text{-}3'}$	0.832454	0.743968	-2957.76200310	-2956.87845710	-2957.01803510	-2957.00513010	-407.54
$6L_{L26\text{-}3'}$	0.697236	0.743164	-3091.80768010	-3091.06451610	-3091.19353810	-3091.18157810	
$6M\text{-}TS_{L26\text{-}3'}$	0.696705	0.741947	-3091.77670510	-3091.03475810	-3091.16063810	-3091.15007510	-378.30
K_3PO_4	0.017434	0.028491	-2441.56056910	-2441.53207810	-2441.58028410	-2441.57899610	
K_2HPO_4	0.028151	0.037752	-1842.36264510	-1842.32489310	-1842.37010910	-1842.36902510	
KCl	0.000541	0.00435	-1059.90313710	-1059.89878710	-1059.92610110	-1059.92610310	
L24	0.493153	0.518601	-1214.84989410	-1214.33129310	-1214.41092610	-1214.40647510	
L25	0.719659	0.751755	-1545.152444	-1545.14943210	-1544.39767710	-1544.49325610	
L26	0.586366	0.614858	-1311.84589110	-1311.23103310	-1311.31684510	-1311.31219110	
L26-3'	0.586581	0.614977	-1311.84415110	-1311.22917410	-1311.31484210	-1311.31002610	
L28	0.567968	0.593852	-1310.64621110	-1310.05235910	-1310.13423010	-1310.12909610	
L29	0.5670150	0.593256	-1310.64695810	-1310.05370210	-1310.13727110	-1310.13134510	

L32	0.578653	0.60802	-1537.90249810	-1537.29447810	-1537.38372910	-1537.37781510	
1a	0.110713	0.124984	-1651.98112710	-1651.85614310	-1651.91226710	-1651.91022610	
2a	0.146404	0.15455	-326.65219810	-326.49764810	-326.53703710	-326.53692910	
3a	0.246742	0.267245	-1517.97273510	-1517.70549010	-1517.77702910	-1517.77251410	

[a]Zero-point correction(ZPE), thermal correction to enthalpy (tcH), energies(E), enthalpies (H), Gibbs free energies (G) (in Hartree), and quasi-harmonic corrected Gibbs free energy of the structures calculated at the PBE0-D3(BJ)/Def2-TZVP-SMD(dioxane)//B3PW91-D3(BJ)/6-31G(d)-SDD(Pd)-SMD(dioxane) level of theory.

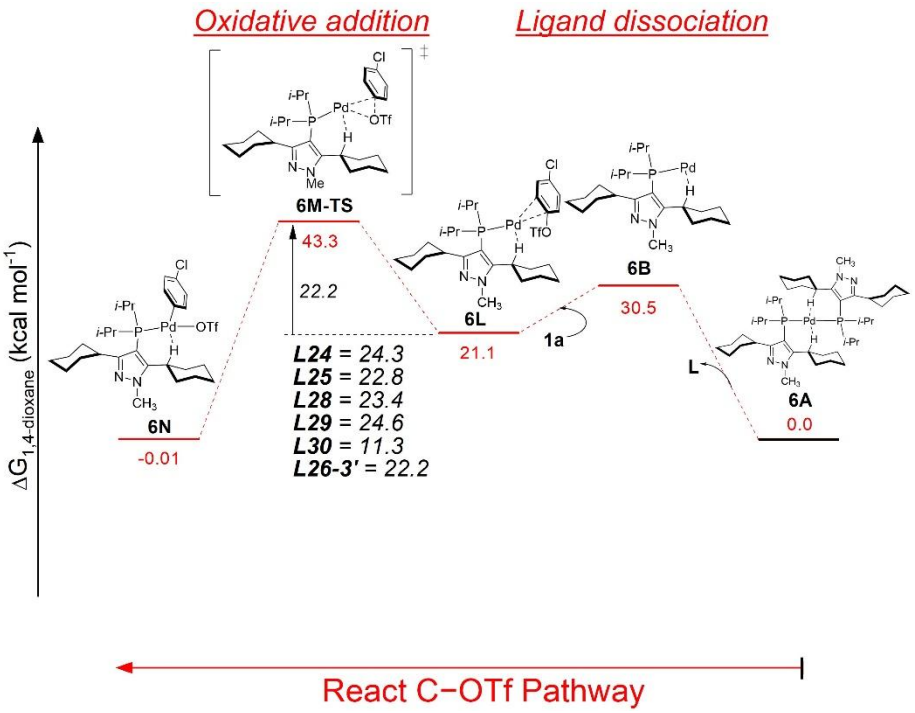

Figure 2.8 Free energy profile calculated for chemoselective palladium-catalyzed amination of chloro phenyltriflate with C–OTf pathway.

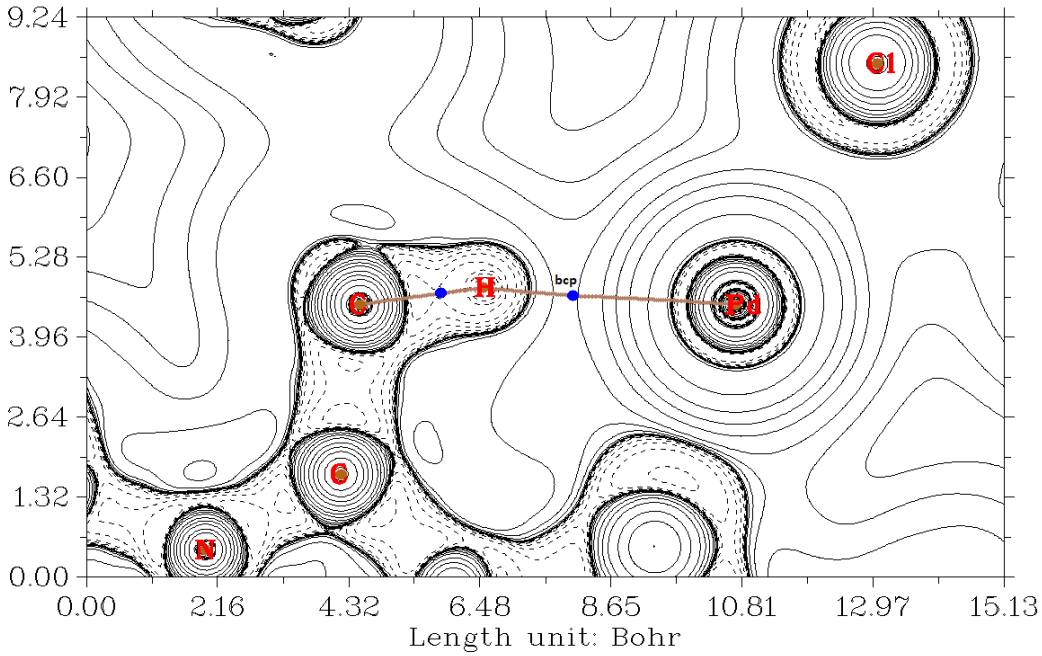

Figure 2.9 Electron density map of **6D-TS**. Laplacian of the electron density at the BCP is [$\nabla^2\varrho$(BCP) = 0.0740 e/bohr^5] and the energy density is [H(BCP) = -0.0056 e/bohr^3]

SECOND ORDER PERTURBATION THEORY ANALYSIS OF FOCK MATRIX IN NBO BASIS

Threshold for printing: 0.50 kcal/mol
(Intermolecular threshold: 0.05 kcal/mol)

Donor (L) NBO	Acceptor (NL) NBO	E(2) kcal/mol	E(NL)-E(L) a.u.	F(L,NL) a.u.
57. LP (1)Pd 1	177. BD*(1) P 2- C 65	0.67	0.44	0.015
57. LP (1)Pd 1	216. BD*(1) C 31- H 34	0.55	0.60	0.016
57. LP (1)Pd 1	228. BD*(1) C 38- H 45	0.07	0.62	0.006
58. LP (2)Pd 1	178. BD*(1) P 2- C 73	0.29	0.45	0.010
58. LP (2)Pd 1	216. BD*(1) C 31- H 34	0.12	0.61	0.008
58. LP (2)Pd 1	249. BD*(1) C 65- C 67	0.12	0.60	0.007
59. LP (3)Pd 1	178. BD*(1) P 2- C 73	0.27	0.45	0.010
59. LP (3)Pd 1	216. BD*(1) C 31- H 34	2.53	0.61	0.035
59. LP (3)Pd 1	225. BD*(1) C 35- H 43	0.14	0.63	0.008
60. LP (4)Pd 1	178. BD*(1) P 2- C 73	2.90	0.45	0.032
60. LP (4)Pd 1	216. BD*(1) C 31- H 34	1.33	0.61	0.026
60. LP (4)Pd 1	259. BD*(1) C 73- H 76	0.07	0.63	0.006
61. LP (5)Pd 1	215. BD*(1) C 31- C 33	0.09	0.59	0.006
61. LP (5)Pd 1	216. BD*(1) C 31- H 34	0.99	0.60	0.022
125. BD (1) C 31- H 34	175. LV (1)Pd 1	4.18	0.71	0.049
125. BD (1) C 31- H 34	266. RY (1)Pd 1	1.02	3.26	0.052

Figure 2.10 Selected NBO parameters for **6D-TS** computed at SMD(1,4-Dioxane)

PBE0-D3(BJ)/Def2-TZVP level

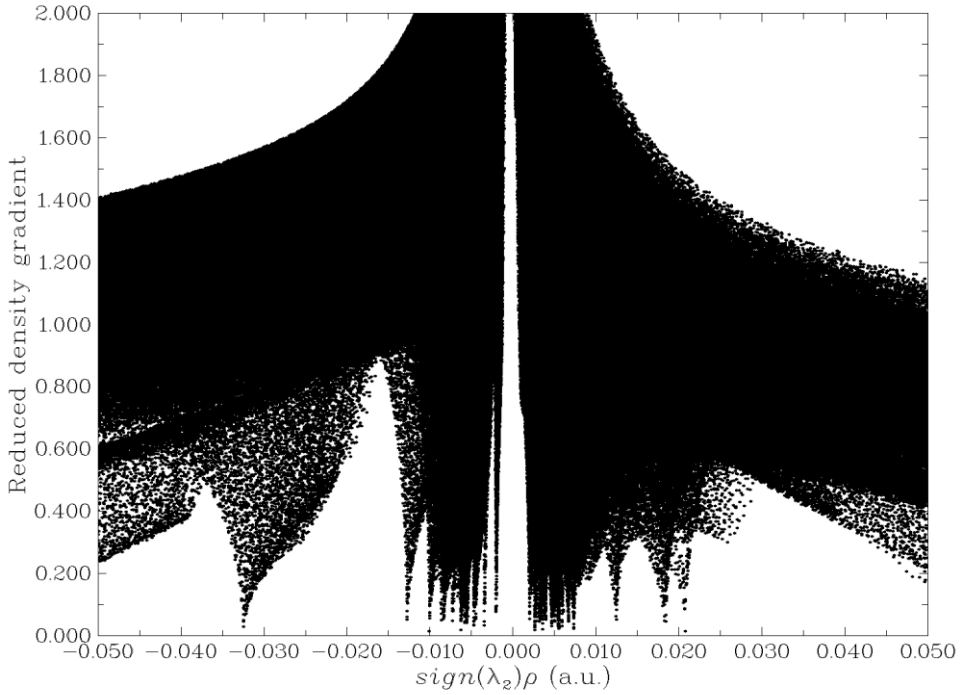

Figure 2.11 Non-covalent interaction (NCI) scatter plots for **6D-TS**

2.5 References

(1) (a) Schlummer, B.; Scholz, U. *Adv. Synth. Catal*. **2004**, *346 (13-15)*, 1599-1626; (b) Corbet, J.-P.; Mignani, G. *Chem. Rev.* **2006**, *106 (7)*, 2651-2710; (c) Torborg, C.; Beller, M. *Adv. Synth. Catal.* **2009**, *351 (18)*, 3027-3043; (d) Welsch, M. E.; Snyder, S. A.; Stockwell, B. R. *Curr. Opin. Chem. Biol.* **2010**, *14 (3)*, 347-361; (e) Roughley, S. D.; Jordan, A. M. *J. Med. Chem.* **2011**, *54 (10)*, 3451-3479; (f) Liang, M.; Chen, *J. Chem.Soc. Rev.* **2013**, *42 (8)*, 3453-3488; (g) Ruiz-Castillo, P.; Buchwald, S. L. *Chem. Rev.* **2016**, *116 (19)*, 12564-12649.

(2) (a) Louie, J.; Hartwig, J. F. *Tetrahedron Lett.* **1995**, *36 (21)*, 3609-3612; (b) Guram, A. S.; Rennels, R. A.; Buchwald, S. L. *Angew. Chem. Int. Ed.* **1995**, *34 (12)*, 1348-1350; (c) Louie, J.; Driver, M. S.; Hamann, B. C.; Hartwig, J. F. *J. Org. Chem.* **1997**, *62 (5)*, 1268-1273; (d) Wolfe, J. P.; Buchwald, S. L. *J. Org. Chem.* **1997**, *62 (5)*, 1264-1267; (e) So, C. M.; Zhou, Z.; Lau, C. P.; Kwong, F. Y. *Angew. Chem. Int. Ed.* **2008**, *47 (34)*, 6402-6406; (f) Shen, Q.; Hartwig, J. F. *Org. Lett.* **2008**, *10 (18)*, 4109-4112; (g) Aubin, Y.; Fischmeister, C.; Thomas, C. M.; Renaud, J.-L. *Chem. Soc. Rev.* **2010**, *39 (11)*, 4130-4145; (h) Fors, B. P.; Buchwald, S. L. *J. Am. Chem. Soc.* **2010**, *132 (45)*, 15914-15917; (i) Gildner, P. G.; DeAngelis, A.; Colacot, T. J. *Org. Lett.* **2016**, *18 (6)*, 1442-1445.

(3) (a) Wolfe, J. P.; Buchwald, S. L. *Org. Synth.* **2003**, *78*, 23; (b) Ji, J.; Li, T.; Bunnelle, W. H. *Org. Lett.* **2003**, *5 (24)*, 4611-4614; (c) Urgaonkar, S.; Nagarajan, M.; Verkade, J. *J. Org. Chem.* **2003**, *68 (2)*, 452-459; (d) Espino, G.; Kurbangalieva, A.; Brown, J. M. *Chem. Commun.* **2007**, *(17)*, 1742-1744; (e) Meiries, S.; Chartoire, A.; Slawin, A.

M.; Nolan, S. P. *Organometallics* **2012**, *31 (8)*, 3402-3409; (f) King, S. M.; Buchwald, S. L. *Org. Lett.* **2016**, *18 (16)*, 4128-4131; (g) Dennis, J. M.; White, N. A.; Liu, R. Y.; Buchwald, S. L. *J. Am. Chem. Soc.* **2018**, *140 (13)*, 4721-4725; (h) Dennis, J. M.; White, N. A.; Liu, R. Y.; Buchwald, S. L. *ACS Catal.* **2019**, *9 (5)*, 3822-3830; (i) Onodera, S.; Kochi, T.; Kakiuchi, F. *J. Org. Chem.* **2019**, *84 (10)*, 6508-6515; (j) Taeufer, T.; Pospech, J. *J. Org. Chem.* **2020**, *85 (11)*, 7097-7111; (k) Kreisel, T.; Mendel, M.; Queen, A. E.; Deckers, K.; Hupperich, D.; Riegger, J.; Fricke, C.; Schoenebeck, F. *Angew. Chem. Int. Ed.* **2022**, *61 (20)*, e202201475.

(4) (a) Fairlamb, I. J. *Chem.Soc. Rev.* **2007**, *36 (7)*, 1036-1045; (b) Reimann, S.; Parpart, S.; Ehlers, P.; Sharif, M.; Spannenberg, A.; Langer, P. *Org. Biomol. Chem.* **2015**, *13 (24)*, 6832-6838; (c) Almond-Thynne, J.; Blakemore, D. C.; Pryde, D. C.; Spivey, A. C. *Chem. Sci.* **2017**, *8 (1)*, 40-62; (d) Kalvet, I.; Magnin, G.; Schoenebeck, F. *Angew. Chem. Int. Ed.* **2017**, *56 (6)*, 1581-1585; (e) Kundu, G.; Sperger, T.; Rissanen, K.; Schoenebeck, F. *Angew. Chem. Int. Ed.* **2020**, *59 (49)*, 21930-21934.

(5) (a) Dobrounig, P.; Trobe, M.; Breinbauer, R. Monatsh. *Chem.* **2017**, *148*, 3-35; (b) Reeves, E. K.; Entz, E. D.; Neufeldt, S. R. *Chem. Eur. J.* **2021**, *27 (20)*, 6161-6177.

(6) (a) Littke, A. F.; Dai, C.; Fu, G. C. *J. Am. Chem. Soc.* **2000**, *122 (17)*, 4020-4028; (b) Schoenebeck, F.; Houk, K. *J. Am. Chem. Soc.* **2010**, *132 (8)*, 2496-2497; (c) Niemeyer, Z. L.; Milo, A.; Hickey, D. P.; Sigman, M. S. *Nat. Chem.* **2016**, *8 (6)*, 610-617; (d) Keaveney, S. T.; Kundu, G.; Schoenebeck, F. *Angew. Chem. Int. Ed.* **2018**, *57 (38)*, 12573-12577; (e) Hu, Z.; Wei, X. J.; Handelmann, J.; Seitz, A. K.; Rodstein, I.; Gessner, V. H.; Gooßen, L. J. *Angew. Chem. Int. Ed.* **2021**, *60 (12)*, 6778-6783; (f) Wei,

X. J.; Xue, B.; Handelmann, J.; Hu, Z.; Darmandeh, H.; Gessner, V. H.; Gooßen, L. J. *Adv. Synth. Catal.* **2022**, *364 (19)*, 3336-3341.

(7) Reeves, E. K.; Humke, J. N.; Neufeldt, S. R. *J. Org. Chem.* **2019**, *84 (18)*, 11799-11812.

(8) (a) So, C. M.; Yuen, O. Y.; Ng, S. S.; Chen, Z. *ACS Catal.* **2021**, *11 (13)*, 7820-7827; (b) Chen, Z.; Gu, C.; Yuen, O. Y.; So, C. M. *Chem. Sci.* **2022**, *13 (17)*, 4762-4769; (c) Ng, S. S.; Chen, Z.; Yuen, O. Y.; So, C. M. *Adv. Synth. Catal.* **2022**, *364 (9)*, 1596-1601; (d) Wang, M.; Pang, W. H.; Yuen, O. Y.; Ng, S. S.; So, C. M. *Org. Lett.* **2023**, *25 (47)*, 8429-8433; (e) Wang, M.; So, C. M. *Org. Lett.* **2022**, *24 (2)*, 681-685; (f) Wang, M.; Yuen, O. Y.; So, C. M. *Chin. J. Chem.* **2023**, *41 (8)*, 909-914; (g) Chen, Z.; Pang, W. H.; Yuen, O. Y.; Ng, S. S.; So, C. M. *J. Org. Chem.* **2024**, Article ASAP.

(9) (a) Stroup, B. W.; Szklennik, P. V.; Forster, C. J.; Serrano-Wu, M. H. *Org. Lett.* **2007**, *9 (10)*, 2039-2042; (b) Keylor, M. H.; Niemeyer, Z. L.; Sigman, M. S.; Tan, K. L. *J. Am. Chem. Soc.* **2017**, *139 (31)*, 10613-10616.

(10) (a) Molnár, Á. *Palladium-catalyzed coupling reactions: practical aspects and future developments;* Wiley-VCH: Weinheim, **2013**; (b) A. de Meijere, S. Bräse, M. Oestreich, *Metal-Catalyzed Cross-Coupling Reactions and More*, *Vol. 1–3*; Wiley-VCH: Weinheim, **2014**; (c) Colacot, T. J. New trends in cross-coupling: theory and applications; Royal Society of Chemistry, 2014; (d) Gildner, P. G.; Colacot, T. J. *Organometallics* **2015**, *34 (23)*, 5497-5508; (e) Hartwig, J. F. *Acc. Chem. Res.* **2008**, *41 (11)*, 1534-1544. (f) Johansson Seechurn, C. C.; Kitching, M. O.; Colacot, T. J.; Snieckus, V. *Angew. Chem. Int. Ed.* **2012**, *51 (21)*, 5062-5085; (g) Lundgren, R. J.;

Stradiotto, M. *Chem. Eur. J.* **2012**, *18 (32)*, 9758-9769; (h) Wong, S. M.; Yuen, O. Y.; Choy, P. Y.; Kwong, F. Y. *Coord. Chem. Rev.* **2015**, *293*, 158-186; (i) Zapf, A.; Beller, M. *Chem. Commun.* **2005**, *(4)*, 431-440.

(11) Fors, B. P.; Watson, D. A.; Biscoe, M. R.; Buchwald, S. L. *J. Am. Chem. Soc.* **2008**, *130 (41)*, 13552-13554.

(12) Handa, S.; Andersson, M. P.; Gallou, F.; Reilly, J.; Lipshutz, B. H. *Angew. Chem. Int. Ed.* **2016**, *55 (16)*, 4914-4918.

(13) Li, P.; Lü, B.; Fu, C.; Ma, S. *Adv. Synth. Catal.* **2013**, *355 (7)*, 1255-1259.

(14) Martin, R.; Buchwald, S. L. *Acc. Chem. Res.* **2008**, *41 (11)*, 1461-1473.

(15) (a) Ansari, A.; Ali, A.; Asif, M. *New. J. Chem.* **2017**, *41 (1)*, 16-41; (b) Fustero, S.; Sánchez-Roselló, M.; Barrio, P.; Simon-Fuentes, A. *Chem. Rev.* **2011**, *111 (11)*, 6984-7034.

(16) (a) House, D.; Steel, P.; Watson, A. *Aust. J. Chem.* **1986**, *39 (10)*, 1525-1536; (b) Kon'kov, S.; Krylov, K.; Bormasheva, K.; Moiseev, I. *Russ. J. Org. Chem.* **2014**, *50*, 1636-1638; (c) Mukherjee, R. *Coord. Chem. Rev.* **2000**, *203 (1)*, 151-218; (d) Rimola, A.; Sodupe, M.; Ros, J.; Pons, J. *A Theoretical Study on PdII Complexes Containing Hemilabile Pyrazole-Derived Ligands*. Wiley Online Library: **2006**; (e) Singer, R. A.; Caron, S.; McDermott, R. E.; Arpin, P.; Do, N. M. *Synthesis* **2003**, *2003 (11)*, 1727-1731.

(17) Knorr, L. *Ber. Dtsch. Chem. Ges.* **1883**, *16 (2)*, 2597-2599.

(18) (a) Berman, A. M.; Johnson, J. S. *J. Org. Chem.* **2006**, *71 (1)*, 219-224; (b) Hung, T. Q.; Thang, N. N.; Dang, T. T.; Villinger, A.; Langer, P. *Org. Biomol. Chem.* **2014**,

12 (16), 2596-2605; (c) Sapountzis, I.; Knochel, P. *Angew. Chem. Int. Ed.* **2004**, *43 (7)*, 897-900.

(19) Wolfe, J. P.; Tomori, H.; Sadighi, J. P.; Yin, J.; Buchwald, S. L. *J. Org. Chem.* **2000**, 65 (4), 1158-1174.

(20) (a) Brookhart, M.; Green, M. L.; Parkin, G. *PANS* **2007**, *104 (17)*, 6908-6914; (b) Lepetit, C.; Poater, J.; Alikhani, M. E.; Silvi, B.; Canac, Y.; Contreras-Garcia, J.; Solà, M.; Chauvin, R. *Inorg. Chem.* **2015**, *54 (6)*, 2960-2969; (c) Scherer, W.; Dunbar, A. C.; Barquera-Lozada, J. E.; Schmitz, D.; Eickerling, G.; Kratzert, D.; Stalke, D.; Lanza, A.; Macchi, P.; Casati, N. P. *Angew. Chem. Int. Ed.* **2015**, *54 (8)*, 2505-2509; (d) Sundquist, W. I.; Bancroft, D. P.; Lippard, S. J. *J. Am. Chem. Soc.* **1990**, *112 (4)*, 1590-1596; (e) Taubmann, C.; Öfele, K.; Herdtweck, E.; Herrmann, W. A. *Organometallics* **2009**, *28 (15)*, 4254-4257.

(21) Miyaura, N.; Suzuki, A. *Chem. Rev.* **1995**, *95 (7)*, 2457-2483.

(22) (a) Braga, D.; Grepioni, F.; Tedesco, E.; Biradha, K.; Desiraju, G. R. *Organometallics* **1997**, *16 (9)*, 1846-1856; (b) Zhang, Y.; Lewis, J. C.; Bergman, R. G.; Ellman, J. A.; Oldfield, E. *Organometallics* **2006**, *25 (14)*, 3515-3519.

(23) Johnson, E. R.; Keinan, S.; Mori-Sánchez, P.; Contreras-García, J.; Cohen, A. J.; Yang, W. *J. Am. Chem. Soc.* **2010**, *132 (18)*, 6498-6506.

(24) (a) Cao, H.-J.; Zhao, Q.; Zhang, Q.-F.; Li, J.; Hamilton, E. J.; Zhang, J.; Wang, L.-S.; Chen, X. *Dalton Trans.* **2016**, *45 (25)*, 10194-10199; (b) Darmandeh, H.; Löffler, J.; Tzouras, N. V.; Dereli, B.; Scherpf, T.; Feichtner, K. S.; Vanden Broeck, S.; Van Hecke, K.; Saab, M.; Cazin, C. S. *Angew. Chem. Int.* Ed. **2021**, *60 (38)*, 21014-21024;

(c) Nielson, A. J.; Harrison, J. A.; Sajjad, M. A.; Schwerdtfeger, P. *Eur. J. Inorg. Chem.* **2017**, *2017 (15)*, 2255-2264.

(25) Armarego, W. L. F.; Perrin, D. D. in *Purification of Laboratory Chemicals, Ed. 6* (Eds: Armarego, W. L. F.; Chai, C. L. L.), Butterworth-Heinemann, Oxford, **2009**, pp. 88–444.

(26) Chung, K. H.; So, C. M.; Wong, S. M.; Luk, C. H.; Zhou, Z.; Lau, C. P.; Kwong, F. Y. *Chem. Commun.* **2012**, *48 (14)*, 1967-1969.

(27) Sawa, M.; Morisaki, K.; Kondo, Y.; Morimoto, H.; Ohshima, T. *Chem. Eur. J.* **2017**, *23 (67)*, 17022-17028.

(28) Ahmed, M.; Kobayashi, K.; Mori, A. *Org. Lett.* **2005**, *7 (20)*, 4487-4489.

(29) Zhao, Z. G.; Wang, Z. X. *Synth. Commun.* **2007**, *37 (1)*, 137-147.

(30) Frisch, M. J.; Trucks, G. W.; Schlegel, H. B.; Scuseria, G. E.; Robb, M. A.; Cheeseman, J. R.; Scalmani, G.; Barone, V.; Petersson, G. A.; Nakatsuji, H.; Li, X.; Caricato, M.; Marenich, A. V.; Bloino, J.; Janesko, B. G.; Gomperts, R.; Mennucci, B.; Hratchian, H. P.; Ortiz, J. V.; Izmaylov, A. F.; Sonnenberg, J. L.; Williams-Young, D.; Ding, F.; Lipparini, F.; Egidi, F.; Goings, J.; Peng, B.; Petrone, A.; Henderson, T.; Ranasinghe, D.; Zakrzewski, V. G.; Gao, J.; Rega, N.; Zheng, G.; Liang, W.; Hada, M.; Ehara, M.; Toyota, K.; Fukuda, R.; Hasegawa, J.; Ishida, M.; Nakajima, T.; Honda, Y.; Kitao, O.; Nakai, H.; Vreven, T.; Throssell, K.; Jr. Montgomery, J. A.; Peralta, J. E.; Ogliaro, F.; Bearpark, M. J.; Heyd, J. J.; Brothers, E. N.; Kudin, K. N.; Staroverov, V. N.; Keith, T. A.; Kobayashi, R.; Normand, J.; Raghavachari, K.; Rendell, A. P.; Burant, J. C.; Iyengar, S. S.; Tomasi, J.; Cossi, M.; Millam, J. M.; Klene, M.; Adamo, C.;

Cammi, R.; Ochterski, J. W.; Martin, R. L.; Morokuma, K.; Farkas, O.; Foresman, J. B.; Fox, D. J. *GAUSSIAN 16* (Revision A.03), Gaussian Inc., Wallingford, CT, **2016**.

(31) (a) Perdew, J. P.; Burke, K.; Wang, Y. *Phys. Rev. B: Condens. Mater. Phys.* **1996**, *54 (23)*, 16533; (b) Perdew, J. P.; Chevary, J. A.; Vosko, S. H.; Jackson, K. A.; Pederson, M. R.; Singh, D. J.; Fiolhais, C. *Phys. Rev. B: Condens. Mater. Phys.* **1992**, *46 (11)*, 6671; (c) Becke, A. D. *J. Chem. Phys.* **1996**, *104 (3)*, 1040-1046.

(32) (a) Arnold, P. L.; Hollis, E.; Nichol, G. S.; Love, J. B.; Griveau, J.-C.; Caciuffo, R.; Magnani, N.; Maron, L.; Castro, L.; Yahia, A. *J. Am. Chem. Soc.* **2013**, *135 (10)*, 3841-3854; (b) Salman, S.; Bredas, J.-L.; Marder, S. R.; Coropceanu, V.; Barlow, S. *Organometallics* **2013**, *32 (20)*, 6061-6068; (c) Montero-Campillo, M. M.; Lamsabhi, A. M.; Mó, O.; Yáñez, M. *Alkyl mercury compounds: an assessment of DFT methods.* In 8th Congress on Electronic Structure: Principles and Applications (ESPA 2012) A Conference Selection from Theoretical Chemistry Accounts, **2014**; Springer: pp 111-118; (d) Ignatov, S.; Panteleev, S.; Maslennikov, S.; Spirina, I. *Russ. J. Gen. Chem.* **2012**, *82*, 1954-1961. (e) Wang, L.; Zhang, Y.; He, H.; Zhang, J. *Synth. Met.* **2013**, *167*, 51-63.

(33) (a) Dolg, M.; Wedig, U.; Stoll, H.; Preuss, H. *J. Chem. Phys.* **1987**, *86 (2)*, 866-872; (b) Schwerdtfeger, P.; Dolg, M.; Schwarz, W.; Bowmaker, G. A.; Boyd, P. D. *J. Chem. Phys.* **1989**, *91 (3)*, 1762-1774; (c) Andrae, D.; Haeussermann, U.; Dolg, M.; Stoll, H.; Preuss, H. *Theor. Chim. Acta* **1990**, *77* 123-141.

(34) Marenich, A. V.; Cramer, C. J.; Truhlar, D. G. *J. Phys. Chem. B* **2009**, *113 (18)*, 6378-6396.

(35) (a) Grimme, S.; Antony, J.; Ehrlich, S.; Krieg, H. *J. Chem. Phys.* **2010**, *132 (15)*. (b) Grimme, S.; Ehrlich, S.; Goerigk, L. *J. Comput. Chem.* **2011**, *32 (7)*, 1456-1465. (c) Risthaus, T.; Grimme, S. *J. Chem. Theory. Comput.* **2013**, *9 (3)*, 1580-1591.

(36) (a) Becke, A. D.; Johnson, E. R. *J. Chem. Phys.* **2007**, *127 (15)*. (b) Becke, A. D.; Johnson, E. R. *J. Chem. Phys.* **2005**, *122 (15)*.

(37) (a) Gonzalez, C.; Schlegel, H. B. *J. Chem. Phys.* **1989**, *90 (4)*, 2154-2161. (b) Gonzalez, C.; Schlegel, H. B. *J.Phy. Chem.* **1990**, *94 (14)*, 5523-5527.

(38) Weigend, F.; Ahlrichs, R. *Phys. Chem. Chem. Phys.* **2005**, *7 (18)*, 3297-3305.

(39) (a) R. S.; Paton, GoodVibes v3.0.1, 2019, bobbypaton/GoodVibes: Calculate quasi-harmonic free energies from Gaussian output files with temperature and other corrections, https://github.com/bobbypaton/GoodVibes, (accessed Feb 20, 2021); (b) Grimme, S. *Chem. –Eur. J.* **2012**, *18 (32)*, 9955-9964.

(40) Glendening, E. D.; Badenhoop, J. K.; Reed, A. E.; Carpenter, J. E.; Bohmann, J. A.; Morales, C. M.; Karafiloglou, P.; Landis, C. R.; Weinhold, F. *NBO 7.0*; Theoretical Chemistry Institute, University of Wisconsin: Madison, **2018**.

(41) (a) Lu, T.; Chen, F. *J. Comput. Chem.* **2012**, *33 (5)*, 580-592. (b) Bader, R. F.; Molecules, A. I. *Atoms in Molecules: A Quantum Theory,* Clarendon: Oxford, UK **1990**, p. 438.

(42) Humphrey, W., Dalke, A. and Schulten, K., "*VMD - Visual Molecular Dynamics*", J. Molec. Graphics, **1996**, *vol. 14*, pp. 33-38.

(43) . C. Y. Legault, CYLview 1.0b, Département de Chimie, Université de Sherbrooke: Quebec, Canada, 2009, http://www.cylview.org, (accessed Feb 20, 2021).

Chapter 3 Palladium-Catalyzed Regio- and Chemoselective Additive-Free Direct C─H Functionalization of Heterocycles with Chloroaryl Triflates Using Pyrazole-Alkyl Phosphine Ligands

3.1 Introduction

Recent progress in transition metal-catalyzed direct C−H arylation of heteroarenes has established a robust methodology for the synthesis of hetero-biaryl motifs, which are prevalent in numerous natural products and pharmaceutical compounds.[1] This transformation is particularly alluring in terms of its environmental and atom economy advantages compared to traditional cross-coupling protocols, which necessitate prefunctionalized coupling reagents.[2] Current research efforts are primarily focused on broadening the scope of C−H bond activation and achieving precise regioselectivity. This is being pursued via the optimization of reaction conditions or the development of novel catalysts designed for regioselective mono- or diarylation of specific sites within the heterocyclic framework (Scheme 3.1A). Although much research has focused on catalysts capable of differentiating between the various C−H bonds on nucleophiles to achieve regioselectivity, there is still a serious lack of research on reaching dual selectivity—realizing both C−H regioselectivity on the nucleophile and chemoselectivity on the electrophile with multiple reactive sites.

Attaining dual selectivity poses a significant challenge due to the conflicting demands placed on the palladium center during various elementary steps of the catalytic

cycle. Tan and Hartwig demonstrated that palladium complexes featuring dimethylacetamide (DMAc) as the ligand promoted C−H bond cleavage in benzene faster than complexes with phosphine ligands.[3] Experimental results and density functional theory (DFT) calculations, indicate a lower activation barrier and enhanced rates of direct arylation for benzene in comparison to reactions involving phosphine ligands.[3-4] The propensity of phosphine ligands to form three-coordinate palladium complexes may render the C−H bond cleavage step of the reaction pathway energetically less favorable.[3, 5] Additionally, polar solvents can aid in the generation of anionic palladium species, which has a lower energy barrier than neutral palladium species coordinated with bulky and electron-rich phosphine ligands.[3, 6]

Regarding the control of chemoselectivity for polyhalogenated aryl triflates, oxidative addition step was deemed as key step to determine the outcomes (Scheme 3.1B).[7] Furthermore, phosphine ligands are critical for the control of the coordination site of the palladium center during oxidative addition, particularly for realizing a C−Cl > C−OTf selectivity order.[8] Palladium catalysts featuring bulky, electron-rich phosphine ligands are known to effectively activate inert C−Cl bonds;[9] however, they may not enhance the rates of C−H activation processes.[10] In fact, in order to suit reaction conditions that promote C−H activation, only less abundant but more active electrophiles,[11] such as aryl iodides (ArI)[10a] and aryl bromides (ArBr),[4c, 12] are usually harnessed in direct C−H arylation of heteroarenes (Scheme 3.1C).[13] Additionally, preferred conditions for C−H activation involve utilizing a phosphine-free palladium catalyst,[4] polar coordinating solvents such as DMAc, dimethyl sulfoxide (DMSO),

dimethylformamide (DMF), hexafluoroisopropanol (HFIP), and *n*-methyl-2-pyrrolidone (NMP),[3, 13b, 14] and adding quaternary ammonium salts (*n*-Bu_4NX) to promote the formation of anionic palladium species.[3, 10b] Moreover, the incorporation of substoichiometric amounts of additives, such as pivalic acid (PivOH),[4a, 15] silver carbonate (Ag_2CO_3),[16] and copper(I) chloride (CuCl),[17] has been demonstrated to promote the C−H activation process. Nonetheless, these conditions have been particularly effective in activating the C−OTf bond.[18] Furthermore, there is an additional challenge in retaining the −OTf group in the product during the chemoselective reaction, as reaction conditions that can promote C−H bond activation, including strong polar solvents, strong alkaline conditions, and high temperatures can promote hydrolysis of triflates to the corresponding phenol.[18c]

A **Pd-catalyzed regioselective C−H arylation of heterocyclic compounds**

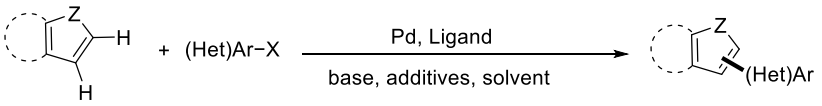

General: X = I, Br or OTf

B **Pd-catalyzed chemoselective coupling reactions**

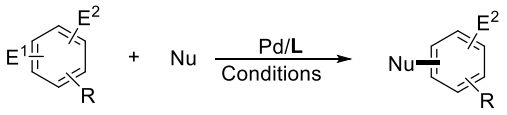

C **Contradicted requirements for the palladium catalyst**

Preferred conditions for promoting the reaction	**Regioselective C-H arylation reaction**	**Chemoselective C-Cl over C-OTf reaction**
Solvent	High polar coordinating solvents, e.g. DMAc, DMF	Noncoordinating solvents, e.g. Tolune, Dioxane, THF
Nature of Pd species	Anionic Pd species to promote C−H activation	Neutral Pd species promote the C−Cl bond activation
Electrophilic sites for reaction to take place	More reactive electrophiles, e.g. ArI, ArBr and ArOTf	ArCl
Phosphine Ligand	Solvent coordinated, phosphine-free Pd center to promote C-H activation	Controlling of the ligation state via phosphine coordination
Additives	PivOH, Ag_2CO_3, CuCl, *n*-Bu_4NBr, and atc.	Additive-free

D **This work: Pd-catalyzed regio- and chemoselective C−H arylation**

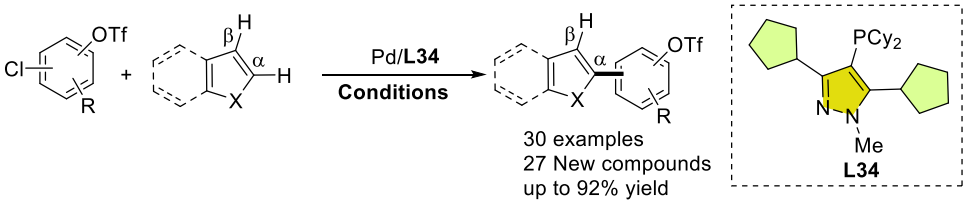

- The first chemoselective C–Cl (over–OTf) C–H arylation of heterarenes
- New alkyl-pyrazole-based ligand
- High α-regioselectivity
- High C–Cl > C–OTf chemoselectivity
- Broad substrate scope
- No additives
- Late-stage functionalizations

Scheme 3.1 Development of alkyl pyrazole phosphine ligands and overcoming challenges in achieving dual selectivity

As far as we know, there are no reports addressing the challenge of bridging the regio- and chemoselective C−H arylation of heterocycles with chloroaryl triflates. Considering the convenience of obtaining highly complex molecules via Pd-catalyzed cross-coupling protocols, developing an efficient, direct regio- and chemoselective C−H arylation methodology with a controllable reaction sequence is of great importance for broadening the scope of C−H activation reactions.[19] One of the most alluring approaches to address these challenges is to control regioselectivity and chemoselectivity via a ligand method. Therefore, in this chapter, we aimed to broaden our ligand library and then overcome the mentioned challenges in achieving dual selectivity, which leads to regio-, and chemoselective C−H arylation of heterocycles with chloroaryl triflates under relatively benign conditions without the requirement for additional additives (Scheme 3.1D).

3.2 Results and Discussion

3.2.1 Ligand Synthesis Route Optimization and Ligand Synthesis

Inspired by our previous development of alkyl-pyrazole-phosphine ligands, which demonstrated exceptional reactivity and chemoselectivity in chemoselective amination reactions,[20] we are confident in further modifying the alkyl groups of these advantageous ligand frameworks. Nevertheless, the protection of the nitrogen atom on pyrazoles requires the use of the methylation reagent dimethyl sulfate, a class of highly toxic reagents. In order to simplify the ligand synthesis route and circumvent the use of highly toxic reagents, we tried to replace hydrazine hydrate with a commercially

available methylhydrazine sulfate, and at the same time, Et_3N was added as a base to neutralize the sulfuric acid to release methylhydrazine, which then underwent a Knorr reaction with alkyl-substituted diketone to afford corresponding *N*-methyl 3,5-dialkyl substituted pyrazoles. Fortunately, we have successfully and efficiently obtained a series of *N*-protected pyrazoles with different sizes of cycloalkyl groups at the C3 and C5 positions, ranging from three-membered to seven-membered just via one step (Table 3.1). Through the improved synthetic ligand route, we then successfully and efficiently synthesized a series of alkyl-pyrazole-based phosphine ligands with varying ring sizes (Table 3.2).

Table 3.1 One-step synthesis for *N*-methyl 3,5-dialkyl substituted pyrazole utilizing diketone as starting materials[a]

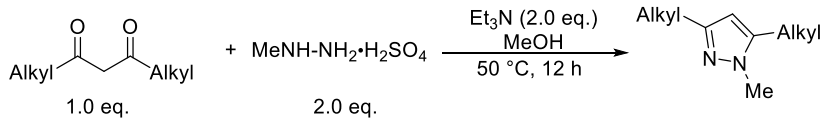

entry	Diketone	product	Yield (%)[b]
1	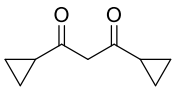	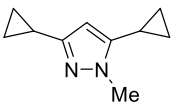	95
2	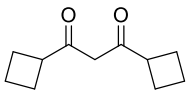	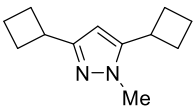	98
3	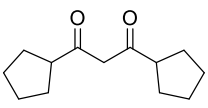	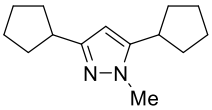	87
4	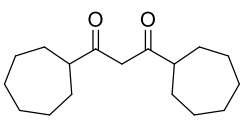	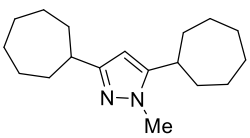	76

[a]Reaction conditions: Methylhydrazine sulfate (2.0 eq.), Di-alkyl substituted diketone (1.0 eq.), Et_3N (2.0 eq.), MeOH, Temperatue = 50 °C, Time = 12 h. [b]Isolated yield.

Table 3.2 Yield of phosphination step and overall yield of 4-step synthesis route[a]

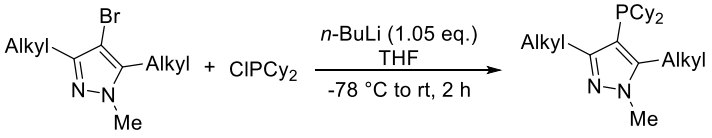

entry	ligand		Yield for phosphination step (%)[b]	Overall yield for 4-step synthesis route (%)
1	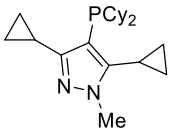	**L32**	40	28
2	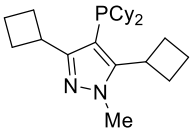	**L33**	62	50
3	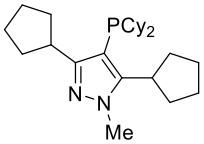	**L34**	62	46
4	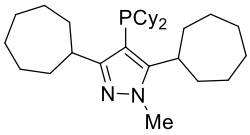	**L35**	67	33

[a]Phosphination step: 4-Bromo-3,5-dialkly-1-methyl-1*H*-pyrazole (1.0 eq.), *n*-BuLi (1.05 eq.), THF, -78 °C, 45 min, then $ClPCy_2$ (1.05 eq.), rt, 1 h.

3.2.2 Assessment of Ligand Impact on Regio-, and Chemoselective C–H Arylation of Heterocycles

After synthesizing a series of pyrazole-based phosphine ligands featuring varying cycloalkyl ring sizes, we then chose 4-chlorophenyl triflate **1a** and benzo[*b*]thiophene **4a** as model substrates to evaluate the efficacy of ligands in regio- and chemoselective C–H arylation (Table 3.3). Before that, we first examined some preferred conditions[3, 10b] for C–H activation of heterocyclic compounds using $Pd(dba)_2$ as a catalyst, which included the use of polar and coordinating solvent DMAc with or without *n*-Bu_4NBr as

an additive (Table 3.3, entries **1** and **2**). However, rather than yielding the desired product **5a**, only the hydrolysis of the triflate group was observed. This outcome highlighted the inherent challenges in achieving dual selectivity.

Subsequently, we investigated a series of commercially available phosphine ligands for this reaction harnessing dioxane as the solvent. PPh_3 (**L1**) and P(*o*-tolyl)$_3$ (**L7**) demonstrated efficacy as ligands in the direct C–H arylation of aryl iodides with heteroarenes.[21] Nevertheless, it produced only trace amounts and showed selectivity towards the C–OTf bond (Table 3.3, entries **3** and **8**). PCy_3 (**L2**) and P*t*-Bu_3 (**L3**) were identified as pivotal ligands in Fu's seminal reports[22] and in subsequent theoretical investigations[23] by Houk, Schoenebeck, and Sigman, which investigated the chemoselectivity of C–Cl and C–OTf bonds. These studies revealed that the chemoselectivity of C–Cl and C–OTf originates from the ligation modes of the palladium center with the ligand. For instance, PCy_3 (**L2**), which can form a bisligated L_2Pd complex, prefers to activate the C–OTf bond, whereas P*t*-Bu_3 (**L3**), which can form a monoligated LPd complex, favors the activation of C–Cl bond. Intriguingly, PCy_3 (**L2**) provided a C–Cl > C–OTf reactivity order yet resulted in low yield and poor C–H regioselectivity, suggesting the complexity of the reaction process (Table 3.3, entry **4**). P*t*-Bu_3·HBF_4 (**L5**) has been reported to afford C–Cl bond selectivity [22] and allow C–H functionalization of heteroarenes, [24] we hypothesized that this ligand could be effective in our reaction. Nevertheless, it produced only trace amounts of the desired product **5a** (Table 3.3, entry **5**). We hypothesized that the reaction conditions might not be optimal for the current transformation. Continued endeavors, utilizing the reported

reaction conditions[24] (i.e., LiO*t*-Bu$_3$ with or without DMF as the solvent), gave rise to no desired product **5a** but in complete hydrolysis of the chlorophenyl triflates to the corresponding phenols (Table 3.3, entries **6** and **7**). This outcome underscores the challenge of bridging chemoselectivity and regioselectivity in the current transformation. Some Buchwald-type ligands were tested,[25] including CyJohnPhos (**L8**), DavePhos (**L9**), SPhos (**L10**), and XPhos (**L12**) (Table 3.3 entries **9**–**12**). Nevertheless, only **L9** was capable of producing a reaction, albeit with poor yield and chemoselectivity (Table 3.3, entry **10**). In addition, for the test of diphosphine ligands such as Cy-XantPhos (**L36**) and dppb (**L37**), still poor results were obtained (Table 3.3, entries **13** and **14**). The NHC carbene ligand SIPr·HCl[26] (**L38**) and CySelectPhos[27] (**L42**) demonstrated efficacy in achieving C–Cl over C–OTf chemoselectivity. Nevertheless, they were found to be ineffective in facilitating the C–H arylation reaction (Table 3.3, entries **15** and **16**).

We next examined our prepared alkyl-pyrazole-based phosphine ligands. To our satisfaction, preliminary tests with the ligand bearing a cyclohexyl group (**L25**) demonstrated high efficacy, achieving remarkable chemoselectivity favoring the C–Cl bond over the C–OTf bond (Table 3.3, entry **21**). Additionally, it demonstrated excellent α/β regioselectivity, yielding the α-arylated product selectively without the need for additives. Ligands with five-membered rings (**L34**) delivered superior results (Table 3.3, entry **19**), enabling the reaction to proceed effectively at 90°C (Table 3.3, entry **20**), a remarkably low temperature that still produced excellent outcomes with prolonged reaction time. To the best of our knowledge, this is the lowest recorded temperature for

activating the C–Cl bond in Pd-catalyzed C–H arylation reactions. Nevertheless, further decreasing it to a four-membered ring (**L33**) or increasing the ring size to a seven-membered ring (**L35**) resulted in reduced reactivity (Table 3.3, entries **18** and **22**). In addition, the ligand with a cyclopropane ring (**L32**) showed no reactivity, even with an extended reaction time of 18 hours (Table 3.3, entry **17**). Furthermore, substituting the cycloalkyl group with the phenyl group (**L30**) also led to no reactivity (Table 3.3, entry **23**), highlighting the critical role of the alkyl group in achieving this C–H arylation reaction.

Table 3.3 Ligands' effects on regio- and chemoselective C–H arylation

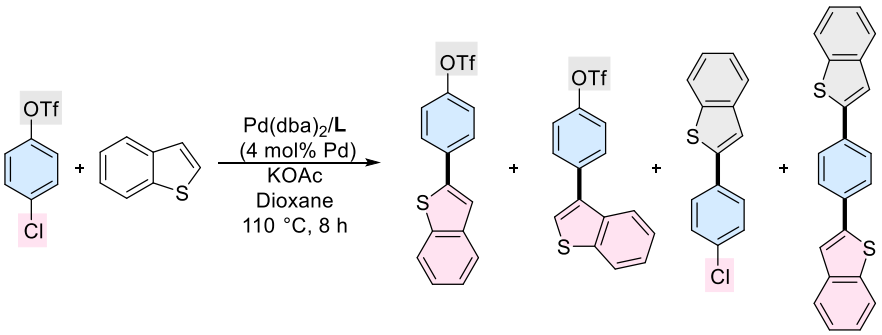

1a **6a** **7a** **7a'** **8a** **9a**

Entry	L	7a (%)	7a: 7a'	7a: 8a: 9a
1[b]	None	0	-	-
2[b,c]	None	0	-	-
3	**L1** = PPh_3	1	-	6: 94: 0
4	**L2** = PCy_3	34	99: 1	90: 10: 0
5	**L5** = P*t*-Bu_3•HBF_4	<1	-	-
6[d]	**L5** = P*t*-Bu_3•HBF_4	0	-	-
7[d,e]	**L5** = P*t*-Bu_3•HBF_4	0	-	-
8[f]	**L7** = P(*o*-tolyl)$_3$	0	-	-
9	**L8** = CyJohnPhos	<1	-	-
10	**L9** = DavePhos	4	100: 0	53: 47: 0
11	**L10** = SPhos	0	-	-
12	**L12** = XPhos	0	-	-
13	**L36** = Cy-XantPhos	0	-	-
14	**L37** = dppb	<1	-	5: 95: 0
15	**L38** = SIPr•HCl	0	-	-
16	**L42** = CySelectPhos	<1	-	-
17[f]	**L32**	0	-	-
18	**L33**	60	99: 1	99: 1: 0
19	**L34**	**96** (**84**)[h]	99: 1	100: 0: 0
20[g]	**L34**	99	99: 1	100: 0: 0
21	**L25**	85	99: 1	99: 1: 0
22	**L35**	66	98: 0	99: 1: 0
23	**L30**	0	-	-

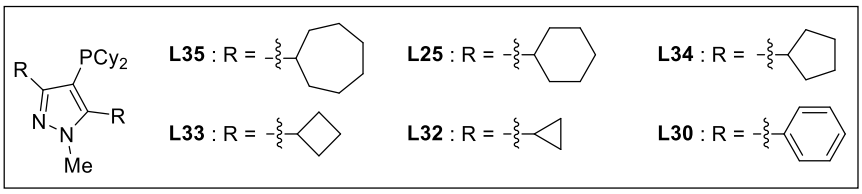

[a]Reaction condition: 4-chlorophenyltriflate **1a** (0.20 mmol), benzo[*b*]thiophene **6a** (0.30 mmol), $Pd(dba)_2$ (4.0 mol%), **L** (8.0 mol%), KOAc (0.40 mmol) and dioxane (1.0 mL) were stirred at 110 °C for 8 h. Calibrated GC-FID yields are reported using dodecane as an internal standard. The regioselectivity ratio **7a**: **7a'** and the chemoselectivity ratio **7a**: **8a**: **9a** were determined by GC-MS. "-" represents the ratio cannot be determined. [b]DMAc (1.0 mL) as solvent. [c]*n*-Bu_4NBr (0.20 mmol) was added. [d]LiO*t*-Bu (0.6 mmol) as base. [e]DMF (1.0 mL) as solvent. [f]18 h. [g]90°C for 18 h. [h]Isolated yield.

3.2.3 Mechanism Investigations

Inspired by promising results, we commenced a preliminary mechanistic investigation into the regio- and chemoselective C–H arylation reaction harnessing the Pd/**L34** system, aiming to elucidate the intricacies of the ligand effects and reaction pathway involved in the C–H activation process (Scheme 3.2). We first carried out competition experiments utilizing pairs of chloroaryl triflates, each featuring either an electron-donating or an electron-withdrawing group (Scheme 3.2 A, $–CF_3$ vs. –Me).

The results that substrate bearing electron-withdrawing group **1u** exhibited similar reactivity compared to those bearing electron-donating group **1k**, indicating that the rate-determining step of this reaction might not be the oxidative addition step. The C–H functionalization step can usually proceed via one of three pathways: (a) an electrophilic aromatic substitution (S_EAr) pathway; (b) a concerted metalation-deprotonation (CMD) pathway; or (c) a Heck-type pathway. To study the possible pathway, we carried out competition experiments utilizing 1-(thiophen-2-yl)ethan-1-

one (**6e**) and 2-butylthiophene (**6h**) as substrates (Scheme 3.2 B). The generation of products **7s** and **7v** in a 1.2:1 ratio indicates that the relatively electron-rich heterocycle did not exhibit preferential reactivity over the electron-poor substrate. This observation implies that the reaction might not proceed via the S_EAr mechanism, which is typically preferred for electron-rich heteroarenes. In order to explore the possibility of the reaction occurring via the Heck-type mechanism or CMD pathway, we performed a series of deuterium-labeling investigations (Scheme 3.2 C–E). The hydrogen/deuterium exchange experiment indicated that the cleavage of the C–H bond at the α-position was a reversible process (Scheme 3.2 C). Furthermore, the parallel KIE competition reactions (Scheme 3.2 D) produced a KIE value of 2.2, while the KIE experiment performed in the same vessel (Scheme 3E) yielded a KIE value of 2.7. The observed primary kinetic isotopic effect indicates that the C–H bond cleavage is associated with the rate-determining step. These experimental outcomes support the conclusion that the C–H bond activation pathway in the Pd/**L34** system proceeds through the CMD process.

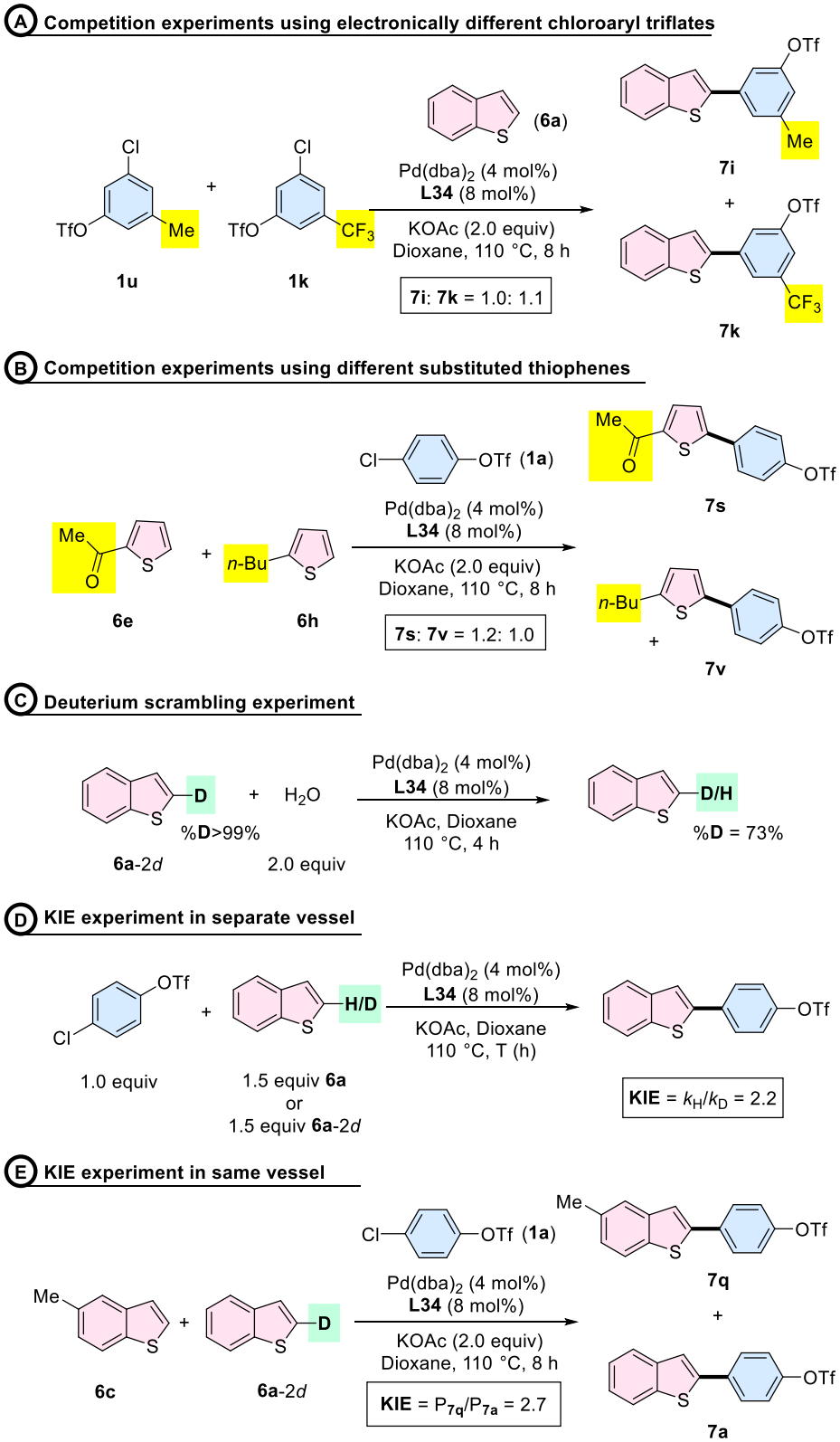

Scheme 3.2 Mechanism investigations

In order to further investigate the effect of ligands on the bridging of regio- and

chemoselective C–H arylation processes, we carried out a density functional theory (DFT) study of the reaction process at the B3LYP-D3(BJ)/Def2-TZVP-SMD(1,4-dioxane)//B3PW91-D3(BJ)/6-31G(d)-SDD(Pd)-PCM(1,4-dioxane) level of theory (see **3.5** section-computational details).[13b] The reaction system under scrutiny involved the palladium complex Pd–**L34** reacting with 4-chlorophenyl triflate, using benzo[*b*]thiophene as the substrate (Figure 3.1). The calculated outcomes reveal that the pivotal transition state in the reaction mechanism is associated with the C–H bond activation step. This step was found to favor the CMD pathway (**12H-TS**, 19.8 kcal/mol) over the Heck-type pathway (**12Q-TS**, 38.5 kcal/mol). The regioselectivity of the reaction was elucidated by the preference for CMD at the C-2 position (**12H-TS**, 19.8 kcal/mol) rather than the C-3 position (**12P-TS**, 21.0 kcal/mol), which is consistent with experimental results and explains the observed regioselectivity in the C–H arylation process. In addition, the lower energy barrier for the oxidative addition step of C–Cl (**12D-TS**, 9.5 kcal/mol) compared to C–OTf (**12N-TS**, 14.0 kcal/mol) indicates that the reaction favors the C–Cl pathway, which could be the chemoselectivity-determining step early in the reaction.[7] Finally, **12I** undergoes reductive elimination of the transition state **12K-TS** to produce the arylation product with activation energies of 9.0 kcal/mol. Due to the relatively endothermic characteristic of the metalation/deprotonation step, **12I** possesses higher energy than **12E**, making **12K-TS** the highest energy point. The total barrier is 25.7 kcal/mol, which encompasses both the energy required for C–H activation and that for reductive elimination, which becomes the rate-determining state.

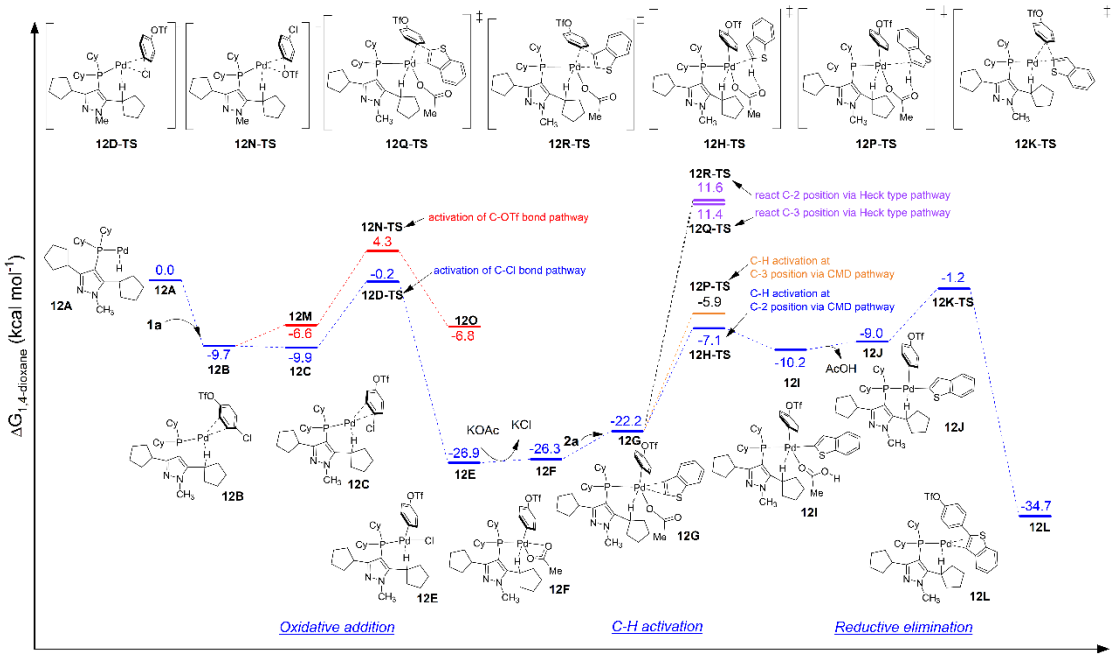

Figure 3.1 Free energy profiles calculated for the chemoselective Pd-**L34** cross-coupling reaction of 4-chlorophenyltriflate with benzo[*b*]thiophene.

To further elucidate the high reactivity of the Pd/**L34** system, we also investigated the Pd–P*t*-Bu$_3$ system (Figure 3.2, see **3.5** section-figure **3.6** for details), known for its ability to give C–Cl chemoselectivity[22] and to facilitate C–H functionalization of heteroarenes.[24] In agreement with previous findings, the Pd–P*t*-Bu$_3$ system exhibited a preference for the C–Cl bonding (**18D-TS**, 10.4 kcal/mol) over the C–OTf bonding (**18N-TS**, 13.8 kcal/mol). Nevertheless, the energy required for the lowest energy pathway of the Pd/P*t*-Bu$_3$ system (**18H-TS**, 28.1 kcal/mol) is higher than that of the Pd/**L34** system (**12K-TS**, 25.1 kcal/mol), which may explain its inactivity when a strong base is not utilized in this reaction.

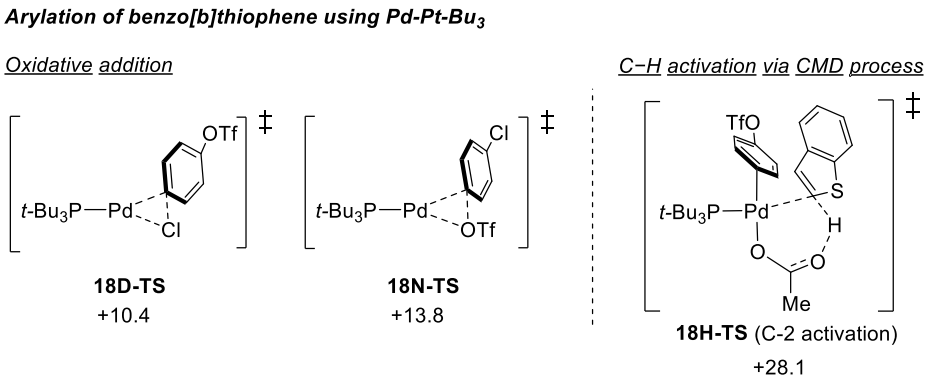

Figure 3.2 Calculated transition structures of the oxidative addition step for Pd/P*t*-Bu$_3$

We made a preliminary attempt to investigate the effect of the nature and size of the cycloalkyl ring on the reactivity of the reaction. We utilized **L25**, **L32**–**L35**, and **L39** as ligands to calculate the C–H bond activation step via the CMD pathway and the reductive elimination step, as these steps were deemed to be involved in the rate-determining state in the direct C–H functionalization of heterocycles. Interestingly, the calculation results revealed that the substituent group *ortho* to the phosphino group has a considerably influence on the energy barrier of the C–H activation step and the whole reaction process (Figure 3.3). **L39** lacking the cycloalkyl group exhibits a high energy barrier, which diminishes with increasing cycloalkyl ring size, commencing from a three-membered ring and reaching a minimum at the five/six-membered ring. However, the energy barrier started to rise again when the ring size was further expanded to seven members.

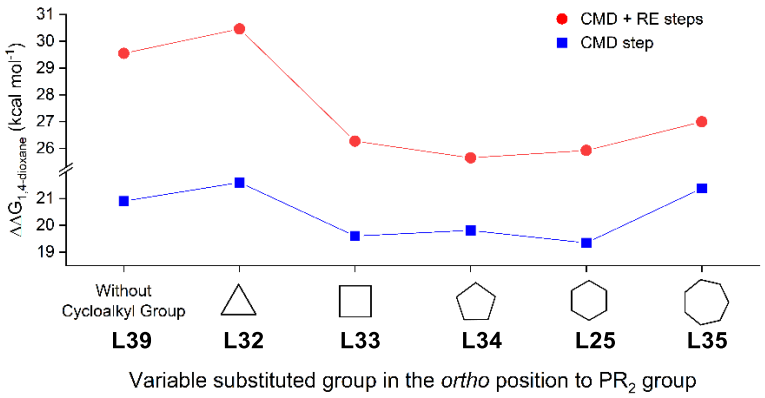

Figure 3.3 Effect of cycloalkyl ring size on the free energy barrier of direct C–H activation of benzo[*b*]thiophene via the CMD and reductive elimination process.

Considering the considerable effects of the degree and geometry on the Pd···H–C interaction, an additional investigation was undertaken to analyze the angle of this interaction in the DFT-calculated structures of the palladium complexes after the oxidative addition step for ligands **L25**, **L32**–**L35**, and **L39**. This step was also identified as the starting point of the C–H activation process in the reaction coordinate. The Pd···H–C interaction's angle exhibited a gradual increase from the cyclopropyl group (84.1°) to the cyclohexyl group (162.1°), then decreased with the cycloheptyl group (134.2°). Angles of Pd···H–C separation formed by four- to seven-membered ring structures generally lie within a standard range of 110-170°. Furthermore, a series of LPd(η^3-C_3H_5)Cl complexes (**L32**–**L35**) were prepared, and NMR investigations were conducted to ascertain the chemical shift of the methide hydrogen within the cycloalkyl group. A downfield shift (4.05–4.60 ppm) was observed for the methide hydrogen as the ring size increased from four to seven members. The obtained computational structures and NMR results provide evidence for the presence of anagostic/preagostic Pd···H–C interactions in **L33**–**L35**.[28] Nevertheless, the observed

angle for the cyclopropyl group (84.1°) deviated significantly from the typical range of 110-170°. Additionally, the absence of a downfield shift (2.25 ppm) in the methide hydrogen of the cyclopropyl group in **L32**-Pd(η^3-C_3H_5)Cl may suggest a potential absence of anagostic/preagostic interactions.[29]

It is imperative to highlight that the observed trends in these findings, including the observed inertness in **L32** and the progressive enhancement in reactivity for **L34**, are generally consistent with the experimental observations (Table 3.3). To gain preliminary insights into the underlying factors driving this observed trend, we investigated the evolution of the Pd···H–C distance throughout the reaction. Our findings reveal significant variations in the Pd···H–C distance, ranging from 1.97 Å to 2.32 Å for L34, whereas the Pd···H–C distance for **L32** exhibits a greater extent, spanning from 2.62 Å to 3.77 Å. Furthermore, we conducted a detailed analysis of the critical transition state structures associated with the CMD and reductive elimination steps for ligands **L25**, **L32**–**L35**, and **L39** (Figure 3.4). The analysis using natural bond orbital (NBO) revealed that the Pd···H–C interaction contributes to the second-order perturbation energy via Pd to antibonding sp^3 C−H backdonation, as well as electronic donation from the C−C bond of the aryl group in the substrate to the Pd center. Moreover, the stabilization energy provided by the Pd···H–C interaction exhibits variation based on the cycloalkyl group size. It becomes negligible for the 3-membered ring, reaches its peak at the 5/6-membered ring, and decreases with the 7-membered ring. This observed variation aligns with the trend depicted in Figure 3.3. Notably, this observation provides evidence for the first time that Pd···H–C interactions, facilitated

by the optimal size of the cycloalkyl group, may assist in reducing the high energy barrier associated with the C–H activation step and subsequent reductive elimination step, which might account for the occurrence of the reaction under relatively mild and additive-free conditions.[30]

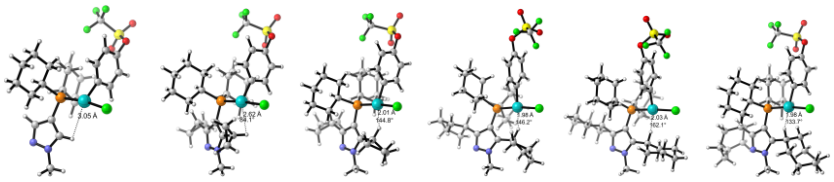

17E d(Pd–H–Ar)=3.05Å | **13E** d(Pd–H)=2.62Å Pd–H–C=84.1° | **14E** d(Pd–H)=2.01Å Pd–H–C=144.8° | **12E** d(Pd–H)=1.98Å Pd–H–C=146.2° | **15E** d(Pd–H)=2.03Å Pd–H–C=162.1° | **16E** d(Pd–H)=1.98Å Pd–H–C=133.7°

		H	c-Propyl	c-Butyl	c-Pentyl	c-Hexyl	c-Heptyl
CMD Step	Optimized Structure	17H-TS	13H-TS	14H-TS	12H-TS	15H-TS	16H-Ts
	d(Pd···H–C) at CMD step [Å]	-	3.44	2.28	2.24	2.25	2.16
	[a]E(2) Pd LP to C–H σ* [kcal/mol]	-	-	2.15	3.56	2.35	2.16
	[b]E(2) C–Pd σ to C–H σ* [kcal/mol]	-	-	2.09	2.53	2.38	2.05
Reductive Elimination	Optimized Structure	17H-TS	13H-TS	14H-TS	12H-TS	15H-TS	16H-Ts
	d(Pd···H–C) at RE step [Å]	-	3.37	2.06	2.07	2.10	2.14
	[a]E(2) Pd LP to C–H σ* [kcal/mol]	-	-	3.42	4.54	4.63	3.57
	[a]E(2) C–H σ to Pd LP* [kcal/mol]	-	0.29	5.09	5.12	5.35	4.54
	[b]E(2) C–C σ to C–H σ* [kcal/mol]	-	-	0.35	0.48	0.62	0.67
	[b]E(2) C–C π to C–H σ* [kcal/mol]	-	-	0.27	0.61	0.46	0.41

Figure 3.4 NBO second-order perturbation stabilization energy E(2) analysis of the optimized transition state structures. [a]Stabilization energy contributed from the interaction between H–C and Pd. [b]Stabilization energy contributed from the interaction between H–C and the oxidative added aryl substrate.

3.2.4 Evaluation of Reaction Parameters

We then tested the effect of other reaction parameters on the regio- and chemoselective C–H arylation reaction (Table 3.4). We investigated various palladium sources (Table 3.3, entries **1**–**6**), solvents (Table 3.4, entries **7**–**11**) and inorganic bases (Table 3.4, entries **12**–**15**) and found that the combination of $Pd(dba)_2$, KOAc, and

dioxane, as used in the mother reaction, remained optimal. Reducing the equivalents of **2a**, the Pd/ligand ratio or the loading of palladium led to varying degrees of yield reduction (Table 3.4, entries **16**–**18**), while regio- and chemoselectivity remained unaffected. Furthermore, even at a reaction temperature of 90 °C for 24 hours, a yield of 63% and excellent selectivity were still obtained (Table 3.4, entry **19**).

Table 3.4 Evaluation of reaction conditions[a]

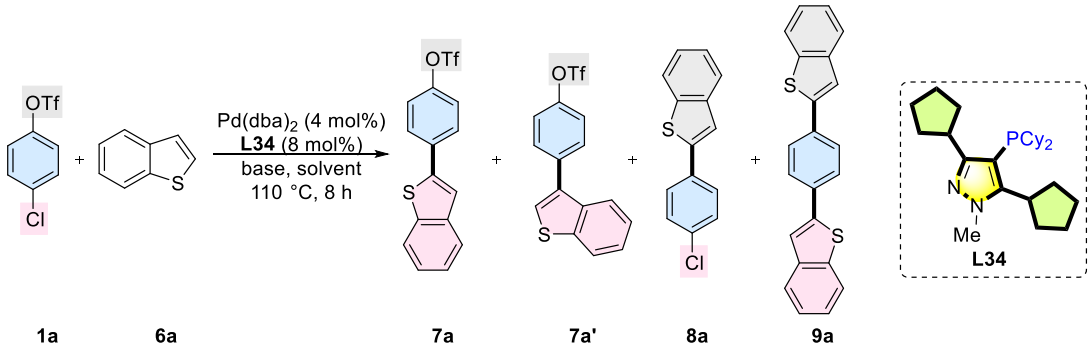

1a **6a** **7a** **7a'** **8a** **9a**

Entry	Pd source	Solvent	Base	**7a** (%)[b]	**7a**: **8a**: **9a**[c]	**7a**: **7a'**[c]	**1a** (%)[b]
1	$Pd(OAc)_2$	Dioxane	KOAc	72	99: 1: 0	99: 1	13
2	$PdCl_2$	Dioxane	KOAc	36	98: 2: 0	99: 1	53
3	$[Pd(\pi\text{-cinnamyl})Cl]_2$	Dioxane	KOAc	60	99: 1: 0	99: 1	28
4	$[Pd(2\text{-butenyl})Cl]_2$	Dioxane	KOAc	79	99: 1: 0	99: 1	11
5	$[Pd(2\text{-allyl})Cl]_2$	Dioxane	KOAc	41	99: 1: 0	99: 1	50
6	$Pd2(dba)_3$	Dioxane	KOAc	85	99: 1: 0	99: 1	21
7	$Pd(dba)_2$	THF	KOAc	64	99: 1: 0	99: 1	31
8	$Pd(dba)_2$	CPME	KOAc	61	99: 1: 0	99: 1	26

9	$Pd(dba)_2$	Hexane	KOAc	48	99: 1: 0	99: 1	38
10	$Pd(dba)_2$	Toluene	KOAc	48	99: 1: 0	99: 1	39
11	$Pd(dba)_2$	*t*-BuOH	KOAc	43	99: 1: 0	99: 1	46
12	$Pd(dba)_2$	Dioxane	NaOAc	20	100: 0: 0	100: 0	72
13	$Pd(dba)_2$	Dioxane	K_2CO_3	13	100: 0: 0	98: 2	73
14	$Pd(dba)_2$	Dioxane	K_3PO_4	<1	N.A.	N.A.	49
15	$Pd(dba)_2$	Dioxane	CsOAc	87	100: 0: 0	99: 1	<1
16[d]	$Pd(dba)_2$	Dioxane	KOAc	59	99: 1: 0	99: 1	24
17[e]	$Pd(dba)_2$	Dioxane	KOAc	63	99: 1: 0	99: 1	24
18[f]	$Pd(dba)_2$	Dioxane	KOAc	31	99: 1: 0	99: 1	66
19[g]	$Pd(dba)_2$	Dioxane	KOAc	63	99: 1: 0	99: 1	28

[a]Reaction condition: 4-chlorophenyltriflate (0.20 mmol), benzo[*b*]thiophene (0.30 mmol), Pd source (4.0 mol%), **L34** (8.0 mol%), base (0.40 mmol) and solvent (1.0 mL) were stirred at 110 °C for 8 h. [b]Calibrated GC-FID yields are reported using dodecane as an internal standard and remaining of **1a** was recorded. [c]The regioselectivity ratio **7a**: **7a'** and the chemoselectivity ratio **7a**: **8a**: **9a** were determined by GC-MS. [d]1.2 equiv. **6a**. [e]Pd: **L34** = 1: 1.5. [f]2 mol% $Pd(dba)_2$ was used. [g]90 °C.

3.2.5 Exploration of the Scope of Chloroaryl Triflates

Subsequently, an investigation into the substrate scope of chloroaryl triflates was undertaken (Table 3.5). Chloroaryl triflates, irrespective of the positional variations of –Cl and –OTf groups (*ortho*, *meta*, or *para*), regio- and chemoselectively coupled with benzo[*b*]thiophene, producing α-arylation products in good to excellent yields (Table 3.5, **7a**, **7g**, and **7o**). Substrates bearing electron-donating and electron-withdrawing

groups such as –Me, –OMe, –Bn, –CN, –CF_3, and –F underwent conversion to the corresponding products with notable yields, accompanied by excellent α-regioselectivity (Table 3.5, **7d**, **7h**, **7i**, **7j**, **7k**, and **7f**). Despite known challenges associated with utilizing sterically hindered aryl halides for direct C–H activation, which often exhibits reduced reactivity[31] and poses potential α/β regioselectivity issues, especially in the absence of additives, the Pd/**L34** system allowed chemoselective reactions at the sterically hindered –Cl site, including with *ortho*- and di-*ortho*-substituted groups, to give C–H arylation products with excellent regioselectivity (Table 3.5, **7e** and **7n**). Furthermore, electronically biased chloroaryl triflates, wherein the reactivity of the –OTf group was augmented by electron-withdrawing groups (–CF_3, –CHO, and –F) *ortho* to the –OTf group, selectively reacted at the C–Cl bond, affording products with outstanding α-regioselectivity (Table 3.5, **7b**, **7c**, and **7m**). The relatively low yield observed for **7l** could be attributed to the decomposition of both the starting material and the product.

Table 3.5 Palladium-catalyzed regio- and chemoselective C–H arylation of benzo[*b*]thiophene[a]

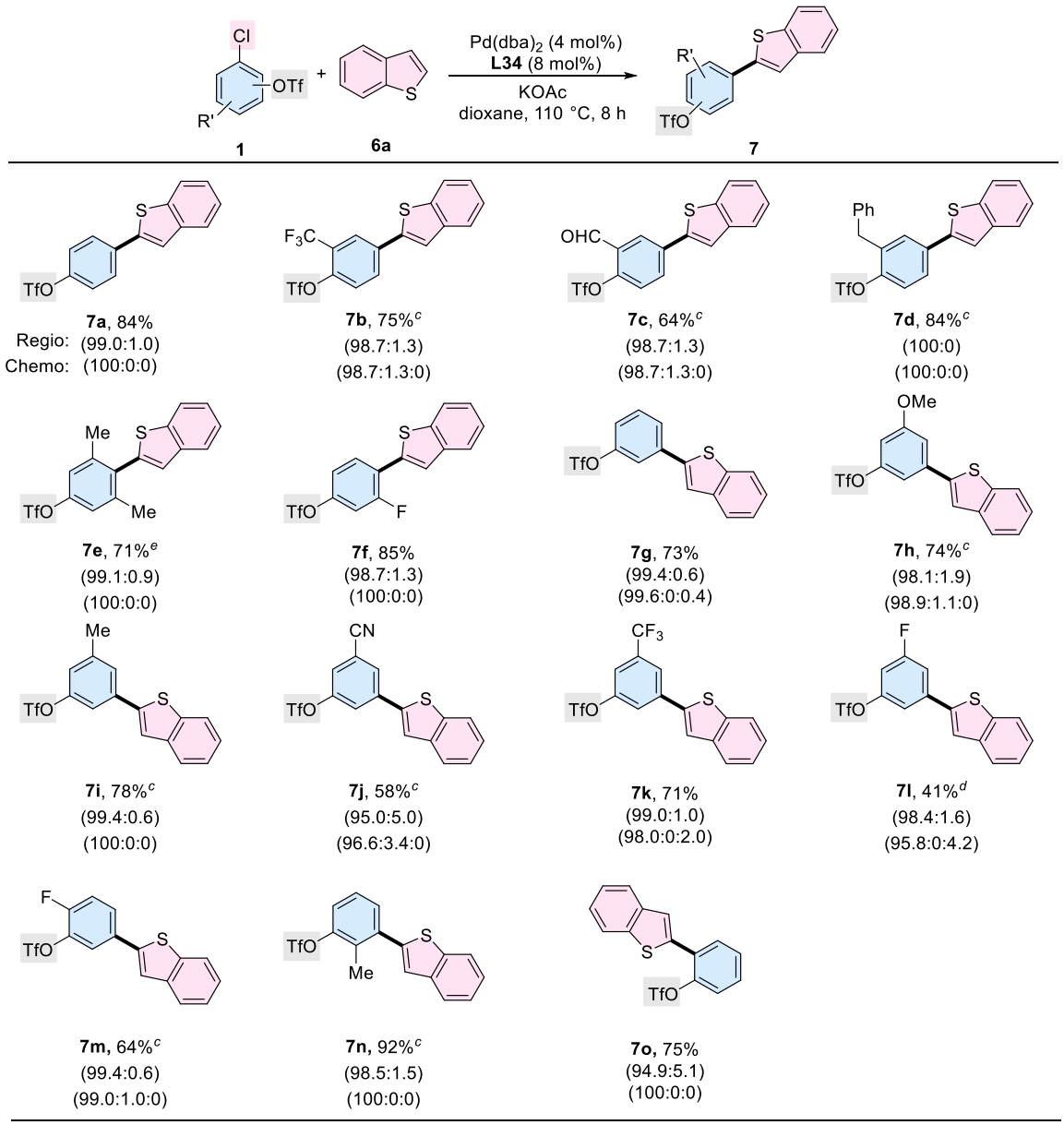

[a]Reaction conditions: 4-chlorophenyltriflate (0.20 mmol), benzo[*b*]thiophene (0.30 mmol), $Pd(dba)_2$ (4.0 mol%), **L34** (8.0 mol%), KOAc (0.40 mmol) and dioxane (1.0 mL) were stirred at 110 °C for 8 h. Isolated yields are reported. The ratio in the first parentheses represents the chemoselectivity ratio in a crude reaction mixture (products from reacting on the C–Cl site: C–OTf site: both sites). The ratio in the second parentheses represents the regioselectivity ratio in a crude reaction mixture (products from reacting on the α site: β site). [b]10 h. [c]12 h. [d]14 h. [e]16 h.

3.2.6 Exploration of the Scope of Heterocycles and Relative Derivatives

We subsequently conducted an investigation involving a variety of heterocycles and their derivatives (Table 3.6). Benzo[*b*]thiophene derivatives and thiophenes

containing electron-donating groups (Me, *n*-Bu, *n*-Hex, and –OMe) or electron-withdrawing groups (esters, ketones, and Py) underwent smooth coupling with 4-chlorophenyl triflate, exclusively at the C–Cl bond, resulting in the formation of α-regioselective products in good yield (Table 3.6, **7p**–**7x**). Furan, known for its high p*Ka* value of the C–H bond (p*Ka* = 35 in DMSO)[32] and generally needing high temperatures (130-150 °C) to active,[33] underwent regio- and chemoselective C–H arylation at a milder 110 °C utilizing a weak base KOAc in the Pd/**L34** catalytic system (Table 3.6, **7y** and **7z**). In the case of benzofuran, which generally exhibits poor regioselectivity because of comparable activation energies at the α and β positions of the C–H bond,[6a, 34] we achieved good yields with excellent regioselectivity and exclusive C–Cl chemoselectivity by utilizing **L34** as the ligand (Table 3.6, **7aa**). As for thiazole, we obtained exclusively C2 regioselective products without observing the generation of di-arylated products (Table 3.6, **7ab**). In addition, **L-menthol** derivatives and caffeine proved amenable to facile modifications, as they yielded C–H arylated products in moderate to good yields, exhibiting exclusive C–Cl chemoselectivity (Table 3.6, **7ac** and **7ad**).

Table 3.6 Palladium-catalyzed chemoselective C–Cl (over C–OTf) and regioselective C–H arylation of heterocycles[a]

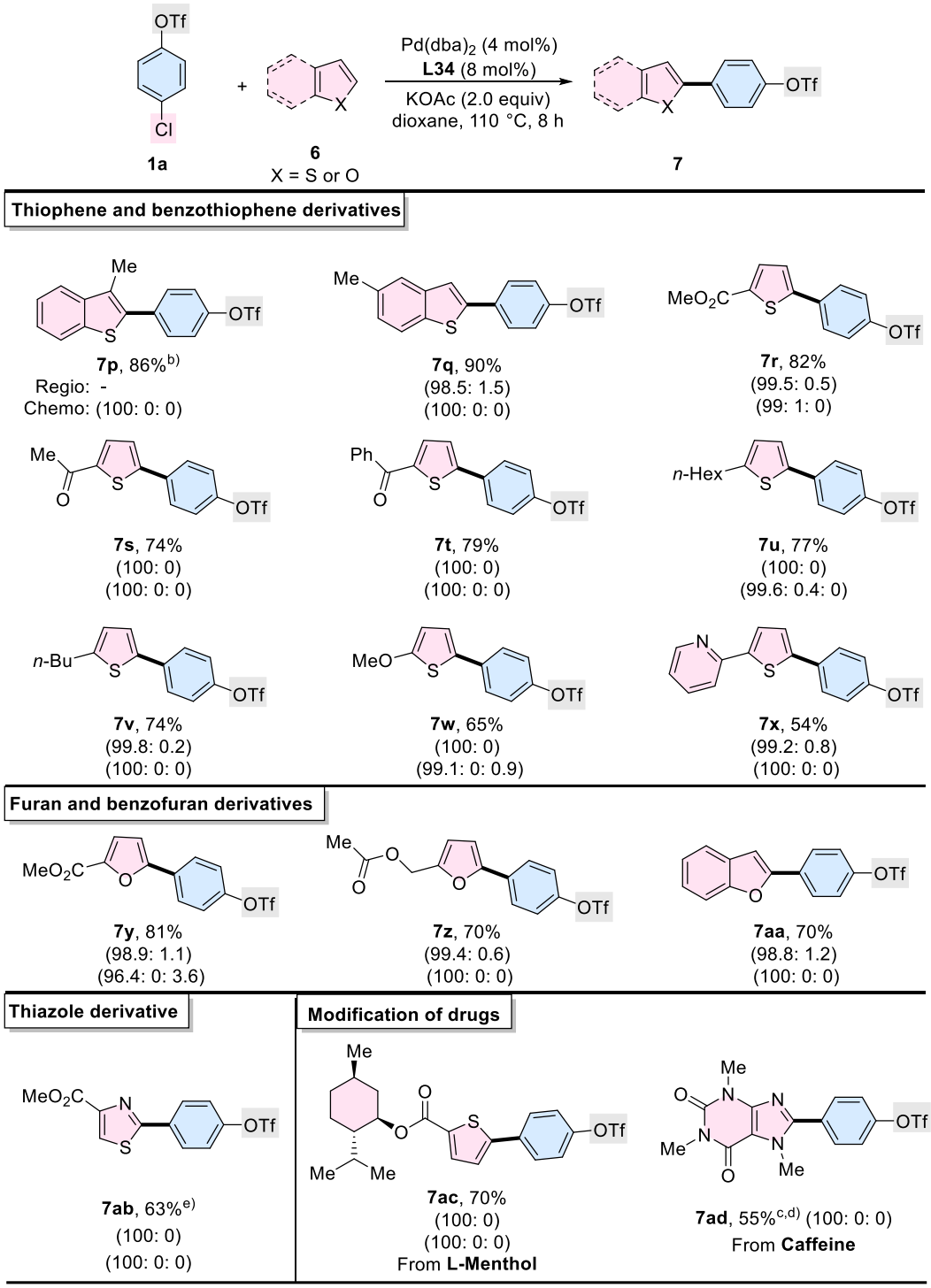

[a]Reaction conditions: 4-chlorophenyltriflate (0.20 mmol), heterocycles (0.30 mmol), $Pd(dba)_2$ (4.0 mol%), **L34** (8.0 mol%), KOAc (0.40 mmol), and dioxane (1.0 mL) were stirred at 110 °C for 8 h. Isolated yields are reported. The ratio in the first parentheses represents the chemoselectivity ratio in a crude reaction mixture (products from reacting on the C–Cl site: C–OTf site: both sites). The ratio in the second parentheses represents the regioselectivity ratio in a crude reaction mixture (products from reacting on the α site: β site). [b]12 h. [c]24 h. [d]2.0 equiv. K_2CO_3 as base. [e]**1a**: **6** = 1.0: 2.0.

3.2.7 Gram-Scale Regio- and Chemoselective C–H arylation

To demonstrate the scalability of the present reaction conditions, we conducted a gram-scale regio- and chemoselective C–H arylation of benzo[*b*]thiophene and 4-chlorophenyltriflate (Scheme 3.3). The reaction could be readily upscaled by a factor of 50, resulting in the production of the coupling product with a yield of 56%.

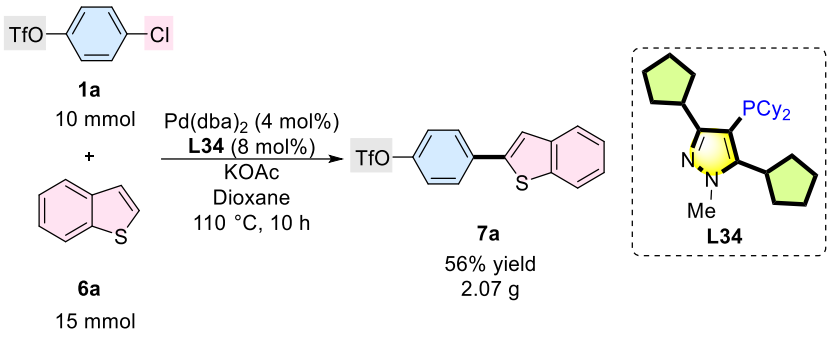

Scheme 3.3 Gram-scale synthesis. Reaction conditions: 4-chlorophenyltriflate (10 mmol), benzo[*b*]thiophene (15 mmol), $Pd(dba)_2$ (4.0 mol%), **L34** (8.0 mol%), KOAc (20 mmol), and dioxane (50 mL) were stirred at 110 °C for 8 h. Isolated yield is reported. The ratios of **7a**:**8a**:**9a** and **7a**:**7a'** are 100:0:0 and 98:2, respectively.

3.2.8 Synthetic Applications

The potential synthetic utility was additionally demonstrated by the synthesis of the optical materials (Scheme 3.4, compound **11a**),[35] along with its analogues (compounds **11b** and **11c**)[36] via a straightforward functionalization of highly reactive Ar–OTf from compound **7a**.

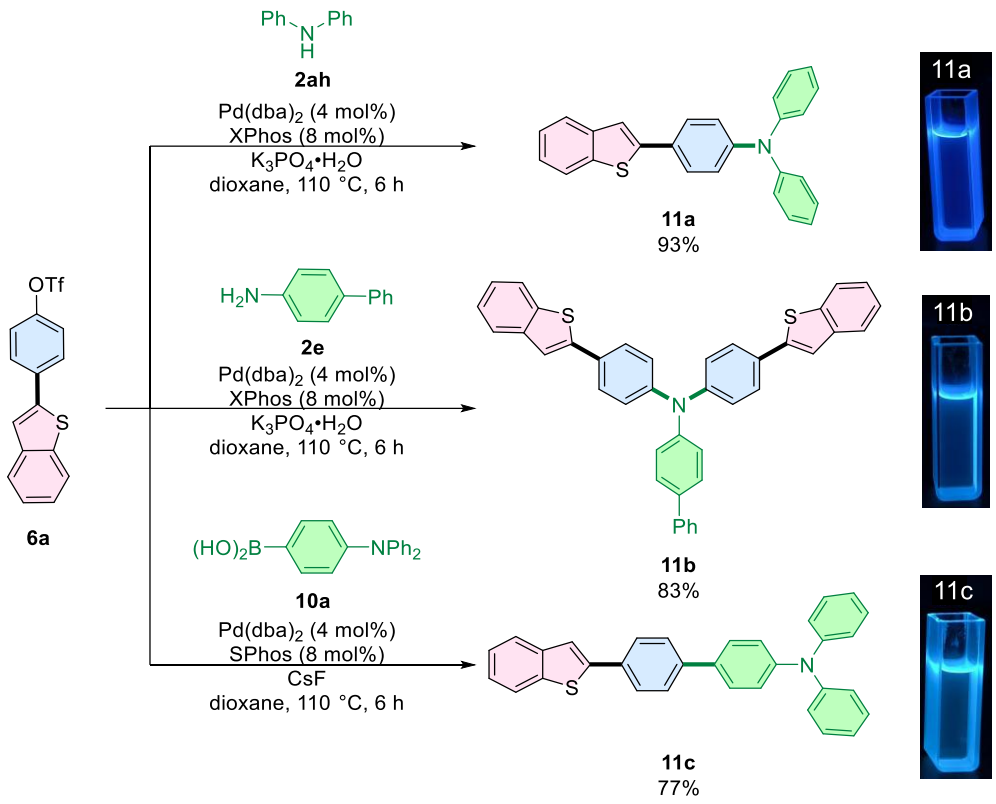

Scheme 3.4 Synthetic application for synthesis of optical materials. (Photographs taken under 365 nm UV light for the compounds dissolved in DCM.)

3.3 Conclusion

We have successfully improved the synthetic route for pyrazole-alkyl-phosphine ligands, leading to the synthesis of a series of such ligands with varying cycloalkyl ring sizes in a facile and highly efficient way. We subsequently investigated a novel methodology for regio- and chemoselective C–H arylation of heterocycles, utilizing innovative newly developed ligands. These ligands have demonstrated promising efficacy in facilitating additive-free arylation of various heterocycles including benzo[*b*]thiophene, thiophene, furan, benzofuran, and thiazole, with diverse chloroaryl triflates, resulting in good to excellent yields under relatively mild conditions. The

distinctiveness of this approach is ascribed to the varying cycloalkyl ring sizes within the ligand motif, which seem to play a crucial role in providing high reactivity for regio- and chemoselective reactions. Notable findings include notable α/β selectivity in the arylation of heterocycles and a remarkable chemoselective arylation of C–Cl instead of C–OTf, paving the way for an efficient and selective preparation of hetero-biaryl compounds. Supported by experimental evidence and DFT calculation results, we propose that the optimally sized pyrazole phosphine ligands may reduce the energy barrier in the C–H activation step through a CMD and reductive elimination pathway. The potential of these ligands to facilitate C–H arylation under relatively mild conditions, without the requirement of additional additives may represent a meaningful advance in heterocycle functionalization. This approach may provide advantages for sustainable methodologies of organic synthesis, especially in areas such as pharmaceuticals and natural products.

3.4 Experimental Section

3.4.1 General Consideration

Unless otherwise noted, all reagents were purchased from commercial suppliers and used without purification. All Pd-catalyzed reactions were carried out in a resealable screw cap Schlenk tube (approx. 20 mL volume) in the presence of a Teflon-coated magnetic stirrer bar (5 mm x 10 mm). Dioxane, cyclopentyl methyl ether (CPME) and toluene were freshly distilled from sodium under nitrogen. Tetrahydrofuran (THF) was freshly distilled from sodium benzophenone ketyl under nitrogen. tert-Butanol (*t*-

BuOH) and *n*-hexane were freshly distilled from anhydrous CaH_2 under nitrogen. **L1, L2, L5, L7–L10, L12, L36–L38** were purchased from commercial suppliers. CySelectPhos **L24** was prepared according to the reported literature.[27] A new bottle of *n*-butyllithium was used. Thin-layer chromatography was performed on pre-coated silica gel 60 F254 plates. Silica gel (Grace, 60Å, 40-63 μm) was used for column chromatography. Melting points were recorded on an uncorrected Stuart Melting Point SMP30 instrument. ^{1}H, ^{13}C, ^{19}F NMR and ^{31}P spectra were recorded using Brüker spectrometers operating at 400 MHz and 600 MHz, along with a Jeol JMN-ECZ500R/S1 spectrometer at 500 MHz. Spectra were referenced internally to the residual proton resonance in $CDCl_3$ (δ 7.26 ppm) as the internal standard. ^{13}C NMR spectra were referenced to $CDCl_3$ (δ 77.0 ppm, the middle peak). ^{19}F NMR chemical shifts were determined relative to $CFCl_3$ as the external standard and low field is positive. ^{31}P NMR spectra were referenced to 85% H_3PO_4 externally. Coupling constants (J) were reported in Hertz (Hz). Mass spectra (EI-MS) were recorded on an HP 5977A MSD Mass Spectrometer. High-resolution mass spectra (HRMS) were obtained on the Agilent 6540 ESI-QTof-MS or APPI-QTof-MS and a Waters GCT Premier EI-ToF-MS. GC-MS analysis was conducted on a HP 7890B GC system using a HP5MS column (30 m x 0.25 mm). The products described in GC yield were accorded to the authentic samples/dodecane calibration standard from HP 7890B GC-FID system. All yields reported referring to the isolated yield of compounds estimated to be greater than 95% purity as determined by capillary gas chromatography (GC) or 1H NMR. Compounds described in the literature were characterized by a comparison of their ^{1}H,

^{13}C, ^{19}F and/or ^{31}P NMR spectra to the previously reported data. The procedures in this section are representative, and thus the yields may differ from those reported in tables.

3.4.2 General Procedure for Initial Ligand Screening

Benzo[*b*]thiophene (0.30 mmol), $Pd(dba)_2$ (0.0080 mmol), ligand (0.016 mmol), and KOAc (0.40 mmol) were added to the Schlenk tube that was charged with Teflon-coated magnetic stir bar (5 mm x 10 mm) and equipped with screw cap. The tube was carefully evacuated and flushed with nitrogen (3 cycles). 4-Chlorophenyltriflate (0.20 mmol), and the freshly distilled dioxane (1.00 mL) were added via syringes. The tube was sealed and magnetically stirred at a preheated 110 °C oil bath for 8 h. The reaction was then allowed to reach room temperature. Ethyl acetate (~4.0 mL), dodecane (45.2 mL, internal standard), and water (~2.0 mL) were added. The organic layer was subjected to GC analysis. The GC yield was previously calibrated by an authentic sample/dodecane calibration curve.

3.4.3 General Procedure for Screening of Reaction Conditions

Benzo[*b*]thiophene (0.30 mmol), Pd source (0.0080 mmol), **L34** (0.0080-0.032 mmol), and base (0.40 mmol) were added to the Schlenk tube that was charged with Teflon-coated magnetic stir bar (5 mm x 10 mm) and equipped with screw cap. The tube was carefully evacuated and flushed with nitrogen (3 cycles). 4-Chlorophenyltriflate (0.20 mmol), and the freshly distilled solvent (1.00 mL) were added via syringes. The tube was sealed and magnetically stirred at a preheated 110 °C oil bath for 8 h. The reaction was then allowed to reach room temperature. Ethyl acetate

(~4 mL), dodecane (45.2 mL, internal standard), and water (~2 mL) were added. The organic layer was subjected to GC analysis. The GC yield was previously calibrated by an authentic sample/dodecane calibration curve.

3.4.4 Competition Experiments between 3-Chloro-5-methylphenyltriflate and 3-Chloro-5-(trifluoromethyl)phenyltriflate with Benzo[*b*]thiophene

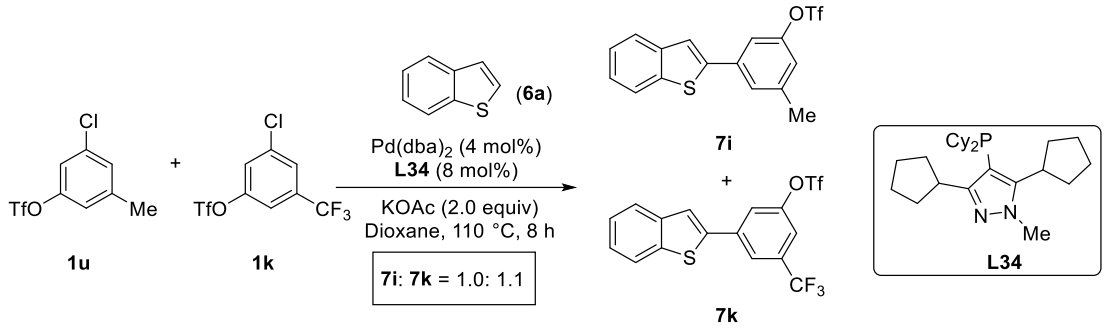

Benzo[*b*]thiophene (40.2 mg, 0.3 mmol), $Pd(dba)_2$ (4.60 mg, 0.0080 mmol), **L34** (6.60 mg, 0.016 mmol), and KOAc (39.0 mg, 0.40 mmol) were added to the Schlenk tube that was charged with Teflon-coated magnetic stir bar (5 mm x 10 mm) and equipped with screw cap. The tube was carefully evacuated and flushed with nitrogen (3 cycles). 3-chloro-5-methylphenyltriflate (27.4 mg, 0.10 mmol), 3-chloro-5-(trifluoromethyl)phenyltriflate (32.8 mg, 0.10 mmol) and the freshly distilled solvent (1.00 mL) were added via syringes. The tube was sealed and magnetically stirred at a preheated 110 °C oil bath for 8 h. The reaction was then allowed to reach room temperature. Ethyl acetate (~4 mL), dodecane (45.2 mL, internal standard), and water (~2 mL) were added. The organic layer was subjected to GC analysis. The ratio of coupling products **7i** and **7k** was determined to be 1.0:1.1 by GC-MS.

3.4.5 Competition Experiments between 2-Acetylthiophene and 2-*n*-

Butylthiophene with 4-Chlorophenyltriflate

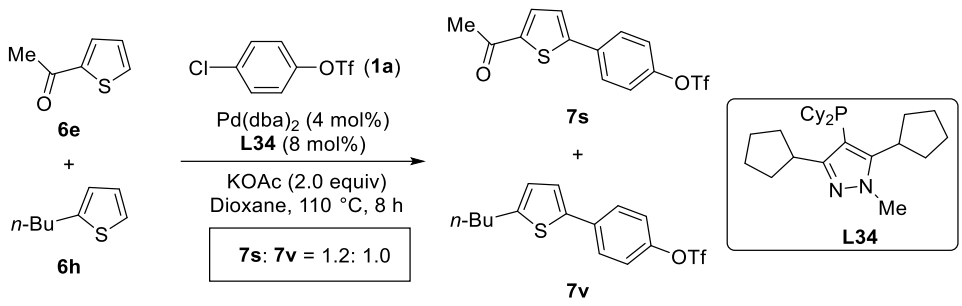

$Pd(dba)_2$ (4.60 mg, 0.0080 mmol), **L34** (6.60 mg, 0.016 mmol), and KOAc (39.0 mg, 0.40 mmol) were added to the Schlenk tube that was charged with Teflon-coated magnetic stir bar (5 mm x 10 mm) and equipped with screw cap. The tube was carefully evacuated and flushed with nitrogen (3 cycles). 4-Chlorophenyltriflate (52.0 mg, 0.20 mmol), 2-acetylthiophene **6e** (12.6 mg, 0.1 mmol), 2-*n*-butylthiophene **6h** (14.0 mg, 0.1 mmol) and the freshly distilled solvent (1.00 mL) were added via syringes. The tube was sealed and magnetically stirred at a preheated 110 ºC oil bath for 8 h. The reaction was then allowed to reach room temperature. Ethyl acetate (~4 mL), dodecane (45.2 mL, internal standard), and water (~2 mL) were added. The organic layer was subjected to GC analysis. The ratio of coupling products **7s** and **7v** was determined to be 1.2:1.0 by GC-MS.

3.4.6 Deuterium Scrambling Experiments

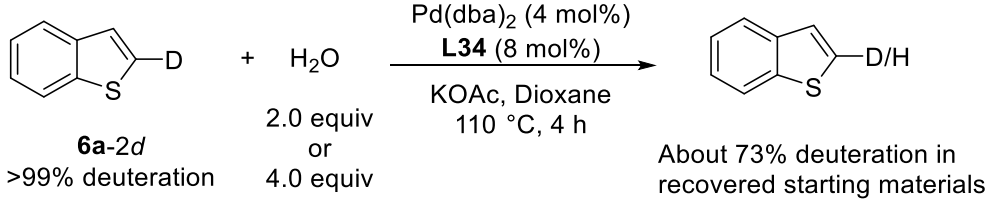

Benzo[*b*]thiophene **6a**-2*d* (13.5 mg, 0.10 mmol, 1.0 equiv), $Pd(dba)_2$ (4.60 mg,

0.0080 mmol), **L34** (6.60 mg, 0.016 mmol), and KOAc (39.0 mg, 0.40 mmol) were added to the Schlenk tube that was charged with Teflon-coated magnetic stir bar (5 mm x 10 mm) and equipped with screw cap. The tube was carefully evacuated and flushed with nitrogen (3 cycles). The water (2.0 equiv or 4.0 equiv) and the freshly distilled solvent (1.00 mL) were added via syringes. The tube was sealed and magnetically stirred at a preheated 110 °C oil bath for 4 h. The resultant mixture was diluted with EtOAc (10.0 mL) and filtered through a plug of silica. The silica plug was flushed with EtOAc (30 mL) and the filtrate was evaporated to dryness under reduced pressure. H/D scrambling was calculated by ^{1}H-NMR in $CDCl_3$ using 1,3,5-trimethoxybenzene as an internal standard.

3.4.7 KIE Determined from Two Parallel Reactions

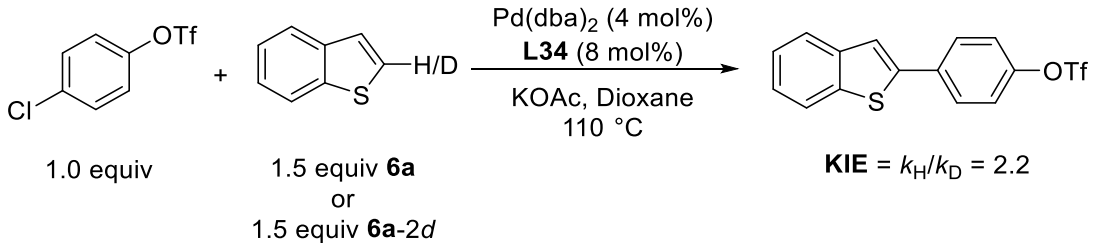

Experiments for the deuterated and non-deuterated substrates were done simultaneously utilizing two Schlenk tubes separately in one set of reactions. Benzo[*b*]thiophene **6a** (40.2 mg, 0.3 mmol, 1.5 equiv) or Benzo[*b*]thiophene **6a-**2*d* (40.5 mg, 0.3 mmol, 1.5 equiv) were added into two Schlenk tubes separately, every tube was then charged with $Pd(dba)_2$ (4.60 mg, 0.0080 mmol), **L34** (6.60 mg, 0.016 mmol), KOAc (39.0 mg, 0.40 mmol), Teflon-coated magnetic stir bar (5 mm x 10 mm) and equipped with screw cap. The tube was carefully evacuated and flushed with

nitrogen (3 cycles). 4-Chlorophenyltriflate (52.0 mg, 0.20 mmol) and the freshly distilled solvent (1.00 mL) were added via syringes. The tube was sealed and magnetically stirred at a preheated 110 °C oil bath for appropriate times. The reaction was then allowed to reach room temperature. Ethyl acetate (~4 mL), dodecane (45.2 mL, internal standard), and water (~2 mL) were added. The organic layer was subjected to GC analysis. The GC yield was previously calibrated by an authentic sample/dodecane calibration curve.

3.4.8 KIE Determined from Two Parallel Reactions

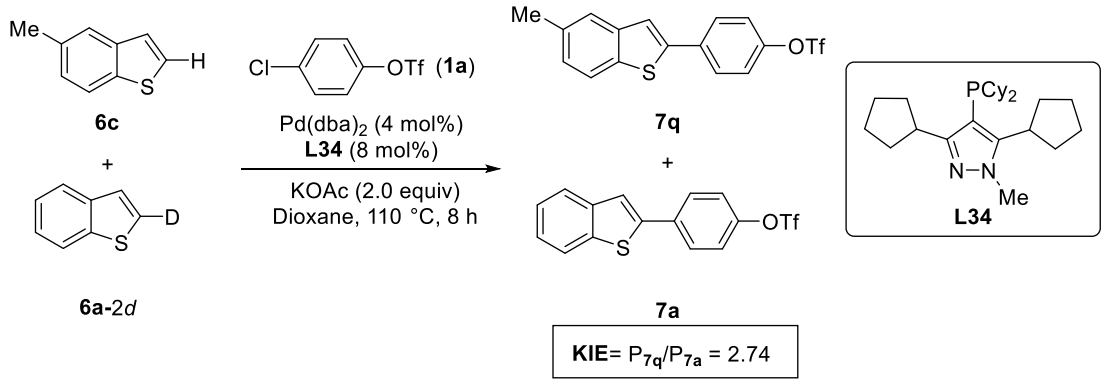

5-Methylbenzo[*b*]thiophene **6c** (22.2 mg, 0.15 mmol), benzo[*b*]thiophene-2-*d* **6a**-2*d* (20.3 mg, 0.15 mmol), $Pd(dba)_2$ (4.60 mg, 0.0080 mmol), **L34** (6.60 mg, 0.016 mmol), and KOAc (39.0 mg, 0.40 mmol) were added to the Schlenk tube that was charged with Teflon-coated magnetic stir bar (5 mm x 10 mm) and equipped with screw cap. The tube was carefully evacuated and flushed with nitrogen (3 cycles). 4-Chlorophenyltriflate (52.0 mg, 0.20 mmol), and the freshly distilled solvent (1.00 mL) were added via syringes. The tube was sealed and magnetically stirred at a preheated 110 °C oil bath for 8 h. The reaction was then allowed to reach room temperature. Ethyl acetate (~4 mL), dodecane (45.2 mL, internal standard), and water (~2 mL) were added.

The organic layer was subjected to GC analysis. The yields of coupling products **7a** and **7q** were determined by GC-FID using dodecane as internal standard. The k_H/k_D was estimated to be 2.74.

3.4.9 The Procedure of Synthetic Applications and Characterization

3.4.9.1 Synthesis of LPd(η^3-C_3H_5)Cl Complexes

General procedure for preparation of LPd(η^3-C_3H_5)Cl complexes: A solution of [Pd(η^3-C_3H_5)Cl]$_2$ (0.0370 g, 0.100 mmol, and **L** (0.0720 g, 0.200 mmol, 1.0 equiv.) in CH_2Cl_2 (1.00 mL) was stirred at room temperature for 30 min. The mixture was treated with rotary evaporator to remove DCM and then was identified by NMR instrument under air.

L32-Pd (η^3-C_3H_5)Cl complex

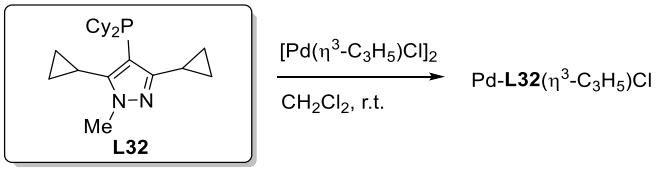

The corresponding **L32**-Pd(η^3-C_3H_5)Cl complex was prepared following the general procedure. **^{1}H NMR** (600 MHz, $CDCl_3$) δ 5.38 (sept, *J* = 6.9 Hz, 1H), 4.55 (t, *J* = 6.9 Hz, 1H), 3.78 (s, 3H), 3.55-3.51 (m, 1H), 3.31 (s, 1H), 2.79 (d, *J* = 9.7 Hz, 1H), 2.71-2.66 (m, 2H), 2.26 (s, 1H), 2.10 (d, *J* = 7.3 Hz, 1H), 2.04 (d, *J* = 6.6 Hz, 1H), 1.95 (s, 1H), 1.85-1.74 (m, 7H), 1.69-1.64 (m, 2H), 1.54-1.49 (m, 1H), 1.35-1.31 (m, 3H), 1.28-1.20 (m, 4H), 1.14-1.09 (m, 1H), 1.05 (d, *J* = 7.7 Hz, 2H), 0.98-0.93 (m, 3H), 0.87-0.83 (m, 3H); **^{31}P NMR** (243 MHz, $CDCl_3$) δ 15.2.

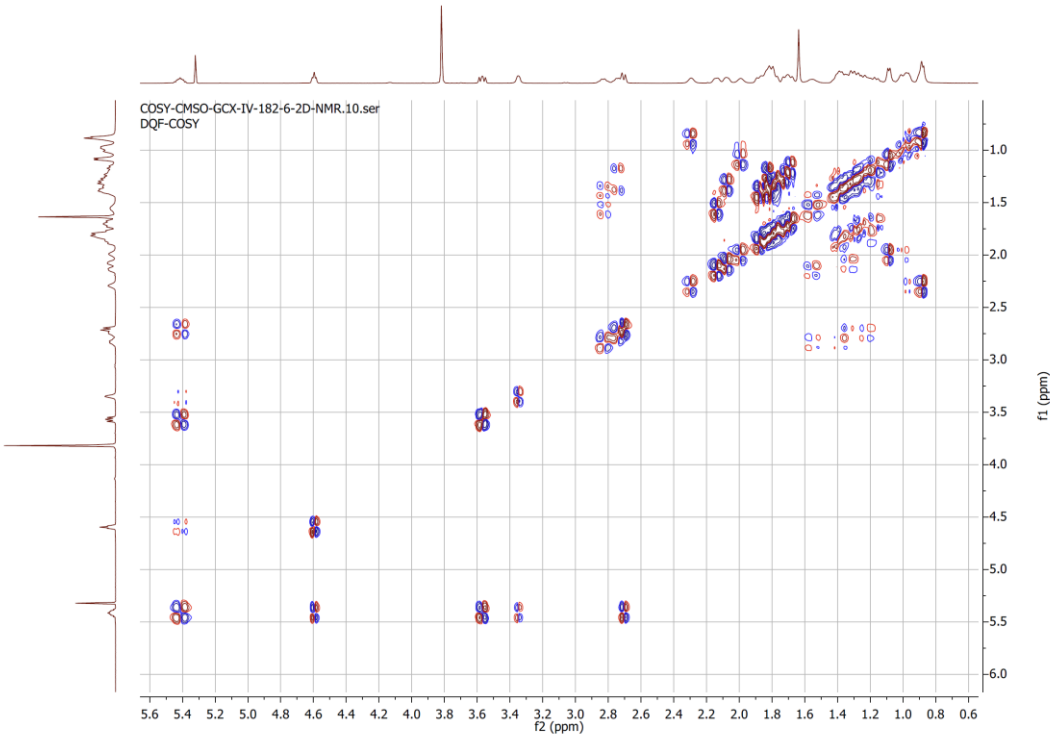

Figure 3.6 Cosy spectra of **L32**-Pd(η^3-C_3H_5)Cl complex

L33-Pd (η^3-C_3H_5)Cl complex

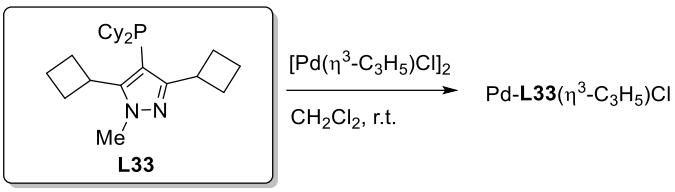

The corresponding **L33**-Pd(η^3-C_3H_5)Cl complex was prepared following the general procedure. **^{1}H NMR** (600 MHz, $CDCl_3$) δ 5.45 (sept, *J* = 6.7 Hz, 1H), 4.66 (t, *J* = 6.7 Hz, 1H), 4.60 (s, 1H), 4.14 (s, 3H), 3.62-3.59 (m, 2H), 3.21 (s. 1H), 2.54-2.34 (m, 7H), 2.23-2.18 (m, 4H), 2.09-2.01 (m, 3H), 1.95-1.80 (m, 4H), 1.73-1.62 (m, 9H), 1.41-1.35 (m, 2H), 1.31-1.25 (m, 2H), 1.17-1.13 (m, 2H), 1.04 (d, *J* = 11.1 Hz, 1H), 0.99-0.93 (m, 1H); **^{31}P NMR** (243 MHz, $CDCl_3$) δ 14.9.

L34-Pd (η^3-C_3H_5)Cl complex

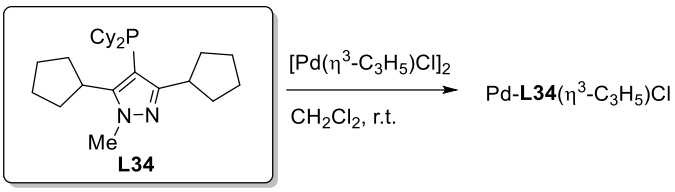

The corresponding **L34**-Pd(η^3-C_3H_5)Cl complex was prepared following the general procedure. **^{1}H NMR** (600 MHz, $CDCl_3$) δ 5.36 (sept, *J* = 6.7 Hz, 1H), 4.61 (t, *J* = 6.7 Hz, 1H), 4.19 (s, 1H), 3.80 (s, 3H), 3.61-3.57 (m, 2H), 3.18 (s, 1H), 2.65 (d, *J* = 11.7 Hz, 1H), 2.44-2.38 (m, 1H), 1.94-1.92 (m, 5H), 1.85-1.58 (m, 23H), 1.49-1.44 (m, 1H), 1.39-1.31 (m, 3H), 1.22-1.19 (m, 3H), 1.16-1.07 (m, 2H); **^{31}P NMR** (243 MHz, $CDCl_3$) δ 12.7.

L25-Pd (η^3-C_3H_5)Cl complex

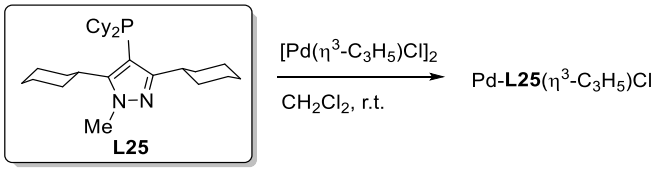

The corresponding **L25**-Pd(η^3-C_3H_5)Cl complex was prepared following the general procedure.**^{1}H NMR** (400 MHz, $CDCl_3$) δ 5.47 (sept, *J* = 7.1 Hz, 1H), 4.65 (t, *J* = 7.1 Hz, 1H), 4.05 (s, 1H), 3.90 (s, 3H), 3.71-3.78 (m, 2H), 2.69-2.84 (m, 2H), 2.20-2.35 (m, 2H), 1.55-1.95 (m, 26H), 1.10-1.50 (m, 14H); **^{31}P NMR** (162 MHz, $CDCl_3$) δ 10.4.

L35-Pd (η^3-C_3H_5)Cl complex

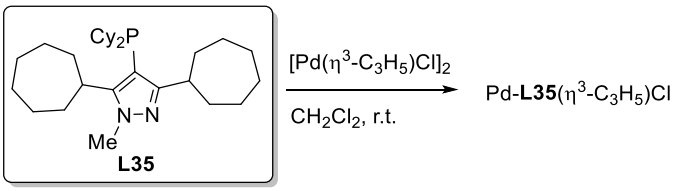

The corresponding **L35**-Pd(η^3-C_3H_5)Cl complex was prepared following the

general procedure. **^{1}H NMR** (600 MHz, $CDCl_3$) δ 5.43 (sept, *J* = 6.8 Hz, 1H), 4.63 (t, *J* = 6.8 Hz, 1H), 4.08 (s, 1H), 3.81 (s, 3H), 3.77 (s, 1H), 3.68 (dd, *J* = 9.7, 3.1 Hz, 1H), 2.91 (s, 1H), 2.70 (d, *J* = 11.8 Hz, 1H), 2.26 (s, 1H), 1.89-1.77 (m, 20H), 1.67-1.55 (m, 14H), 1.47-1.41 (m, 4H), 1.34-1.27 (m, 3H), 1.23-1.16 (m, 4H); **^{31}P NMR** (243 MHz, $CDCl_3$) δ 11.4.

3.4.9.2 Procedure of Synthetic Application and Characterization

4-(Benzo[*b*]thiophen-2-yl)-*N*,*N*-diphenylaniline (Scheme 3.4, compound 11a)

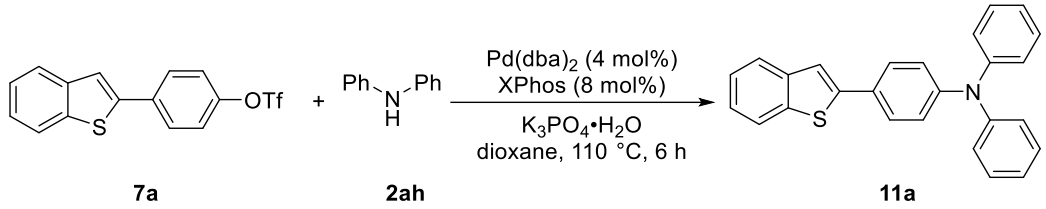

7a **2ah** **11a**

4-(Benzo[*b*]thiophen-2-yl)phenyl triflate **7a** (0.10 mmol, 35.8 mg), diphenylamine **2ah** (0.15 mmol, 25.4 mg), $Pd(dba)_2$ (0.0040 mmol, 2.3 mg), XPhos (0.0080 mmol, 3.8 mg), and $K_3PO_4 \cdot H_2O$ (0.20 mmol, 46 mg) were added to the Schlenk tube that was charged with Teflon-coated magnetic stir bar (5 mm x 10 mm) and equipped with screw cap. The tube was carefully evacuated and flushed with nitrogen (3 cycles). The freshly distilled dioxane (1.00 mL) was added via syringes. The tube was sealed and magnetically stirred at a preheated 110 °C oil bath for 6 h. The reaction was then allowed to reach room temperature. Then ethyl acetate and water were added to the mixture, organic layer was extracted by ethyl acetate, washed with brine and dried by anhydrous sodium sulfate and concentrated under reduced pressure. Purification by column chromatography (Hexane: DCM = 3:1) to afford 4-(benzo[*b*]thiophen-2-yl)-*N*,*N*-diphenylaniline **11a**.

Yield: 93% (34.9 mg), light-yellow solid. **^{1}H NMR** (600 MHz, $CDCl_3$) δ 7.81 (d, *J* = 7.9 Hz, 1H), 7.74 (d, *J* = 7.9 Hz, 1H), 7.57 (d, *J* = 8.5 Hz, 2H), 7.45 (s, 1H), 7.34 (t, *J* = 7.4 Hz, 1H), 7.29 (t, *J* = 7.7 Hz, 5H), 7.15 (d, *J* = 7.7 Hz, 4H), 7.10 (d, *J* = 8.2 Hz, 2H), 7.06 (t, *J* = 7.3 Hz, 2H); **^{13}C NMR** (150 MHz, $CDCl_3$) δ 148.0, 147.3, 144.1, 140.9, 139.1, 129.3, 128.0, 127.2, 124.7, 124.4, 124.0, 123.3, 123.25, 123.21, 122.17, 118.2.

_N_,_N_-Bis(4-(benzo[_b_]thiophen-2-yl)phenyl)-[1,1'-biphenyl]-4-amine (Scheme 3.4, compound 11b)

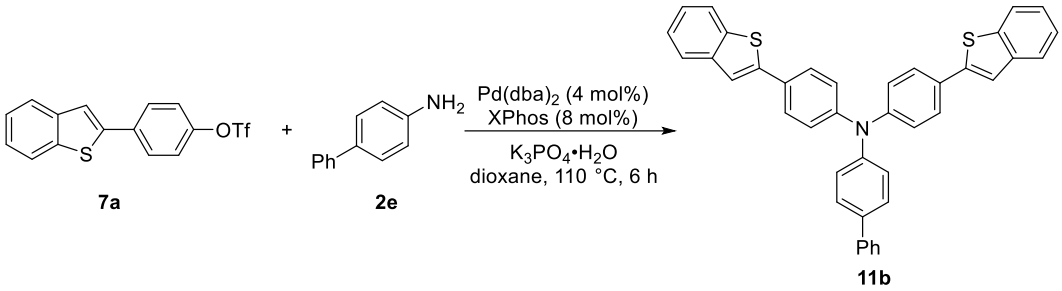

4-(Benzo[*b*]thiophen-2-yl)phenyl triflate **7a** (0.40 mmol, 143.2 mg), 4-aminobiphenyl **2e** (0.20 mmol, 33.8 mg), $Pd(dba)_2$ (0.0080 mmol, 4.6 mg), X-Phos (0.016 mmol, 7.6 mg), and $K_3PO_4 \cdot H_2O$ (0.40 mmol, 92 mg) were added to the Schlenk tube that was charged with Teflon-coated magnetic stir bar (5 mm x 10 mm) and equipped with screw cap. The tube was carefully evacuated and flushed with nitrogen (3 cycles). The freshly distilled dioxane (2.00 mL) was added via syringes. The tube was sealed and magnetically stirred at a preheated 110 °C oil bath for 6 h. The reaction was then allowed to reach room temperature. Then DCM and water were added to the mixture, organic layer was extracted by DCM, washed with brine and dried by anhydrous sodium sulfate and concentrated under reduced pressure. After the solvent

was removed under vacuum, the solid product was washed with a cold mixture solvent (MeOH: DCM = 10:1, 10 ml x 3) to afford *N*,*N*-bis(4-(benzo[*b*]thiophen-2-yl)phenyl)-[1,1'-biphenyl]-4-amine **11b**.

Yield: 83% (97.0 mg). Yellow solid; **^{1}H NMR** (600 MHz, $CDCl_3$) δ 7.82 (d, *J* = 7.7 Hz, 2H), 7.76 (d, *J* = 7.7 Hz, 2H), 7.64 (d, *J* = 7.7 Hz, 4H), 7.61 (d, *J* = 7.4 Hz, 2H), 7.55 (d, *J* = 7.6 Hz, 2H), 7.49 (s, 2H), 7.45 (t, *J* = 7.3 Hz, 2H), 7.37-7.34 (m, 3H), 7.31 (t, *J* = 7.5 Hz, 2H), 7.25 (d, *J* = 8.1 Hz, 2H), 7.21 (d, *J* = 7.7 Hz, 4H); **^{13}C NMR** (150 MHz, $CDCl_3$) δ 147.3, 146.2, 143.9, 140.8, 140.4, 139.2, 136.4, 128.9, 128.8, 128.1, 127.4, 127.0, 126.7, 125.0, 124.5, 124.1, 124.09, 123.3, 122.2, 118.6.

4'-(Benzo[*b*]thiophen-2-yl)-*N*,*N*-diphenyl-[1,1'-biphenyl]-4-amine (Scheme 3.4, compound 11c)

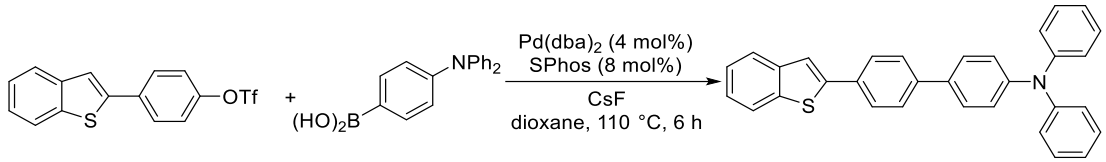

4-(Benzo[*b*]thiophen-2-yl)phenyl triflate **7a** (0.20 mmol, 71.6 mg), 4-(diphenylamino)phenylboronic acid **10a** (0.30 mmol, 86.8 mg), $Pd(dba)_2$ (0.0080 mmol, 4.6 mg), S-Phos (0.016 mmol, 6.6 mg), and CsF (0.40 mmol, 92 mg) were added to the Schlenk tube that was charged with Teflon-coated magnetic stir bar (5 mm x 10 mm) and equipped with screw cap. The tube was carefully evacuated and flushed with nitrogen (3 cycles). The freshly distilled dioxane (2.00 mL) was added via syringes. The tube was sealed and magnetically stirred at a preheated 110 ^{o}C oil bath for 6 h. The reaction was then allowed to reach room temperature. Then DCM and water were added

to the mixture, organic layer was extracted by DCM, washed with brine and dried by anhydrous sodium sulfate and concentrated under reduced pressure. After the solvent was removed under vacuum, the solid product was washed with a cold mixture solvent (MeOH: DCM = 10:1, 10 ml x 3) to afford 4'-(benzo[*b*]thiophen-2-yl)-*N*,*N*-diphenyl-[1,1'-biphenyl]-4-amine **11c**.

Yield: 77% (70.1 mg). Light-yellow solid; **^{1}H NMR** (600 MHz, $CDCl_3$) δ 7.84 (d, *J* = 7.8 Hz, 1H), 7.79-7.76 (m, 3H), 7.64 (d, *J* = 7.7 Hz, 2H), 7.58 (s, 1H), 7.52 (d, *J* = 8.1 Hz, 2H), 7.36 (t, *J* = 7.3 Hz, 1H), 7.32 (t, *J* = 7.6 Hz, 1H), 7.28 (t, *J* = 7.6 Hz, 4H), 7.15 (d, *J* = 8.0 Hz, 6H), 7.05 (t, *J* = 7.3 Hz, 2H); **^{13}C NMR** (150 MHz, $CDCl_3$) δ 147.6, 147.5, 143.9, 140.7, 140.5, 139.4, 134.0, 132.7, 129.3, 127.5, 127.0, 126.8, 124.5, 124.3, 123.7, 123.5, 123.1, 122.2, 119.2.

3.4.9.3 Synthesis of Starting Materials

Preparation of (1*R*,2*S*,5*R*)-2-Isopropyl-5-methylcyclohexyl thiophene-2-carboxylate. Known compound.[37]

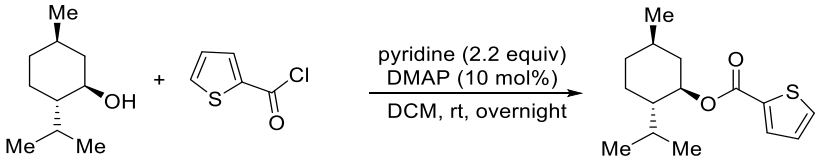

L-Menthol (1.56 g, 10.0 mmol, 1.0 equiv.) and 4-(Dimethylamino) pyridine (122 mg, 1.00 mmol, 0.1 equiv.) were added to a three-neck flask equipped with a magnetic stir bar, and the resultant mixture was degassed and filled with nitrogen gas. DCM (50.0 ml) was added, followed by pyridine (1.78 ml, 22.0 mmol, 2.2 equiv.). 2-Thienylcarbonyl chloride (2.14 ml, 20.0 mmol, 2.0 equiv.) in DCM (10 ml) was dropwise via dropping funnel over 5 min. The mixture was allowed to stir at room

temperature overnight. Then the mixture was treated with saturated $NaHCO_3$ solution, extracted with DCM, washed with brine, and dried over Na_2SO_4, filtered, and concentrated under reduced pressure. The crude product was purified by flash column chromatography, with Hexane: Et_2O = 20:1 as eluent, to afford the product.

Yield: 70% (1.90 g). White liquid; **^{1}H NMR** (600 MHz, $CDCl_3$) δ 7.76 (d, *J* = 3.7 Hz, 1H), 7.70 (d, *J* = 8.0 Hz, 2H), 7.32 (d, *J* = 8.5 Hz, 2H), 7.29 (d, *J* = 3.7 Hz, 1H), 4.89 (dt, *J* = 10.8, 4.0 Hz, 1H), 2.13 (d, *J* = 11.8 Hz, 1H), 1.99-1.94 (m, 1H), 1.72 (d, *J* = 11.3 Hz, 2H), 1.54 (t, *J* = 11.3 Hz, 2H), 1.12 (q, *J* = 11.8 Hz, 2H), 0.93-0.92 (m, 7H), 0.81 (d, *J* = 6.9 Hz, 3H); **^{13}C NMR** (150 MHz, $CDCl_3$) δ 161.9, 134.6, 133.0, 132.0, 127.6, 75.2, 47.1, 40.9, 34.2, 31.4, 26.5, 23.7, 22.0, 20.7, 16.6.

Preparation of benzo[*b*]thiophene-2-*d*.[31]

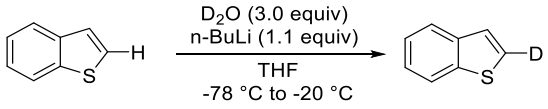

Benzo[*b*]thiophene (0.540 g, 4.00 mmol, 1.0 equiv.) was dissolved in the freshly distilled THF (10.0 mL) at room temperature under a nitrogen atmosphere. The solution was cooled to -78 ºC in a dry ice/acetone bath. Titrated *n*-BuLi (4.40 mmol, 4.4 equiv.) was added dropwise with a syringe. After the reaction mixture was stirred for 1 h at -78 ºC, D_2O (0.220 ml, 12.0 mmol, 3.0 equiv.) was added. The mixture was then diluted with ethyl acetate, washed with brine, dried over Na_2SO_4, filtered, and concentrated under reduced pressure. The crude product was purified by flash column chromatography, with Hexane as eluent, to afford the product as a white solid.

Yield: 87% (0.468 g). **^{1}H NMR** (600 MHz, $CDCl_3$) δ 7.90 (d, *J* = 7.6 Hz, 1H), 7.84 (d, *J* = 7.6 Hz, 1H), 7.40-7.36 (m, 3H).

3.4.9.4 Synthesis of Ligand Precursors and Ligands

1,3-Dicyclopropyl-3-hydroxyprop-2-en-1-one

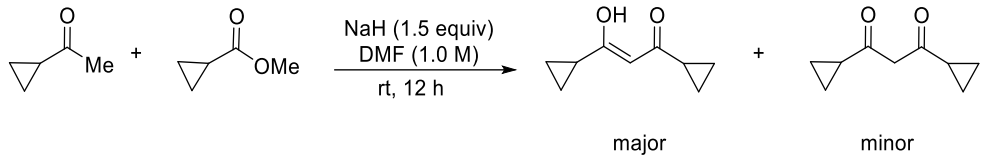

A 500 mL flask was equipped with a magnetic stir bar, which was dried under vacuum with a heat gun and refilled with nitrogen. Sodium hydride (3.00 g, 75.0 mmol, 1.5 equiv, 60% in mineral oil) and DMF (50.0 mL) were added to the flask, and the mixture was stirred. 1-cyclopropylethan-1-one (5.00 mL, 50.0 mmol, 1.0 equiv) and methyl cyclopropanecarboxylate (5.60 mL, 55.0 mmol, 1.1 equiv) were added dropwise to the mixture for 30 min, and the resulting mixture was stirred at room temperature for 12 h. After completion, the solution was quenched with ice water. Then 1 M HCl solution was added to the mixture and adjust the pH to 5, followed by adding saturated Na_2CO_3 solution to adjust pH to 7.5, and extracted three times with ethyl acetate. The combined organic layer was washed with water and brine, and dried over Na_2SO_4, and evaporated under reduced pressure. The crude product was purified by column chromatography, with Hexanes: Ethyl acetate = 20:1, to afford a mixture product of 1,3-dicyclopropyl-3-hydroxyprop-2-en-1-one as major product and 1,3-dicyclopropylpropane-1,3-dione as minor product.

Total yield of two isomers: 76% (5.80 g). Yellow liquid. **Major**: **^{1}H NMR** (600 MHz, $CDCl_3$) δ 5.72 (s, 1H), 1.58-1.54 (m, 2H), 1.08-1.06 (m, 4H), 0.90-0.87 (m, 4H); **^{13}C**

NMR (150 MHz, $CDCl_3$) δ 193.2, 97.9, 21.2, 17.3, 11.7, 9.5; **HRMS** (ESI): $[M+Na]^+$ calcd. for $C_9H_{12}O_2Na^+$: 175.0730, found 175.0733.

3,5-Dicyclopropyl-1-methyl-1*H*-pyrazole

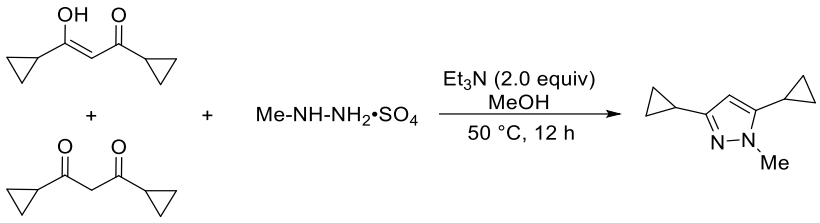

To a mixture of Methylhydrazine sulfate (5.76 g. 40.0 mmol, 2.0 equiv) and MeOH (10.0 ml), Et_3N (5.60 ml, 40.0 mmol, 2.0 equiv) was added. After stirring for a while until all the solids disappeared, this solution was added to a mixture (3.04 g, 20.0 mmol, 1.0 equiv) of 1,3-dicyclopropyl-3-hydroxyprop-2-en-1-one and 1,3-dicyclopropylpropane-1,3-dione of methanol (50.0 ml), and the resulting mixture was stirred at 50 ºC for 12 h (as monitored by GC-MS). The reaction mixture was evaporated under reduced pressure to remove MeOH, and then ethyl acetate and water were added, and extracted with ethyl acetate three times. The combined organic layers were washed with brine, dried over Na_2SO_4, and evaporated under reduced pressure. The crude product was purified by column chromatography, with Hexanes: Ethyl acetate = 4:1, to afford the product.

Yield: 95% (3.08 g, yield). Yellow liquid. **^{1}H NMR** (400 MHz, $CDCl_3$) δ 5.46 (s, 1H), 3.79 (s, 3H), 1.87-1.80 (m, 1H), 1.67-1.61 (m, 1H), 0.93-0.88 (m, 2H), 0.86-0.82 (m, 2H), 0.65-0.63 (m, 2H), 0.61-0.58 (m, 2H); **^{13}C NMR** (100 MHz, $CDCl_3$) δ 153.5, 145.6, 98.4, 35.8, 9.0, 7.7, 6.6, 6.1; **HRMS** (ESI): $[M+H]^+$ calcd. for $C_{10}H_{15}N_2^+$: 163.1230, found 163.1232.

4-Bromo-3,5-dicyclopropyl-1-methyl-1*H*-pyrazole

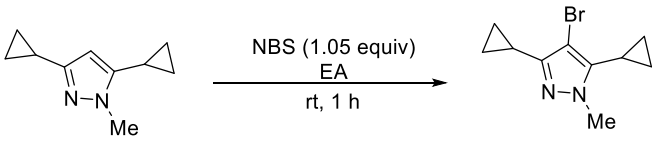

N-Bromosuccinimide (3.46 g, 19.4 mmol, 1.05 equiv) was added to a solution of 3,5-dicyclopropyl-1-methyl-1*H*-pyrazole (3.09 g, 18.5 mmol, 1.0 equiv) in ethyl acetate (40.0 mL) in portion at room temperature. After stirring for 60 min, the solvent was removed by vacuum. DCM and water were added to the mixture and the organic phase was separated. The organic layer was washed with water three times. The combined organic layer was then concentrated to afford the product.

Yield: 98% (4.29 g). Yellow liquid. **^{1}H NMR** (400 MHz, $CDCl_3$) δ 3.77 (s, 3H), 1.83-1.76 (m, 1H), 1.59-1.52 (m, 1H), 1.00-0.95 (m, 2H),0.85-0.81 (m, 6H); **^{13}C NMR** (100 MHz, $CDCl_3$) δ 150.2 140.1, 93.9, 36.9, 7.5, 6.8, 5.4, 5.2; **HRMS** (ESI): $[M+H]^+$ calcd. for $C_{10}H_{14}BrN_2^+$: 241.0335, found 241.0334.

3,5-Dicyclopropyl-4-(dicyclohexylphosphaneyl)-1-methyl-1*H*-pyrazole (L32)

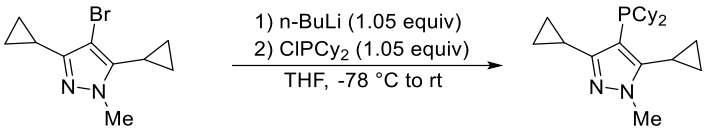

4-Bromo-3,5- dicyclopropyl-1-methyl-1*H*-pyrazole (1.20 g, 5.00 mmol, 1.0 equiv) was dissolved in freshly distilled THF (15.0 mL) at room temperature under nitrogen atmosphere. The solution was cooled to -78 ºC in a dry ice/acetone bath. Titrated *n*-BuLi (5.25 mmol, 1.05 equiv) was added dropwise with a syringe. After the reaction mixture was stirred for 45 min at -78 ºC, chlorodicyclohexylphosphine (1.20 mL, 5.25 mmol, 1.05 equiv) was added. The reaction was allowed to warm to room temperature

and stirred for 60 min. The solvent was removed under reduced pressure. After the solvent was removed under vacuum, the solid product was washed with methanol/degassed water = 5:1 (8.0 mL x 3). The white solid was collected by filtration and dried over vacuum to afford the **L32**.

Yield: 40% (0.71 g). White solid. **^{1}H NMR** (600 MHz, $CDCl_3$) δ 3.77 (s, 3H), 2.17-2.13 (m, 2H), 1.89 (d, *J* = 6.7 Hz, 2H), 1.85-1.81 (m, 1H), 1.75 (d, *J* = 11.6 Hz, 2H), 1.66-1.63 (m, 4H), 1.59-1.57 (m, 1H), 1.51 (d, *J* = 12.5 Hz, 2H), 1.31-1.21 (m, 4H), 1.19-1.14 (m, 4H), 1.01-0.96 (m, 4H), 0.87-0.83 (m, 6H); **^{13}C NMR** (150 MHz, $CDCl_3$) δ 155.3 (d, *J* = 4.8 Hz, 1C), 150.0 (d, *J* = 32.9 Hz, 1C), 107.6 (d, *J* = 15.2 Hz, 1C), 36.6, 34.4 (d, *J* = 7.7 Hz, 1C), 32.5, 32.3, 30.5 (d, *J* = 8.3 Hz, 1C), 27.2, 27.1 (d, *J* = 1.9 Hz, 1C), 27.06, 26.3, 9.7, 7.8, 7.3 (d, *J* = 9.5 Hz, 1C), 6.4 (d, *J* = 3.5 Hz, 1C); ^{31}P NMR (243 MHz, $CDCl_3$) δ -25.5; **HRMS** (ESI): $[M+H]^+$ calcd. for $C_{22}H_{36}N_2P^+$: 359.2611, found 359.2618.

1,3-Dicyclobutyl-3-hydroxyprop-2-en-1-one

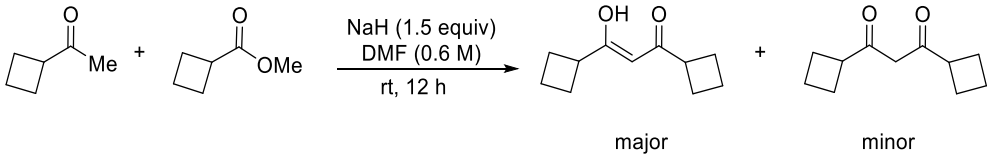

A 500 mL flask was equipped with a magnetic stir bar, which was dried under vacuum with a heat gun and refilled with nitrogen. Sodium hydride (3.00 g, 75.0 mmol, 1.5 equiv, 60% in mineral oil) and DMF (50.0 mL) were added to the flask, and the mixture was stirred. 1-cyclobutylethan-1-one (5.43 mL, 50.0 mmol, 1.0 equiv) and methyl cyclobutanecarboxylate (6.06 mL, 55.0 mmol, 1.1 equiv) were added dropwise to the mixture for 30 min, and the resulting mixture was stirred at room temperature for

12 h. After completion, the solution was quenched with ice water. Then 1 M HCl solution was added to the mixture and adjust the pH to 5, followed by adding saturated Na_2CO_3 solution to adjust pH to 7.5, and extracted three times with ethyl acetate. The combined organic layer was washed with water and brine, and dried over Na_2SO_4, and evaporated under reduced pressure. The crude product was purified by column chromatography, with Hexanes: Ethyl acetate = 20:1, to afford a mixture product of 1,3-dicyclobutyl-3-hydroxyprop-2-en-1-one as major product and 1,3-dicyclobutylpropane-1,3-dione as minor product as yellow liquid.

Total yield of two isomers: 88% (7.90 g). **Major**: **^{1}H NMR** (600 MHz, $CDCl_3$) δ 15.53 (s, 1H), 5.38 (s, 1H), 3.14-3.05 (m, 2H), 2.25-2.14 (m, 8H), 2.00-1.91 (m, 2H), 1.86-1.79 (m, 2H); **^{13}C NMR** (150 MHz, $CDCl_3$) δ 205.1, 195.7, 95.5, 46.0, 41.7, 25.4, 24.1, 18.0, 17.4; **HRMS** (ESI): $[M+Na]^+$ calcd. for $C_{11}H_{16}O_2Na^+$: 203.1043, found 203.1048.

3,5-Dicyclobutyl-1-methyl-1*H*-pyrazole

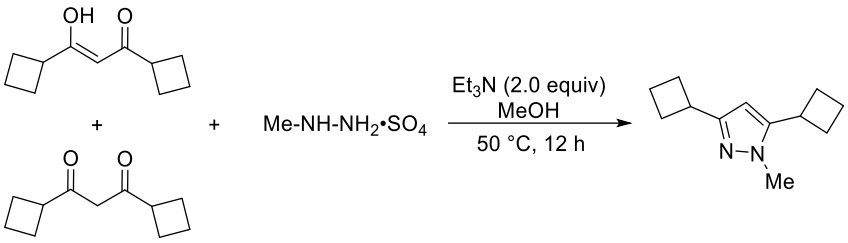

To a mixture of methylhydrazine sulfate (5.76 g. 40.0 mmol, 2.0 equiv) and MeOH (10.0 ml), Et_3N (5.60 ml, 40.0 mmol, 2.0 equiv) was added. After stirring for a while until all the solids disappeared, this solution was added to a mixture (3.60 g, 20.0 mmol, 1.0 equiv) of 1,3-dicyclobutyl-3-hydroxyprop-2-en-1-one and 1,3-dicyclobutylpropane-1,3-dione of methanol (50.0 ml), and the resulting mixture was stirred at 50 ºC for 12 h (as monitored by GC-MS). The reaction mixture was evaporated

under reduced pressure to remove MeOH, and then ethyl acetate and water were added, and extracted with ethyl acetate three times. The combined organic layers were washed with brine, dried over Na_2SO_4, and evaporated under reduced pressure. The crude product was purified by column chromatography, with Hexanes: Ethyl acetate = 4:1, to afford the product as a yellow liquid.

Yield: 98% (3.90 g). **^{1}H NMR** (600 MHz, $CDCl_3$) δ 5.95 (s, 1H), 3.63 (s, 3H), 3.52-3.39 (m, 2H), 2.40-2.46 (m, 4H), 2.22-2.10 (m, 4H), 2.06-1.82 (m, 4H); **^{13}C NMR** (150 MHz, $CDCl_3$) δ 155.6, 147.7, 99.8, 35.8, 34.1, 31.3, 29.5, 28.4, 18.59, 18.57; **HRMS** (ESI): $[M+H]^+$ calcd. for $C_{12}H_{19}N_2^+$: 191.1543, found 191.1546.

4-Bromo-3,5-dicyclobutyl-1-methyl-1*H*-pyrazole

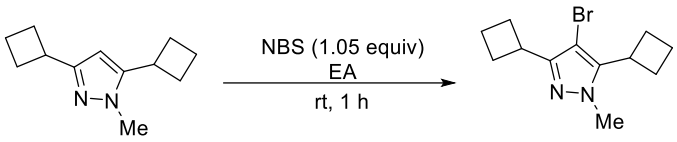

N-Bromosuccinimide (3.81 g, 21.4 mmol, 1.05 equiv) was added to a solution of 3,5-dicyclobutyl-1-methyl-1*H*-pyrazole (3.87 g, 20.3 mmol, 1.0 equiv) in ethyl acetate (40.0 mL) in portion at room temperature. After stirring for 60 min, the solvent was removed by vacuum. DCM and water were added to the mixture and the organic phase was separated. The organic layer was washed with water three times. The combined organic layer was then concentrated to afford the product as an orange liquid.

Yield: 93% (5.08 g). **^{1}H NMR** (400 MHz, $CDCl_3$) δ 3.75 (s, 3H), 3.61-3.47 (m, 2H), 2.65-2.55 (m, 2H), 2.35-2.27 (m, 6H), 2.08-1.97 (m, 2H), 1.94-1.82 (m, 2H); **^{13}C NMR** (100 MHz, $CDCl_3$) δ 152.5, 141.7, 90.8, 37.7, 32.6, 31.7, 27.9, 27.6, 19.1, 18.6; **HRMS** (ESI): $[M+H]^+$ calcd. for $C_{12}H_{18}BrN_2^+$: 269.0648, found 269.0651.

3,5-Dicyclobutyl-4-(dicyclohexylphosphaneyl)-1-methyl-1*H*-pyrazole (L33)

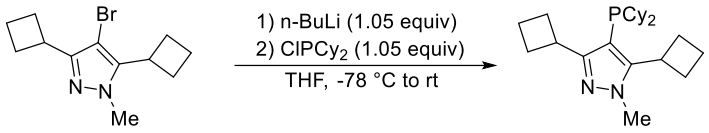

4-Bromo-3,5-dicyclobutyl-1-methyl-1*H*-pyrazole (1.61 g, 6.00 mmol, 1.0 equiv) was dissolved in freshly distilled THF (15.0 mL) at room temperature under nitrogen atmosphere. The solution was cooled to -78 ºC in a dry ice/acetone bath. Titrated n-BuLi (6.30 mmol, 1.05 equiv) was added dropwise with a syringe. After the reaction mixture was stirred for 45 min at -78 ºC, chlorodicyclohexylphosphine (1.40 mL, 6.30 mmol, 1.05 equiv) was added. The reaction was allowed to warm to room temperature and stirred for 60 min. The solvent was removed under reduced pressure. After the solvent was removed under vacuum, the solid product was washed with methanol (5.0 mL x 2). The white solid was collected by filtration and dried over vacuum to afford the **L33**.

Yield: 62% (2.06 g). White solid, m.p.= 79.0–81.1 °C. **^{1}H NMR** (600 MHz, $CDCl_3$) δ 3.98-3.95 (m, 4H), 3.51 (s, 1H), 2.57-2.50 (m, 2H), 2.35-2.32 (m, 2H), 2.28-2.19 (m, 4H), 2.02-1.85 (m, 8H), 1.76 (d, J = 12.0 Hz, 2H), 1.63-1.62 (m, 4H), 1.39 (d, J = 12.0 Hz, 2H), 1.33-1.27 (m, 2H), 1.22-1.11 (m, 6H), 0.90-0.83 (m, 2H); **^{13}C NMR** (150 MHz, C_6D_6) δ 157.8-157.6 (m, 1C), 151.3-151.2 (m, 1C), 106.1 (d, *J* = 15.7 Hz, 1C), 37.6, 35.6 (d, *J* = 9.6 Hz, 1C), 35.2, 33.4, 33.2, 32.4 (d, *J* = 7.6 Hz, 1C), 31.1 (d, *J* = 8.3 Hz, 1C), 30.3, 29.9, 27.5, 27.4 (d, *J* = 23.3 Hz, 1C), 26.9, 19.0-18.8 (m, 1C), 18.7; **^{31}P NMR** (243 MHz, $CDCl_3$) δ -25.8; **HRMS** (ESI): $[M+H]^+$ calcd. for $C_{24}H_{40}N_2P^+$: 387.2924, found 387.2932.

1,3-Dicyclopentyl-3-hydroxyprop-2-en-1-one

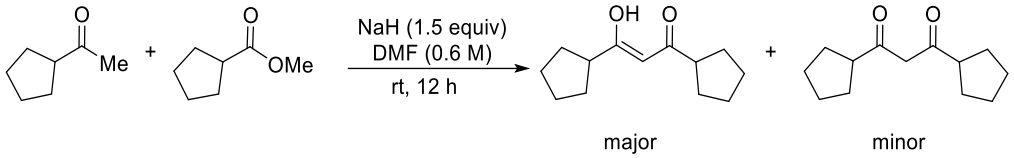

A 500 mL flask was equipped with a magnetic stir bar, which was dried under vacuum with a heat gun and refilled with nitrogen. Sodium hydride (3.00 g, 75.0 mmol, 1.5 equiv, 60% in mineral oil) and DMF (80.0 mL) were added to the flask, and the mixture was stirred. 1-cyclopentylethan-1-one (6.20 mL, 50.0 mmol, 1.0 equiv) and methyl cyclopentanecarboxylate (6.95 mL, 55.0 mmol, 1.1 equiv) were added dropwise to the mixture for 30 min, and the resulting mixture was stirred at room temperature for 12 h. After completion, the solution was quenched with ice water. Then 1 M HCl solution was added to the mixture and adjust the pH to 5, followed by adding saturated Na_2CO_3 solution to adjust pH to 7.5, and extracted three times with ethyl acetate. The combined organic layer was washed with water and brine, and dried over Na_2SO_4, and evaporated under reduced pressure. The crude product was purified by column chromatography, with Hexanes: Ethyl acetate = 20:1, to afford a mixture product of 1,3-dicyclopentyl-3-hydroxyprop-2-en-1-one as major product and 1,3-dicyclopentylpropane-1,3-dione as minor product as an orange liquid.

Total yield of two isomers: 87% (9.07 g). **Major**: **^{1}H NMR** (600 MHz, $CDCl_3$) δ 15.66 (s, 1H), 5.52 (s, 1H), 2.70-2.62 (m, 2H), 1.92-1.82 (m, 4H), 1.76-1.68 (m, 7H), 1.64-1.56 (m, 5H); **^{13}C NMR** (150 MHz, $CDCl_3$) δ 197.4, 97.1, 47.6, 30.3, 30.0. **HRMS** (ESI): $[M+Na]^+$ calcd. for $C_{13}H_{20}O_2Na^+$: 231.1356, found 231.1357.

3,5-Dicyclopentyl-1-methyl-1*H*-pyrazole

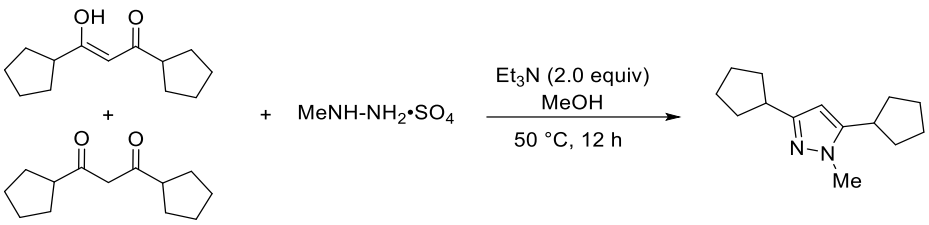

To a mixture of Methylhydrazine sulfate (6.12 g. 42.5 mmol, 2.0 equiv) and MeOH (10.0 ml), Et_3N (5.9 ml, 42.5 mmol, 2.0 equiv) was added. After stirring for a while until all the solids disappeared, this solution was added to a mixture (4.42 g, 21.3 mmol, 1.0 equiv) of 1,3-dicyclopentyl-3-hydroxyprop-2-en-1-one and 1,3-dicyclopentylpropane-1,3-dione of methanol (50.0 ml), and the resulting mixture was stirred at 50 °C for 12 h (as monitored by GC-MS). The reaction mixture was evaporated under reduced pressure to remove MeOH, and then ethyl acetate and water were added, and extracted with ethyl acetate three times. The combined organic layers were washed with brine, dried over Na_2SO_4, and evaporated under reduced pressure. The crude product was purified by column chromatography, with Hexanes: Ethyl acetate =10:1 to 5:1, to afford the product.

Yield: 87% (3.98 g). Yellow liquid; **^{1}H NMR** (600 MHz, $CDCl_3$) δ 5.78 (s, 1H), 3.71 (s, 3H), 3.01-2.88 (m, 2H), 2.04-1.97 (m, 4H), 1.77-1.68 (m, 4H), 1.65-1.51 (m, 8H); **^{13}C NMR** (150 MHz, $CDCl_3$) δ 155.7, 147.8, 99.0, 39.0, 36.3, 35.8, 33.4, 32.5, 25.3, 25.0; **HRMS** (ESI): $[M+H]^+$ calcd. for $C_{14}H_{23}N_2^+$: 219.1856, found 219.1859.

4-Bromo-3,5-dicyclopentyl-1-methyl-1*H*-pyrazole

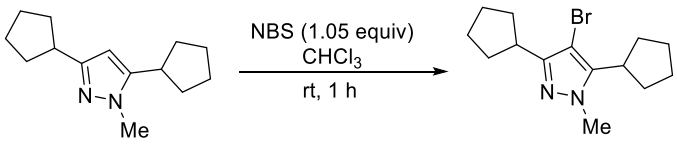

N-Bromosuccinimide (3.41 g, 19.2 mmol, 1.05 equiv) was added to a solution of 3,5-Dicyclopentyl-1-methyl-1*H*-pyrazole (3.98 g, 18.3 mmol, 1.0 equiv) in anhydrous chloroform (40.0 mL) in portion at room temperature. After stirring for 50 min, the solvent was removed by vacuum. DCM and water were added to the mixture and the organic phase was separated. The organic layer was washed with water three times. The combined organic layer was then concentrated to afford the product.

Yield: 99% (5.60 g). Orange liquid. **^{1}H NMR** (600 MHz, $CDCl_3$) δ 3.76 (s, 3H), 3.17-3.10 (m, 1H), 3.07-3.01 (m, 1H), 2.00-1.97 (m, 2H), 1.96-1.90 (m, 4H), 1.89-1.85 (m, 2H), 1.80-1.72 (m, 4H), 1.69-1.65 (m, 2H), 1.64-1.61 (m, 2H); **^{13}C NMR** (150 MHz, $CDCl_3$) δ 152.7, 142.7, 91.2, 37.7, 37.5, 36.1, 31.7, 30.6, 26.2, 25.5; **HRMS** (ESI): $[M+H]^+$ calcd. for $C_{14}H_{22}BrN_2^+$: 297.0961, found 297.0964.

3,5-Dicyclopentyl-4-(dicyclohexylphosphaneyl)-1-methyl-1*H*-pyrazole (L34)

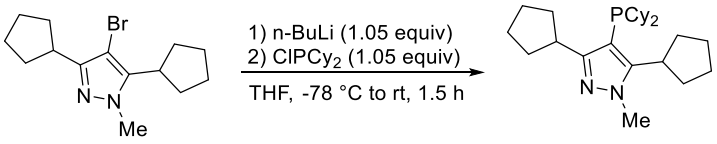

4-Bromo-3,5-dicyclopentyl-1-methyl-1*H*-pyrazole (2.37 g, 8.00 mmol, 1.0 equiv) was dissolved in freshly distilled THF (30.0 mL) at room temperature under nitrogen atmosphere. The solution was cooled to -78 ºC in a dry ice/acetone bath. Titrated n-BuLi (8.40 mmol, 1.05 equiv) was added dropwise with a syringe. After the reaction mixture was stirred for 60 min at -78 ºC, chlorodicyclohexylphosphine (1.90 mL, 8.40 mmol, 1.05 equiv) was added. The reaction was allowed to warm to room temperature and stirred for 70 min. The solvent was removed under reduced pressure. After the solvent was removed under vacuum, the solid product was washed with methanol (10.0

mL), 90% methanol/water mixture (10.0 mL x 2), and methanol (10.0 mL). The white solid was collected by filtration and dried over vacuum to afford the **L34**.

Yield: 62% (2.06 g). White solid, m.p.= 145.6–147.3 °C. **^{1}H NMR** (600 MHz, $CDCl_3$) δ 3.79 (s, 3H), 1.96-1.63 (m, 28H), 1.46 (d, *J*= 12.7 Hz, 2H), 1.32-1.13 (m, 8H), 0.92-0.90 (m, 2H); **^{13}C NMR** (150 MHz, C_6D_6) δ 158.3, 151.9 (d, *J* = 37.6 Hz, 1C), 106.2 (d, *J* = 12.1 Hz, 1C), 39.5, 37.8, 35.9, 35.0, 34.6, 32.7 (d, *J* = 22.1 Hz, 1C), 31.9, 30.6 (d, *J* = 8.5 Hz, 1C), 27.0, 26.97 (d, *J* = 5.7 Hz, 1C), 26.3, 25.7; **^{31}P NMR** (243 MHz, C_6D_6) δ -26.7; **HRMS** (ESI): $[M+H]^+$ calcd. for $C_{26}H_{44}N_2P^+$: 415.3237, found 415.3243.

1,3-Dicycloheptyl-3-hydroxyprop-2-en-1-one

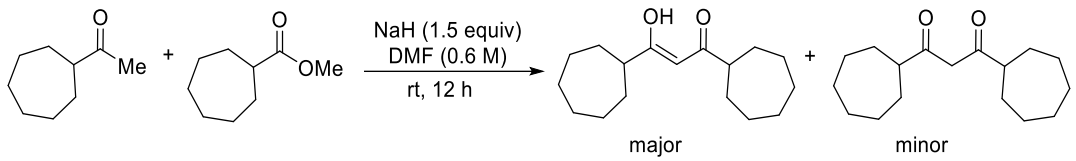

A 100 mL flask was equipped with a magnetic stir bar, which was dried under vacuum with a heat gun and refilled with nitrogen. Sodium hydride (60% in mineral oil, 0.900 g, 22.5 mmol, 1.5 equiv) and DMF (25.0 mL) were added to the flask, and the mixture was stirred. 1-Cycloheptylethan-1-one (2.10 g, 15.0 mmol, 1.0 equiv) and methyl cycloheptanecarboxylate (2.57 g, 16.5 mmol, 1.1 equiv) were added dropwise to the mixture for 10 min, and the resulting mixture was stirred at room temperature for 12 h. The solution was quenched by ice water. Then 1 M HCl solution was added to the mixture and adjust the pH to 5, followed by adding saturated Na_2CO_3 solution to adjust pH to 7.5, and extracted three times with ethyl acetate. The combined organic layer was washed with water and brine, and dried over Na_2SO_4, and evaporated under reduced

pressure. The crude product was purified by column chromatography, with Hexanes: Ethyl acetate = 20: 1, to afford a mixture product of 1,3-Dicycloheptyl-3-hydroxyprop-2-en-1-one as major product and 1,3-dicycloheptylpropane-1,3-dione as minor product. **Total yield of two isomers**: 72% (2.86 g). Light-yellow solid, m.p.= 71.1–73.2 ºC. **Major**: **^{1}H NMR** (600 MHz, $CDCl_3$) δ 15.65 (s, 1H), 5.44 (s, 1H), 2.33-2.29 (m, 2H), 1.87-1.85 (m, 4H), 1.77-1.74 (m, 4H), 1.63-1.56 (m, 10H), 1.54-1.52 (m, 5H), 1.51-1.44 (m, 5H); **^{13}C NMR** (150 MHz, $CDCl_3$) δ 199.3, 95.5, 48.6, 31.5, 28.1, 26.7; **HRMS** (ESI): $[M+Na]^+$ calcd. for $C_{17}H_{28}O_2Na^+$: 287.1982, found 287.1985.

3,5-Dicycloheptyl-1-methyl-1*H*-pyrazole

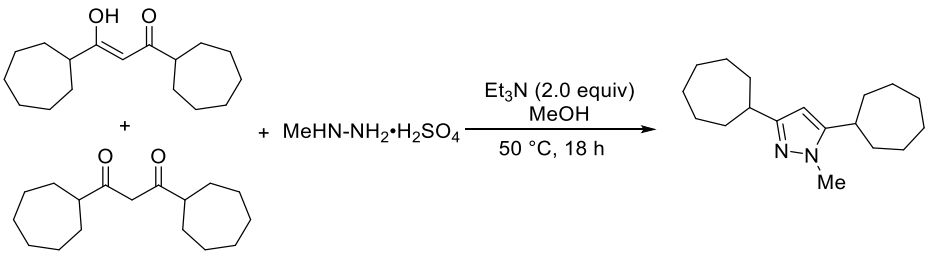

To a mixture of Methylhydrazine sulfate (3.11 g. 21.6 mmol, 2.0 equiv) and MeOH (20.0 ml), Et_3N (3.00 ml, 21.6 mmol, 2.0 equiv) was added. After stirring for a while until all the solids disappeared, this solution was added to a mixture (2.86 g, 10.8 mmol, 1.0 equiv) of 1,3-dicycloheptyl-3-hydroxyprop-2-en-1-one and 1,3-dicycloheptylpropane-1,3-dione of methanol (30.0 ml), and the resulting mixture was stirred at 50 ºC for 12 h (as monitored by GC-MS). The reaction mixture was evaporated under reduced pressure to remove MeOH, and then ethyl acetate and water were added, and extracted with ethyl acetate three times. The combined organic layers were washed with brine, dried over Na_2SO_4, and evaporated under reduced pressure. The crude

product was purified by column chromatography, with Hexanes: Ethyl acetate = 10: 1, to afford the product.

Yield: 76% (2.25 g). Yellow liquid. **^{1}H NMR** (600 MHz, $CDCl_3$) δ 5.78 (s, 1H), 3.70 (s, 3H), 2.76-2.66 (m, 2H), 2.00-1.90 (m, 4H), 1.77-1.48 (m, 20H); **^{13}C NMR** (150 MHz, $CDCl_3$) δ 158.1, 149.7, 98.7, 39.7, 37.0, 35.6, 35.4, 34.5, 28.09, 28.05, 26.7, 26.5; **HRMS** (ESI): $[M+H]^+$ calcd. for $C_{18}H_{31}N_2^+$: 275.2482, found 275.2488.

4-Bromo-3,5-dicycloheptyl-1-methyl-1*H*-pyrazole

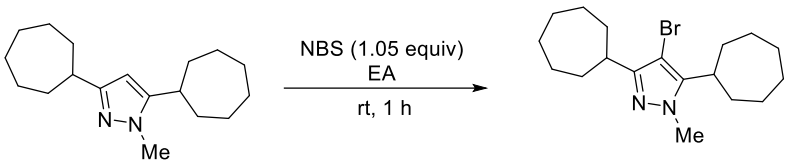

N-Bromosuccinimide (1.54 g, 8.62 mmol, 1.05 equiv) was added to a solution of 3,5-dicyclohexyl-1-methyl-1*H*-pyrazole (2.25 g, 8.21 mmol, 1.0 equiv) in ethyl acetate (20.0 mL) in portion at room temperature. After stirring for 60 min, the solvent was removed by vacuum. DCM and water were added to the mixture and the organic phase was separated. The organic layer was washed with water three times. The combined organic layer was then concentrated to afford the product.

Yield: 91% (2.64 g). Yellow solid, m.p.= 70.3–71.9 ºC. **^{1}H NMR** (400 MHz, $CDCl_3$) δ 3.77 (s, 3H), 2.90 (t, *J* = 11.0 Hz, 1H), 2.79 (t, *J* = 10.4 Hz, 1H), 1.96-1.88 (m, 4H), 1.83-1.64 (m, 12H), 1.61-1.49 (m, 8H); **^{13}C NMR** (100 MHz, $CDCl_3$) δ 155.0, 145.7, 90.0, 38.5, 37.9, 37.8, 33.7, 32.3, 27.9, 27.8, 27.6, 27.0; **HRMS** (ESI): $[M+H]^+$ calcd. for $C_{18}H_{30}BrN_2^+$: 353.1587, found 353.1590.

3,5-Dicycloheptyl-4-(dicyclohexylphosphaneyl)-1-methyl-1*H*-pyrazole (L35)

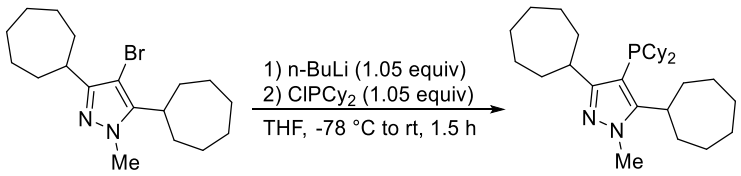

4-Bromo-3,5-dicycloheptyl-1-methyl-1*H*-pyrazole (1.40 g, 4.00 mmol, 1.0 equiv) was dissolved in freshly distilled THF (15.0 mL) at room temperature under nitrogen atmosphere. The solution was cooled to -78 ºC in a dry ice/acetone bath. Titrated n-BuLi (4.20 mmol, 1.05 equiv) was added dropwise with a syringe. After the reaction mixture was stirred for 60 min at -78 ºC, chlorodicyclohexylphosphine (0.924 mL, 4.20 mmol, 1.05 equiv) was added. The reaction was allowed to warm to room temperature and stirred for 70 min. The solvent was removed under reduced pressure. After the solvent was removed under vacuum, the solid product was washed with methanol (10.0 mL x 3). The white solid was collected by filtration and dried over vacuum to afford the **L35**.

Yield: 67% (1.26 g). White solid, m.p.= 140.2–142.1 °C. **^{1}H NMR** (600 MHz, C_6D_6) δ 3.45 (s, 3H), 2.29-2.23 (m, 4H), 2.18-2.14 (m, 2H), 2.07 (d, *J* = 11.8 Hz, 2H), 1.95-1.92 (m, 2H), 1.79-1.61 (m, 22H), 1.55-1.41 (m, 7H), 1.38-1.18 (m, 9H); **^{13}C NMR** (150 MHz, C_6D_6) δ 160.9-160.8 (m, 1C), 155.2 (d, *J* = 40.5 Hz, 1C), 103.7 (d, *J* = 13.8 Hz, 1C), 40.6, 37.9-37.7 (m, 1C), 36.5, 36.0-35.9 (m, 1C), 34.0-33.7 (m, 1C), 33.3 (d, *J* = 22.1 Hz, 1C), 31.6 (d, *J* = 9.3 Hz, 1C), 28.7 (d, *J* = 33.4 Hz, 1C), 28.1 (d, *J* = 32.0 Hz, 1C), 27.7, 27.6 (d, *J* = 13.1 Hz, 1C), 26.9; **^{31}P NMR** (243 MHz, C_6D_6) δ -27.2, -25.7; **HRMS** (ESI): $[M+H]^+$ calcd. for $C_{30}H_{52}N_2P^+$: 471.3863, found 471.3868.

3.4.9.5 Characterization of Products

4-(Benzo[*b*]thiophen-2-yl)phenyl trifluoromethanesulfonate (Table 3.5, compound 7a)

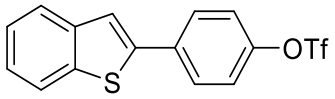

Yield: 84% (60.0 mg). White solid, m.p. = 154.7–157.2 °C. Eluents (R_f = 0.6, Pentane = 100) was used for flash column chromatography. **^{1}H NMR** (600 MHz, $CDCl_3$) δ 7.84 (d, *J* = 7.7 Hz, 1H), 7.80 (d, *J* = 7.6 Hz, 1H), 7.76 (d, *J* = 8.5 Hz, 2H), 7.55 (s, 1H), 7.40-7.36 (m, 2H), 7.33 (d, *J* = 8.6 Hz, 2H); **^{13}C NMR** (150 MHz, $CDCl_3$) δ 149.1, 141.7, 140.4, 139.7, 134.8, 128.1, 124.9, 124.8, 123.9, 122.3, 121.9, 120.8, 118.7 (q, *J* = 318.8 Hz, 1C); **^{19}F NMR** (565 MHz, $CDCl_3$) δ -72.7; **HRMS** (EI): $[M]^+$ calcd. for $C_{15}H_9F_3O_3S_2^+$: 357.9940, found 357.9932.

4-(Benzo[*b*]thiophen-2-yl)-2-(trifluoromethyl)phenyl trifluoromethanesulfonate (Table 3.5, compound 7b)

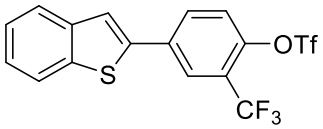

Yield: 75% (64.5 mg). Light-yellow solid, m.p. = 95.0–99.2 °C. Eluents (R_f = 0.5, Hexane: Ethyl acetate = 30: 1) was used for flash column chromatography. **^{1}H NMR** (600 MHz, $CDCl_3$) δ 8.01 (s, 1H), 7.87 (d, *J* = 8.7 Hz, 1H), 7.84 (d, *J* = 7.5 Hz, 1H), 7.81 (d, *J* = 7.6 Hz, 1H), 7.58 (s, 1H), 7.54 (d, *J* = 8.7 Hz, 1H), 7.43-7.35 (m, 2H); **^{13}C NMR** (150 MHz, $CDCl_3$) δ 145.2, 140.2 140.0, 139.8, 134.8, 131.1, 125.43 (q, *J* = 4.7 Hz, 1C), 125.42, 125.0, 124.2, 123.7 (q, *J* = 32.7 Hz, 1C), 123.0, 122.4, 121.8, 121.6

(q, J = 271.6 Hz, 1C), 118.2 (q, J = 318.2 Hz, 1C); **^{19}F NMR** (565 MHz, $CDCl_3$) δ -73.4, -60.9; **HRMS** (EI): $[M]^+$ calcd. for $C_{16}H_8F_6O_3S_2^+$: 425.9814, found 425.9817.

4-(Benzo[*b*]thiophen-2-yl)-2-formylphenyl trifluoromethanesulfonate (Table 3.5, compound 7c)

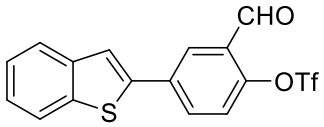

Yield: 75% (64.5 mg). Light-yellow solid, m.p. = 121.2–125.0 ºC. Eluents (R_f = 0.5, Hexane: Ethyl acetate = 30: 1) was used for flash column chromatography. **^{1}H NMR** (600 MHz, $CDCl_3$) δ 10.3 (s, 1H), 8.03 (d, J = 8.0 Hz, 1H), 7.87-7.83 (m, 3H), 7.73 (s, 1H), 7.69 (s, 1H), 7.43-7.40 (m, 2H); **^{13}C NMR** (150 MHz, $CDCl_3$) δ 185.7, 150.2 142.1, 140.2, 140.0, 139.99, 131.3, 127.1, 126.2, 125.9, 125.2, 124.5, 123.1, 122.4, 119.5, 118.6 (q, J = 318.6 Hz, 1C); **^{19}F NMR** (565 MHz, $CDCl_3$) δ -72.7; **HRMS** (EI): $[M]^+$ calcd. for $C_{16}H_9F_3O_4S_2^+$: 385.9889, found 385.9883.

4-(Benzo[*b*]thiophen-2-yl)-2-benzylphenyl trifluoromethanesulfonate (Table 3.5, compound 7d)

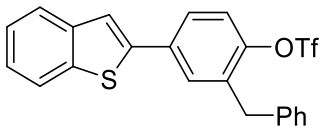

Yield: 84% (75.5 mg). White liquid. Eluents (R_f = 0.4, Hexane = 100) was used for flash column chromatography. **^{1}H NMR** (600 MHz, $CDCl_3$) δ 7.76 (d, J = 7.8 Hz, 1H), 7.71 (d, J = 7.7 Hz, 1H), 7.54 (d, J = 8.5 Hz, 1H), 7.49 (s, 1H), 7.40 (s, 1H), 7.33-7.28 (m, 5H), 7.60 (s, 1H), 7.25 (d, J = 7.1 Hz, 1H), 7.22 (d, J = 7.5 Hz, 2H), 1.98 (s, 2H);

^{13}C NMR (150 MHz, $CDCl_3$) δ 147.5, 141.8, 140.4, 139.6, 138.1, 134.7, 134.6, 129.5, 129.0, 128.7, 126.8, 126.0, 124.8, 124.7, 123.8, 122.2, 121.9, 120.7, 118.6 (q, J = 318.3 Hz, 1C), 35.9; **^{19}F NMR** (565 MHz, $CDCl_3$) δ -73.6; **HRMS** (EI): $[M]^+$ calcd. for $C_{22}H_{15}F_3O_3S_2^+$:448.0409, found 448.0410.

4-(Benzo[*b*]thiophen-2-yl)-3,5-dimethylphenyl trifluoromethanesulfonate (Table 3.5, compound 7e)

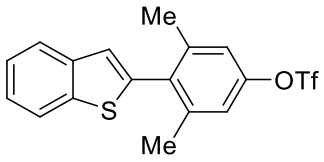

Yield: 71% (54.5 mg). Light-yellow liquid; Eluents (R_f = 0.4, Hexane = 100) was used for flash column chromatography. **^{1}H NMR** (600 MHz, $CDCl_3$) δ 7.89 (d, J = 7.9 Hz, 1H), 7.84 (d, J = 7.7 Hz, 1H), 7.43 (t, J = 7.2 Hz, 1H), 7.39 (t, J = 7.2 Hz, 1H), 7.09 (s, 1H), 7.07 (s, 2H), 2.26 (s, 6H); **^{13}C NMR** (150 MHz, $CDCl_3$) δ 149.0, 141.1, 140.6, 140.1, 140.0, 134.4, 124.4, 124.3, 123.6, 123.5, 122.2, 119.8, 118.7 (q, J = 318.4 Hz, 1C), 20.9; **^{19}F NMR** (565 MHz, $CDCl_3$) δ -72.9; **HRMS** (EI): $[M]^+$ calcd. For $C_{17}H_{13}F_3O_3S_2^+$: 386.0253, found 386.0250.

4-(Benzo[*b*]thiophen-2-yl)-3-fluorophenyl trifluoromethanesulfonate (Table 3.5, compound 7f)

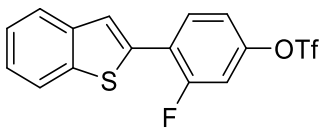

Yield: 85% (64.0 mg). Light-yellow solid, m.p. = 117.9–121.8 °C. Eluents (R_f = 0.4, Hexane = 100) was used for flash column chromatography. **^{1}H NMR** (600 MHz, $CDCl_3$)

δ 7.86 (d, *J* = 7.1 Hz, 1H), 7.83 (d, *J* = 7.1 Hz, 1H), 7.76-7.74 (m, 2H), 7.47-7.38 (m, 2H), 7.19-7.16 (m, 2H); **^{13}C NMR** (150 MHz, $CDCl_3$) δ 159.1 (d, *J* = 254.8 Hz, 1C), 148.4 (d, *J* = 100.9 Hz, 1C), 140.1, 139.5 (d, *J* = 3.0 Hz, 1C), 135.0 (d, *J* = 33.5 Hz, 1C), 130.4 (d, *J* = 4.3 Hz, 1C), 125.2, 124.8, 124.4 (d, *J* = 8.7 Hz, 1C), 124.2, 123.0 (d, *J* = 12.2 Hz, 1C), 122.0, 118.7 (q, *J* = 318.8 Hz, 1C), 117.7 (d, *J* = 3.5 Hz, 1C), 110.6 (d, *J* = 26.9 Hz, 1C); **^{19}F NMR** (565 MHz, $CDCl_3$) δ -107.7, -72.6; **HRMS** (EI): $[M]^+$ calcd. for $C_{15}H_8F_4O_3S_2^+$: 375.9845, found 375.9854.

3-(Benzo[*b*]thiophen-2-yl)phenyl trifluoromethanesulfonate (Table 3.5, compound 7g)

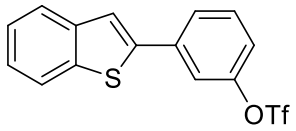

Yield: 73% (52.2 mg). White solid, m.p. = 86.3–88.9 °C. Eluents (R_f = 0.4, Hexane = 100) was used for flash column chromatography. **^{1}H NMR** (600 MHz, $CDCl_3$) δ 7.81 (d, *J* = 7.7 Hz, 1H), 7.77 (d, *J* = 7.5 Hz, 1H), 7.66 (d, *J* = 7.8 Hz, 1H), 7.57 (s, 1H), 7.54 (s, 1H), 7.45 (t, *J* = 8.1 Hz, 1H), 7.37-7.32 (m, 2H), 7.21 (d, *J* = 8.3 Hz, 1H); **^{13}C NMR** (150 MHz, $CDCl_3$) δ 149.9, 141.4, 140.3, 139.4, 136.9, 130.7, 126.3, 125.0, 124.8, 124.0, 122.3, 121.1, 120.5, 119.1, 118.7 (q, *J* = 318.7 Hz, 1C); **^{19}F NMR** (565 MHz, $CDCl_3$) δ -72.7; **HRMS** (EI): $[M]^+$ calcd. for $C_{15}H_9F_3O_3S_2^+$: 357.9940, found 357.9935.

3-(Benzo[*b*]thiophen-2-yl)-5-methoxyphenyl trifluoromethanesulfonate (Table 3.5, compound 7h)

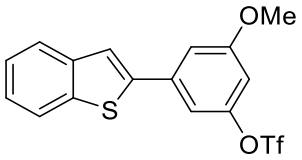

Yield: 74% (57.6 mg). Light-yellow solid, m.p. = 58.4–61.2 ºC. Eluents (R_f = 0.6, Hexane: Ethyl acetate = 10: 1) was used for flash column chromatography. **^{1}H NMR** (600 MHz, $CDCl_3$) δ 7.84 (d, *J* = 7.6 Hz, 1H), 7.80 (d, *J* = 7.6 Hz, 1H), 7.60 (s, 1H), 7.40-7.35 (m, 2H), 7.22 (s, 1H), 7.21 (s, 1H), 6.78 (s, 1H), 3.89 (s, 3H); **^{13}C NMR** (150 MHz, $CDCl_3$) δ 161.0, 150.4, 141.6, 140.2, 139.6, 137.2, 125.0, 124.8, 124.0, 122.3, 121.1, 118.7 (q, *J* = 319.0 Hz, 1C), 112.2, 111.3, 106.7, 55.8; **^{19}F NMR** (565 MHz, $CDCl_3$) δ-72.8; **HRMS** (EI): $[M]^+$ calcd. for $C_{16}H_{11}F_3O_4S_2^+$: 388.0045, found 388.0050

3-(Benzo[*b*]thiophen-2-yl)-5-methylphenyl trifluoromethanesulfonate (Table 3.5, compound 7i)

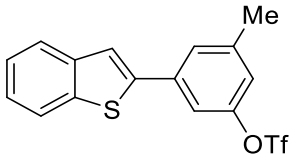

Yield: 78% (57.7 mg). White liquid; Eluents (R_f = 0.5, Hexane = 100) was used for flash column chromatography. **^{1}H NMR** (600 MHz, $CDCl_3$) δ 7.84 (d, *J* = 7.6 Hz, 1H), 7.80 (d, *J* = 7.4 Hz, 1H), 7.56 (s, 1H), 7.51 (s, 1H), 7.41 (s, 1H), 7.39-7.34 (m, 2H), 7.06 (s, 1H), 2.46 (s, 3H); **^{13}C NMR** (150 MHz, $CDCl_3$) δ 149.8, 141.7, 141.1, 140.3, 139.6, 136.5, 127.0, 124.9, 124.8, 123.9, 122.3, 121.1, 120.9, 118.7 (q, *J* = 319.0 Hz, 1C), 116.1, 21.4; **^{19}F NMR** (565 MHz, $CDCl_3$) δ -72.8; **HRMS** (EI): $[M]^+$ calcd. for $C_{16}H_{11}F_3O_3S_2^+$: 372.0096, found 372.0090.

3-(Benzo[*b*]thiophen-2-yl)-5-cyanophenyl trifluoromethanesulfonate (Table 3.5, compound 7j)

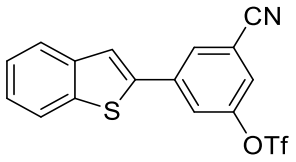

Yield: 58% (44.4 mg). White solid, m.p. = 105.9–107.3 ºC. Eluents (R_f = 0.7, Hexane = 100) was used for flash column chromatography. **^{1}H NMR** (600 MHz, $CDCl_3$) δ 7.94 (s, 1H), 7.86-7.82 (m, 2H), 7.78 (s, 1H), 7.64 (s, 1H), 7.49 (s, 1H), 7.42-7.40 (m, 2H); **^{13}C NMR** (150 MHz, $CDCl_3$) δ 149.6, 139.93, 139.87, 138.7, 138.5, 129.4, 125.9, 125.3, 124.4, 123.4, 123.3, 122.7, 122.4, 118.6 (q, *J* = 318.9 Hz, 1C), 116.5, 115.1; **^{19}F NMR** (565 MHz, $CDCl_3$) δ -72.4; **HRMS** (EI): $[M]^+$ calcd. for $C_{16}H_8FNO_3S_2^+$: 382.9892, found 382.9901.

3-(Benzo[*b*]thiophen-2-yl)-5-(trifluoromethyl)phenyl trifluoromethanesulfonate (Table 3.5, compound 7k)

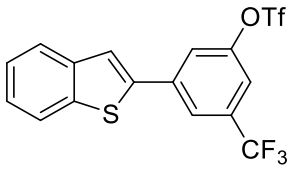

Yield: 71% (60.5 mg). Light-yellow liquid. Eluents (R_f = 0.6, Hexane = 100) was used for flash column chromatography. **^{1}H NMR** (600 MHz, $CDCl_3$) δ 7.94 (s, 1H), 7.85 (d, *J* = 7.7 Hz, 1H), 7.82 (d, *J* = 6.8 Hz, 1H), 7.75 (s, 1H), 7.64 (s, 1H), 7.48 (s, 1H), 7.42-7.38 (m, 2H); **^{13}C NMR** (150 MHz, $CDCl_3$) δ 149.7, 140.0, 139.6, 138.1, 133.5 (q, *J* = 33.4 Hz, 1C), 125.7, 125.1, 124.3, 122.9 (q, *J* = 3.4 Hz, 1C), 122.7 (q, *J* = 271.3 Hz, 1C), 122.4, 122.3, 122.2, 118.7 (q, *J* = 318.8 Hz, 1C), 117.5 (q, *J* = 3.5 Hz, 1C); **^{19}F**

NMR (565 MHz, $CDCl_3$) δ -72.6, -62.9; **HRMS** (EI): $[M]^+$ calcd. for $C_{16}H_8F_6O_3S_2^+$: 425.9814, found 425.9819.

3-(Benzo[*b*]thiophen-2-yl)-5-fluorophenyl trifluoromethanesulfonate (Table 3.5, compound 7l)

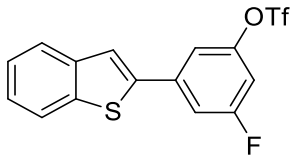

Yield: 41% (30.6 mg). White solid, m.p. = 85.3–90.0 °C. Eluents (R_f = 0.7, Hexane = 100) was used for flash column chromatography. **^{1}H NMR** (600 MHz, $CDCl_3$) δ 7.94 (s, 1H), 7.85 (d, *J* = 7.7 Hz, 1H), 7.81 (d, *J* = 7.2 Hz, 1H), 7.60 (s, 1H), 7.44-7.37 (m, 4H), 7.00 (d, *J* = 8.0 Hz, 1H); **^{13}C NMR** (150 MHz, $CDCl_3$) δ 162.9 (d, *J* = 249.6 Hz, 1C), 149.9 (d, *J* = 11.7 Hz, 1C), 140.2 (d, *J* = 7.2 Hz, 1C), 140.1, 139.7, 138.1 (d, *J* = 9.5 Hz, 1C), 125.5, 125.0, 124.2, 122.4, 121.9, 118.7 (q, *J* = 319.1 Hz, 1C), 115.1 (d, *J* = 3.4 Hz, 1C), 113.5 (d, *J* = 22.8 Hz, 1C), 108.8 (d, *J* = 25.8 Hz, 1C); **^{19}F NMR** (565 MHz, $CDCl_3$) δ -107.5, -72.6; **HRMS** (EI): $[M]^+$ calcd. for $C_{15}H_8F_4O_3S_2^+$: 375.9845, found 375.9833.

5-(Benzo[*b*]thiophen-2-yl)-2-fluorophenyl trifluoromethanesulfonate (Table 3.5, compound 7m)

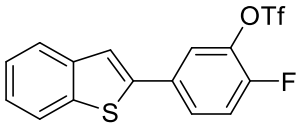

Yield: 64% (47.8 mg). White solid, m.p. = 72.5–75.3 °C. Eluents (R_f = 0.6, Petane = 100) was used for flash column chromatography. **^{1}H NMR** (600 MHz, $CDCl_3$) δ 7.83

(d, *J* = 7.7 Hz, 1H), 7.79 (d, *J* = 7.4 Hz, 1H), 7.66-7.64 (m, 2H), 7.50 (s, 1H), 7.40-7.35 (m, 2H), 7.31 (t, *J* = 8.6 Hz, 1H); **^{13}C NMR** (150 MHz, $CDCl_3$) δ 153.2 (d, *J* = 253.9 Hz, 1C), 140.5, 140.3, 139.6, 137.0 (d, *J* = 14.0 Hz, 1C), 132.2 (d, *J* = 4.0 Hz, 1C), 127.5 (d, *J* = 7.0 Hz, 1C), 125.1, 124.9, 123.9, 122.3, 121.3, 120.9, 118.7 (q, *J* = 318.5 Hz, 1C), 118.1 (d, *J* = 18.6 Hz, 1C); **^{19}F NMR** (565 MHz, $CDCl_3$) δ -127.9, -73.0; **HRMS** (EI): $[M]^+$ calcd. for $C_{15}H_8F_4O_3S_2^+$: 375.9845, found 375.9849.

3-(Benzo[*b*]thiophen-2-yl)-2-methylphenyl trifluoromethanesulfonate (Table 3.5, compound 7n)

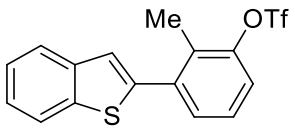

Yield: 92% (68.8 mg), white solid, m.p. = 53.3–56.1 °C; Eluents (R_f = 0.7, Hexane = 100) was used for flash column chromatography; **^{1}H NMR** (600 MHz, $CDCl_3$) δ 7.86 (d, *J* = 7.8 Hz, 1H), 7.82 (d, *J* = 7.8 Hz, 1H), 7.49 (d, *J* = 7.3 Hz, 1H), 7.42-7.36 (m, 2H), 7.34-7.30 (m, 2H), 7.26 (d, *J* = 8.3 Hz, 1H), 2.45 (s, 3H); **^{13}C NMR** (150 MHz, $CDCl_3$) δ 148.9, 140.9, 140.2, 139.8, 137.4, 130.7, 130.1, 127.0, 124.6, 124.2, 123.8, 122.1, 121.3, 118.6 (q, *J* = 318.1 Hz, 1C), 14.5; **^{19}F NMR** (565 MHz, $CDCl_3$) δ -73.7; **HRMS** (EI): $[M]^+$ calcd for $C_{16}H_{11}F_3O_3S_2^+$: 372.0096, found 372.0104.

2-(Benzo[*b*]thiophen-2-yl)phenyl trifluoromethanesulfonate (Table 3.5, compound 7o)

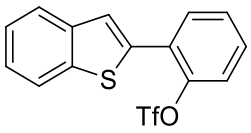

Yield: 75% (53.6 mg), light-yellow liquid; Eluents (R_f = 0.4, Hexane = 100) was used for flash column chromatography; **^{1}H NMR** (600 MHz, $CDCl_3$) δ 7.85 (d, *J* = 7.6 Hz, 1H), 7.82 (d, *J* = 7.3 Hz, 1H), 7.69-7.67 (m, 1H), 7.60 (s, 1H), 7.43-7.40 (m, 3H), 7.39-7.34 (m, 2H); **^{13}C NMR** (150 MHz, $CDCl_3$) δ 146.6, 140.1, 140.0, 136.4, 131.9, 129.5, 128.6, 128.3, 125.0, 124.9, 124.7, 124.1, 122.2, 122.1, 118.5 (q, *J* = 318.9 Hz, 1C); **^{19}F NMR** (565 MHz, $CDCl_3$) δ -73.6; **HRMS** (EI): $[M]^+$ calcd for $C_{15}H_9F_3O_3S_2^+$:357.9940, found 357.9949.

4-(3-Methylbenzo[*b*]thiophen-2-yl)phenyl trifluoromethanesulfonate (Table 3.6, compound 7p)

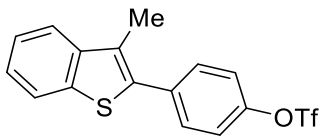

Yield: 86% (64.2 mg), light-yellow solid, m.p. = 82.2–84.3 ºC; Eluents (R_f = 0.5, Hexane = 100) was used for flash column chromatography; **^{1}H NMR** (600 MHz, $CDCl_3$) δ 7.85 (d, *J* = 8.0 Hz, 1H), 7.75 (d, *J* = 8.0 Hz, 1H), 7.62 (d, *J* = 8.3 Hz, 2H), 7.46 (t, *J* = 7.3 Hz, 1H), 7.40-7.37 (m, 3H), 2.47 (s, 3H); **^{13}C NMR** (150 MHz, $CDCl_3$) δ 148.9, 140.9, 138.9, 135.6, 135.3, 131.4, 128.6, 124.8, 124.4, 122.4, 122.2, 121.5, 118.7 (q, *J* = 319.0 Hz, 1C), 12.6; **^{19}F NMR** (565 MHz, $CDCl_3$) δ -72.7; **HRMS** (EI): $[M]^+$ calcd. for $C_{16}H_{11}F_3O_3S_2^+$: 372.0096, found 372.0086.

4-(5-Methylbenzo[*b*]thiophen-2-yl)phenyl trifluoromethanesulfonate (Table 3.6, compound 7q)

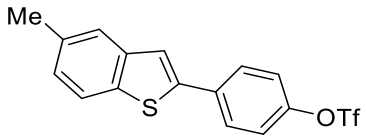

Yield: 90% (67.3 mg), white solid, m.p. = >173 ºC; Eluents (R_f = 0.6, Hexane = 100) was used for flash column chromatography. **^{1}H NMR** (600 MHz, $CDCl_3$) δ 7.75 (d, *J* = 8.5 Hz, 2H), 7.72 (d, *J* = 8.2 Hz, 1H), 7.59 (s, 1H), 7.48 (s, 1H), 7.33 (d, *J* = 8.5 Hz, 2H), 7.19 (d, *J* = 8.2 Hz, 1H), 2.48 (s, 3H); **^{13}C NMR** (150 MHz, $CDCl_3$) δ 149.0, 141.8, 140.8, 136.9, 134.9, 134.6, 128.0, 126.7, 123.8, 121.9, 121.87, 120.5, 118.7 (q, *J* = 319.2 Hz, 1C), 21.4; **^{19}F NMR** (565 MHz, $CDCl_3$) δ -72.7; **HRMS** (EI): $[M]^+$ calcd. for $C_{16}H_{11}F_3O_3S_2^+$: 372.0096, found 372.0097.

Methyl 5-(4-(((trifluoromethyl)sulfonyl)oxy)phenyl)thiophene-2-carboxylate (Table 3.6, compound 7r)

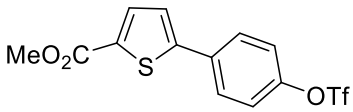

Yield: 82% (60.3 mg), light-yellow solid, m.p. = 86.5–91.2 ºC; Eluents (R_f = 0.5, Hexane: Ethyl acetate: DCM = 10: 1: 1) was used for flash column chromatography. **^{1}H NMR** (600 MHz, $CDCl_3$) δ 7.77 (d, *J* = 3.8 Hz, 1H), 7.70 (d, *J* = 8.5 Hz, 2H), 7.33 (d, *J* = 8.5 Hz, 2H), 7.30 (d, *J* = 3.8 Hz, 1H), 3.91 (s, 3H); **^{13}C NMR** (150 MHz, $CDCl_3$) δ 162.4, 149.1, 148.5, 134.4, 133.8, 133.3, 127.9, 124.7, 122.1, 118.7 (q, *J* = 319.1 Hz, 1C), 52.3; **^{19}F NMR** (565 MHz, $CDCl_3$) δ -72.7; **HRMS** (EI): $[M]^+$ calcd. for $C_{13}H_9F_3O_5S_2^+$: 365.9838, found 365.9839.

4-(5-Acetylthiophen-2-yl)phenyl trifluoromethanesulfonate (Table 3.6, compound 7s)

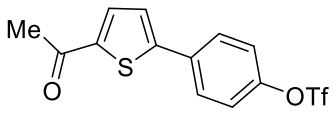

Yield: 74% (52.0 mg), light-yellow solid, m.p. = 100.8–103.4 ºC; Eluents (R_f = 0.3, Hexane: Ethyl acetate = 5: 1) was used for flash column chromatography. **^{1}H NMR** (600 MHz, $CDCl_3$) δ 7.70 (d, *J* = 8.5 Hz, 2H), 7.66 (d, *J* = 3.7 Hz, 1H), 7.33-7.32 (m, 3H), 2.57 (s, 3H); **^{13}C NMR** (150 MHz, $CDCl_3$) δ 190.5, 149.9, 149.5, 144.2, 133.7, 133.3, 128.0, 125.0, 122.1, 118.7 (q, *J* = 319.1 Hz, 1C), 26.5; **^{19}F NMR** (565 MHz, $CDCl_3$) δ -72.7; **HRMS** (EI): $[M]^+$ calcd. for $C_{13}H_9F_3O_4S_2^+$: 349.9889, found 349.9892.

4-(5-Benzoylthiophen-2-yl)phenyl trifluoromethanesulfonate (Table 3.6, compound 7t)

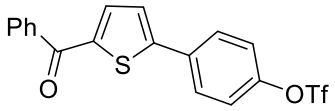

Yield: 54% (41.9 mg), light-yellow solid, m.p. = 109.9–114.0 ºC; Eluents (R_f = 0.5, Hexane: DCM = 20: 1) was used for flash column chromatography; **^{1}H NMR** (600 MHz, $CDCl_3$) δ 7.88 (d, *J* = 8.6 Hz, 2H), 7.76 (d, *J* = 8.3 Hz, 2H), 7.63-7.61 (m, 2H), 7.52 (*t*, J = 7.5 Hz, 2H), 7.37-7.34 (m, 3H); **^{13}C NMR** (150 MHz, $CDCl_3$) δ 187.9, 150.3, 149.6, 143.5, 137.7, 135.7, 133.7, 132.4, 129.1, 128.5, 128.1, 124.9, 122.2, 118.7 (q, *J* = 319.4 Hz, 1C); **^{19}F NMR** (565 MHz, $CDCl_3$) δ-72.7; **HRMS** (EI): $[M]^+$ calcd. for $C_{18}H_{11}F_3O_4S_2^+$: 412.0045, found 412.0049.

4-(5-Pentylthiophen-2-yl)phenyl trifluoromethanesulfonate (Table 3.6, compound 7u)

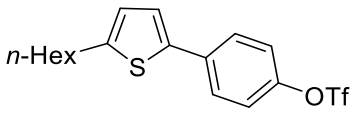

Yield: 77% (60.2 mg), white solid, m.p. = 38.7–41.2 °C; Eluents (R_f = 0.5, Hexane = 100) was used for flash column chromatography; **^{1}H NMR** (600 MHz, $CDCl_3$) δ 7.58 (d, *J* = 8.6 Hz, 2H), 7.24 (d, *J* = 8.6 Hz, 2H), 7.12 (d, *J* = 3.2 Hz, 1H), 6.75 (d, *J* = 2.8 Hz, 1H), 2.81 (t, *J* = 7.6 Hz, 2H), 1.71-1.67 (m, 2H), 1.39-1.37 (m, 2H), 1.32- 1.30 (m, 4H), 0.89 (t, *J* = 6.1 Hz, 3H); **^{13}C NMR** (150 MHz, $CDCl_3$) δ 148.2, 147.2, 139.2, 135.2, 126.9, 125.3, 123.9, 121.7, 118.7 (q, *J* = 318.7 Hz, 1C), 31.5, 30.2, 28.7, 22.6, 14.0; **^{19}F NMR** (565 MHz, $CDCl_3$) δ -72.8; **HRMS** (EI): $[M]^+$ calcd. for $C_{17}H_{17}F_3O_3S_2^+$: 392.0722, found 392.0726.

4-(5-Butylthiophen-2-yl)phenyl trifluoromethanesulfonate (Table 3.6, compound 7v)

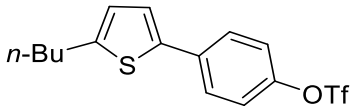

Yield: 74% (53.7 mg), white solid, m.p. = 47.2–50.2 °C; Eluents (R_f = 0.4, Hexane = 100) was used for flash column chromatography; **^{1}H NMR** (600 MHz, $CDCl_3$) δ 7.58 (d, *J* = 8.7 Hz, 2H), 7.24 (d, *J* = 8.6 Hz, 2H), 7.16 (d, *J* = 3.4 Hz, 1H), 6.75 (d, *J* = 2.6 Hz, 1H), 2.82 (t, *J* = 7.6 Hz, 2H), 1.70-1.65 (m, 2H), 1.44-1.38 (m, 2H), 0.95 (t, *J* = 7.4 Hz, 3H); **^{13}C NMR** (150 MHz, $CDCl_3$) δ 148.2, 147.1, 139.2, 135.2, 126.9, 125.3, 123.9, 121.7, 118.7 (q, *J* = 318.9 Hz, 1C), 33.7, 29.9, 22.1, 13.8; **^{19}F NMR** (565 MHz, $CDCl_3$) δ -72.8; **HRMS** (EI): $[M]^+$ calcd. for $C_{15}H_{15}F_3O_3S_2^+$: 364.0406, found 364.0409.

4-(5-Methoxythiophen-2-yl)phenyl trifluoromethanesulfonate (Table 3.6,

compound 7w)

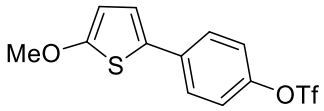

Yield: 65% (45.8 mg), light-yellow solid, m.p. = 80.6–85.0 ºC; Eluents (R_f = 0.3, Hexane = 100) was used for flash column chromatography; **^{1}H NMR** (600 MHz, $CDCl_3$) δ 7.51 (d, *J* = 8.6 Hz, 2H), 7.23 (d, *J* = 8.6 Hz, 2H), 6.97 (d, *J* = 3.8 Hz, 1H), 6.20 (d, *J* = 3.8 Hz, 1H), 3.93 (s, 3H); **^{13}C NMR** (150 MHz, $CDCl_3$) δ 167.0, 147.9, 135.2, 127.7, 126.1, 122.0, 121.7, 118.7 (q, *J* = 319.1 Hz, 1C), 104.9, 60.2; **^{19}F NMR** (565 MHz, $CDCl_3$) δ -72.8; **HRMS** (EI): $[M]^+$ calcd. for $C_{12}H_9F_3O_4S_2^+$:337.9889, found 337.9883.

4-(5-(Pyridin-2-yl)thiophen-2-yl)phenyl trifluoromethanesulfonate (Table 3.6, compound 7x)

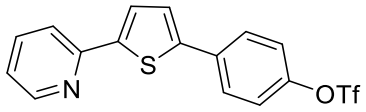

Yield: 54% (41.9 mg), light-yellow solid, m.p. = 154.8–158.2 ºC; Eluents (R_f = 0.5, Hexane: DCM = 20: 1) was used for flash column chromatography. **^{1}H NMR** (600 MHz, $CDCl_3$) δ 8.58 (d, *J* = 4.2 Hz, 1H), 7.70-7.68 (m, 3H), 7.65 (d, *J* = 7.9 Hz, 1H), 7.53 (d, *J* = 3.1 Hz, 1H), 7.31 (d, *J* = 4.0 Hz, 1H), 7.29 (d, *J* = 7.6 Hz, 2H), 7.17-7.15 (m, 1H); **^{13}C NMR** (150 MHz, $CDCl_3$) δ 152.0, 149.6, 148.7, 145.2, 143.5, 136.7, 134.7, 127.2, 125.4, 125.1, 122.2, 121.9, 118.7 (q, *J* = 318.9 Hz, 1C), 118.5; **^{19}F NMR** (565 MHz, $CDCl_3$) δ -72.7; **HRMS** (EI): $[M]^+$ calcd. for $C_{16}H_{10}F_3NO_3S_2^+$: 385.0049, found 385.0037.

Methyl 5-(4-(((trifluoromethyl)sulfonyl)oxy)phenyl)furan-2-carboxylate (Table

3.6, compound 7y)

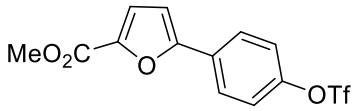

Yield: 81% (53.9 mg), white liquid; Eluents (R_f = 0.5, Hexane: Ethyl acetate = 10: 1) was used for flash column chromatography. **^{1}H NMR** (600 MHz, $CDCl_3$) δ 7.84 (d, *J* = 8.5 Hz, 2H), 7.32 (d, *J* = 8.5 Hz, 2H), 7.24 (d, *J* = 3.1 Hz, 1H), 6.77 (d, *J* = 3.1 Hz, 1H), 3.91 (s, 3H); **^{13}C NMR** (150 MHz, $CDCl_3$) δ 158.9, 155.3, 149.4, 144.3, 129.7, 126.5, 121.9, 119.9, 118.7 (q, *J* = 318.8 Hz, 1C), 108.1, 52.0; **^{19}F NMR** (565 MHz, $CDCl_3$) δ -72.8; **HRMS** (EI): $[M]^+$ calcd. for $C_{13}H_9F_3O_6S^+$: 350.0066, found 350.0071.

(5-(4-(((Trifluoromethyl)sulfonyl)oxy)phenyl)furan-2-yl)methyl acetate (Table 3.6, compound 7z)

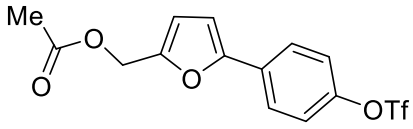

Yield: 70% (51.2 mg), light-yellow liquid; Eluents (R_f = 0.5, Hexane: Ethyl acetate = 10: 1) was used for flash column chromatography; **^{1}H NMR** (600 MHz, $CDCl_3$) δ 7.73 (d, *J* = 8.6 Hz, 2H), 7.28 (d, *J* = 8.6 Hz, 2H), 6.60 (d, *J* = 3.2 Hz, 1H), 6.50 (d, *J* = 3.2 Hz, 1H), 5.10 (s, 2H), 2.10 (s, 3H); **^{13}C NMR** (150 MHz, $CDCl_3$) δ 170.6, 152.6, 149.9, 148.6, 130.7, 125.5, 121.7, 118.7 (q, *J* = 318.6 Hz, 1C), 112.9, 107.2, 58.0, 20.9; **^{19}F NMR** (565 MHz, $CDCl_3$) δ -72.8; **HRMS** (EI): $[M]^+$ calcd. for $C_{14}H_{11}F_3O_6S^+$: 364.0223, found 364.0225.

4-(Benzofuran-2-yl)phenyl trifluoromethanesulfonate (Table 3.6, compound 7aa)

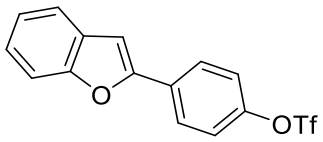

Yield: 70% (48.3 mg), white solid, m.p. = 123.7–125.5 ºC; Eluents (R_f = 0.5, Pentane = 100) was used for flash column chromatography. **^{1}H NMR** (600 MHz, $CDCl_3$) δ 7.92 (d, *J* = 8.1 Hz, 2H), 7.61 (d, *J* = 7.7 Hz, 1H), 7.54 (d, *J* = 8.2 Hz, 1H), 7.37-7.32 (m, 3H), 7.26 (t, *J* = 7.6 Hz, 1H), 7.07 (s, 1H); **^{13}C NMR** (150 MHz, $CDCl_3$) δ 155.1, 153.8, 149.2, 130.8, 128.8, 126.6, 125.0, 123.2, 121.8, 121.2, 118.7 (q, *J* = 319.0 Hz, 1C), 111.3, 102; **^{19}F NMR** (565 MHz, $CDCl_3$) δ -72.7; **HRMS** (EI): $[M]^+$ calcd. for $C_{15}H_9F_3O_4S^+$: 342.0168, found 342.0171.

(1R,2S,5R)-2-Isopropyl-5-methylcyclohexyl 5-(4-(((trifluoromethyl)sulfonyl)oxy)phenyl)thiophene-2-carboxylate (Table 3.6, compound 7ab)

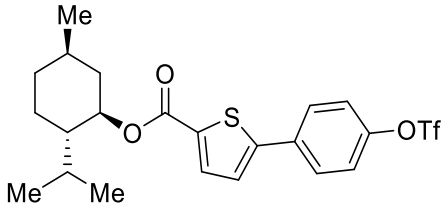

Yield: 70% (68.8 mg), white solid; Eluents (R_f = 0.2, Hexane: Et_2O = 10:1) was used for flash column chromatography. **^{1}H NMR** (600 MHz, $CDCl_3$) δ 7.76 (d, *J* = 3.7 Hz, 1H), 7.70 (d, *J* = 8.0 Hz, 2H), 7.32 (d, *J* = 8.5 Hz, 2H), 7.29 (d, *J* = 3.7 Hz, 1H), 4.89 (dt, *J* = 10.8, 4.0 Hz, 1H), 2.13 (d, *J* = 11.8 Hz, 1H), 1.99-1.94 (m, 1H), 1.72 (d, *J* = 11.3 Hz, 2H), 1.54 (t, *J* = 11.3 Hz, 2H), 1.12 (q, *J* = 11.8 Hz, 2H), 0.93-0.92 (m, 7H), 0.81 (d, *J* = 6.9 Hz, 3H); **^{13}C NMR** (150 MHz, $CDCl_3$) δ 161.5, 149.3, 148.1, 134.3, 134.0, 133.9, 127.9, 124.6, 122.1, 118.7 (q, *J* = 319.2 Hz, 1C), 75.5, 47.1, 40.9, 34.2,

31.4, 26.6, 23.7, 22.0, 20.6, 16.6; **^{19}F NMR** (565 MHz, $CDCl_3$) δ -72.7; **HRMS** (EI): $[M]^+$ calcd. for $C_{22}H_{25}F_3O_5S_2^+$: 490.1090, found 490.1096.

4-(1,3,7-Trimethyl-2,6-dioxo-2,3,6,7-tetrahydro-1*H*-purin-8-yl)phenyl trifluoromethanesulfonate (Table 3.6, compound 7ac)

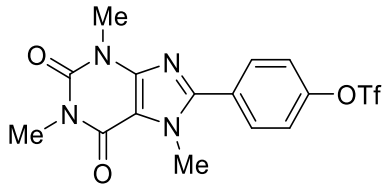

Yield: 55% (46.0 mg), white solid, m.p. = 197.2–199.9 °C; Eluents (R_f = 0.5, DCM: Ethyl acetate = 10: 1) was used for flash column chromatography; **^{1}H NMR** (600 MHz, $CDCl_3$) δ 7.82 (d, *J* = 8.4 Hz, 2H), 7.45 (d, *J* = 8.4 Hz, 2H), 4.08 (s, 3H), 3.60 (s, 3H), 3.42 (s, 3H); **^{13}C NMR** (150 MHz, $CDCl_3$) δ 155.5, 151.6, 150.5, 149.8, 148.1, 131.2, 128.8, 122.1, 118.7 (q, *J* = 319.0 Hz, 1C), 108.9, 34.0, 29.7, 28.0; **^{19}F NMR** (565 MHz, $CDCl_3$) δ -72.7; **HRMS** (ESI): $[M+H]^+$ calcd. for $C_{15}H_{14}F_3O_5N_4S^+$: 419.0632, found 419.0639.

3.5 Computational details

All density functional theory (DFT) calculations were performed using the Gaussian 16 software.[38] The B3PW91[39] functional has been used in this study. This hybrid functional has been shown to perform well in modeling a range of reactions involving transition metals.[40] Geometry optimizations of all the minima and transition states were fully optimized at the B3PW91-D3(BJ) level of theory, with the SDD[41] pseudopotential for Pd and the 6-31G(d) for other atoms using the Polarizable

Continuum Model (PCM) model[42] with 1,4-dioxane as the solvent. Dispersion corrections according to Grimmes's DFT-D3 scheme,[43] including Becke–Johnson damping, were utilized.[44] Vibrational frequencies were calculated at the same level of theory to evaluate its zero-point vibrational energy and thermal corrections at 298.15K, and to check whether each optimized structure is an energy minimum or a transition state. Intrinsic reaction coordinates (IRC) calculations were performed to confirm whether the located transition state connect the correct reactant and product.[45] On the basis of the optimized structures, the single point energies were calculated at the B3LYP-D3(BJ)/Def2-TZVP[13b, 46] level, and solvation energy corrections were calculated using the Solvation Model Based on Density (SMD) model[47] with 1,4-dioxane as the solvent. The reported Gibbs free energies were corrected using the quasi-harmonic model[48] with a cut-off frequency of 100 cm^{-1}. The Gibbs free energies were further corrected to standard state from 1 atm to 1 mol/L, a correction of RTLn(cs/cg) (1.89 kcal/mol) was added to the energies of all species. cs is the standard molar concentration in solution (1 mol/L), cg is the standard molar concentration in the gas phase (0.0446 mol/L), and R is the gas constant. Conformational searches are conducted to ensure that the most stable conformers are located. The NBO calculations were performed with the NBO7.0 package.[49] The images of computed species were generated using CYLView.[50]

Table 3.7: Table of energies of minimum energy structures[a]

Structure	*ZPE*	*tcH*	*E caled*	*H*	*G*	*qh-G*	*Imaginary frequency*

							(cm^{-1})
12A	0.661459	0.693856	-1596.14420313	-1595.45034713	-1595.54938613	-1595.54104913	
12B	0.772666	0.820211	-3249.32653308	-3248.50632208	-3248.64030008	-3248.62675108	
12C	0.772108	0.819944	-3249.32504973	-3248.50510573	-3248.64197773	-3248.62713473	
12D-TS	0.771897	0.819216	-3249.30973605	-3248.49052005	-3248.62620605	-3248.61164405	-111.25
12E	0.774036	0.821475	-3249.35473803	-3248.53326303	-3248.66747303	-3248.65417003	
12F	0.825986	0.876729	-3017.70474056	-3016.82801156	-3016.96939056	-3016.95494456	
12G	0.943212	1.001468	-3724.56158010	-3723.56011210	-3723.71481910	-3723.70019310	
12H-TS	0.936912	0.995481	-3724.52977410	-3723.53429310	-3723.69250710	-3723.67601410	-510.33
12I	0.944026	1.002867	-3724.54172661	-3723.53885961	-3723.69707961	-3723.68103361	
12J	0.877061	0.930279	-3495.31462884	-3494.38434984	-3494.52955684	-3494.51543084	
12K-TS	0.875292	0.92831	-3495.30070219	-3494.37239219	-3494.51745819	-3494.50298619	-338.04
12L	0.878021	0.93117	-3495.35706995	-3494.42589995	-3494.57081895	-3494.55640295	
12M	0.773303	0.820558	-3249.32328367	-3248.50272567	-3248.63417667	-3248.62186367	
12N-TS	0.770478	0.817888	-3249.30210395	-3248.48421595	-3248.61788695	-3248.60445195	-155.07
12O	0.774546	0.821029	-3249.32563948	-3248.50461048	-3248.63367448	-3248.62221548	
12P-TS	0.935833	0.994694	-3724.52658438	-3723.53189038	-3723.69102238	-3723.67420538	-1319.04
12Q-TS	0.941015	0.999044	-3724.50552101	-3723.50647701	-3723.66168801	-3723.64667001	-390.23
12R-TS	0.940818	0.998915	-3724.50453118	-3723.50561618	-3723.66169918	-3723.64621718	-459.00
13A	0.542291	0.570712	-1438.74356194	-1438.17284994	-1438.26103594	-1438.25515694	
13E	0.655911	0.698957	-3091.96308503	-3091.26412803	-3091.38419203	-3091.37502203	
13F	0.706674	0.753329	-2860.30646974	-2859.55314074	-2859.68387174	-2859.67178174	
13G	0.823144	0.877768	-3567.16207910	-3566.28431110	-3566.43011410	-3566.41734310	
13H-TS	0.817743	0.872204	-3567.13242510	-3566.26022110	-3566.40877810	-3566.39401710	-571.90
13I	0.822332	0.87737	-3567.14492334	-3566.26755334	-3566.41785034	-3566.40271534	
13J	0.758012	0.807448	-3337.91186536	-3337.10441736	-3337.24190636	-3337.22860536	
13K-TS	0.756409	0.805506	-3337.89867780	-3337.09317180	-3337.22883580	-3337.21616980	-371.19
13L	0.759977	0.80883	-3337.95431880	-3337.14548880	-3337.27932080	-3337.26744180	
14A	0.601459	0.631709	-1517.41562191	-1516.78391291	-1516.87675791	-1516.87005491	
14E	0.714718	0.759684	-3170.62821335	-3169.86852935	-3169.99352735	-3169.98330435	
14F	0.765135	0.813885	-2938.97713059	-2938.16324559	-2938.29881859	-2938.28595859	
14G	0.882767	0.939053	-3645.83549540	-3644.89644240	-3645.04654240	-3645.03282640	
14H-TS	0.8763	0.932821	-3645.80265127	-3644.86983027	-3645.02294127	-3645.00748227	-843.16
14I	0.88126	0.938202	-3645.81583880	-3644.87763680	-3645.03191080	-3645.01648380	
14J	0.817076	0.86829	-3416.58509441	-3415.71680441	-3415.85796241	-3415.84417941	
14K-TS	0.815105	0.866113	-3416.57130356	-3415.70519056	-3415.84604056	-3415.83216556	-371.19
14L	0.819389	0.8703	-3416.62760900	-3415.75730900	-3415.89688100	-3415.88363600	
15A	0.720442	0.754418	-1674.83177331	-1674.07735531	-1674.17797631	-1674.17022731	
15E	0.833102	0.882178	-3328.04149137	-3327.15931337	-3327.29571737	-3327.28258437	
15F	0.884277	0.936689	-3096.39248830	-3095.45579930	-3095.59805530	-3095.58474330	

15G	1.003932	1.063399	-3803.24636959	-3802.18297059	-3802.33918859	-3802.32495559	
15H-TS	0.995506	1.055645	-3803.21752356	-3802.16187856	-3802.32162356	-3802.30571656	-839.21
15I	1.000957	1.061384	-3803.23168404	-3802.17030004	-3802.33079004	-3802.31483804	
15J	0.935701	0.990816	-3573.99836523	-3573.00754923	-3573.15768523	-3573.14241923	
15K-TS	0.93408	0.988919	-3573.98601161	-3572.99709261	-3573.14700261	-3573.13150461	-300.46
15L	0.936948	0.991886	-3574.04372966	-3573.05184366	-3573.20135466	-3573.18613566	
16A	0.779667	0.815807	-1753.46525901	-1752.64945201	-1752.75421101	-1752.74643701	
16E	0.892968	0.943795	-3406.67987416	-3405.73607916	-3405.87230116	-3405.86130916	
16F	0.944709	0.998946	-3175.02741161	-3174.02846561	-3174.17392061	-3174.16059161	
16G	1.061338	1.123437	-3881.88015409	-3880.75671709	-3880.91919609	-3880.90387709	
16H-TS	1.054524	1.117013	-3881.84939876	-3880.73238576	-3880.89716476	-3880.88065276	-827.53
16I	1.059949	1.122698	-3881.86368924	-3880.74099124	-3880.90640624	-3880.88984624	
16J	0.99586	1.052721	-3652.63539742	-3651.58267642	-3651.73371842	-3651.71983242	
16K-TS	0.993151	1.050232	-3652.61948475	-3651.56925275	-3651.72390175	-3651.70798375	-346.17
16L	0.997357	1.053978	-3652.67939710	-3651.62541910	-3651.77500910	-3651.76148710	
17A	0.416475	0.43866	-1205.22412785	-1204.78546785	-1204.86072185	-1204.85573585	
17E	0.529226	0.566459	-2858.43475339	-2857.86829439	-2857.97802539	-2857.96868439	
17F	0.580551	0.620988	-2626.78650420	-2626.16551620	-2626.28327820	-2626.27228420	
17G	0.697113	0.745501	-3333.64352280	-3332.89802180	-3333.03204380	-3333.01949180	
17H-TS	0.690347	0.739117	-3333.60636271	-3332.86724571	-3333.00550371	-3332.99077871	-970.20
17I	0.695483	0.74469	-3333.62067675	-3332.87598675	-3333.01651675	-3333.00086575	
17J	0.631627	0.675089	-3104.38699473	-3103.71190573	-3103.83701173	-3103.82468973	
17K-TS	0.630204	0.673229	-3104.37464639	-3103.70141739	-3103.82550639	-3103.81327339	-340.85
17L	0.632693	0.675752	-3104.42929239	-3103.75354039	-3103.87639939	-3103.86473739	
18A	0.374038	0.394366	-943.17167579	-942.77730979	-942.84192379	-942.84128079	
18B	0.484799	0.520543	-2596.35115904	-2595.83061604	-2595.93448204	-2595.92696204	
18C	0.484568	0.520439	-2596.34922968	-2595.82879068	-2595.93280168	-2595.92540468	
18D-TS	0.484432	0.519686	-2596.33490369	-2595.81521769	-2595.91688069	-2595.91037769	-103.92
18E	0.486534	0.522011	-2596.38080845	-2595.85879745	-2595.96000045	-2595.95406745	
18F	0.538091	0.5767	-2364.72551042	-2364.14881042	-2364.25727542	-2364.25009042	
18G	0.655208	0.701469	-3071.57426069	-3070.87279169	-3070.99677269	-3070.98824969	
18H-TS	0.649594	0.695861	-3071.54255683	-3070.84669583	-3070.97220483	-3070.96271383	-867.00
18I	0.654292	0.701168	-3071.55630708	-3070.85513908	-3070.98234408	-3070.97244208	
18J	0.588457	0.630336	-2842.33537189	-2841.70503589	-2841.82257789	-2841.81338389	
18K-TS	0.587919	0.629087	-2842.32326499	-2841.69417799	-2841.80817999	-2841.80033299	-310.51
18L	0.589874	0.631325	-2842.37958349	-2841.74825849	-2841.86300149	-2841.85481649	
18M	0.484403	0.520155	-2596.34694942	-2595.82679442	-2595.92941842	-2595.92255342	
18N-TS	0.48251	0.51813	-2596.32689568	-2595.80876568	-2595.91218468	-2595.90482268	-150.71
18O	0.483566	0.519616	-2596.34946499	-2595.82984899	-2595.93603999	-2595.92760899	
18P-TS	0.653383	0.699396	-3071.52074750	-3070.82135150	-3070.94537350	-3070.93665550	-477.87
***P*t-Bu$_3$**	0.372926	0.391376	-815.16857649	-814.77720049	-814.83653349	-814.83631049	

L32	0.540982	0.567606	-1310.74190862	-1310.17430262	-1310.25811162	-1310.25248362	
L33	0.600623	0.628831	-1389.41091227	-1388.78208127	-1388.86881927	-1388.86331427	
L34	0.660725	0.691149	-1468.13981760	-1467.44866860	-1467.54195160	-1467.53471260	
L25	0.719744	0.751755	-1546.82664522	-1546.07489022	-1546.17035122	-1546.16342422	
L35	0.778251	0.812628	-1625.47030943	-1624.65768143	-1624.75728043	-1624.75043143	
L39	0.415207	0.43546	-1077.22085732	-1076.78539732	-1076.85536132	-1076.85109432	
1a	0.110556	0.124942	-1653.14065615	-1653.01571415	-1653.07295215	-1653.07030815	
4a	0.114885	0.122302	-706.83566109	-706.71335909	-706.75179509	-706.75180009	
KCl	0.000491	0.004332	-1060.25738701	-1060.25305501	-1060.28048001	-1060.28048101	
KOAc	0.050151	0.056576	-828.60252704	-828.54595104	-828.58266704	-828.58209504	
AcOH	0.06222	0.067706	-229.19910432	-229.13139832	-229.16402132	-229.16371932	

[a]Zero-point correction (ZPE), thermal correction to enthalpy (tcH), energies(E), enthalpies (H), Gibbs free energies (G) (in Hartree), and quasi-harmonic corrected Gibbs free energy of the structures calculated at the B3LYP-D3(BJ)/Def2-TZVP-SMD(1,4-dioxane)//B3PW91-D3(BJ)/6-31G(d)-SDD(Pd)-PCM(1,4-dioxane) level of theory.

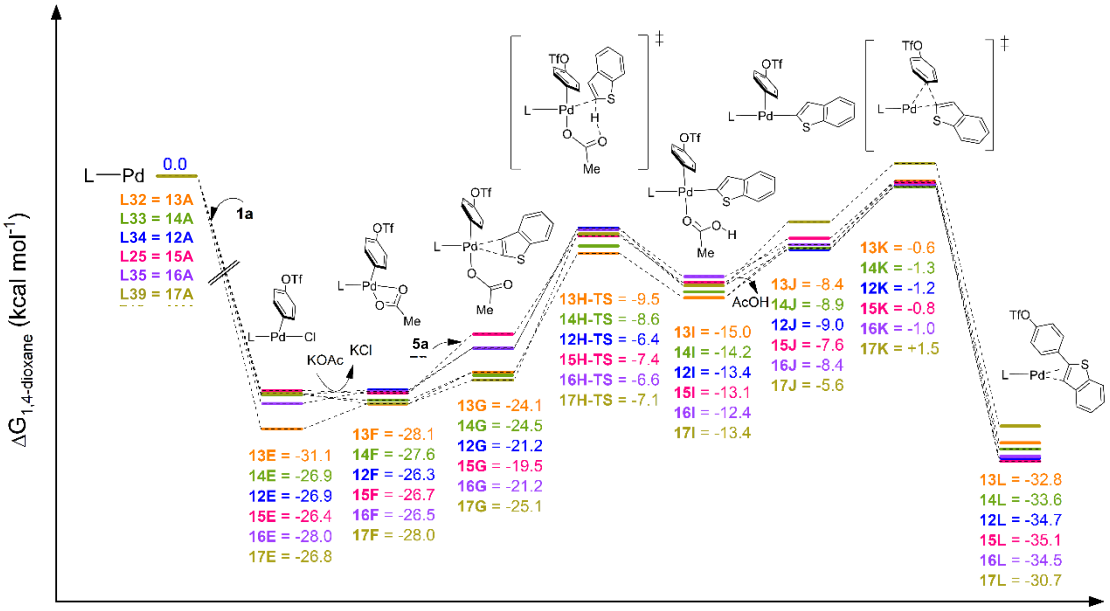

Figure 3.5 Free energy profiles calculated for the CMD process of chemoselective cross-coupling reaction using Pd/(**L25**, **L32**–**L35,** and **L39**) catalysts.

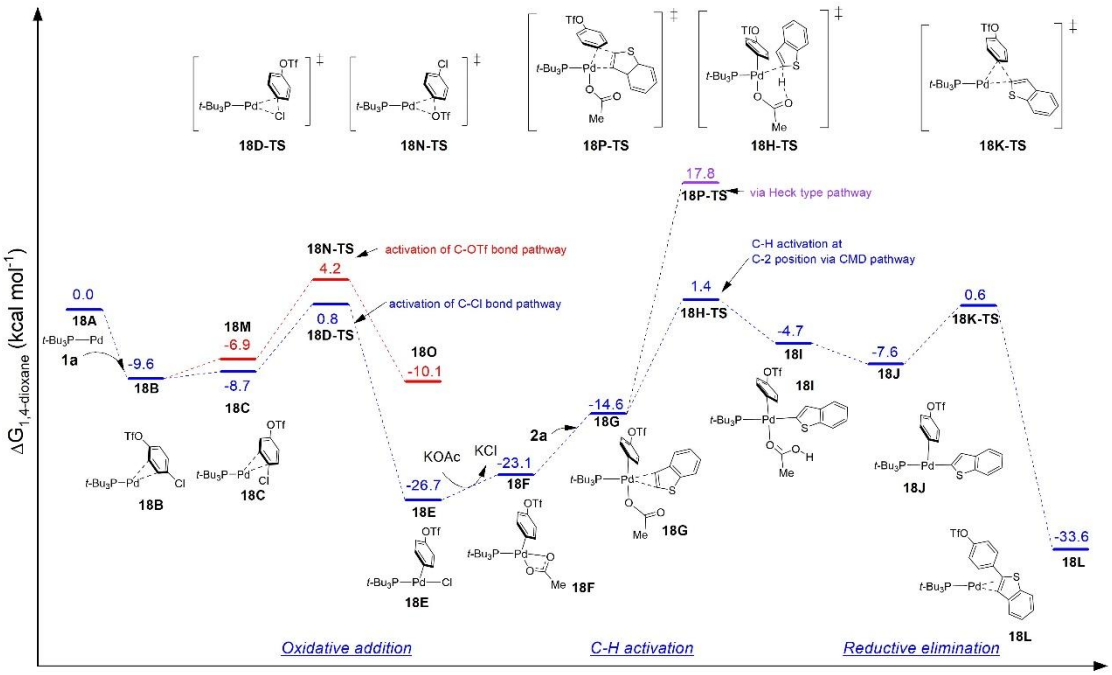

Figure 3.6 Free energy profiles calculated for the chemoselective Pd-P*t*-Bu_3 cross-coupling reaction of 4-chlorophenyltriflate with benzo[*b*]thiophene.

Table 3.8 Selected NBO parameters for optimized structures computed at SMD(1,4-dioxane) B3LYP-D3(BJ)/Def2-TZVP level.

SECOND ORDER PERTURBATION THEORY ANALYSIS OF FOCK MATRIX IN NBO BASIS

Threshold for printing: 0.50 kcal/mol
(Intermolecular threshold: 0.05 kcal/mol)

	Donor (L) NBO	Acceptor (NL) NBO	E(2) kcal/mol	E(NL)-E(L) a.u.	F(L,NL) a.u.
13K-TS	152. BD (1) C 53- H 56	199. LV (1)Pd 61	0.29	0.86	0.01
14H-TS	91. LP (2)Pd 63	325. BD*(1) C 86- H 89	2.15	0.6	0.033
	92. LP (3)Pd 63	325. BD*(1) C 86- H 89	1.09	0.65	0.024
	105. BD (1) C 1-Pd 63	325. BD*(1) C 86- H 89	2.09	0.66	0.033
	120. BD (1) P 11-Pd 63	325. BD*(1) C 86- H 89	2.76	0.69	0.039
	203. BD (1) C 86- H 89	242. BD*(1) P 11-Pd 63	0.62	0.84	0.020
14K-TS	87. LP (1)Pd 63	301. BD*(1) C 78- H 81	1.20	0.61	0.024
	88. LP (2)Pd 63	301. BD*(1) C 78- H 81	0.56	0.60	0.016
	89. LP (3)Pd 63	301. BD*(1) C 78- H 81	0.89	0.62	0.021
	90. LP (4)Pd 63	301. BD*(1) C 78- H 81	0.09	0.61	0.007
	91. LP (5)Pd 63	301. BD*(1) C 78- H 81	3.42	0.61	0.041
	96. BD (2) C 1- C 3	301. BD*(1) C 78- H 81	0.27	0.61	0.011
	97. BD (1) C 1- C 64	301. BD*(1) C 78- H 81	0.35	0.74	0.014
	187. BD (1) C 78- H 81	210. BD*(2) C 1- C 3	0.13	0.48	0.007
	187. BD (1) C 78- H 81	211. BD*(1) C 1- C 64	0.25	0.48	0.010
	187. BD (1) C 78- H 81	281. BD*(2) C 64- C 75	0.21	0.48	0.009
	187. BD (1) C 78- H 81	207. LV (1)Pd 63	5.09	0.90	0.060
12H-TS	93. LP (2)Pd 91	321. BD*(1) C 77- H 80	3.56	0.62	0.042
	107. BD (1) C 1-Pd 91	321. BD*(1) C 77- H 80	2.53	0.65	0.036
	122. BD (1) P 11-Pd 91	321. BD*(1) C 77- H 80	3.31	0.68	0.042
	193. BD (1) C 77- H 80	235. BD*(1) C 1-Pd 91	0.92	0.71	0.023
	193. BD (1) C 77- H 80	250. BD*(1) P 11-Pd 91	1.02	0.80	0.026
12K-TS	89. LP (1)Pd 91	304. BD*(1) C 77- H 80	0.27	0.61	0.011
	91. LP (3)Pd 91	304. BD*(1) C 77- H 80	0.18	0.63	0.010
	92. LP (4)Pd 91	304. BD*(1) C 77- H 80	0.32	0.62	0.013
	93. LP (5)Pd 91	304. BD*(1) C 77- H 80	4.54	0.61	0.047
	98. BD (2) C 1- C 3	304. BD*(1) C 77- H 80	0.48	0.62	0.015
	99. BD (1) C 1- C 92	304. BD*(1) C 77- H 80	0.61	0.74	0.019
	197. BD (2) C 92- C103	304. BD*(1) C 77- H 80	0.06	0.63	0.006
	184. BD (1) C 77- H 80	218. BD*(2) C 1- C 3	0.13	0.48	0.007
	184. BD (1) C 77- H 80	219. BD*(1) C 1- C 92	0.32	0.48	0.011
	184. BD (1) C 77- H 80	317. BD*(2) C 92- C103	0.16	0.48	0.008
	184. BD (1) C 77- H 80	215. LV (1)Pd 91	5.12	0.89	0.060
15H-TS	95. LP (2)Pd 63	341. BD*(1) C 86- H 89	2.35	0.63	0.034
	96. LP (3)Pd 63	341. BD*(1) C 86- H 89	1.13	0.6	0.027
	109. BD (1) C 1-Pd 63	341. BD*(1) C 86- H 89	2.38	0.65	0.035
	124. BD (1) P 11-Pd 63	341. BD*(1) C 86- H 89	3.48	0.68	0.043
	207. BD (1) C 86- H 89	258. BD*(1) P 11-Pd 63	0.87	0.82	0.024
	207. BD (1) C 86- H 89	243. BD*(1) C 1-Pd 63	0.77	0.71	0.021
15K-TS	91. LP (1)Pd 63	317. BD*(1) C 78- H 81	0.17	0.61	0.009
	93. LP (3)Pd 63	317. BD*(1) C 78- H 81	0.11	0.62	0.007
	94. LP (4)Pd 63	317. BD*(1) C 78- H 81	0.26	0.61	0.011
	95. LP (5)Pd 63	317. BD*(1) C 78- H 81	4.63	0.60	0.047
	100. BD (2) C 1- C 3	317. BD*(1) C 78- H 81	0.46	0.61	0.015
	101. BD (1) C 1- C 64	317. BD*(1) C 78- H 81	0.62	0.73	0.019
	171. BD (2) C 64- C 75	317. BD*(1) C 78- H 81	0.07	0.63	0.006
	191. BD (1) C 78- H 81	226. BD*(2) C 1- C 3	0.13	0.48	0.007
	191. BD (1) C 78- H 81	227. BD*(1) C 1- C 64	0.29	0.47	0.010
	191. BD (1) C 78- H 81	297. BD*(2) C 64- C 75	0.11	0.48	0.007
	191. BD (1) C 78- H 81	223. LV (1)Pd 63	5.35	0.89	0.062
16H-TS	97. LP (2)Pd 63	369. BD*(1) C106- H109	2.16	0.65	0.033
	98. LP (3)Pd 63	369. BD*(1) C106- H109	2.17	0.65	0.033
	104. LP (2) O 78	369. BD*(1) C106- H109	0.13	0.76	0.009
	105. LP (3) O 78	369. BD*(1) C106- H109	0.49	0.66	0.016
	111. BD (1) C 1-Pd 63	369. BD*(1) C106- H109	2.05	0.66	0.033
	126. BD (1) P 11-Pd 63	369. BD*(1) C106- H109	3.28	0.68	0.042
	229. BD (1) C106- H109	251. BD*(1) C 1-Pd 63	1.13	0.71	0.025
	229. BD (1) C106- H109	266. BD*(1) P 11-Pd 63	0.87	0.83	0.024
16K-TS	95. LP (3)Pd 63	345. BD*(1) C 98- H101	0.11	0.62	0.007
	96. LP (4)Pd 63	345. BD*(1) C 98- H101	0.09	0.61	0.007
	97. LP (5)Pd 63	345. BD*(1) C 98- H101	3.57	0.60	0.041
	102. BD (2) C 1- C 3	345. BD*(1) C 98- H101	0.41	0.61	0.014
	103. BD (1) C 1- C 64	345. BD*(1) C 98- H101	0.67	0.74	0.020
	213. BD (1) C 98- H101	234. BD*(2) C 1- C 3	0.11	0.47	0.006
	213. BD (1) C 98- H101	235. BD*(1) C 1- C 64	0.25	0.47	0.010
	213. BD (1) C 98- H101	305. BD*(2) C 64- C 75	0.10	0.47	0.006
	213. BD (1) C 98- H101	231. LV (1)Pd 63	4.54	0.86	0.056

3.6 References

(1) (a) Lu, R.-J.; Tucker, J. A.; Pickens, J.; Ma, Y.-A.; Zinevitch, T.; Kirichenko, O.; Konoplev, V.; Kuznetsova, S.; Sviridov, S.; Brahmachary, E. *J. Med. Chem.* **2009**, *52 (14)*, 4481-4487; (b) Hu, X.; Wu, J.-W.; Wang, M.; Yu, M.-H.; Zhao, Q.-S.; Wang, H.-Y.; Hou, A.-J. *J. Nat. Prod.* **2012**, *75 (1)*, 82-87; (c) Liang, H.; Zhu, G.; Pu, X.; Qiu, L. *Org. Lett.* **2021**, *23 (23)*, 9246-9250.

(2) Bheeter, C. B.; Chen, L.; Soulé, J.-F.; Doucet, H. *Catal. Sci. Technol.* **2016**, *6 (7)*, 2005-2049.

(3) Tan, Y.; Hartwig, J. F. *J. Am. Chem. Soc.* **2011**, *133 (10)*, 3308-3311.

(4) (a) Fujinami, Y.; Kuwabara, J.; Lu, W.; Hayashi, H.; Kanbara, T. *ACS Macro Lett.* **2012**, *1 (1)*, 67-70; (b) Kuwabara, J.; Sakai, M.; Zhang, Q.; Kanbara, T. *Org. Chem. Front.* **2015**, *2 (5)*, 520-525; (c) Požgan, F.; Roger, J.; Doucet, H. *ChemSusChem.* **2008**, *1 (5)*, 404-407; (d) Yamamoto, Y.; Tokuji, S.; Tanaka, T.; Yorimitsu, H.; Osuka, A. *Asian J. Org. Chem.* **2013**, *2 (4)*, 320-324.

(5) Yamashita, M.; Hartwig, J. F. *J. Am. Chem. Soc.* **2004**, *126 (17)*, 5344-5345.

(6) (a) Gorelsky, S. I.; Lapointe, D.; Fagnou, K. *J. Org. Chem.* **2012**, *77 (1)*, 658-668; (b) Liegault, B.; Lapointe, D.; Caron, L.; Vlassova, A.; Fagnou, K. *J. Org. Chem.* **2009**, *74 (5)*, 1826-1834.

(7) (a) Chen, Z.; Gu, C.; Yuen, O. Y.; So, C. M. *Chem. Sci.* **2022**, *13 (17)*, 4762-4769; (b) Miyaura, N.; Suzuki, A. *Chem. Rev.* **1995**, *95 (7)*, 2457-2483; (c) Niemeyer, Z. L.; Milo, A.; Hickey, D. P.; Sigman, M. S. *Nat. Chem.* **2016**, *8 (6)*, 610-617.

(8) Ng, S. S.; Pang, W. H.; Yuen, O. Y.; So, C. M. *Org. Chem. Front.* **2023**, *10 (17)*, 4408-4436.

(9) Littke, A. F.; Fu, G. C. *Angew. Chem. Int. Ed.* **2002**, *41 (22)*, 4176-4211.

(10) (a) Rene, O.; Fagnou, K. *Adv. Syn. Catal.* **2010**, *352 (13)*, 2116-2120; (b) Roy, D.; Mom, S.; Royer, S.; Lucas, D.; Hierso, J.-C.; Doucet, H. *ACS Catal.* **2012**, *2 (6)*, 1033-1041.

(11) Chen, S.; Ranjan, P.; Voskressensky, L. G.; Van der Eycken, E. V.; Sharma, U. K. *Molecules.* **2020**, *25 (21)*, 4970.

(12) Chen, L.; Bruneau, C.; Dixneuf, P. H.; Doucet, H. *Green Chem.* **2012**, *14 (4)*, 1111-1124.

(13) (a) Bellina, F.; Calandri, C.; Cauteruccio, S.; Rossi, R. *Tetrahedron* **2007**, *63 (9)*, 1970-1980; (b) Colletto, C.; Islam, S.; Julia-Hernandez, F.; Larrosa, I. *J. Am. Chem. Soc.* **2016**, *138 (5)*, 1677-1683; (c) Lebrasseur, N.; Larrosa, I. *J. Am. Chem. Soc.* **2008**, *130 (10)*, 2926-2927; (d) Matsuda, S.; Takahashi, M.; Monguchi, D.; Mori, A. *Synlett* **2009**, *2009 (12)*, 1941-1944; (e) Wang, L.; Yi, W.-b.; Cai, C. *Chem. Commun.* **2011**, *47 (2)*, 806-808; (f) Xu, Z.; Xu, Y.; Lu, H.; Yang, T.; Lin, X.; Shao, L.;

Ren, F. *Tetrahedron* **2015**, *71 (18)*, 2616-2621.

(14) Wakioka, M.; Nakamura, Y.; Wang, Q.; Ozawa, F. *Organometallics* **2012**, *31 (13)*, 4810-4816.

(15) Choi, S. J.; Kuwabara, J.; Kanbara, T. *ACS Sustainable Chem. Eng.* **2013**, *1 (8)*, 878-882.

(16) (a) Athavan, G.; Tanner, T. F.; Whitwood, A. C.; Fairlamb, I. J.; Perutz, R. N. *Organometallics* **2022**, *41 (22)*, 3175-3184; (b) Bay, K. L.; Yang, Y.-F.; Houk, K. *J. Organomet. Chem.* **2018**, *864* 19-25; (c) Whitaker, D.; Bures, J.; Larrosa, I. *J. Am. Chem. Soc.* **2016**, *138 (27)*, 8384-8387.

(17) (a) Fairlamb, I. J. S.; Scott, N. W. J. *Nanoparticles in Catalysis* (Ed: S. Kobayashi), Springer International Publishing, Cham **2020**, pp. 171–205; (b) Wang, X.; Truesdale, L.; Yu, J.-Q. *J. Am. Chem. Soc.* **2010**, *132 (11)*, 3648-3649; (c) Faarasse, S.; El Brahmi, N.; Guillaumet, G.; El Kazzouli, S. *Molecules.* **2021**, *26 (19)*, 5763.

(18) (a) Elias, E. K.; Rehbein, S. M.; Neufeldt, S. R. *Chem. Sci.* **2022**, *13 (6)*, 1618-1628; (b) Reeves, E. K.; Bauman, O. R.; Mitchem, G. B.; Neufeldt, S. R. *Isr. J. Chem.* **2020**, *60 (3-4)*, 406-409; (c) Roger, J.; Doucet, H. *Org. Biomol. Chem.* **2008**, *6 (1)*, 169-174; (d) Roy, A. H.; Hartwig, J. F. *Organometallics* **2004**, *23 (2)*, 194-202.

(19) (a) Fairlamb, I. J. *Chem. Soc. Rev.* **2007**, *36 (7)*, 1036-1045; (b) Schröter, S.; Stock, C.; Bach, T. *Tetrahedron* **2005**, *61* 2245-2267.

(20) Gu, C.; Yuen, O. Y.; Ng, S. S.; So, C. M. *Adv. Syn. Catal.* **2024**, *366 (7)*, 1565-1574.

(21) Shibahara, F.; Murai, T. *Asian J. Org. Chem.* **2013**, *2 (8)*, 624-636.

(22) Littke, A. F.; Dai, C.; Fu, G. C. *J. Am. Chem. Soc.* **2000**, *122 (17)*, 4020-4028.

(23) Schoenebeck, F.; Houk, K. *J. Am. Chem. Soc.* **2010**, *132 (8)*, 2496-2497.

(24) Tamba, S.; Okubo, Y.; Tanaka, S.; Monguchi, D.; Mori, A. *J. Org. Chem.* **2010**, *75 (20)*, 6998-7001.

(25) Verrier, C.; Martin, T.; Hoarau, C.; Marsais, F. *J. Org. Chem.* **2008**, *73 (18)*, 7383-7386.

(26) Reeves, E. K.; Humke, J. N.; Neufeldt, S. R. *J. Org. Chem.* **2019**, *84 (18)*, 11799-11812.

(27) So, C. M.; Yuen, O. Y.; Ng, S. S.; Chen, Z. *ACS Catal.* **2021**, *11 (13)*, 7820-7827.

(28) (a) Brookhart, M.; Green, M. L.; Parkin, G. *Proc. Natl. Acad. Sci. USA* **2007**, *104 (17)*, 6908-6914; (b) Lepetit, C.; Poater, J.; Alikhani, M. E.; Silvi, B.; Canac, Y.; Contreras-Garcia, J.; Solà, M.; Chauvin, R. *Inorg. Chem.* **2015**, *54 (6)*, 2960-2969; (c) Scherer, W.; Dunbar, A. C.; Barquera-Lozada, J. E.; Schmitz, D.; Eickerling, G.; Kratzert, D.; Stalke, D.; Lanza, A.; Macchi, P.; Casati, N. P. *Angew. Chem. Int. Ed.* **2015**, *54 (8)*, 2505-2509; (d) Taubmann, C.; Öfele, K.; Herdtweck, E.; Herrmann, W.

A. *Organometallics.* **2009**, *28 (15)*, 4254-4257.

(29) Barquera-Lozada, J. E.; Obenhuber, A.; Hauf, C.; Scherer, W. *J. Phys. Chem. A.* **2013**, *117 (20)*, 4304-4315.

(30) (a) Cao, H.-J.; Zhao, Q.; Zhang, Q.-F.; Li, J.; Hamilton, E. J.; Zhang, J.; Wang, L.-S.; Chen, X. *Dalton Trans.* **2016**, *45 (25)*, 10194-10199; (b) Darmandeh, H.; Löffler, J.; Tzouras, N. V.; Dereli, B.; Scherpf, T.; Feichtner, K. S.; Vanden Broeck, S.; Van Hecke, K.; Saab, M.; Cazin, C. S. *Angew. Chem. Int. Ed.* **2021**, *60 (38)*, 21014-21024; (c) Wei, X. J.; Xue, B.; Handelmann, J.; Hu, Z.; Darmandeh, H.; Gessner, V. H.; Gooßen, L. J. *Adv. Syn. Catal.* **2022**, *364 (19)*, 3336-3341.

(31) Ghosh, D.; Lee, H. M. *Org. Lett.* **2012**, *14 (21)*, 5534-5537.

(32) (a) Bordwell, F. G. *Acc. Chem. Res.* **1988**, *21 (12)*, 456-463; (b) Shen, K.; Fu, Y.; Li, J.-N.; Liu, L.; Guo, Q.-X. *Tetrahedron* **2007**, *63 (7)*, 1568-1576.

(33) (a) Fu, H. Y.; Doucet, H. *Methyl 2-Furoate: An Alternative Reagent to Furan for Palladium-Catalysed Direct Arylation.* Wiley Online Library: **2011**; (b) Battace, A.; Lemhadri, M.; Zair, T.; Doucet, H.; Santelli, M. *Organometallics* **2007**, *26 (3)*, 472-474.

(34) (a) Chiong, H. A.; Daugulis, O. *Org. Lett.* **2007**, *9 (8)*, 1449-1451; (b) Dao-Huy, T.; Haider, M.; Glatz, F.; Schnürch, M.; Mihovilovic, M. D. *Eur. J. Org. Chem.* **2014**, *2014 (36)*, 8119-8125; (c) Loukotova, L.; Yuan, K.; Doucet, H. *ChemCatChem.* **2014**, *6 (5)*, 1303-1309; (d) Pereira, K. C.; Porter, A. L.; Potavathri, S.; LeBris, A. P.; DeBoef, B. *Tetrahedron* **2013**, *69 (22)*, 4429-4435; (e) Shibahara, F.; Yamaguchi, E.; Murai, T. *Chem. Commun.* **2010**, *46 (14)*, 2471-2473.

(35) Yamaguchi, E.; Wang, C.; Fukazawa, A.; Taki, M.; Sato, Y.; Sasaki, T.; Ueda, M.; Sasaki, N.; Higashiyama, T.; Yamaguchi, S. *Angew. Chem. Int. Ed.* **2015**, *127 (15)*, 4622-4626.

(36) Seok, M. K.; Kim, M. S.; Park, Y. P.; Han, K. J.; Oh, E. G. in *World Intellectual Property Organization*, Vol. *WO2022080696*, **2022**, https://patentimages.storage.googleapis.com/b0/f5/d5/ff13058d717abe/WO2022080696A1.pdf (accessed: November 2023).

(37) Donohoe, T. J.; Jahanshahi, A.; Tucker, M. J.; Bhatti, F. L.; Roslan, I. A.; Kabeshov, M.; Wrigley, G. *Chem. Commun.* **2011**, *47 (20)*, 5849-5851.

(38) Frisch, M.; Trucks, G.; Schlegel, H.; Scuseria, G.; Robb, M.; Cheeseman, J.; Scalmani, G.; Barone, V.; Petersson, G.; Nakatsuji, H. *Gaussian16 (Revision A. 03)* **2016**.

(39) (a) Becke, A. D. *J. Chem. Phys.* **1996**, *104 (3)*, 1040-1046; (b) Perdew, J. P.; Burke, K.; Wang, Y. *Phys. Rev. B: Condens. Matter Mater. Phys.* **1996**, *54 (23)*, 16533-16539; (c) Perdew, J. P.; Chevary,

J. A.; Vosko, S. H.; Jackson, K. A.; Pederson, M. R.; Singh, D. J.; Fiolhais, C. *Phys. Rev. B: Condens. Matter Mater. Phys.* **1992**, *46 (11)*, 6671-6687.

(40) (a) Arnold, P. L.; Hollis, E.; Nichol, G. S.; Love, J. B.; Griveau, J.-C.; Caciuffo, R.; Magnani, N.; Maron, L.; Castro, L.; Yahia, A. *J. Am. Chem. Soc.* **2013**, *135 (10)*, 3841-3854; (b) Ignatov, S.; Panteleev, S.; Maslennikov, S.; Spirina, I. *Russ. J. Gen. Chem.* **2012**, *82* 1954-1961; (c) Montero-Campillo, M. M.; Lamsabhi, A. M.; Mó, O.; Yáñez, M. *Alkyl mercury compounds: an assessment of DFT methods.* In *8th Congress on Electronic Structure: Principles and Applications (ESPA 2012) A Conference Selection from Theoretical Chemistry Accounts*, **2014**; Springer: pp 111-118; (d) Salman, S.; Bredas, J.-L.; Marder, S. R.; Coropceanu, V.; Barlow, S. *Organometallics* **2013**, *32 (20)*, 6061-6068; (e) Wang, L.; Zhang, Y.; He, H.; Zhang, J. *Synth. Met.* **2013**, *167* 51-63.

(41) (a) Dolg, M.; Wedig, U.; Stoll, H.; Preuss, H. *J. Chem. Phys.* **1987**, *86 (2)*, 866-872; (b) Schwerdtfeger, P.; Dolg, M.; Schwarz, W.; Bowmaker, G. A.; Boyd, P. D. *J. Chem. Phys.* **1989**, *91 (3)*, 1762-1774; (c) Andrae, D.; Haeussermann, U.; Dolg, M.; Stoll, H.; Preuss, H. *Theor. Chim. Acta* **1990**, *77* 123-141.

(42) (a) Mennucci, B.; Tomasi, J.; Cammi, R.; Cheeseman, J.; Frisch, M.; Devlin, F.; Gabriel, S.; Stephens, P. *J. Phys. Chem. A.* **2002**, *106 (25)*, 6102-6113; (b) Tomasi, J.; Mennucci, B.; Cammi, R. *Chem. Rev.* **2005**, *105 (8)*, 2999-3094.

(43) Marenich, A. V.; Cramer, C. J.; Truhlar, D. G. *J. Phys. Chem, B* **2009**, *113 (18)*, 6378-6396.

(44) (a) Grimme, S.; Antony, J.; Ehrlich, S.; Krieg, H. *J. Chem. Phys.* **2010**, *132 (15)* ; (b) Grimme, S.; Ehrlich, S.; Goerigk, L. *J. Comput. Chem.* **2011**, *32 (7)*, 1456-1465; (c) Risthaus, T.; Grimme, S. *J. Chem. Theory Comput.* **2013**, *9 (3)*, 1580-1591.

(45) (a) Becke, A. D.; Johnson, E. R. *J. Chem. Phys.* **2007**, *127 (15)* ; (b) Johnson, E. R.; Becke, A. D. *J. Chem. Phys.* **2006**, *124 (17)*.

(46) (a) Becke, A. D. *J. Chem. Phys.* **1992**, *96 (3)*, 2155-2160; (b) Lee, C.; Yang, W.; Parr, R. G. *Phys. Rev. B: Condens. Matter Mater. Phys.* **1988**, *37 (2)*, 785.

(47) Weigend, F.; Ahlrichs, R. *Phys. Chem. Chem. Phys.* **2005**, *7 (18)*, 3297-3305.

(48) (a) Paton, R. S. GoodVibes v3.0.1, 2019, bobbypaton/GoodVibes: Calculate quasi-harmonic free energies from Gaussian output files with temperature and other corrections, https://github.com/bobbypaton/GoodVibes, (accessed Feb 20, 2021); (b) Grimme, S. *Chem. Eur. J.* **2012**, *18 (32)*, 9955-9964.

(49) Glendening, E. D.; Badenhoop, J. K.; Reed, A. E.; Carpenter, J. E.; Bohmann, J. A.; Morales, C. M. P.; Karafiloglou, C. R.; Landis, F. Weinhold, *NBO 7.0*; Theoretical Chemistry Institute, University of Wisconsin: Madison, **2018**.

(50) Legault, C. Y. CYLview 1.0b, Département de Chimie, Université de Sherbrooke: Quebec, Canada, 2009, http://www.cylview.org, (accessed Feb 20, 2021).

Chapter 4 Alkyl-Pyrazole-Phosphine Ligands Featuring Pd···H–C Interaction Enabled Pd-Catalyzed Decarboxylative Cross-Coupling at Moderate Temperature and Late-Stage Functionalization of Drugs

4.1 Introduction

Carboxylic acids, known for their vast structural diversity and stability, are readily available either commercially or synthetically,[1] and are easy to handle. Decarboxylative cross-coupling reaction, which harnesses carboxylic acids as surrogates for more expensive and less stable nucleophilic coupling partners such as organozinc reagents or organotin reagents, becomes a fascinating strategy.[2] The past two decades have witnessed a flourishing development of redox-neutral decarboxylative cross-coupling reactions promoted by a bimetallic catalytic system, which typically rely on the copper or silver to facilitate the decarboxylation step and the palladium to promote the oxidative addition, transmetalation, and reductive elimination steps, thereby expanding both the substrate scope of the arene carboxylic acids and electrophiles.[3] However, many developed methodologies generally necessitate higher reaction temperatures (150–190 ºC), which may lead to narrow substrate scope, experimental safety concerns, and high energy consumption.

Over the past decade, chemists have made considerable endeavors in lowering the reaction temperature of redox-neutral decarboxylative cross-coupling reactions. Based on the discovery guided by DFT calculations that protodecarboxylation of *ortho*-

substituted benzoates at only 120 °C when utilizing silver as the catalyst,[4] Gooßen *et al.* consequently leveraged the Pd/Ag catalytic system to finish the decarboxylative cross-coupling reactions at 130 °C.[5] Cahiez and co-works disclosed that harnessing tetramethylethylenediamine (TMEDA) as the copper ligand could lead to the cross-coupling of cesium 2-nitrobenzoates with aryl bromides at 120–140 °C.[6] Later, Gooßen et al. via DFT calculations and experiments found that in the Cu/Pd bimetallic catalytic system, the transmetalation step may replace the decarboxylation step as the rate-determining step of the reaction.[7] This has led to the development of bridging ligands[8] to facilitate the transmetalation step, then enabled the reaction temperature to be lowered to only 100 °C.

However, the optimization of a suitable bimetallic catalytic system, which requires the fine-tuning of both catalytic cycles as well as ensuring their compatibility, renders the process rather tedious and time-consuming. Therefore, monometallic catalytic systems demonstrate some complementary advantages compared to bimetallic catalytic systems. In recent years, palladium catalysts, as promising metals, have been employed by chemists to develop decarboxylative cross-coupling reactions due to their capability to independently catalyze such reactions. Although satisfactory progress has been made in this area, many achievements have been realized through the decarboxylative cross-coupling of expensive aryl iodides or bromides with aryl carboxylic acids under high temperatures (170–190 °C).[9] The ability to perform decarboxylative cross-coupling reactions with inexpensive and readily available aryl chlorides and aryl carboxylic acids is of significant importance for both the industry and academia. Currently, while there

are a few successful examples (Scheme 4.1A),10 limitations were obviously included (i) the narrow substrate scope, (ii) the requirement for additives, and (iii) especially the need for high reaction temperatures, which remains a persistent and significant scientific challenge hindering the broader applicability of decarboxylative cross-coupling transformations.

According to some mechanism investigations of the palladium-catalyzed decarboxylation step, electron-deficient Pd(II) species was the advantageous intermediate for decarboxylation,[11] whereas electron-rich Pd(II) species, composed of electron-donating phosphine ligands and palladium, require higher activate energy to finish the decarboxylation step[12] (Scheme 4.1B). However, the activation of aryl chlorides typically necessitates electron-rich phosphine ligands,[13] which then poses a contradiction for lowering the reaction temperatures. Promoted by our previous work that achieved newly developed pyrazole phosphine ligands can bridge the regio-, and chemoselective C–H arylation process,[14] which solved the contradiction between the requirements of oxidative addition step and C–H activation step. We anticipated such alkyl-based pyrazole phosphine ligands which could interact with palladium and then generate Pd···H–C interactions could tackle the mentioned challenge. In this study, we developed another new type of pyrazole ligand and investigated the decarboxylative cross-coupling reaction under mild reaction conditions (Scheme 4.1 C).

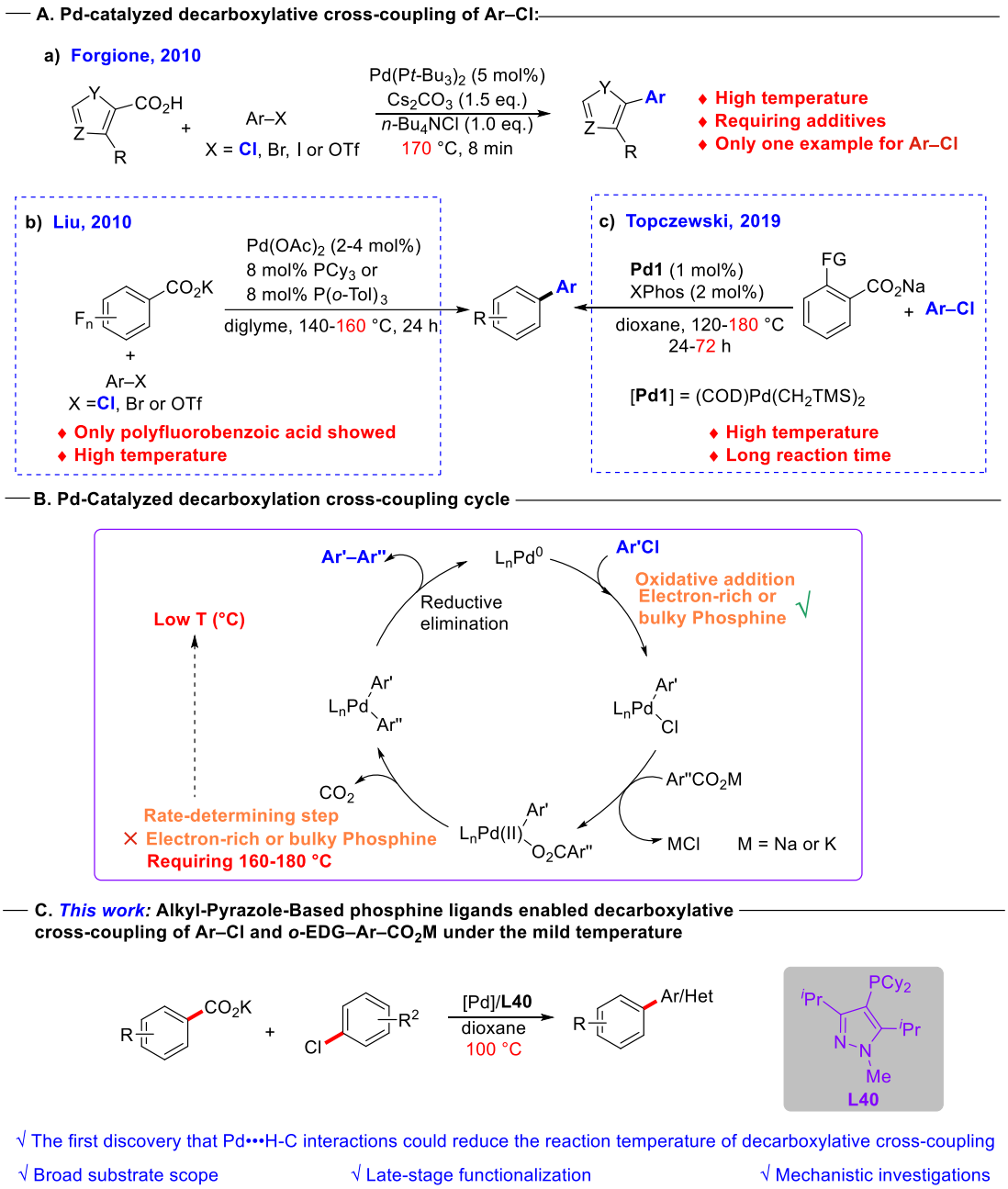

Scheme 4.1 Pd-catalyzed decarboxylative cross-coupling reactions using aryl chlorides

4.2 Results and Discussion

4.2.1 Synthesis of L40

Inspired by previous investigations that the angles and distances of Pd···H–C interaction can influence the reactivity of palladium catalyst,[14] further modification of

cycloalkyl ring to non-cycloalkyl group featuring methine hydrogen might fine-tuning these parameters and then enhance the reactivity. Utilizing the modified method for the synthesis of pyrazole-alkyl-based phosphine ligands, we synthesized the phosphine ligand **L40** containing non-cycloalkyl group *i*-Pr (Scheme 4.2). A simple three-step synthetic route starting from commercially available reagents 2,6-dimethylheptane-3,5-dione and methylhydrazine sulfate afforded the *N*-methyl-protected 3,5-diisopropyl-substituted pyrazole compound via Knorr reaction, followed by selective bromination and phosphorylation, which conveniently afforded **L40** with an overall 33% yield. After obtaining the new ligand, we attempted to obtain the crystal of the **L40** as well as the Pd-**L40** complex to know the spatial structure of the ligand, the spatial configuration of the complex, and the existence of Pd···H–C interaction. However, no satisfactory results have been obtained yet. To our delight, a downfield shift (4.26 ppm) of the methine hydrogen indicates the existence of anagostic/preagostic interactions of the Pd···H–C separation in this new phosphine ligand.[14-15]

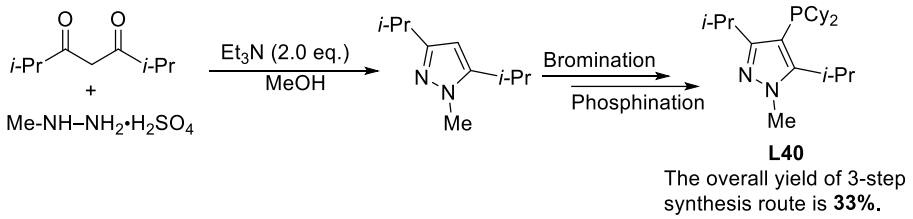

Scheme 4.2 Synthetic protocols for **L40**

4.2.2 Evaluating of Ligands' Effect on Decarboxylative Cross-Coupling Reaction Under Relatively Low Reaction Temperature

We began our investigation utilizing a challenging substrate potassium 2,6-

dimethoxybenzoate **12a**[10c] and 2-chloronaphthalene **13a** as model substrates to test the effect of ligands for the decarboxylative cross-coupling reaction at 110 °C (Table 4.1). PCy_3 (**L2**), P*t*-Bu_3·HBF_4 (**L5**), SPhos (**L10**), and XPhos (**L12**) proved to be efficient ligands in the decarboxylative cross-coupling reaction of aromatic carboxylic acids with aryl chlorides.10 However, they provided only trace amounts of product **14a** at 110 °C (Table 4.1, entries **1**–**4**), which accentuated the difficulty in achieving such a reaction under such a low temperature. We then tested our developed alkyl-pyrazole-based phosphine ligands. Fortunately, almost pyrazole-based phosphine ligands with cycloalkyl groups were able to provide product **14a** in moderate to good yields at 110 °C (Table 4.1, entries **5**–**8**), and ligand with non-cyclic alkyl groups (**L40**) afforded the cross-coupling product in near-equivalent yield. These outcomes indicated that ligands (**L25**, **L33**–**L35** and **L40**) that can provide Pd···H–C interaction all showed better reactivity than Buchwald-type phosphine ligands, highlighting the importance of such interaction in lowering the reaction temperature. This is also demonstrated by harnessing a pyrazole-based phosphine ligand with cyclopropyl group (**L32**), which was previously shown to be incapable of providing Pd···H–C interaction[14] and thus also afforded a bad result (Table 4.1, entry **9**).

Table 4.1 Effect of ligands on decarboxylative cross-coupling reaction at 110 °C[a]

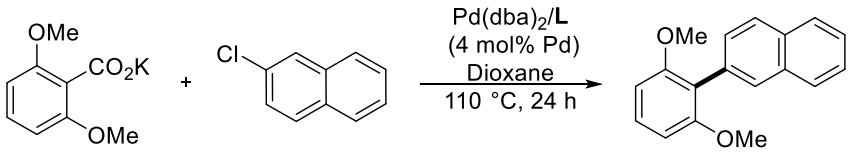

12a **13a** **14a**

Entry	L	14a (%)[b]	Remaining of 13a (%)[b]
1	**L2** = PCy_3	5	77
2	**L5** = P*t*-Bu_3•HBF_4	5	69
3	**L10** = SPhos	2	82
4	**L12** = XPhos	4	75
5	**L35**	50	6
6	**L25**	77	0
7	**L34**	84	0
8	**L33**	44	37
9	**L32**	<1	81
10	**L40**	**90 (97)[c]**	<1

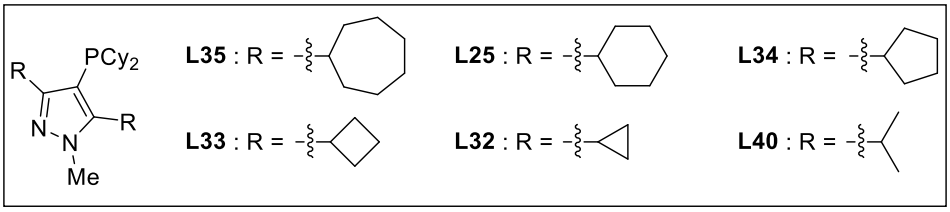

[a]Reaction condition: potassium 2,6-dimethoxybenzoate **12a** (0.30 mmol), 2-chloronaphthalene **13a** (0.20 mmol), $Pd(dba)_2$ (4 mol%), **L** (8 mol%) and dioxane (2.0 mL) were stirred at 110 °C for 24 h. [b]Calibrated GC yields were reported by using dodecane as an internal standard. [c]Isolated yield.

Promoted by these results, we attempted to further lower the reaction temperature to 100 °C (Table 4.2). After temperature reduction, **L1**–**L4** undoubtedly still could provide only traces of product **14a** (Table 4.2, entries **1**–**4**). We also tested several bidentate ligands including dppe, BINAP, and PCy_2-XantPhos and they gave no yield of decarboxylative cross-coupling product (Table 4.2, entries **5**–**7**). NHC ligands like IMes·HCl exhibited no reactivity at such low reaction temperature (Table 4.2, entry **8**).

To our surprise, **L5**–**L8**, which previously provided satisfactory results, afforded only low yields at the reduced reaction temperature (Table 4.2, entries **9**–**12**), while the ligand with three-membered (**L9**) ring afforded no cross-coupling product at this temperature (Table 4.2, entry **13**). To our delight, **L10** still gave rise to good yields, albeit with some reduction in yield (Table 4.2, entry **14**). Another evidence to show the necessity of Pd···H–C interaction was the use of **L11** lacking methine hydrogen and **L12** bearing the phenyl group, which gave rise to no yield of biaryl product **14a** due to the lack of Pd···H–C interaction (Table 4.2, entries **15** and **16**).

Table 4.2 Effect of ligands on decarboxylative cross-coupling reaction at 100 ºC[a]

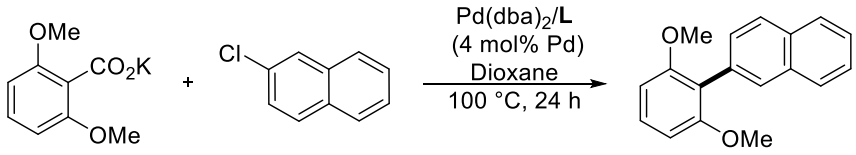

12a **13a** **14a**

Entry	L	14a (%)[b]
1	**L2** = PCy_3	2
2	**L5** = P*t*-Bu_3•HBF_4	3
3	**L10** = SPhos	1
4	**L12** = XPhos	4
5	**L17** = dppe	0
6	**L20** = BINAP	0
7	**L36** = PCy_2-XantPhos	0
8	**L22** = IMes•HCl	0
9	**L35**	17
10	**L25**	21
11	**L34**	22
12	**L33**	11
13	**L32**	0
14	**L40**	**63**
15	**L31**	0
16	**L30**	0

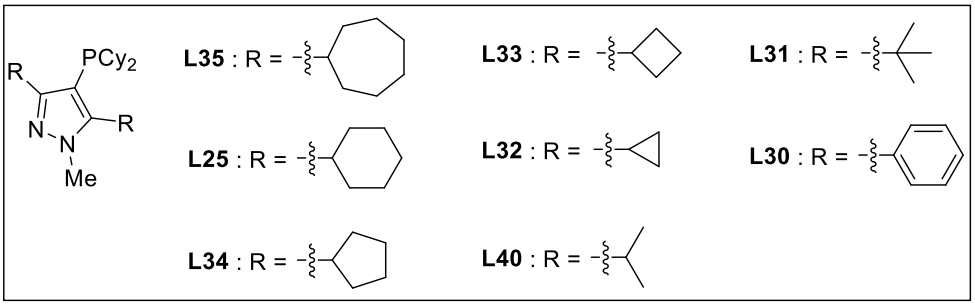

[a]Reaction condition: dimethoxybenzoate **12a** (0.30 mmol), 2-chloronaphthalene **13a** (0.20 mmol), potassium 2,6- $Pd(dba)_2$ (4 mol%), **L** (8 mol%) and dioxane (2.0 mL) were stirred at 100 °C for 24 h. [b]Calibrated GC yields were reported by using dodecane as an internal standard.

4.2.3 Optimization of Reaction Parameters

We then chose **L40** to further optimize the reaction conditions (Table 4.3). The change in the carboxylate substrate used from potassium to sodium salt resulted in a significant decrease in yield (Table 4.3, entry **1**). Evaluation of the ligand ratio showed that lowering or increasing the Pd: L ratio resulted in lower yields (Table 4.3, entries **2**–**4**). Regarding the screening of solvents, the combination of THF and Toluene with a ratio of 1:1 gave the best yield of **14a** among the THF, Toluene, DMF, and NMP (Table 4.3, entries **5**–**9**). Delightfully, $[Pd(2\text{-butenyl})Cl]_2$ was found to be the best palladium source which enhanced yield up to 98% isolated yield of **14a** (Table 4.3, entries **13**), while other palladium sources resulted in reduced yield (Table 4.3, entries **10**–**12**). Attempts to reduce the catalyst loading of $[Pd(2\text{-butenyl})Cl]_2$ from 4% to 2% resulted in a significant decrease in the yield of product **14a** (Table 4.3, entry **14**). Remarkably, a reasonable yield was also obtained already at 90 °C with a prolonged reaction time (Table 4.2, entry **15**), which is an extremely low temperature for a redox-neutral decarboxylative cross-coupling reaction using aryl chloride as reagent.

Table 4.3 Optimization of reaction conditions[a]

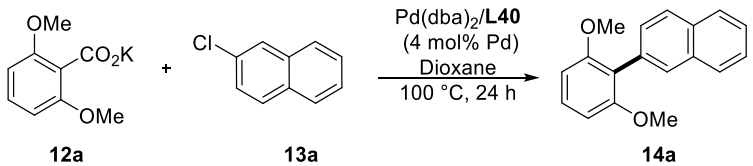

12a 13a 14a

entry	Pd source	Pd: L	Solvent	Yield of **14a** (%)[b]
1[c]	$Pd(dba)_2$	1:2	Dioxane	<1

2	$Pd(dba)_2$	1:1	Dioxane	19
3	$Pd(dba)_2$	1:3	Dioxane	14
4	$Pd(dba)_2$	1:4	Dioxane	8
5	$Pd(dba)_2$	1:2	THF	52
6	$Pd(dba)_2$	1:2	Toluene	63
7	$Pd(dba)_2$	1:2	THF + Toluene	75
8	$Pd(dba)_2$	1:2	DMF	45
9	$Pd(dba)_2$	1:2	NMP	43
10	$[Pd(\pi\text{-cinnamyl})Cl]_2$	1:2	Dioxane	8
11	$[Pd(2\text{-allyl})Cl]_2$	1:2	Dioxane	10
12	$(COD)Pd(CH_2TMS)_2$	1:2	Dioxane	48
13	$[Pd(2\text{-butenyl})\ Cl]_2$	1:2	Dioxane	88 (98%)[d]
14[e]	$[Pd(2\text{-butenyl})\ Cl]_2$	1:2	Dioxane	18
15[f,g]	$[Pd(2\text{-butenyl})\ Cl]_2$	1:2	Dioxane	35

[a]Reaction condition: potassium 2,6-dimethoxybenzoate **12a** (0.30 mmol), 2-chloronaphthalene **13a** (0.20 mmol), $Pd(dba)_2$ (4 mol%), **L40** (8 mol%) and dioxane (2.0 mL) were stirred at 100 °C for 24 h. [b]Calibrated GC yields were reported by using dodecane as an internal standard. [c]sodium 2,6-dimethoxy benzoate was used. [d]Isolated yield. [e]2 mol% $[Pd(2\text{-butenyl})\ Cl]_2$ was used. [f]90 °C. [g]48 h.

4.2.4 Scope of Aryl or Heteroaryl Chlorides

With the optimum conditions in hand, we next tested the substrates scope starting with the variations of aryl chlorides. As shown in Table 4.4, a series of aryl chlorides containing electron-withdrawing groups or electron-donating groups at *para*, *meta*, or *ortho* positions were competent coupling partners and can be converted to the

corresponding products under relatively low reaction temperatures in 85-99% yields (**14b**–**14o**). Noting that substrates containing reactive functional groups such as nitro (**14e**), ester (**14f**), aldehyde (**14g**), and amide (**14l**) were tolerated well. The mild catalytic system also allowed a wide of heterocycles chlorides that containing serious of heterocycles including quinoline, 9*H*-thioxanthen-9-one, benzo[*d*]thiazole, substituted thiophene and pyridine to react smoothly with benzoate acid affording corresponding products in 79-99% yields (**14o**–**14s**).

Table 4.4 Aryl or heteroaryl chlorides scope for decarboxylative cross-coupling reaction[a]

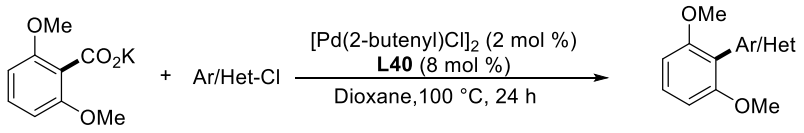

12a **13** **14**

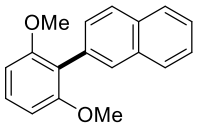

14a, 98 %

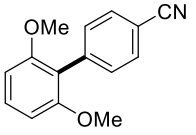

14b, 99 %

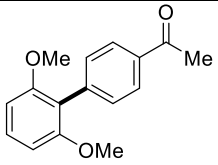

14c, 98 %

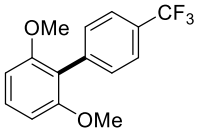

14d, 96 %

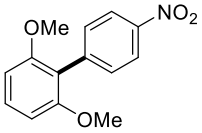

14e, 95 %

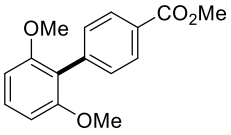

14f, 89 %

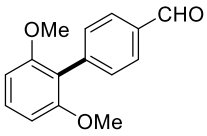

14g, 99 %

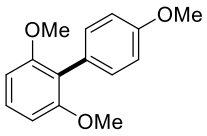

14h, 85%[c,d]

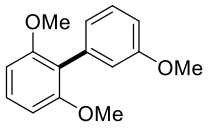

14i, 93%[b]

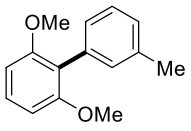

14j, 87%[b]

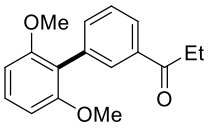

14k, 99 %

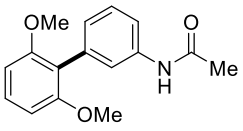

14l, 99%[c,d]

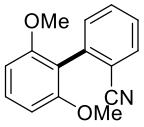

14m, 99%

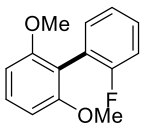

14n, 87% yield

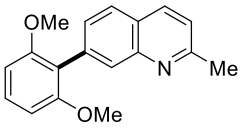

14o, 97 %

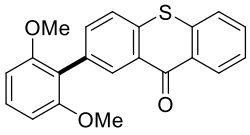

14p, 79 %

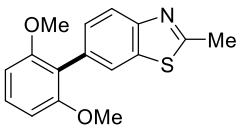

14q, 92 %[b]

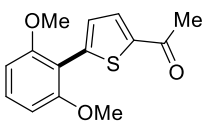

14r, 95 %

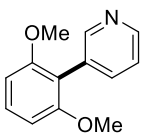

14s, 99 %[b,e]

[a]Reaction condition: potassium 2,6-dimethoxybenzoate or potassium 1-phenyl-1*H*-pyrrole-2-carboxylate (0.30 mmol), aryl/heteroaryl chlorides (0.20 mmol), [Pd(2-butenyl)Cl]$_2$ (2 mol%), **L40** (8 mol%) and dioxane (2.0 mL) were stirred at 100 ºC for 24 h. Yields are those of the isolated products. [b]110 ºC. [c]120 ºC. [d]48 h. [e]Dioxane (1 ml)

and toluene (1 ml) as solvent.

4.2.5 Scope of Aryl or Heteroaryl Carboxylates

The scope of potassium carboxylates that participate in this decarboxylative coupling was also investigated (Table 4.5). Potassium 2,4,6-trimethoxy benzoate was tolerated providing near-quantitative yield (Table 4.5, **14t**). 2-Fluoro-6-(trifluoromethyl)benzoate and 2-fluoro-6-methoxybenzoate were proved to be challenging substrates that needed to be activated at 160 °C.[10c] These substrates can react efficiently with 2-chloronaphthalene providing corresponding products in 97-98% yield only at 100–110 °C with our developed catalytic system (Table 4.5, **14v** and **14w**). Some fluorine-containing benzoates were compatible under mild conditions (Table 4.5, **14u,** and **14x**–**14ab**). The catalytic system also allowed some heterocyclic carboxylic acids to be competent coupling partners (Table 4.5, **14ac** and **14ad**), which previously required a high temperature of 180 °C to activate.[10c]

Table 4.5 Aryl or heteroaryl carboxylates scope for decarboxylative cross-coupling reaction[a]

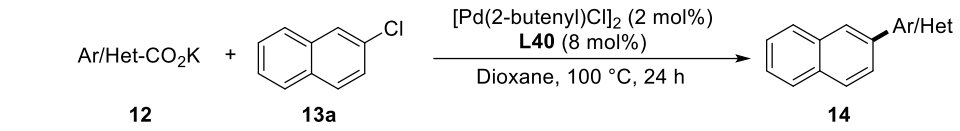

12 **13a** **14**

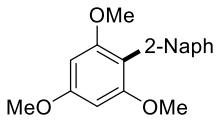

14t, 99%

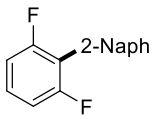

14u, 93%

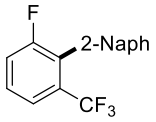

14v, 97%[b]

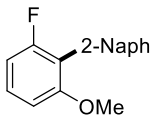

14w, 98%

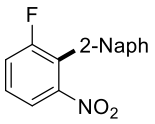

14x, 96%[b]

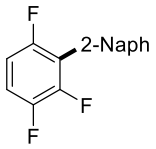

14y, 84%[b,c]

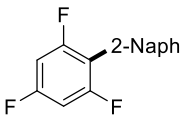

14z, 91%[b]

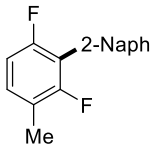

14aa, 97%

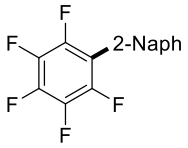

14ab, 90%

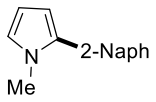

14ac, 54%[b]

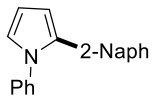

14ad,97%[d]

[a]Reaction condition: Potassium aryl (hetro) carboxylates (0.30 mmol), 2-chloronaphthalene **13a** (0.20 mmol), [Pd(2-butenyl)Cl]$_2$ (2 mol%), **L40** (8 mol%) and dioxane (2.0 mL) were stirred at 100 °C for 24 h. Yields are those of the isolated products. [b]110 °C. [c]Dioxane (1 ml) and Toluene (1 ml). [d]8h.

4.2.6 Late-Stage Functionalization

Inspired by these excellent results, we then focused on the challenging late-stage functionalization of some drugs containing –Cl, which have not been utilized as coupling partners in redox-neutral decarboxylative cross-coupling reactions due to their inert properties and the compatibility in reactions. Fortunately, some drugs that can be used to treat vascular diseases such as Fenofibrate,[16] Clofibrate, and Rivaroxaban, and some insecticide drugs like ChlorFenson or Fenson were competent substrates which can be easily modified to more complex molecular in 84-99% yield only at 100-120 °C (Table 4.6, **14ae**, **14ag**, **14ah**, and **14am**). Loratadine is used to treat Kimura's disease,[17]

Chlorpromazine is used as the psychotropic medicine, and H1 receptor-blocking medication (Azelastine)[18] can react with potassium 1-phenyl-1*H*-pyrrole-2-carboxylate well to afford heterocycle substituted molecular in 90-97% yield at 120 °C (Table 4.6, **14aj**–**14al**). An elevated reaction temperature was required for the smooth transformations of the antifungal drug Grisefulvin and the nonsteroidal anti-inflammatory drug Indomethacin (Table 4.6, **14ai** and **14an**). It is noted that the active hydrogen proton of indomethacin can be preserved well.

Table 4.6 Late-stage functionalization of some drugs containing chloride

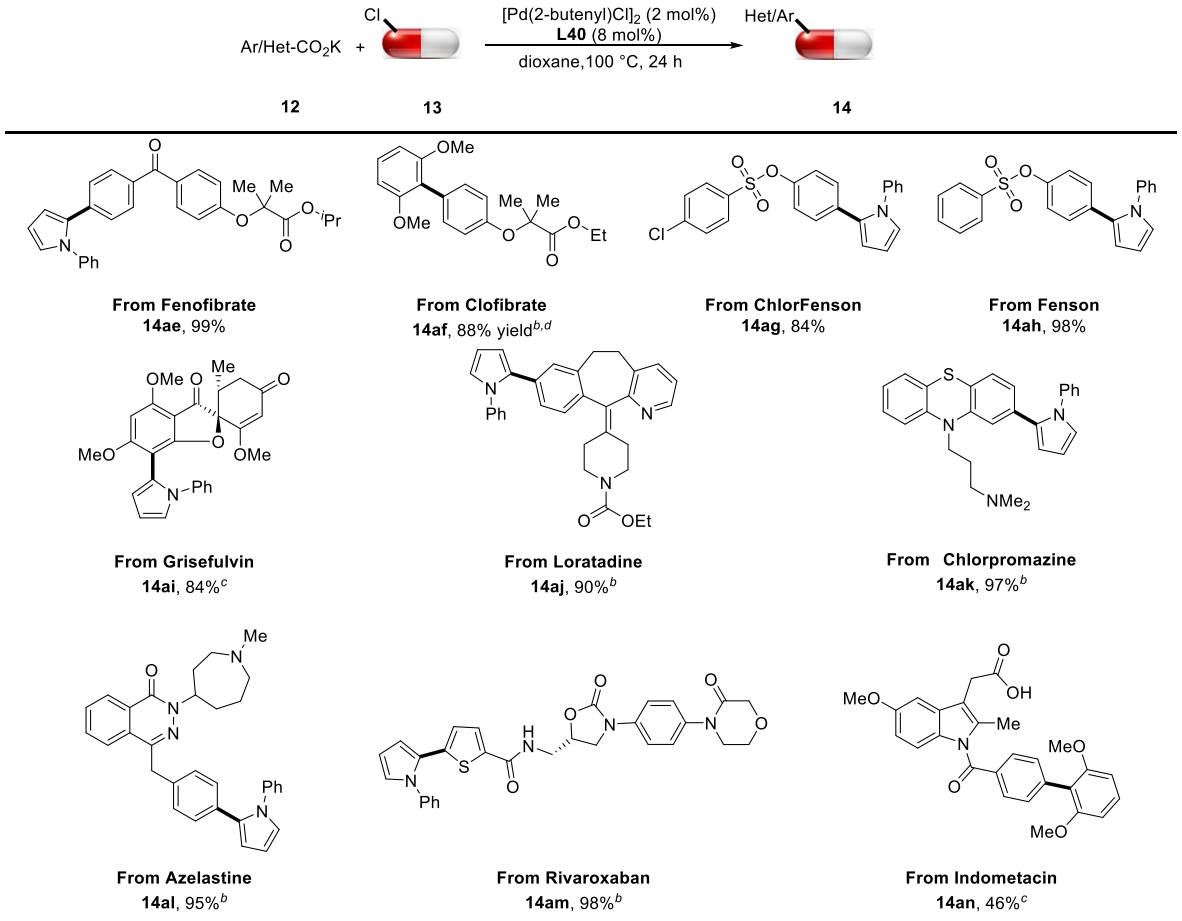

[a]Reaction condition: Potassium 2,6-dimethoxybenzoate or potassium 1-phenyl-1*H*-pyrrole-2-carboxylate (0.30 mmol), aryl/heteroaryl chlorides (0.20 mmol), [Pd(2-butenyl)Cl]$_2$ (2 mol%), **L40** (8 mol%) and dioxane (2.0 mL) were stirred at 100 °C for 24 h. Yields are those of the isolated products. [b]110 °C. [c]140 °C. [d]48 h.

4.2.7 Synthesis of Tetra-*Ortho*-Substituted Biaryls

We then attempted to synthesize synthetically challenging sterically tetra-*ortho*-substituted biaryls scaffolds, which are attractive motifs in pharmaceutical intermediates and biologically active compounds.[19] The methodologies that could obtain tetra-*ortho*-substituted biaryl motifs were only limited to the Suzuki,[20] Negishi[21], and Kumada[22] coupling protocols. Herein, we demonstrated that such attractive bialy motifs could also be obtained via redox-neutral decarboxylative cross-coupling reactions (Table 4.7). Sterically hindered aryl or heterocycles and anthracene chlorides coupled well with 2,6-disubstituted potassium aryl carboxylates and provided reasonable to good yields with enhanced reaction temperatures (Table 4.7, **14ap**–**14as**, **14au** and **14av**, 39%–89%). Polyfluorinated electron-deficient aryl chlorides reacted smoothly and afforded corresponding products in good yields (Table 4.7, **14ao** and **14at**). Noting compounds similar to **14aq** bearing acridine core can be harnessed as photocatalysts to active photoinduced organic transformations,[23] which shows the practicality of the method we developed.

Table 4.7 Synthesis of tetra-*ortho*-substituted biayls via decarboxylative coupling[a]

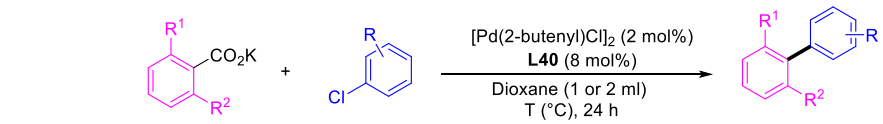

12 13 14

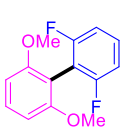

14ao, 69%
140 °C

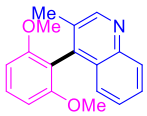

14ap, 39%
140 °C

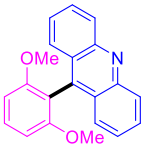

14aq, 57%
140 °C

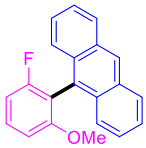

14ar, 83%
140 °C

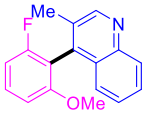

14as, 89%
120 °C

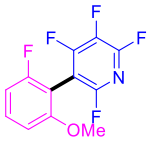

14at, 73%
120 °C

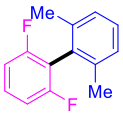

14au, 77%
140 °C

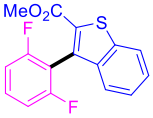

14av, 89%
120 °C

[a]Reaction condition: potassium aryl carboxylates (0.30 mmol), aryl/heteroaryl chlorides (0.20 mmol), [Pd(2-butenyl)Cl]$_2$ (2 mol%), **L40** (8 mol%) and dioxane (1.0 or 2.0 mL) were stirred at 120 °C or 140 °C for 24 h. Yields are those of the isolated products.

4.3 Mechanism Investigations

Motivated by promising results, we embarked on mechanism investigations of the redox-neutral decarboxylative cross-coupling reactions under lower temperatures. Based on the mechanism studies by Liu and Topczewski,[10a, 24] the most probable catalytic cycle involves (i) precatalyst activation; (ii) oxidative addition; (iii) rate-determining decarboxylative step; and (iv) reductive elimination. A Hammett plot, which was commonly used to explore the oxidative addition step in palladium-catalyzed reactions,[25] was generated utilizing the methodology of initial rate (Scheme 4.3-I).[26] Compared to the traditional Hammett series, the Hammett constant-ρ value (0.39) was not large enough to prove that the oxidative addition step might be the rate-determining step. This is aligned with Liu and Topczewski's mechanism results that decarboxylation is rate-determining step rather than oxidative addition. However, the

better linear relationship indicates that the electronic effects on the aryl chlorides have a certain impact on the reaction. That is, electron-rich aryl chlorides react more slowly, whereas electron-deficient substrates react more quickly. This result is also consistent with the observation in substrate scope extension that electron-rich aryl chloride substrates require slightly higher temperatures for activation.

According to the obtained results, oxidative addition appears not to be rate-determining, making decarboxylation the likely rate-determining step. To explore the activation barriers of the reactions, an Eyring plot[27] was constructed by measuring the initial rate at different temperatures with **12a** and **13a** as substrates. Based on the slope and intercept (Scheme 4.3-II), the activation barriers were calculated [$\Delta G_{298.15k}$ = 26.8 kcal/mol, ΔH = 9.0 kcal/mol and ΔS = -58.8 cal/(mol·K)], which were consistent with the reaction temperature requiring to be only 100 ºC. To explain that the Buchwald-type ligands were incapable of catalyzing the decarboxylative reactions efficiently under only 100 ºC, another Eyring plot was formed with the same method (Scheme 4.3-III). Much higher activation barriers ($\Delta G_{298.15k}$ = 36.3 kcal/mol) which was similar to that was calculated by Topczewski elucidated that palladium species featuring Pd···π interaction disfavored to catalyze decarboxylative cross-coupling reaction under lower temperature than that featuring Pd···H–C interaction. We also compared the initial rates of the coupling of 2,6-dimethoxy benzoate with 2-chloronaphthalene catalyzed by the combination of $[Pd(2\text{-butenyl})Cl]_2$ and **L40** to that catalyzed by $[Pd(2\text{-butenyl})Cl]_2$ and SPhos. The plots showed that the initial rate of the reaction catalyzed by the combination of $[Pd(2\text{-butenyl})Cl]_2$ and **L40** ($k = 9.66 \times 10^{-7}$ M·s^{-1}) under 110 ºC is

higher than that by the combination of $[Pd(2\text{-butenyl})Cl]_2$ and SPhos ($k = 2.07 \times 10^{-8}$ $M \cdot s^{-1}$) by approximately a factor of 47.

I. Hammett plot.

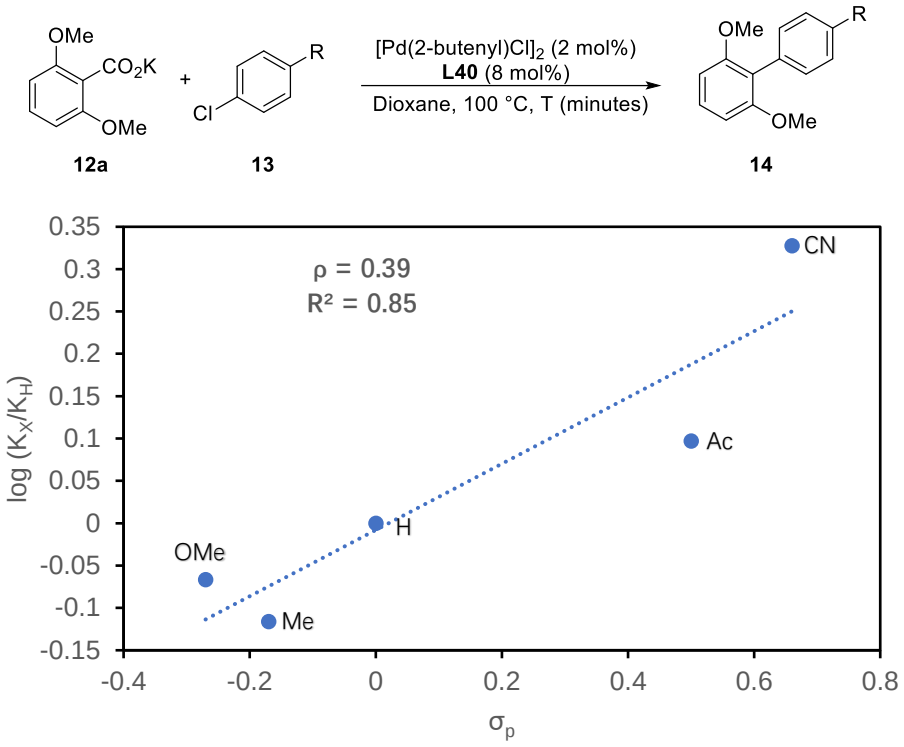

(II) (a) Eyring plot-**L40**

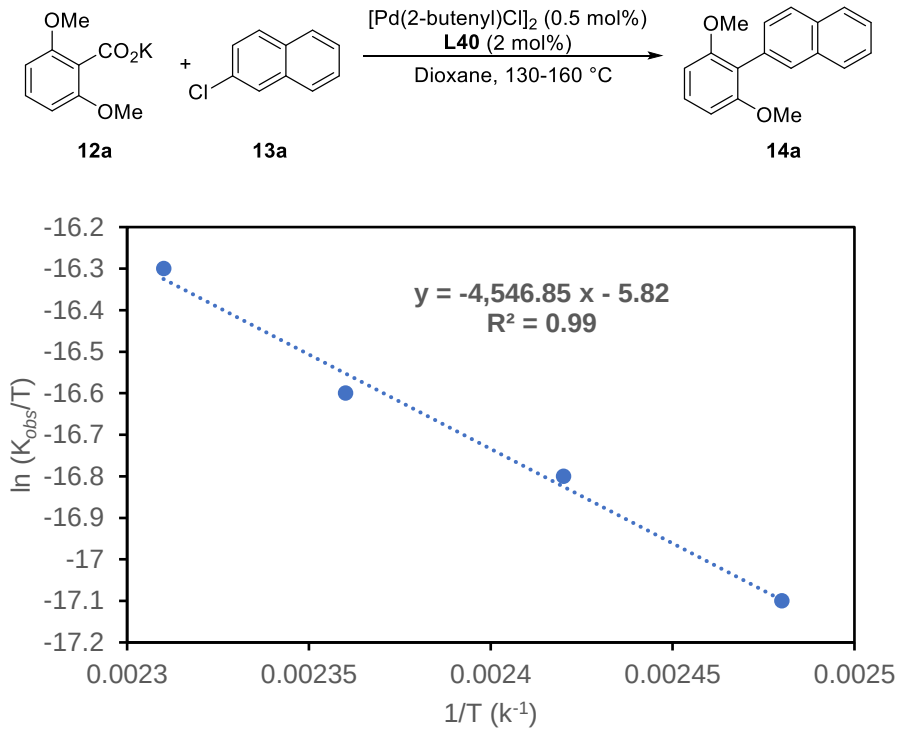

(b) Eyring plot-**SPhos**

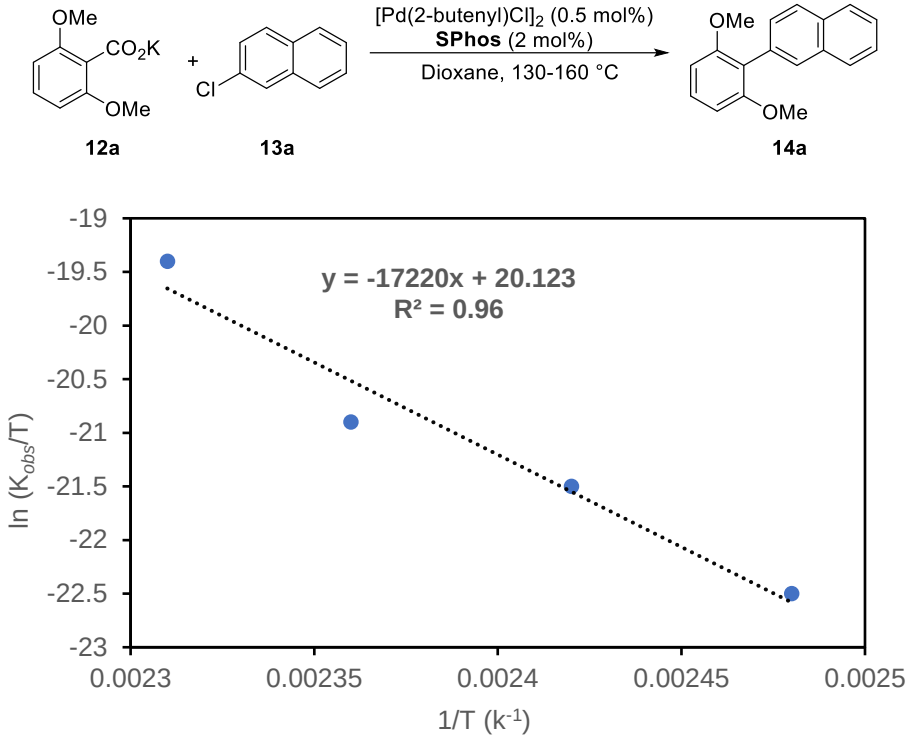

Scheme 4.3 Mechanistic investigations: (I) Hammett plot. Values for k_{obs} were calculated based on the method of initial rates with product [3] measured via calibrated GC-FID. Each point reflects the average of duplicate trials with a given chloroarene. Reactions conducted with potassium 2,6-dimethoxybenzoate **12a** (0.30 mmol), chloroarene (0.20 mmol), in dioxane (0.1 M), with 0.5 mol % $[Pd(2\text{-butenyl})Cl]_2$ and 2 mol% **L40**. (II)-(a) Eyring plot-**L40**. Values for k_{obs} were calculated based on the method of initial rates with [**14a**] measured via calibrated GC-FID. Each point reflects the average of duplicate trials at a given temperature. Reactions conducted with potassium 2,6-dimethoxybenzoate **12a** (0.30 mmol), 2-chloronaphthalene **13a** (0.20 mmol), in dioxane (0.1 M), with 0.5 mol % $[Pd(2\text{-butenyl})Cl]_2$ and 2 mol% **L40**. (II)-(b) Eyring plot-**SPhos**. The manipulates are the same as (II)-(a) except that using **SPhos** as ligand at this stage.

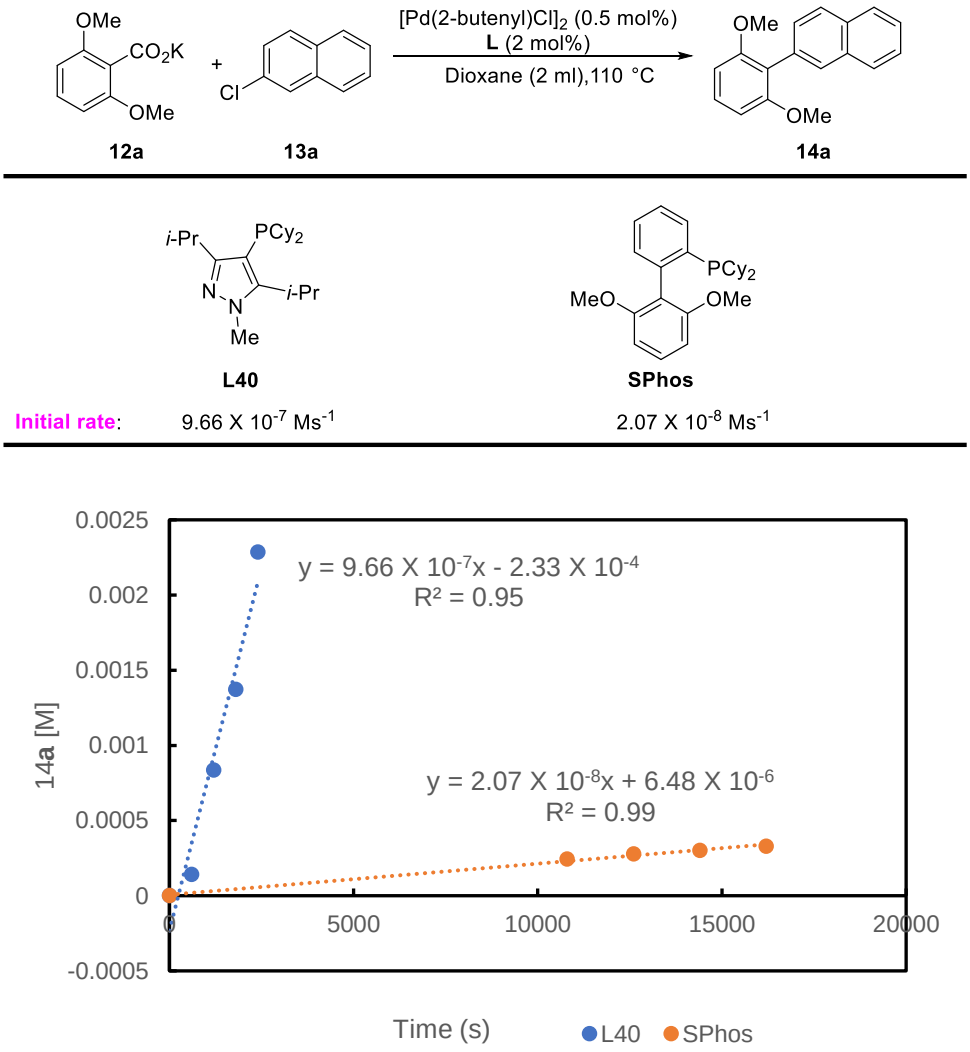

Figure 4.1 Comparison of the kinetic behavior of the pyrazole-phosphine ligand (**L40**) vs. the SPhos in Pd-catalyzed decarboxylative cross-coupling reaction.

4.4 Conclusion

In summary, we developed another alkyl-pyrazole-based phosphine ligand bearing non-cycloalkyl group to fine-tune the angle and distance of Pd···H–C interaction, which might play a key role in controlling the reactivity of the palladium center. The results of Hammett plots indicated that the oxidative addition step is not the rate-determining step of the reaction, while decarboxylation is the likely rate-determining step. However, the electronic properties of the substrates exert a certain influence on

the reaction kinetics, which manifests as electron-rich substrates decreasing the reaction rate, while electron-deficient substrates enhance the rate of the reaction. The comparison of activation energies and initial rates between **L40** and SPhos demonstrated that the palladium center featuring Pd···H–C interaction was the better interaction than that featuring Pd···π interaction for significantly lowering the reaction temperatures of redox-neutral decarboxylative cross-coupling reactions. Utilizing the Pd/**L40** catalytic system, a variety of commercially available aryl chlorides as well as some chloro-containing drugs were successfully coupled with potassium carboxylates under mild conditions to provide the corresponding products, which indicates the importance of this method for the discovery of new drugs. The practicality of the developed methodology was also demonstrated by the synthesis of sterically challenging tetra-*ortho*-substituted biaryl compounds. It is worth to note that the 24 out of 48 compounds synthesized in Tables 4.4 to 4.7 are new compounds. Remarkably, the newly developed method can reduce the activation temperature of previously challenging substrates by about 60–80 ^{o}C, which is a big improvement. We anticipate that such a discovery will further advance the development of methodologies for modulating ligand-metal interactions, to achieve lower reaction temperatures in subsequent investigations.

4.5 Experiment Section

4.5.1 General Consideration

Unless otherwise noted, all reagents were purchased from commercial suppliers

and used without purification. All Pd-catalyzed reactions were performed in a resealable screw cap Schlenk tube (approx. 20 mL volume) in the presence of a Teflon-coated magnetic stirrer bar (5 mm x 10 mm). Dioxane and toluene were freshly distilled from sodium under nitrogen. Tetrahydrofuran (THF) was freshly distilled from sodium benzophenone ketyl under nitrogen. *N*-Methyl-2-pyrrolidone (NMP) and *N*, *N*-Dimethylformamide (DMF) were freshly distilled from anhydrous CaH_2 under nitrogen.[28] K_3PO_4, $K_3PO_4 \cdot H_2O$, $K_3PO_4 \cdot 3H_2O$, K_2CO_3, Cs_2CO_3, and Na_3PO_4 were purchased from Dieckmann and used as received. $Pd(OAc)_2$, $Pd(dba)_2$, Pd_2dba_3, and $[Pd(\pi\text{-cinnamyl})Cl]_2$ were purchased from Strem. $PdCl_2$ and $[Pd(2\text{-butenyl})Cl]_2$ were purchased from Energy. Ligands **L2**, **L5**, **L10**, **L12**, **L17**, **L20**, **L22**, and **L36** were purchased from commercial suppliers. **L32**–**L35** were prepared according to the reported literature.[14] **L25**, **L30**, and **L31** were prepared according to the reported literature.[15] A new bottle of n-butyllithium was used. Thin-layer chromatography was performed on pre-coated silica gel 60 F254 plates. Silica gel (Grace, 60Å, 40-63 μm) was used for column chromatography. Melting points were recorded on an uncorrected Stuart Melting Point SMP30 instrument. NMR spectra were recorded on a Brüker spectrometer (400 MHz for ^1H, 100 MHz for ^{13}C, 376 MHz for ^{19}F and 162 MHz for ^{31}P) and Jeol JMN-ECZ500R/S1 spectrometer (465.89 MHz for ^{19}F and 200.43 MHz for ^{31}P). Spectra were referenced internally to the residual proton resonance in $CDCl_3$ (δ 7.26 ppm) as the internal standard. ^{13}C NMR spectra were referenced to $CDCl_3$ (δ 77.0 ppm, the middle peak). ^{19}F NMR chemical shifts were determined relative to $CFCl_3$ as the external standard and low field is positive. ^{31}P NMR spectra were

referenced to 85% H_3PO_4 externally. Coupling constants (J) were reported in Hertz (Hz). Mass spectra (EI-MS) were recorded on an HP 5977A MSD Mass Spectrometer. High-resolution mass spectra (HRMS) were obtained on the Agilent 6540 ESI-QTof-MS or APPI-QTof-MS and a Waters GCT Premier EI-ToF-MS. GC-MS analysis was conducted on a HP 7890B GC system using a HP5MS column (30 m × 0.25 mm). The products described in GC yield were accorded to the authentic samples/dodecane calibration standard from HP 7890B GC-FID system. All yields reported referring to the isolated yield of compounds estimated to be greater than 95% purity as determined by capillary gas chromatography (GC) or ^{1}H NMR. Compounds described in the literature were characterized by a comparison of their ^{1}H, ^{13}C, ^{19}F and/or ^{31}P NMR spectra to the previously reported data. The procedures in this section are representative, and thus the yields may differ from those reported in tables.

4.5.2 General Procedure for Ligand Screening

2,6-Dimethoxybenzoate **12a** (0.30 mmol, 66.0 mg), 2-chloronaphthalene **13a** (0.20 mmol, 32.4 mg), Pd $(dba)_2$ (0.0080 mmol, 4.60 mg), and ligand (0.0160 mmol) were added to the Schlenk tube that was charged with Teflon-coated magnetic stir bar (5 mm x 10 mm) and equipped with screw cap. The tube was carefully evacuated and flushed with nitrogen (3 cycles). The freshly distilled dioxane (2.0 mL) was added via syringes. The tube was sealed and magnetically stirred at a preheated 100 °C or 110 °C oil bath for 24 h. The reaction was then allowed to reach room temperature. Ethyl acetate (~4 mL), dodecane (45.2 mL, internal standard), and water (~2 mL) were added.

The organic layer was subjected to GC analysis. The GC yield was previously calibrated by an authentic sample/dodecane calibration curve.

4.5.3 General Procedure for Optimization of Reaction Condition

Pd source (0.0080 mmol), **L40** (0.0080-0.032 mmol), potassium 2,6-dimethoxybenzoate **12a** (0.3 mmol, 66.0 mg) and 2-chloronaphthalene **13a** (0.2 mmol, 32.4 mg) were added to the Schlenk tube that was charged with Teflon-coated magnetic stir bar (5 mm x 10 mm) and equipped with screw cap. The tube was carefully evacuated and flushed with nitrogen (3 cycles). The freshly distilled solvent (2.0 mL) was added via syringes. The tube was sealed and magnetically stirred at a preheated 100 ºC oil bath for 24 h. The reaction was then allowed to reach room temperature. Ethyl acetate (~4 mL), dodecane (45.2 μL, internal standard), and water (~2 mL) were added. The organic layer was subjected to GC analysis. The GC yield was previously calibrated by an authentic sample/dodecane calibration curve.

4.5.4 General Procedure for Broaden of Substrate Scope

Potassium aryl benzoate (0.3 mmol), $[Pd(2\text{-butenyl})\ Cl]_2$ (0.0040 mmol, 1.60 mg), **L40** (0.016 mmol, 5.80 mg), and aryl chloride (0.2 mmol) were added to the Schlenk tube that was charged with Teflon-coated magnetic stir bar (5 mm x 10 mm) and equipped with screw cap. The tube was carefully evacuated and flushed with nitrogen (3 cycles). Freshly distillated dioxane (2.0 mL) were added to the tube via syringe. The tube was resealed and magnetically stirred in a preheated 100 ºC oil bath for 24 h. The reaction was allowed to reach room temperature. Ethyl acetate (~4 mL) and water (~2

mL) were added. The organic layer was subjected to GC analysis. The aqueous layer was washed with ethyl acetate. The organic layers were combined and concentrated. The crude products were purified by column chromatography on silica gel (230-400 mesh) to afford the desired product.

4.5.5 Hammett Plot

Data Summary:

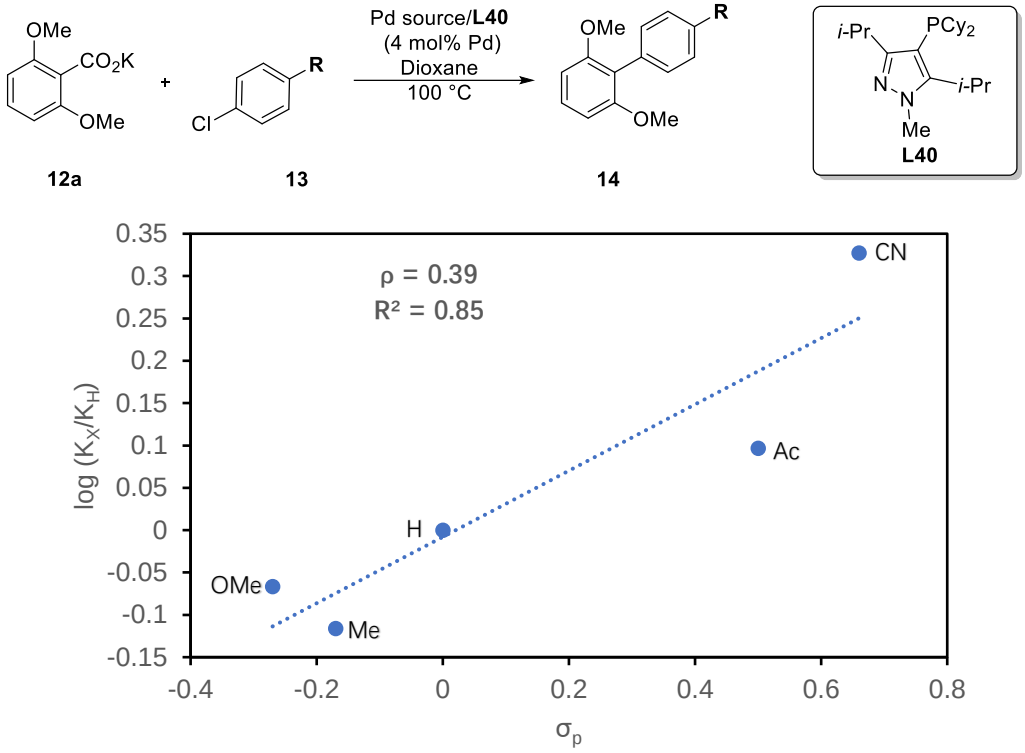

Figure 4.2 Linear fit of initial rate kinetics for conversion of aryl chloride **13** to biaryl **14**

Table 4.8 Summary of results from GC-FID kinetics using Microsoft Excel software to fit initial rate data. Initial [ArCl] = 0.1 M, Initial [**12a**] = 0.15 M, Initial Temperature = 373 K

	Trial
R =	k(M/s) x 10^{-6}

OMe	0.892
Me	0.796
H	1.04
Ac	1.3
CN	2.21

Raw Kinetic Date:

Aryl Chloride (R = CN)

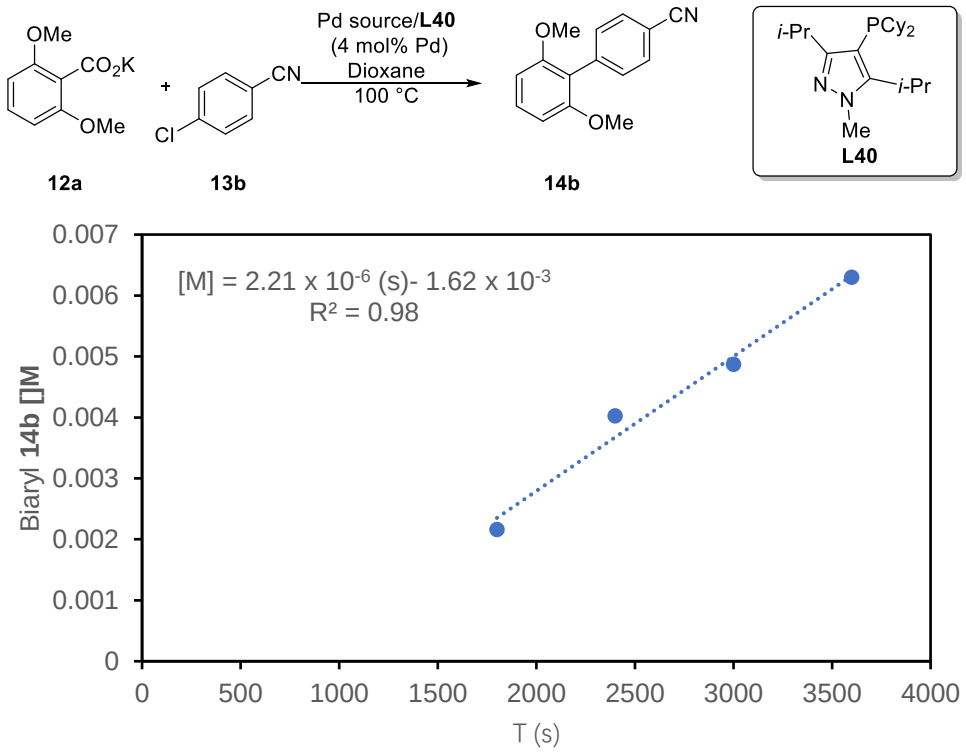

Figure 4.3 Linear fit of initial rate kinetics for conversion of aryl chloride **13b** to biaryl **14b**

Table 4.9 Tabulated molarity data obtained from GC-FID integration for the conversion of aryl chloride **13b** to biaryl **14b**

Time (s)	[Biaryl **14b**] (M)
1800	0.002162
2400	0.004023

3000	0.004869
3600	0.006296

Aryl Chloride (R = Ac)

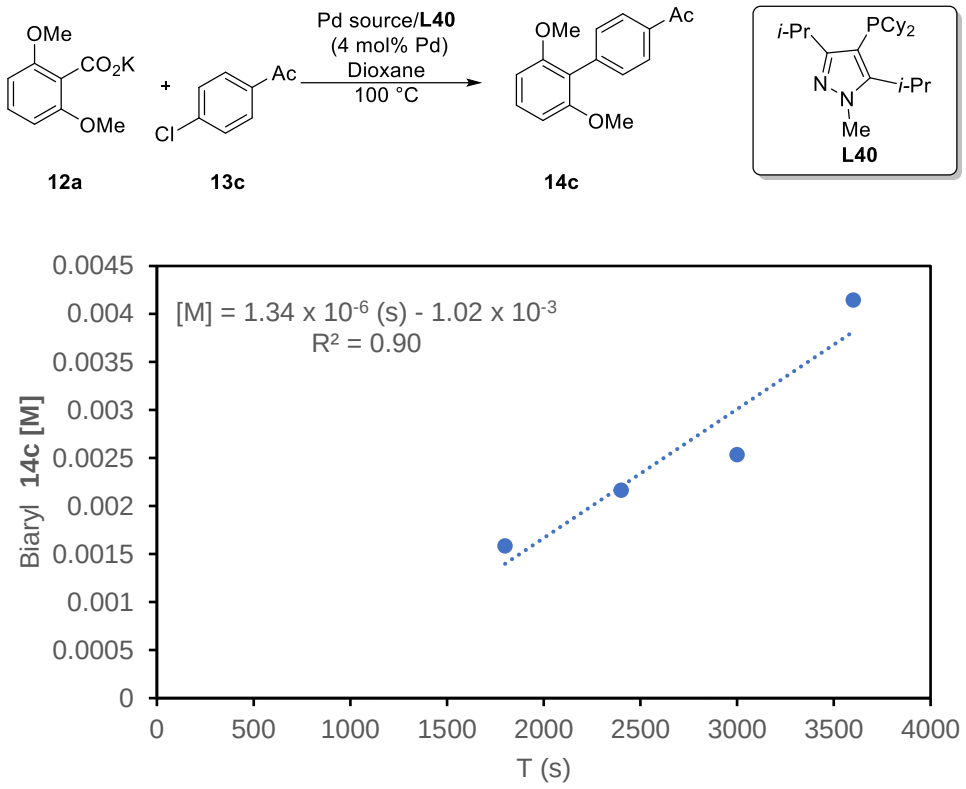

Figure 4.4 Linear fit of initial rate kinetics for conversion of aryl chloride **13c** to biaryl **14c**

Table 4.10 Tabulated molarity data obtained from GC-FID integration for the conversion of aryl chloride **13c** to biaryl **14c**

Time (s)	[Biaryl **14c**] (M)
1800	0.001583
2400	0.002165
3000	0.002546
3600	0.004145

Aryl Chloride (R = H)

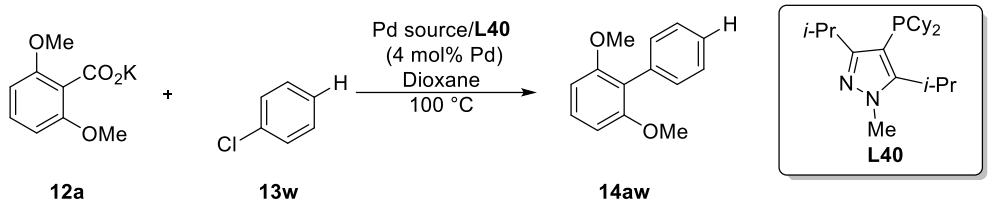

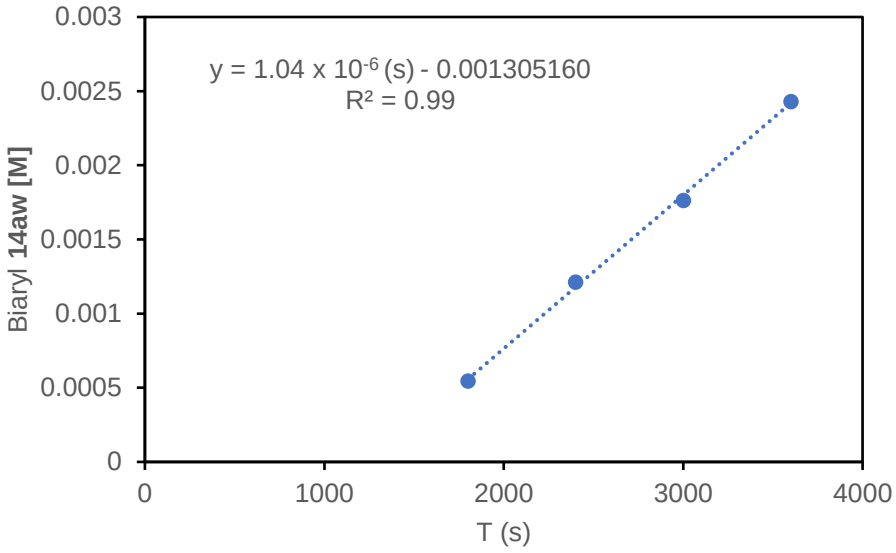

Figure 4.5 Linear fit of initial rate kinetics for conversion of aryl chloride **13w** to biaryl **14aw**

Table 4.11 Tabulated molarity data obtained from GC-FID integration for the conversion of aryl chloride **13w** to biaryl **14aw**

Time (s)	[Biaryl **14aw**] (M)
1800	0.000545
2400	0.001213
3000	0.001764
3600	0.002431

Aryl Chloride (R = Me)

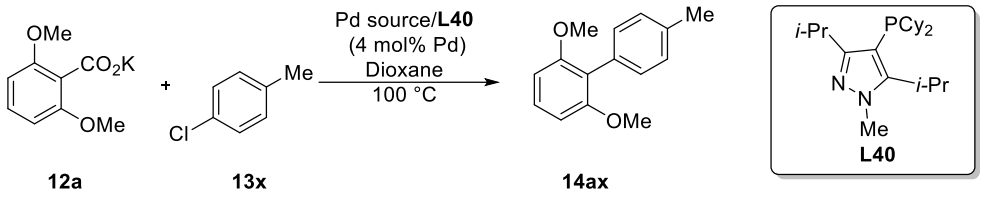

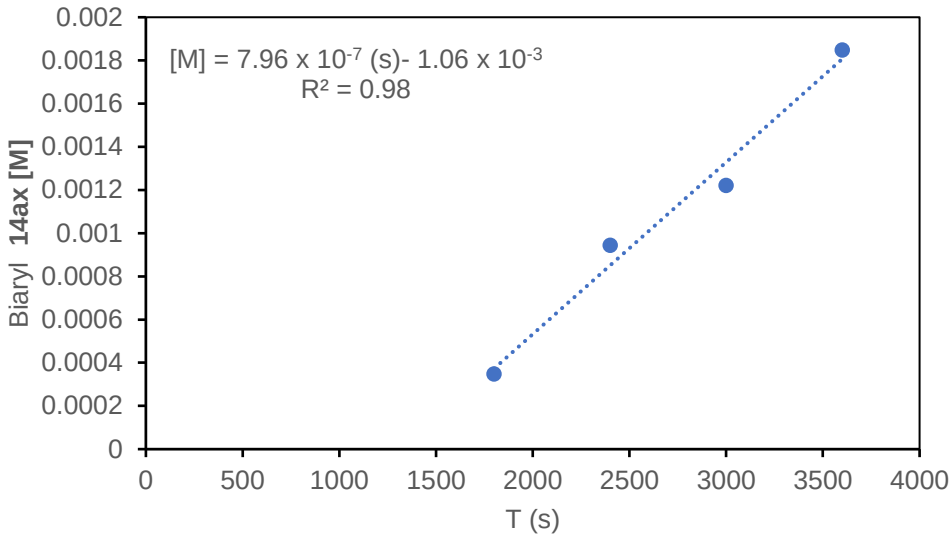

Figure 4.6 Linear fit of initial rate kinetics for conversion of aryl chloride **13x** to biaryl **14ax**

Table 4.12 Tabulated molarity data obtained from GC-FID integration for the conversion of aryl chloride **13x** to biaryl **14ax**

Time (s)	[Biaryl **14ax**] (M)
1800	0.0003472
2400	0.00009440
3000	0.001220
3600	0.001848

Aryl Chloride (R = OMe)

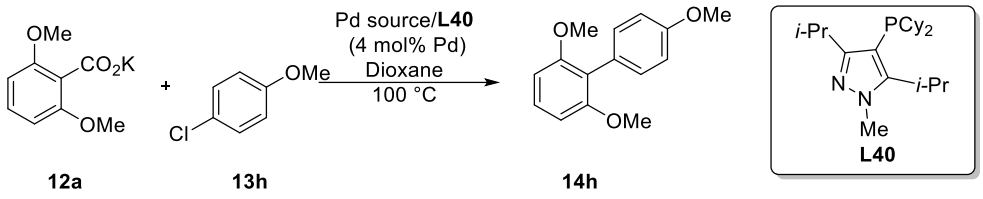

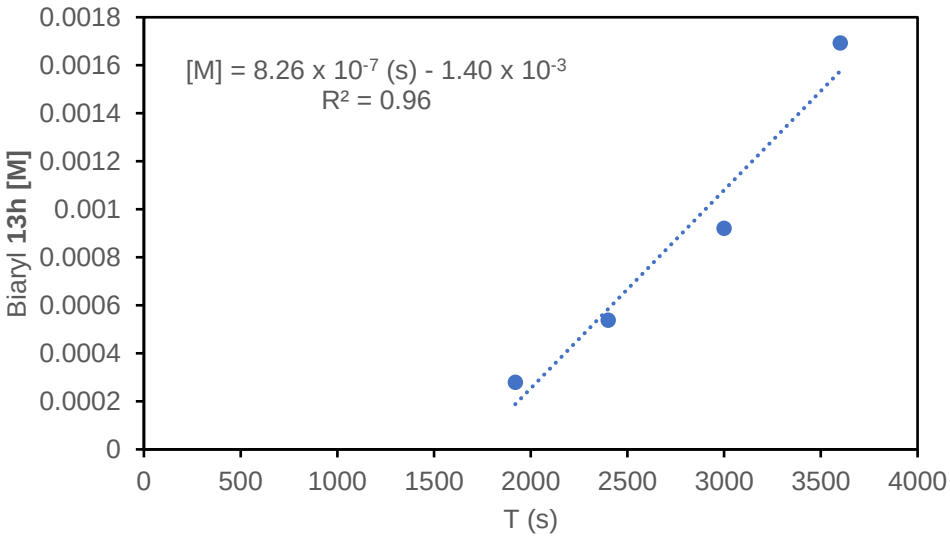

Figure 4.7 Linear fit of initial rate kinetics for conversion of aryl chloride **13h** to biaryl **14h**

Table 4.13 Tabulated molarity data obtained from GC-FID integration for the conversion of aryl chloride **13h** to biaryl **14h**

Time (s)	[Biaryl **14h**] (M)
1800	0.0002789
2400	0.0005370
3000	0.000920
3600	0.001692

4.5.6 Eyring Plot

Data Summary:

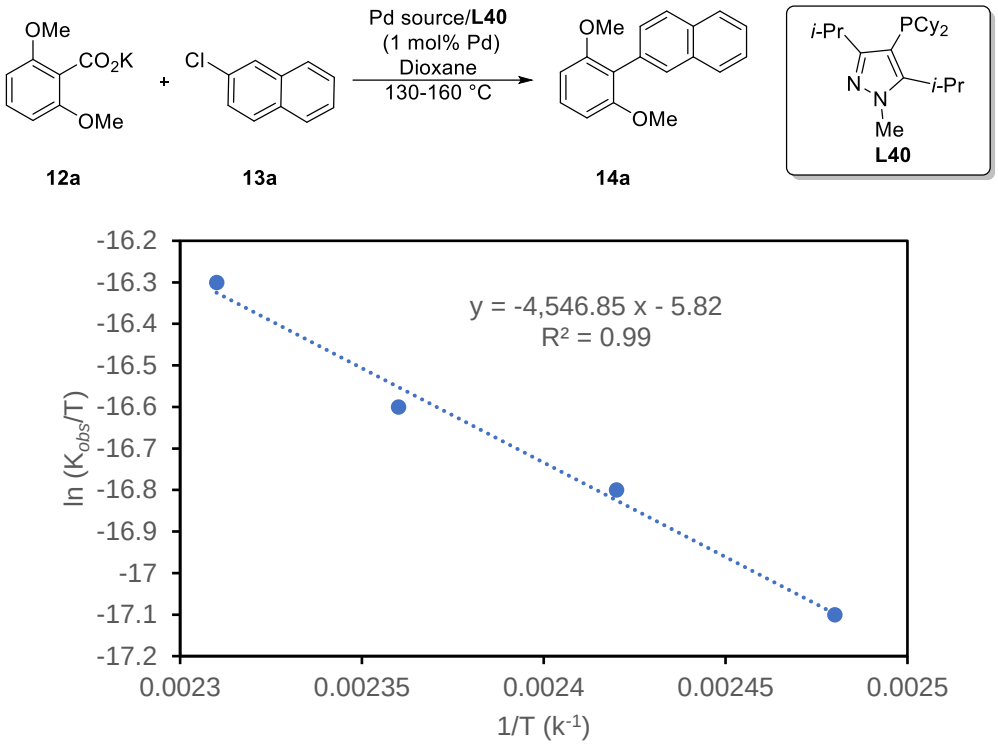

Figure 4.8 Eyring Plot with **L40**

Table 4.14 Summary of results from GC-FID kinetics using Microsoft Excel software to fit initial rate data. Initial [**13a**] = 0.1 M, Initial [**12a**] = 0.15 M, Initial Temperature = 403 K

	Trial	**1/T**	**ln(k_{obs}/T)**
Temp(K)	k(M/s) x 10^{-5}	(K^{-1}) X 10^{-3}	
403	1.51	2.48	-17.1
413	2.04	2.42	-16.8
423	2.56	2.36	-16.6
433	3.76	2.31	-16.3

Raw Kinetic Data:
Temp. = 130 °C (403 K)

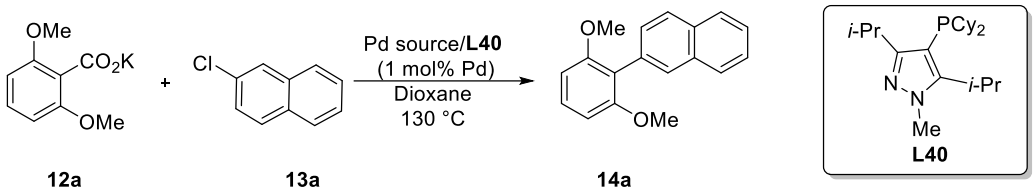

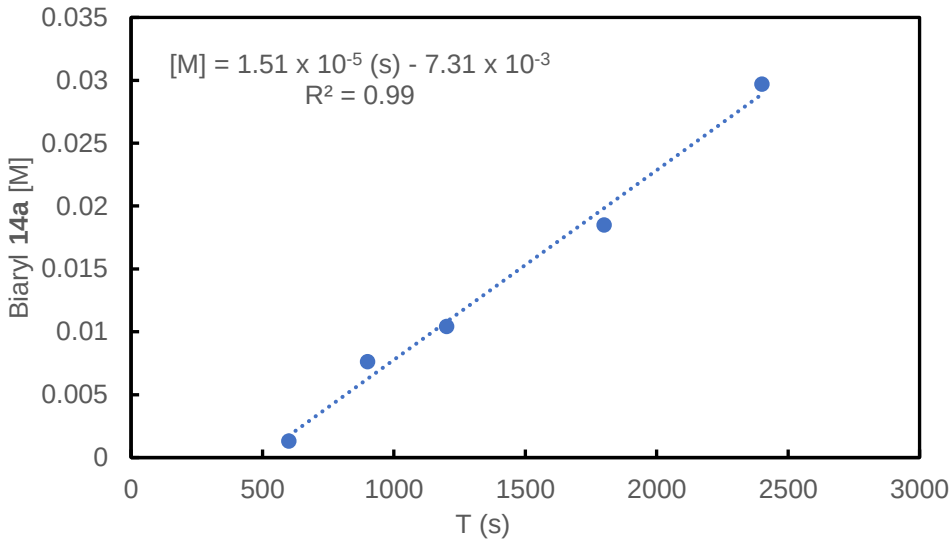

Figure 4.9 Linear fit of initial rate kinetics for conversion of aryl chloride **13a** to biaryl **14a**

Table 4.15 Tabulated molarity data obtained from GC-FID integration for the conversion of aryl chloride **13a** to biaryl **14a**

Time (s)	[Biaryl **14a**] (M)
600	0.001308
900	0.007616
1200	0.01042
1800	0.01849
2400	0.02968

Temp. = 140 °C (413 K)

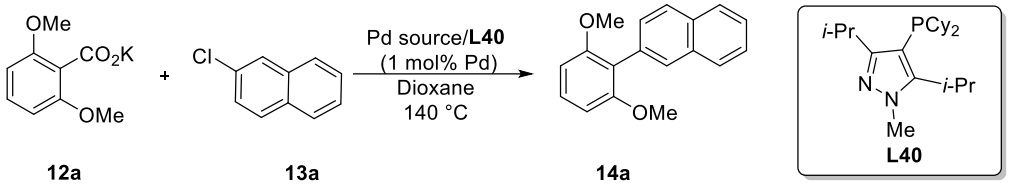

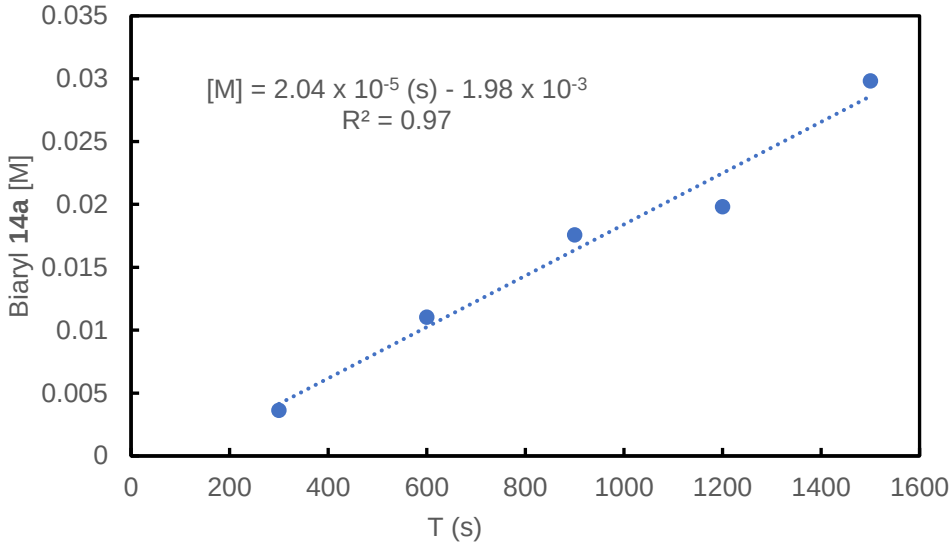

Figure 4.10 Linear fit of initial rate kinetics for conversion of aryl chloride **13a** to biaryl **14a**

Table 4.16 Tabulated molarity data obtained from GC-FID integration for the conversion of aryl chloride **13a** to biaryl **14a**

Time (s)	[Biaryl **14a**] (M)
300	0.003627
600	0.01102
900	0.01757
1200	0.01981
1500	0.02981

Temp. = 150 °C (423 K)

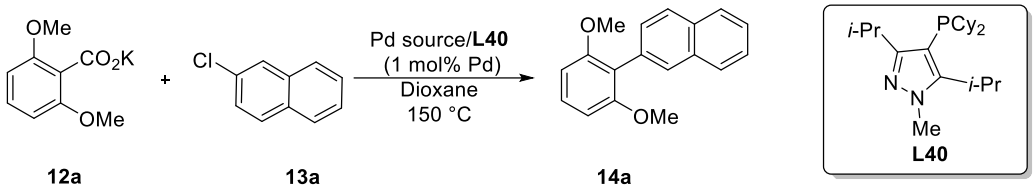

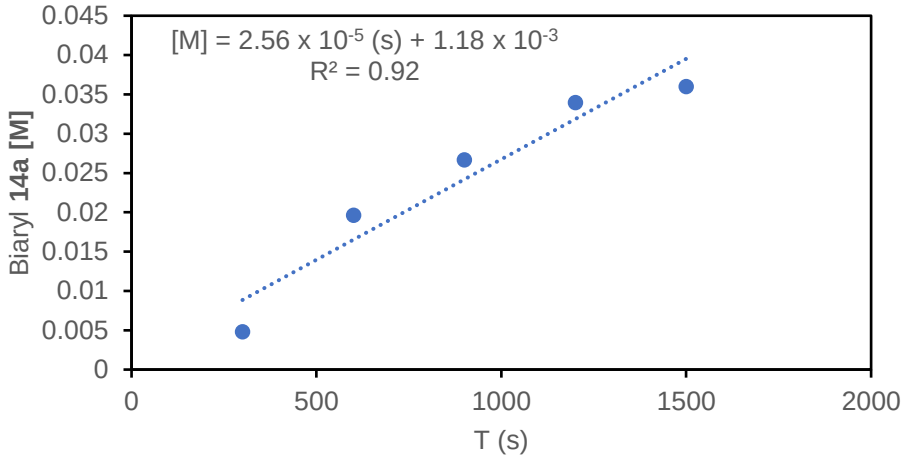

Figure 4.11 Linear fit of initial rate kinetics for conversion of aryl chloride **13a** to biaryl **14a**

Table 4.17 Tabulated molarity data obtained from GC-FID integration for the conversion of aryl chloride **13a** to biaryl **14a**

Time (s)	[Biaryl **14a**] (M)
300	0.004798
600	0.01959
900	0.02665
1200	0.03393
1500	0.03597

Temp. = 160 °C (433 K)

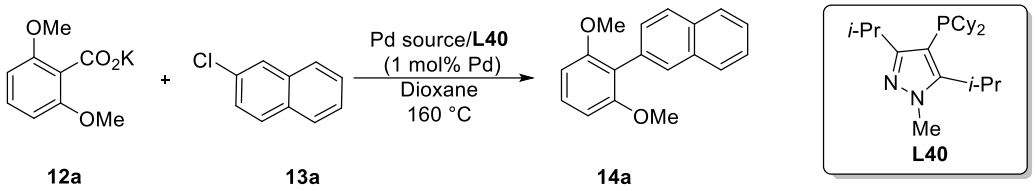

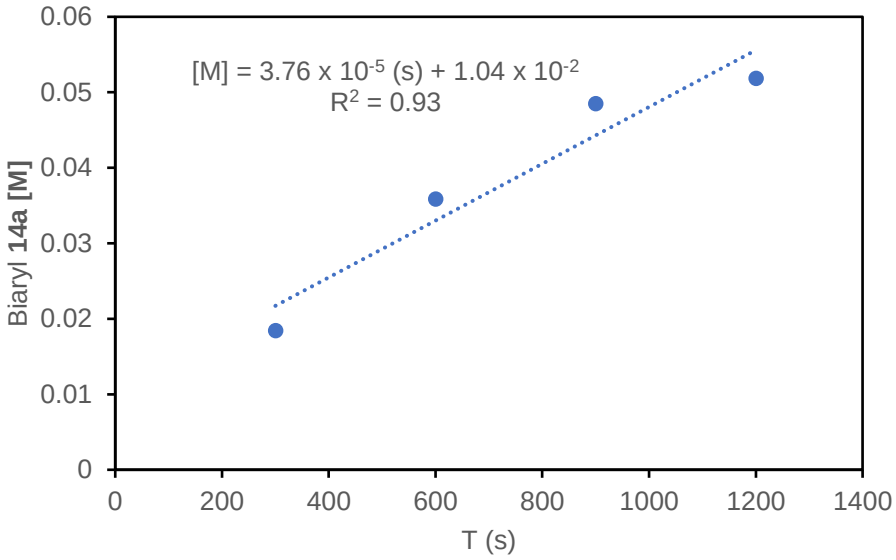

Figure 4.12 Linear fit of initial rate kinetics for conversion of aryl chloride **13a** to biaryl **14a**

Table 4.18 Tabulated molarity data obtained from GC-FID integration for the conversion of aryl chloride **13a** to biaryl **14a**

Time (s)	[Biaryl **14a**] (M)
300	0.01841
600	0.03587
900	0.04847
1200	0.05184

Eyring Plot with SPhos

Data Summary:

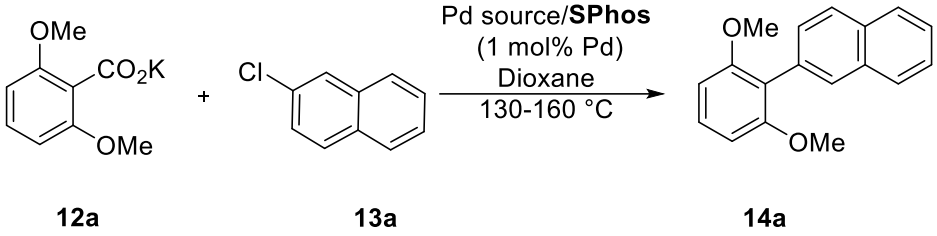

12a **13a** **14a**

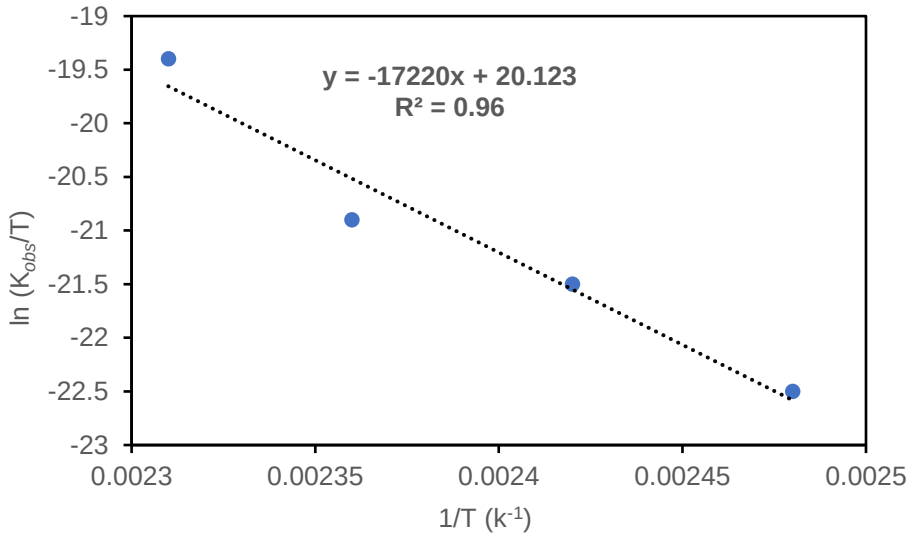

Figure 4.13 Eyring Plot with **SPhos**

Table 4.19 Summary of results from GC-FID kinetics using Microsoft Excel software to fit initial rate data. Initial [**13a**] = 0.1 M, Initial [**12a**] = 0.15 M, Initial Temperature = 403 K

	Trial	**1/T**	**ln(k_{obs}/T)**
Temp(K)	**k(M/s) x 10^{-7}**	**(K^{-1}) X 10^{-3}**	
403	0.71	2.48	-22.5
413	1.89	2.42	-21.5
423	3.58	2.36	-20.9
433	16.9	2.31	-19.4

Temp. = 130 °C (403 K)

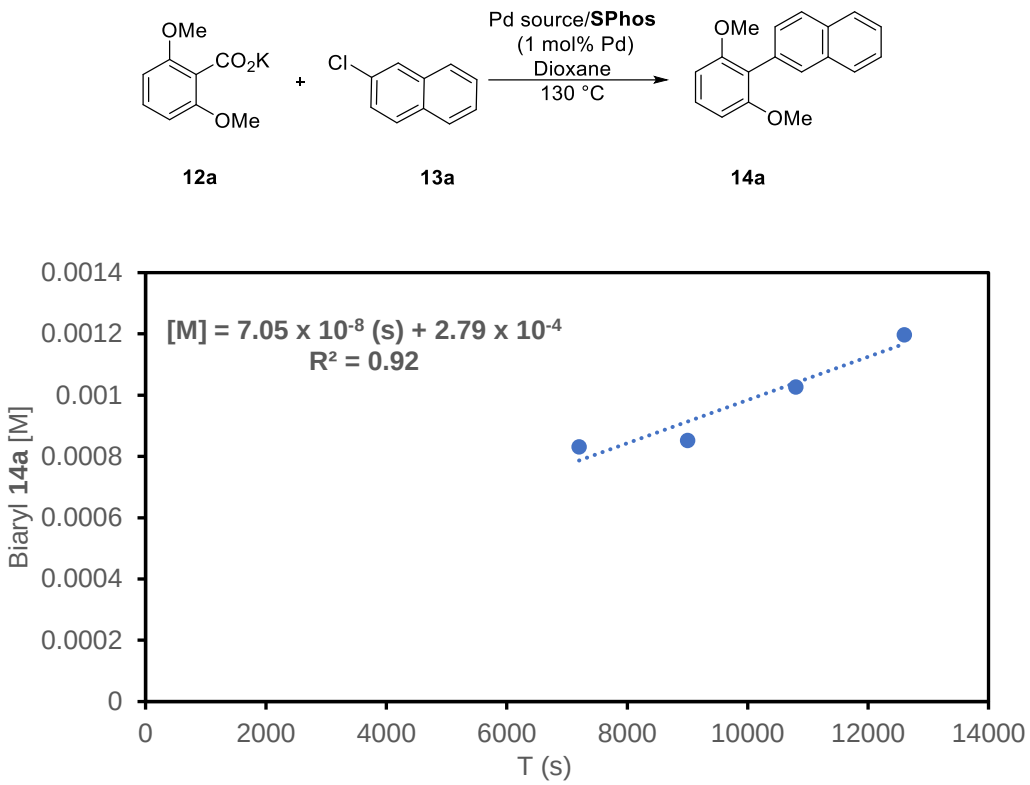

Figure 4.14 Linear fit of initial rate kinetics for conversion of aryl chloride **13a** to biaryl **14a**

Table 4.20 Tabulated molarity data obtained from GC-FID integration for the conversion of aryl chloride **13a** to biaryl **14a**

Time (s)	[Biaryl **14a**] (M)
7200	0.000832
9000	0.000852
10800	0.00103
12600	0.00120

Temp. = 140 °C (413 K)

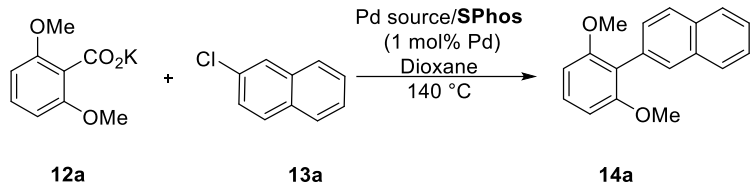

12a **13a** **14a**

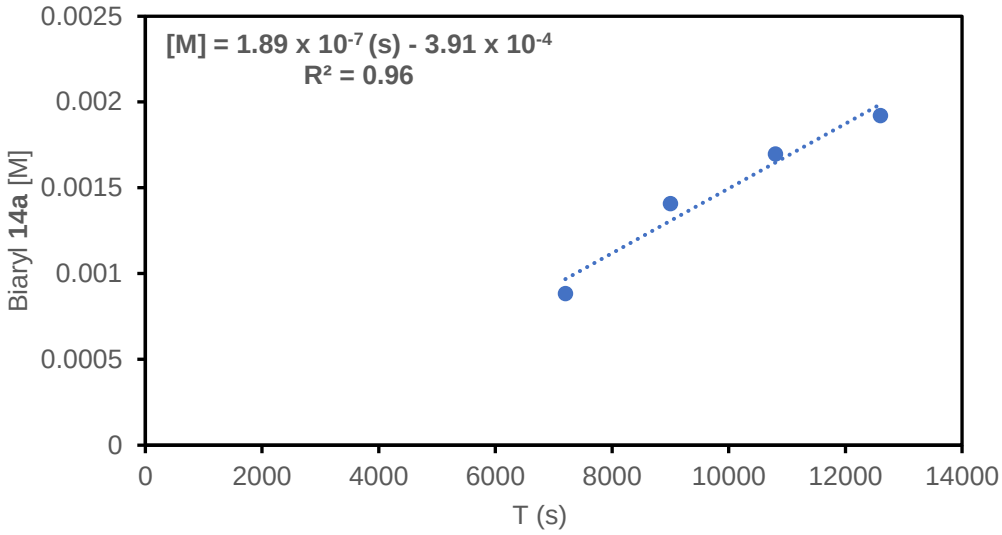

Figure 4.14 Linear fit of initial rate kinetics for conversion of aryl chloride **13a** to biaryl **14a**

Table 4.20 Tabulated molarity data obtained from GC-FID integration for the conversion of aryl chloride **13a** to biaryl **14a**

Time (s)	[Biaryl **14a**] (M)
7200	0.000884
9000	0.00141
10800	0.00170
12600	0.00192

Temp. = 150 °C (423 K)

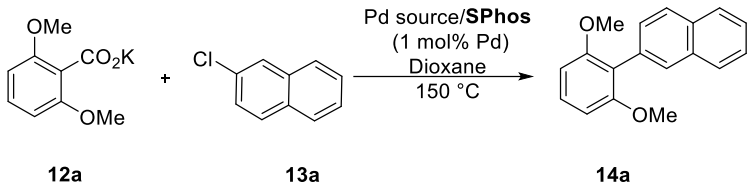

12a **13a** **14a**

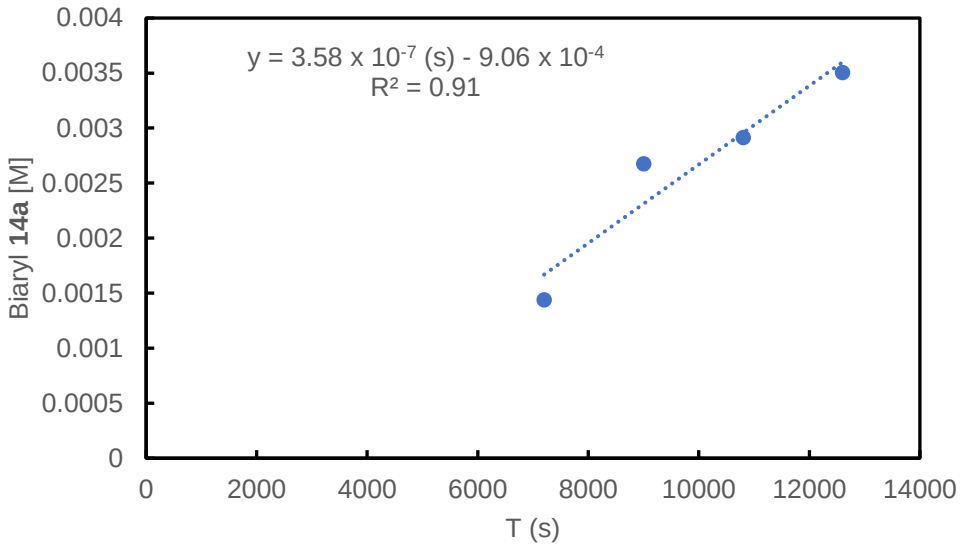

Figure 4.15 Linear fit of initial rate kinetics for conversion of aryl chloride **13a** to biaryl **14a**

Table 4.21 Tabulated molarity data obtained from GC-FID integration for the conversion of aryl chloride **13a** to biaryl **14a**

Time (s)	[Biaryl **14a**] (M)
7200	0.00144
9000	0.002676
10800	0.002913
12600	0.003506

Temp. = 160 °C (433 K)

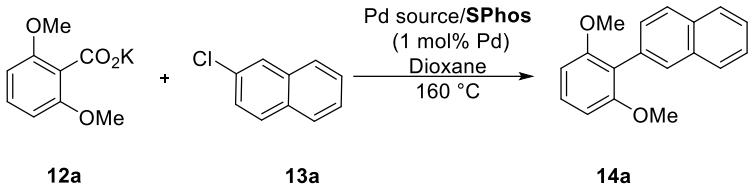

12a **13a** **14a**

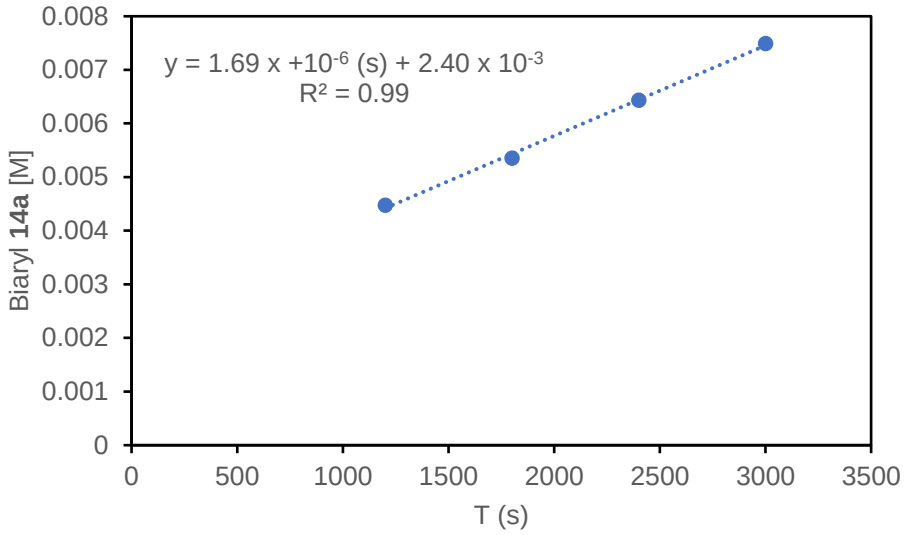

Figure 4.16 Linear fit of initial rate kinetics for conversion of aryl chloride **13a** to biaryl **14a**

Table 4.22 Tabulated molarity data obtained from GC-FID integration for the conversion of aryl chloride **13a** to biaryl **14a**

Time (s)	[Biaryl **14a**] (M)
1200	0.004477
1800	0.005351
2400	0.006432
3000	0.007489

4.5.7 Rate Comparison between L40 and SPhos

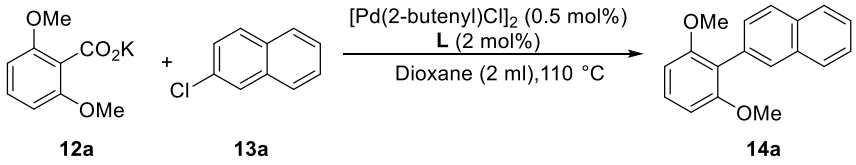

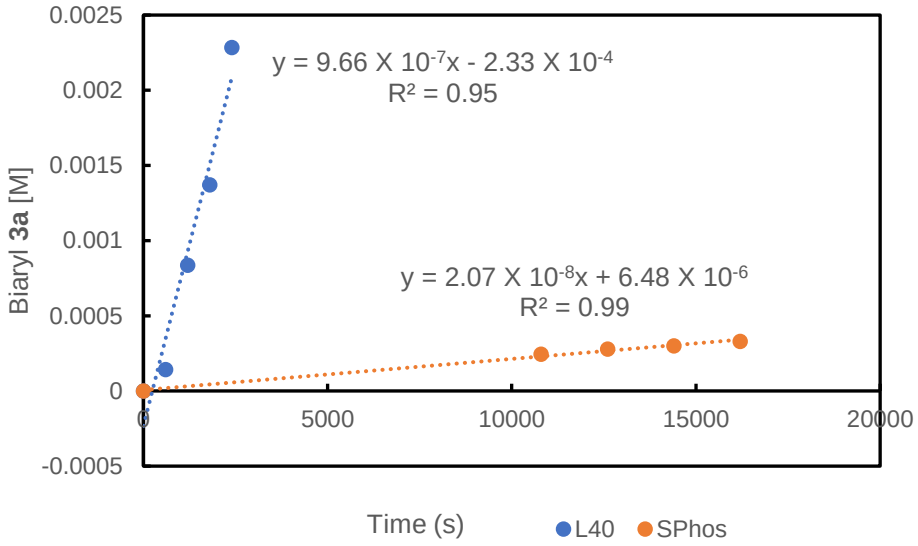

Figure 4.1 Comparison of the kinetic behavior of the pyrazole-phosphine ligand (**L40**) vs. the **SPhos** in Pd-catalyzed decarboxylative cross-coupling reaction

Table 4.23 Tabulated molarity data obtained from GC-FID integration for the conversion of aryl chloride **13a** to biaryl **14a** using **L40** as ligand

Time (s)	[Biaryl **14a**] (M)
0	0
600	0.000141
1200	0.000835
1800	0.001371
2400	0.00228

Table 4.24 Tabulated molarity data obtained from GC-FID integration for the conversion of aryl chloride **13a** to biaryl **14a** using **SPhos** as ligand

Time (s)	[Biaryl **14a**] (M)
0	0
10800	0.000244
12600	0.000277
14400	0.000300
16200	0.000328

4.5.8 Synthesis and Characterization Data

3,5-Diisopropyl-1-methyl-1*H*-pyrazole

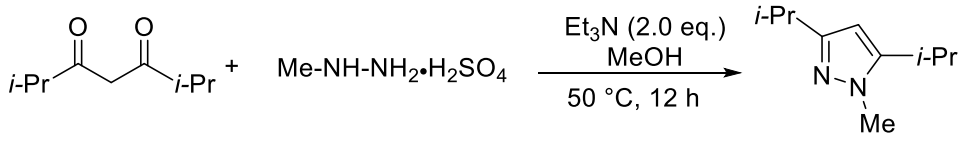

A clear solution of methylhydrazine sulfate (2.0 eq.) and Et_3N (2.0 eq.) in MeOH was added to a solution of 2,6-dimethylheptane-3,5-dione in MeOH. Resulted mixture was heated at 50 ^oC for 12 h. After the completion of the reaction monitored by GC-MS, the reaction mixture was evaporated under reduced pressure to remove MeOH, and then ethyl acetate and water were added, and extracted with ethyl acetate three times. The combined organic layers were washed with brine, dried over Na_2SO_4, and evaporated under reduced pressure. The crude product was purified by column chromatography, with Hexanes: Ethyl acetate = 4:1, to afford the product.

^{1}H NMR (400 MHz, $CDCl_3$) δ 5.82 (s, 1H), 3.74 (s, 3H), 2.95-2.85 (m, 2H), 1.24 (d, *J* = 2.0 Hz, 6H), 1.23 (d, *J* = 2.0 Hz, 6H); **^{13}C NMR** (150 MHz, $CDCl_3$) δ 157.7, 149.5,

98.1, 35.6, 27.8, 25.4, 22.9, 22.5. ^{1}H was in agreement with the literature.[29]

4-Bromo-3,5-diisopropyl-1-methyl-1*H*-pyrazole

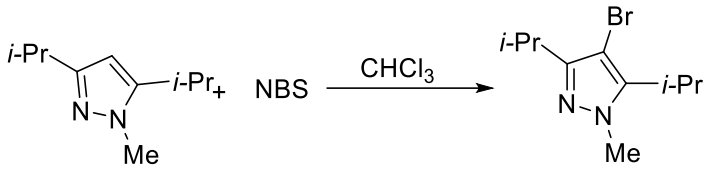

N-Bromosuccinimide (1.90 g, 10.7 mmol) was added to a solution of 3,5-diisopropyl-1-methyl-1*H*-pyrazole (1.69 g, 10.2 mmol) in anhydrous chloroform (30 mL) in portion at room temperature. After stirring for 60 min, solvent was removed by vacuum. DCM and water were added to the mixture and the organic phase was separated. The organic layer was washed with water for several times. The combined organic layer was then concentrated and yield 4-bromo-3,5-diisopropyl-1-methyl-1*H*-pyrazole as yellow liquid product.

Yield: 96% (2.38 g). **^{1}H NMR** (400 MHz, $CDCl_3$) δ 3.80 (s, 3H), 3.16 (hept, J = 7.1 Hz, 1H), 2.98 (hept, J = 7.1 Hz, 1H), 1.36 (s, 3H), 1.34 (s, 3H), 1.27 (s, 3H), 1.25 (s, 3H); **^{13}C NMR** (100 MHz, $CDCl_3$) δ 154.4, 144,5, 90.3, 37.7, 26.6, 25.9, 21.5, 20.1; **HRMS** (ESI): calcd. for $C_{10}H_{18}BrN_2^+$: 245.0648, found 245.0654.

4-(Dicyclohexylphosphaneyl)-3,5-diisopropyl-1-methyl-1*H*-pyrazole (L40)

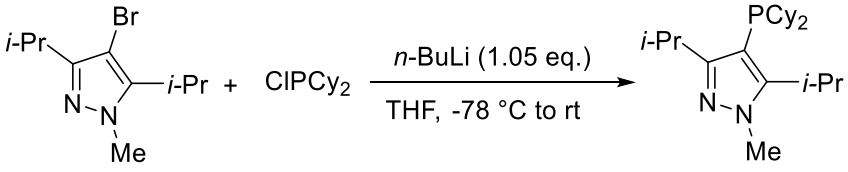

4-Bromo-3,5-diisopropyl-1-methyl-1*H*-pyrazole (0.98 g, 4.0 mmol) was dissolved in freshly distilled THF (20 mL) at room temperature under nitrogen atmosphere. The

solution was cooled to -78 °C in a dry ice/acetone bath. Titrated *n*-BuLi (4.20 mmol) was added dropwise with a syringe. After the reaction mixture was stirred for 35 min at -78 °C, chlorodicyclohexylphosphine (1.0 mL, 4.50 mmol) was added. The reaction was allowed to warm to room temperature and stirred for 65 min. The solvent was removed under reduced pressure. After the solvent was removed under vacuum, the solid product was washed with 90% methanol/water mixture (10 mL x3). The white solid was collected by filtration and dried over vacuum to afford 4-(dicyclohexylphosphaneyl)-3,5-diisopropyl-1-methyl-1*H*-pyrazole.

Yield: 57% (0.82 g). White solid, m.p. = 132.6–134.3 °C. **^{1}H NMR** (600 MHz, C_6D_6) δ 3.81 (s, 3H), 3.68-3.60 (m, 1H), 3.00-2.93 (m, 1H), 2.00-1.96 (m, 2H), 1.92-1.89 (m, 2H), 1.76-1.73 (m, 2H), 1.65-1.61 (m, 4H), 1.45-1.42 (m, 2H), 1.28-1.15 (m, 20H), 0.94-0.88 (m, 2H); **^{13}C NMR** (150 MHz, $CDCl_3$) δ 160.0-159.9 (m, 1C), 154.2 (d, J = 35.3 Hz, 1C), 104.4 (d, J = 11.9 Hz, 1C), 37.9, 35.0, 32.8 (d, J = 21.6 Hz, 1C), 30.8 (d, J = 9.2 Hz, 1C), 27.8, 27.0 (d, J = 32.9 Hz, 1C), 25.3-25.2 (m, 1C), 23.3, 21.2; **^{31}P NMR** (200 MHz, C_6D_6) δ -26.8; **HRMS** (ESI): calcd. for $C_{22}H_{40}N_2P^+$: 363.2924, found 363.2928.

2-(2,6-Dimethoxyphenyl) naphthalene (Table 4.4, compound 14a)[30]

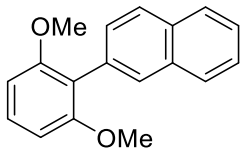

Yield: 98% (51.8 mg). White solid. Eluents (R_f = 0.5, Hexane: Ethyl acetate = 20:1) was used for flash column chromatography; **^{1}H NMR** (400 MHz, $CDCl_3$) δ 7.98-7.89

(m, 4H), 7.59-7.52 (m, 3H), 7.39 (t, *J* = 8.4 Hz, 1H), 6.76 (d, *J* = 8.4 Hz, 2H), 3.80 (s, 6H); **^{13}C NMR** (100 MHz, $CDCl_3$) δ 157.8, 133.3, 132.4, 131.7, 129.7, 129.3, 128.8, 128.1, 127.6, 126.8, 125.51, 125.49, 119.4, 104.2, 55.9; **HRMS** (EI): calcd for $C_{18}H_{16}O_2^+$: 264.1145, found 264.1150.

2',6'-Dimethoxy-[1,1'-biphenyl]-4-carbonitrile (Table 4.4, compound 14b)[31]

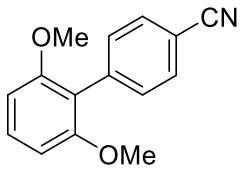

Yield: 99% (47.5 mg). Light-yellow solid. Eluents (R_f = 0.2, Hexane: Ethyl acetate = 20:1) was used for flash column chromatography. **^{1}H NMR** (400 MHz, $CDCl_3$) δ 7.68 (d, *J* = 7.7 Hz, 2H), 7.49 (d, *J* = 7.7 Hz, 2H), 7.35 (t, *J* = 8.2 Hz, 1H), 6.69 (d, *J* = 8.3 Hz, 2H), 3.76 (s, 6H). **^{13}C NMR** (100 MHz, $CDCl_3$) δ 157.2, 139.5, 131.8, 131.2, 129.7, 119.3, 117.3, 110.1, 104.0, 55.7; **HRMS** (EI): calcd for $C_{15}H_{13}NO_2^+$: 239.0941, found 239.0942.

1-(2',6'-Dimethoxy-[1,1'-biphenyl]-4-yl) ethan-1-one (Table 4.4, compound 14c)[32]

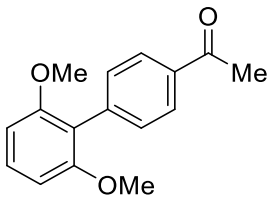

Yield: 93% (50.3 mg). White solid. Eluents (R_f = 0.2, Hexane: Ethyl acetate: DCM = 10:1:1) was used for flash column chromatography. **^{1}H NMR** (400 MHz, $CDCl_3$) δ 8.02 (d, *J* = 8.3 Hz, 2H), 7.49 (d, *J* = 8.3 Hz, 2H), 7.33 (t, *J* = 8.4 Hz, 1H), 6.68 (d, *J* = 8.4 Hz, 2H), 3.75 (s, 6H), 2.64 (s, 3H); **^{13}C NMR** (100 MHz, $CDCl_3$) δ 197.9, 157.3, 139.6,

135.3, 131.2, 129.3, 127.6, 118.1, 104.0, 55.8, 26.5; **HRMS** (ESI): calcd for $C_{16}H_{17}O_3^+$: 257.1172, found 257.1173.

2,6-Dimethoxy-4'-(trifluoromethyl)-1,1'-biphenyl (Table 4.4, compound 14d)[32]

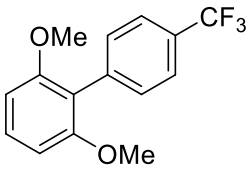

Yield: 96% (54.3 mg). White solid, m.p.= 75.6–78.6 °C. Eluents (R_f = 0.2, Hexane: Ethyl acetate = 20:1) was used for flash column chromatography. **^{1}H NMR** (400 MHz, $CDCl_3$) δ 7.65 (d, *J* = 8.1 Hz, 2H), 7.47 (d, *J* = 8.0 Hz, 2H), 7.32 (t, *J* = 8.4 Hz, 1H), 6.67 (d, *J* = 8.4 Hz, 2H), 3.75 (s, 6H); **^{13}C NMR** (100 MHz, $CDCl_3$) δ 157.5, 138.1, 131.4, 129.4, 128.6 (q, *J* = 31.3 Hz), 124.52 (q, *J* = 3.7 Hz), 124.45 (q, *J* = 270.4 Hz), 118.0, 104.1, 55.8; **^{19}F NMR** (565 MHz, $CDCl_3$) δ -62.3; **HRMS** (EI): calcd for $C_{15}H_{13}F_3NO_2^+$: 282.0862, found 282.0868.

2,6-Dimethoxy-4'-nitro-1,1'-biphenyl (Table 4.4, compound 14e)[33]

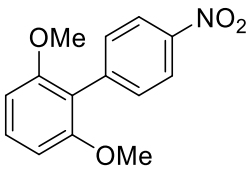

Yield: 95% (49.4 mg). Light-yellow liquid. Eluents (R_f = 0.6, Hexane: Ethyl acetate = 5:1) was used for flash column chromatography. **^{1}H NMR** (400 MHz, $CDCl_3$) δ 8.26 (d, *J* = 8.7 Hz, 2H), 7.55 (d, *J* = 8.7 Hz, 2H), 7.36 (t, *J* = 8.4 Hz, 1H), 6.70 (d, *J* = 8.4 Hz, 2H), 3.77 (s, 6H); **^{13}C NMR** (100 MHz, $CDCl_3$) δ 157.2, 146.4, 141.7, 132.0, 130.0, 122.7, 117.0, 104.1, 55.8; **HRMS** (EI): calcd for $C_{14}H_{13}NO_4^+$: 259.0839, found

259.0849.

Methyl 2',6'-dimethoxy-[1,1'-biphenyl]-4-carboxylate (Table 4.4, compound 14f)[32]

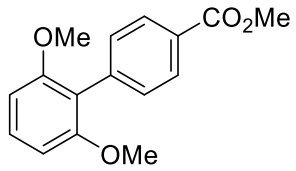

Yield: 89% (48.3 mg). Light-yellow solid. Eluents (R_f = 0.2, Hexane: Ethyl acetate = 20:1) was used for flash column chromatography. **^{1}H NMR** (400 MHz, $CDCl_3$) δ 8.12-8.07 (m, 2H), 7.48-7.44 (m, 2H), 7.32 (t, *J* = 8.4 Hz, 1H), 6.68 (d, *J* = 8.4 Hz, 2H), 3.94 (s, 3H), 3.74 (s, 6H); **^{13}C NMR** (100 MHz, $CDCl_3$) δ 167.2, 157.4, 139.4, 131.0, 129.2, 128.9, 128.3, 118.3, 104.1, 55.8, 51.9; **HRMS** (EI): calcd for $C_{16}H_{16}O_4^+$: 272.1043, found 272.1048.

2',6'-Dimethoxy-[1,1'-biphenyl]-4-carbaldehyde (Table 4.4, compound 14g)[32]

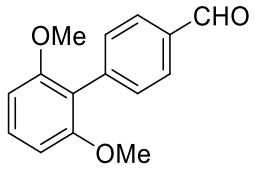

Yield: 99% (47.8 mg). Light-yellow liquid. Eluents (R_f = 0.5, Hexane: Ethyl acetate = 5:1) was used for flash column chromatography. **^{1}H NMR** (400 MHz, $CDCl_3$) δ 10.05 (s, 1H), 7.93 (d, *J* = 8.1 Hz, 2H), 7.55 (d, *J* = 8.1 Hz, 2H), 7.34 (t, *J* = 8.4 Hz, 1H), 6.69 (d, *J* = 8.4 Hz, 2H), 3.75 (s, 6H); **^{13}C NMR** (100 MHz, $CDCl_3$) δ 192.2, 157.3, 141.2, 134.7, 131.7, 129.5, 129.0, 118.0, 104.1, 55.8; **HRMS** (ESI): calcd for $C_{15}H_{15}O_3^+$: 243.1016, found 243.1017.

2,4',6-Trimethoxy-1,1'-biphenyl (Table 4.4, compound 14h)[34]

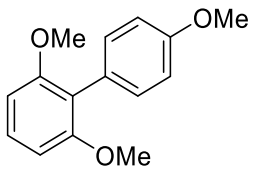

Yield: 85% (41.4 mg). White solid. Eluents (R_f = 0.6, Hexane: Ethyl acetate: DCM = 10:1:1) was used for flash column chromatography. **^{1}H NMR** (400 MHz, $CDCl_3$) δ 7.29 (dd, *J* = 16.2, 8.3 Hz, 3H), 6.98 (d, *J* = 8.6 Hz, 2H), 6.67 (d, *J* = 8.4 Hz, 2H), 3.86 (s, 3H), 3.76 (s, 6H); **^{13}C NMR** (100 MHz, $CDCl_3$) δ 158.2, 157.7, 131.9, 128.3, 126.0, 119.0, 113.2, 104.1, 55.8, 55.0; **HRMS** (ESI): calcd for $C_{15}H_{17}O_3^+$: 245.1172, found 245.1170.

2,3',6-Trimethoxy-1,1'-biphenyl (Table 4.4, compound 14i)[35]

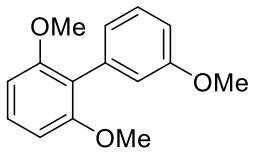

Yield: 93% (45.4 mg). Light-yellow liquid. Eluents (R_f = 0.8, Hexane: Ethyl acetate: DCM = 10:1:1) was used for flash column chromatography. **^{1}H NMR** (400 MHz, $CDCl_3$) δ 7.40-7.31 (m, 2H), 7.01-6.92 (m, 3H), 6.70 (dd, *J* = 8.5, 2.3 Hz, 2H), 3.86 (s, 3H), 3.78 (s, 6H); **^{13}C NMR** (100 MHz, $CDCl_3$) δ 158.9, 157.6, 135.4, 128.6, 128.5, 123.3, 119.3, 116.6, 112.2, 104.1, 55.8, 55.0; **HRMS** (EI): calcd for $C_{15}H_{16}O_3^+$: 244.1094, found 244.1096.

2,6-Dimethoxy-3'-methyl-1,1'-biphenyl (Table 4.4, compound 14j)[36]

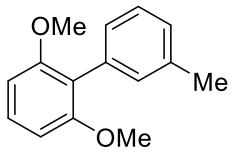

Yield: 87% (39.8 mg). Light-yellow liquid. Eluents (R_f = 0.7, Hexane: Ethyl acetate: DCM = 10:1:1) was used for flash column chromatography. **^{1}H NMR** (400 MHz, $CDCl_3$) δ 7.41-7.31 (m, 2H), 7.24-7.18 (m, 3H), 6.72 (d, *J* = 8.4 Hz, 2H), 3.79 (s, 6H), 2.46 (s, 3H); **^{13}C NMR** (100 MHz, $CDCl_3$) δ 157.6, 137.0, 133.9, 131.5, 128.5, 127.8, 127.6, 127.5, 119.6, 104.1, 55.8, 21.5.

1-(2',6'-Dimethoxy-[1,1'-biphenyl]-4-yl) propan-1-one (Table 4.4, compound 14k)

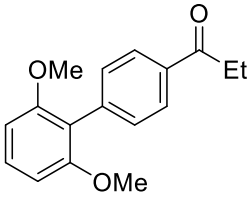

Yield: 99% (53.6 mg). Light-yellow solid, m.p.= 75.6–78.6 ºC. Eluents (R_f = 0.6, Hexane: Ethyl acetate: DCM = 10:1:2) was used for flash column chromatography. **^{1}H NMR** (400 MHz, $CDCl_3$) δ 8.00 (s, 1H), 7.96 (d, *J* = 7.7 Hz, 1H), 7.58 (d, *J* = 7.6 Hz, 1H), 7.51 (t, *J* = 7.6 Hz, 1H), 7.33 (t, *J* = 8.4 Hz, 1H), 6.69 (d, *J* = 8.4 Hz, 2H), 3.75 (s, 6H), 3.04 (q, *J* = 7.3 Hz, 2H), 1.26 (t, *J* = 7.3 Hz, 3H); **^{13}C NMR** (100 MHz, $CDCl_3$) δ 157.5, 136.3, 134.5, 130.9, 129.1, 127.8, 126.3, 118.3, 104.0, 55.8, 31.7, 8.3; **HRMS** (ESI): calcd for $C_{17}H_{19}O_3^+$: 271.1329, found 271.1332.

***N*-(2',6'-dimethoxy-[1,1'-biphenyl]-3-yl) acetamide (Table 4.4, compound 14l)**

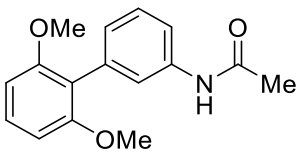

Yield: 93% (50.4 mg). Light-yellow solid, m.p.= 152.8–157.3 °C. Eluents (R_f = 0.2, Hexane: Ethyl acetate: DCM = 2:2:1) was used for flash column chromatography. **^{1}H NMR** (400 MHz, $CDCl_3$) δ 7.80 (s, 1H), 7.56 (d, *J* = 8.1 Hz, 1H), 7.37 (s, 1H), 7.31 (t, *J* = 6.2 Hz, 1H), 7.27 (t, *J* = 6.6 Hz, 1H), 7.07 (d, *J* = 7.6 Hz, 1H), 6.64 (d, *J* = 8.4 Hz, 2H), 3.71 (s, 6H), 2.06 (s, 3H); **^{13}C NMR** (100 MHz, $CDCl_3$) δ 168.5, 157.5, 137.6, 134.8, 128.7, 128.1, 126.7, 122.1, 119.0, 118.5, 104.1, 55.7, 24.3; **HRMS** (EI): calcd for $C_{16}H_{17}NO_3^+$: 271.1203, found 271.1211.

2',6'-Dimethoxy-[1,1'-biphenyl]-2-carbonitrile (Table 4.4, compound 14m)[37]

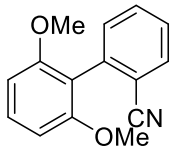

Yield: 99% (47.4 mg). Light-yellow solid. Eluents (R_f = 0.6, Hexane: Ethyl acetate: DCM = 10:1:1) was used for flash column chromatography. **^{1}H NMR** (400 MHz, $CDCl_3$) δ 7.74 (d, *J* = 7.7 Hz, 1H), 7.62 (t, *J* = 7.7 Hz, 1H), 7.44-7.35 (m, 3H), 6.69 (d, *J* = 8.4 Hz, 2H), 3.77 (s, 6H); **^{13}C NMR** (100 MHz, $CDCl_3$) δ 157.4, 138.7, 132.4, 132.1, 131.9, 130.3, 127.1 118.6, 115.5, 114.3, 104.1, 55.7; **HRMS** (ESI): calcd for $C_{15}H_{14}NO_2^+$: 240.1019, found 240.1017.

2'-Fluoro-2,6-dimethoxy-1,1'-biphenyl (Table 4.4, compound 14n)[38]

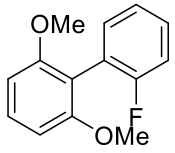

Yield: 87% (40.3 mg). White solid. Eluents (R_f = 0.8, Hexane: Ethyl acetate: DCM = 10:1:1) was used for flash column chromatography. **^{1}H NMR** (400 MHz, $CDCl_3$) δ

7.36-7.32 (m, 3H), 7.22 (t, *J* = 7.5 Hz, 1H), 7.16 (t, *J* = 8.9 Hz, 1H), 6.69 (d, *J* = 8.4 Hz, 2H), 3.78 (s, 6H); **^{13}C NMR** (100 MHz, $CDCl_3$) δ 160.3 (d, *J* = 245.1 Hz), 158.0, 132.9 (d, *J* = 4.2 Hz), 129.5, 128.8 (d, *J* = 8.1 Hz), 123.3(d, *J* = 3.4 Hz), 121.9 (d, *J* = 16.9 Hz), 115.2 (d, *J* = 22.4 Hz), 113.2, 104.0, 55.9.

7-(2,6-Dimethoxyphenyl)-2-methylquinoline (Table 4.4, compound 14o)[39]

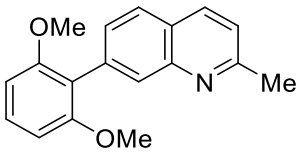

Yield: 97% (54.3 mg). Light-yellow solid, m.p.= 110.8–115.1 ^{o}C. Eluents (R_f = 0.4, Hexane: Ethyl acetate: DCM = 5:2:1) was used for flash column chromatography. **^{1}H NMR** (400 MHz, $CDCl_3$) δ 8.07 (s, 1H), 8.03 (d, *J* = 8.4 Hz, 1H), 7.78 (d, *J* = 8.3 Hz, 1H), 7.51 (dd, *J* = 8.3, 1.2 Hz, 1H), 7.33 (t, *J* = 8.4 Hz, 1H), 7.25 (d, *J* = 8.4 Hz, 1H), 6.69 (d, *J* = 8.4 Hz, 2H), 3.74 (s, 6H), 2.75 (s, 3H); **^{13}C NMR** (100 MHz, $CDCl_3$) δ 158.5, 157.6, 147.6, 135.8, 130.6, 129.2, 129.0, 126.2, 125.3, 121.6, 118.7, 104.1, 55.8, 25.3; **HRMS** (ESI): calcd for $C_{18}H_{18}O_2N^+$: 280.1332, found 280.1335.

2-(2,6-Dimethoxyphenyl)-9H-thioxanthen-9-one (Table 4.4, compound 14p)[40]

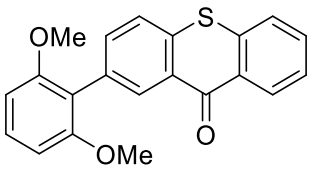

Yield: 79% (55.2 mg). Light-yellow solid. Eluents (R_f = 0.4, Hexane: Ethyl acetate: DCM = 10:1:1) was used for flash column chromatography. **^{1}H NMR** (400 MHz, $CDCl_3$) δ 8.66-8.62 (m, 2H), 7.67-7.59 (m, 4H), 7.47 (t, *J* = 7.0 Hz, 1H), 7.32 (t, *J* =

8.4 Hz, 1H), 6.68 (d, *J* = 8.4 Hz, 2H), 3.76 (s, 6H); **^{13}C NMR** (100 MHz, $CDCl_3$) δ 179.9, 157.5, 137.2, 135.4, 135.4, 132.5, 132.2, 132.0, 129.7, 129.2, 128.7, 126.0, 125.9, 125.1, 117.7, 104.0, 55.8; **HRMS** (ESI): calcd for $C_{21}H_{17}O_3S^+$: 349.0893, found 349.0898.

5-(2,6-Dimethoxyphenyl)-2-methylbenzo[d]thiazole (Table 4.4, compound 14q)

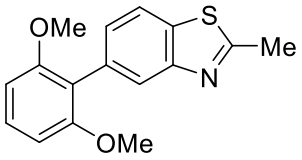

Yield: 92% (52.4 mg). Light-yellow solid, m.p.= 77.6–80.1 ºC. Eluents (R_f = 0.4, Hexane: Ethyl acetate: DCM = 5:1:1) was used for flash column chromatography. **^{1}H NMR** (400 MHz, $CDCl_3$) δ 8.00 (d, *J* = 1.1 Hz, 1H), 7.85 (d, *J* = 8.2 Hz, 1H), 7.39 (dd, *J* = 8.2, 1.4 Hz, 1H), 7.33 (t, *J* = 8.4 Hz, 1H), 6.70 (d, *J* = 8.4 Hz, 2H), 3.75 (s, 6H), 2.85 (s, 3H); **^{13}C NMR** (100 MHz, $CDCl_3$) δ 166.5, 157.6, 153.2, 134.0, 131.9, 128.8, 127.8, 124.7, 120.3, 118.7, 104.1, 55.7, 20.0; **HRMS** (ESI): calcd for $C_{16}H_{16}NO_2S^+$: 286.0896, found 286.0902.

1-(5-(2,6-Dimethoxyphenyl) thiophen-2-yl) ethan-1-one (Table 4.4, compound 14r)[41]

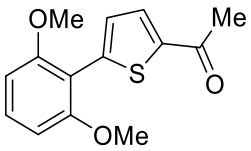

Yield: 95% (50.0 mg). Light-yellow solid, m.p.= 123.6–125.3 ºC. Eluents (R_f = 0.4, Hexane: Ethyl acetate = 5:1) was used for flash column chromatography. **^{1}H NMR** (400 MHz, $CDCl_3$) δ 7.67 (d, *J* = 4.0 Hz, 1H), 7.50 (d, *J* = 4.0 Hz, 1H), 7.28 (t, *J* = 8.4 Hz,

1H), 6.65 (d, *J* = 8.4 Hz, 2H), 3.85 (s, 6H), 2.57 (s, 3H); **^{13}C NMR** (100 MHz, $CDCl_3$) δ 191.0, 157.7, 143.4, 142.7, 131.7, 129.8, 111.3, 104.1, 55.8, 26.6; **HRMS** (ESI): calcd for $C_{14}H_{15}O_3S^+$: 263.0736, found 263.0738.

3-(2,6-Dimethoxyphenyl) pyridine (Table 4.4, compound 14s)[36]

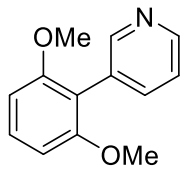

Yield: 99% (42.4 mg). Yellow liquid. Eluents (R_f = 0.3, Hexane: Ethyl acetate: DCM = 5:2:1) was used for flash column chromatography. **^{1}H NMR** (400 MHz, $CDCl_3$) δ 8.60 (s, 1H), 8.51 (d, *J* = 3.9 Hz, 1H), 7.68 (d, *J* = 7.8 Hz, 1H), 7.31 (dd, *J* = 10.9, 5.5 Hz, 2H), 6.65 (d, *J* = 8.4 Hz, 2H), 3.72 (s, 6H); **^{13}C NMR** (100 MHz, $CDCl_3$) δ 157.5, 151.7, 147.5, 138.3, 129.9, 129.4, 122.5, 115.5, 104.0, 55.7; **HRMS** (ESI): calcd for $C_{13}H_{14}NO_2^+$: 216.1019, found 216.1023.

2-(2,4,6-Trimethoxyphenyl) naphthalene (Table 4.5, compound 14t)[42]

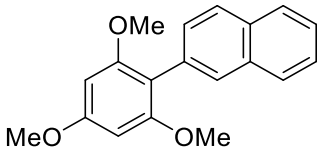

Yield: 99% (58.2 mg). White solid. Eluents (R_f = 0.6, Hexane: Ethyl acetate: DCM = 10:1:1) was used for flash column chromatography. **^{1}H NMR** (400 MHz, $CDCl_3$) δ 7.93-7.90 (m, 4H), 7.53 (ddd, *J* = 14.5, 7.3, 2.2 Hz, 3H), 6.34 (s, 2H), 3.94 (s, 3H), 3.78 (s, 6H); **^{13}C NMR** (100 MHz, $CDCl_3$) δ 160.6, 158.4, 133.3, 132.2, 131.6, 129.8, 129.7, 128.0, 127.5, 126.7, 125.4, 125.4, 112.3, 90.9, 55.8, 55.3; **HRMS** (ESI): calcd for

$C_{19}H_{18}O_3$: 294.1256, found 294.1256.

2-(2,6-Difluorophenyl) naphthalene (Table 4.5, compound 14u)[43]

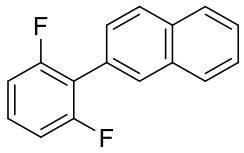

Yield: 93% (44.4 mg). White solid. Eluents (R_f = 0.7, Hexane = 100) was used for flash column chromatography. **^{1}H NMR** (400 MHz, $CDCl_3$) δ 8.03-7.92 (m, 4H), 7.65-7.54 (m, 3H), 7.35-7.31 (m, 1H), 7.09-7.04 (m, 2H); **^{13}C NMR** (100 MHz, $CDCl_3$) δ 160.2 (dd, *J* = 247.1, 7.0 Hz, 1C), 133.1, 132.9, 129.8, 128.9 (t, *J* = 10.3 Hz, 1C), 128.2, 127.8, 127.75, 127.65, 126.56, 126.49, 126.21, 118.5 (t, *J* = 18.8 Hz, 1C), 111.7 (dd, *J* = 12.4, 6.9 Hz, 1C); **^{19}F NMR** (565 MHz, $CDCl_3$) δ -114.18-114.24 (m, 2F); **HRMS** (EI): calcd for $C_{16}H_{10}F_2^+$: 240.0745, found 240.0748.

2-(2-Fluoro-6-(trifluoromethyl) phenyl) naphthalene (Table 4.5, compound 14v)

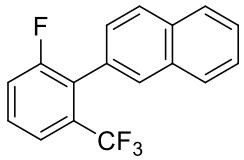

Yield: 97% (56.0 mg). Colorless liquid. Eluents (R_f = 0.7, Hexane = 100) was used for flash column chromatography. **^{1}H NMR** (400 MHz, $CDCl_3$) δ 7.97-7.90 (m, 3H), 7.86 (s, 1H), 7.64 (d, *J* = 7.9 Hz, 1H), 7.58-7.56 (m, 2H), 7.50-7.45 (m, 2H), 7.38 (t, *J* = 8.5 Hz, 1H); **^{13}C NMR** (100 MHz, $CDCl_3$) δ 160.4 (d, *J* = 244.6 Hz, 1C), 132.9, 132.8, 131.1 (qd, *J* = 30.8, 2.4 Hz, 1C), 129.3, 129.2, 129.13, 129.06, 128.9 (d, *J* = 2.1 Hz, 1C), 128.2, 127.8, 127.4, 126.5, 126.3, 123.4 (qd, *J* = 273.1, 3.6 Hz, 1C), 121.7 (m,

1C), 119.1 (d, J = 23.6 Hz, 1C); **^{19}F NMR** (565 MHz, $CDCl_3$) δ -57.1, -111.3; **HRMS** (EI): calcd for $C_{17}H_{10}F_4^+$: 290.0713, found 290.0718.

2-(2-Fluoro-6-methoxyphenyl) naphthalene (Table 4.5 compound 14w)

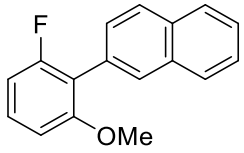

Yield: 98% (49.5 mg). Colorless liquid. Eluents (R_f = 0.3, Hexane = 100) was used for flash column chromatography. **^{1}H NMR** (400 MHz, $CDCl_3$) δ 7.97-7.93 (m, 4H), 7.60-7.54 (m, 3H), 7.35 (dd, J = 14.8, 8.0 Hz, 1H), 6.93-6.84 (m, 2H), 3.82 (s, 3H); **^{13}C NMR** (100 MHz, $CDCl_3$) δ 160.5 (d, J = 243.3 Hz, 1C), 158.0 (d, J = 7.1 Hz, 1C), 133.1, 132.6, 129.7, 129.02, 128.95, 128.9, 128.6, 128.1, 127.6, 127.2, 125.9 (d, J = 14.3 Hz, 1C), 118.7 (d, J = 17.8 Hz, 1C), 108.3 (d, J = 23.3 Hz, 1C), 106.7, 56.0; **^{19}F NMR** (376 MHz, $CDCl_3$) δ -115.2; **HRMS** (EI): calcd for $C_{15}H_{13}FO^+$: 252.0945, found 252.0944.

2-(2-Fluoro-6-nitrophenyl) naphthalene (Table 4.5, compound 14x)

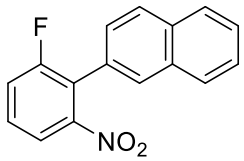

Yield: 96% (51.3 mg). Brown solid, m.p.= 66.8–69.0 ^{o}C. Eluents (R_f = 0.2, Hexane = 100) was used for flash column chromatography. **^{1}H NMR** (400 MHz, $CDCl_3$) δ 7.95 (d, J = 8.5 Hz, 1H), 7.92-7.86 (m, 2H), 7.83 (s, 1H), 7.73 (d, J = 7.9 Hz, 1H), 7.58 - 7.52 (m, 2H), 7.50-7.40 (m, 3H); ^{13}C NMR (100 MHz, $CDCl_3$) δ 159.9 (d, J = 248.7

Hz, 1C), 150.4 (d, *J* = 4.0 Hz, 1C), 133.0 (d, *J* = 2.5 Hz, 1C), 129.2 (d, *J* = 8.9 Hz, 1C), 128.3, 128.3 (d, *J* = 1.4 Hz, 1C), 128.2, 127.8, 127.5, 126.8, 126.5, 126.3 (d, *J* = 0.8 Hz, 1C), 124.7 (d, *J* = 20.1 Hz, 1C), 120.1, 119.8, 119.7 (d, *J* = 3.7 Hz, 1C); ^{19}F NMR (376 MHz, $CDCl_3$) δ -110.9; HRMS (EI): calcd for $C_{16}H_{10}FNO_2^+$: 267.0690, found 267.0692.

2-(2,3,6-Trifluorophenyl) naphthalene (Table 4.5 compound 14y)[43]

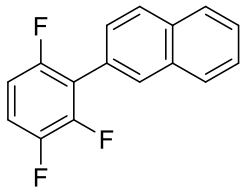

Yield: 84% (43.6 mg). White solid. Eluents (R_f = 0.6, Hexane = 100) was used for flash column chromatography. **^{1}H NMR** (400 MHz, $CDCl_3$) δ 8.01-7.91 (m, 4H), 7.60-7.56 (m, 3H), 7.17 (qd, *J* = 9.1, 4.9 Hz, 1H), 6.98 (tdd, *J* = 9.1, 3.7, 2.2 Hz, 1H); **^{13}C NMR** (100 MHz, $CDCl_3$) δ 155.4 (dm, *J* = 243.7 Hz, 1C), 148.0 (dm, *J* = 248.5 Hz, 1C), 147.5 (dm, *J* = 242.2 Hz, 1C), 133.1 (d, *J* = 1.5 Hz, 1C), 129.9 (t, *J* = 1.8 Hz, 1C), 128.3, 128.0, 127.7, 127.4 (t, *J* = 1.7 Hz, 1C), 126.8, 126.4, 125.73, 125.71, 120.3 (dd, *J* = 20.5, 15.2 Hz, 1C), 115.7 (ddd, *J* = 19.4, 10.0, 1.1 Hz, 1C), 110.9 (dm, *J* = 25.4 Hz, 1C); **^{19}F NMR** (376 MHz, $CDCl_3$) δ -119.52- -119.54 (m, 1F), -137.60- -137.64 (m, 1F), -141.88- -141.95 (m, 1F); **HRMS** (EI): calcd for $C_{16}H_9F_3^+$: 258.0651, found 258.0650.

2-(2,4,6-Trifluorophenyl) naphthalene (Table 4.5, compound 14z)[10c]

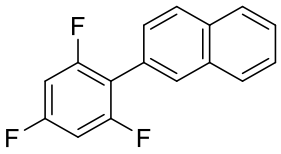

Yield: 91% (47.1 mg). White solid. Eluents (R_f = 0.6, Hexane = 100) was used for flash column chromatography. **^{1}H NMR** (400 MHz, $CDCl_3$) δ 7.97-7.90 (m, 4H), 7.57-7.55 (m, 3H), 6.84 (t, *J* = 8.2 Hz, 2H); **^{13}C NMR** (100 MHz, $CDCl_3$) δ 161.8 (dt, *J* = 247.8, 15.6 Hz, 1C), 160.4 (ddd, *J* = 248.1, 14.7, 9.8 Hz, 1C), 133.1, 132.9, 129.8, 128.2, 127.9, 127.7, 127.6, 126.6, 126.3, 125.7, 115.0 (dt, *J* = 19.2, 4.8 Hz, 1C), 100.8-100.2 (m, 1C); **^{19}F NMR** (565 MHz, $CDCl_3$) δ -108.8, -111.1; **HRMS** (EI): calcd for $C_{16}H_9F_3^+$: 258.0651, found 258.0657.

2-(2,6-Difluoro-3-methylphenyl) naphthalene (Table 4.5, compound 14aa)

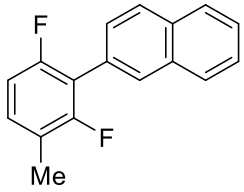

Yield: 97% (49.2 mg). White solid, m.p.= 120.9–123.9 °C. Eluents (R_f = 0.7, Hexane = 100) was used for flash column chromatography. **^{1}H NMR** (400 MHz, $CDCl_3$) δ 8.00-7.88 (m, 4H), 7.60 (dd, *J* = 8.4, 1.3 Hz, 1H), 7.55-7.53 (m, 2H), 7.17 (dd, *J* = 14.8, 8.3 Hz, 1H), 6.95 (t, *J* = 8.8 Hz, 1H), 2.34 (s, 3H); **^{13}C NMR** (100 MHz, $CDCl_3$) δ 158.4 (dd, *J* = 244.3, 6.7 Hz, 1C), 158.2 (dd, *J* = 245.7, 6.6 Hz, 1C), 133.1, 132.8, 130.1 (dd, *J* = 9.7, 6.9 Hz, 1C), 129.8, 128.2, 127.9, 127.7, 127.1, 126.4, 126.2, 120.9 (d, *J* = 3.8 Hz, 1C), 120.8 (d, *J* = 3.6 Hz, 1C), 117.9 (t, *J* = 19.1 Hz, 1C), 110.9 (dd, *J* = 22.6, 3.9 Hz, 1C), 14.4 (d, *J* = 3.9 Hz, 1C); **^{19}F NMR** (376 MHz, $CDCl_3$) δ -117.10- -117.13 (m,

1F), -118.19- -118.24 (m, 1F); **HRMS** (EI): calcd for $C_{17}H_{12}F_2^+$: 254.0902, found 254.0911.

2-(Perfluorophenyl) naphthalene (Table 4.5, compound 14ab)[43]

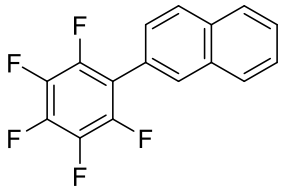

Yield: 90% (53.0 mg). Light-yellow solid. Eluents (R_f = 0.6, Hexane = 100) was used for flash column chromatography. ^{1}H NMR (600 MHz, $CDCl_3$) δ 7.96 (d, *J* = 8.4 Hz, 1H), 7.94 (s, 1H), 7.91 (t, *J* = 5.7 Hz, 2H), 7.57 (m, 2H), 7.50 (d, *J* = 8.2 Hz, 1H); ^{19}F NMR (565 MHz, $CDCl_3$) δ -143.0 (dd, *J* = 24.1, 9.1 Hz, 2F), -155.4 (t, *J* = 21.8 Hz, 1F), -162.1 (m, 2F).

1-Methyl-2-(naphthalen-2-yl)-1*H*-pyrrole (Table 4.5, compound 14ac)[44]

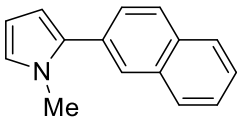

Yield: 54% (22.3 mg). Yellow liquid. Eluents (R_f = 0.5, Hexane: Ethyl acetate = 20:1) was used for flash column chromatography. **^{1}H NMR** (400 MHz, $CDCl_3$) δ 7.90-7.87 (m, 4H), 7.59 (dd, *J* = 8.4, 1.3 Hz, 1H), 7.55-7.48 (m, 2H), 6.80 (t, *J* = 2.4 Hz, 1H), 6.39 (dd, *J* = 3.4, 1.7 Hz, 1H), 6.29 (t, *J* = 3.1 Hz, 1H), 3.76 (s, 3H); **^{13}C NMR** (100 MHz, $CDCl_3$) δ 134.5, 133.3, 132.1, 130.7, 127.9, 127.9, 127.6, 127.1, 126.9, 126.3, 125.8, 123.9, 109.1, 107.9, 35.2; **HRMS** (ESI): calcd for $C_{15}H_{14}N^+$: 208.1121, found 208.1120.

2-(Naphthalen-2-yl)-1-phenyl-1*H*-pyrrole (Table 4.5, compound 14ad)[45]

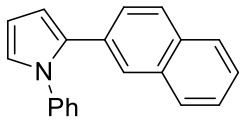

Yield: 97% (52.1 mg). Light-yellow liquid. Eluents (R_f = 0.4, Hexane = 100) was used for flash column chromatography. **^{1}H NMR** (400 MHz, $CDCl_3$) δ 7.83-7.81 (m, 1H), 7.77-7.74 (m, 2H), 7.71 (d, *J* = 8.6 Hz, 1H), 7.51-7.46 (m, 2H), 7.39-7.28 (m, 6H), 7.08 (t, *J* = 2.8 Hz, 1H), 6.66 (dd, *J* = 3.5, 1.7 Hz, 1H), 6.51 (t, *J* = 3.2 Hz, 1H); **^{13}C NMR** (100 MHz, $CDCl_3$) δ 140.5, 133.3, 133.3, 131.8, 130.5, 129.0, 127.8, 127.5, 127.4, 126.7, 126.6, 126.5, 126.0, 125.6, 125.6, 124.6, 111.2, 109.4; **HRMS** (ESI): calcd for $C_{20}H_{16}N^+$: 270.1277, found 270.1280.

Isopropyl 2-methyl-2-(4-(4-(1-phenyl-1*H*-pyrrol-2-yl) benzoyl) phenoxy) propanoate (Table 4.6, compound 14ae)

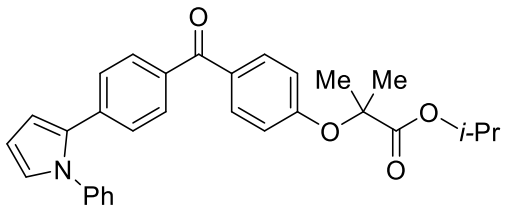

Yield: 99% (92.0 mg). Yellow solid, m.p.= 104.3–107.4 ºC. Eluents (R_f= 0.5, Hexane: Ethyl acetate = 10:1) was used for flash column chromatography. **^{1}H NMR** (400 MHz, $CDCl_3$) δ 7.75-7.73 (m, 2H), 7.62 (d, *J* = 8.3 Hz, 2H), 7.35-7.30 (m, 3H), 7.20 (t, *J* = 8.4 Hz, 4H), 6.99-6.98 (m, 1H), 6.86 (d, *J* = 8.8 Hz, 2H), 6.57 (dd, *J* = 3.6, 1.7 Hz, 1H), 6.40 (t, *J* = 3.2 Hz, 1H), 5.09 (t, *J* = 12.5, Hz, 1H), 1.66 (s, 6H), 1.21 (s, 3H), 1.19 (s, 3H); **^{13}C NMR** (100 MHz, $CDCl_3$) δ 194.8, 173.0, 159.2, 140.2, 136.5, 135.2, 132.5,

131.7, 130.6, 129.8, 129.1, 127.3, 126.9, 125.6, 117.0, 112.0, 109.6, 79.2, 69.2, 53.3, 25.2, 21.4; **HRMS** (ESI): calcd for $C_{30}H_{29}NO_4Na^+$: 490.1989, found 490.1998.

Ethyl 2-((2',6'-dimethoxy-[1,1'-biphenyl]-4-yl)oxy)-2-methylpropanoate (Table 4.6, compound 14af)

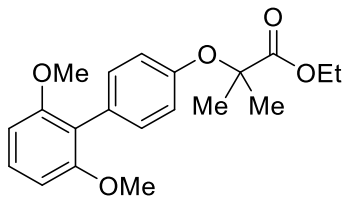

Yield: 88% (60.4 mg). Yellow liquid. Eluents (R_f = 0.3, Hexane: Ethyl acetate = 10:1) was used for flash column chromatography. **^{1}H NMR** (400 MHz, $CDCl_3$) δ 7.26-7.22 (m, 3H), 6.86 (d, *J* = 8.6 Hz, 2H), 6.63 (d, *J* = 8.4 Hz, 2H), 4.25 (q, *J* = 7.1 Hz, 2H), 3.70 (s, 6H), 1.64 (s, 6H), 1.25 (t, *J* = 7.1 Hz, 3H); **^{13}C NMR** (100 MHz, $CDCl_3$) δ 174.4, 157.6, 154.1, 131.6, 128.3, 127.3, 118.9, 117.9, 104.2, 78.8, 61.2, 55.8, 25.4, 13.9; **HRMS** (ESI): calcd for $C_{20}H_{25}O_5^+$: 345.1697, found 345.1699.

4-(1-Phenyl-1*H*-pyrrol-2-yl) phenyl 4-chlorobenzenesulfonate (Table 4.6, compound 14ag)

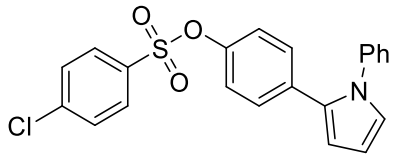

Yield: 84% (69.1 mg). Yellow liquid. Eluents (R_f = 0.4, Hexane: Ethyl acetate = 10:1) was used for flash column chromatography. **^{1}H NMR** (400 MHz, $CDCl_3$) δ 7.61 (d, *J* = 8.5 Hz, 2H), 7.41-7.35 (m, 3H), 7.25 (m, *J* = 3.2 Hz, 2H), 7.23 (d, *J* = 2.9 Hz, 2H), 7.17-7.15 (m, 2H), 7.02 (t, *J* = 1.8 Hz, 1H), 6.94-6.90 (m, 2H), 6.63 (dd, *J* = 2.0, 1.4

Hz, 1H), 6.42 (t, *J* = 3.1 Hz, 1H); **^{13}C NMR** (100 MHz, $CDCl_3$) δ 147.9, 139.8, 138.9, 132.7, 131.3, 131.3, 129.6, 129.3, 128.3, 127.8, 127.4, 126.8, 125.7, 123.7, 113.1, 110.0; **HRMS** (EI): calcd for $C_{22}H_{16}NO_3SCl$: 409.0539, found 409.0558.

4-(1-Phenyl-1*H*-pyrrol-2-yl) phenyl benzenesulfonate (Table 4.6, compound 14ah)

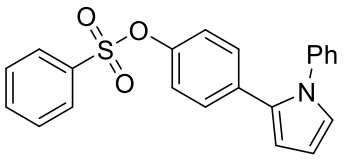

Yield: 98% (73.3 mg). Yellow solid, m.p. = 119.5–122.4 ºC. Eluents (R_f = 0.2, Hexane: Ethyl acetate = 10:1) was used for flash column chromatography. **^{1}H NMR** (400 MHz, $CDCl_3$) δ 7.81 (d, *J* = 7.7 Hz, 2H), 7.65 (t, *J* = 7.4 Hz, 1H), 7.52-7.48 (m, 2H), 7.34-7.29 (m, 3H), 7.12 (d, *J* = 6.9 Hz, 2H), 7.04 (d, *J* = 8.6 Hz, 2H), 6.94 (t, *J* = 2.2 Hz, 1H), 6.82 (d, *J* = 8.6 Hz, 2H), 6.44-6.43 (m, 1H), 6.36 (t, *J* = 3.0 Hz, 1H); **^{13}C NMR** (100 MHz, $CDCl_3$) δ 147.7, 140.1, 135.2, 134.1, 132.2, 132.0, 129.1, 129.0, 129.0, 128.4, 126.8, 125.6, 124.8, 121.9, 111.1, 109.3; **HRMS** (EI): calcd for $C_{22}H_{17}NO_3S$: 375.0928, found 375.0946.

(6'R)-2',4,6-Trimethoxy-6'-methyl-7-(1-phenyl-1*H*-pyrrol-2-yl)-3H-spiro[benzofuran-2,1'-cyclohexan]-2'-ene-3,4'-dione (Table 4.6, compound 14al)

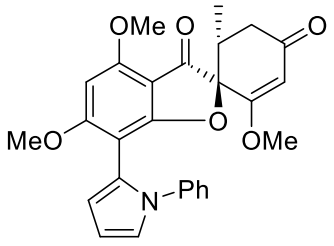

Yield: 84% (77.1 mg). Light-yellow solid, m.p.= 128.6–133.3 °C. Eluents (R_f = 0.3, Hexane: Ethyl acetate = 10:1) was used for flash column chromatography. **^{1}H NMR** (400 MHz, $CDCl_3$) δ 7.28-7.24 (m, 2H), 7.21-7.16 (m, 3H), 7.02 (s, 1H), 6.42 (t, *J* = 3.1 Hz, 1H), 6.36 (dd, *J* = 3.2, 1.5 Hz, 1H), 5.90 (s, 1H), 5.46 (s, 1H), 3.92 (s, 3H), 3.56 (s, 3H), 3.53 (s, 3H), 3.00 (t, *J* = 15.2 Hz, 1H), 2.66 (s, 1H), 2.34 (dd, *J* = 16.7, 4.3 Hz, 1H), 0.87-0.82 (m, 3H); **^{13}C NMR** (100 MHz, $CDCl_3$) δ 197.3, 193.0, 172.8, 171.4, 167.2, 159.2, 140.8, 128.6, 126.2, 124.1, 122.6, 121.4, 112.3, 109.1, 104.4, 104.0, 99.7, 89.8, 88.4, 56.4, 56.0, 56.0, 40.0, 36.1, 14.0; **HRMS** (ESI): calcd for $C_{27}H_{26}NO_6^+$: 460.1755, found 460.1754.

Ethyl 4-(8-(1-phenyl-1*H*-pyrrol-2-yl)-5,6-dihydro-11H-benzo [5,6] cyclohepta[1,2-b] pyridin-11-ylidene) piperidine-1-carboxylate (Table 4.6, compound 14aj)

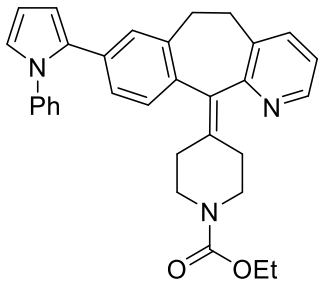

Yield: 90% (87.7 mg). Light-yellow solid, m.p.= 79.4–83.8 °C. Eluents (R_f = 0.4, DCM: MeOH = 20:1) was used for flash column chromatography. **^{1}H NMR** (400 MHz, $CDCl_3$) δ 8.37 (d, *J* = 4.5 Hz, 1H), 7.41 (d, *J* = 7.6 Hz, 1H), 7.30-7.24 (m, 3H), 7.14 (d, *J* = 7.2 Hz, 2H), 7.07-6.85 (m, 5H), 6.41-6.32 (m, 2H), 4.12 (q, *J* = 7.0 Hz, 2H), 3.79 (s, 2H), 3.29 (td, *J* = 9.9, 2.5 Hz, 2H), 3.13 (qd, *J* = 12.8, 5.0 Hz, 2H), 2.77-2.61 (m, 2H), 2.49-2.40 (m, 1H), 2.35 (t, *J* = 5.3 Hz, 2H), 2.26 (d, *J* = 14.2 Hz, 1H), 1.23 (t, *J* = 7.1 Hz, 3H); **^{13}C NMR** (100 MHz, $CDCl_3$) δ157.6, 155.3, 146.3, 140.3, 137.1, 136.5, 136.5,

134.8, 133.7, 133.2, 131.8, 129.0, 128.8, 128.6, 126.5, 125.7, 124.2, 122.0, 110.4, 109.1, 61.1, 44.7, 44.6, 31.8, 31.4, 30.5, 30.4, 14.5; **HRMS** (ESI): calcd for $C_{32}H_{32}N_3O_2^+$: 490.2489, found 490.2496.

***N*, *N*-Dimethyl-3-(2-(1-phenyl-1*H*-pyrrol-2-yl)-10H-phenothiazin-10-yl) propan-1-amine (Table 4.6, compound 14ak)**

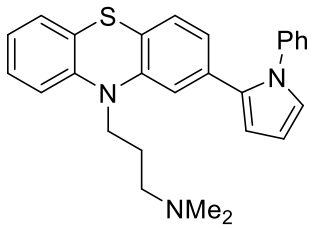

Yield: 97% (82.1 mg). Light-yellow solid, m.p.= 113.9–115.8 °C. Eluents (R_f = 0.6, Hexane: Ethyl acetate: Et_3N = 10:10:1) was used for flash column chromatography. **^{1}H NMR** (400 MHz, $CDCl_3$) δ 7.40-7.36 (m, 2H), 7.32 (d, *J* = 7.2 Hz, 1H), 7.23 (d, *J* = 7.4 Hz, 2H), 7.14 (t, *J* = 7.3 Hz, 2H), 7.00 (d, *J* = 7.9 Hz, 1H), 6.98-6.96 (m, 1H), 6.91 (t, *J* = 7.4 Hz, 1H), 6.84 (d, *J* = 8.2 Hz, 1H), 6.78 (dd, *J* = 7.9, 1.0 Hz, 1H), 6.63 (s, 1H), 6.47 (dd, *J* = 3.2, 1.5 Hz, 1H), 6.40 (t, *J* = 3.1 Hz, 1H), 3.62 (t, *J* = 7.0 Hz, 2H), 2.31 (t, *J* = 7.1 Hz, 2H), 2.22 (s, 6H), 1.79-1.72 (m, 2H); **^{13}C NMR** (100 MHz, $CDCl_3$) δ 144.8, 140.4, 133.2, 132.0, 129.0, 127.2, 127.1, 126.9, 126.6, 125.6, 124.6, 124.3, 122.6, 122.2, 122.2, 115.4, 115.4, 110.6, 109.2, 57.0, 45.5, 45.1, 24.8; **HRMS** (ESI): calcd for $C_{27}H_{28}N_3S^+$: 426.1998, found 426.2005.

2-(1-Methylazepan-4-yl)-4-(4-(1-phenyl-1*H*-pyrrol-2-yl) benzyl) phthalazin-1(2H)-one (Table 4.6, compound 14al)

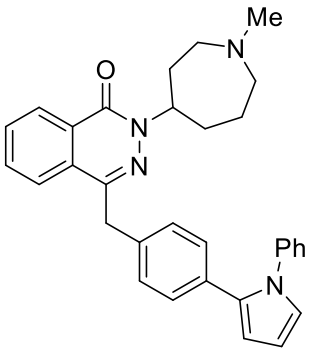

Yield: 95% (92.7 mg). Light-yellow solid, m.p.= 104.7–107.8 ^{o}C. Eluents (R_f = 0.6, DCM: MeOH = 10:1) was used for flash column chromatography. **^{1}H NMR** (400 MHz, $CDCl_3$) δ 8.46-8.42 (m, 1H), 7.70-7.63 (m, 3H), 7.33-7.23 (m, 3H), 7.16-7.02 (m, 6H), 6.93- 6.90 (m, 1H), 6.39 (dd, *J* = 3.5, 1.7 Hz, 1H), 6.33 (t, *J* = 3.2 Hz, 1H), 5.35 (tt, *J* = 9.1, 5.4 Hz, 1H), 4.23 (s, 2H), 2.85 (ddd, *J* = 13.2, 7.4, 2.0 Hz, 1H), 2.76-2.57 (m, 3H), 2.40 (s, 3H), 2.31-2.21 (m, 1H), 2.17-1.92 (m, 4H), 1.77 (tdd, *J* = 12.2, 6.2, 3.2 Hz, 1H); **^{13}C NMR** (100 MHz, $CDCl_3$) δ 158.4, 144.9, 140.4, 135.9, 133.3, 132.6, 131.4, 130.9, 128.9, 128.7, 128.4, 128.2, 128.1, 127.4, 126.6, 125.6, 124.8, 124.4, 110.6, 109.2, 58.8, 56.1, 54.4, 46.9, 38.7, 33.0, 32.2, 24.6; **HRMS** (ESI): calcd for $C_{32}H_{33}N_4O^+$: 489.2649, found 489.2646.

(*S*)-N-((2-oxo-3-(4-(3-oxomorpholino) phenyl) oxazolidin-5-yl) methyl)-5-(1-phenyl-1*H*-pyrrol-2-yl) thiophene-2-carboxamide (Table 4.6, compound 14am)

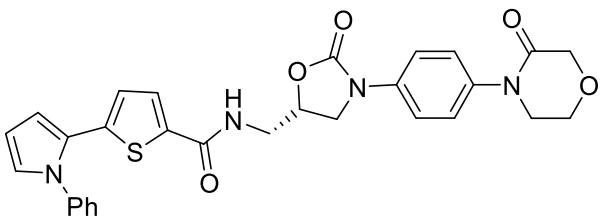

Yield: 98% (106.1 mg). Yellow solid, m.p.= 128.8–133.2 ^{o}C. Eluents (DCM: MeOH = 20:1, R_f = 0.5) was used for flash column chromatography. **^{1}H NMR** (400 MHz, $CDCl_3$)

δ 7.51-7.48 (m, 2H), 7.40-7.35 (m, 3H), 7.29-7.28 (m, 1H), 7.26-7.22 (m, 4H), 6.89-6.85 (m, 2H), 6.54 (dd, *J* = 3.5, 1.6 Hz, 1H), 6.39 (d, *J* = 4.0 Hz, 1H), 6.31 (t, *J* = 3.2 Hz, 1H), 4.78-4.72 (m, 1H), 4.30 (s, 2H), 4.01-3.96 (m, 3H), 3.80-3.68 (m, 4H), 3.65-3.58 (m, 1H); **^{13}C NMR** (100 MHz, $CDCl_3$) δ 166.9, 162.7, 154.4, 140.5, 139.5, 137.1, 136.7, 134.9, 129.2, 128.9, 128.0, 126.6, 126.2, 125.8, 124.5, 119.0, 112.0, 109.6, 71.9, 68.5, 64.0, 49.6, 47.6, 42.2; **HRMS** (ESI): calcd for $C_{29}H_{26}N_4O_5SNa^+$: 565.1516, found 565.1517.

2-(1-(2',6'-Dimethoxy-[1,1'-biphenyl]-4-carbonyl)-5-methoxy-2-methyl-1*H*-indol-3-yl) acetic acid (Table 4.6, compound 14an)

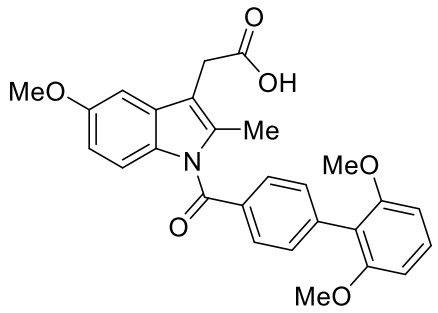

Yield: 46% (42.0 mg). Light-yellow solid, m.p.= 82.2–85.9 °C. Eluents (R_f = 0.3, Hexane: Ethyl acetate = 10:1) was used for flash column chromatography. **^{1}H NMR** (400 MHz, $CDCl_3$) δ 7.76 (d, *J* = 7.9 Hz, 2H), 7.48 (d, *J* = 7.9 Hz, 2H), 7.33 (t, *J* = 8.4 Hz, 1H), 7.06 (d, *J* = 9.0 Hz, 1H), 6.99 (s, 1H), 6.72-6.67 (m, 3H), 3.84 (s, 3H), 3.76 (s, 6H), 3.72 (s, 2H), 2.43 (s, 3H); **^{13}C NMR** (100 MHz, $CDCl_3$) δ 176.8, 169.6, 157.4, 155.7, 139.6, 136.3, 133.2, 131.5, 131.0, 130.2, 129.4, 129.1, 118.1, 115.2, 111.6, 111.2, 104.2, 100.8, 55.8, 55.6, 30.1, 13.2; **HRMS** (ESI): calcd for $C_{27}H_{26}NO_6^+$: 460.1755, found 460.1758.

2,6-Difluoro-2',6'-dimethoxy-1,1'-biphenyl (Table 4.7, 14ao)

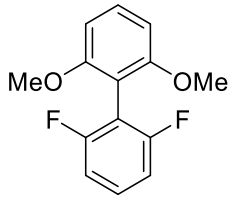

Yield: 69% (34.6 mg). Light-yellow solid, m.p.= 107.2–110.4 °C. Eluents (R_f = 0.5, Hexane: Ethyl acetate = 10: 1) was used for flash column chromatography. **^{1}H NMR** (600 MHz, $CDCl_3$) δ 7.38 (d, *J* = 8.3 Hz, 1H), 7.33-7.28 (m, 1H), 6.99-6.95 (m, 2H), 6.68 (d, *J* = 8.4 Hz, 2H), 3.78 (s, 6H); **^{13}C NMR** (150 MHz, $CDCl_3$) δ 160.9 (dd, *J* = 246.3, 7.9 Hz, 1C), 158.3, 130.3, 128.9 (t, *J* = 10.0 Hz, 1C), 111.4 (t, *J* = 21.4 Hz, 1C), 110.9 (dd, *J* = 21.3 Hz, 5.2 Hz, 1C), 106.8, 103.9, 55.9; **^{19}F NMR** (565 MHz, $CDCl_3$) δ -110.0; **HRMS** (APPI): calcd for $C_{14}H_{12}F_2O_2^+$: 250.0800, found 250.0791.

4-(2,6-Dimethoxyphenyl)-3-methylquinoline (Table 4.7, 14ap)

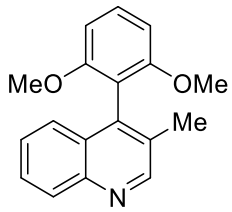

Yield: 39% (22.0mg). Light-yellow solid, m.p.= 136.6–138.9 °C. Eluents (R_f = 0.3, Hexane: Ethyl acetate = 4: 1) was used for flash column chromatography. **^{1}H NMR** (600 MHz, $CDCl_3$) δ 8.86 (s, 1H), 8.09 (d, *J* = 8.4 Hz, 1H), 7.60-7.57 (m, 1H), 7.37-7.35 (m, 2H), 6.72 (d, *J* = 8.4 Hz, 2H), 3.61 (s, 6H), 2.20 (s, 3H); **^{13}C NMR** (150 MHz, $CDCl_3$) δ 157.6, 152.4, 146.7, 140.3, 129.9, 129.8, 129.3, 127.8, 127.7, 128.0, 125.4, 113.5, 104.0, 55.7, 17.2; **HRMS** (ESI): calcd for $C_{18}H_{18}O_2N^+$: 280.1332, found

280.1337.

9-(2,6-Dimethoxyphenyl)acridine (Table 4.7, 14aq)

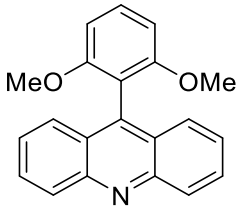

Yield: 57% (36.3 mg). Light-yellow solid, m.p.= 238.4–239.8 °C. Eluents (R_f = 0.3, DCM: MeOH = 20: 1) was used for flash column chromatography. **^{1}H NMR** (600 MHz, $CDCl_3$) δ 8.27 (d, *J* = 8.7 Hz, 2H), 7.76-7.72 (m, 2H), 7.61 (d, *J* = 8.6 Hz, 2H), 7.52 (t, *J* = 8.4 Hz, 1H), 7.40-7.37 (m, 2H), 6.79 (d, *J* = 8.4 Hz, 2H), 3.54 (s, 6H); **^{13}C NMR** (150 MHz, $CDCl_3$) δ 158.3, 148.9, 141.9, 130.5, 129.7, 129.6, 126.7, 125.9, 125.1, 112.8, 104.1, 55.8; **HRMS** (ESI): calcd for $C_{21}H_{18}O_2N^+$: 316.1332, found 316.1336.

9-(2-Fluoro-6-methoxyphenyl)anthracene (Table 4.7, 14ar)

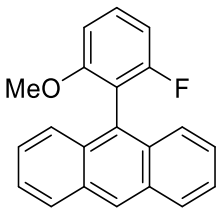

Yield: 83% (50.2 mg). Light-yellow solid, m.p.= 232.8–235.7 °C. Eluents (R_f = 0.7, Hexane: Ethyl acetate = 10: 1) was used for flash column chromatography. **^{1}H NMR** (600 MHz, $CDCl_3$) δ 8.53 (s, 1H), 8.06 (d, *J* = 8.5 Hz, 2H), 7.60 (d, *J* = 8.8 Hz, 2H), 7.53-7.49 (m, 1H), 7.46 (t, *J* = 7.1 Hz, 2H), 7.39-7.37 (m, 2H), 6.97-6.94 (m, 2H), 3.61 (s, 3H); **^{13}C NMR** (150 MHz, $CDCl_3$) δ 161.3 (d *J* = 242.9 Hz, 1C), 159.3 (d *J* = 7.2 Hz, 1C), 131.4, 130.6, 129.9 (d, *J* = 10.0 Hz, 1C), 128.6, 127.3, 126.7, 126.0, 125.6,

125.1, 115.0 (d, J = 20.5 Hz, 1C), 108.3 (d, J = 22.9 Hz, 1C), 106.8 (d, J = 2.7 Hz, 1C), 56.1; **^{19}F NMR** (565 MHz, $CDCl_3$) δ -111.8; **HRMS** (APPI): calcd for $C_{21}H_{16}FO^+$: 303.1180, found 303.1169.

4-(2-Fluoro-6-methoxyphenyl)-3-methylquinoline (Table 4.7, 14as)

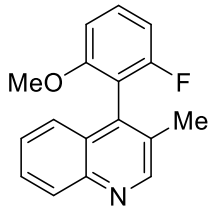

Yield: 89% (47.3 mg). Light-yellow solid, m.p.= 108.4–112.8 °C. Eluents (R_f = 0.4, Hexane: Ethyl acetate = 3: 1) was used for flash column chromatography. **^{1}H NMR** (600 MHz, $CDCl_3$) δ 8.87 (s, 1H), 8.12 (d, J = 8.4 Hz, 1H), 7.63-7.60 (m, 1H), 7.45-7.37 (m, 3H), 6.89-6.84 (m, 2H), 3.66 (s, 3H), 2.25 (m, 3H); **^{13}C NMR** (150 MHz, $CDCl_3$) δ 160.0 (d, J = 243.8 Hz, 1C), 157.9 (d J = 7.4 Hz, 1C), 152.3, 146.6, 137.1, 130.3 (d, J = 10.6 Hz, 1C), 130.0, 129.3, 128.1, 127.4, 126.5, 125.1, 113.0 (d, J = 20.0 Hz, 1C), 108.2 (d, J = 22.3 Hz, 1C), 106.7 (d, J = 3.0 Hz, 1C), 55.9, 17.2; **^{19}F NMR** (565 MHz, $CDCl_3$) δ -112.6; **HRMS** (ESI): calcd for $C_{17}H_{15}FNO^+$: 268.1132, found 268.1134.

2,3,4,6-Tetrafluoro-5-(2-fluoro-6-methoxyphenyl)pyridine (Table 4.7, 14at)

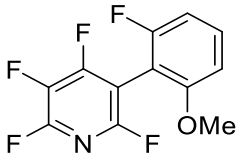

Yield: 73% (40.0 mg). Yellow liquid. Eluents (R_f = 0.7, Hexane: DCM = 5: 1) was used for flash column chromatography. **^{1}H NMR** (600 MHz, $CDCl_3$) δ 7.46-7.42 (m, 1H),

6.85-6.81 (m, 2H), 3.83 (s, 3H); **^{13}C NMR** (150 MHz, $CDCl_3$) δ 160.7 (d *J* = 247.6 Hz, 1C), 158.3 (d, *J* = 6.2 Hz, 1C), 157.9 (dm, *J* = 265.3 Hz, 1C), 152.7 (dm, *J* = 241.9 Hz, 1C), 149.3 (dm, *J* = 240.6 Hz, 1C), 133.0 (dm, *J* = 242.8 Hz, 1C), 132.2, 132.1, 108.1 (d, *J* = 21.8 Hz, 1C), 106.8 (d, *J* = 3.1 Hz, 1C), 103.3-103.0 (m, 1C), 56.2; **^{19}F NMR** (565 MHz, $CDCl_3$) δ -68.9- -69.0 (m, 1F), -85.2- -85.3 (m, 1F), -112.0- -112.01 (m, 1F), -112.1- -112.2 (m, 1F), -167.4- -167.5 (m, 1F); **HRMS** (APPI): calcd for $C_{12}H_6F_5NO^+$: 275.0364, found 275.0362.

2,6-Difluoro-2',6'-dimethyl-1,1'-biphenyl (Table 4.7, 14au)[46]

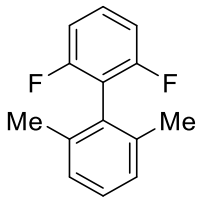

Yield: 77% (33.3mg). Light-yellow liquid. Eluents (R_f = 0.7, Hexane = 100) was used for flash column chromatography. **^{1}H NMR** (600 MHz, $CDCl_3$) δ7.38-7.33 (m, 1H), 7.27 (t, *J* = 7.6 Hz, 1H), 7.18 (d, *J* = 7.6 Hz, 2H), 7.04-7.00 (m, 2H), 2.12 (s, 6H); **^{13}C NMR** (150 MHz, $CDCl_3$) δ 160.0 (dd, J = 245.1, 7.9 Hz, 1C), 137.3, 129.2 (t, *J* = 10.1 Hz, 1C), 128.7, 128.4, 127.3, 116.9 (t, *J* = 22.4 Hz, 1C), 111.5 (d, *J* = 4.8 Hz, 1C), 111.3 (d, *J* = 5.1 Hz, 1C), 20.1; **^{19}F NMR** (565 MHz, $CDCl_3$) δ -112.2.

Methyl 3-(2,6-difluorophenyl)benzo[*b*]thiophene-2-carboxylate (Table 4.7, 14av)

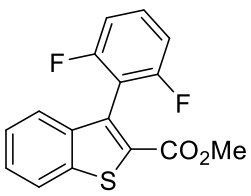

Yield: 82% (49.7mg). Light-yellow solid, m.p.= 132.4–134.9 °C. Eluents (R_f = 0.4,

Hexane: DCM = 5: 1) was used for flash column chromatography. **^{1}H NMR** (600 MHz, $CDCl_3$) δ 7.91 (d, *J* = 8.3 Hz, 1H), 7.52-7.50 (m, 2H), 7.47-7.39 (m, 2H), 7.09-7.05 (m, 2H), 3.84 (s, 3H); **^{13}C NMR** (150 MHz, $CDCl_3$) δ 162.3, 160.3 (dd, *J* = 247.8, 7.1 Hz, 1C), 140.3, 138.8, 130.8, 130.4, 130.3 (t, *J* = 10.0 Hz, 1C), 127.4, 125.1, 124.5, 122.6, 111.6 (t, *J* = 20.6 Hz, 1C), 111.3 (dd, *J* = 20.9, 4.5 Hz, 1C), 52.3; **^{19}F NMR** (565 MHz, $CDCl_3$) δ -110.5; **HRMS** (ESI): calcd for $C_{16}H_{10}F_2O_2SNa^+$: 327.0262, found 327.0265.

4.6 References

(1) Hegedus, L.; Wade, L. Preparation of carboxylic acids, acid halides and anhydrides. John Wiley & Sons Hoboken, NJ: **1977**; *Vol. 3*, pp. 8-32.

(2) (a) Goossen, L. J.; Deng, G.; Levy, L. M. *Science* **2006**, *313 (5787)*, 662-664; (b) Rodríguez, N.; Goossen, L. J. *Chem. Soc. Rev.* **2011**, *40 (10)*, 5030-5048; (c) Wei, Y.; Hu, P.; Zhang, M.; Su, W. *Chem. Rev.* **2017**, *117 (13)*, 8864-8907; (d) Cornella, J.; Larrosa, I. *Synthesis* **2012**, 653-676; (e) Dzik, W. I.; Lange, P. P.; Goossen, L. J. *Chem. Sci.* **2012**, *3 (9)*, 2671-2678; (f) Gooßen, L. J.; Rodríguez, N.; Gooßen, K. *Angew. Chem. Int, Ed.* **2008**, *47 (17)*, 3100-3120.

(3) (a) Goossen, L. J.; Rodríguez, N.; Linder, C. *J. Am. Chem. Soc.* **2008**, *130 (46)*, 15248-15249; (b) Gooßen, L. J.; Zimmermann, B.; Knauber, T. *Angew. Chem. Int, Ed.* **2008**, *47 (37)*, 7103-7106; (c) Wang, Z.; Ding, Q.; He, X.; Wu, J. *Tetrahedron* **2009**, *65 (24)*, 4635-4638; (d) Tang, J.; Biafora, A.; Goossen, L. J. *Angew. Chem. Int, Ed.* **2015**, *54 (44)*, 13130-13133; (e) Wang, S.; Lu, H.; Li, J.; Zou, D.; Wu, Y.; Wu, Y. *Tetrahedron lett.* **2017**, *58 (12)*, 1107-1111.

(4) Gooßen, L. J.; Rodríguez, N.; Linder, C.; Lange, P. P.; Fromm, A. *ChemCatChem* **2010**, *2 (4)*, 430-442.

(5) Gooßen, L. J.; Lange, P. P.; Rodríguez, N.; Linder, C. *Chem. Eur. J.* **2010**, *13 (16)*, 3906-3909.

(6) Cahiez, G.; Moyeux, A.; Gager, O.; Poizat, M. *Adv. Syn. Catal.* **2013**, *355 (4)*, 790-796.

(7) Fromm, A.; van Wüllen, C.; Hackenberger, D.; Goossen, L. J. *J. Am. Chem. Soc.*

2014, *136 (28)*, 10007-10023.

(8) Hackenberger, D.; Song, B.; Grünberg, M. F.; Farsadpour, S.; Menges, F.; Kelm, H.; Groß, C.; Wolff, T.; Niedner-Schatteburg, G.; Thiel, W. R. *ChemCatChem* **2015**, *7 (21)*, 3579-3588.

(9) (a) Forgione, P.; Brochu, M.-C.; St-Onge, M.; Thesen, K. H.; Bailey, M. D.; Bilodeau, F. *J. Am. Chem. Soc.* **2006**, *128 (35)*, 11350-11351; (b) Voutchkova, A.; Coplin, A.; Leadbeater, N. E.; Crabtree, R. H. *Chem. Commun.* **2008**, *(47)*, 6312-6314; (c) Shen, Z.; Ni, Z.; Mo, S.; Wang, J.; Zhu, Y. *Chemistry (Weinheim an der Bergstrasse, Germany)* **2012**, *18 (16)*, 4859-4865; (d) Arroyave, F. A.; Reynolds, J. R. *Org. Lett.* **2010**, *12 (6)*, 1328-1331; (e) Messina, C.; Douglas, L. Z.; Liu, J. T.; Forgione, P. *Eur. J. Org. Chem.* **2020**, *2020 (32)*, 5182-5191; (f) Liu, J. T.; Hase, H.; Taylor, S.; Salzmann, I.; Forgione, P. *Angew. Chem. Int, Ed.* **2020**, *59 (18)*, 7146-7153; (g) Chen, F.; Wong, N. W.; Forgione, P. *Adv. Syn. Catal.* **2014**, *356 (8)*, 1725-1730.

(10) (a) Shang, R.; Xu, Q.; Jiang, Y.-Y.; Wang, Y.; Liu, L. *Org. Lett.* **2010**, *12 (5)*, 1000-1003; (b) Bilodeau, F.; Brochu, M.-C.; Guimond, N.; Thesen, K. H.; Forgione, P. *J. Org. Chem.* **2010**, *75 (5)*, 1550-1560; (c) Daley, R. A.; Liu, E.-C.; Topczewski, J. J. *Org. Lett.* **2019**, *21 (12)*, 4734-4738.

(11) Tanaka, D.; Romeril, S. P.; Myers, A. G. *J. Am. Chem. Soc.* **2005**, *127 (29)*, 10323-10333.

(12) Zhang, S.-L.; Fu, Y.; Shang, R.; Guo, Q.-X.; Liu, L. *J. Am. Chem. Soc.* **2010**, *132 (2)*, 638-646.

(13) Littke, A. F.; Fu, G. C. *Angew. Chem. Int, Ed.* **2002**, *41 (22)*, 4176-4211.

(14) Gu, C.; So, C. M. *Adv. Sci.* **2024**, *11 (21)*, 2309192.

(15) Gu, C.; Yuen, O. Y.; Ng, S. S.; So, C. M. *Adv. Syn. Catal.* **2024**, *366 (7)*, 1565-1574.

(16) Yang, L. P.; Keating, G. M. *Am. J. Cardiovascular. Drugs* **2009**, *9* 401-409.

(17) Ueda, T.; Arai, S.; Amoh, Y.; Katsuoka, K. *Eur. J. Dermatol.* **2012**, *21 (6)*, 1020-1021.

(18) Al-Qahtani, A.; Haidar, H.; Larem, A. *Textbook of clinical otolaryngology*; Springer Nature, 2020.

(19) (a) Bringmann, G.; Gulder, T.; Gulder, T. A.; Breuning, M. *Chem. Rev.* **2011**, *111 (2)*, 563-639; (b) Kozlowski, M. C.; Morgan, B. J.; Linton, E. C. *Chem. Soc. Rev.* **2009**, *38 (11)*, 3193-3207; (c) Nicolaou, K.; Bulger, P. G.; Sarlah, D. *Angew. Chem. Int, Ed.* **2005**, *44 (29)*, 4442-4489.

(20) (a) Altenhoff, G.; Goddard, R.; Lehmann, C. W.; Glorius, F. *J. Am. Chem. Soc.* **2004**, *126 (46)*, 15195-15201; (b) Fu, W. C.; Zhou, Z.; Kwong, F. Y. *Org. Chem. Front.* **2016**, *3 (2)*, 273-276; (c) To, S.; Kwong, F. *Chem. Commun.* **2011**, *47 (17)*, 5079-5081; (d) Tu, T.; Sun, Z.; Fang, W.; Xu, M.; Zhou, Y. *Org. Lett.* **2012**, *14 (16)*, 4250-4253; (e) Yin, J.; Rainka, M. P.; Zhang, X.-X.; Buchwald, S. L. *J. Am. Chem. Soc.* **2002**, *124 (7)*, 1162-1163; (f) Lu, D.-D.; He, X.-X.; Liu, F.-S. *J. Org. Chem.* **2017**, *82 (20)*, 10898-10911.

(21) (a) Çalimsiz, S.; Sayah, M.; Mallik, D.; Organ, M. G. *Angew. Chem. Int, Ed.* **2010**, *11 (49)*, 2014-2017; (b) Milne, J. E.; Buchwald, S. L. *J. Am. Chem. Soc.* **2004**, *126 (40)*, 13028-13032; (c) Zhilyaev, K. A.; Lipilin, D. L.; Kosobokov, M. D.; Samigullina, A. I.;

Dilman, A. D. *Adv. Syn. Catal.* **2022**, *364 (18)*, 3295-3301.

(22) Lesieur, M.; Slawin, A. M.; Cazin, C. S. *Org. Biomol. Chem.* **2014**, *12 (30)*, 5586-5589.

(23) (a) Dang, H. T.; Nguyen, V. D.; Haug, G. C.; Arman, H. D.; Larionov, O. V. *JACS Au* **2023**, *3 (3)*, 813-822; (b) Korpusik, A. B.; Adili, A.; Bhatt, K.; Anatot, J. E.; Seidel, D.; Sumerlin, B. S. *J. Am. Chem. Soc.* **2023**, *145 (19)*, 10480-10485.

(24) Humke, J. N.; Daley, R. A.; Morrenzin, A. S.; Neufeldt, S. R.; Topczewski, J. J. *J. Org. Chem.* **2021**, *86 (17)*, 11419-11433.

(25) Amatore, C.; Pfluger, F. *Organometallics* **1990**, *9 (8)*, 2276-2282.

(26) Espenson, J. H. *Chemical kinetics and reaction mechanisms*; Citeseer, 1995.

(27) Eyring, H. *J. Chem. Phys.* **1935**, *3 (2)*, 107-115.

(28) Armarego, W. L. *Purification of laboratory chemicals: Part 2 inorganic chemicals, catalysts, biochemicals, physiologically active chemicals, nanomaterials*; Butterworth-Heinemann, **2022**.

(29) Dastrup, D. M.; Yap, A. H.; Weinreb, S. M.; Henry, J. R.; Lechleiter, A. J. *Tetrahedron* **2004**, *60 (4)*, 901-906.

(30) Asako, S.; Nakajima, H.; Takai, K. *Nat. Catal.* **2019**, *2 (4)*, 297-303.

(31) Liu, Z.; Dong, N.; Xu, M.; Sun, Z.; Tu, T. *J. Org. Chem.* **2013**, *78 (15)*, 7436-7444.

(32) Liu, C.; Ji, C.-L.; Qin, Z.-X.; Hong, X.; Szostak, M. *iScience* **2019**, *19* 749-759.

(33) Vignesh, A.; Shalini, C.; Dharmaraj, N.; Kaminsky, W.; Karvembu, R. *Eur. J. Inorg. Chem.* **2019**, *2019 (34)*, 3869-3882.

(34) Milne, J. E.; Buchwald, S. L. *J. Am. Chem. Soc.* **2004**, *126 (40)*, 13028-13032.

(35) Becht, J.-M.; Catala, C.; Le Drian, C.; Wagner, A. *Org. Lett.* **2007**, *9 (9)*, 1781-1783.

(36) Voutchkova, A.; Coplin, A.; Leadbeater, N. E.; Crabtree, R. H. *Chem. Commun.* **2008**, *(47)*, 6312-6314.

(37) Kim, Y.; Tae, J.; Lee, K.; Rhim, H.; Choo, I. H.; Cho, H.; Park, W.-K.; Keum, G.; Choo, H. *Bioorg. Med. Chem.* **2014**, *22 (17)*, 4587-4596.

(38) Schaarschmidt, D.; Grumbt, M.; Hildebrandt, A.; Lang, H. *Eur. J. Org. Chem.* **2014**, *2014 (30)*, 6676-6685.

(39) Yin, Y.-B.; Peng, X.-S.; Wong, H. N. C. *Synthesis* **2023**, *55 (14)*, 2253-2260.

(40) Schmidt, T. A.; Sparr, C. *Angew. Chem., Int. Ed.* **2021**, *60 (44)*, 23911-23916.

(41) Hu, P.; Zhang, M.; Jie, X.; Su, W. *Angew. Chem., Int. Ed.* **2012**, *51 (1)*, 227-231.

(42) Dai, J.-J.; Liu, J.-H.; Luo, D.-F.; Liu, L. *Chem. Commun.* **2011**, *47 (2)*, 677-679.

(43) Chen, Q.; Wu, A.; Qin, S.; Zeng, M.; Le, Z.; Yan, Z.; Zhang, H. *Adv. Syn. Catal.* **2018**, *360 (17)*, 3239-3244.

(44) Shen, N.; Li, R.; Liu, C.; Shen, X.; Guan, W.; Shang, R. *ACS Catal.* **2022**, *12 (5)*, 2788-2795.

(45) Wang, J.; Tang, M.; Gu, W.; Huang, S.; Xie, L.-G. *J. Org. Chem.* **2022**, *87 (18)*, 12482-12490.

(46) Timsina, Y. N.; Xu, G.; Colacot, T. J. *ACS Catal.* **2023**, *13 (12)*, 8106-8118.

Chapter 5 Palladium-Catalyzed Chemoselective Decarboxylative Cross-Coupling of Polyfluorobenzoates with Chloroaryl Triflates at C–Cl Site under Mild Conditions

5.1 Introduction

Redox-neutral decarboxylative cross-coupling reactions have been widely used as potent synthetic methodologies for the regioselective construction of C–C bonds.[1] The most salient advantage of this category of reactions lies in the utilization of stable, easy-handle, ubiquitously available, and cost-effective carboxylic acids as surrogates to some expensive and less stable nucleophilic coupling partners. Over the last two decades, investigations on redox-neutral decarboxylative cross-coupling reactions have mainly focused on expanding the scope of carboxylic acids[2] and electrophiles,[3] as well as on lowering the reaction temperatures.[4] However, chemoselectivity of electrophiles bearing several reactive sites remains underexplored.

In 2009, Wu achieved chemoselective decarboxylative cross-coupling reaction in C–I > C–Cl or C–Br > C–Cl order utilizing palladium as the catalyst and silver salt as additive (Scheme 5.1 A). However, merely two examples have been documented, accompanied by limitations necessitating high reaction temperatures and low efficiency. Subsequently, the implementation of mechanism investigations[5] by Gooßen promoted the development of efficient Pd/Ag[4a] and Pd/Cu[4b] bimetallic catalytic systems to realize chemoselective C–C bond formation in C–OTf > C–Cl order under relatively low

reaction temperatures (Scheme 5.1B and 5.1C). Nevertheless, the number of reported cases remains insufficient, and the completion of the catalytic cycle still relies on the involvement of two metals, which further complicates the optimization of the reaction system. To the best of our knowledge, there has been no chemoselective redox-neutral decarboxylative cross-coupling reaction catalyzed by a monometallic system in C–Cl > C–OTf order so far. Based on our previous discovery that pyrazole-based phosphine ligand bearing *i*-Pr group at C3 and C5 positions can reduce the temperature of the decarboxylative cross-coupling reaction to 100 °C, and the ligand has also been shown to form Pd···H–C interaction with palladium, a key interaction that has been demonstrated to provide C–Cl > C–OTf reactivity order.[6] Therefore, we anticipated the ligand to be able to achieve chemoselective decarboxylative cross-coupling under mild conditions in C–Cl > C–OTf reactivity order (Scheme 5.1D).

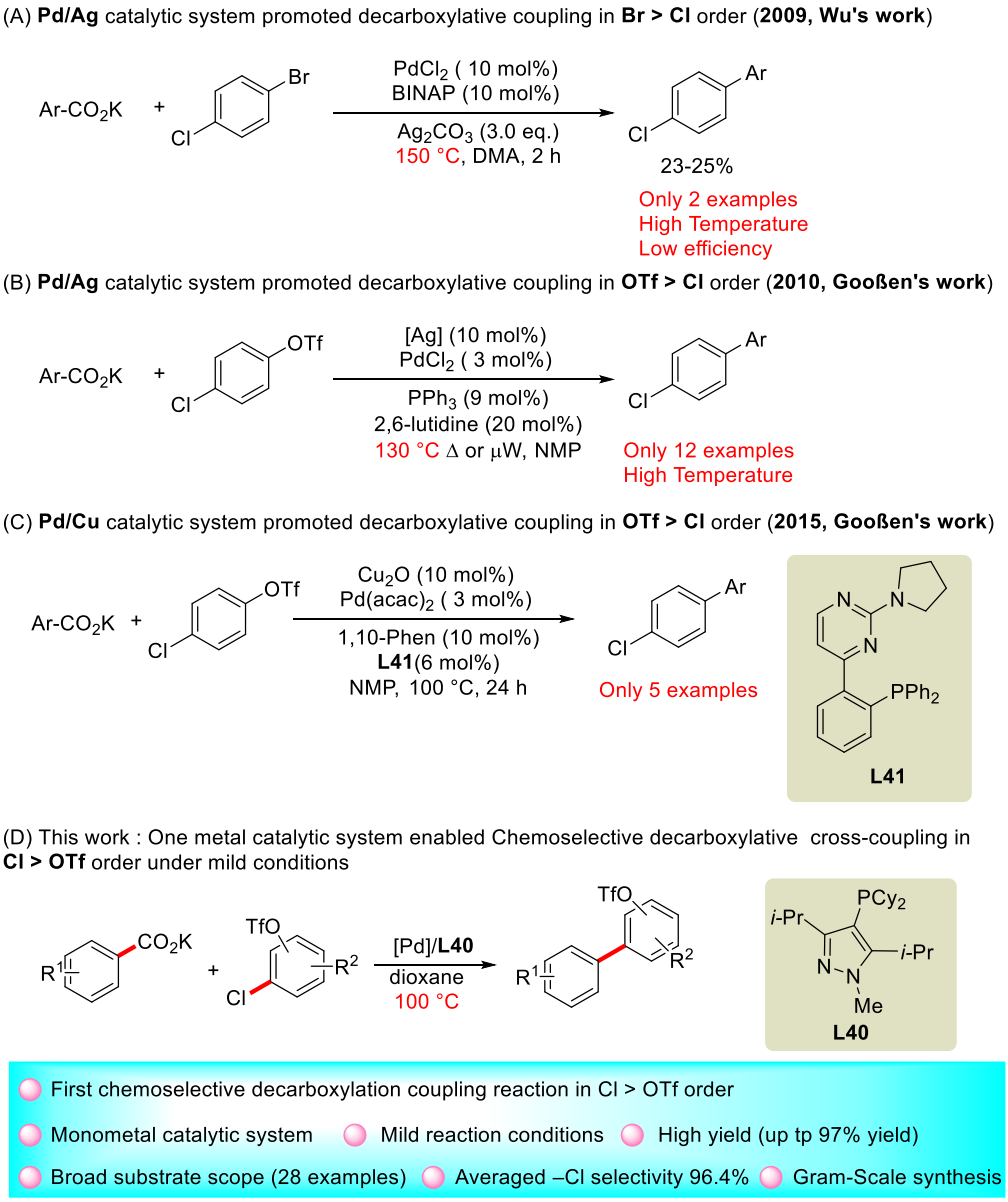

Scheme 5.1 Chemoselective decarboxylative cross-coupling reactions

5.2 Results and Discussion

5.2.1 Evaluation of Ligand Effect on Chemoselective Decarboxylative Cross-Coupling Reaction

We embarked on investigations by evaluating the effect of ligands on the chemoselective coupling of potassium 2,6-difluorobenzoate (**12c**) and 4-chlorophenyl triflate (**1a**) under 100 ºC (Table 5.1). Commercially available ligands were screened

first (Table 5.1, entries **1**–**9**). In the evaluation of mono-phosphine ligands, P*t*-Bu_3·HBF_4 (**L5**) and MordalPhos (**L16**) lead to C–Cl bond activation but with poor efficiency (Table 5.1, entries **3** and **9**). Other ligands including PPh_3 (**L1**), PCy_3 (**L2**), P(*o*-tolyl)$_3$ (**L6**) and Buchwald-type ligands (**L8**, **L10**, **L12**, and **L13**), preferred to activate the C–OTf bond but also showed poor reactivity (Table 5.1, entries **1**–**2** and entries **4**–**8**). Testing of bidentate ligands showed that both dppe (**L17**) and dppf (**L18**) preferentially activated the C–OTf bond, while BINAP (**L20**) gave mixed results. However, all these bidentate ligands exhibited poor reactivity (Table 5.1, entries **10**–**12**). Although the utilized NHC ligands (IMes·HCl and IPr·HCl) exhibited selectivity for C–Cl, extremely poor reactivity was obtained (Table 5.1, entries **13** and **14**). SelectPhos (**L24**)[6a-d] and BirdPhos (**L25**)[6e], both potent ligands capable of efficiently achieving a series of chemoselective cross-coupling reactions in the reactivity order of C–Cl > C–OTf, also exhibited low reactivity at this stage (Table 5.1, entries **15** and **16**). These results indicated that achieving efficient decarboxylative cross-coupling reactions at relatively low temperatures in the reactivity order of C–Cl > C–OTf is challenging. To our delight, the use of **L40** resulted in selective cleavage of the C–Cl bond, affording product **15a** in 86% yield, with only trace amounts of starting material remaining (Table 5.1, entry **17**).

Table 5.1 Ligand screening[a]

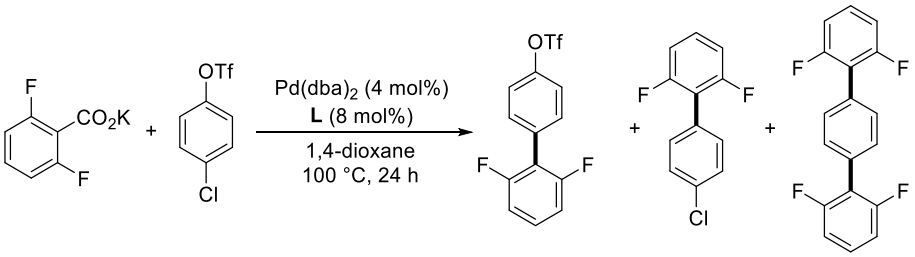

12c **1a** **15a** **16a** **17a**

entry	L	**15a** (%)[b]	**16a** (%)[b]	**17a** (%)[b]	Remaining of **1a** (%)[b]
1	**L1** = PPh_3	0	1	0	87
2	**L2** = PCy_3	0	1	0	83
3	**L5** = P*t*-Bu_3•HBF_4	29	0	0	70
4	**L6** = P(*p*-tolyl)$_3$	0	4	0	80
5	**L8** = Cy-JohnPhos	1	3	0	75
6	**L10** = SPhos	0	4	0	80
7	**L12** = XPhos	1	19	0	69
8	**L13** = BrettPhos	0	10	0	80
9	**L16** = MorDalPhos	1	0	0	90
10	**L17** = dppe	0	4	0	53
11	**L18** = dppf	1	18	0	78
12	**L20** = BINAP	1	1	0	81
13	**L22** = IMes•HCl	1	0	0	88
14	**L23** = IPr•HCl	1	0	0	87
15	**L24** = SelectPhos	12	0	0	80
16	**L25**	24	1	0	71
17	**L40**	**86**	0	0	3

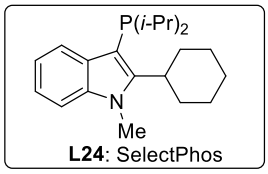

L24: SelectPhos

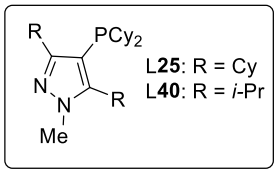

L25: R = Cy
L40: R = *i*-Pr

[a]Conditions: potassium 2,6-difluorobenzoate **12c** (0.3 mmol), 4-chlorophenyl triflate **1a** (0.2 mmol), $Pd(dba)_2$ (4 mol%), **L** (8 mol%), and 1,4-dioxane (1.0 ml) were stirred at 100 ºC for 24 h under a nitrogen atmosphere. [b]Yield determined by calibrated GC-FID analysis using dodecane as an internal standard.

5.2.2 Optimization of Reaction Condition

We then chose **L40** to further evaluate the effect of reaction conditions on the

reaction (Table 5.2). We initially investigated the influence of various metal species of benzoic acid on the reaction. The lithium salt of benzoic acid failed to yield any target products, whereas its sodium salt led to a slight reduction in yield (Table 5.2, entries **1** and **2**). These observations indicate that the nature of the metal salt of benzoic acid significantly impacts the reaction outcome. We endeavored to modify the Pd/L ratio and observed that both decreasing and increasing this ratio resulted in varying extents of yield reduction (Table 5.2, entries **3**–**5**). Screening of solvents revealed that other solvents including CPME, THF, and Toluene provided lower yields than Dioxane (Table 5.2, entries **6**–**8**), while the use of mixed solvents showed comparable or superior reactivity to dioxane (Table 5.2, entries **9**–**10**). For the screening of the palladium source (Table 5.2, entries **11**, **12**, and **14**–**16**), $[Pd(2\text{-butenyl})Cl]_2$ was found to complete the reaction more efficiently, which shortened the reaction time to 16 h and provided 95% isolated yield of **15a** (Table 5.2, entry **13**).

Table 5.2 Optimization of reaction conditions[a]

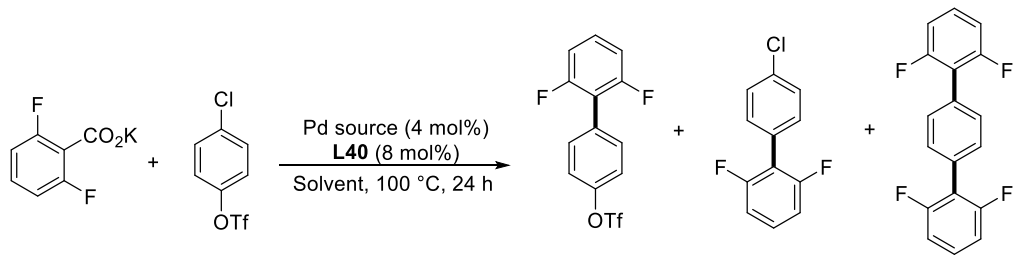

12c **1a** **15a** **16a** **17a**

Entry	Pd source	Pd: L	Solvent	**15a**(%)[b]	**16a** (%)[b]	**17a** (%)[b]
1[c]	$Pd(dba)_2$	1:2	Dioxane	0	0	0

2[d]	$Pd(dba)_2$	1:2	Dioxane	53	0	<1
3	$Pd(dba)_2$	1:1	Dioxane	71	0	0
4	$Pd(dba)_2$	1:3	Dioxane	61	0	<1
5	$Pd(dba)_2$	1:4	Dioxane	49	0	<1
6	$Pd(dba)_2$	1:2	CPME	46	0	0
7	$Pd(dba)_2$	1:2	Toluene	42	0	0
8	$Pd(dba)_2$	1:2	THF	77	0	<1
9	$Pd(dba)_2$	1:2	Dioxane+Toluene	84	0	<1
10	$Pd(dba)_2$	1:2	Dioxane+THF	91	0	<1
11	$Pd(OAc)_2$	1:2	Dioxane	32	0	0
12	$[Pd(\pi\text{-cinnamyl})Cl]_2$	1:2	Dioxane	32	0	0
13[h]	$[Pd(2\text{-butenyl})Cl]_2$	1:2	Dioxane	88 (**95** [e])	0	1
14	$[Pd(2\text{-allyl})Cl]_2$	1:2	Dioxane	37	0.1	0
15	Pd_2dba_3	1:2	Dioxane	58	0	0
16	$Pd_2dba_3 \cdot CHCl_3$	1:2	Dioxane	77	0.2	4
17[f,i]	$Pd(dba)_2$	1:2	Dioxane+THF	97	0	0
18[g,i]	$Pd(dba)_2$	1:2	Dioxane+THF	18	0	0

[a]Reaction condition: potassium 2,6-difluorobenzoate **12c** (0.3 mmol), 4-chlorophenyl triflate **1a** (0.2 mmol), [Pd] (4 mol%), **L40** (8 mol%) and solvent (1.0 mL) were stirred at 100 °C for 24 h. [b]Calibrated GC yields were reported by using dodecane as an internal standard. [c]$ArCO_2Li$ was used. [d]$ArCO_2Na$ was used. [e]Isolated yield. [f]90 °C. [g]80 °C. [h]16 h. [i]48 h.

5.2.3 Substrate Scope of Chloroaryl Triflates

We then initially explored the substrate scope of chloroaryl triflates (Table 5.3). A variety of chloroaryl triflates bearing electron-donating groups (–Me, –OMe, and –Bn) and electron-withdrawing groups (–F, $–CF_3$, –CHO, and ketone) were coupled with potassium 2,6-difluorobenzoate smoothly and afforded corresponding products in excellent yields as well as chemoselectivity at –Cl (Table 5.3, **15c**–**15p**). It is worth noting that substrates containing reactive functional groups such as aldehyde were tolerated well (Table 5.3, **15n**). Regardless of the positional variation of the –Cl and –OTf groups (*ortho*, *meta*, or *para*), the chloroaryl triflates underwent chemoselective decarboxylative coupling with potassium 2,6-difluorobenzoate to yield C–C bond coupling products in excellent yields as well as chemoselectivity (**15a**, **15b** and **15i**).

Table 5.3 Substrate scope of chloroaryl triflates[a]

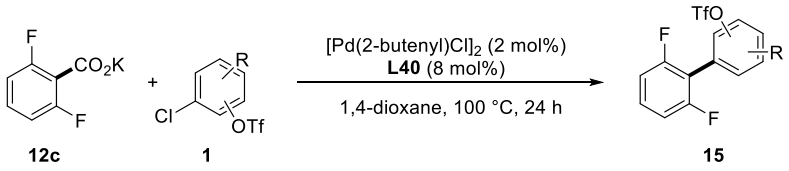

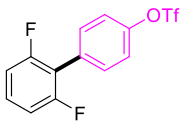

15a, 95%[f]
(97.9 : 0 : 2.1)

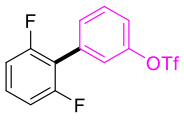

15b, 91%
(97.9 : 0 : 2.1)

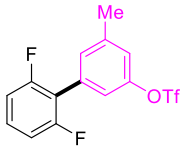

15c, 80%
(98.9 : 0 : 1.1)

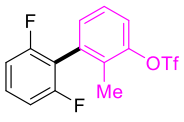

15d, 97%[b,f]
(97.0 : 0 : 3.0)

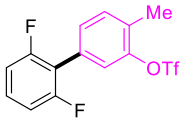

15e, 91%
(98.6 : 0.2 : 1.2)

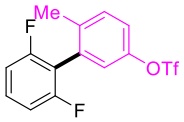

15f, 89%[b,g]
(98.9 : 0 : 1.1)

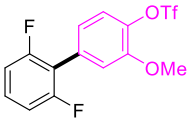

15g, 98%[b,f]
(99.0 : 0 : 1.0)

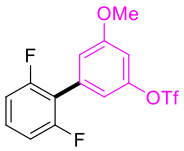

15h, 94%
(97.0 : 0 : 3.0)

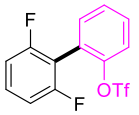

15i, 86%[c]
(98.7 : 0.9 : 0.4)

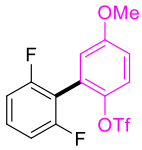

15j, 88%[c]
(100 : 0 : 0)

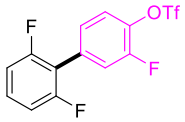

15k, 94%[c,i]
(96.6 : 0 : 3.4)

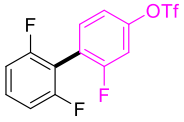

15l, 86%
(97.0 : 0 : 3.0)

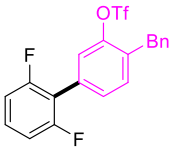

15m, 96%[i]
(99.0 : 0 : 1.0)

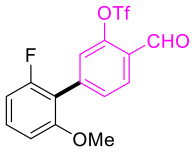

15n, 90%[d,i]
(94.8 : 0.8 : 4.4)

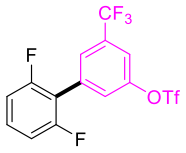

15o, 86%
(98.1 : 0 : 1.9)

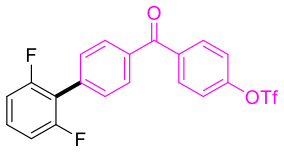

15p, 92%
(100 : 0 : 0)

[a]Conditions: potassium 2,6-difluorobenzoate **12c** (0.3 mmol), Cl−Ar−OTf **1** (0.2 mmol), Pd(2-butenyl)Cl]$_2$ (2 mol%), **L40** (8 mol%) and 1,4-dioxane (1.0 ml) were stirred at 100 °C for 24 h under a nitrogen atmosphere. Isolated yields were reported. [b]110 °C. [c]120 °C. [d]3 h. [e]14 h. [f]16 h. [g]18 h. [h]20 h. [i]1.2 eq. **1a** was used.

5.2.4 Substrate Scope of (Hetero)aryl Carboxylates

We next investigated an array of potassium benzoates (Table 5.4). A series of *ortho*-difluorobenzoic acid substrates bearing electron-donating groups such as –Me or electron-withdrawing groups like –F groups, reacted efficiently with 4-chlorophenyl

triflate **1a**, yielding the corresponding products with excellent chemoselectivity and yields (Table 5.4, **15q**–**15u**). Previous works have identified substrates such as *ortho*-fluorobenzoic acids bearing only one –F group or those with electron-donating groups such as –OMe in the *ortho* position as challenging substrates.[7] Delightfully, our catalytic system enables the chemoselective decarboxylative cross-coupling reactions at –Cl under relatively mild temperatures, giving rise to coupling products in 85-95% yields (Table 5.4, **15v**–**15z**). The high-performance catalyst Pd/**L40** also allowed heterocyclic benzoates such as *N*-substituted pyrrole and indole carboxylates to react well with 4-chlorophenyl triflate **1a**, providing corresponding products in moderate to excellent yields (Table 5.4, **15aa** and **15ab**).

Table 5.4 Substrate scope of (hetero)aryl carboxylates[a]

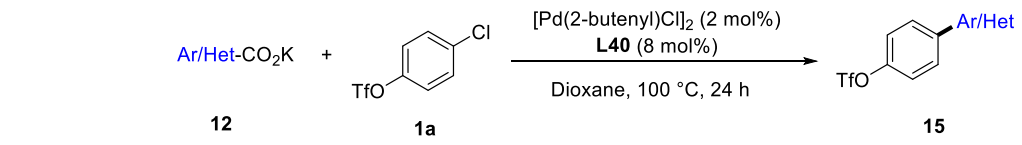

12 1a 15

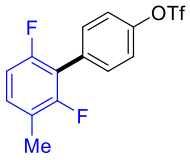

15q, 97%[b,h]
(98.1 : 0 : 1.9)

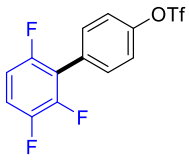

15r, 94%[b,g]
(94.6 : 0 : 5.4)

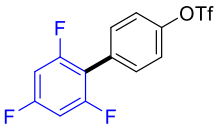

15s, 84%[b,g]
(95.9 : 0 : 4.1)

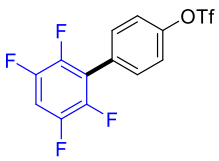

15t, 86%[c,i]
(97.8 : 0 : 2.2)

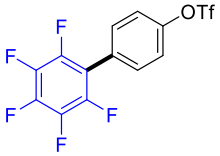

15u, 89%
(96.2 : 0 : 3.8)

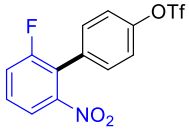

15v, 85%[b,g]
(92.5 : 0 : 7.5)

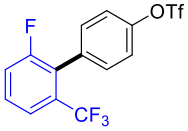

15w, 92%[b,f]
(98.4 : 0 : 1.6)

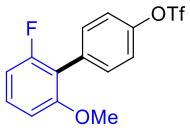

15x, 94%
(94.1 : 0 : 5.9)

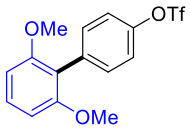

15y, 95%
(98.5 : 0 : 1.5)

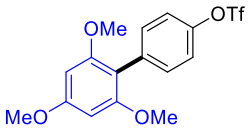

15z, 94%
(100 : 0 : 0)

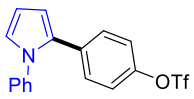

15aa, 93%[h]
(93.8 : 0 : 6.2)

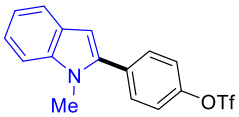

15ab, 44%[d]
(100 : 0 : 0)

[a]Conditions: **12** (0.3 mmol), 4-chlorophenyl triflate **1a** (0.2 mmol), $[Pd(2\text{-butenyl})Cl]_2$ (2 mol%), **L40** (8 mol%), and 1,4-dioxane (1.0 ml) were stirred at 100 °C for 24 h under a nitrogen atmosphere. Isolated yields were reported. [b]110 °C. [c]120 °C. [d]140 °C. [e]14 h. [f]18 h. [g]20 h. [h]1.2 eq. **12** was used. [i]1.0 eq. **12** was used.

5.2.5 Gram-Scale Chemoselective Decarboxylative Cross-Coupling Reaction

To explore the feasibility of scaling up the current reaction conditions, we carried out a gram-scale reaction of potassium 2,6-difluorobenzoate **12c** with 4-chlorophenyl triflate **1a** (Scheme 5.2). It provided the desired coupling product **15a** in 89% isolated yield with prolonged reaction time, without any erosion of the previously observed chemoselectivity.

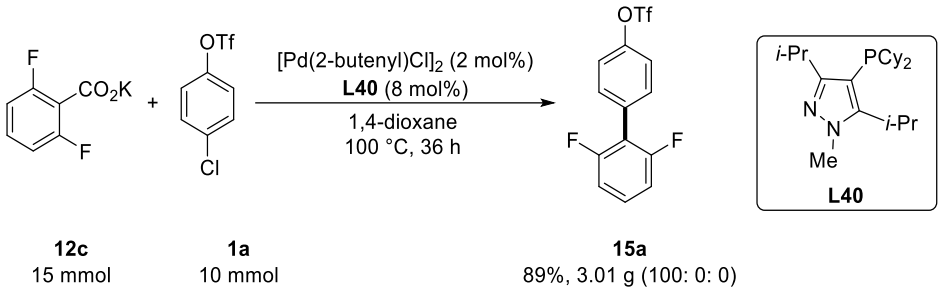

Scheme 5.2 Gram-scale chemoselective C–Cl (over C–OTf) decarboxylative cross-coupling reaction

5.3 Conclusion

In summary, we have demonstrated a palladium-catalyzed ligand-controlled chemoselective decarboxylative cross-coupling reaction of a wide spectrum of benzoates including *ortho*-di- or mono-fluoro substituted, *ortho*-methoxy substituted benzoic acids, or some heteroaromatic carboxylic acids with chloroaryl triflates, can be achieved utilizing a novel alkyl-pyrazole-based ligand (**L40**). We also utilized the Pd/**L40** catalytic system to achieve gram-scale synthesis of biaryls with excellent chemoselectivity at the C–Cl bond. In the redox-neutral decarboxylative cross-coupling reactions, the inert C–Cl bond undergoes preferential functionalization in the presence of the more active C–OTf bond, thereby establishing a reverse reactivity sequence of C–Cl > C–OTf, distinct from those previously reported. Additionally, the remaining reactive C–OTf group in the newly formed aromatic coupling products possesses substantial potential for further downstream functionalization. Moreover, our catalytic system operates under relatively mild conditions, which also allows for compatibility with some sensitive functional groups such as aldehydes and ketones. Further

functional group modification of the products and investigation into the reaction mechanism will be conducted in subsequent studies.

5.4 Experimental Section

5.4.1 General Consideration

Unless otherwise noted, all reagents were purchased from commercial suppliers and used without purification. All Pd-catalyzed reactions were performed in a resealable screw cap Schlenk tube (approx. 20 mL volume) in the presence of a Teflon-coated magnetic stirrer bar (5 mm x 10 mm). Dioxane, CPME, and toluene were freshly distilled from sodium under nitrogen. Tetrahydrofuran (THF) was freshly distilled from sodium benzophenone ketyl under nitrogen. $Pd(OAc)_2$, $Pd(dba)_2$, Pd_2dba_3, and $[Pd(\pi\text{-cinnamyl})Cl]_2$ were purchased from Strem. $PdCl_2$ and $[Pd(2\text{-butenyl})Cl]_2$ were purchased from Energy. A new bottle of n-butyllithium was used. Thin-layer chromatography was performed on pre-coated silica gel 60 F254 plates. Silica gel (Grace, 60Å, 40-63 mm) was used for column chromatography. Melting points were recorded on an uncorrected Stuart Melting Point SMP30 instrument. NMR spectra were recorded on a Brüker spectrometer (400 MHz for ^{1}H, 100 MHz for ^{13}C, 376 MHz for ^{19}F and 162 MHz for ^{31}P) and Jeol JMN-ECZ500R/S1 spectrometer (465.89 MHz for ^{19}F and 200.43 MHz for ^{31}P). Spectra were referenced internally to the residual proton resonance in $CDCl_3$ (δ 7.26 ppm) as the internal standard. ^{13}C NMR spectra were referenced to $CDCl_3$ (δ 77.0 ppm, the middle peak). ^{19}F NMR chemical shifts were determined relative to $CFCl_3$ as the external standard and low field is positive. ^{31}P NMR

spectra were referenced to 85% H_3PO_4 externally. Coupling constants (J) were reported in Hertz (Hz). Mass spectra (EI-MS) were recorded on an HP 5977A MSD Mass Spectrometer. High-resolution mass spectra (HRMS) were obtained on the Agilent 6540 ESI-QTof-MS or APPI-QTof-MS and a Waters GCT Premier EI-ToF-MS. GC-MS analysis was conducted on a HP 7890B GC system using a HP5MS column (30 m × 0.25 mm). The products described in GC yield were accorded to the authentic samples/dodecane calibration standard from HP 7890B GC-FID system. All yields reported referring to the isolated yield of compounds estimated to be greater than 95% purity as determined by capillary gas chromatography (GC) or ^{1}H NMR. Compounds described in the literature were characterized by a comparison of their ^{1}H, ^{13}C, ^{19}F and/or ^{31}P NMR spectra to the previously reported data. The procedures in this section are representative, and thus the yields may differ from those reported in tables.

5.4.2 General Procedure for Ligand Screening

Potassium 2,6-difluorobenzoate **12c** (0.30 mmol, 59.8 mg), Pd $(dba)_2$ (0.0080 mmol, 4.60 mg), and ligand (0.0160 mmol) were added to the Schlenk tube that was charged with Teflon-coated magnetic stir bar (5 mm x 10 mm) and equipped with screw cap. The tube was carefully evacuated and flushed with nitrogen (3 cycles). 4-Chlorophenyltriflate **1a** (0.20 mmol, 52.0 mg) and the freshly distilled dioxane (1.0 mL) were added via syringes. The tube was sealed and magnetically stirred at a preheated 100 ºC bath for 24 h. The reaction was then allowed to reach room temperature. Ethyl acetate (~4 mL), dodecane (45.2 mL, internal standard), and water (~2 mL) were added.

The organic layer was subjected to GC analysis. The GC yield was previously calibrated by an authentic sample/dodecane calibration curve.

5.4.3 General Procedure for Reaction Condition Screening

Pd source (0.0080 mmol), **L40** (0.0080-0.032 mmol), and potassium 2,6-difluorobenzoate (0.30 mmol, 58.8 mg) were added to the Schlenk tube that was charged with Teflon-coated magnetic stir bar (5 mm x 10 mm) and equipped with screw cap. The tube was carefully evacuated and flushed with nitrogen (3 cycles). 4-Chlorophenyltriflate (0.20 mmol, 52.0 mg) and the freshly distilled solvent (1.0 mL) were added via syringes. The tube was sealed and magnetically stirred in a preheated 100 °C oil bath for 24 h. The reaction was then allowed to reach room temperature. Ethyl acetate (~4 mL), dodecane (45.2 mL, internal standard), and water (~2 mL) were added. The organic layer was subjected to GC analysis. The GC yield was previously calibrated by an authentic sample/dodecane calibration curve.

5.4.4 General Procedure for Exploring the Substrate Scope

Potassium aryl benzoate (0.30 mmol), **L40** (0.016 mmol, 5.80 mg), and [Pd(2-butenyl) Cl]$_2$ (0.0040 mmol, 1.60 mg) were added to the Schlenk tube that was charged with Teflon-coated magnetic stir bar (5 mm x 10 mm) and equipped with screw cap. The tube was carefully evacuated and flushed with nitrogen (3 cycles). Chloroaryl triflates (0.20 mmol) and the freshly distilled dioxane (1.0 mL) were added to the tube via syringe. The tube was resealed and magnetically stirred in a preheated 100 °C oil bath for 24 h. The reaction was allowed to reach room temperature. Ethyl acetate (~4

mL) and water (~2 mL) were added. The organic layer was subjected to GC analysis. The aqueous layer was washed with ethyl acetate. The organic layers were combined and concentrated. The crude products were purified by column chromatography on silica gel (230-400 mesh) to afford the desired product.

5.4.5 Characterization Data

2',6'-Difluoro-[1,1'-biphenyl]-4-yl trifluoromethanesulfonate (Table 5.3, compound 15a)[8]

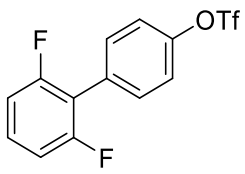

Yield: 95% (64.6 mg). White solid, m.p. = 64.3–66.0 °C. Eluent (R_f = 0.5, Hexane = 100) was used for flash column chromatography. **^{1}H NMR** (400 MHz, $CDCl_3$) δ 7.57 (d, *J* = 8.4 Hz, 2H), 7.39-7.30 (m, 3H), 7.04-7.00 (m, 2H); **^{13}C NMR** (150 MHz, $CDCl_3$) δ 159.9 (dd, *J* = 6.6, 248.2 Hz, 1C), 149.2, 132.3 (t, *J* = 2.6 Hz, 1C), 129.8 (d, *J* = 20.7 Hz, 1C), 129.7 (d, *J* = 19.1 Hz, 1C), 121.2, 118.8 (q, *J* = 318.7 Hz, 1C), 116.6 (t, *J* = 18.1 Hz, 1C), 111.9-111.8 (m, 1C); **^{19}F NMR** (565 MHz, $CDCl_3$) δ -72.8, -114.5.

2',6'-Difluoro-[1,1'-biphenyl]-3-yl trifluoromethanesulfonate (Table 5.3, compound 15b)

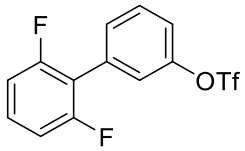

Yield: 91% (61.7 mg). Colorless liquid. Eluent (R_f = 0.7, Hexane: Ethyl acetate = 20:1)

was used for flash column chromatography. **^{1}H NMR** (600 MHz, $CDCl_3$) δ 7.56 -7.51 (m, 2H), 7.43 (s, 1H), 7.36-7.32 (m, 2H), 7.04-7.01 (m, 2H); **^{13}C NMR** (150 MHz, $CDCl_3$) δ 159.8 (dd, *J* = 6.6, 248.6 Hz, 1C), 149.4, 131.6, 130.4, 129.99 (d, *J* = 20.6 Hz, 1C), 129.98, 123.3, 121.1, 118.8 (q, *J* = 318.8 Hz, 1C), 116.3 (t, *J* = 17.8 Hz, 1C), 111.9 (dd, *J* = 21.5, 5.0 Hz, 1C); **^{19}F NMR** (565 MHz, $CDCl_3$) δ -72.20– -74.12 (m, 1F), -113.31– -116.03 (m, 2F); **HRMS** (EI): calcd for $C_{13}H_7SF_5O_3^+$: 338.0031, found 338.0035.

2',6'-Difluoro-5-methyl-[1,1'-biphenyl]-3-yl trifluoromethanesulfonate (Table 5.3, compound 15c)

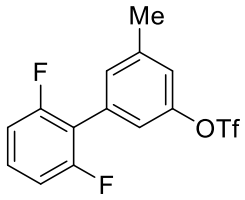

Yield: 80% (56.5 mg). Colorless liquid. Eluent (R_f = 0.6, Hexane: Ethyl acetate = 20:1) was used for flash column chromatography. **^{1}H NMR** (600 MHz, $CDCl_3$) δ 7.35-7.31 (m, 2H), 7.22 (s, 1H), 7.15 (s, 1H), 7.01 (t, *J* = 7.7 Hz, 2H), 2.46 (s, 3H); **^{13}C NMR** (100 MHz, $CDCl_3$) δ 159.9 (dd, *J* = 6.6, 248.3 Hz, 1C), 149.3, 140.7, 131.2, 131.1, 129.8 (t, *J* = 10.3 Hz, 1C), 121.6, 120.2, 118.8 (q, *J* = 318.9 Hz, 1C), 116.6 (t, *J* = 18.2 Hz, 1C), 111.8 (dd, *J* = 21.5, 5.0 Hz, 1C), 21.3; **^{19}F NMR** (565 MHz, $CDCl_3$) δ -72.9, -114.4; **HRMS** (EI): calcd for $C_{14}H_9SF_5O_3^+$: 352.0187, found 352.0175.

1-(2',6'-Dimethoxy-[1,1'-biphenyl]-4-yl) propan-1-one (Table 5.3, compound 15d)

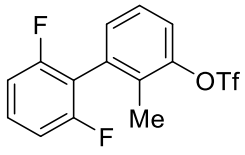

Yield: 97% yield (68.1 mg). Light-yellow liquid. Eluents (R_f = 0.5, Hexane = 100) was used for flash column chromatography. **^{1}H NMR** (600 MHz, $CDCl_3$) δ 7.41-7.37 (m, 1H), 7.36-7.35 (m, 2H), 7.30-7.28 (m, 1H), 7.04-7.00 (m, 2H), 2.20 (s, 3H); ^{13}C NMR (150 MHz, $CDCl_3$) δ 159.9 (dd, *J* = 247.2, 6.8 Hz, 1C), 148.8, 132.1, 130.9, 130.8, 130.1 (t, *J* = 10.2 Hz, 1C), 126.9, 121.5, 118.7 (q, *J* = 318.2 Hz, 1C), 116.3 (t, *J* = 20.6 Hz, 1C), 111.7-111.5 (m, 1C), 13.7; **^{19}F NMR** (565 MHz, $CDCl_3$) δ -73.8, -112.1; **HRMS** (EI): calcd for $C_{14}H_9SF_5O_3^+$: 352.0187, found 352.0194.

2',6'-Difluoro-4-methyl-[1,1'-biphenyl]-3-yl trifluoromethanesulfonate (Table 5.3, compound 15e)

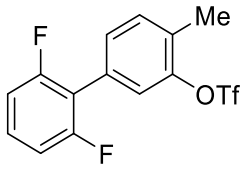

Yield: 91% (64.2 mg). Light-yellow liquid. Eluent (R_f = 0.5, Hexane = 100) was used for flash column chromatography. **^{1}H NMR** (400 MHz, $CDCl_3$) δ 7.42-7.39 (m, 3H), 7.36-7.28 (m, 1H), 7.04-6.98 (m, 2H), 2.45 (s, 3H); **^{13}C NMR** (100 MHz, $CDCl_3$) δ 159.9 (dd, *J* = 6.6, 248.0 Hz, 1C), 148.2, 131.9, 130.9, 130.17 (t, *J* = 2.1 Hz, 1C), 129.7 (t, *J* = 10.4 Hz, 1C), 128.9, 123.2, 118.7 (q, *J* = 318.3 Hz, 1C), 116.40 (t, *J* = 18.1 Hz, 1C), 112.0-111.0 (m, 1C), 16.2; **^{19}F NMR** (565 MHz, $CDCl_3$) δ -73.7, -114.6; **HRMS** (EI): calcd for $C_{14}H_9SF_5O_3^+$: 352.0187, found 352.0189.

2',6'-Difluoro-6-methyl-[1,1'-biphenyl]-3-yl trifluoromethanesulfonate (Table 5.3, compound 15f)

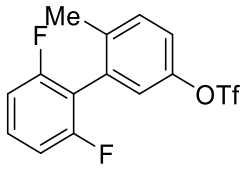

Yield: 89% (62.7 mg). Light-yellow liquid. Eluent (R_f = 0.6, Hexane = 100) was used for flash column chromatography. **^{1}H NMR** (400 MHz, $CDCl_3$) δ 7.40-7.34 (m, 2H), 7.26 (dd, *J* = 8.5, 2.6 Hz, 1H), 7.18 (d, *J* = 2.1 Hz, 1H), 7.04-6.98 (m, 2H), 2.21 (s, 3H); **^{13}C NMR** (150 MHz, $CDCl_3$) δ 159.8 (dd, *J* = 247.3, 7.2 Hz, 1C), 147.2, 138.3, 131.7, 131.0, 130.1 (t, *J* = 10.3 Hz, 1C), 123.4, 121.3, 118.8 (q, *J* = 318.6 Hz, 1C), 116.2 (t, *J* = 20.8 Hz, 1C), 111.7-111.5 (m, 1C), 19.3; **^{19}F NMR** (565 MHz, $CDCl_3$) δ -72.8, -112.2; **HRMS** (EI): calcd for $C_{14}H_9SF_5O_3^+$: 352.0187, found 352.0194.

2',6'-Difluoro-3-methoxy-[1,1'-biphenyl]-4-yl trifluoromethanesulfonate (Table 5.3, compound 15g)

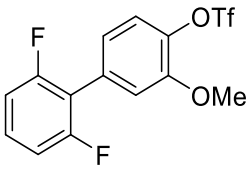

Yield: 98% (72.3 mg). Light-yellow liquid. Eluent (R_f = 0.2, Hexane = 100) was used for flash column chromatography. **^{1}H NMR** (600 MHz, $CDCl_3$) δ 7.36-7.32 (m, 1H), 7.30 (d, *J* = 8.4 Hz, 1H), 7.14 (s, 1H), 7.09 (d, *J* = 8.4 Hz, 1H), 7.03-6.99 (m, 2H), 3.94 (s, 3H); **^{13}C NMR** (150 MHz, $CDCl_3$) δ 159.9 (dd, *J* = 248.1, 6.6 Hz, 1C), 151.1, 138.4, 130.4, 129.7 (t, *J* = 10.1 Hz, 1C), 123.0, 122.2, 118.7 (q, *J* = 318.2 Hz, 1C), 117.0 (t, *J* = 18.0 Hz, 1C), 115.4, 111.9-111.7 (m, 1C), 56.2; **^{19}F NMR** (565 MHz, $CDCl_3$) δ -72.9, -114.0; **HRMS** (EI): calcd for $C_{14}H_9SF_5O_4^+$: 368.0136, found 368.0123.

2',6'-Difluoro-5-methoxy-[1,1'-biphenyl]-3-yl trifluoromethanesulfonate (Table 5.3, compound 15h)

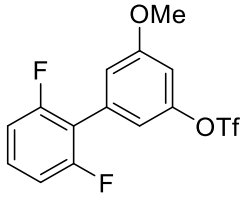

Yield: 94% (69.3 mg). Light-yellow liquid. Eluent (R_f = 0.2, Hexane = 100) was used for flash column chromatography. **^{1}H NMR** (400 MHz, $CDCl_3$) δ 7.37-7.30 (m, 1H), 7.05 (s, 1H), 7.01 (t, *J* = 8.1 Hz, 3H), 6.87 (t, *J* = 2.1 Hz, 1H), 3.86 (s, 3H); **^{13}C NMR** (100 MHz, $CDCl_3$) δ 160.5, 159.8 (dd, *J* = 248.4, 6.5 Hz, 1C), 149.9, 131.9, 130.0 (t, *J* = 10.3 Hz, 1C), 118.7 (q, *J* = 318.9 Hz, 1C), 116.5 (t, *J* = 18.0 Hz, 1C), 116.3 (t, *J* = 2.2 Hz, 1C), 115.3, 112.0-111.7 (m, 1C), 107.3, 55.8; **^{19}F NMR** (565 MHz, $CDCl_3$) δ -72.8, -114.1; **HRMS** (EI): calcd for $C_{14}H_9SF_5O_4^+$: 368.0136, found 368.0138.

2',6'-Difluoro-[1,1'-biphenyl]-2-yl trifluoromethanesulfonate (Table 5.3, compound 15i)

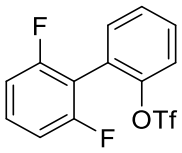

Yield: 86% (58.0 mg). Light-yellow liquid. Eluent (R_f = 0.5, Hexane = 100) was used for flash column chromatography. **^{1}H NMR** (600 MHz, $CDCl_3$) δ 7.55-7.51 (m, 1H), 7.50-7.48 (m, 2H), 7.45 (d, *J* = 8.3 Hz, 1H), 7.43-7.39 (m, 1H), 7.06-7.01 (m, 2H); **^{13}C NMR** (150 MHz, $CDCl_3$) δ 160.1 (dd, *J* = 249.0, 6.6 Hz, 1C), 147.5, 133.0, 130.9 (t, *J* = 10.4 Hz, 1C), 130.6, 128.2, 123.2, 121.8, 118.4 (q, *J* = 318.5 Hz, 1C), 112.4 (t, *J* = 19.7 Hz, 1C), 111.6-111.5 (m, 1C); **^{19}F NMR** (565 MHz, $CDCl_3$) δ -74.2, -112.0;

HRMS (APPI): calcd for $C_{13}H_7SF_5O_3^+$: 338.0031, found 338.0021.

2',6'-Difluoro-5-methoxy-[1,1'-biphenyl]-2-yl trifluoromethanesulfonate (Table 5.3, compound 15j)

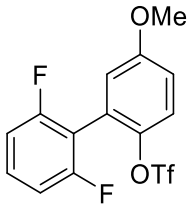

Yield: 88% (64.7 mg). Light-yellow liquid. Eluent (R_f = 0.2, Hexane = 100) was used for flash column chromatography. **^{1}H NMR** (400 MHz, $CDCl_3$) δ 7.44-7.38 (m, 1H), 7.35 (d, *J* = 9.1 Hz, 1H), 7.06-7.02 (m, 2H), 7.00 (d, *J* = 3.8 Hz, 1H), 6.97 (d, *J* = 2.8 Hz, 1H), 3.84 (s, 3H); **^{13}C NMR** (100 MHz, $CDCl_3$) δ 160.1 (dd, *J* = 249.1, 6.4 Hz, 1C), 158.7, 141.0, 130.9 (t, *J* = 10.1 Hz, 1C), 124.2, 122.7, 118.4 (q, *J* = 318.5 Hz, 1C), 117.6, 115.5, 112.5 (t, *J* = 19.5 Hz, 1C), 111.7-111.4 (m, 1C), 55.8; **^{19}F NMR** (565 MHz, $CDCl_3$) δ -74.1, -111.9; **HRMS** (EI): calcd for $C_{14}H_9SF_5O_4^+$: 368.0136, found 368.0139.

2',3,6'-Trifluoro-[1,1'-biphenyl]-4-yl trifluoromethanesulfonate (Table 5.3, compound 15k)

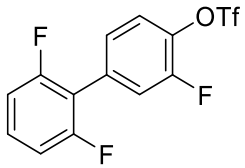

Yield: 88% (63.0 mg). White solid, m.p. = 50.5–52.8 ºC. Eluent (R_f = 0.4, Hexane = 100) was used for flash column chromatography. **^{1}H NMR** (400 MHz, $CDCl_3$) δ 7.52-7.49 (m, 2H), 7.38-7.31 (m, 2H), 7.02 (t, *J* = 8.0 Hz, 2H); **^{13}C NMR** (100 MHz, $CDCl_3$) δ 159.8 (dd, *J* = 6.4, 248.3 Hz, 1C), 153.3 (d, *J* = 253.8 Hz, 1C), 136.5 (d, *J* = 13.7 Hz,

1C), 131.8 (d, *J* = 7.1 Hz, 1C), 130.1 (t, *J* = 10.4 Hz, 1C), 126.5 (d, *J* = 4.2 Hz, 1C), 125.6, 118.7 (q, *J* = 318.8 Hz, 1C), 117.4 (d, *J* = 18.4 Hz, 1C), 115.6 (t, *J* = 17.9 Hz, 1C), 112.0 (dd, *J* = 12.9, 6.5 Hz, 1C); **^{19}F NMR** (565 MHz, $CDCl_3$) δ -73.2, -114.8, -127.5; **HRMS** (EI): calcd for $C_{13}H_6SF_6O_3^+$: 355.9936, found 355.9946.

2,2',6'-Trifluoro-[1,1'-biphenyl]-4-yl trifluoromethanesulfonate (Table 5.3, compound 15l)

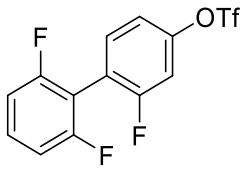

Yield: 86% (61.4 mg). White solid, m.p. = 76.0–78.4 ºC. Eluent (R_f = 0.6, Hexane = 100) was used for flash column chromatography. **^{1}H NMR** (600 MHz, $CDCl_3$) δ 7.50 (t, *J* = 7.6 Hz, 1H), 7.43-7.38 (m, 1H), 7.22-7.18 (m, 2H), 7.04-7.02 (m, 2H); **^{13}C NMR** (100 MHz, $CDCl_3$) δ 160.09 (dd, *J* = 249.3, 6.4 Hz, 1C), 159.95 (d, *J* = 253.2 Hz, 1C), 149.7 (d, *J* = 10.8 Hz, 1C), 133.5 (d, *J* = 4.1 Hz, 1C), 130.8 (t, *J* = 10.2 Hz, 1C), 118.7 (q, *J* = 319.0 Hz, 1C), 117.8 (d, *J* = 16.2 Hz, 1C), 117.1 (t, *J* = 3.8 Hz, 1C), 111.8-111.5 (m, 1C), 111.0 (t, *J* = 2.0 Hz, 1C), 110.1 (d, *J* = 26.7 Hz, 1C); **^{19}F NMR** (565 MHz, $CDCl_3$) δ -72.8, -106.9 (d, *J* = 10.3 Hz, 1F), -112.2 (d, *J* = 10.3 Hz, 1F) ; **HRMS** (EI): calcd for $C_{13}H_6SF_6O_3^+$: 355.9936, found 355.9937.

4-Benzyl-2',6'-difluoro-[1,1'-biphenyl]-3-yl trifluoromethanesulfonate (Table 5.3, compound 15m)

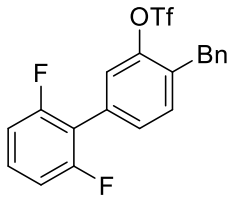

Yield: 96% (82.4 mg). White solid, m.p. = 71.7–73.8 ºC. Eluent (R_f = 0.4, Hexane = 100) was used for flash column chromatography. **^{1}H NMR** (400 MHz, $CDCl_3$) δ 7.46-7.26 (m, 9H), 7.00 (t, *J* = 1.9 Hz, 2H), 4.18 (s, 2H); **^{13}C NMR** (100 MHz, $CDCl_3$) δ 159.9 (dd, *J* = 247.9, 6.7 Hz, 1C), 147.6, 138.2, 133.9, 133.8, 130.2, 129.59 (t, *J* = 10.4 Hz, 1C), 129.56, 129.0, 128.7, 126.7, 121.2, 118.6 (q, *J* = 318.2 Hz, 1C), 116.7 (t, *J* = 18.4 Hz, 1C), 111.9-111.6 (m, 1C), 35.8; **^{19}F NMR** (565 MHz, $CDCl_3$) δ -73.7, -114.4; **HRMS** (EI): calcd for $C_{20}H_{13}SF_5O_3^+$: 428.0500, found 428.0501.

2'-Fluoro-4-formyl-6'-methoxy-[1,1'-biphenyl]-3-yl trifluoromethanesulfonate (Table 5.3, compound 15n)

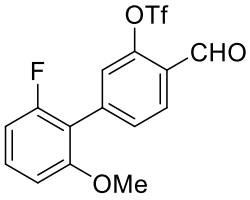

Yield: 90% (68.1 mg). Light-yellow liquid. Eluent (R_f = 0.4, Hexane: DCM = 5: 1) was used for flash column chromatography. **^{1}H NMR** (600 MHz, $CDCl_3$) δ 10.28 (s, 1H), 8.02 (d, *J* = 8.0 Hz, 1H), 7.64 (d, *J* = 8.0 Hz, 1H), 7.52 (s, 1H), 7.38-7.35 (m, 1H), 6.85-6.82 (m, 2H), 3.82 (s, 3H); **^{13}C NMR** (150 MHz, $CDCl_3$) δ 186.4, 160.0 (d, *J* = 246.1 Hz, 1C), 157.4 (d, *J* = 6.2 Hz, 1C), 149.2, 140.2, 131.3 (d, *J* = 2.0 Hz, 1C), 130.8 (d, J = 10.9 Hz, 1C), 130.1, 127.0, 124.9, 118.6 (q, *J* = 319.2 Hz, 1C), 115.4 (d, *J* = 16.3 Hz, 1C), 108.5 (d, *J* = 22.9 Hz, 1C), 107.0 (d, *J* = 2.5 Hz, 1C), 56.0; **^{19}F NMR** (565 MHz, $CDCl_3$) δ -72.8, -115.1; **HRMS** (APPI): calcd for $C_{15}H_{10}SF_4O_5^+$: 378.0180, found

378.0169.

2',6'-Difluoro-5-(trifluoromethyl)-[1,1'-biphenyl]-3-yl trifluoromethanesulfonate (Table 5.3, compound 15o)

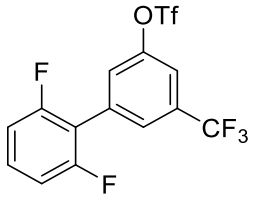

Yield: 86% (70.1 mg). Light-yellow liquid. Eluent (R_f = 0.6, Hexane = 100) was used for flash column chromatography. **^{1}H NMR** (400 MHz, $CDCl_3$) δ 7.82 (s, 1H), 7.63 (s, 1H), 7.59 (s, 1H). 7.43-7.38 (m, 1H), 7.08-7.04 (m, 2H); **^{13}C NMR** (100 MHz, $CDCl_3$) δ 159.7 (dd, *J* = 249.4, 6.2 Hz, 1C), 149.2, 132.9 (q, *J* = 33.8 Hz, 1C), 132.89, 130.9 (t, *J* = 10.4 Hz, 1C), 127.4-127.3 (m, 1C), 126.8, 122.8 (q, *J* = 271.3 Hz, 1C), 118.7 (q, *J* = 318.9 Hz, 1C), 118.4 (q, *J* = 3.8 Hz, 1C), 115.1 (t, *J* = 17.7 Hz, 1C), 112.3-112.0 (m, 1C); **^{19}F NMR** (565 MHz, $CDCl_3$) δ -62.9, -72.7, -114.6; **HRMS** (EI): calcd for $C_{14}H_6SF_8O_3^+$: 405.9904, found 405.9915.

4-(2',6'-Difluoro-[1,1'-biphenyl]-4-carbonyl)phenyl trifluoromethanesulfonate (Table 5.3, compound 15p)

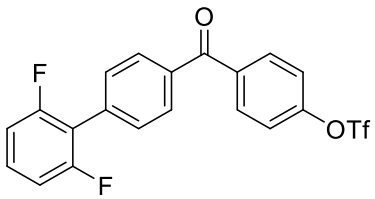

Yield: 92% (81.0 mg). White solid m.p. = 99.2–101.1 ºC. Eluent (R_f = 0.5, Hexane: Ethyl acetate = 20: 1) was used for flash column chromatography. **^{1}H NMR** (600 MHz, $CDCl_3$) δ 7.97-7.95 (m, 2H), 7.89-7.87 (m, 2H), 7.62 (d, *J* = 8.3 Hz, 2H), 7.44-7.42 (m,

2H), 7.37-7.32 (m, 1H), 7.05-7.01 (m, 2H); **^{13}C NMR** (150 MHz, $CDCl_3$) δ 194.2, 159.9 (dd, *J* = 248.2, 6.7 Hz, 1C), 152.0, 137.4, 136.1, 134.1, 132.1, 130.5, 129.84 (d, *J* = 20.6 Hz, 1C), 129.83, 121.4, 118.7 (q, *J* = 318.5 Hz, 1C), 117.2 (t, *J* = 17.9 Hz, 1C), 111.9-111.7 (m, 1C); **^{19}F NMR** (565 MHz, $CDCl_3$) δ-72.7, -114.2; **HRMS** (EI): calcd for $C_{20}H_{11}SF_5O_4^+$: 442.0293, found 442.0310.

2',6'-Difluoro-3'-methyl-[1,1'-biphenyl]-4-yl trifluoromethanesulfonate (Table 5.4, compound 15q)

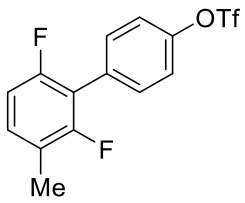

Yield: 98% yield (69.6 mg). Light-yellow liquid. Eluent (R_f = 0.5, Hexane = 100) was used for flash column chromatography. **^{1}H NMR** (600 MHz, $CDCl_3$) δ 7.56 (d, *J* = 8.5 Hz, 2H), 7.37 (d, *J* = 8.8 Hz, 2H), 7.19-7.15 (m, 1H), 6.91 (t, *J* = 8.9 Hz, 1H), 2.30 (s, 3H); ^{13}C NMR (150 MHz, $CDCl_3$) δ 158.0 (dd, *J* = 245.2, 6.3 Hz, 1C), 157.8 (dd, *J* = 246.3, 6.5 Hz, 1C), 149.1, 132.3, 130.9-130.8 (m, 1C), 130.2, 121.1, 121.0 (d, *J* = 3.4 Hz, 1C), 118.8 (q, *J* = 319.1 Hz, 1C), 116.0 (t, *J* = 18.6 Hz, 1C), 111.1-111.0 (m, 1C), 14.3 (d, *J* = 3.8 Hz, 1C); ^{19}F NMR (565 MHz, $CDCl_3$) δ -72.9, -117.5 (d, *J* = 6.3 Hz, 1F), -118.6 (d, *J* = 6.3 Hz, 1F); **HRMS** (EI): calcd for $C_{14}H_9SF_5O_3^+$: 352.0187, found 352.0197.

2',3',6'-Trifluoro-[1,1'-biphenyl]-4-yl trifluoromethanesulfonate (Table 5.4, compound 15r)

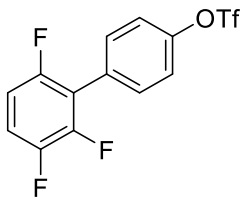

Yield: 94% (68.5 mg). White solid, m.p. = 62.2–64.8 ºC. Eluent (R_f = 0.5, Hexane: Ethyl acetate = 20: 1) was used for flash column chromatography. **^{1}H NMR** (400 MHz, $CDCl_3$) δ 7.57 (d, *J* = 8.4 Hz, 2H), 7.40 (d, *J* = 8.6 Hz, 1H), 7.22-7.14 (m, 1H), 6.96 (t, *J* = 8.6 Hz, 1H); **^{13}C NMR** (100 MHz, $CDCl_3$) δ 155.1 (dm, *J* = 245.0 Hz, 1C), 149.6, 147.6 (dm, *J* = 240.9 Hz, 1C), 132.2, 130.1 (d, *J* = 2.2 Hz, 1C), 128.8 (d, *J* = 2.0 Hz, 1C), 121.5, 118.8 (q, *J* = 318.7 Hz, 1C), 118.5-118.2 (m, 1C), 116.8-116.5 (m, 1C), 111.2 (dm, *J* = 24.9 Hz, 1C); **^{19}F NMR** (565 MHz, $CDCl_3$) δ -72.8, -119.7 (t, *J* = 15.5 Hz, 1F), -137.7 (t, *J* = 23.3 Hz, 1F), -141.4 (dd, *J* = 18.1, 22.2 Hz, 1F); **HRMS** (EI): calcd for $C_{13}H_6SF_6O_3^+$: 355.9936, found 355.9944.

2',4',6'-Trifluoro-[1,1'-biphenyl]-4-yl trifluoromethanesulfonate (Table 5.4, compound 15s)

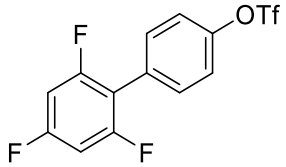

Yield: 84% (61.0 mg). White solid, m.p. = 50.9–52.9 ºC. Eluent (R_f = 0.4, Hexane = 100) was used for flash column chromatography. **^{1}H NMR** (400 MHz, $CDCl_3$) δ 7.52 (d, *J* = 8.6 Hz, 2H), 7.38 (d, *J* = 8.8 Hz, 1H), 6.83-6.75 (m, 2H); **^{13}C NMR** (100 MHz, $CDCl_3$) δ 162.2 (dt, *J* = 249.3, 15.3 Hz, 1C), 160.1 (ddd, *J* = 248.9, 9.6, 5.3 Hz, 1C), 149.3, 132.2, 128.9, 121.4, 118.8 (q, *J* = 318.8 Hz, 1C), 113.1 (d, *J* = 4.7 Hz, 1C), 101.0-

100.5 (m, 1C); **^{19}F NMR** (565 MHz, $CDCl_3$) δ -72.9, -107.4 (t, *J* = 7.2 Hz, 1F), -111.3 (d, *J* = 7.0 Hz, 1F); **HRMS** (EI): calcd for $C_{13}H_6SF_6O_3^+$: 355.9936, found 355.9946..

2',3',5',6'-Tetrafluoro-[1,1'-biphenyl]-4-yl trifluoromethanesulfonate (Table 5.4, compound 15t)

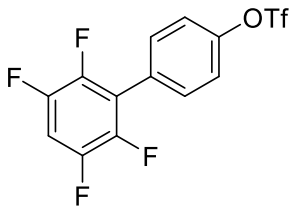

Yield: 86% (64.1 mg). White solid, m.p. = 98.2–100.6 °C. Eluent (R_f = 0.5, Hexane = 100) was used for flash column chromatography. **^{1}H NMR** (400 MHz, $CDCl_3$) δ 7.58 (d, *J* = 8.5 Hz, 2H), 7.42 (d, *J* = 8.8 Hz, 2H), 7.17-7.08 (m, 1H); **^{13}C NMR** (100 MHz, $CDCl_3$) δ 149.9, 146.3 (dm, *J* = 246.9 Hz, 1C), 143.6 (dm, *J* = 246.5 Hz, 1C), 132.2 (t, *J* = 2.5 Hz, 1C), 127.9 (t, *J* = 2.9 Hz, 1C), 121.7, 119.5, 118.7 (q, *J* = 318.8 Hz, 1C), 105.8 (t, *J* = 22.7 Hz, 1C); **^{19}F NMR** (565 MHz, $CDCl_3$) δ -72.9, -138.4 (dd, *J* = 9.9, 13.1 Hz, 1F), -143.8 (dd, *J* = 13.9, 9.1 Hz, 1F) ; **HRMS** (EI): calcd for $C_{13}H_5SF_7O_3^+$: 373.9842, found 373.9848.

2',3',4',5',6'-Pentafluoro-[1,1'-biphenyl]-4-yl trifluoromethanesulfonate (Table 5.4, compound 15u)

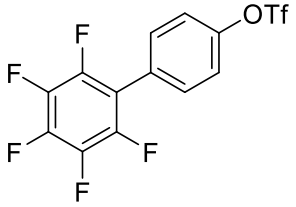

Yield: 89% (69.9 mg). White solid, m.p. = 39.1–41.0 ºC. Eluent (R_f = 0.5, Hexane = 100) was used for flash column chromatography. **^{1}H NMR** (400 MHz, $CDCl_3$) δ 7.55 (d, *J* = 8.5 Hz, 2H), 7.42 (d, *J* = 8.8 Hz, 2H); **^{13}C NMR** (100 MHz, $CDCl_3$) δ 149.9, 144.1 (dm, *J* = 246.7 Hz, 1C), 140.9 (dm, *J* = 249.1 Hz, 1C), 138.0 (dm, *J* = 252.0 Hz, 1C), 132.2, 126.9, 121.9, 118.7 (q, *J* = 318.8 Hz, 1C), 114.2-113.9 (m, 1C); **^{19}F NMR** (565 MHz, $CDCl_3$) δ -72.9, -143.1 (dd, *J* = 8.0, 23.6 Hz, 2F), -153.9 (t, *J* = 22.2 Hz, 1F), -161.5 (dt, *J* = 6.9, 22.7 Hz, 2F); **HRMS** (EI): calcd for $C_{13}H_4SF_8O_3^+$: 391.9748, found 391.9747.

2'-Fluoro-6'-nitro-[1,1'-biphenyl]-4-yl trifluoromethanesulfonate (Table 5.4, compound 15v)

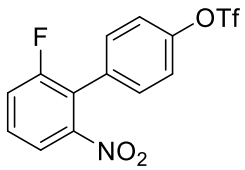

Yield: 85% (61.7 mg). Light-yellow liquid. Eluent (R_f = 0.3, Hexane: Ethyl acetate = 20: 1) was used for flash column chromatography. **^{1}H NMR** (400 MHz, $CDCl_3$) δ 7.77 (d, *J* = 8.1 Hz, 1H), 7.58-7.52 (m, 1H), 7.46-7.36 (m, 5H); **^{13}C NMR** (100 MHz, $CDCl_3$) δ 159.6 (d, *J* = 249.5 Hz, 1C), 149.9, 149.7, 131.0, 130.7, 130.1 (d, *J* = 8.9 Hz, 1C), 123.0 (d, *J* = 20.3 Hz, 1C), 121.6, 120.4 (d, *J* = 23.2 Hz, 1C), 120.0 (d, *J* = 3.6 Hz, 1C), 118.7 (q, *J* = 318.6 Hz, 1C); **^{19}F NMR** (565 MHz, $CDCl_3$) δ -72.8, -110.7; **HRMS** (EI): calcd for $C_{13}H_7SF_4O_5N^+$: 364.9976, found 364.9972.

2'-Fluoro-6'-(trifluoromethyl)-[1,1'-biphenyl]-4-yl trifluoromethanesulfonate (Table 5.4, compound 15w)

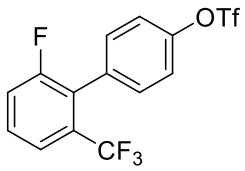

Yield: 92% (71.3 mg). Light-yellow liquid. Eluent (R_f = 0.3, Hexane = 100) was used for flash column chromatography. **^{1}H NMR** (400 MHz, $CDCl_3$) δ 7.59 (d, *J* = 7.9 Hz, 2H), 7.54-7.49 (m, 2H), 7.41-7.34 (m, 5H); **^{13}C NMR** (100 MHz, $CDCl_3$) δ 160.0 (d, *J* = 245.7 Hz, 1C), 149.5, 132.3, 131.8, 130.9 (q, *J* = 30.3 Hz, 1C), 129.9 (d, *J* = 8.7 Hz, 1C), 126.9 (d, *J* = 17.7 Hz, 1C), 123.1 (q, *J* = 272.7 Hz, 1C), 122.0-121.8 (m, 1C), 120.9, 119.4 (d, *J* = 23.2 Hz, 1C), 118.8 (q, *J* = 318.9 Hz, 1C); **^{19}F NMR** (565 MHz, $CDCl_3$) δ -57.3, -72.9, -111.4; **HRMS** (EI): calcd for $C_{14}H_7SF_7O_3^+$: 388.0004, found 388.0006.

2'-Fluoro-6'-methoxy-[1,1'-biphenyl]-4-yl trifluoromethanesulfonate (Table 5.4, compound 15x)

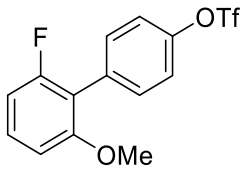

Yield: 94% (65.5 mg). White solid, m.p. = 66.4–67.4 ºC. Eluent (R_f = 0.3, Hexane: Ethyl acetate = 20: 1) was used for flash column chromatography. **^{1}H NMR** (400 MHz, $CDCl_3$) δ 7.52 (d, *J* = 8.1 Hz, 2H), 7.34 (d, *J* = 8.5 Hz, 2H), 7.31 (t, *J* = 7.4 Hz, 1H), 6.84 (d, *J* = 7.7 Hz, 1H), 6.81 (d, *J* = 7.8 Hz, 1H), 3.80 (s, 3H); **^{13}C NMR** (100 MHz, $CDCl_3$) δ 160.2 (d, *J* = 244.2 Hz, 1C), 157.6 (d, *J* = 6.7 Hz, 1C), 148.7, 132.6 (d, *J* = 1.7 Hz, 1C), 132.1, 129.6 (d, *J* = 10.7 Hz, 1C), 120.7, 118.8 (q, *J* = 318.9 Hz, 1C), 116.7 (d, *J* = 17.1 Hz, 1C), 108.3 (d, *J* = 23.2 Hz, 1C), 106.8 (d, *J* = 2.8 Hz, 1C), 56.0; **^{19}F**

NMR (565 MHz, $CDCl_3$) δ -72.9, -115.4; **HRMS** (EI): calcd for $C_{14}H_{10}SF_4O_4^+$: 350.0230, found 350.0231.

2',6'-Dimethoxy-[1,1'-biphenyl]-4-yl trifluoromethanesulfonate (Table 5.4, compound 15y)

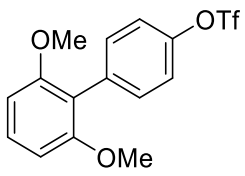

Yield: 95% (68.5 mg). Light-yellow solid, m.p. = 117.8–119.3 ºC. Eluent (R_f = 0.5, Hexane: Ethyl acetate = 10: 1) was used for flash column chromatography. **^{1}H NMR** (400 MHz, $CDCl_3$) δ 7.47 (d, *J* = 8.6 Hz, 2H), 7.34 (d, *J* = 8.4 Hz, 1H), 7.31 (d, *J* = 8.4 Hz, 2H), 6.70 (d, *J* = 8.4 Hz, 2H), 3.76 (s, 3H); **^{13}C NMR** (100 MHz, $CDCl_3$) δ 157.4, 148.2, 134.6, 132.9, 129.4, 123.6, 120.3, 118.7 (q, *J* = 318.7 Hz, 1C), 104.1, 55.7; **^{19}F NMR** (565 MHz, $CDCl_3$) δ -73.0; **HRMS** (EI): calcd for $C_{15}H_{13}SF_3O_5^+$: 362.0430, found 362.0435.

2',4',6'-Trimethoxy-[1,1'-biphenyl]-4-yl trifluoromethanesulfonate (Table 5.4, compound 15z)

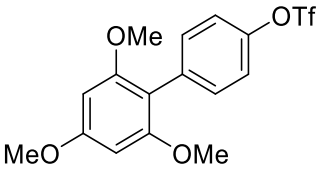

Yield: 94% (73.9 mg). Yellow solid, m.p. = 141.2–143.8 ºC. Eluent (R_f = 0.2, Hexane: Ethyl acetate = 10: 1) was used for flash column chromatography. **^{1}H NMR** (400 MHz, $CDCl_3$) δ 7.44 (d, *J* = 6.4 Hz, 2H), 7.29 (d, *J* = 6.4 Hz, 2H), 6.26 (s, 2H), 3.89 (s, 3H),

3.75 (s, 6H); **^{13}C NMR** (100 MHz, $CDCl_3$) δ 161.0, 158.1, 148.0, 134.7, 133.1, 120.2, 118.7 (q, *J* = 318.2 Hz, 1C), 110.2, 90.7, 55.7, 55.3; **^{19}F NMR** (565 MHz, $CDCl_3$) δ -73.0; **HRMS** (EI): calcd for $C_{16}H_{15}SF_3O_6^+$: 392.0536, found 392.0544.

4-(1-Phenyl-1*H*-pyrrol-2-yl)phenyl trifluoromethanesulfonate (Table 5.4, compound 15aa)

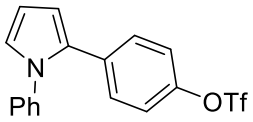

Yield: 93% (68.2 mg). Yellow liquid. Eluent (R_f = 0.3, Hexane = 100) was used for flash column chromatography. **^{1}H NMR** (400 MHz, $CDCl_3$) δ 7.40-7.31 (m, 3H), 7.22-7.16 (m, 4H), 7.15-7.13 (m, 2H), 6.99 (t, *J* = 2.4 Hz, 1H), 6.52 (dd, *J* = 1.7, 3.6 Hz, 1H), 6.41 (t, *J* = 3.2 Hz, 1H); **^{13}C NMR** (100 MHz, $CDCl_3$) δ 147.8, 140.0, 133.4, 131.7, 129.5, 129.2, 127.1, 125.7, 125.3, 121.0, 118.7 (q, *J* = 318.8 Hz, 1C), 111.7, 109.5; **^{19}F NMR** (565 MHz, $CDCl_3$) δ -72.9; **HRMS** (EI): calcd for $C_{17}H_{12}SF_3O_3N^+$: 367.0485, found 367.0497.

4-(1-Methyl-1*H*-indol-2-yl)phenyl trifluoromethanesulfonate (Table 5.4, compound 15ab)

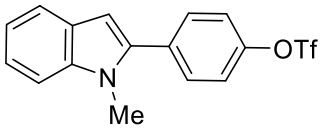

Yield: 44% (30.9 mg). Light-yellow solid. Eluent (R_f = 0.5, Hexane: Ethyl acetate = 20: 1) was used for flash column chromatography. **^{1}H NMR** (600 MHz, $CDCl_3$) δ 7.67 (d, *J* = 7.6 Hz, 1H), 7.60 (d, *J* = 8.6 Hz, 2H), 7.40 (d, *J* = 8.6 Hz, 3H), 7.31 (t, *J* = 7.6 Hz, 1H), 7.19 (d, *J* = 7.3 Hz, 1H), 6.62 (s, 1H), 3.76 (s, 3H); **^{13}C NMR** (150 MHz, $CDCl_3$)

δ 149.0, 139.3, 138.6, 133.3, 130.9, 127.7, 122.3, 121.5, 120.7, 120.2, 118.7 (q, J = 318.7 Hz, 1C), 109.7, 102.7, 31.2; **^{19}F NMR** (565 MHz, $CDCl_3$) δ -72.7; **HRMS** (APPI): calcd for $C_{16}H_{13}SNF_3O_3^+$: 355.0563, found 350.0557.

5.5 References

(1) (a) Cornella, J.; Larrosa, I. *Synthesis* **2012**, 653-676; (b) Dzik, W. I.; Lange, P. P.; Goossen, L. J. *Chem. Sci.* **2012**, *3 (9)*, 2671-2678; (c) Gooßen, L. J.; Rodríguez, N.; Gooßen, K. *Angew. Chem. Int. Ed.* **2008**, *47 (17)*, 3100-3120. (d) Rodríguez, N.; Goossen, L. J. *Chem. Soc. Rev.* **2011**, *40 (10)*, 5030-5048.

(2) (a) Hackenberger, D.; Weber, P.; Blakemore, D. C.; Goossen, L. J. *J. Org. Chem.* **2017**, *82 (7)*, 3917-3925; (b) Haley, C. K.; Gilmore, C. D.; Stoltz, B. M. *Tetrahedron* **2013**, *69 (27-28)*, 5732-5736; (c) Le Pham, N. S.; Lee, J.; Shin, H.; Sohn, J.-H. *Tetrahedron* **2018**, *74 (28)*, 3843-3851; (d) Li, X.; Zou, D.; Leng, F.; Sun, C.; Li, J.; Wu, Y.; Wu, Y. *Chem. Commun.* **2013**, *49 (3)*, 312-314; (e) Messaoudi, S.; Brion, J.-D.; Alami, M. *Org. Lett.* **2012**, *14 (6)*, 1496-1499; (f) Rouchet, J. B.; Schneider, C.; Spitz, C.; Lefevre, J.; Dupas, G.; Fruit, C.; Hoarau, C. *Chem. Eur. J.* **2014**, *20 (13)*, 3610-3615; (g) Tang, J.; Biafora, A.; Goossen, L. J. *Angew. Chem. Int. Ed.* **2015**, *54 (44)*, 13130-13133; (h) Wang, S.; Lu, H.; Li, J.; Zou, D.; Wu, Y.; Wu, Y. *Tetrahedron Lett.* **2017**, *58 (12)*, 1107-1111; (i) Wang, S.; Lu, H.; Li, J.; Zou, D.; Wu, Y.; Wu, Y. *Tetrahedron Lett.* **2017**, *58 (28)*, 2723-2726.

(3) (a) Becht, J.-M.; Drian, C. L. *Org. Lett.* **2008**, *10 (14)*, 3161-3164; (b) Goossen, L. J.; Rodriguez, N.; Linder, C. *J. Am. Chem. Soc.* **2008**, *130 (46)*, 15248-15249; (c) Goossen, L. J.; Rodríguez, N.; Melzer, B.; Linder, C.; Deng, G.; Levy, L. M. *J. Am. Chem. Soc.* **2007**, *129 (15)*, 4824-4833; (d) Gooßen, L. J.; Zimmermann, B.; Knauber, T. *Angew. Chem. Int. Ed.* **2008**, *47 (37)*, 7103-7106; (e) Song, B.; Knauber, T.; Goossen,

L. J. *Angew. Chem. Int. Ed.* **2013**, *52 (10)*.

(4) (a) Gooßen, L. J.; Lange, P. P.; Rodríguez, N.; Linder, C. *Chem. -Eur. J.* **2010**, *13 (16)*, 3906-3909; (b) Hackenberger, D.; Song, B.; Grünberg, M. F.; Farsadpour, S.; Menges, F.; Kelm, H.; Groß, C.; Wolff, T.; Niedner-Schatteburg, G.; Thiel, W. R. *ChemCatChem* **2015**, *7 (21)*, 3579-3588; (c) Wang, J.; Cui, Y.; Xie, S.; Zhang, J.-Q.; Hu, D.; Shuai, S.; Zhang, C.; Ren, H. *Org. Lett.* **2024**, *26 (1)*, 137-141.

(5) (a) Fromm, A.; van Wüllen, C.; Hackenberger, D.; Goossen, L. J. *J. Am. Chem. Soc.* **2014**, *136 (28)*, 10007-10023; (b) Gooßen, L. J.; Rodríguez, N.; Linder, C.; Lange, P. P.; Fromm, A. *ChemCatChem* **2010**, *2 (4)*, 430-442.

(6) (a) Chen, Z.; Gu, C.; Yuen, O. Y.; So, C. M. *Chem. Sci.* **2022**, *13 (17)*, 4762-4769; (b) Chen, Z.; Pang, W. H.; Yuen, O. Y.; Ng, S. S.; So, C. M. *J. Org. Chem.* **2024**, Article ASAP; (c) Ng, S. S.; Chen, Z.; Yuen, O. Y.; So, C. M. *Adv. Syn. Catal.* **2022**, *364 (9)*, 1596-1601; (d) So, C. M.; Yuen, O. Y.; Ng, S. S.; Chen, Z. *ACS Catal.* **2021**, *11 (13)*, 7820-7827; (e) Gu, C.; Yuen, O. Y.; Ng, S. S.; So, C. M. *Adv. Syn. Catal.* **2024**.

(7) Daley, R. A.; Liu, E.-C.; Topczewski, J. J. *Org. Lett.* **2019**, *21 (12)*, 4734-4738.

(8) Liu, K.; Li, N.; Ning, Y. Y.; Zhu, C. J.; Xie, J. *Chem* **2019**, *5 (10)*, 2718-2730.

Chapter 6 Conclusion

We have successfully designed and investigated novel classes of alkyl-pyrazole-based phosphine ligands that utilize the pyrazole skeleton. The pyrazole templates are readily available and easily modified into target substrates. The C3 and C5 substituted with alkyl groups of pyrazole scaffolds could be easily synthesized from commercially available alkyl-substituted diketone and methylhydrazine sulfate via Knorr condensation reaction. Leveraging this facile synthetic methodology, we were able to prepare a series of novel phosphine ligands with a wide variety of alkyl groups at C3 and C5 positions, including three- to seven-membered cycloalkyl groups, *t*-Bu and *i*-Pr groups.

In **Chapter 2**, We initially found that pyrazole scaffold bearing two Cy groups at the C3 and C5 positions enables chemoselective amination reactions well and provides an unconventional C–Cl > C–OTf reactivity order. The developed catalytic system enables the chemoselective amination to tolerate a wide range of chloro(hetero)aryl triflates as well as an array of amines. In addition, the high-performance also allowed the intermolecular chemoselective amination reactions, gram-scale reaction and late-stage functionalization of some drugs, which demonstrated its versatility and practicability. A combination of results of DFT and Pd···H–C interaction which was demonstrated by single X-ray results as well as NMR results elucidated the origination of excellent chemoselectivity. Moreover, the successful implementation of DFT also explained the high reactivity of the $Pd(dba)_2$/**BirdPhos** catalytic system compared to

the $Pd(dba)_2$/**SelectPhos** catalytic system, which might underscore the importance of exploring new scaffold ligands.

In **Chapter 3**, further investigations to vary the ring size of cycloalkyl ring within the pyrazole scaffold to evaluate their effect on achieving challenging dual reactivity reaction—regio-, and chemoselective C–H arylation of the heterocyclic compounds found that ligands with cyclopentyl groups at the C3 and C5 positions of the pyrazole provided the best results. Density functional theory (DFT) results revealed that modifying the ring size of the cycloalkyl groups impacts the angle and length of the Pd···H–C interaction, thereby inducing differential stabilizing effects on the critical intermediates across the reaction. Mechanistic investigations supported by both experimental and DFT results suggest that the alkyl-pyrazole-based phosphine ligands bearing optimal ring sizes enable the reaction to proceed with a lower energy barrier through a concerted metalation–deprotonation (CMD) pathway.

In **Chapter 4**, we then continued to modify the cycloalkyl ring within the pyrazole ligand to non-cycloalkyl group—*i*-Pr, which could also provide Pd···H–C interaction. To our delight, such modified ligand was proven to lower the reaction temperature of redox-neutral decarboxylative cross-coupling reaction by 60–80 °C compared to Buchwald-type ligands such as SPhos. Newly developed catalytic system tolerated a wide range of aryl chlorides and benzoate acids. Moreover, late-stage functionalization of some Cl-containing drugs and synthesis of challenging tetra-*ortho*-substituted biaryls were also demonstrated feasible. The results of the Hammett plot

and Eyring plot revealed that the rate-determining step might be the decarboxylative step.

In **Chapter 5**, we subsequently utilized similar catalytic system achieving the first chemoselective decarboxylative cross-coupling of chloroaryl triflates under relatively mild conditions, in which C–Cl > C–OTf in reactivity. With the developed methodology, various chloroaryl triflates coupled well with a series of fluorine-containing benzoate acids, providing corresponding biaryl compounds containing the reactive OTf groups with excellent yield and chemoselectivity.

In summary, our research focuses on developing novel phosphine ligands for palladium-catalyzed chemoselective cross-coupling reactions. We successfully achieved various reactions, including amination, C–H arylation, and decarboxylative coupling, demonstrating improved chemoselectivity, reactivity, and functional group tolerance, highlighting the potential for milder and environmentally friendly conditions.

Appendix

NMR & HRMS Spectra of Chapter 2

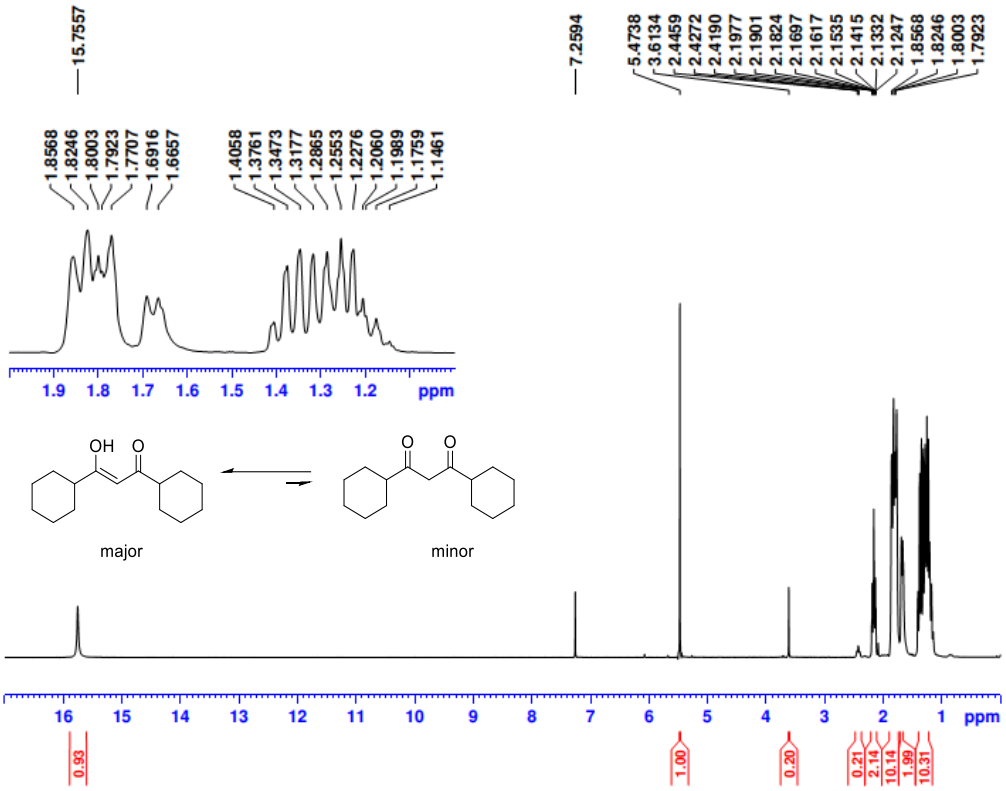

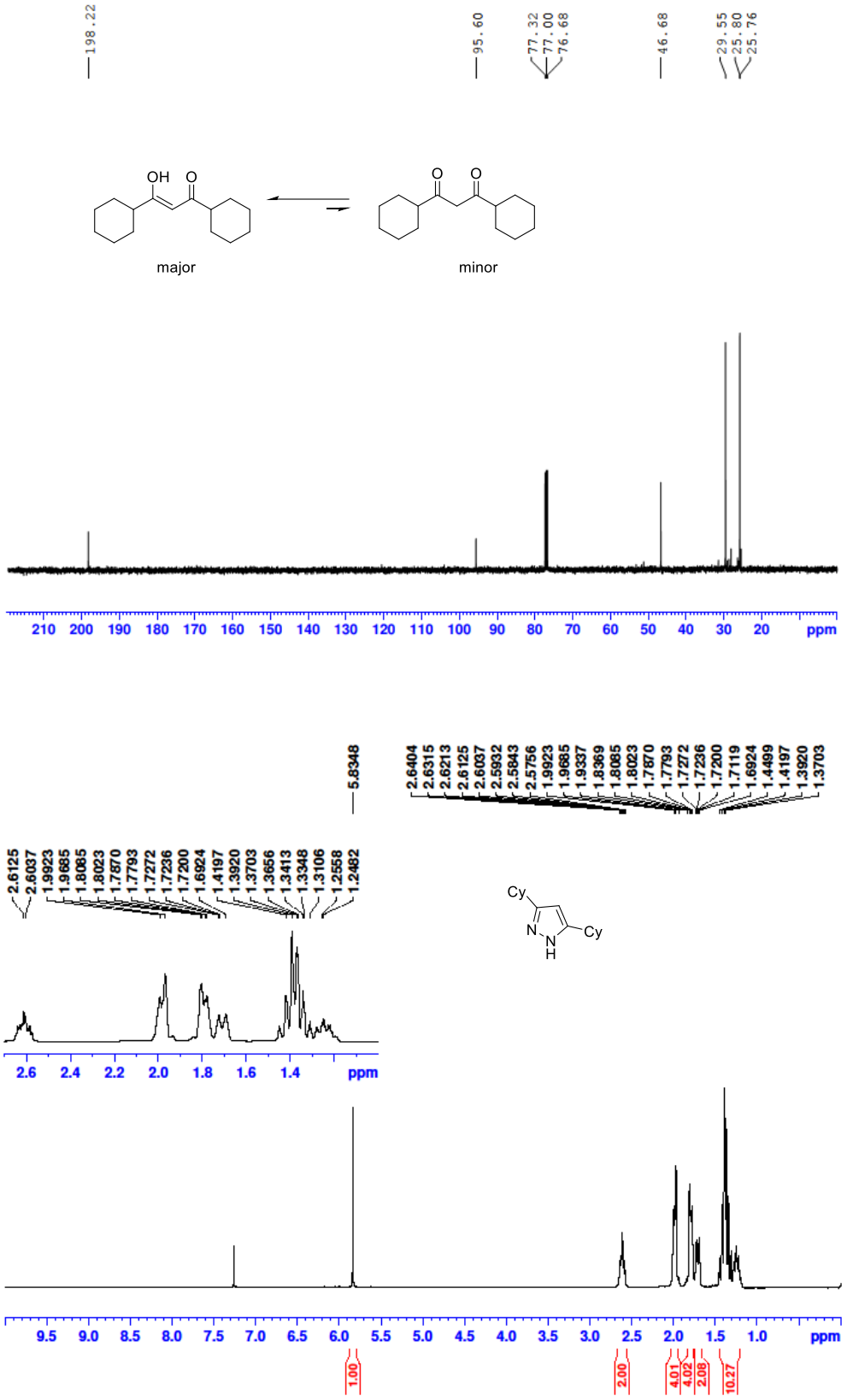
198.22
95.60
77.32
77.00
76.68
46.68
29.55
25.80
25.76
OH
O
O
O
major
minor
210 200 190 180 170 160 150 140 130 120 110 100 90 80 70 60 50 40 30 20 ppm
5.8348
2.6404
2.6315
2.6213
2.6125
2.6037
2.5932
2.5843
2.5756
1.9923
1.9685
1.9337
1.8369
1.8085
1.8023
1.7870
1.7793
1.7272
1.7236
1.7200
1.7119
1.6924
1.4499
1.4197
1.3920
1.3703
2.6125
2.6037
1.9923
1.9685
1.8085
1.8023
1.7870
1.7793
1.7272
1.7236
1.7200
1.6924
1.4197
1.3920
1.3703
1.3656
1.3413
1.3348
1.3106
1.2558
1.2482
Cy
N
N
H
Cy
2.6 2.4 2.2 2.0 1.8 1.6 1.4 ppm
9.5 9.0 8.5 8.0 7.5 7.0 6.5 6.0 5.5 5.0 4.5 4.0 3.5 3.0 2.5 2.0 1.5 1.0 ppm
1.00
2.00
4.01
4.02
2.08
10.27

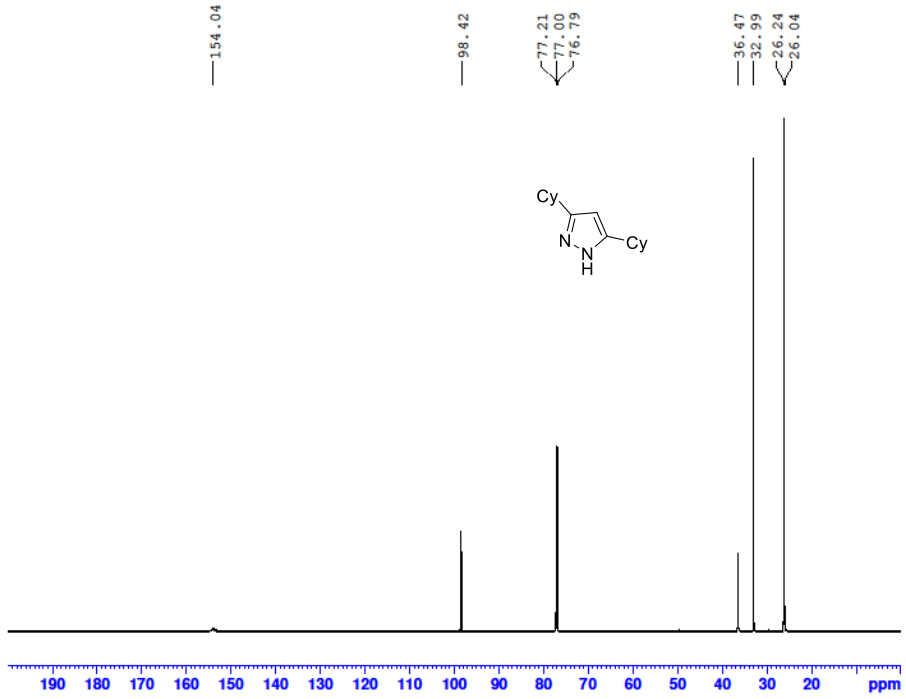

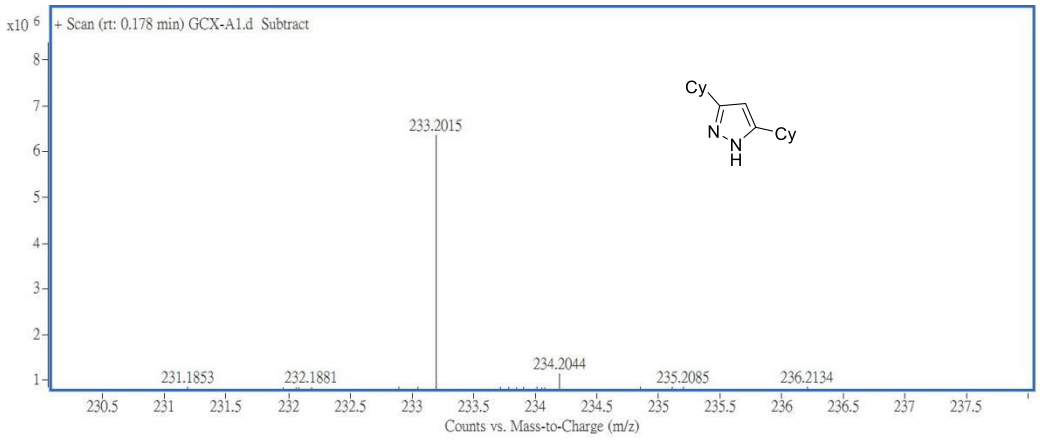

Mass	m/z (Calc)	Diff (mDa)	Diff (ppm)	Formula
233.2015	233.2012	-0.27	-1.18	C15 H25 N2

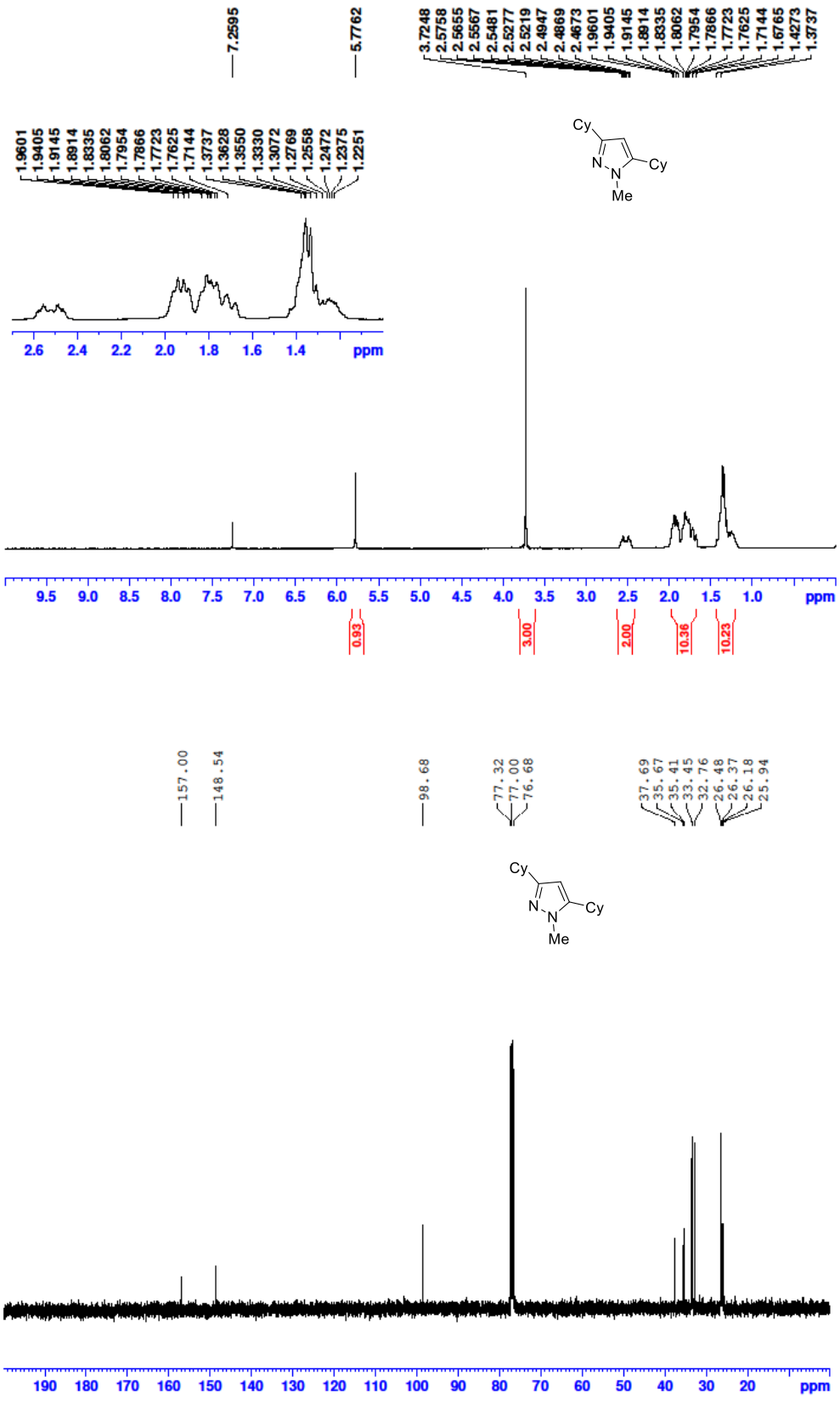
7.2595
5.7762
3.7248
2.5758
2.5655
2.5567
2.5481
2.5277
2.5219
2.4947
2.4869
2.4673
1.9601
1.9405
1.9145
1.8914
1.8335
1.8062
1.7954
1.7866
1.7723
1.7625
1.7144
1.6765
1.4273
1.3737
1.3628
1.3550
1.3330
1.3072
1.2769
1.2558
1.2472
1.2375
1.2251
Cy
N
N
Cy
Me
2.6
2.4
2.2
2.0
1.8
1.6
1.4
ppm
9.5
9.0
8.5
8.0
7.5
7.0
6.5
6.0
5.5
5.0
4.5
4.0
3.5
3.0
2.5
2.0
1.5
1.0
ppm
0.93
3.00
2.00
10.36
10.23
157.00
148.54
98.68
77.32
77.00
76.68
37.69
35.67
35.41
33.45
32.76
26.48
26.37
26.18
25.94
Cy
N
N
Cy
Me
190
180
170
160
150
140
130
120
110
100
90
80
70
60
50
40
30
20
ppm

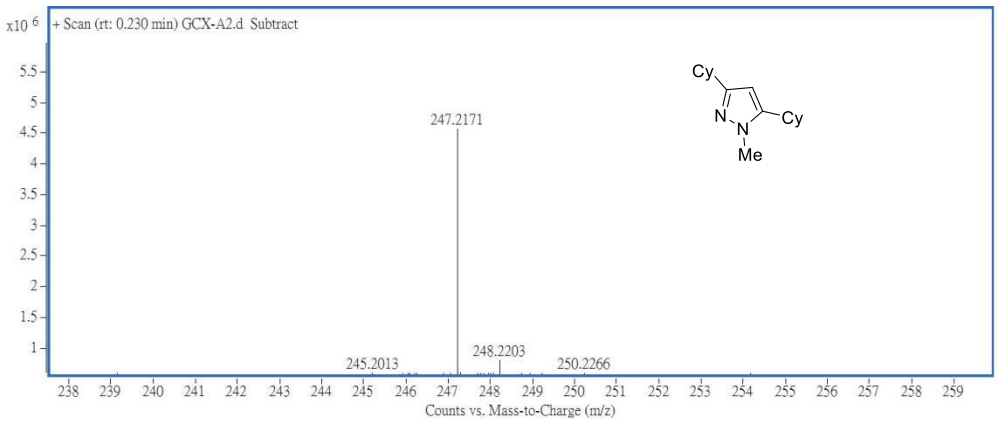

Mass	m/z (Calc)	Diff (mDa)	Diff (ppm)	Formula
247.2171	247.2169	-0.22	-0.91	C16 H27 N2

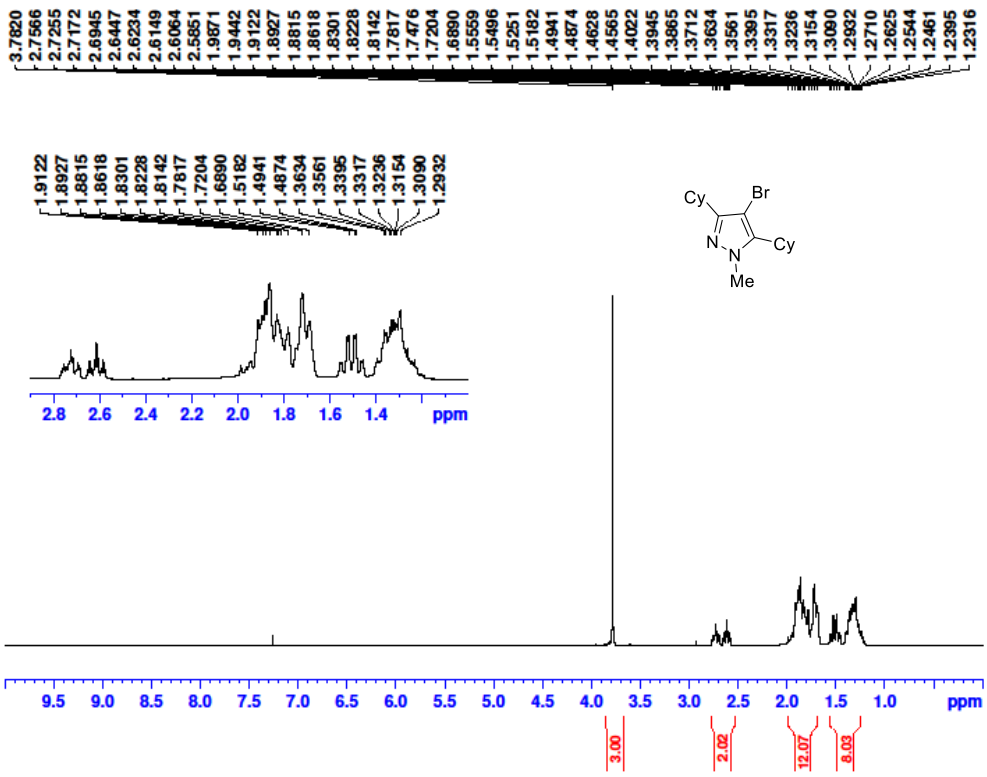

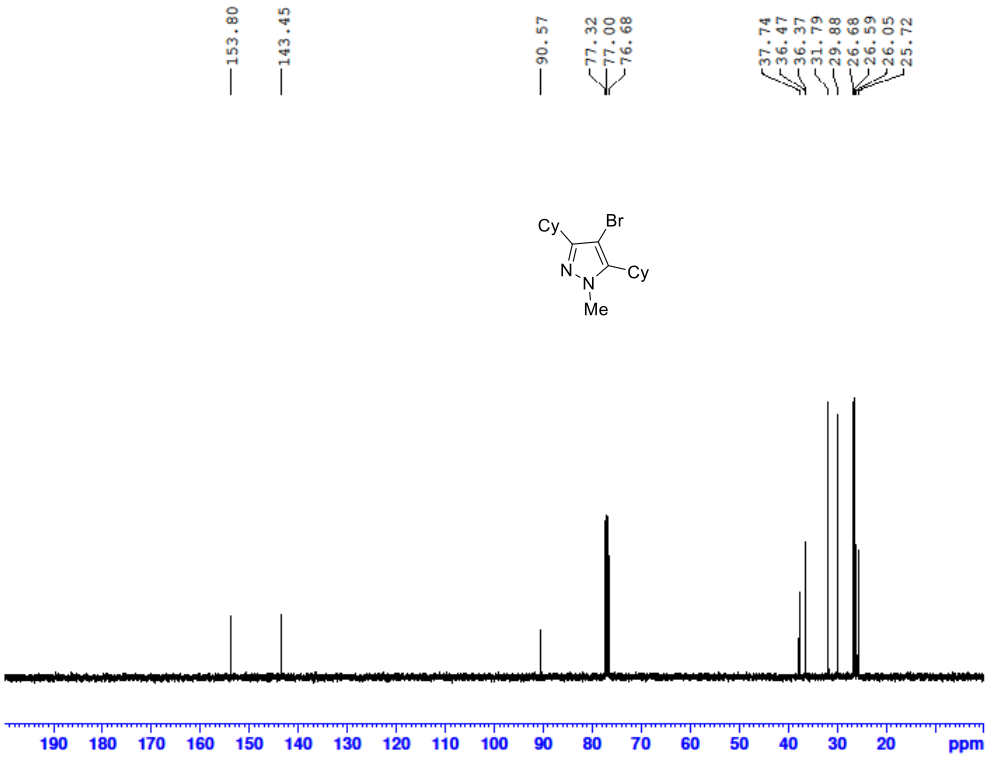

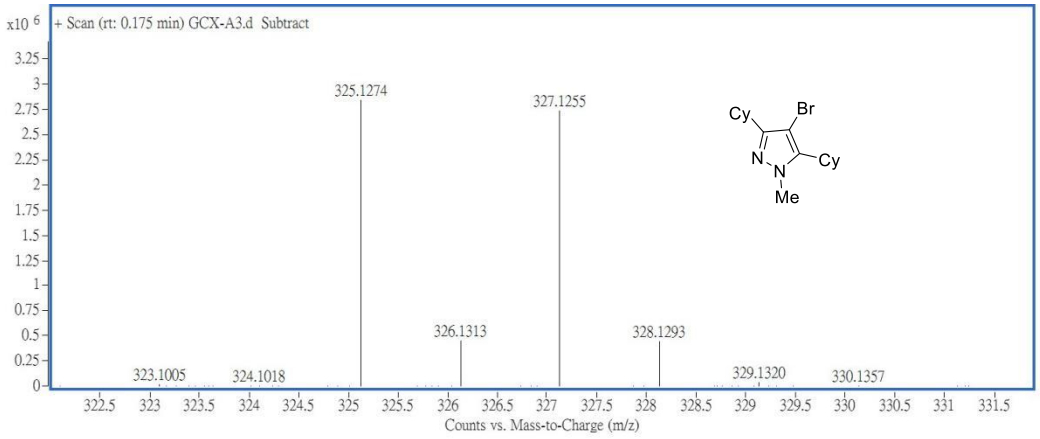

Mass	m/z (Calc)	Diff (mDa)	Diff (ppm)	Formula
325.1274	325.1274	-0.01	-0.04	C16 H26 Br N2

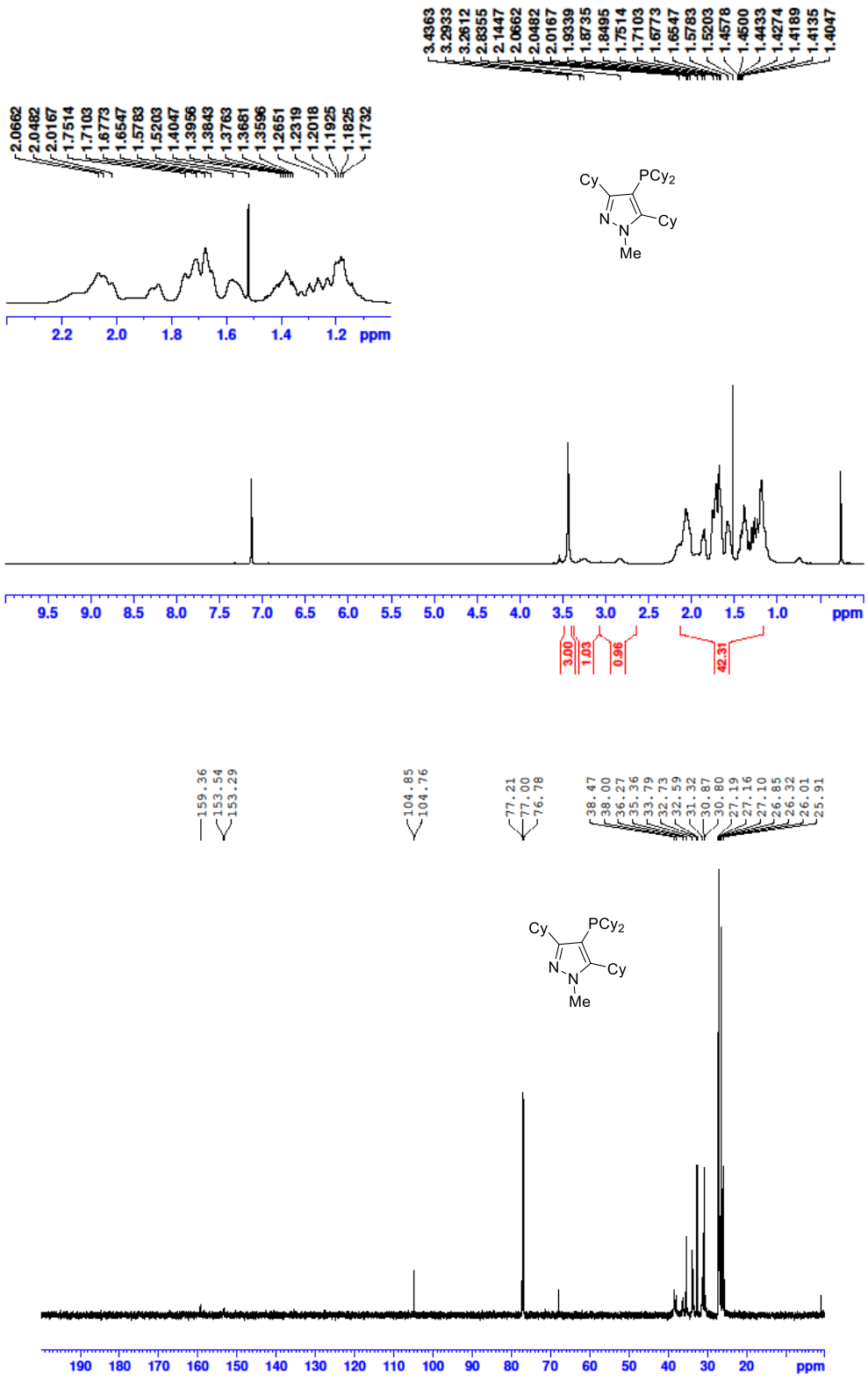
3.4363
3.2933
3.2612
2.8355
2.1447
2.0662
2.0482
2.0167
1.9339
1.8735
1.8495
1.7514
1.7103
1.6773
1.6547
1.5783
1.5203
1.4578
1.4500
1.4433
1.4274
1.4189
1.4135
1.4047
2.0662
2.0482
2.0167
1.7514
1.7103
1.6773
1.6547
1.5783
1.5203
1.4047
1.3956
1.3843
1.3763
1.3681
1.3596
1.2651
1.2319
1.2018
1.1925
1.1825
1.1732
Cy
PCy2
N
N
Cy
Me
2.2
2.0
1.8
1.6
1.4
1.2
ppm
9.5
9.0
8.5
8.0
7.5
7.0
6.5
6.0
5.5
5.0
4.5
4.0
3.5
3.0
2.5
2.0
1.5
1.0
ppm
3.00
1.03
0.96
42.31
159.36
153.54
153.29
104.85
104.76
77.21
77.00
76.78
38.47
38.00
36.27
35.36
33.79
32.73
32.59
31.32
30.87
30.80
27.19
27.16
27.10
26.85
26.32
26.01
25.91
Cy
PCy2
N
N
Cy
Me
190
180
170
160
150
140
130
120
110
100
90
80
70
60
50
40
30
20
ppm

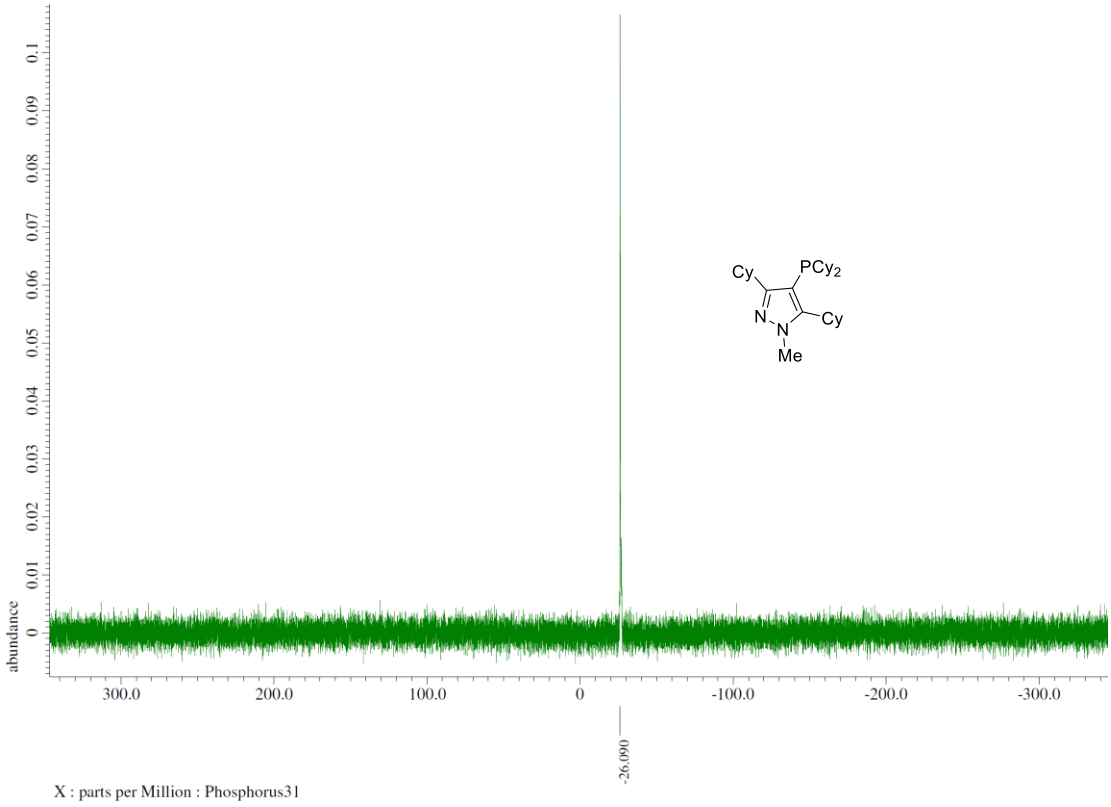

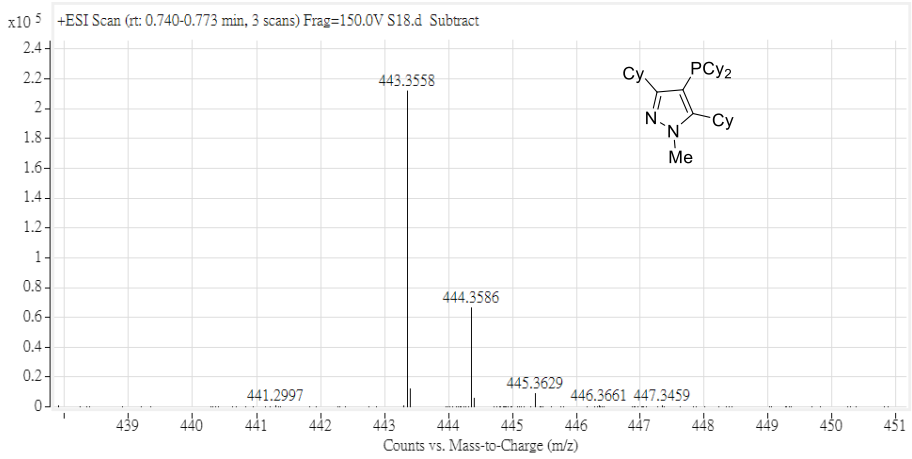

Mass	Calc. Mass	mDa	PPM	Formula
443.3558	443.3550	-0.84	-1.89	C28 H48 N2 P

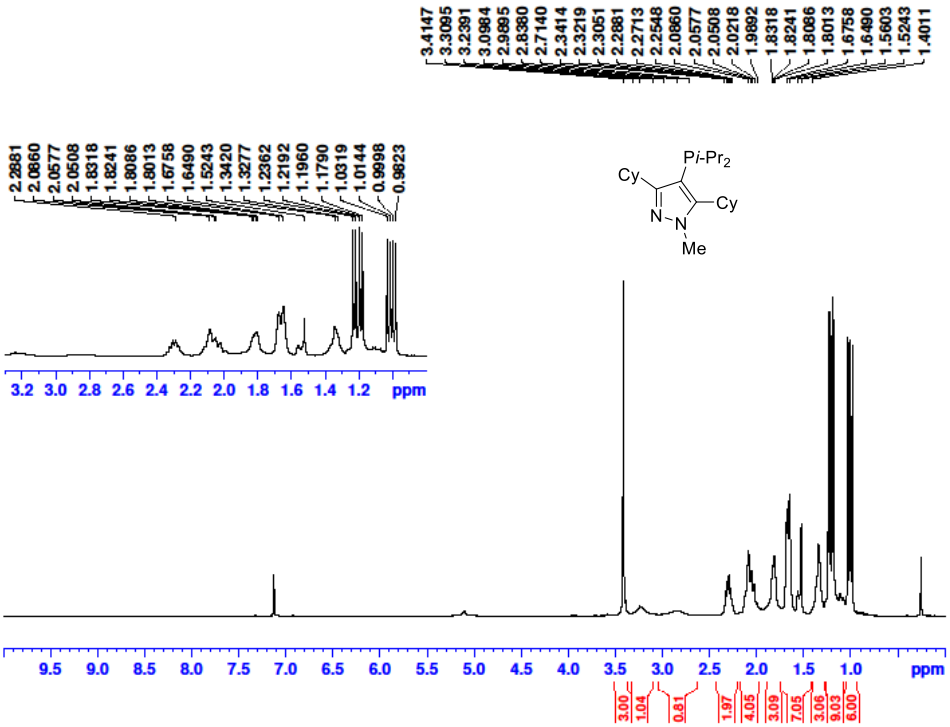
3.4147
3.3095
3.2391
3.0984
2.9895
2.8380
2.7140
2.3414
2.3219
2.3051
2.2881
2.2713
2.2548
2.0860
2.0577
2.0508
2.0218
1.9892
1.8318
1.8241
1.8086
1.8013
1.6758
1.6490
1.5603
1.5243
1.4011
2.2881
2.0860
2.0577
2.0508
1.8318
1.8241
1.8086
1.8013
1.6758
1.6490
1.5243
1.3420
1.3277
1.2362
1.2192
1.1960
1.1790
1.0319
1.0144
0.9998
0.9823
P*i*-Pr2
Cy
Cy
N
N
Me
3.2 3.0 2.8 2.6 2.4 2.2 2.0 1.8 1.6 1.4 1.2 ppm
9.5 9.0 8.5 8.0 7.5 7.0 6.5 6.0 5.5 5.0 4.5 4.0 3.5 3.0 2.5 2.0 1.5 1.0 ppm
3.00
1.04
0.81
1.97
4.05
3.09
7.05
3.06
9.03
6.00

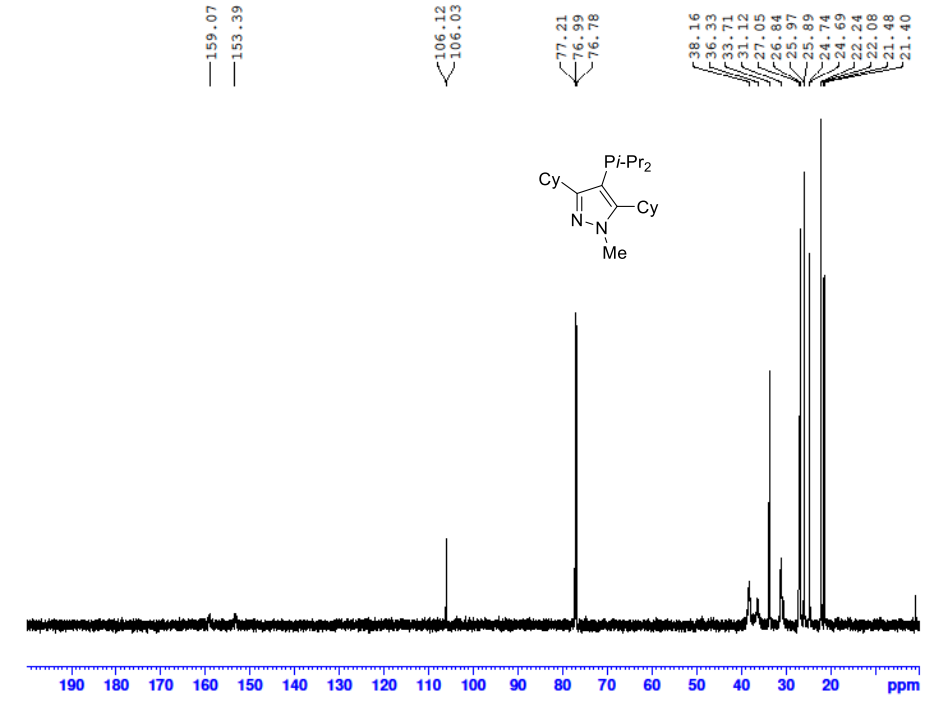
159.07
153.39
106.12
106.03
77.21
76.99
76.78
38.16
36.33
33.71
31.12
27.05
26.84
25.97
25.89
24.74
24.69
22.24
22.08
21.48
21.40
P*i*-Pr2
Cy
Cy
N
N
Me
190 180 170 160 150 140 130 120 110 100 90 80 70 60 50 40 30 20 ppm

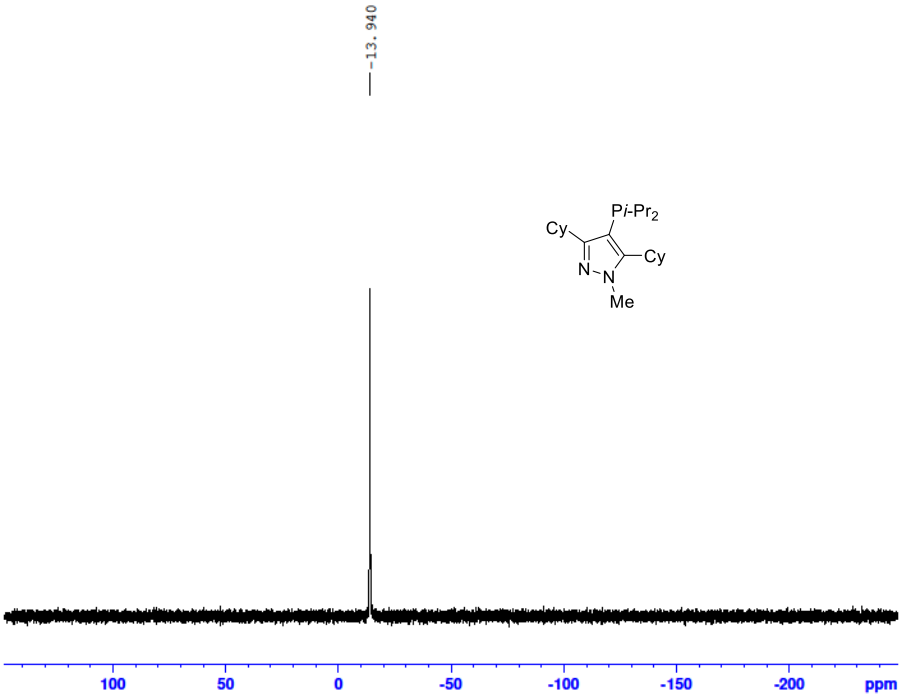

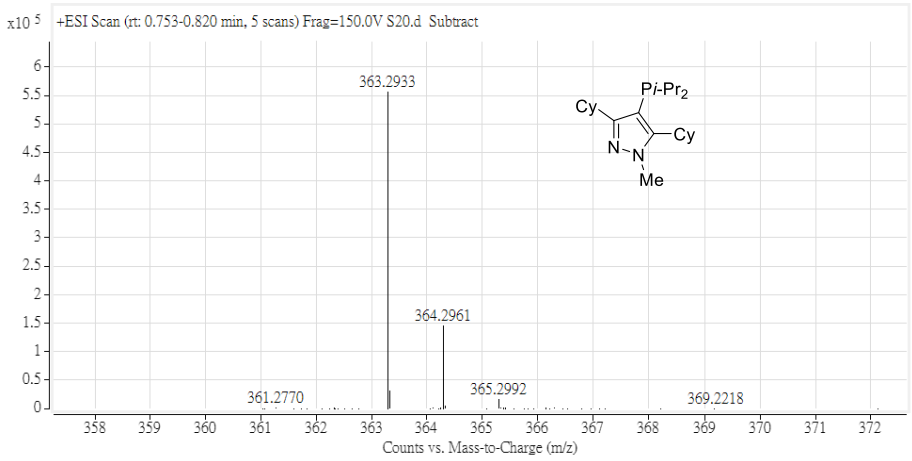

Mass	Calc. Mass	mDa	PPM	Formula
363.2933	363.2924	-0.94	-2.59	C22 H40 N2 P

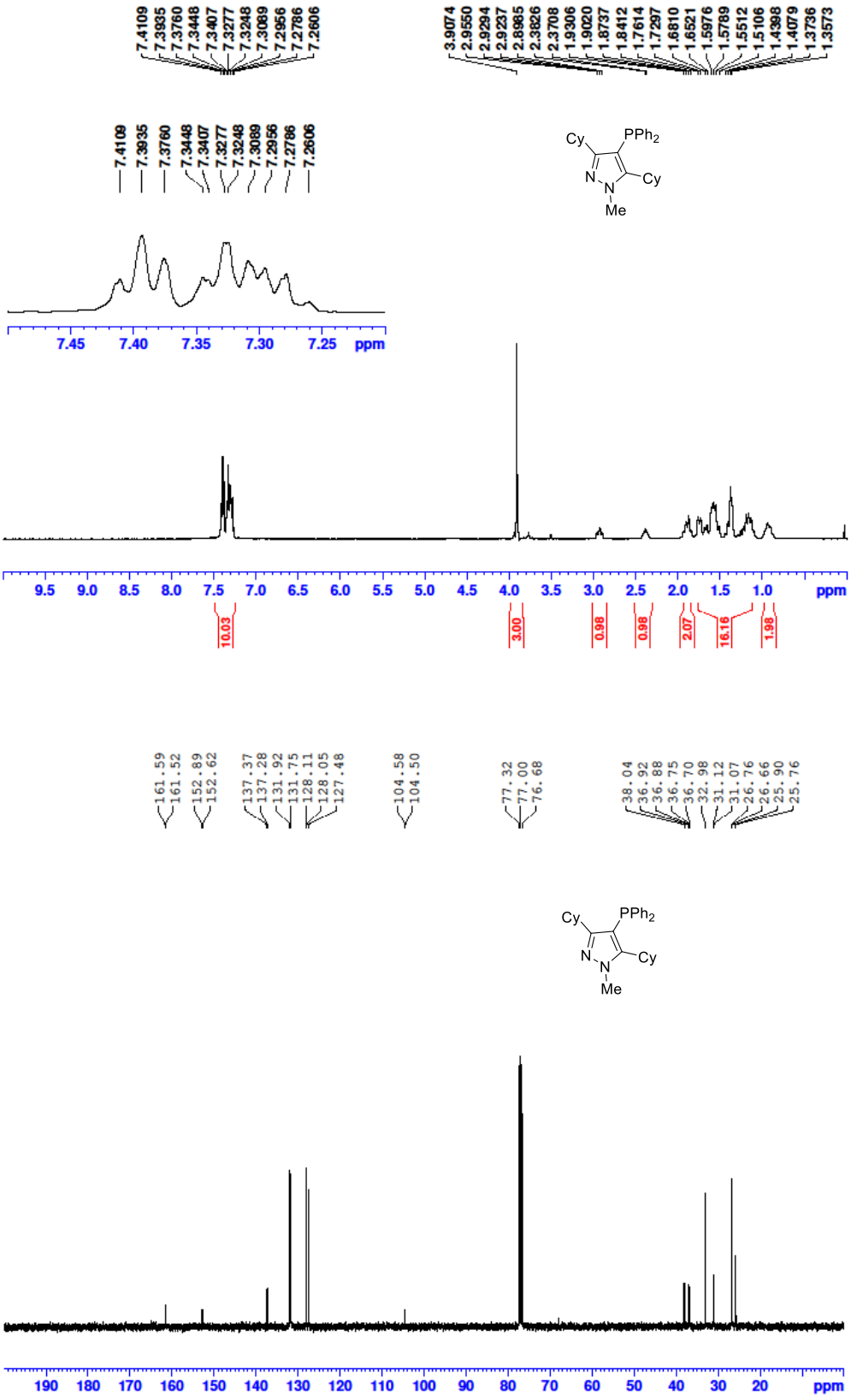
7.4109
7.3935
7.3760
7.3448
7.3407
7.3277
7.3248
7.3089
7.2956
7.2786
7.2606
3.9074
2.9550
2.9294
2.9237
2.8985
2.3826
2.3708
1.9306
1.9020
1.8737
1.8412
1.7614
1.7297
1.6810
1.6521
1.5976
1.5789
1.5512
1.5106
1.4398
1.4079
1.3736
1.3573
Cy
PPh2
Cy
N
N
Me
7.45
7.40
7.35
7.30
7.25
ppm
9.5
9.0
8.5
8.0
7.5
7.0
6.5
6.0
5.5
5.0
4.5
4.0
3.5
3.0
2.5
2.0
1.5
1.0
ppm
10.03
3.00
0.98
0.98
2.07
16.16
1.98
161.59
161.52
152.89
152.62
137.37
137.28
131.92
131.75
128.11
128.05
127.48
104.58
104.50
77.32
77.00
76.68
38.04
36.92
36.88
36.75
36.70
32.98
31.12
31.07
26.76
26.66
25.90
25.76
Cy
PPh2
Cy
N
N
Me
190
180
170
160
150
140
130
120
110
100
90
80
70
60
50
40
30
20
ppm

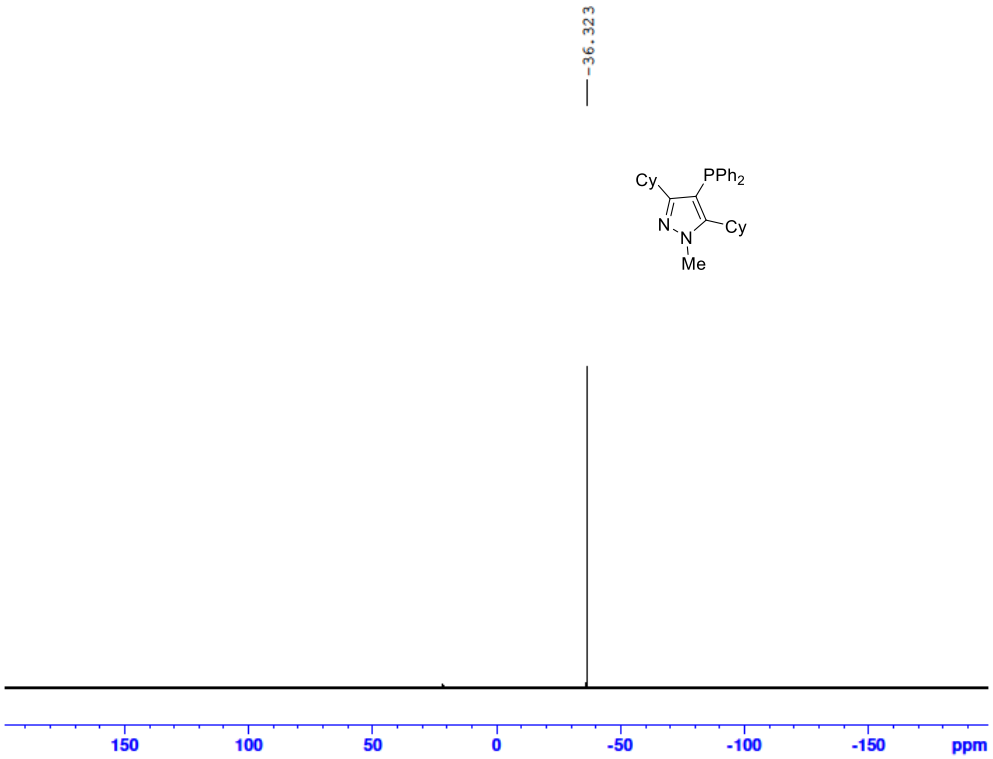

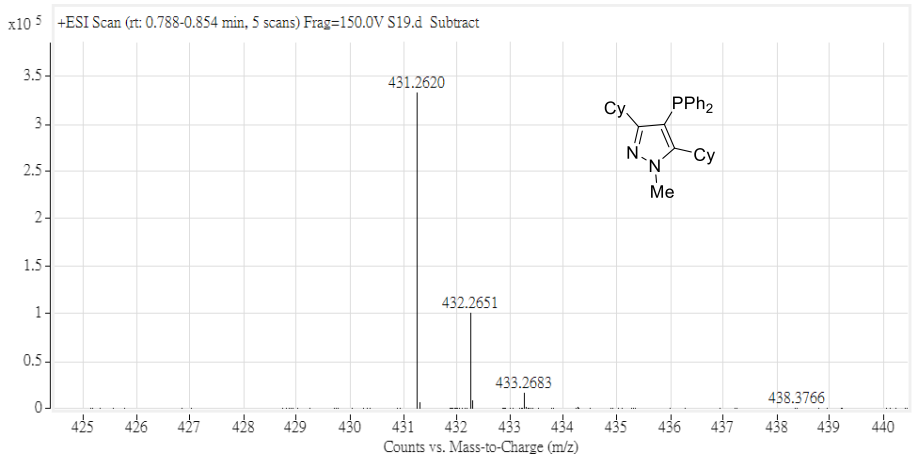

Mass	Calc. Mass	mDa	PPM	Formula
431.2620	431.2611	-0.94	-2.18	C28 H36 N2 P

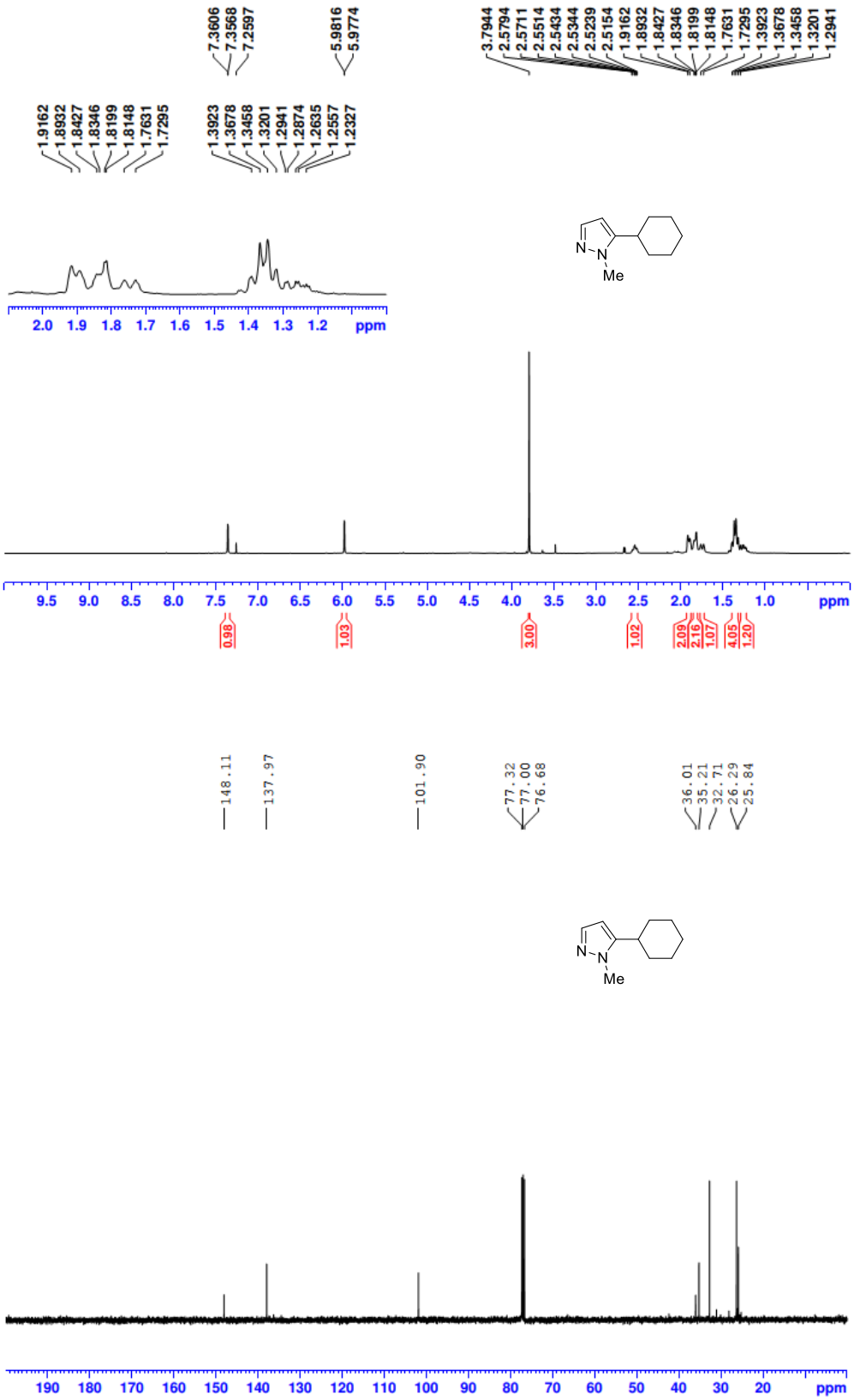
7.3606
7.3568
7.2597
5.9816
5.9774
3.7944
2.5794
2.5711
2.5514
2.5434
2.5344
2.5239
2.5154
1.9162
1.8932
1.8427
1.8346
1.8199
1.8148
1.7631
1.7295
1.3923
1.3678
1.3458
1.3201
1.2941
1.2874
1.2635
1.2557
1.2327
N
N
Me
2.0 1.9 1.8 1.7 1.6 1.5 1.4 1.3 1.2 ppm
9.5 9.0 8.5 8.0 7.5 7.0 6.5 6.0 5.5 5.0 4.5 4.0 3.5 3.0 2.5 2.0 1.5 1.0 ppm
0.98
1.03
3.00
1.02
2.09
2.16
1.07
4.05
1.20
148.11
137.97
101.90
77.32
77.00
76.68
36.01
35.21
32.71
26.29
25.84
N
N
Me
190 180 170 160 150 140 130 120 110 100 90 80 70 60 50 40 30 20 ppm

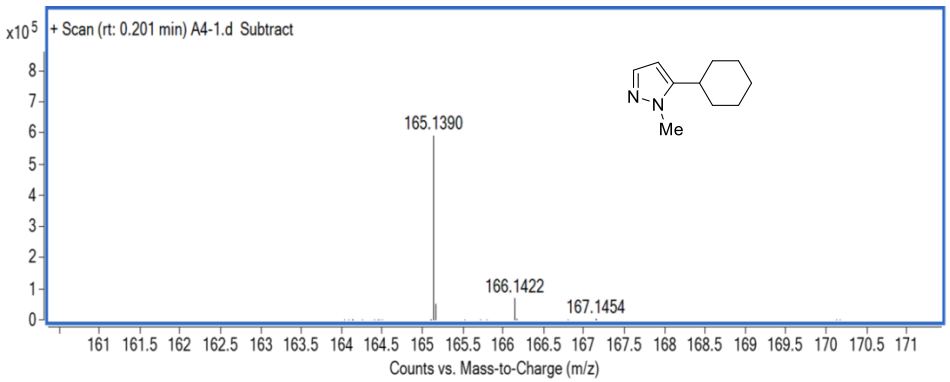

Mass	m/z (Calc)	Diff (mDa)	Diff (ppm)	Formula
165.1390	165.1386	-0.38	-2.28	C10 H17 N2

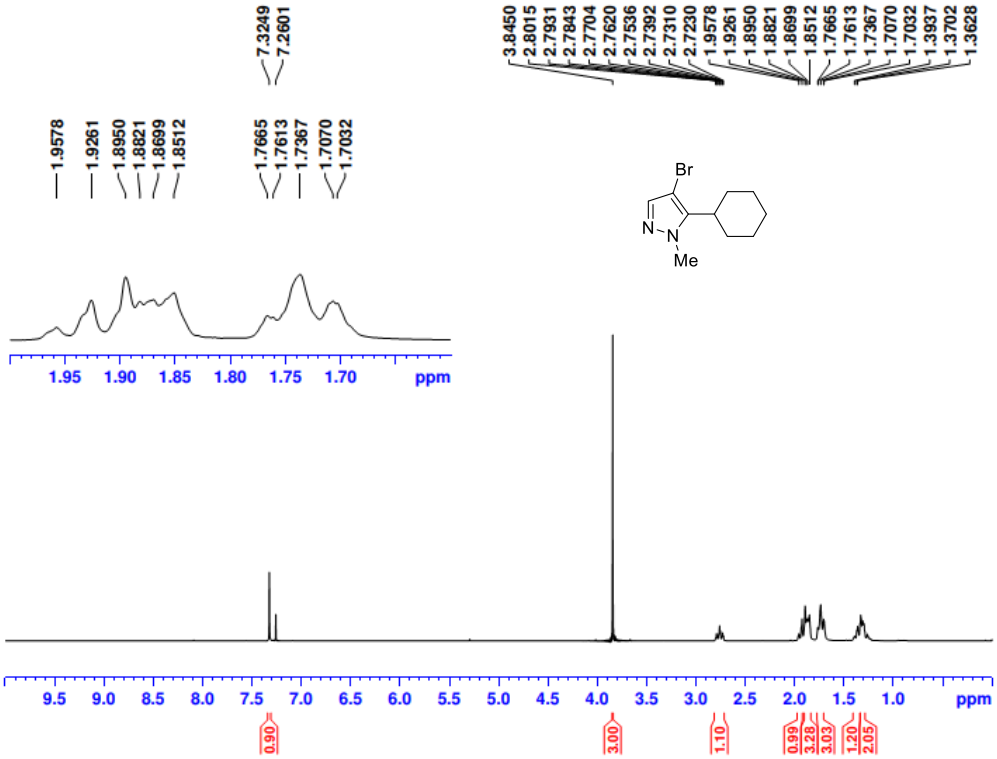

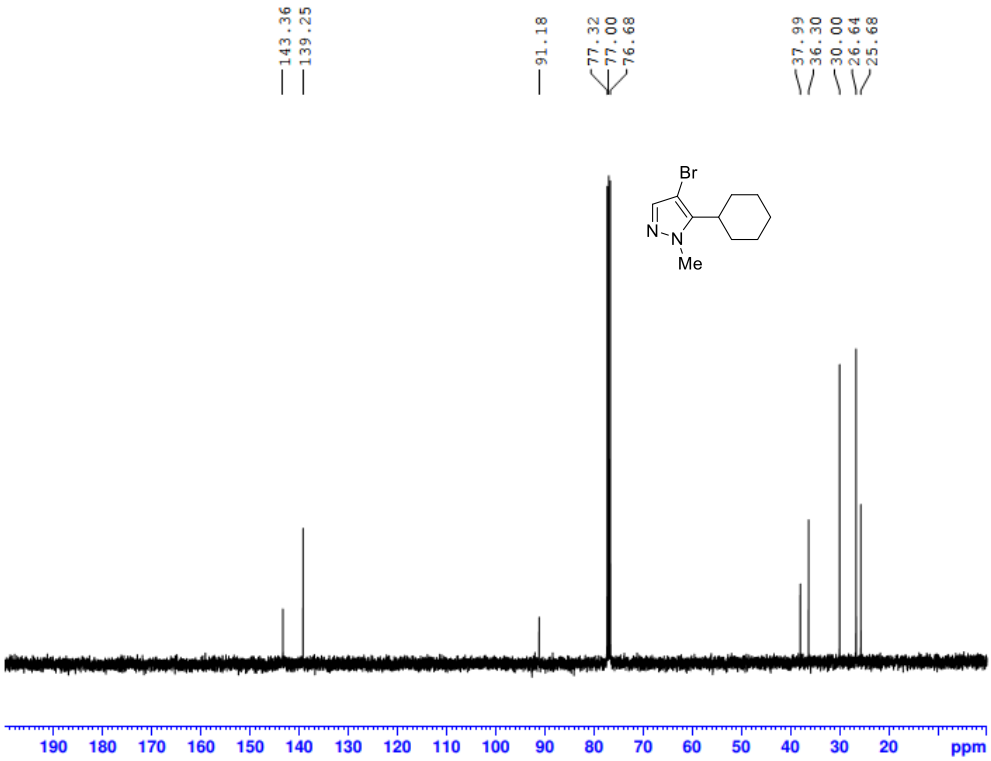

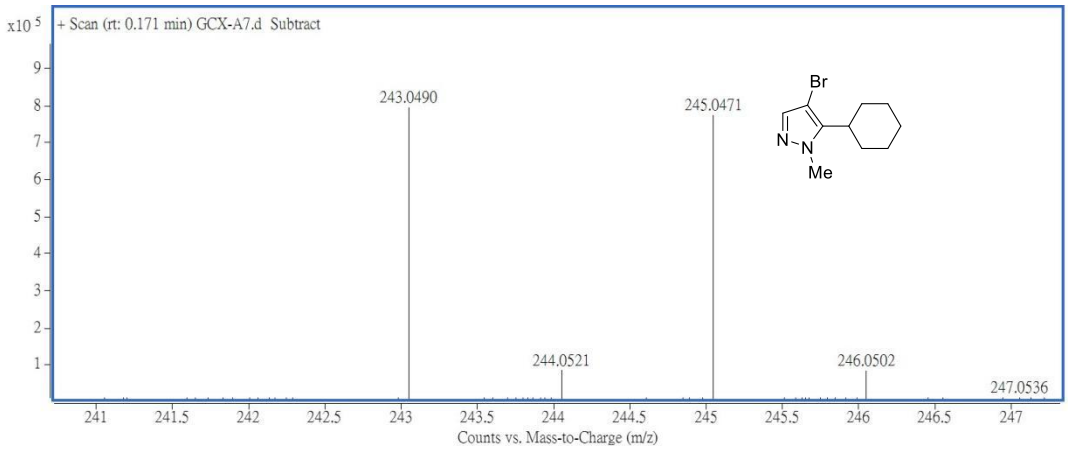

Mass	m/z (Calc)	Diff (mDa)	Diff (ppm)	Formula
243.0490	243.0491	0.14	0.57	C10 H16 Br N2

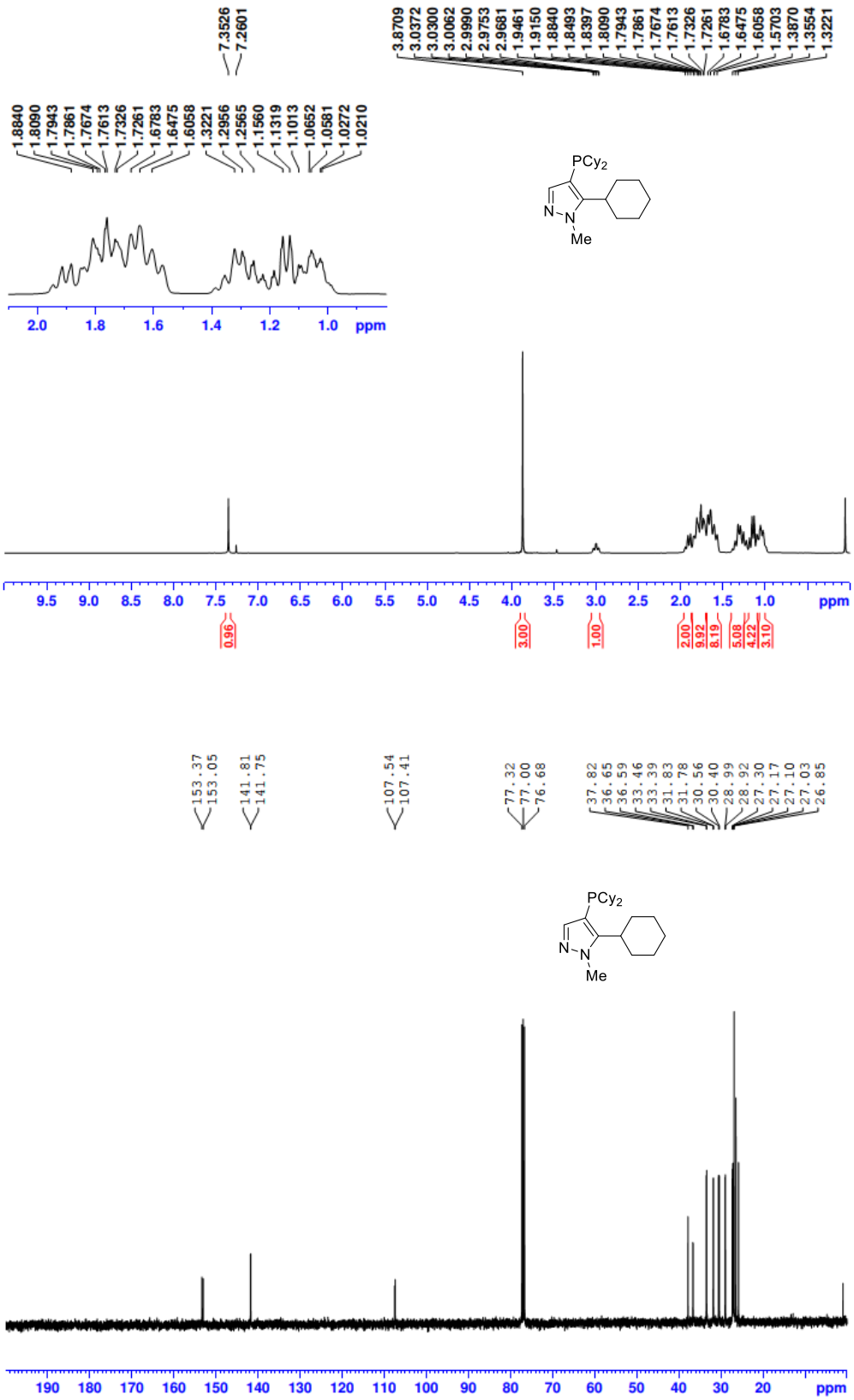
7.3526
7.2601
3.8709
3.0372
3.0300
3.0062
2.9990
2.9753
2.9681
1.9461
1.9150
1.8840
1.8493
1.8397
1.8090
1.7943
1.7861
1.7674
1.7613
1.7326
1.7261
1.6783
1.6475
1.6058
1.5703
1.3870
1.3554
1.3221
1.8840
1.8090
1.7943
1.7861
1.7674
1.7613
1.7326
1.7261
1.6783
1.6475
1.6058
1.3221
1.2956
1.2565
1.1560
1.1319
1.1013
1.0652
1.0581
1.0272
1.0210
PCy2
N
N
Me
2.0
1.8
1.6
1.4
1.2
1.0
ppm
9.5
9.0
8.5
8.0
7.5
7.0
6.5
6.0
5.5
5.0
4.5
4.0
3.5
3.0
2.5
2.0
1.5
1.0
ppm
0.96
3.00
1.00
2.00
9.92
8.19
5.08
4.22
3.10
153.37
153.05
141.81
141.75
107.54
107.41
77.32
77.00
76.68
37.82
36.65
36.59
33.46
33.39
31.83
31.78
30.56
30.40
28.99
28.92
27.30
27.17
27.10
27.03
26.85
PCy2
N
N
Me
190
180
170
160
150
140
130
120
110
100
90
80
70
60
50
40
30
20
ppm

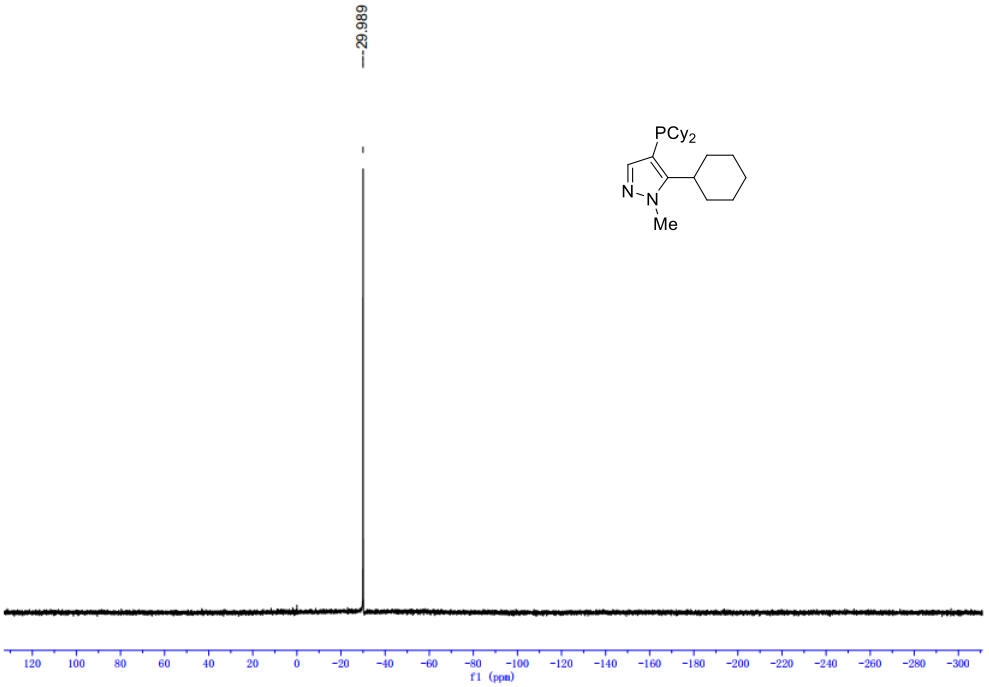

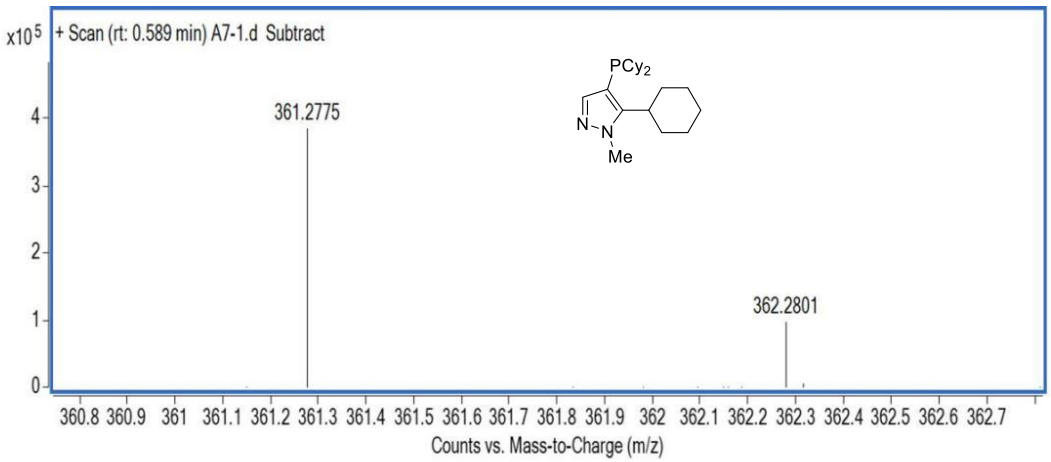

Mass	m/z (Calc)	Diff (mDa)	Diff (ppm)	Formula
361.2775	361.2767	-0.79	-2.19	C22 H38 P N2

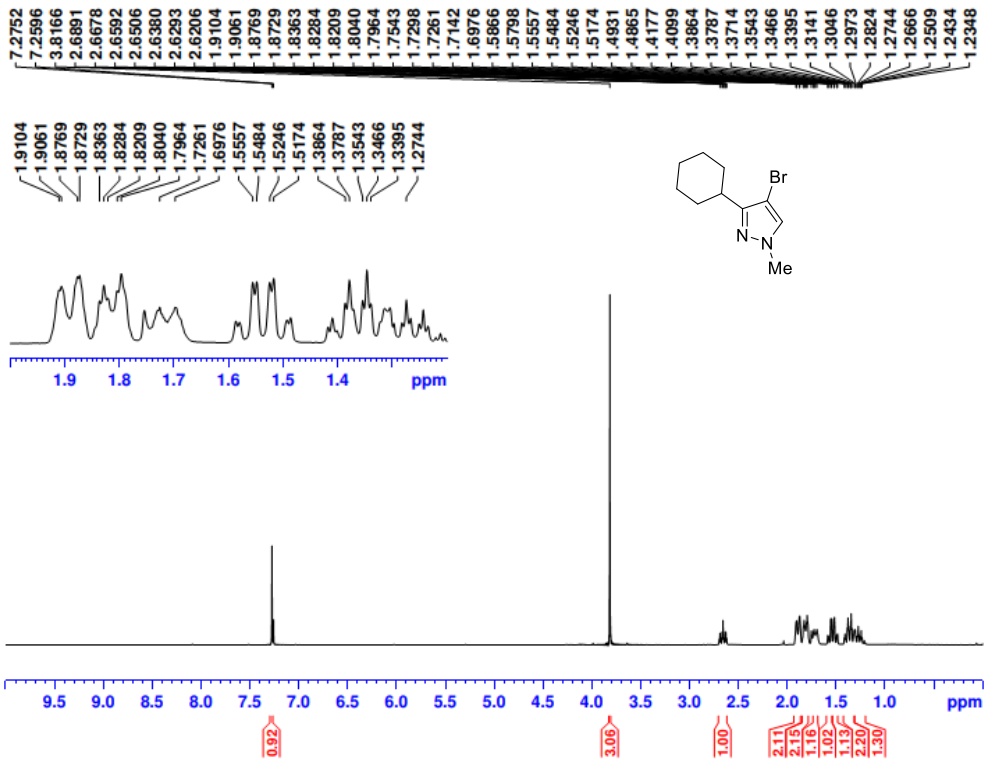
7.2752 7.2596 3.8166 2.6891 2.6678 2.6592 2.6506 2.6380 2.6293 2.6206 1.9104 1.9061 1.8769 1.8729 1.8363 1.8284 1.8209 1.8040 1.7964 1.7543 1.7298 1.7261 1.7142 1.6976 1.5866 1.5798 1.5557 1.5484 1.5246 1.5174 1.4931 1.4865 1.4177 1.4099 1.3864 1.3787 1.3714 1.3543 1.3466 1.3395 1.3141 1.3046 1.2973 1.2824 1.2744 1.2666 1.2509 1.2434 1.2348
1.9104 1.9061 1.8769 1.8729 1.8363 1.8284 1.8209 1.8040 1.7964 1.7261 1.6976 1.5557 1.5484 1.5246 1.5174 1.3864 1.3787 1.3543 1.3466 1.3395 1.2744
Br
N
N
Me
1.9 1.8 1.7 1.6 1.5 1.4 ppm
9.5 9.0 8.5 8.0 7.5 7.0 6.5 6.0 5.5 5.0 4.5 4.0 3.5 3.0 2.5 2.0 1.5 1.0 ppm
0.92 3.06 1.00 2.11 2.15 1.16 1.02 1.13 2.20 1.30

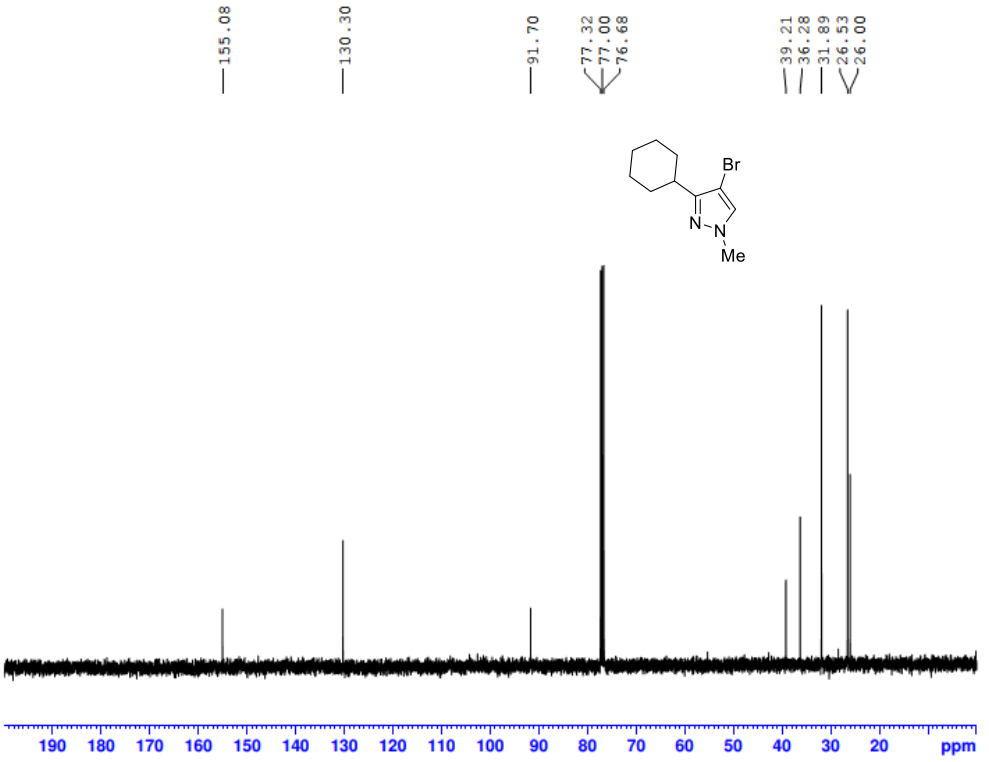
155.08
130.30
91.70
77.32
77.00
76.68
39.21
36.28
31.89
26.53
26.00
Br
N
N
Me
190 180 170 160 150 140 130 120 110 100 90 80 70 60 50 40 30 20 ppm

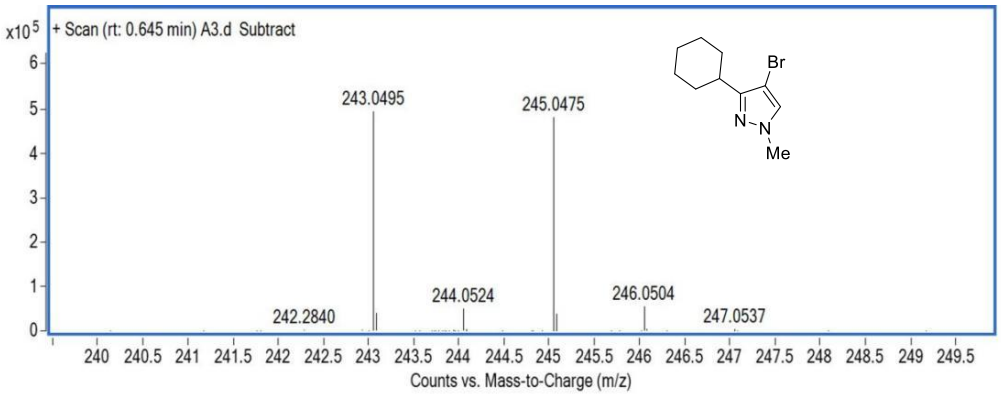

Mass	m/z (Calc)	Diff (mDa)	Diff (ppm)	Formula
243.0495	243.0491	-0.36	-1.51	C10 H16 BrN2

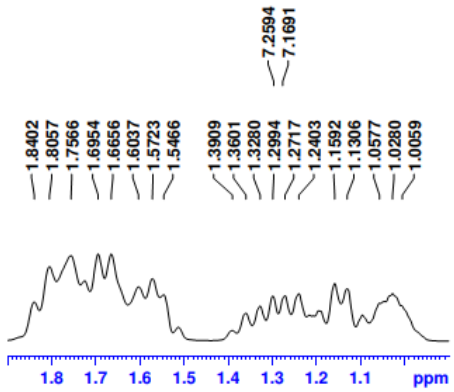

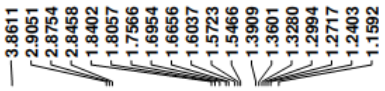

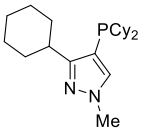

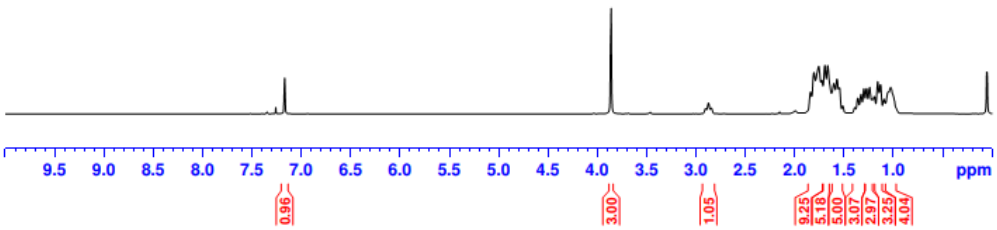

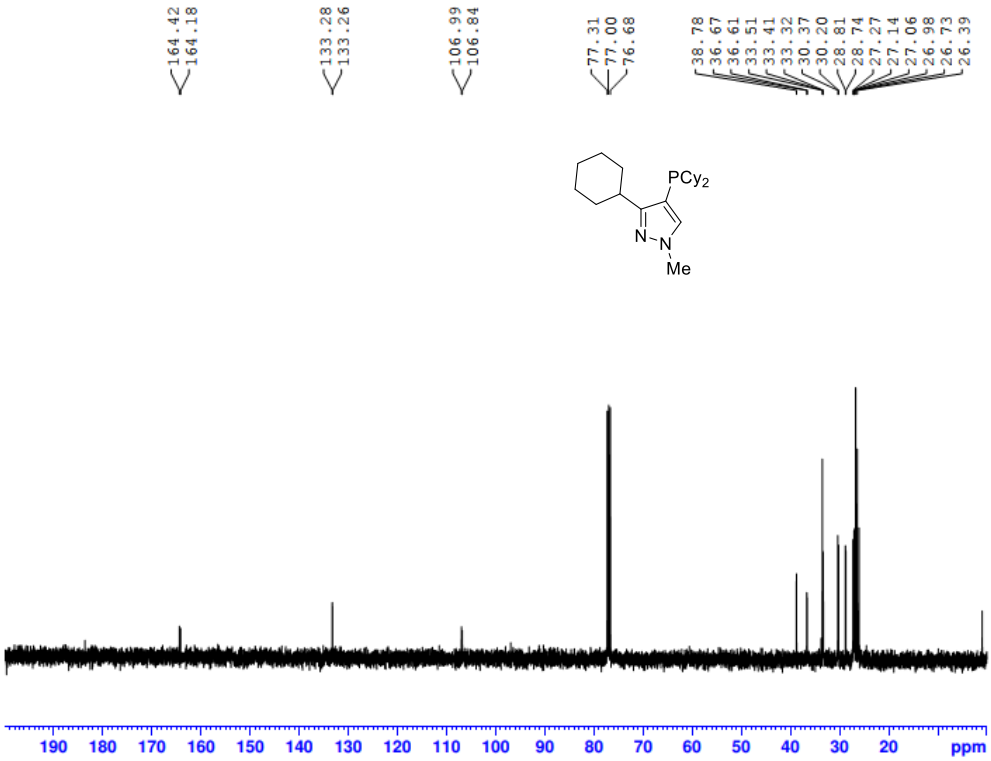
164.42
164.18
133.28
133.26
106.99
106.84
77.31
77.00
76.68
38.78
36.67
36.61
33.51
33.41
33.32
30.37
30.20
28.81
28.74
27.27
27.14
27.06
26.98
26.73
26.39
PCy2
N
N
Me
190 180 170 160 150 140 130 120 110 100 90 80 70 60 50 40 30 20 ppm

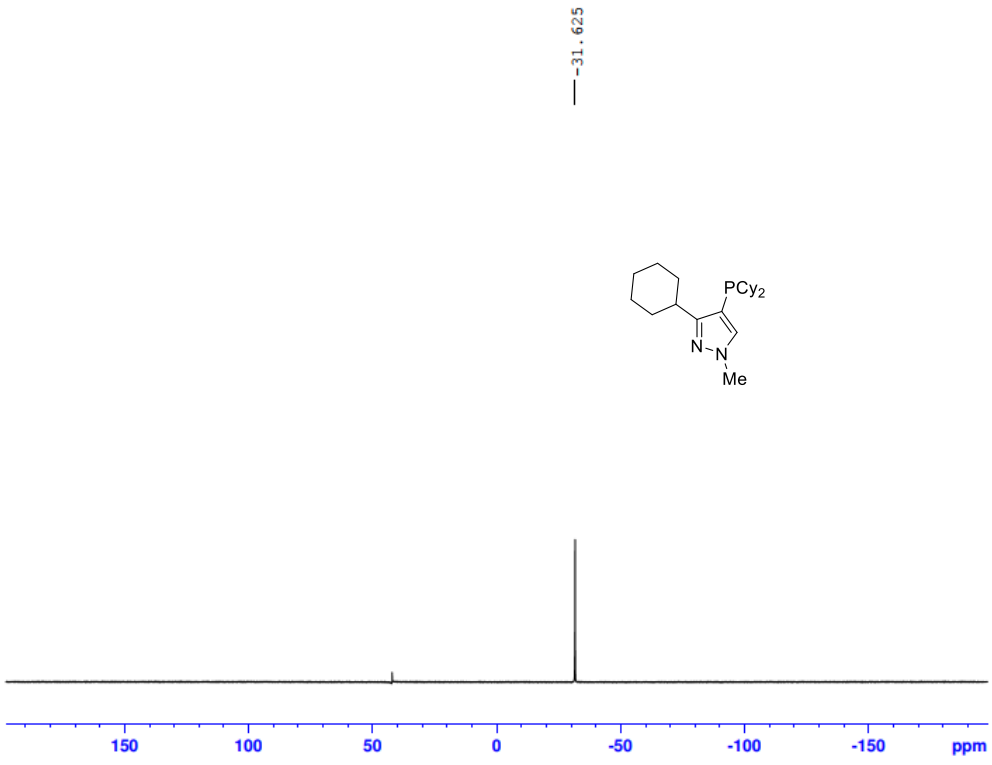
-31.625
PCy2
N
N
Me
150 100 50 0 -50 -100 -150 ppm

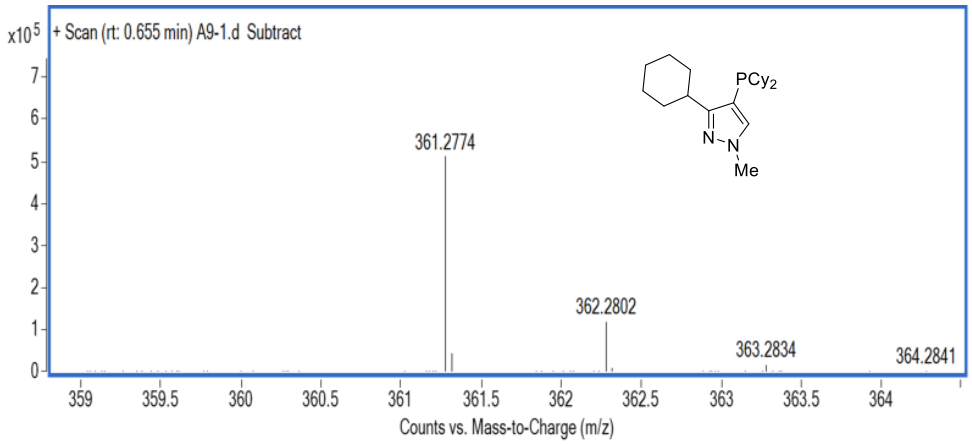

Mass	m/z (Calc)	Diff (mDa)	Diff (ppm)	Formula
361.2774	361.2767	-0.69	-1.91	C22 H38 P N2

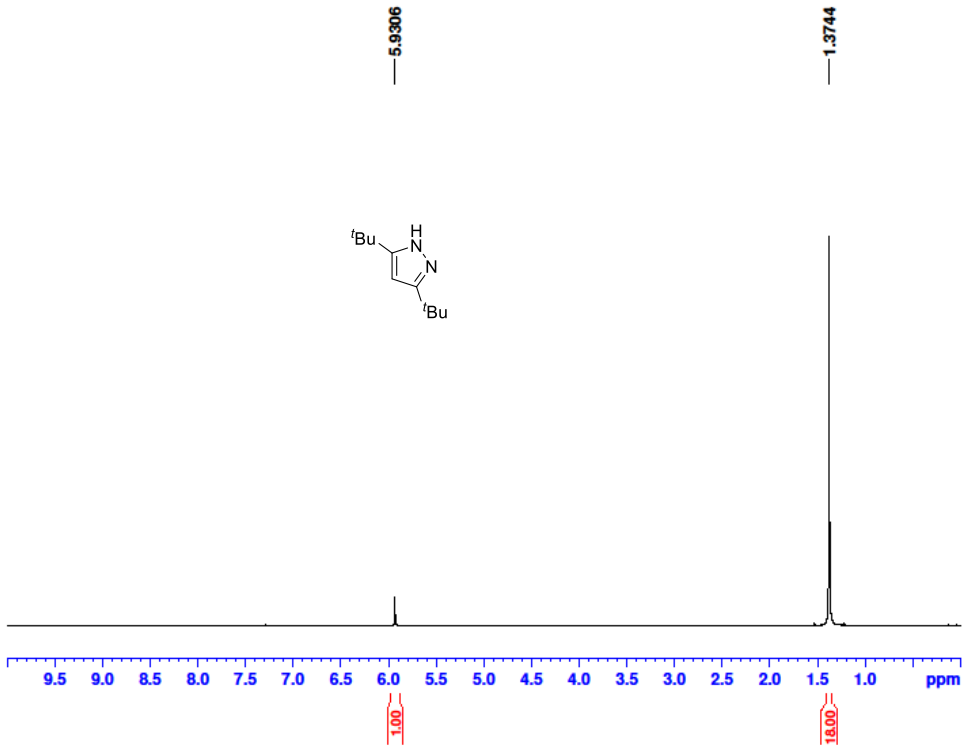

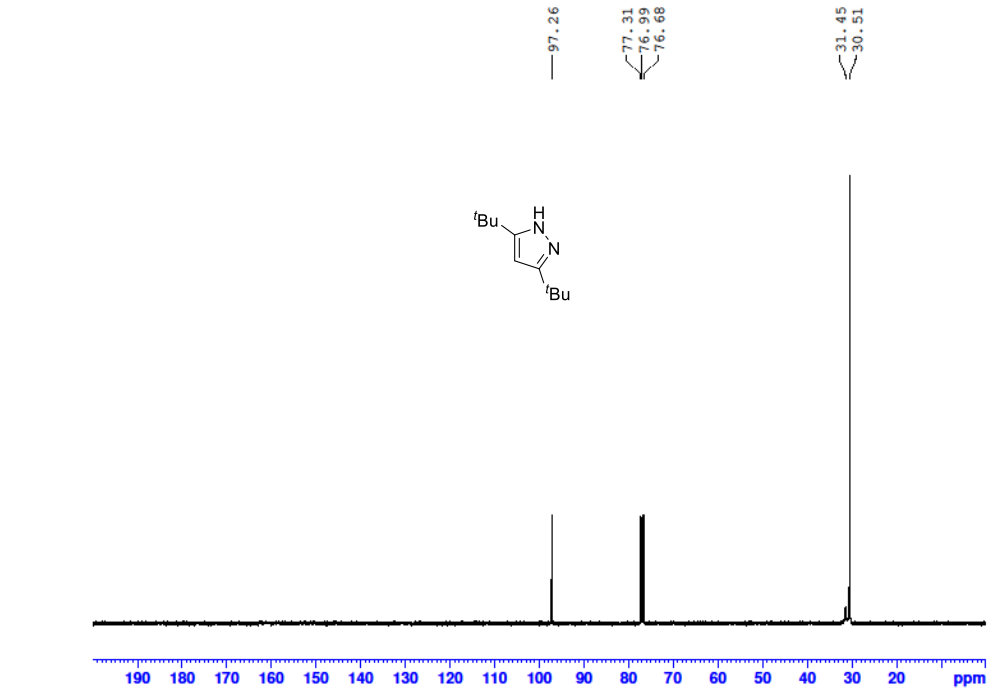
97.26
77.31
76.99
76.68
31.45
30.51
tBu
H
N
N
tBu
190 180 170 160 150 140 130 120 110 100 90 80 70 60 50 40 30 20 ppm

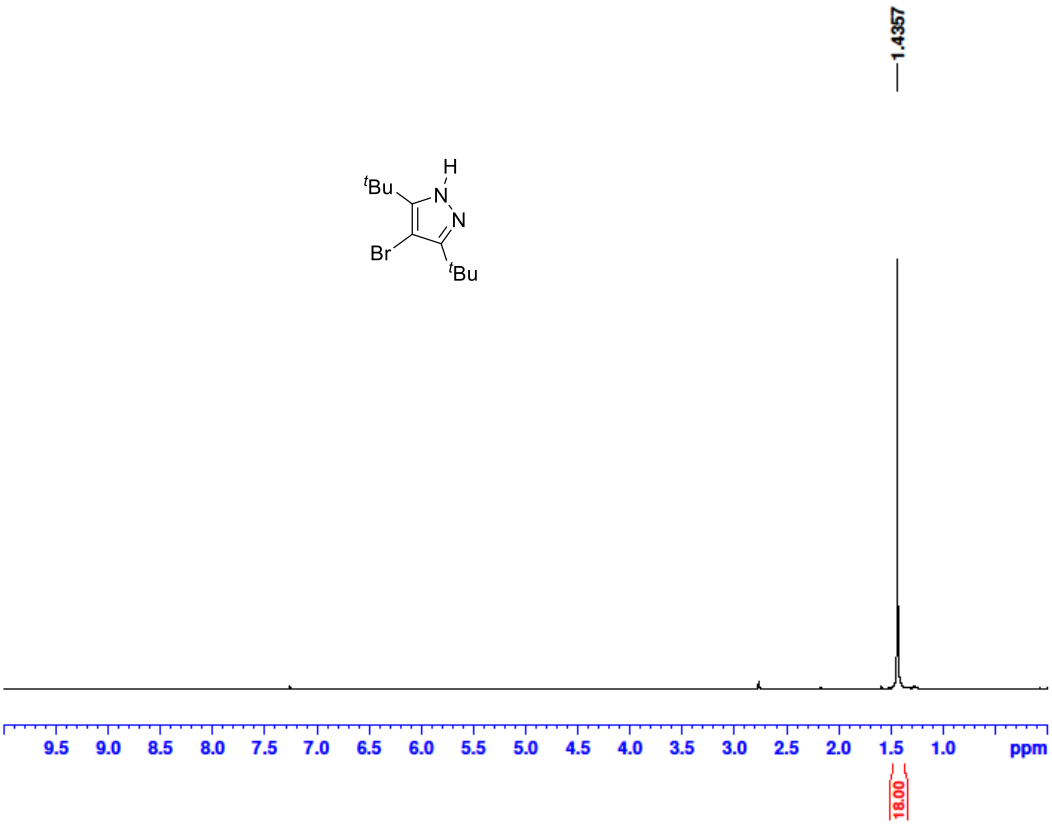
1.4357
tBu
H
N
N
Br
tBu
9.5 9.0 8.5 8.0 7.5 7.0 6.5 6.0 5.5 5.0 4.5 4.0 3.5 3.0 2.5 2.0 1.5 1.0 ppm
18.00

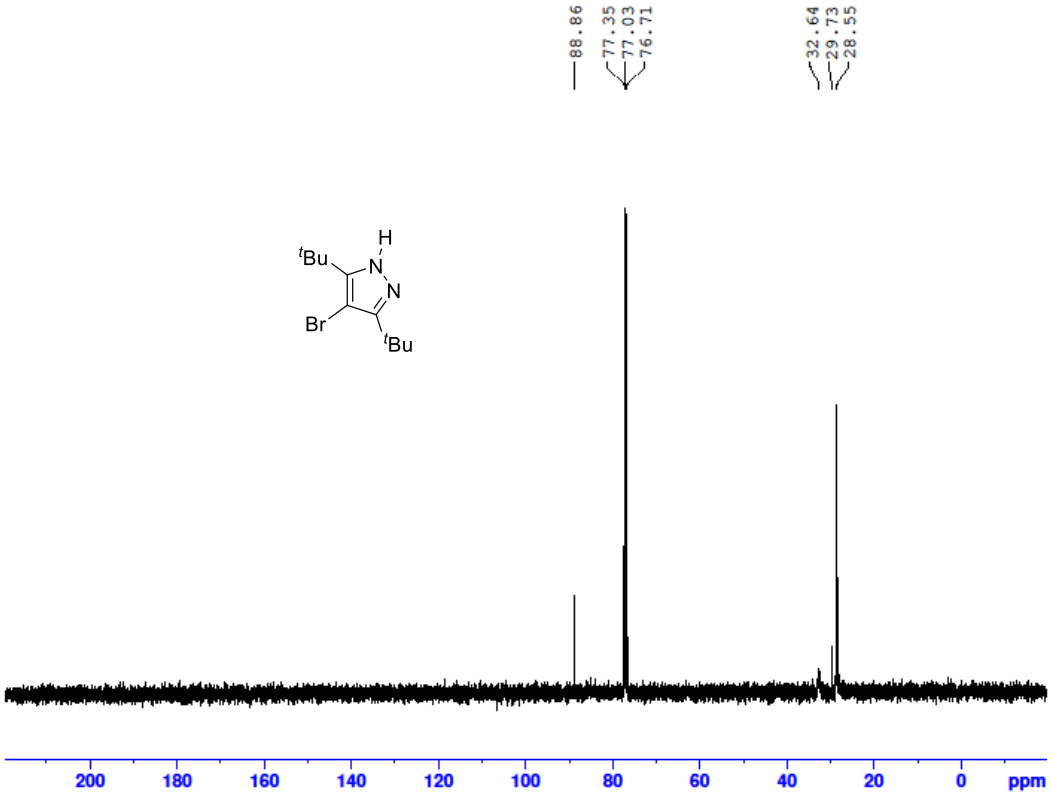
88.86
77.35
77.03
76.71
32.64
29.73
28.55
H
tBu
N
N
Br
tBu
200
180
160
140
120
100
80
60
40
20
0
ppm

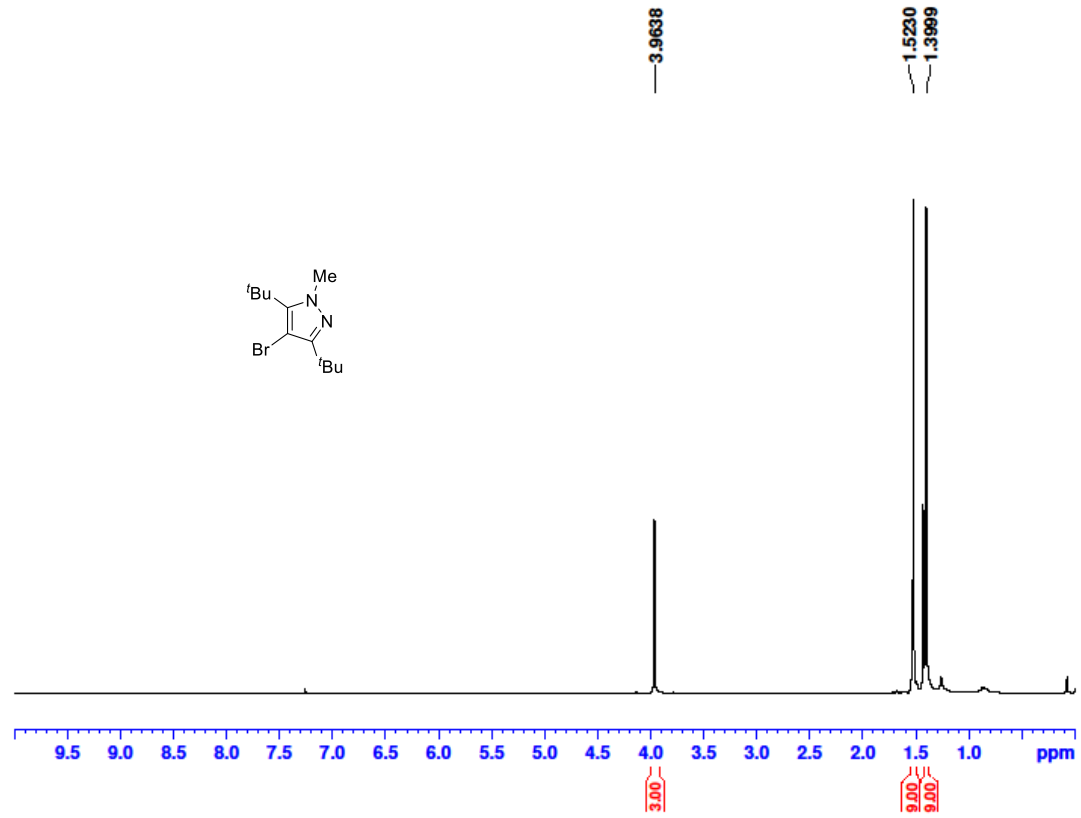
3.9638
1.5230
1.3999
Me
tBu
N
N
Br
tBu
9.5
9.0
8.5
8.0
7.5
7.0
6.5
6.0
5.5
5.0
4.5
4.0
3.5
3.0
2.5
2.0
1.5
1.0
ppm
3.00
9.00
9.00

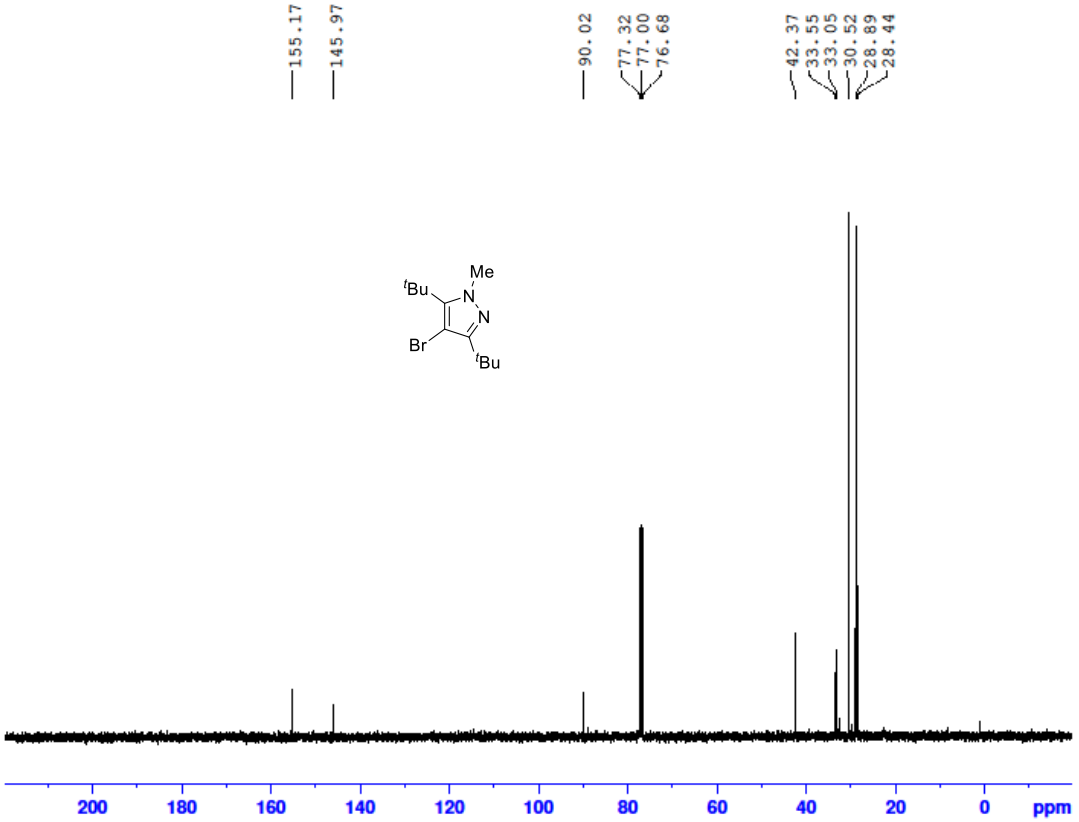

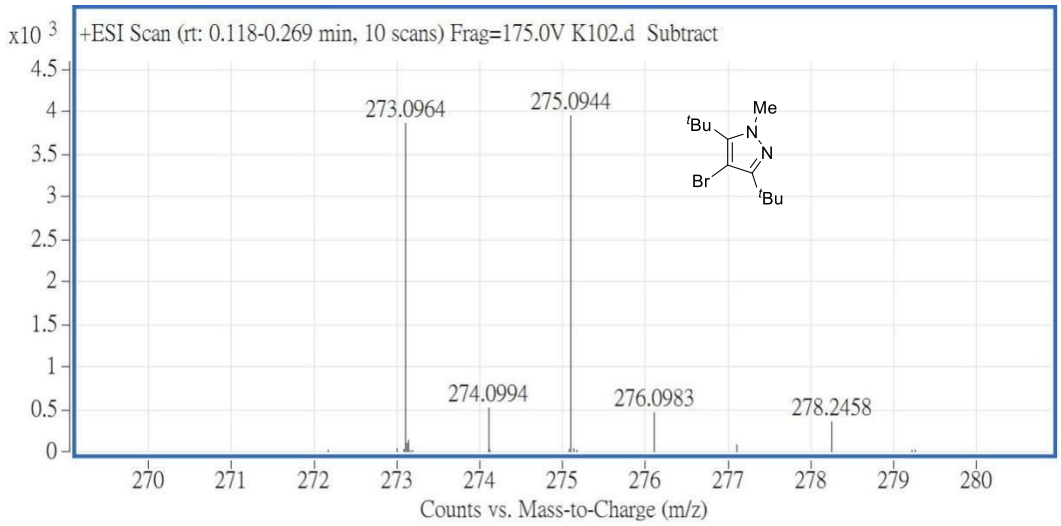

Mass	Calc. Mass	mDa	PPM	Formula
273.0964	273.0961	-0.31	-1.15	C12 H22 Br N2

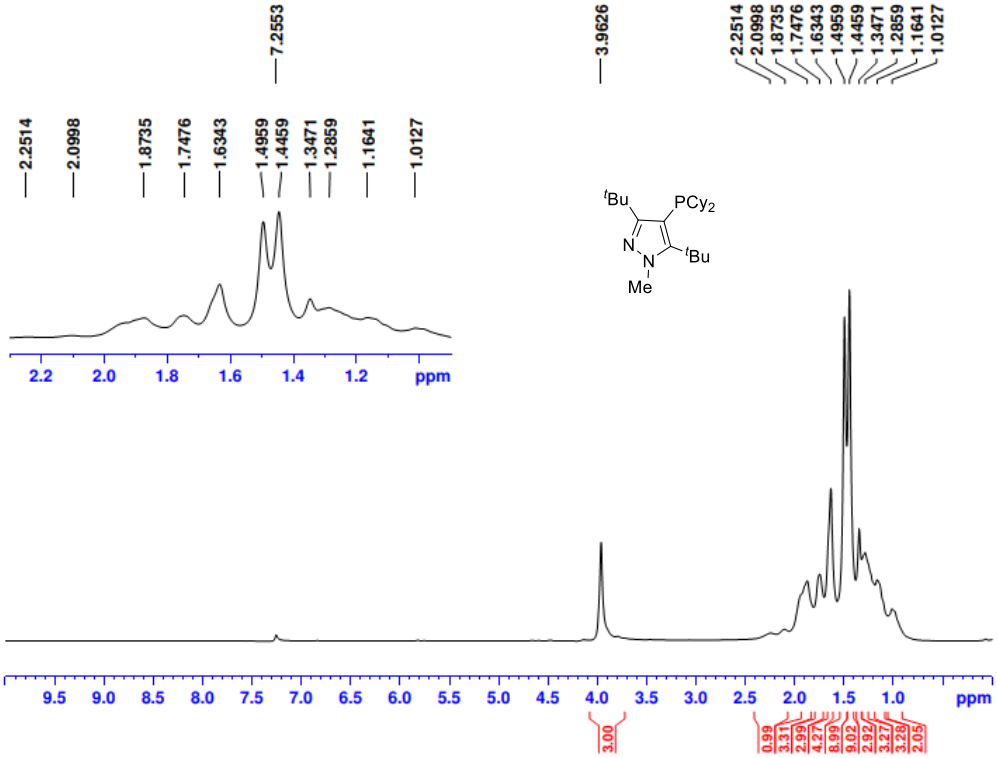
7.2553
3.9626
2.2514
2.0998
1.8735
1.7476
1.6343
1.4959
1.4459
1.3471
1.2859
1.1641
1.0127
tBu
PCy2
tBu
N
N
Me
2.2 2.0 1.8 1.6 1.4 1.2 ppm
9.5 9.0 8.5 8.0 7.5 7.0 6.5 6.0 5.5 5.0 4.5 4.0 3.5 3.0 2.5 2.0 1.5 1.0 ppm
3.00
0.99 3.31 2.99 4.27 8.99 9.02 2.92 3.27 3.28 2.05

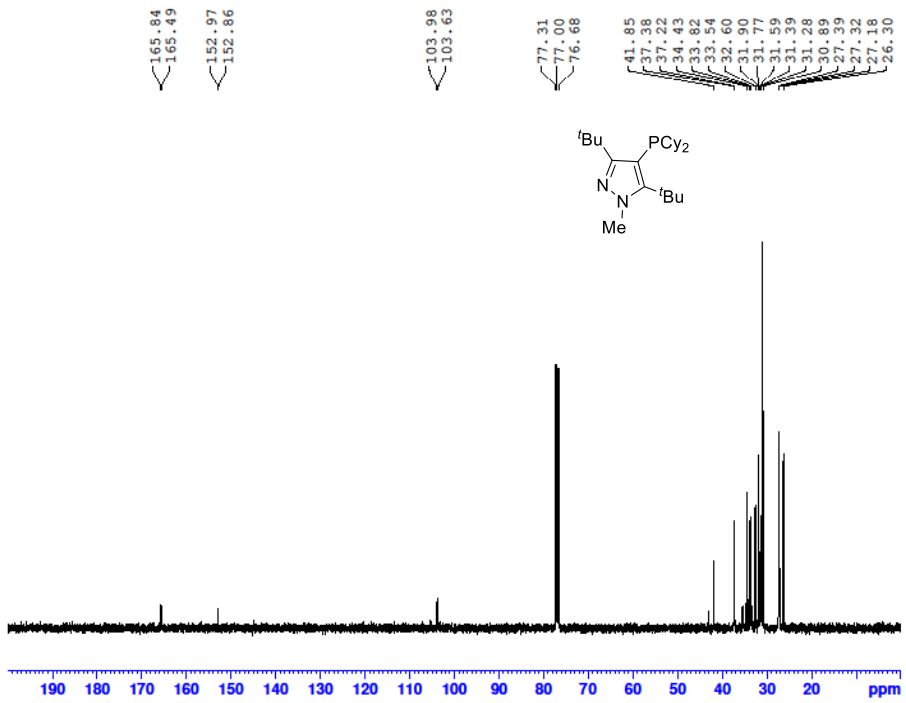
165.84
165.49
152.97
152.86
103.98
103.63
77.31
77.00
76.68
41.85
37.38
37.22
34.43
33.82
33.54
32.60
31.90
31.77
31.59
31.39
31.28
30.89
27.39
27.32
27.18
26.30
tBu
PCy2
tBu
N
N
Me
190 180 170 160 150 140 130 120 110 100 90 80 70 60 50 40 30 20 ppm

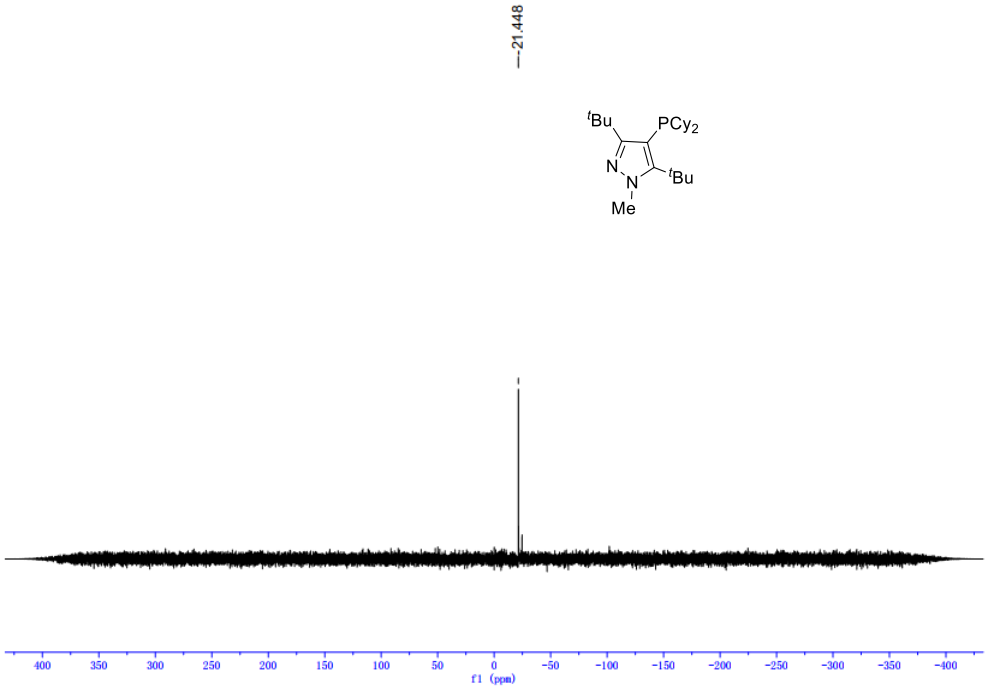

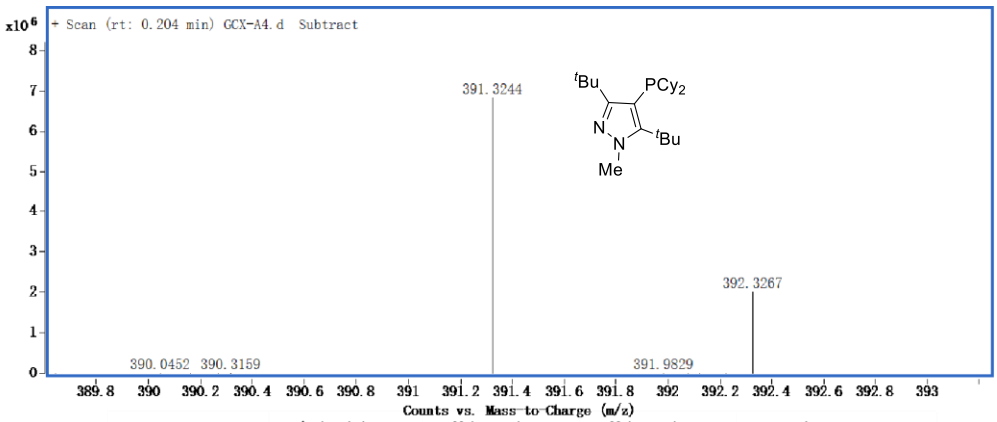

Mass	m/z (Calc)	Diff (mDa)	Diff (ppm)	Formula
391.3244	391.3237	-0.74	-1.89	C24 H44 N2 P

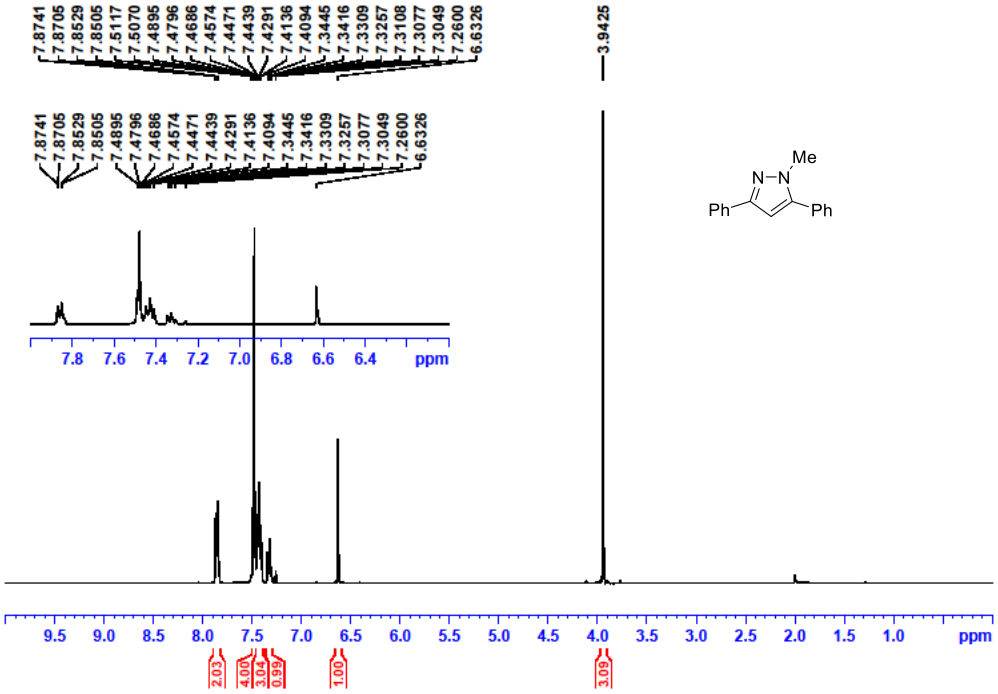
7.8741
7.8705
7.8529
7.8505
7.5117
7.5070
7.4895
7.4796
7.4686
7.4574
7.4471
7.4439
7.4291
7.4136
7.4094
7.3445
7.3416
7.3309
7.3257
7.3108
7.3077
7.3049
7.2600
6.6326
3.9425
Me
N–N
Ph
Ph
7.8 7.6 7.4 7.2 7.0 6.8 6.6 6.4 ppm
9.5 9.0 8.5 8.0 7.5 7.0 6.5 6.0 5.5 5.0 4.5 4.0 3.5 3.0 2.5 2.0 1.5 1.0 ppm
2.03
4.00
3.04
0.99
1.00
3.09

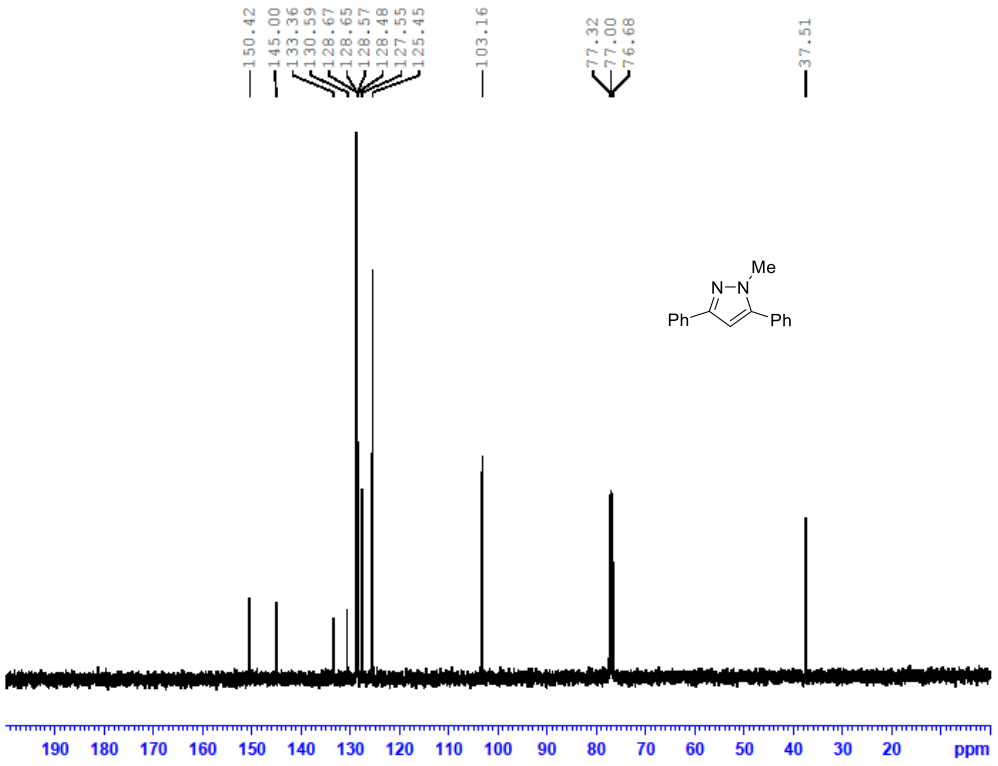
150.42
145.00
133.36
130.59
128.67
128.65
128.57
128.48
127.55
125.45
103.16
77.32
77.00
76.68
37.51
Me
N–N
Ph
Ph
190 180 170 160 150 140 130 120 110 100 90 80 70 60 50 40 30 20 ppm

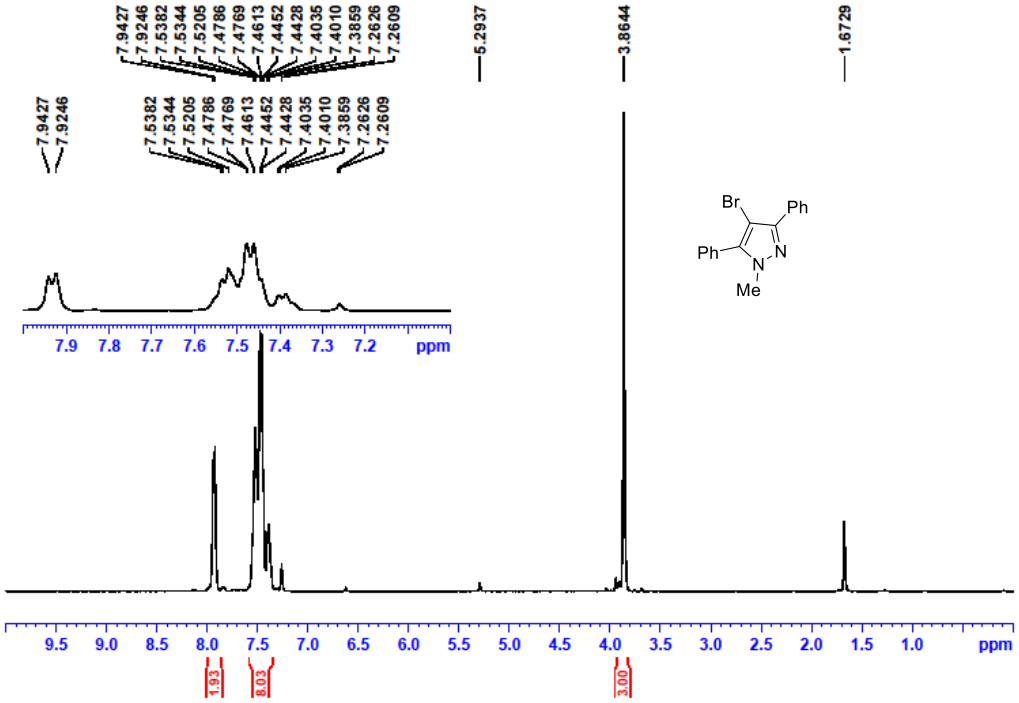
7.9427
7.9246
7.5382
7.5344
7.5205
7.4786
7.4769
7.4613
7.4452
7.4428
7.4035
7.4010
7.3859
7.2626
7.2609
5.2937
3.8644
1.6729
Br
Ph
Ph
N
N
Me
7.9 7.8 7.7 7.6 7.5 7.4 7.3 7.2 ppm
9.5 9.0 8.5 8.0 7.5 7.0 6.5 6.0 5.5 5.0 4.5 4.0 3.5 3.0 2.5 2.0 1.5 1.0 ppm
1.93
8.05
3.00

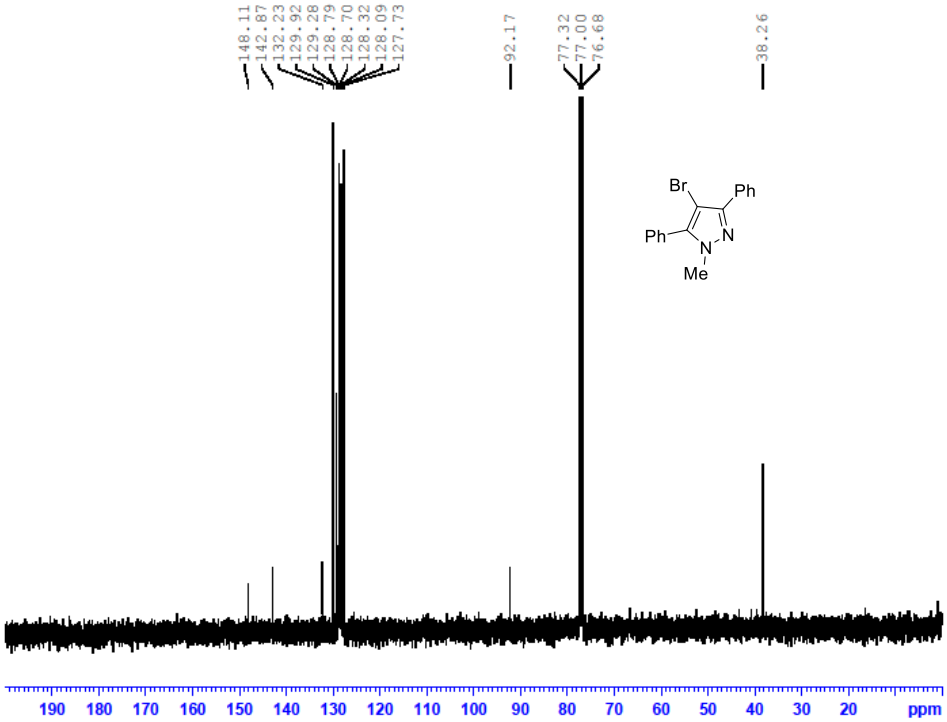
148.11
142.87
132.23
129.92
129.28
128.79
128.70
128.32
128.09
127.73
92.17
77.32
77.00
76.68
38.26
Br
Ph
Ph
N
N
Me
190 180 170 160 150 140 130 120 110 100 90 80 70 60 50 40 30 20 ppm

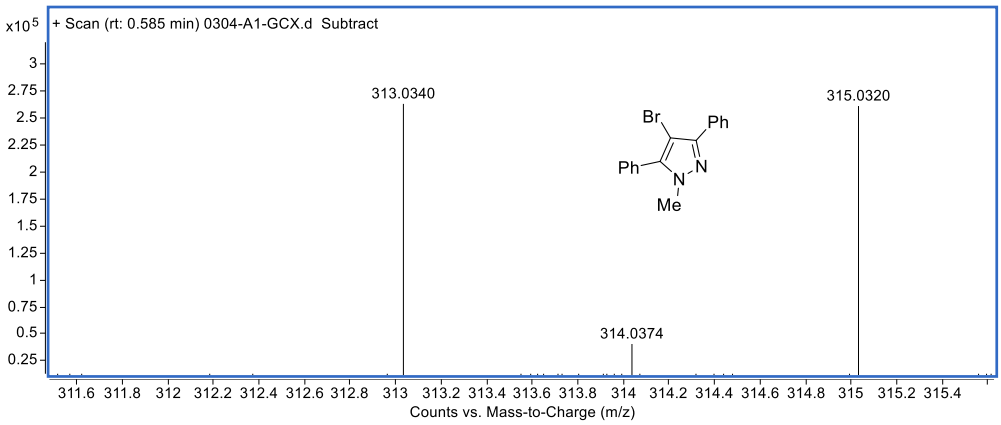

Mass	m/z (Calc)	Diff (mDa)	Diff (ppm)	Formula
313.0340	313.0335	-0.51	-1.64	C16 H14 BrN2

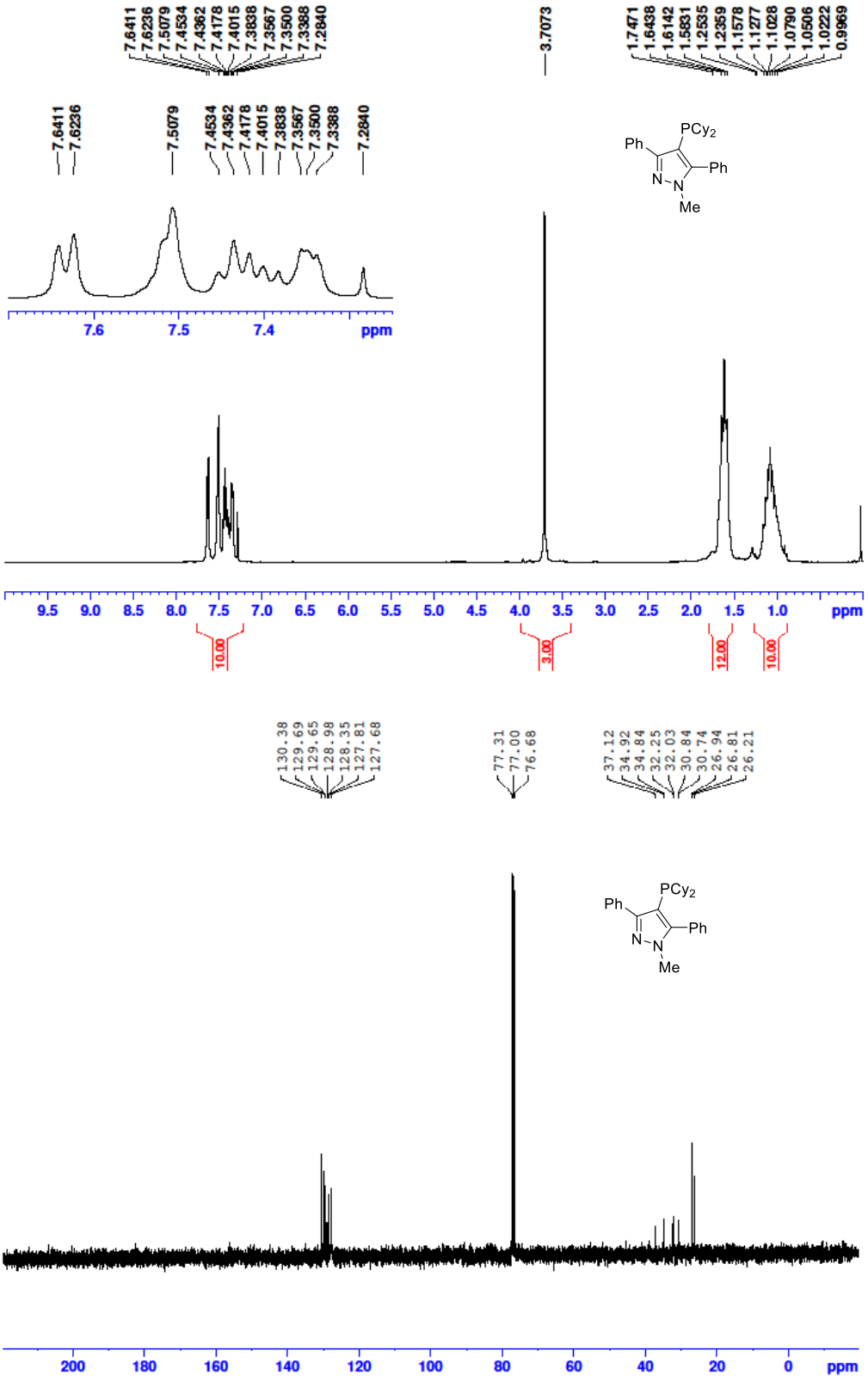
7.6411
7.6236
7.5079
7.4534
7.4362
7.4178
7.4015
7.3838
7.3567
7.3500
7.3388
7.2840
3.7073
1.7471
1.6438
1.6142
1.5831
1.2535
1.2359
1.1578
1.1277
1.1026
1.0790
1.0506
1.0222
0.9969
PCy2
Ph
Ph
N
N
Me
7.6
7.5
7.4
ppm
9.5
9.0
8.5
8.0
7.5
7.0
6.5
6.0
5.5
5.0
4.5
4.0
3.5
3.0
2.5
2.0
1.5
1.0
ppm
10.00
3.00
12.00
10.00
130.38
129.69
129.65
128.98
128.35
127.81
127.68
77.31
77.00
76.68
37.12
34.92
34.84
32.25
32.03
30.84
30.74
26.94
26.81
26.21
PCy2
Ph
Ph
N
N
Me
200
180
160
140
120
100
80
60
40
20
0
ppm

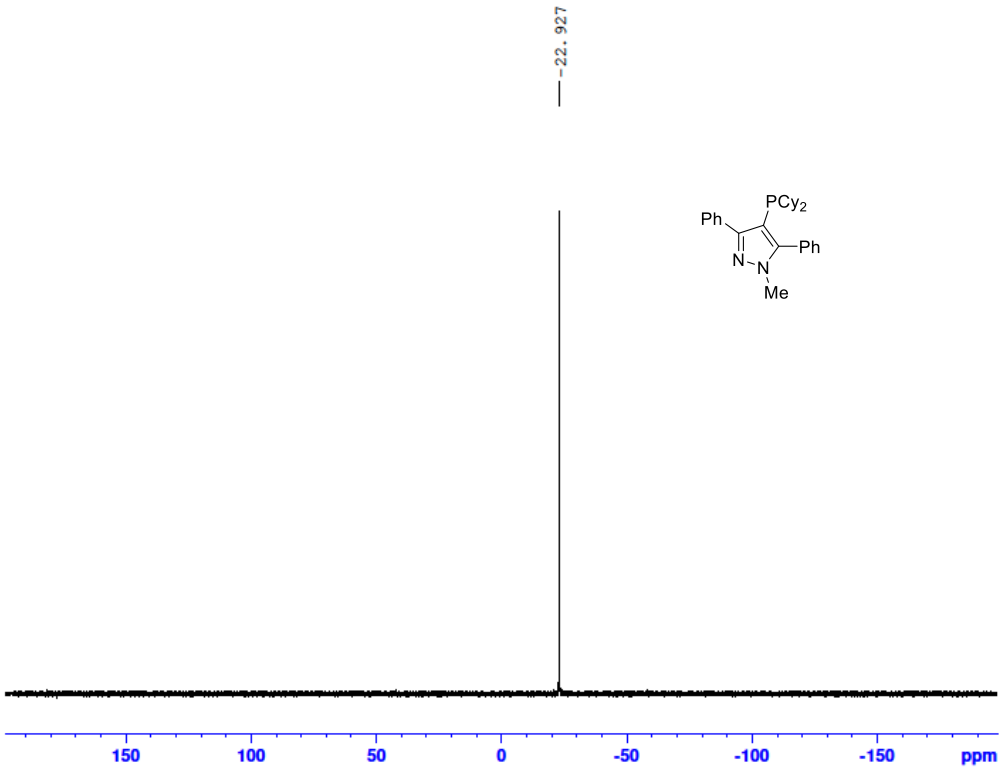

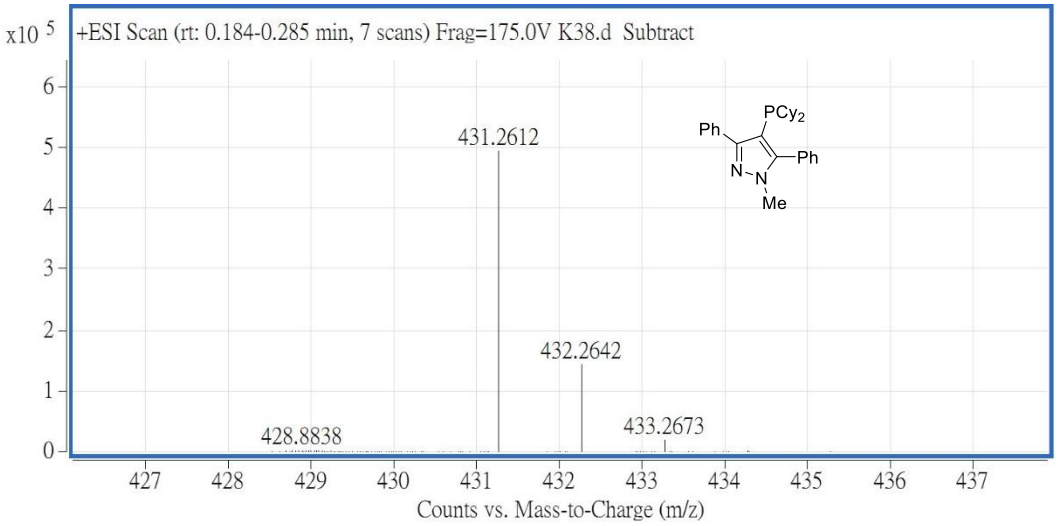

Mass	Calc. Mass	mDa	PPM	Formula
431.2612	431.2611	-0.14	-0.32	C28 H36 N2 P

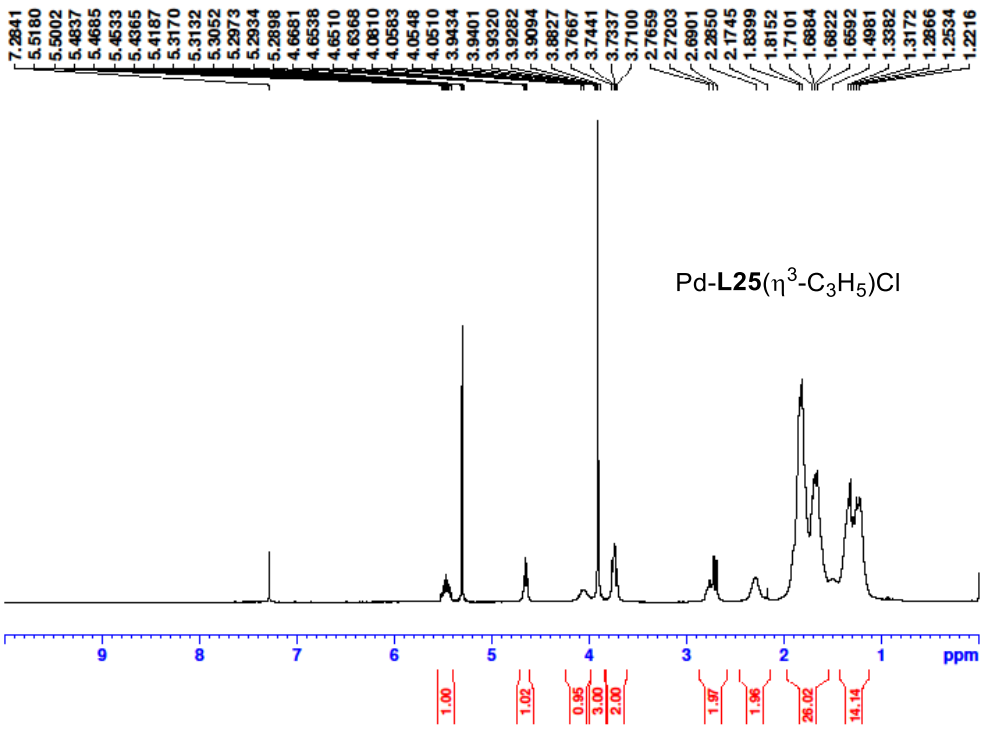
7.2841
5.5180
5.5002
5.4837
5.4685
5.4533
5.4365
5.4187
5.3170
5.3132
5.3052
5.2973
5.2934
5.2898
4.6681
4.6538
4.6510
4.6368
4.0610
4.0583
4.0548
4.0510
3.9434
3.9401
3.9320
3.9282
3.9094
3.8827
3.7667
3.7441
3.7337
3.7100
2.7659
2.7203
2.6901
2.2850
2.1745
1.8399
1.8152
1.7101
1.6884
1.6822
1.6592
1.4981
1.3382
1.3172
1.2866
1.2534
1.2216
Pd-L25(η3-C3H5)Cl
9
8
7
6
5
4
3
2
1
ppm
1.00
1.02
0.95
3.00
2.00
1.97
1.96
26.02
14.14

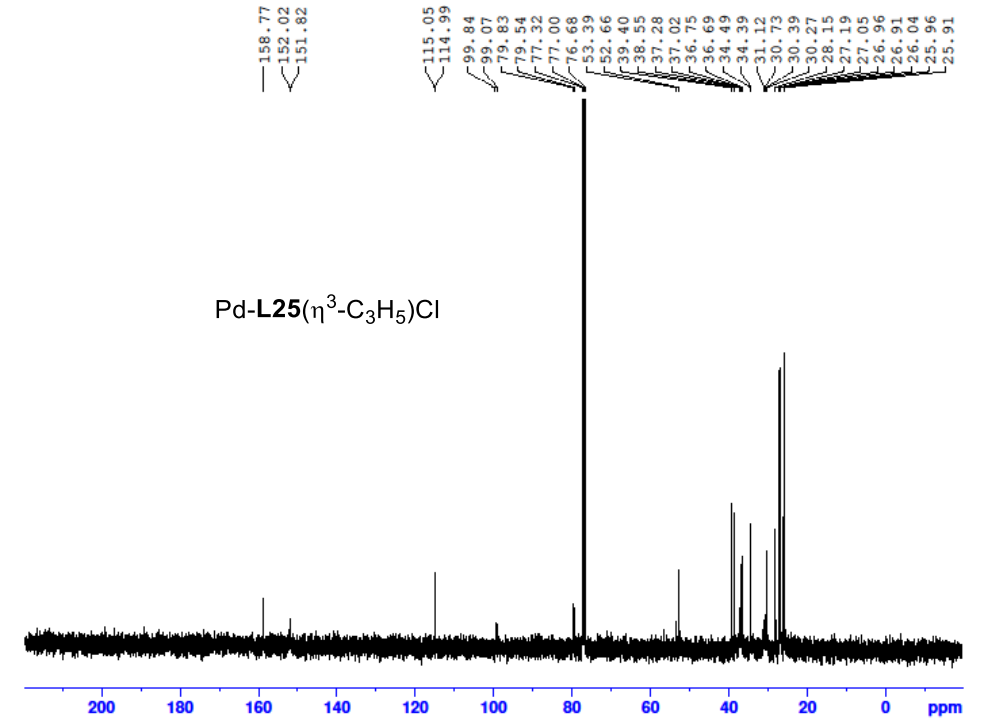
158.77
152.02
151.82
115.05
114.99
99.84
99.07
79.83
79.54
77.32
77.00
76.68
53.39
52.66
39.40
38.55
37.28
37.02
36.75
36.69
34.49
34.39
31.12
30.73
30.39
30.27
28.15
27.19
27.05
26.96
26.91
26.04
25.96
25.91
Pd-L25(η3-C3H5)Cl
200
180
160
140
120
100
80
60
40
20
0
ppm

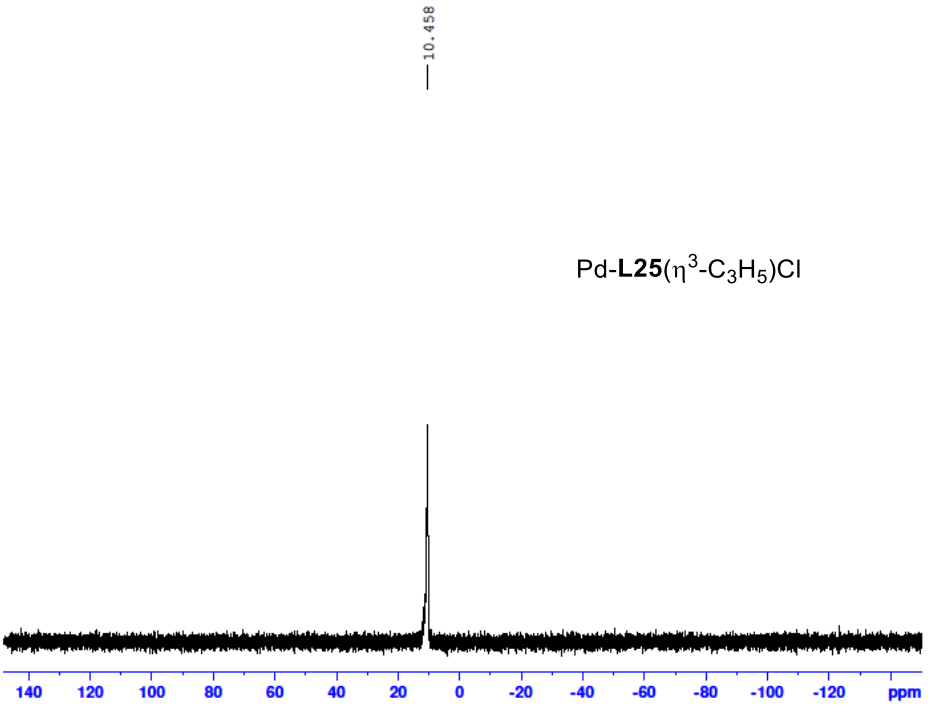
10.458
Pd-L25(η3-C3H5)Cl
140 120 100 80 60 40 20 0 -20 -40 -60 -80 -100 -120 ppm

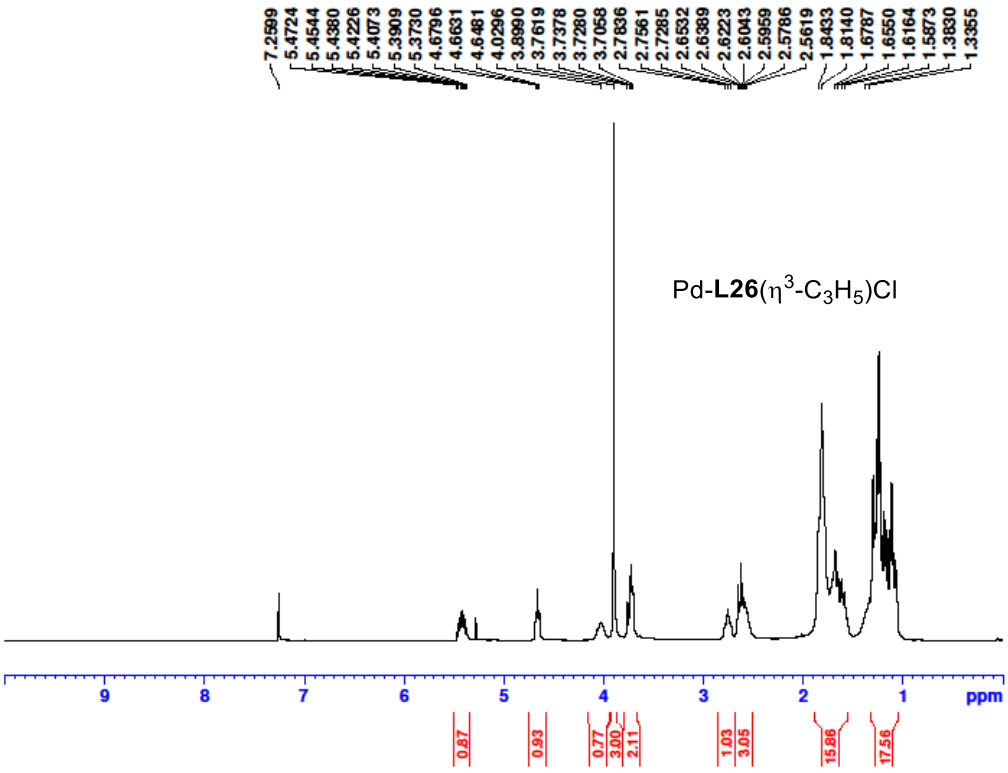
7.2599
5.4724
5.4544
5.4380
5.4226
5.4073
5.3909
5.3730
4.6796
4.6631
4.6481
4.0296
3.8990
3.7619
3.7378
3.7280
3.7058
2.7836
2.7561
2.7285
2.6532
2.6389
2.6223
2.6043
2.5959
2.5786
2.5619
1.8433
1.8140
1.6787
1.6550
1.6164
1.5873
1.3830
1.3355
Pd-L26(η3-C3H5)Cl
9 8 7 6 5 4 3 2 1 ppm
0.87
0.93
0.77
3.00
2.11
1.03
3.05
15.86
17.56

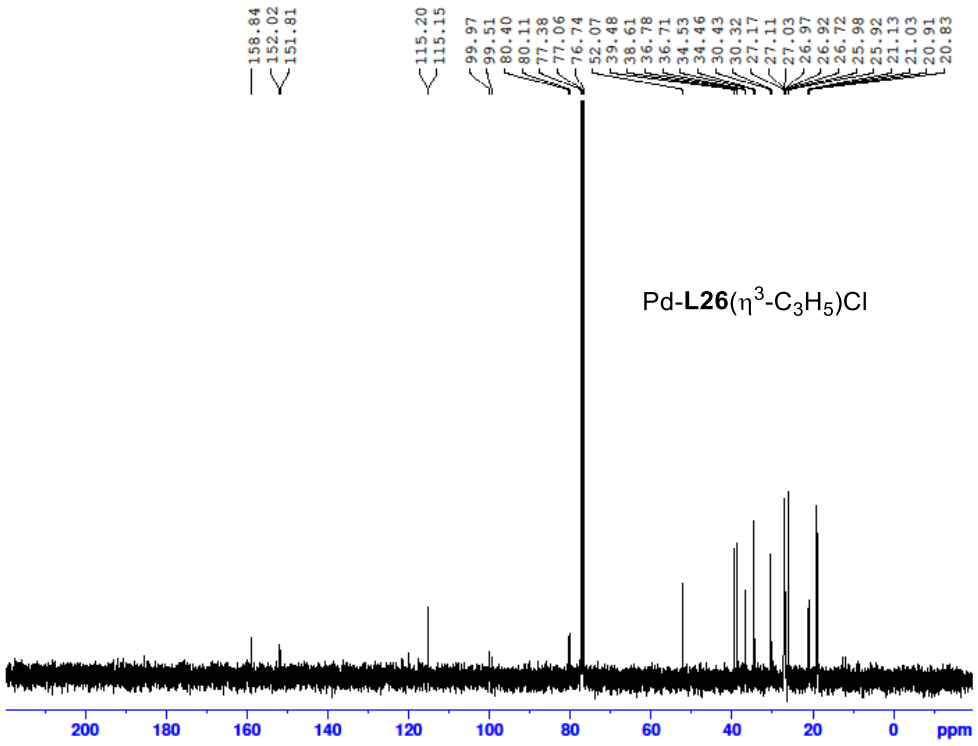
158.84
152.02
151.81
115.20
115.15
99.97
99.51
80.40
80.11
77.38
77.06
76.74
52.07
39.48
38.61
36.78
36.71
34.53
34.46
30.43
30.32
27.17
27.11
27.03
26.97
26.92
26.72
25.98
25.92
21.13
21.03
20.91
20.83
Pd-L26(η3-C3H5)Cl
200
180
160
140
120
100
80
60
40
20
0
ppm

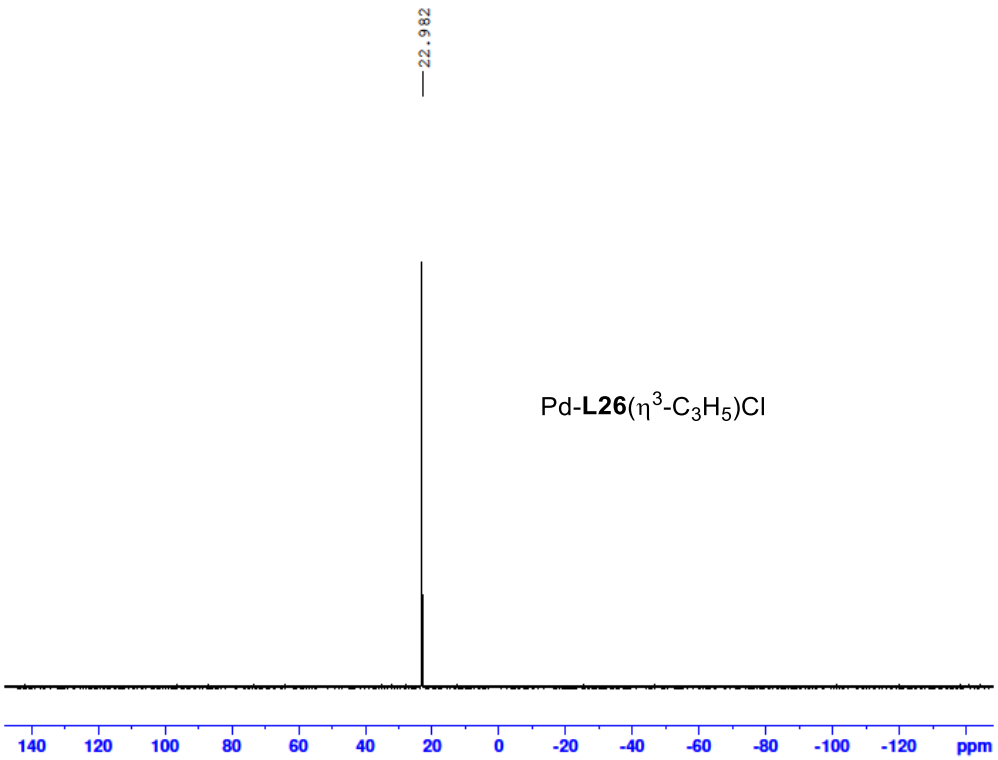
22.982
Pd-L26(η3-C3H5)Cl
140
120
100
80
60
40
20
0
-20
-40
-60
-80
-100
-120
ppm

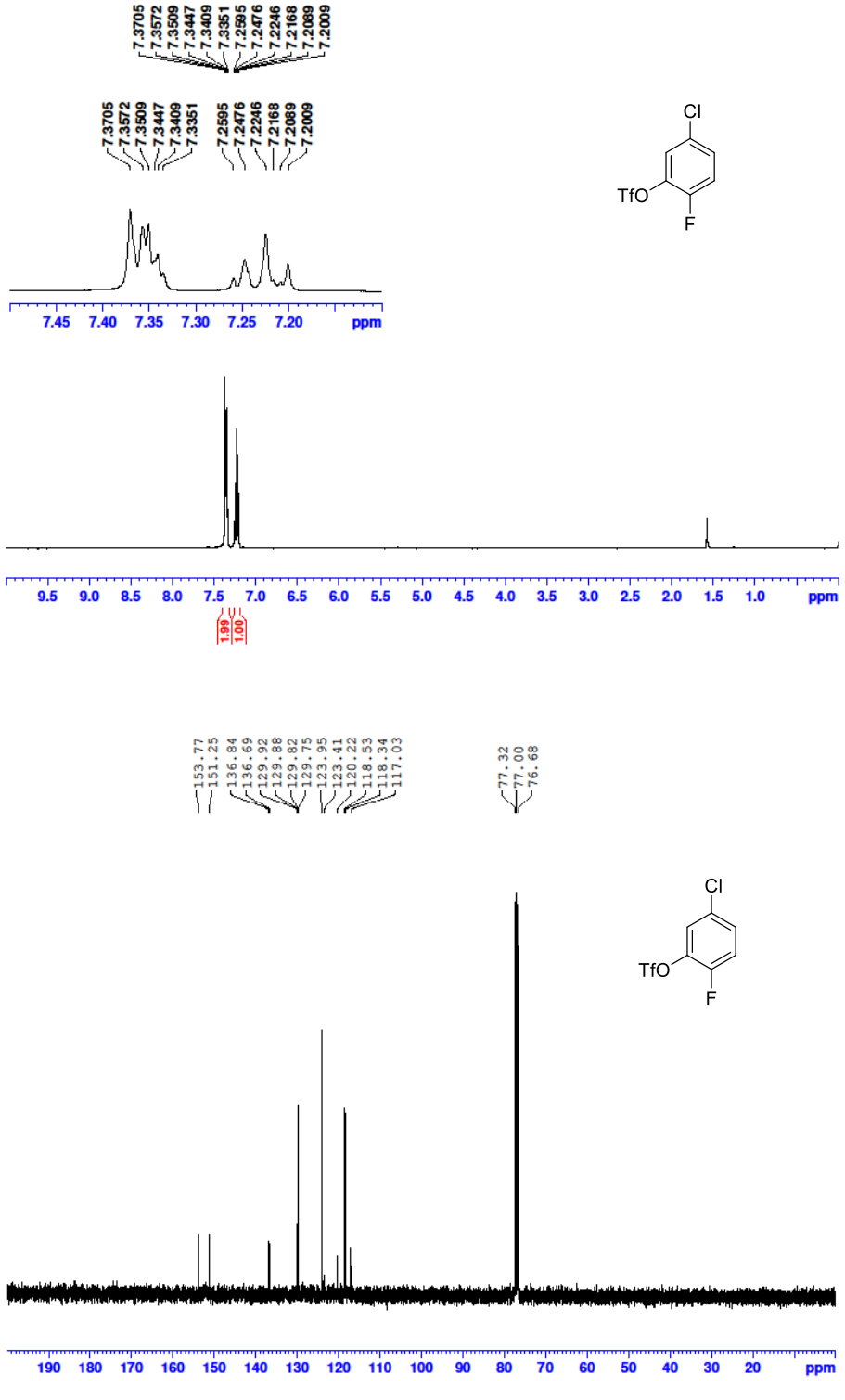
7.3705
7.3572
7.3509
7.3447
7.3409
7.3351
7.2595
7.2476
7.2246
7.2168
7.2089
7.2009
Cl
TfO
F
7.45 7.40 7.35 7.30 7.25 7.20 ppm
9.5 9.0 8.5 8.0 7.5 7.0 6.5 6.0 5.5 5.0 4.5 4.0 3.5 3.0 2.5 2.0 1.5 1.0 ppm
1.99
1.00
153.77
151.25
136.84
136.69
129.92
129.88
129.82
129.75
123.95
123.41
120.22
118.53
118.34
117.03
77.32
77.00
76.68
190 180 170 160 150 140 130 120 110 100 90 80 70 60 50 40 30 20 ppm

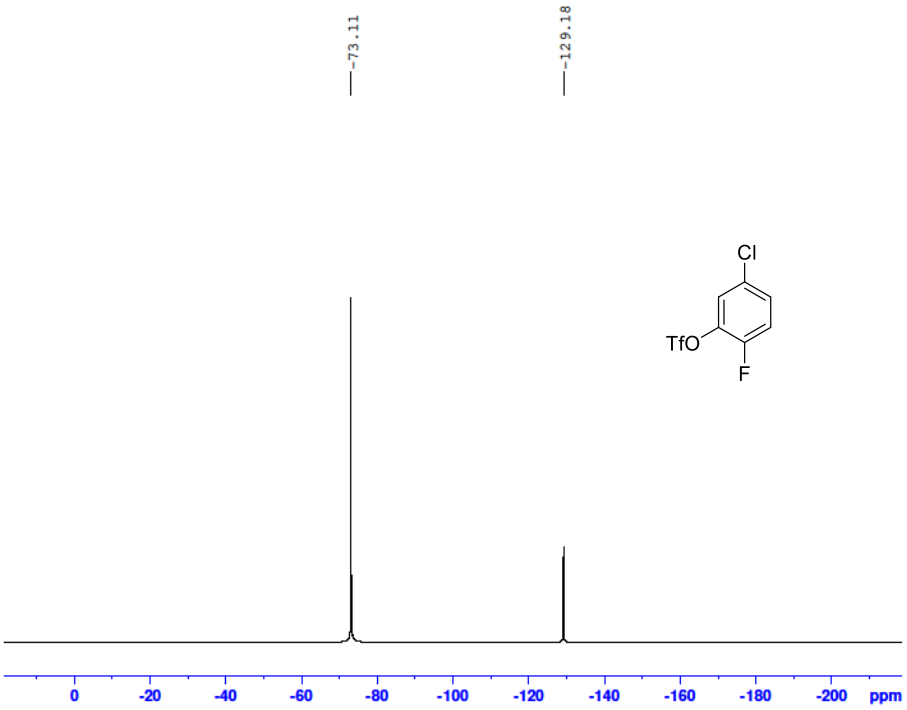

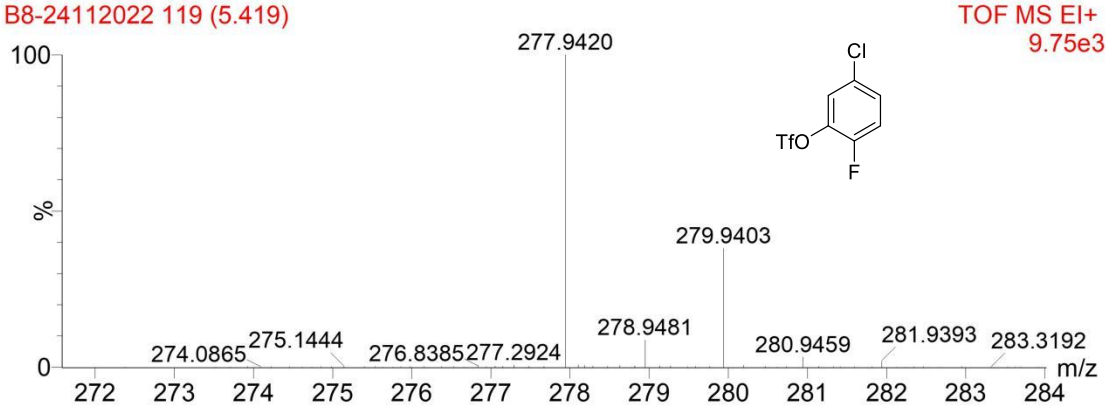

Mass	Calc. Mass	mDa	PPM	Ion Formula
277.9420	277.9422	0.21	0.74	C7H3F4O3ClS

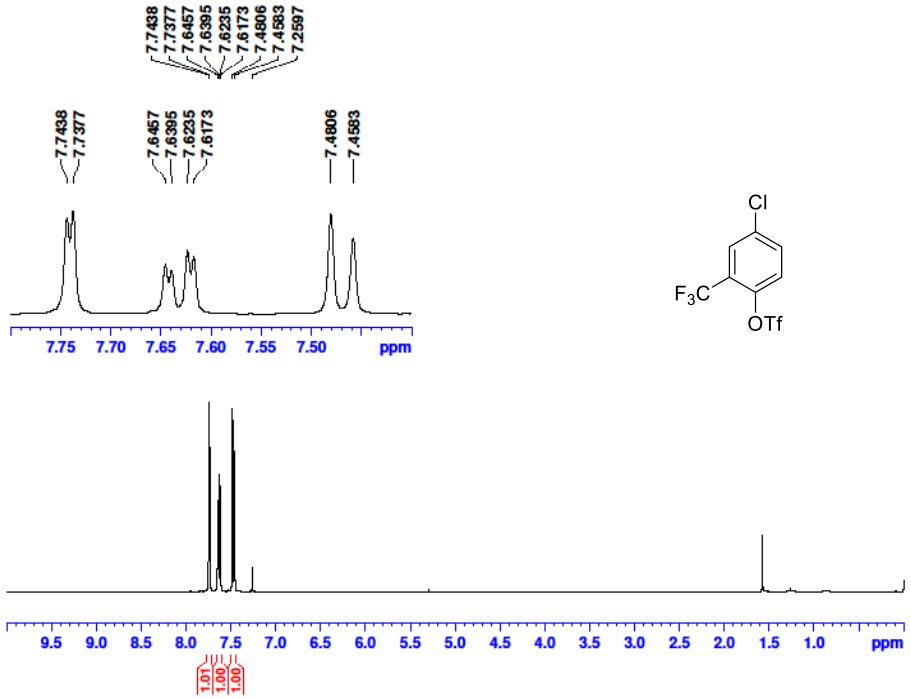
7.7438
7.7377
7.6457
7.6395
7.6235
7.6173
7.4806
7.4583
7.2597
7.75 7.70 7.65 7.60 7.55 7.50 ppm
Cl
F3C
OTf
9.5 9.0 8.5 8.0 7.5 7.0 6.5 6.0 5.5 5.0 4.5 4.0 3.5 3.0 2.5 2.0 1.5 1.0 ppm
1.01
1.00
1.00

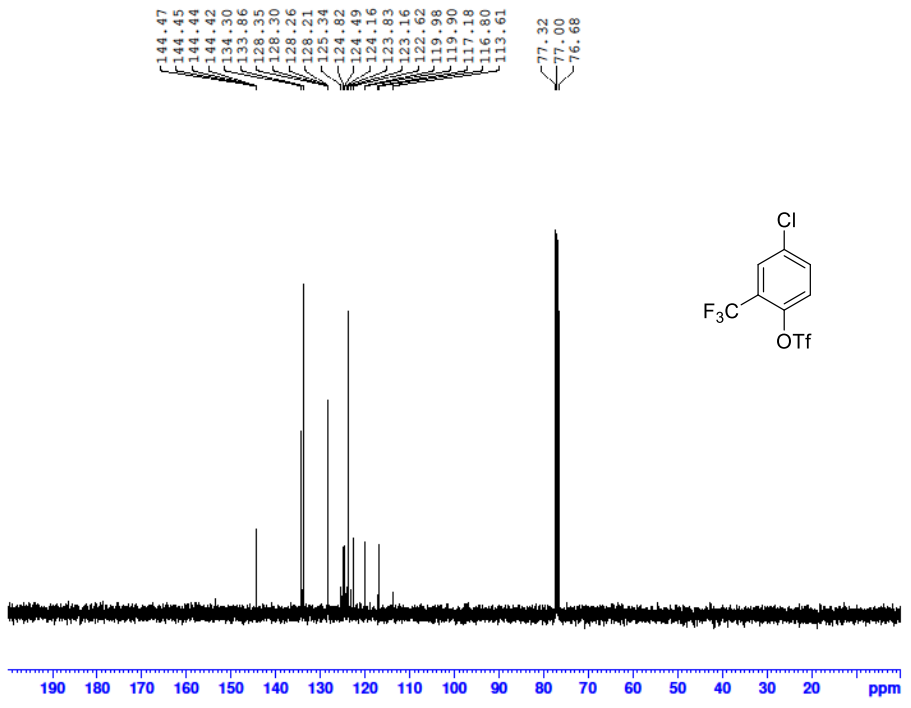
144.47
144.45
144.44
144.42
134.30
133.86
128.35
128.30
128.26
128.21
125.34
124.82
124.49
124.16
123.83
123.16
122.62
119.98
119.90
117.18
116.80
113.61
77.32
77.00
76.68
Cl
F3C
OTf
190 180 170 160 150 140 130 120 110 100 90 80 70 60 50 40 30 20 ppm

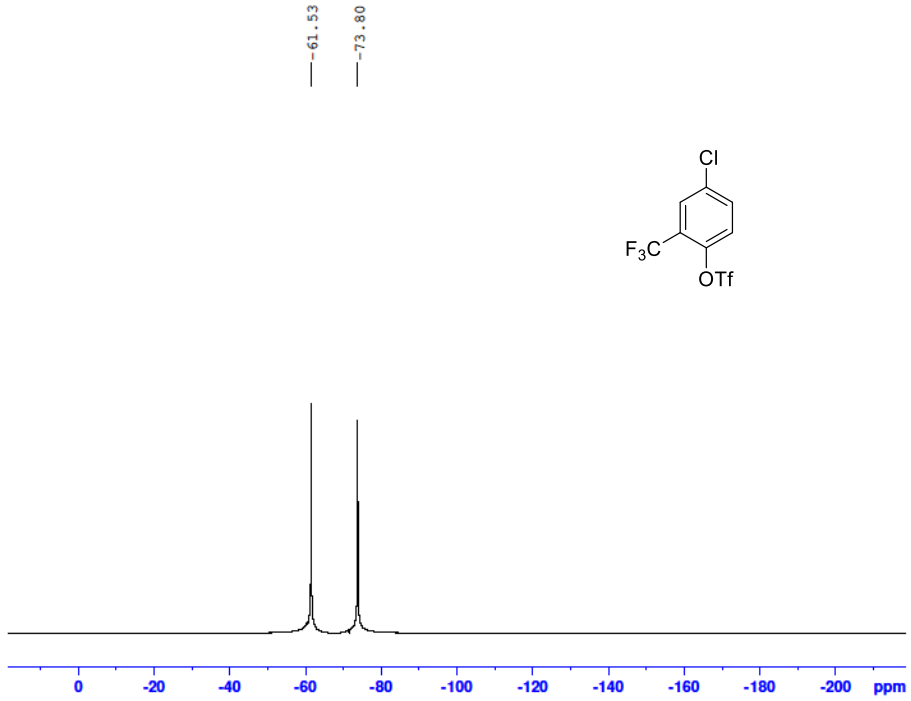

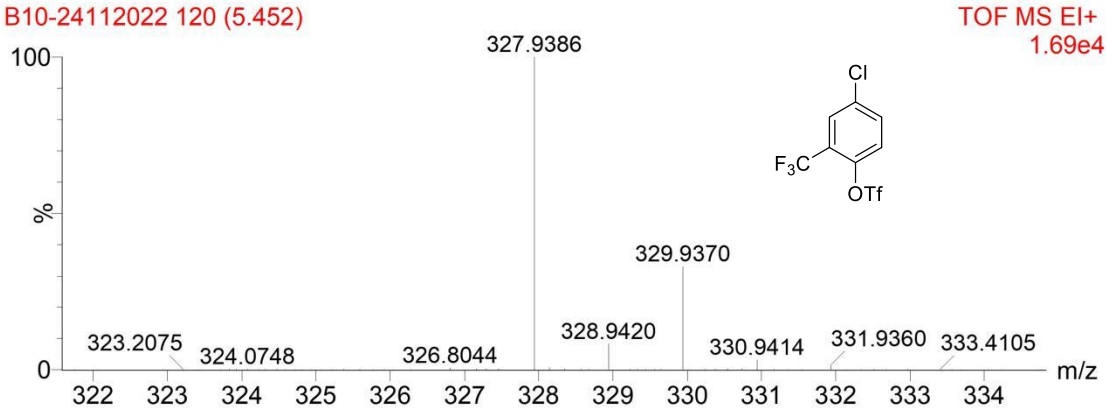

Mass	Calc. Mass	mDa	PPM	Ion Formula
327.9386	327.9390	0.41	1.26	C8H3F6O3ClS

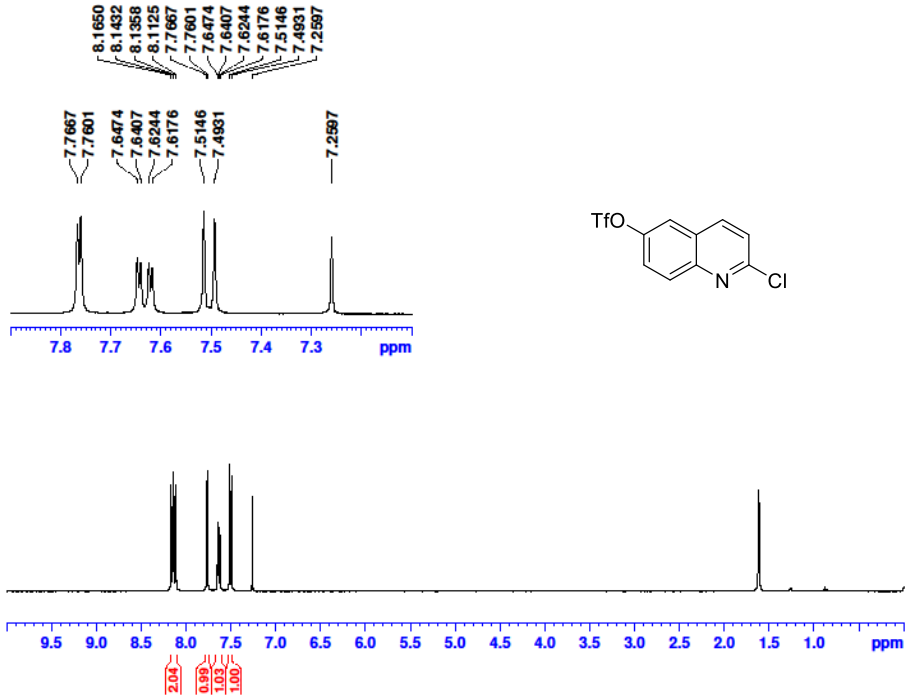
8.1650
8.1432
8.1358
8.1125
7.7667
7.7601
7.6474
7.6407
7.6244
7.6176
7.5146
7.4931
7.2597
TfO
N
Cl
ppm
2.04
0.99
1.03
1.00

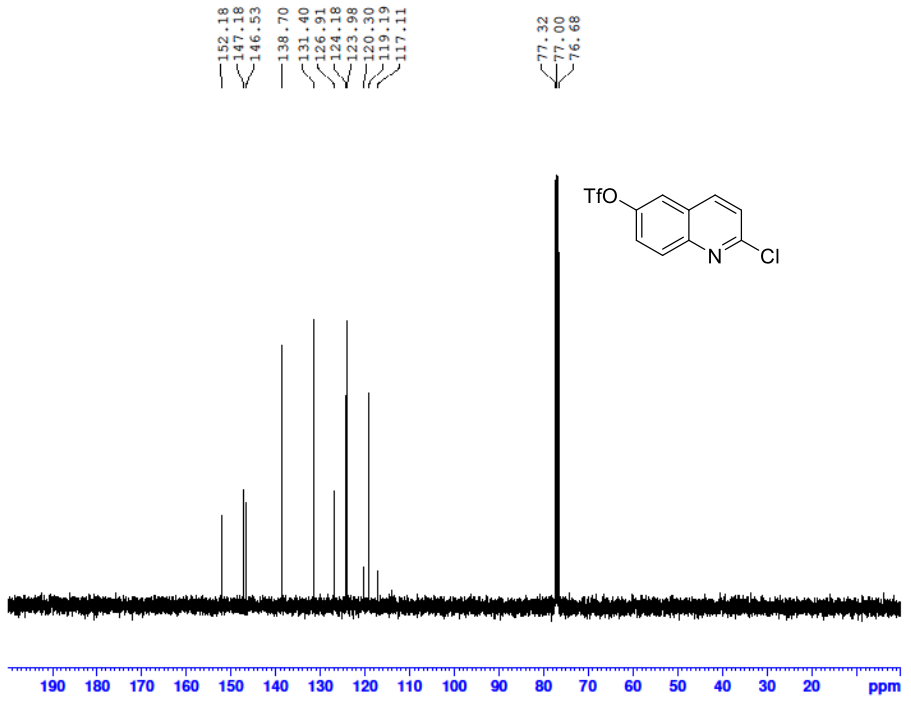
152.18
147.18
146.53
138.70
131.40
126.91
124.18
123.98
120.30
119.19
117.11
77.32
77.00
76.68
TfO
N
Cl
ppm

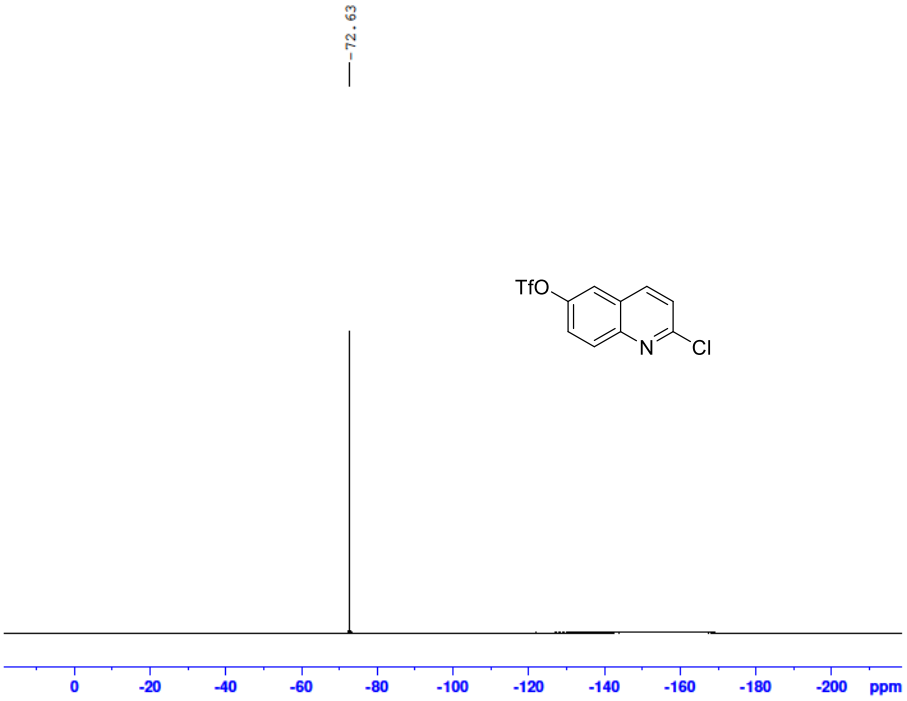
-72.63
TfO
N
Cl
0
-20
-40
-60
-80
-100
-120
-140
-160
-180
-200
ppm

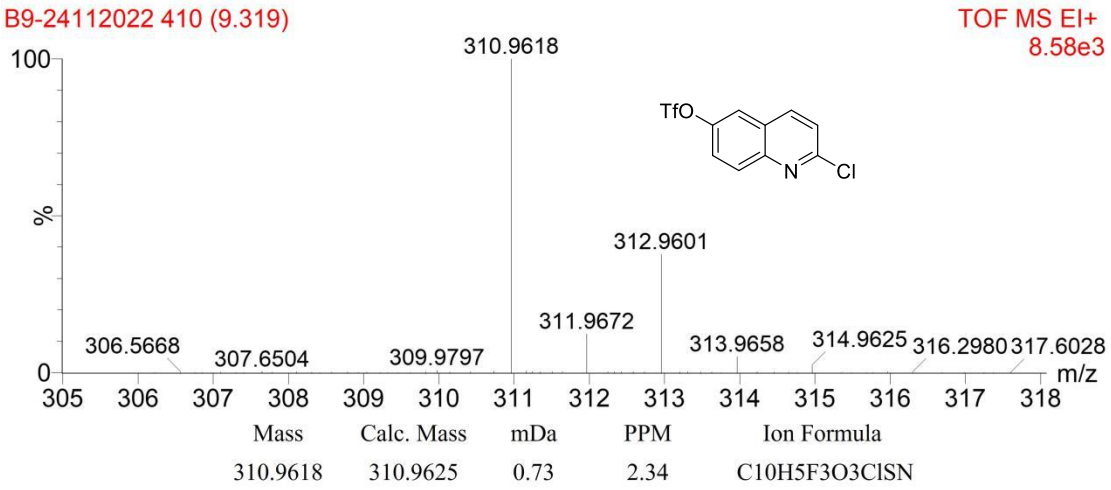
B9-24112022 410 (9.319)
TOF MS EI+
8.58e3
100
%
0
310.9618
312.9601
311.9672
306.5668
307.6504
309.9797
313.9658
314.9625
316.2980
317.6028
TfO
N
Cl
305
306
307
308
309
310
311
312
313
314
315
316
317
318
m/z
Mass
Calc. Mass
mDa
PPM
Ion Formula
310.9618
310.9625
0.73
2.34
C10H5F3O3ClSN

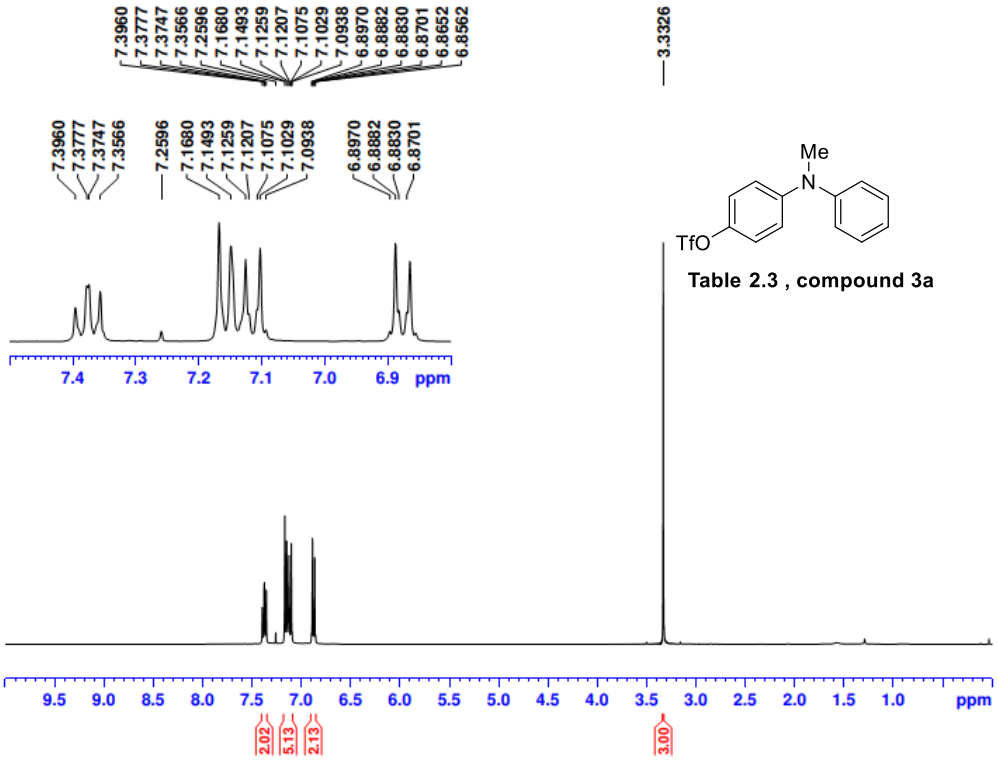

Table 2.3 , compound 3a

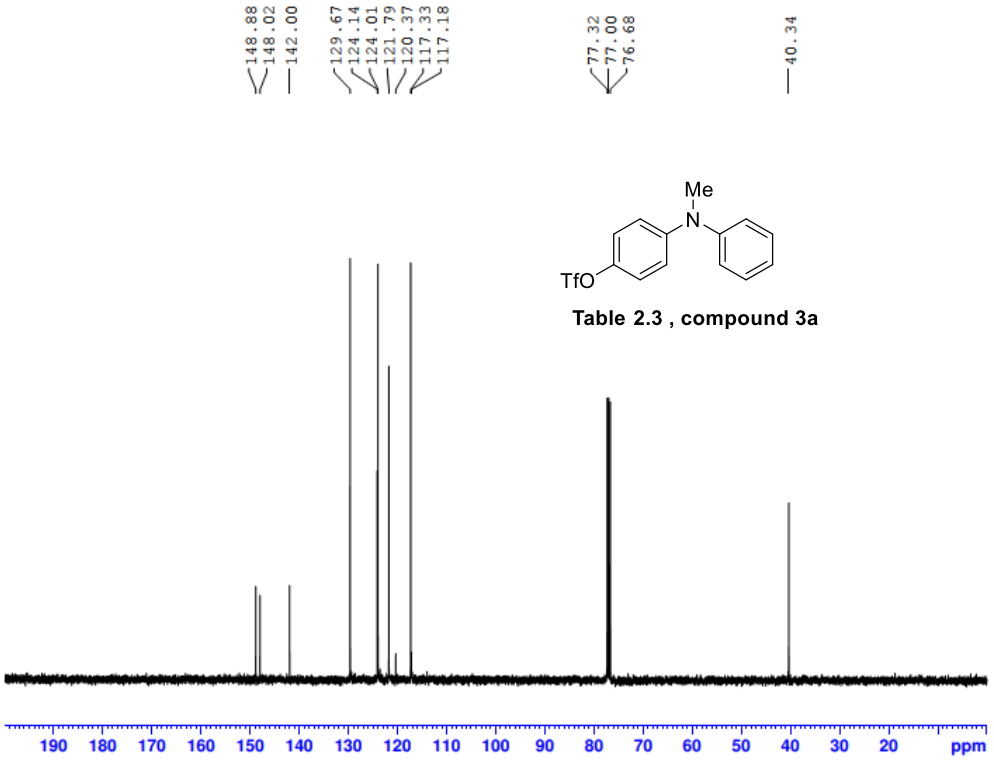

Table 2.3 , compound 3a

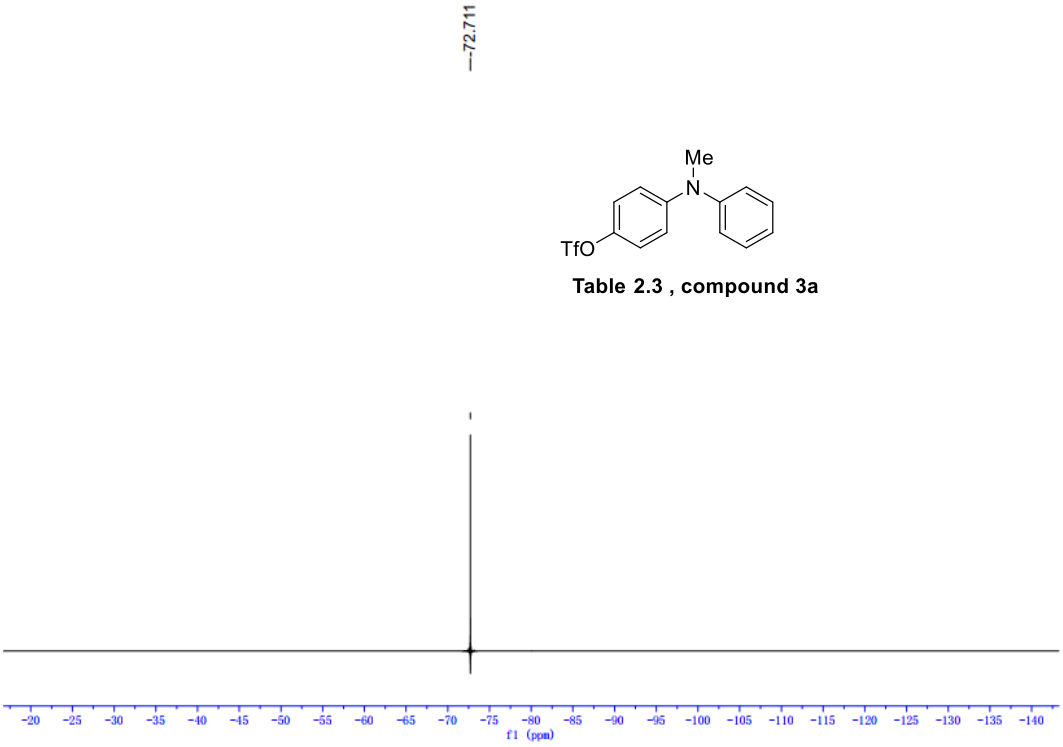

Table 2.3 , compound 3a

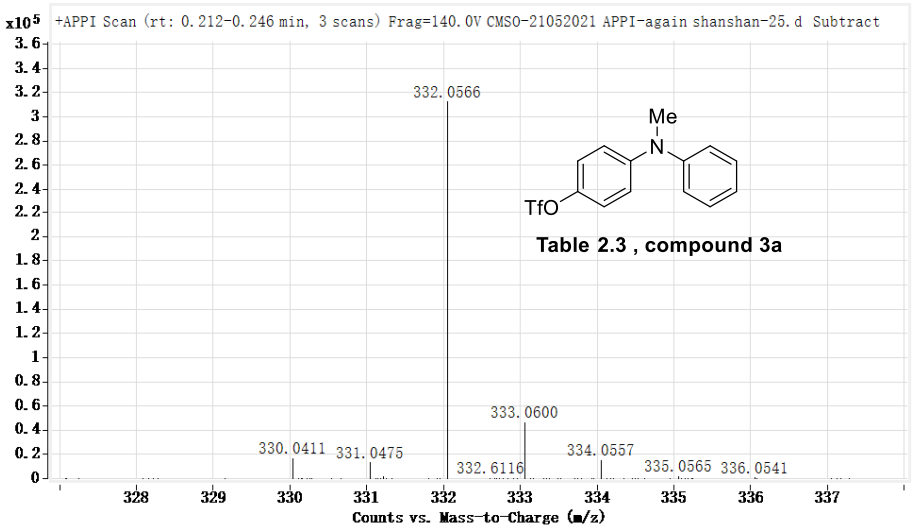

Table 2.3 , compound 3a

Mass	Calc. Mass	mDa	PPM	Formula
332.0566	332.0563	-0.32	-0.98	C14 H13 F3 N O3 S

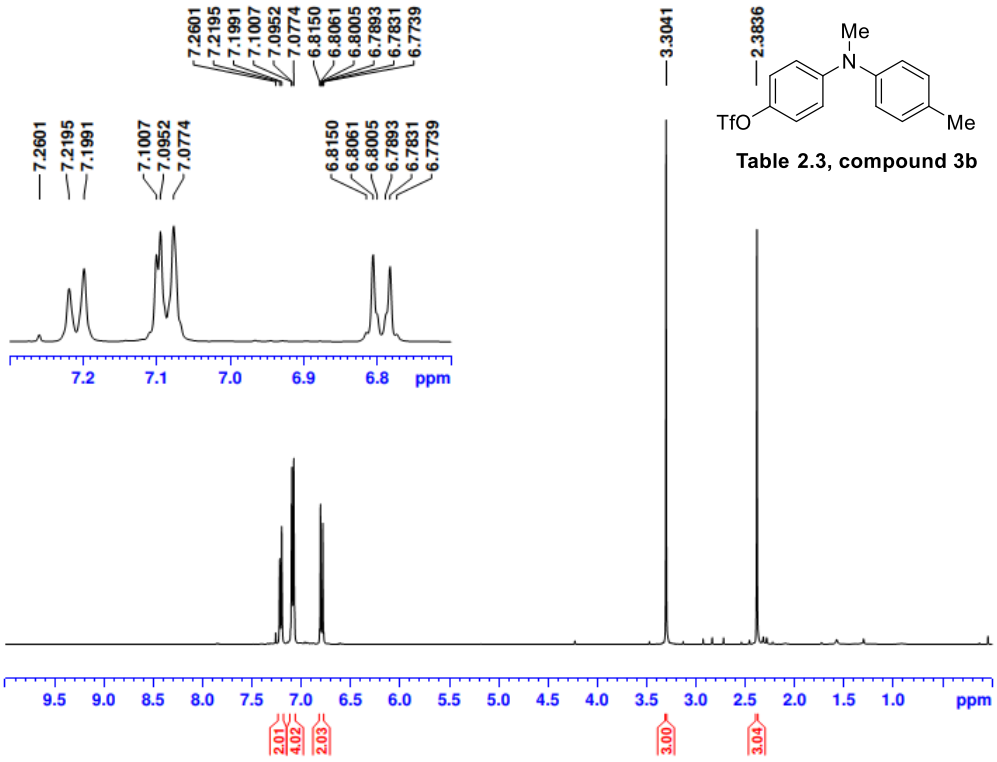

Table 2.3, compound 3b

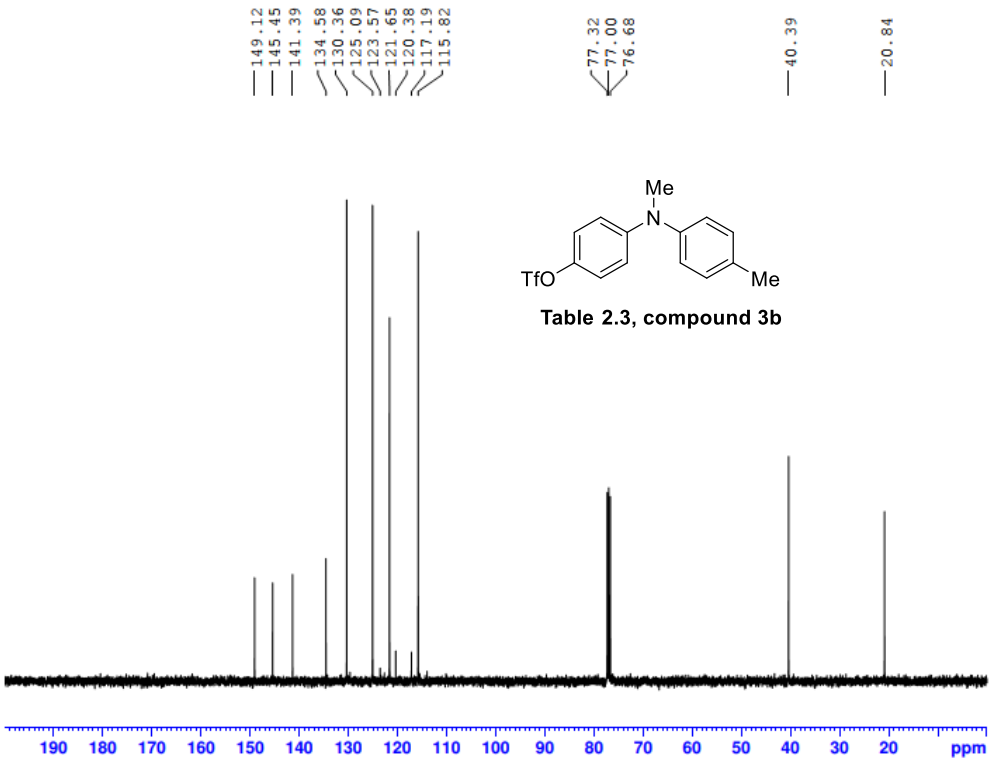

Table 2.3, compound 3b

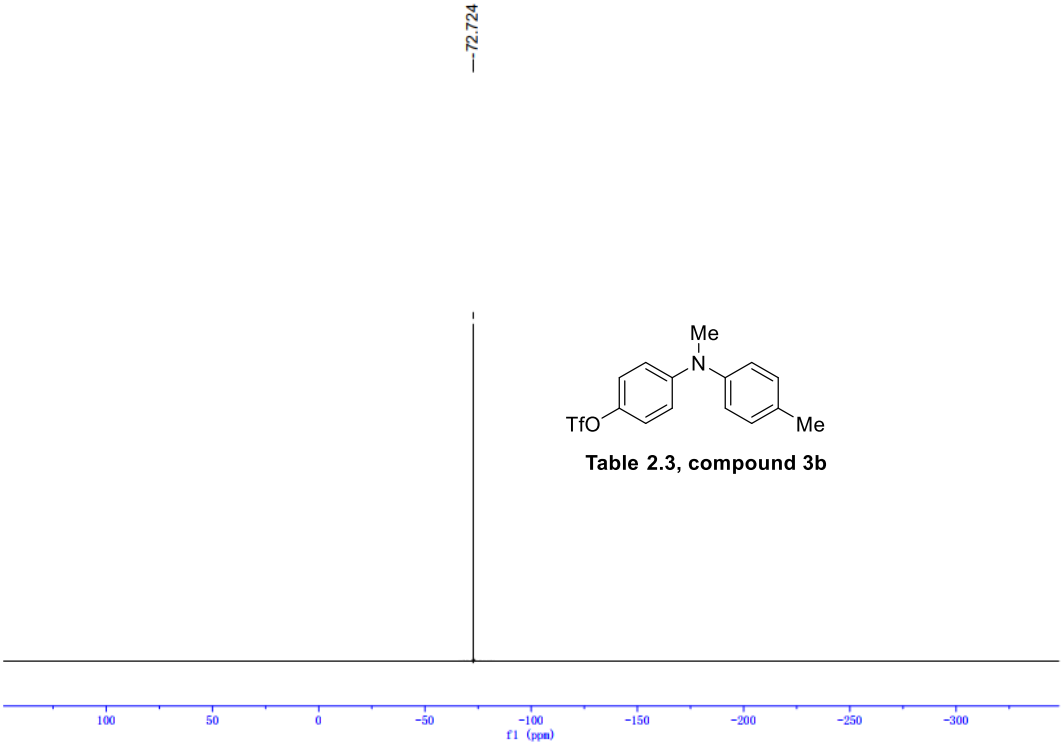

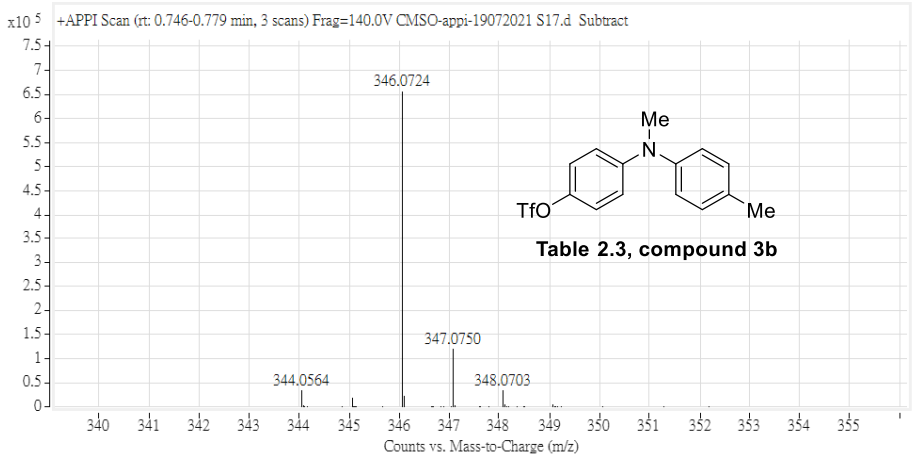

Mass	Calc. Mass	mDa	PPM	Formula
346.0724	346.0719	-0.47	-1.38	C15 H15 F3 N O3 S

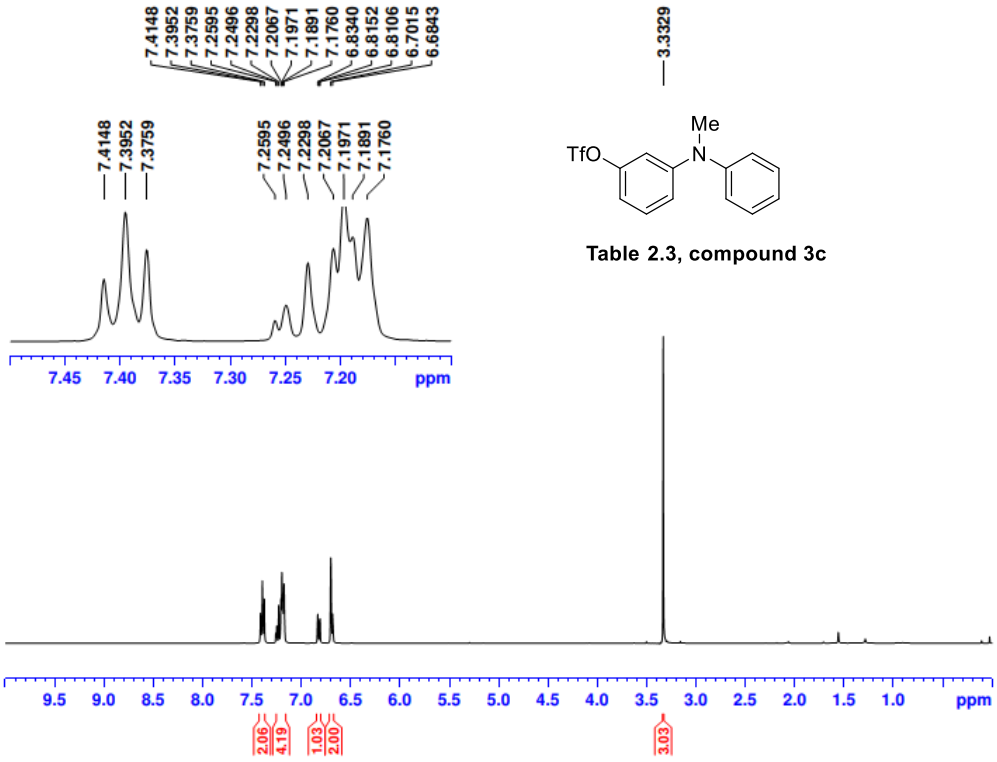

Table 2.3, compound 3c

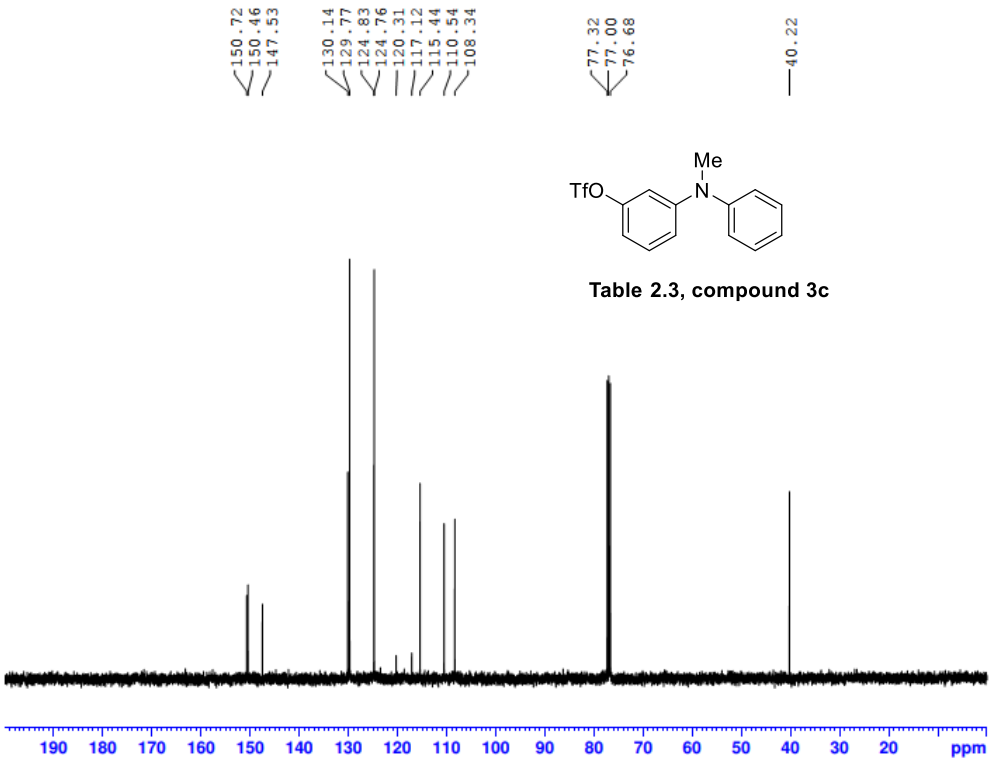

Table 2.3, compound 3c

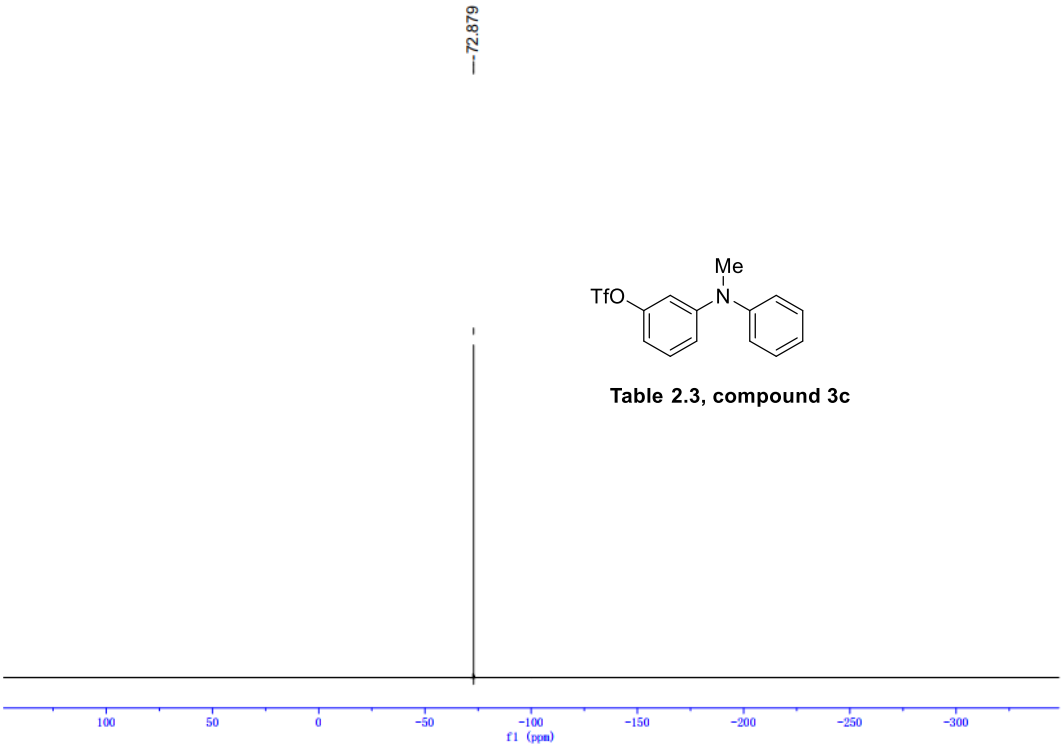

Table 2.3, compound 3c

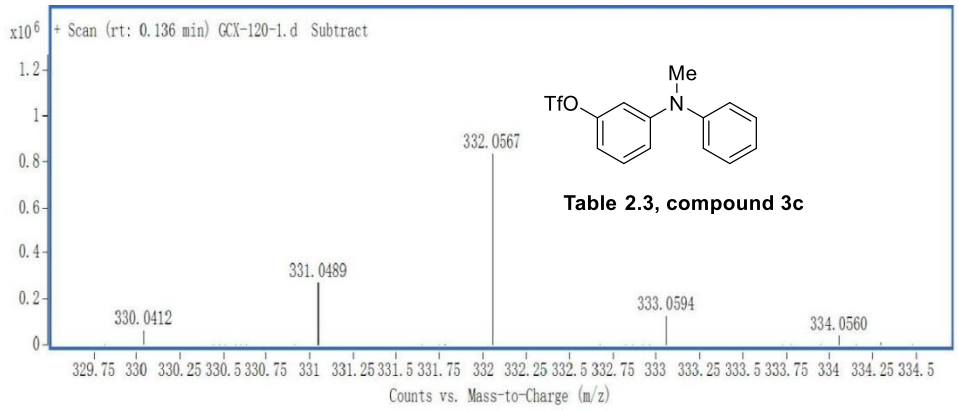

Table 2.3, compound 3c

Mass	m/z (Calc)	Diff (mDa)	Diff (ppm)	Formula
332.0567	332.0563	-0.42	-1.28	C14 H13 N F3 O3 S

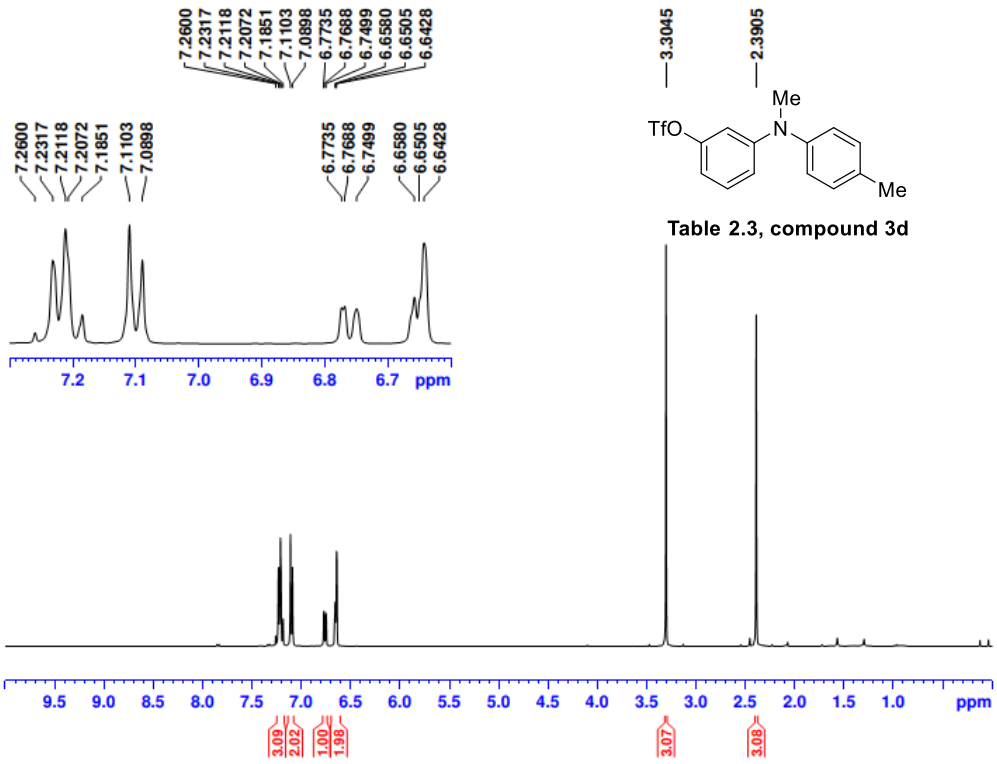

Table 2.3, compound 3d

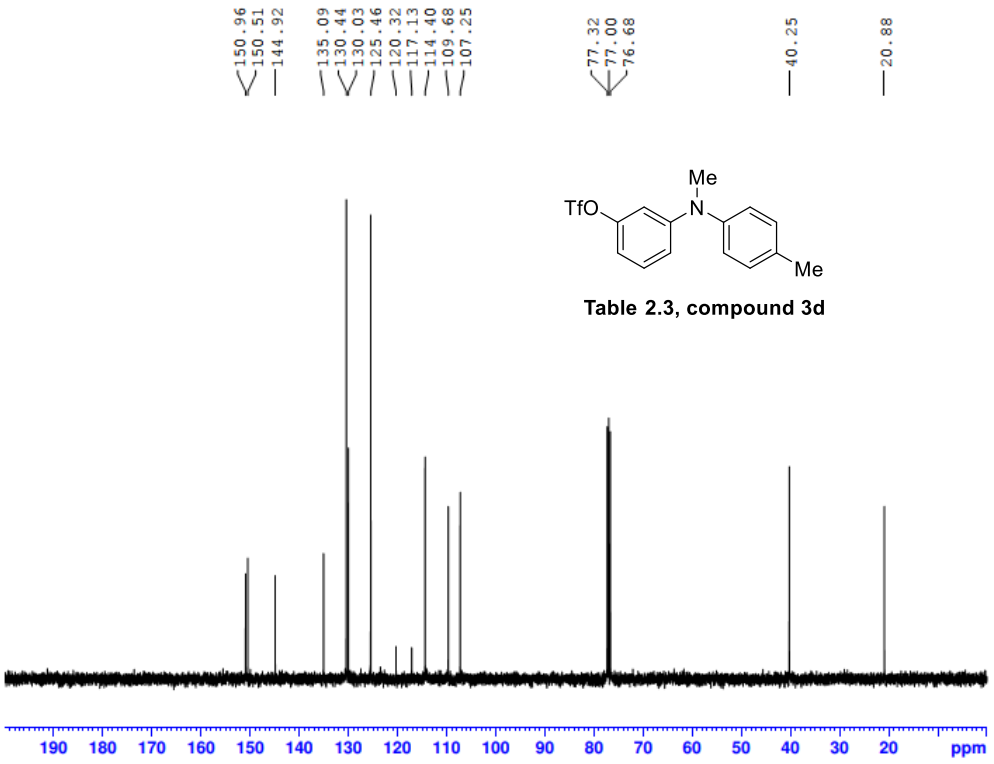

Table 2.3, compound 3d

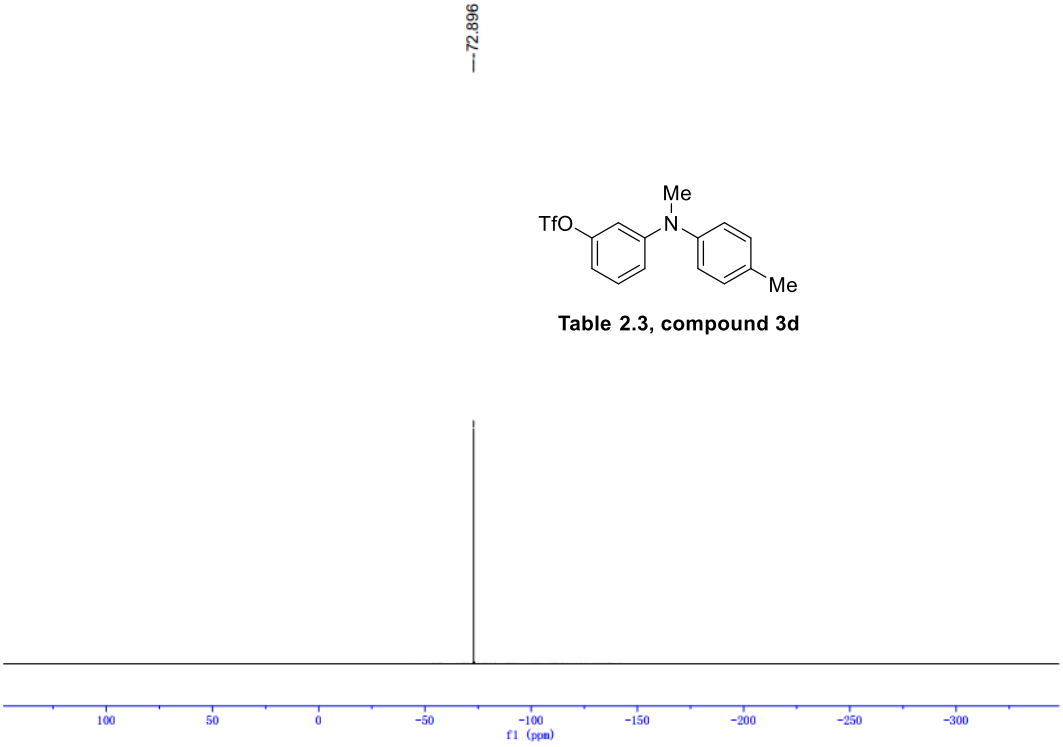

Table 2.3, compound 3d

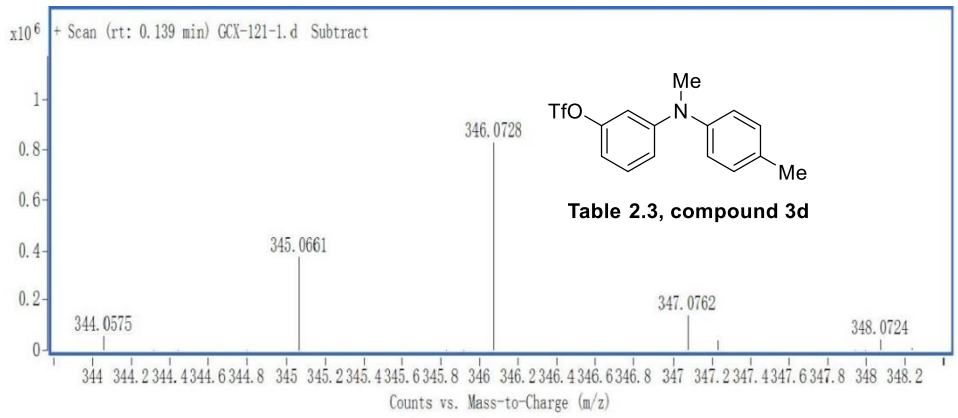

Table 2.3, compound 3d

Mass	m/z (Calc)	Diff (mDa)	Diff (ppm)	Formula
346.0728	346.0719	-0.87	-2.54	C15 H15 N F3 O3 S

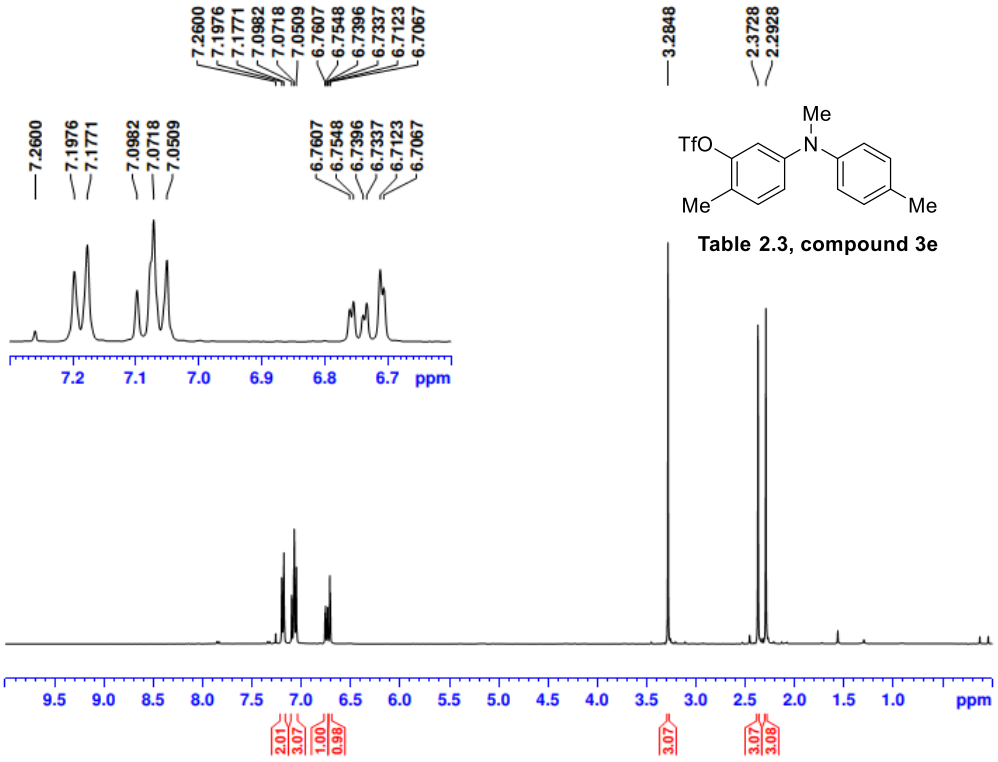

Table 2.3, compound 3e

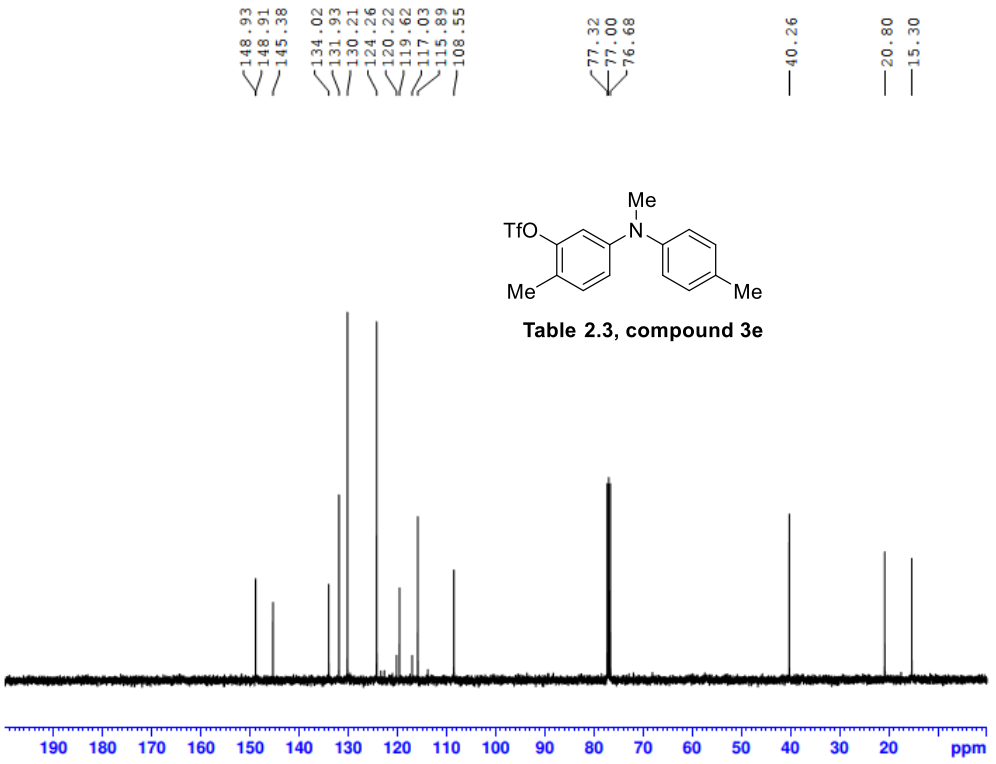

Table 2.3, compound 3e

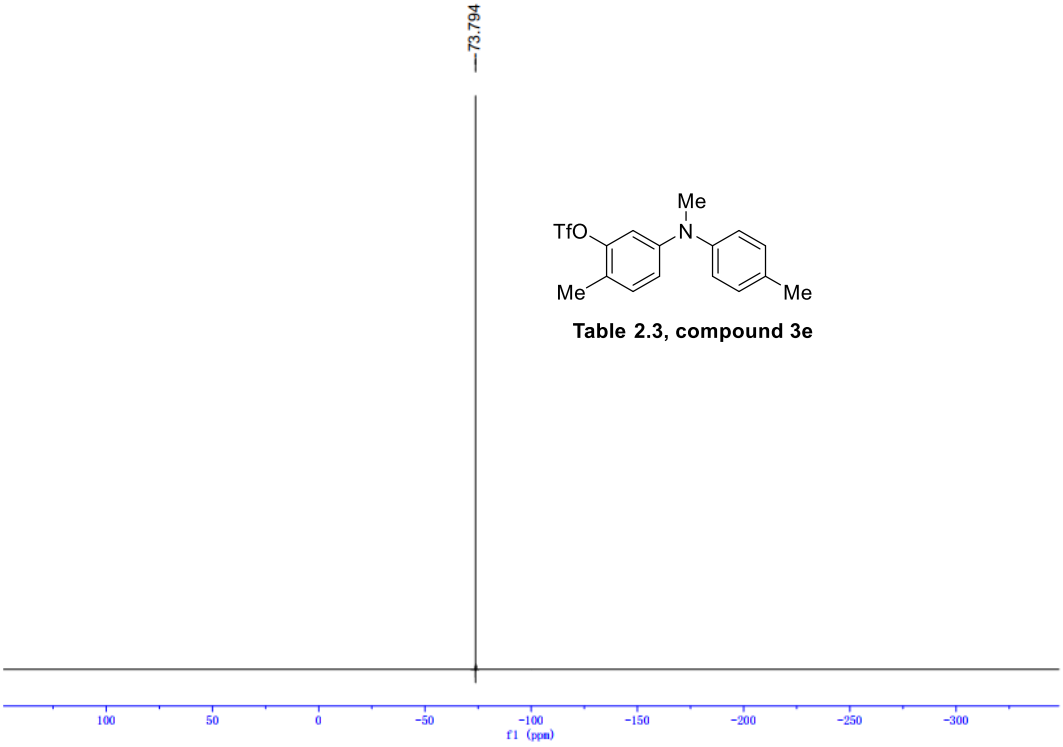

Table 2.3, compound 3e

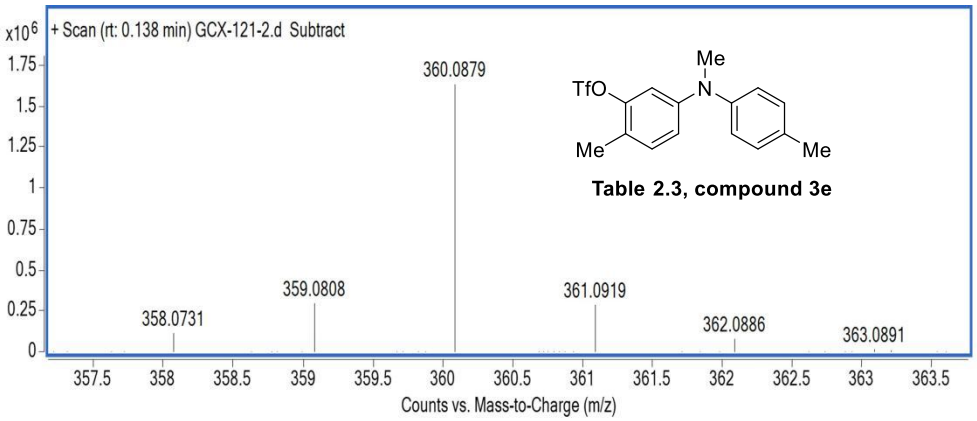

Table 2.3, compound 3e

Mass	m/z (Calc)	Diff (mDa)	Diff (ppm)	Formula
360.0879	360.0876	-0.32	-0.90	C16 H17 N F3 O3 S

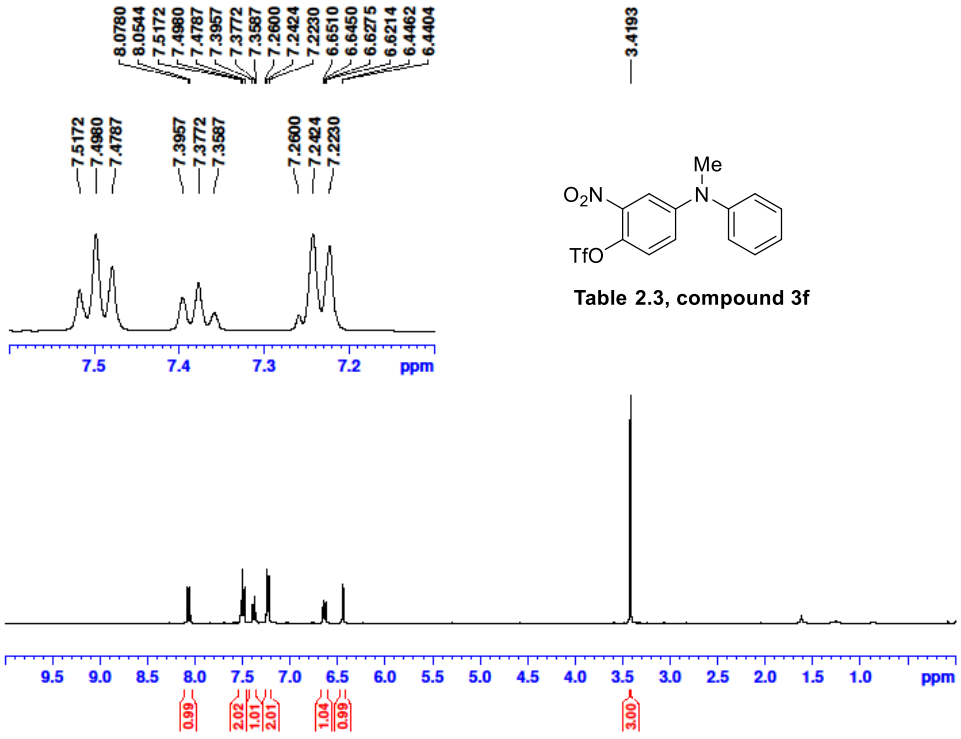

Table 2.3, compound 3f

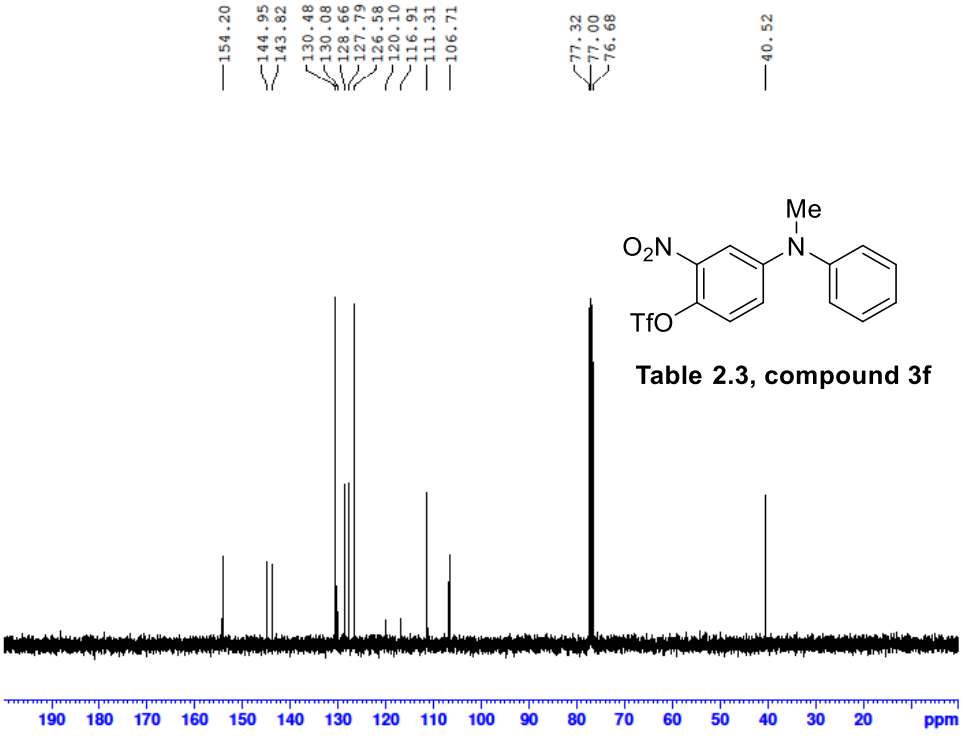

Table 2.3, compound 3f

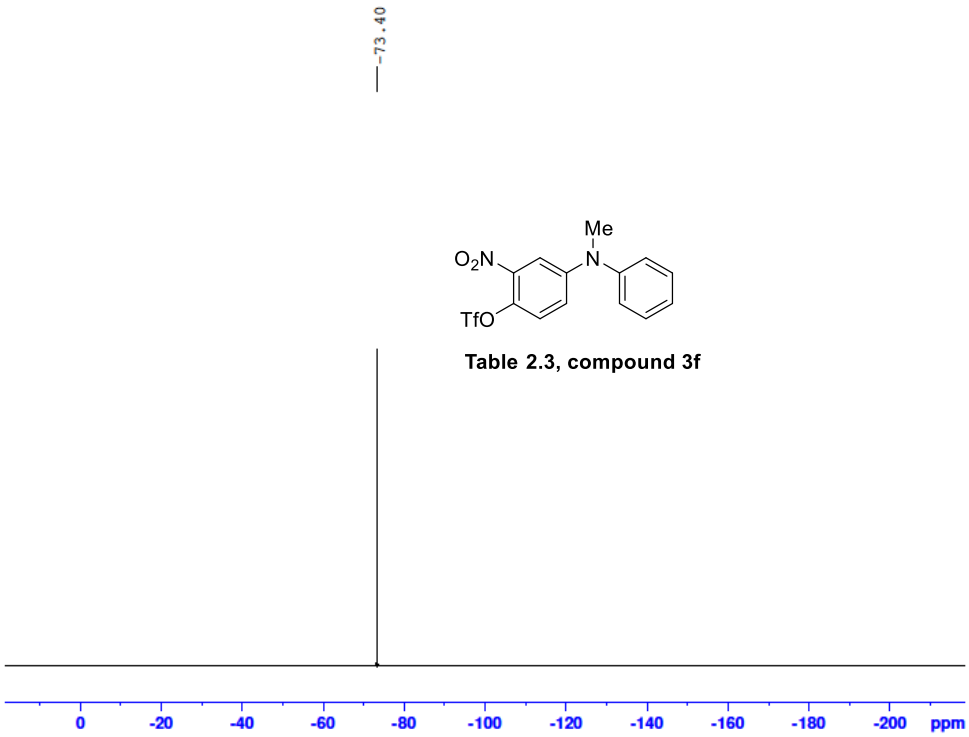

Table 2.3, compound 3f

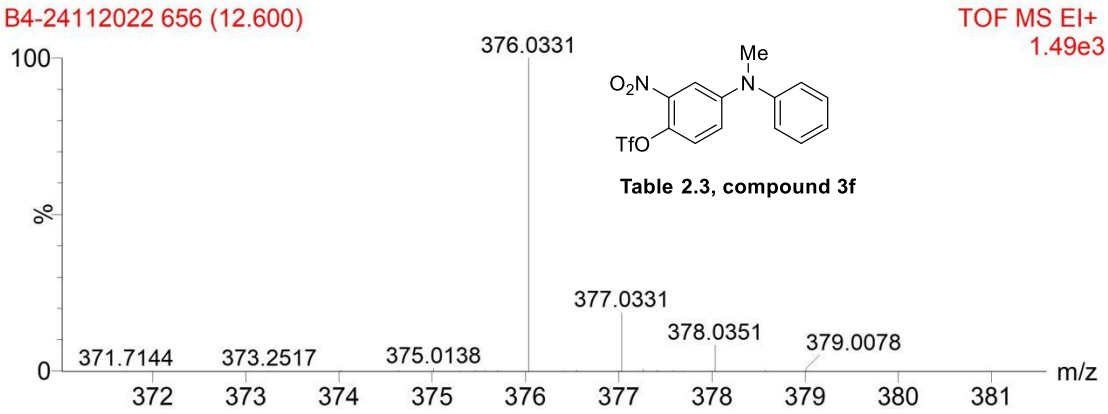

Table 2.3, compound 3f

Mass	Calc. Mass	mDa	PPM	Ion Formula
376.0331	376.0335	0.43	1.14	C14H11F3O5N2S

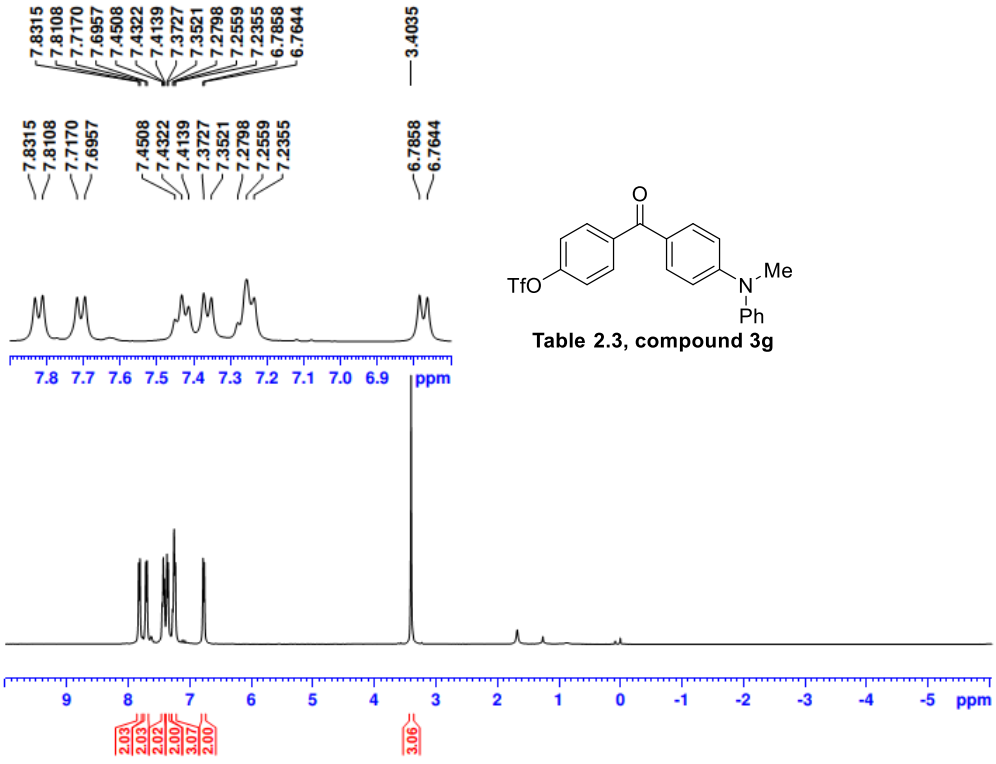

Table 2.3, compound 3g

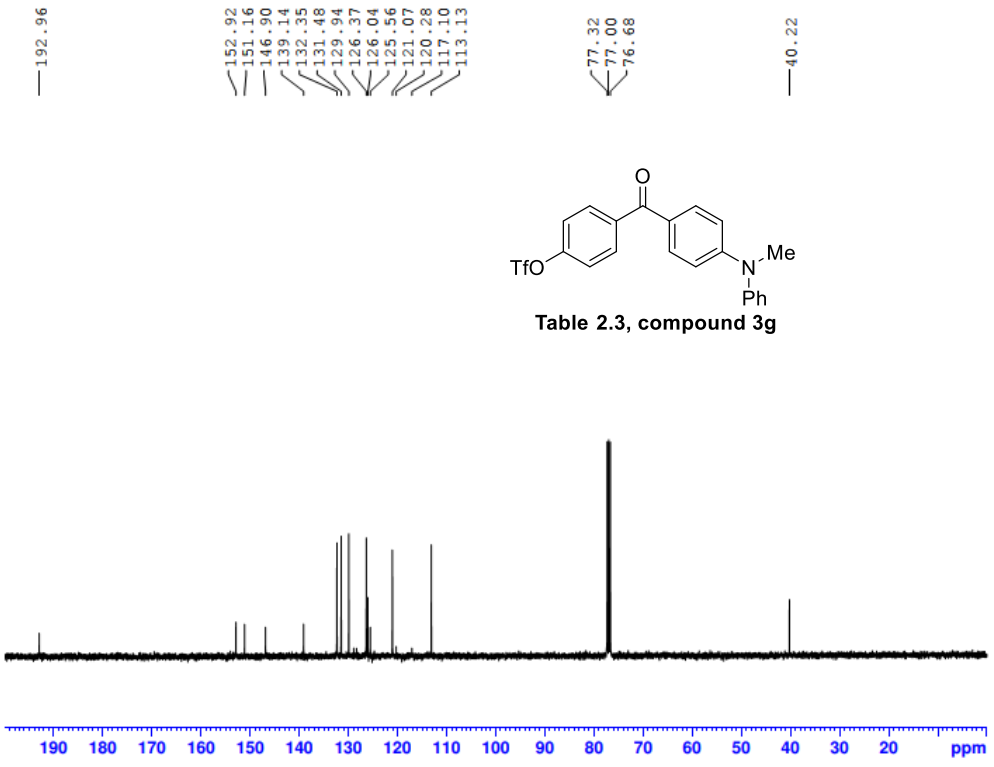

Table 2.3, compound 3g

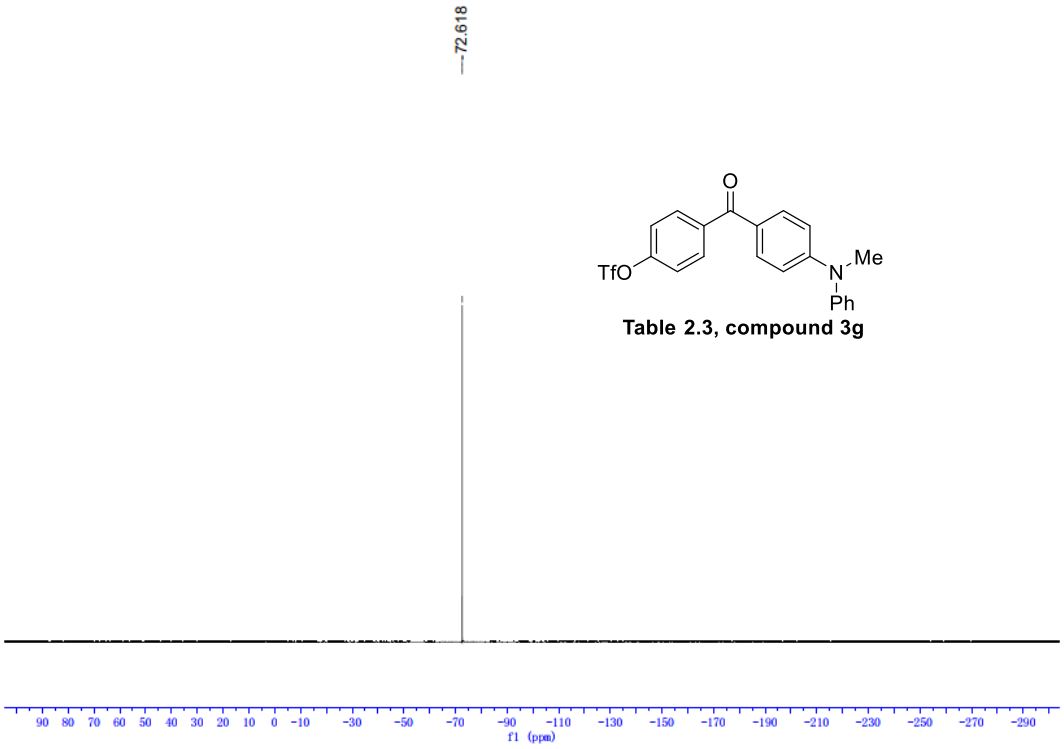

Table 2.3, compound 3g

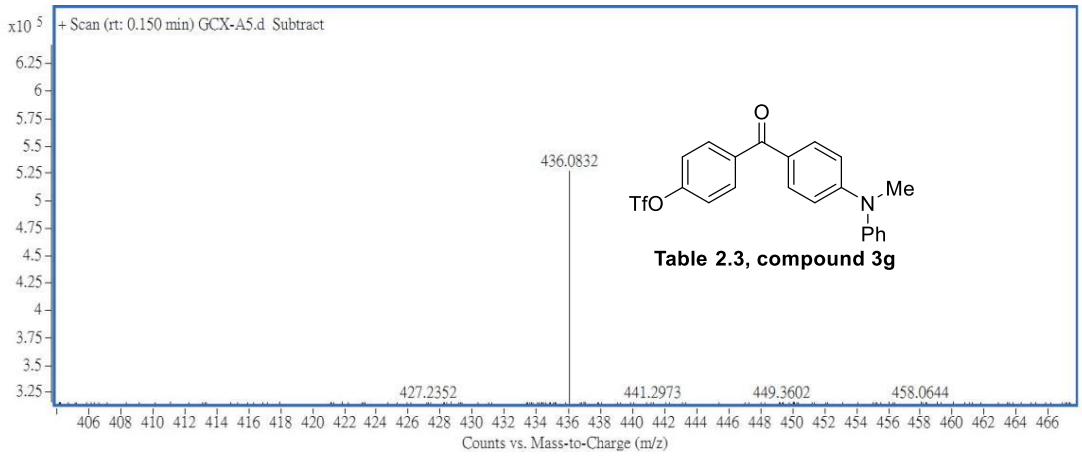

Table 2.3, compound 3g

Mass	m/z (Calc)	Diff (mDa)	Diff (ppm)	Formula
436.0832	436.0825	-0.71	-1.63	C21 H17 F3 N O4 S

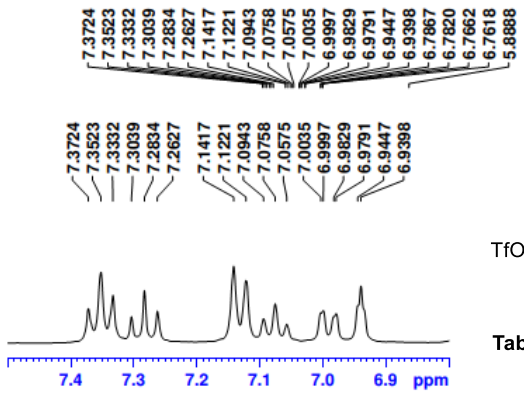

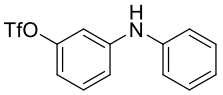

Table 2.3, compound 3h

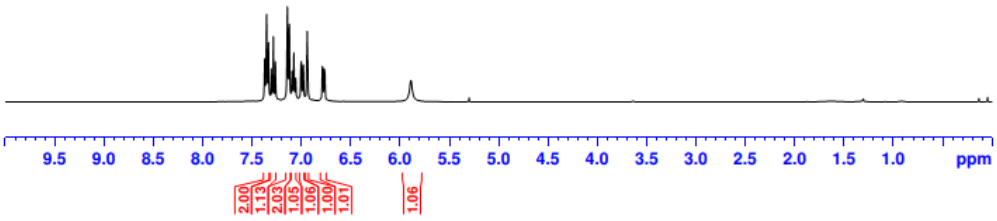

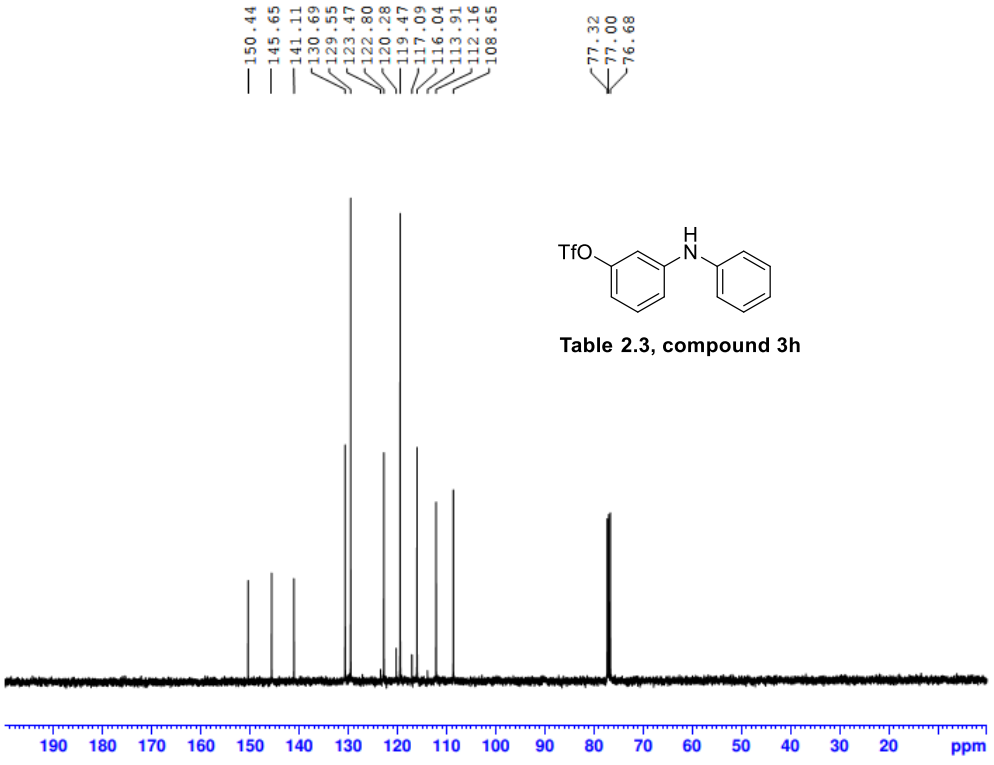

Table 2.3, compound 3h

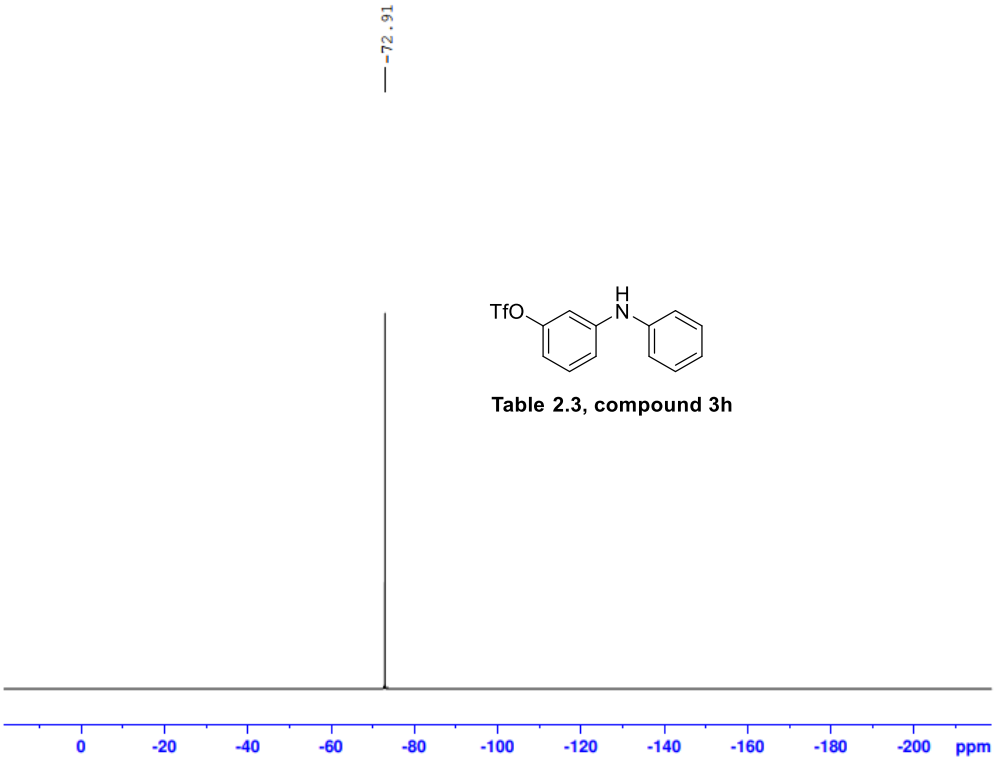

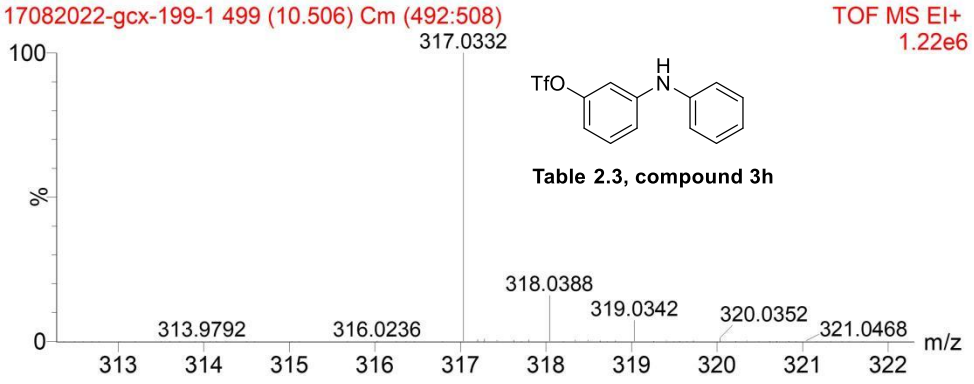

Mass	Calc. Mass	mDa	PPM	Formula
317.0332	317.0328	-1.26	-0.40	C13 H10 F3NO3S

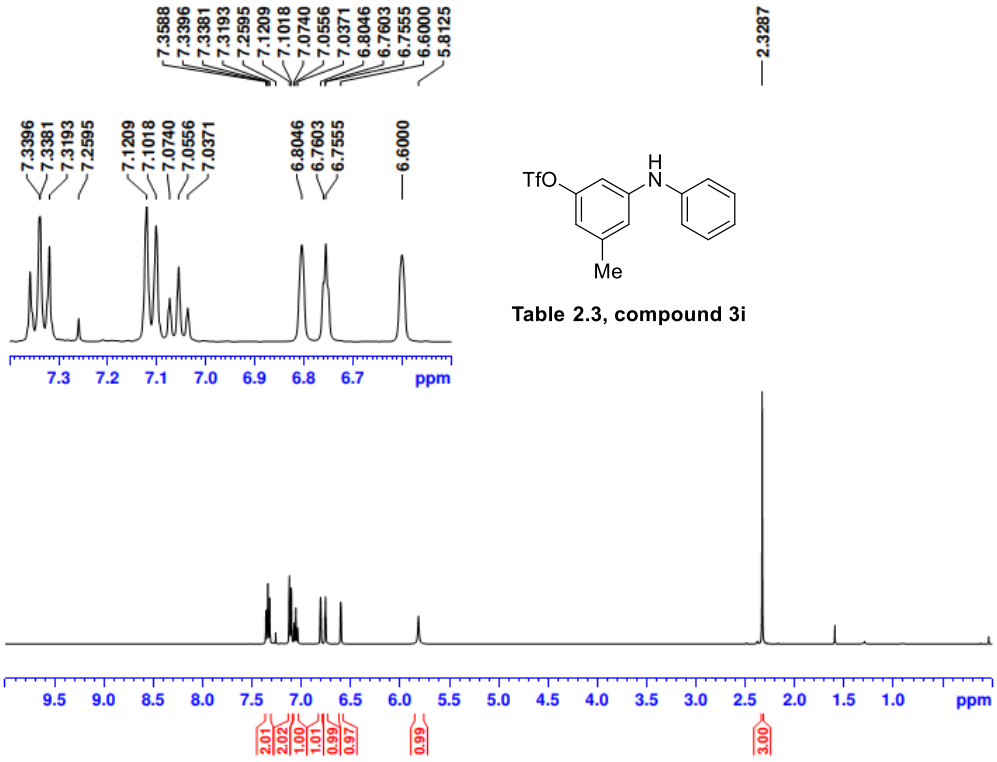

Table 2.3, compound 3i

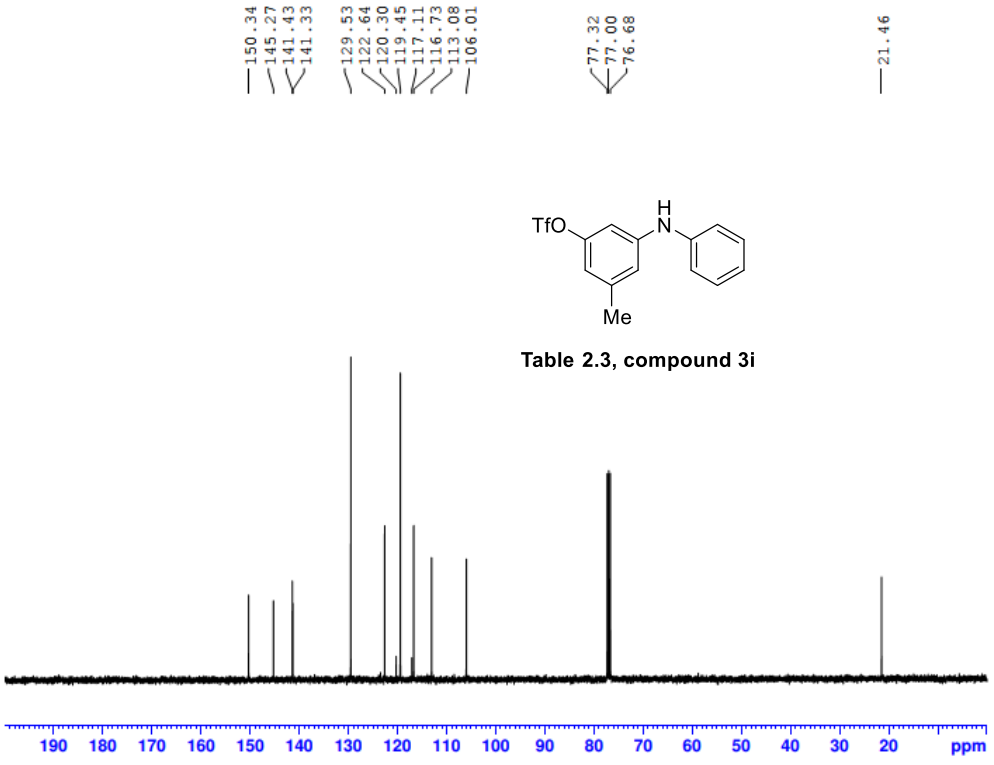

Table 2.3, compound 3i

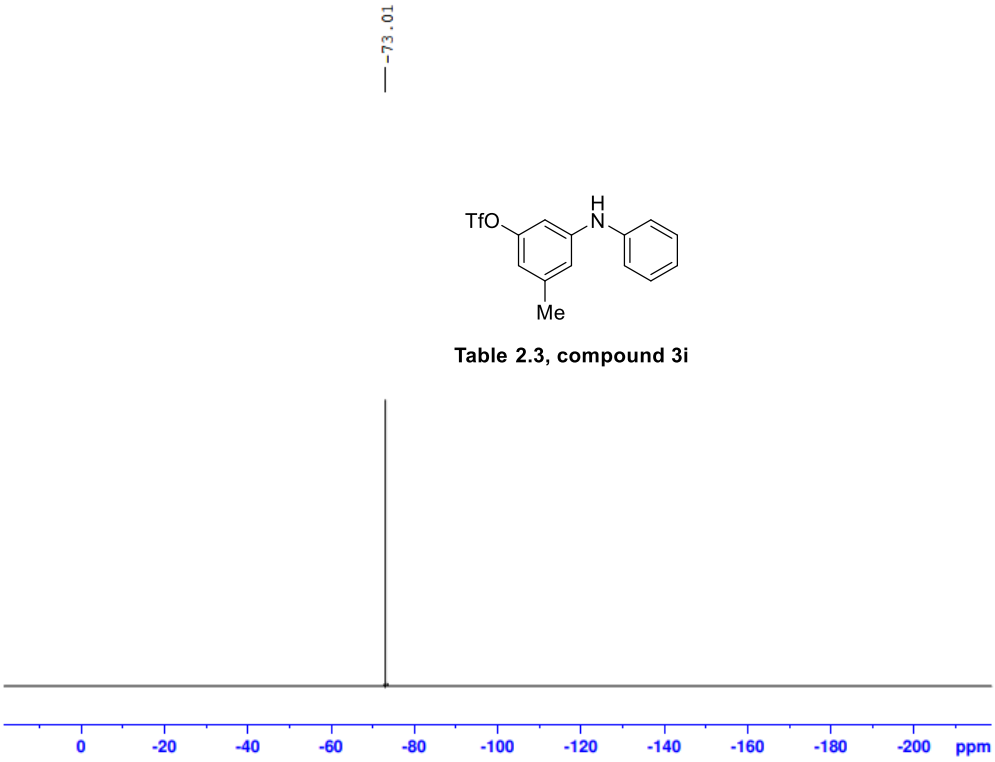

Table 2.3, compound 3i

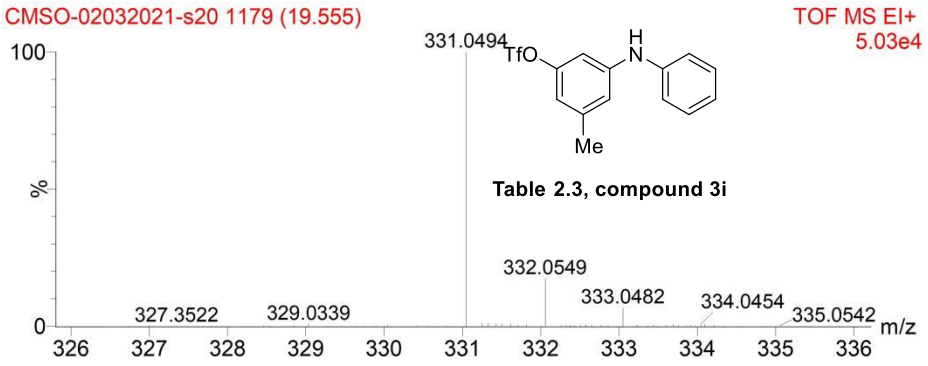

Table 2.3, compound 3i

Mass	Calc. Mass	mDa	PPM	Formula
331.0494	331.0485	-0.95	-2.87	C14H12 F3NO3S

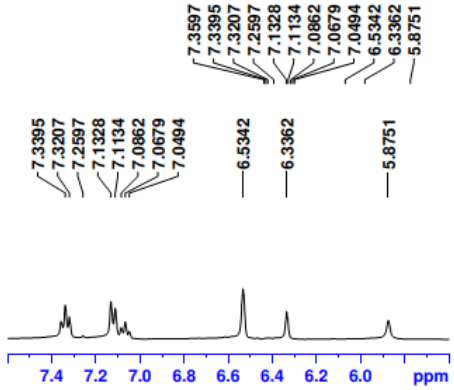

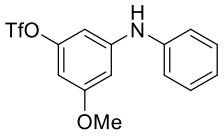

Table 2.3, compound 3j

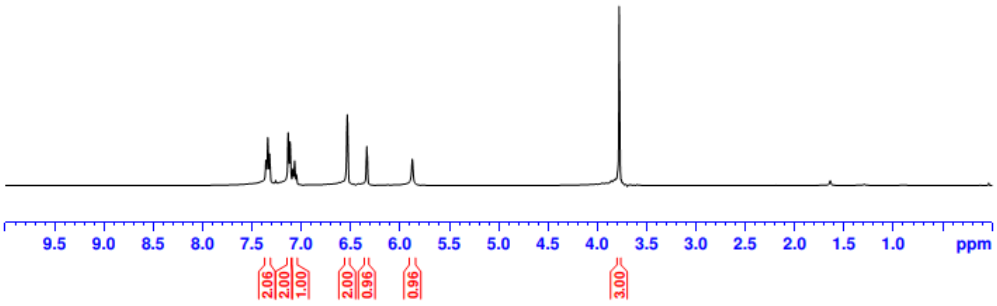

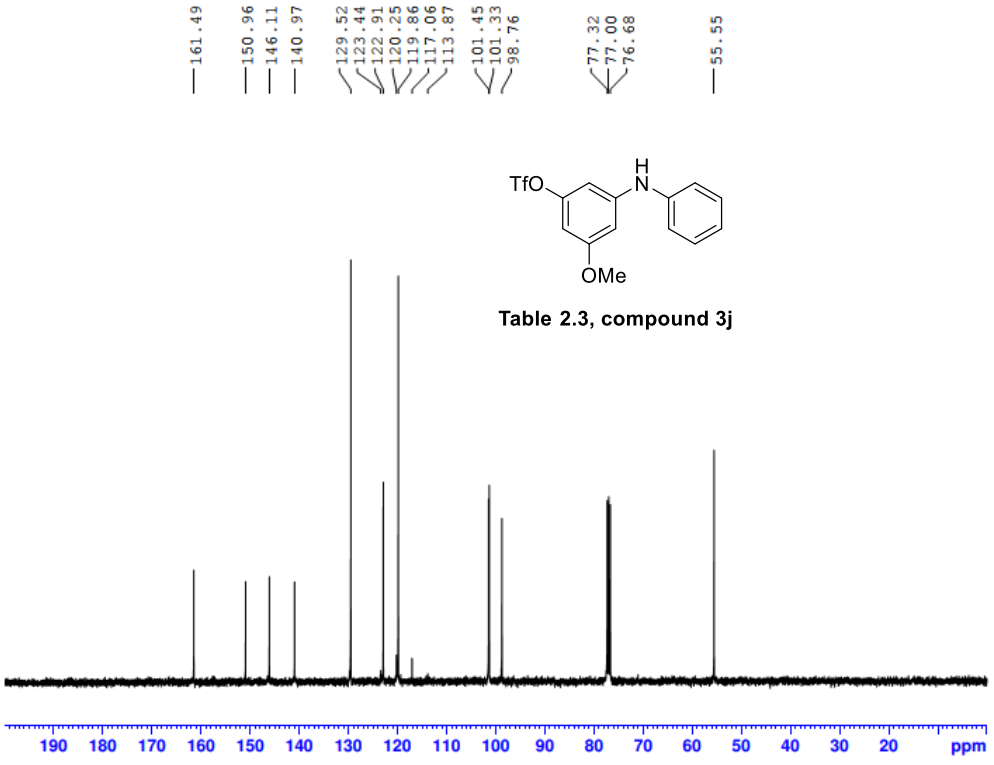

Table 2.3, compound 3j

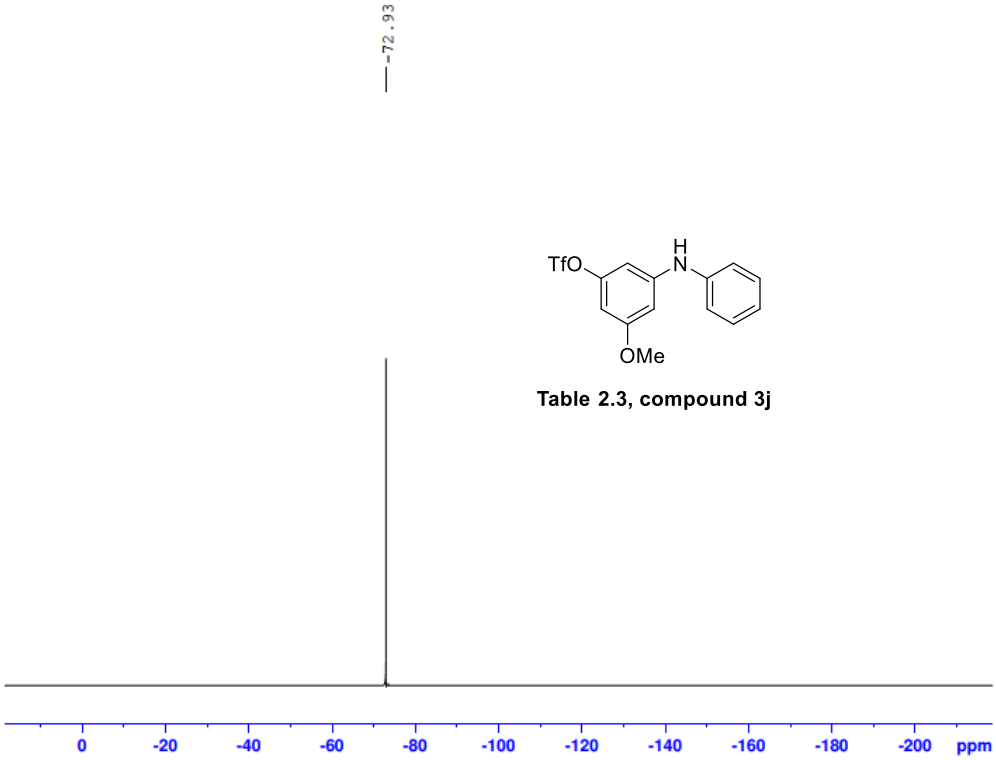

Table 2.3, compound 3j

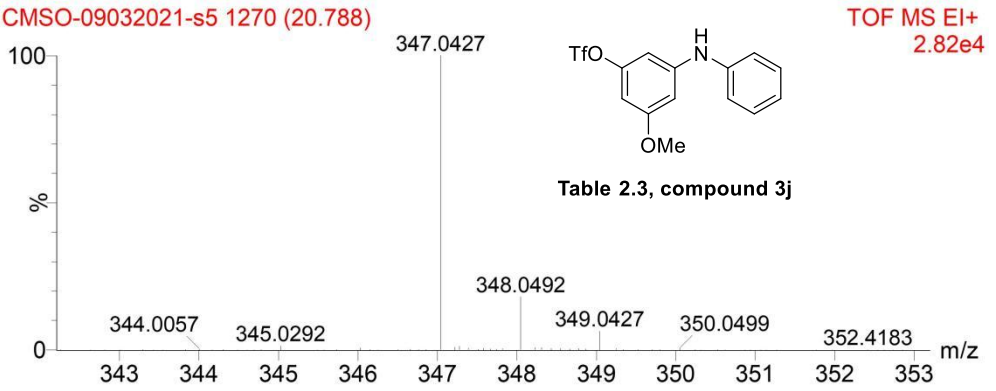

Table 2.3, compound 3j

Mass	Calc. Mass	mDa	PPM	Formula
347.0427	347.0434	0.66	1.92	C14 H12 F3NO4S

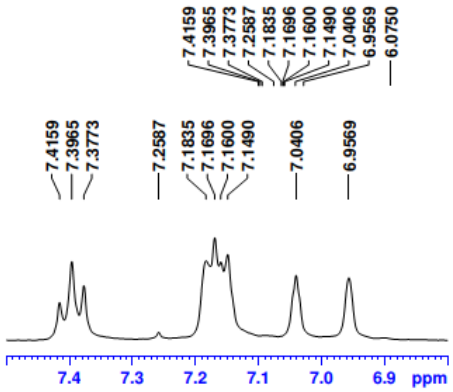

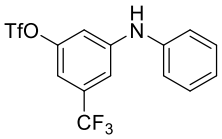

Table 2.3, compound 3k

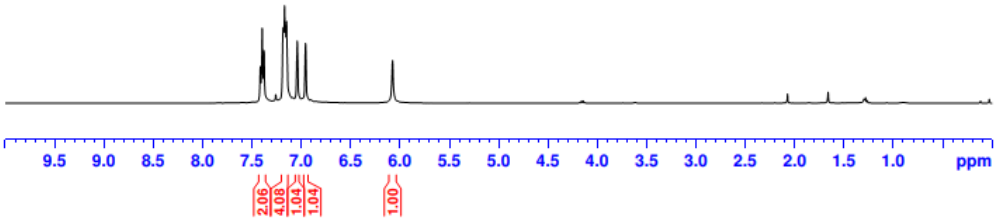

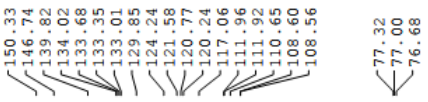

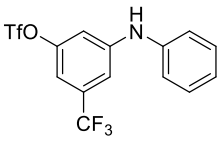

Table 2.3, compound 3k

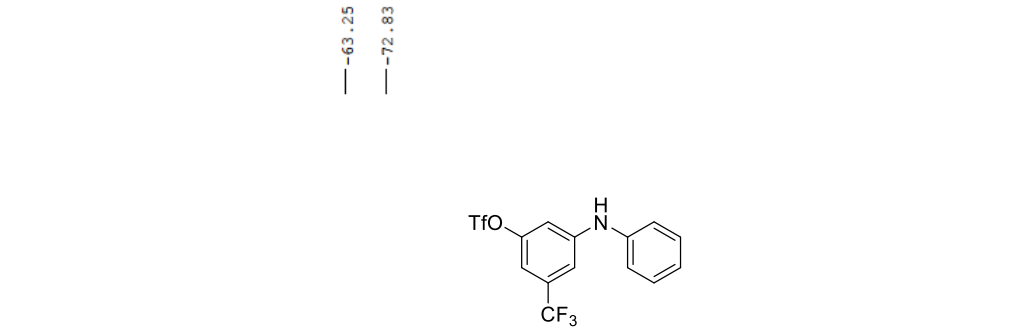

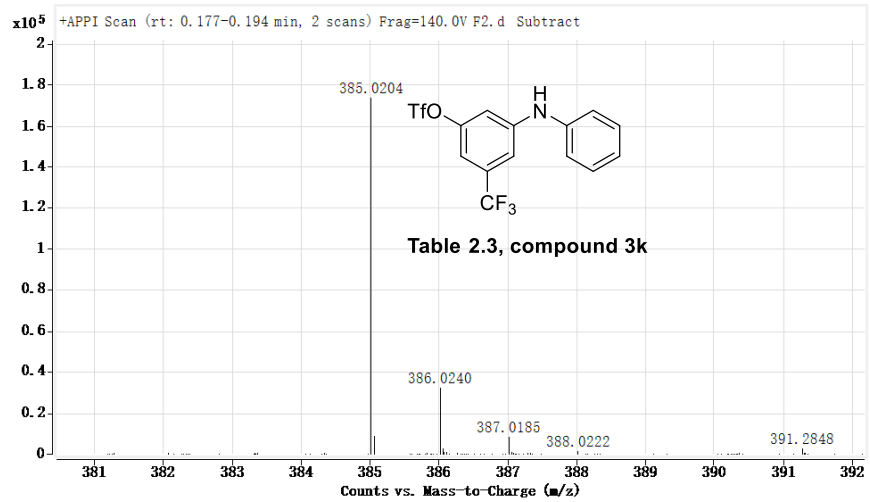

Mass	Calc. Mass	mDa	PPM	Formula
385.0204	385.0202	-0.22	-0.56	C14 H9 F6 N O3 S

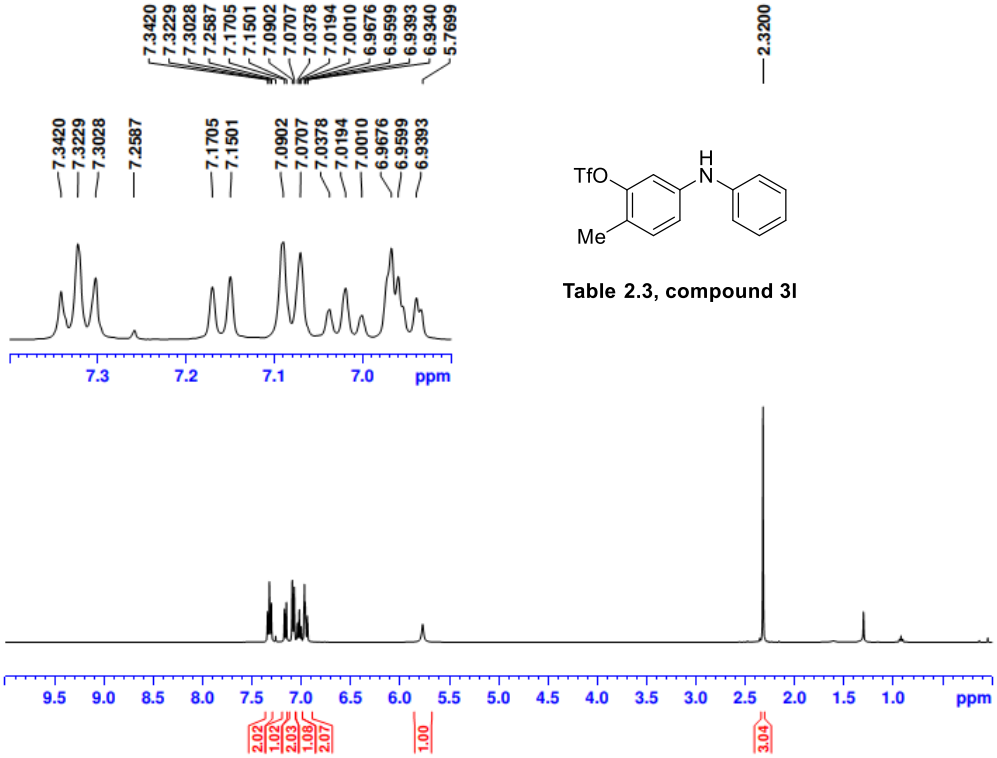

Table 2.3, compound 3l

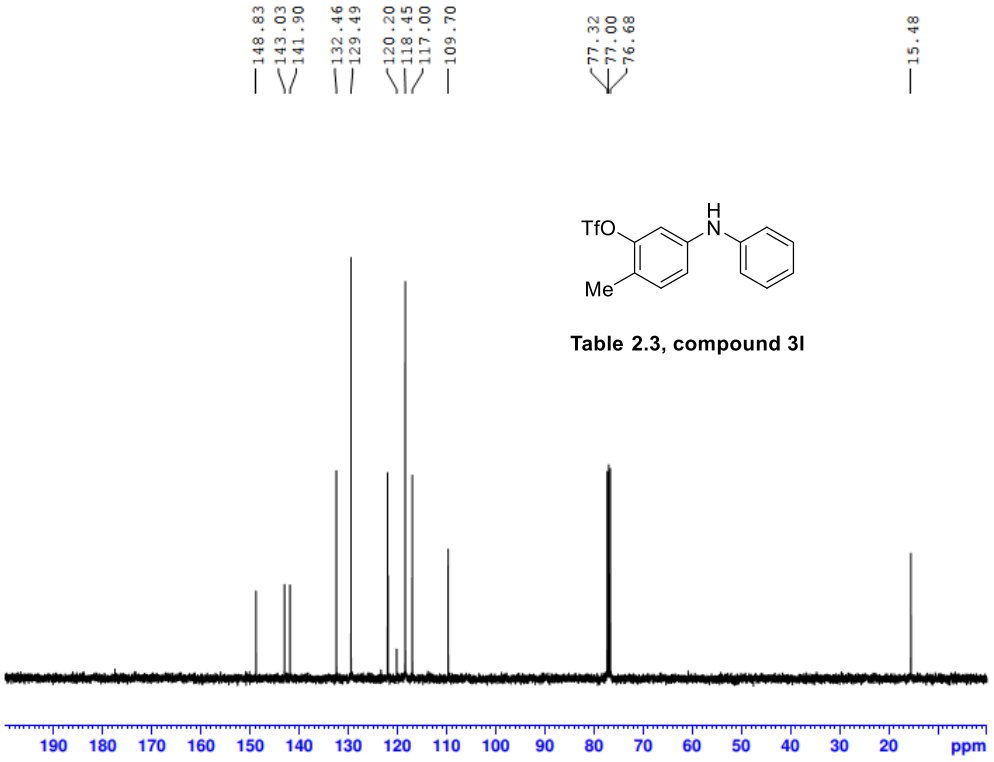

Table 2.3, compound 3l

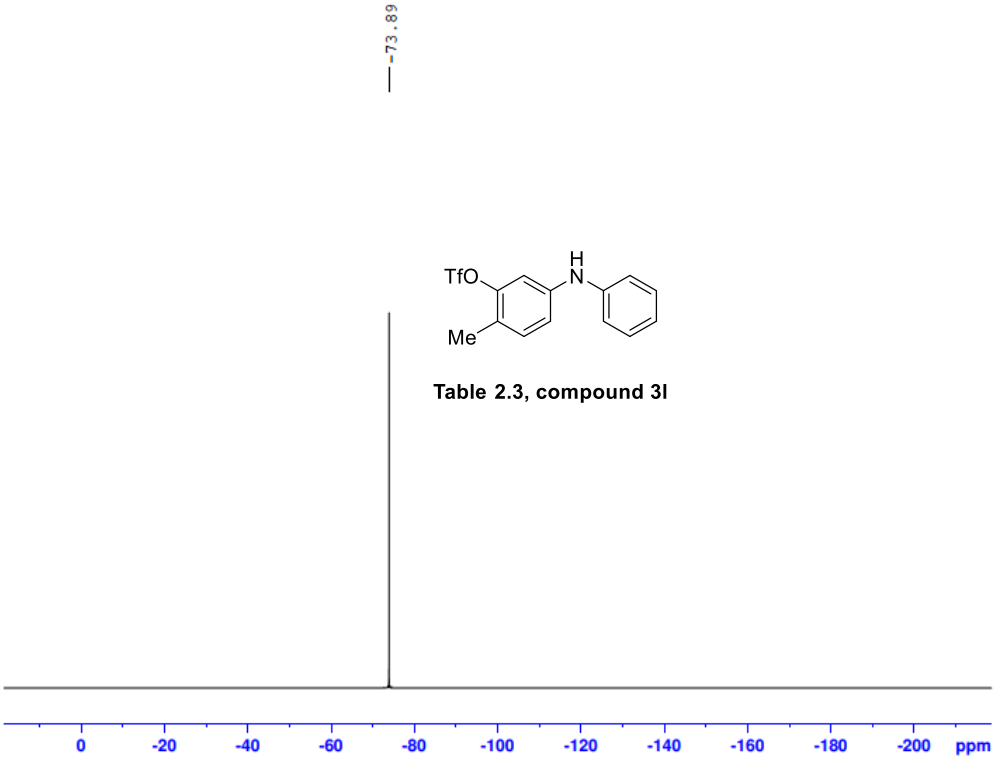

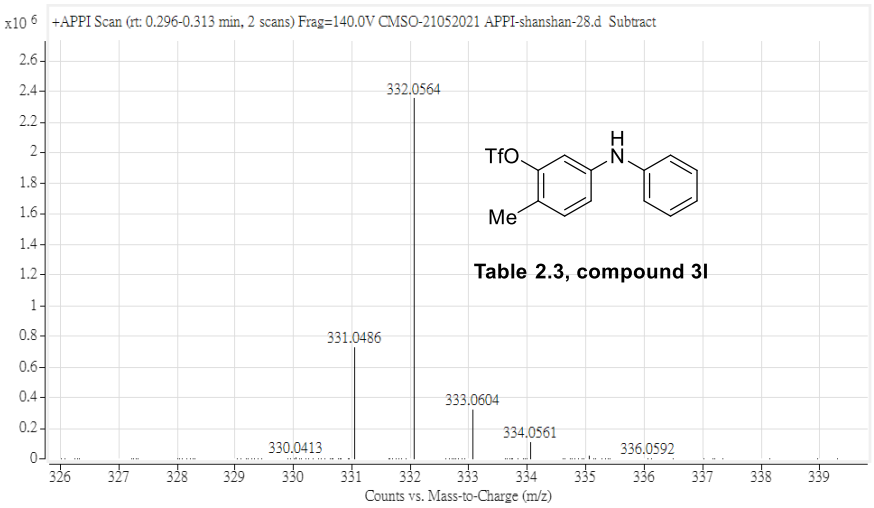

Mass	Calc. Mass	mDa	PPM	Formula
332.0564	332.0563	-0.12	-0.38	C14 H13 F3 N O3 S

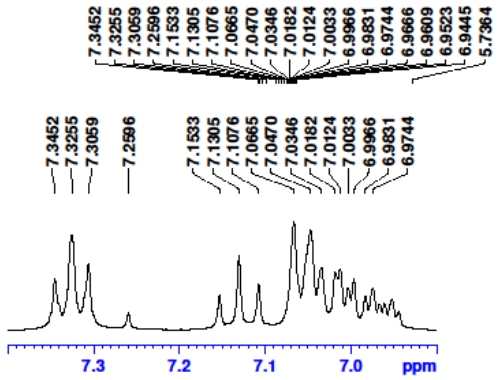

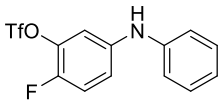

Table 2.3, compound 3m

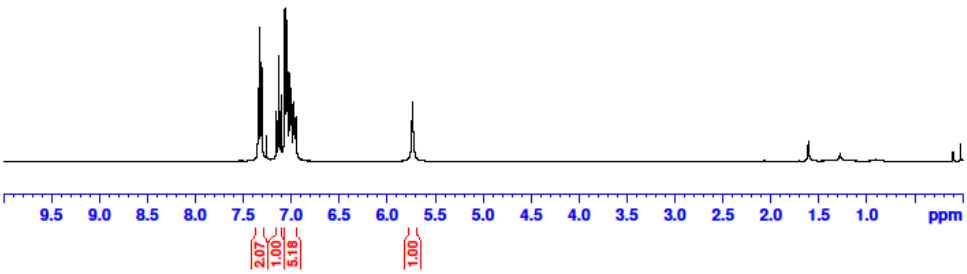

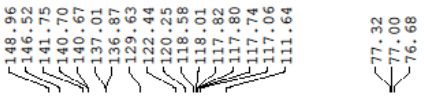

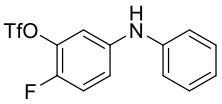

Table 2.3, compound 3m

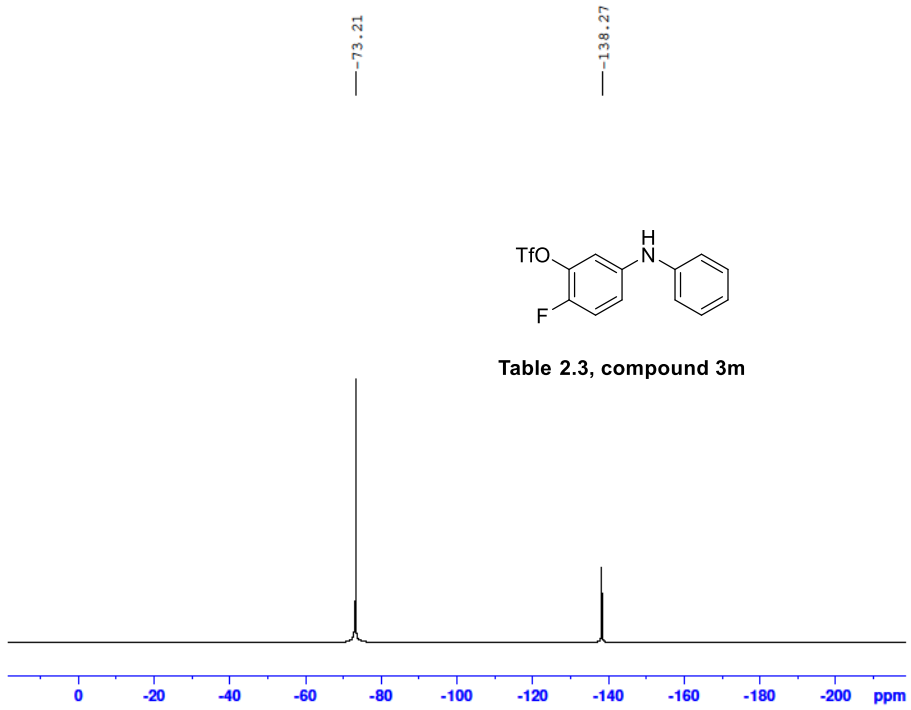

Table 2.3, compound 3m

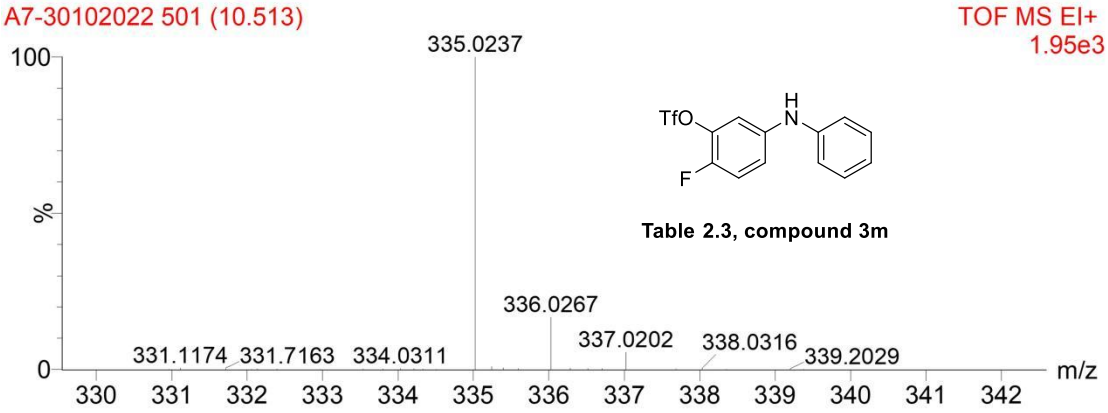

Table 2.3, compound 3m

Mass	Calc. Mass	mDa	PPM	Ion Formula
335.0237	335.0234	-0.32	-0.96	C13H9NF4O3S

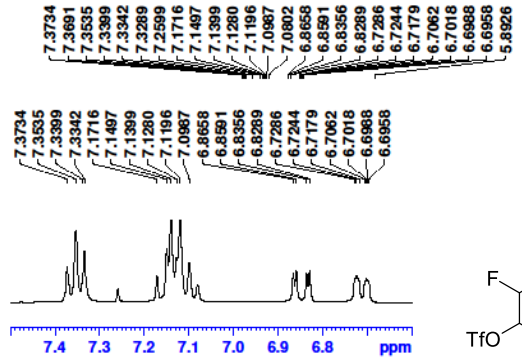

Table 2.3, compound 3n

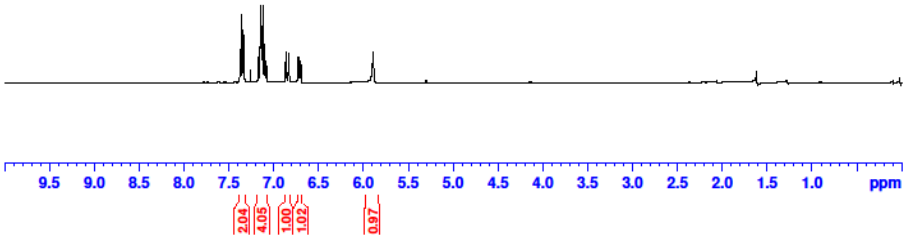

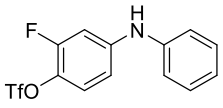

Table 2.3, compound 3n

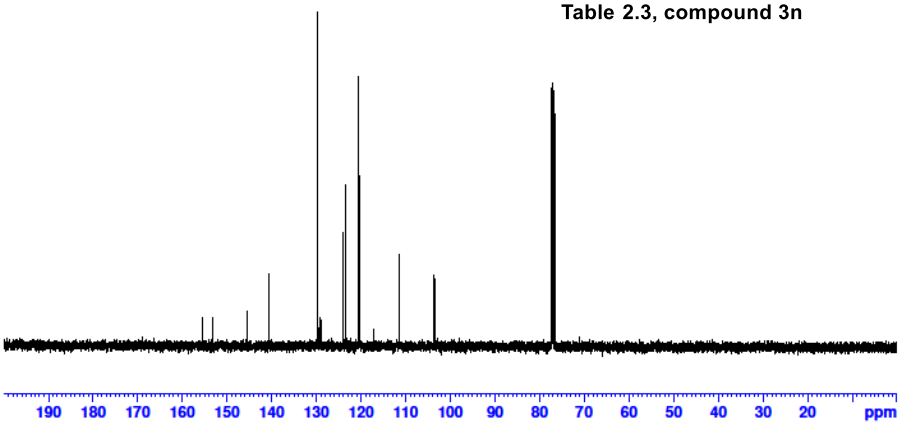

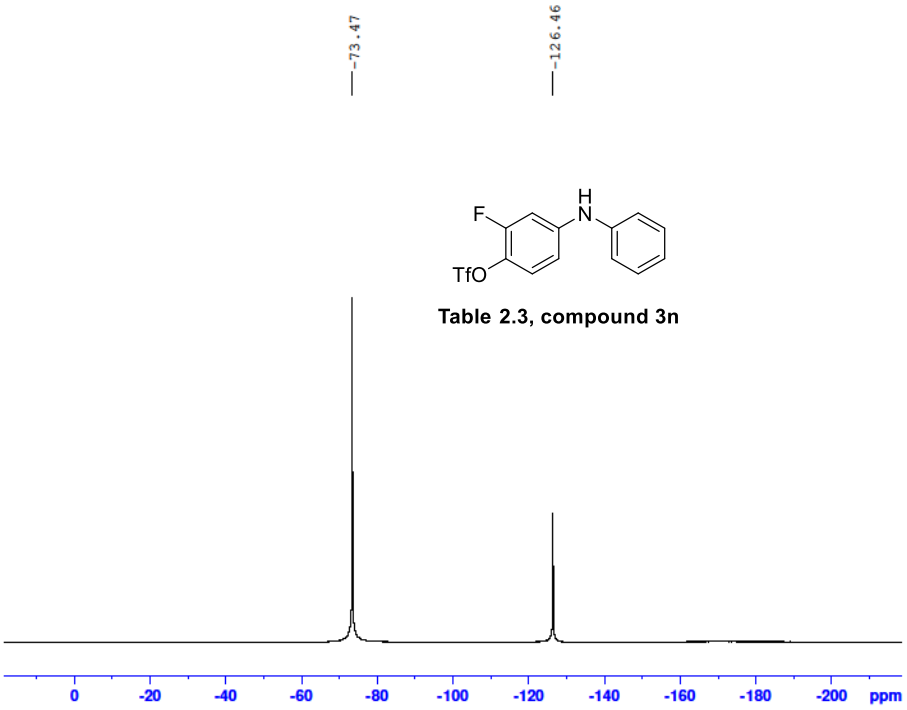

Table 2.3, compound 3n

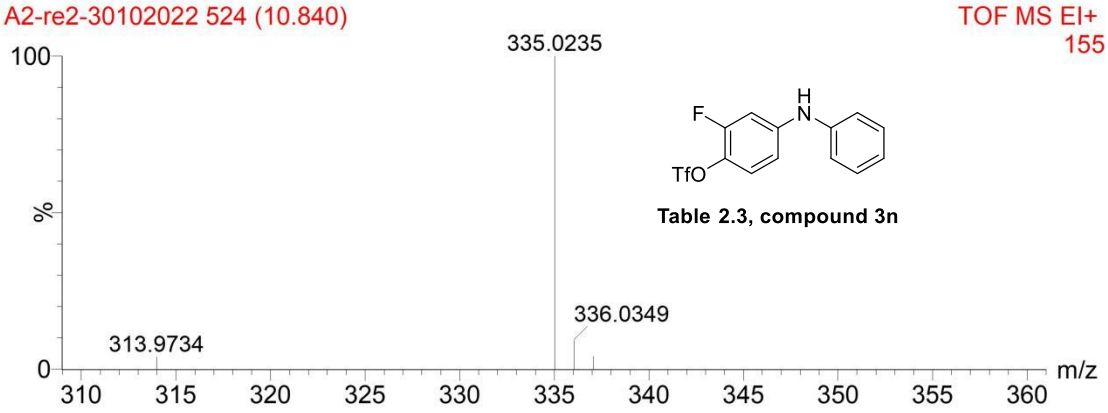

Table 2.3, compound 3n

Mass	Calc. Mass	mDa	PPM	Ion Formula
335.0235	335.0234	-0.12	-0.36	C13H9NF4O3S

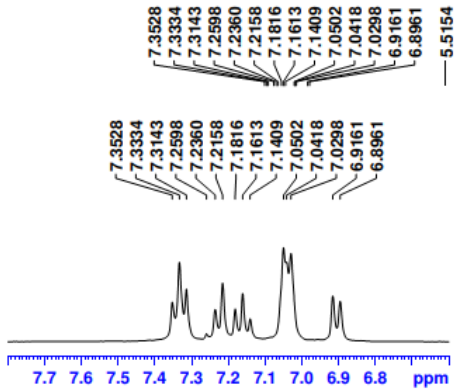

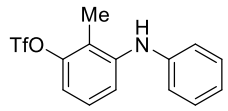

Table 2.3, compound 3o

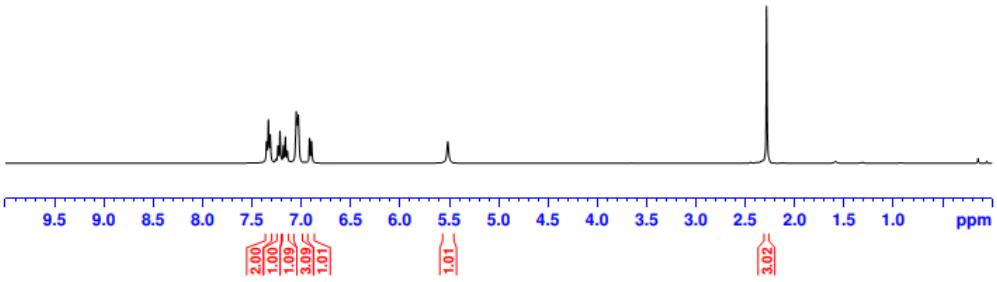

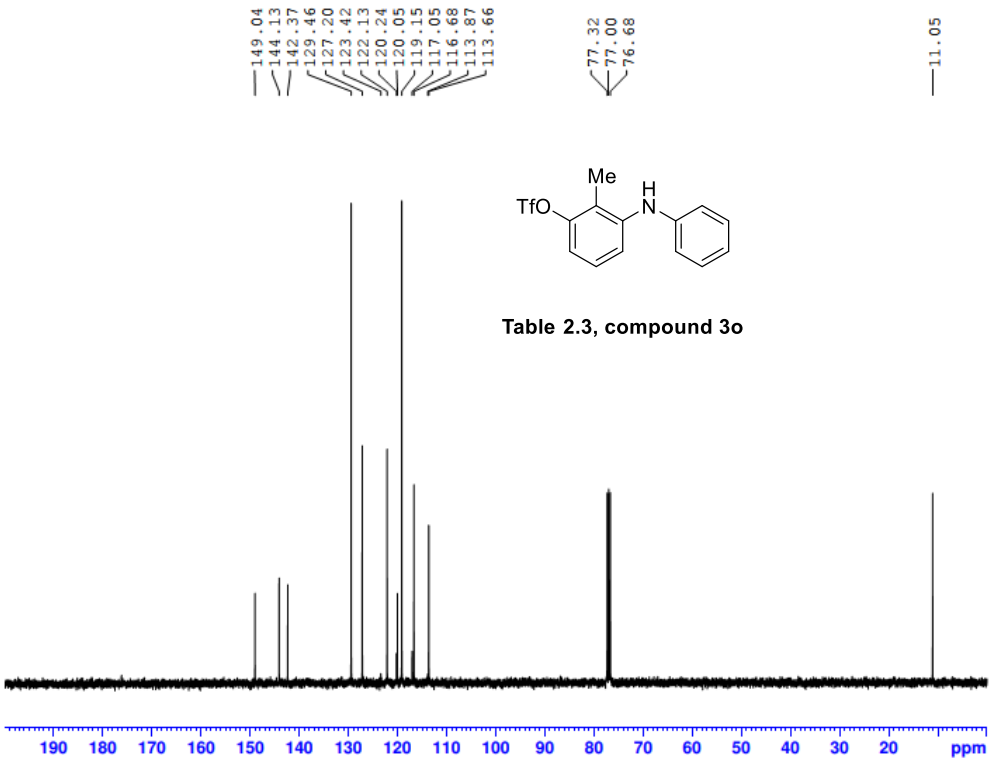

Table 2.3, compound 3o

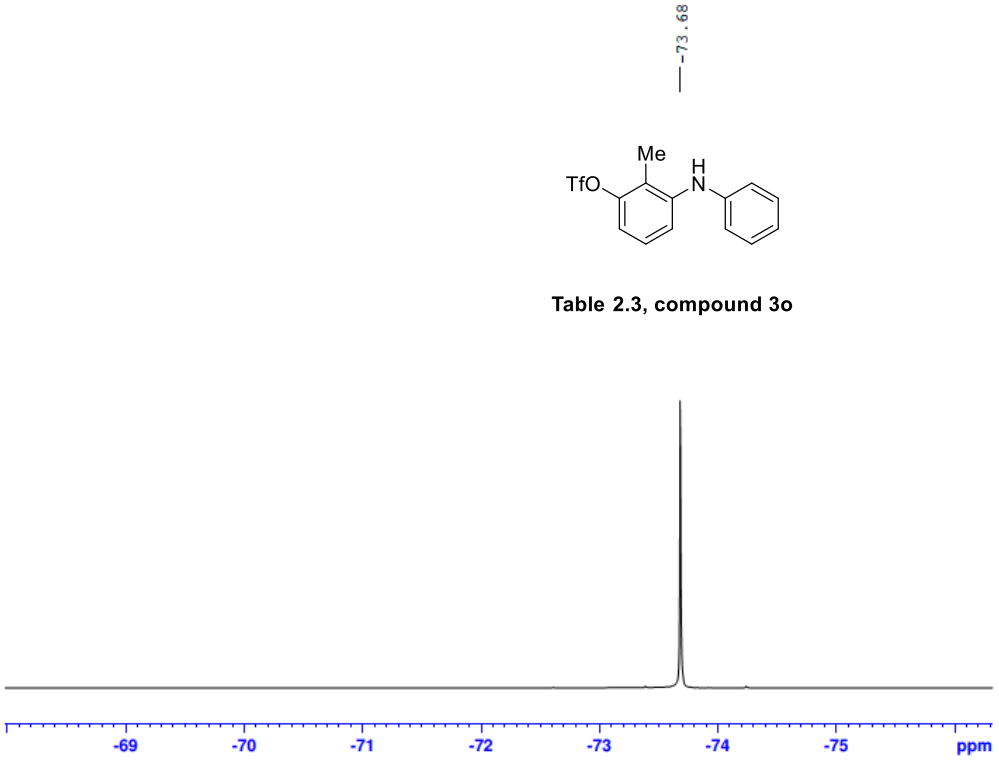

Table 2.3, compound 3o

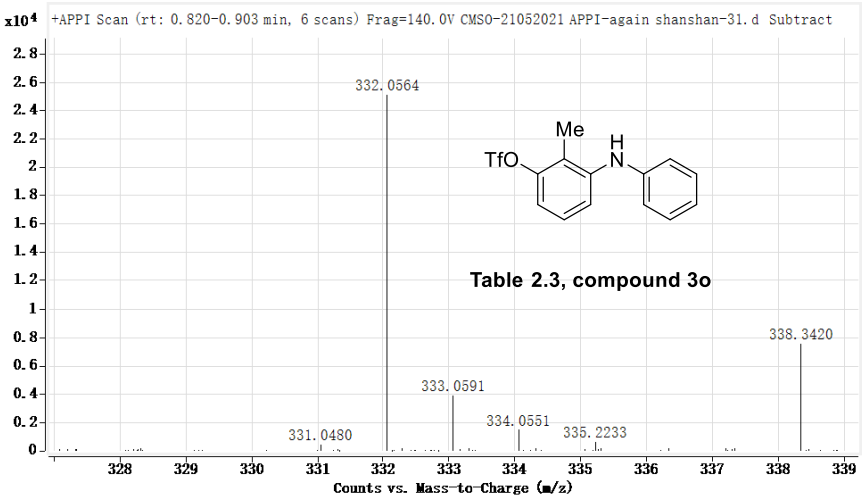

Table 2.3, compound 3o

Mass	Calc. Mass	mDa	PPM	Formula
332.0564	332.0563	-0.12	-0.38	C14 H13 F3 N O3 S

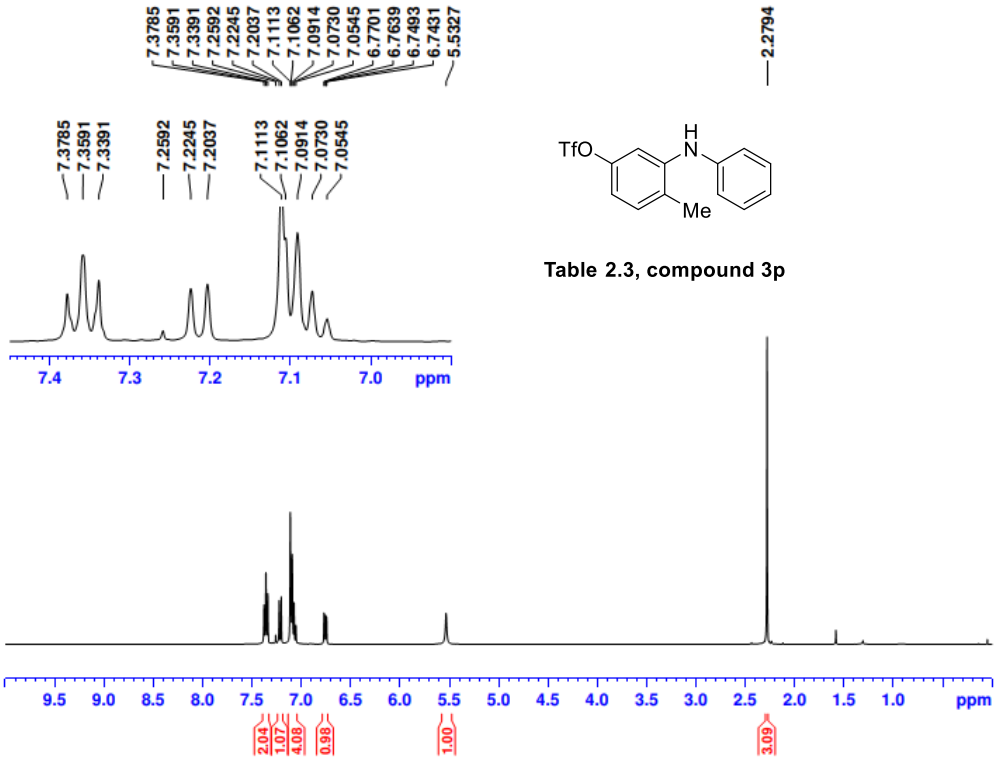

Table 2.3, compound 3p

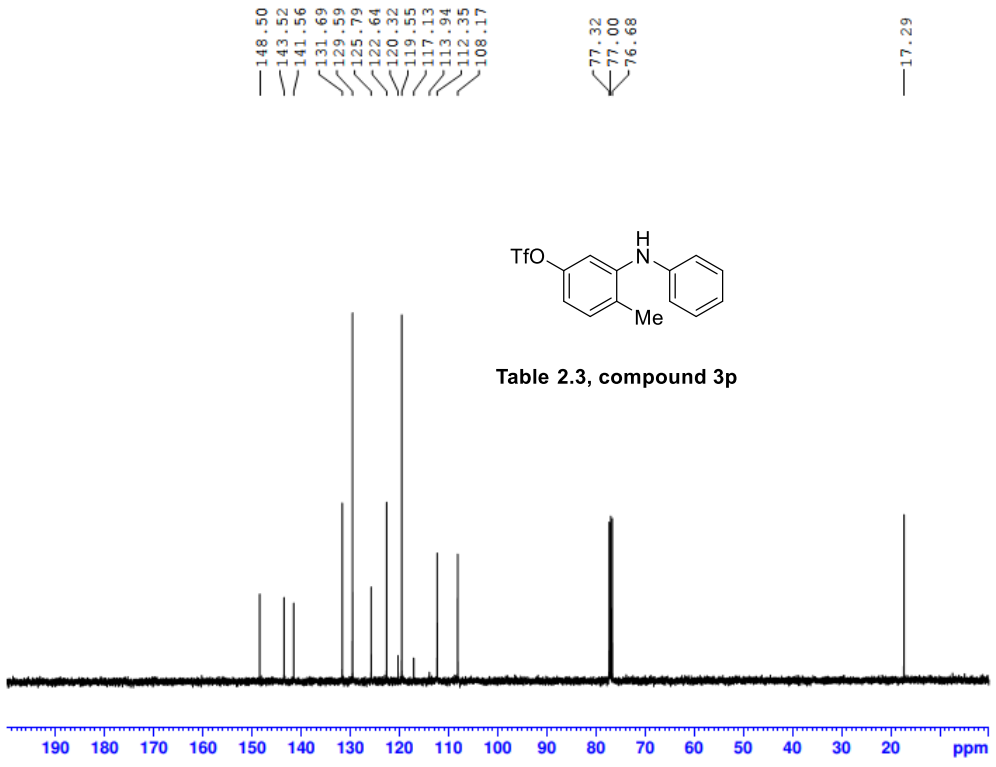

Table 2.3, compound 3p

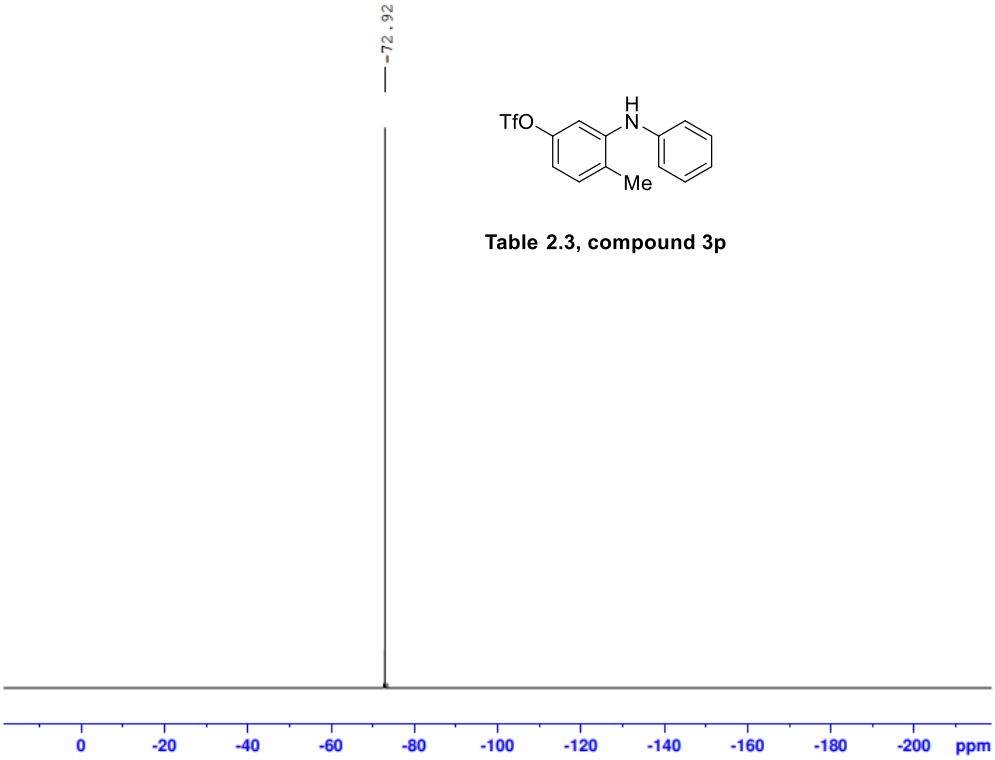

Table 2.3, compound 3p

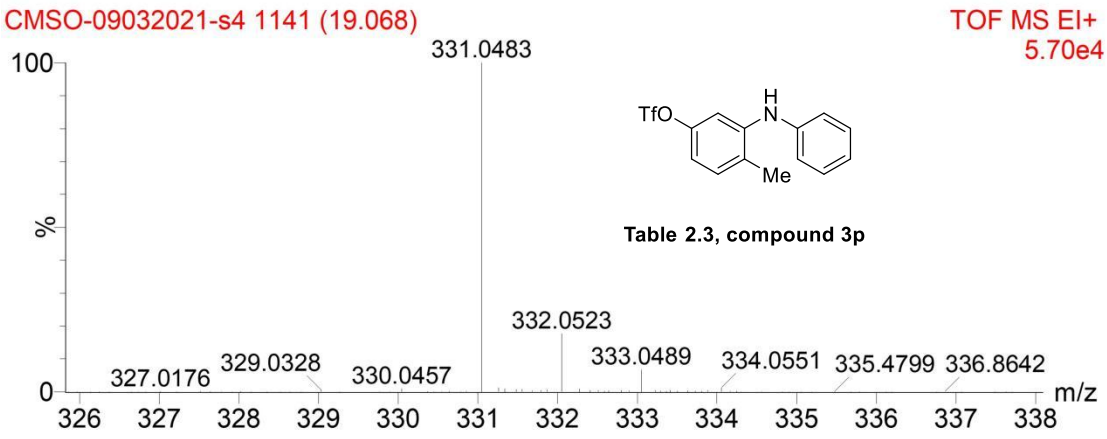

Table 2.3, compound 3p

Mass	Calc. Mass	mDa	PPM	Formula
331.0483	331.0485	0.15	0.45	C14 H12 F3NO3S

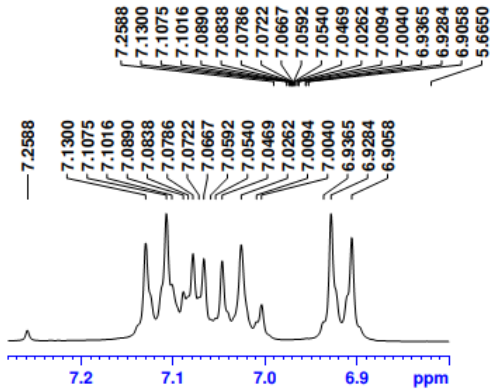

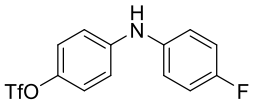

Table 2.3, compound 3q

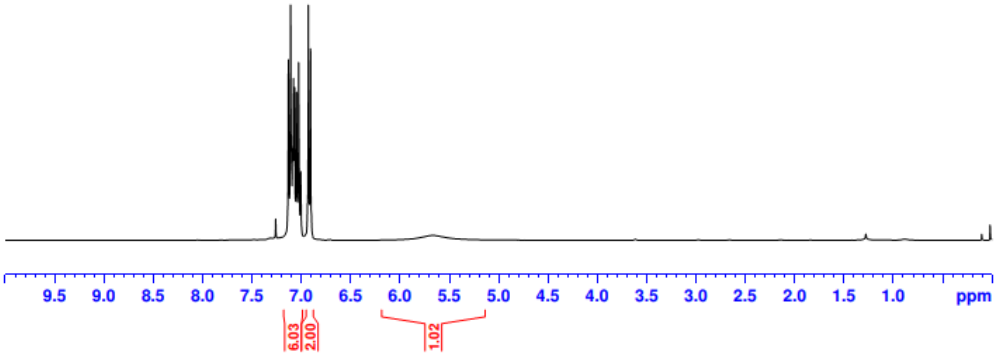

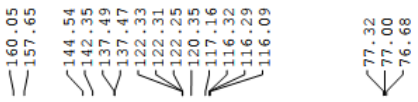

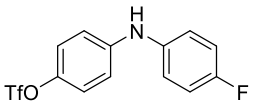

Table 2.3, compound 3q

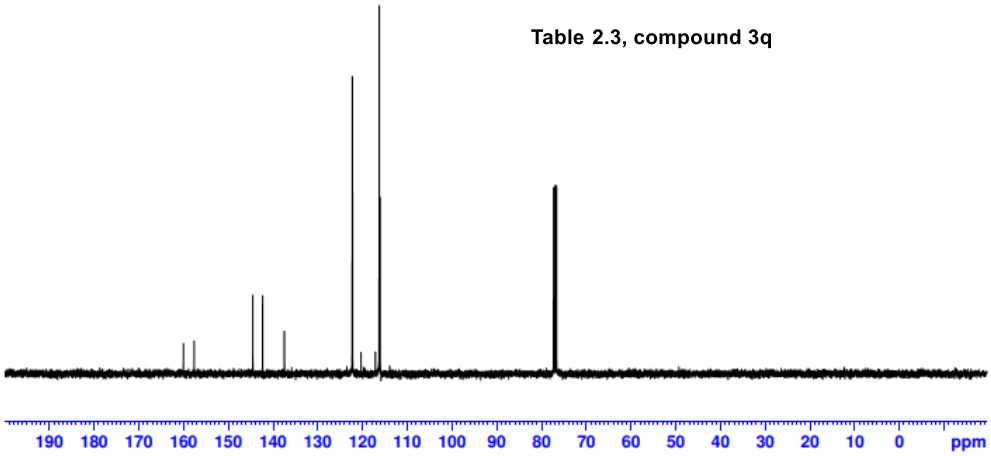

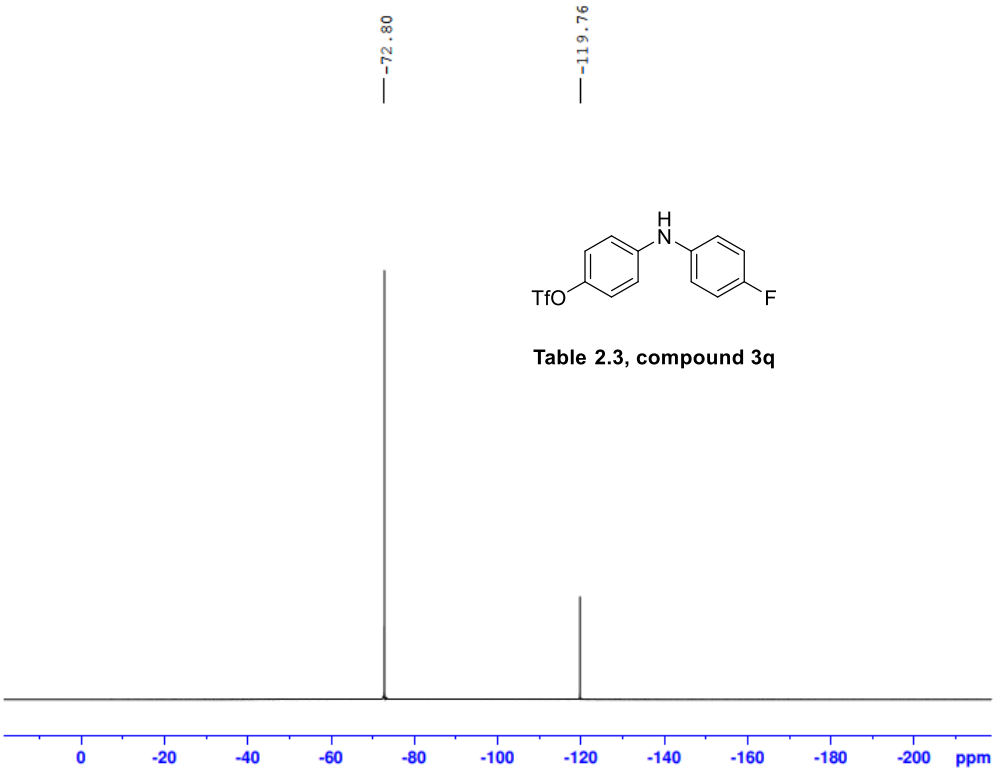

Table 2.3, compound 3q

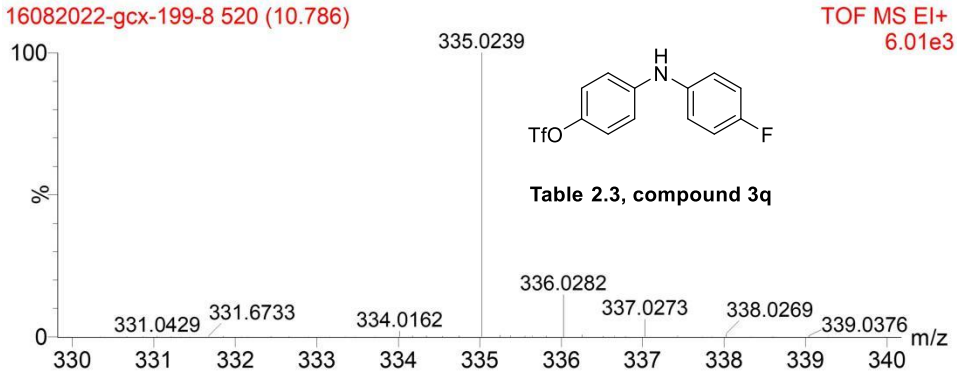

Table 2.3, compound 3q

Mass	Calc. Mass	mDa	PPM	Formula
335.0239	335.0234	-0.52	-1.56	C13 H9 F4NO3S

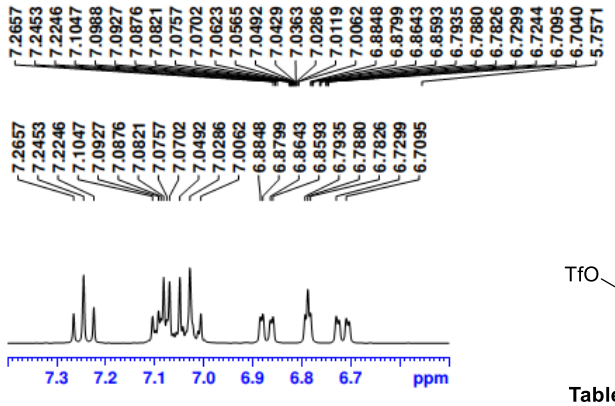

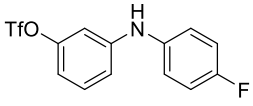

Table 2.3, compound 3r

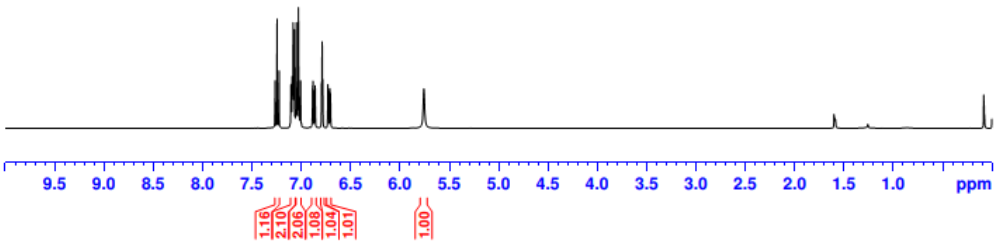

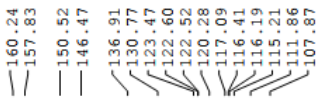

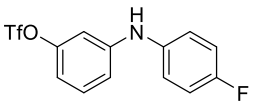

Table 2.3, compound 3r

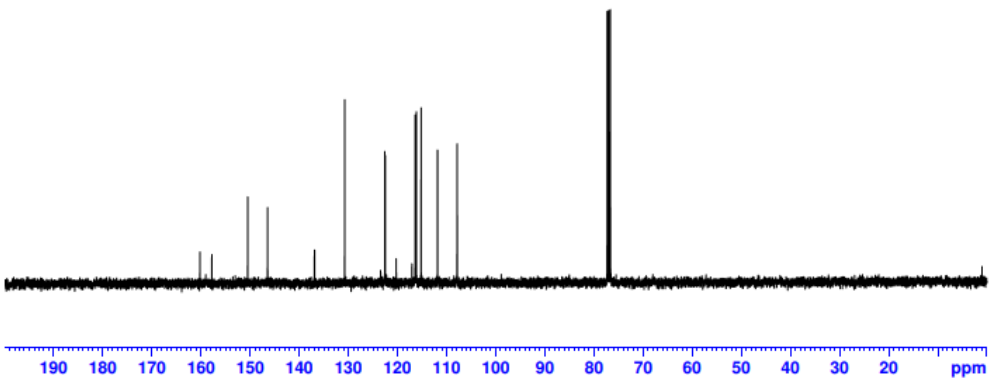

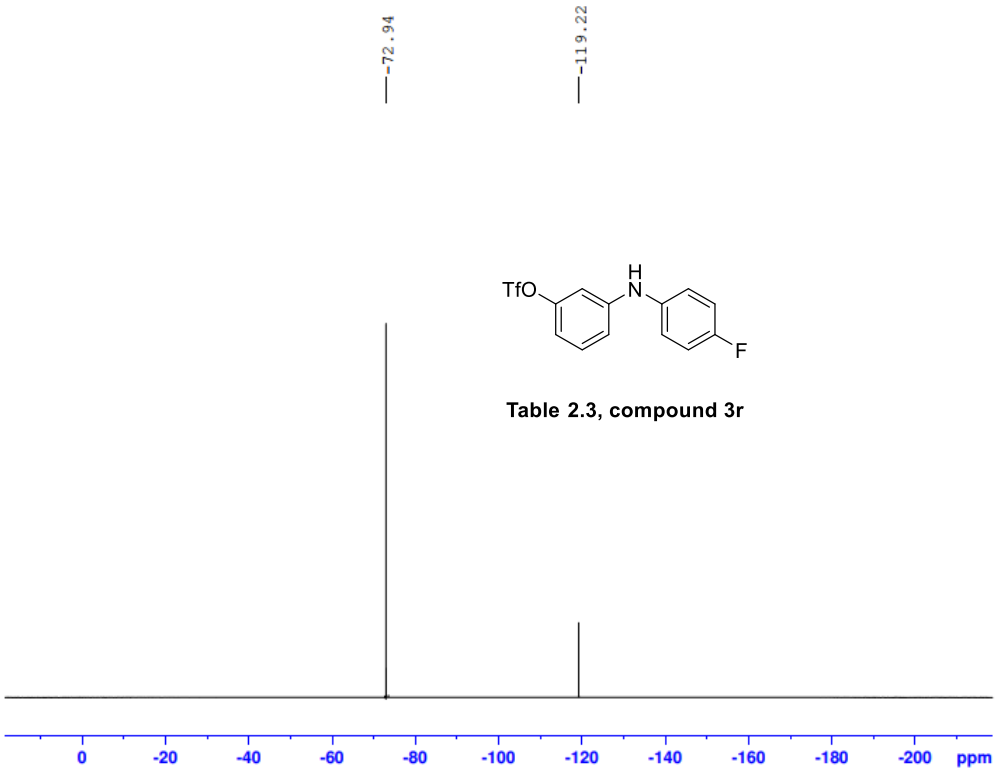

Table 2.3, compound 3r

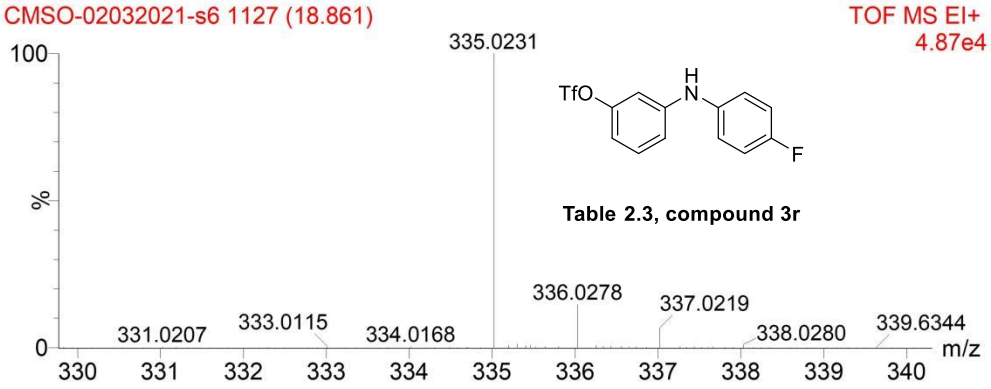

Table 2.3, compound 3r

Mass	Calc. Mass	mDa	PPM	Formula
335.0231	335.0234	0.28	0.83	C13H9 F4NO3S

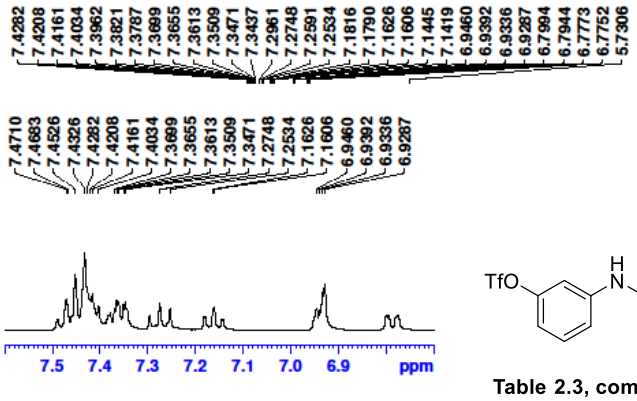

Table 2.3, compound 3s

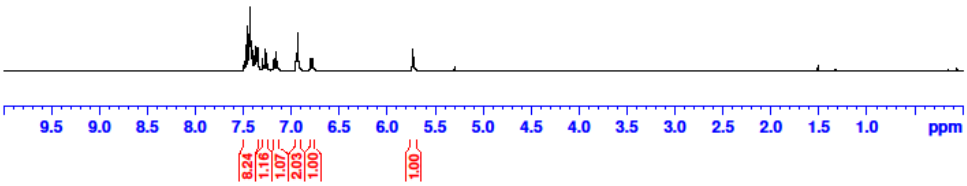

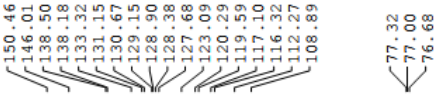

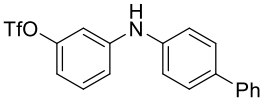

Table 2.3, compound 3s

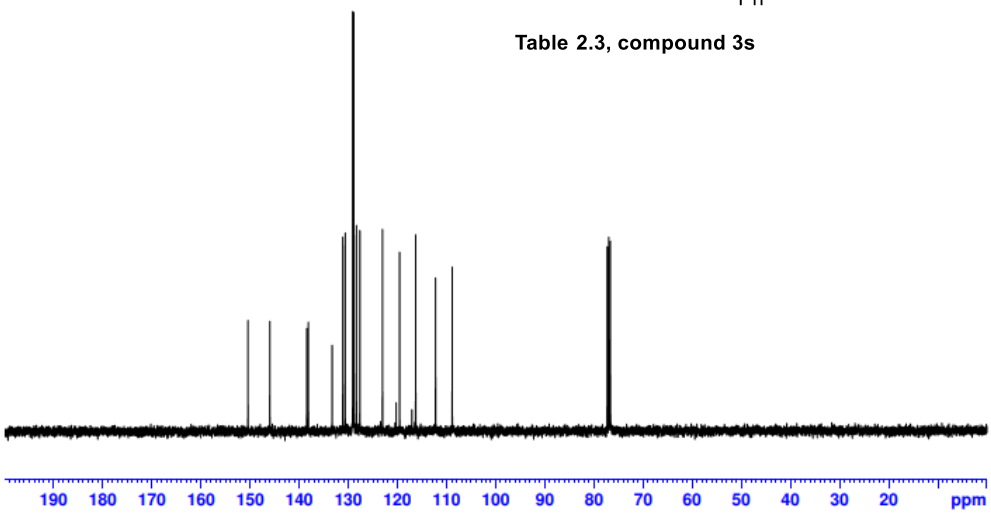

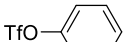

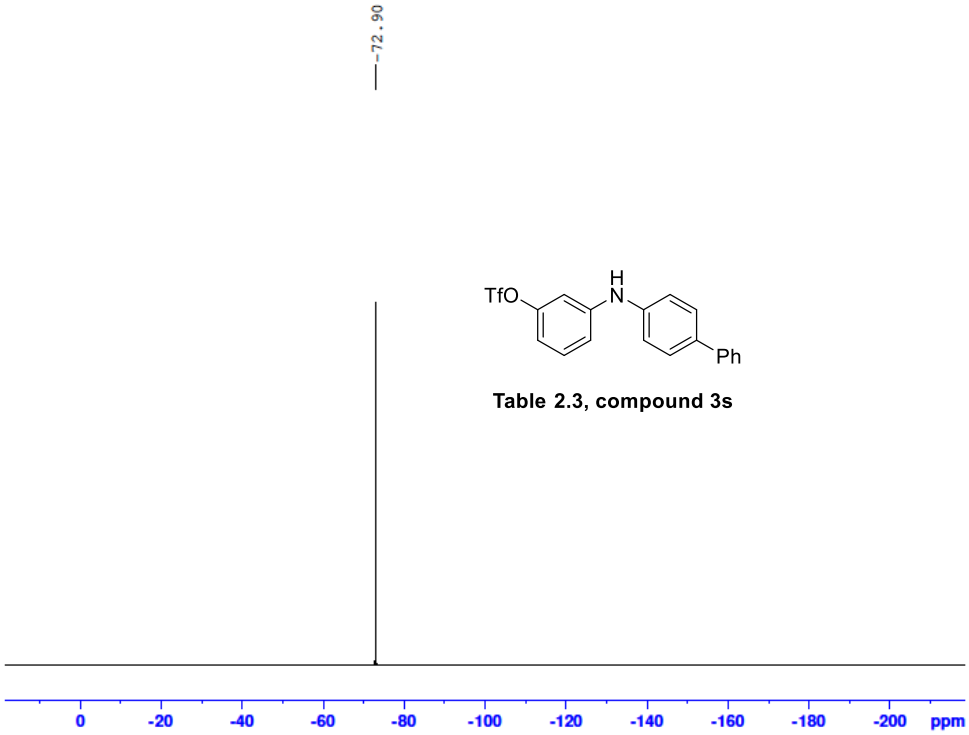

Table 2.3, compound 3s

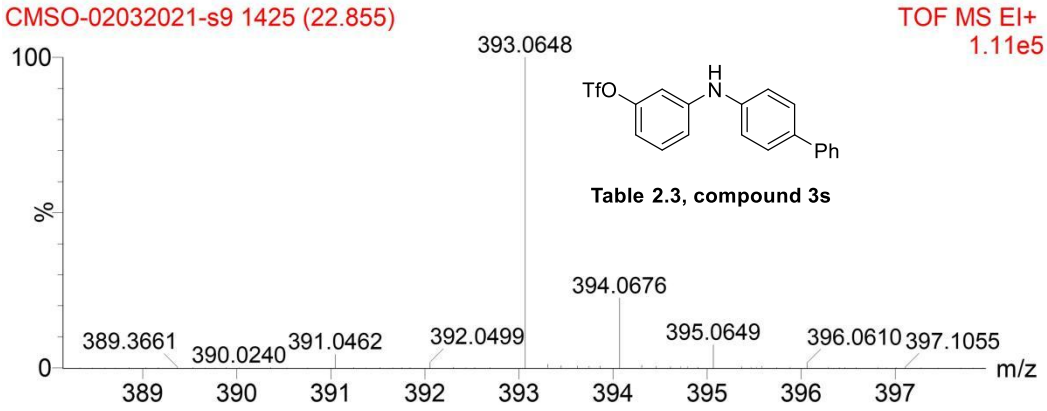

Table 2.3, compound 3s

Mass	Calc. Mass	mDa	PPM	Formula
393.0648	393.0641	-0.70	-1.78	C19H14 F3NO3S

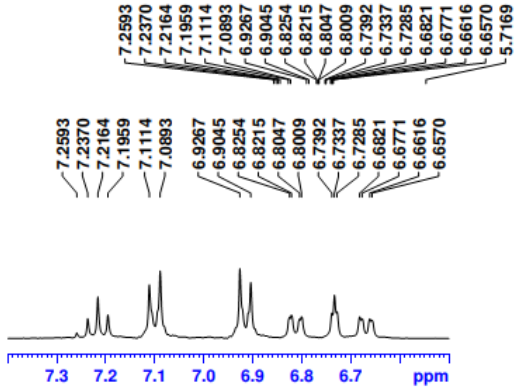

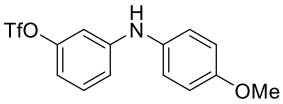

Table 2.3, compound 3t

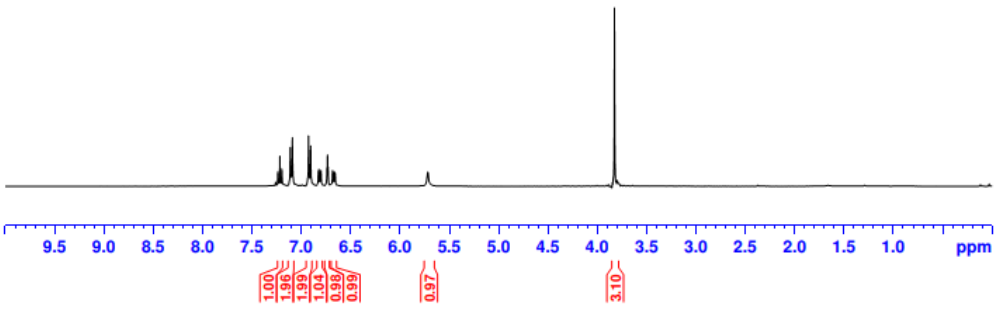

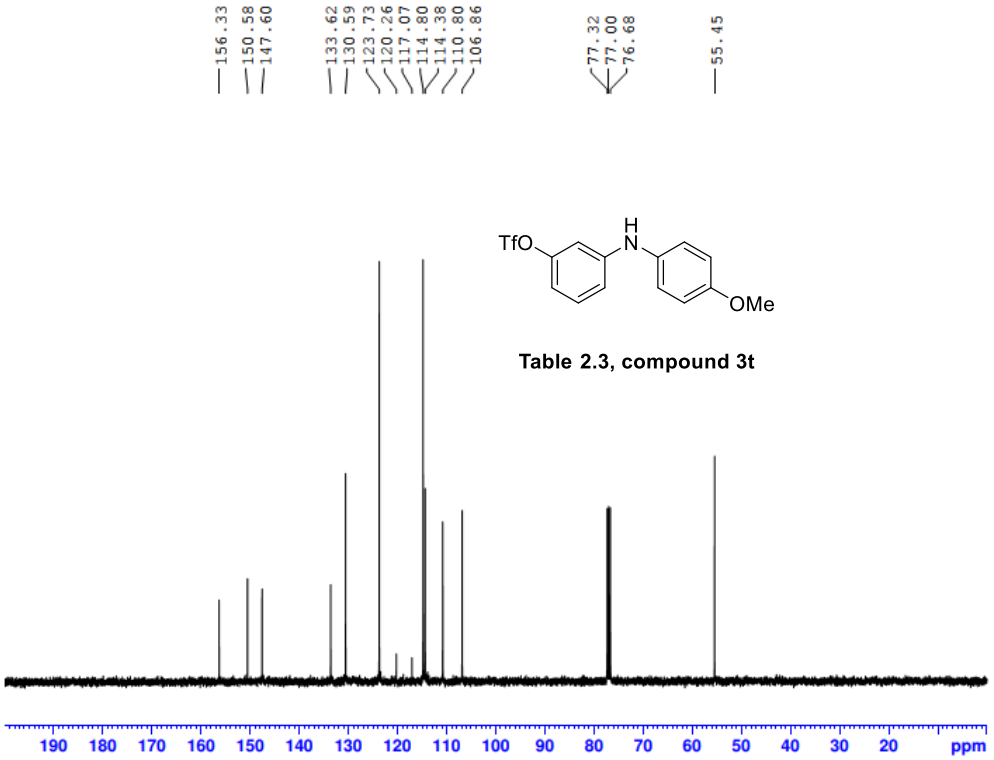

Table 2.3, compound 3t

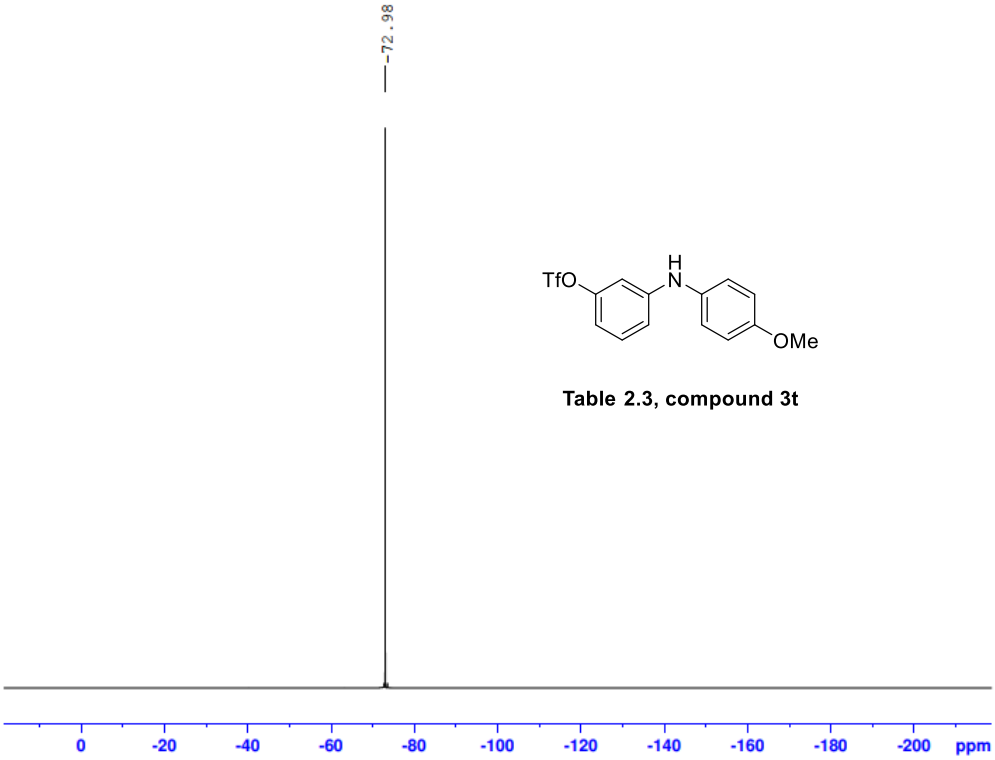

Table 2.3, compound 3t

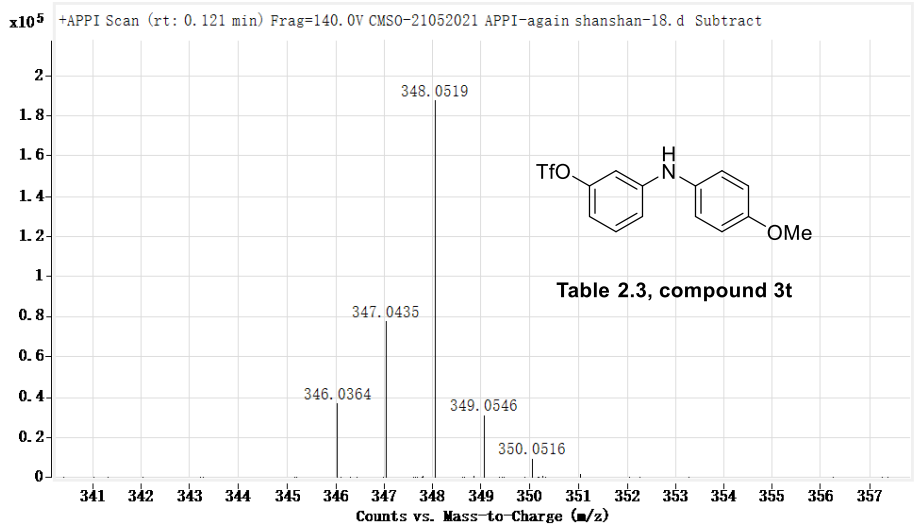

Table 2.3, compound 3t

Mass	Calc. Mass	mDa	PPM	Formula
348.0519	348.0512	-0.71	-2.05	C14 H13 F3 N O4 S

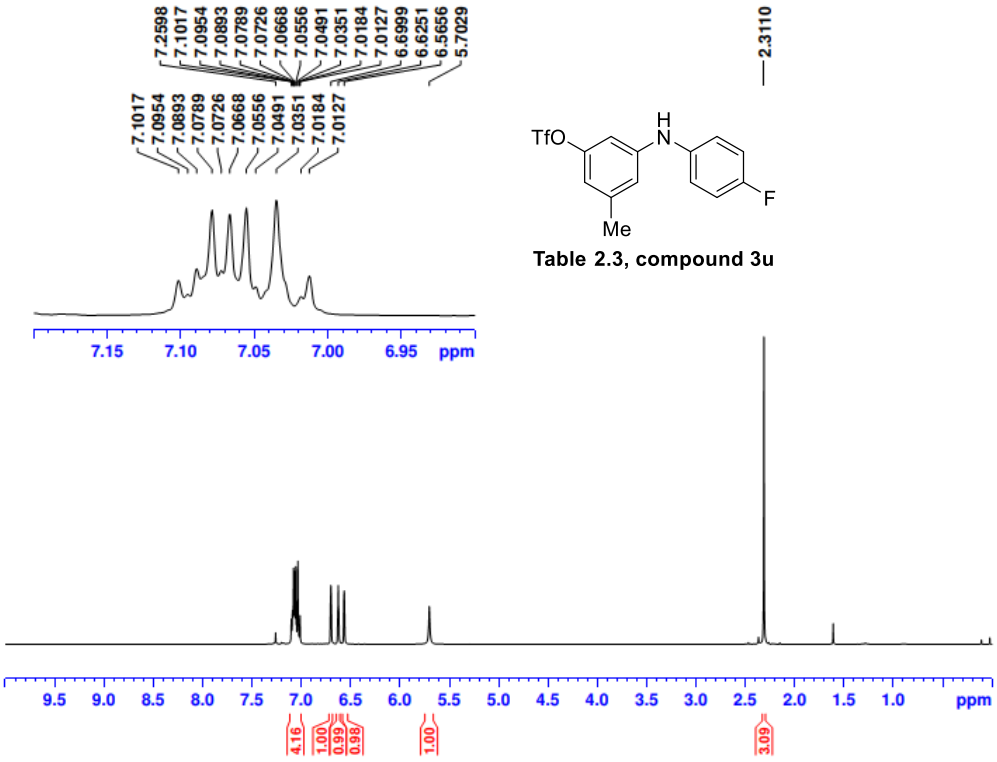

Table 2.3, compound 3u

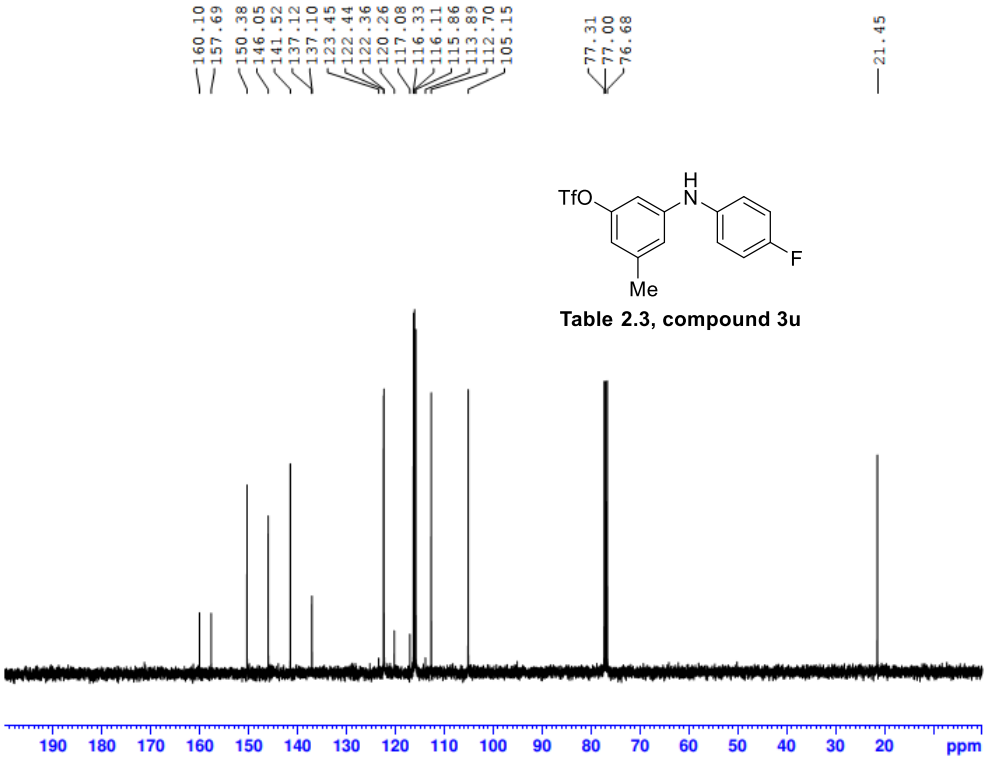

Table 2.3, compound 3u

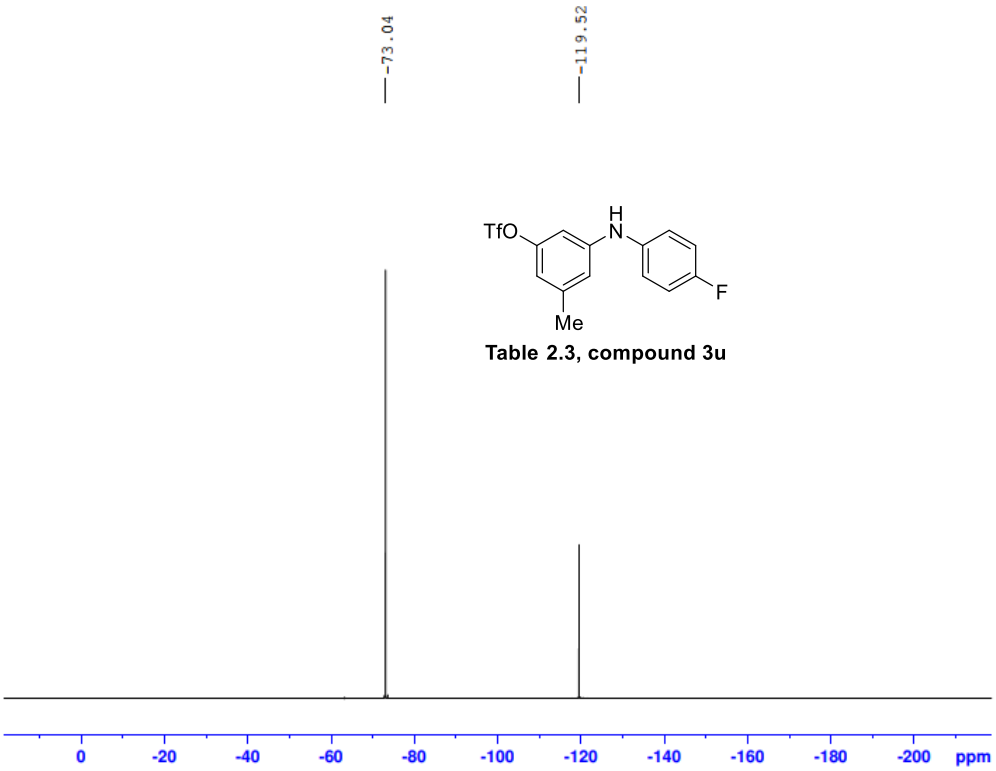

Table 2.3, compound 3u

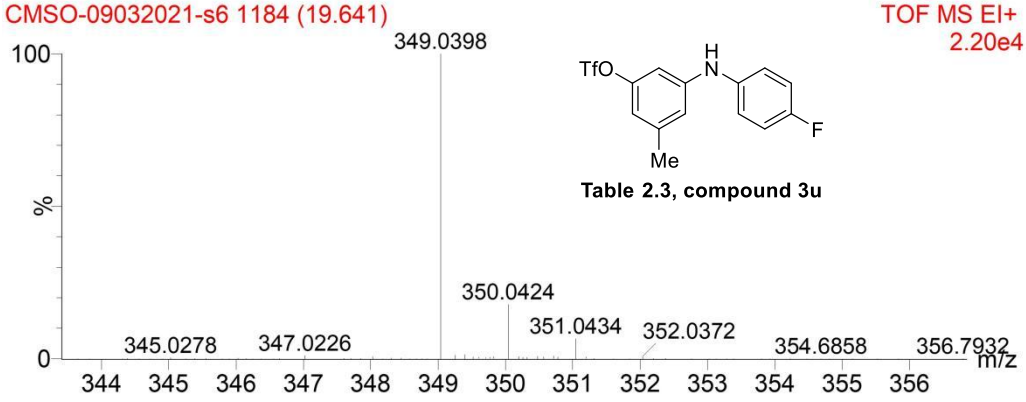

Table 2.3, compound 3u

Mass	Calc. Mass	mDa	PPM	Formula
349.0398	349.0390	-0.77	-2.21	C14 H11 F4NO4S

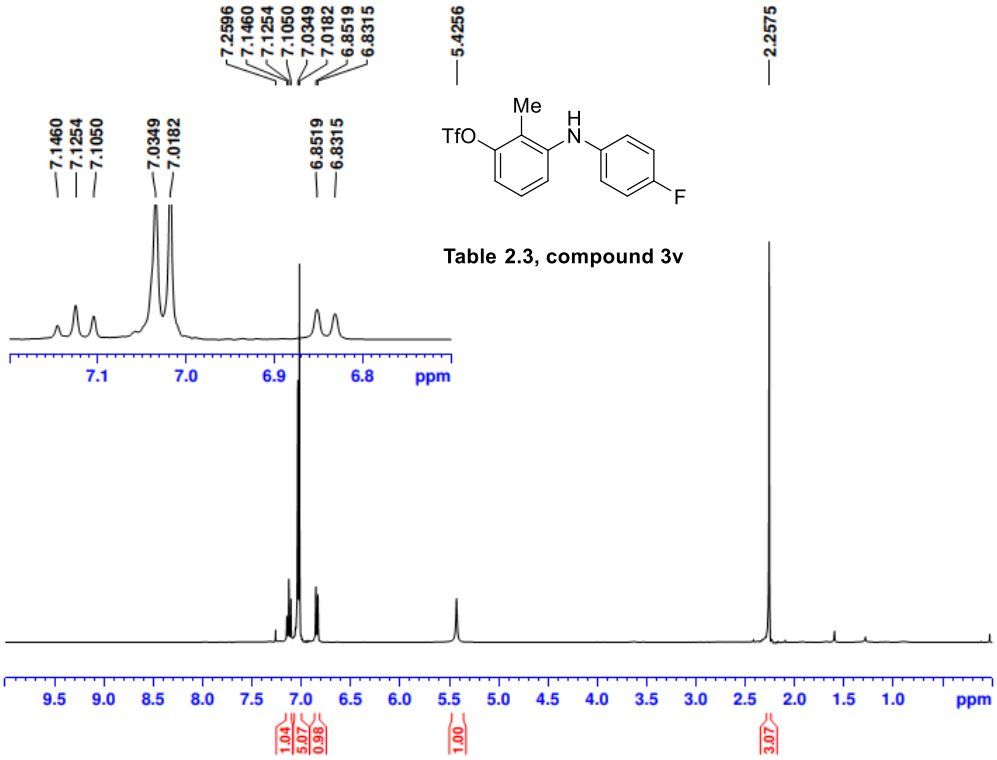
7.2596
7.1460
7.1254
7.1050
7.0349
7.0182
6.8519
6.8315
5.4256
2.2575
Me
TfO
H
N
F
Table 2.3, compound 3v
ppm
1.04
5.07
0.98
1.00
3.07

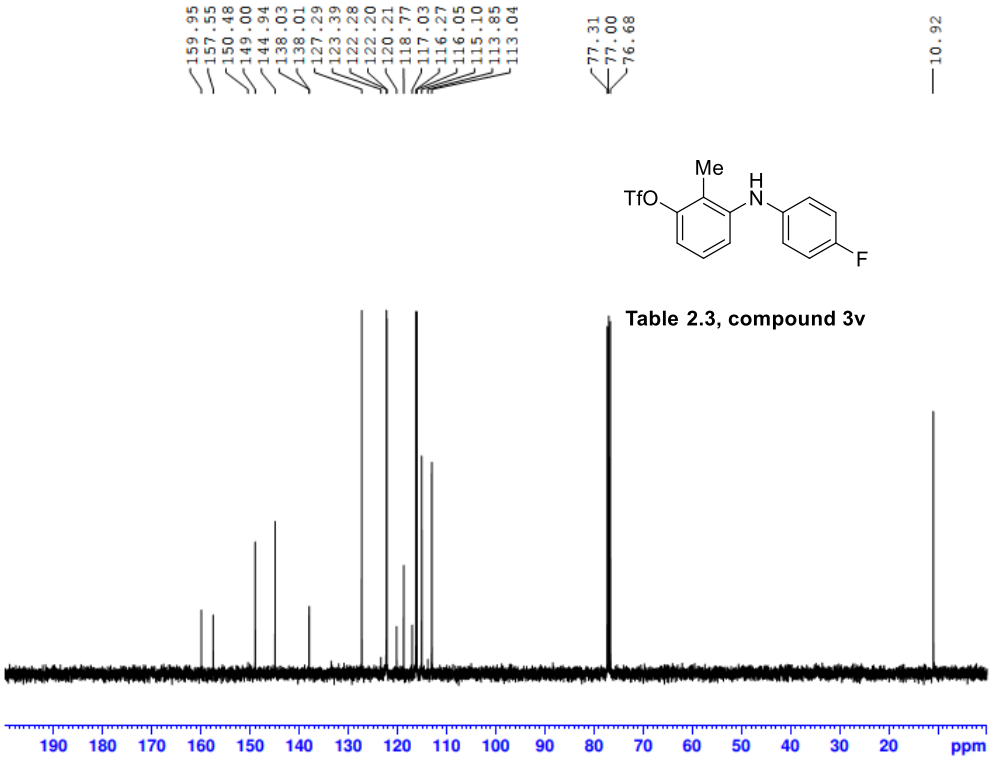
159.95
157.55
150.48
149.00
144.94
138.03
138.01
127.29
123.39
122.28
122.20
120.21
118.77
117.03
116.27
116.05
115.10
113.85
113.04
77.31
77.00
76.68
10.92
Me
TfO
H
N
F
Table 2.3, compound 3v
ppm

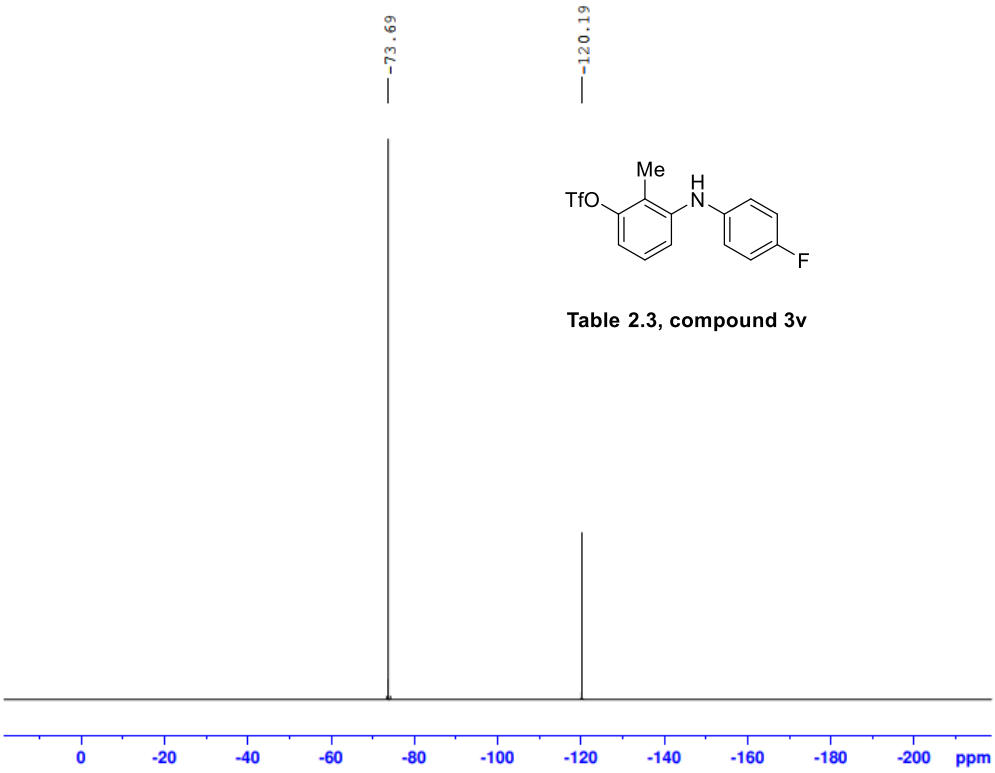

Table 2.3, compound 3v

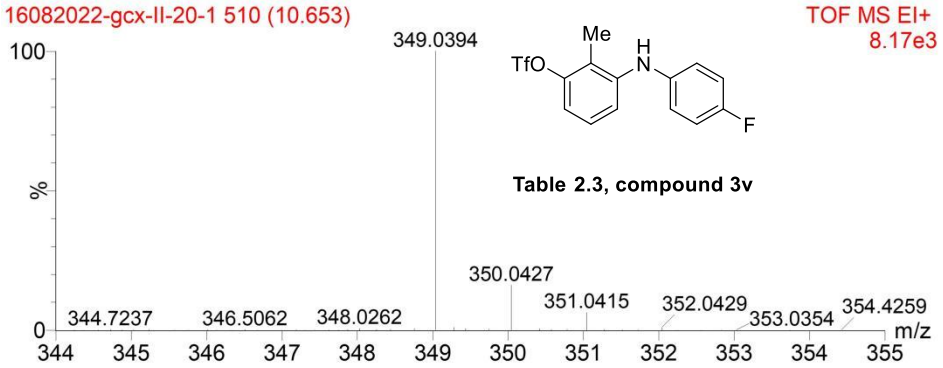

Table 2.3, compound 3v

Mass	Calc. Mass	mDa	PPM	Formula
349.0394	349.0390	-0.37	-1.07	C14 H11 F4NO3S

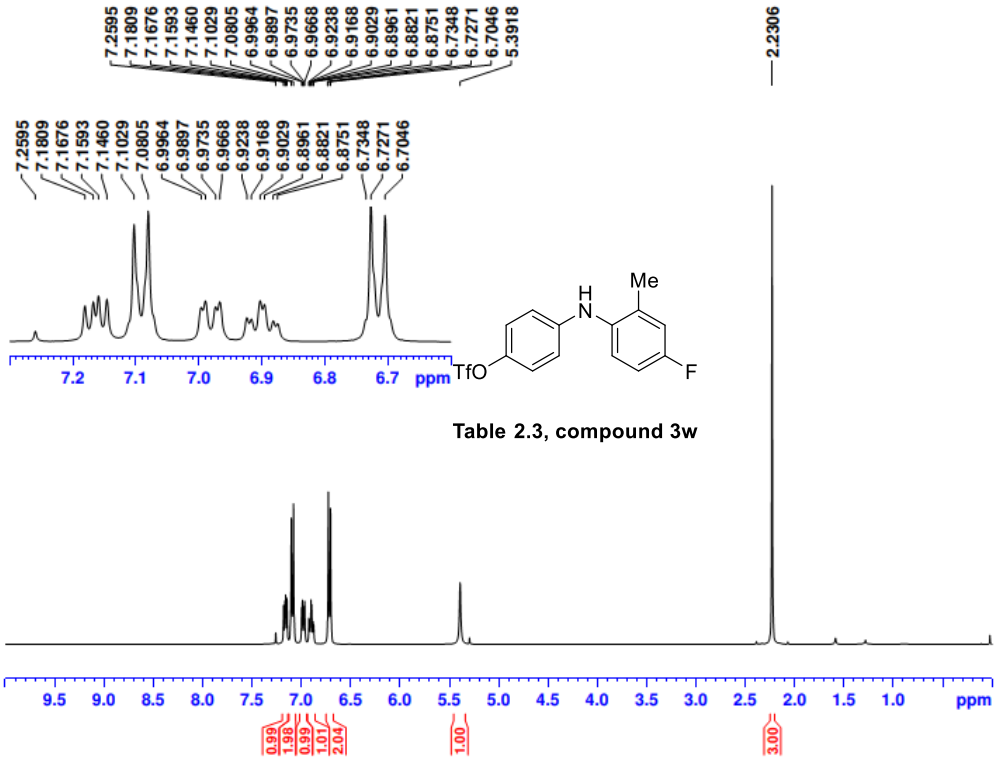

Table 2.3, compound 3w

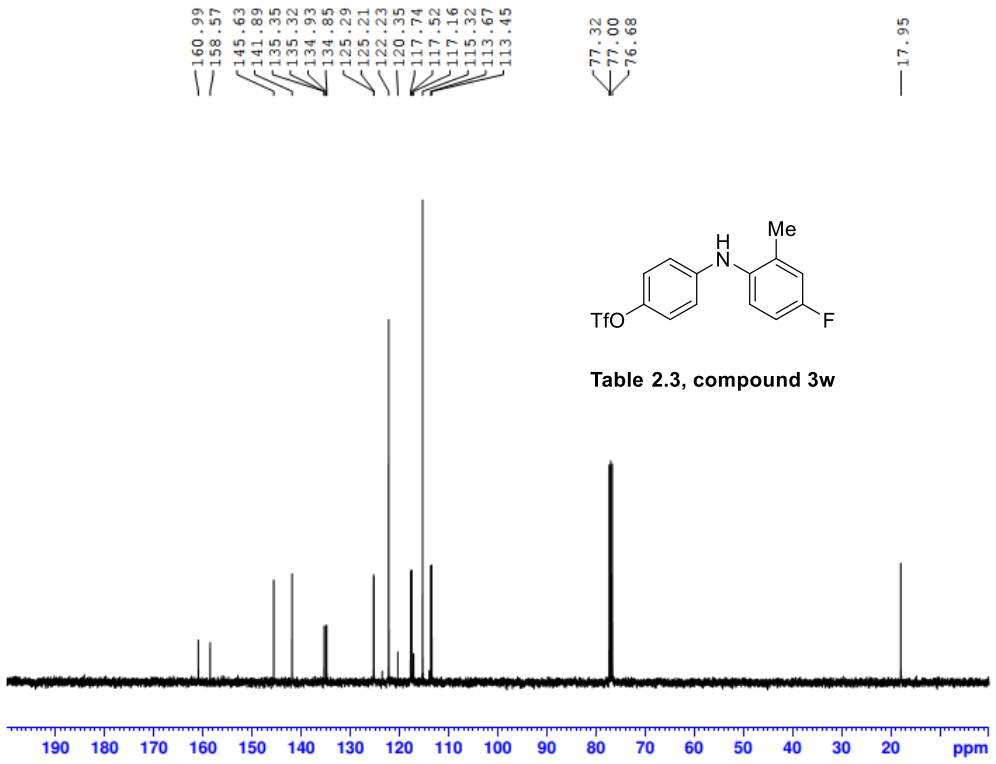

Table 2.3, compound 3w

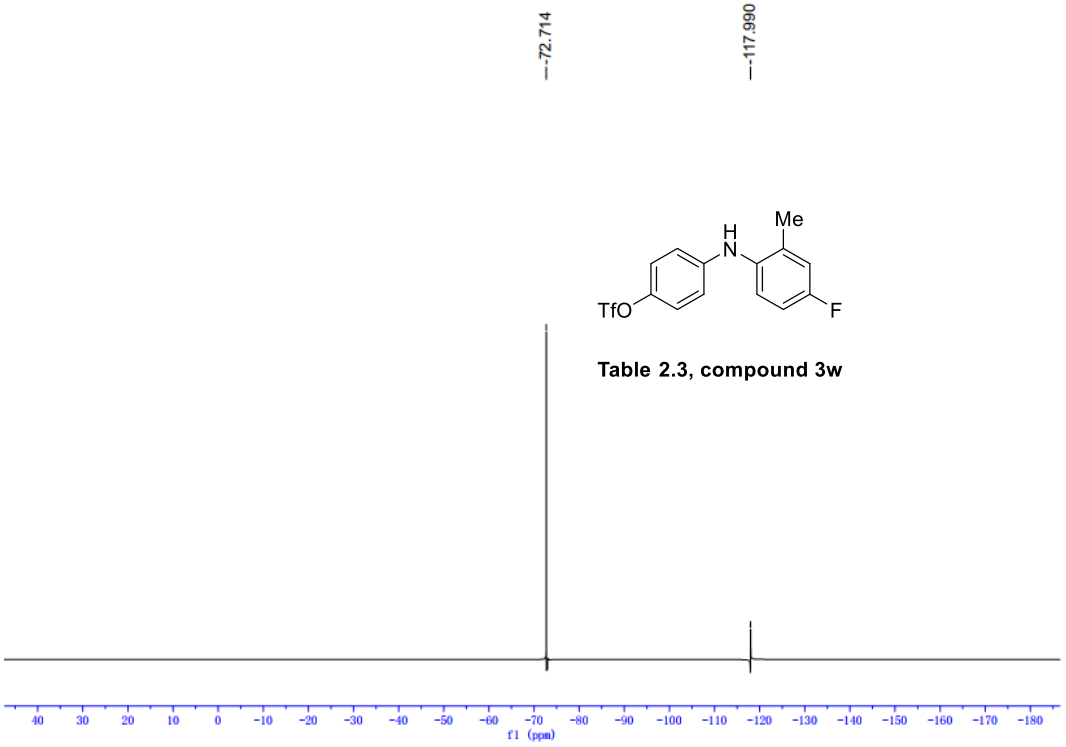

Table 2.3, compound 3w

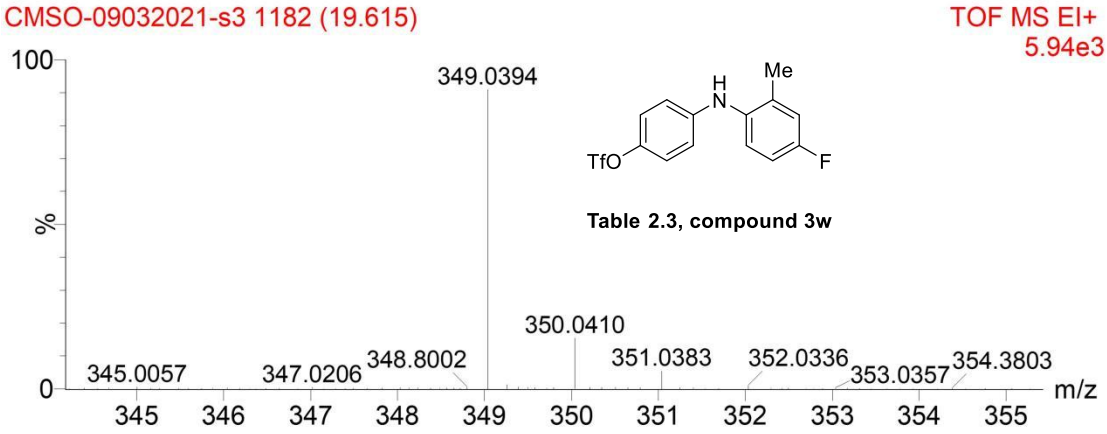

Table 2.3, compound 3w

Mass	Calc. Mass	mDa	PPM	Formula
349.0394	349.0390	-0.37	-1.07	C14 H11 F4NO3S

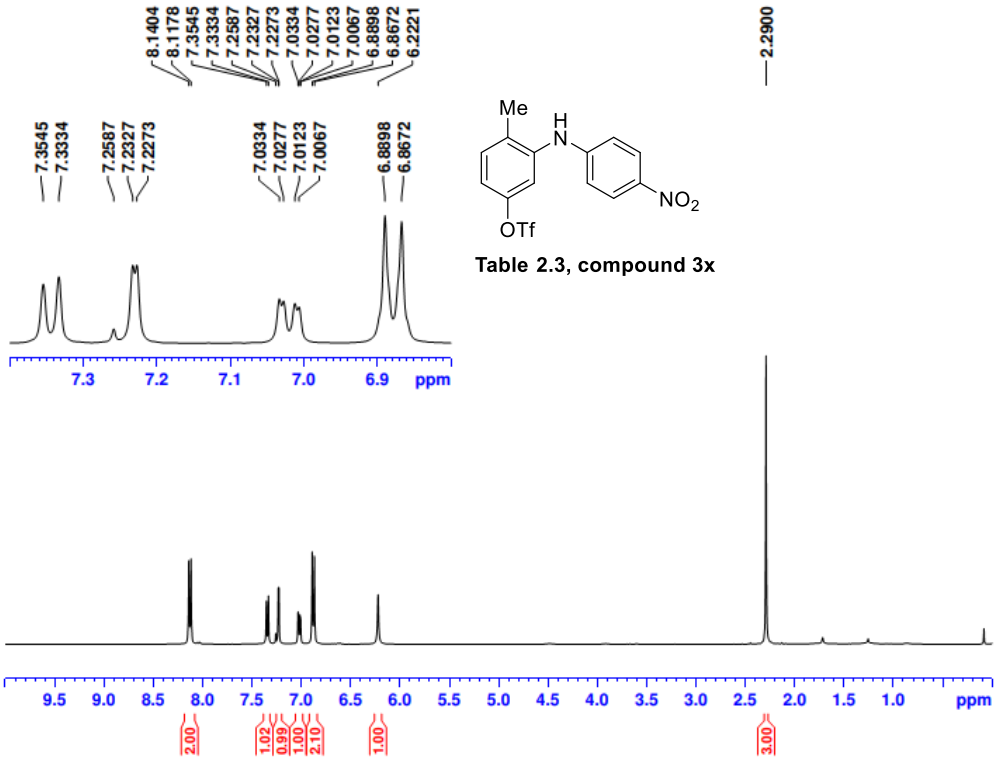

Table 2.3, compound 3x

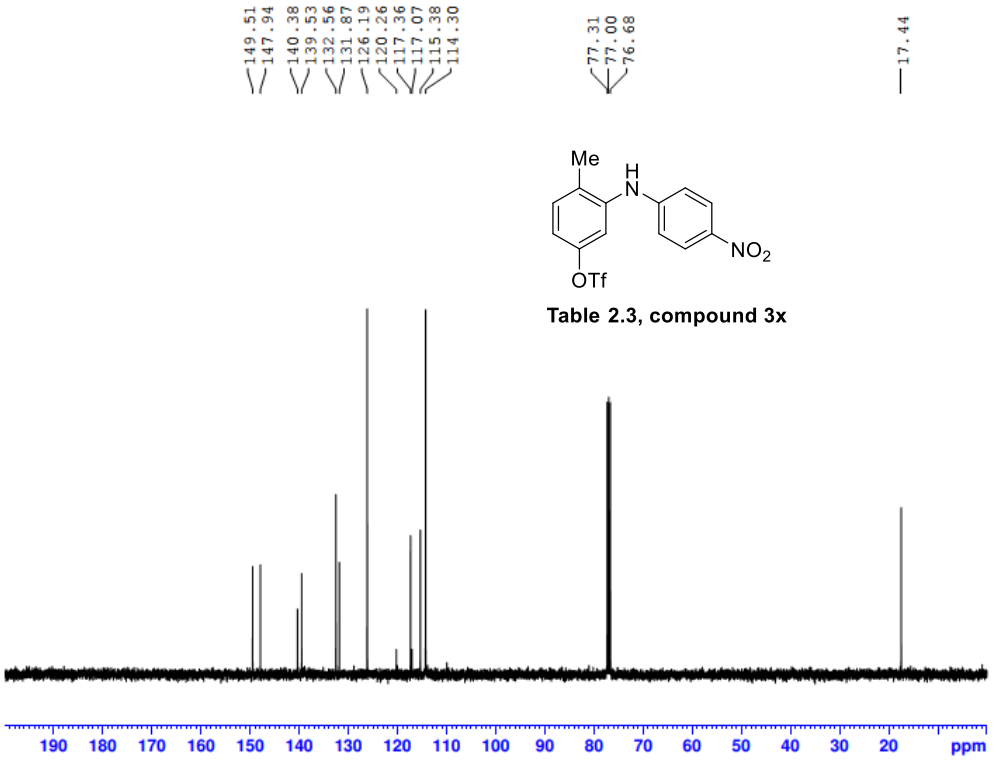

Table 2.3, compound 3x

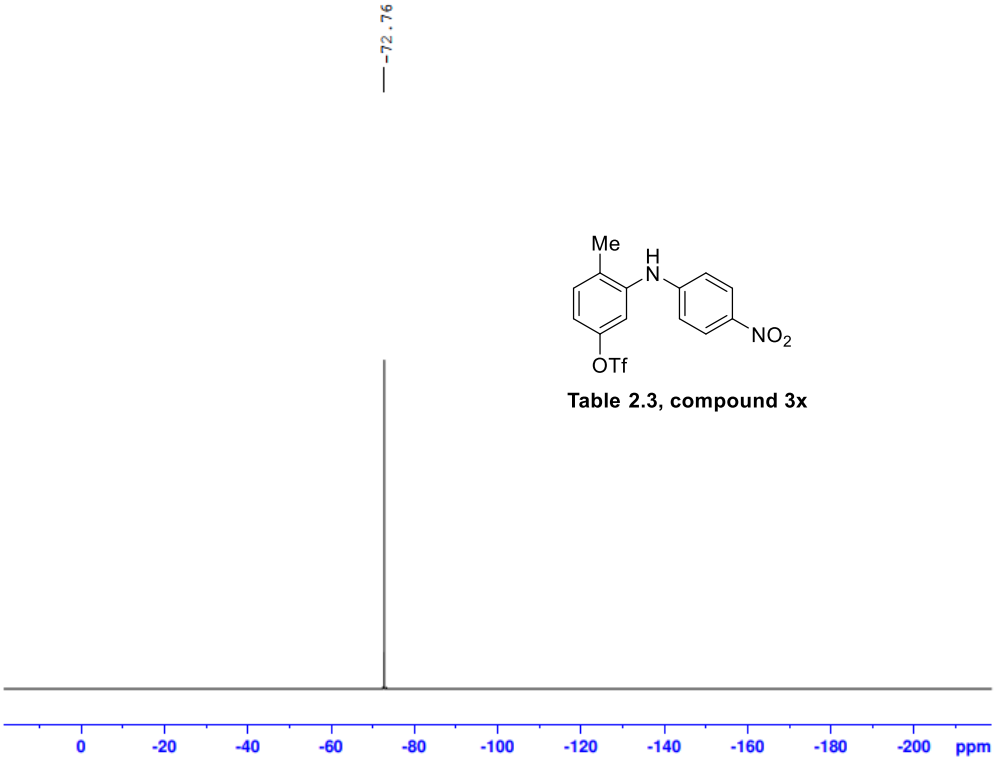

Table 2.3, compound 3x

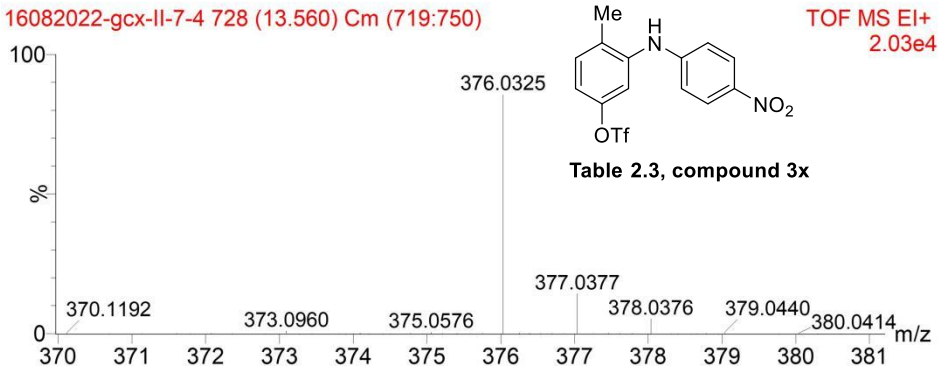

Table 2.3, compound 3x

Mass	Calc. Mass	mDa	PPM	Formula
376.0325	376.0335	1.03	2.73	C14 H11 F3N2O5S

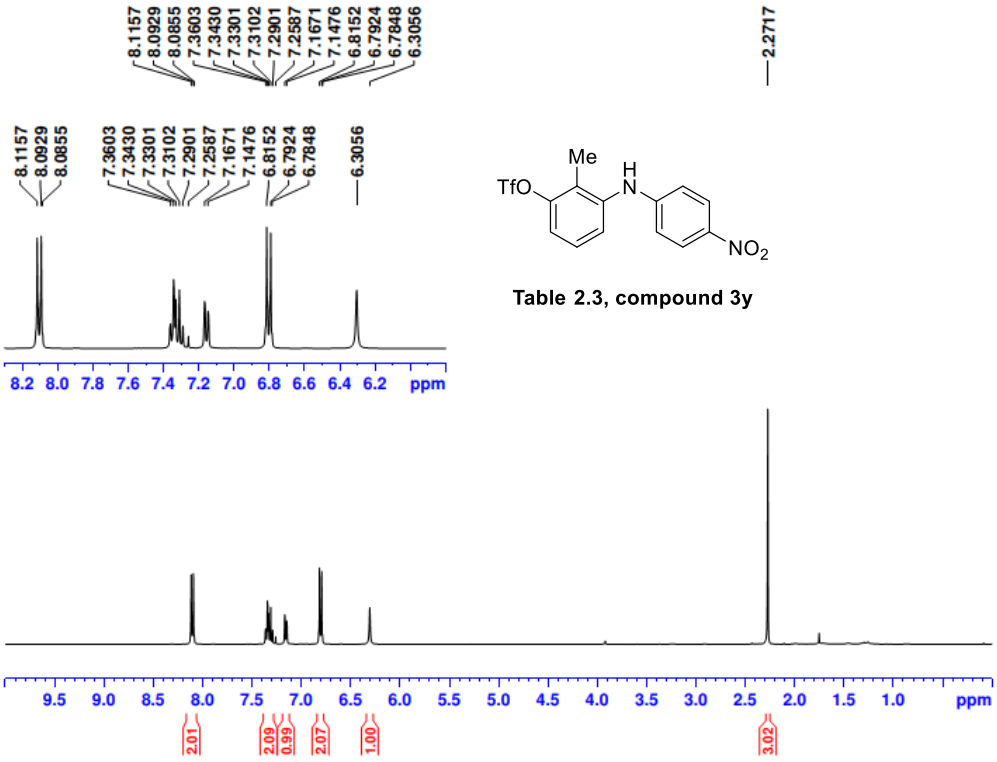

Table 2.3, compound 3y

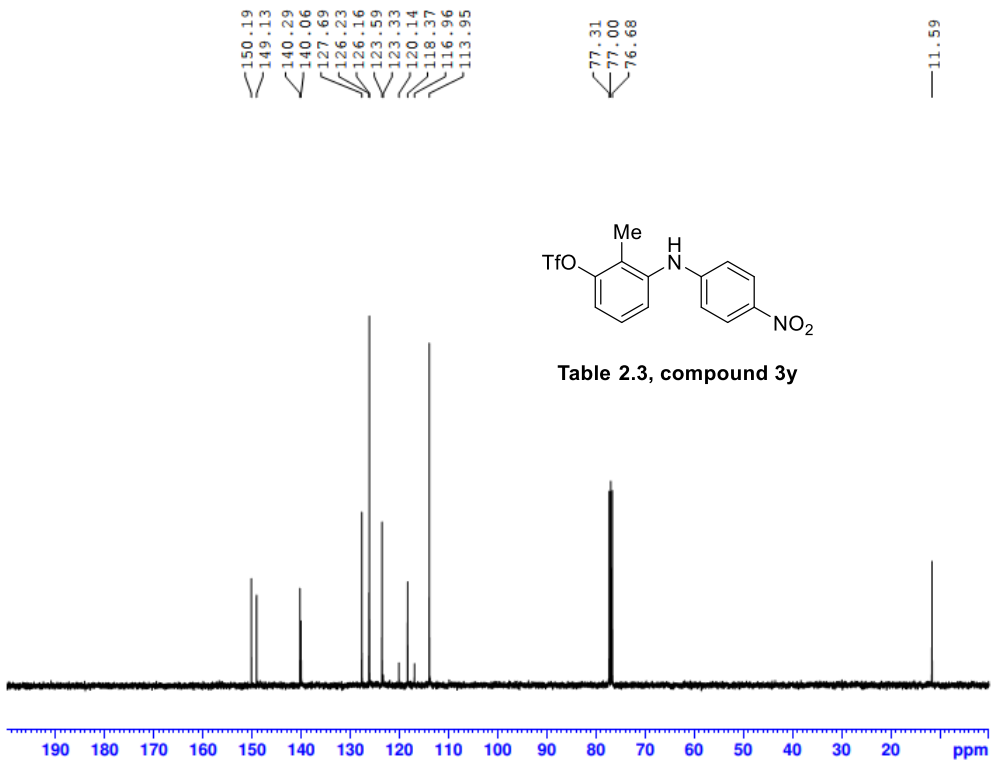

Table 2.3, compound 3y

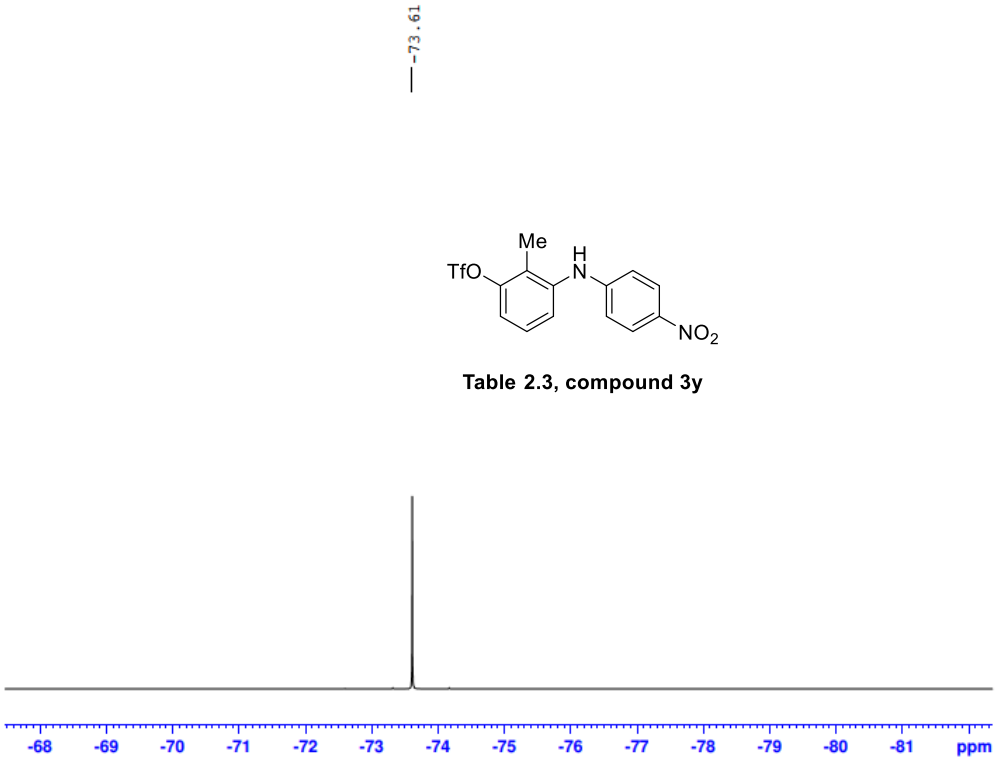

Table 2.3, compound 3y

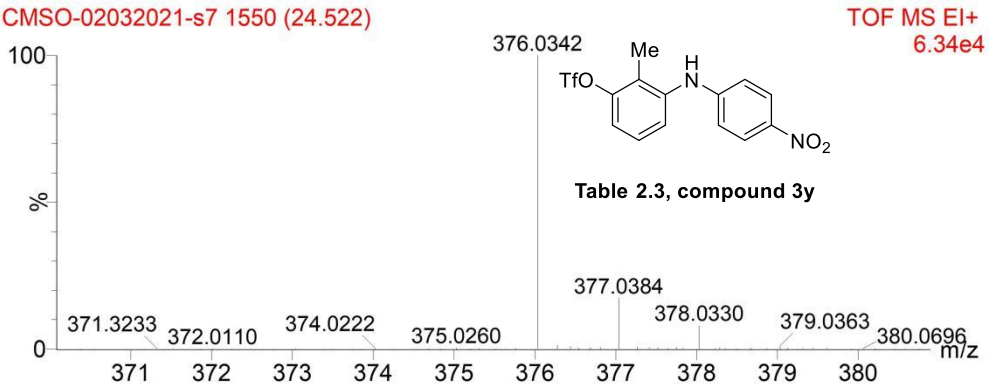

Table 2.3, compound 3y

Mass	Calc. Mass	mDa	PPM	Formula
376.0342	376.0335	-0.67	-1.79	C14H11 F3N2O5S

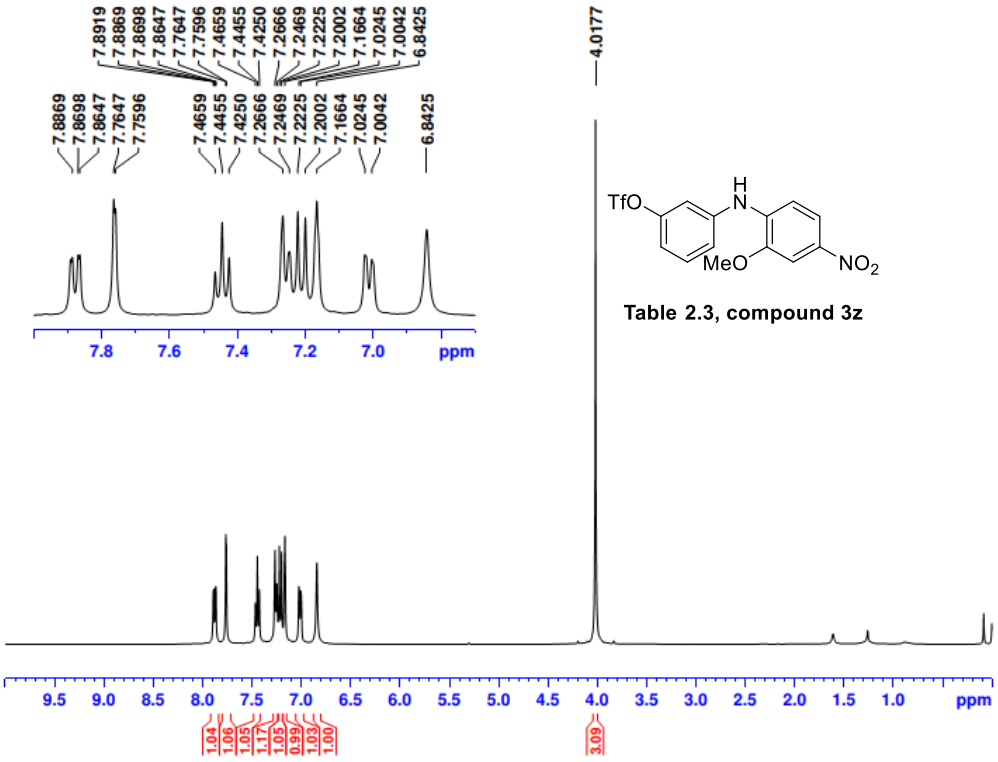
7.8919
7.8869
7.8698
7.8647
7.7647
7.7596
7.4659
7.4455
7.4250
7.2666
7.2469
7.2225
7.2002
7.1664
7.0245
7.0042
6.8425
4.0177
TfO
H
N
MeO
NO2
Table 2.3, compound 3z
ppm
1.04
1.06
1.05
1.17
1.05
0.99
1.03
1.00
3.09

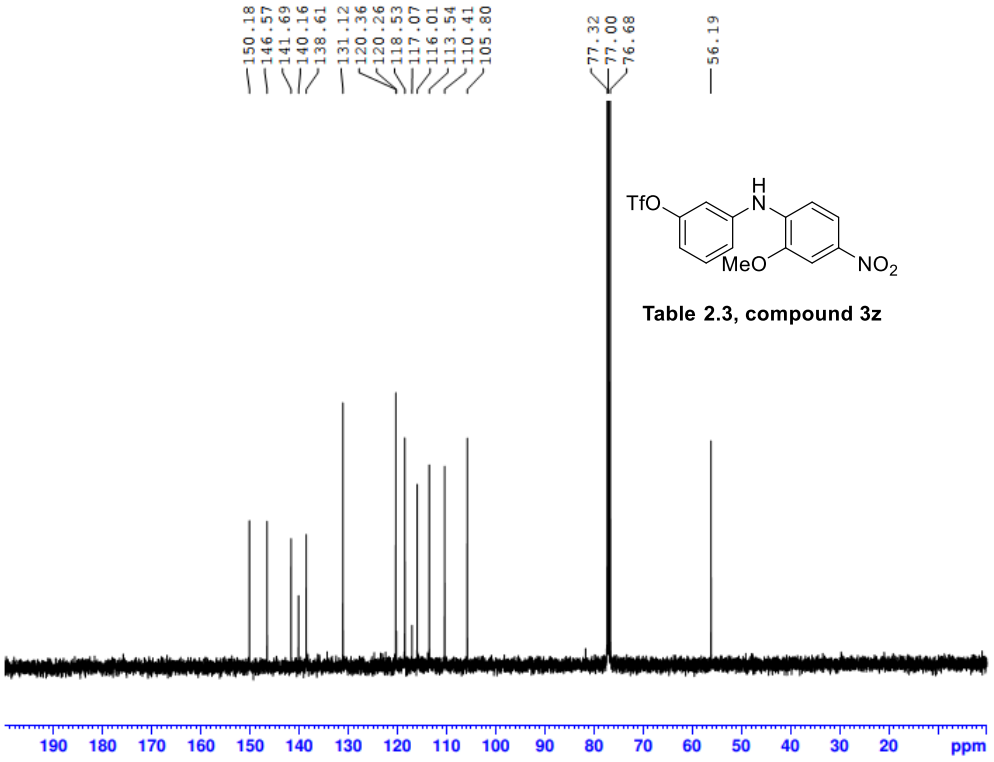
150.18
146.57
141.69
140.16
138.61
131.12
120.36
120.26
118.53
117.07
116.01
113.54
110.41
105.80
77.32
77.00
76.68
56.19
TfO
H
N
MeO
NO2
Table 2.3, compound 3z
ppm

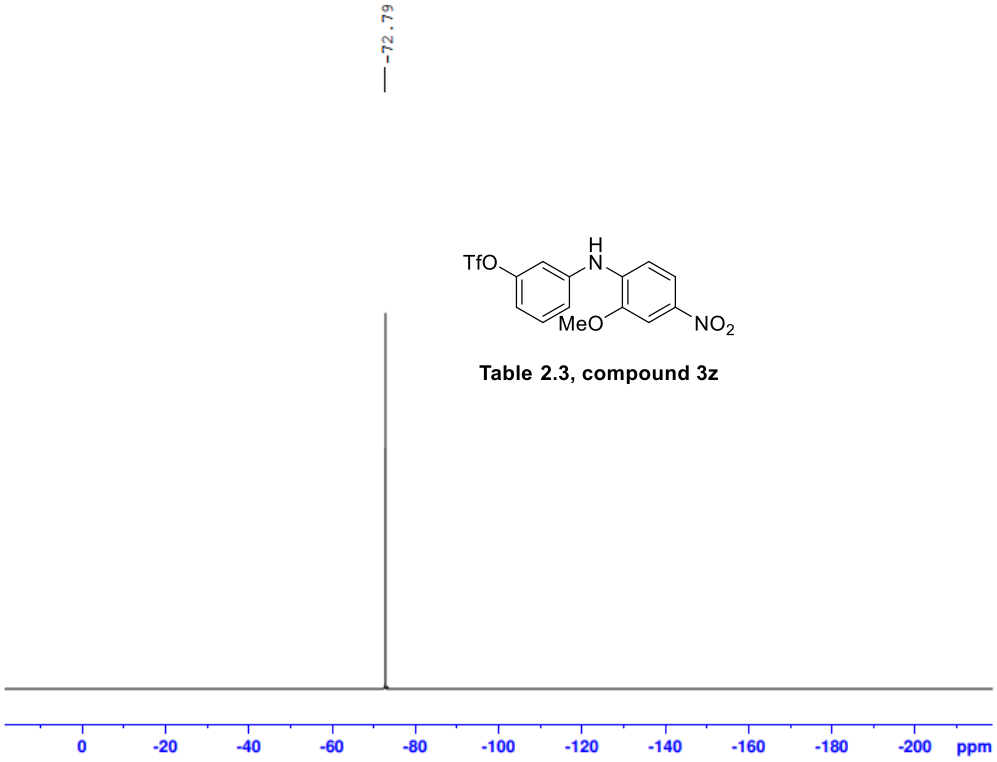

Table 2.3, compound 3z

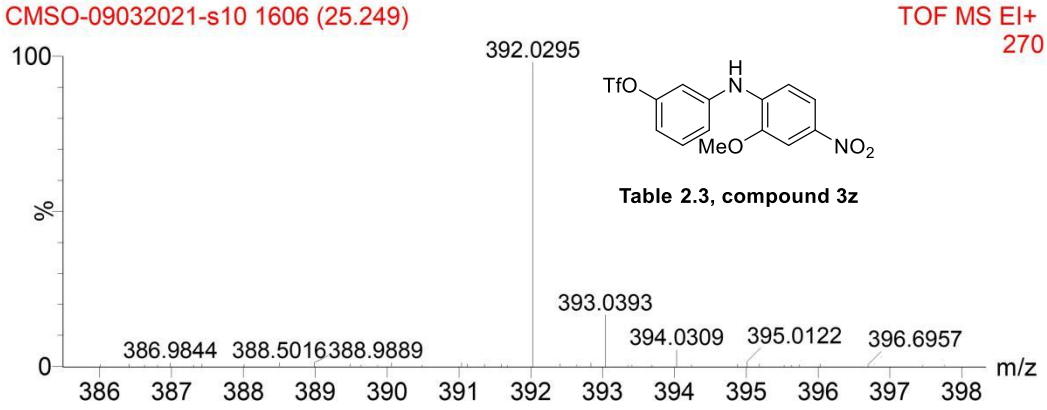

Table 2.3, compound 3z

Mass	Calc. Mass	mDa	PPM	Formula
392.0295	392.0284	-1.06	-2.70	C14 H11 F3N2O6S

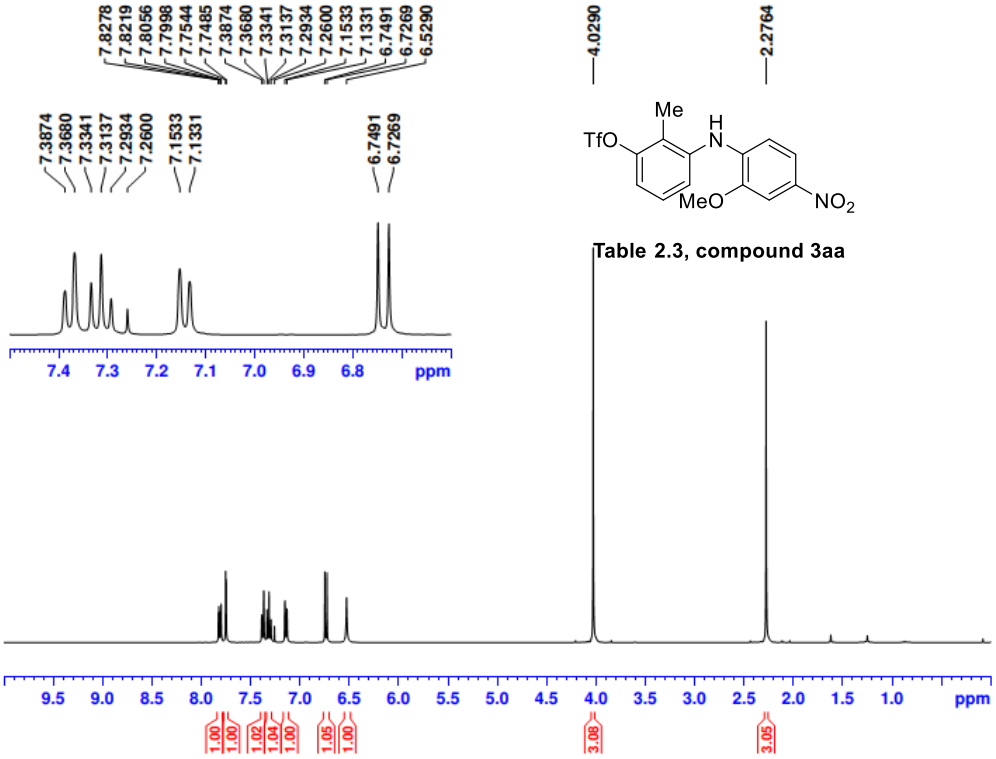
7.8278
7.8219
7.8056
7.7998
7.7544
7.7485
7.3874
7.3680
7.3341
7.3137
7.2934
7.2600
7.1533
7.1331
6.7491
6.7269
6.5290
4.0290
2.2764
Me
H
N
TfO
MeO
NO2
Table 2.3, compound 3aa
ppm

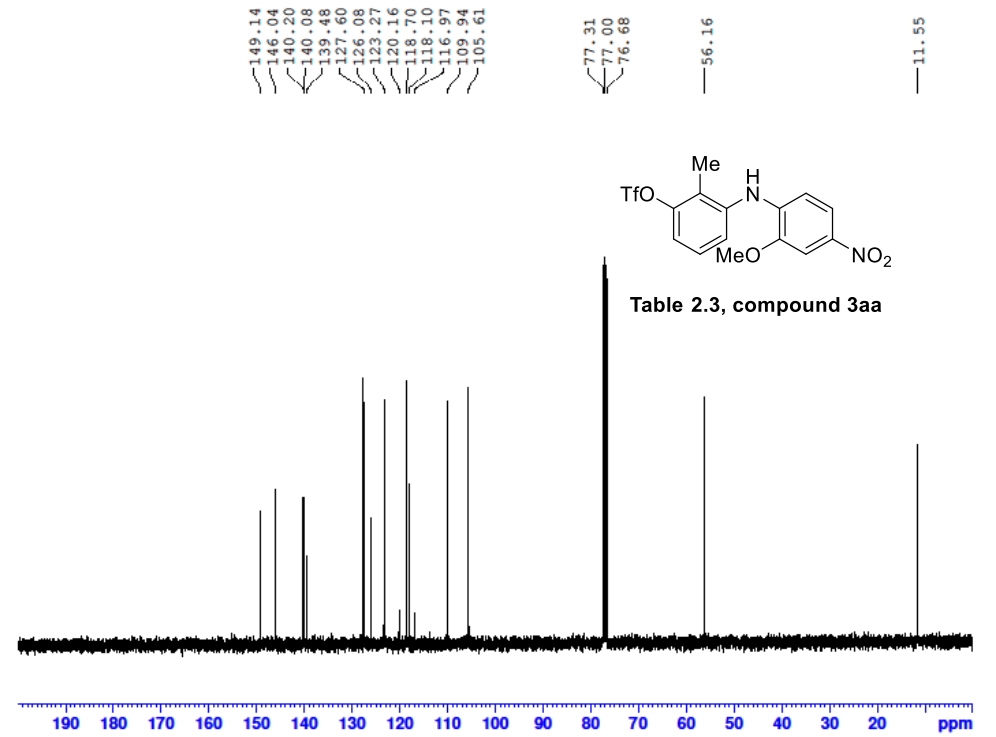
149.14
146.04
140.20
140.08
139.48
127.60
126.08
123.27
120.16
118.70
118.10
116.97
109.94
105.61
77.31
77.00
76.68
56.16
11.55
Me
H
N
TfO
MeO
NO2
Table 2.3, compound 3aa
ppm

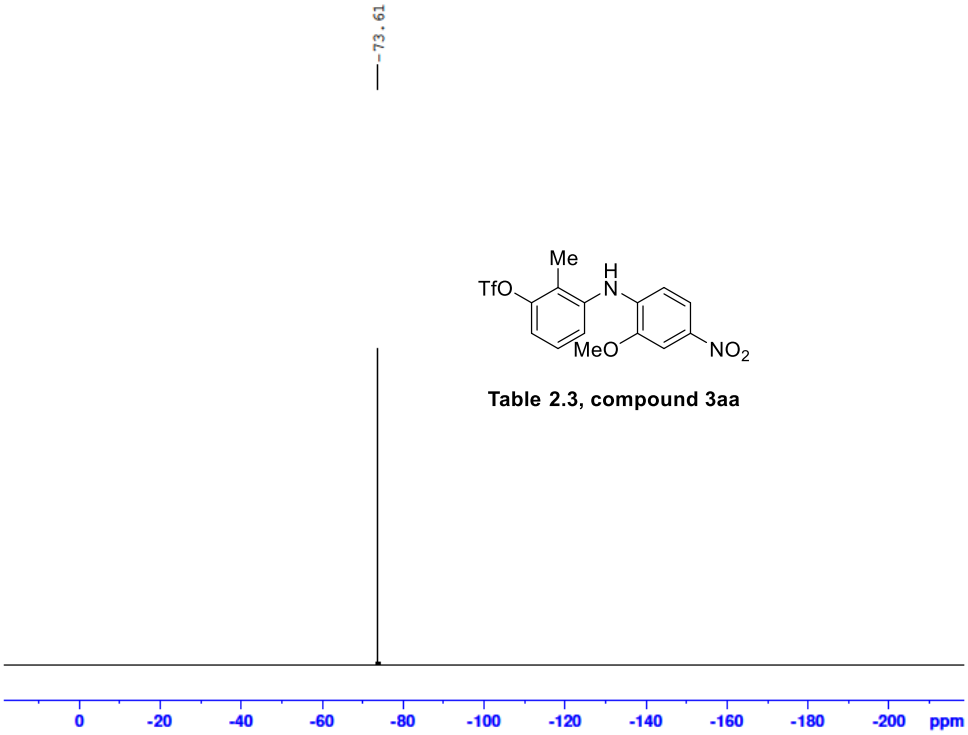

Table 2.3, compound 3aa

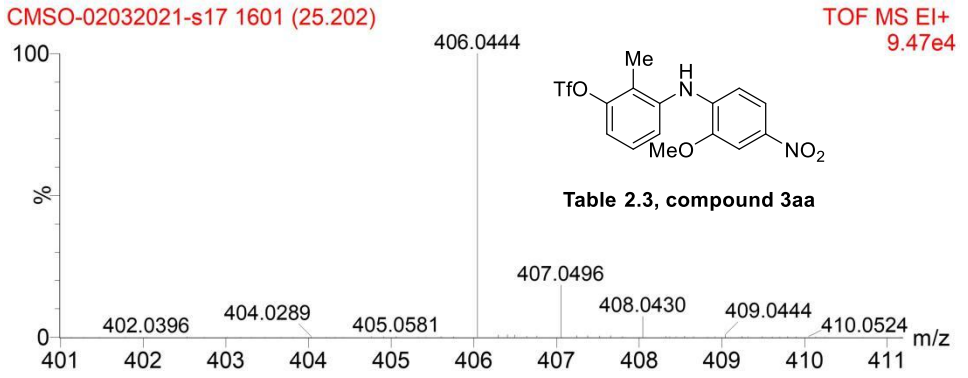

Table 2.3, compound 3aa

Mass	Calc. Mass	mDa	PPM	Formula
406.0444	406.0441	-0.31	-0.76	C15H13 F3N2O6S

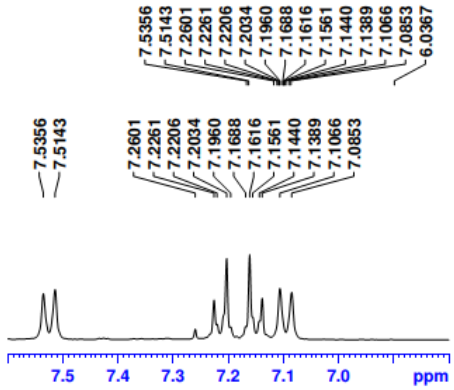

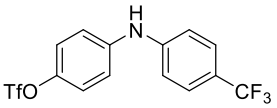

Table 2.3, compound 3ab and Table 2.7, compound 3bo

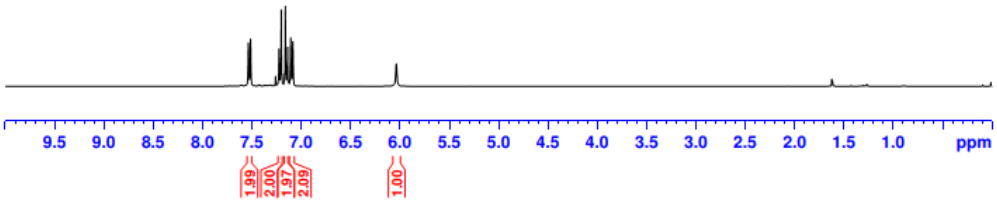

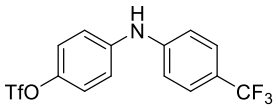

Table 2.3, compound 3ab and Table 2.7, compound 3bo

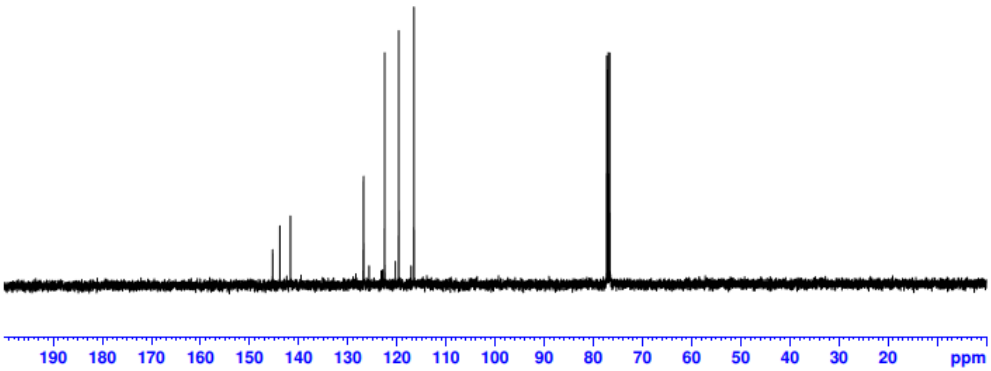

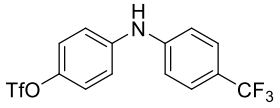

Table 2.3, compound 3ab and
Table 2.7, compound 3bo

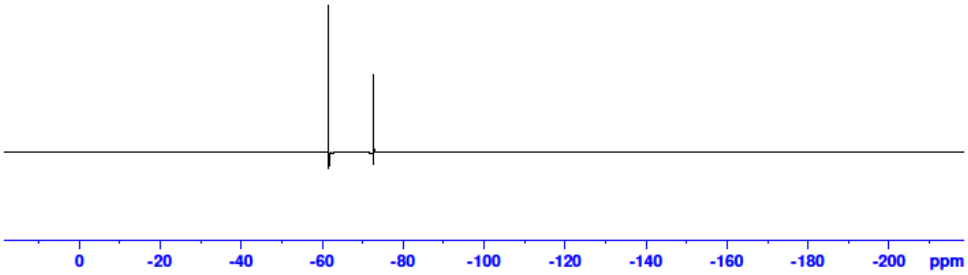

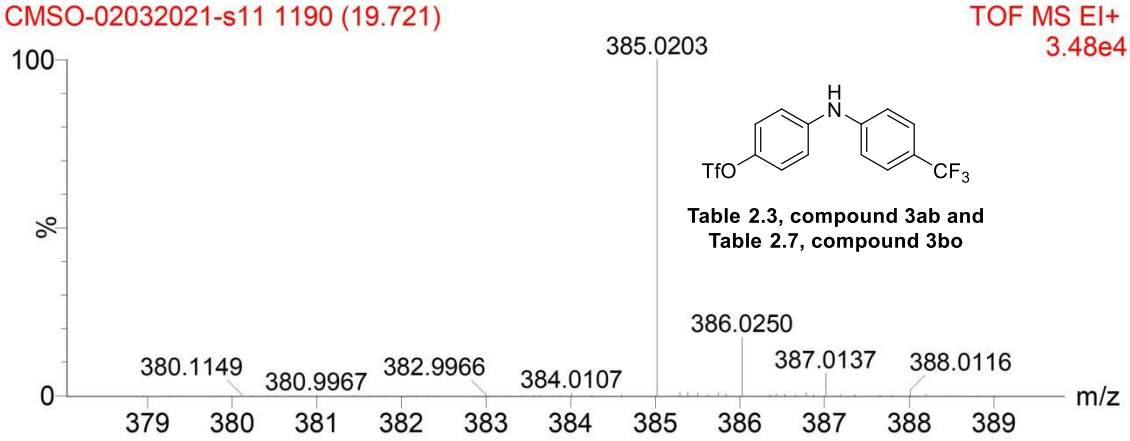

Table 2.3, compound 3ab and
Table 2.7, compound 3bo

Mass	Calc. Mass	mDa	PPM	Formula
385.0203	385.0202	-0.12	-0.30	C14H9 F6NO3S

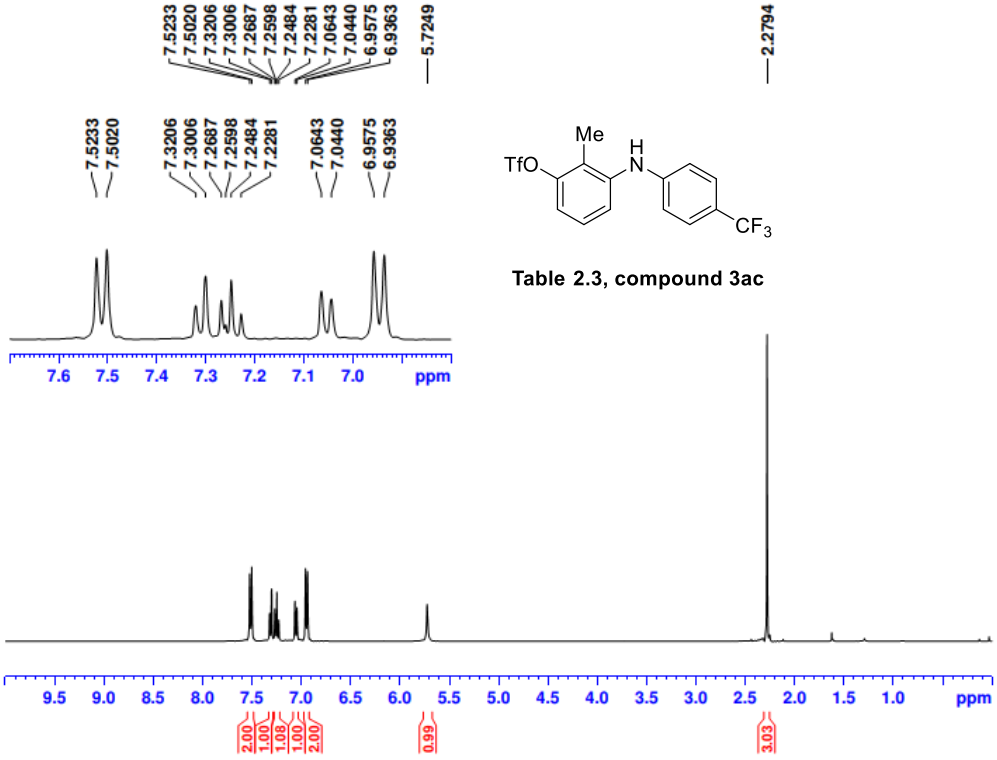

Table 2.3, compound 3ac

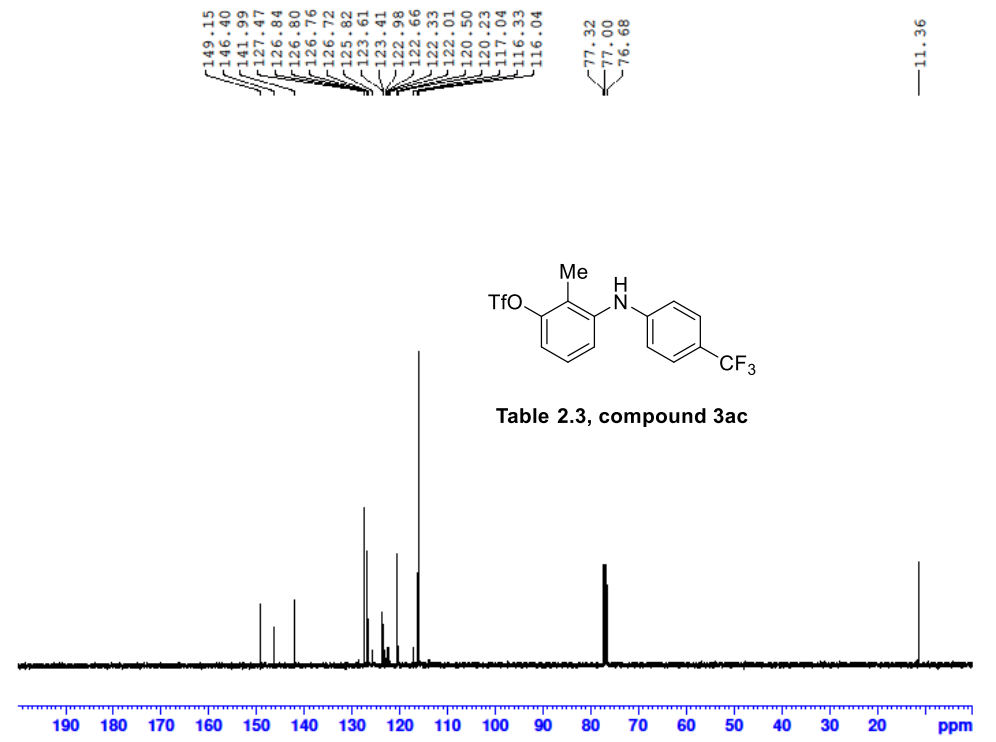

Table 2.3, compound 3ac

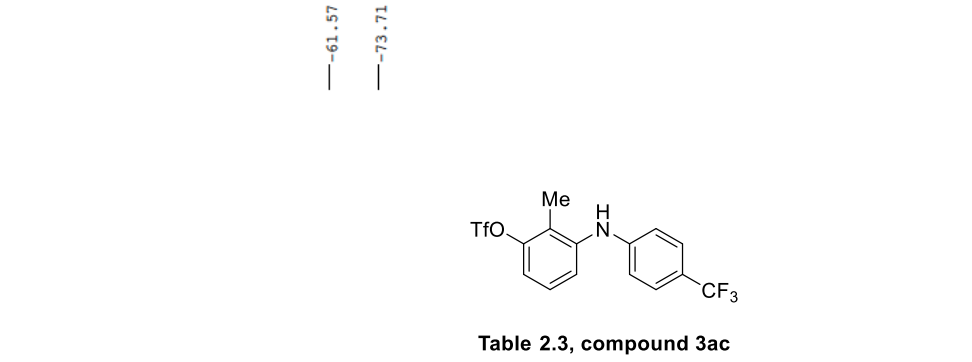

Table 2.3, compound 3ac

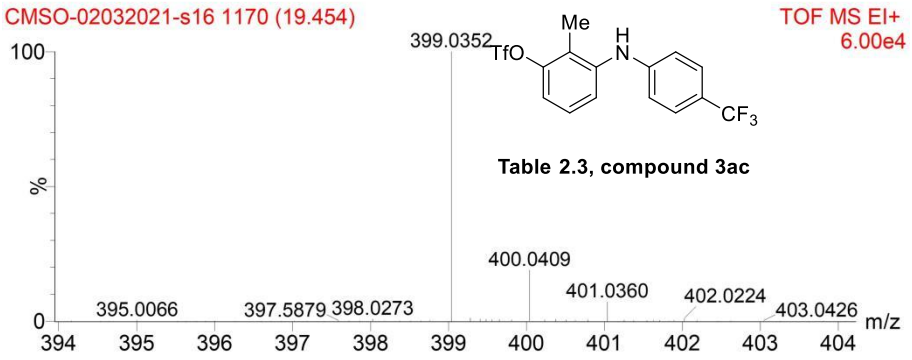

Table 2.3, compound 3ac

Mass	Calc. Mass	mDa	PPM	Formula
399.0352	399.0358	0.63	1.59	C15H11 F6NO3S

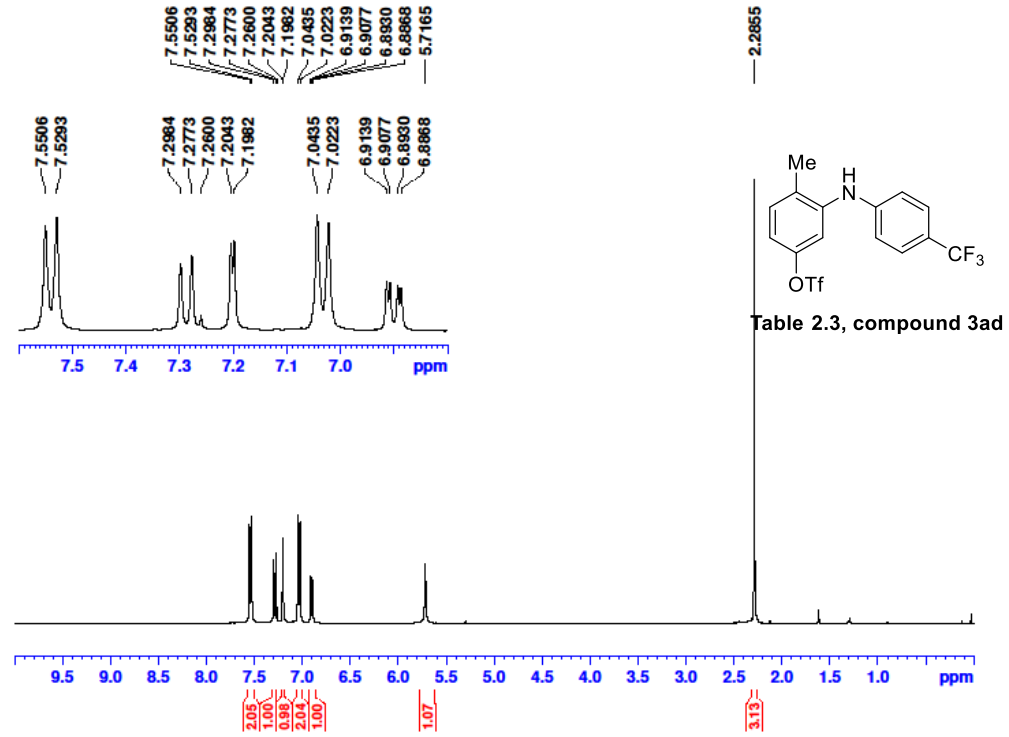

Table 2.3, compound 3ad

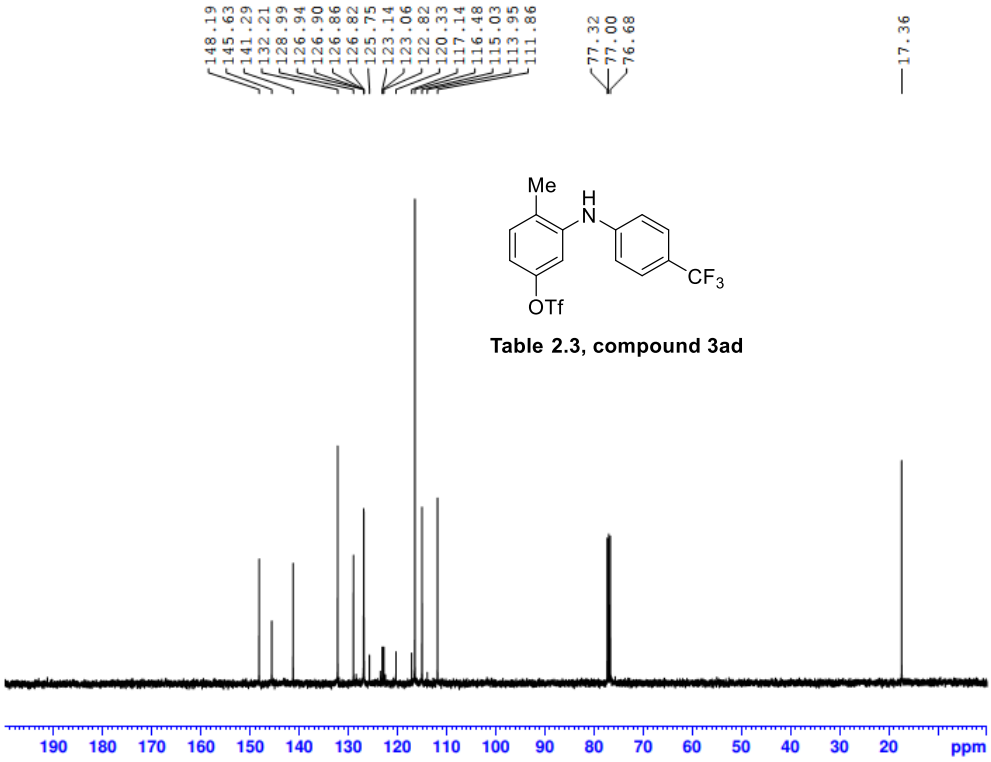

Table 2.3, compound 3ad

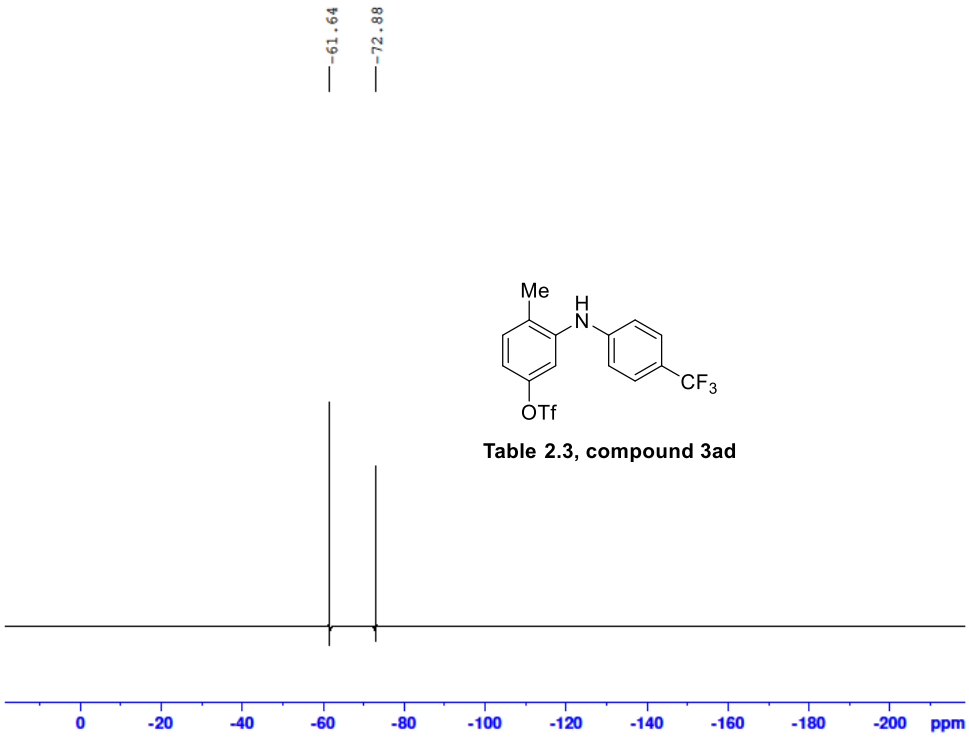

Table 2.3, compound 3ad

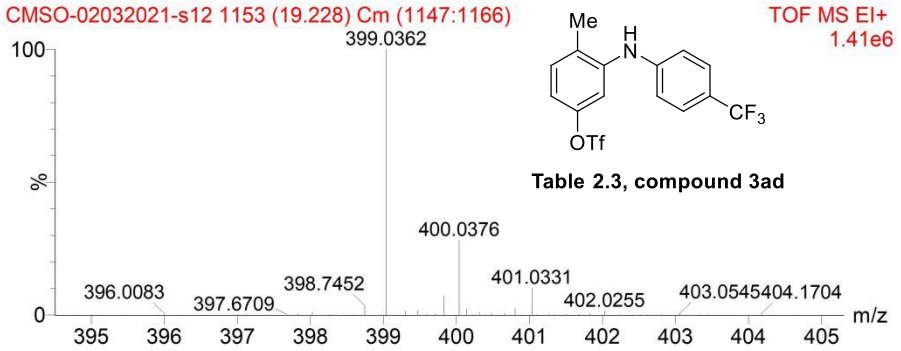

Table 2.3, compound 3ad

Mass	Calc. Mass	mDa	PPM	Formula
399.0362	399.0358	-0.37	-0.92	C15H11 F6NO3S

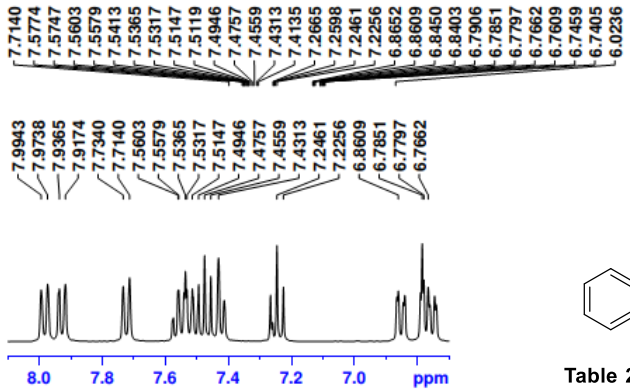

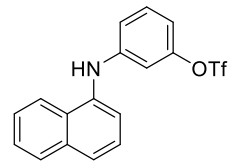

Table 2.3, compound 3ae

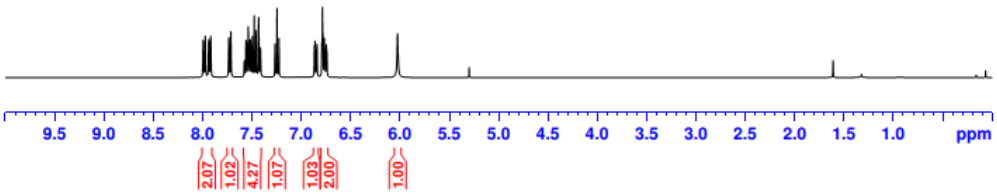

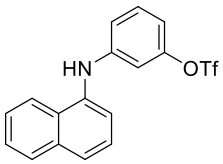

Table 2.3, compound 3ae

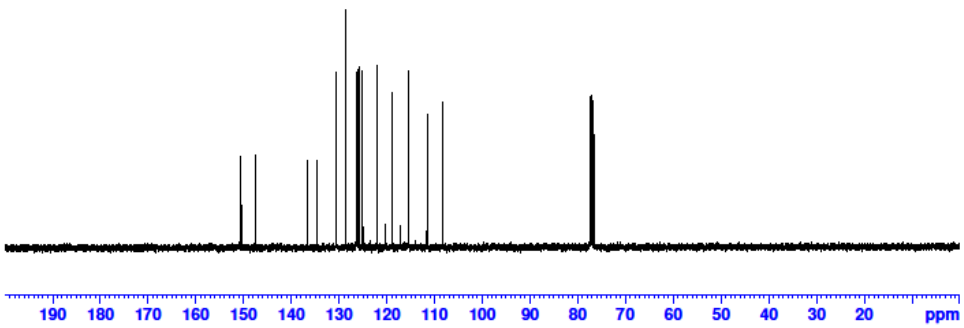

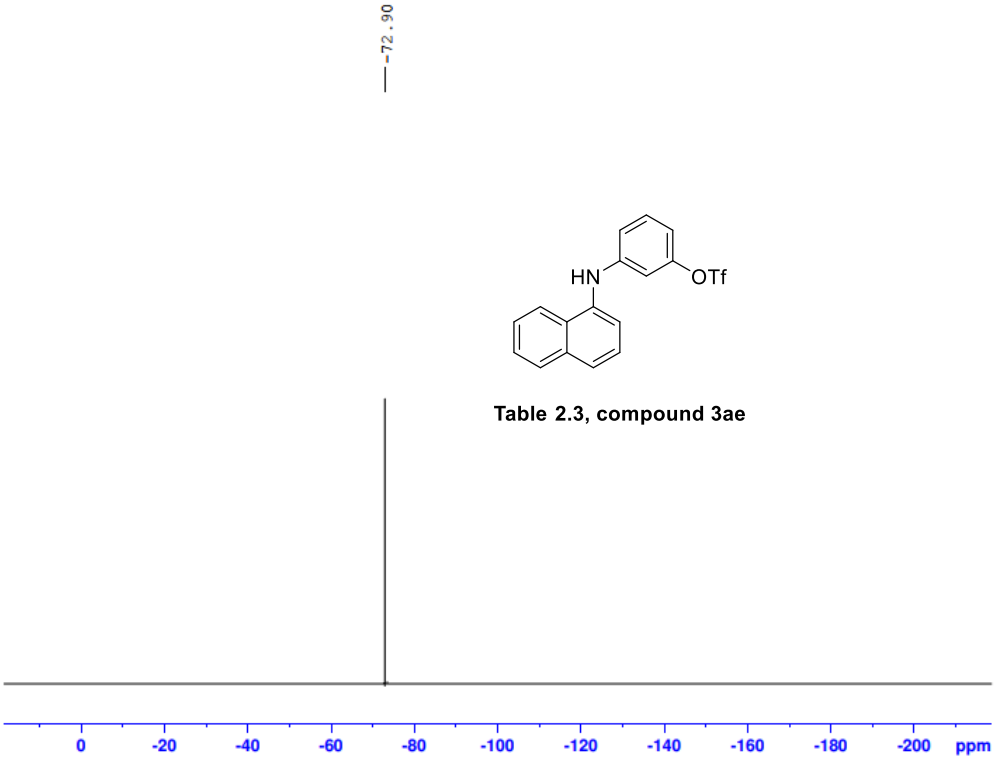

Table 2.3, compound 3ae

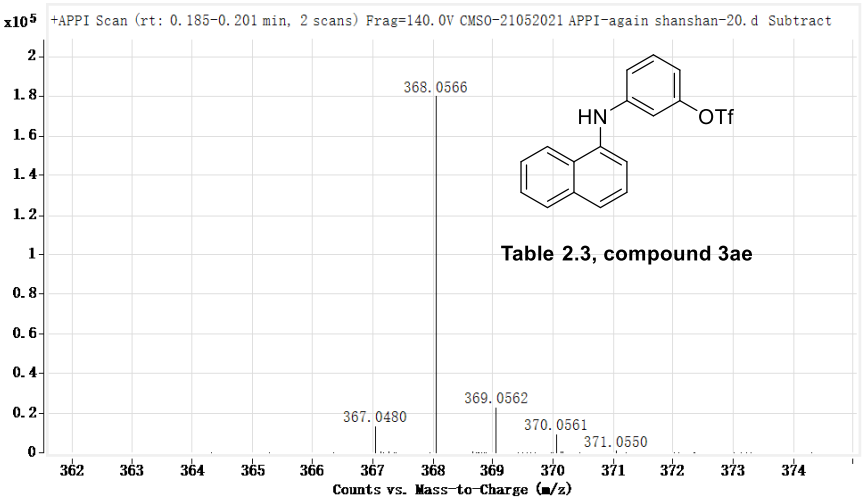

Table 2.3, compound 3ae

Mass	Calc. Mass	mDa	PPM	Formula
368.0566	368.0563	-0.32	-0.89	C17 H13 F3 N O3 S

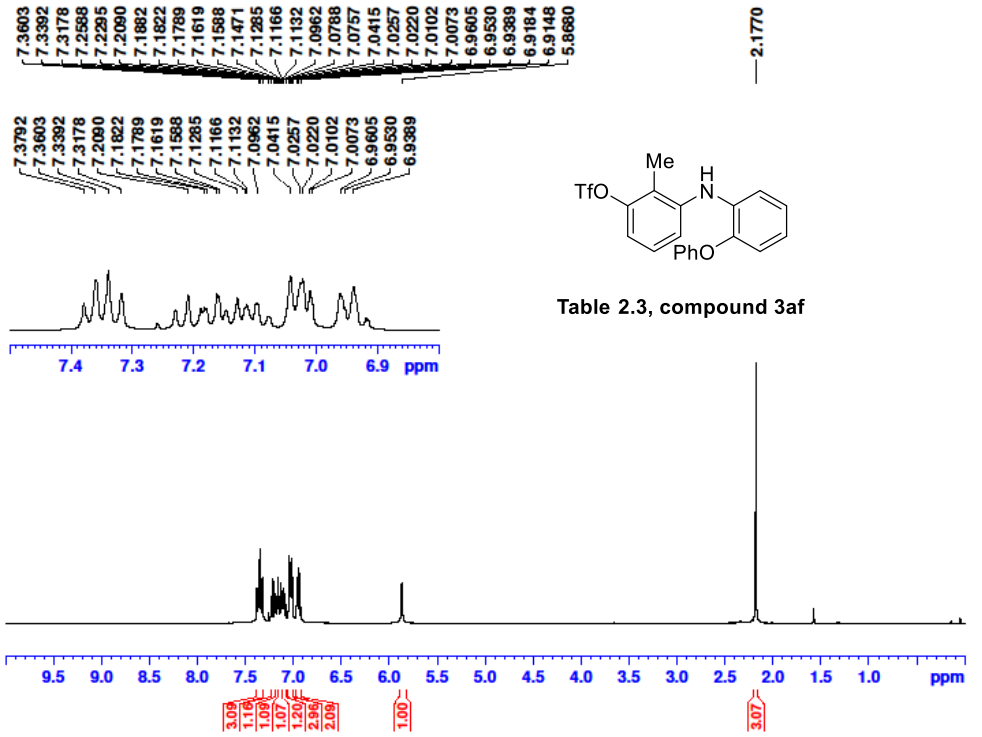

Table 2.3, compound 3af

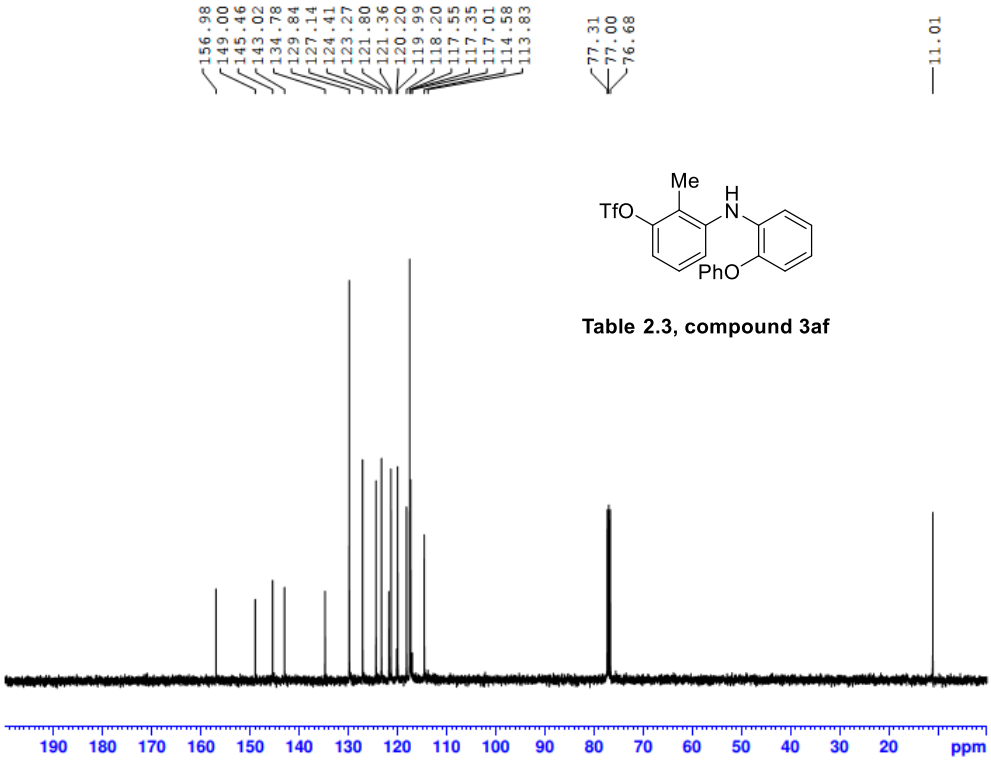

Table 2.3, compound 3af

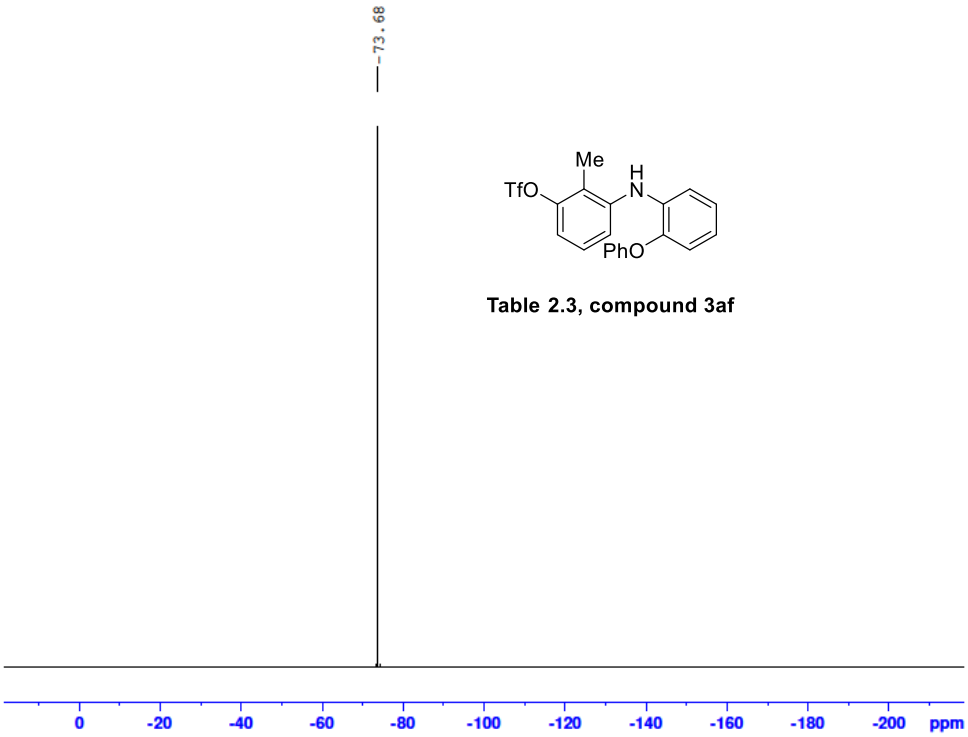

Table 2.3, compound 3af

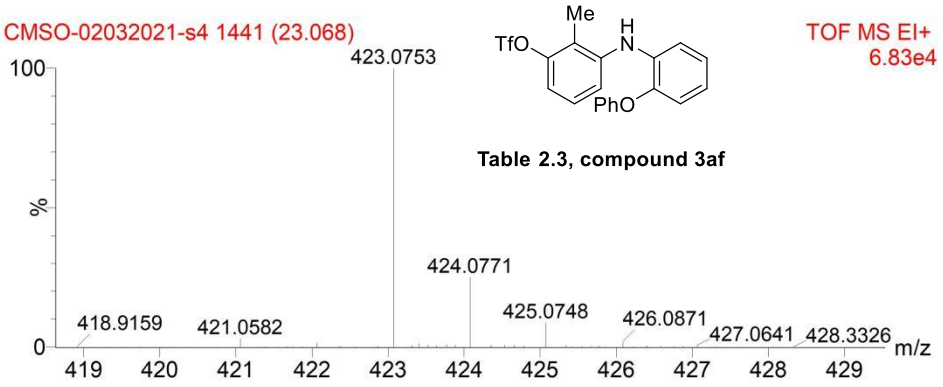

Table 2.3, compound 3af

Mass	Calc. Mass	mDa	PPM	Formula
423.0753	423.0747	-0.64	-1.50	C20 H16 F3NO4S

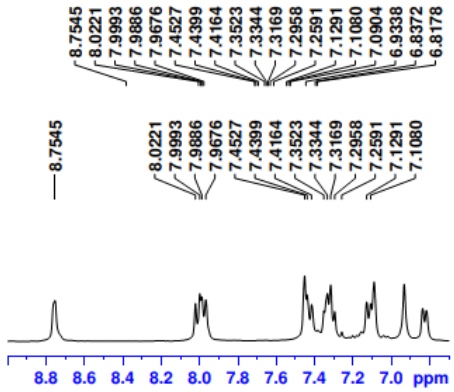

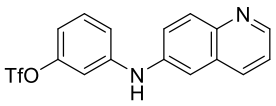

Table 2.4, compound 3ag

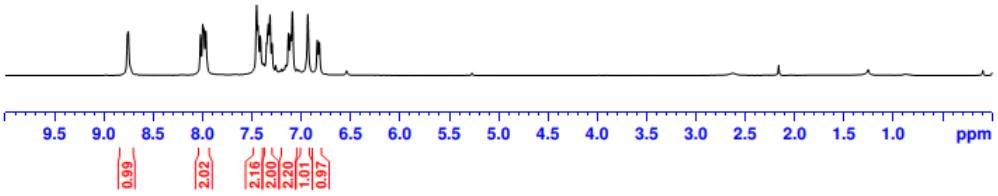

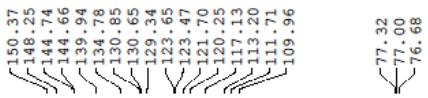

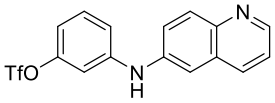

Table 2.4, compound 3ag

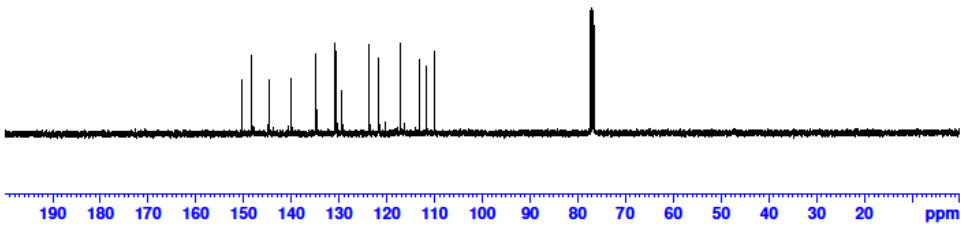

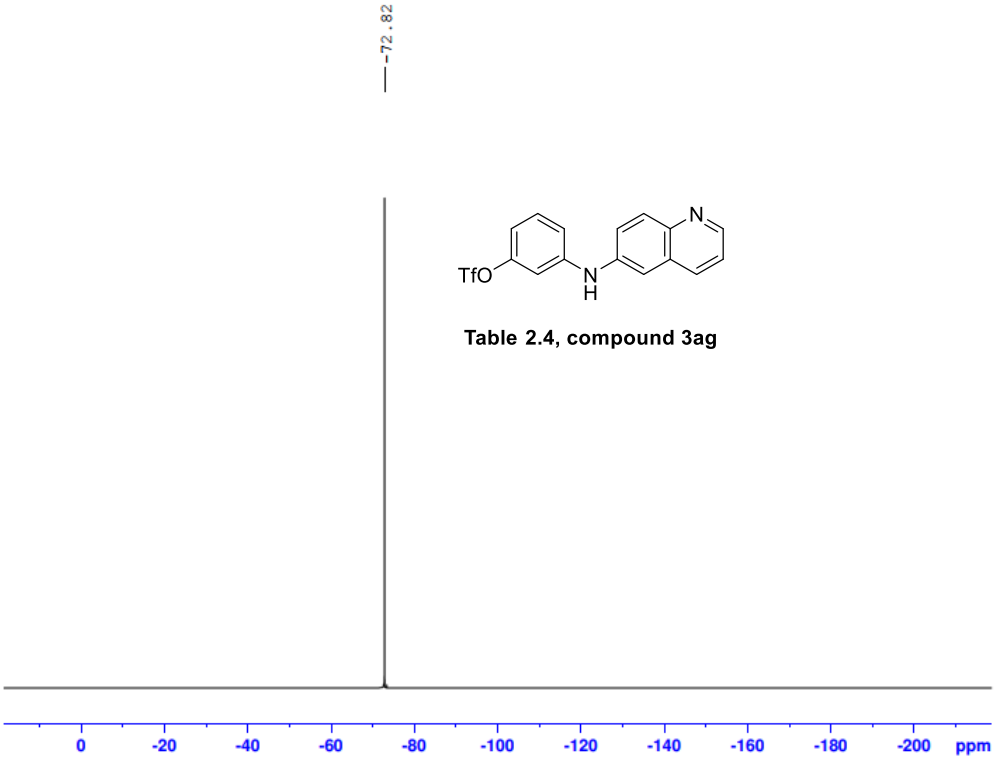

Table 2.4, compound 3ag

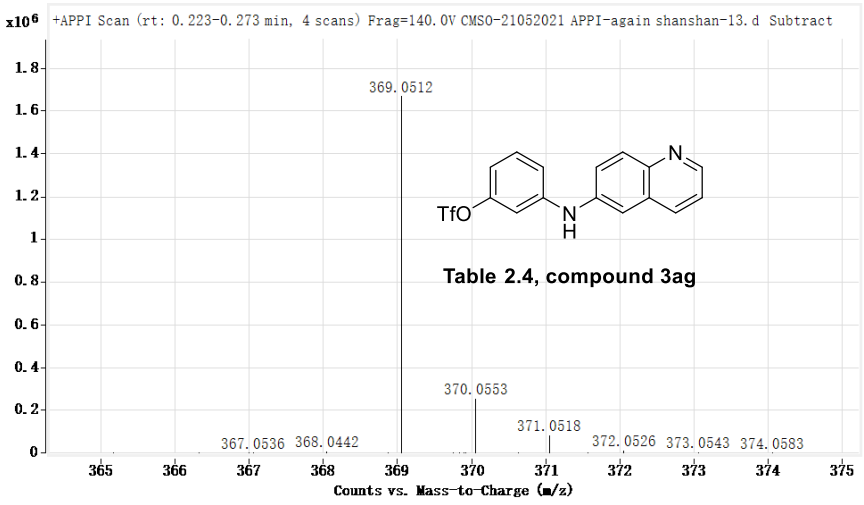

Table 2.4, compound 3ag

Mass	Calc. Mass	mDa	PPM	Formula
369.0512	369.0515	0.32	0.88	C16 H12 F3 N2 O3 S

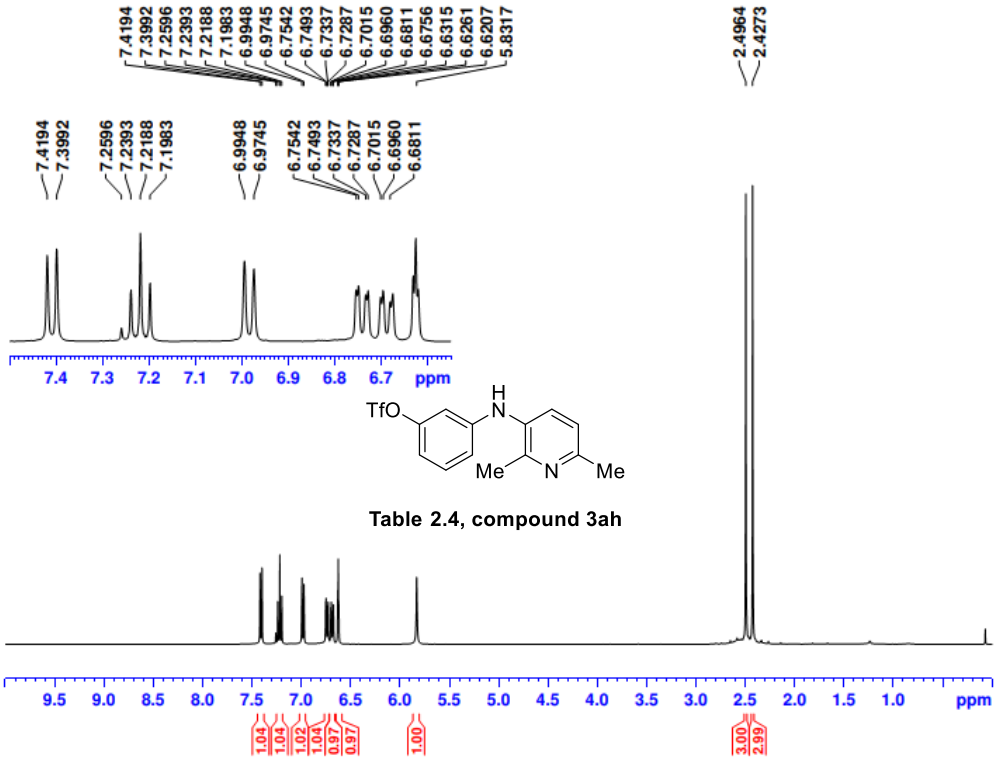

Table 2.4, compound 3ah

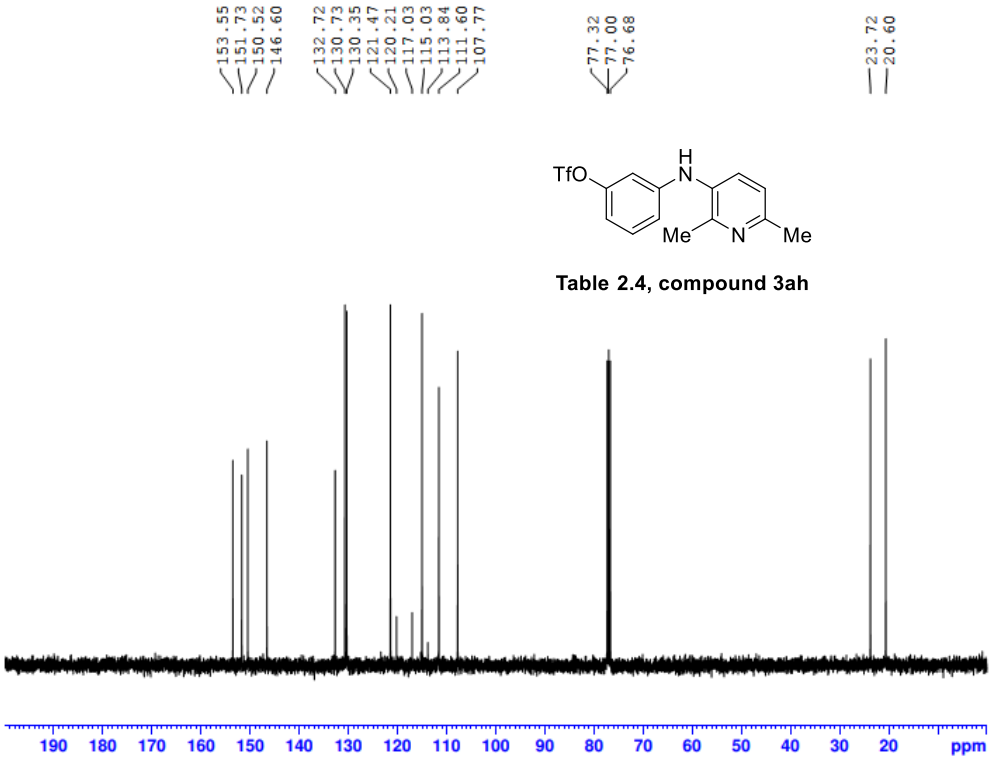

Table 2.4, compound 3ah

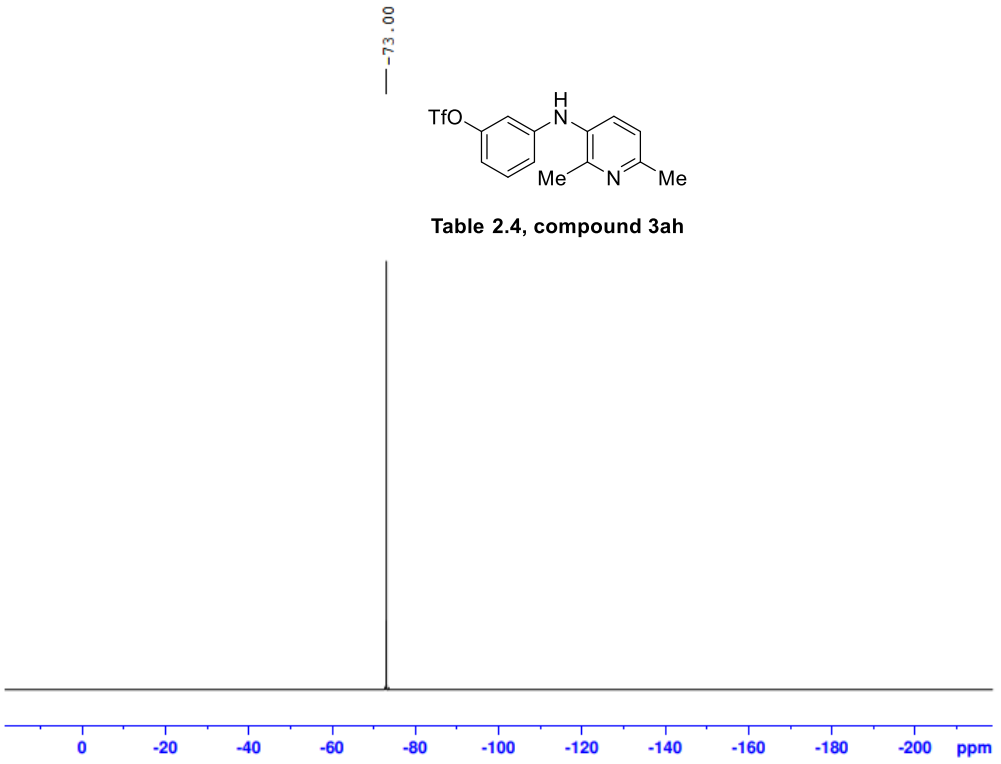

Table 2.4, compound 3ah

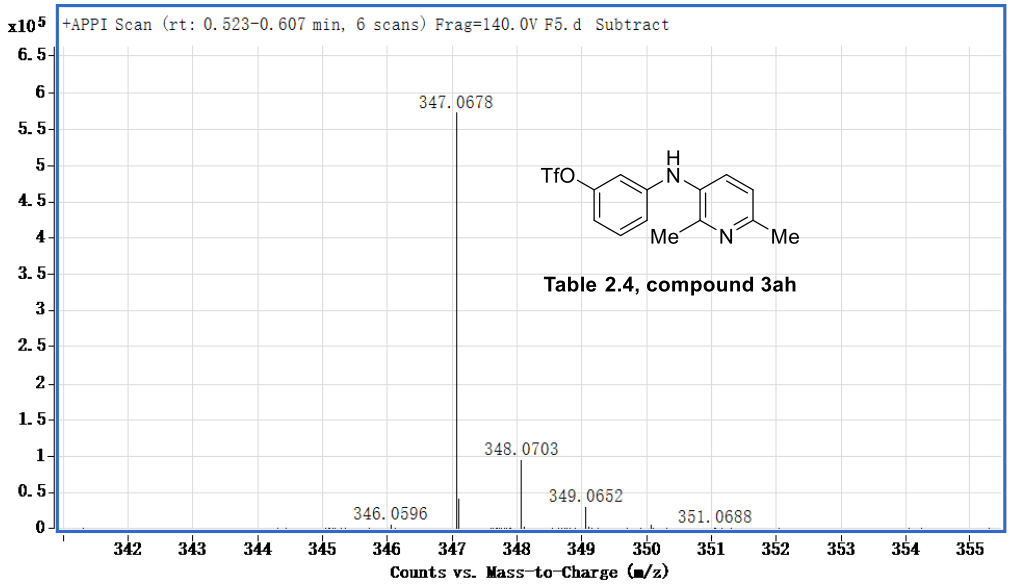

Table 2.4, compound 3ah

Mass	Calc. Mass	mDa	PPM	Formula
347.0678	347.0672	-0.63	-1.81	C14 H14 F3 N2 O3 S

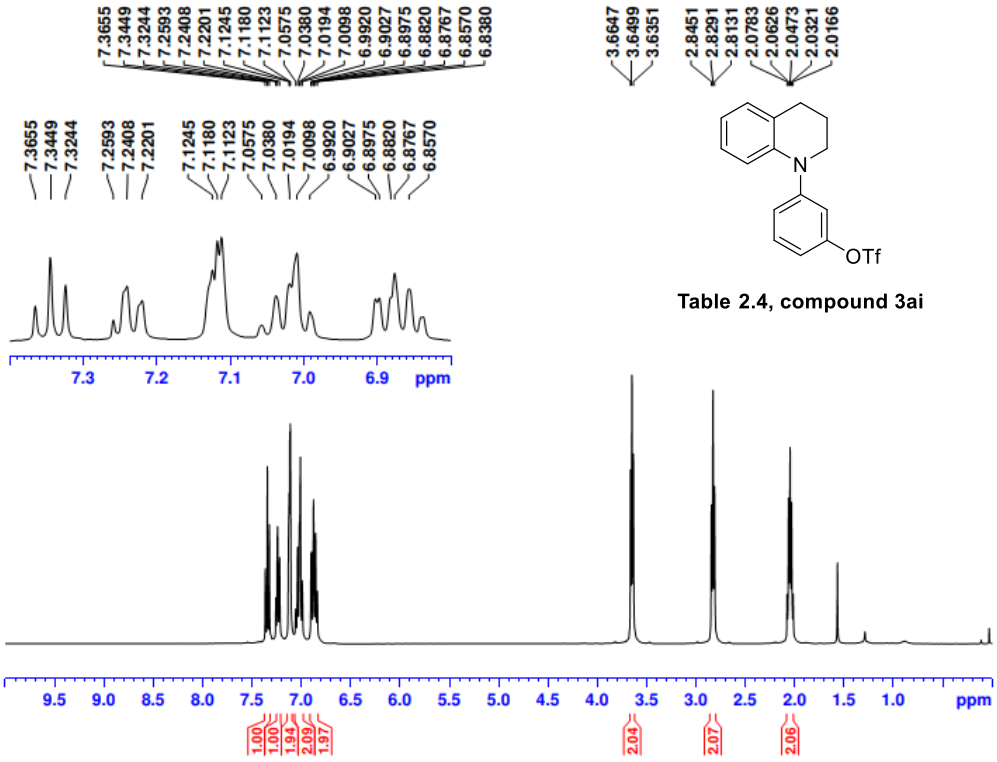

Table 2.4, compound 3ai

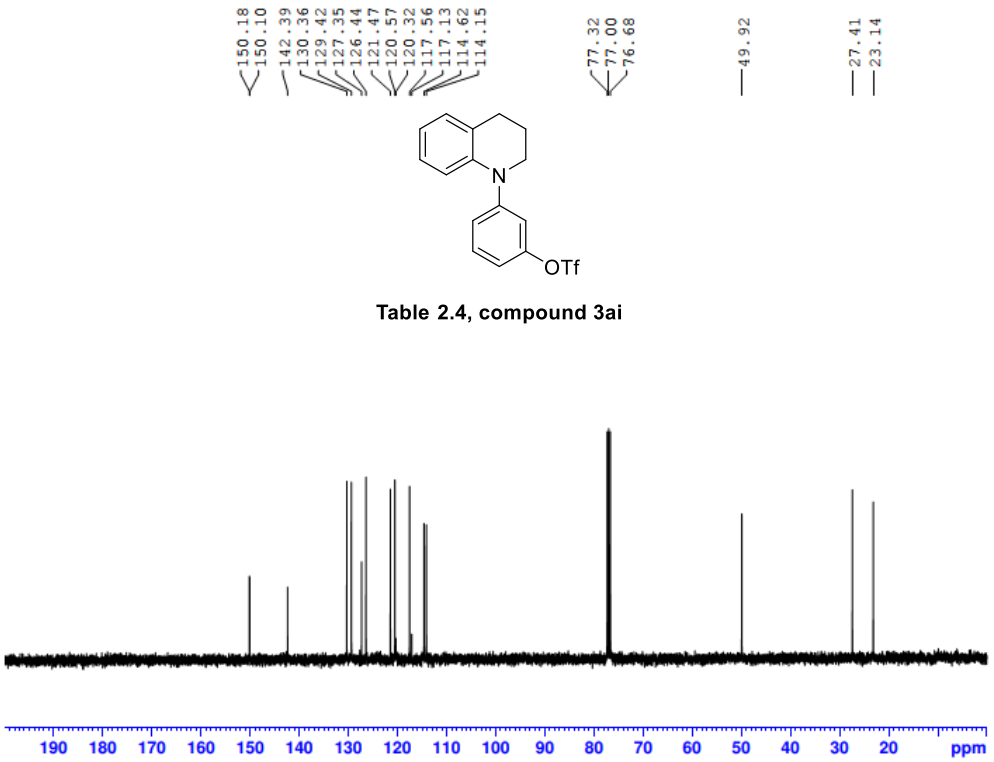

Table 2.4, compound 3ai

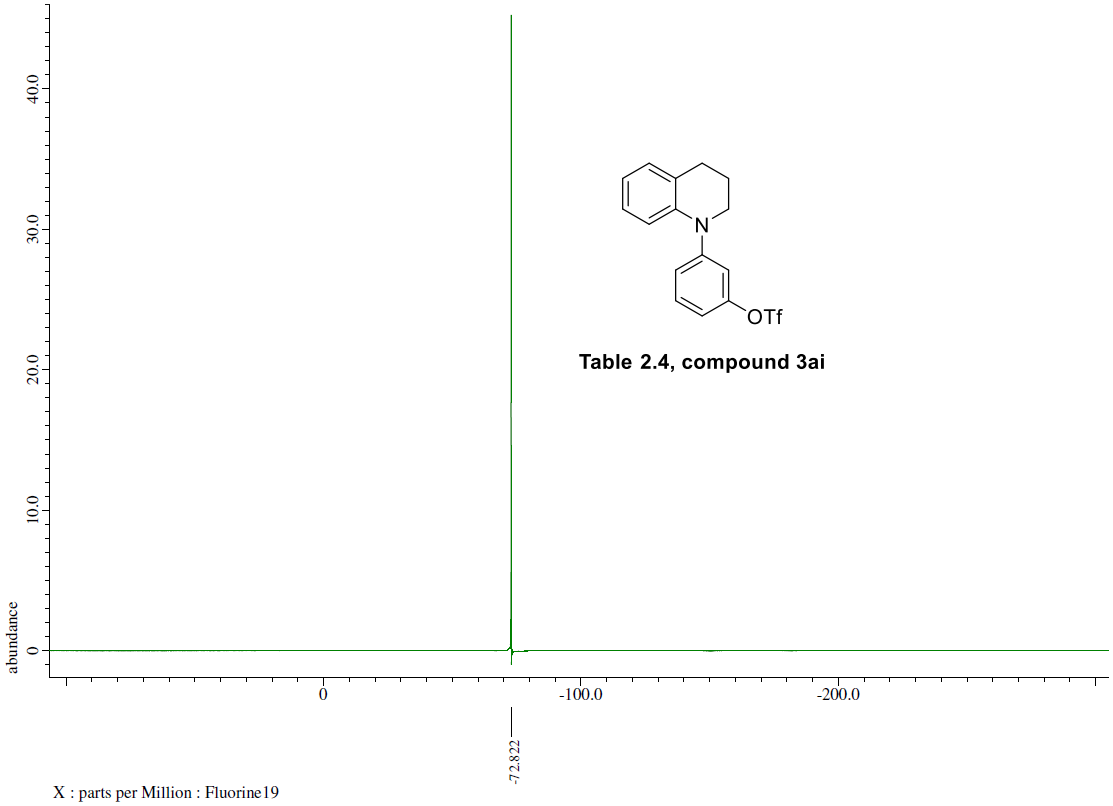

Table 2.4, compound 3ai

X : parts per Million : Fluorine19

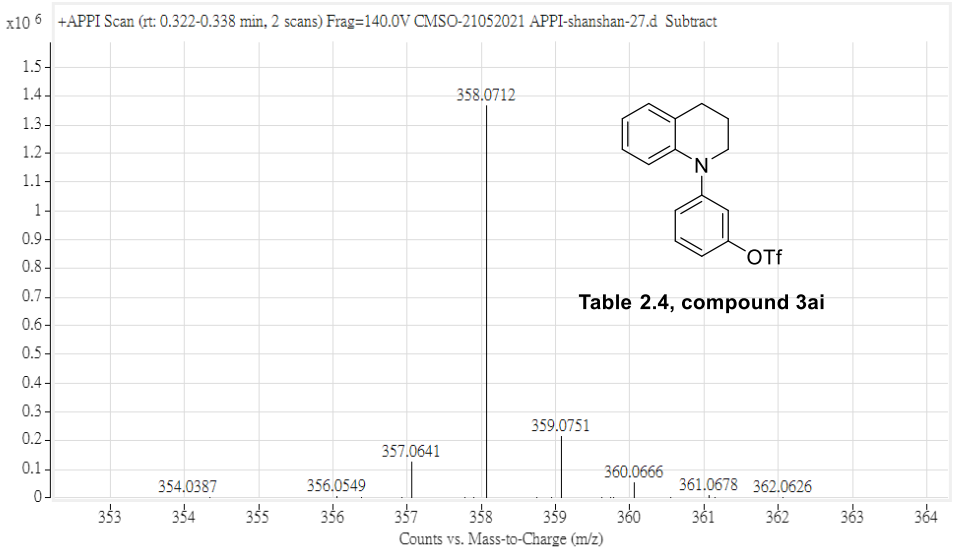

Table 2.4, compound 3ai

Mass	Calc. Mass	mDa	PPM	Formula
358.0712	358.0719	0.73	2.03	C16 H15 F3 N O3 S

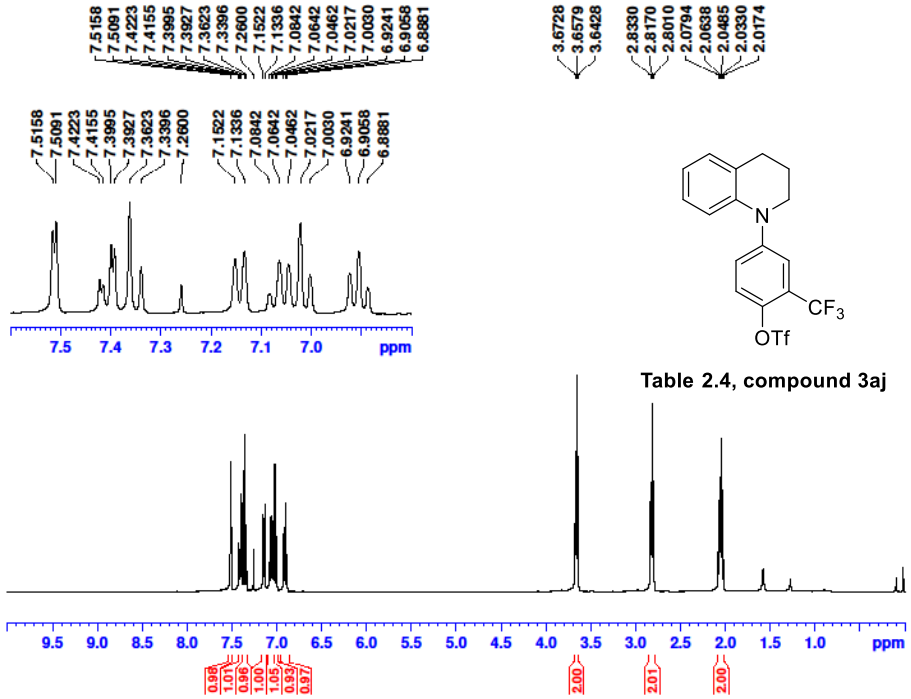

Table 2.4, compound 3aj

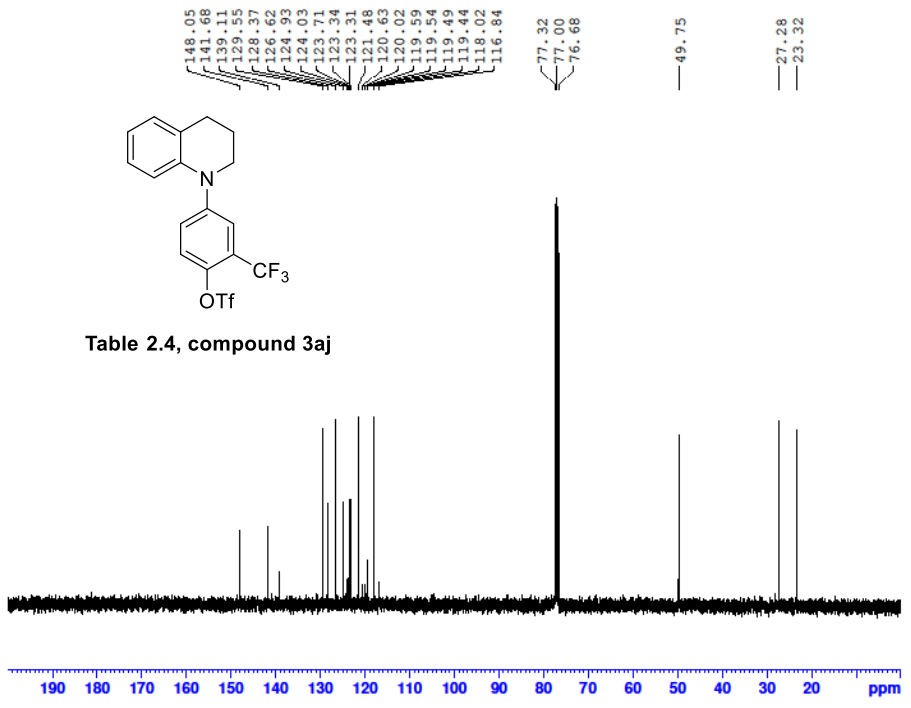

Table 2.4, compound 3aj

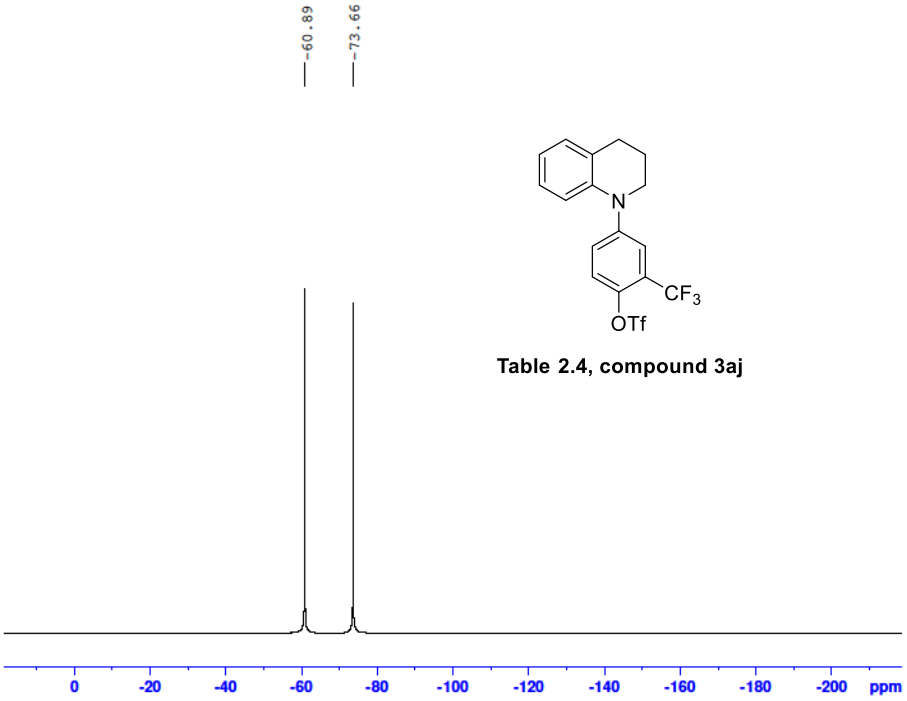

Table 2.4, compound 3aj

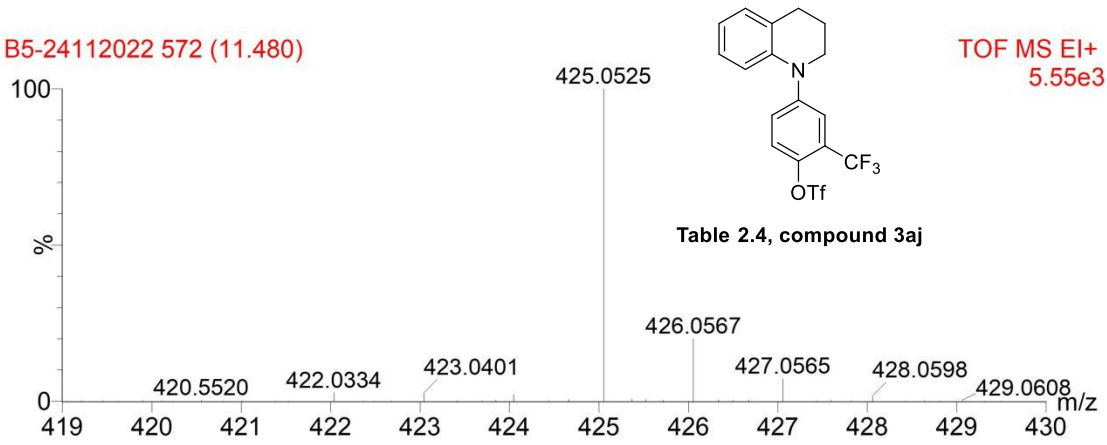

Table 2.4, compound 3aj

Mass	Calc. Mass	mDa	PPM	Ion Formula
425.0525	425.0515	-1.02	-2.39	C17H13F6O3NS

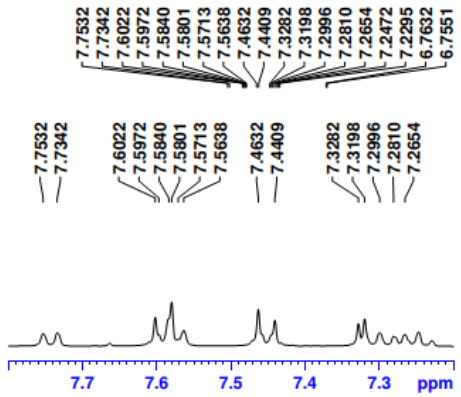

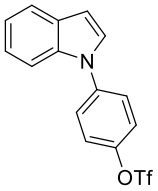

Table 2.4, compound 3ak

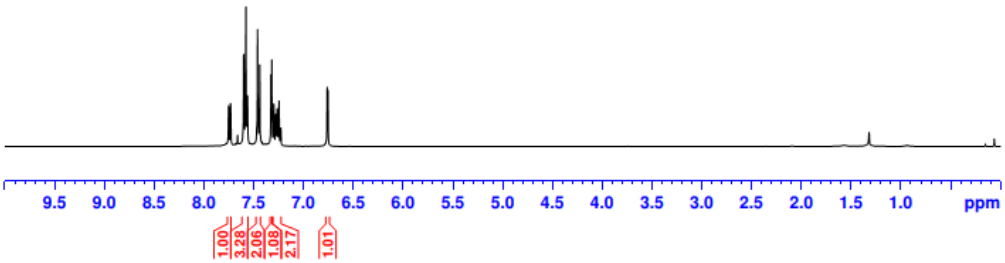

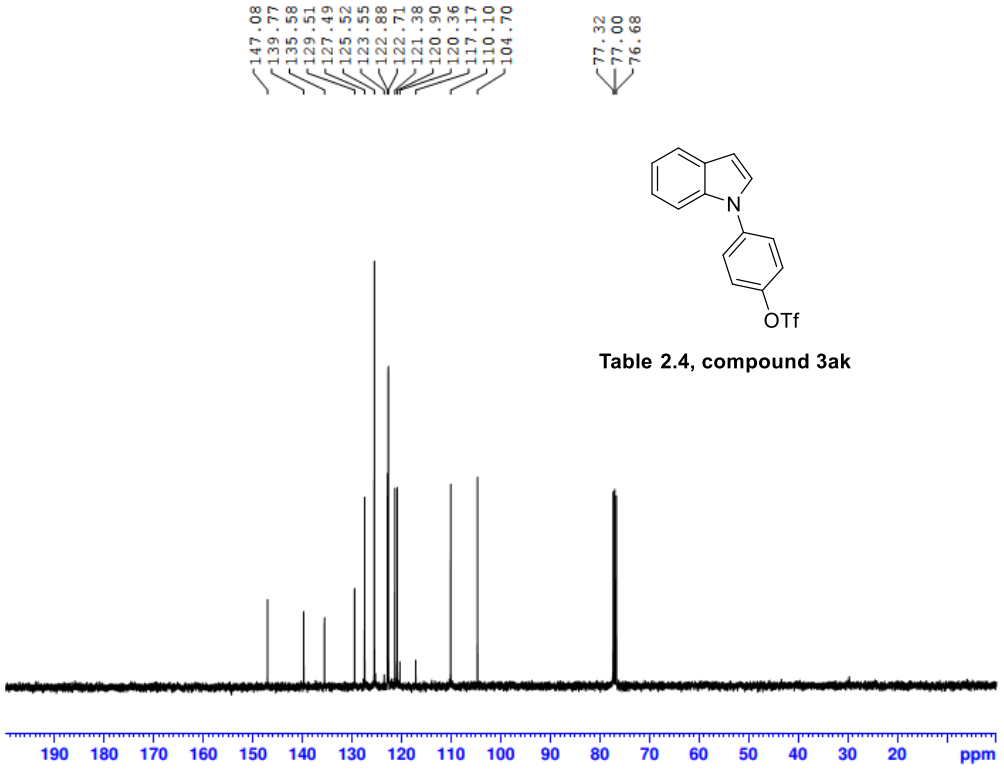

Table 2.4, compound 3ak

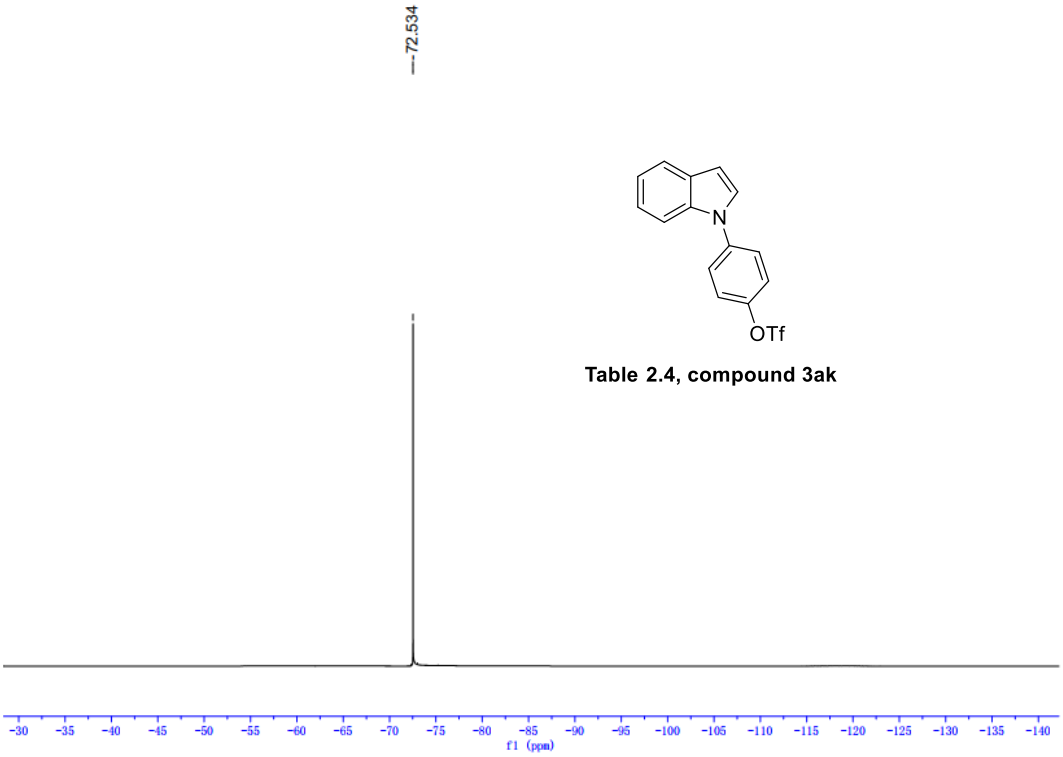

Table 2.4, compound 3ak

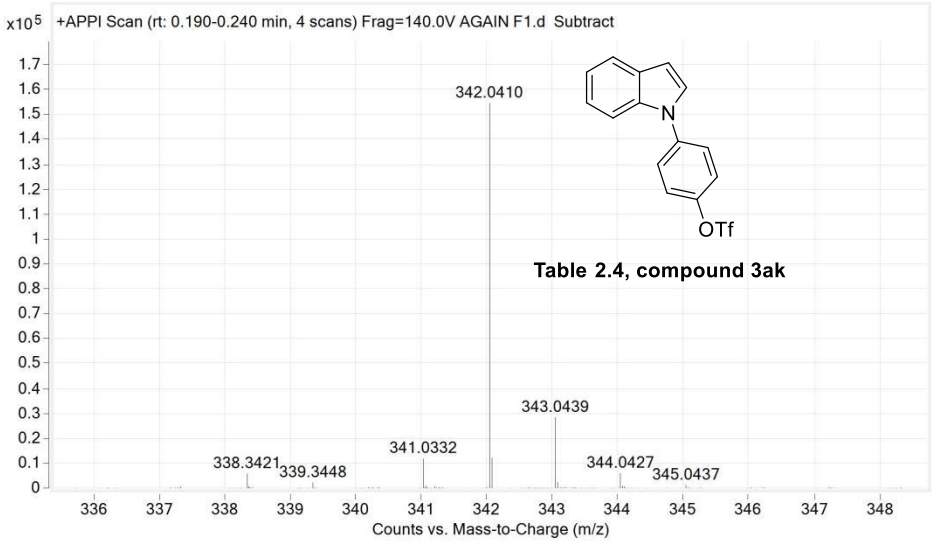

Table 2.4, compound 3ak

Mass	Calc. Mass	mDa	PPM	Formula
342.0410	342.0406	-0.38	-1.10	C15 H11 F3 N O3 S

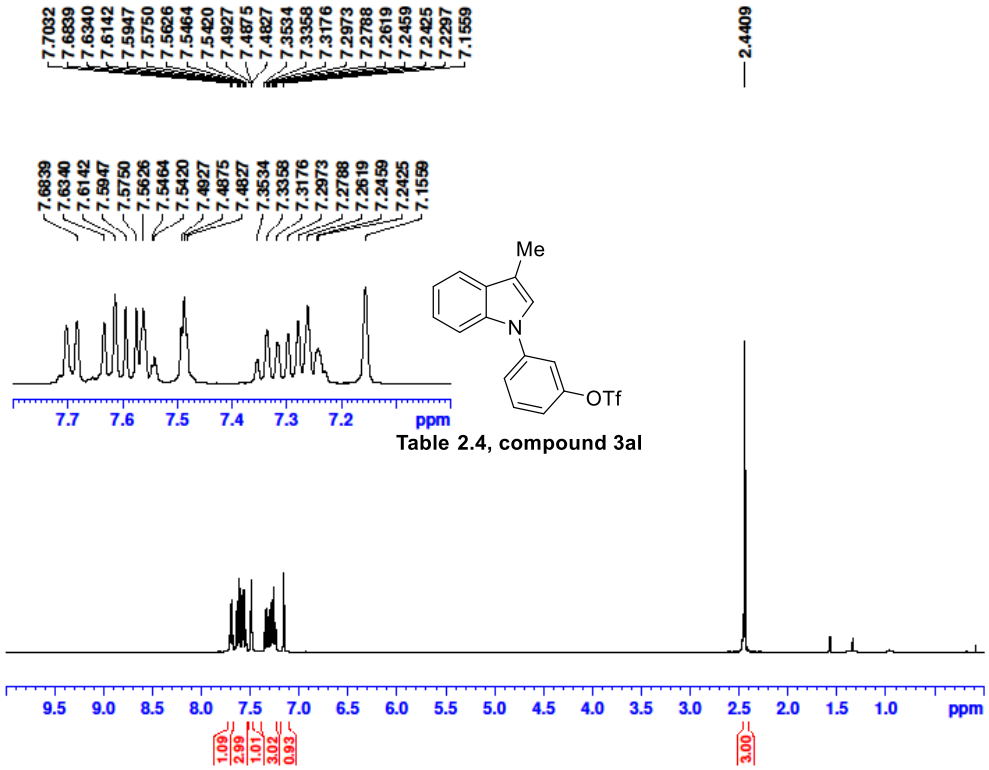

Table 2.4, compound 3al

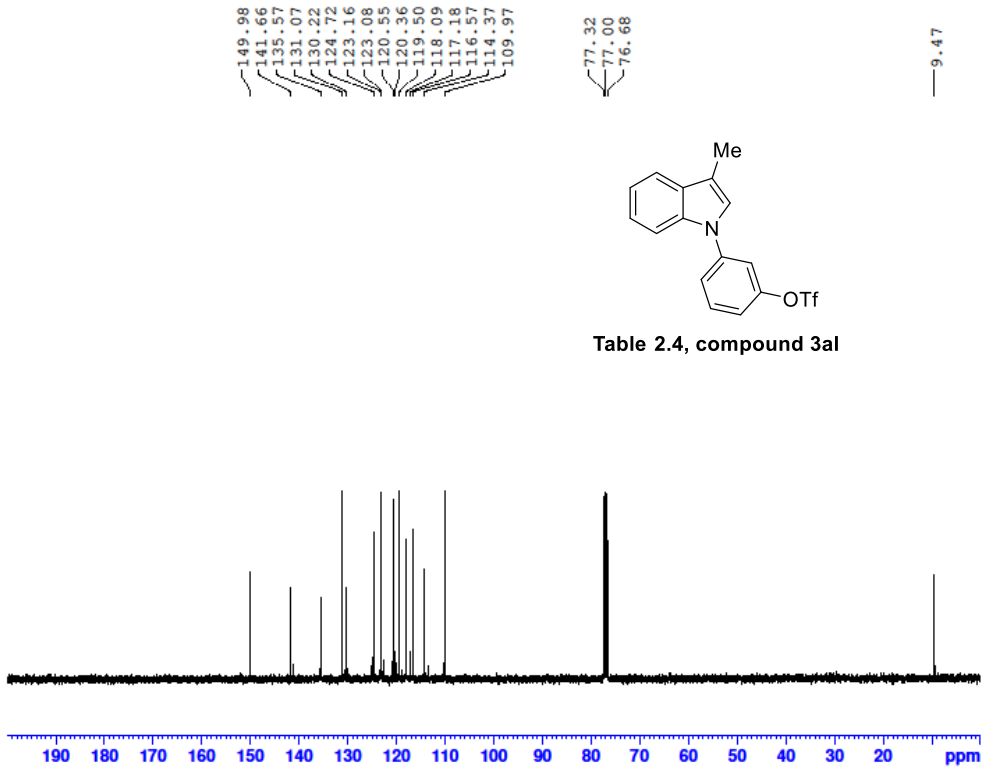

Table 2.4, compound 3al

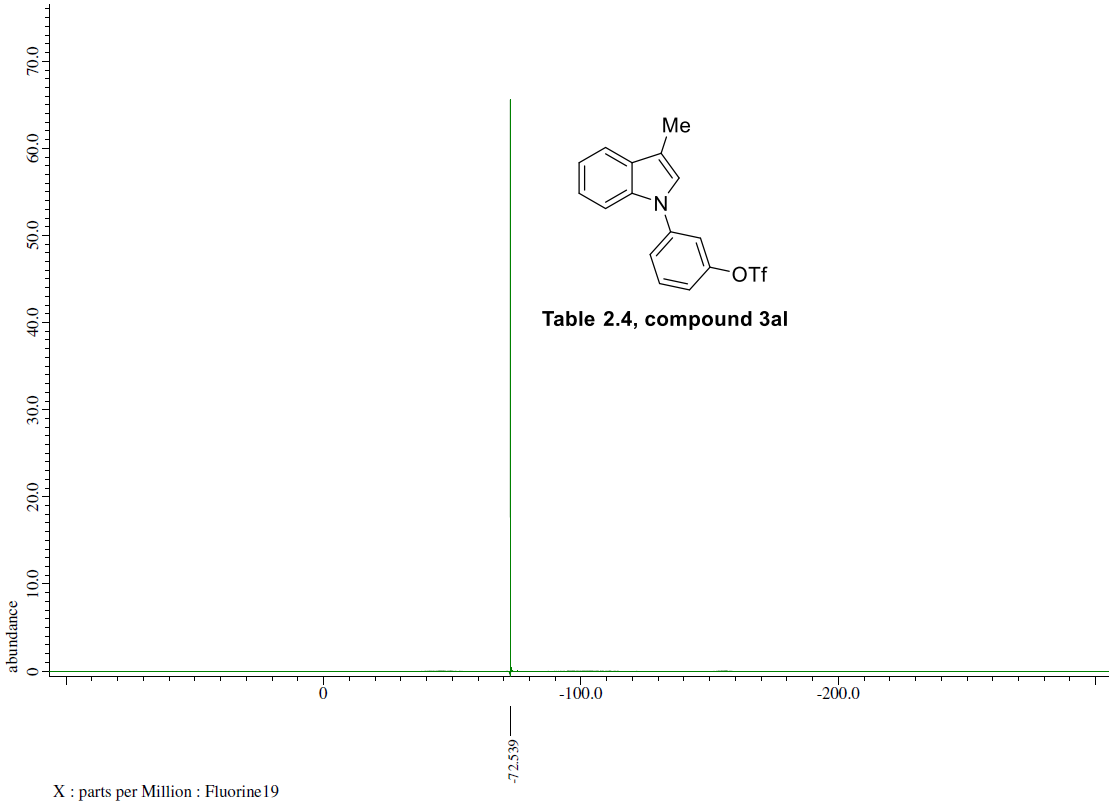

Table 2.4, compound 3al

X : parts per Million : Fluorine19

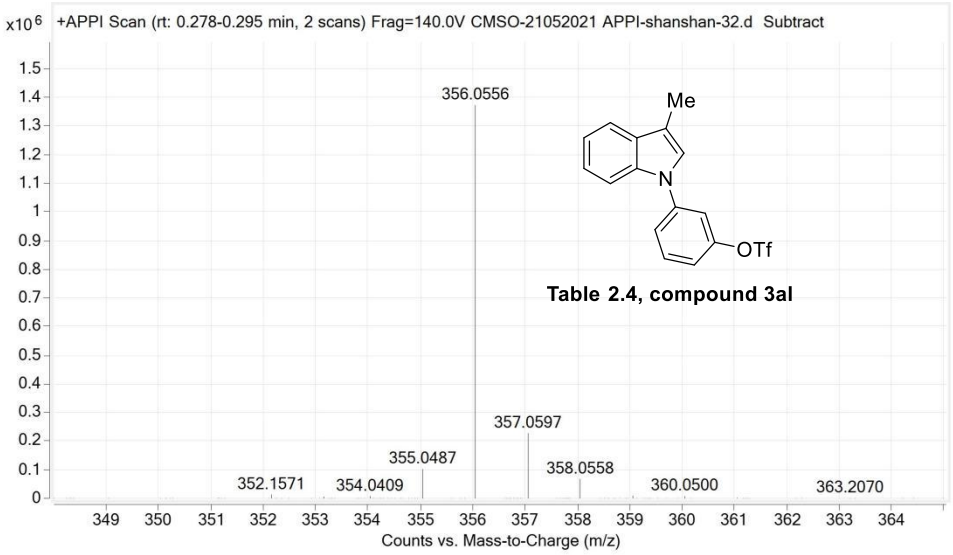

Table 2.4, compound 3al

Mass	Calc. Mass	mDa	PPM	Formula
356.0556	356.0563	0.68	1.90	C16 H13 F3 N O3 S

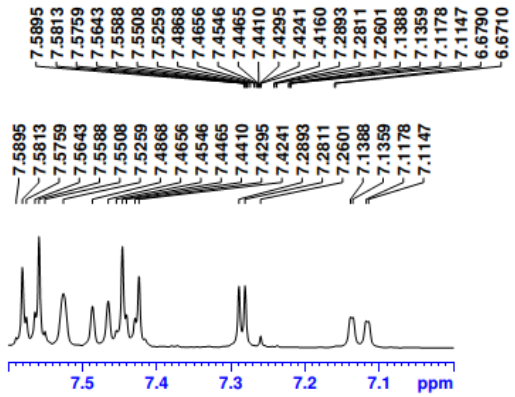

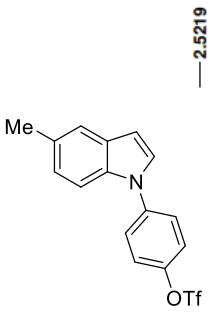

Table 2.4, compound 3am

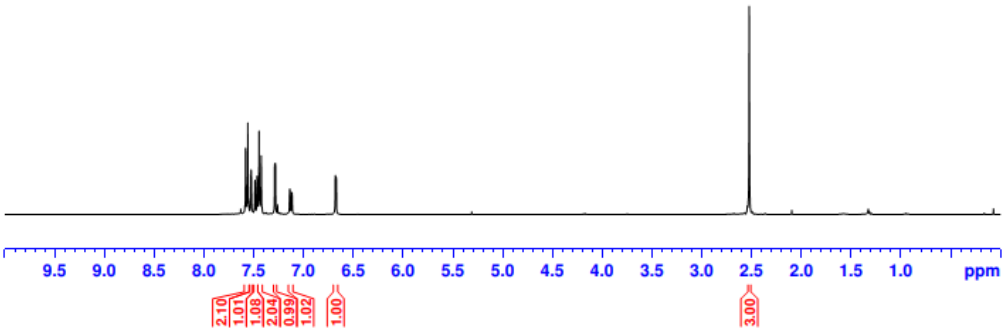

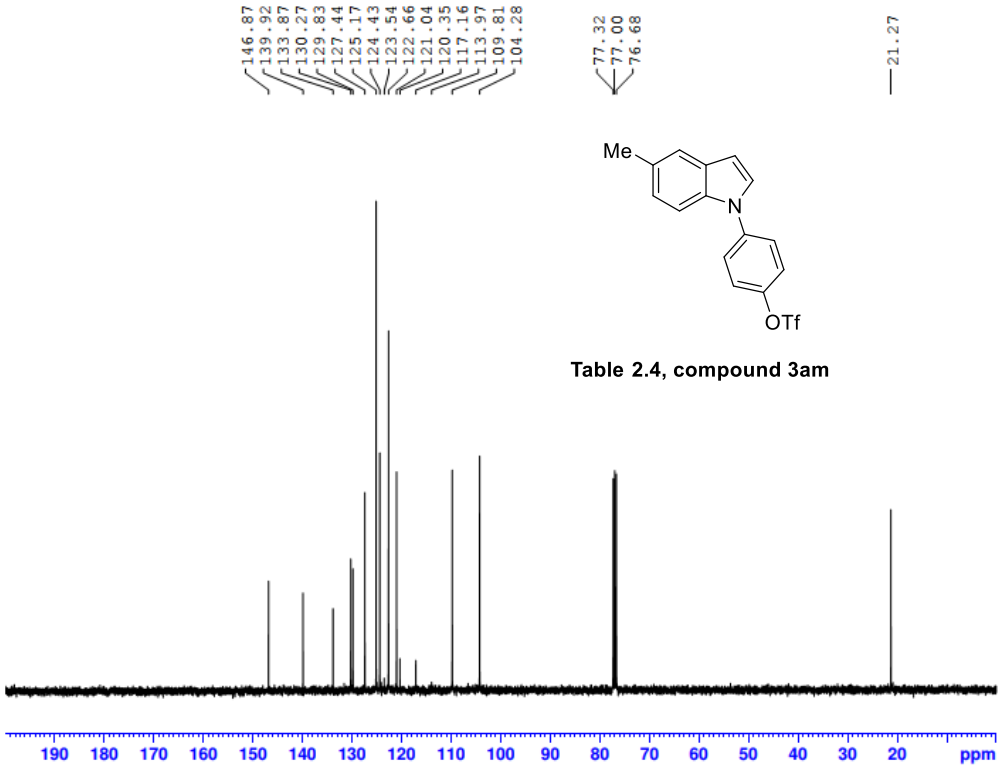

Table 2.4, compound 3am

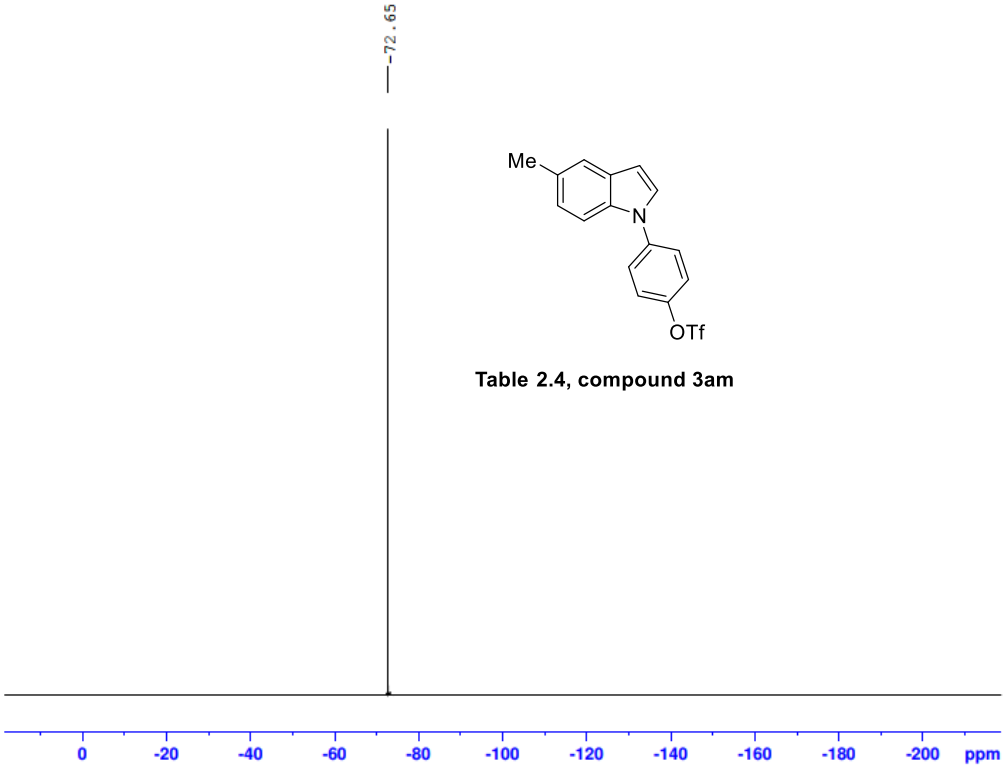

Table 2.4, compound 3am

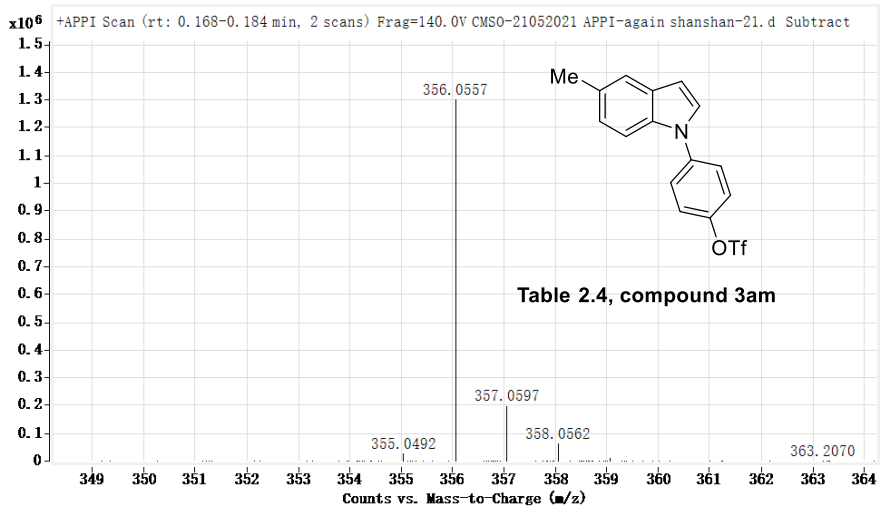

Table 2.4, compound 3am

Mass	Calc. Mass	mDa	PPM	Formula
356.0557	356.0563	0.58	1.62	C16 H13 F3 N O3 S

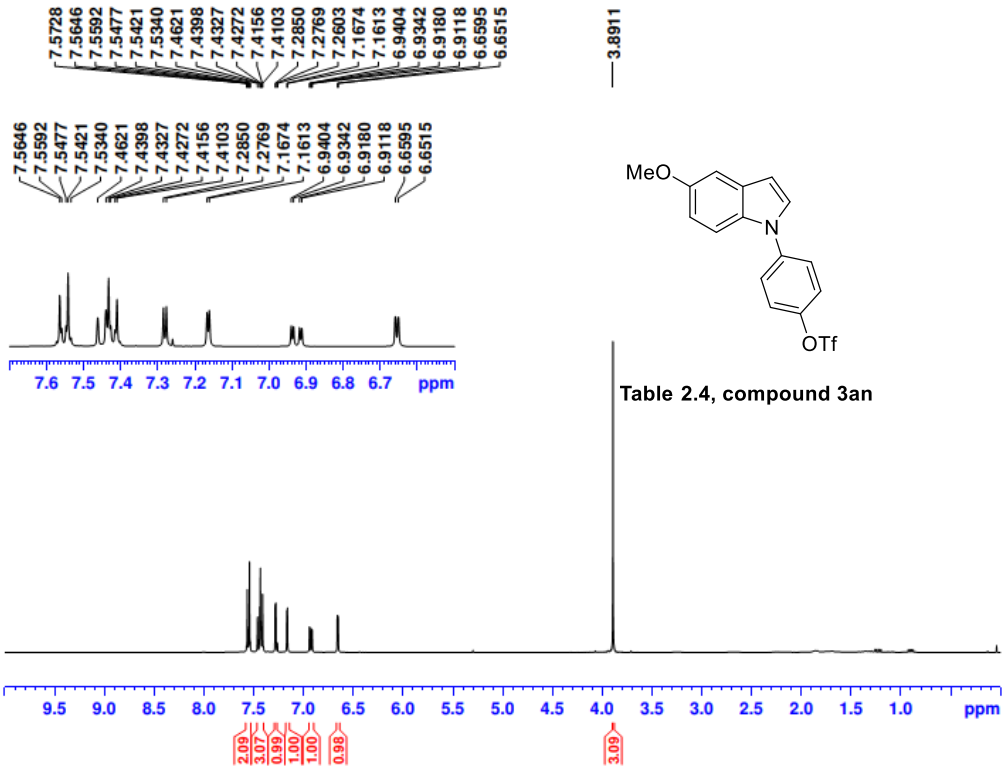

Table 2.4, compound 3an

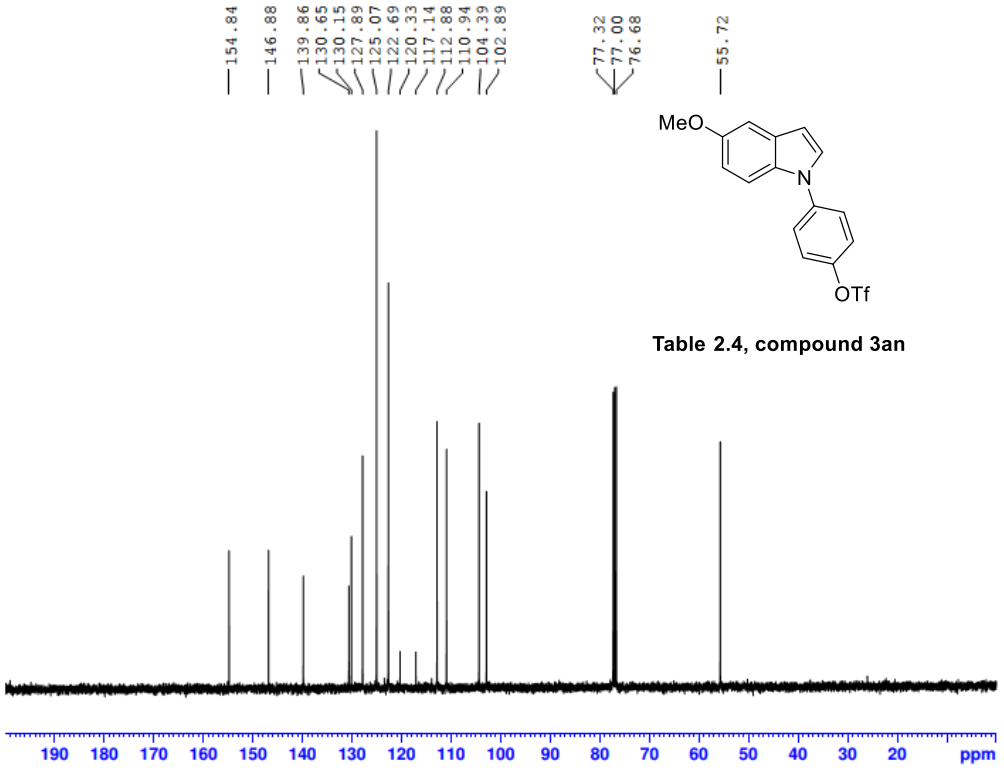

Table 2.4, compound 3an

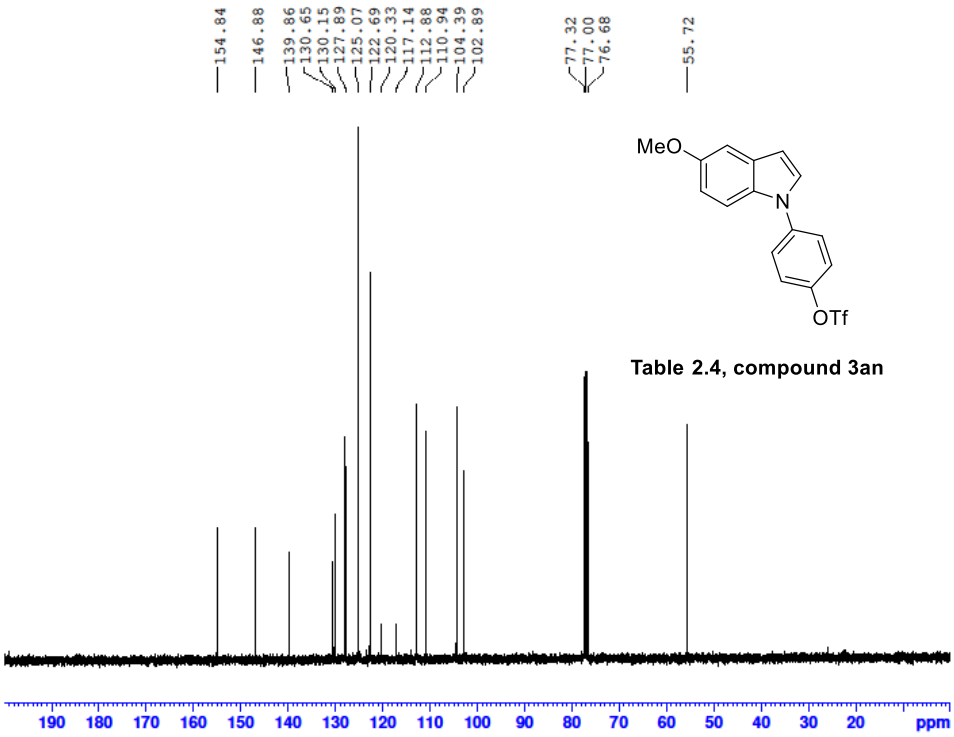

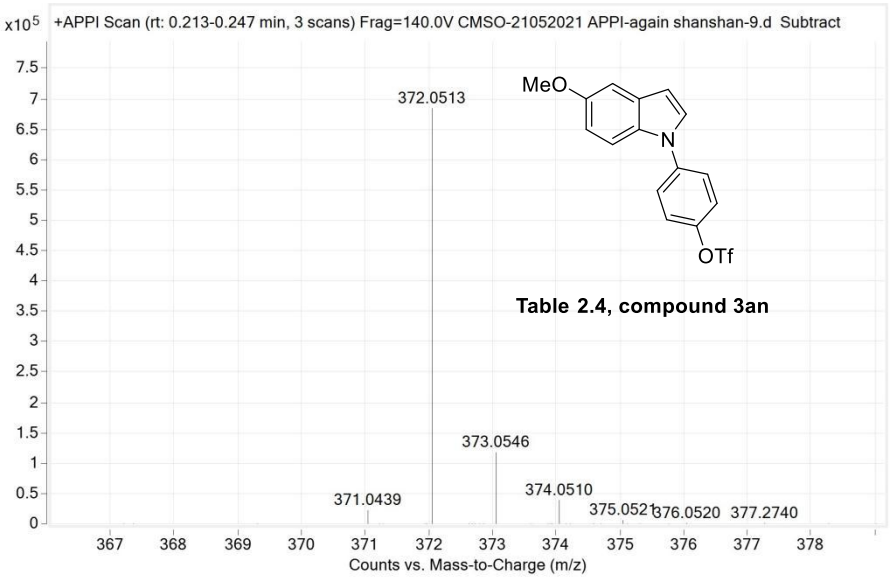

Mass	Calc. Mass	mDa	PPM	Formula
372.0513	372.0512	-0.11	-0.30	C16 H13 F3 N O4 S

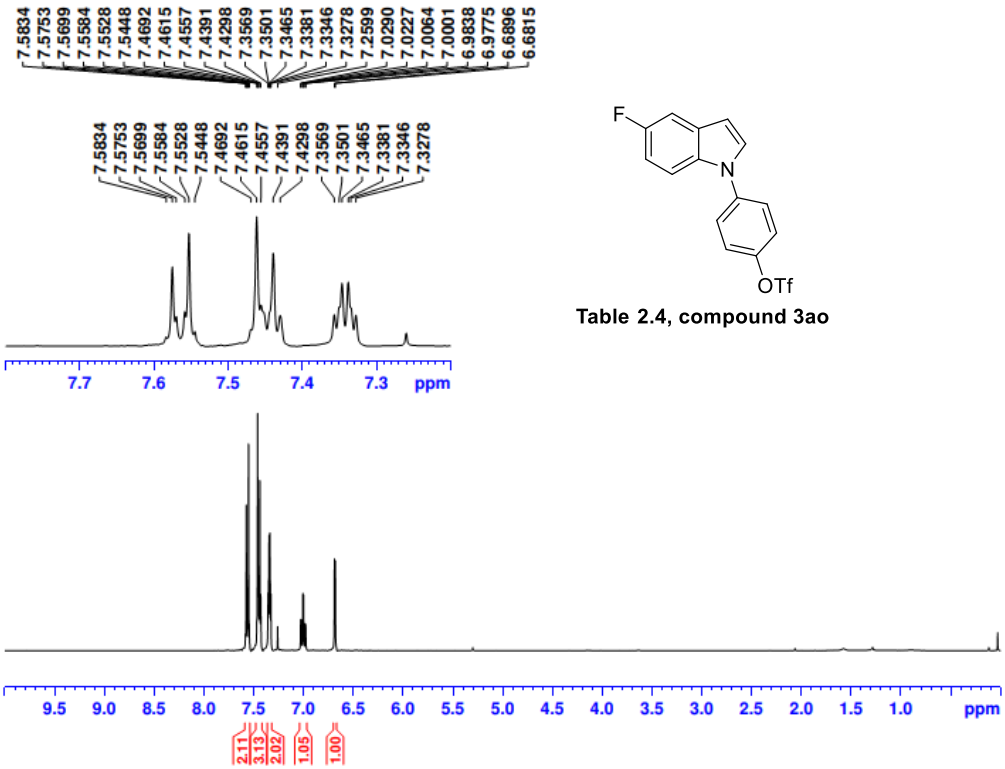

Table 2.4, compound 3ao

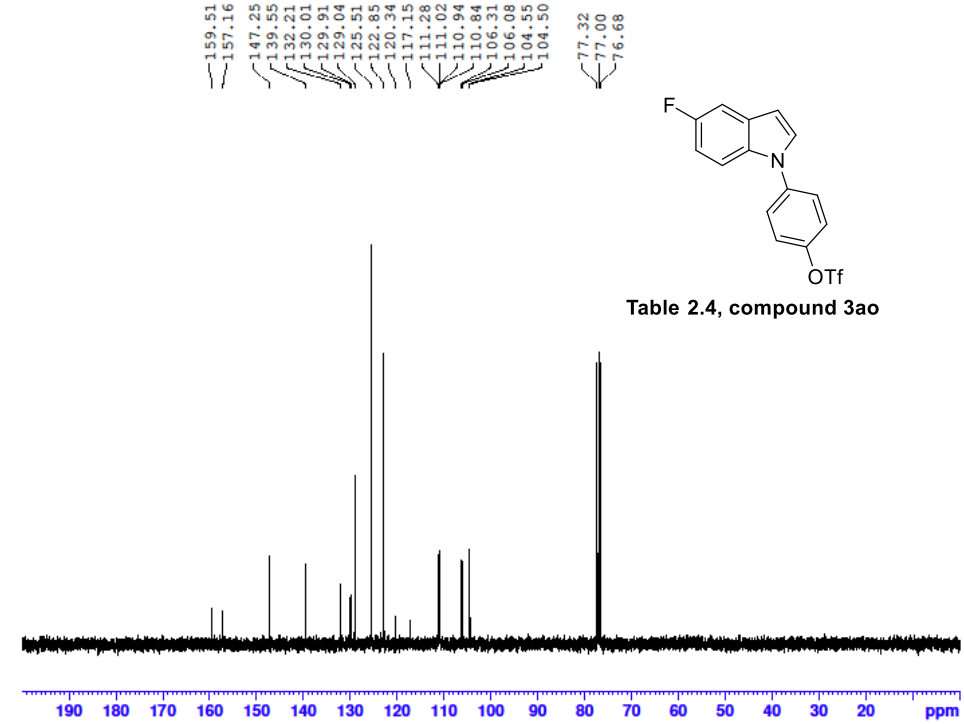

Table 2.4, compound 3ao

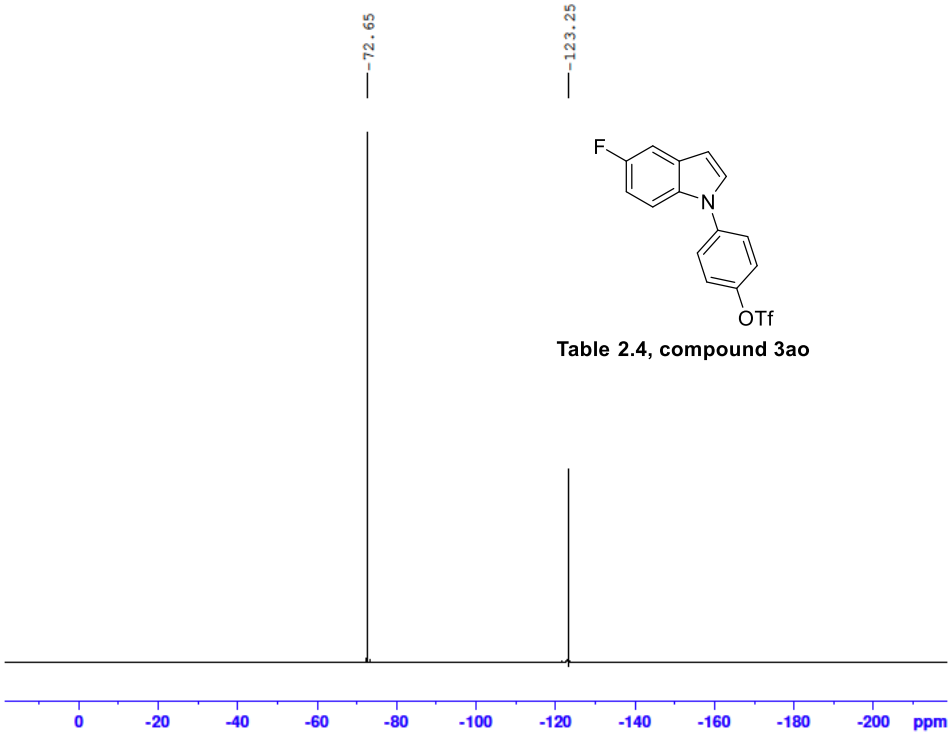

Table 2.4, compound 3ao

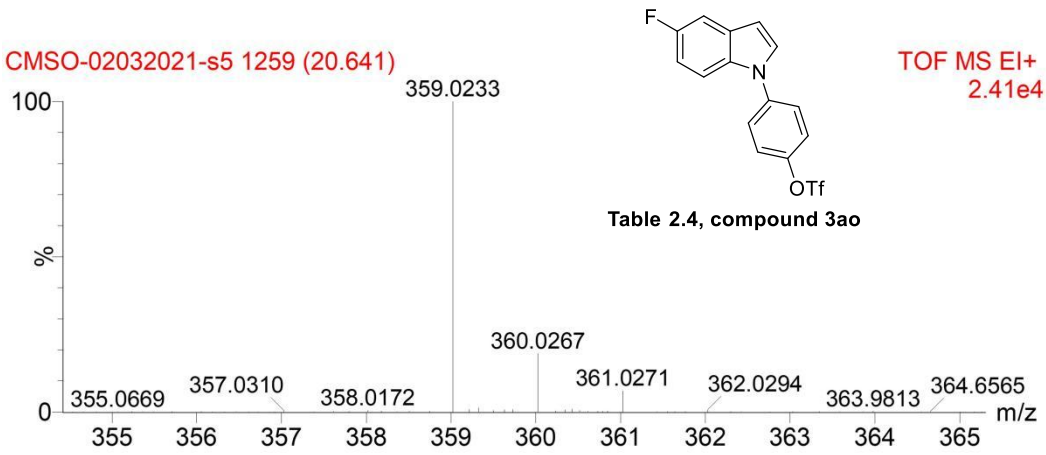

Table 2.4, compound 3ao

Mass	Calc. Mass	mDa	PPM	Formula
359.0233	359.0234	0.08	0.22	C15H9 F4NO3S

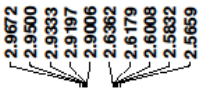

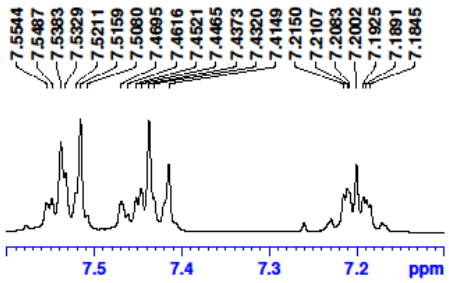

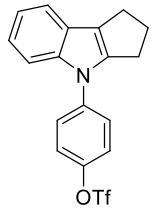

Table 2.4, compound 3ap

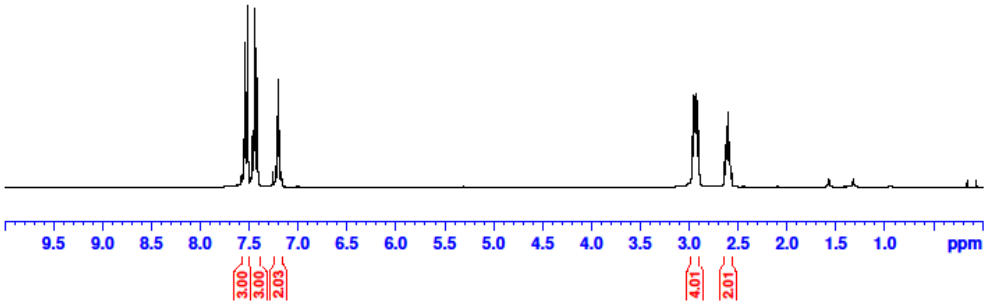

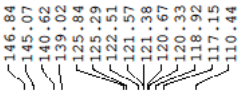

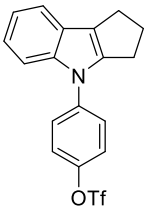

Table 2.4, compound 3ap

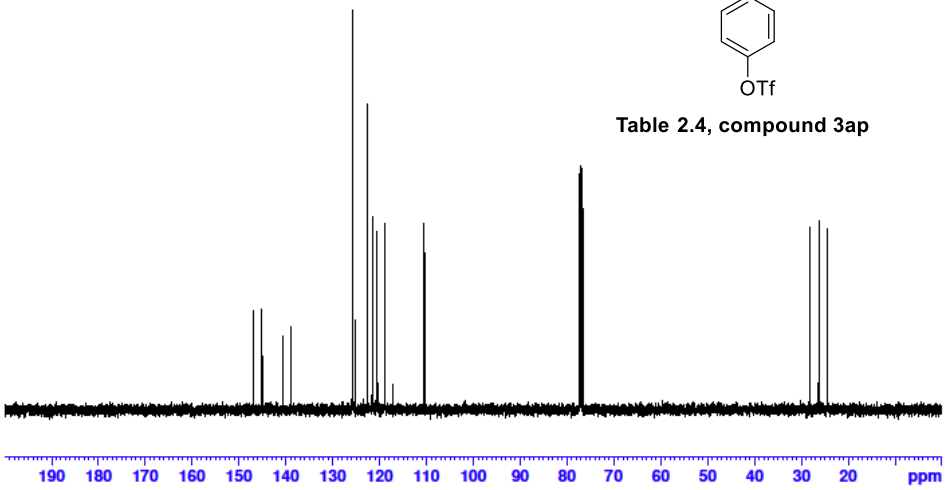

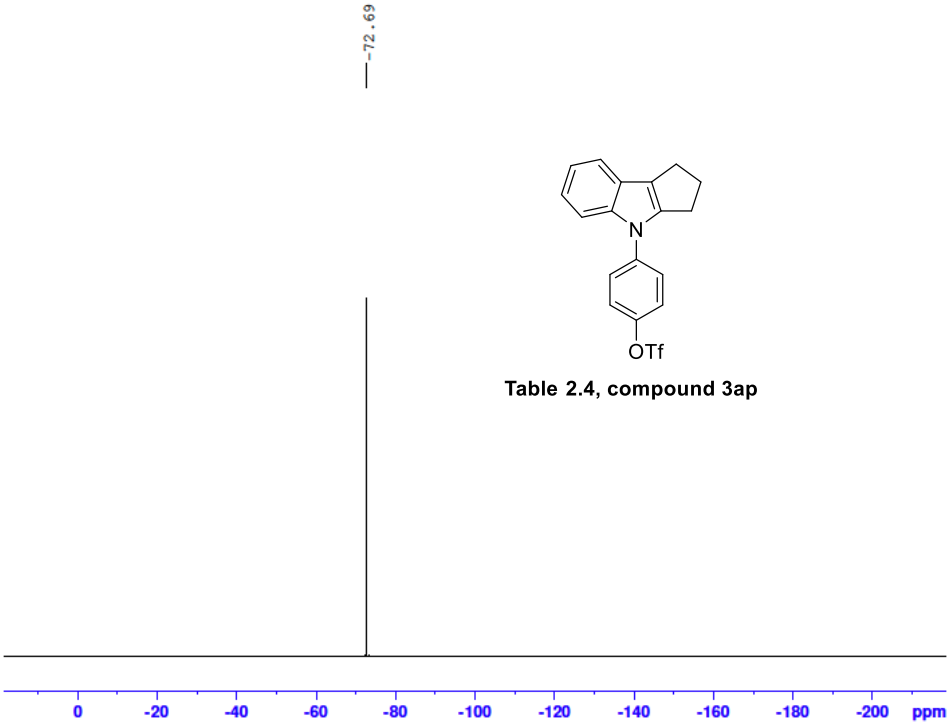

Table 2.4, compound 3ap

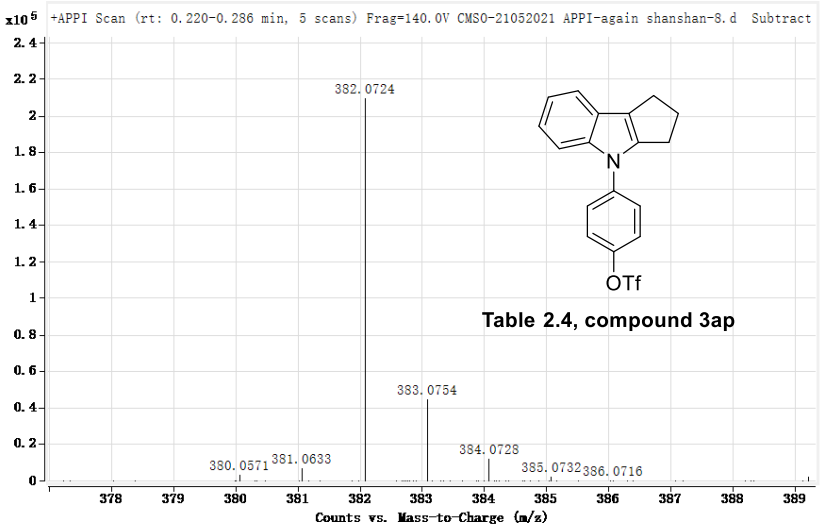

Table 2.4, compound 3ap

Mass	Calc. Mass	mDa	PPM	Formula
382.0724	382.0719	-0.47	-1.25	C18 H15 F3 N O3 S

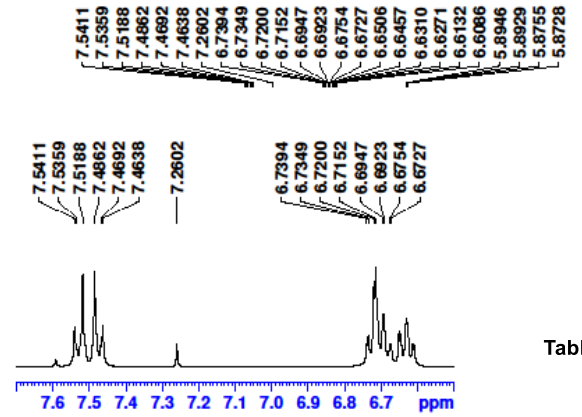

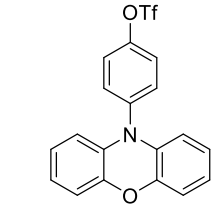

Table 2.4, compound 3aq

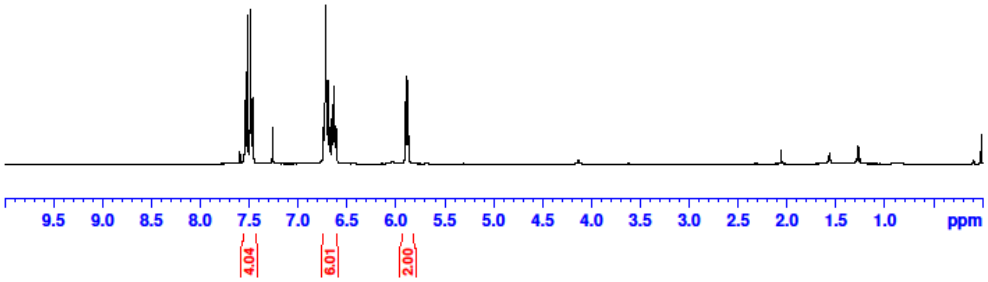

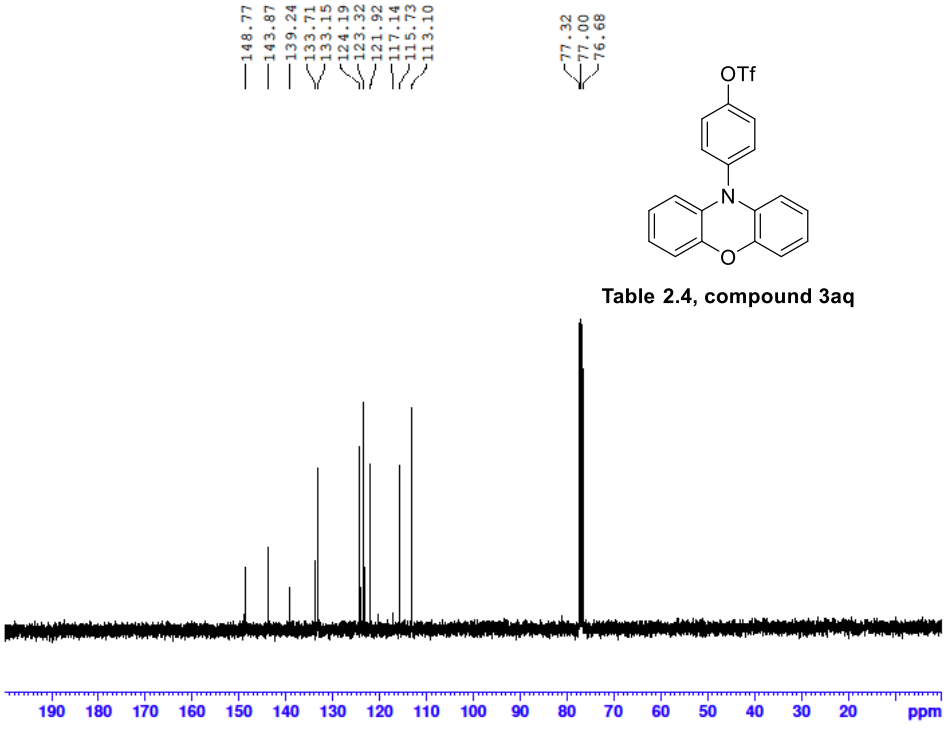

Table 2.4, compound 3aq

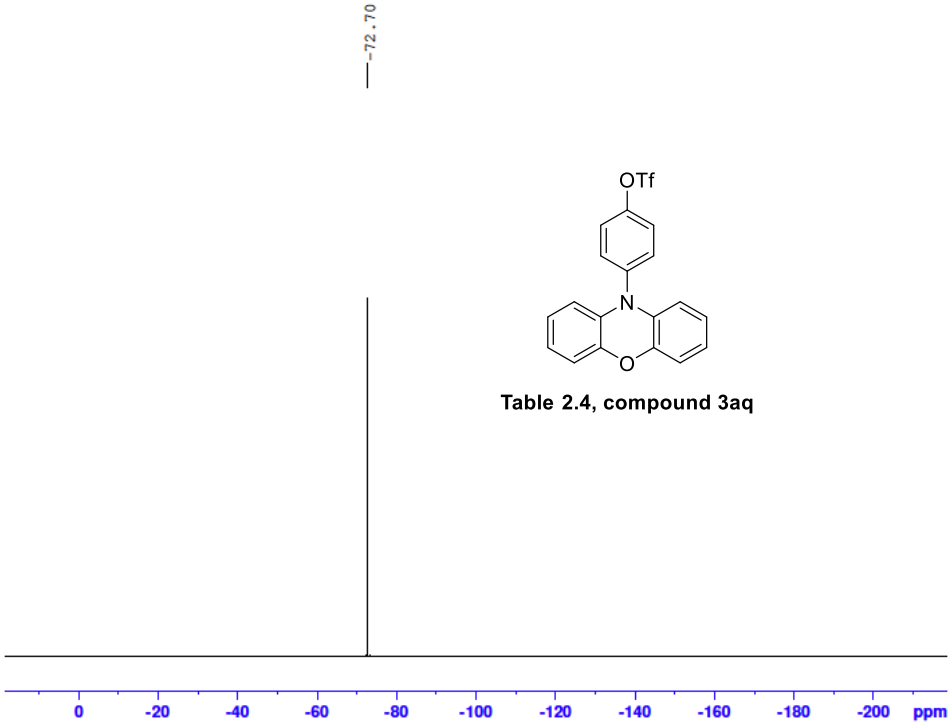

Table 2.4, compound 3aq

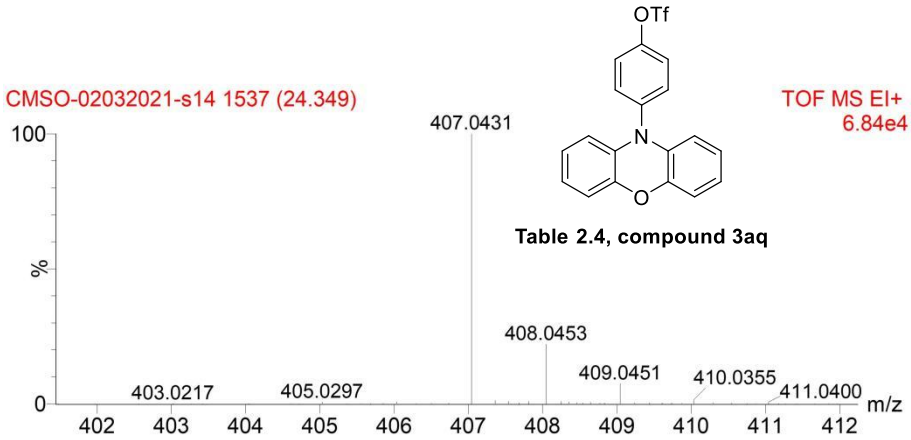

Table 2.4, compound 3aq

Mass	Calc. Mass	mDa	PPM	Formula
407.0431	407.0434	0.26	0.65	C19H12 F3NO4S

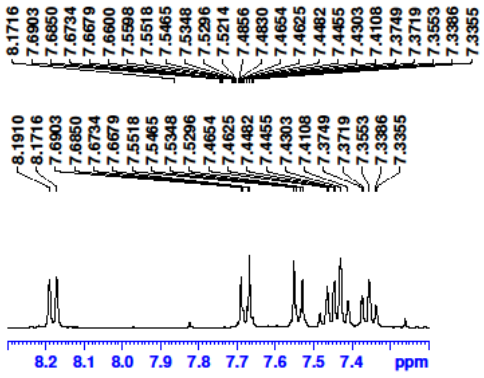

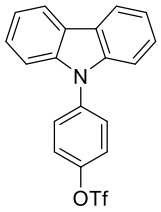

Table 2.4, compound 3ar

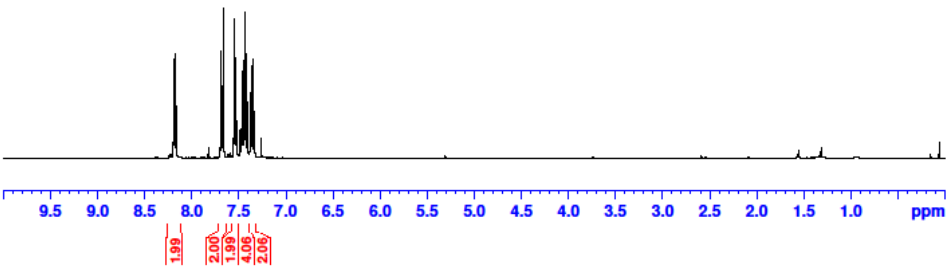

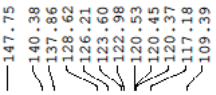

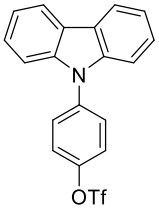

Table 2.4, compound 3ar

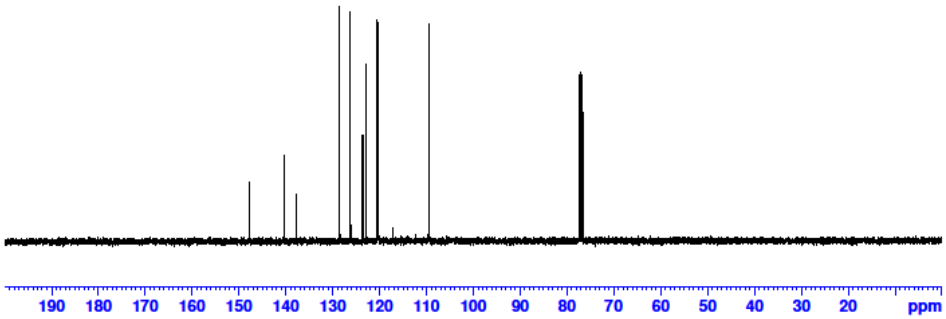

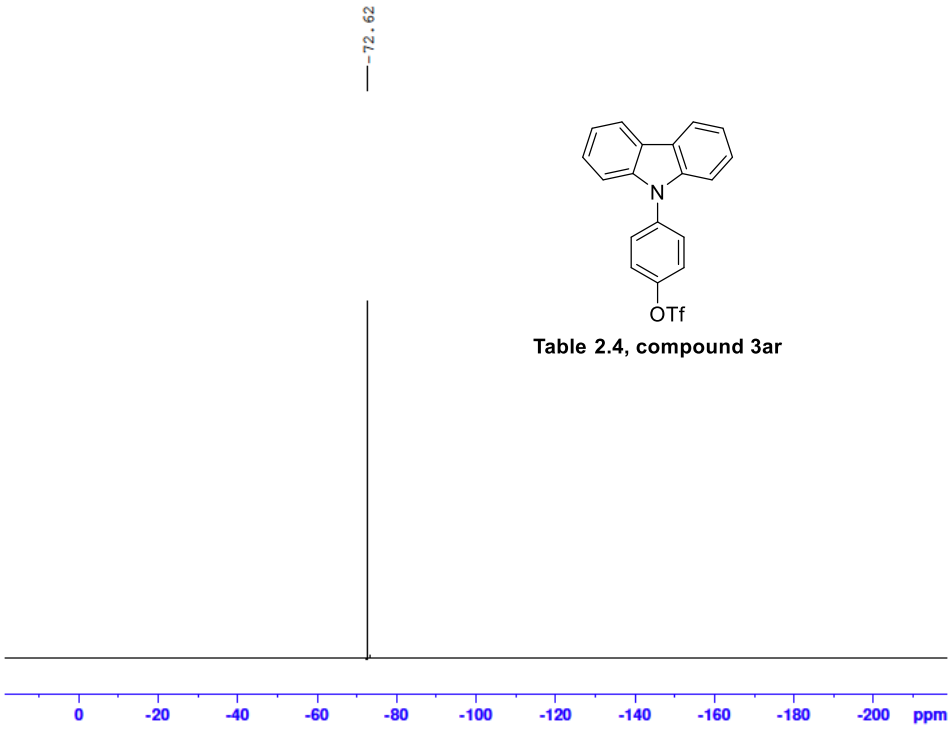

Table 2.4, compound 3ar

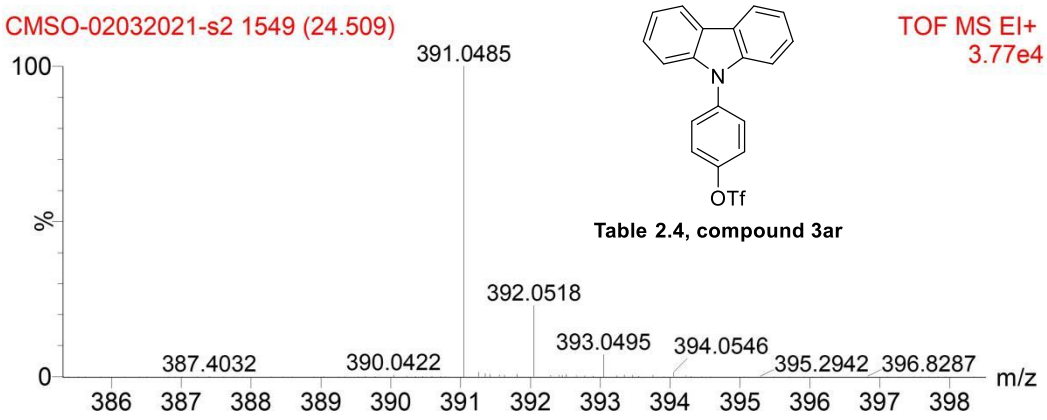

Table 2.4, compound 3ar

Mass	Calc. Mass	mDa	PPM	Formula
391.0485	391.0485	-0.05	-0.13	C19 H12 F3NO3S

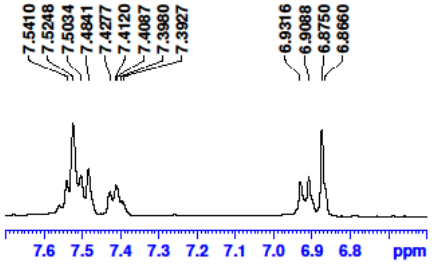

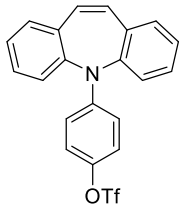

Table 2.4, compound 3as

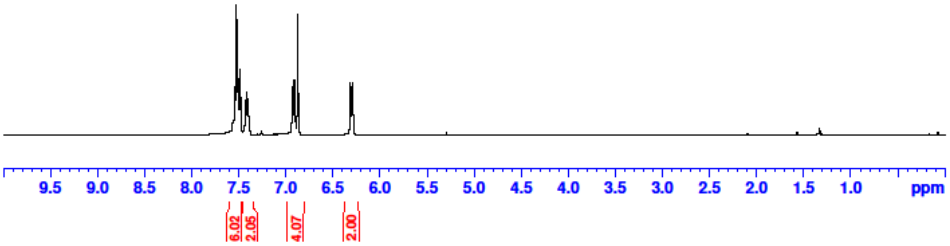

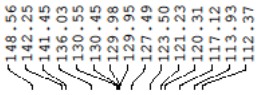

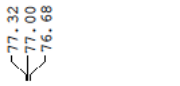

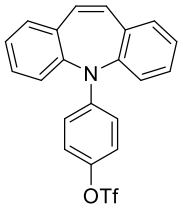

Table 2.4, compound 3as

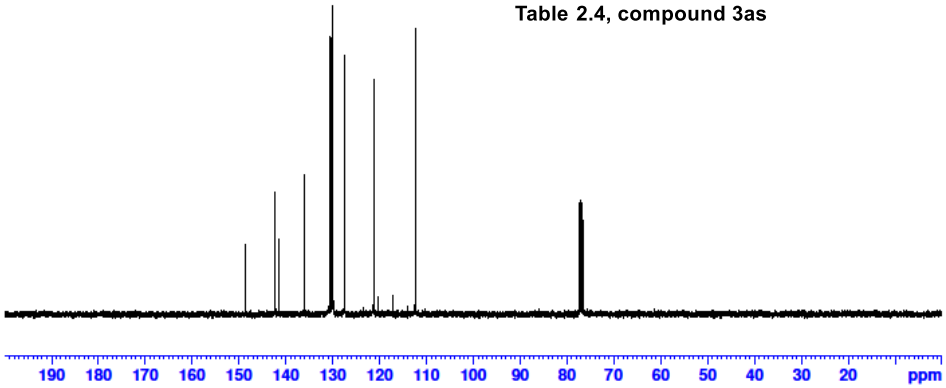

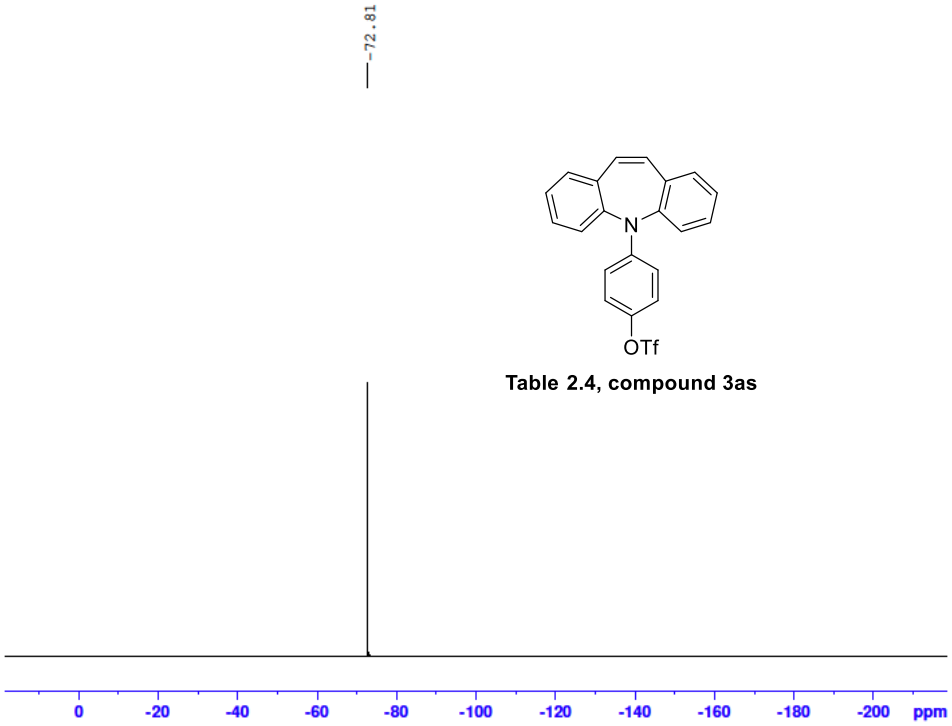

Table 2.4, compound 3as

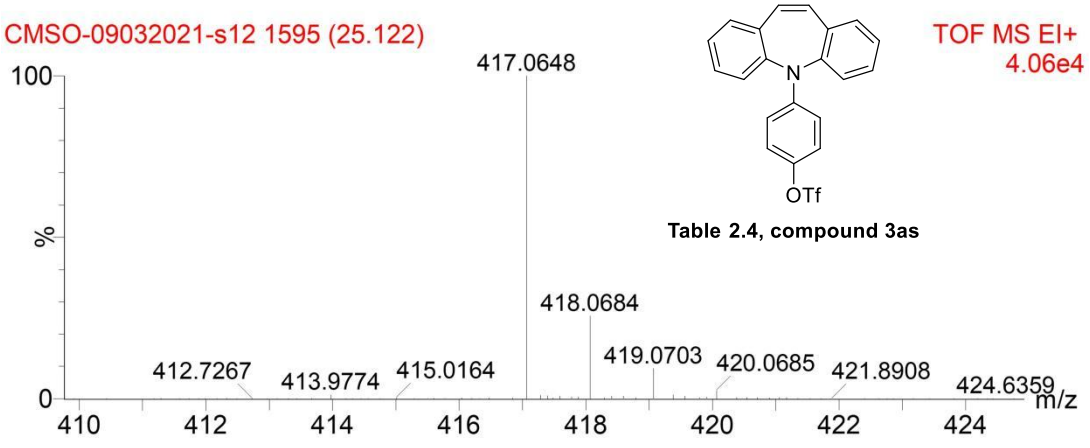

Table 2.4, compound 3as

Mass	Calc. Mass	mDa	PPM	Formula
417.0648	417.0641	-0.70	-1.68	C21 H14 F3NO3S

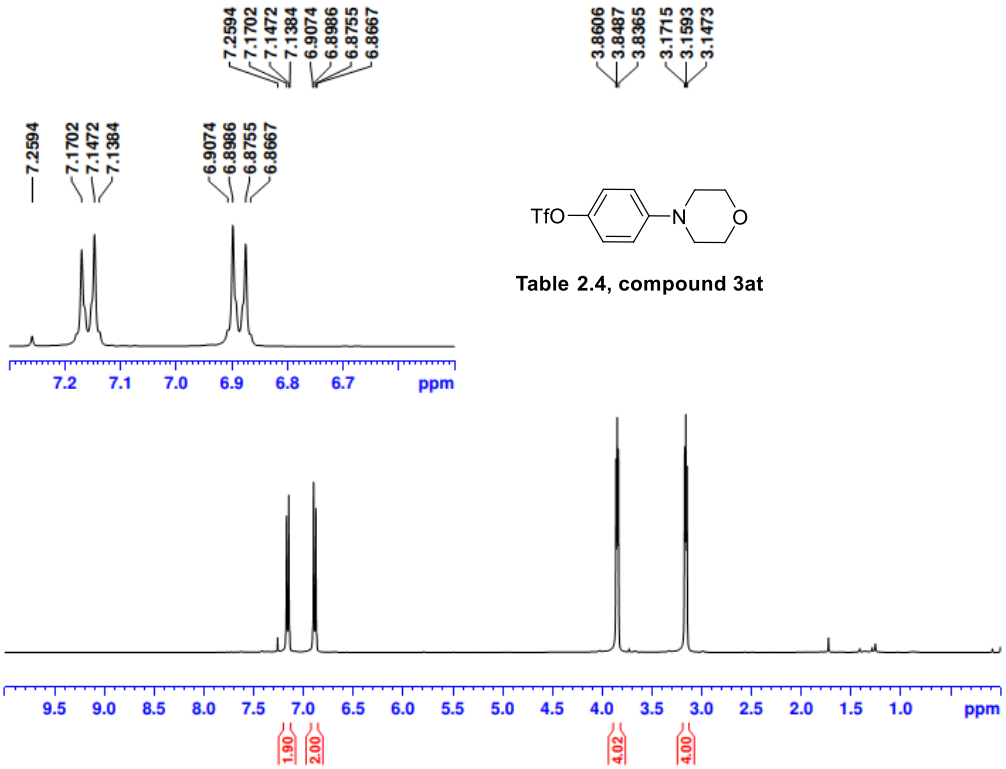

Table 2.4, compound 3at

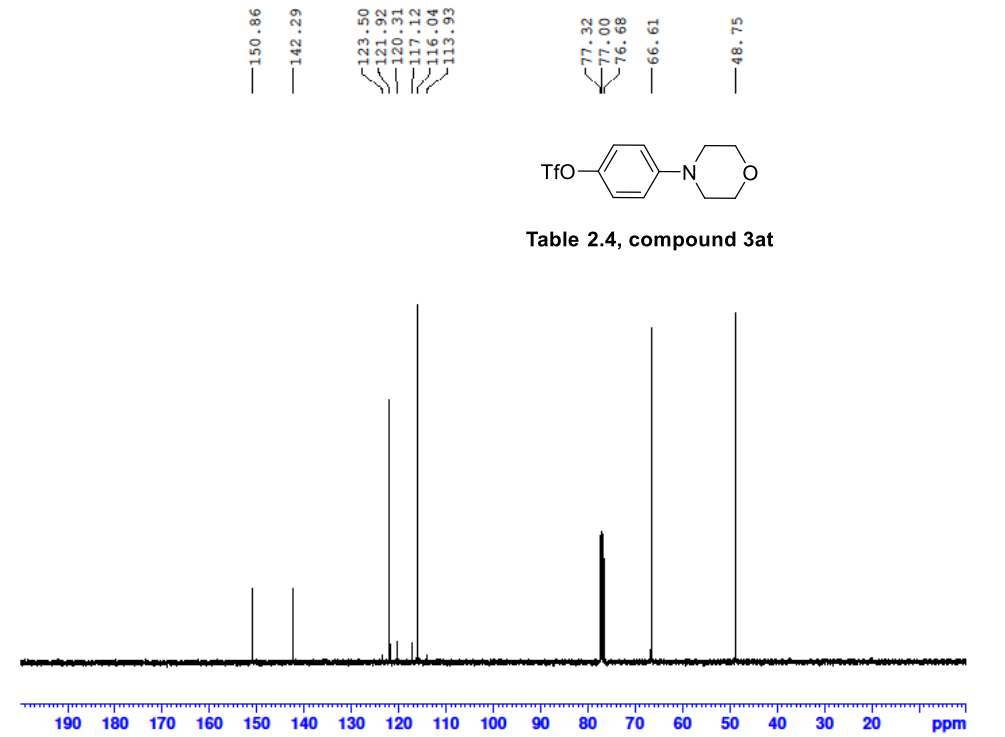

Table 2.4, compound 3at

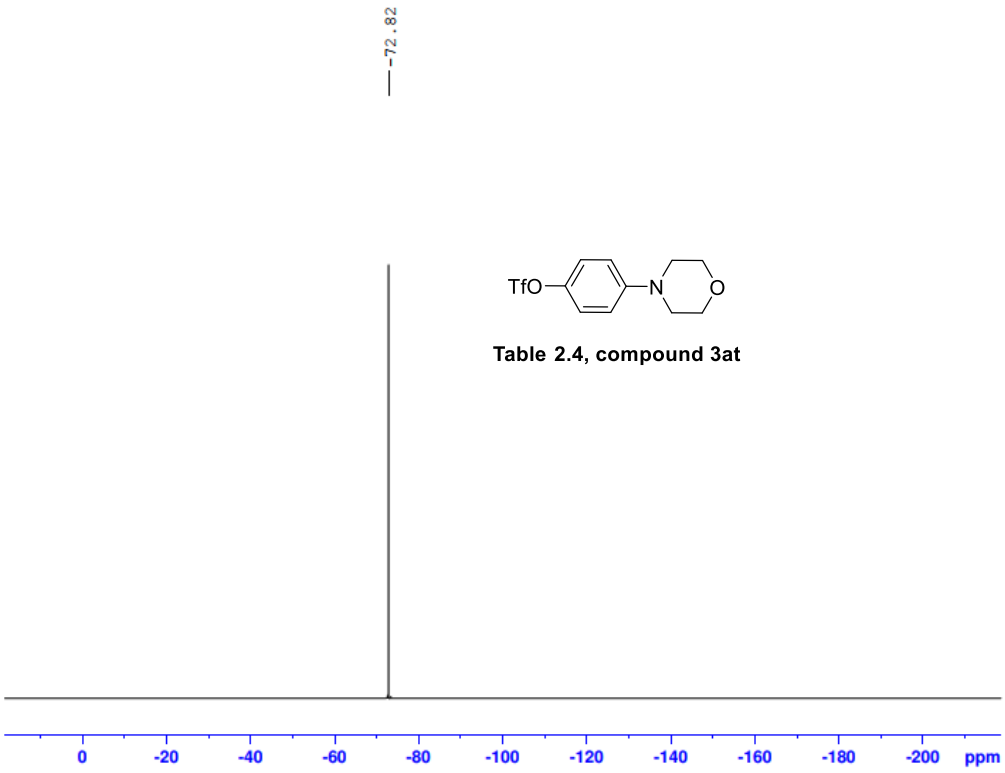

Table 2.4, compound 3at

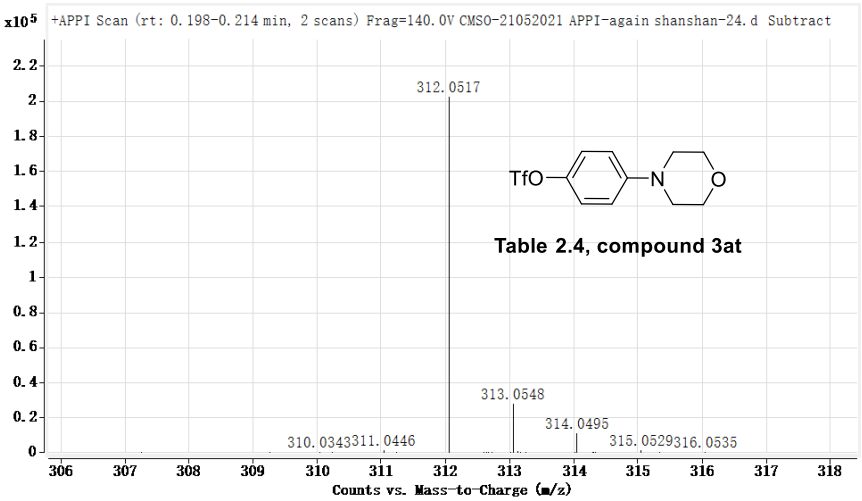

Table 2.4, compound 3at

Mass	Calc. Mass	mDa	PPM	Formula
312.0517	312.0512	-0.51	-1.64	C11 H13 F3 N O4 S

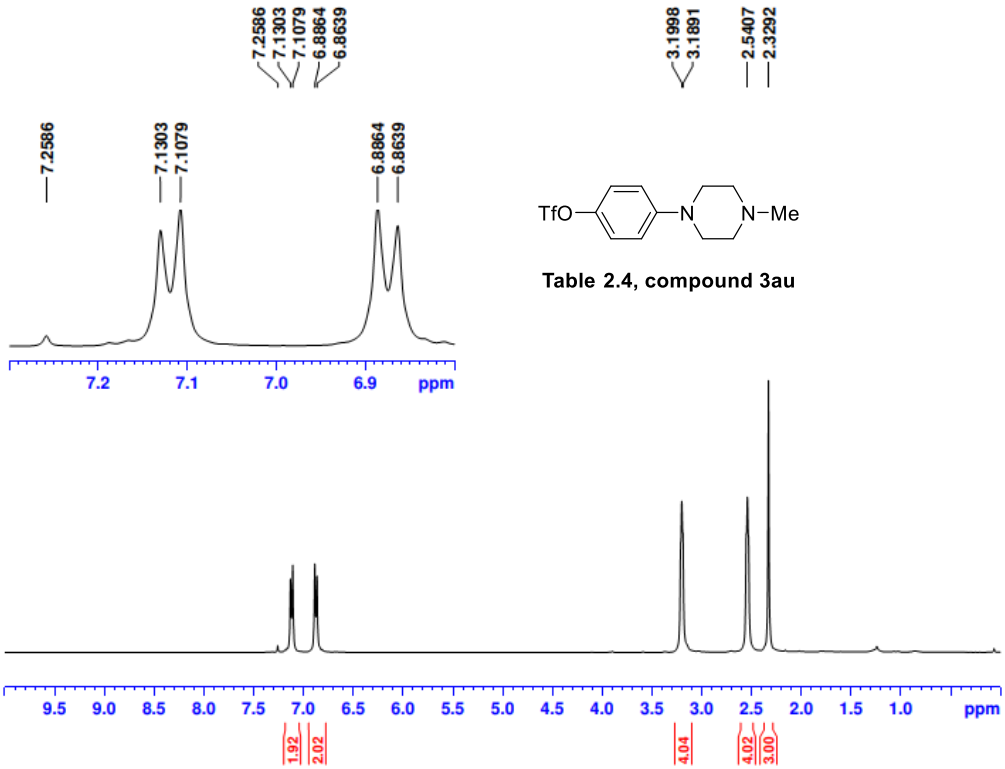

Table 2.4, compound 3au

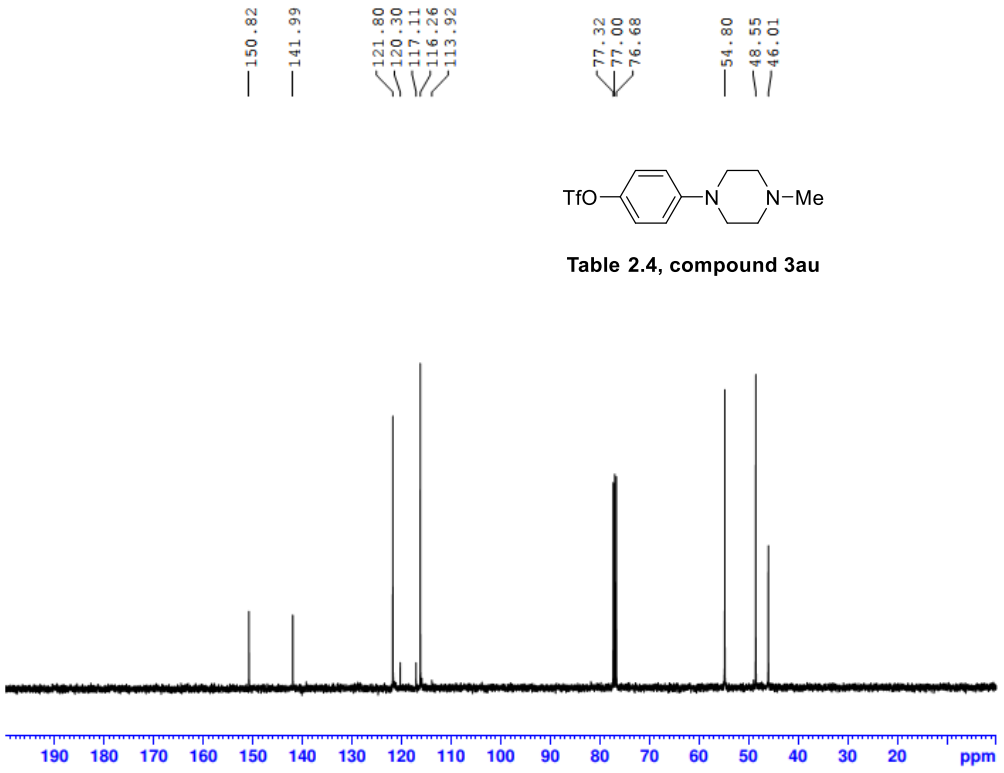

Table 2.4, compound 3au

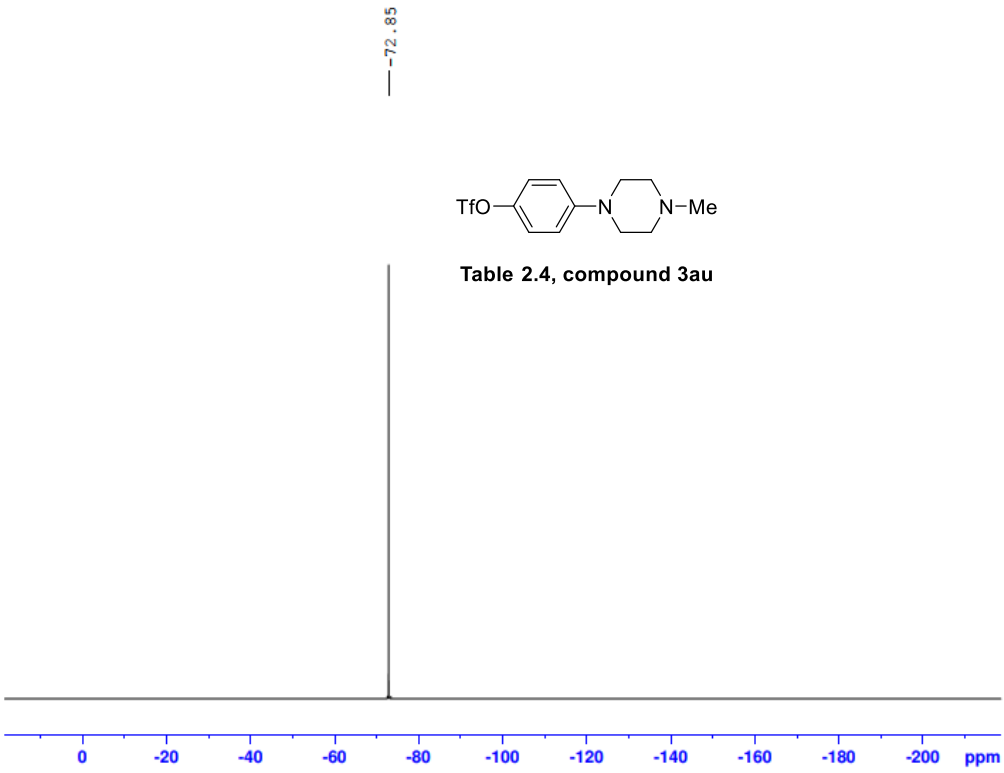

Table 2.4, compound 3au

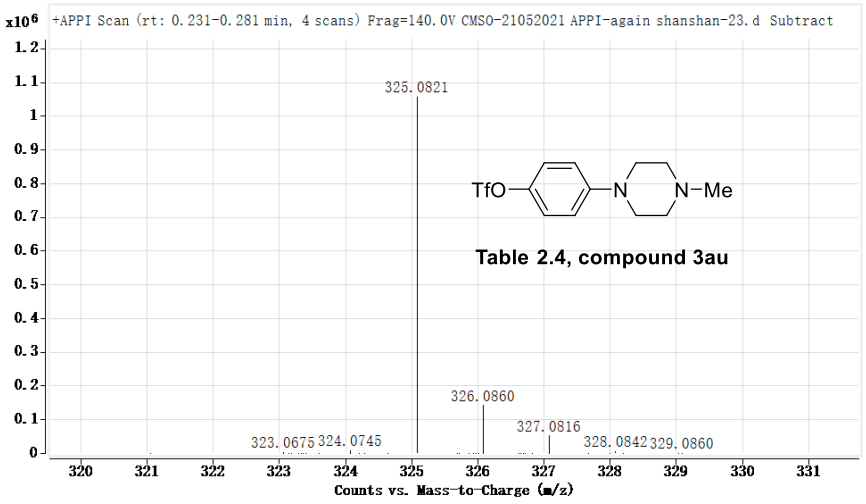

Table 2.4, compound 3au

Mass	Calc. Mass	mDa	PPM	Formula
325.0821	325.0828	0.72	2.23	C12 H16 F3 N2 O3 S

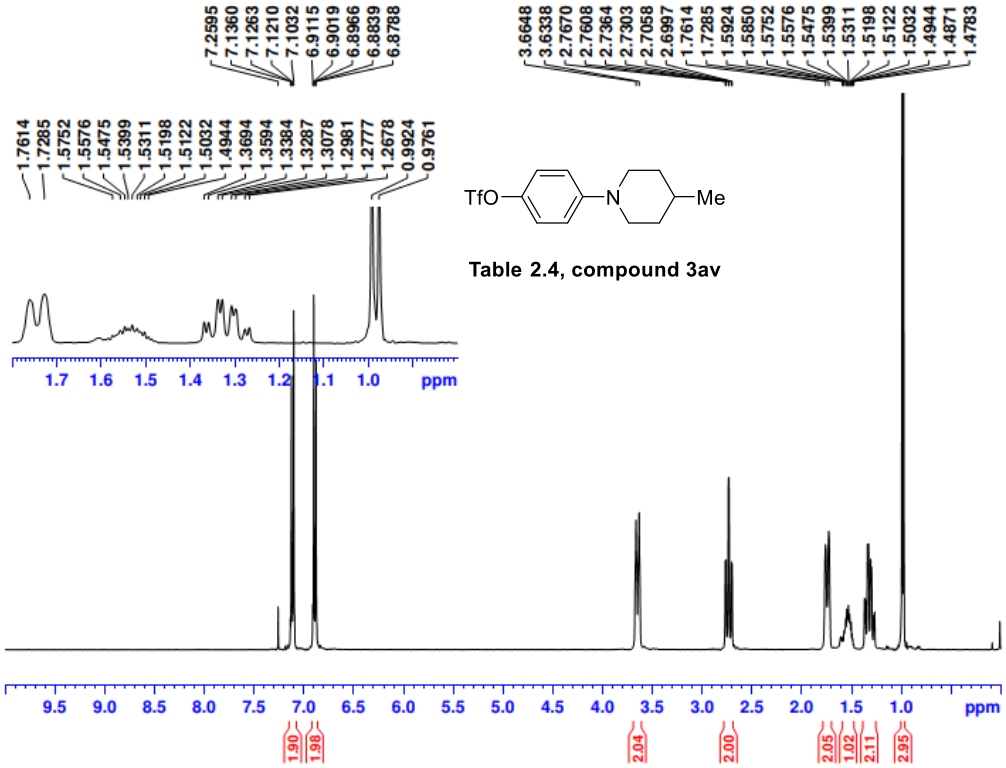

Table 2.4, compound 3av

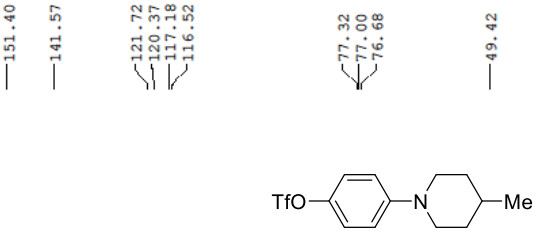

Table 2.4, compound 3av

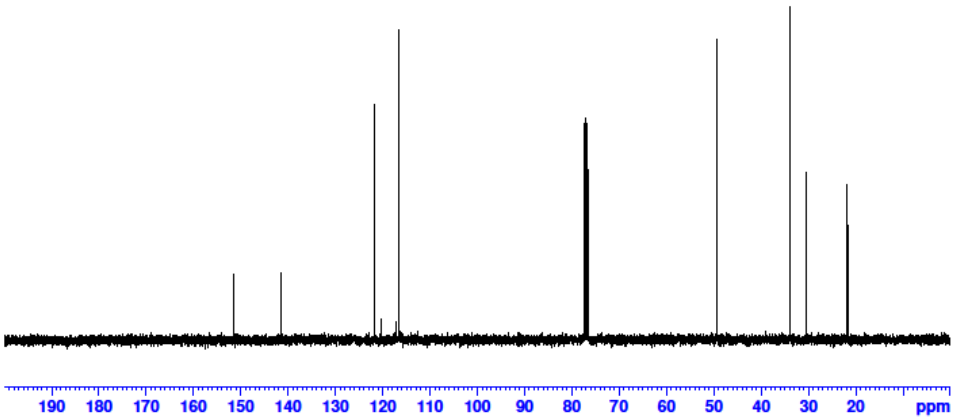

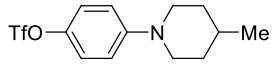

Table 2.4, compound 3av

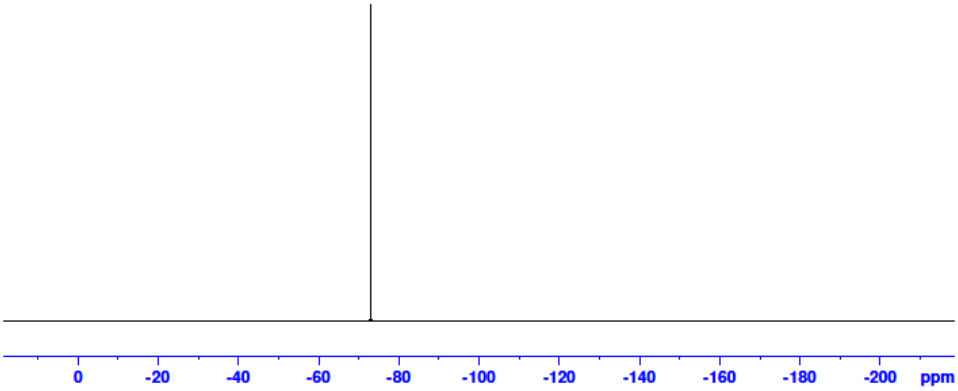

CMSO-09032021-s9 1066 (18.067)

TOF MS EI+
194

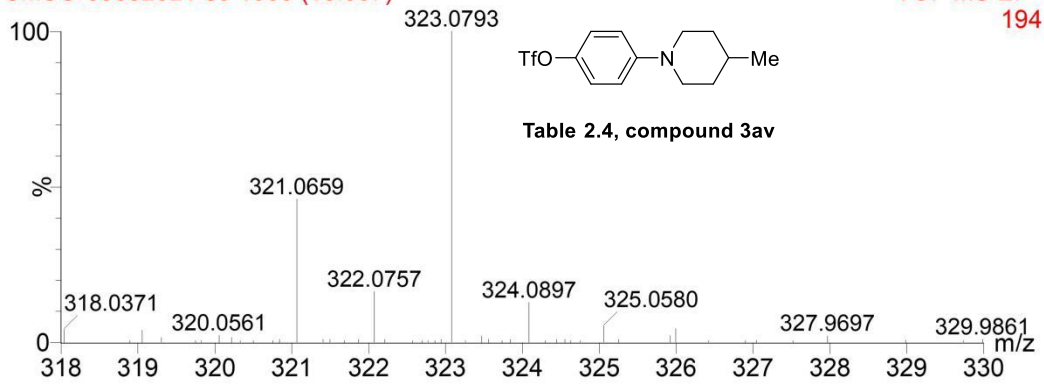

Table 2.4, compound 3av

Mass	Calc. Mass	mDa	PPM	Formula
323.0793	323.0798	0.45	1.39	C13 H16 F3NO4S

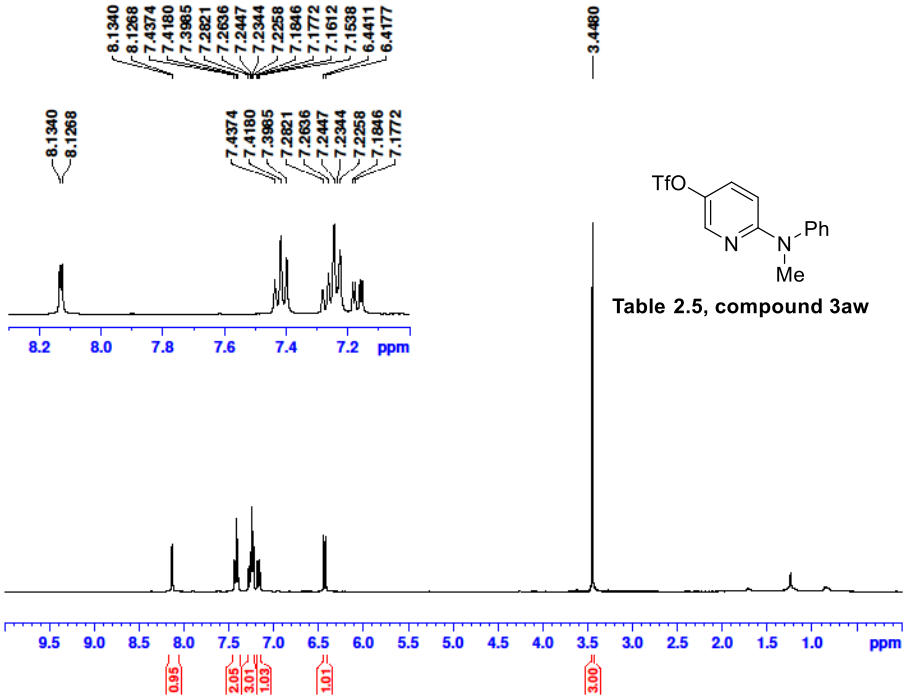

Table 2.5, compound 3aw

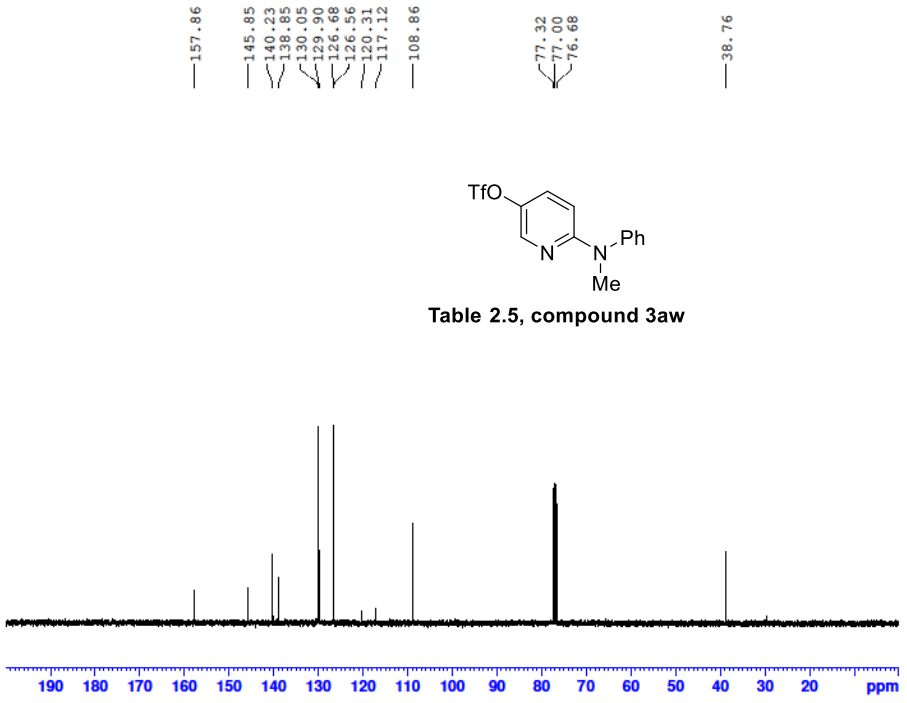

Table 2.5, compound 3aw

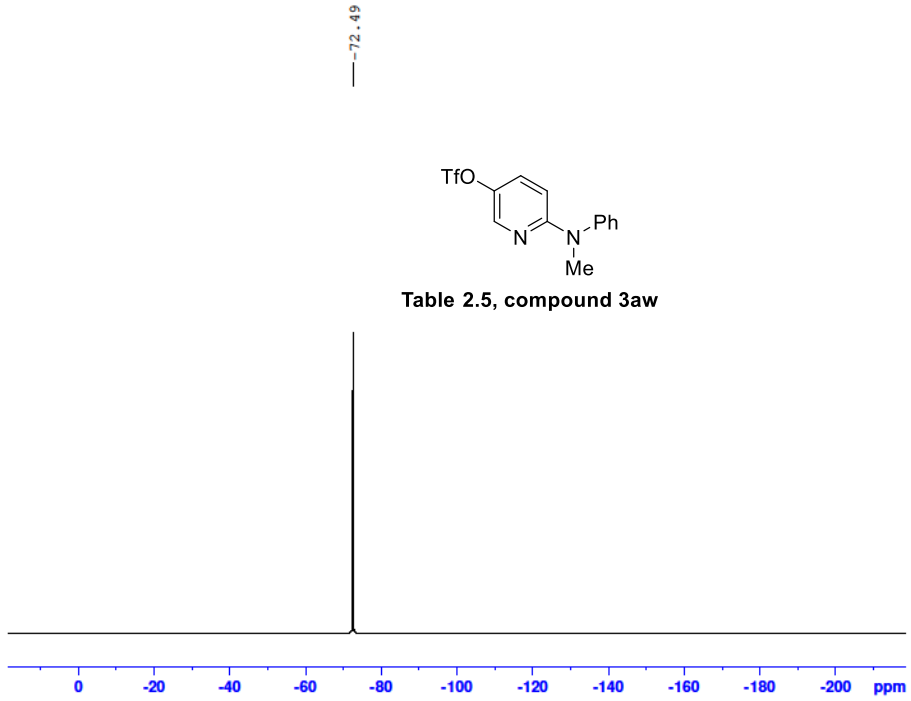

Table 2.5, compound 3aw

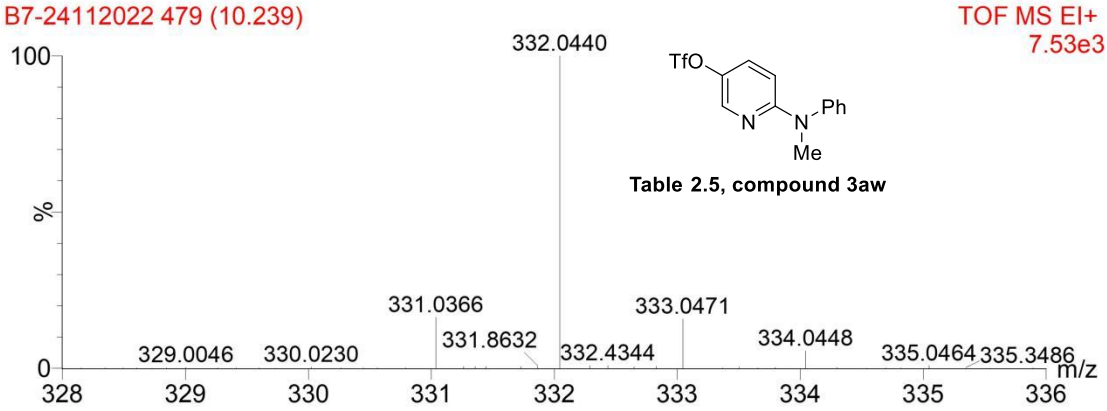

Table 2.5, compound 3aw

Mass	Calc. Mass	mDa	PPM	Ion Formula
332.0440	332.0437	-0.30	-0.91	C13H11F3O3N2S

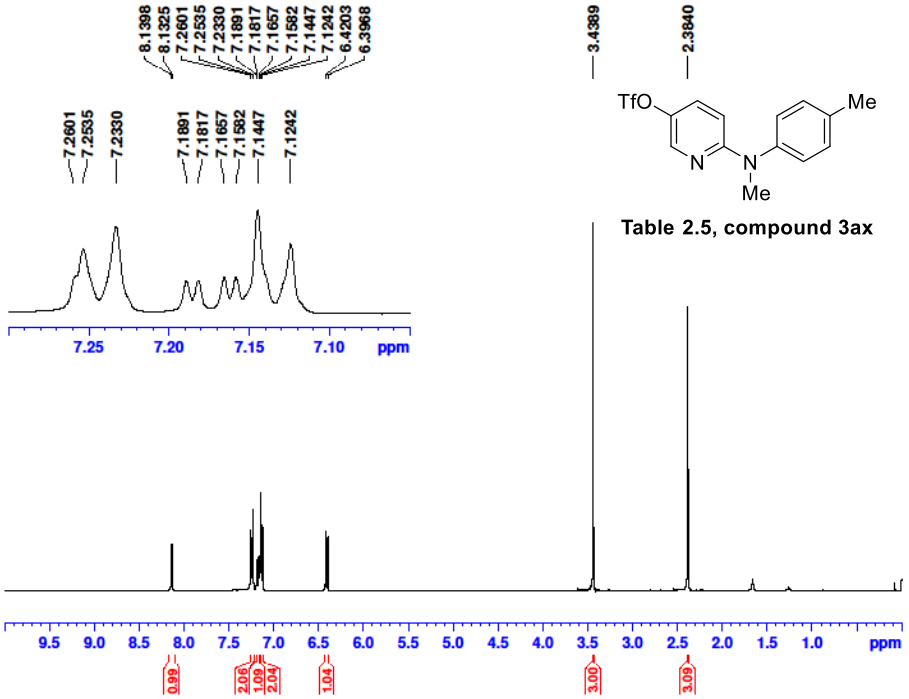

Table 2.5, compound 3ax

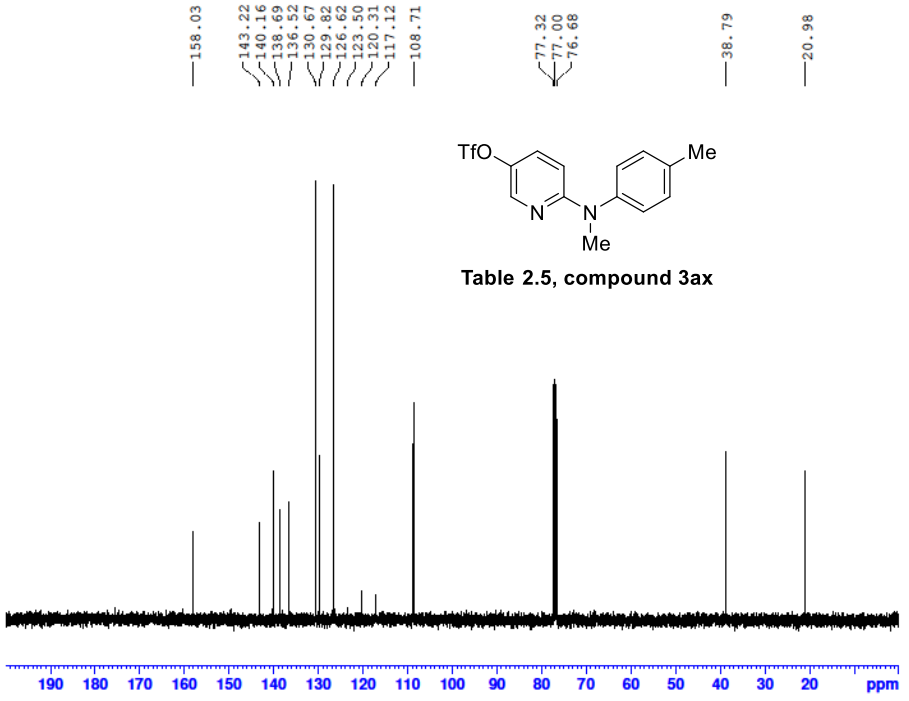

Table 2.5, compound 3ax

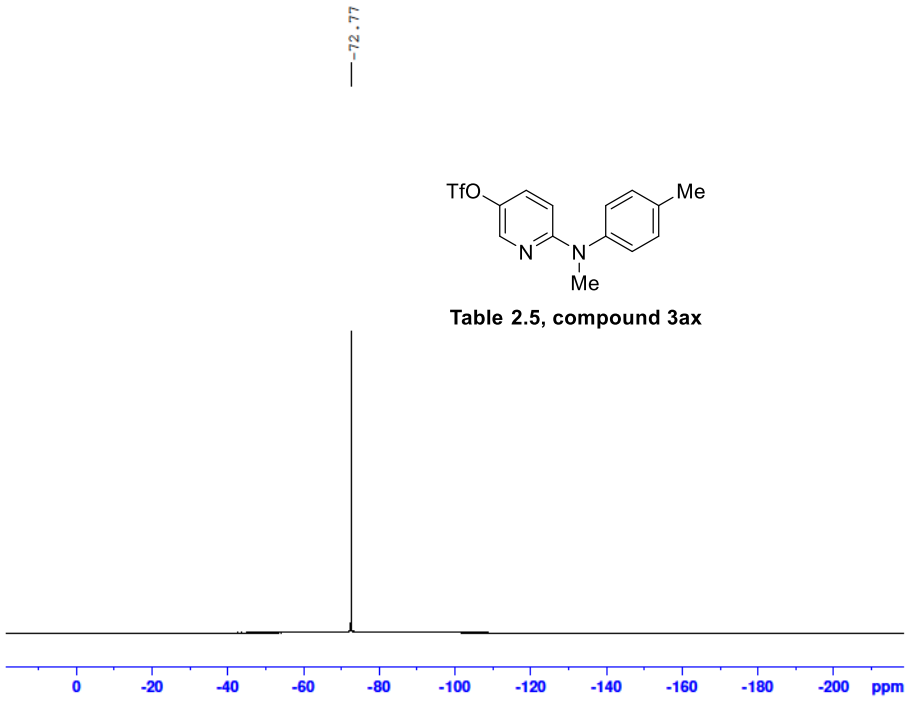

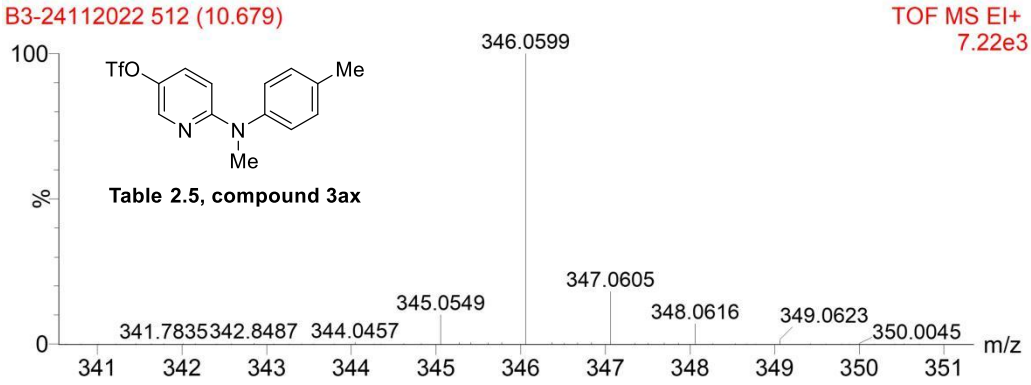

Mass	Calc. Mass	mDa	PPM	Ion Formula
346.0599	346.0593	-0.55	-1.59	C14H13F3O3N2S

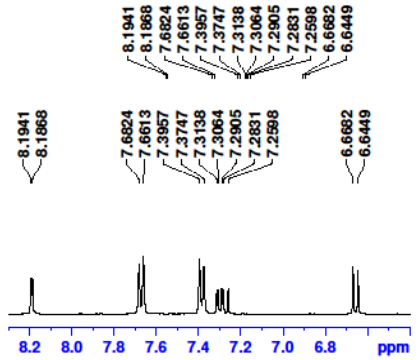

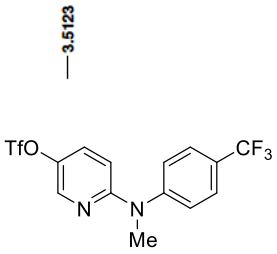

Table 2.5, compound 3ay

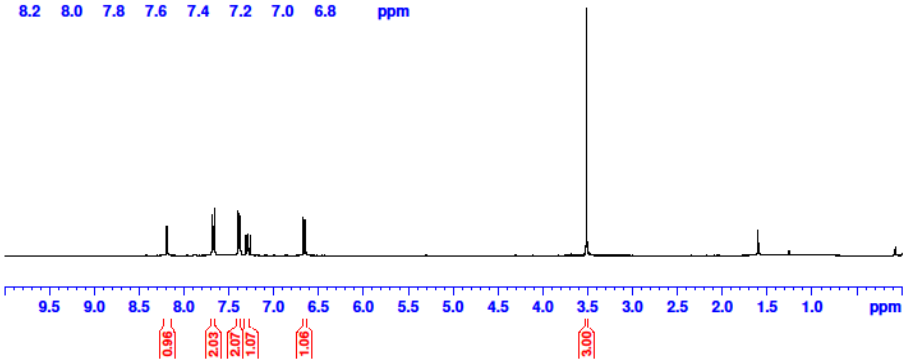

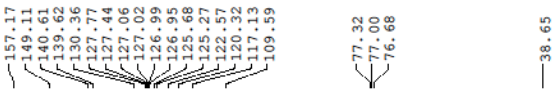

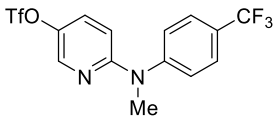

Table 2.5, compound 3ay

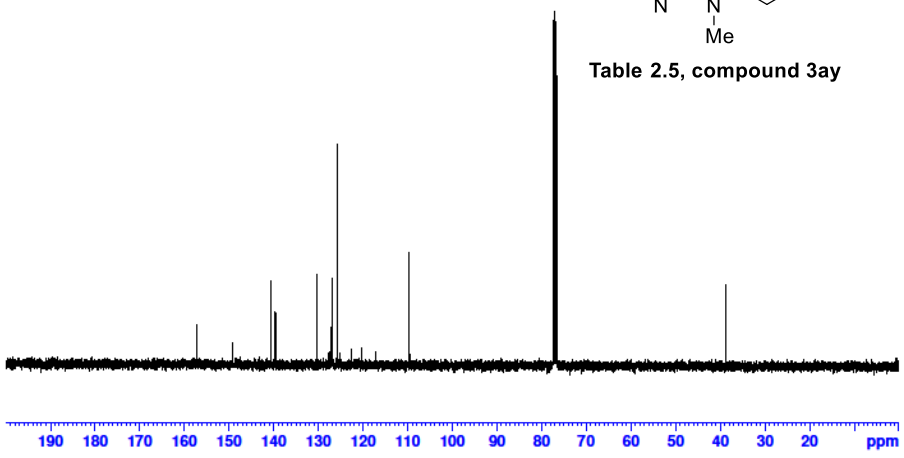

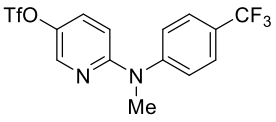

Table 2.5, compound 3ay

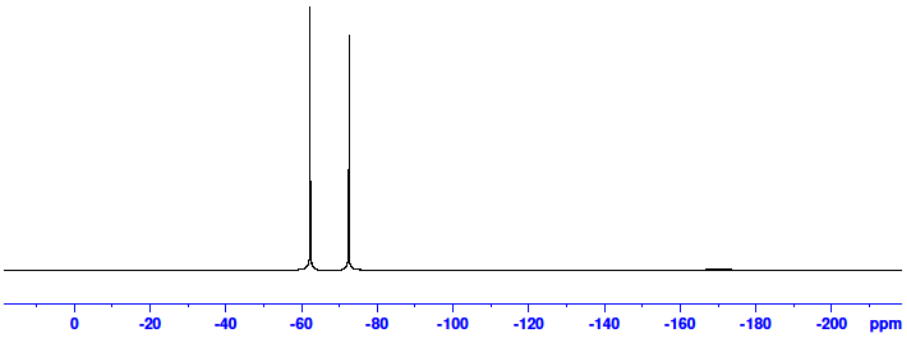

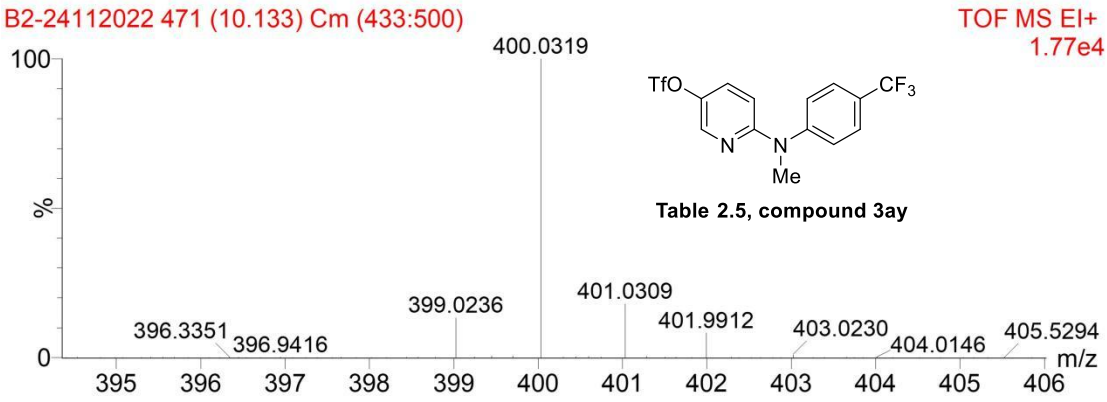

Table 2.5, compound 3ay

Mass	Calc. Mass	mDa	PPM	Ion Formula
400.0319	400.0311	-0.82	-2.04	C14H10F6O3N2S

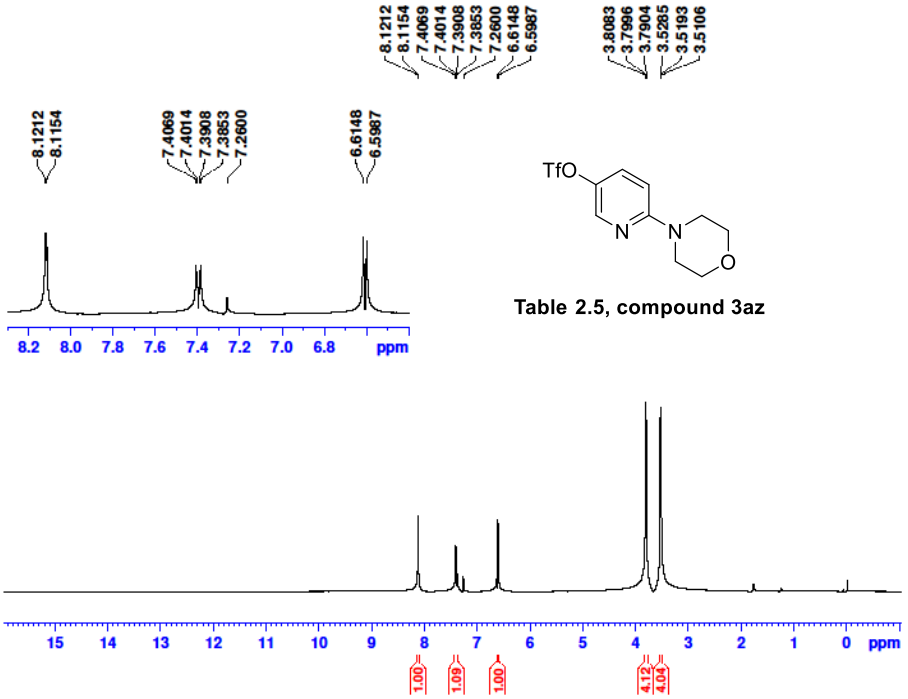

Table 2.5, compound 3az

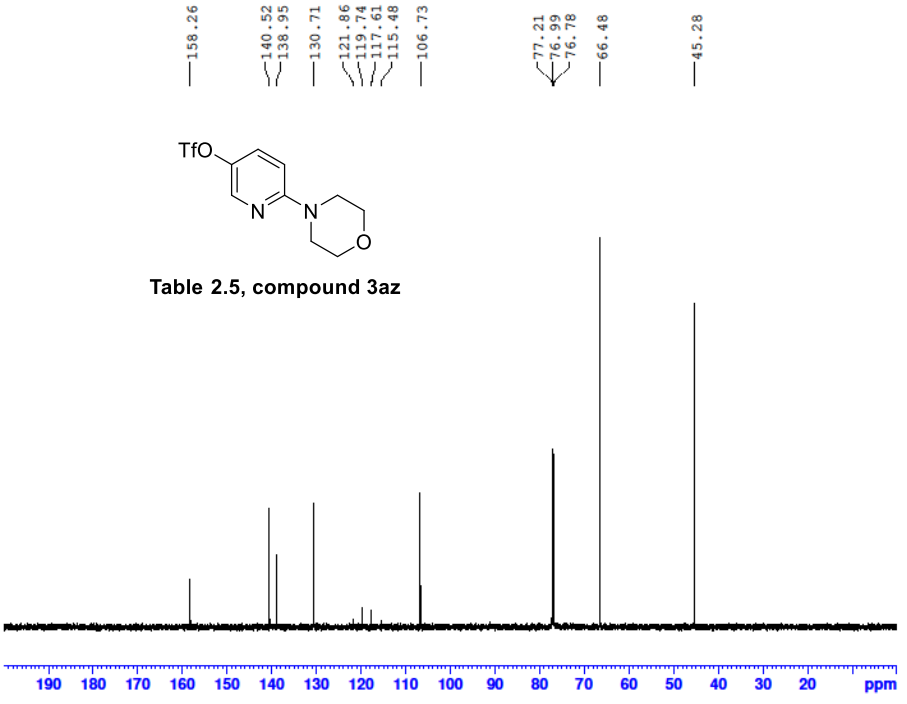

Table 2.5, compound 3az

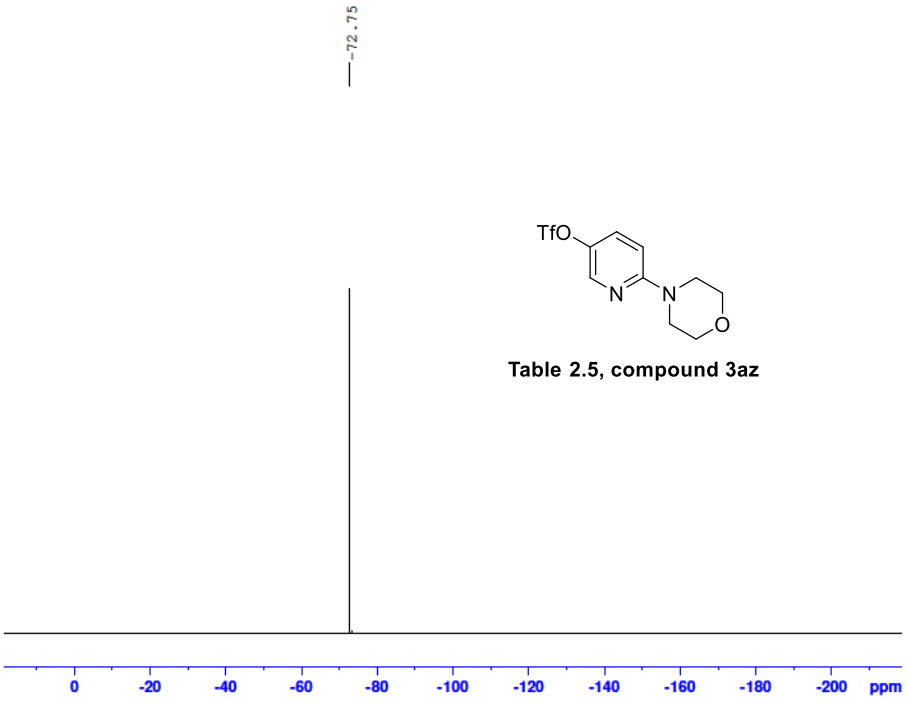

Table 2.5, compound 3az

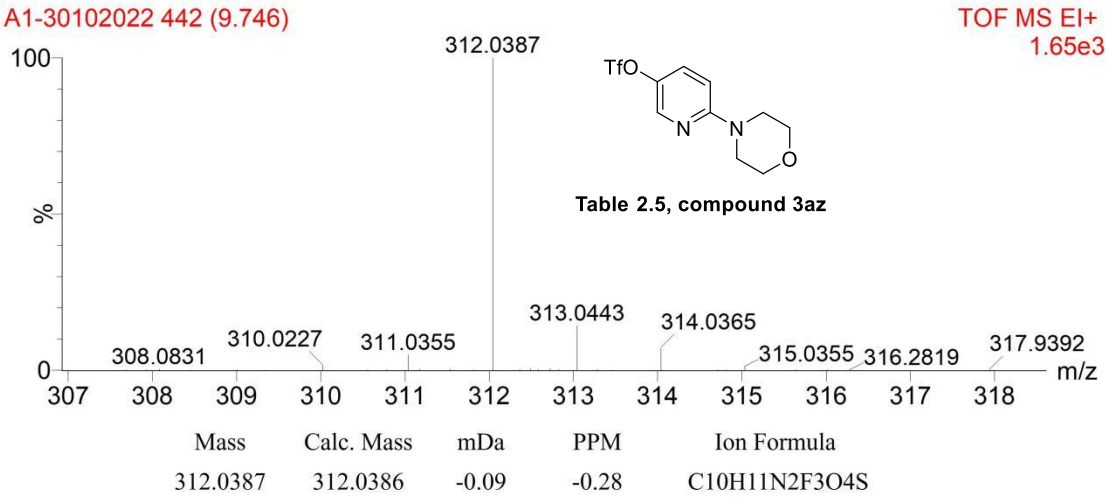

Table 2.5, compound 3az

Mass	Calc. Mass	mDa	PPM	Ion Formula
312.0387	312.0386	-0.09	-0.28	C10H11N2F3O4S

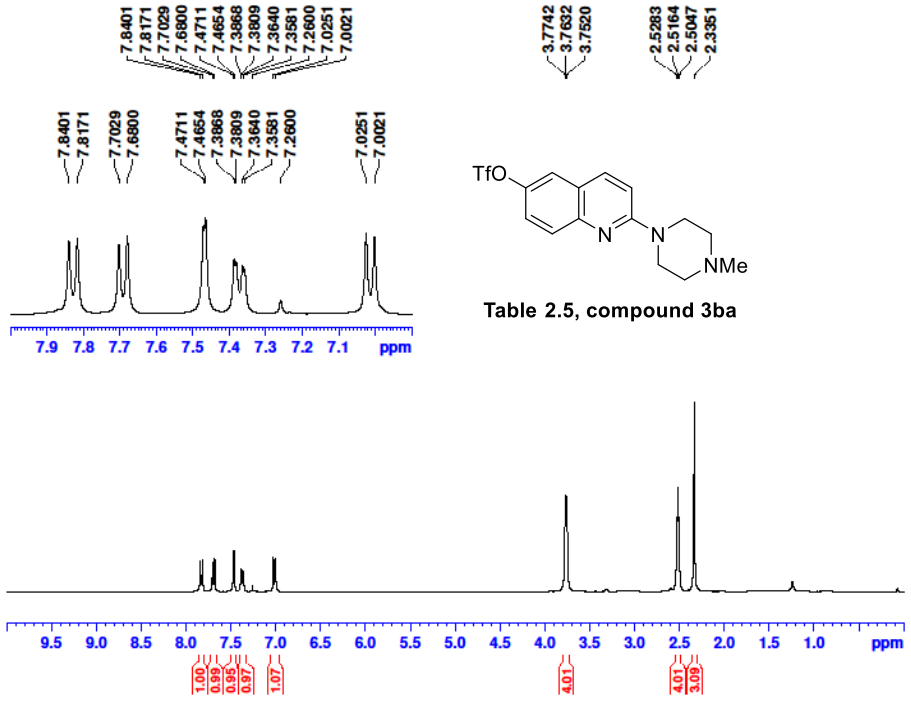

Table 2.5, compound 3ba

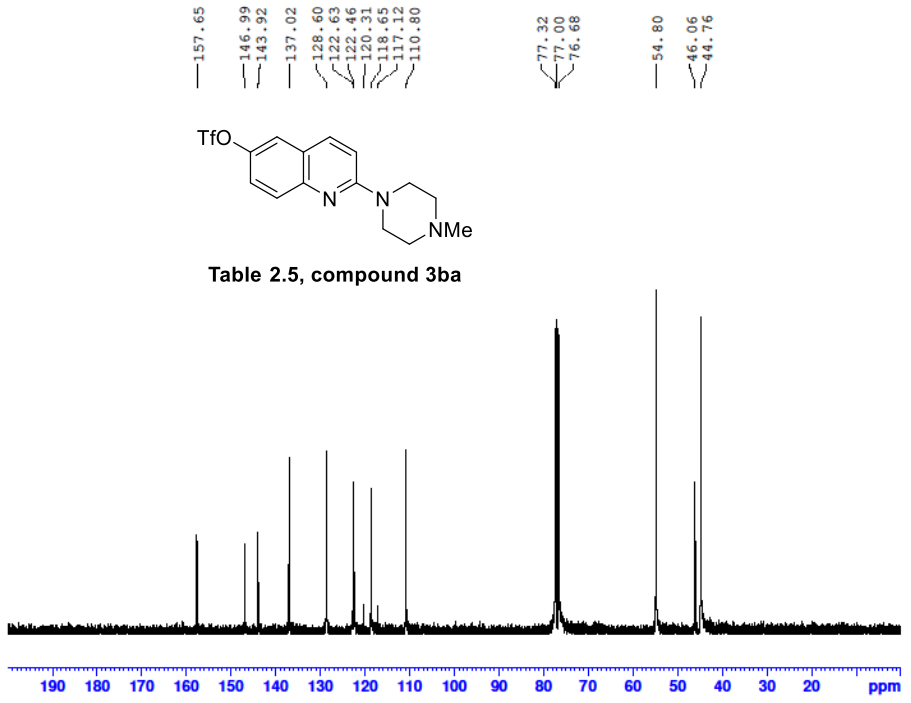

Table 2.5, compound 3ba

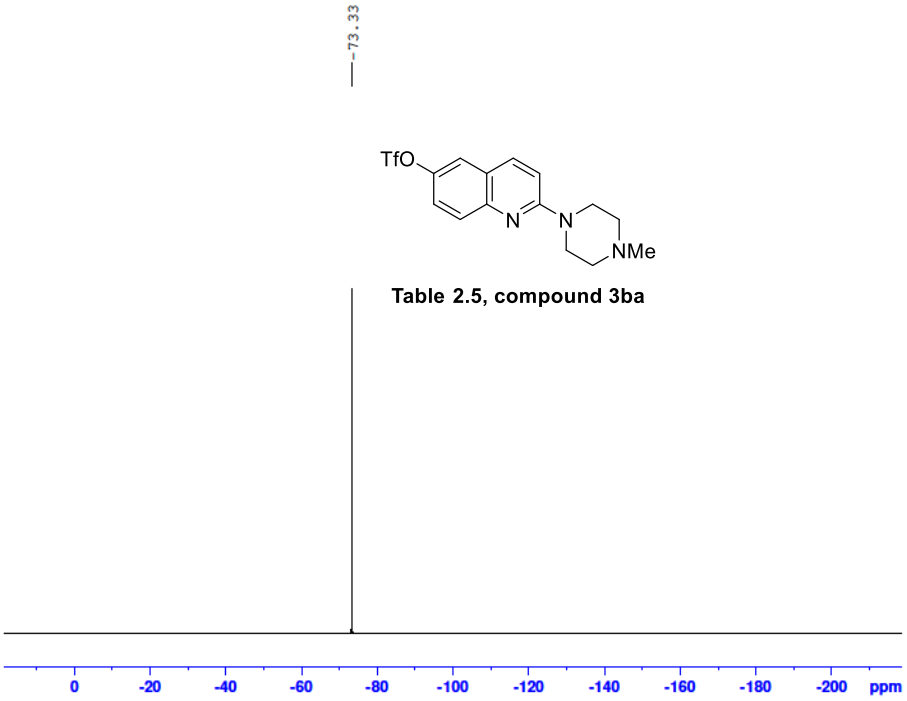

Table 2.5, compound 3ba

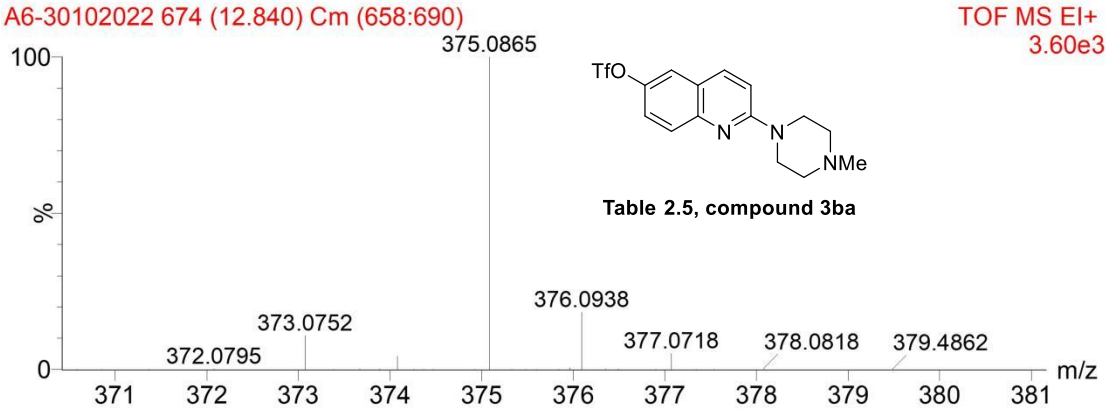

Table 2.5, compound 3ba

Mass	Calc. Mass	mDa	PPM	Ion Formula
375.0865	375.0864	-0.60	-1.60	C15H16N3F3O3S

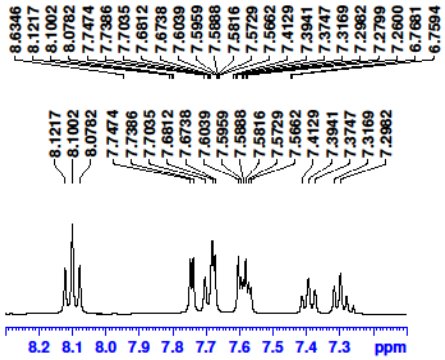

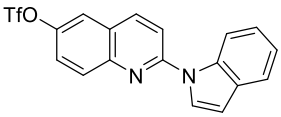

Table 2.5, compound 3bb

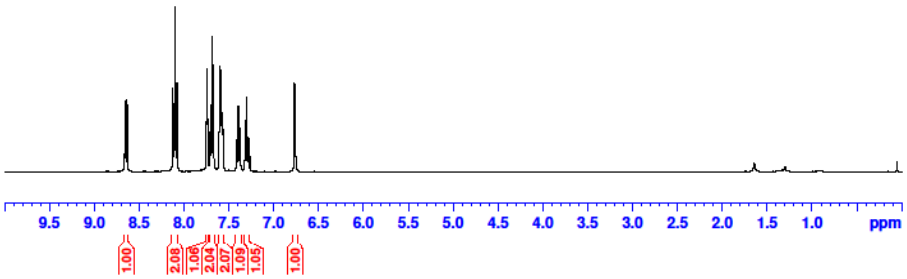

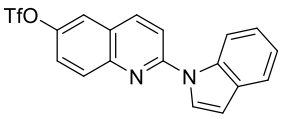

Table 2.5, compound 3bb

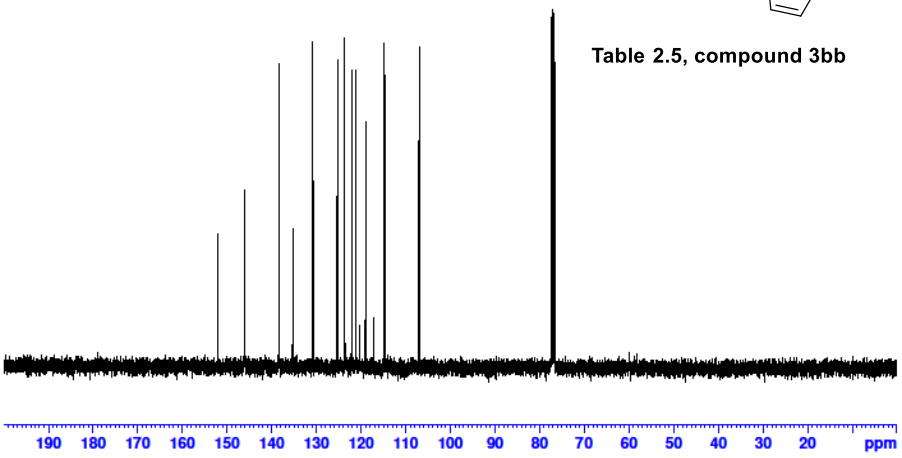

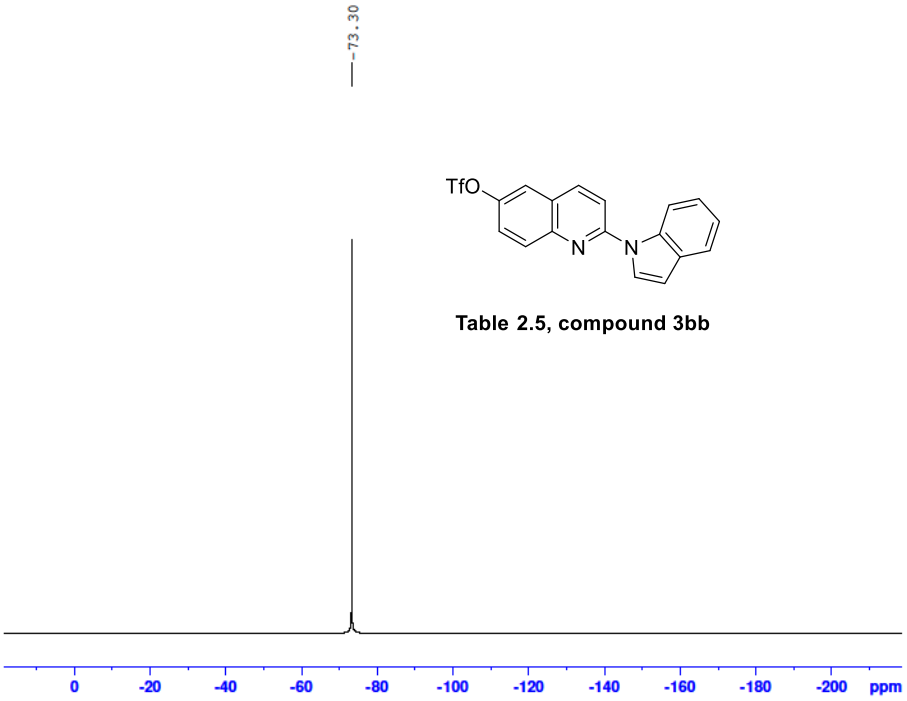

Table 2.5, compound 3bb

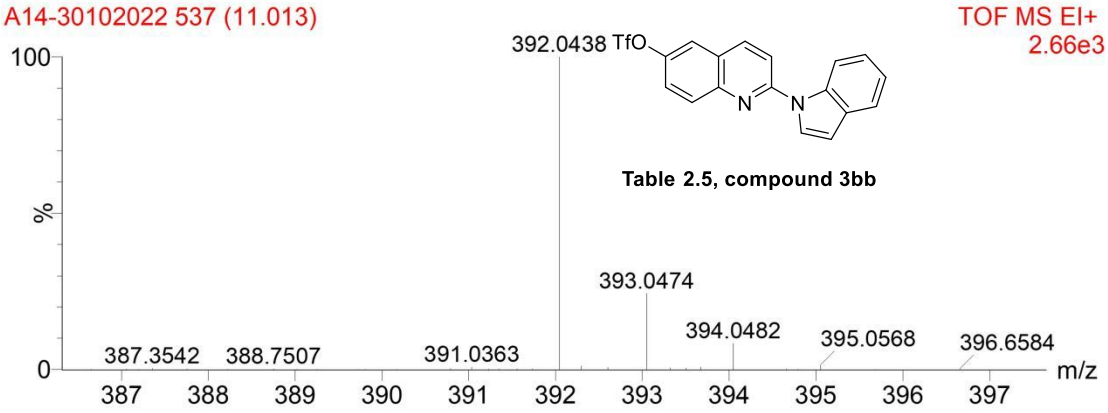

Table 2.5, compound 3bb

Mass	Calc. Mass	mDa	PPM	Ion Formula
392.0438	392.0437	-0.10	-0.26	C18H11N2F3O3S

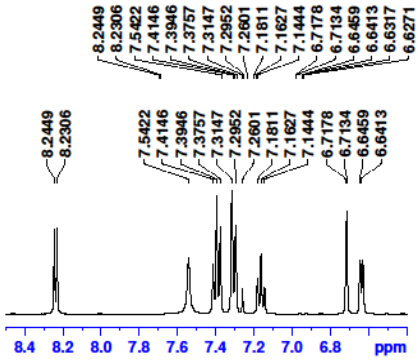

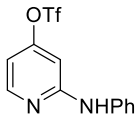

Table 2.5, compound 3bc

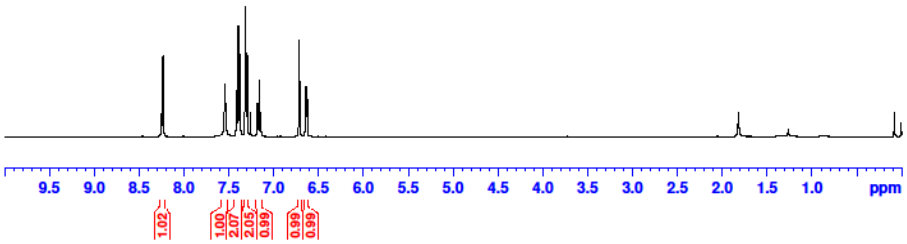

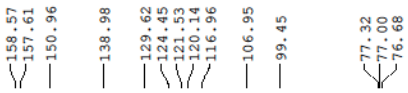

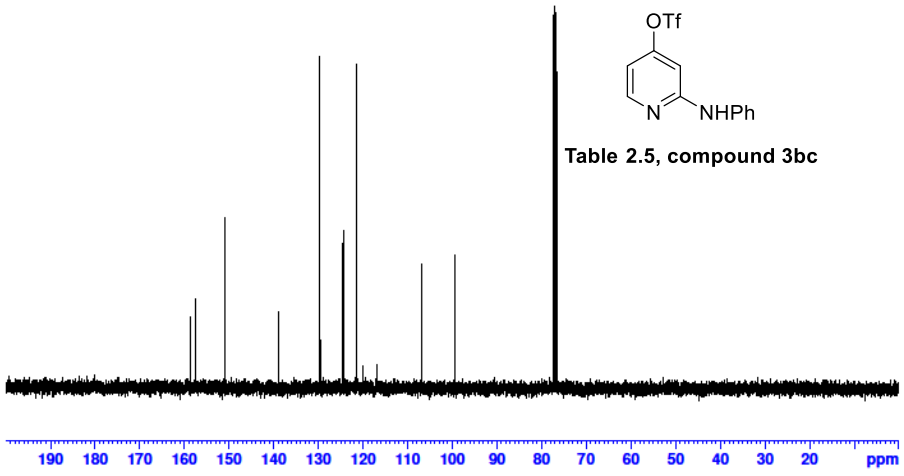

Table 2.5, compound 3bc

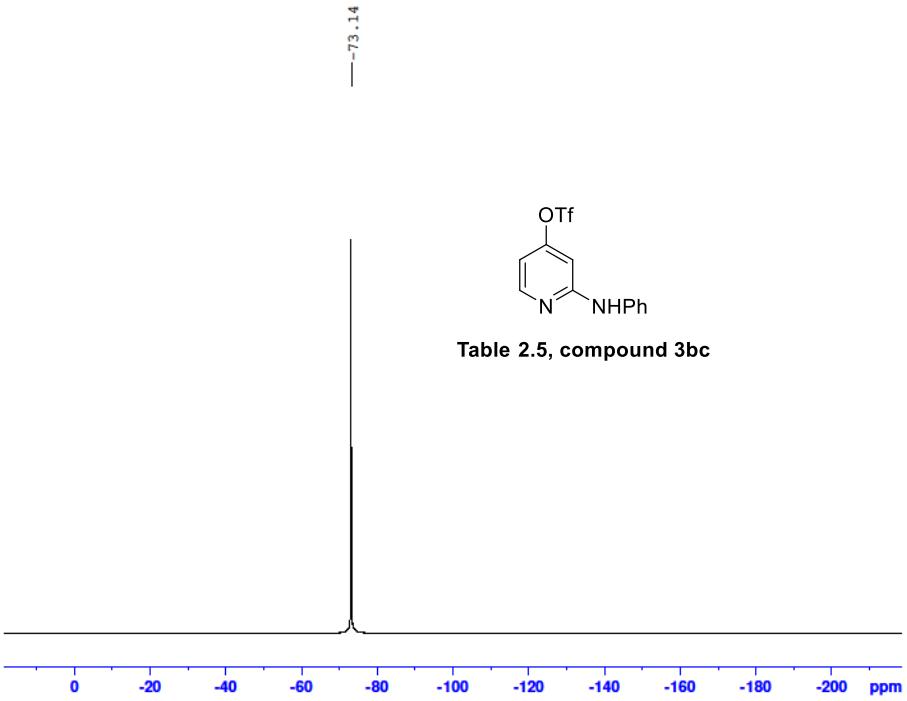

Table 2.5, compound 3bc

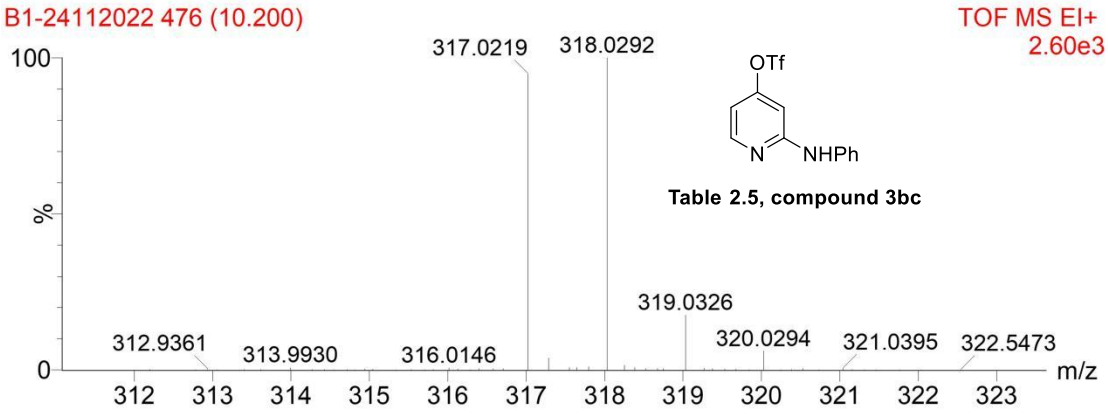

Table 2.5, compound 3bc

Mass	Calc. Mass	mDa	PPM	Ion Formula
318.0292	318.0280	-1.15	-3.62	C12H9F3O3N2S

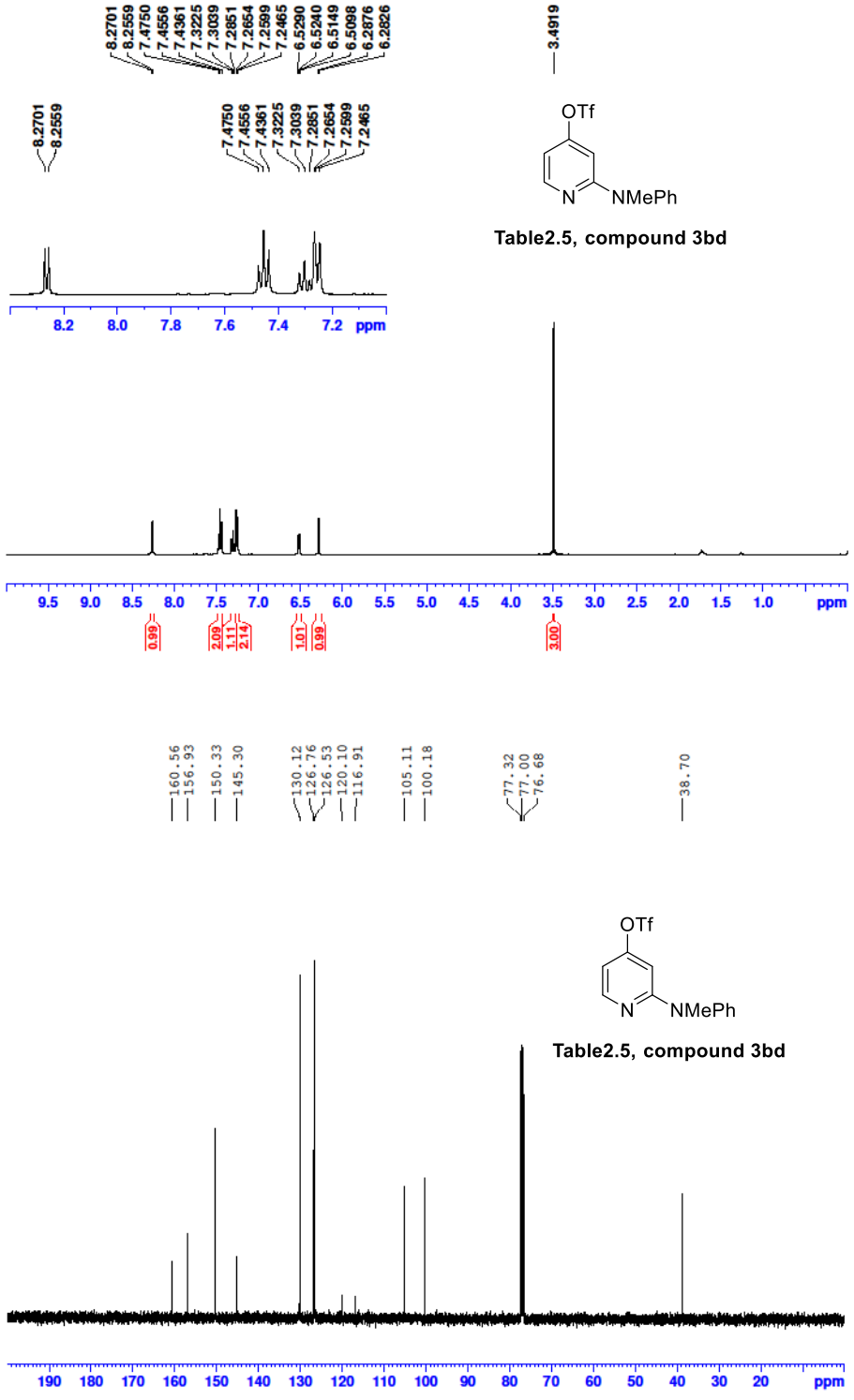

Table2.5, compound 3bd

Table2.5, compound 3bd

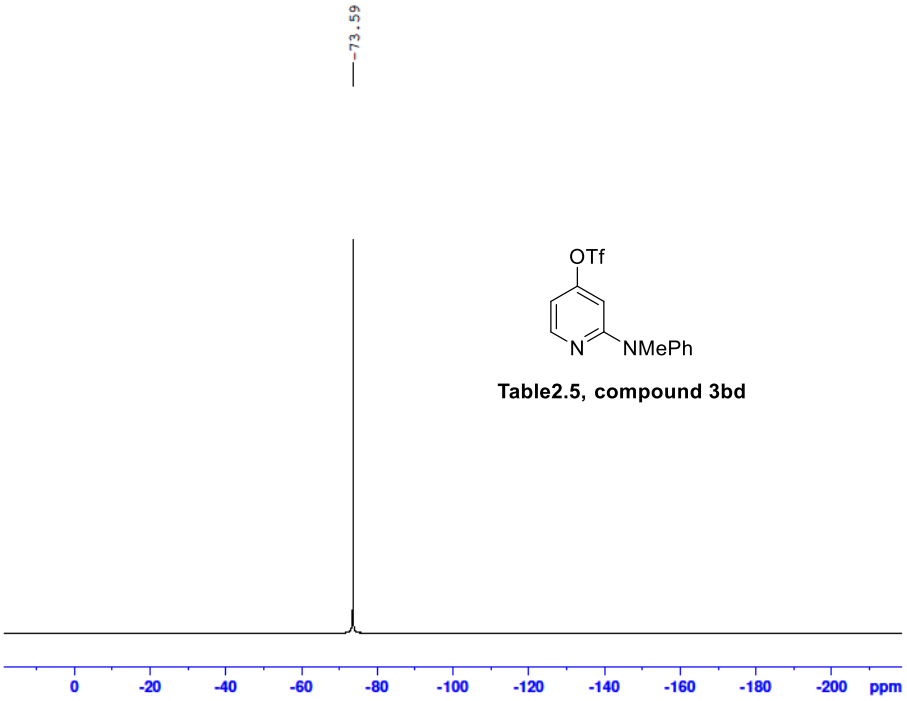

Table2.5, compound 3bd

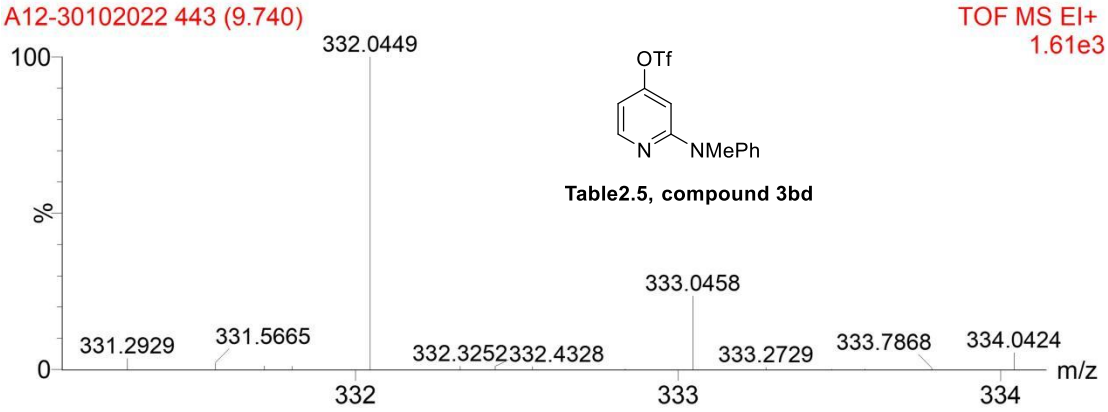

OTf
N
NMePh

Table2.5, compound 3bd

Mass	Calc. Mass	mDa	PPM	Ion Formula
332.0449	332.0437	-1.20	-3.62	C13H11N2F3O3S

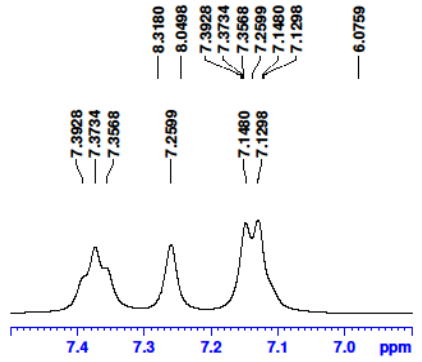

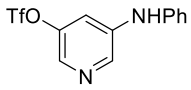

Table 2.5, compound 3be

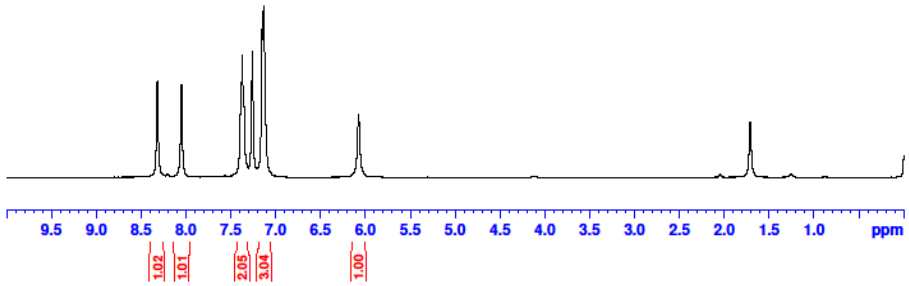

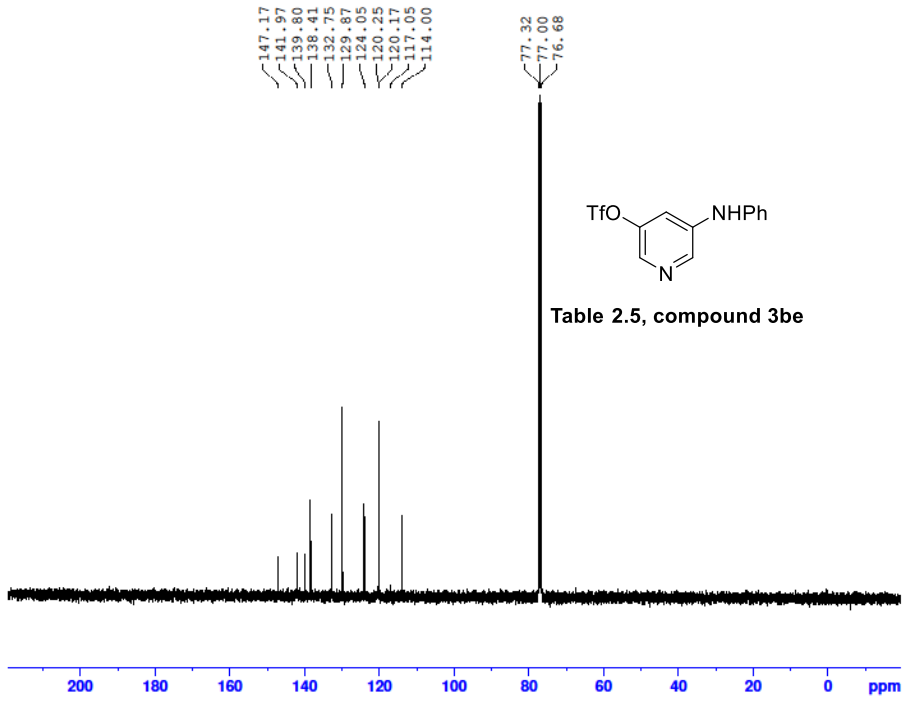

Table 2.5, compound 3be

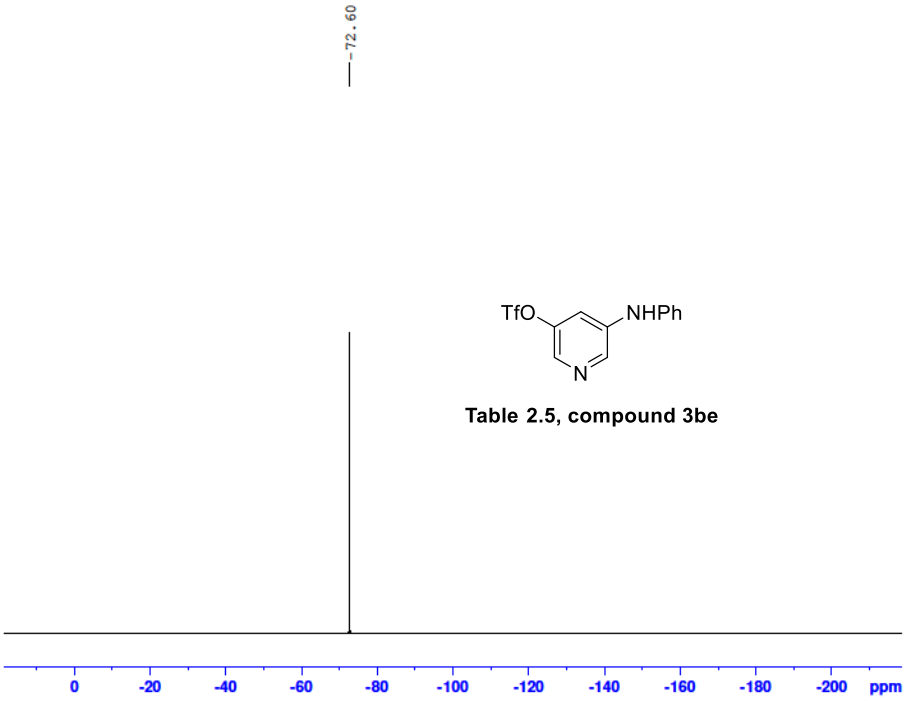

Table 2.5, compound 3be

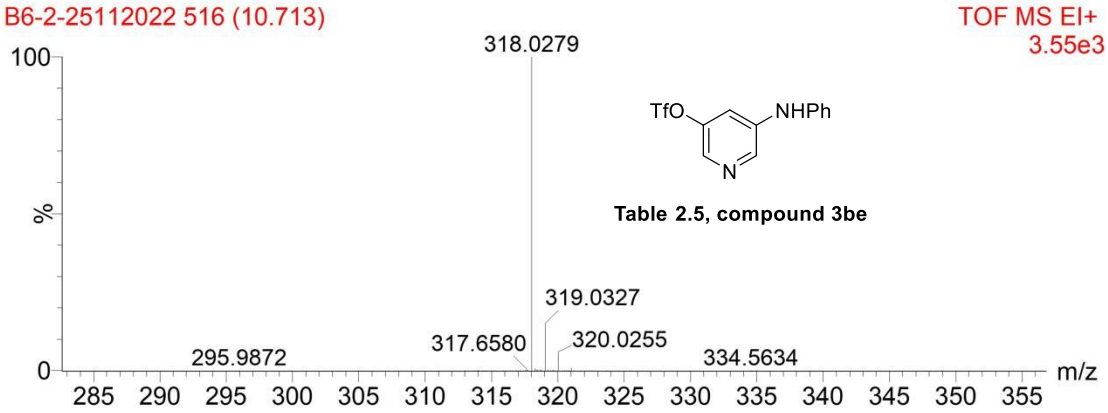

Table 2.5, compound 3be

Mass	Calc. Mass	mDa	PPM	Ion Formula
318.0279	318.0280	0.15	0.47	C12H9F3O3N2S

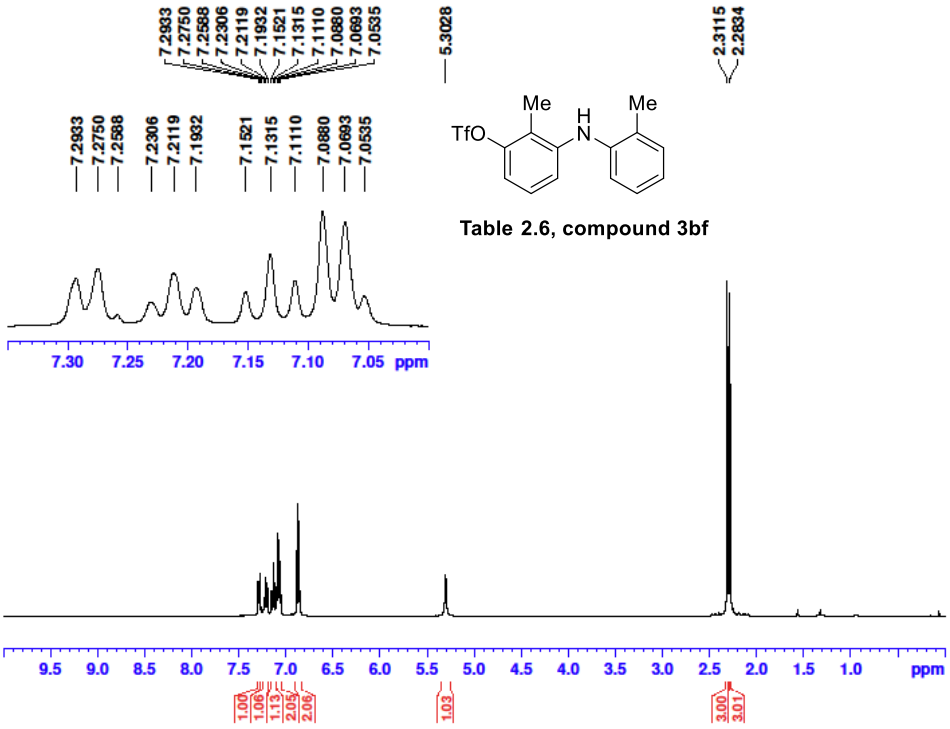

Table 2.6, compound 3bf

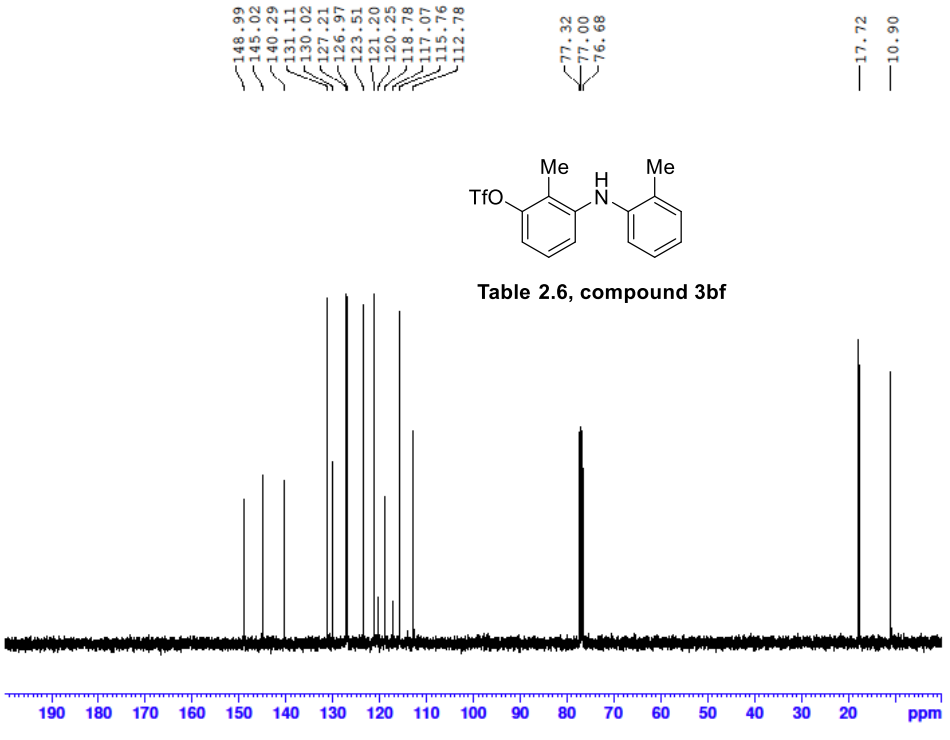

Table 2.6, compound 3bf

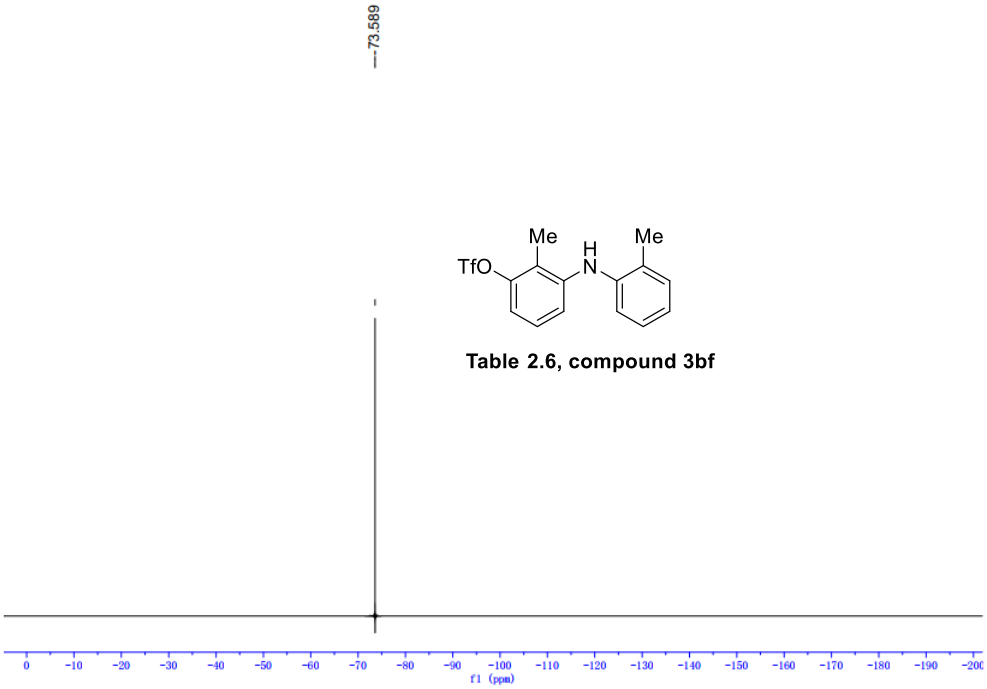

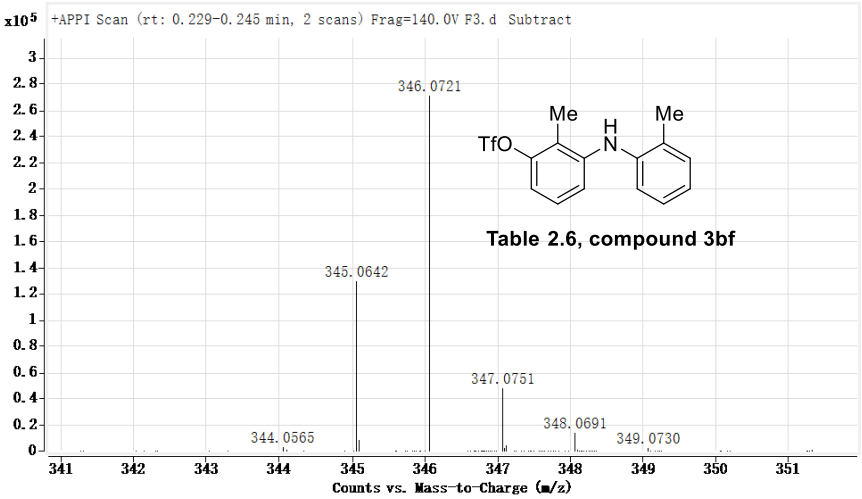

Mass	Calc. Mass	mDa	PPM	Formula
346.0721	346.0719	-0.17	-0.51	C15 H15 F3 N O3 S

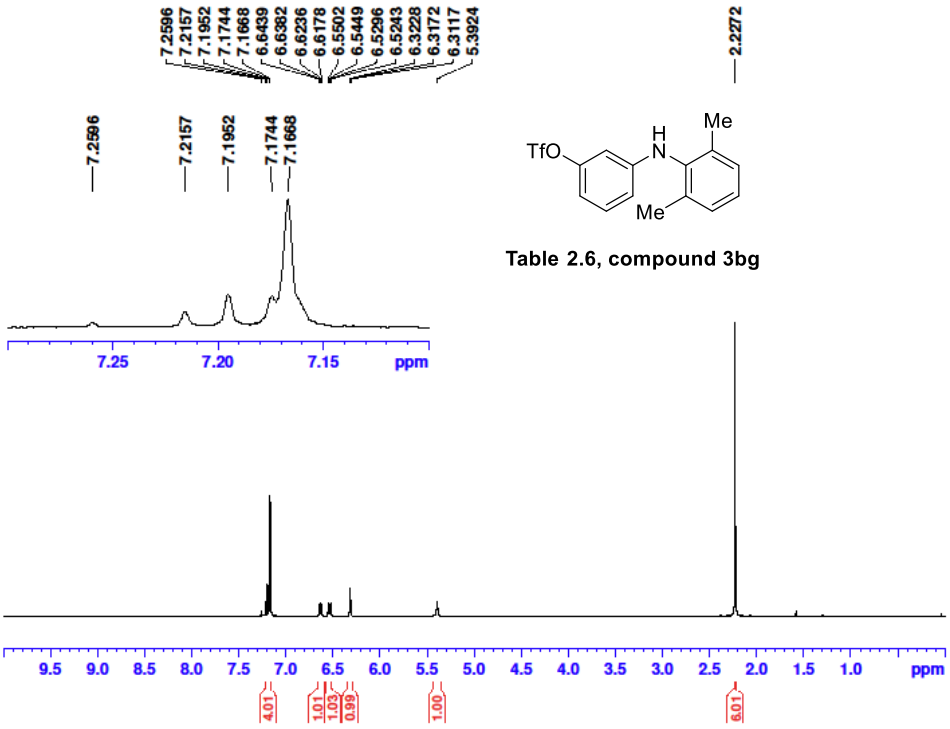

Table 2.6, compound 3bg

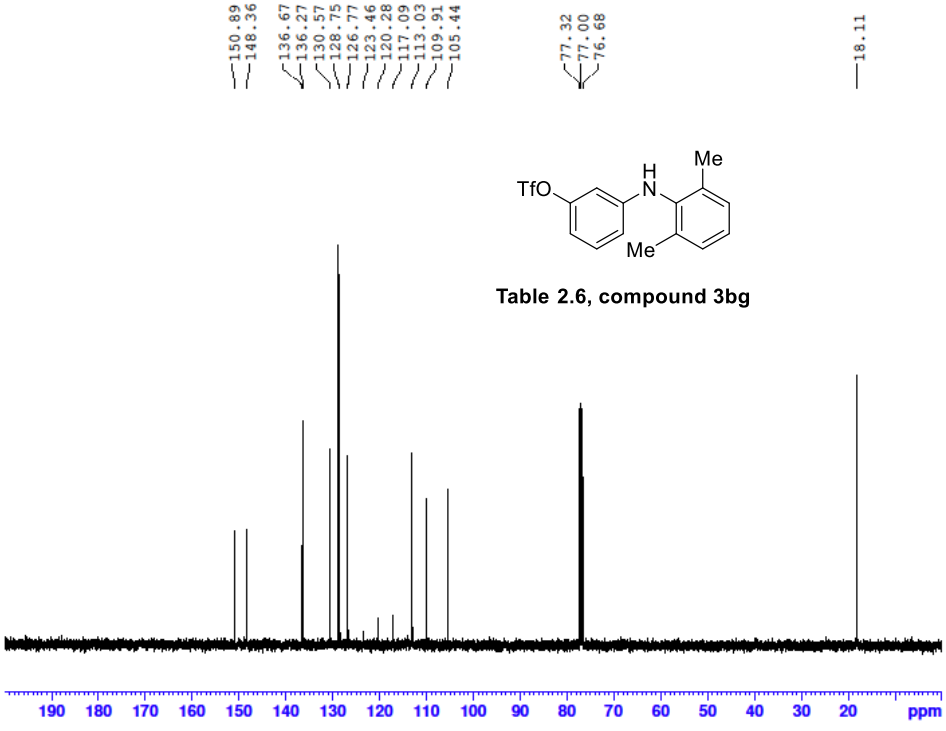

Table 2.6, compound 3bg

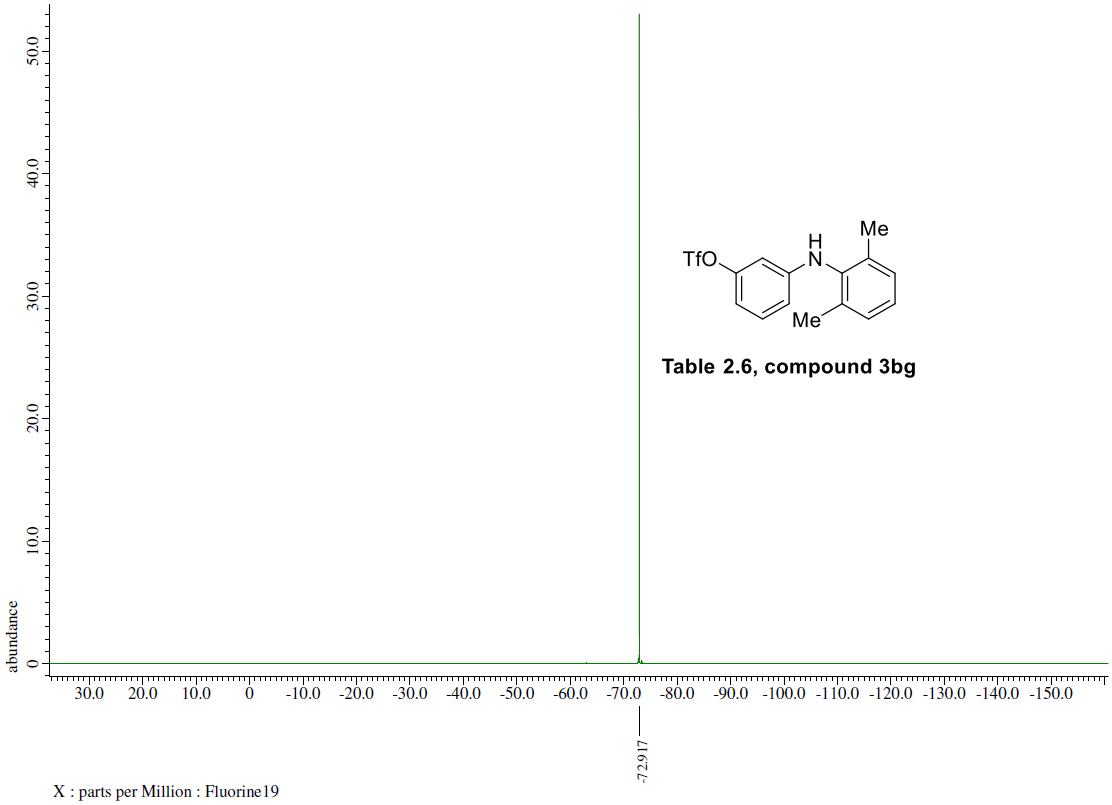

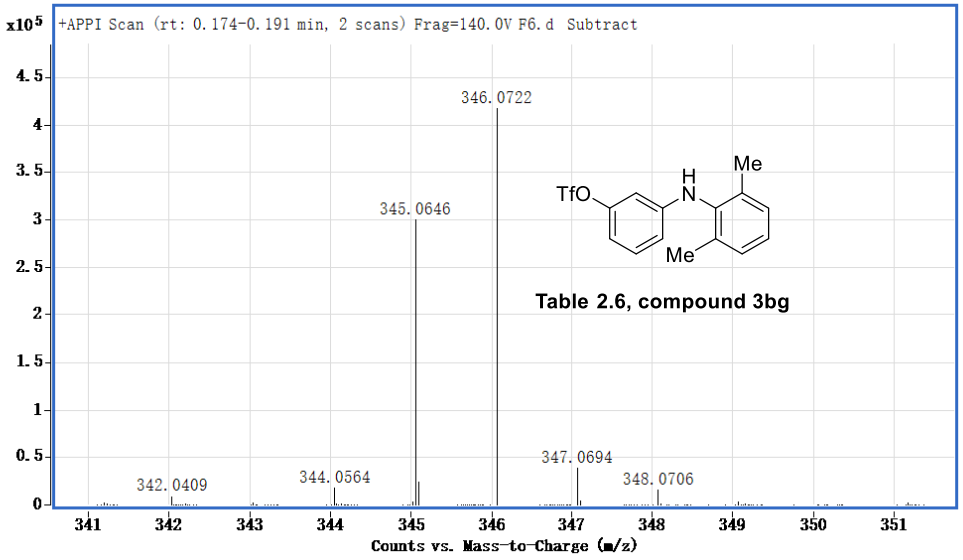

Mass	Calc. Mass	mDa	PPM	Formula
346.0722	346.0719	-0.27	-0.8	C15 H15 F3 N O3 S

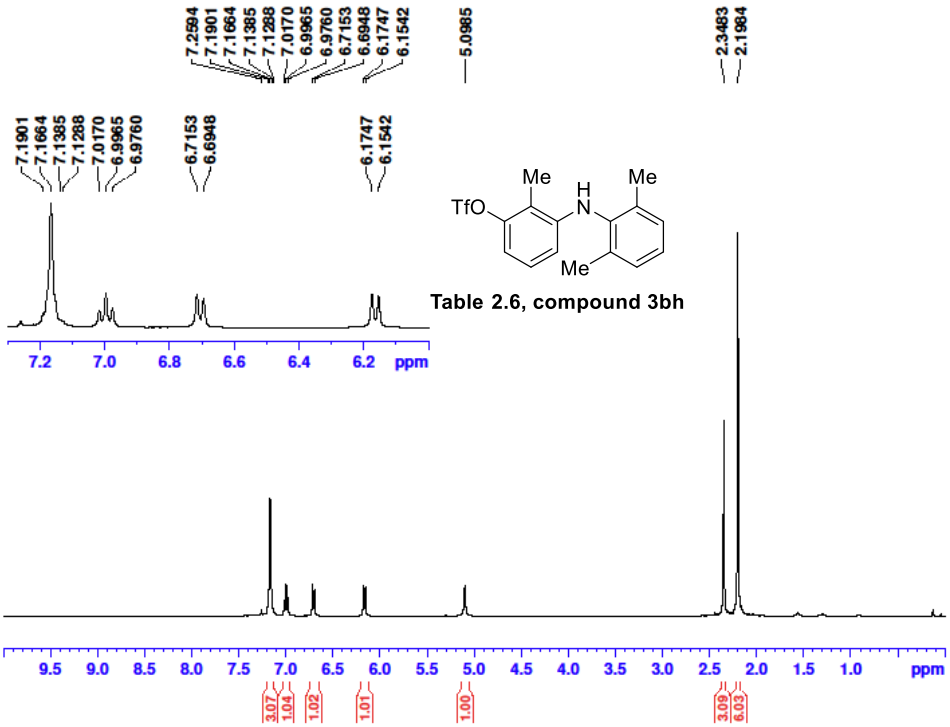

Table 2.6, compound 3bh

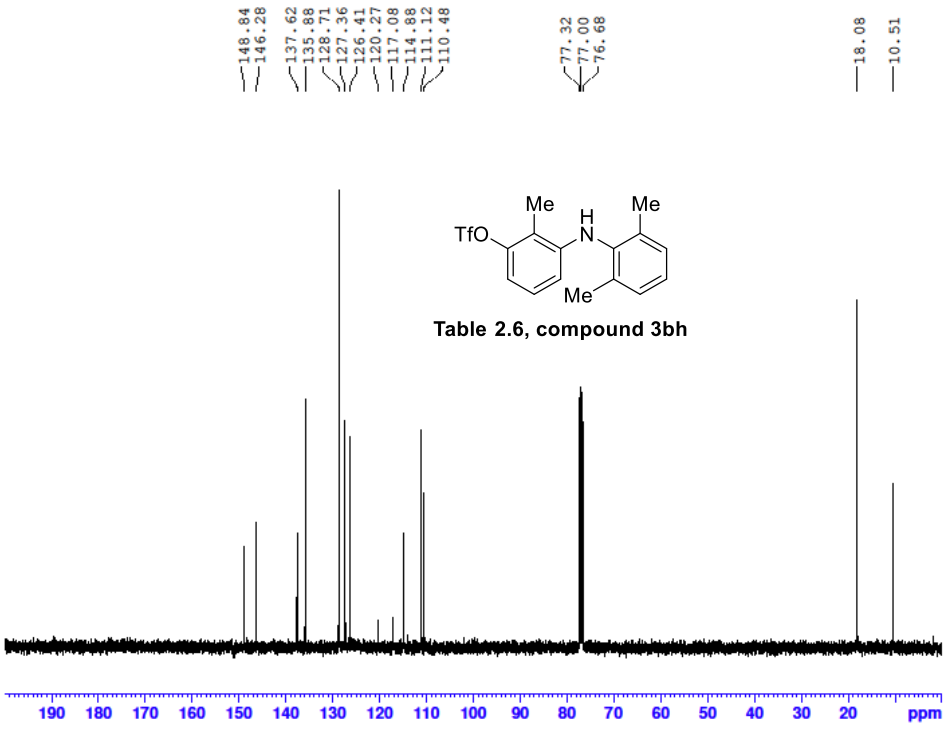

Table 2.6, compound 3bh

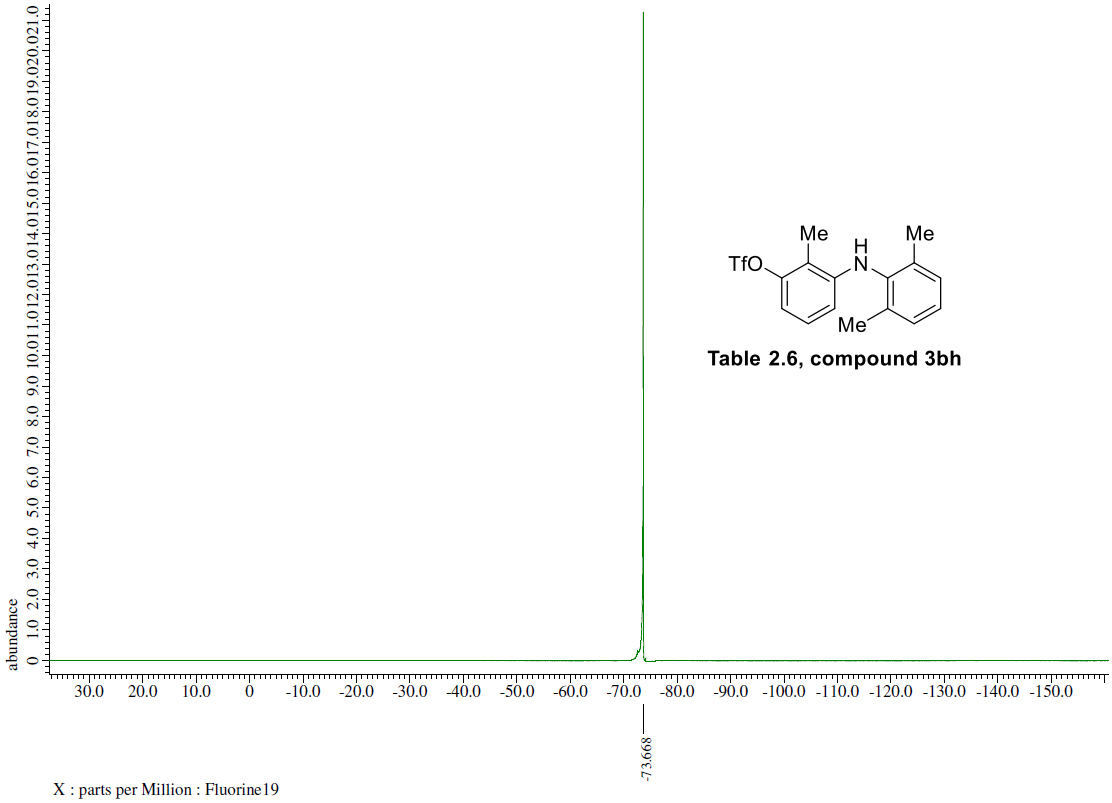

Table 2.6, compound 3bh

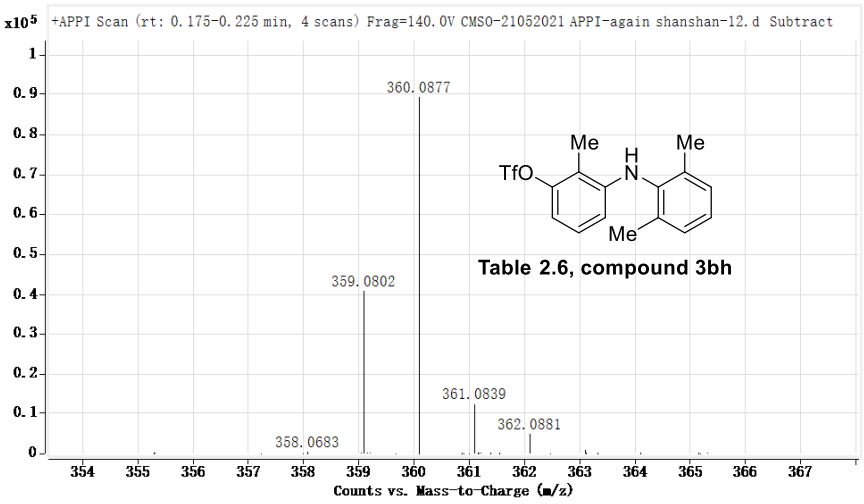

Table 2.6, compound 3bh

Mass	Calc. Mass	mDa	PPM	Formula
360.0877	360.0876	-0.12	-0.35	C16 H17 F3 N O3 S

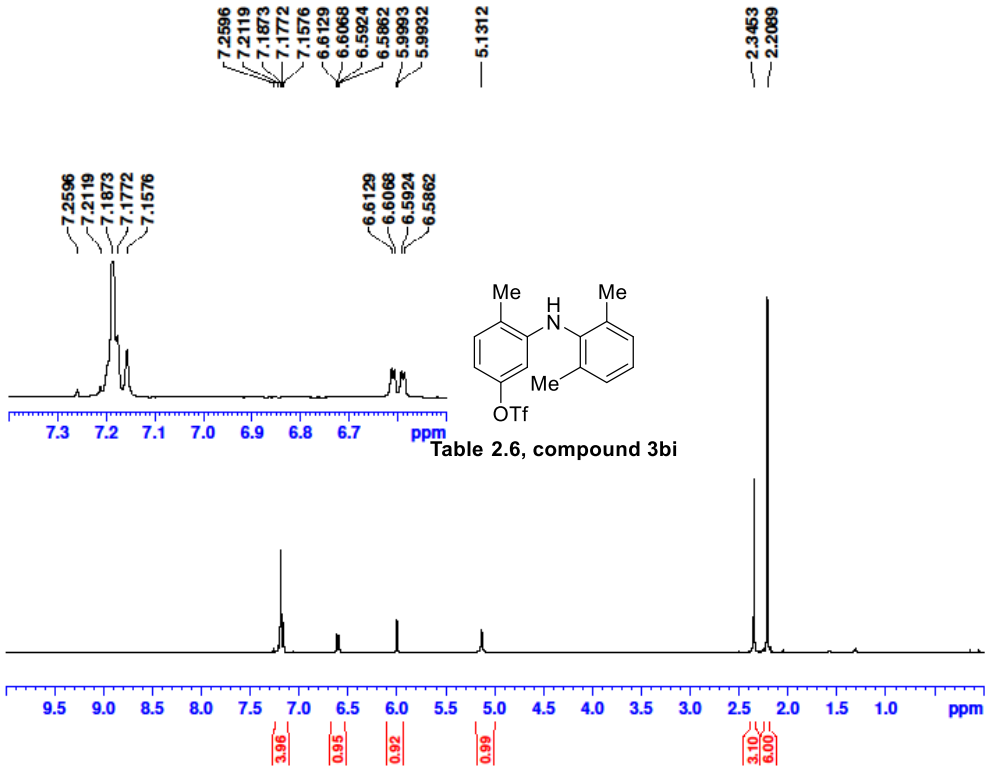

Table 2.6, compound 3bi

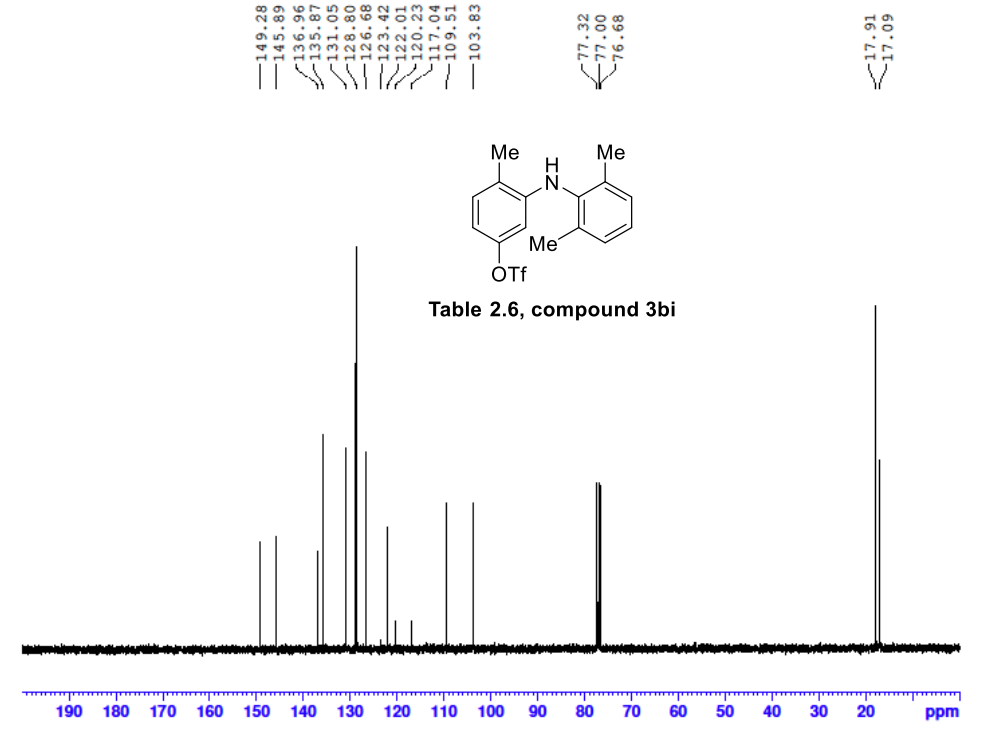

Table 2.6, compound 3bi

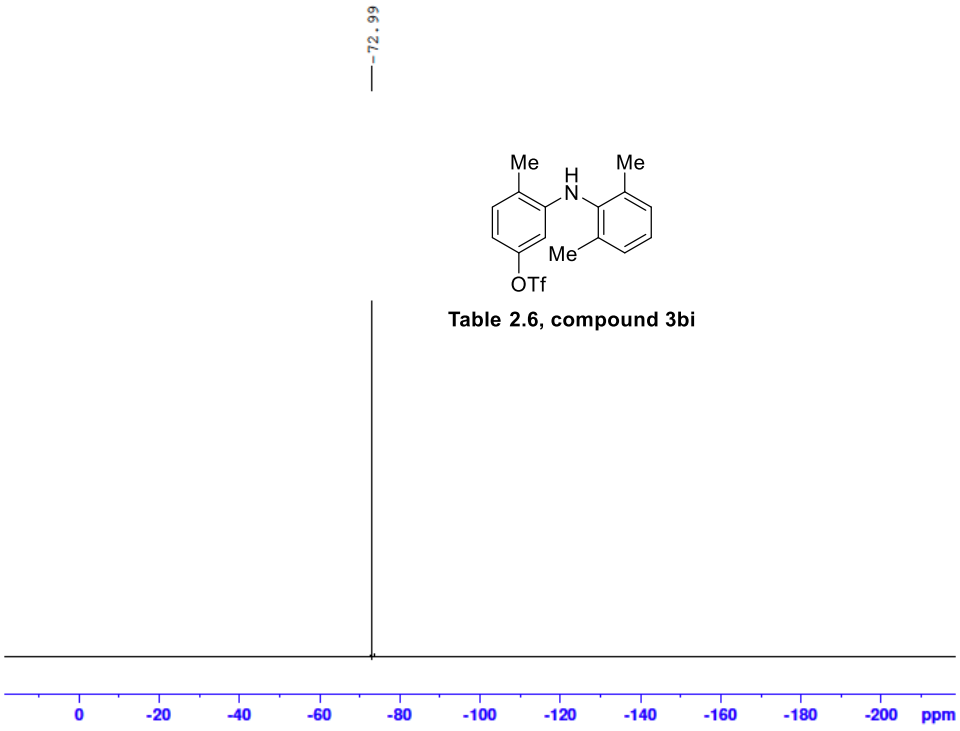

Table 2.6, compound 3bi

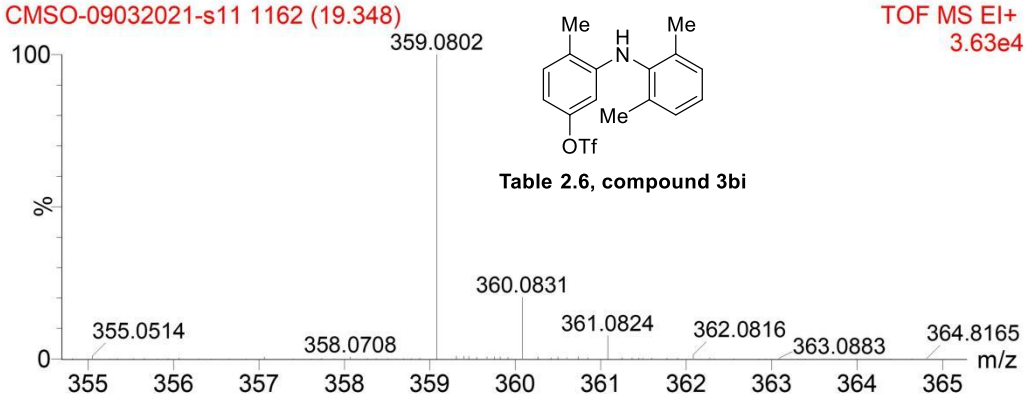

Table 2.6, compound 3bi

Mass	Calc. Mass	mDa	PPM	Formula
359.0802	359.0798	-0.45	1.25	C16 H16 F3NO3S

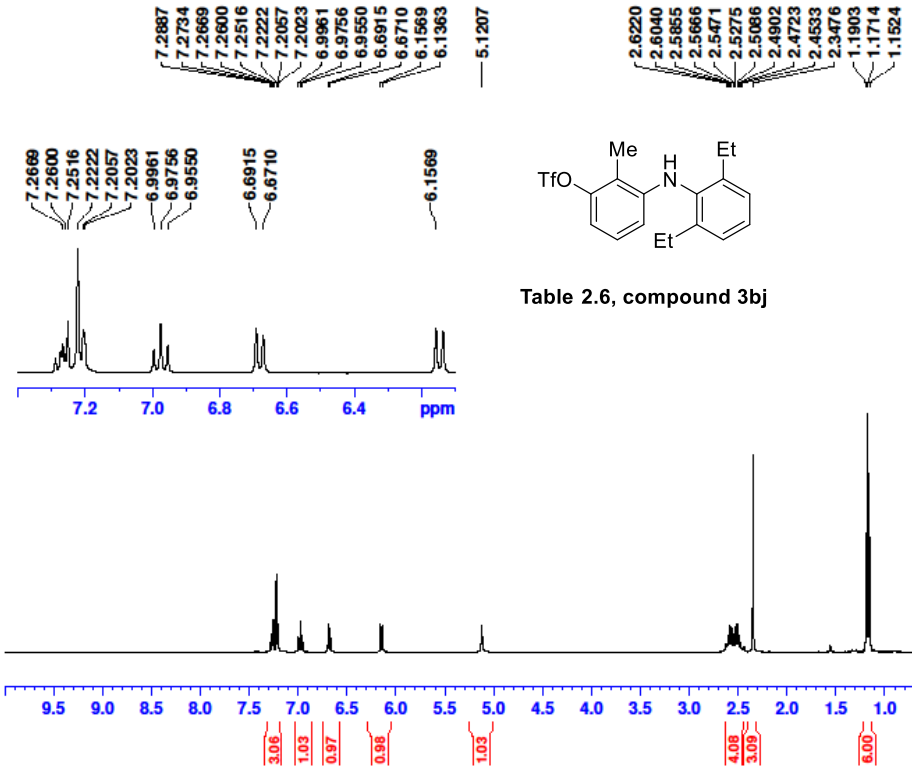

Table 2.6, compound 3bj

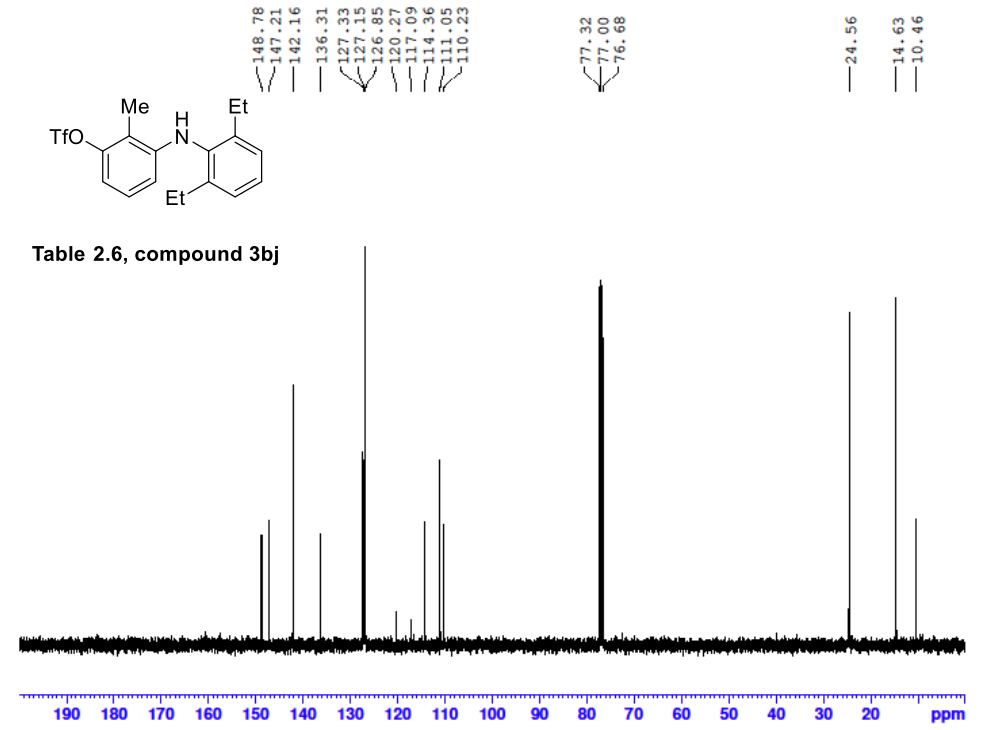

Table 2.6, compound 3bj

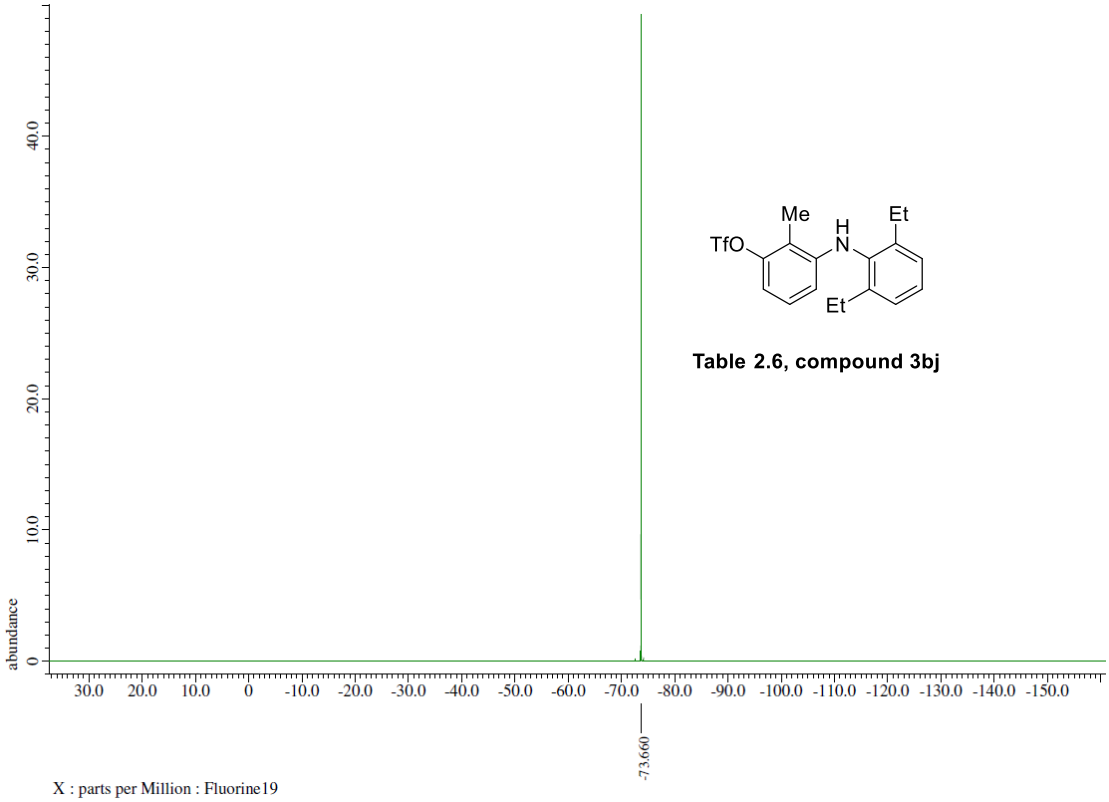

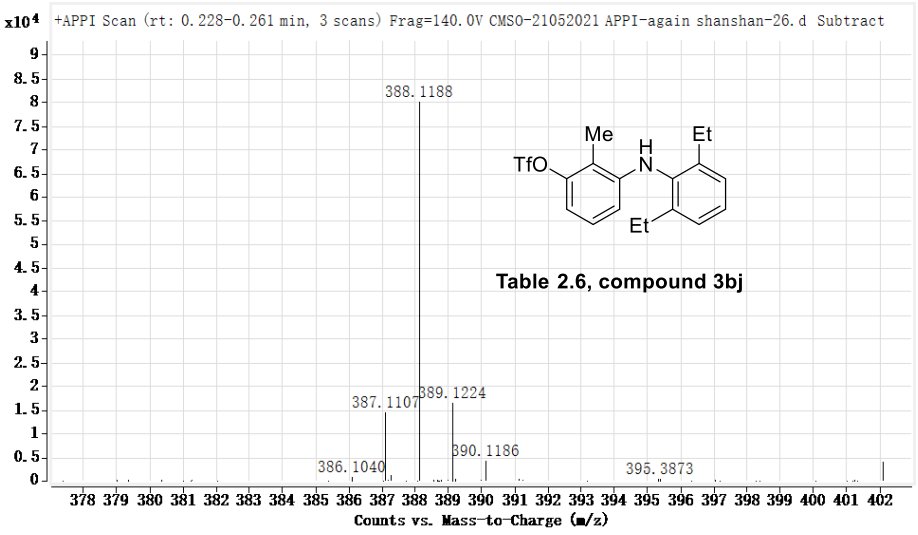

Mass	Calc. Mass	mDa	PPM	Formula
388.1188	388.1189	0.08	0.19	C18 H21 F3 N O3 S

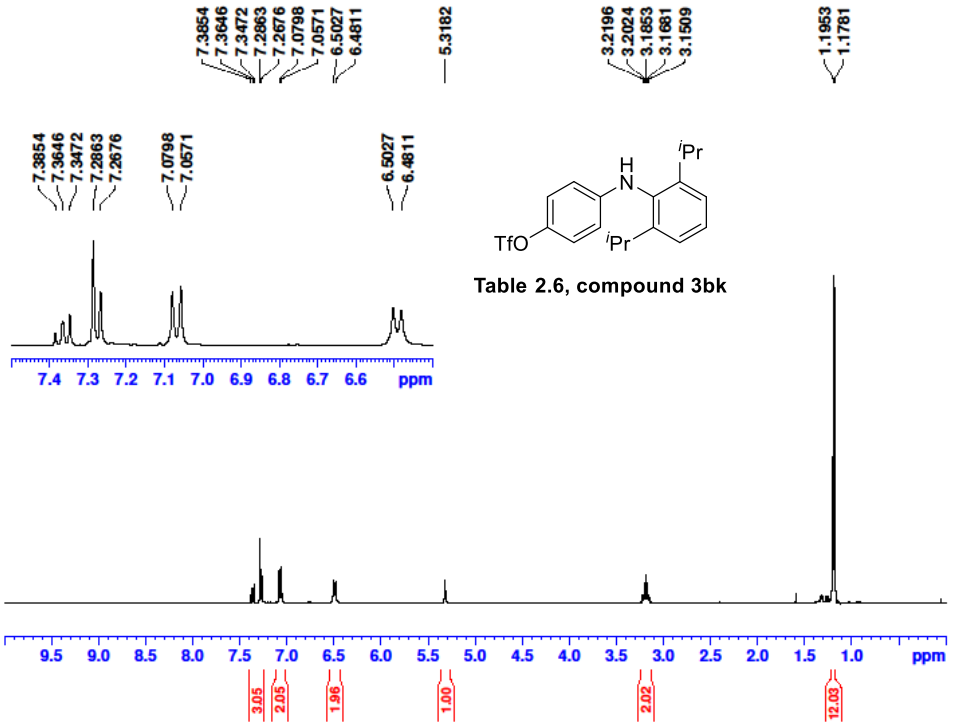

Table 2.6, compound 3bk

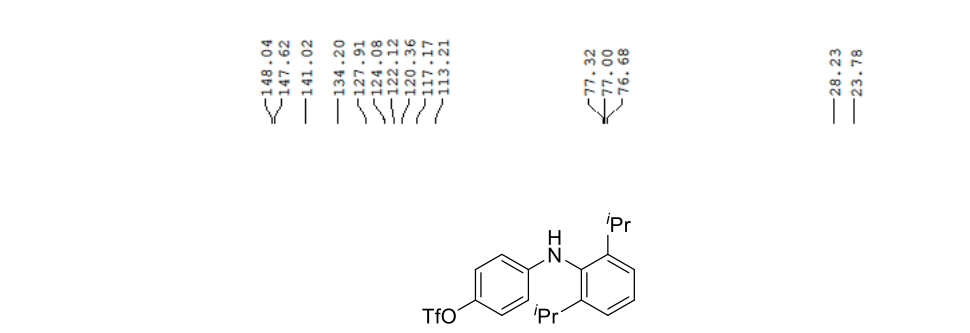

Table 2.6, compound 3bk

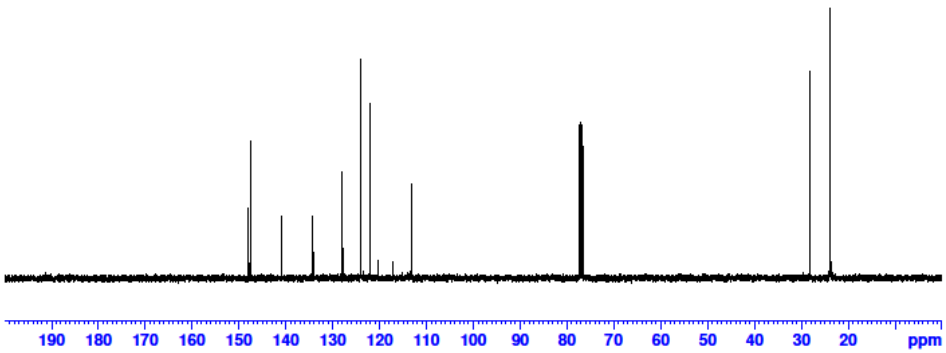

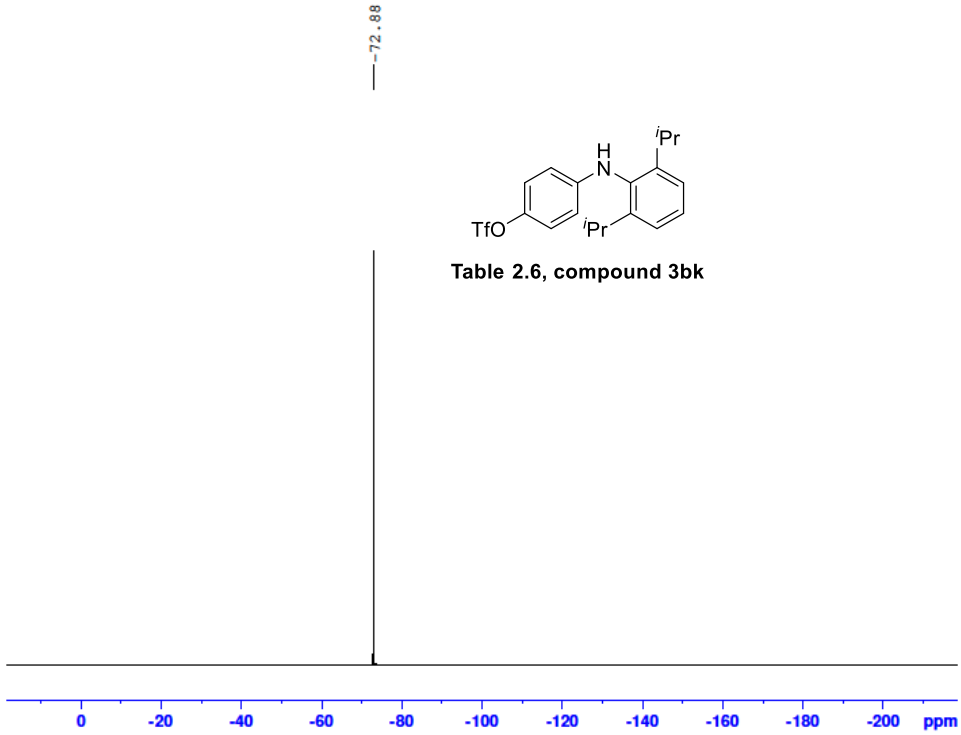

Table 2.6, compound 3bk

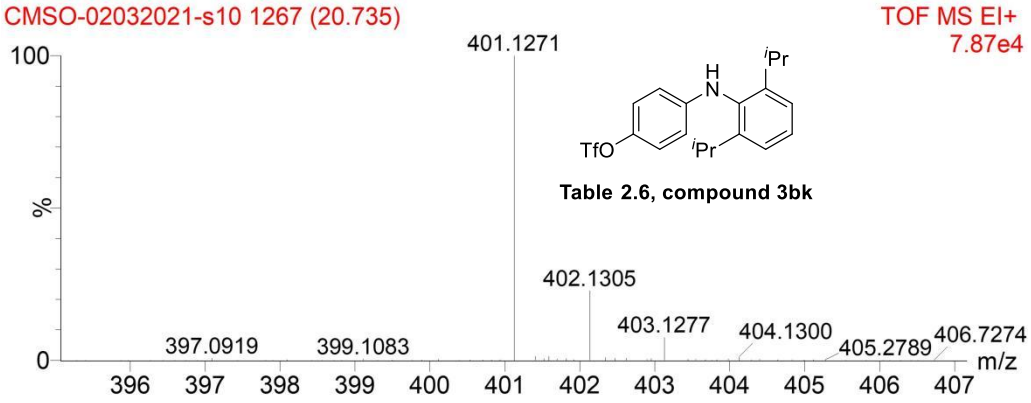

Table 2.6, compound 3bk

Mass	Calc. Mass	mDa	PPM	Formula
401.1271	401.1267	-0.40	-1.00	C19H22 F3NO3S

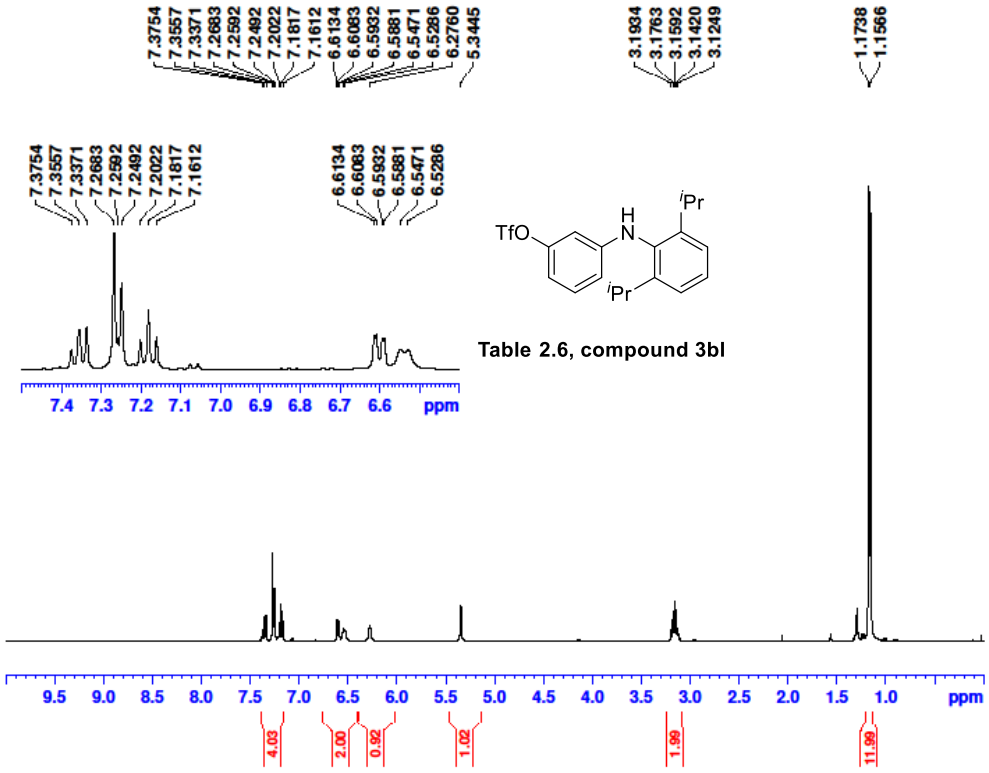

Table 2.6, compound 3bl

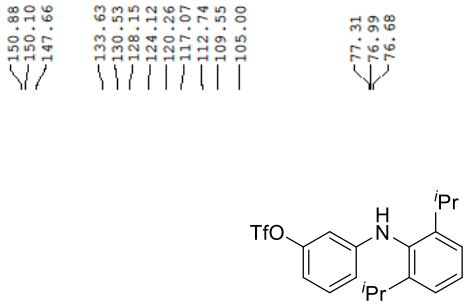

Table 2.6, compound 3bl

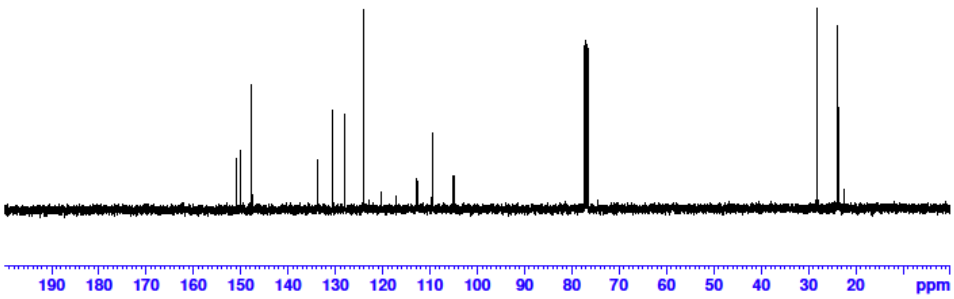

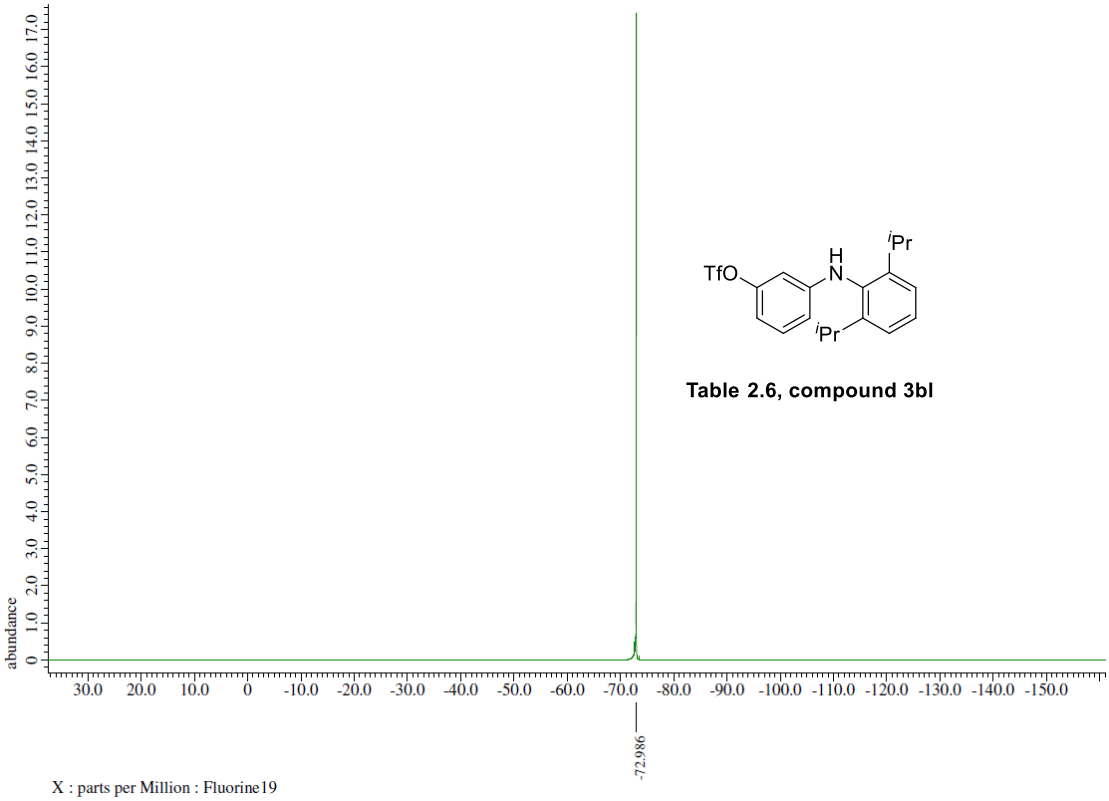

Table 2.6, compound 3bl

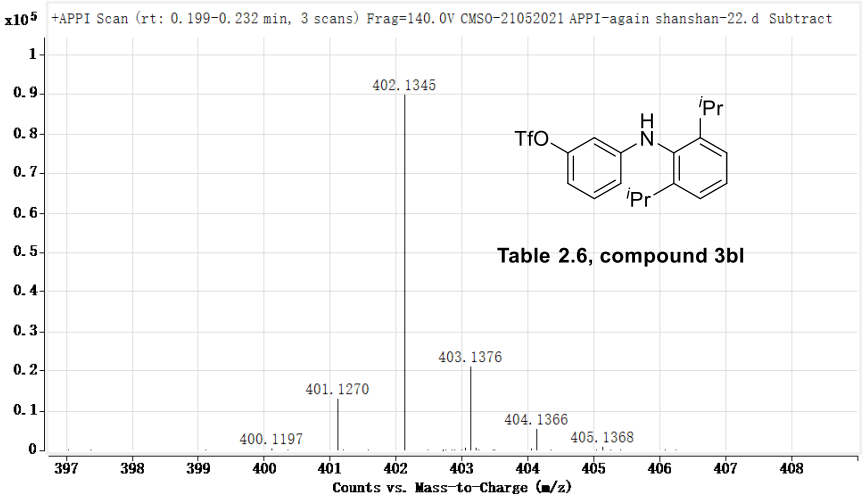

Table 2.6, compound 3bl

Mass	Calc. Mass	mDa	PPM	Formula
402.1345	402.1345	0.03	0.06	C19 H23 F3 N O3 S

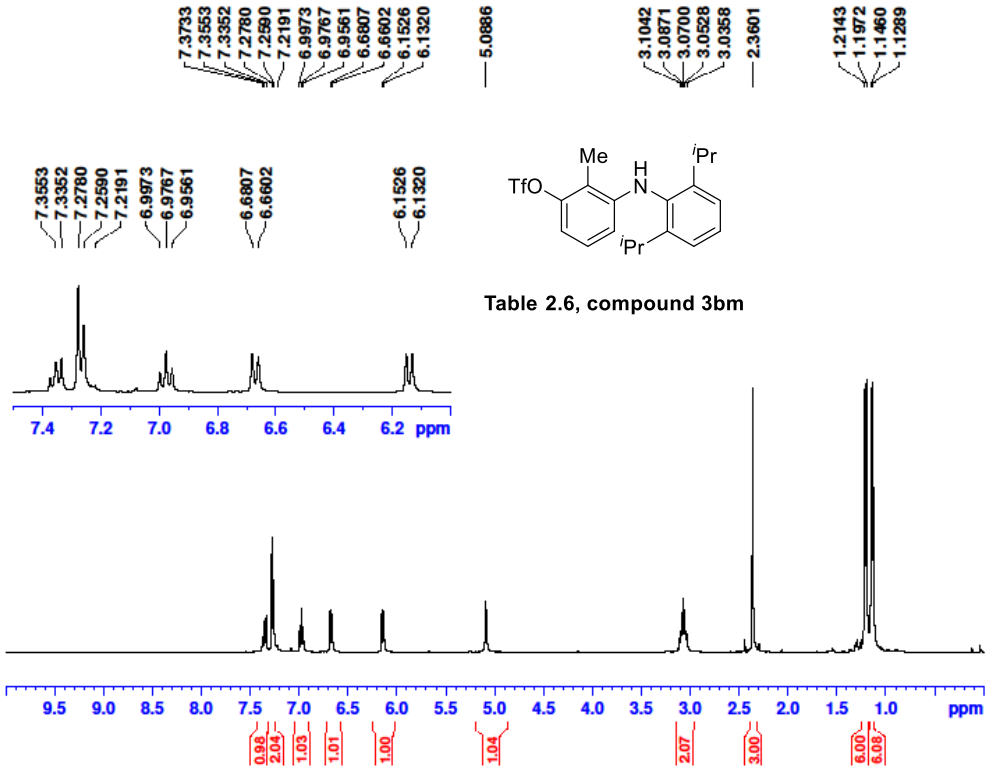

Table 2.6, compound 3bm

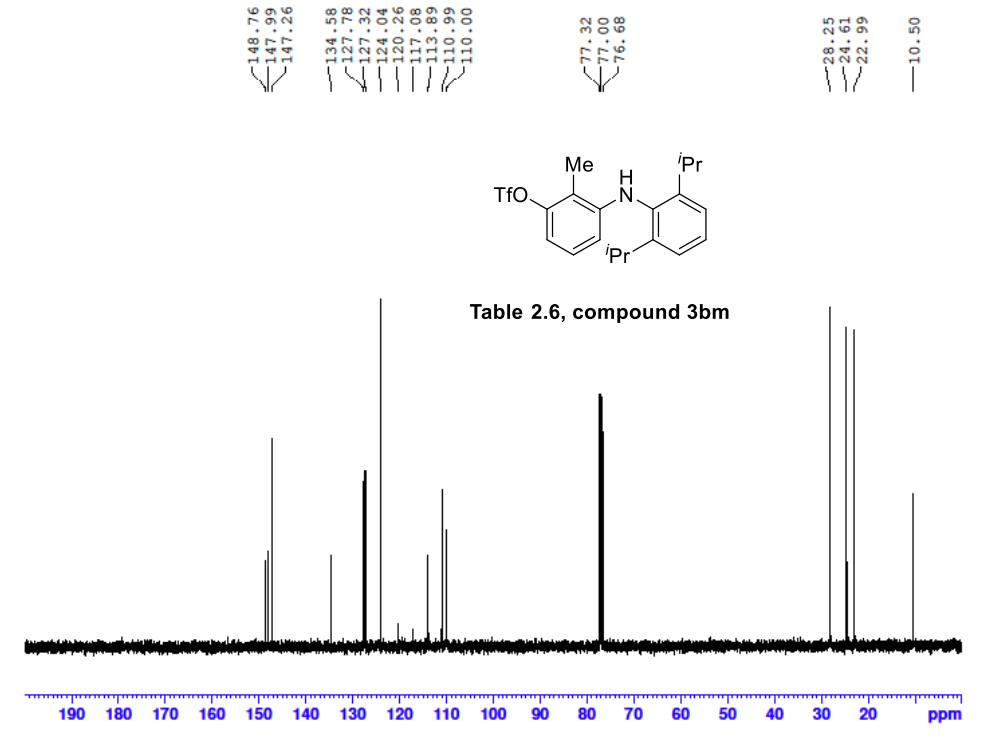

Table 2.6, compound 3bm

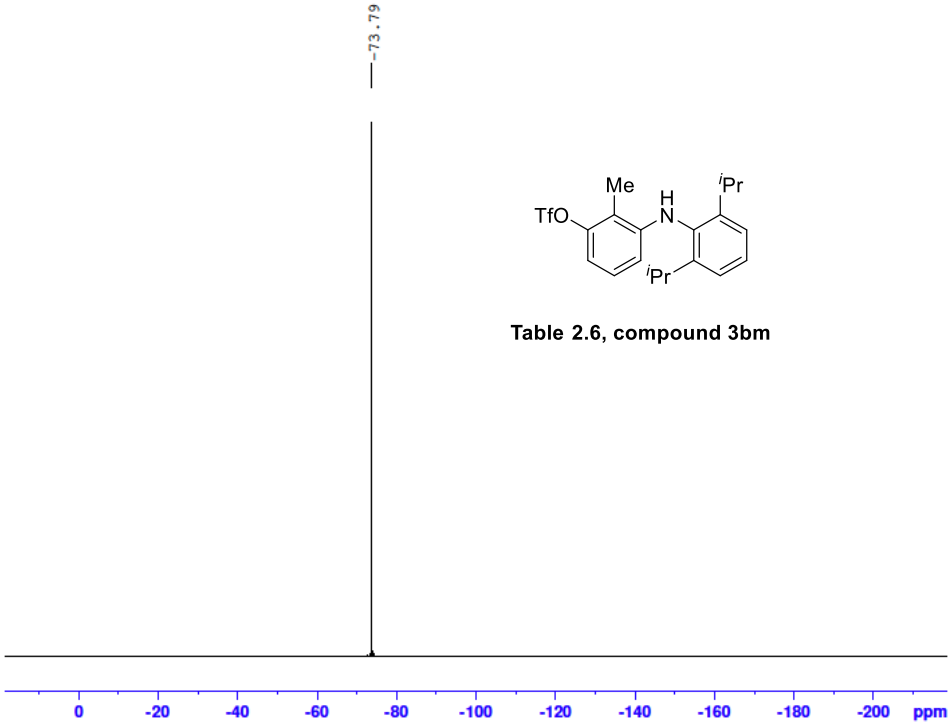

Table 2.6, compound 3bm

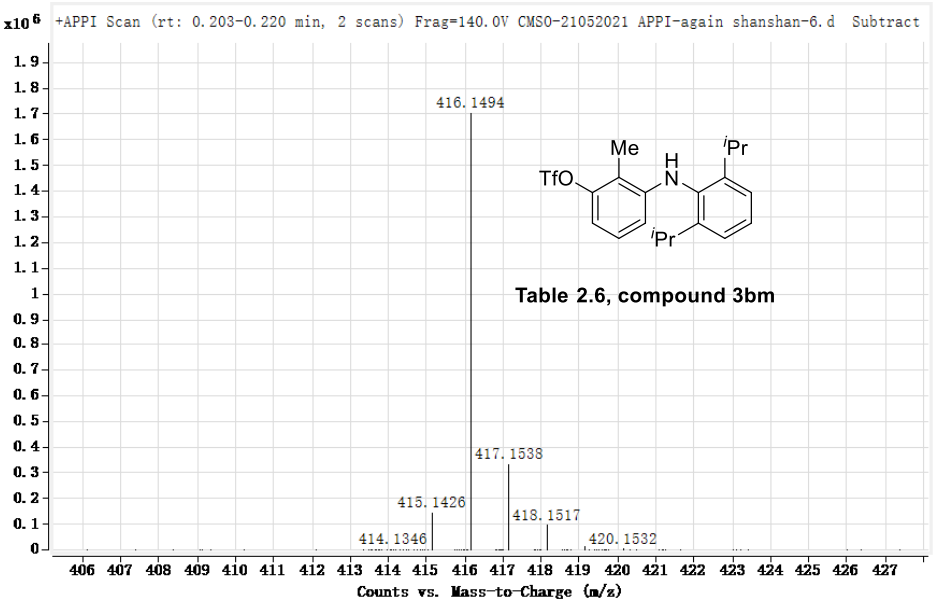

Table 2.6, compound 3bm

Mass	Calc. Mass	mDa	PPM	Formula
416.1494	416.1502	0.78	1.87	C20 H25 F3 N O3 S

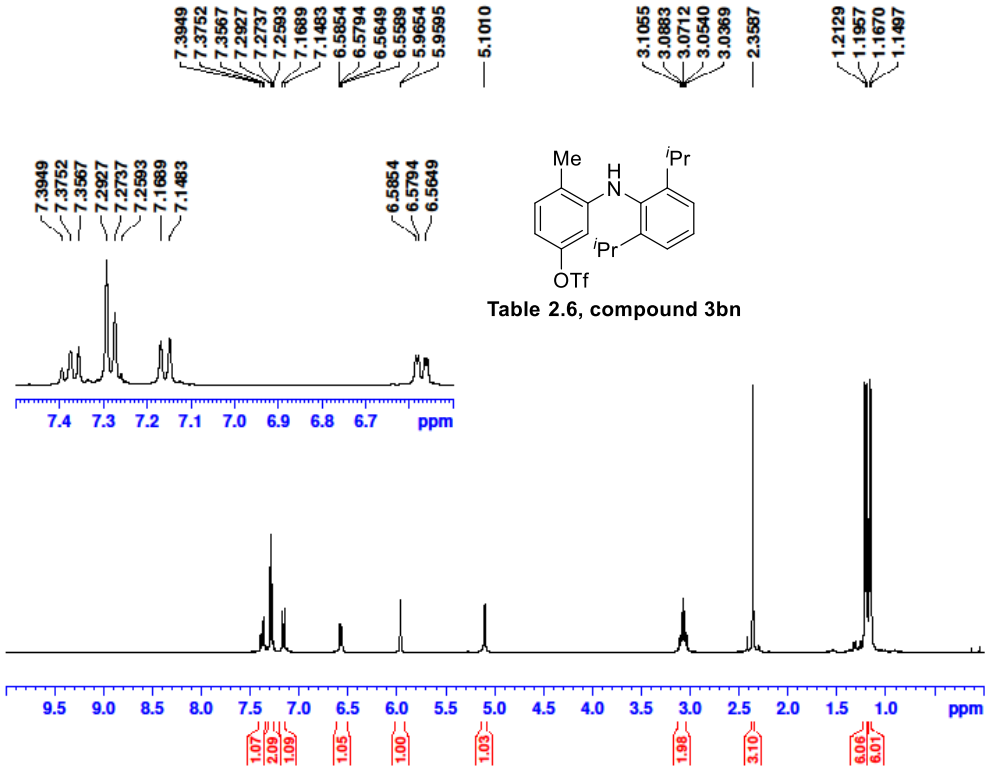

Table 2.6, compound 3bn

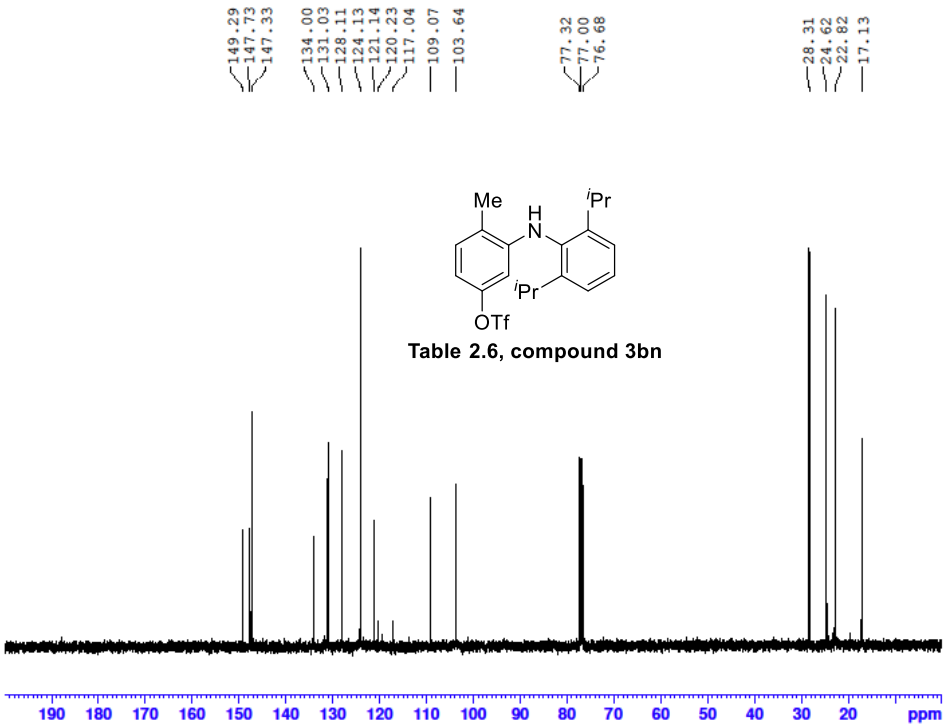

Table 2.6, compound 3bn

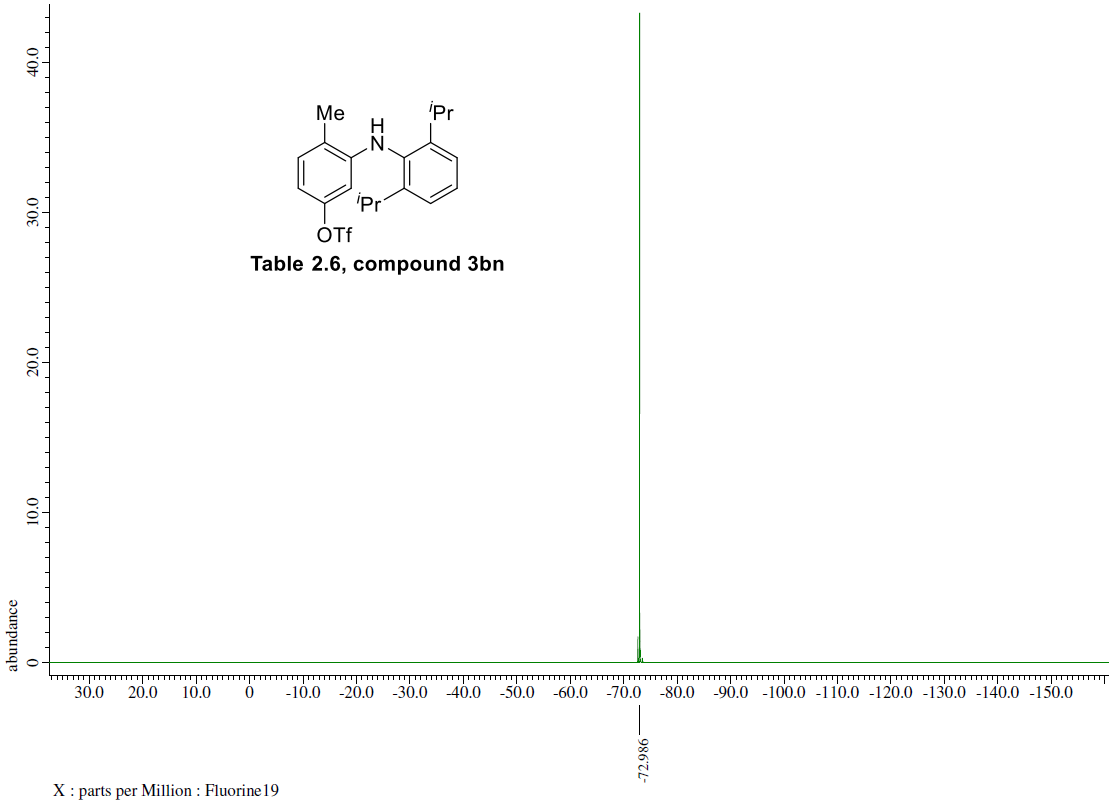

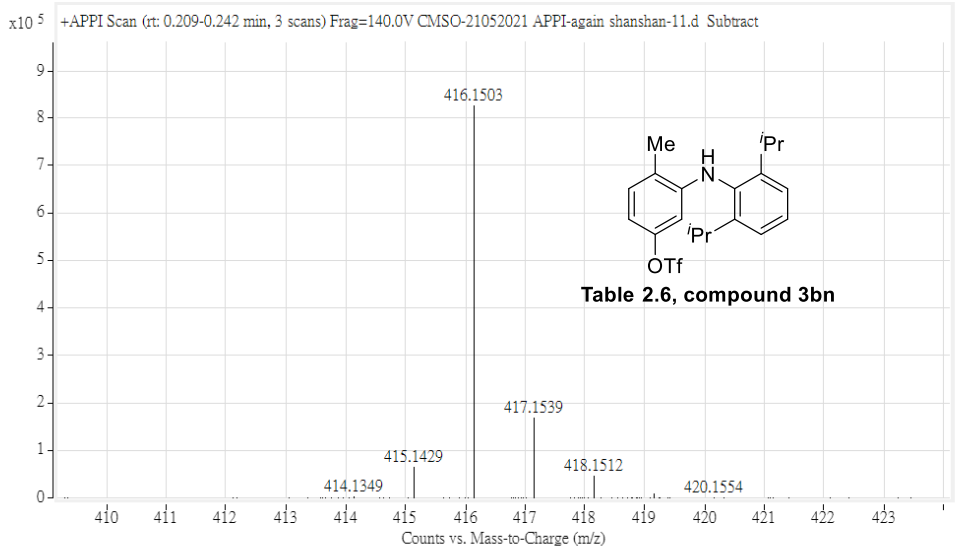

Mass	Calc. Mass	mDa	PPM	Formula
416.1503	416.1502	-0.12	-0.3	C20 H25 F3 N O3 S

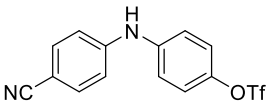

Table 2.7, compound 3bp

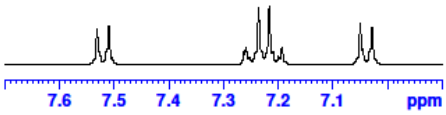

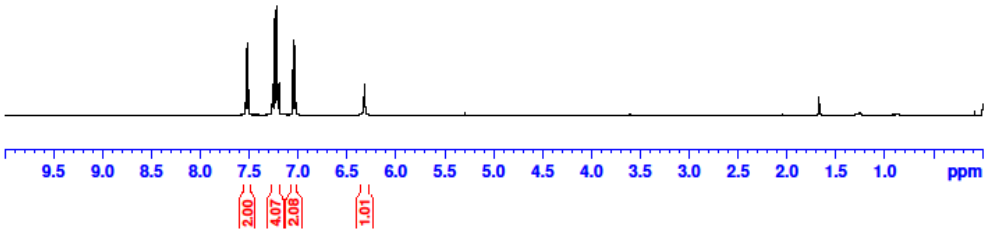

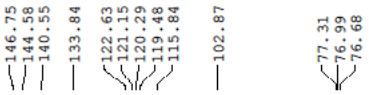

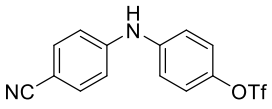

Table 2.7, compound 3bp

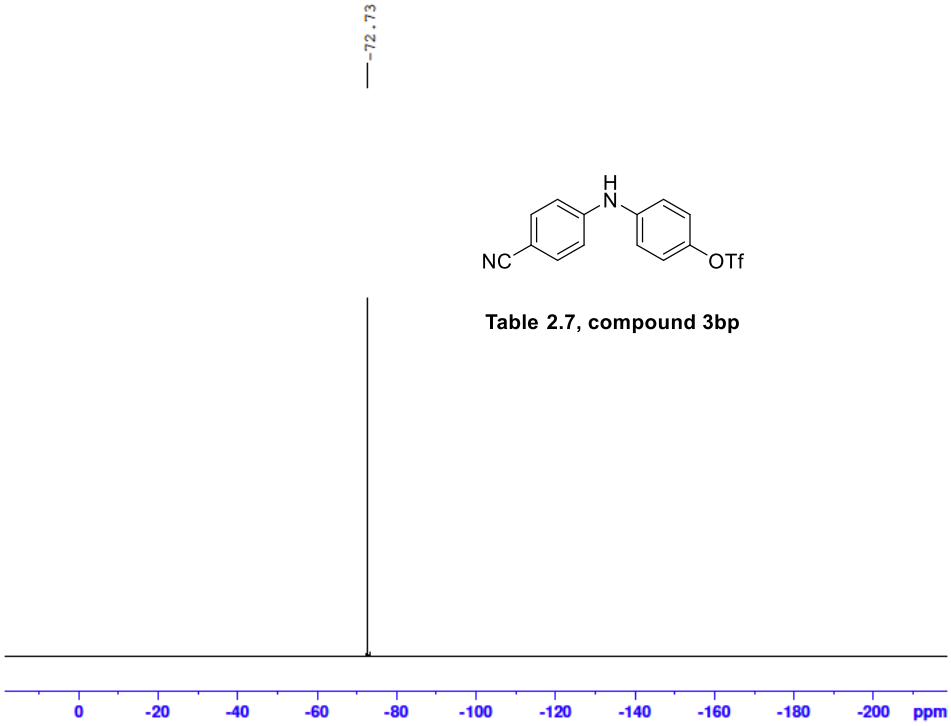

Table 2.7, compound 3bp

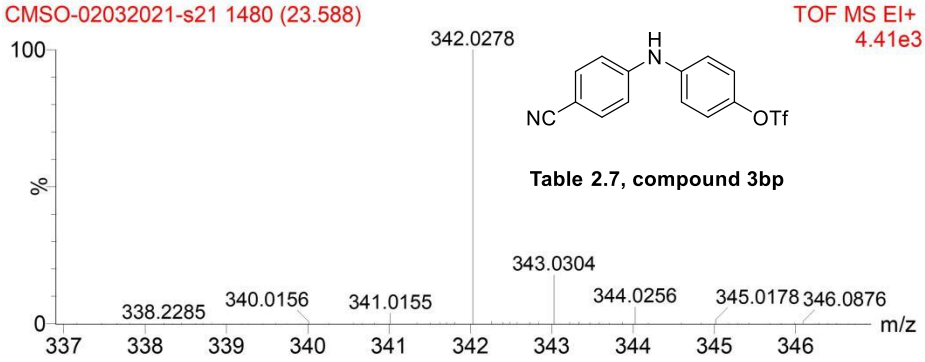

Table 2.7, compound 3bp

Mass	Calc. Mass	mDa	PPM	Formula
342.0278	342.0280	0.25	0.73	C14H9 F3N2O3S

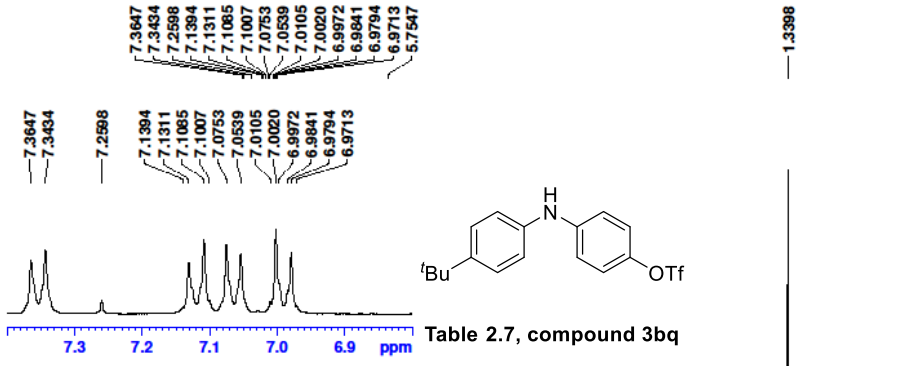

Table 2.7, compound 3bq

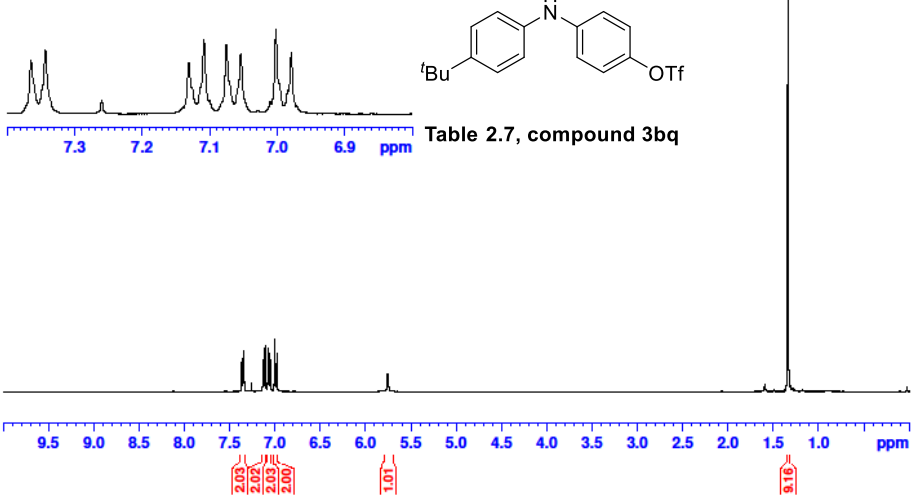

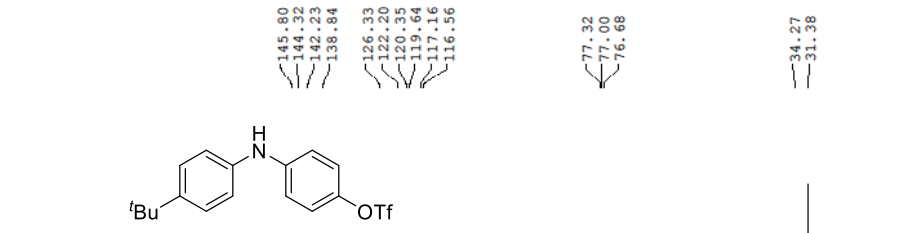

Table 2.7, compound 3bq

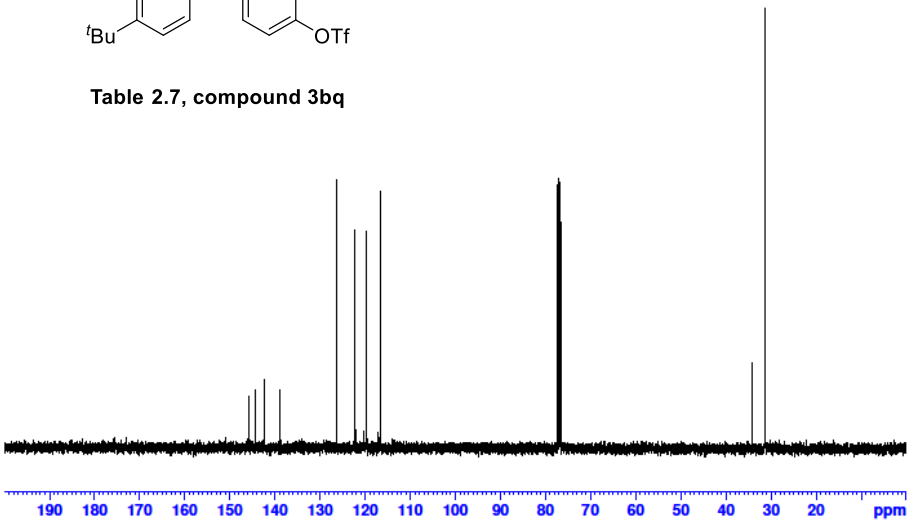

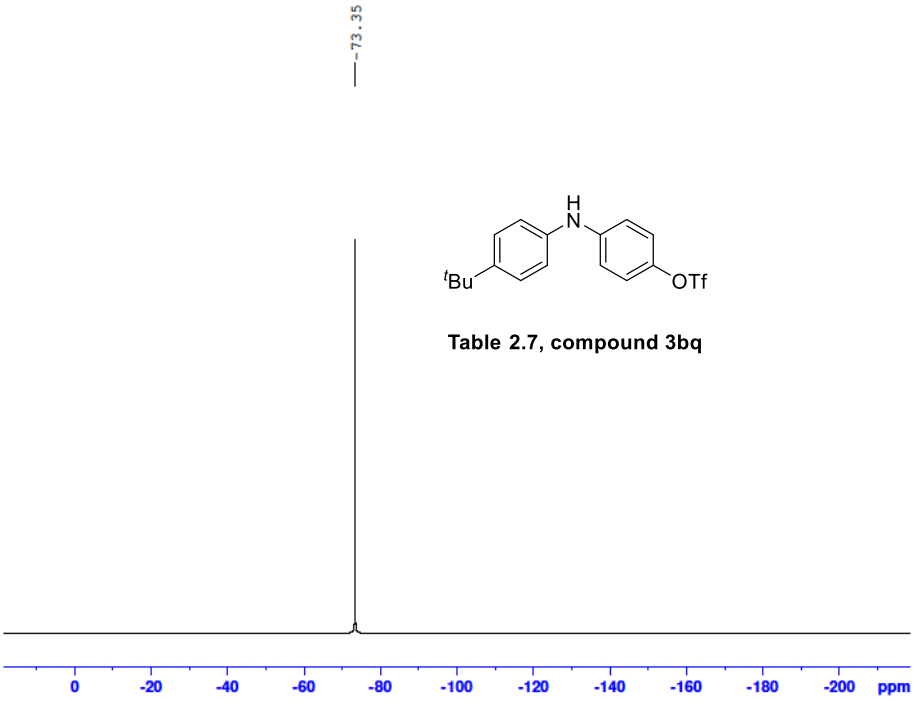

Table 2.7, compound 3bq

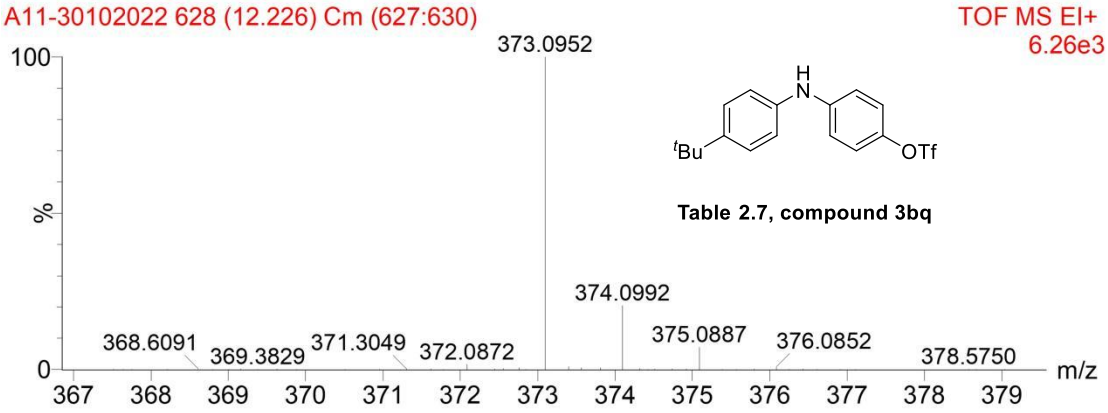

Table 2.7, compound 3bq

Mass	Calc. Mass	mDa	PPM	Ion Formula
373.0952	373.0954	0.20	0.54	C17H18NF3O3S

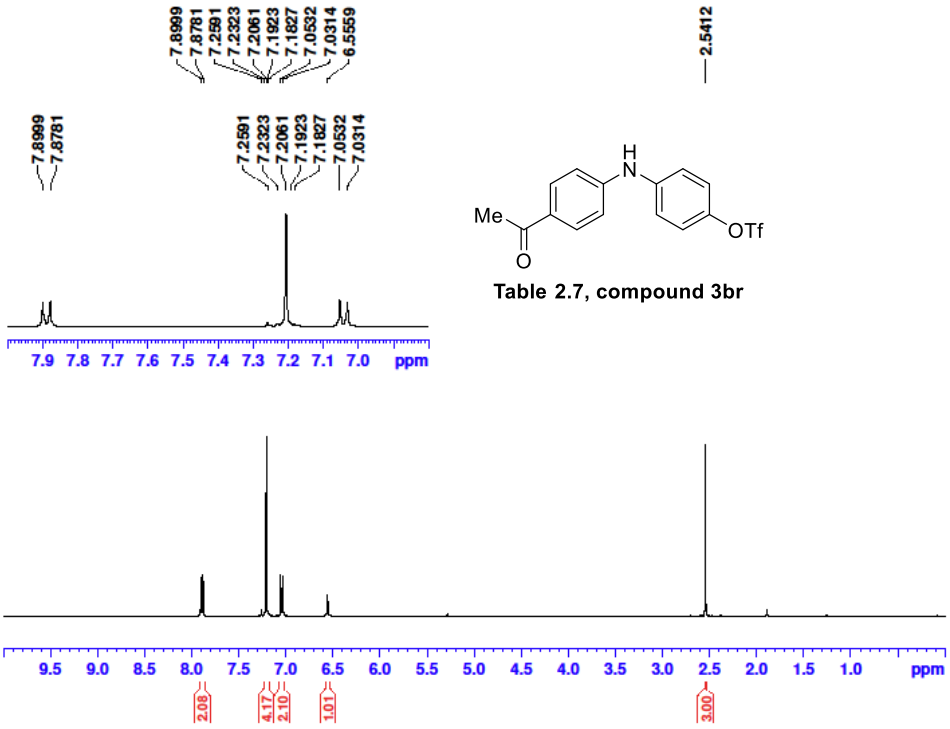

Table 2.7, compound 3br

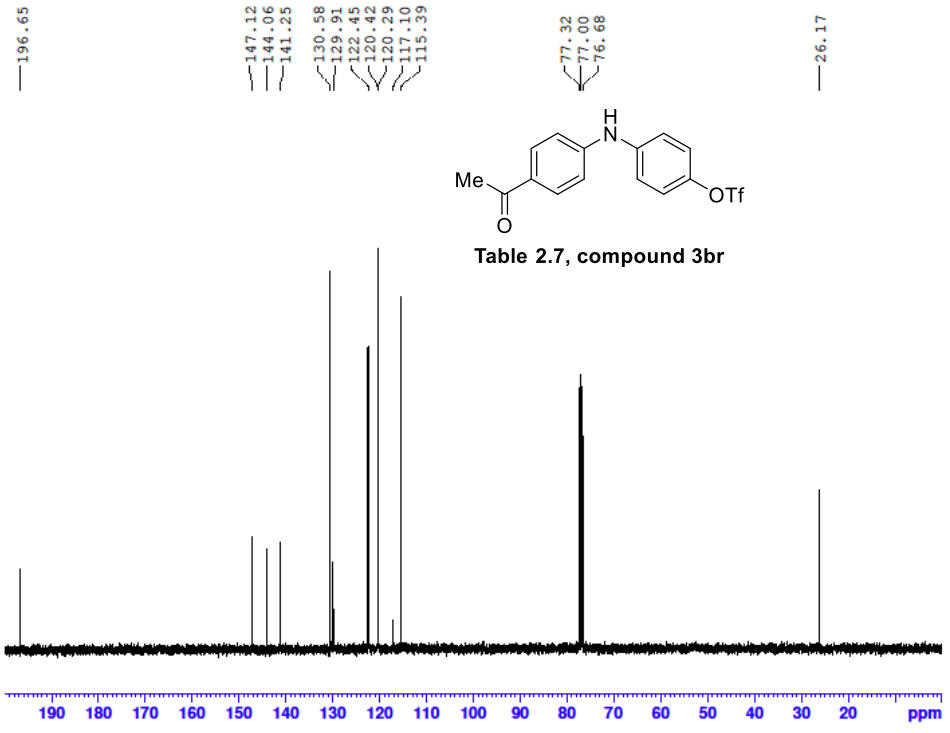

Table 2.7, compound 3br

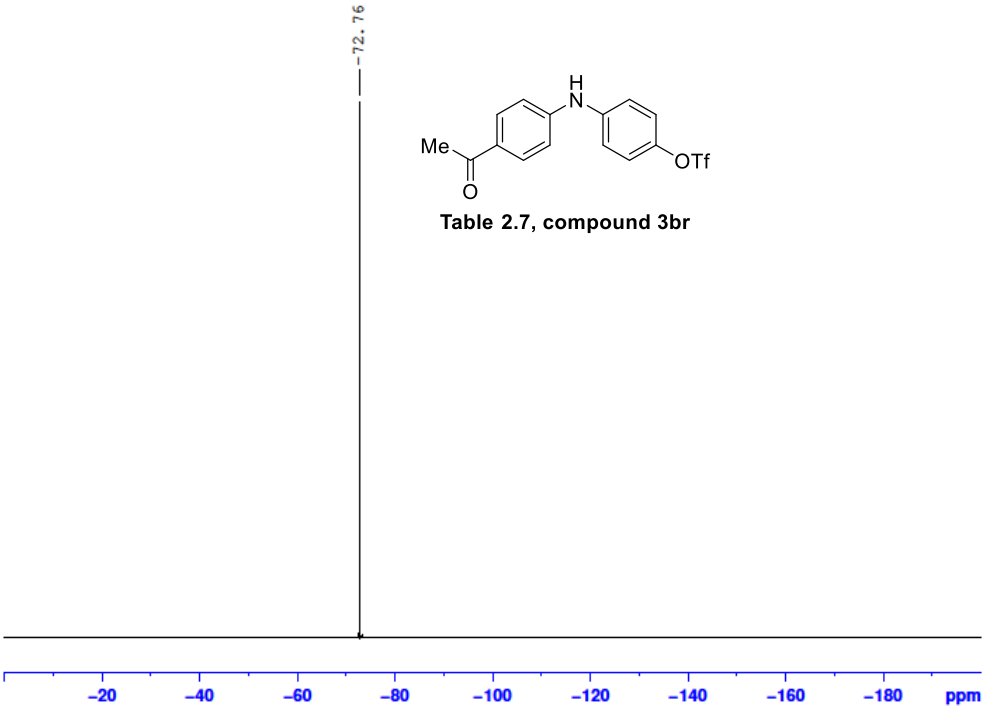

Table 2.7, compound 3br

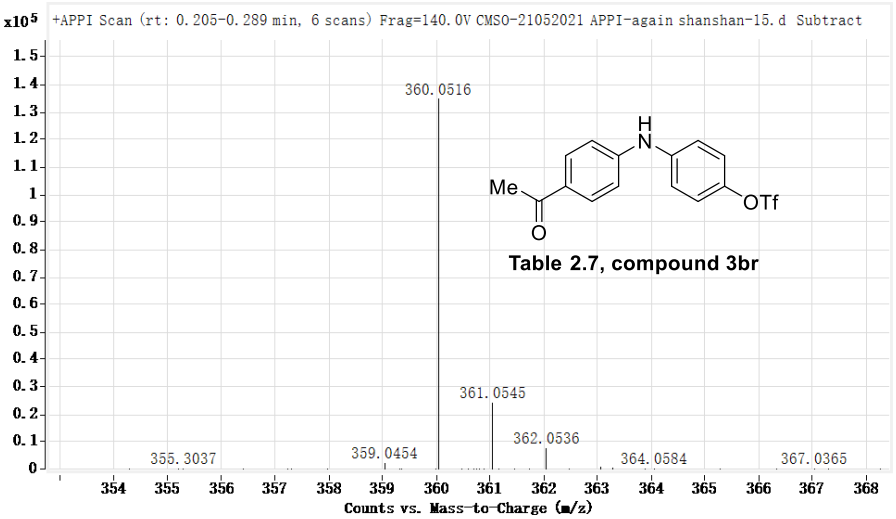

Table 2.7, compound 3br

Mass	Calc. Mass	mDa	PPM	Formula
360.0516	360.0512	-0.41	-1.14	C15 H13 F3 N O4 S

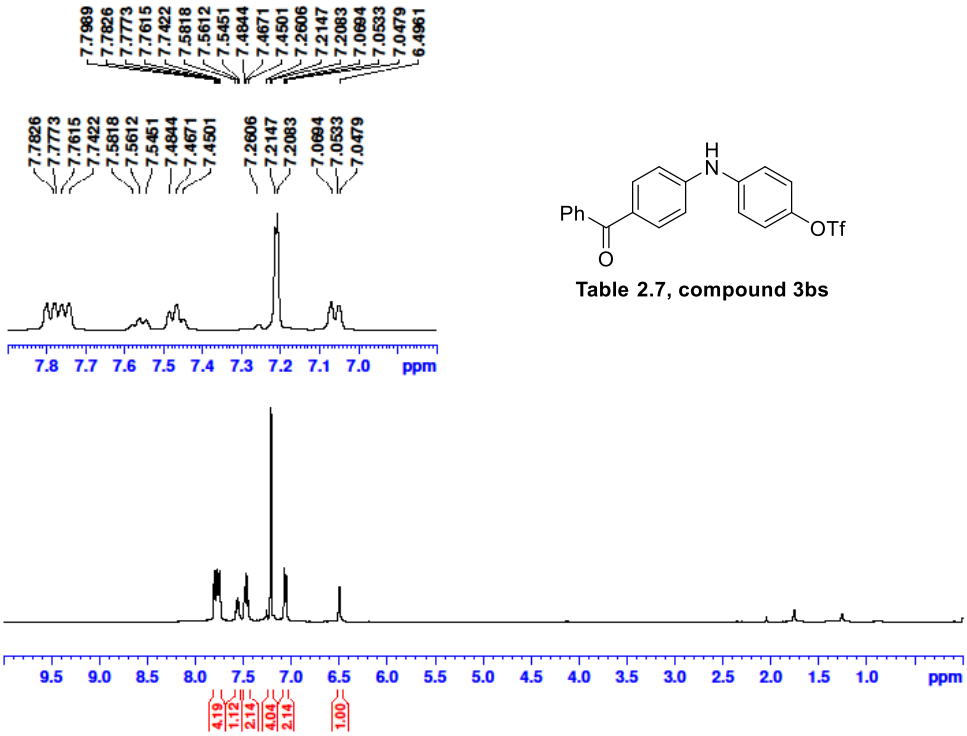

Table 2.7, compound 3bs

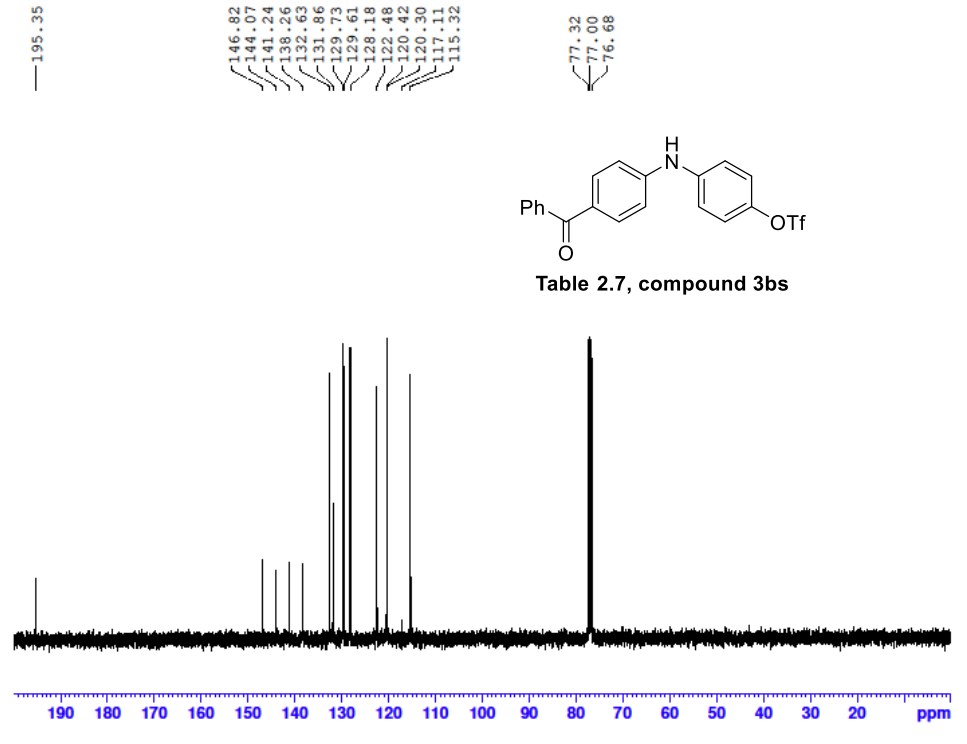

Table 2.7, compound 3bs

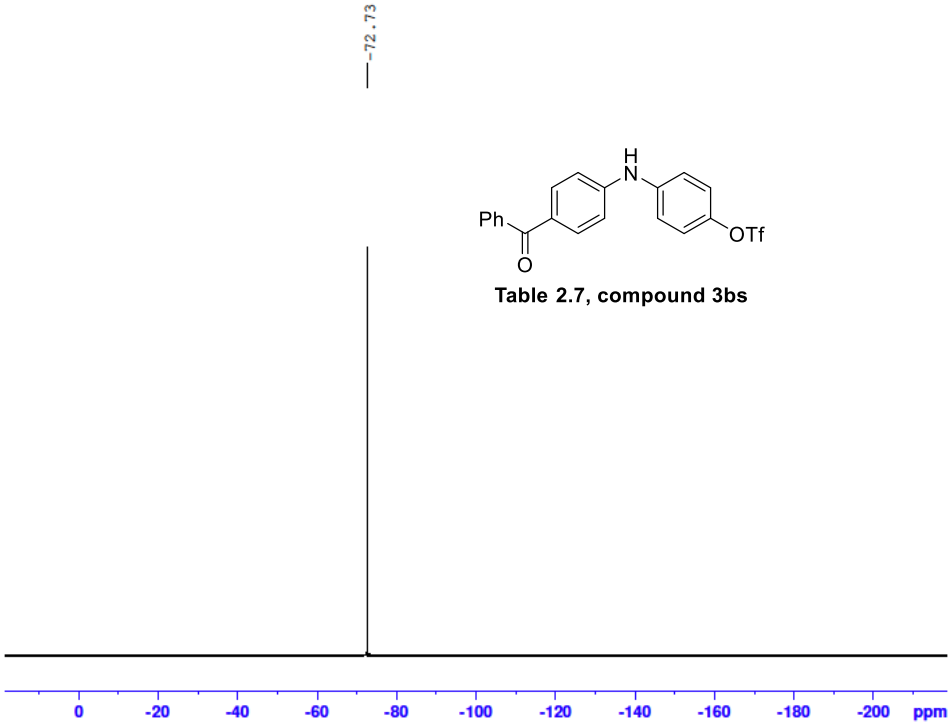

Table 2.7, compound 3bs

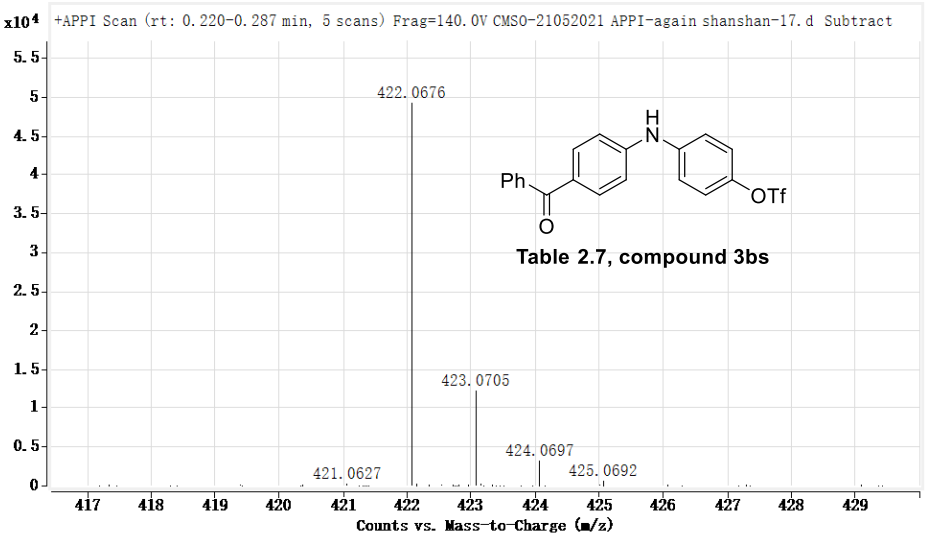

Table 2.7, compound 3bs

Mass	Calc. Mass	mDa	PPM	Formula
422.0676	422.0668	-0.76	-1.81	C20 H15 F3 N O4 S

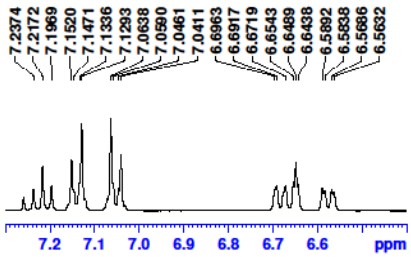

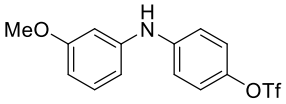

Table 2.7, compound 3bt

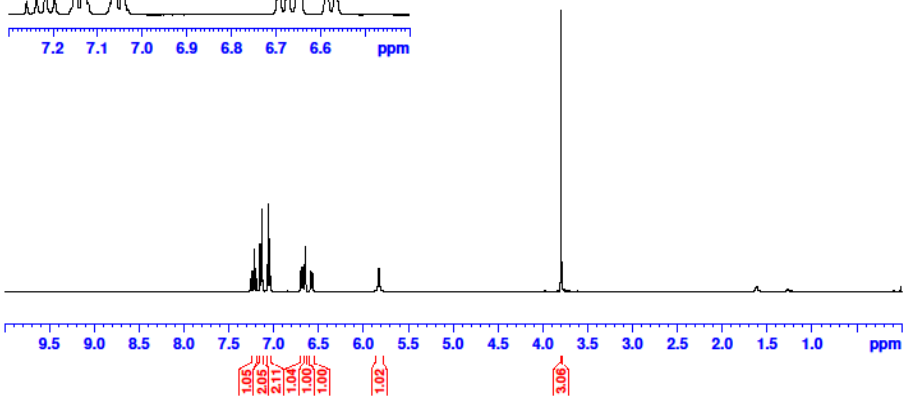

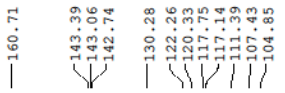

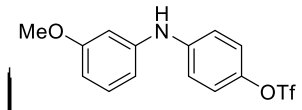

Table 2.7, compound 3bt

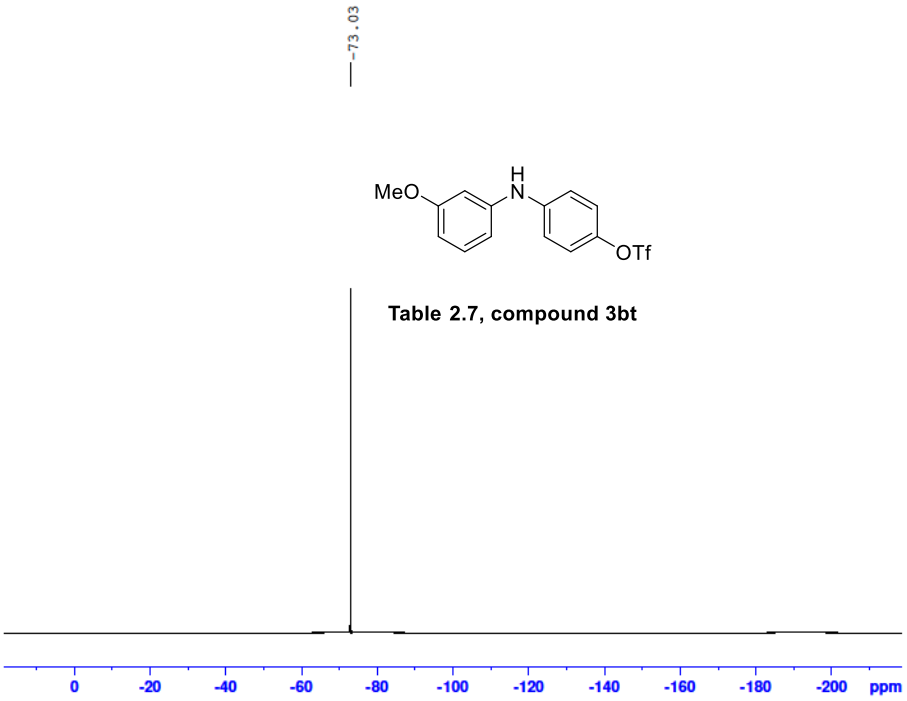

Table 2.7, compound 3bt

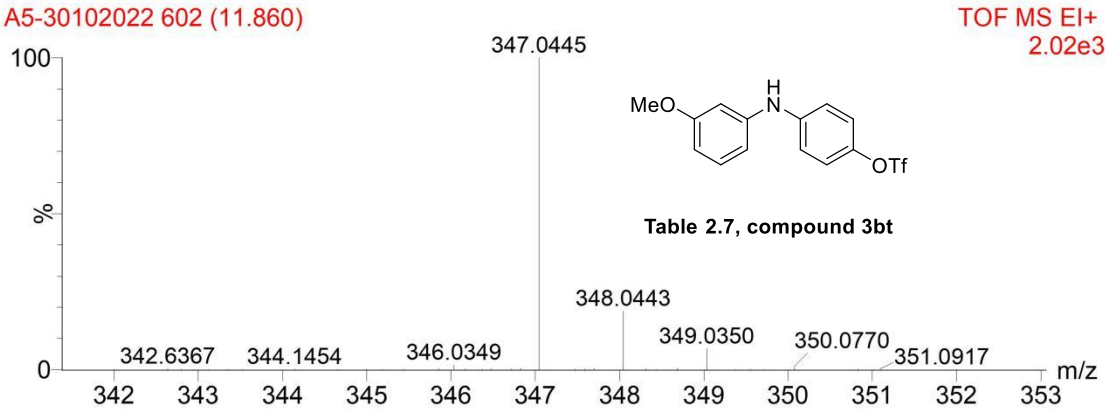

Table 2.7, compound 3bt

Mass	Calc. Mass	mDa	PPM	Ion Formula
347.0445	347.0434	-1.14	-3.27	C14H12NF3O4S

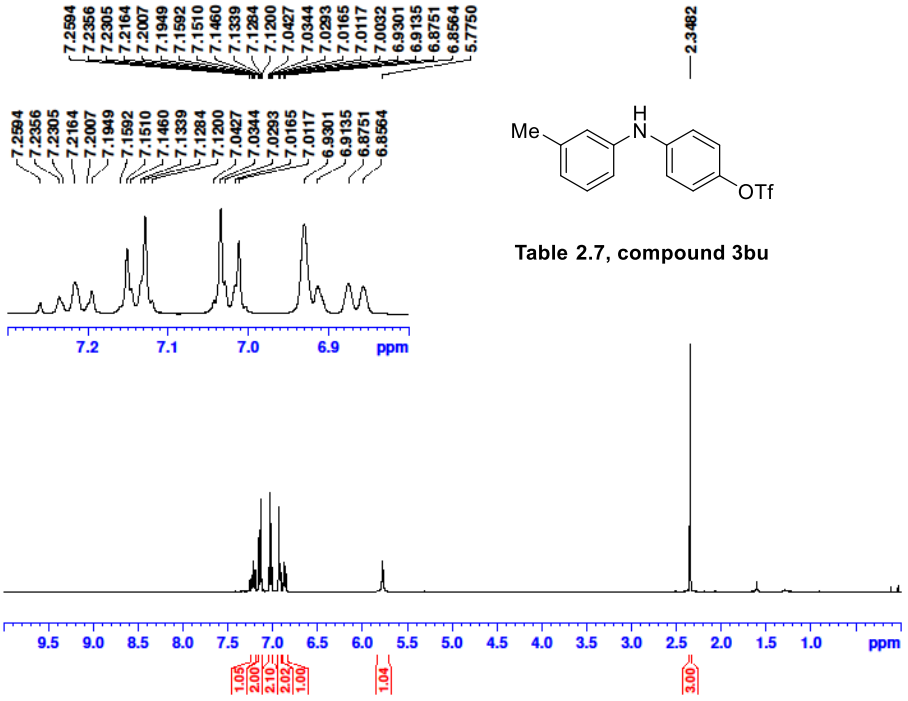

Table 2.7, compound 3bu

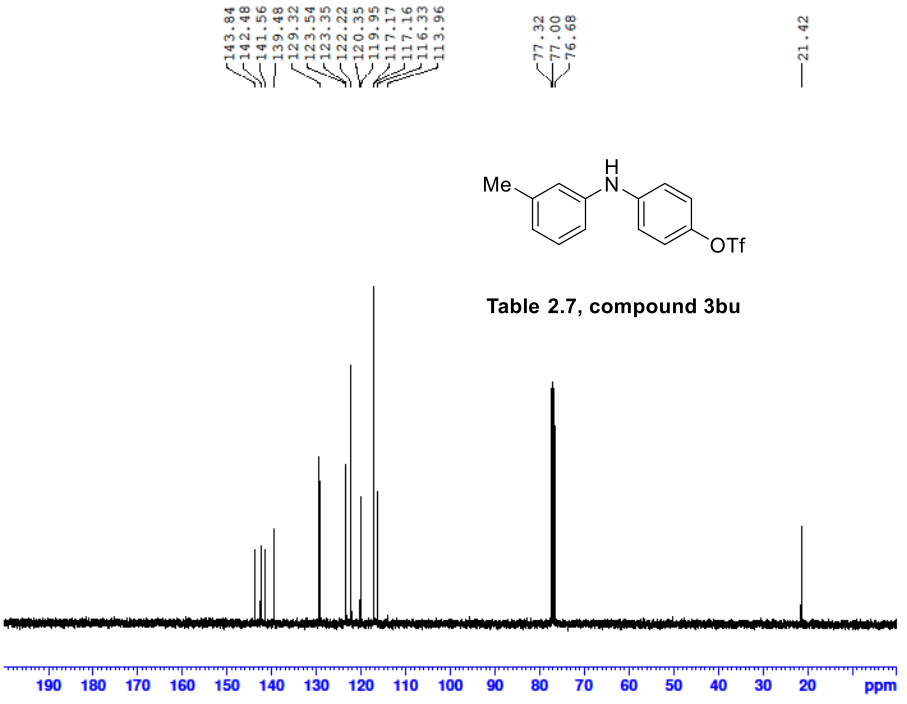

Table 2.7, compound 3bu

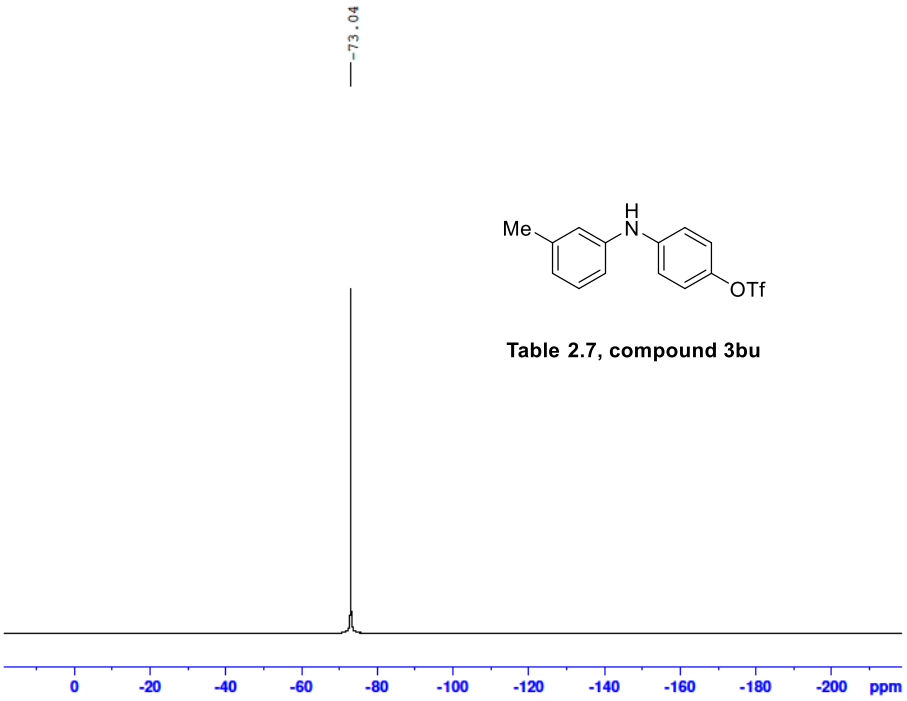

Table 2.7, compound 3bu

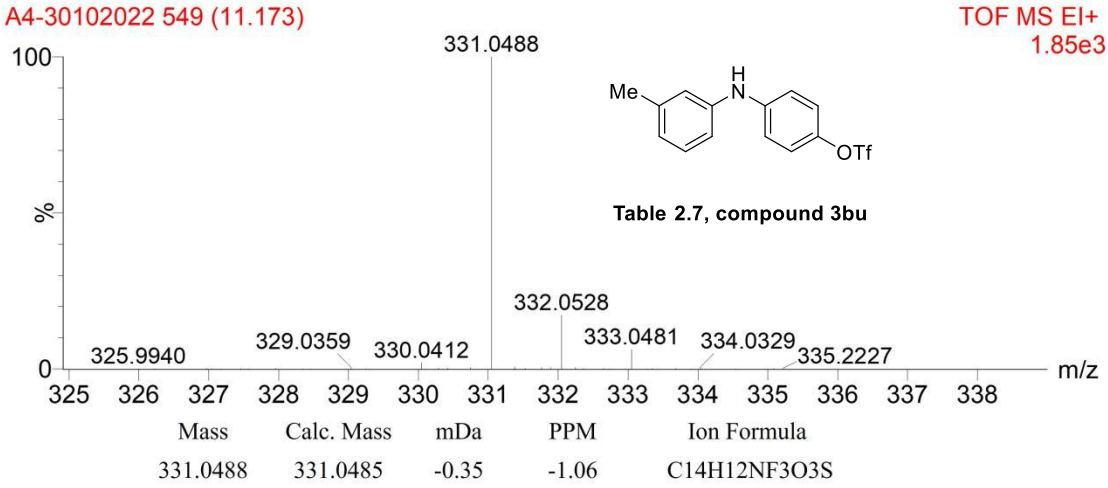

Me
H
N
OTf

Table 2.7, compound 3bu

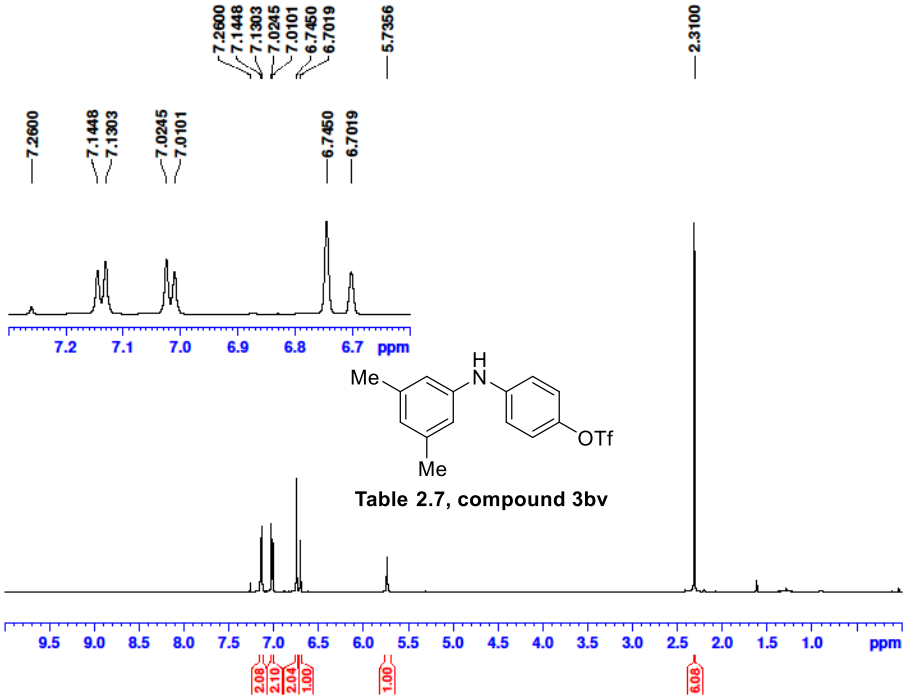

Table 2.7, compound 3bv

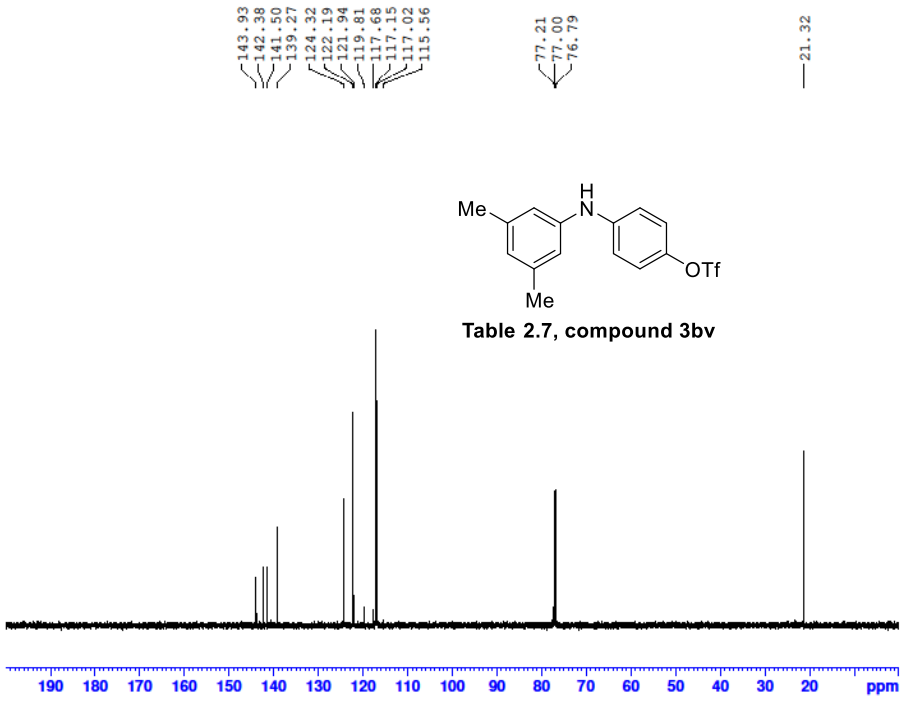

Table 2.7, compound 3bv

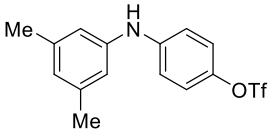

Table 2.7, compound 3bv

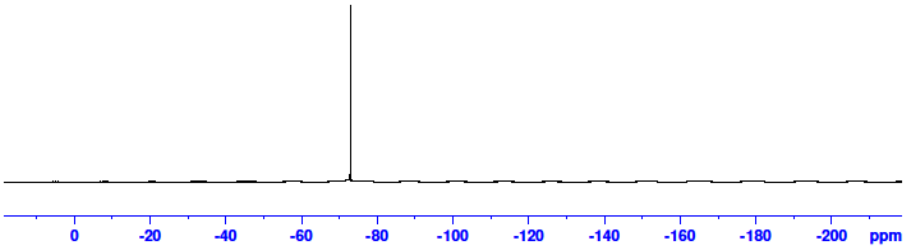

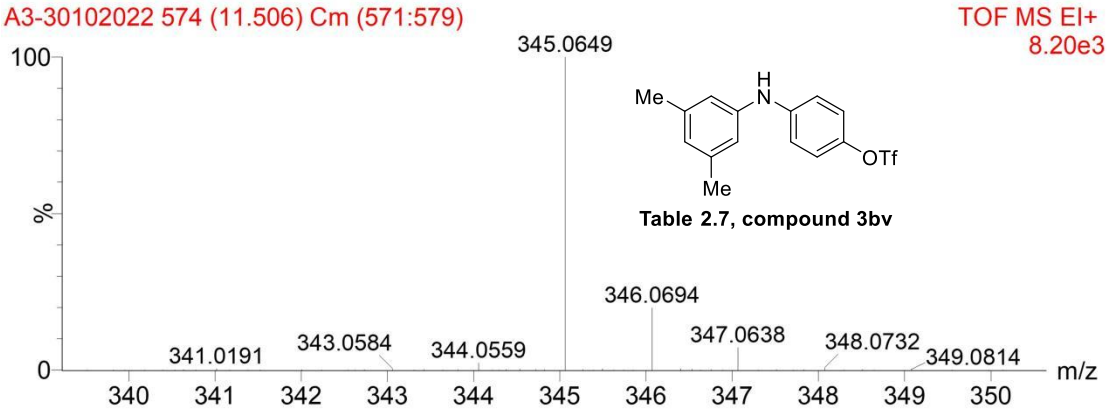

Table 2.7, compound 3bv

Mass	Calc. Mass	mDa	PPM	Ion Formula
345.0649	345.0641	-0.80	-2.32	C15H14NF3O3S

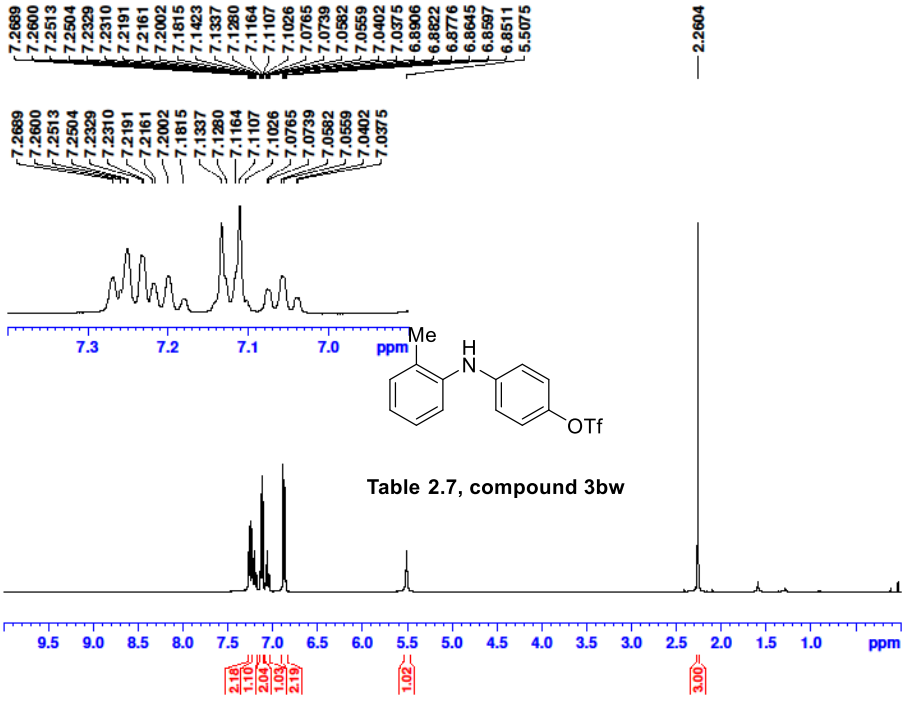

Table 2.7, compound 3bw

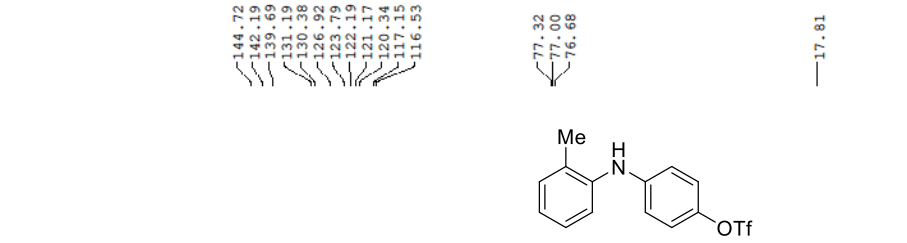

Table 2.7, compound 3bw

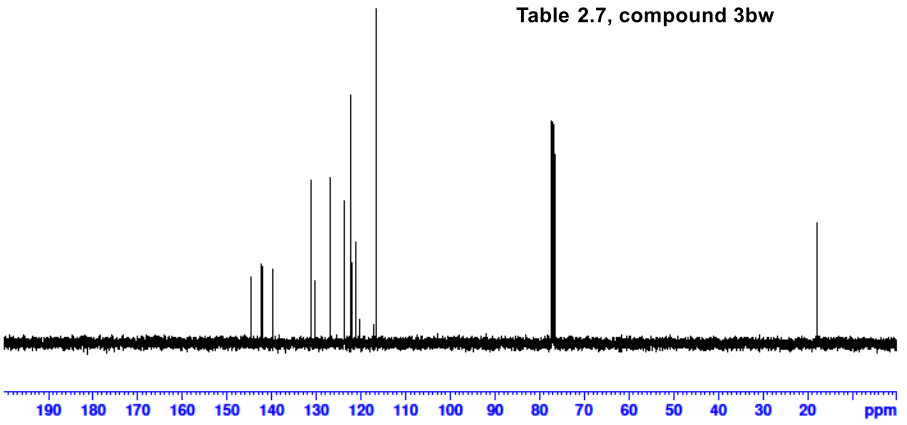

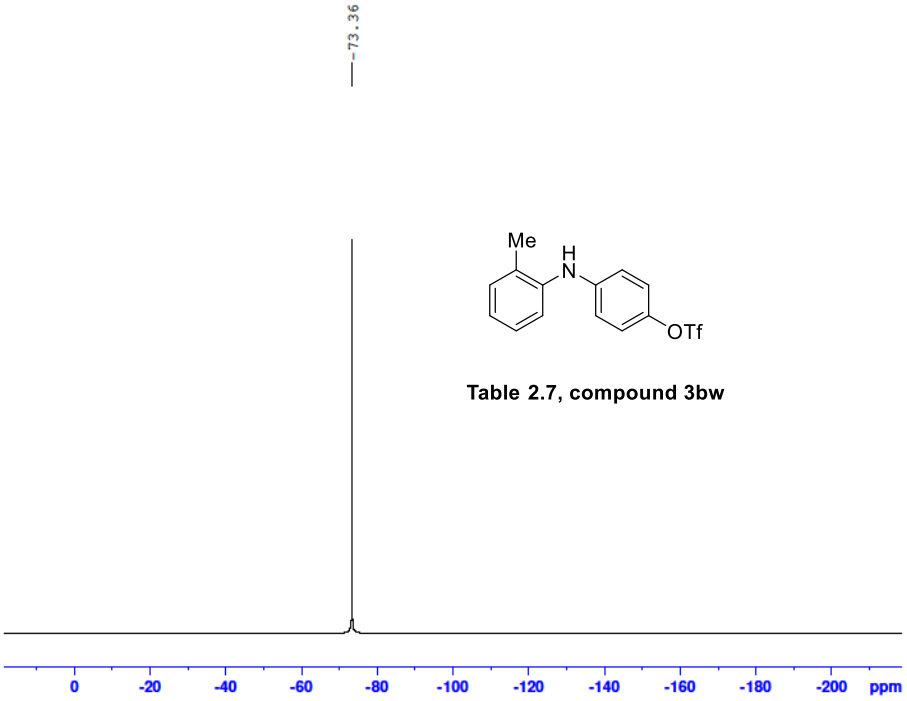

Table 2.7, compound 3bw

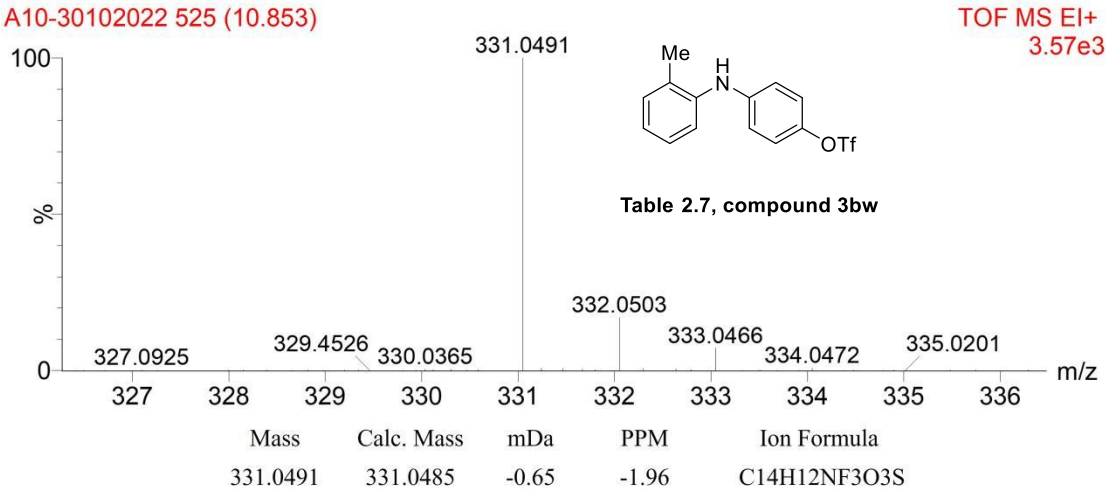

Table 2.7, compound 3bw

Mass	Calc. Mass	mDa	PPM	Ion Formula
331.0491	331.0485	-0.65	-1.96	C14H12NF3O3S

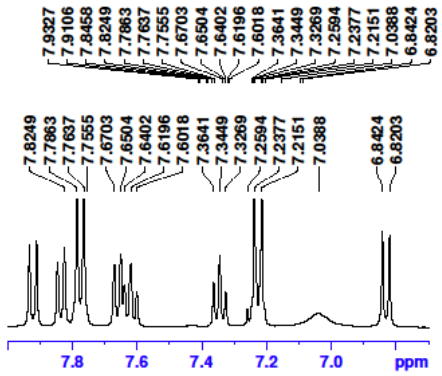

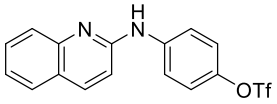

Table 2.7, compound 3bx

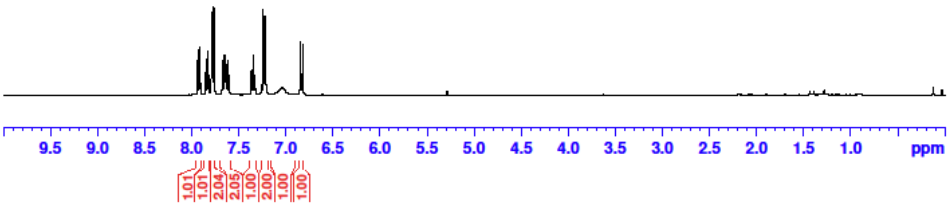

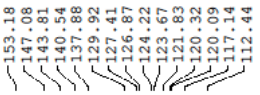

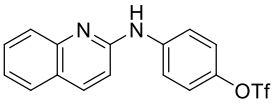

Table 2.7, compound 3bx

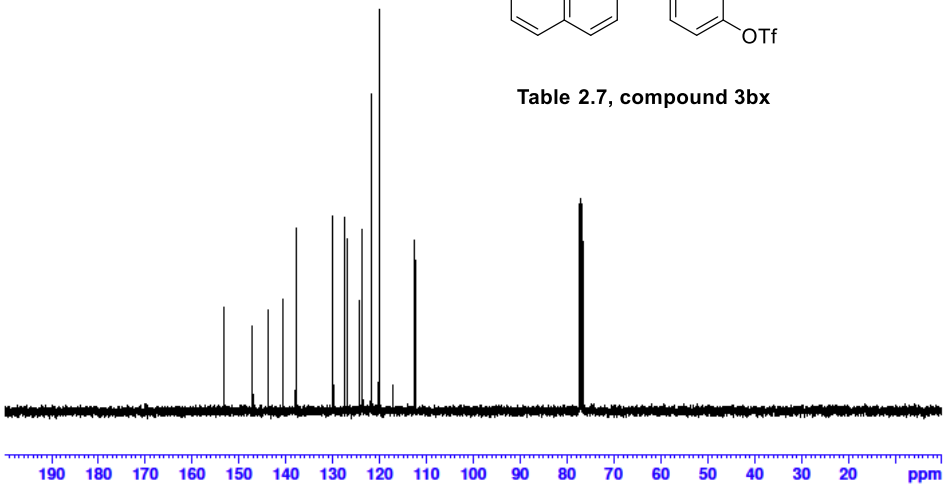

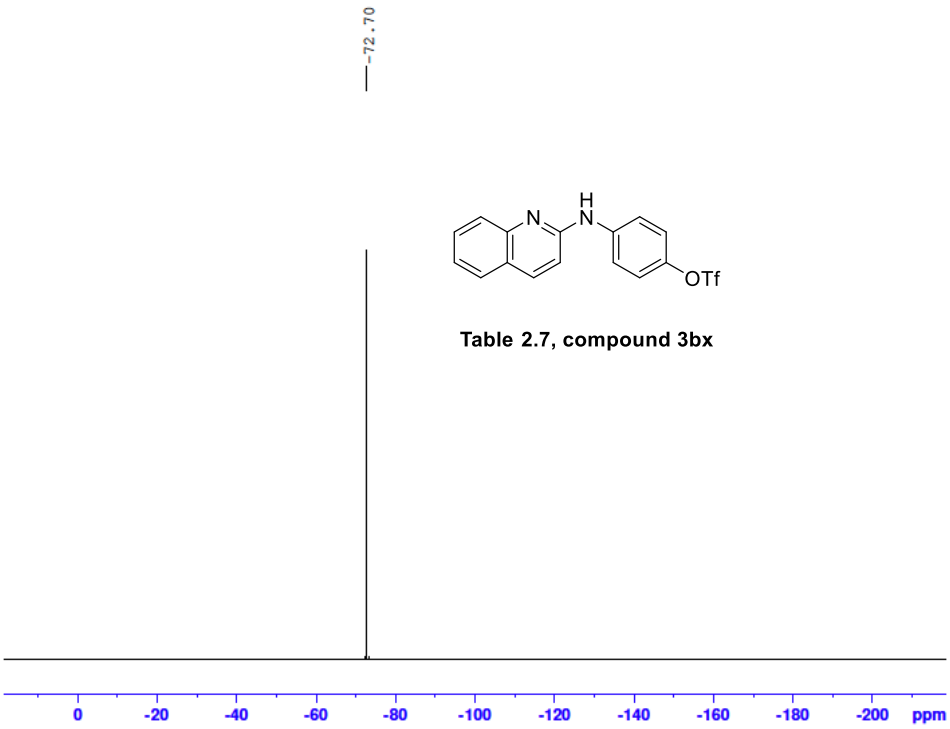

Table 2.7, compound 3bx

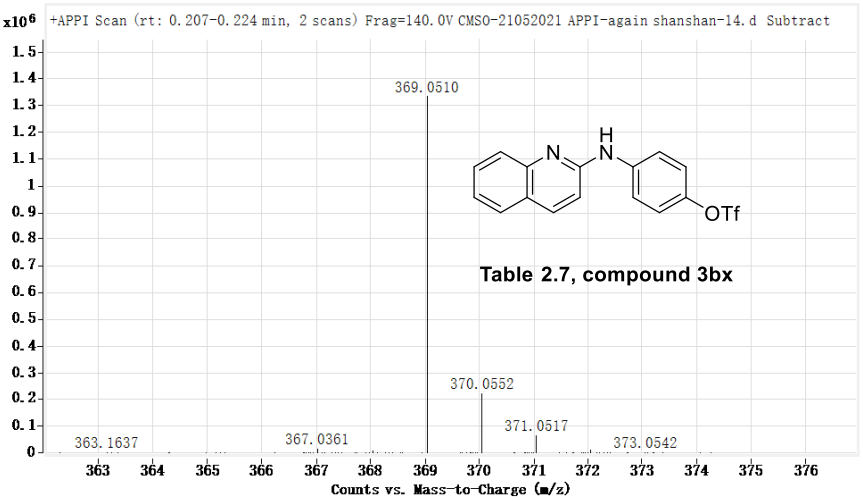

Table 2.7, compound 3bx

Mass	Calc. Mass	mDa	PPM	Formula
369.051	369.0515	0.52	1.42	C16 H12 F3 N2 O3 S

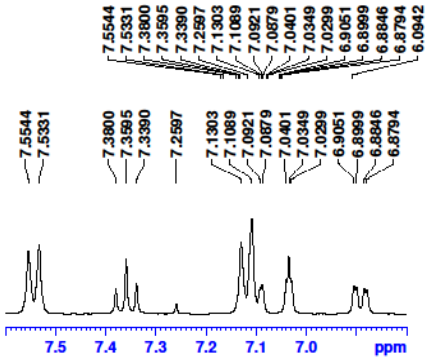

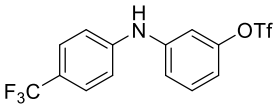

Table 2.7, compound 3by

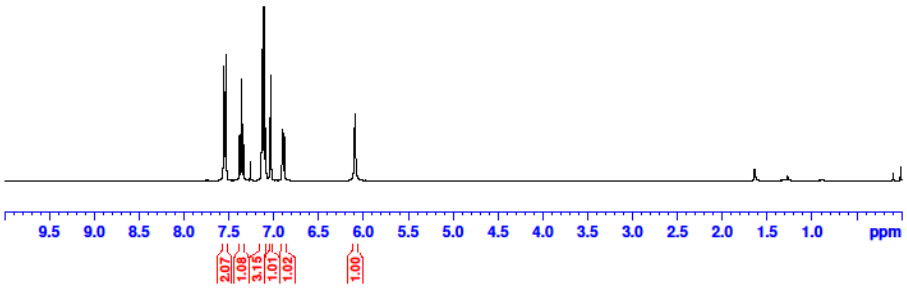

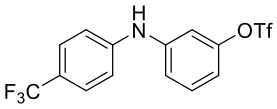

Table 2.7, compound 3by

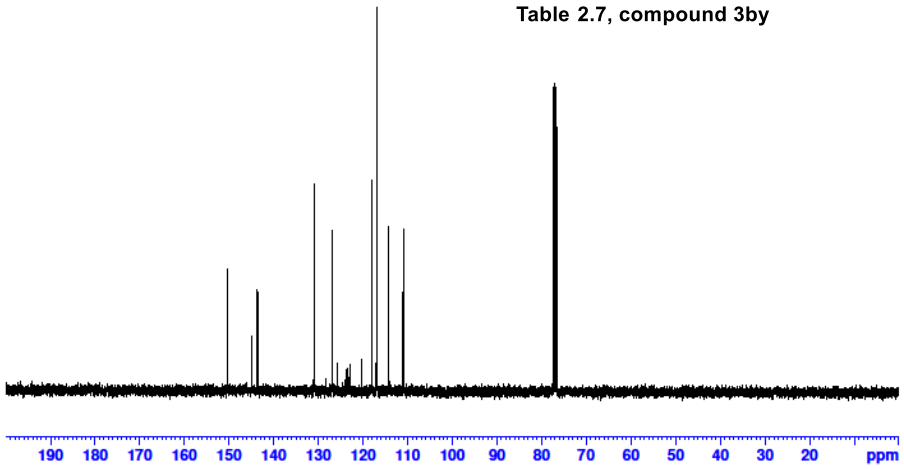

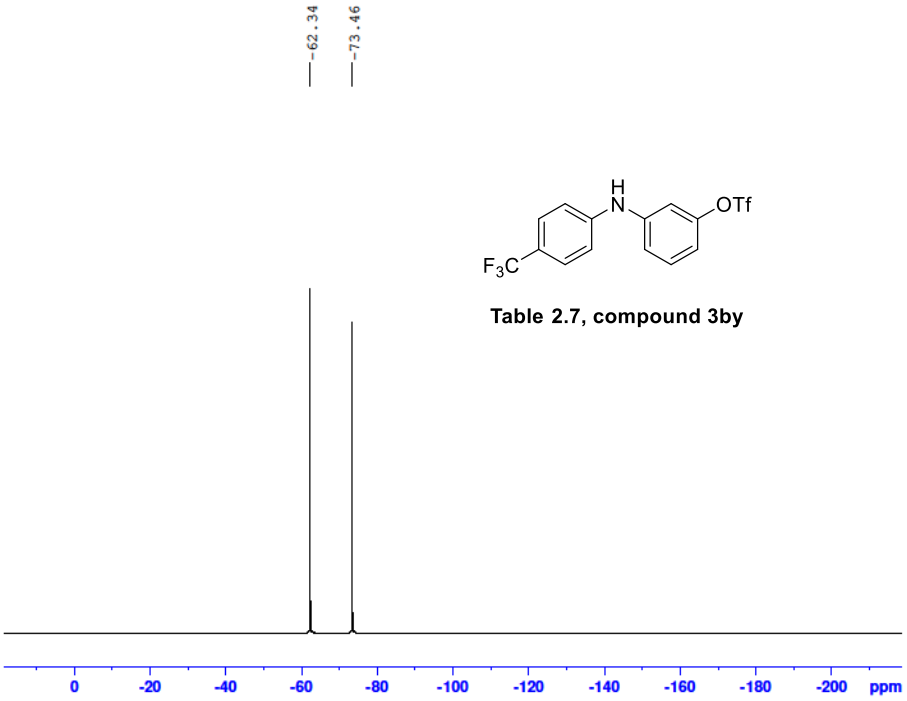

Table 2.7, compound 3by

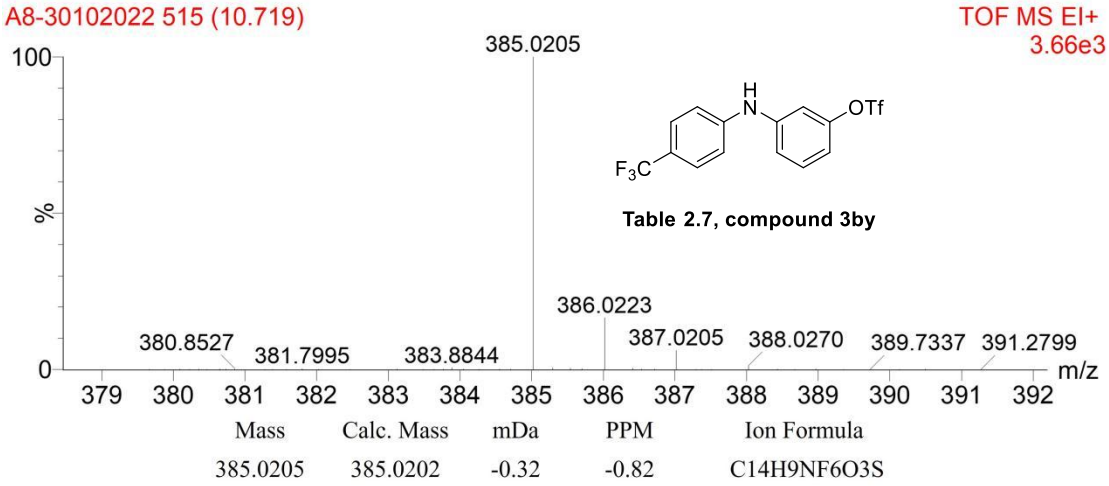

Table 2.7, compound 3by

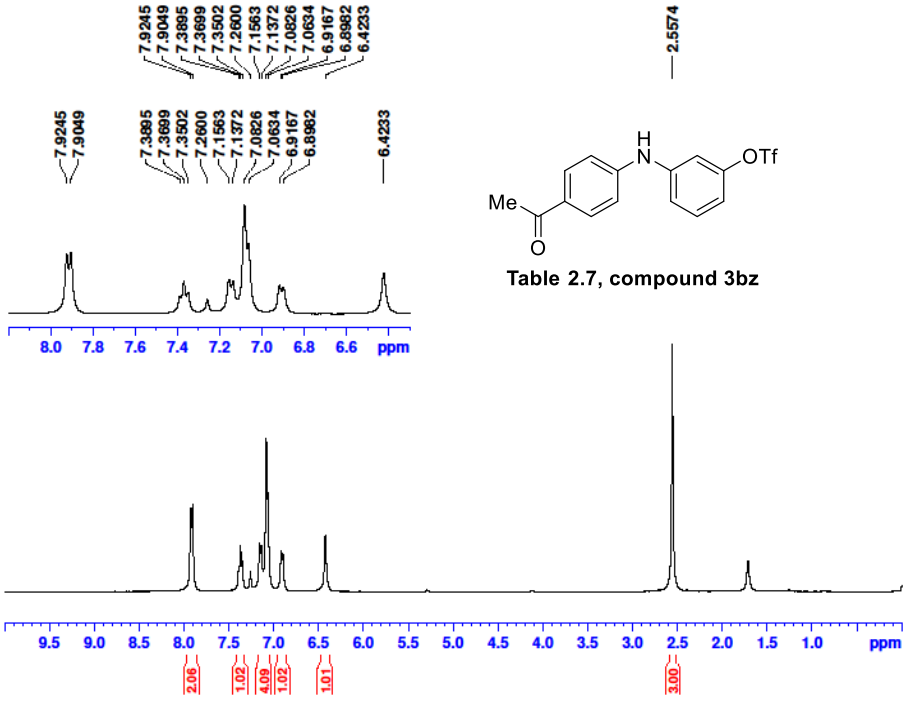

Table 2.7, compound 3bz

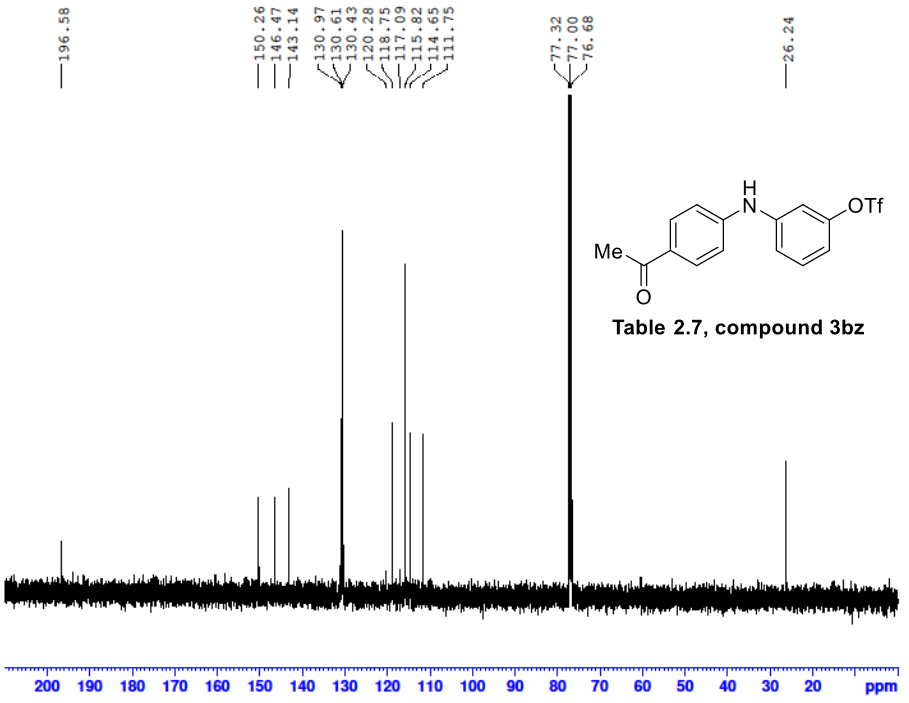

Table 2.7, compound 3bz

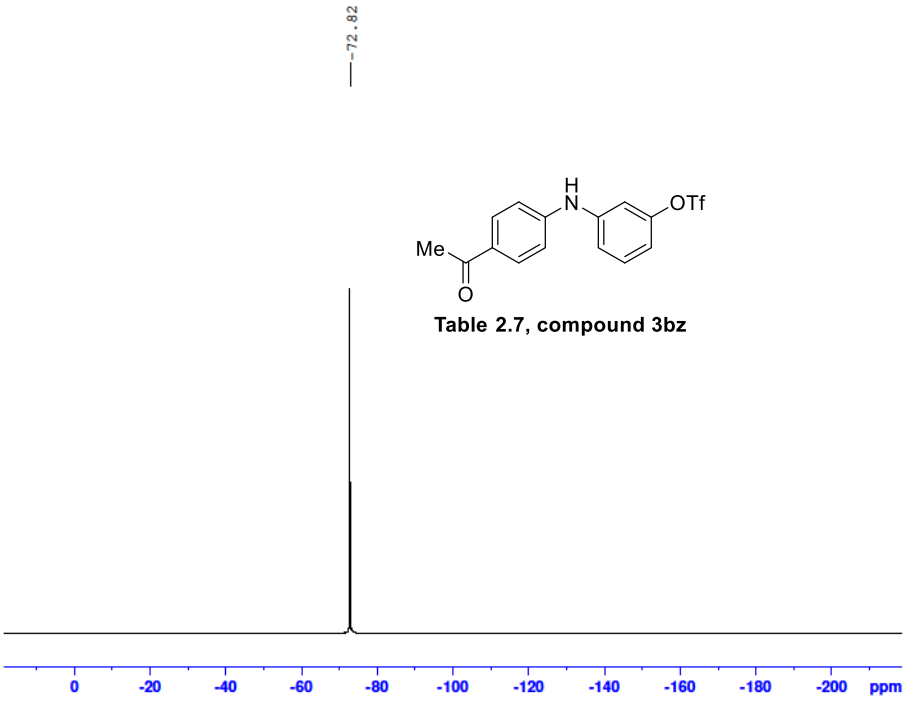

Table 2.7, compound 3bz

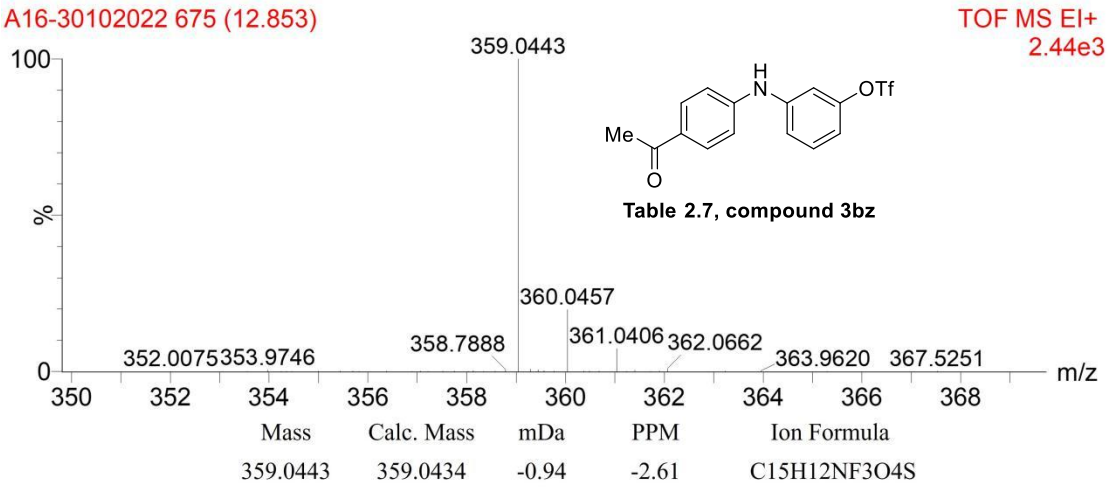

Table 2.7, compound 3bz

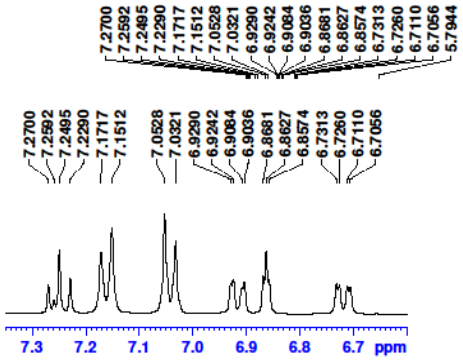

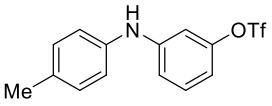

Table 2.7, compound 3ca

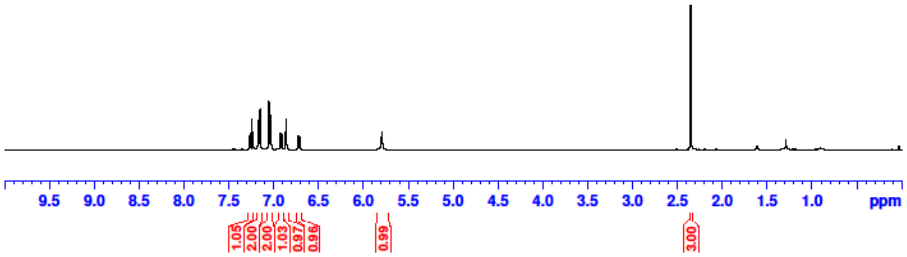

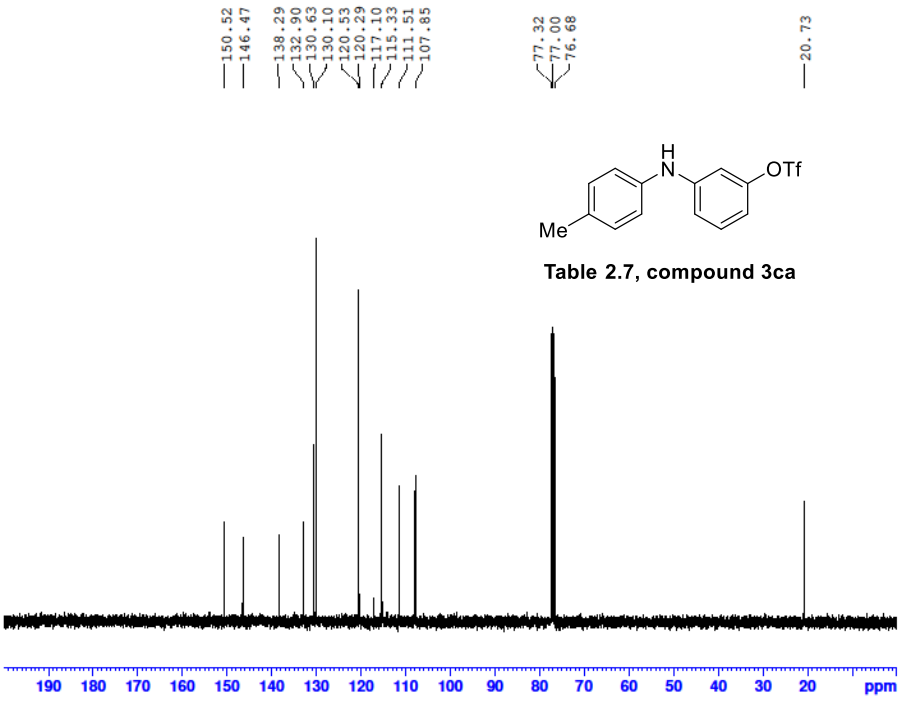

Table 2.7, compound 3ca

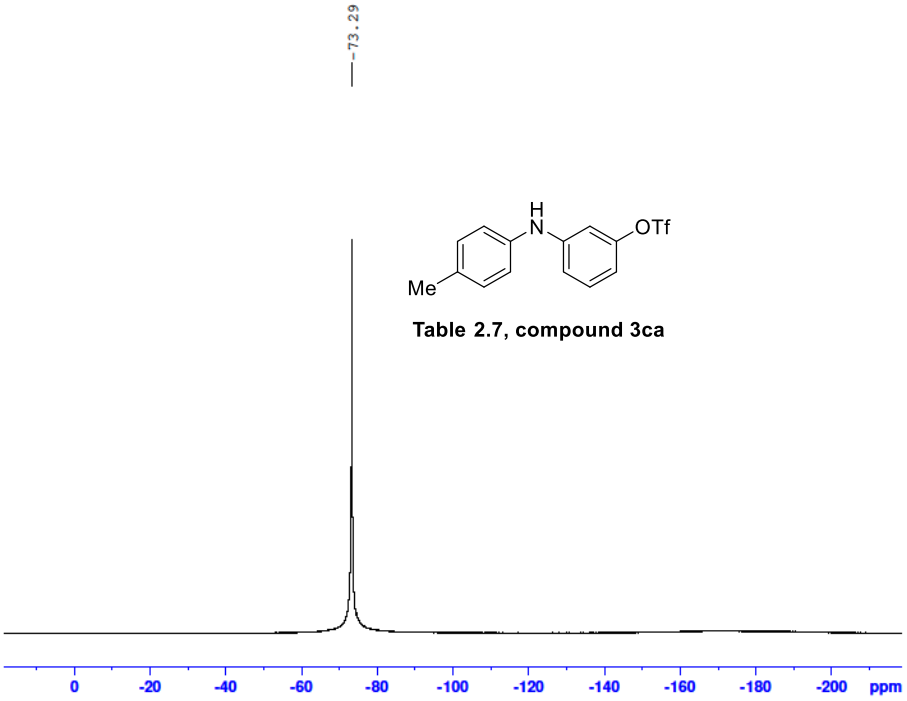

Table 2.7, compound 3ca

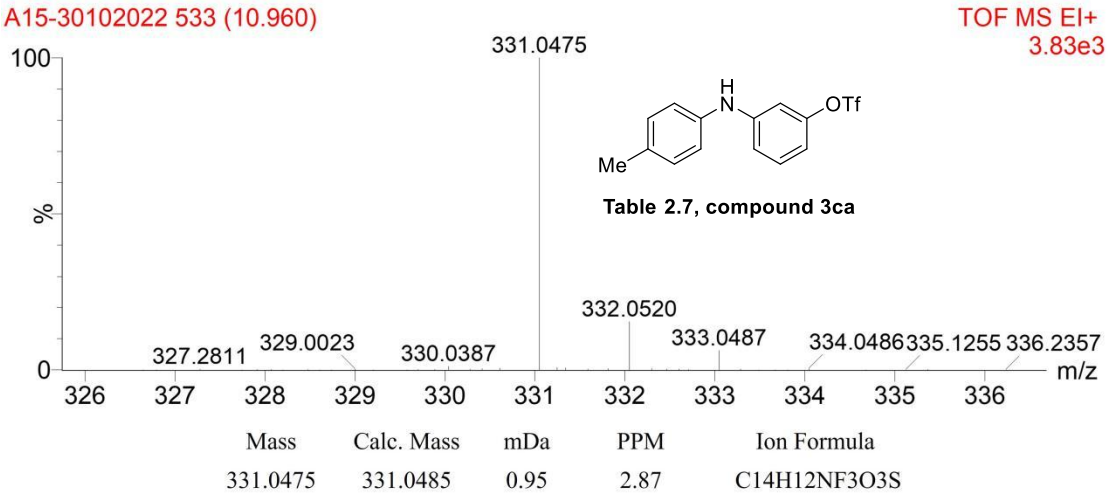

Table 2.7, compound 3ca

Mass	Calc. Mass	mDa	PPM	Ion Formula
331.0475	331.0485	0.95	2.87	C14H12NF3O3S

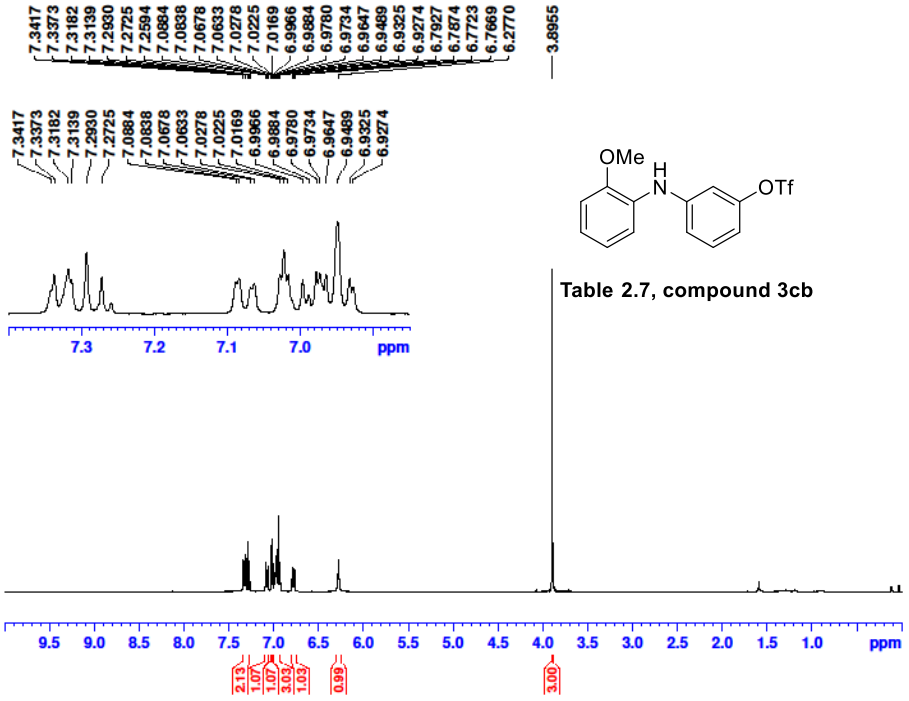

Table 2.7, compound 3cb

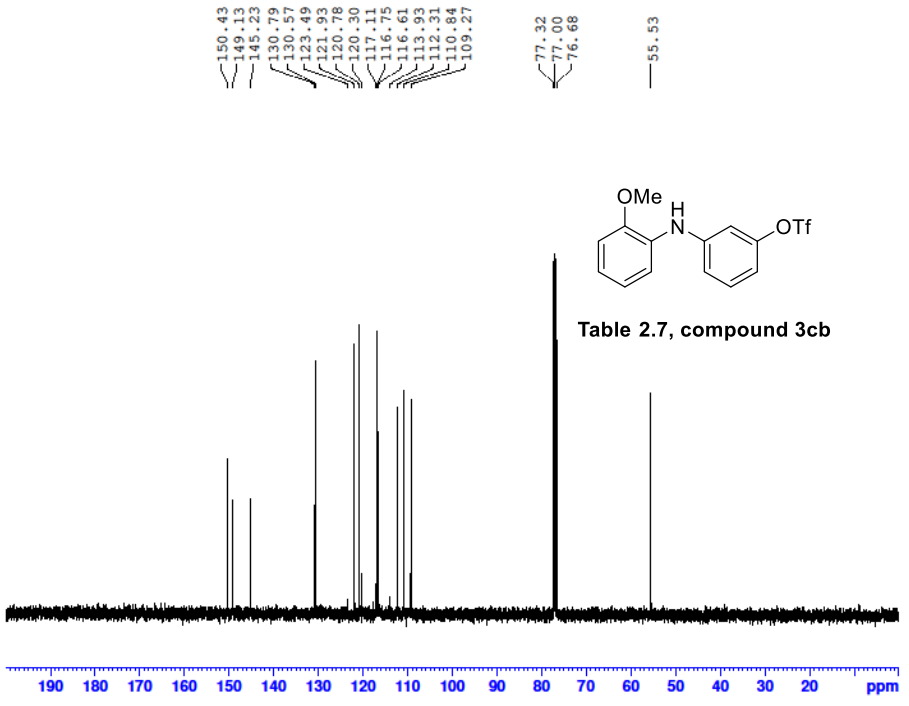

Table 2.7, compound 3cb

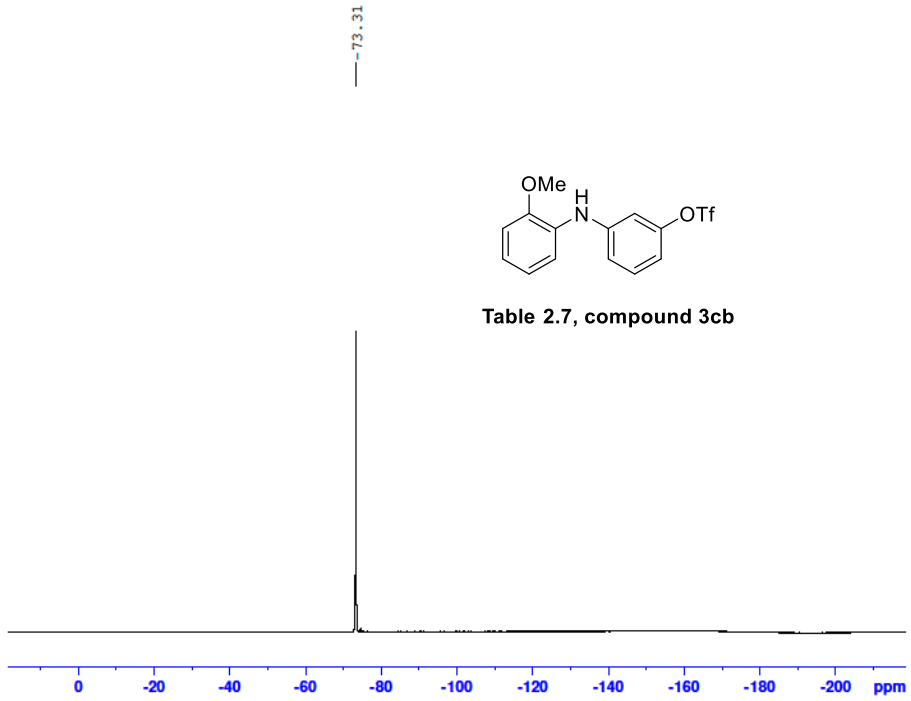

Table 2.7, compound 3cb

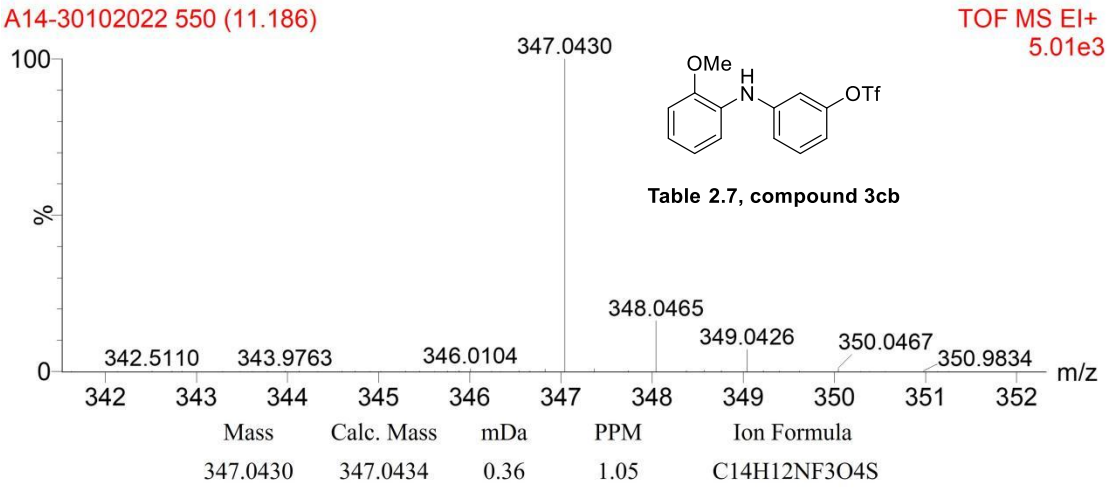

Table 2.7, compound 3cb

Mass	Calc. Mass	mDa	PPM	Ion Formula
347.0430	347.0434	0.36	1.05	C14H12NF3O4S

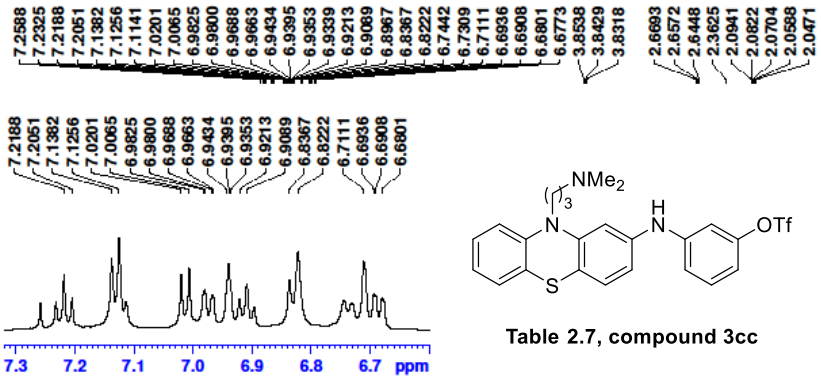

Table 2.7, compound 3cc

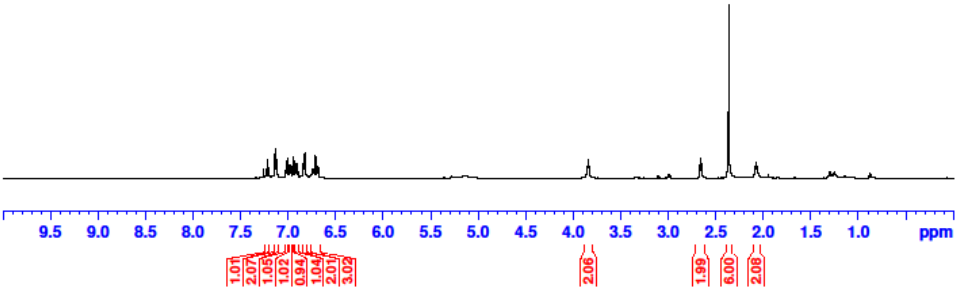

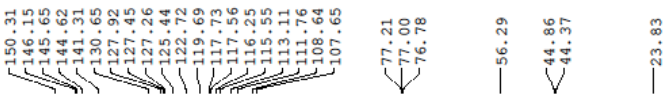

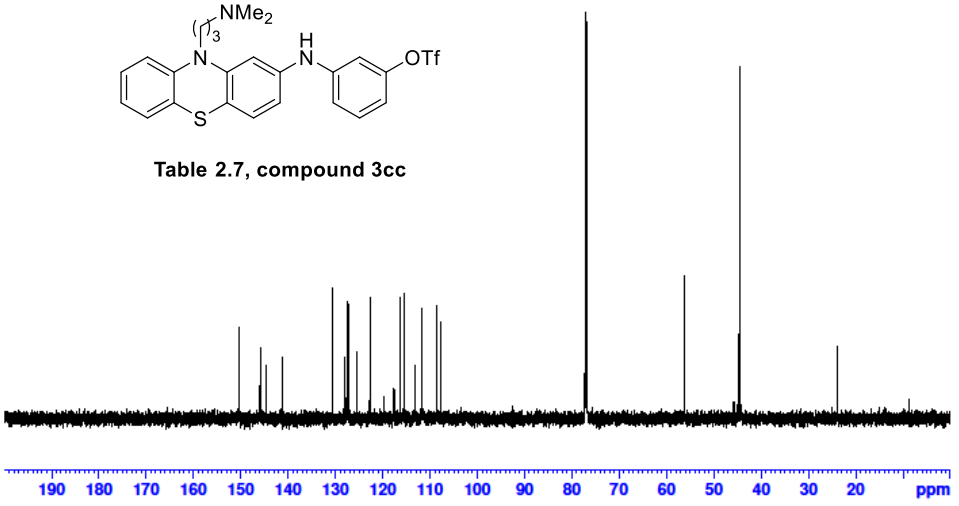

Table 2.7, compound 3cc

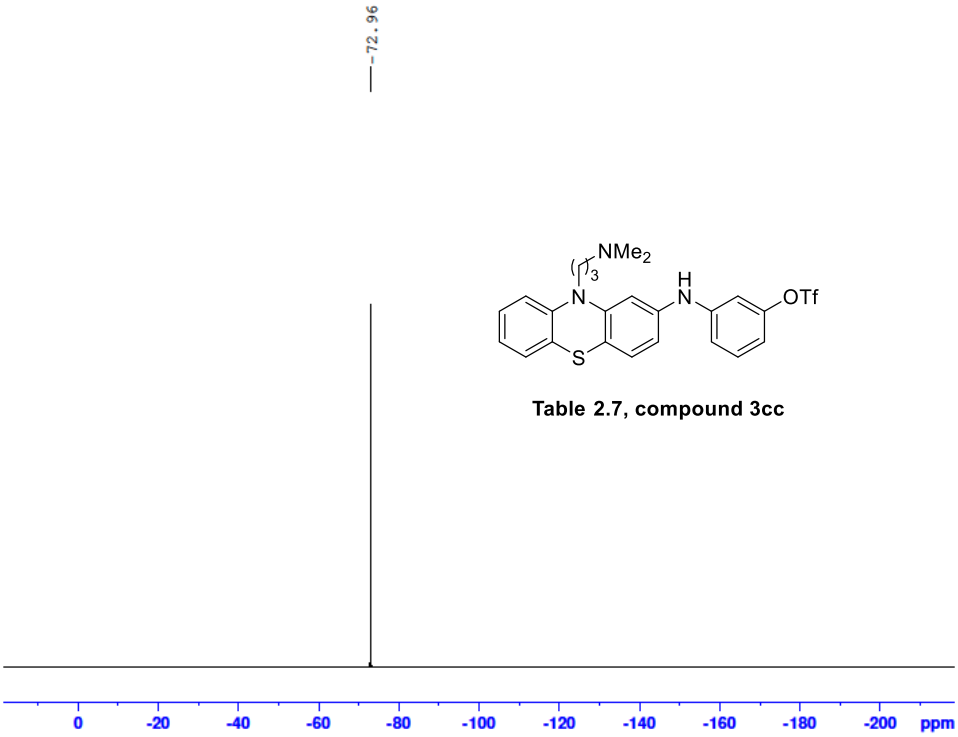

Table 2.7, compound 3cc

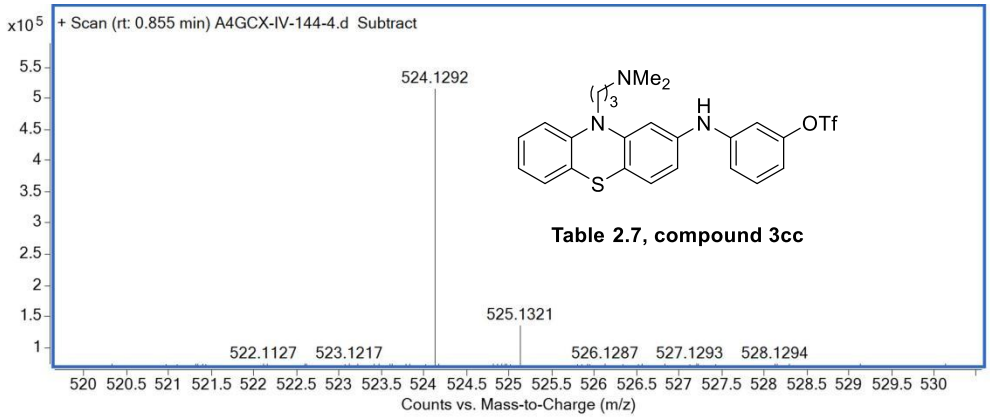

Table 2.7, compound 3cc

Mass	Calc. Mass	mDa	PPM	Ion Formula
524.1284	524.1292	-0.81	-1.54	C24H25F3O3N3S2

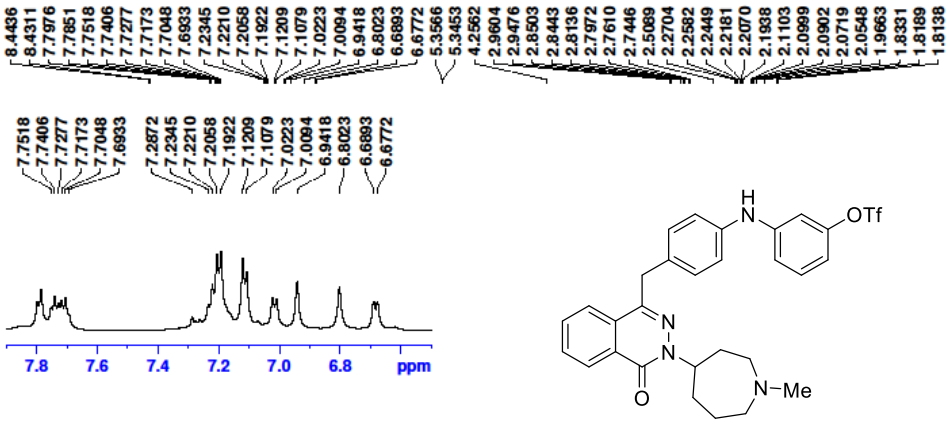

Table 2.7, compound 3cd

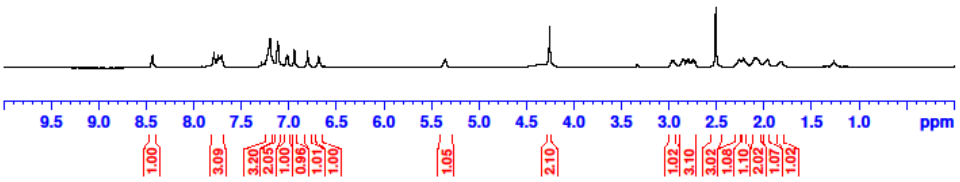

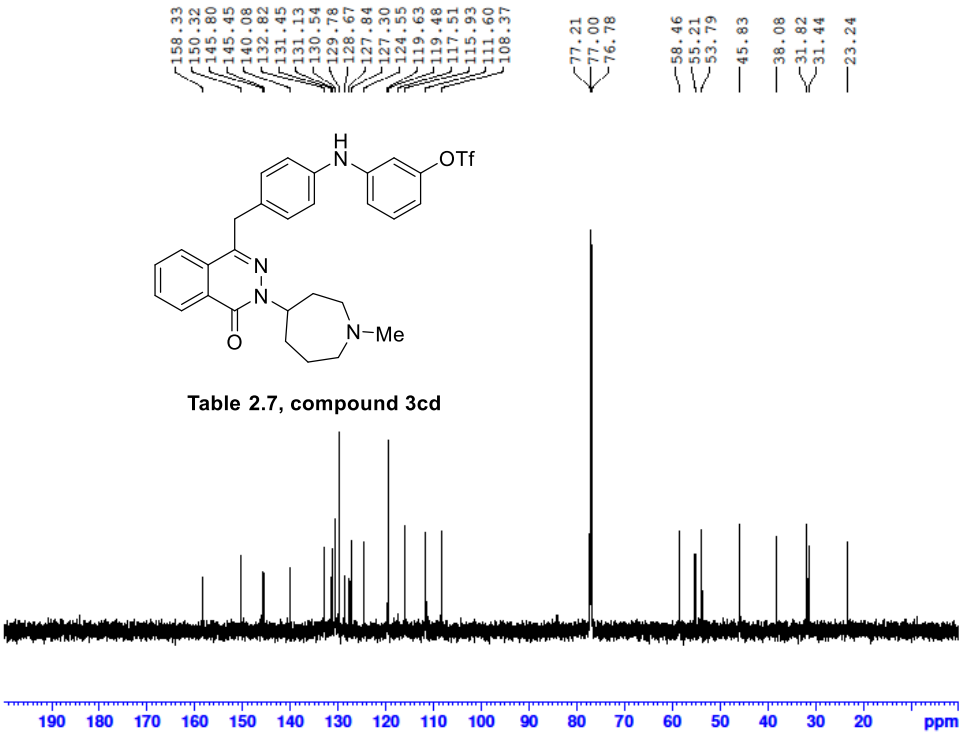

Table 2.7, compound 3cd

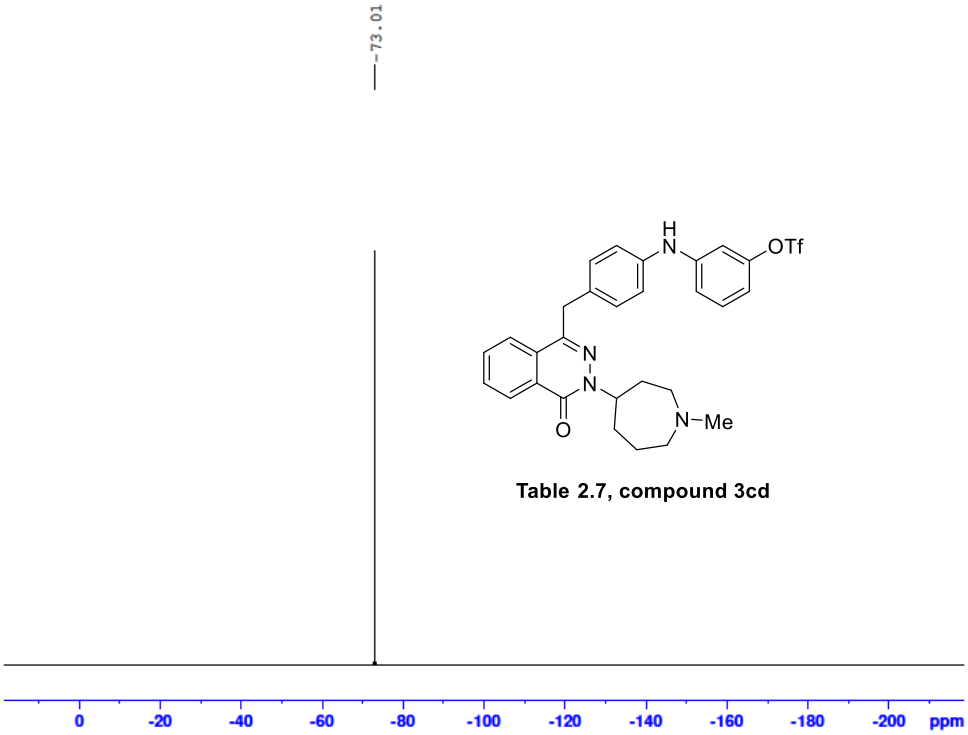

Table 2.7, compound 3cd

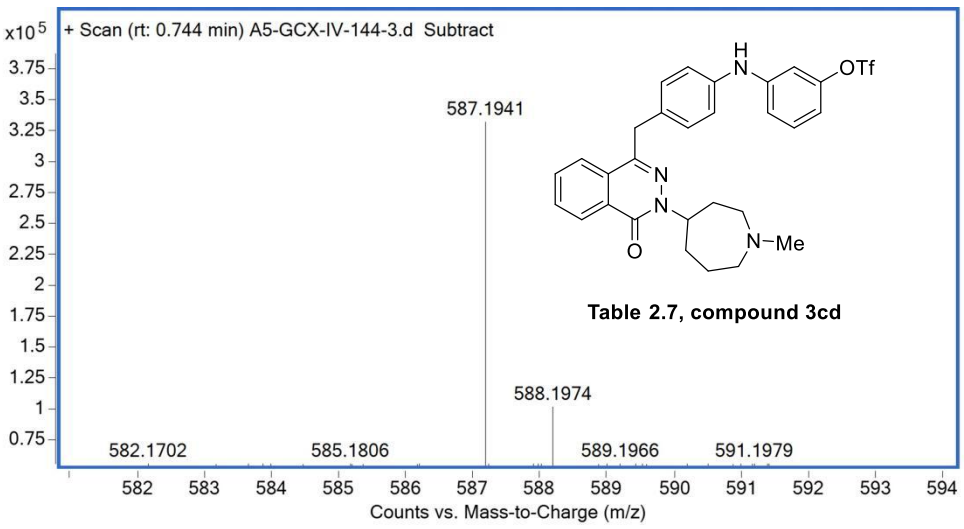

Table 2.7, compound 3cd

Mass	Calc. Mass	mDa	PPM	Ion Formula
587.1934	587.1941	-0.66	-1.13	C29H30F3O4N4S

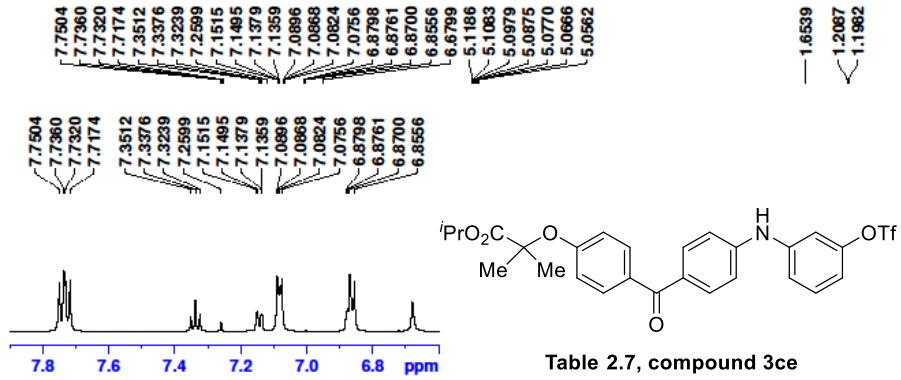

Table 2.7, compound 3ce

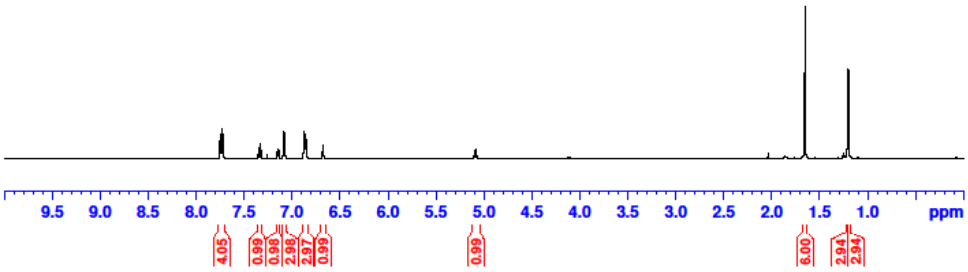

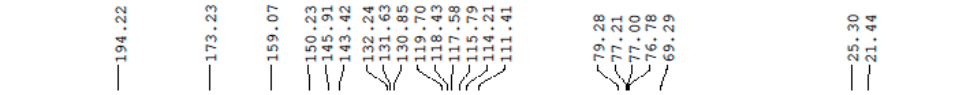

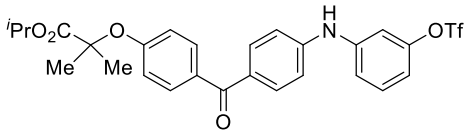

Table 2.7, compound 3ce

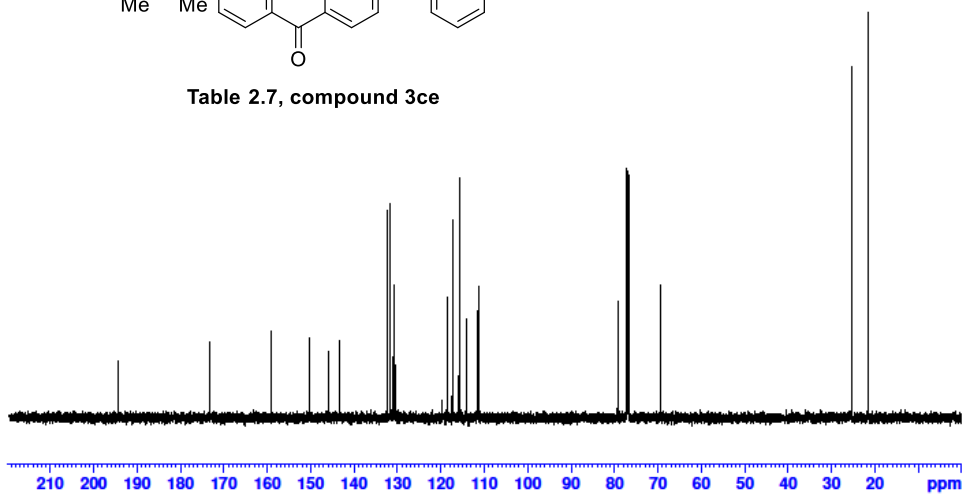

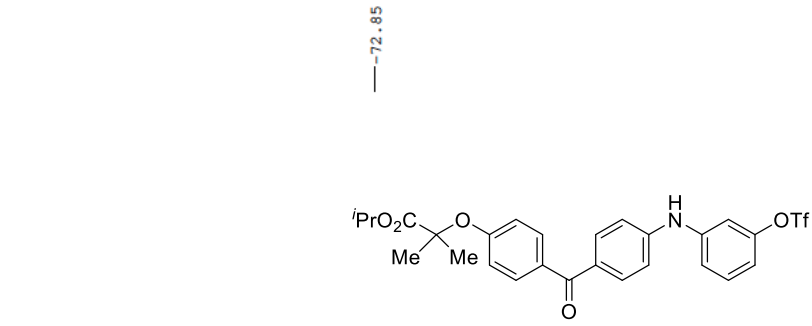

Table 2.7, compound 3ce

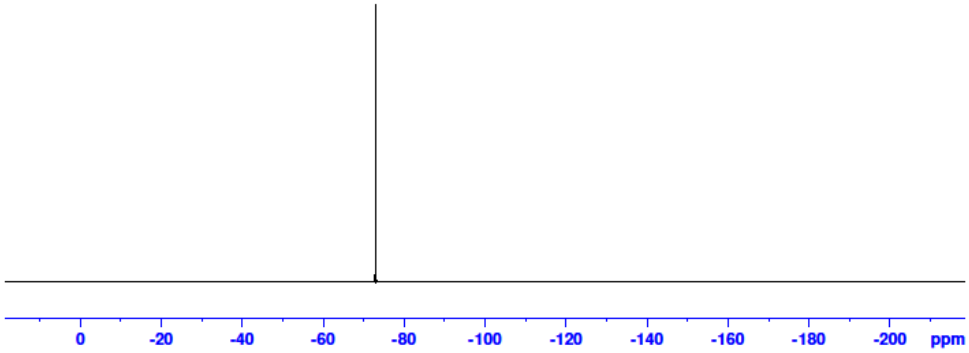

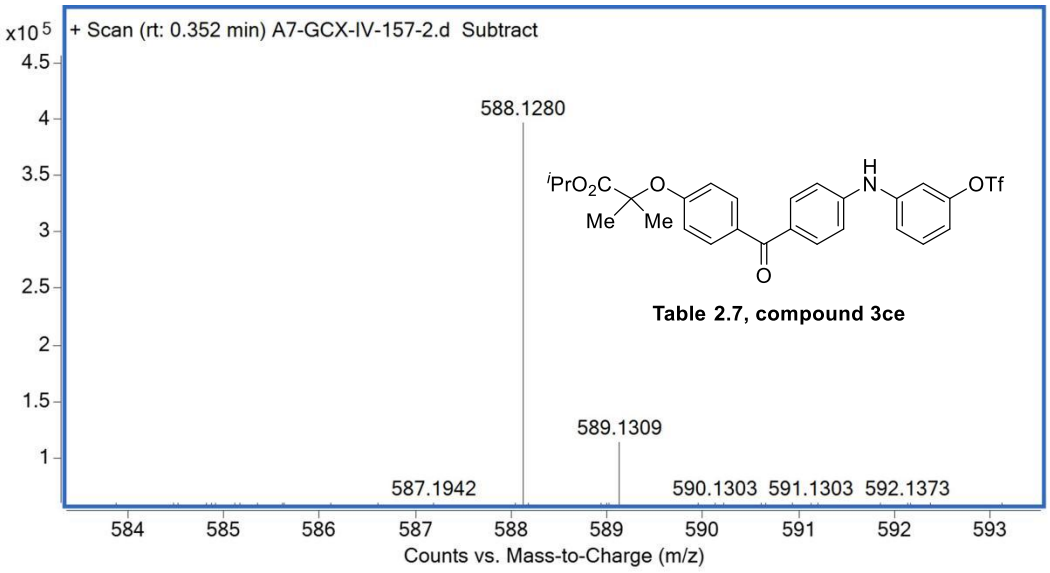

Table 2.7, compound 3ce

Mass	Calc. Mass	mDa	PPM	Ion Formula
588.1274	588.1280	-0.57	-1.01	C27H26F3O7NSNa

NMR & HRMS Spectra of Chapter 3

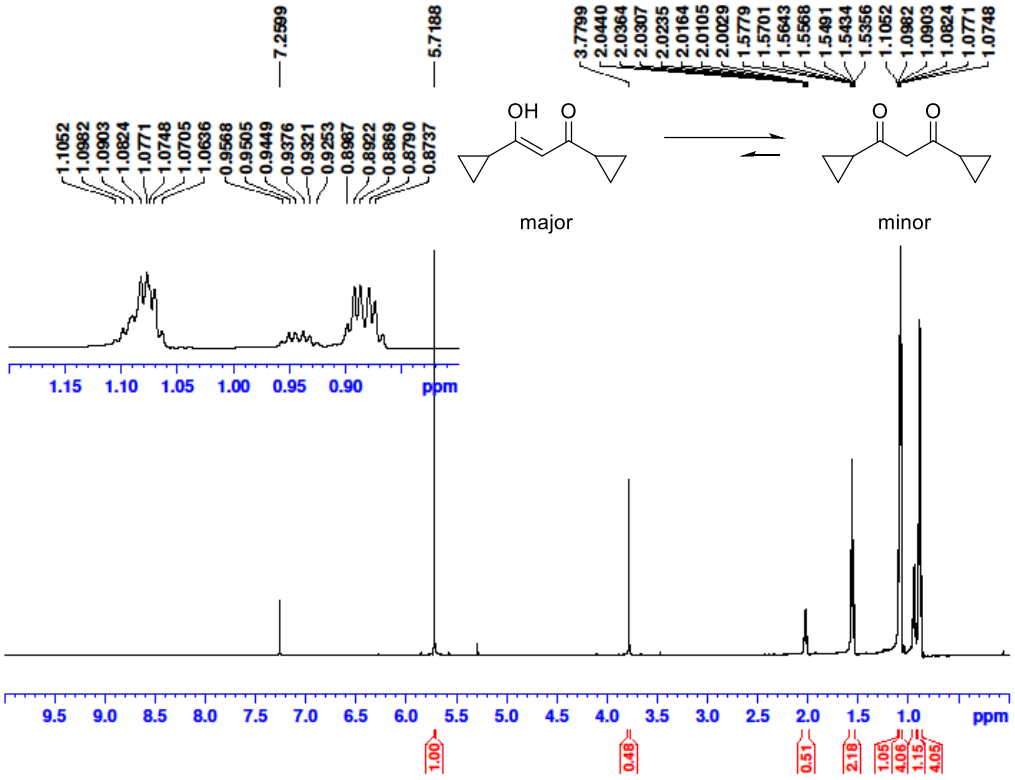

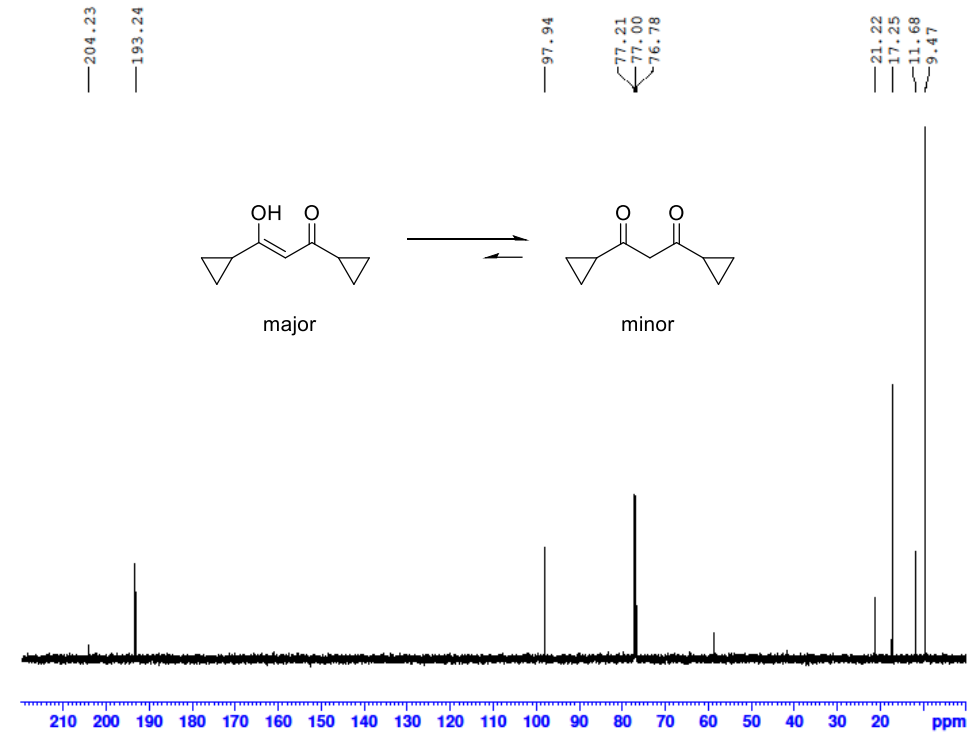

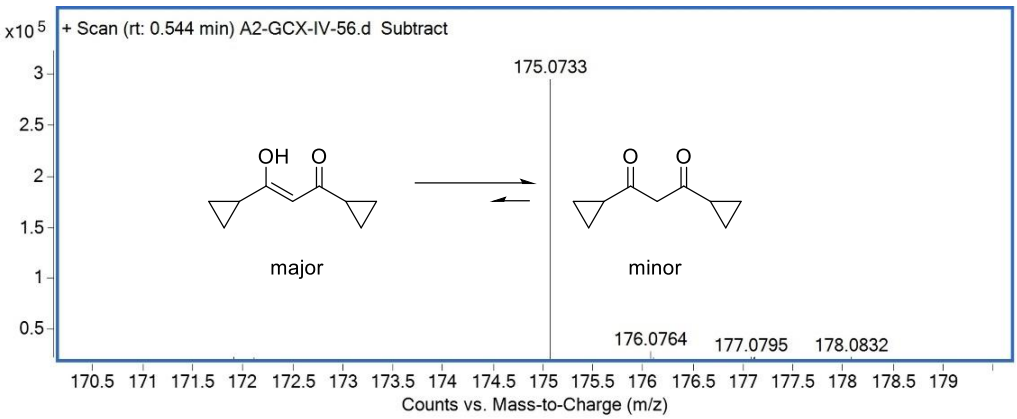

Mass	m/z (Calc)	Diff (mDa)	Diff (ppm)	Formula
175.0733	175.0730	-0.35	-2.30	C9 H12 O2Na

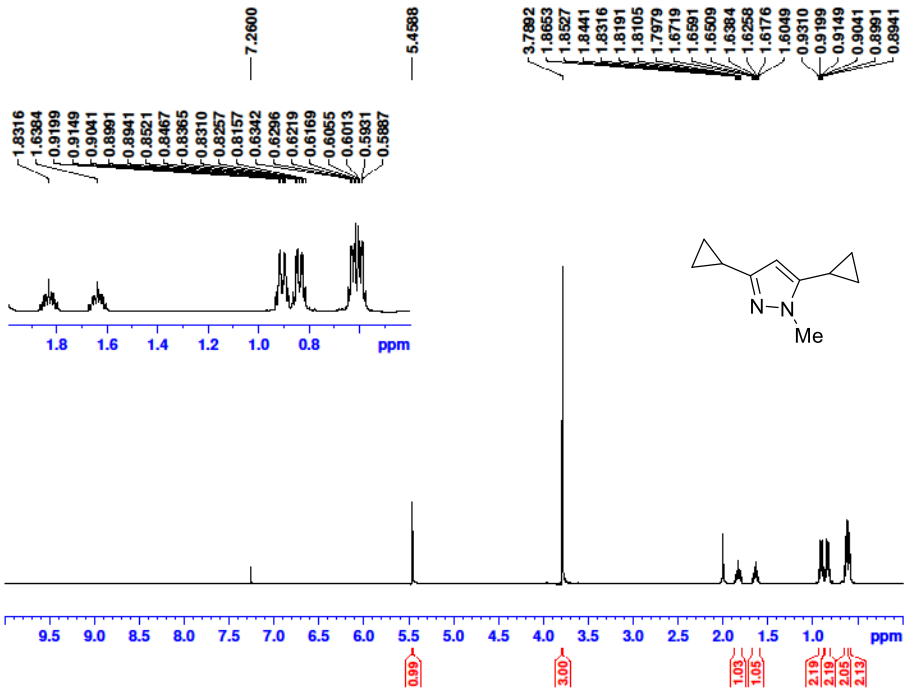

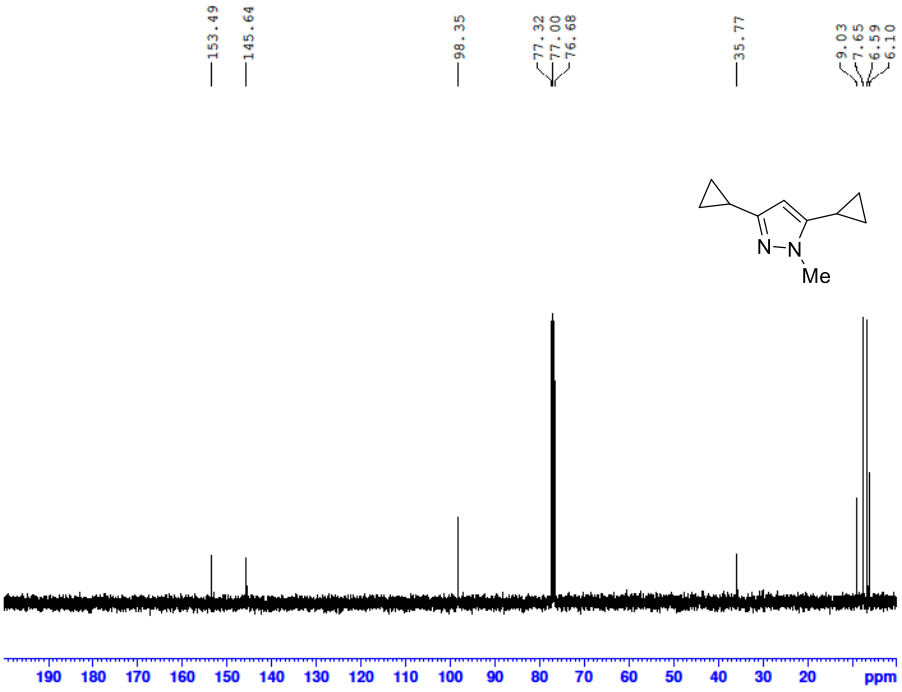

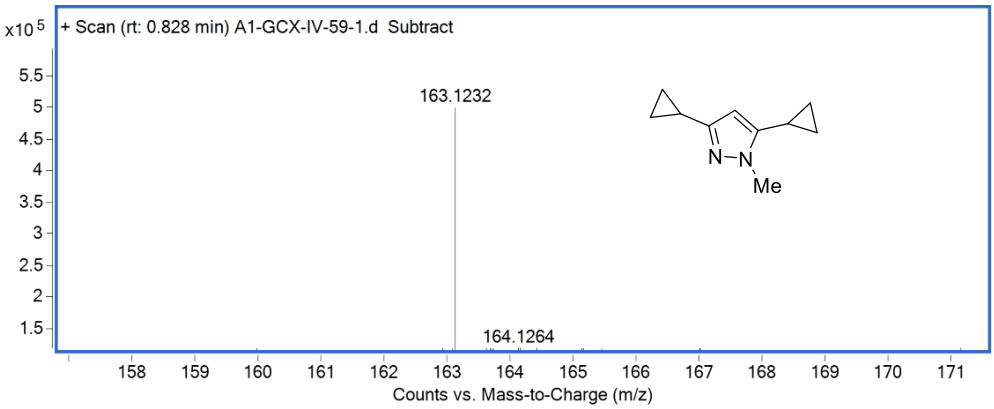

Mass	m/z (Calc)	Diff (mDa)	Diff (ppm)	Formula
163.1232	163.1230	-0.23	-1.39	C10 H15 N2

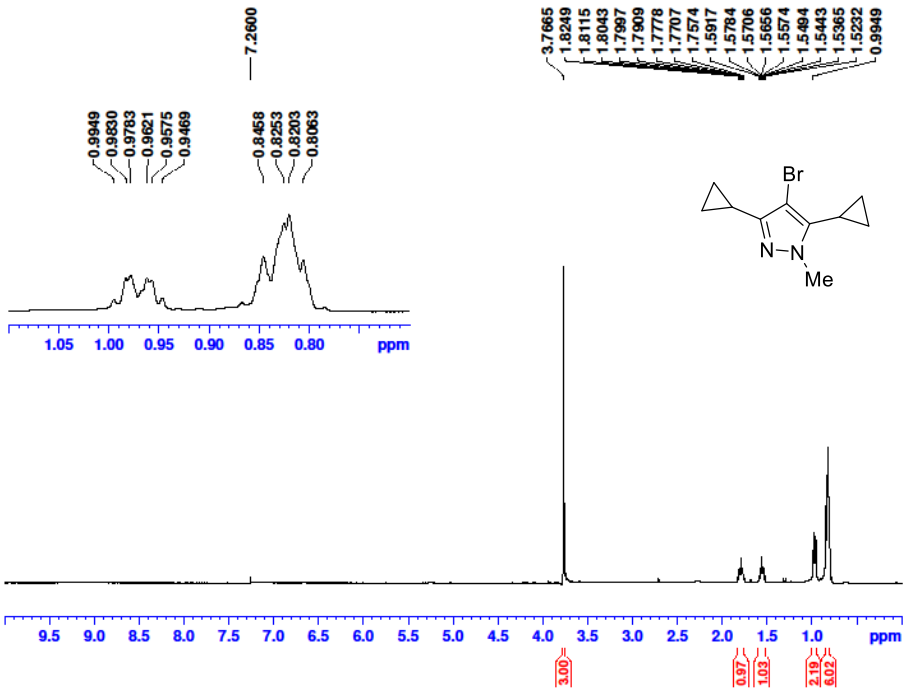
7.2600
3.7665
1.8249
1.8115
1.8043
1.7997
1.7909
1.7778
1.7707
1.7574
1.5917
1.5784
1.5706
1.5656
1.5574
1.5494
1.5443
1.5365
1.5232
0.9949
0.9949
0.9830
0.9783
0.9621
0.9575
0.9469
0.8458
0.8253
0.8203
0.8063
Br
N–N
Me
1.05 1.00 0.95 0.90 0.85 0.80 ppm
9.5 9.0 8.5 8.0 7.5 7.0 6.5 6.0 5.5 5.0 4.5 4.0 3.5 3.0 2.5 2.0 1.5 1.0 ppm
3.00
0.97
1.03
2.19
6.02

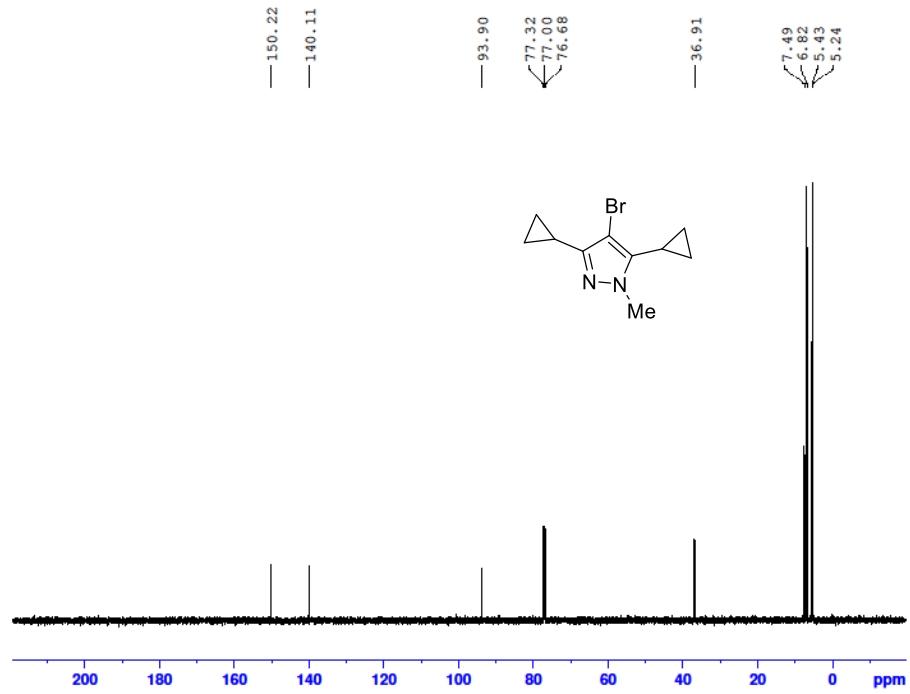
150.22
140.11
93.90
77.32
77.00
76.68
36.91
7.49
6.82
5.43
5.24
Br
N–N
Me
200 180 160 140 120 100 80 60 40 20 0 ppm

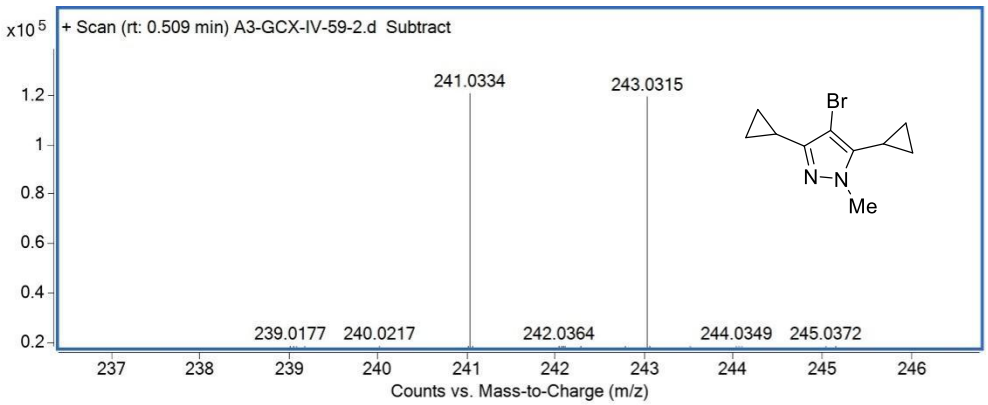

Mass	m/z (Calc)	Diff (mDa)	Diff (ppm)	Formula
241.0334	241.0335	0.09	0.37	C10 H14 BrN2

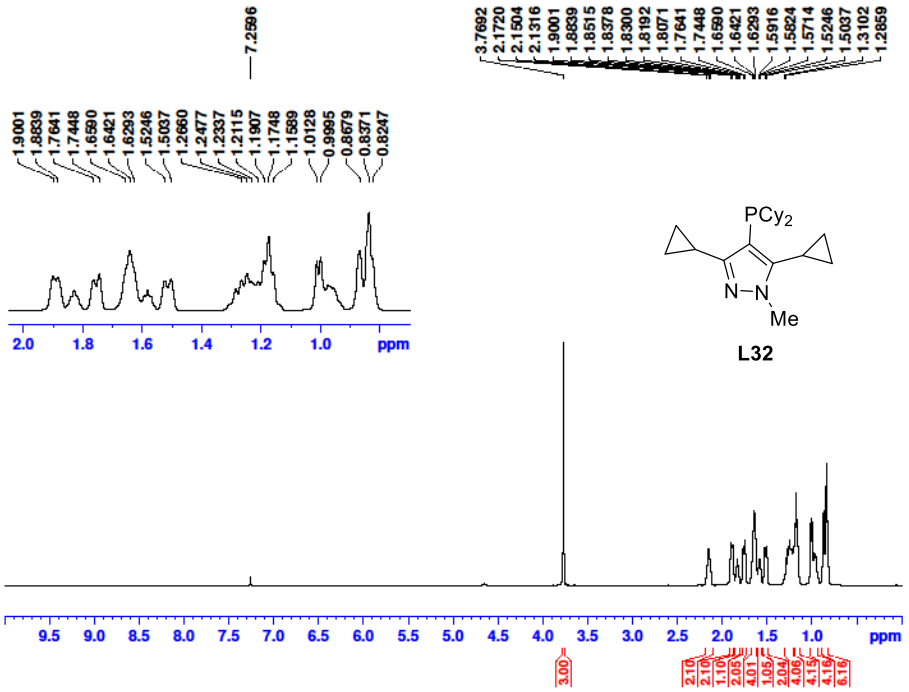

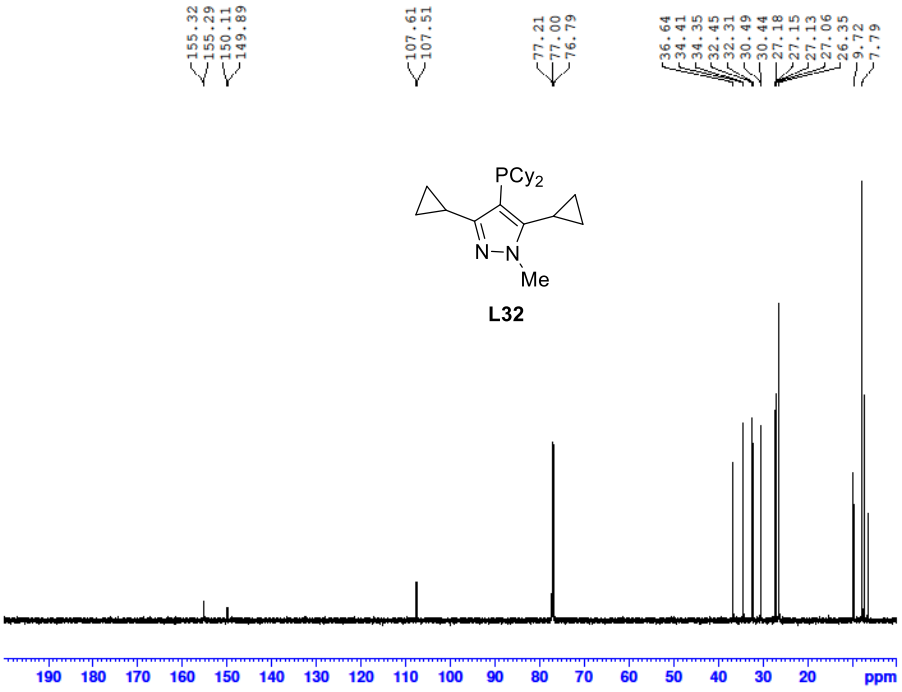
155.32
155.29
150.11
149.89
107.61
107.51
77.21
77.00
76.79
36.64
34.41
34.35
32.45
32.31
30.49
30.44
27.18
27.15
27.13
27.06
26.35
9.72
7.79
PCy2
N–N
Me
190 180 170 160 150 140 130 120 110 100 90 80 70 60 50 40 30 20 ppm

L32

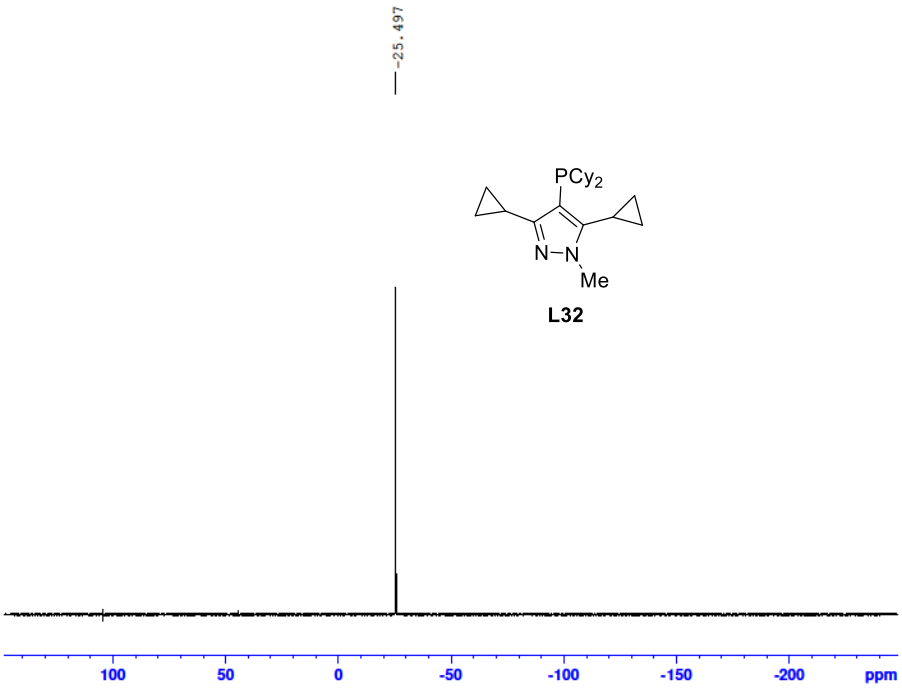
-25.497
PCy2
N–N
Me
100 50 0 -50 -100 -150 -200 ppm

L32

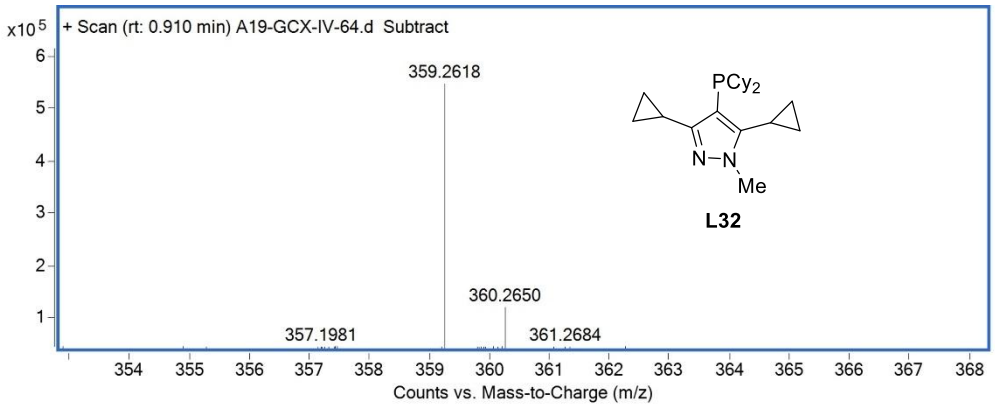

Mass	Calc. Mass	mDa	PPM	Ion Formula
359.2618	359.2611	-0.74	-2.06	C22H36N2P

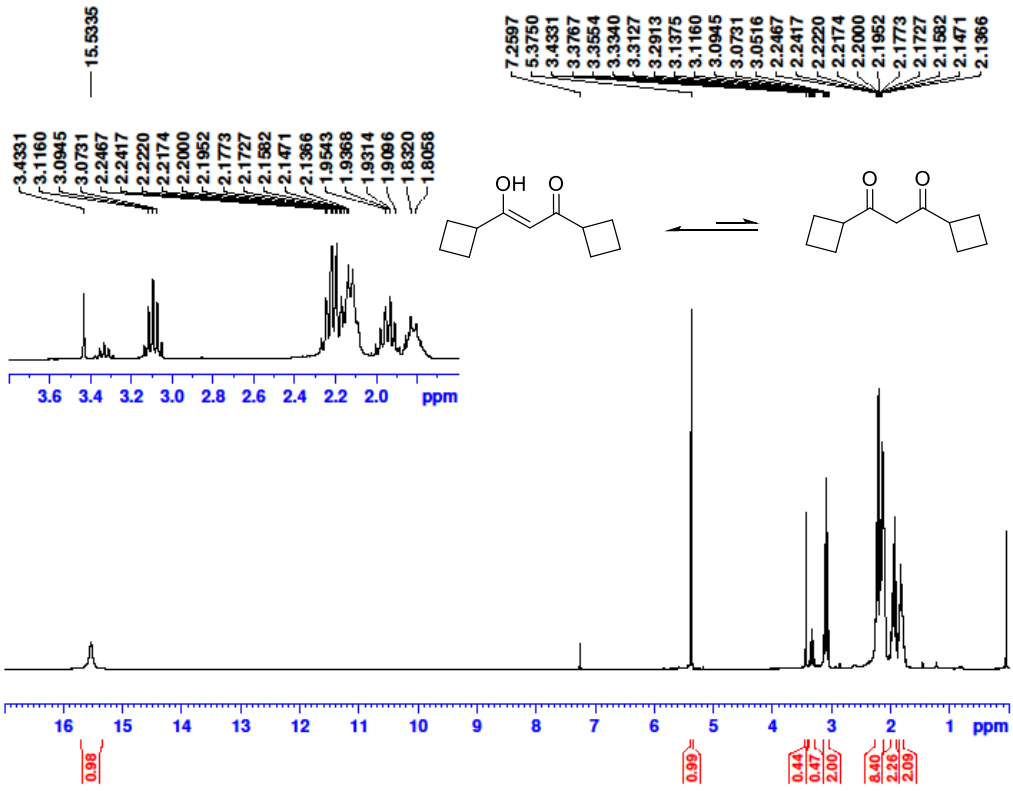

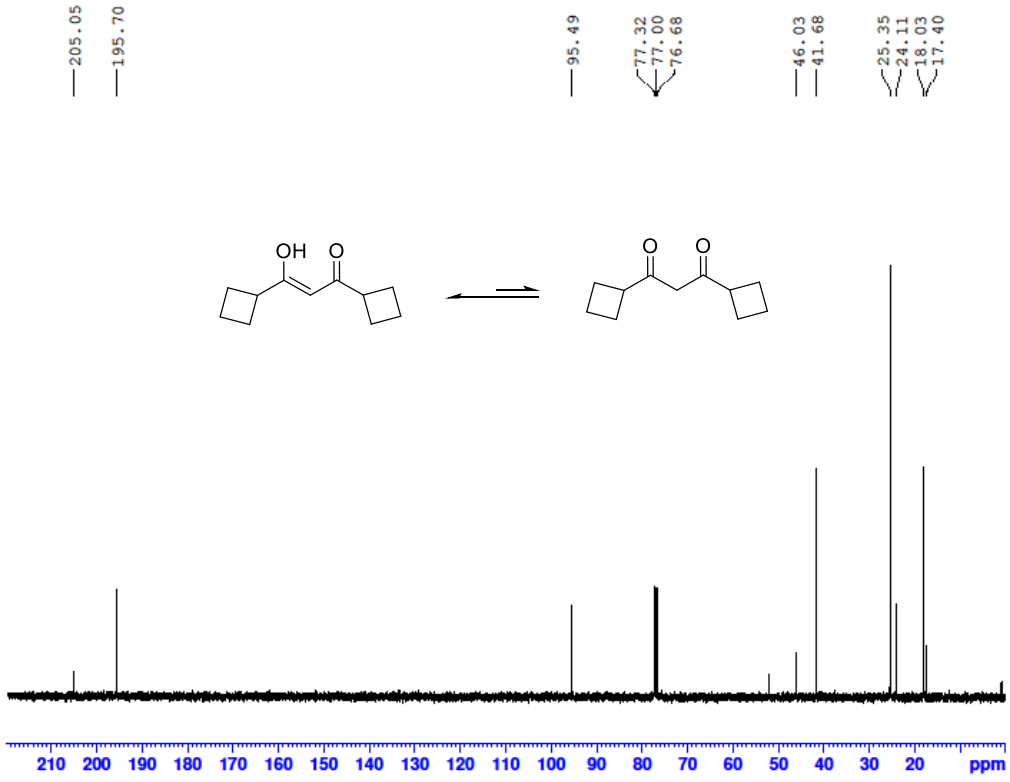

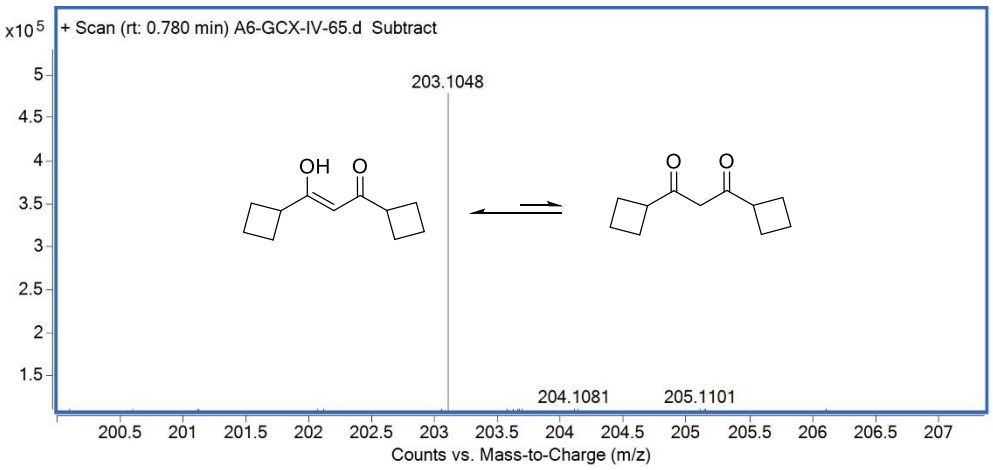

Mass	Calc. Mass	mDa	PPM	Ion Formula
203.1048	203.1043	-0.55	-3.05	C11H16O2Na

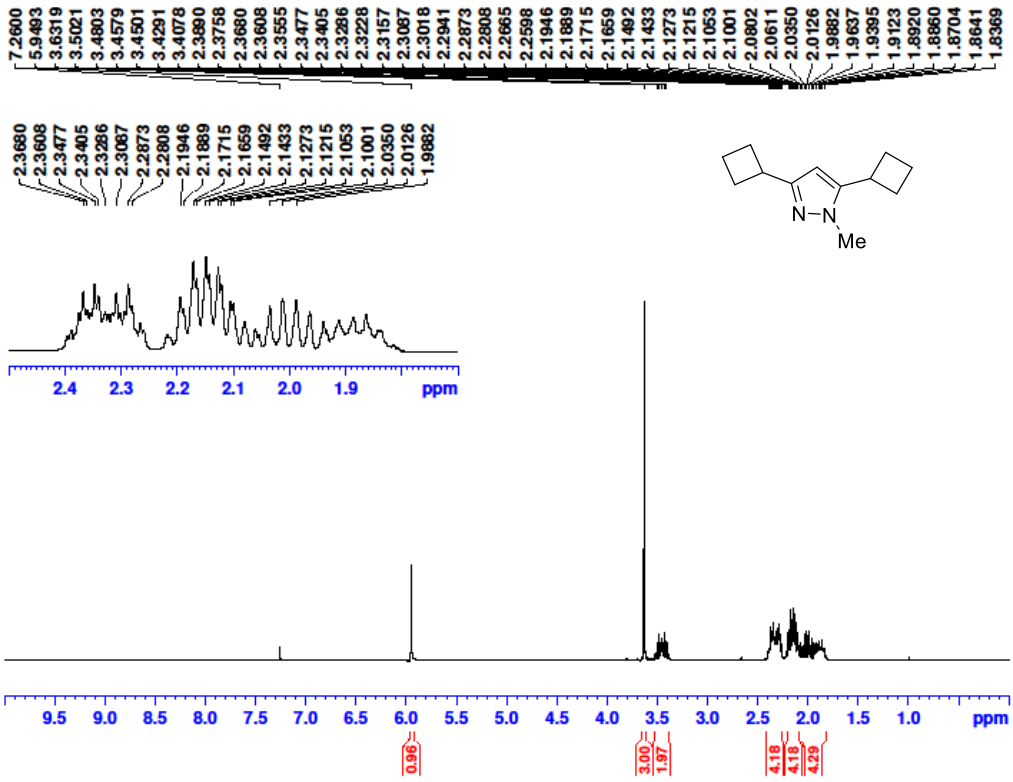
7.2600
5.9493
3.6319
3.5021
3.4803
3.4579
3.4501
3.4291
3.4078
3.3890
3.3758
3.3680
3.3608
3.3555
3.3477
3.3405
3.3286
3.3228
3.3157
3.3087
3.3018
3.2941
3.2873
3.2808
3.2665
3.2598
3.1946
3.1889
3.1715
3.1659
3.1492
3.1433
3.1273
3.1215
3.1053
3.1001
3.0802
3.0611
3.0350
3.0126
1.9882
1.9637
1.9395
1.9123
1.8920
1.8860
1.8704
1.8641
1.8369
N
N
Me
2.4
2.3
2.2
2.1
2.0
1.9
ppm
9.5
9.0
8.5
8.0
7.5
7.0
6.5
6.0
5.5
5.0
4.5
4.0
3.5
3.0
2.5
2.0
1.5
1.0
ppm
0.96
3.00
1.97
4.18
4.18
4.29

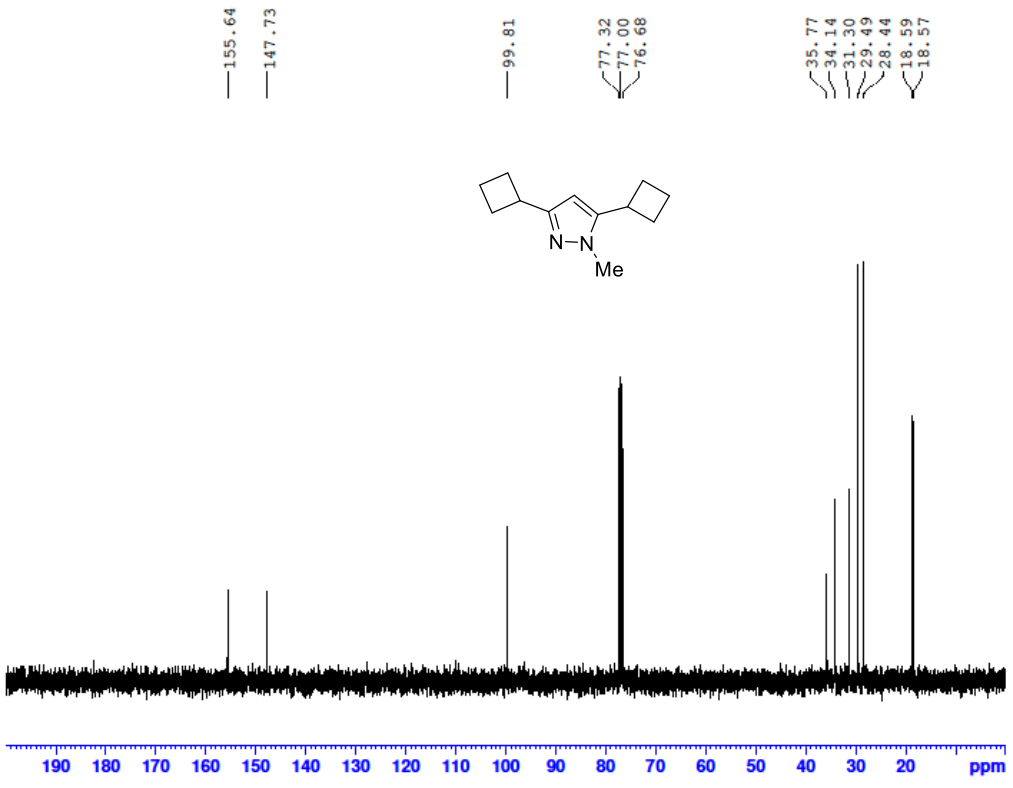
155.64
147.73
99.81
77.32
77.00
76.68
35.77
34.14
31.30
29.49
28.44
18.59
18.57
N
N
Me
190
180
170
160
150
140
130
120
110
100
90
80
70
60
50
40
30
20
ppm

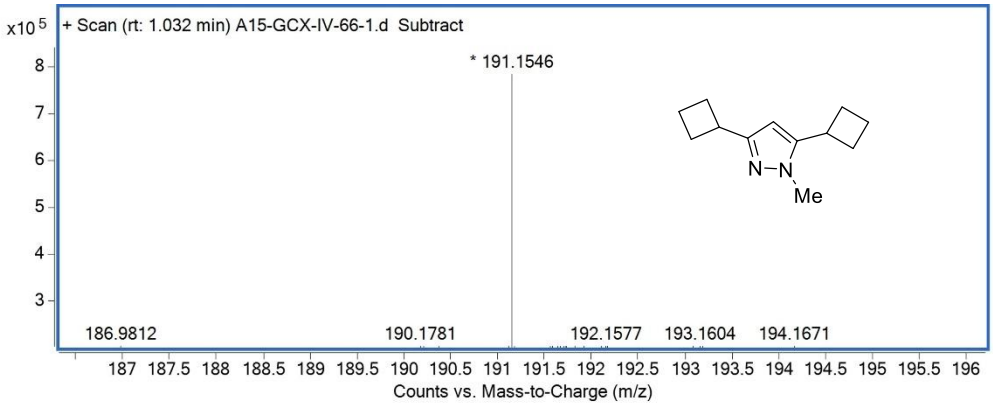

Mass	Calc. Mass	mDa	PPM	Ion Formula
191.1546	191.1543	-0.32	-1.71	C12H19N2

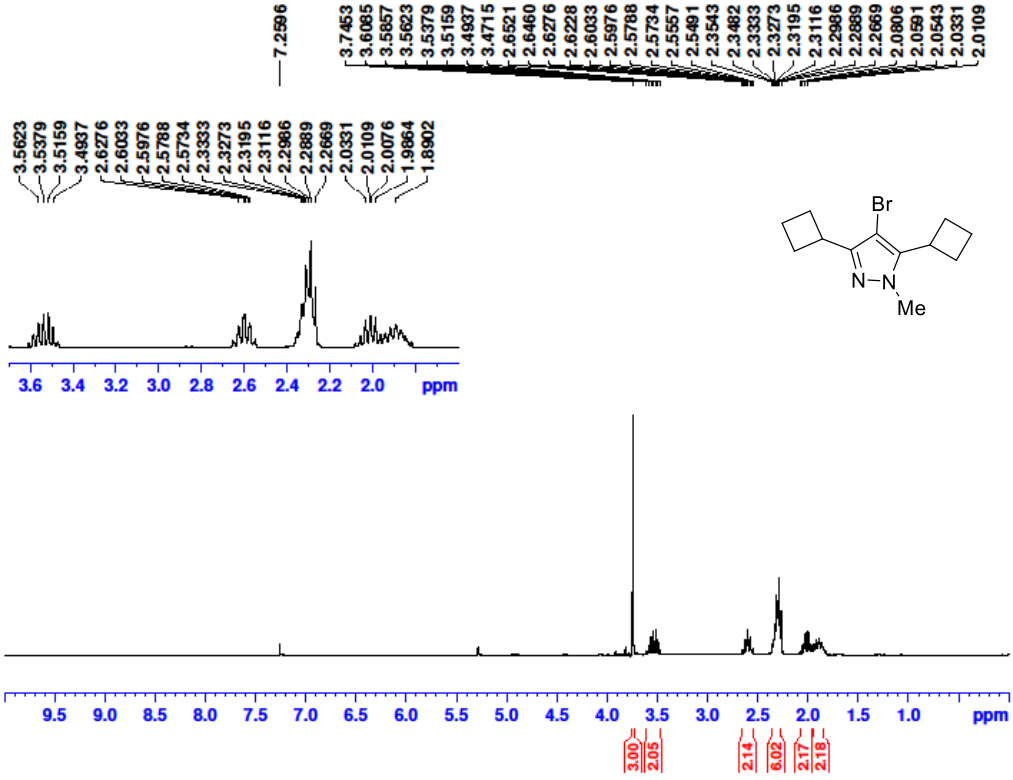

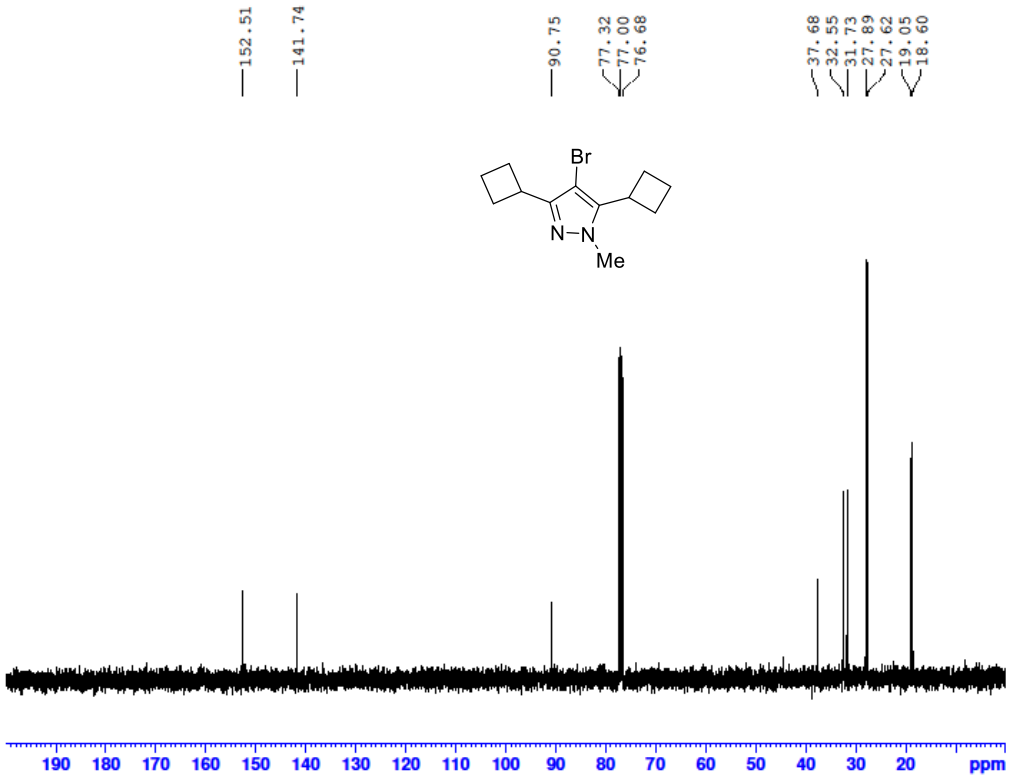

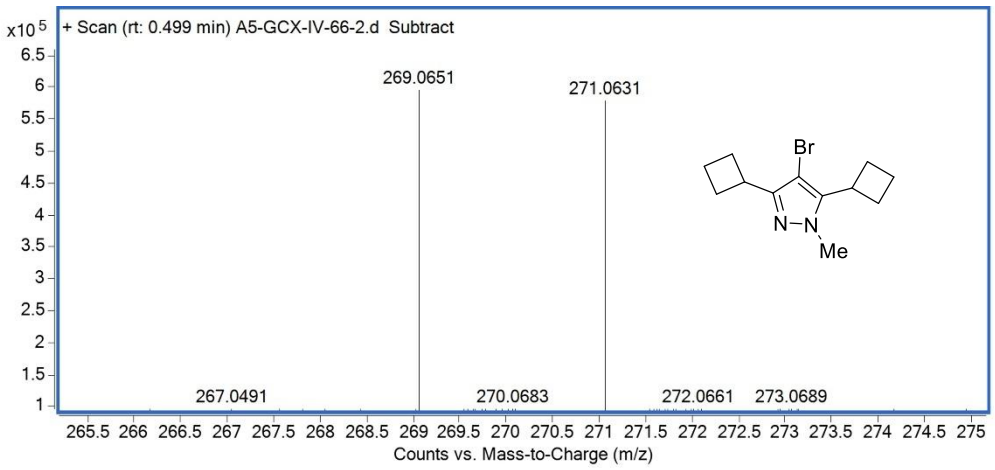

Mass	Calc. Mass	mDa	PPM	Ion Formula
269.0651	269.0648	-0.31	-1.16	C12H18N2Br

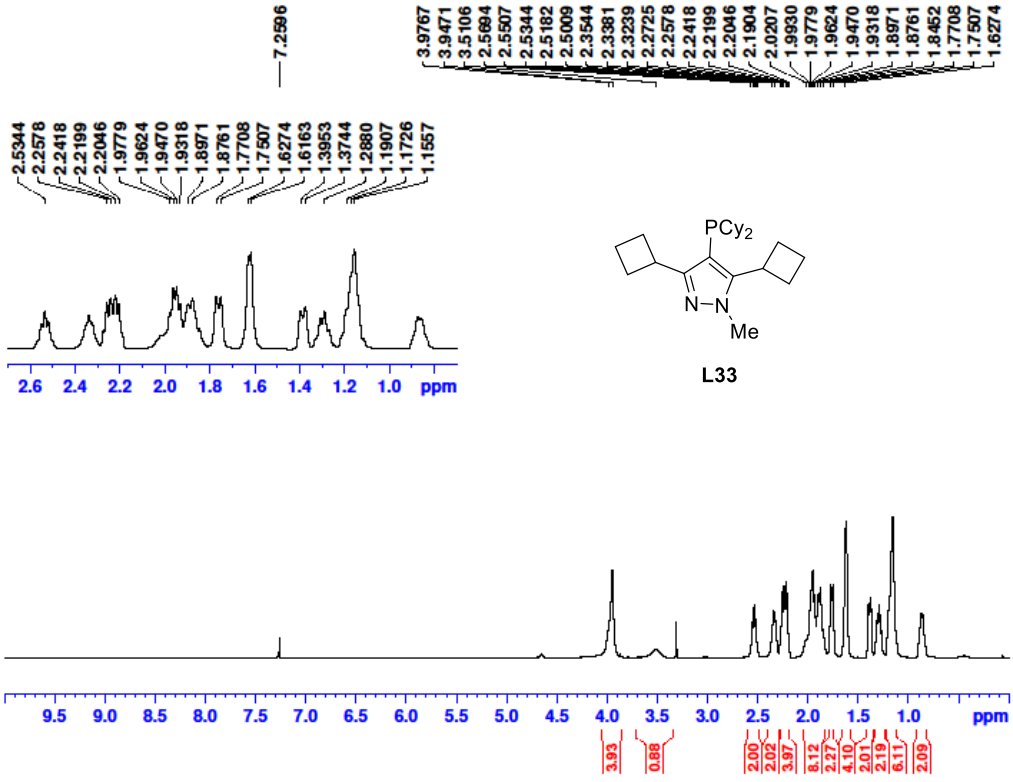
7.2596
3.9767
3.9471
3.5106
2.5684
2.5507
2.5344
2.5182
2.5009
2.3544
2.3381
2.3239
2.2725
2.2578
2.2418
2.2199
2.2046
2.1904
2.0207
1.9930
1.9779
1.9624
1.9470
1.9318
1.8971
1.8761
1.8452
1.7708
1.7507
1.6274
2.5344
2.2578
2.2418
2.2199
2.2046
1.9779
1.9624
1.9470
1.9318
1.8971
1.8761
1.7708
1.7507
1.6274
1.6163
1.3953
1.3744
1.2880
1.1907
1.1726
1.1557
2.6 2.4 2.2 2.0 1.8 1.6 1.4 1.2 1.0 ppm
PCy2
N–N
Me
L33
9.5 9.0 8.5 8.0 7.5 7.0 6.5 6.0 5.5 5.0 4.5 4.0 3.5 3.0 2.5 2.0 1.5 1.0 ppm
3.93
0.88
2.00
2.02
3.97
8.12
2.27
4.10
2.01
2.19
6.11
2.09

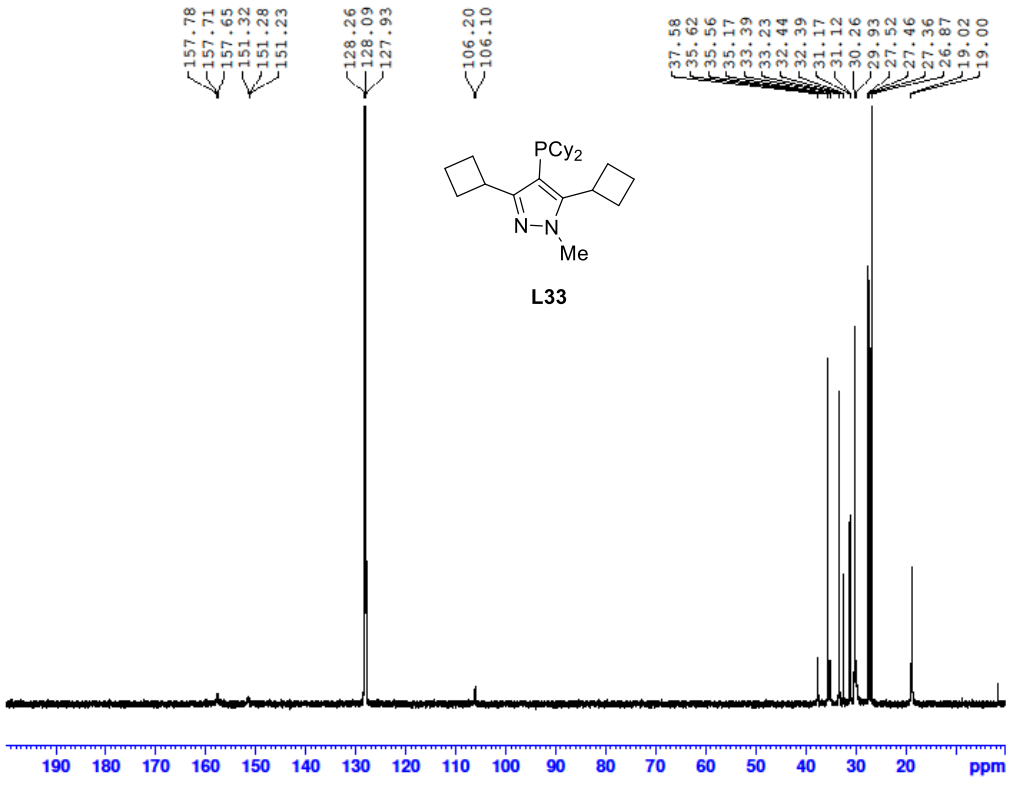
157.78
157.71
157.65
151.32
151.28
151.23
128.26
128.09
127.93
106.20
106.10
37.58
35.62
35.56
35.17
33.39
33.23
32.44
32.39
31.17
31.12
30.26
29.93
27.52
27.46
27.36
26.87
19.02
19.00
PCy2
N–N
Me
L33
190 180 170 160 150 140 130 120 110 100 90 80 70 60 50 40 30 20 ppm

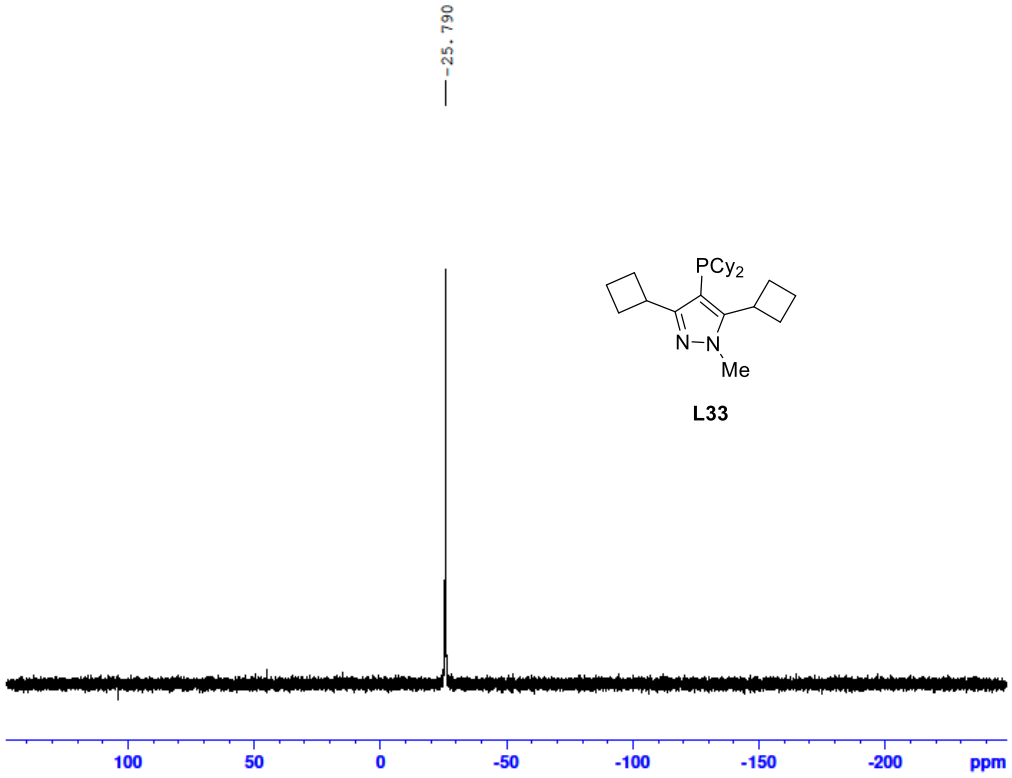

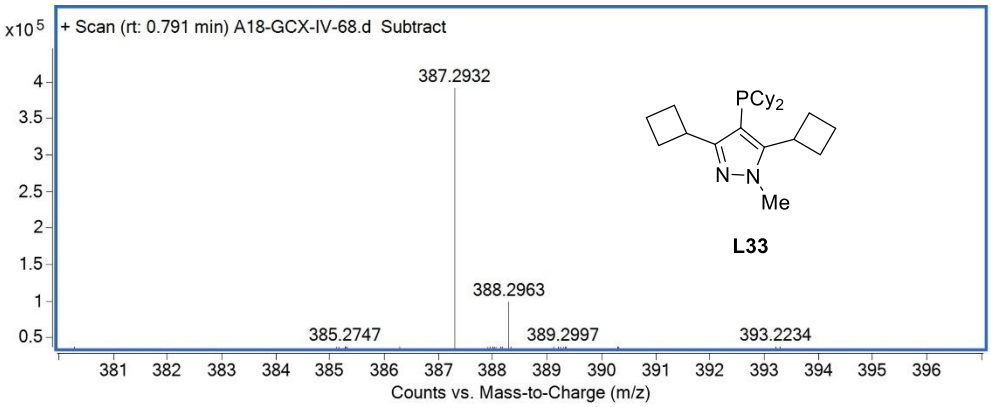

Mass	Calc. Mass	mDa	PPM	Ion Formula
387.2932	387.2924	-0.84	-2.17	C24H40N2P

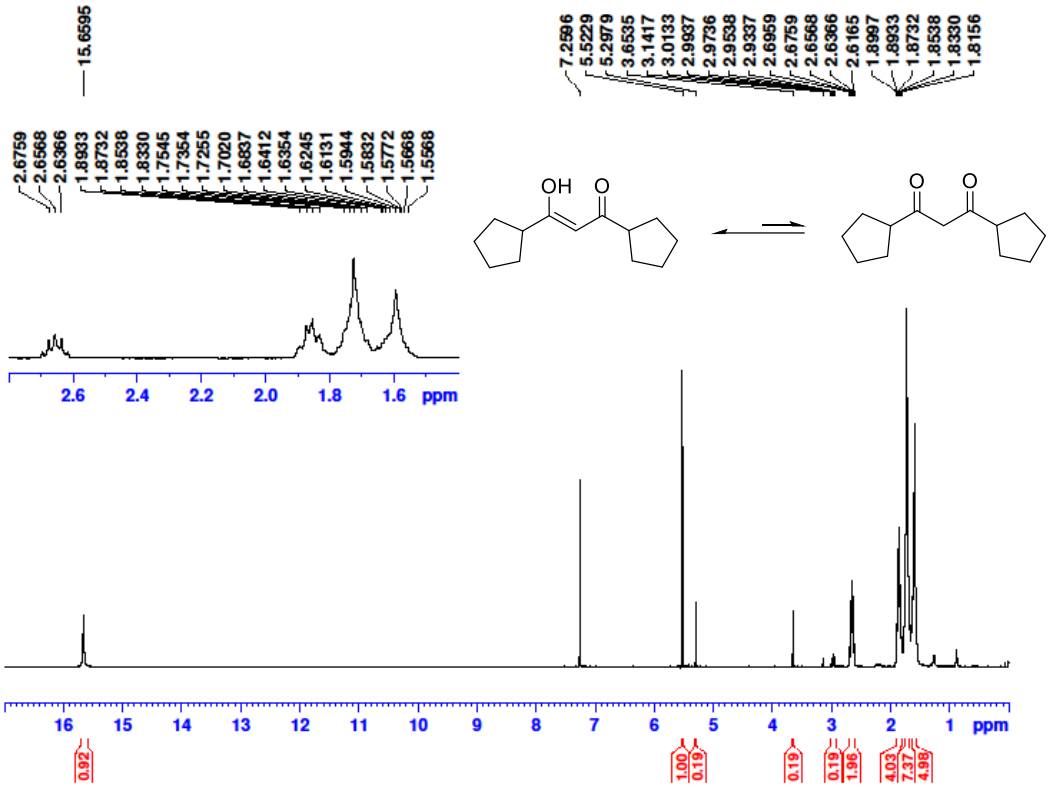
15.6595
7.2596
5.5229
5.2979
3.6535
3.1417
3.0133
2.9937
2.9736
2.9538
2.9337
2.6959
2.6759
2.6568
2.6366
2.6165
1.8997
1.8933
1.8732
1.8538
1.8330
1.8156
2.6759
2.6568
2.6366
1.8933
1.8732
1.8538
1.8330
1.7545
1.7354
1.7255
1.7020
1.6837
1.6412
1.6354
1.6245
1.6131
1.5944
1.5832
1.5772
1.5668
1.5568
OH
O
O
O
2.6
2.4
2.2
2.0
1.8
1.6
ppm
16
15
14
13
12
11
10
9
8
7
6
5
4
3
2
1
ppm
0.92
1.00
0.19
0.19
0.19
1.96
4.03
7.37
4.98

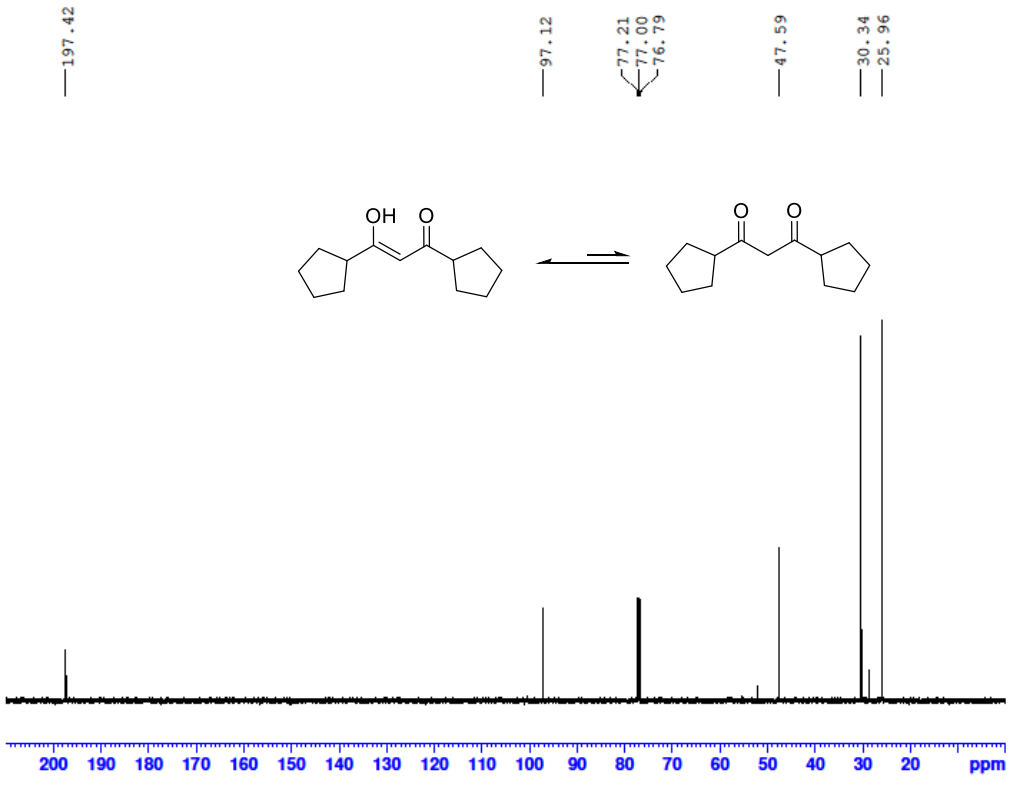
197.42
97.12
77.21
77.00
76.79
47.59
30.34
25.96
OH
O
O
O
200
190
180
170
160
150
140
130
120
110
100
90
80
70
60
50
40
30
20
ppm

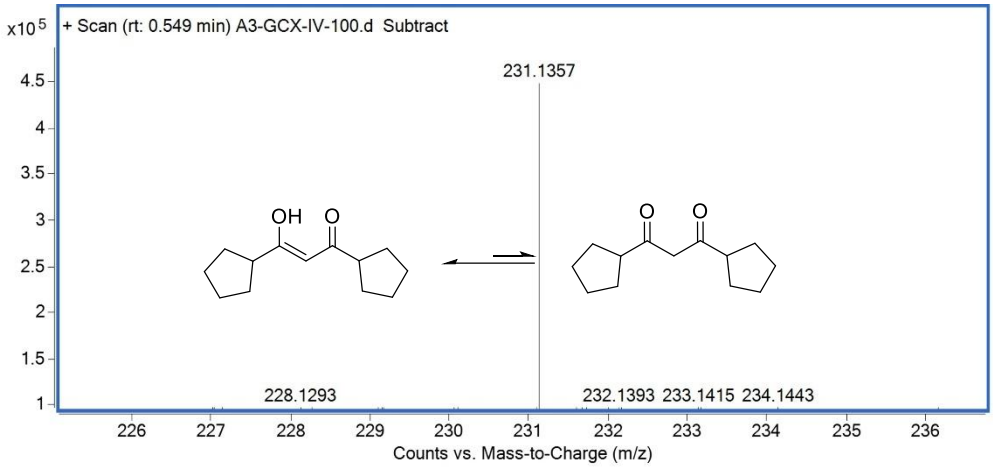

Mass	Calc. Mass	mDa	PPM	Ion Formula
231.1357	231.1356	-0.15	-0.72	C13H20O2Na

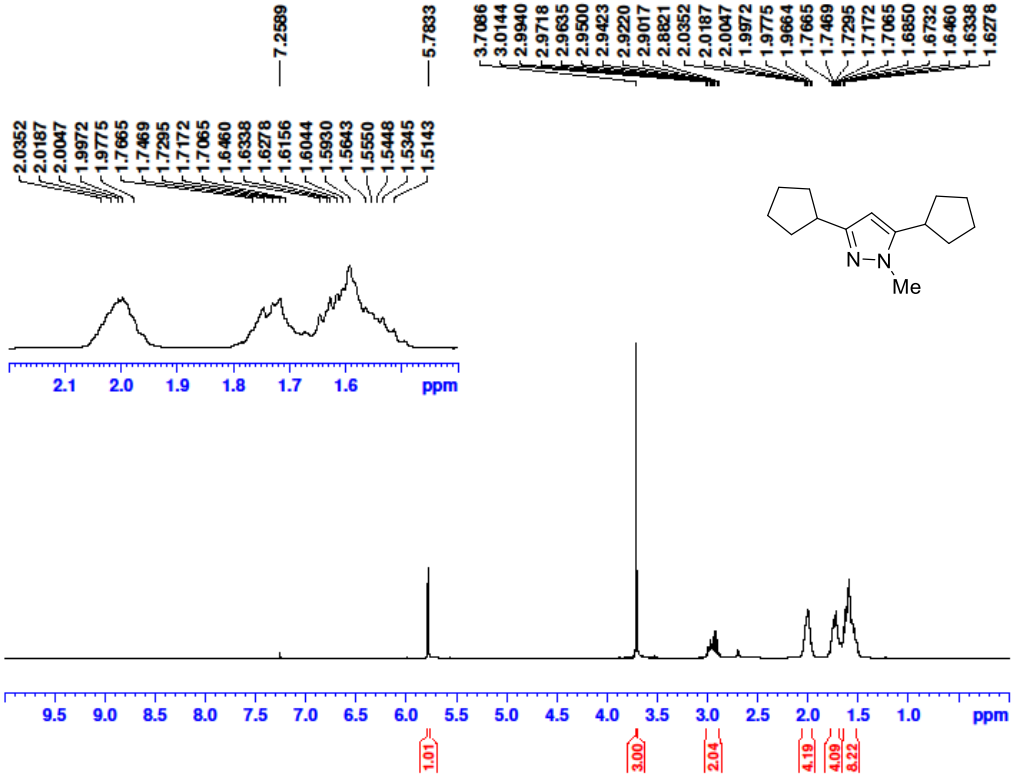

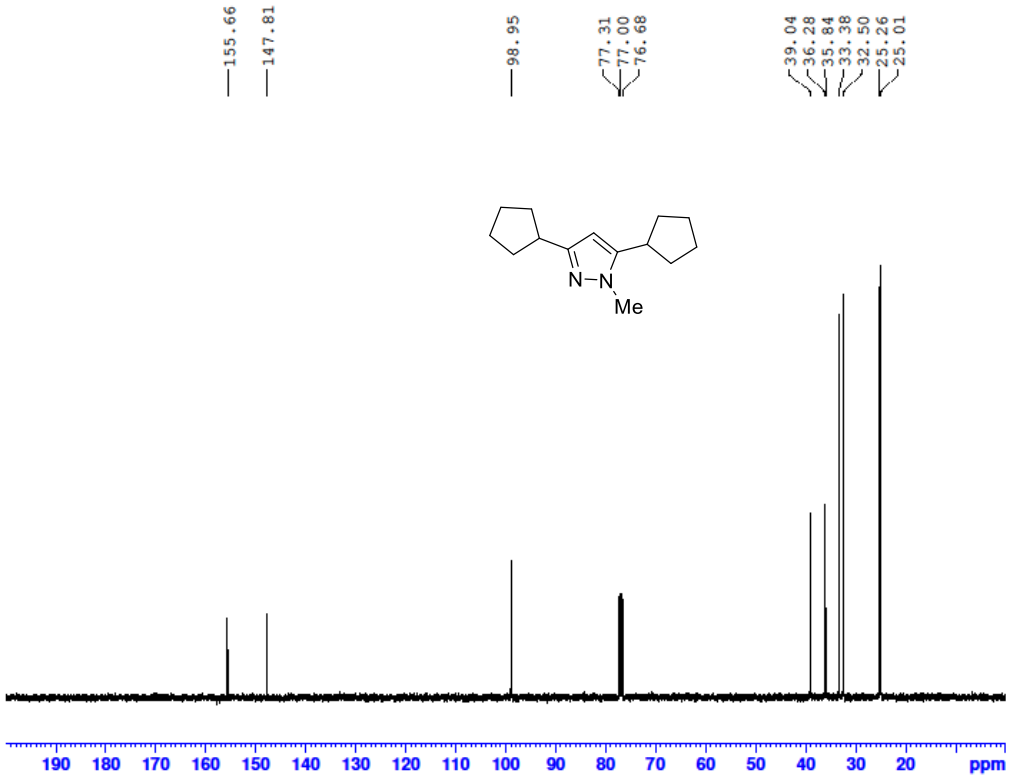

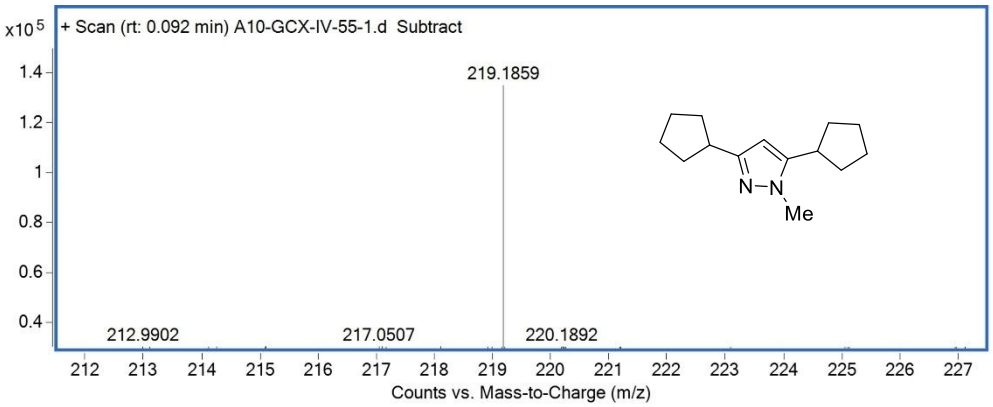

Mass	Calc. Mass	mDa	PPM	Ion Formula
219.1859	219.1856	-0.32	-1.49	C14H23N2

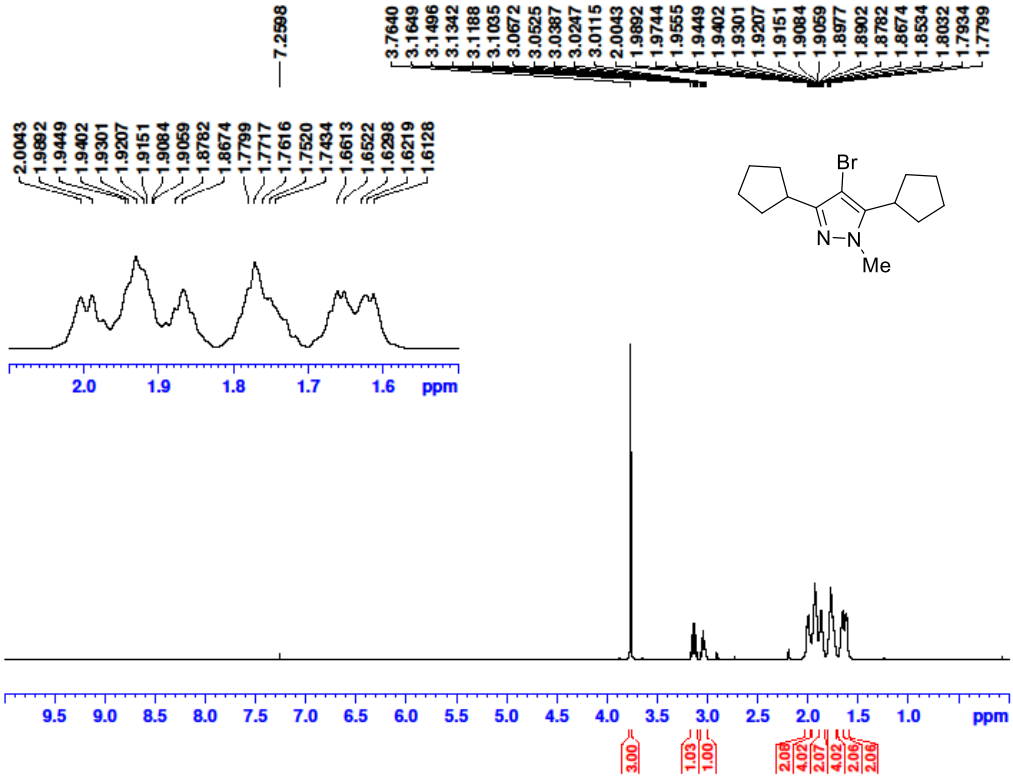
7.2598
3.7640
3.1649
3.1496
3.1342
3.1188
3.1035
3.0672
3.0525
3.0387
3.0247
3.0115
2.0043
1.9892
1.9744
1.9555
1.9449
1.9402
1.9301
1.9207
1.9151
1.9084
1.9059
1.8977
1.8902
1.8782
1.8674
1.8534
1.8032
1.7934
1.7799
Br
N–N
Me
2.0
1.9
1.8
1.7
1.6
ppm
9.5
9.0
8.5
8.0
7.5
7.0
6.5
6.0
5.5
5.0
4.5
4.0
3.5
3.0
2.5
2.0
1.5
1.0
ppm
3.00
1.03
1.00
2.08
4.02
2.07
4.02
2.06
2.06

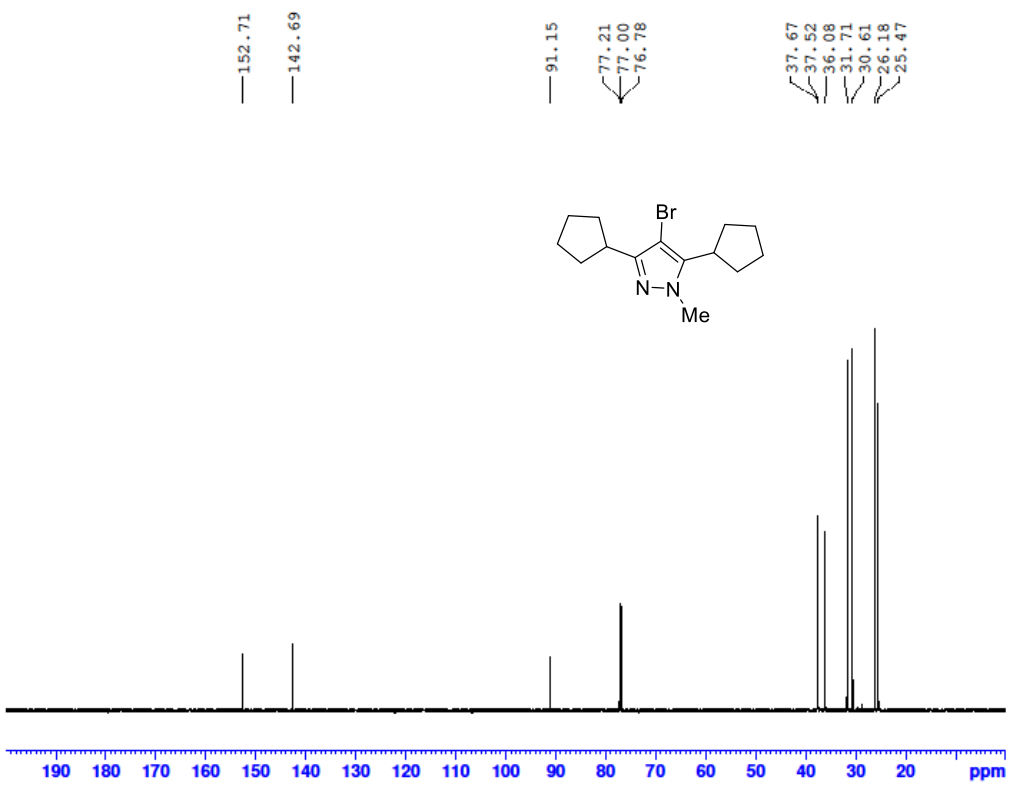
152.71
142.69
91.15
77.21
77.00
76.78
37.67
37.52
36.08
31.71
30.61
26.18
25.47
Br
N–N
Me
190
180
170
160
150
140
130
120
110
100
90
80
70
60
50
40
30
20
ppm

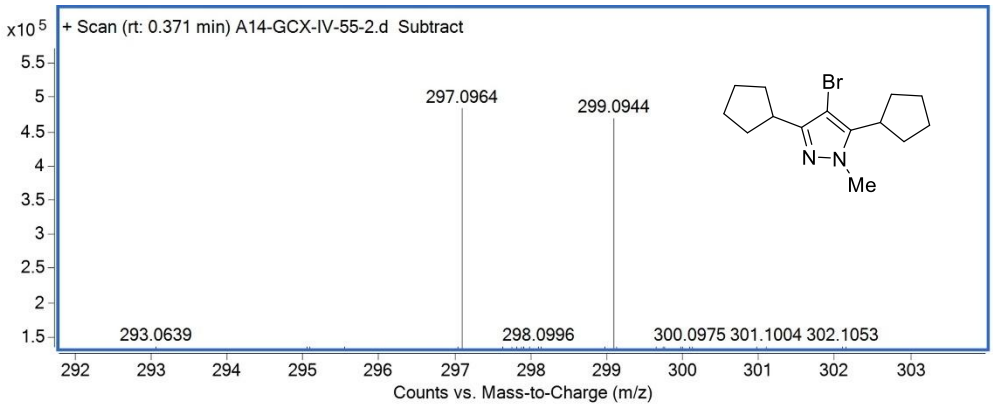

Mass	Calc. Mass	mDa	PPM	Ion Formula
297.0964	297.0961	-0.31	-1.05	C14H22N2Br

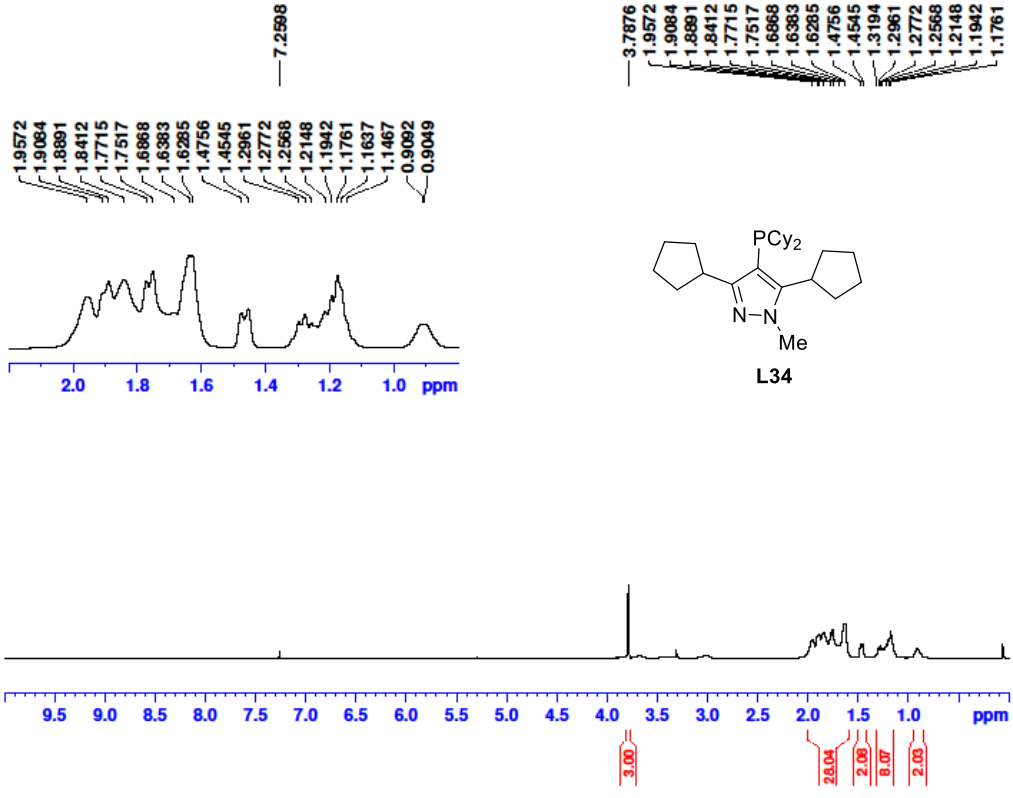

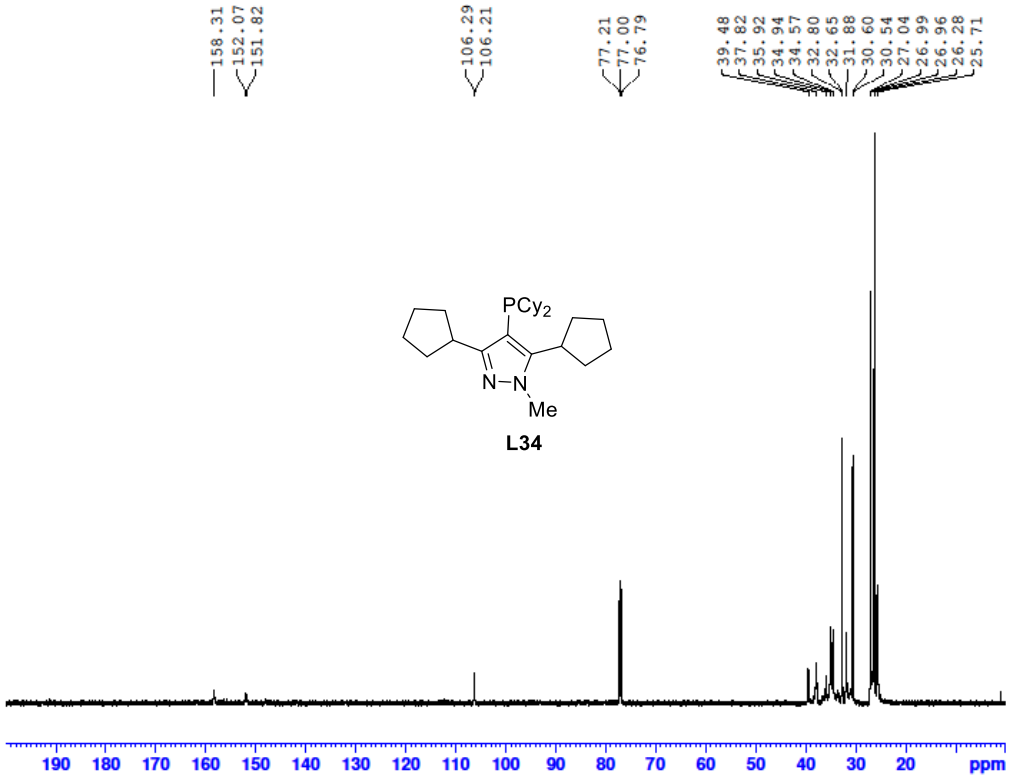
158.31
152.07
151.82
106.29
106.21
77.21
77.00
76.79
39.48
37.82
35.92
34.94
34.57
32.80
32.65
31.88
30.60
30.54
27.04
26.99
26.96
26.28
25.71
PCy2
N–N
Me
190 180 170 160 150 140 130 120 110 100 90 80 70 60 50 40 30 20 ppm

L34

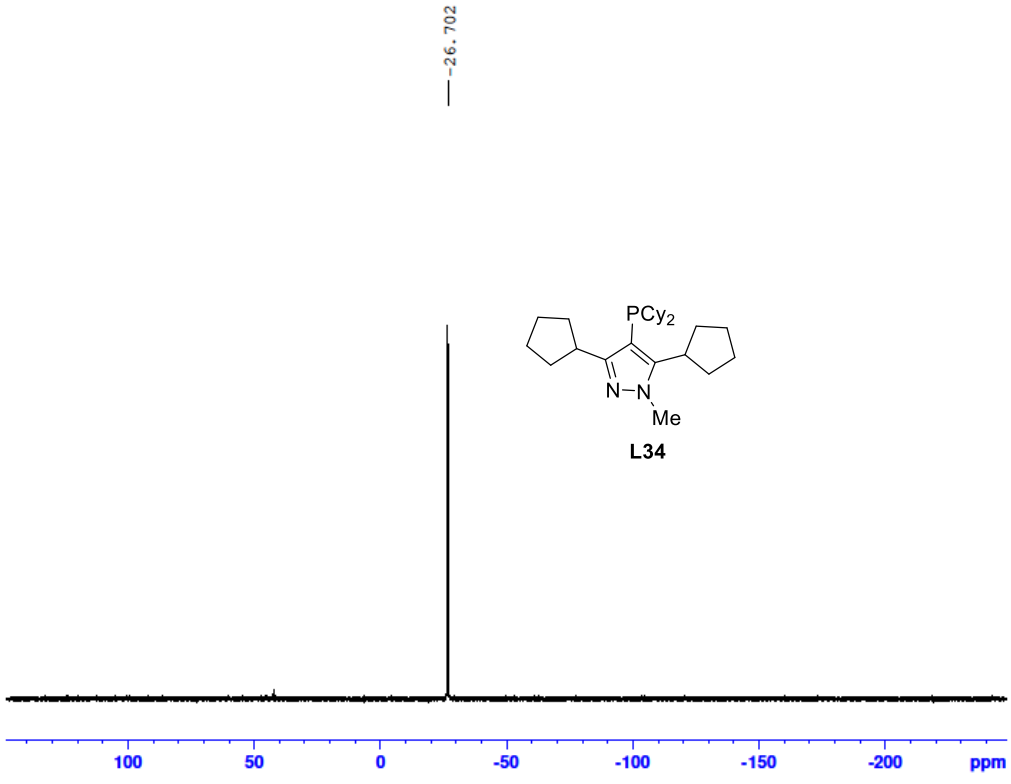
-26.702
PCy2
N–N
Me
100 50 0 -50 -100 -150 -200 ppm

L34

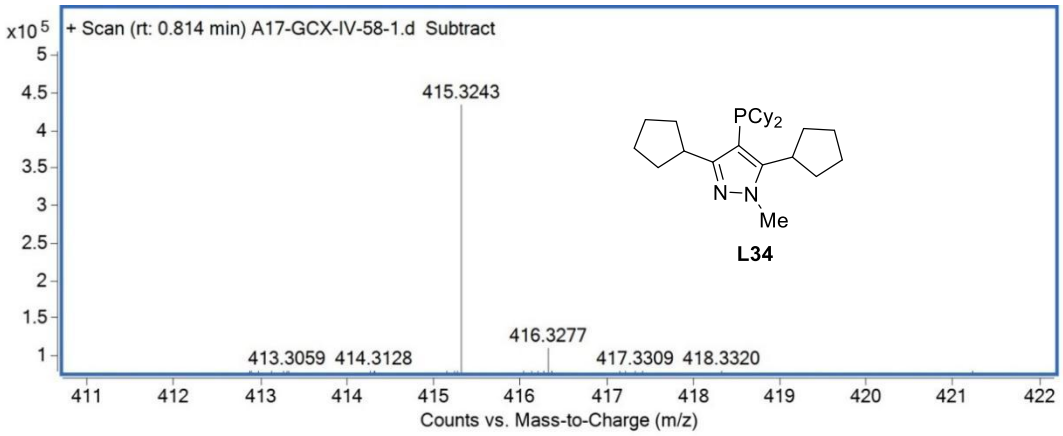

Mass	Calc. Mass	mDa	PPM	Ion Formula
415.3243	415.3237	-0.64	-1.54	C26H44N2P

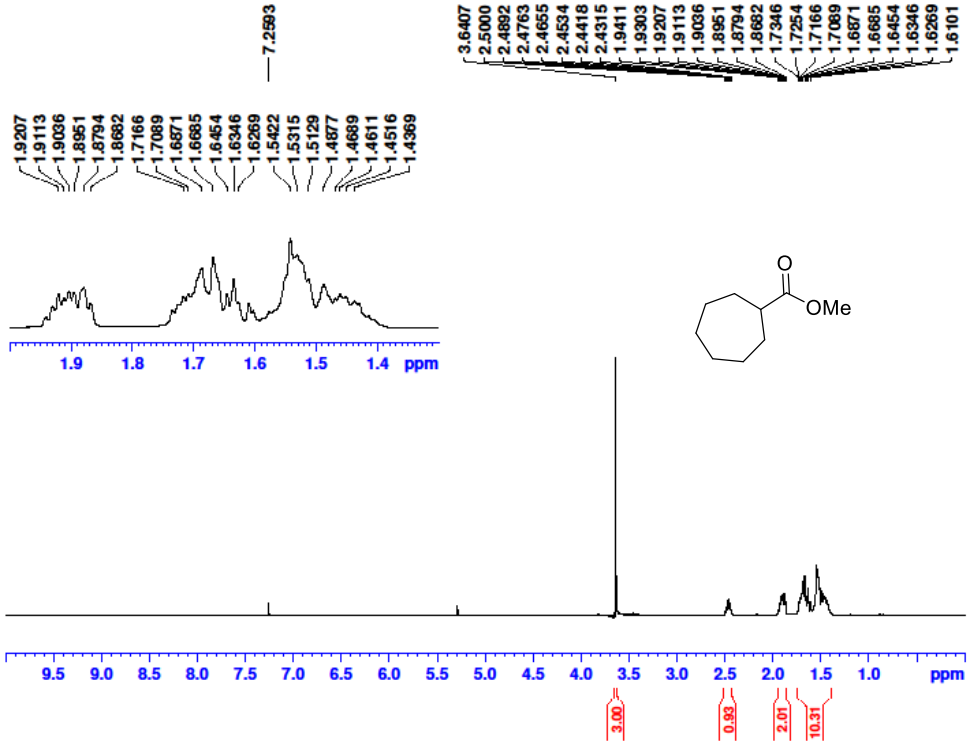

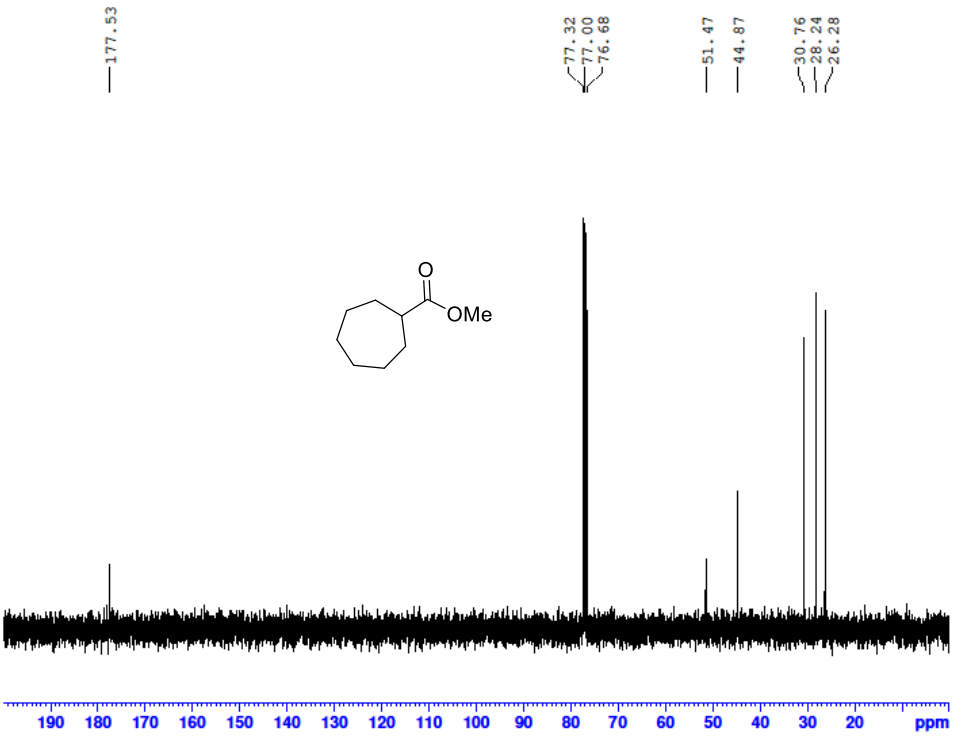
177.53
77.32
77.00
76.68
51.47
44.87
30.76
28.24
26.28
O
OMe
190 180 170 160 150 140 130 120 110 100 90 80 70 60 50 40 30 20 ppm

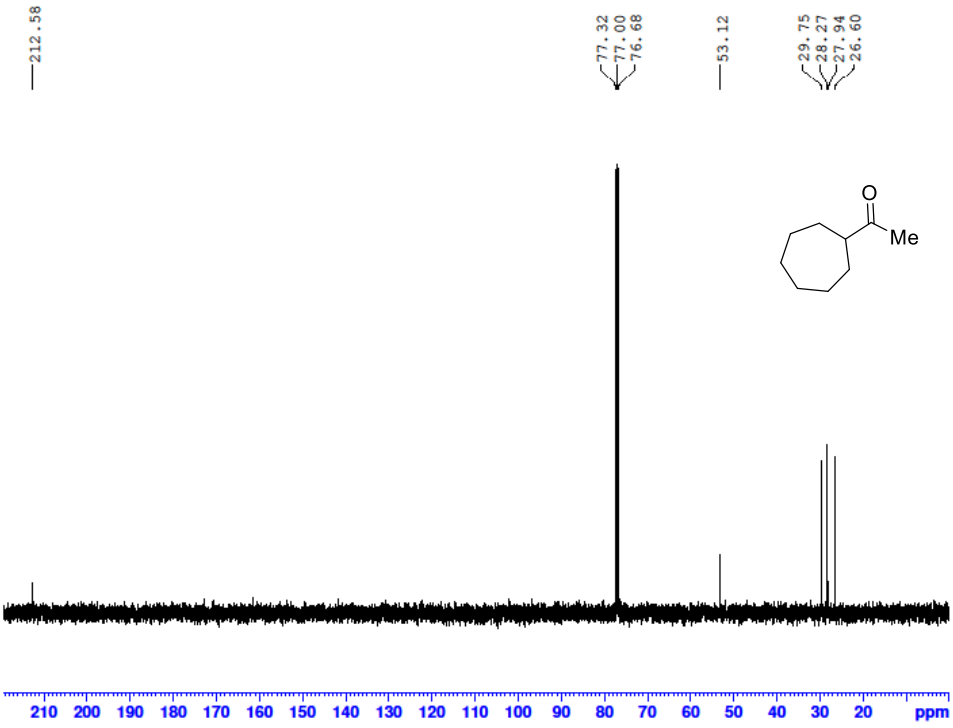
212.58
77.32
77.00
76.68
53.12
29.75
28.27
27.94
26.60
O
Me
210 200 190 180 170 160 150 140 130 120 110 100 90 80 70 60 50 40 30 20 ppm

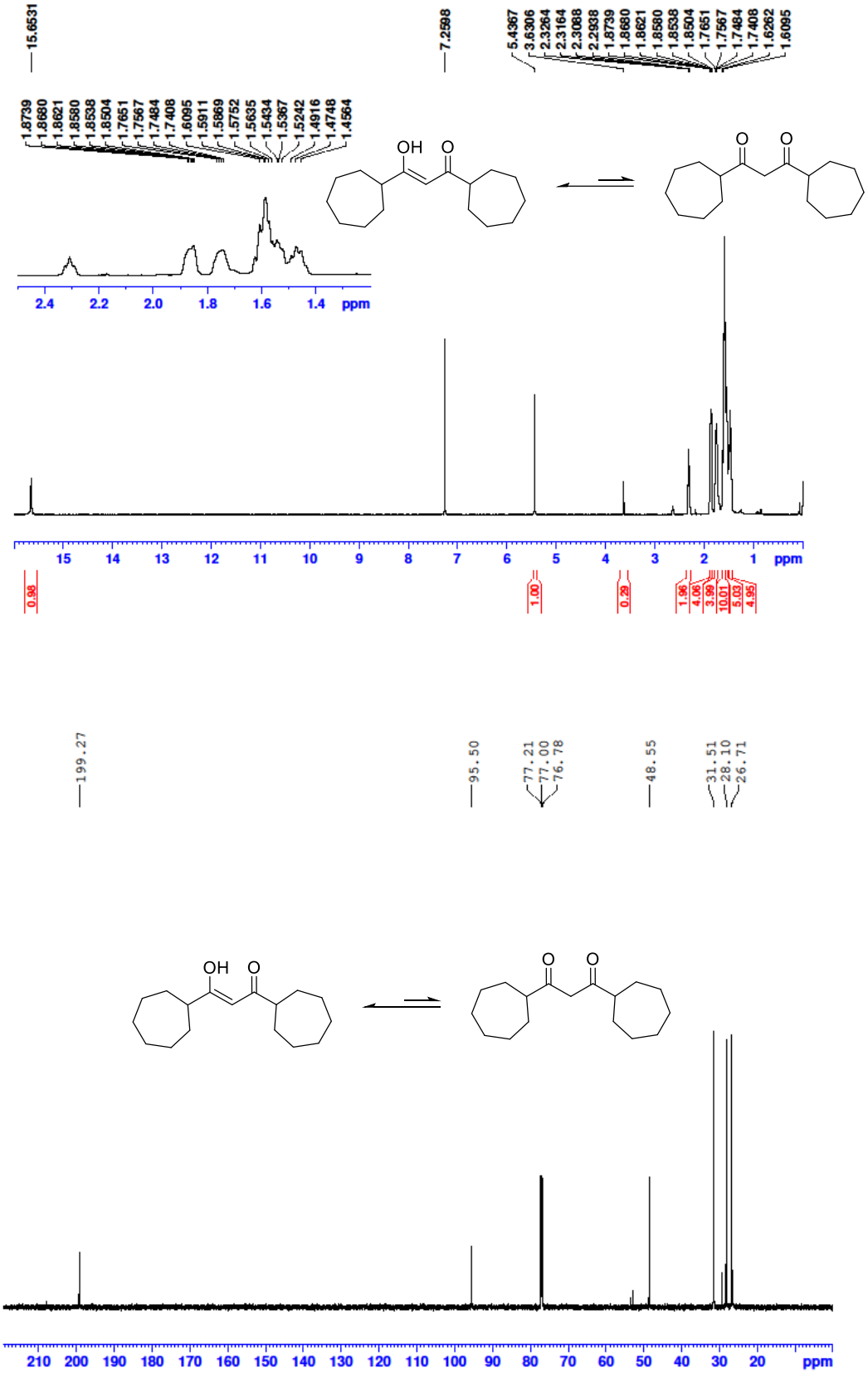
15.6531
7.2598
5.4367
3.6306
2.3264
2.3164
2.3068
2.2938
1.8739
1.8680
1.8621
1.8580
1.8538
1.8504
1.7651
1.7567
1.7484
1.7408
1.6262
1.6095
1.5911
1.5869
1.5752
1.5635
1.5434
1.5367
1.5242
1.4916
1.4748
1.4564
OH
O
O
O
2.4
2.2
2.0
1.8
1.6
1.4
ppm
15
14
13
12
11
10
9
8
7
6
5
4
3
2
1
ppm
0.98
1.00
0.29
1.96
4.06
3.99
10.01
5.03
4.95
199.27
95.50
77.21
77.00
76.78
48.55
31.51
28.10
26.71
OH
O
O
O
210
200
190
180
170
160
150
140
130
120
110
100
90
80
70
60
50
40
30
20
ppm

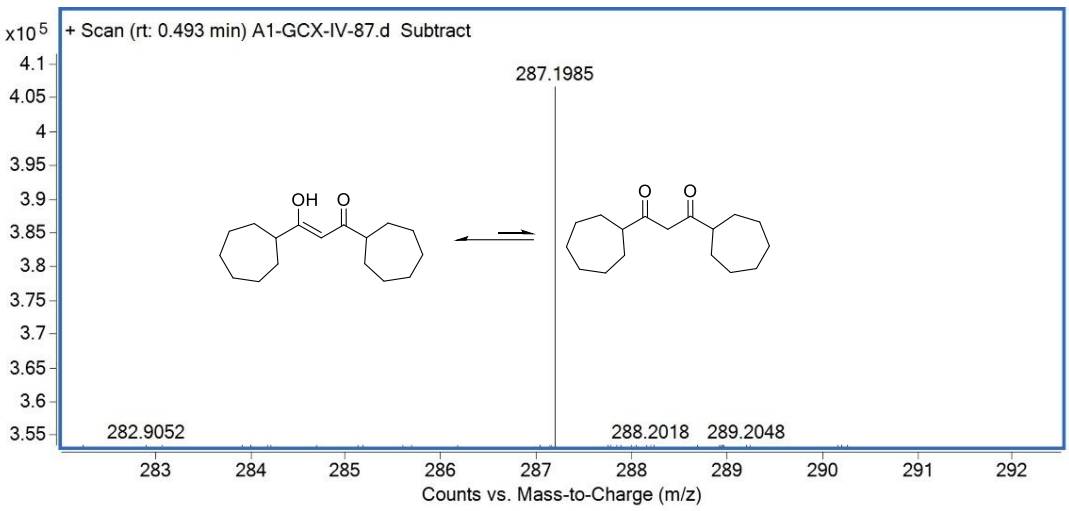

Mass	Calc. Mass	mDa	PPM	Ion Formula
287.1985	287.1982	-0.35	-1.32	C17H28O2Na

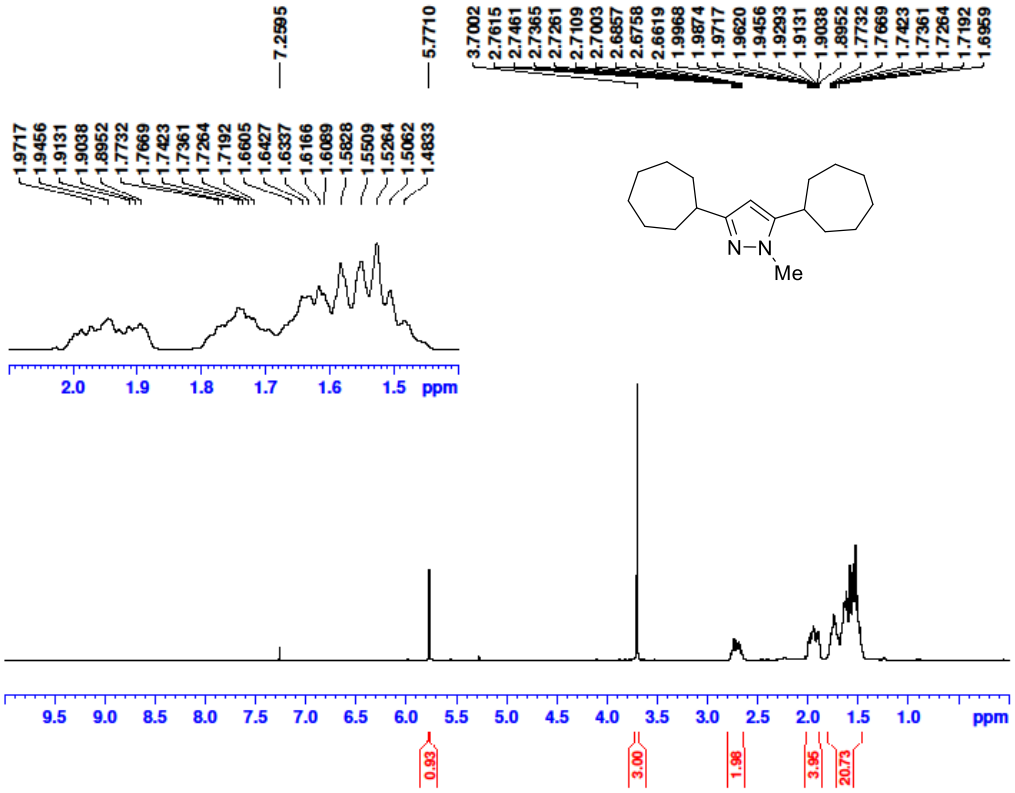

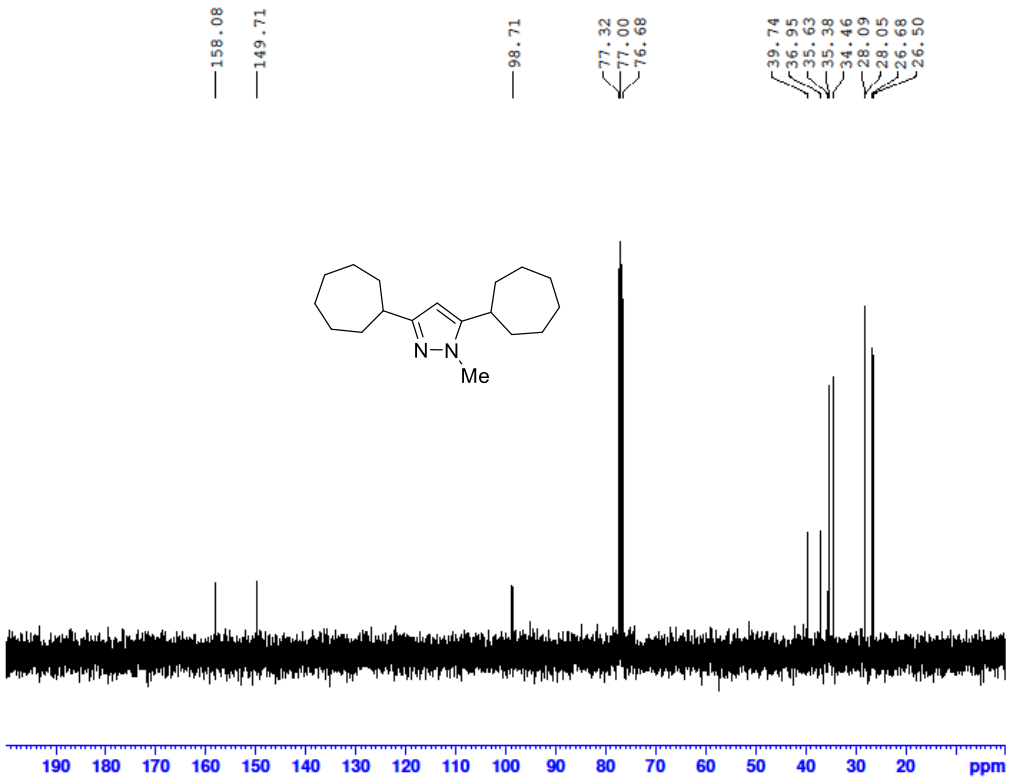

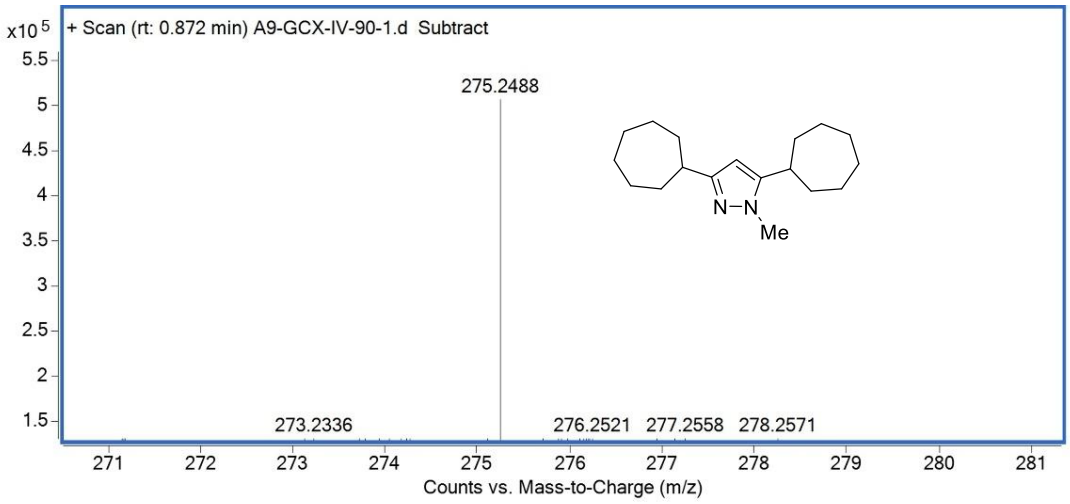

Mass	Calc. Mass	mDa	PPM	Ion Formula
275.2488	275.2482	-0.62	-2.28	C18H31N2

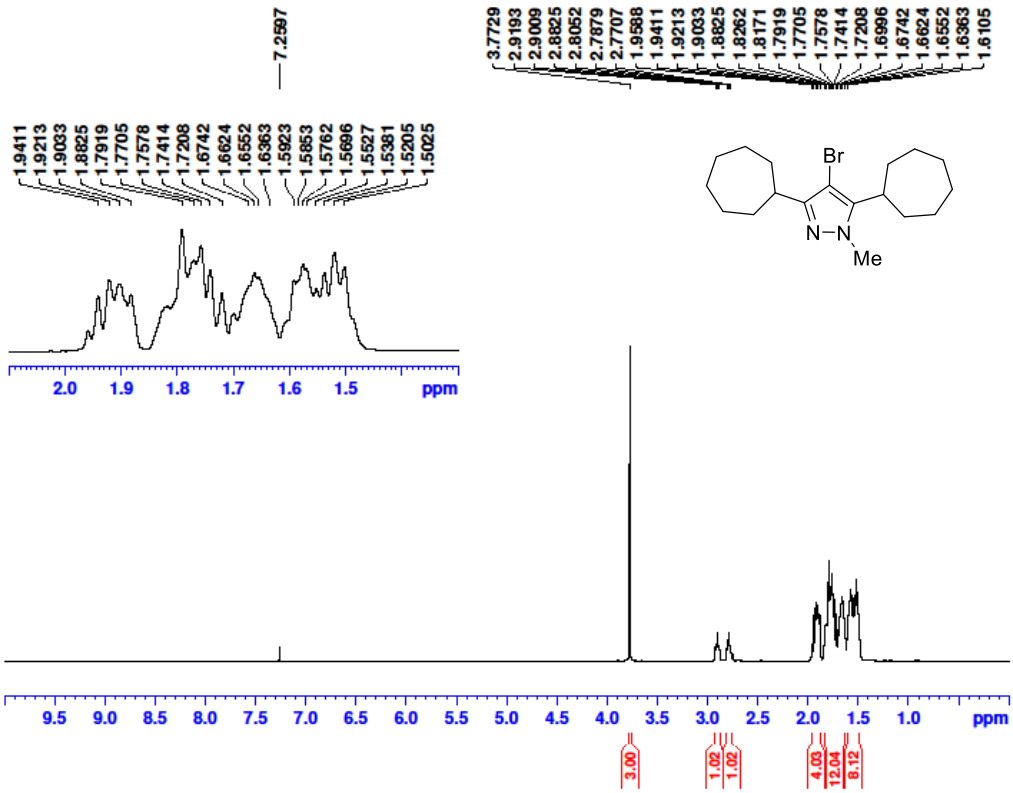
7.2597
3.7729
2.9193
2.9009
2.8825
2.8052
2.7879
2.7707
1.9588
1.9411
1.9213
1.9033
1.8825
1.8262
1.8171
1.7919
1.7705
1.7578
1.7414
1.7208
1.6996
1.6742
1.6624
1.6552
1.6363
1.6105
1.9411
1.9213
1.9033
1.8825
1.7919
1.7705
1.7578
1.7414
1.7208
1.6742
1.6624
1.6552
1.6363
1.5923
1.5853
1.5762
1.5696
1.5527
1.5381
1.5205
1.5025
Br
N–N
Me
2.0
1.9
1.8
1.7
1.6
1.5
ppm
9.5
9.0
8.5
8.0
7.5
7.0
6.5
6.0
5.5
5.0
4.5
4.0
3.5
3.0
2.5
2.0
1.5
1.0
ppm
3.00
1.02
1.02
4.03
12.04
8.12

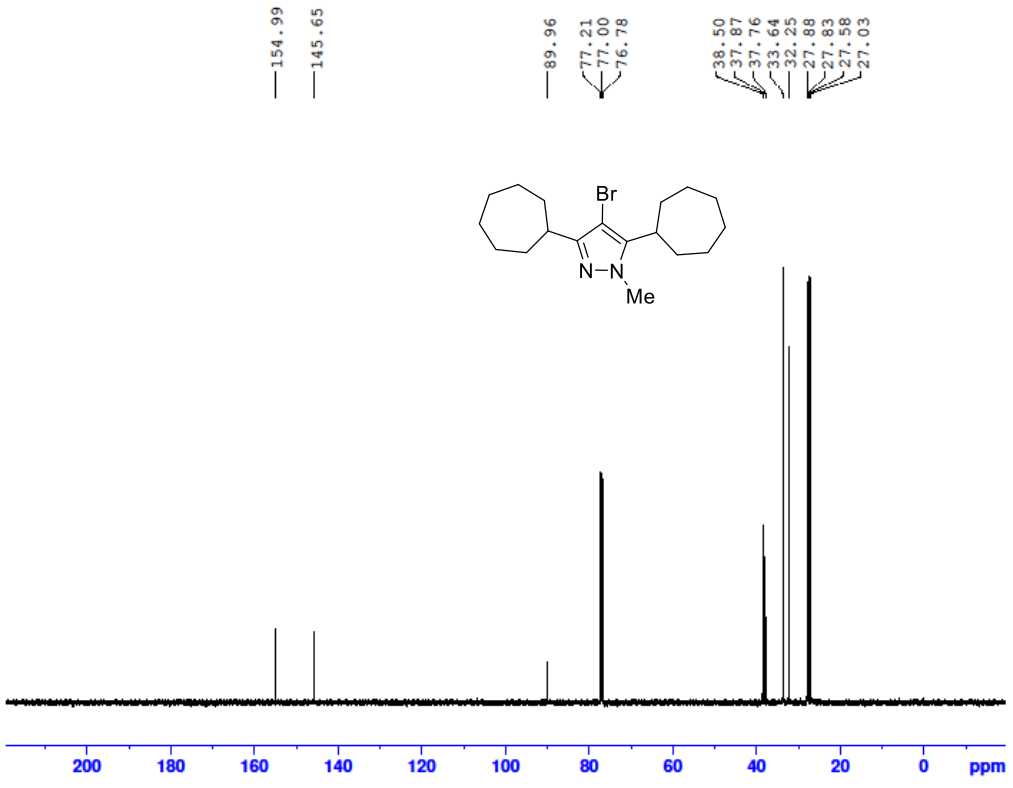
154.99
145.65
89.96
77.21
77.00
76.78
38.50
37.87
37.76
33.64
32.25
27.88
27.83
27.58
27.03
Br
N–N
Me
200
180
160
140
120
100
80
60
40
20
0
ppm

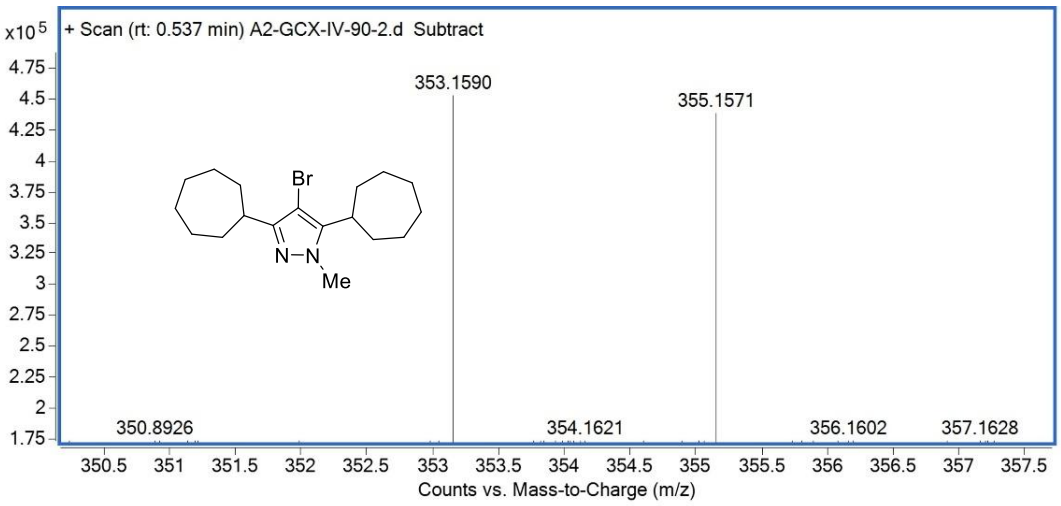

Mass	Calc. Mass	mDa	PPM	Ion Formula
353.1590	353.1587	-0.31	-0.89	C18H30BrN2

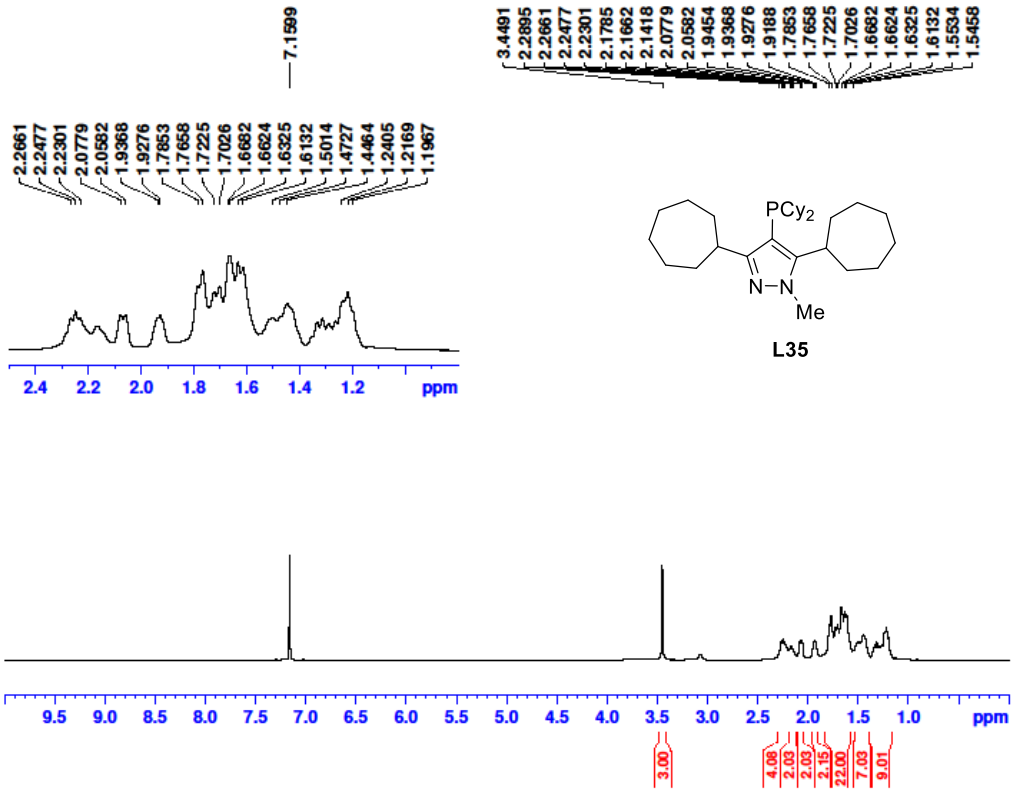

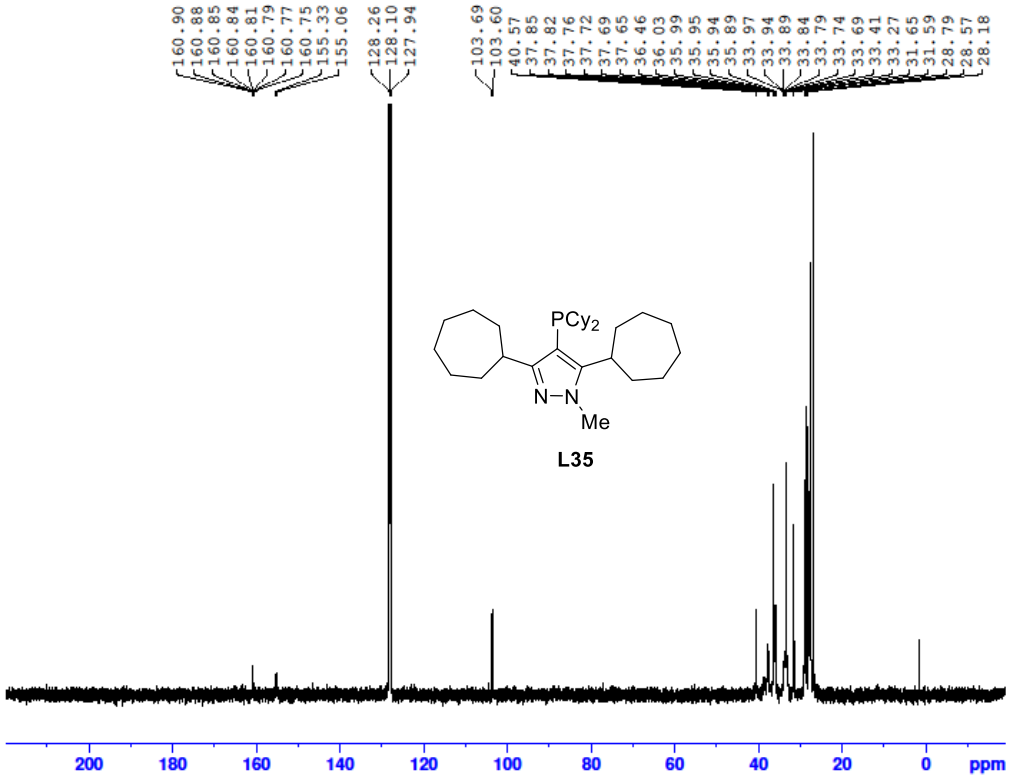
160.90
160.88
160.85
160.84
160.81
160.79
160.77
160.75
155.33
155.06
128.26
128.10
127.94
103.69
103.60
40.57
37.85
37.82
37.76
37.72
37.69
37.65
36.46
36.03
35.99
35.95
35.94
35.89
33.97
33.94
33.89
33.84
33.79
33.74
33.69
33.41
33.27
31.65
31.59
28.79
28.57
28.18
PCy2
N–N
Me
200
180
160
140
120
100
80
60
40
20
0
ppm

L35

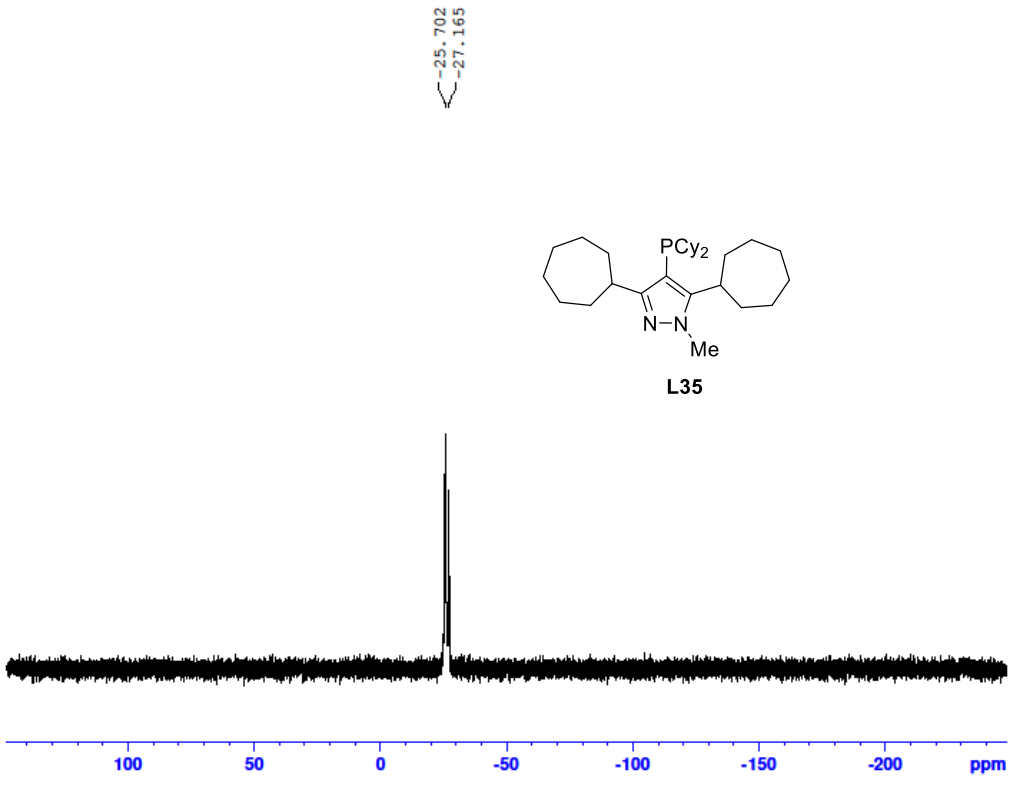
-25.702
-27.165
PCy2
N–N
Me
100
50
0
-50
-100
-150
-200
ppm

L35

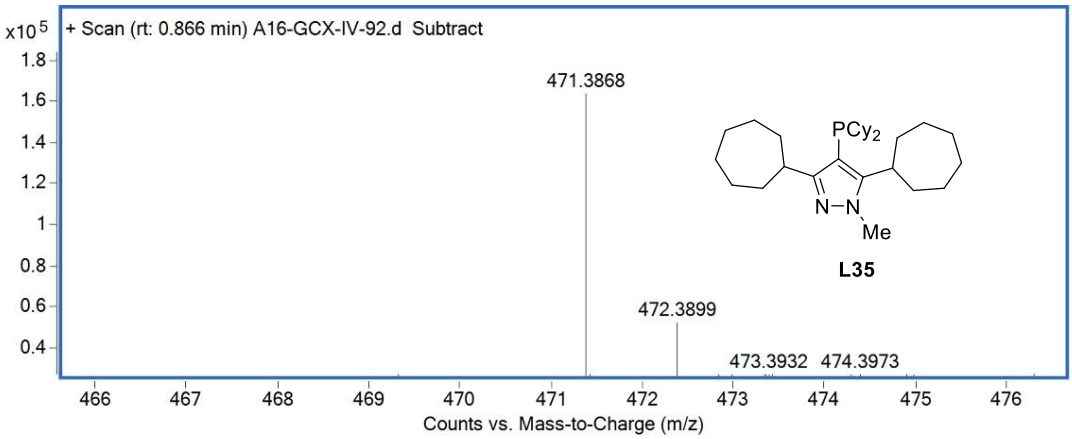

Mass	Calc. Mass	mDa	PPM	Ion Formula
471.3868	471.3863	-0.54	-1.14	C30H52N2P

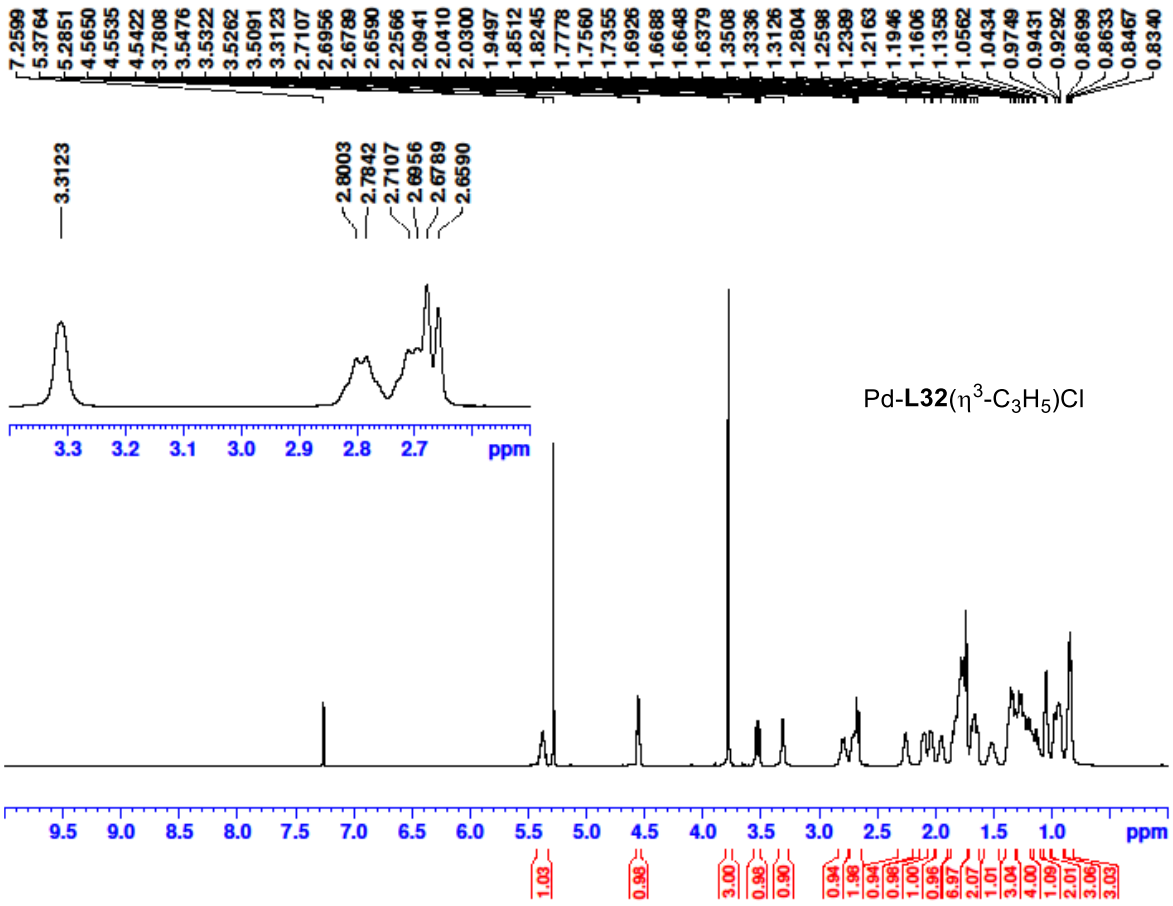

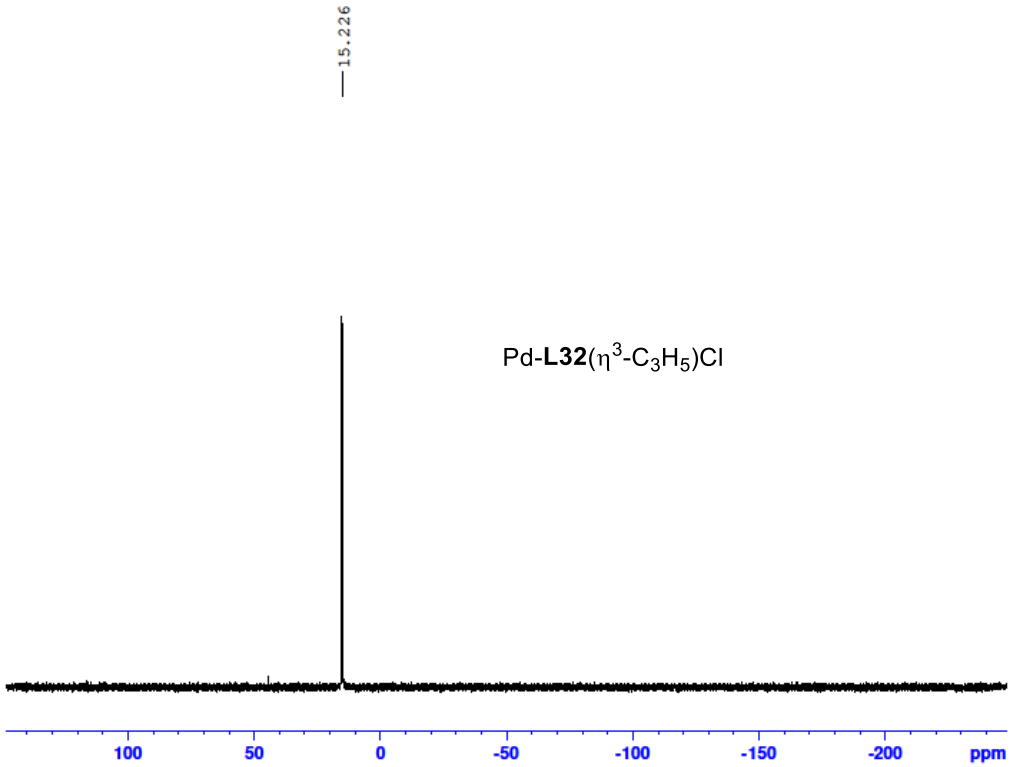
15.226
Pd-L32(η3-C3H5)Cl
100
50
0
-50
-100
-150
-200
ppm

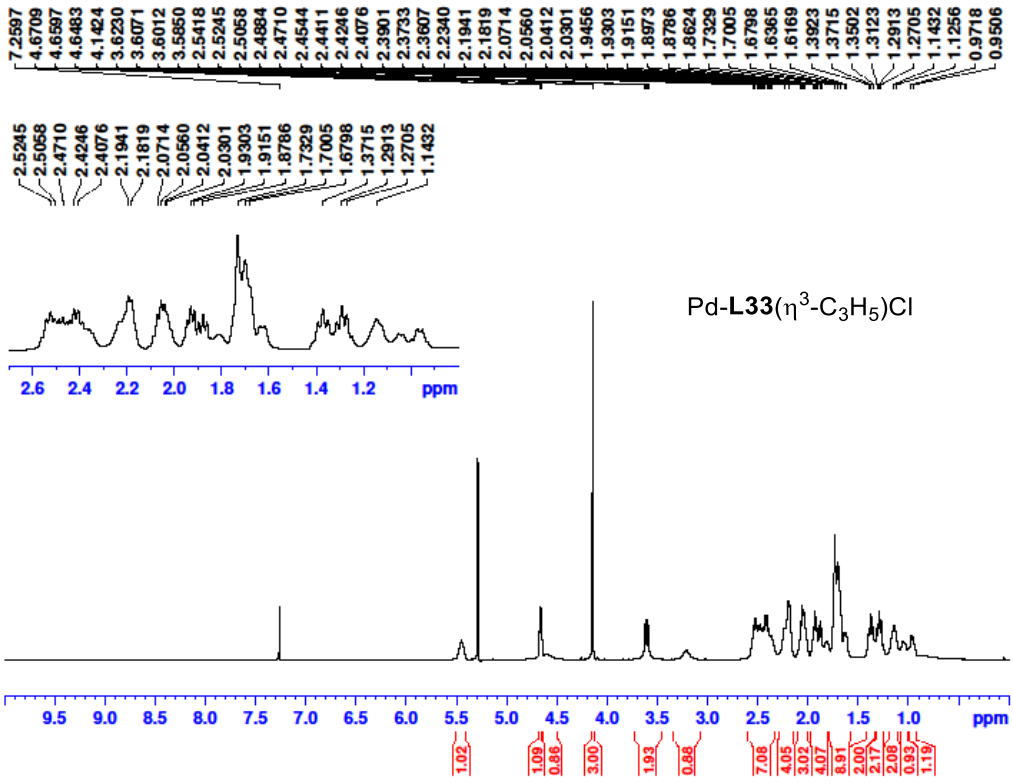
7.2597
4.6709
4.6597
4.6483
4.1424
3.6230
3.6071
3.6012
3.5850
2.5418
2.5245
2.5058
2.4884
2.4710
2.4544
2.4411
2.4246
2.4076
2.3901
2.3733
2.3607
2.2340
2.1941
2.1819
2.0714
2.0560
2.0412
2.0301
1.9456
1.9303
1.9151
1.8973
1.8786
1.8624
1.7329
1.7005
1.6798
1.6365
1.6169
1.3923
1.3715
1.3502
1.3123
1.2913
1.2705
1.1432
1.1256
0.9718
0.9506
2.5245
2.5058
2.4710
2.4246
2.4076
2.1941
2.1819
2.0714
2.0560
2.0412
2.0301
1.9303
1.9151
1.8786
1.7329
1.7005
1.6798
1.3715
1.2913
1.2705
1.1432
2.6
2.4
2.2
2.0
1.8
1.6
1.4
1.2
ppm
Pd-L33(η3-C3H5)Cl
9.5
9.0
8.5
8.0
7.5
7.0
6.5
6.0
5.5
5.0
4.5
4.0
3.5
3.0
2.5
2.0
1.5
1.0
ppm
1.02
1.09
0.86
3.00
1.93
0.88
7.08
4.05
3.02
4.07
8.91
2.00
2.17
2.06
0.93
1.19

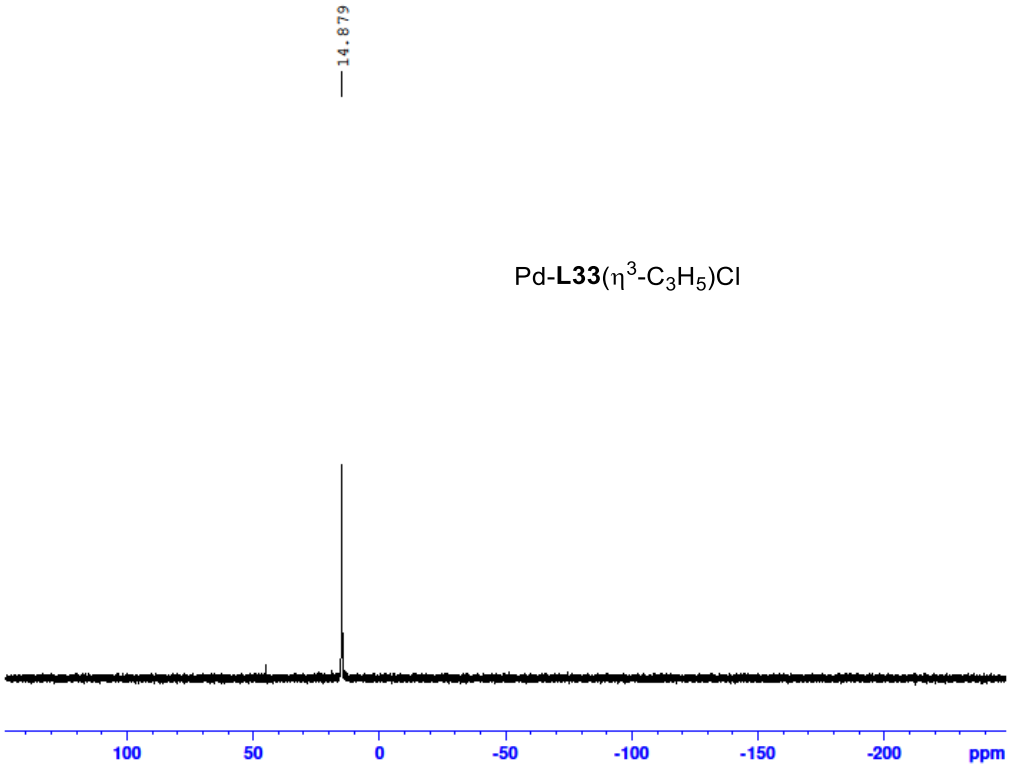

Pd-**L33**(η^3-C_3H_5)Cl

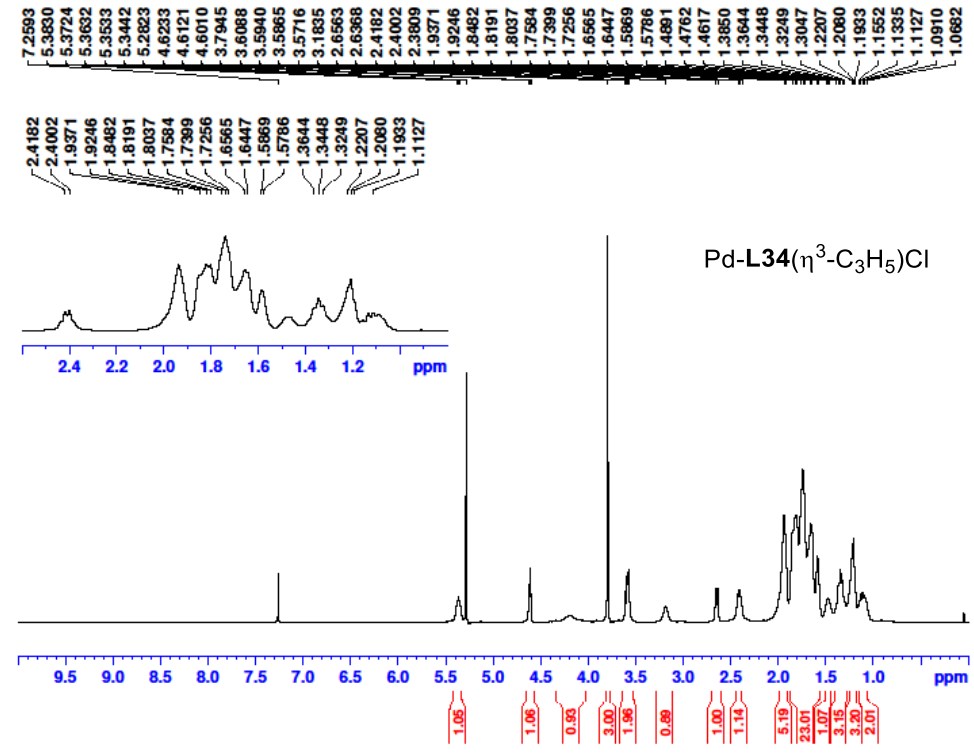

Pd-**L34**(η^3-C_3H_5)Cl

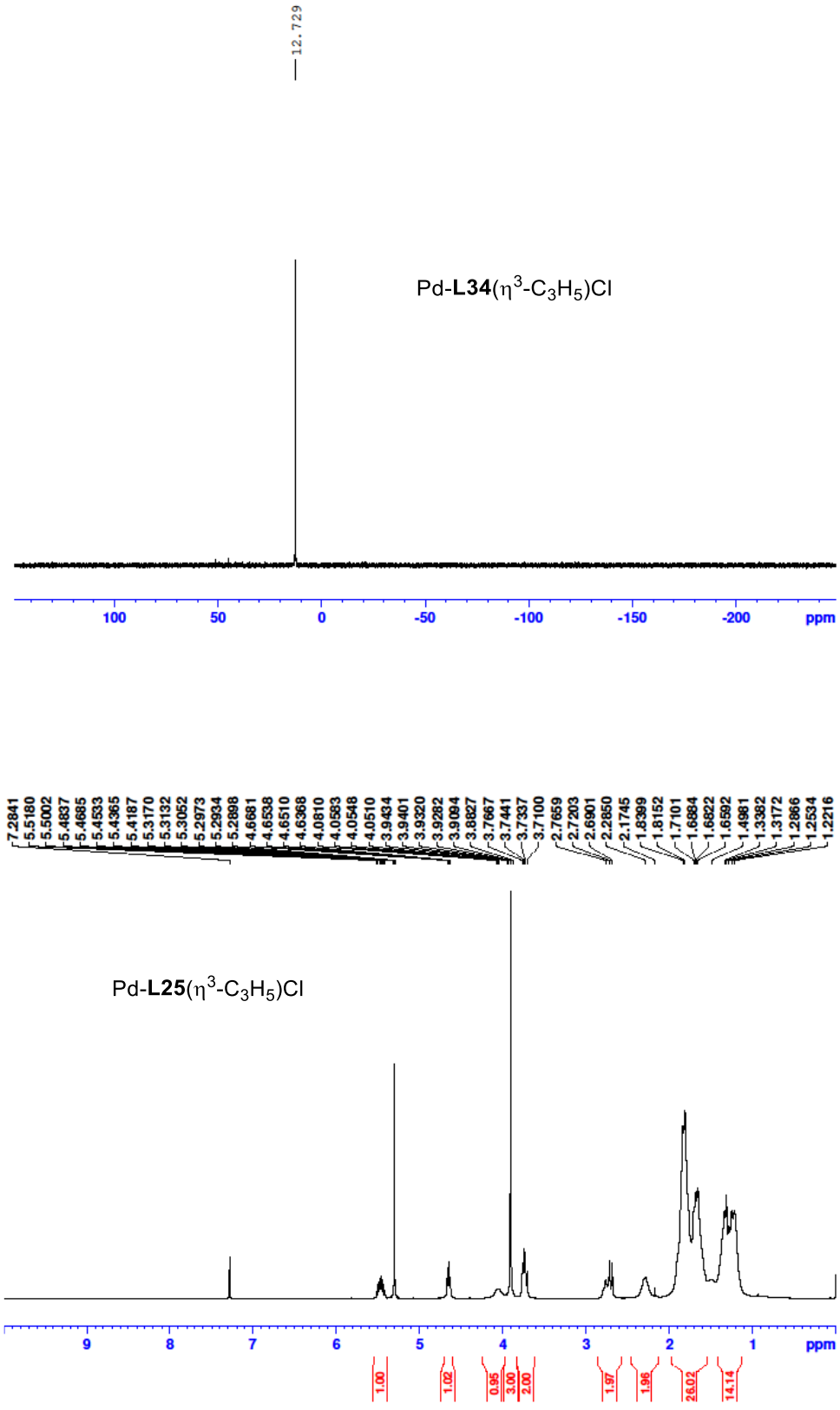
12.729
Pd-L34(η3-C3H5)Cl
100
50
0
-50
-100
-150
-200
ppm
7.2841
5.5180
5.5002
5.4837
5.4685
5.4533
5.4365
5.4187
5.3170
5.3132
5.3052
5.2973
5.2934
5.2898
4.6681
4.6538
4.6510
4.6368
4.0810
4.0583
4.0548
4.0510
3.9434
3.9401
3.9320
3.9282
3.9094
3.8827
3.7667
3.7441
3.7337
3.7100
2.7659
2.7203
2.6901
2.2850
2.1745
1.8399
1.8152
1.7101
1.6884
1.6822
1.6592
1.4981
1.3382
1.3172
1.2866
1.2534
1.2216
Pd-L25(η3-C3H5)Cl
9
8
7
6
5
4
3
2
1
ppm
1.00
1.02
0.95
3.00
2.00
1.97
1.96
26.02
14.14

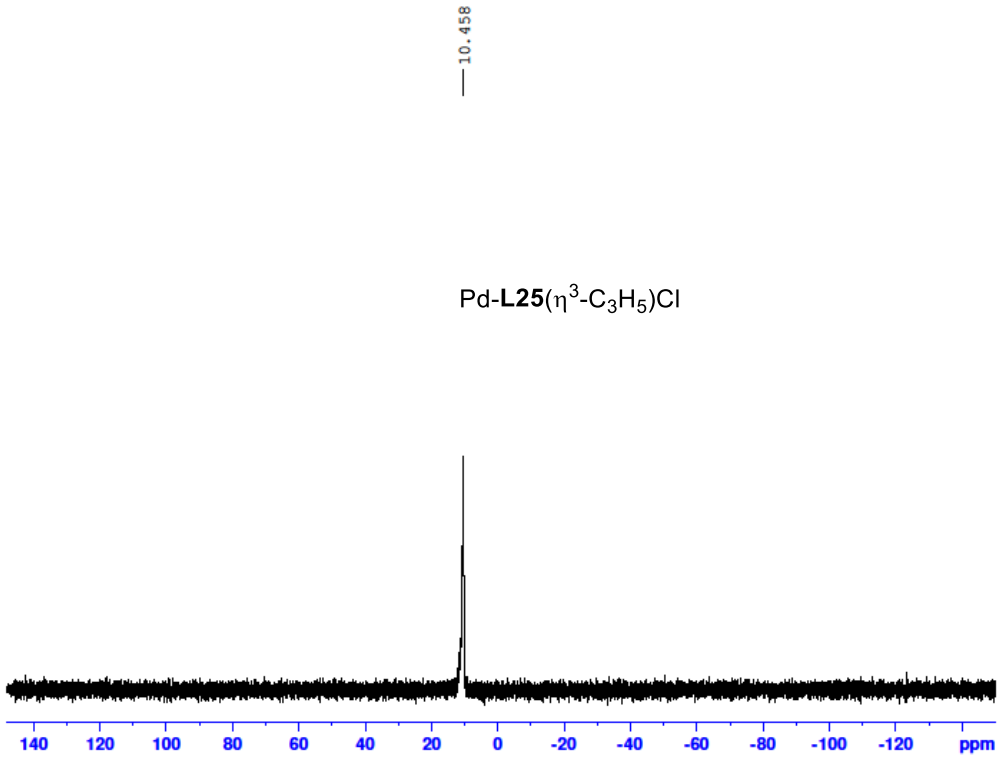
10.458
Pd-L25(η3-C3H5)Cl
140 120 100 80 60 40 20 0 -20 -40 -60 -80 -100 -120 ppm

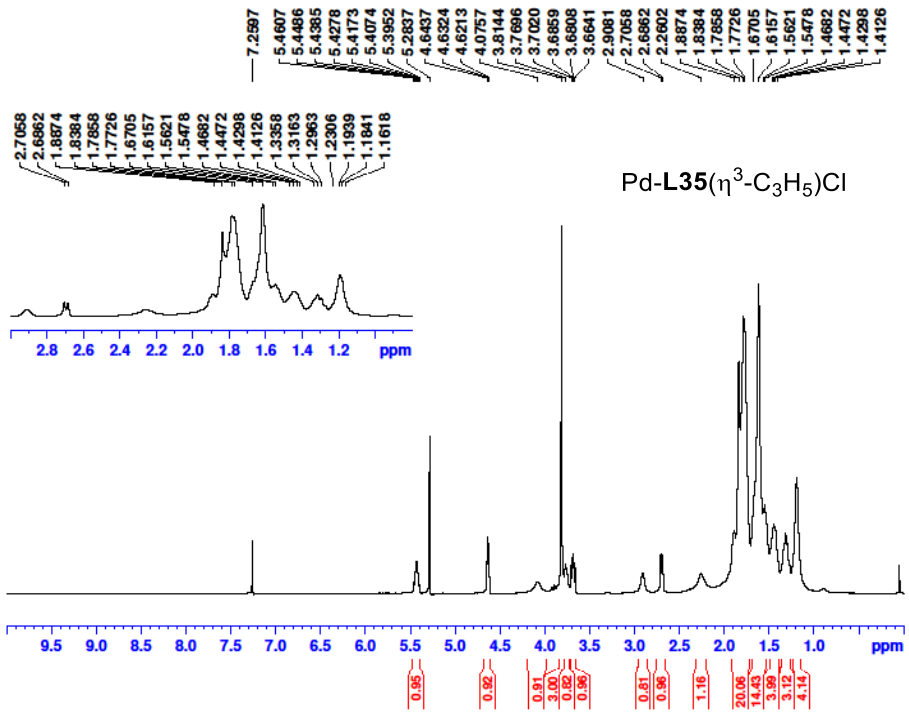
7.2597
5.4607
5.4486
5.4385
5.4278
5.4173
5.4074
5.3952
5.2837
4.6437
4.6324
4.6213
4.0757
3.8144
3.7696
3.7020
3.6859
3.6808
3.6641
2.9081
2.7058
2.6862
2.2602
1.8874
1.8384
1.7858
1.7726
1.6705
1.6157
1.5621
1.5478
1.4682
1.4472
1.4298
1.4126
1.3358
1.3163
1.2963
1.2306
1.1939
1.1841
1.1618
Pd-L35(η3-C3H5)Cl
2.8 2.6 2.4 2.2 2.0 1.8 1.6 1.4 1.2 ppm
9.5 9.0 8.5 8.0 7.5 7.0 6.5 6.0 5.5 5.0 4.5 4.0 3.5 3.0 2.5 2.0 1.5 1.0 ppm
0.95
0.92
0.91
3.00
0.82
0.96
0.81
0.96
1.16
20.06
14.43
3.59
3.12
4.14

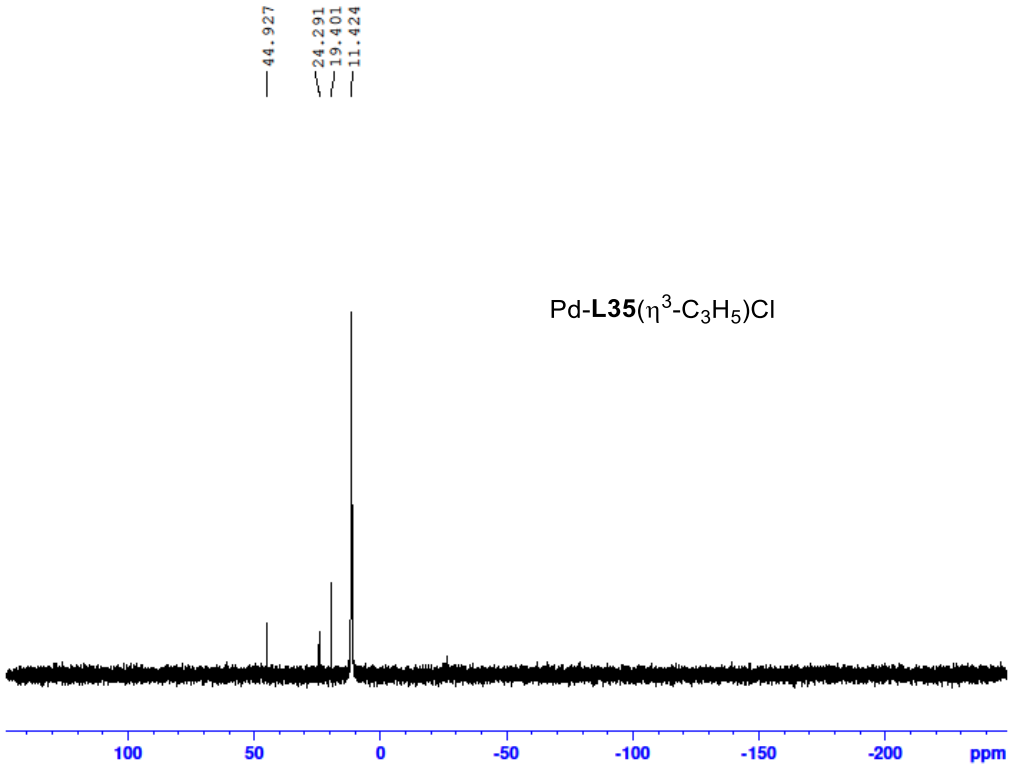

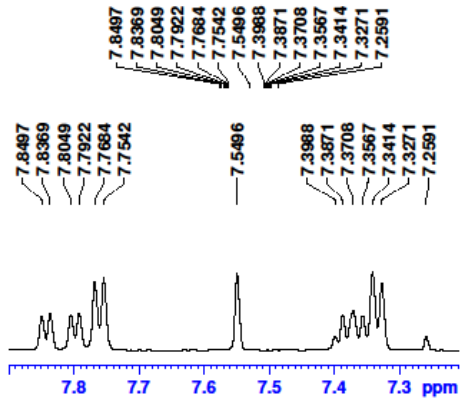

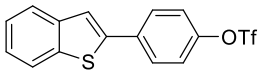

Table 3.5, compound 7a

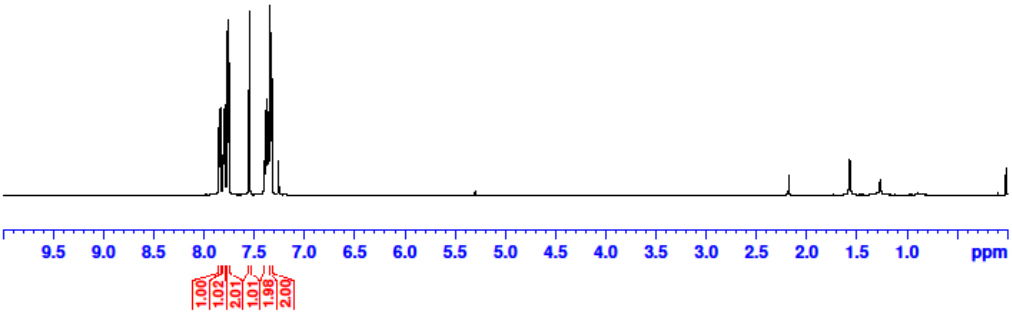

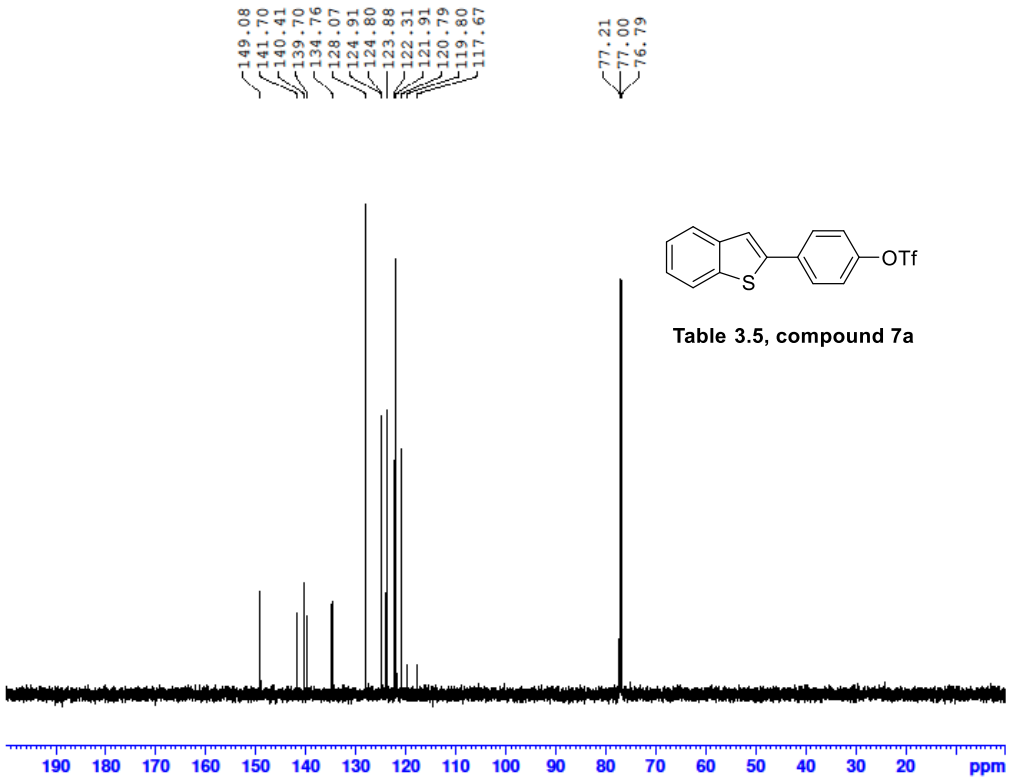

Table 3.5, compound 7a

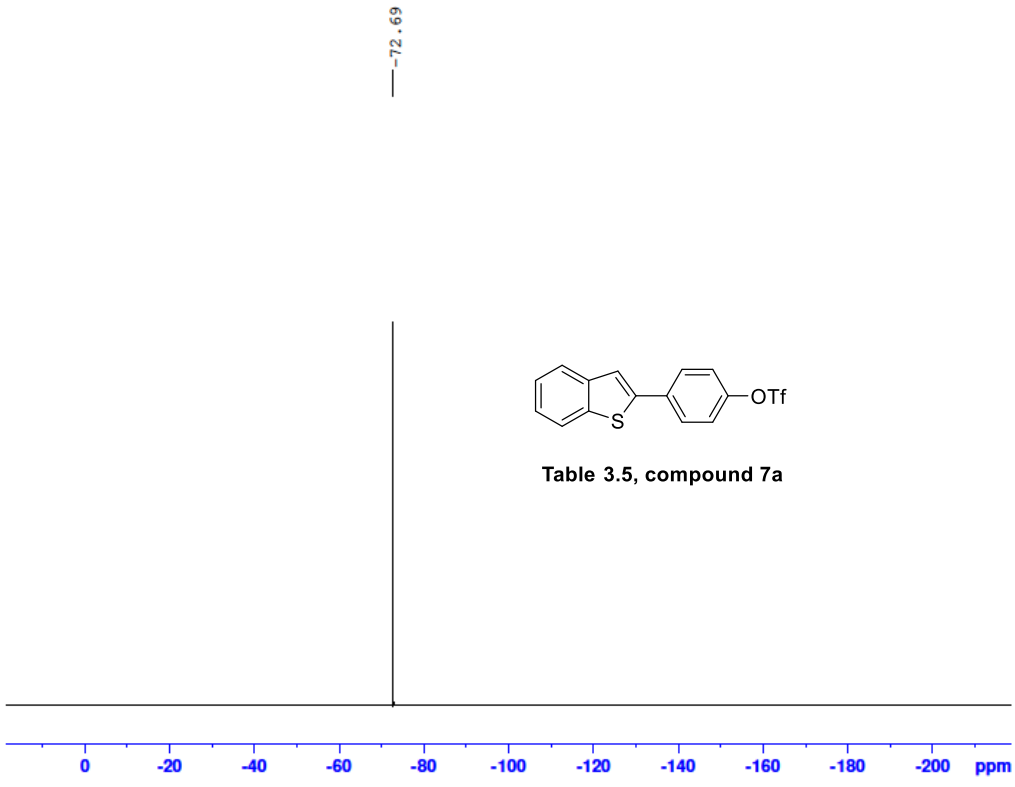

Table 3.5, compound 7a

A25-20230928

A25-GCX-IV-171-1-20230928 640 (12.366)

TOF MS EI+
1.64e3

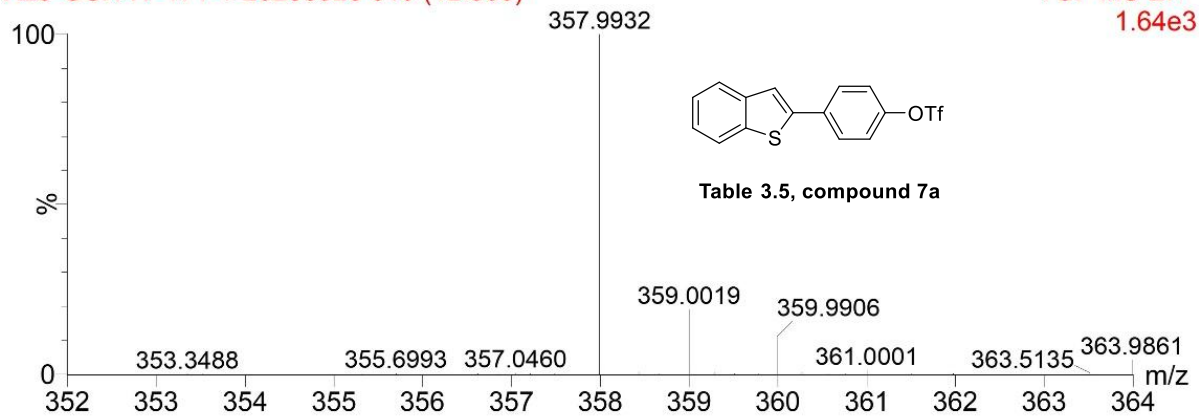

Table 3.5, compound 7a

Mass	Calc. Mass	mDa	PPM	Ion Formula
357.9932	357.9940	2.16	0.77	C15H9F3O3S2

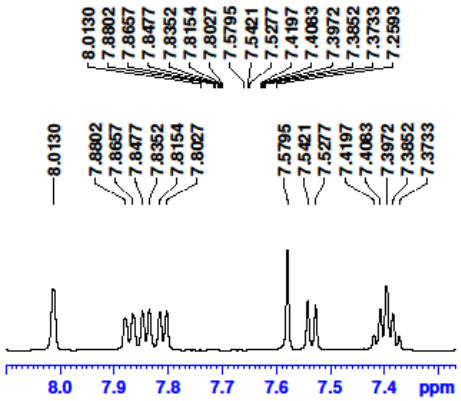

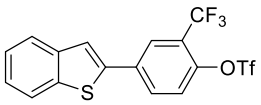

Table 3.5, compound 7b

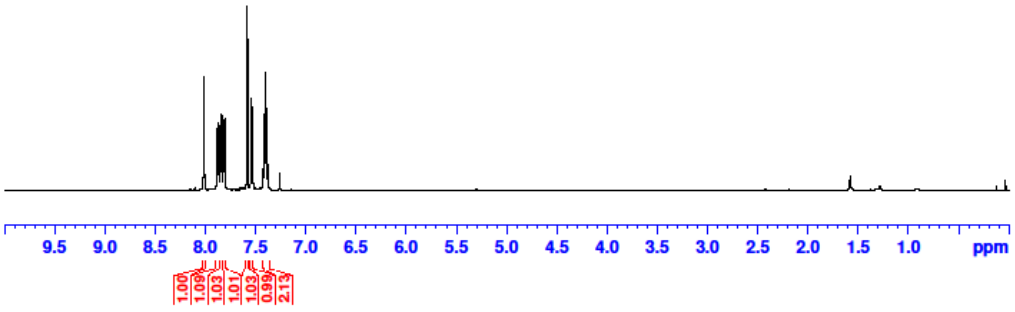

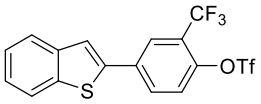

Table 3.5, compound 7b

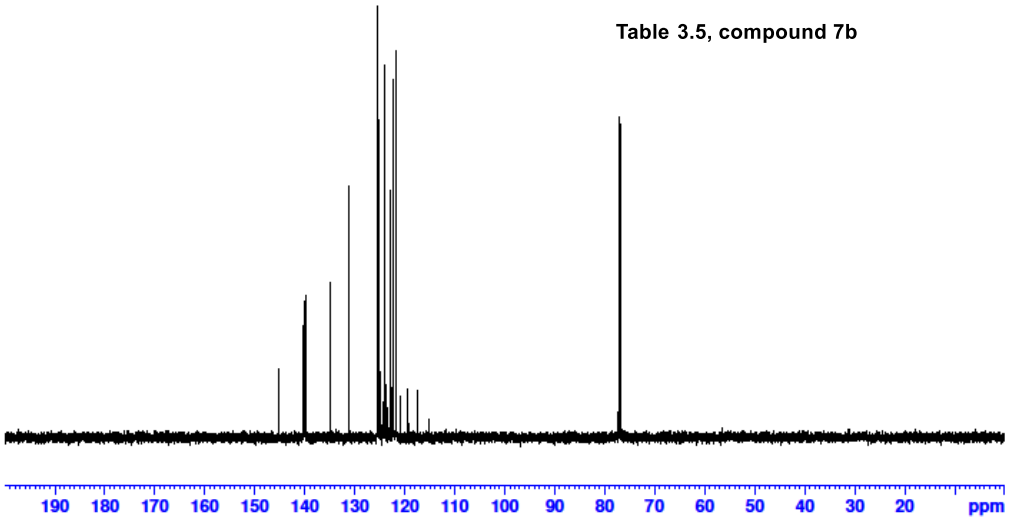

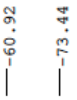

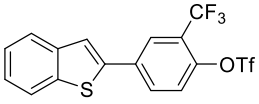

Table 3.5, compound 7b

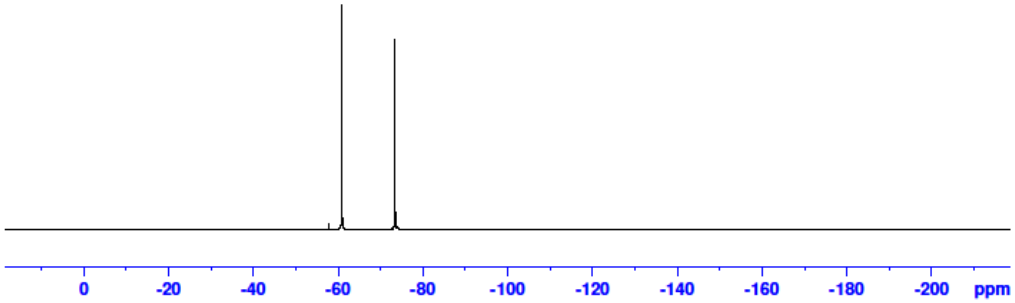

A17-20230928

A17-GCX-IV-116-5-20230928 613 (12.013)

TOF MS EI+
1.27e4

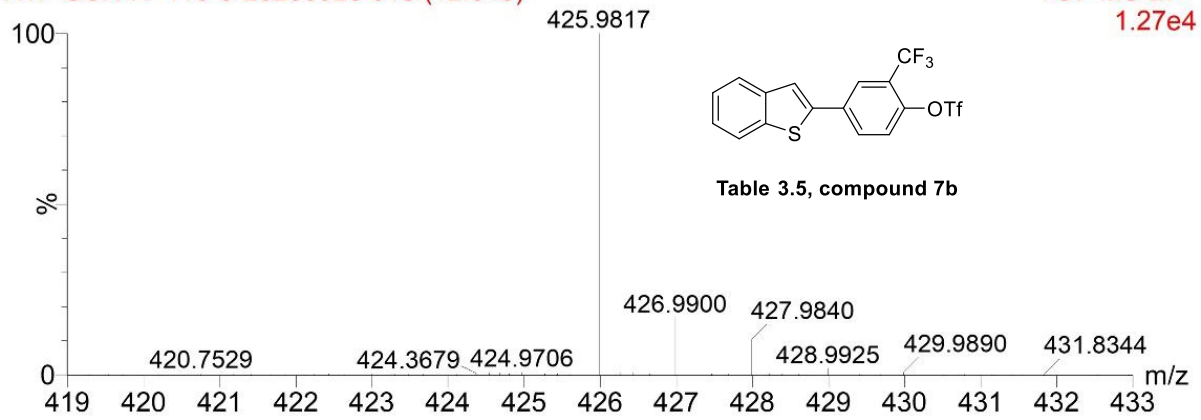

Table 3.5, compound 7b

Mass	Calc. Mass	mDa	PPM	Ion Formula
425.9817	425.9814	-0.81	-0.34	C16H8F6O3S2

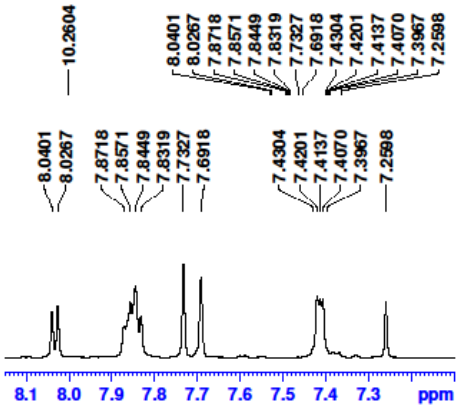

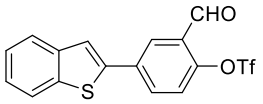

Table 3.5, compound 7c

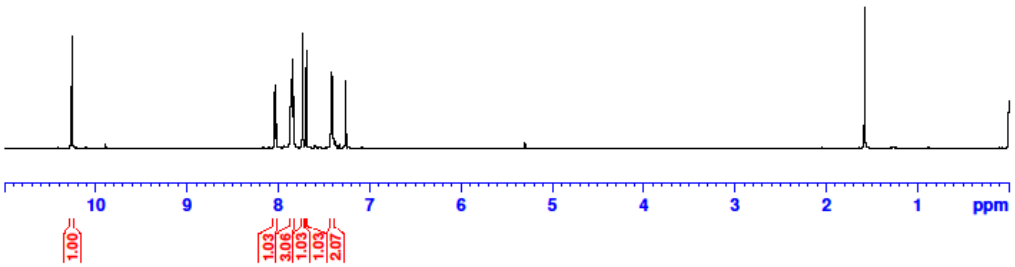

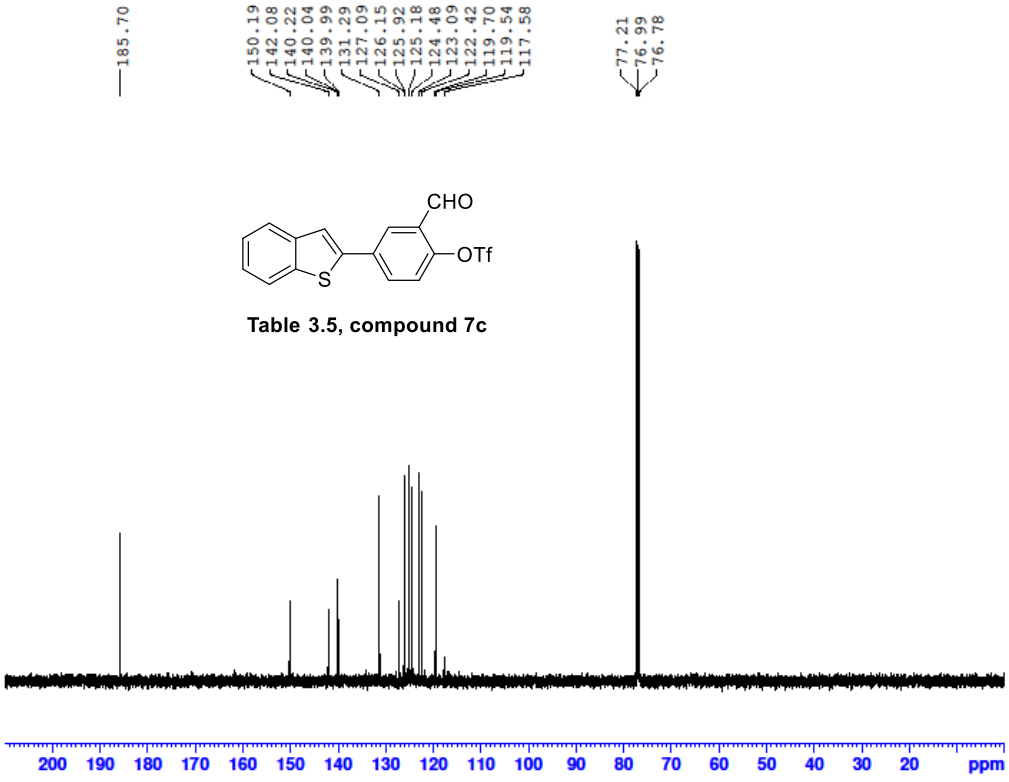

Table 3.5, compound 7c

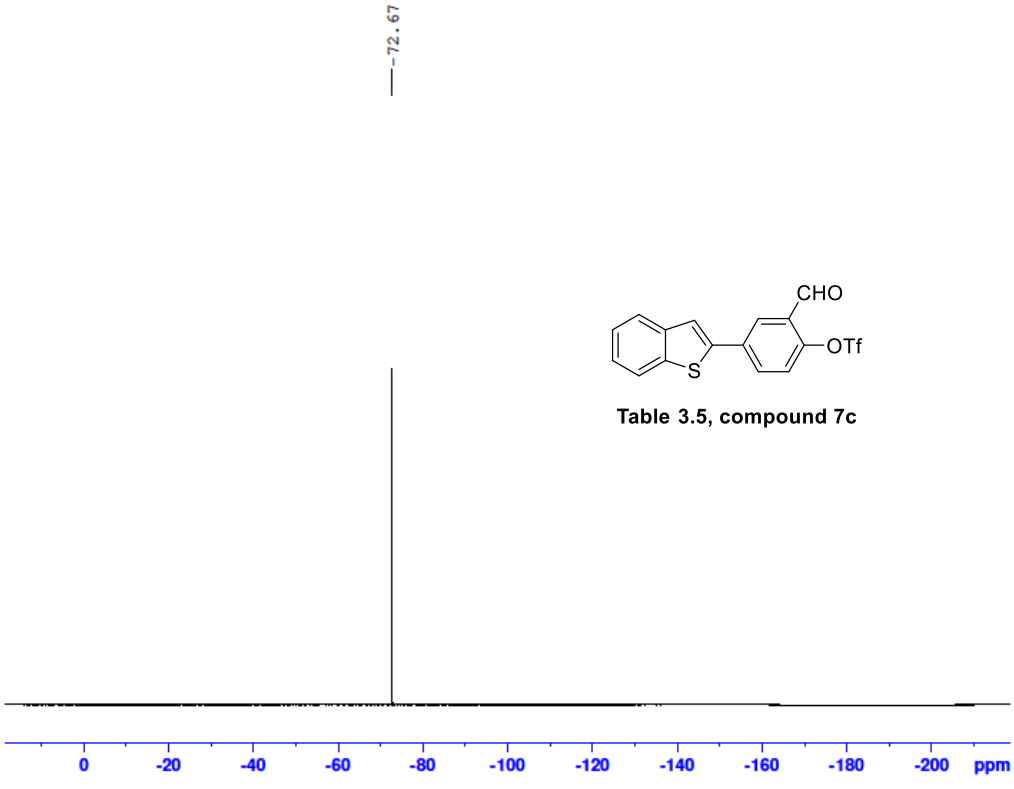

Table 3.5, compound 7c

A29-20230928

A29-GCX-IV-116-7-20230928 708 (13.273)

TOF MS EI+
1.83e4

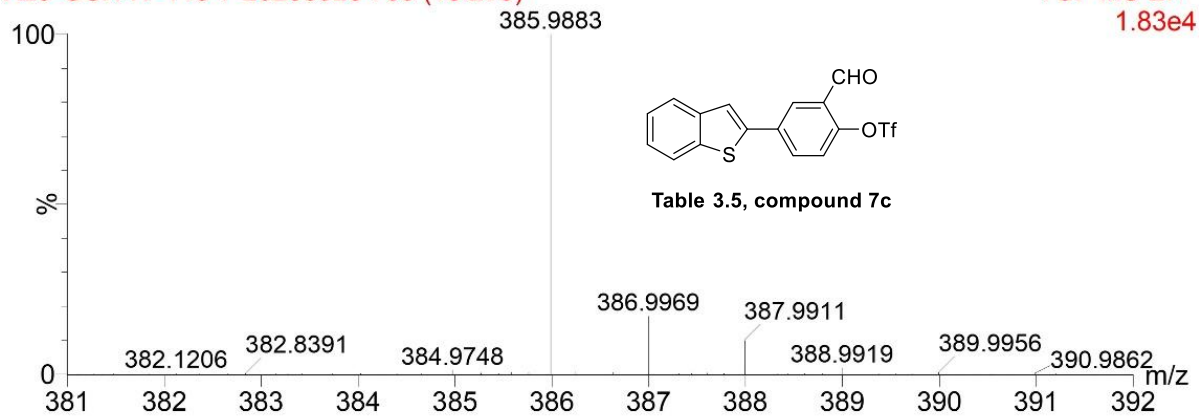

Table 3.5, compound 7c

Mass	Calc. Mass	mDa	PPM	Ion Formula
385.9883	385.9889	1.52	0.59	C16H9F3O4S2

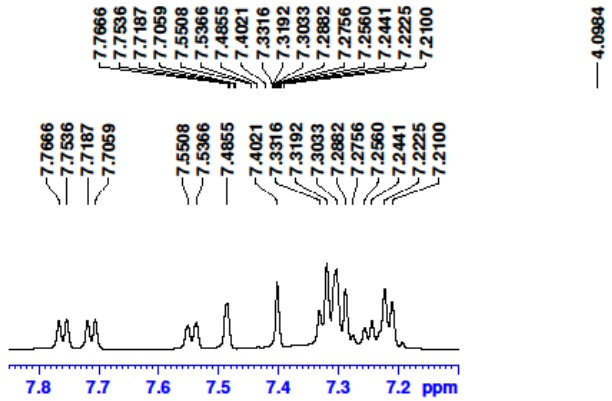

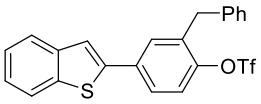

Table 3.5, compound 7d

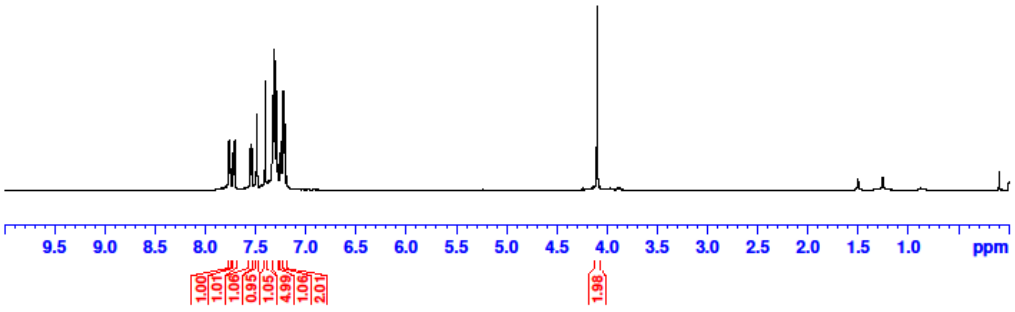

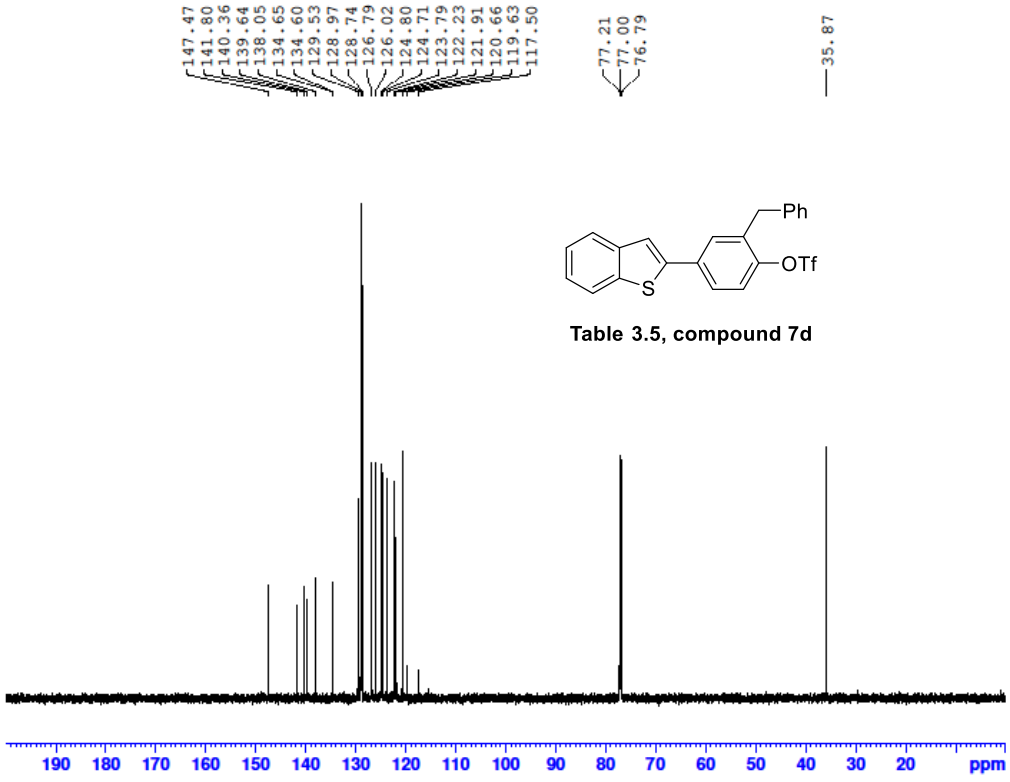

Table 3.5, compound 7d

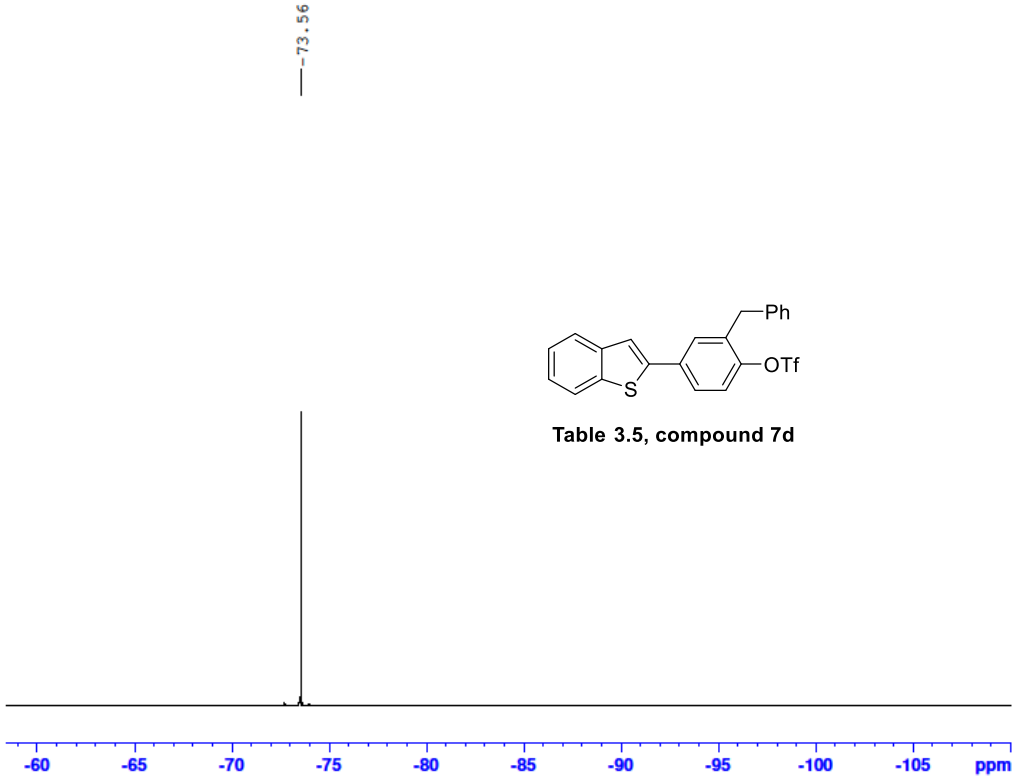

Table 3.5, compound 7d

A11-20230928

A10-GCX-IV-121-6-20230928-1 718 (13.407)

TOF MS EI+
2.14e3

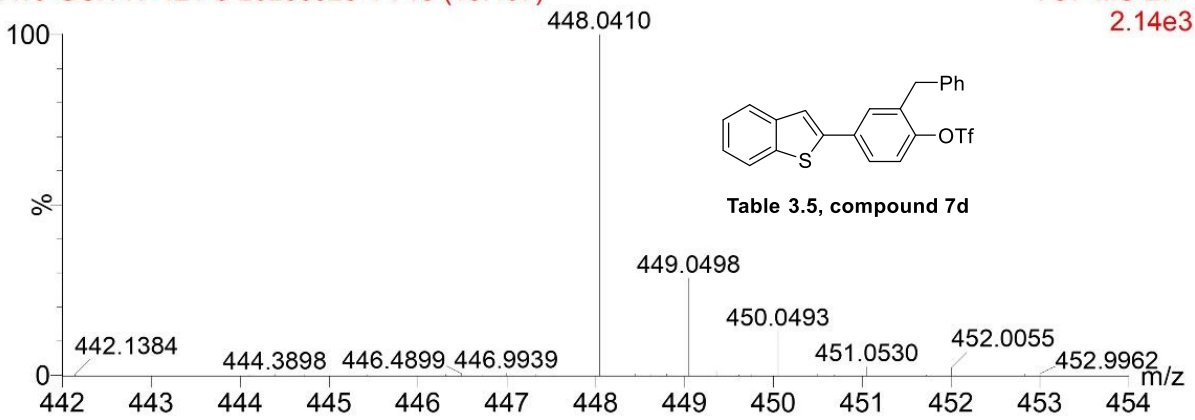

Table 3.5, compound 7d

Mass	Calc. Mass	mDa	PPM	Ion Formula
448.0410	448.0409	-0.17	-0.08	C22H15F3O3S2

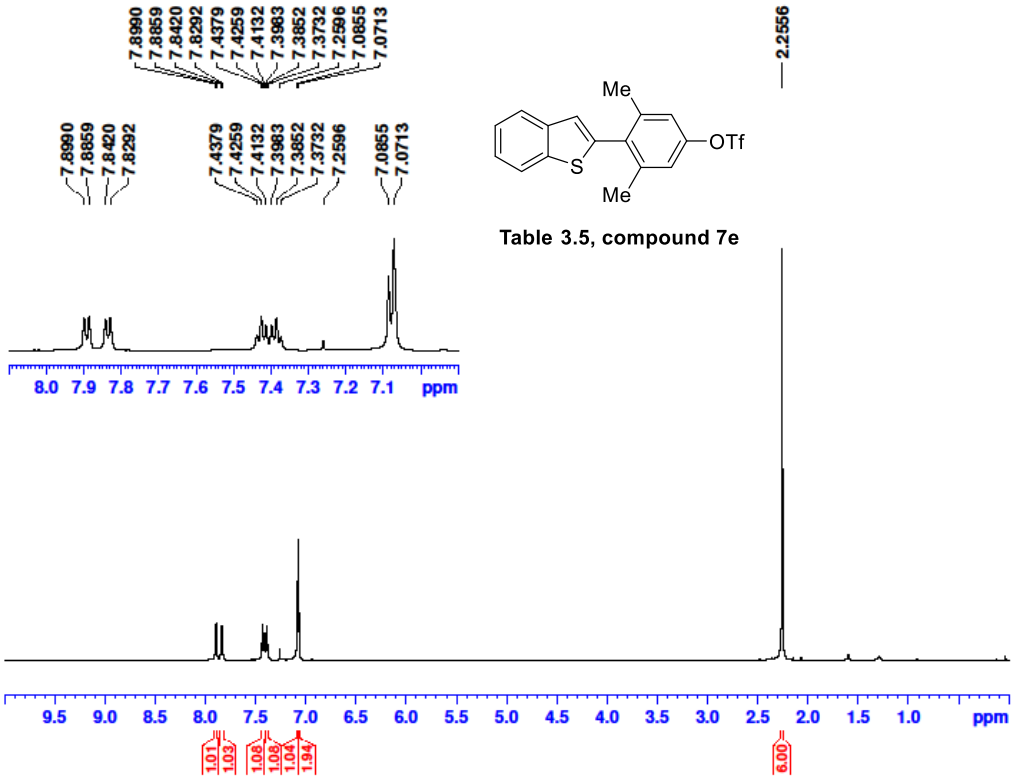

Table 3.5, compound 7e

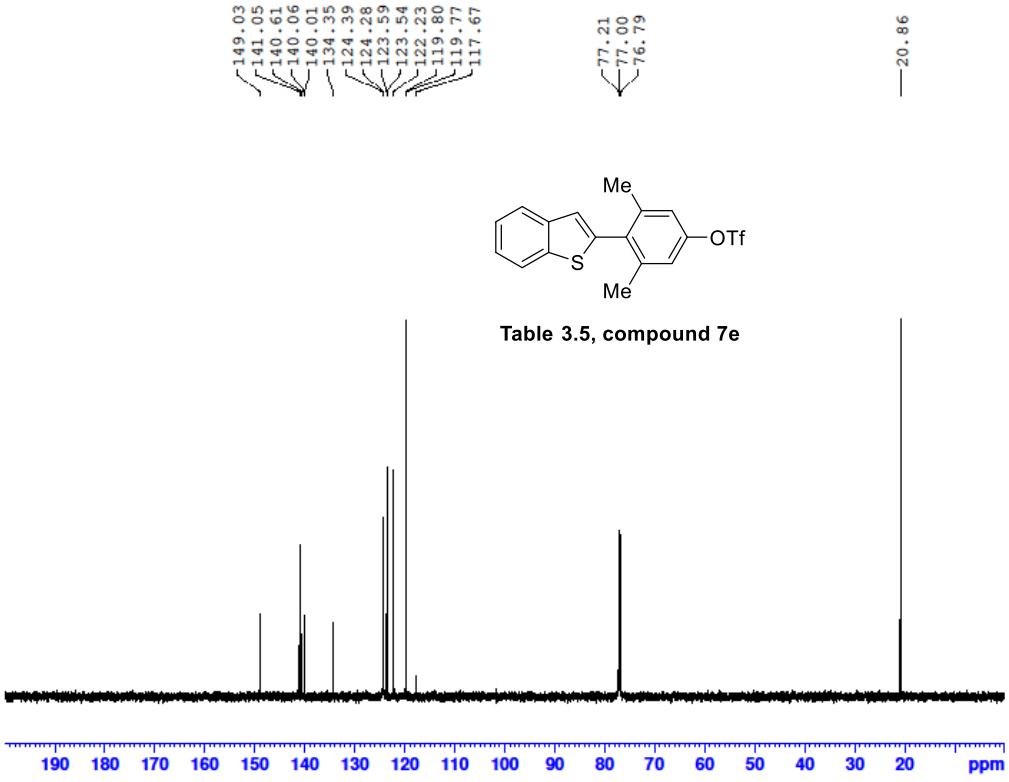

Table 3.5, compound 7e

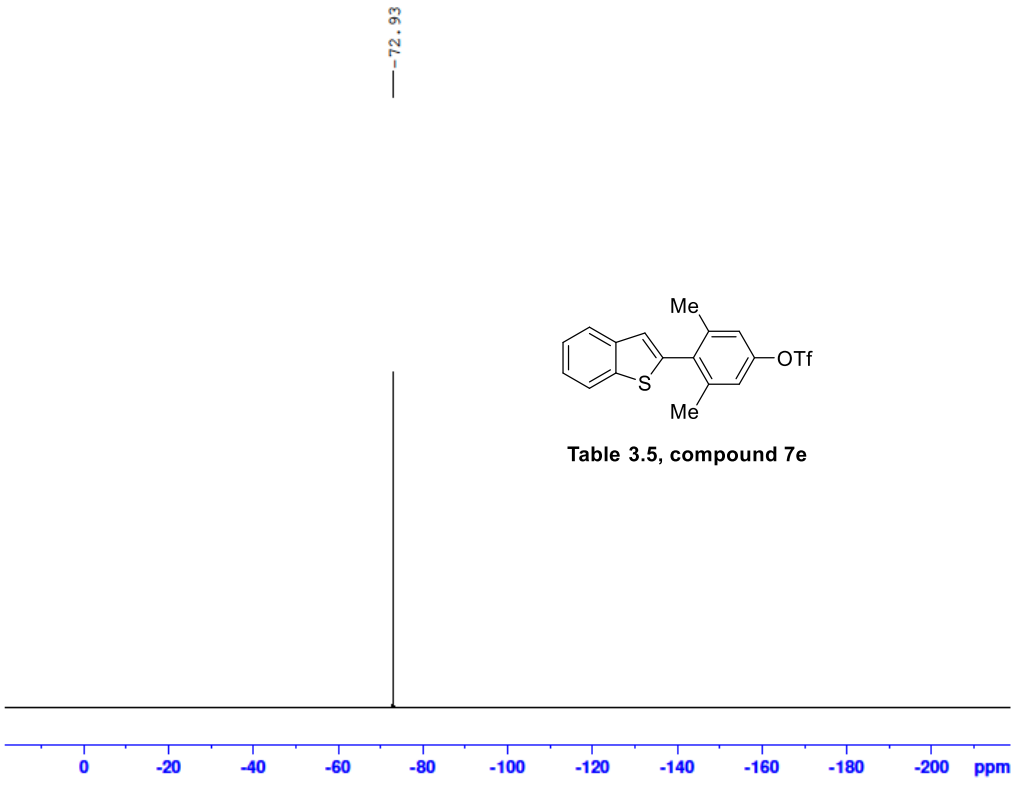

Table 3.5, compound 7e

A31-20230928

A31-GCX-IV-146-1-20230928 624 (12.153)

TOF MS EI+
1.80e3

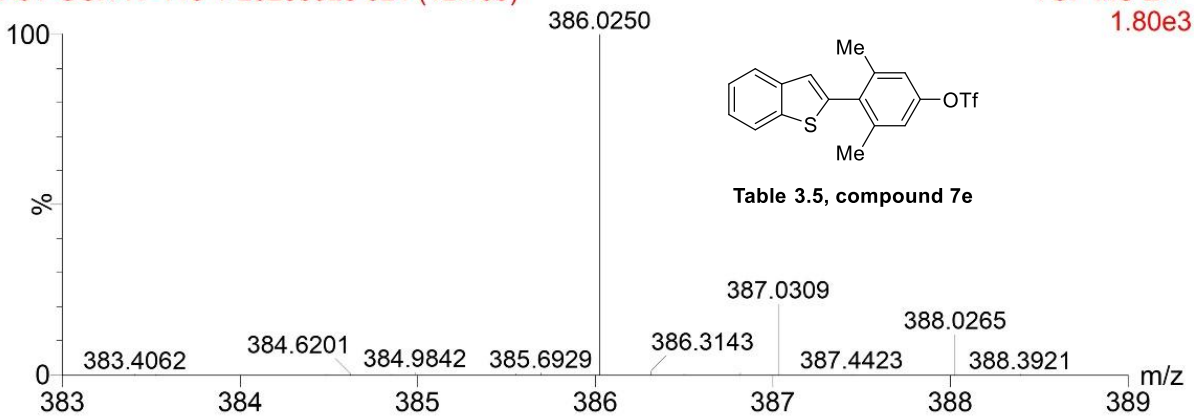

Table 3.5, compound 7e

Mass	Calc. Mass	mDa	PPM	Ion Formula
386.0250	386.0253	0.71	0.27	C17H13F3O3S2

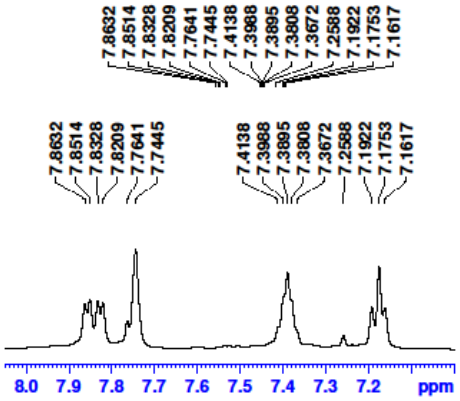

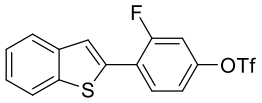

Table 3.5, compound 7f

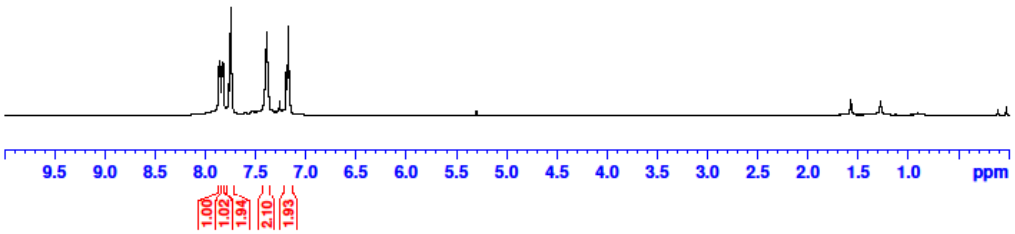

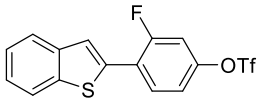

Table 3.5, compound 7f

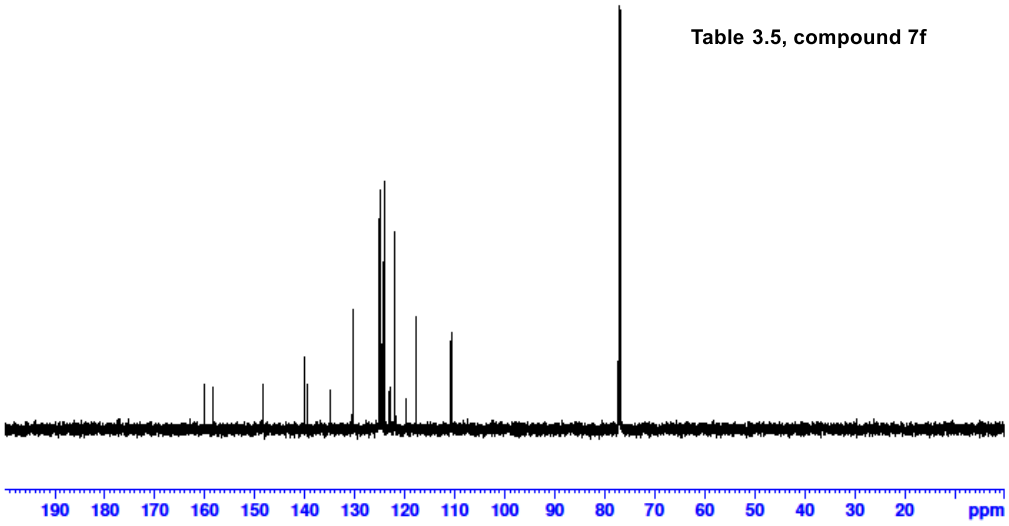

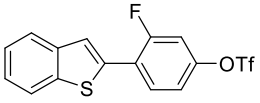

Table 3.5, compound 7f

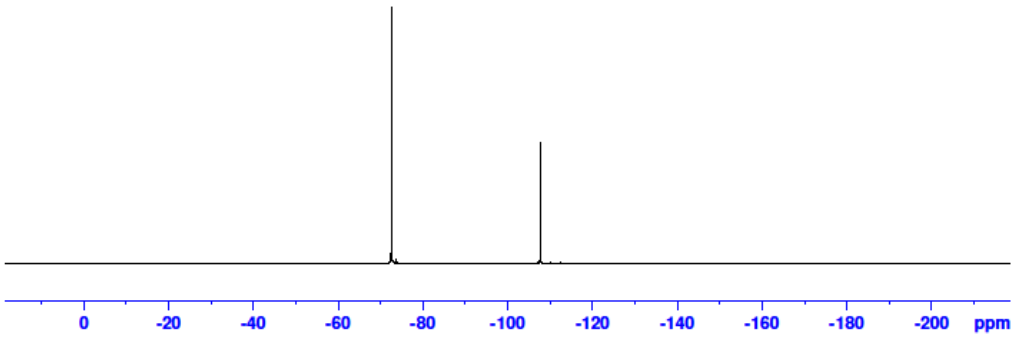

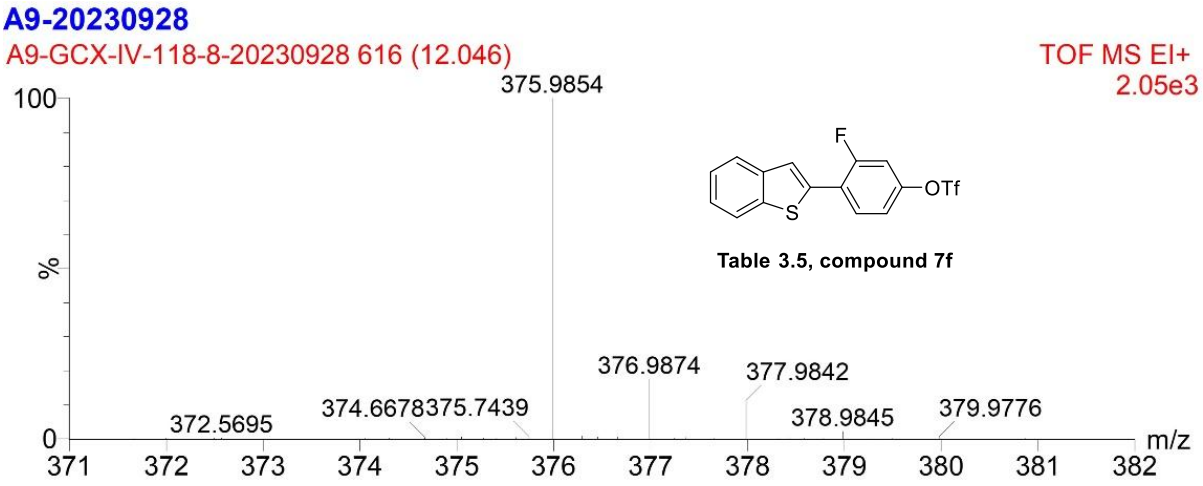

Table 3.5, compound 7f

Mass	Calc. Mass	mDa	PPM	Ion Formula
375.9854	375.9845	-2.27	-0.85	C15H8F4O3S2

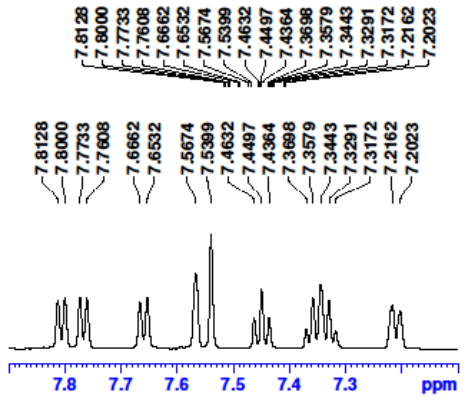

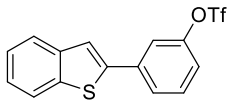

Table 3.5, compound 7g

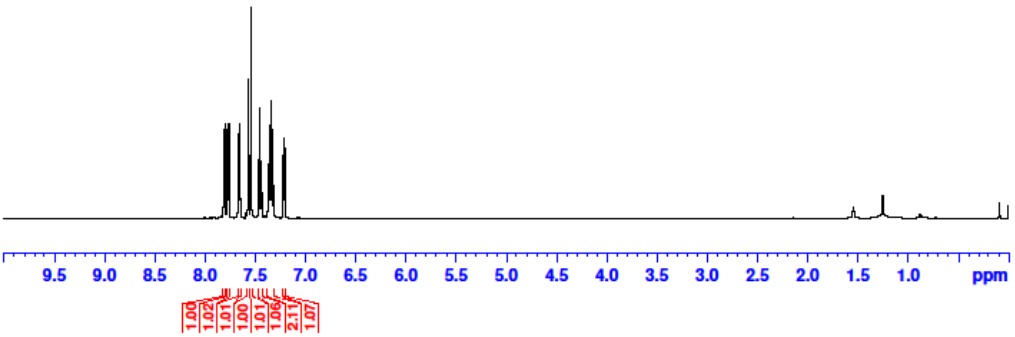

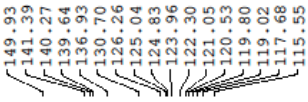

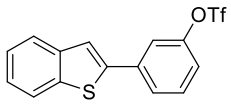

Table 3.5, compound 7g

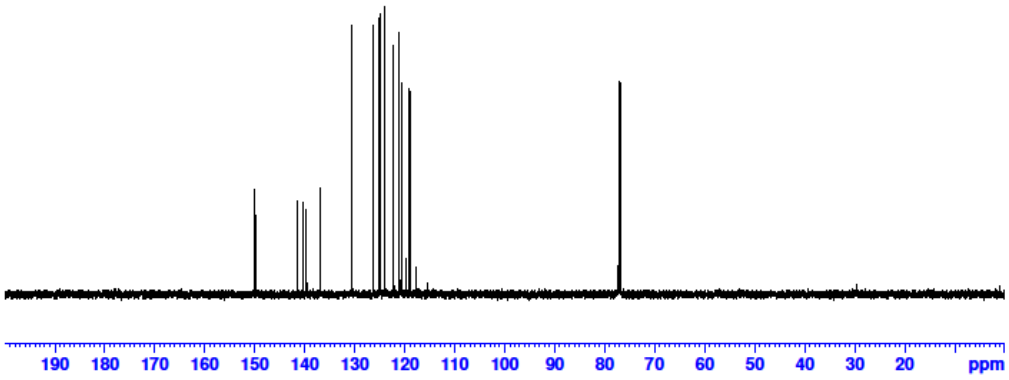

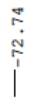

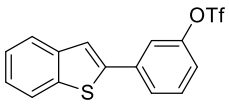

Table 3.5, compound 7g

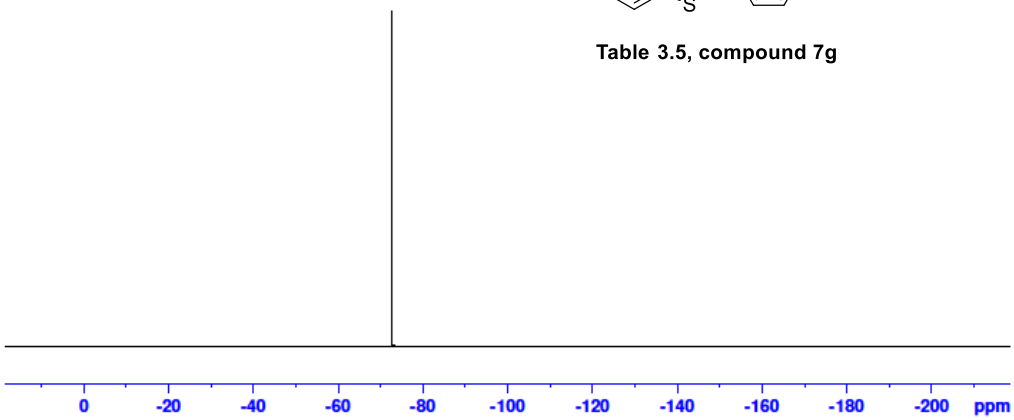

A19-20230928

A19-GCX-IV-118-7-20230928 624 (12.153)

TOF MS EI+
2.67e3

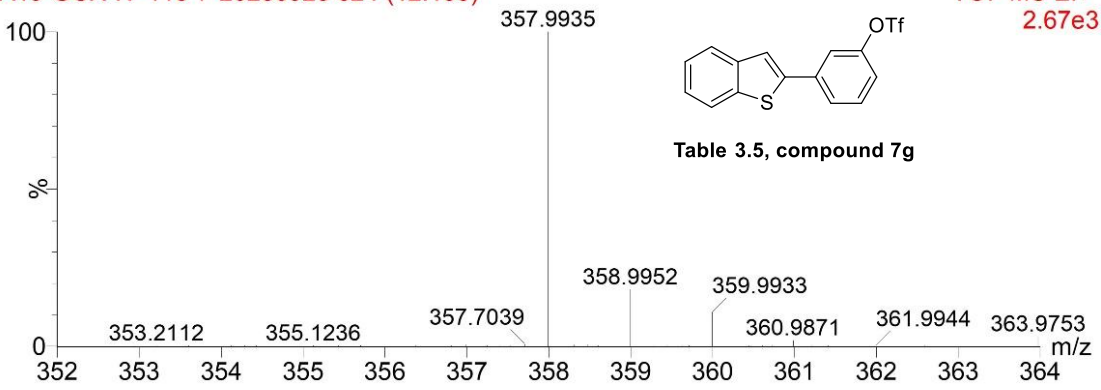

Table 3.5, compound 7g

Mass	Calc. Mass	mDa	PPM	Ion Formula
357.9935	357.9940	1.32	0.47	C15H9F3O3S2

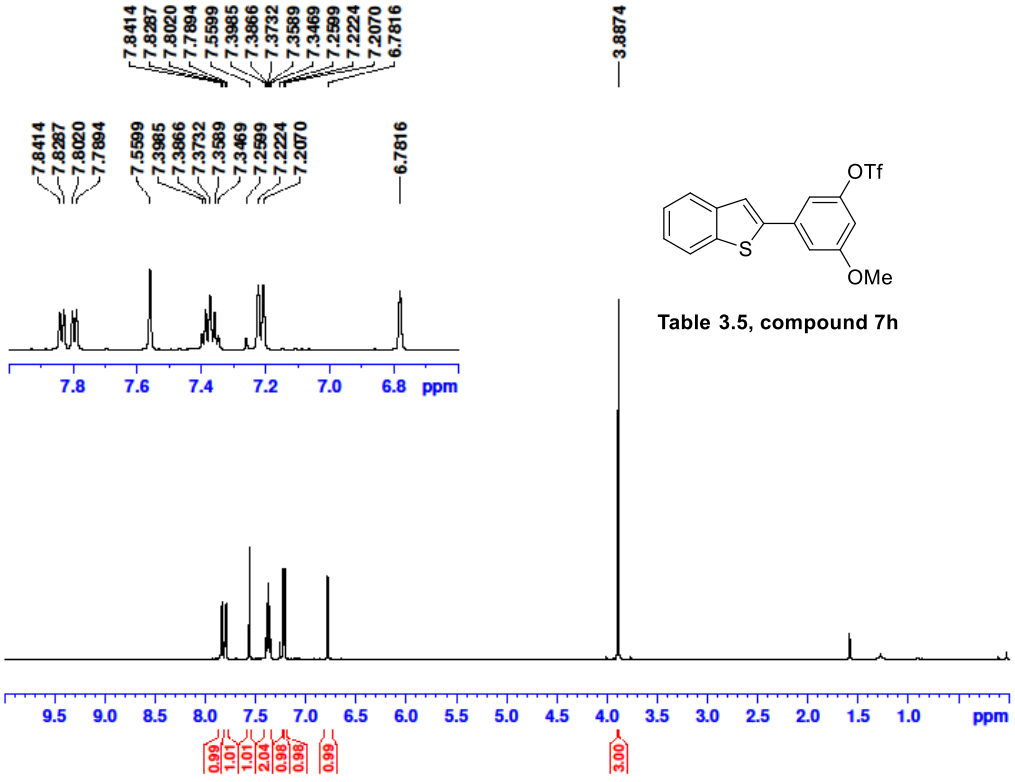

Table 3.5, compound 7h

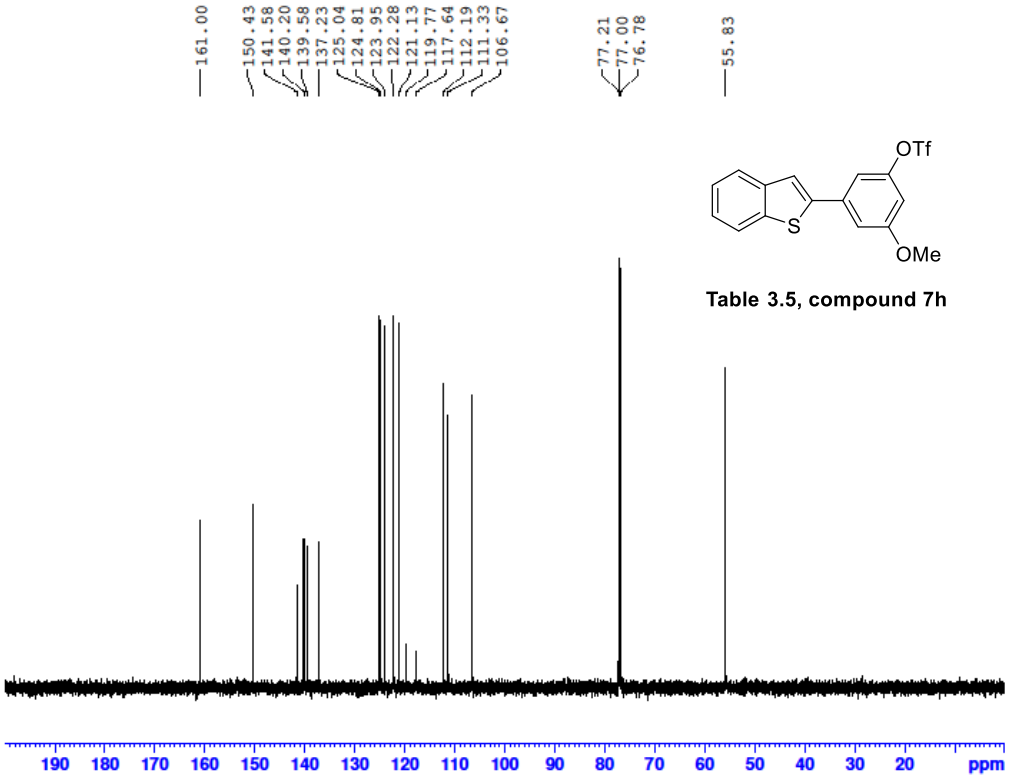

Table 3.5, compound 7h

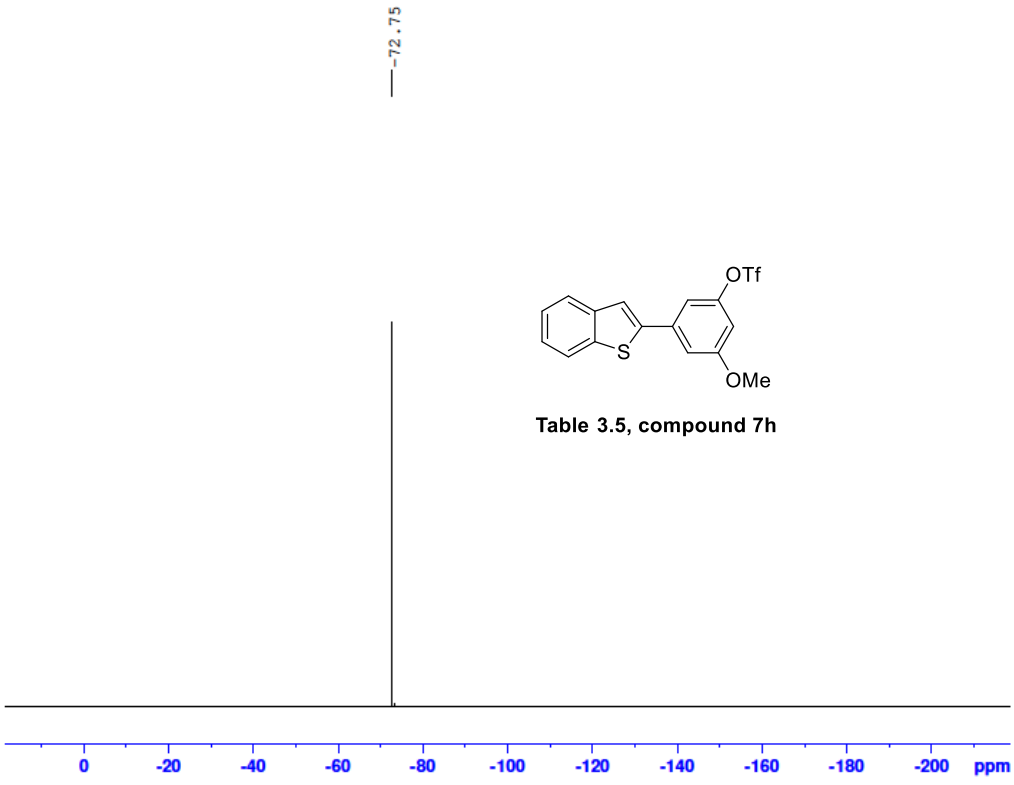

Table 3.5, compound 7h

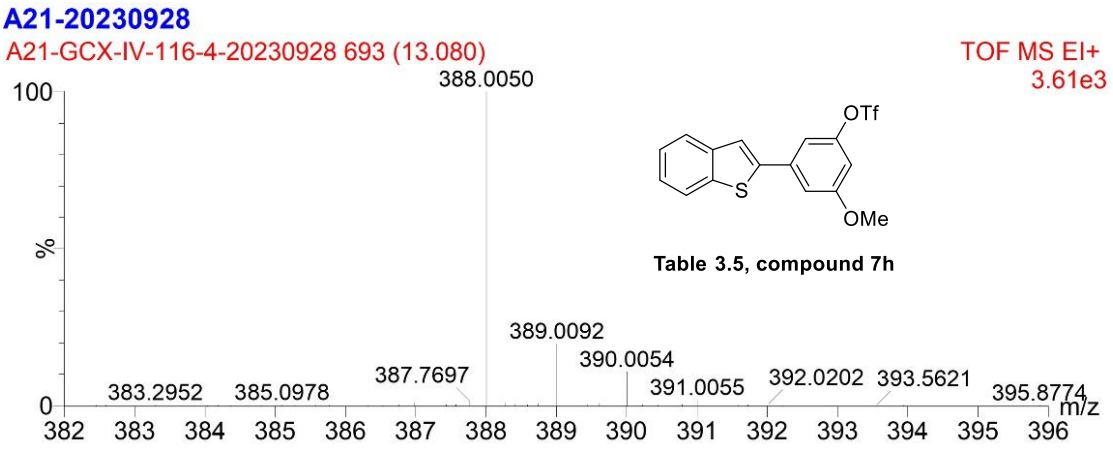

Table 3.5, compound 7h

Mass	Calc. Mass	mDa	PPM	Ion Formula
388.0050	388.0045	-1.20	-0.46	C16H11F3O4S2

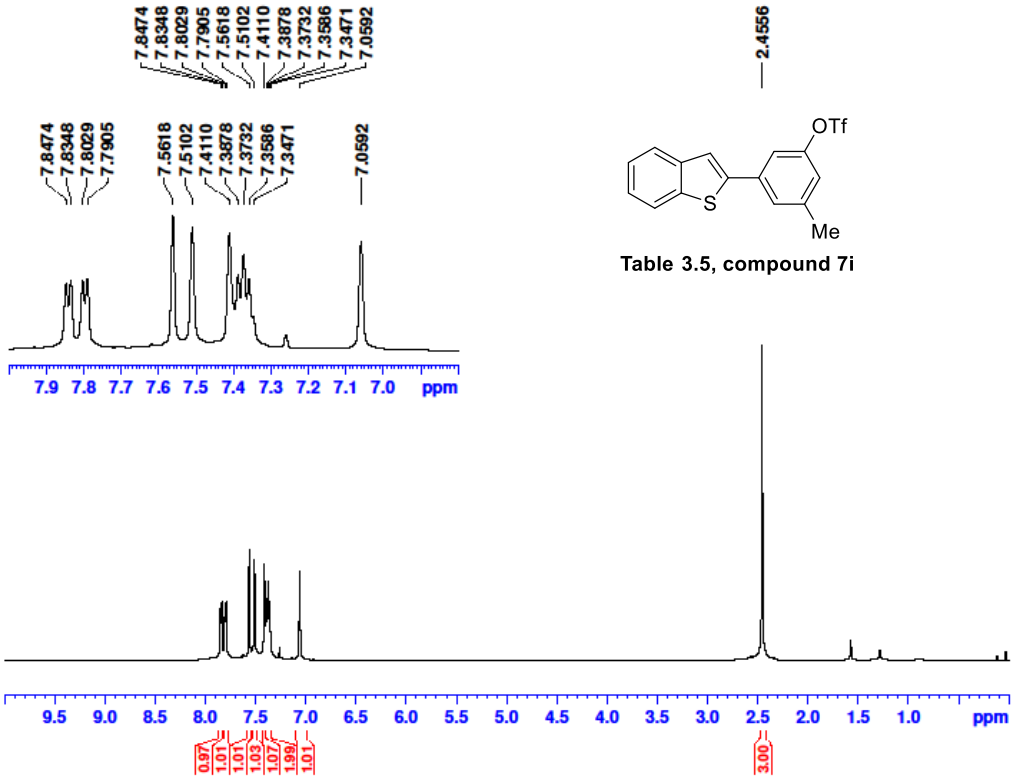

Table 3.5, compound 7i

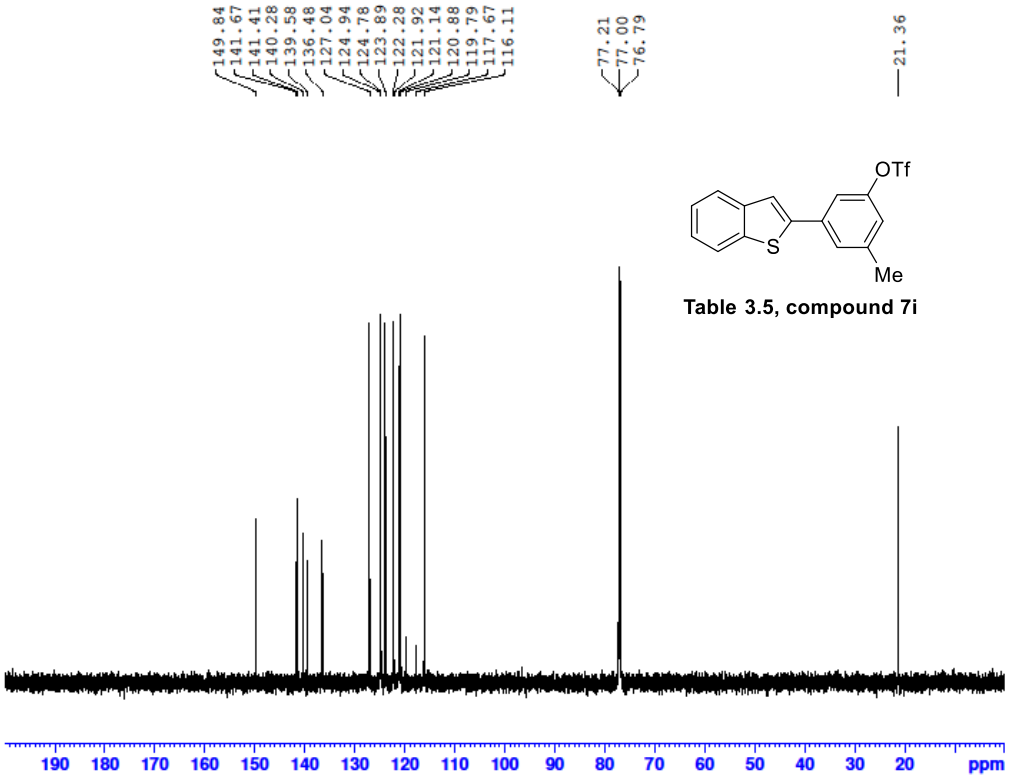

Table 3.5, compound 7i

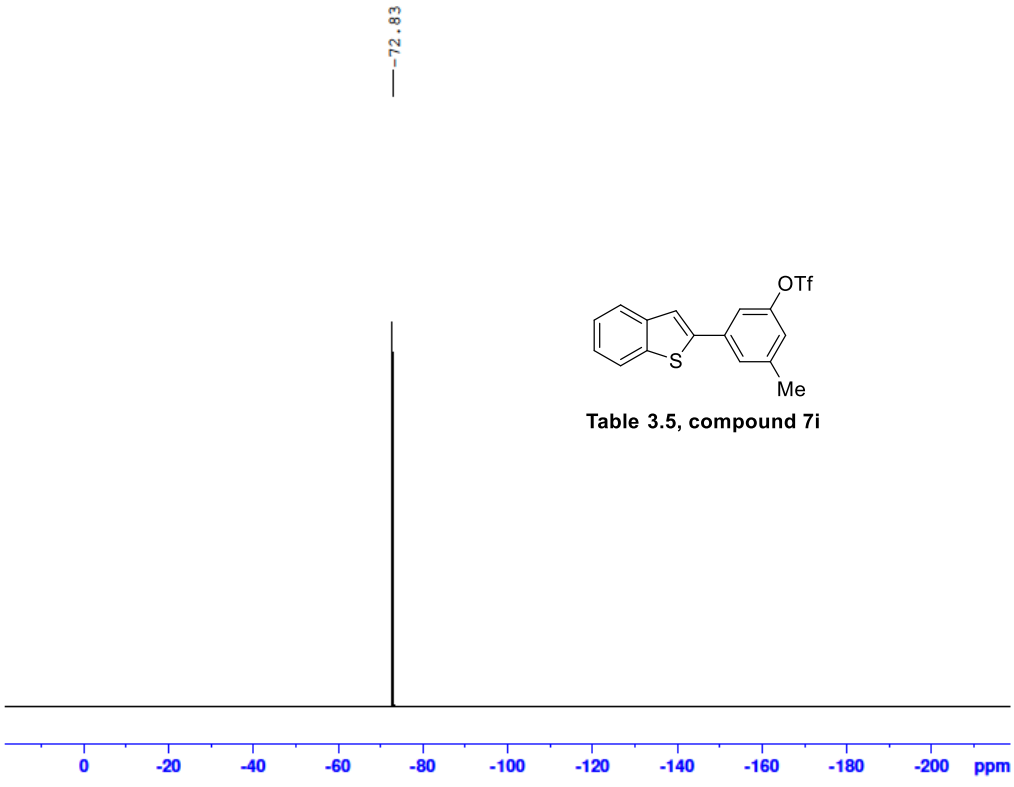

Table 3.5, compound 7i

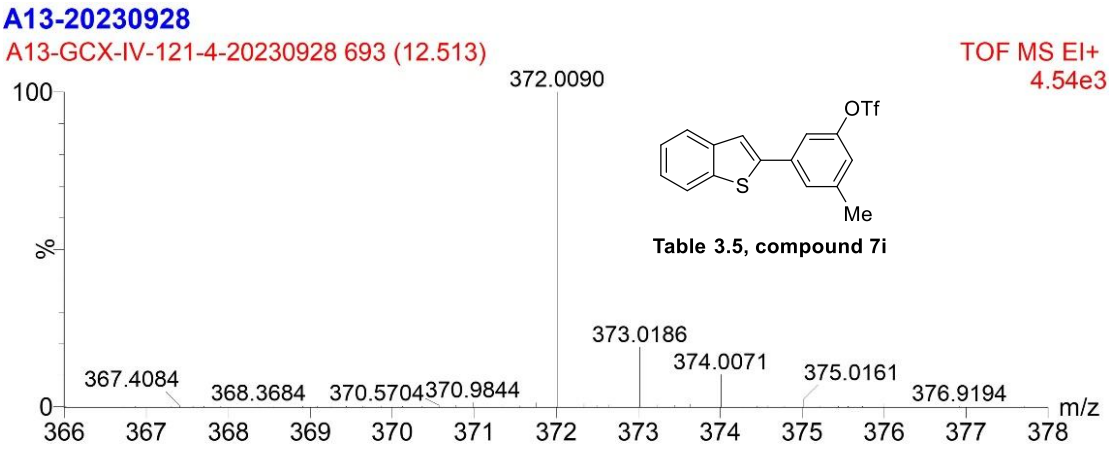

Table 3.5, compound 7i

Mass	Calc. Mass	mDa	PPM	Ion Formula
372.0090	372.0096	1.68	0.62	C16H11F3O3S2

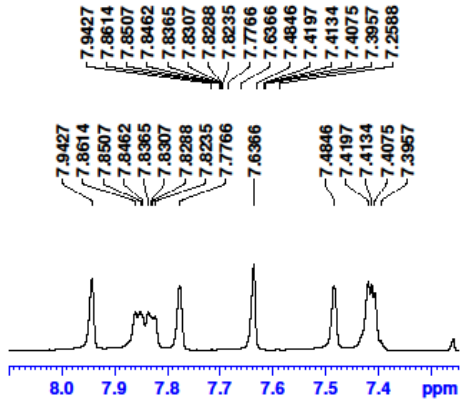

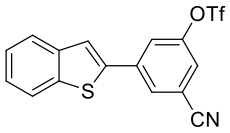

Table 3.5, compound 7j

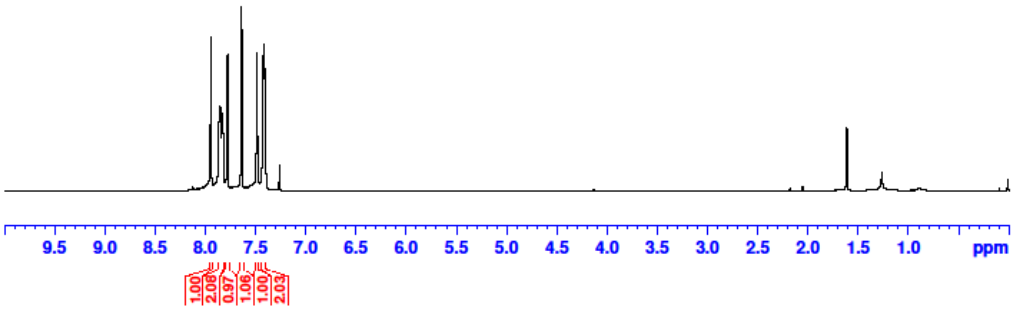

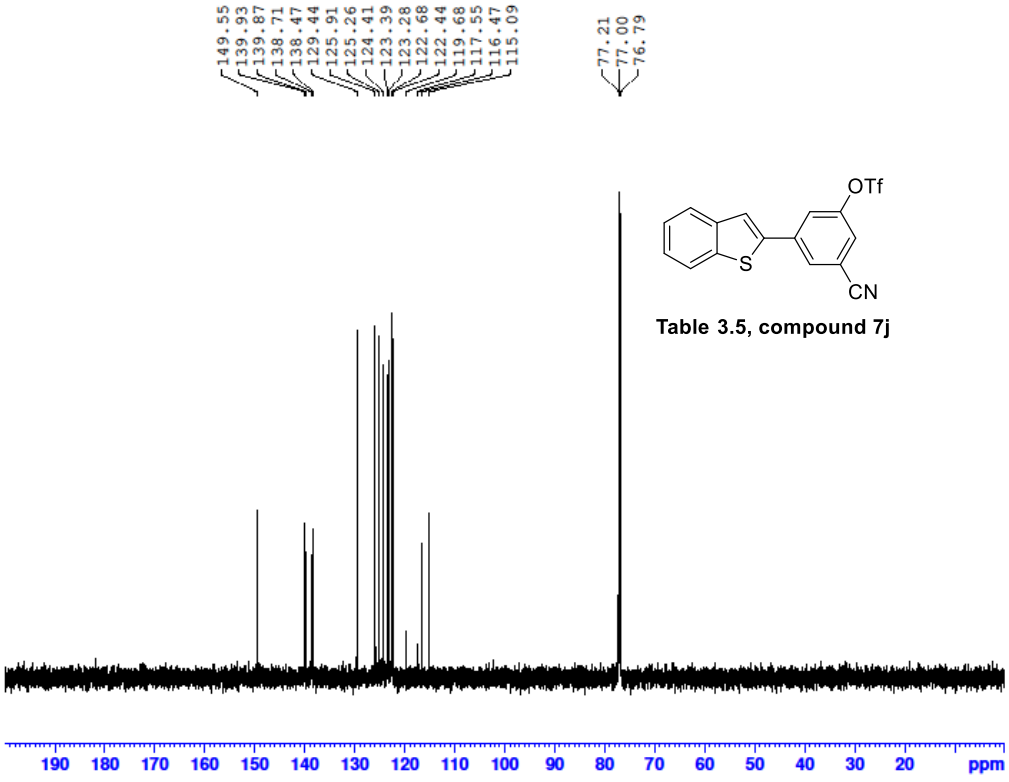

Table 3.5, compound 7j

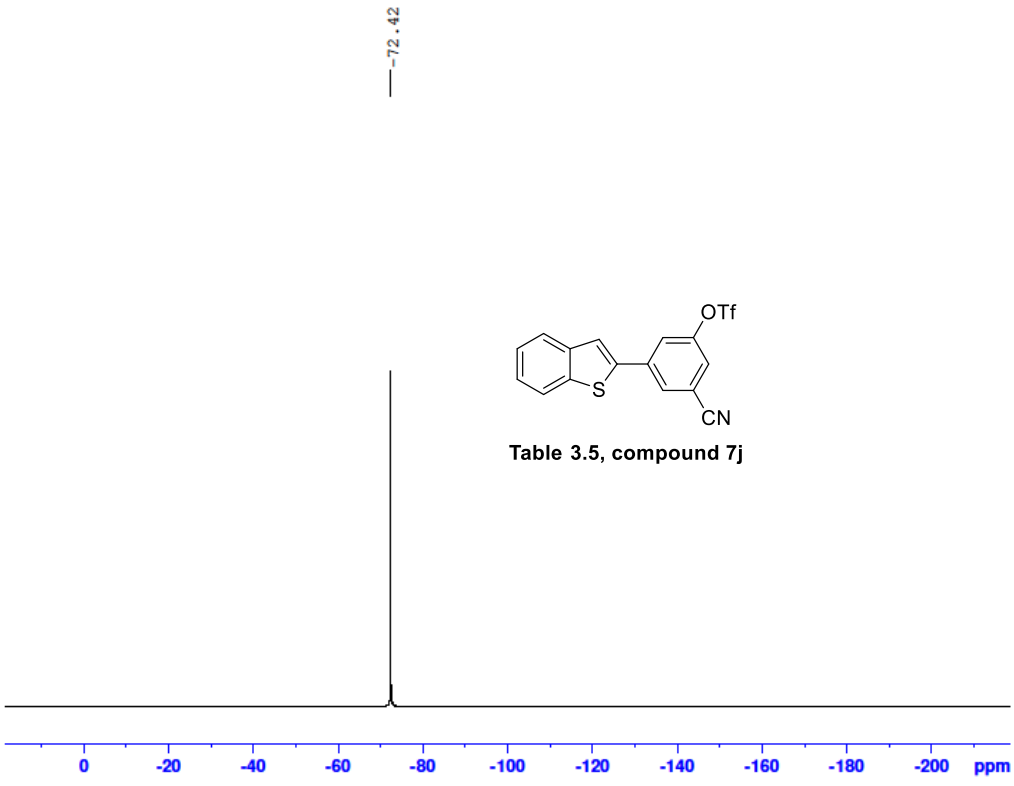

Table 3.5, compound 7j

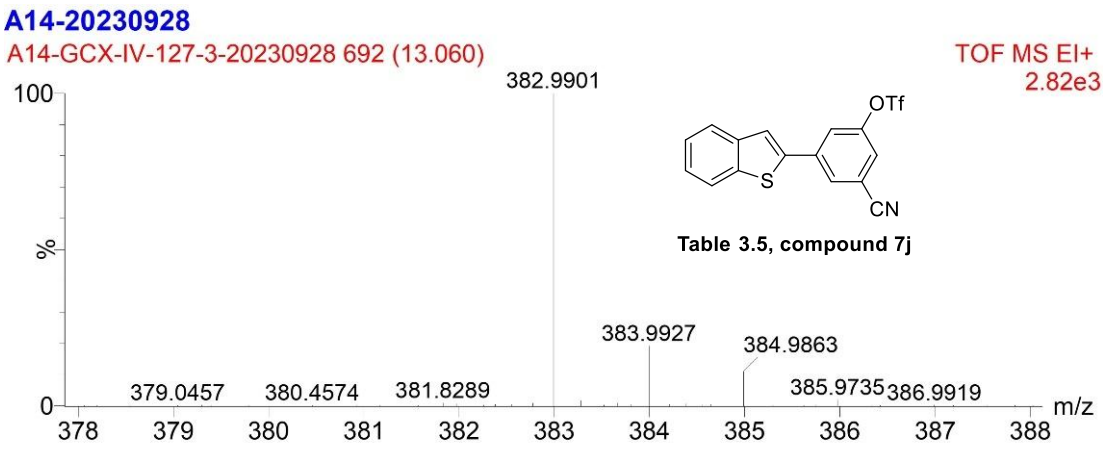

Table 3.5, compound 7j

Mass	Calc. Mass	mDa	PPM	Ion Formula
382.9901	382.9892	-2.30	-0.88	C16H8F3NO3S2

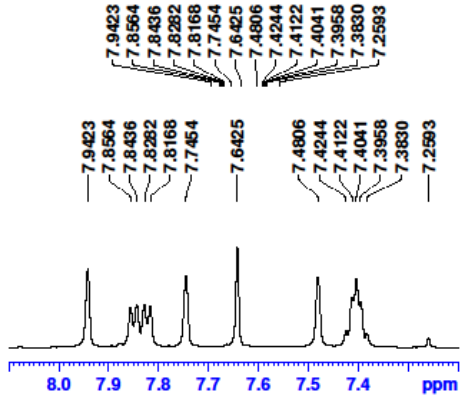

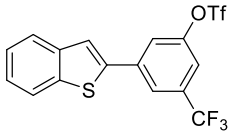

Table 3.5, compound 7k

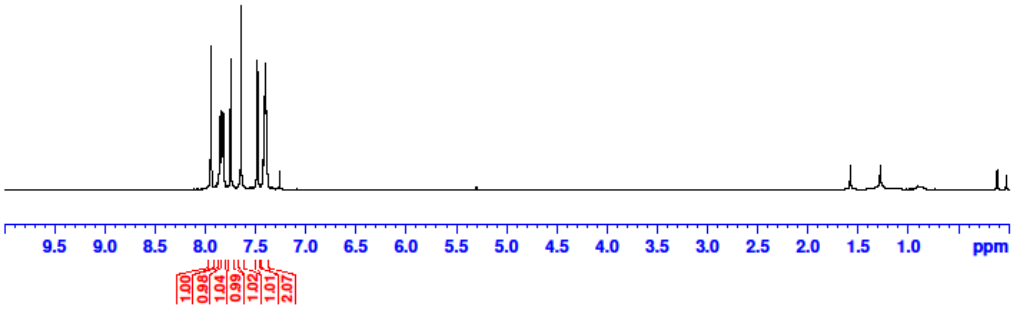

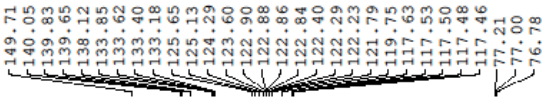

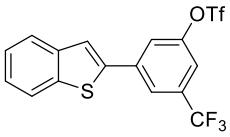

Table 3.5, compound 7k

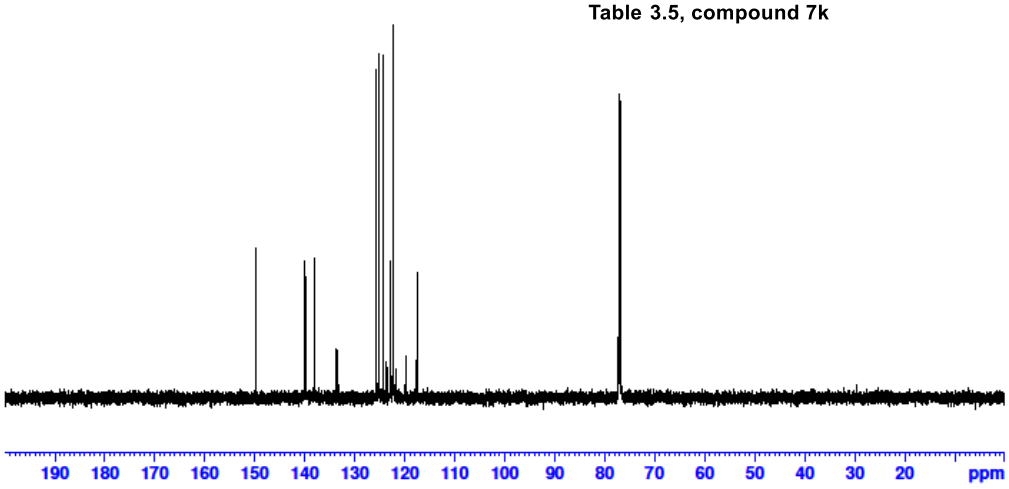

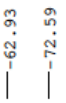

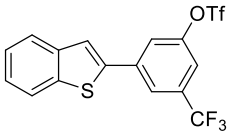

Table 3.5, compound 7k

A3-20230928

A3-GCX-IV-130-1-20230928 556 (11.266) Cm (531:588) TOF MS EI+ 5.74e4

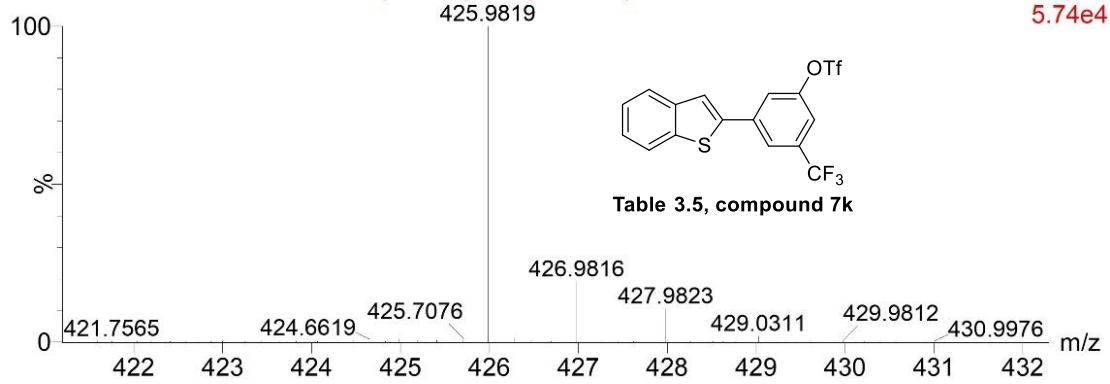

Table 3.5, compound 7k

Mass	Calc. Mass	mDa	PPM	Ion Formula
425.9819	425.9814	-1.28	-0.54	C16H8F6O3S2

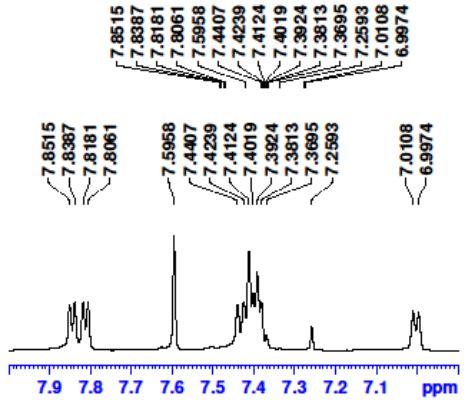

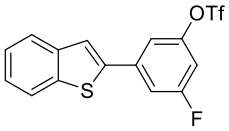

Table 3.5, compund 7l

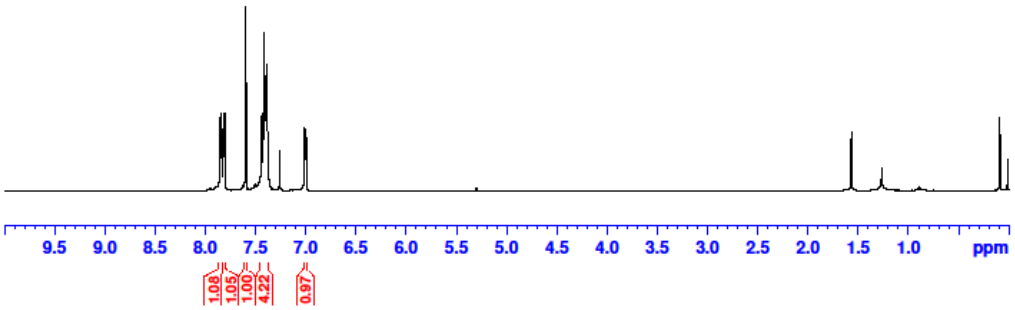

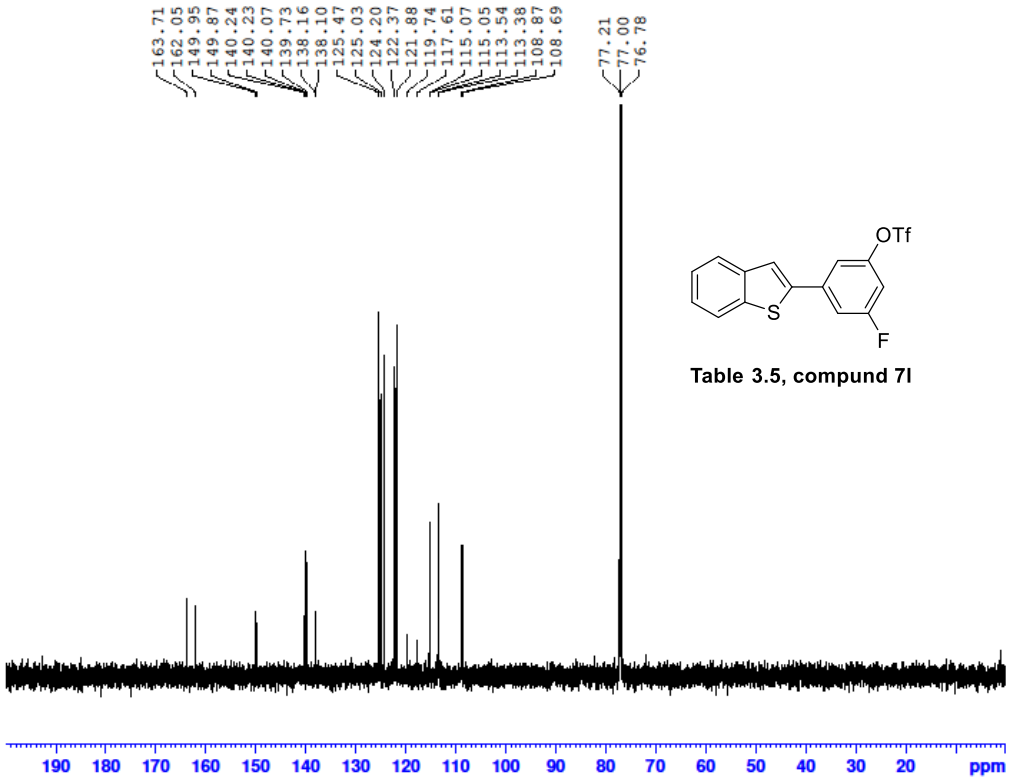

Table 3.5, compund 7l

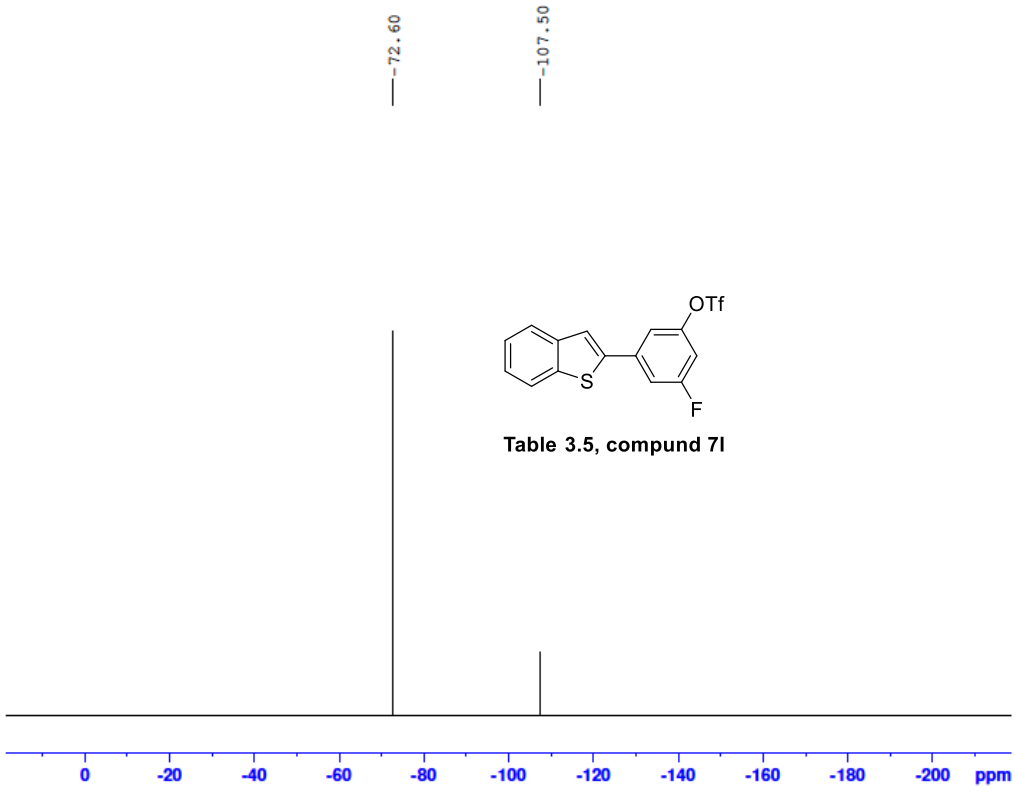

Table 3.5, compund 7l

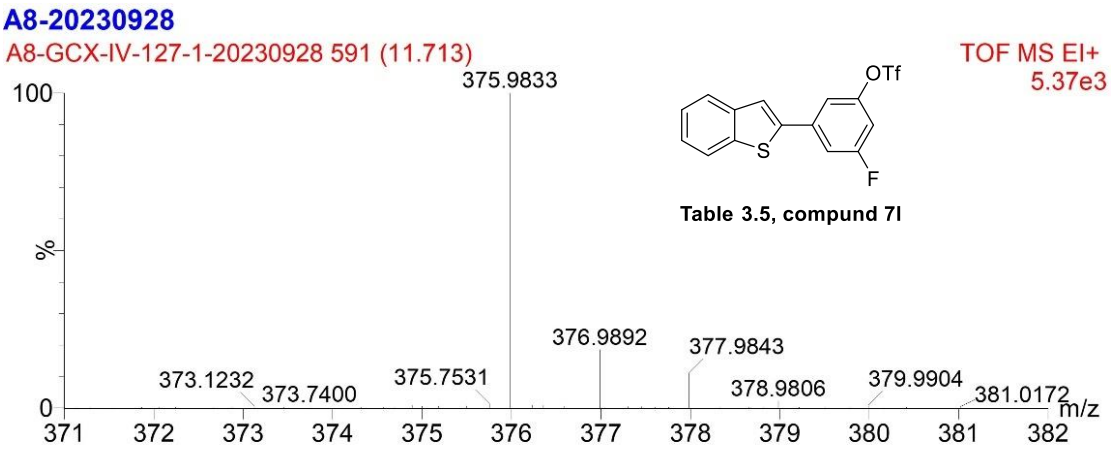

Table 3.5, compund 7l

Mass	Calc. Mass	mDa	PPM	Ion Formula
375.9833	375.9845	3.33	1.25	C15H8F4O3S2

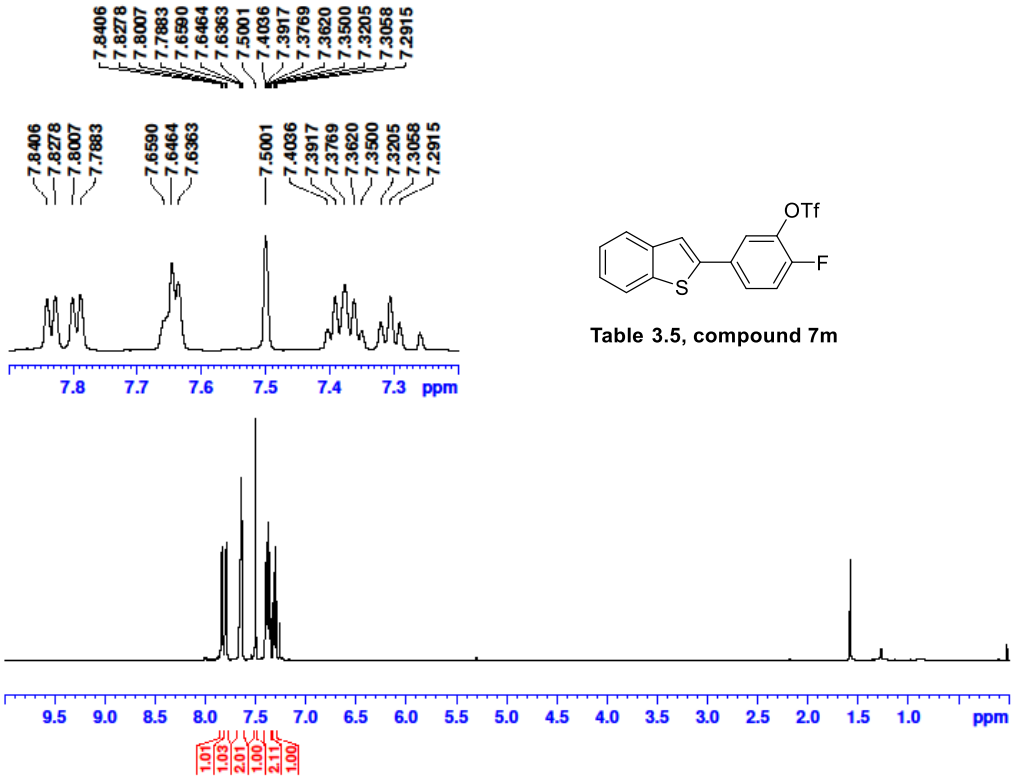

Table 3.5, compound 7m

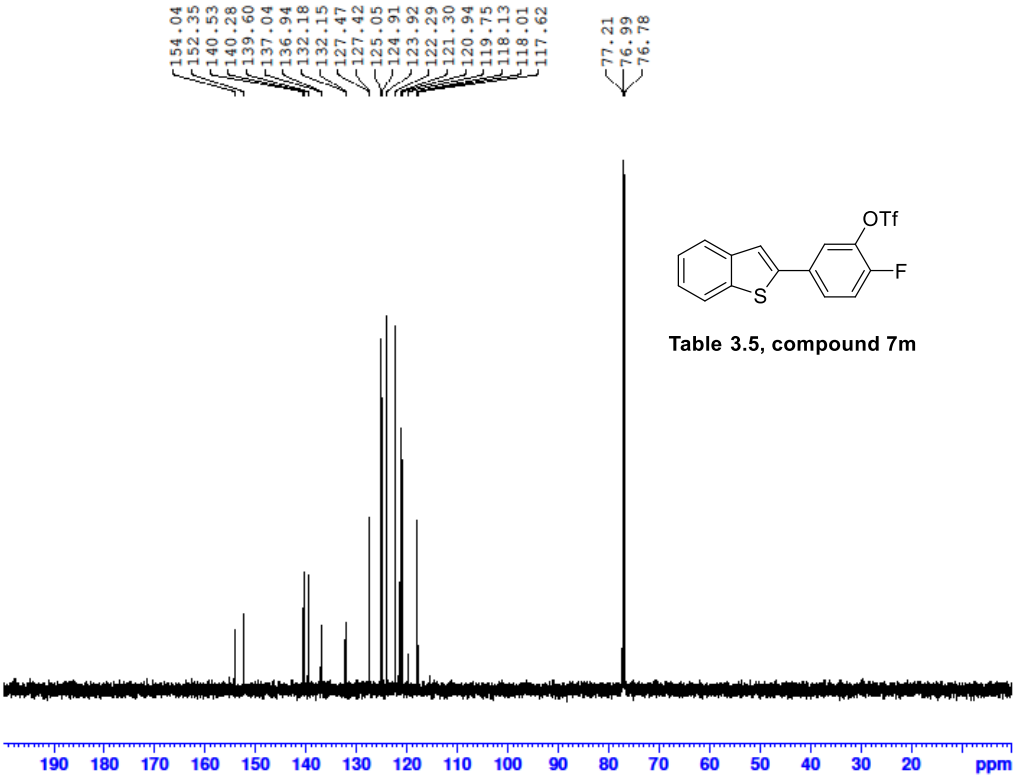

Table 3.5, compound 7m

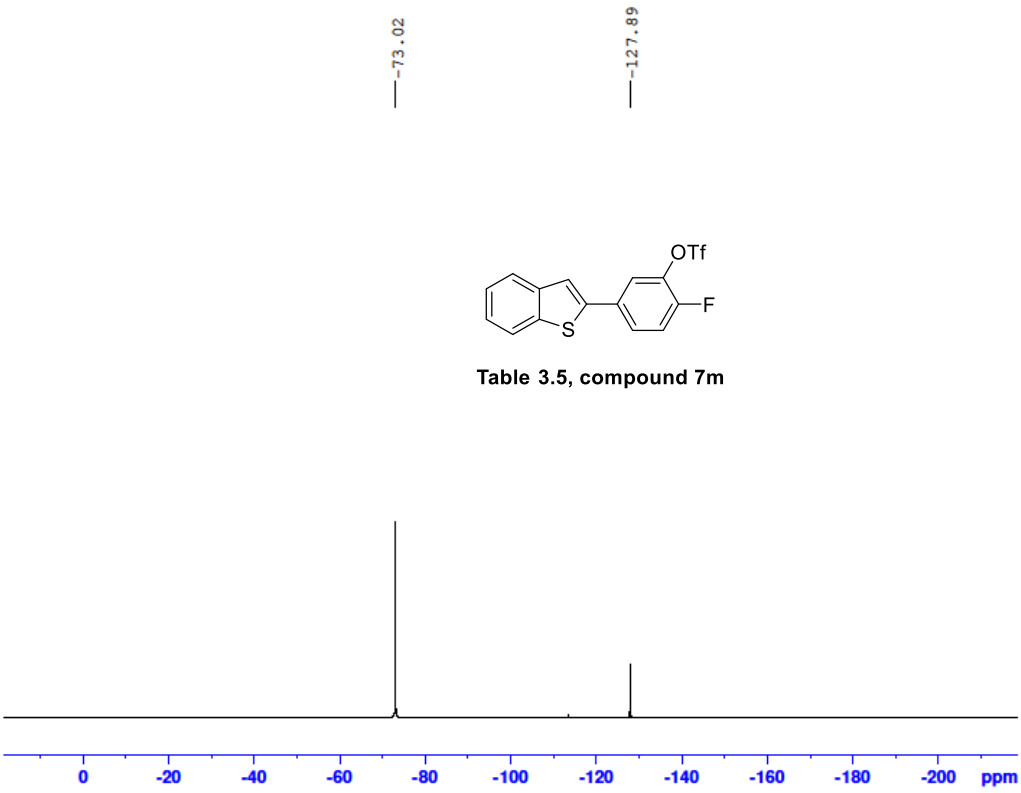

Table 3.5, compound 7m

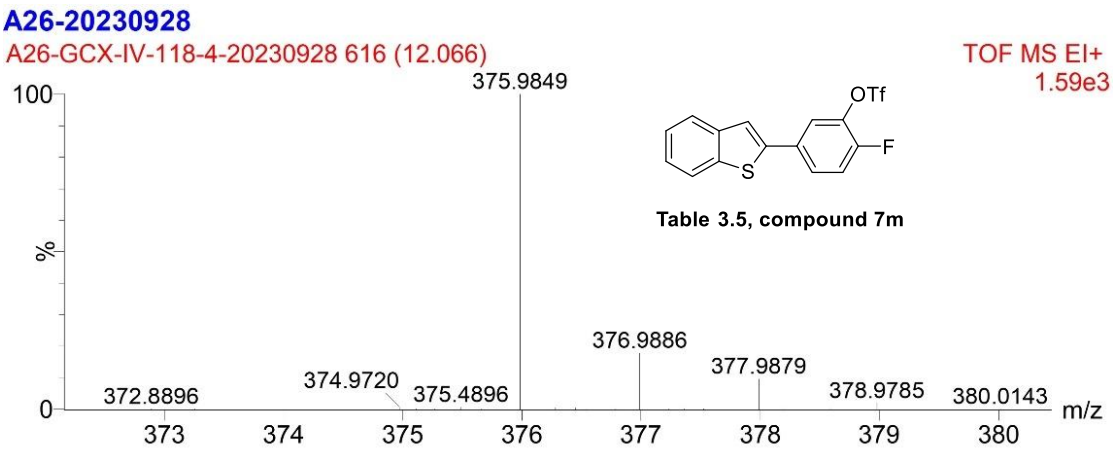

Table 3.5, compound 7m

Mass	Calc. Mass	mDa	PPM	Ion Formula
375.9849	375.9845	-0.93	-0.35	C15H8F4O3S2

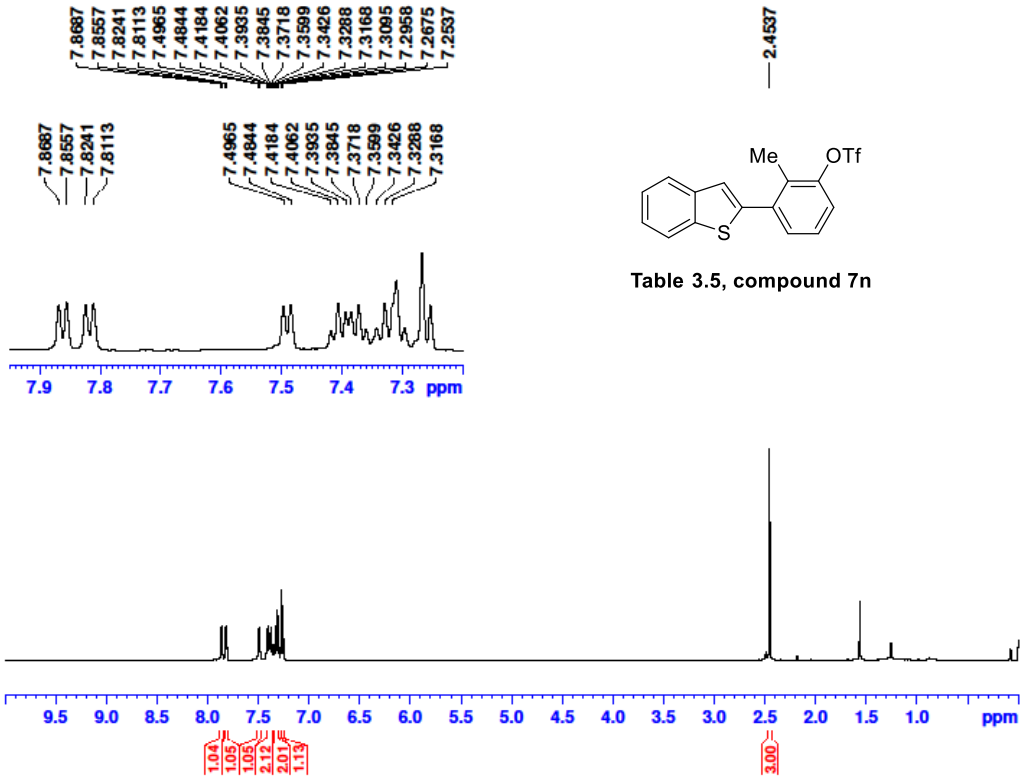

Table 3.5, compound 7n

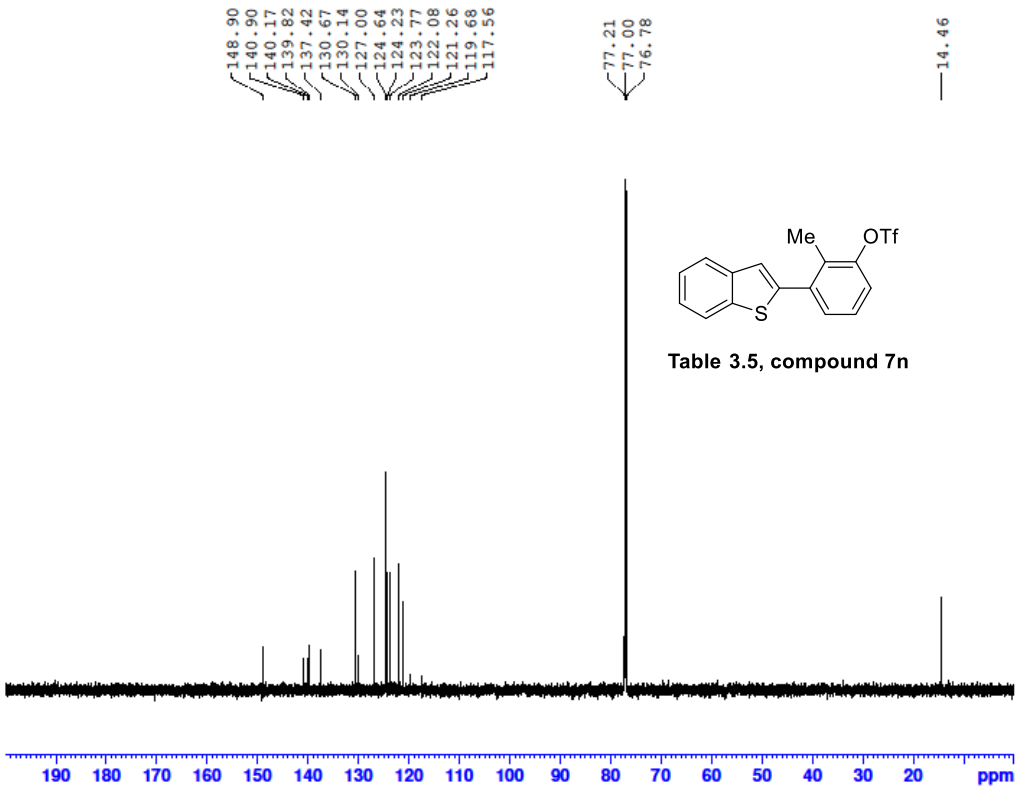

Table 3.5, compound 7n

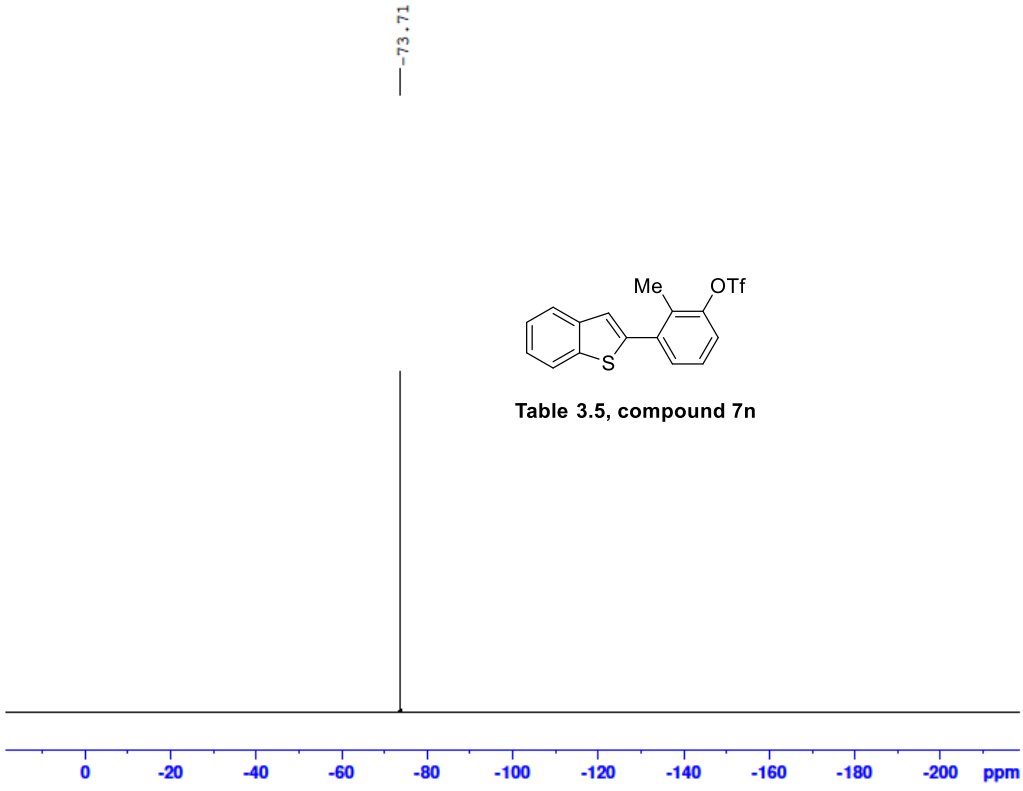

Table 3.5, compound 7n

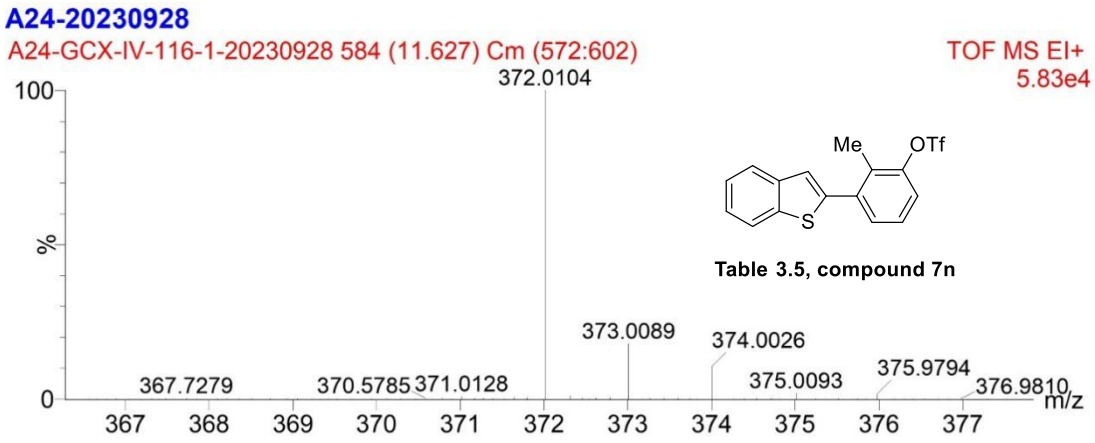

Table 3.5, compound 7n

Mass	Calc. Mass	mDa	PPM	Ion Formula
372.0104	372.0096	-2.10	-0.78	C16H11F3O3S2

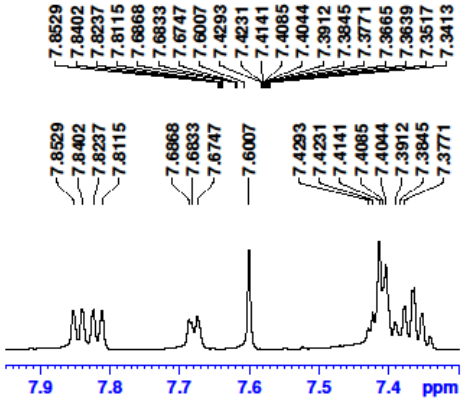

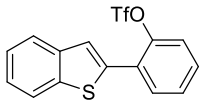

Table 3.5, compound 7o

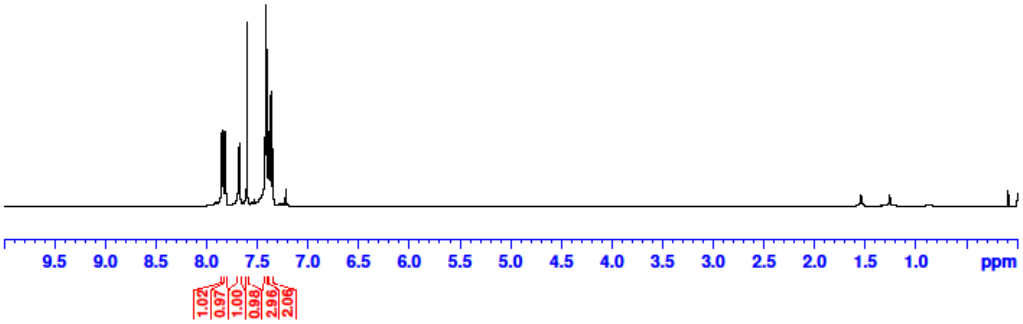

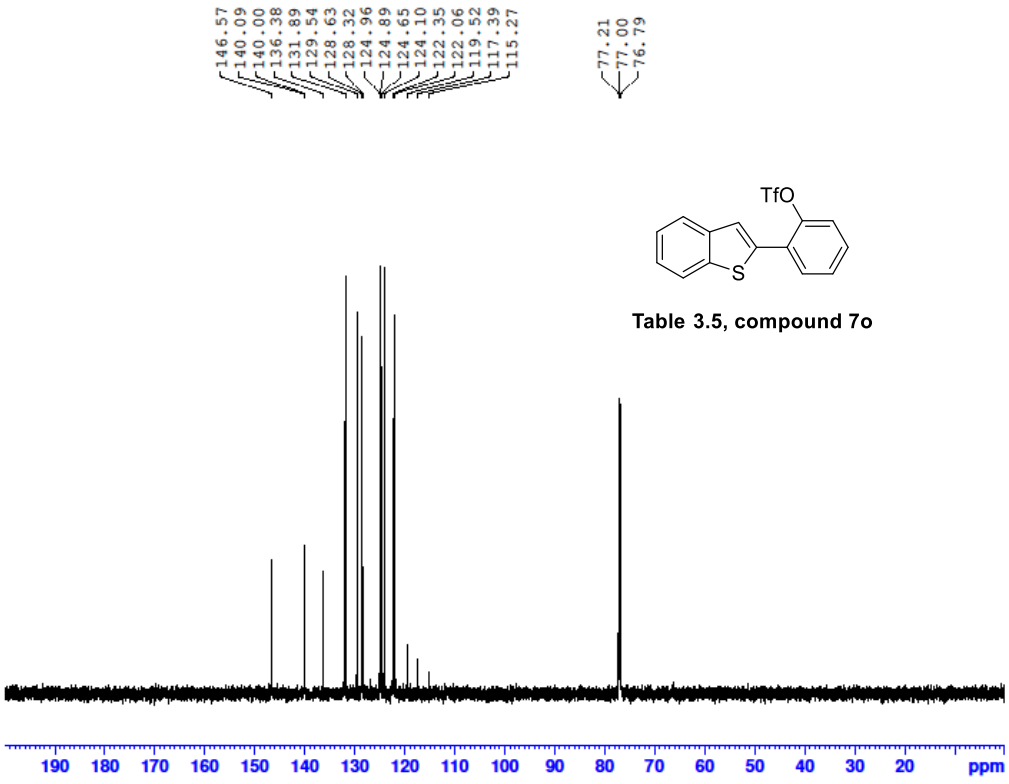

Table 3.5, compound 7o

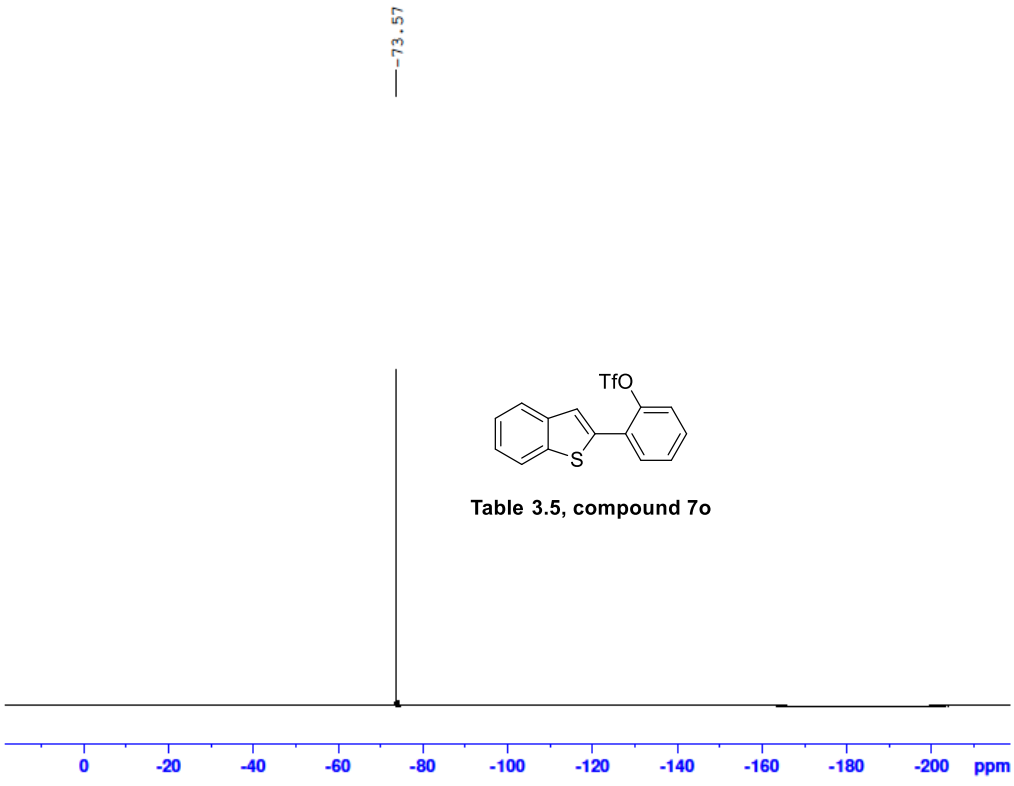

Table 3.5, compound 7o

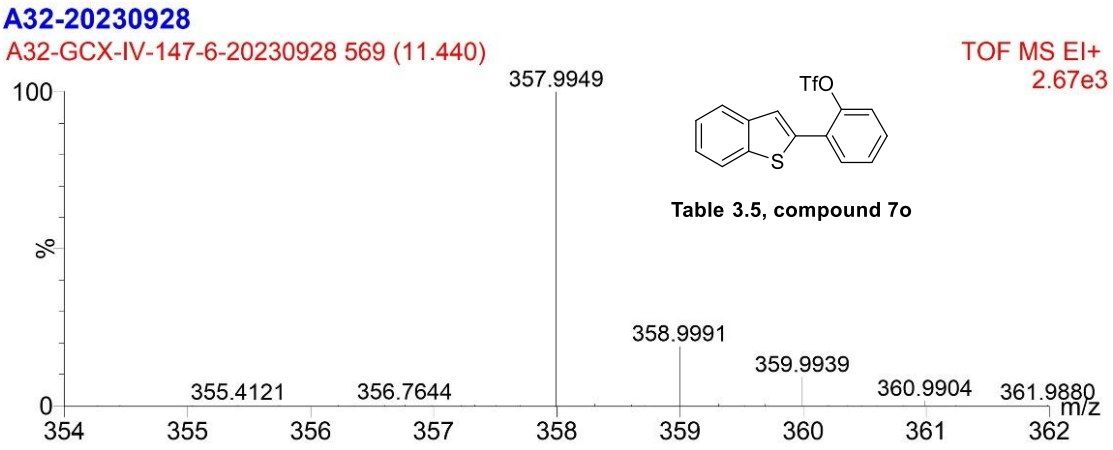

Table 3.5, compound 7o

Mass	Calc. Mass	mDa	PPM	Ion Formula
357.9949	357.9940	-2.60	-0.93	C15H9F3O3S2

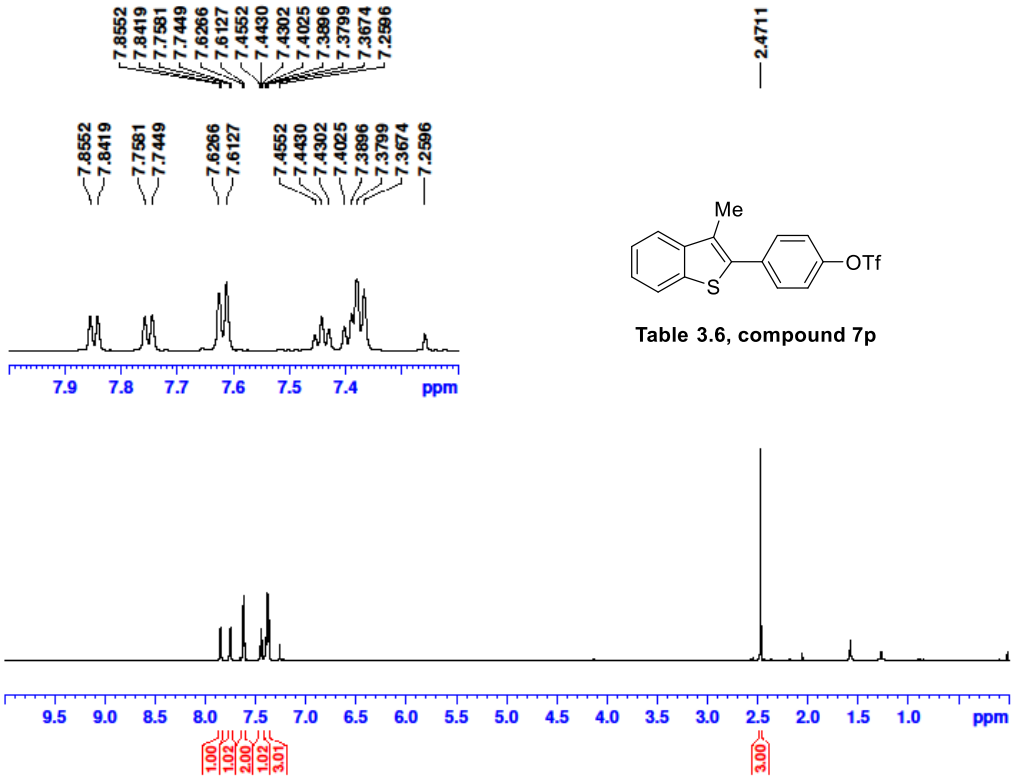

Table 3.6, compound 7p

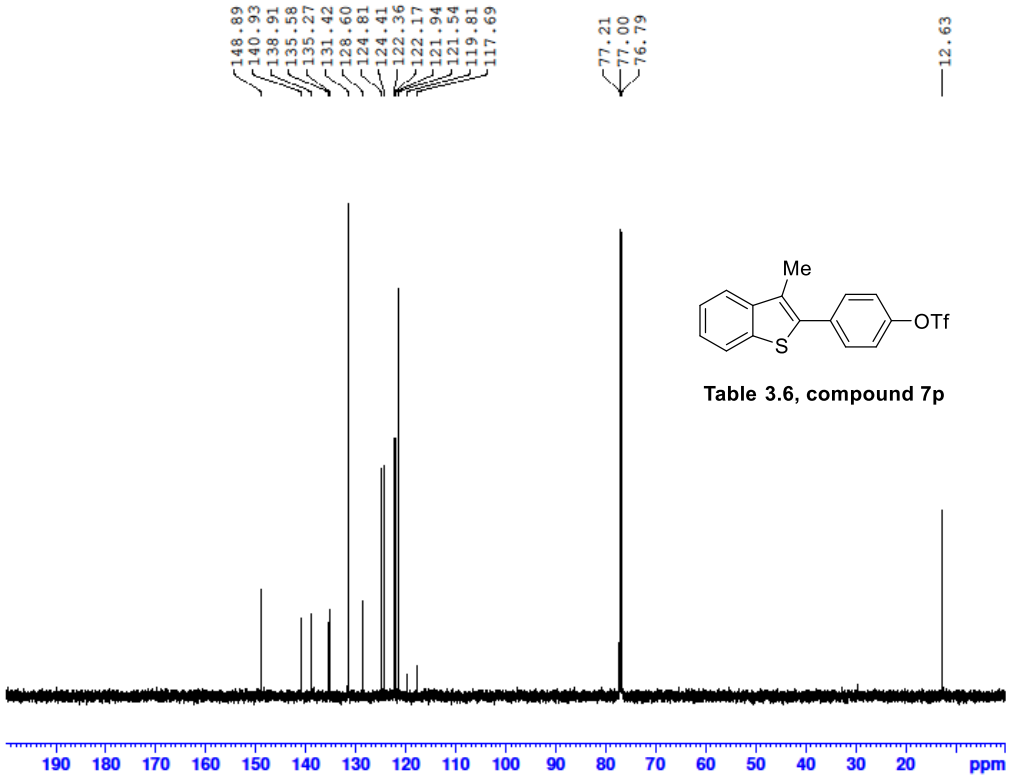

Table 3.6, compound 7p

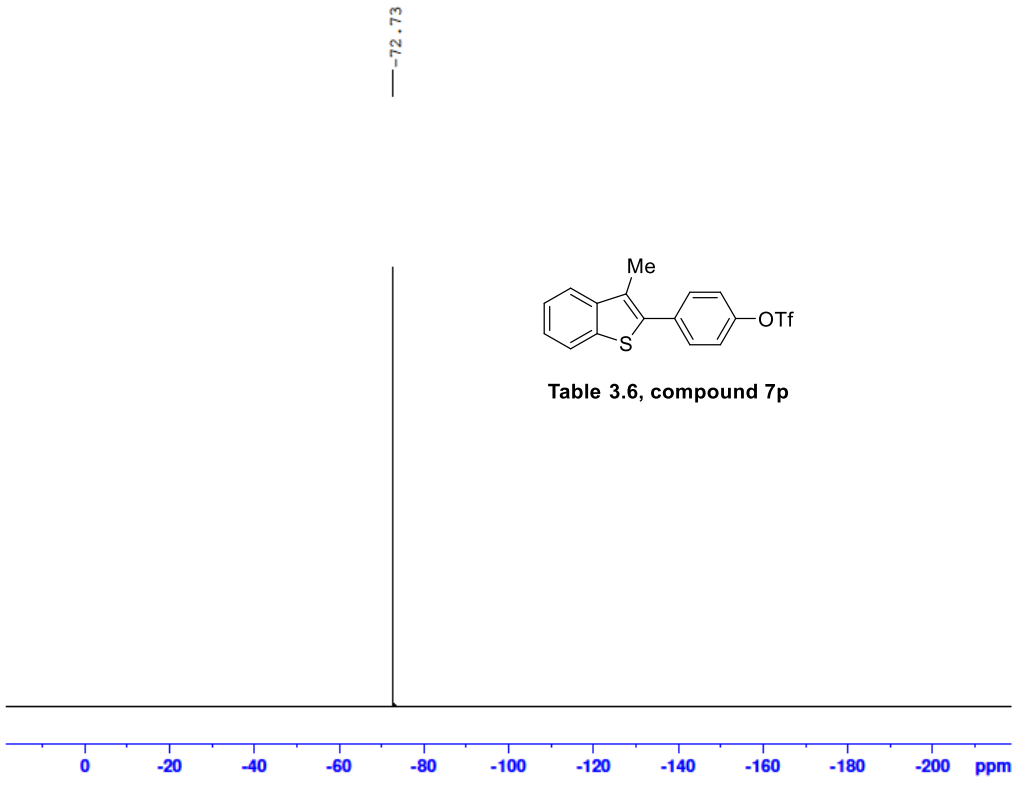

Table 3.6, compound 7p

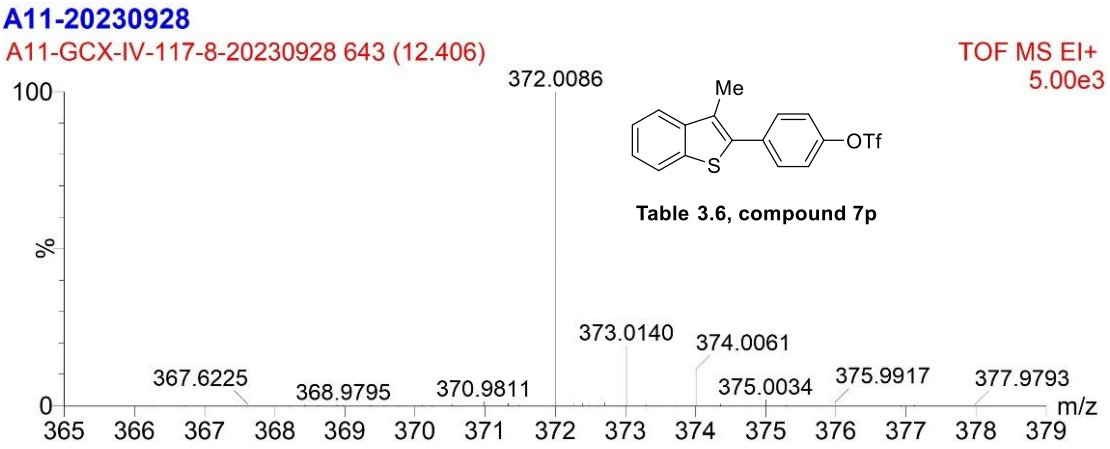

Table 3.6, compound 7p

Mass	Calc. Mass	mDa	PPM	Ion Formula
372.0086	372.0096	2.75	1.02	C16H11F3O3S2

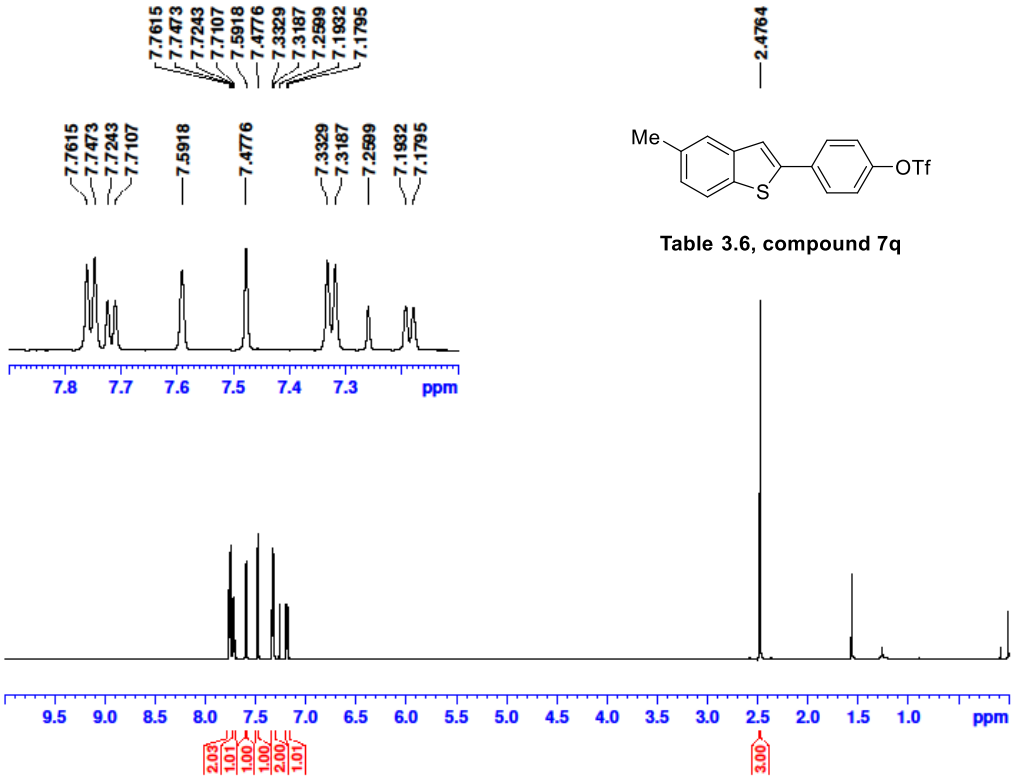

Table 3.6, compound 7q

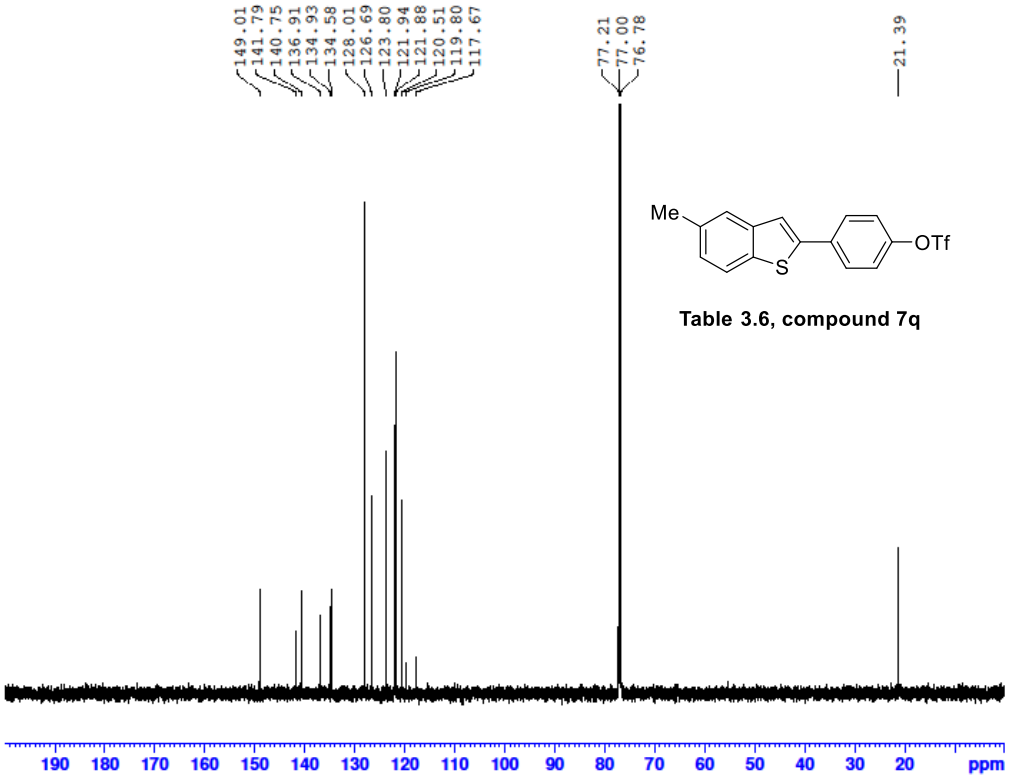

Table 3.6, compound 7q

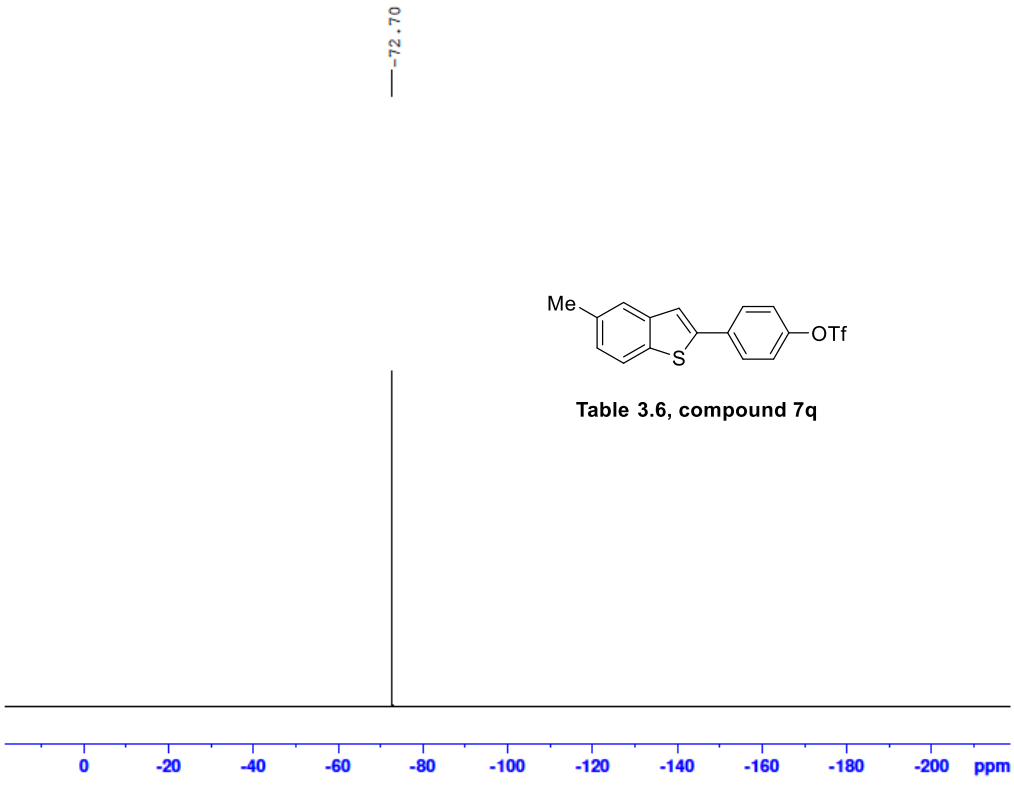

Table 3.6, compound 7q

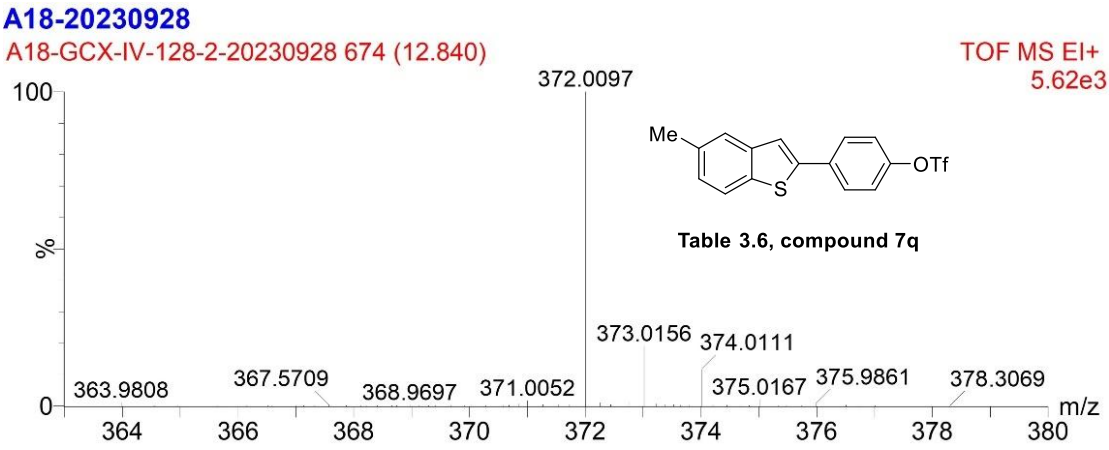

Table 3.6, compound 7q

Mass	Calc. Mass	mDa	PPM	Ion Formula
372.0097	372.0096	-0.21	-0.08	C16H11F3O3S2

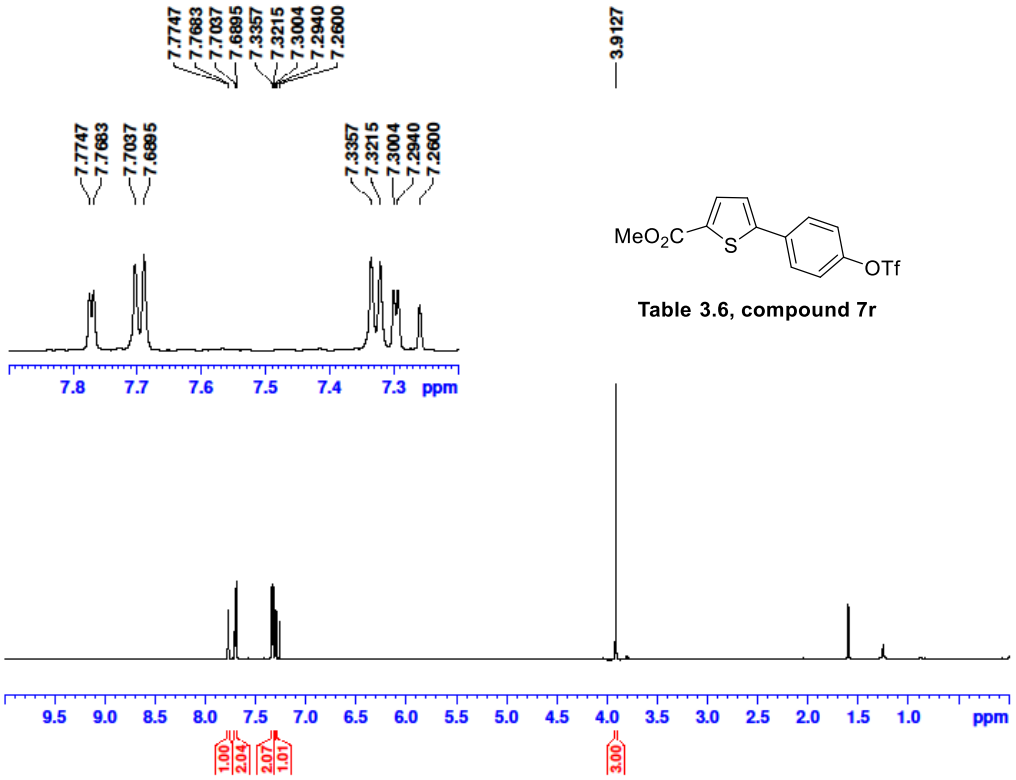

Table 3.6, compound 7r

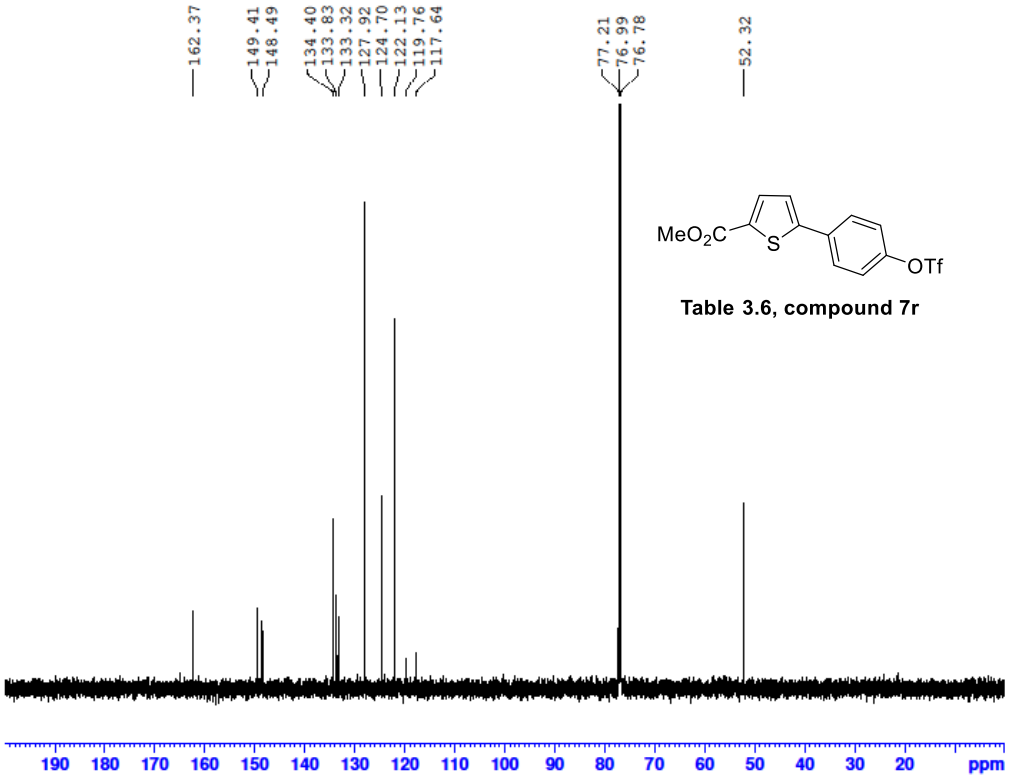

Table 3.6, compound 7r

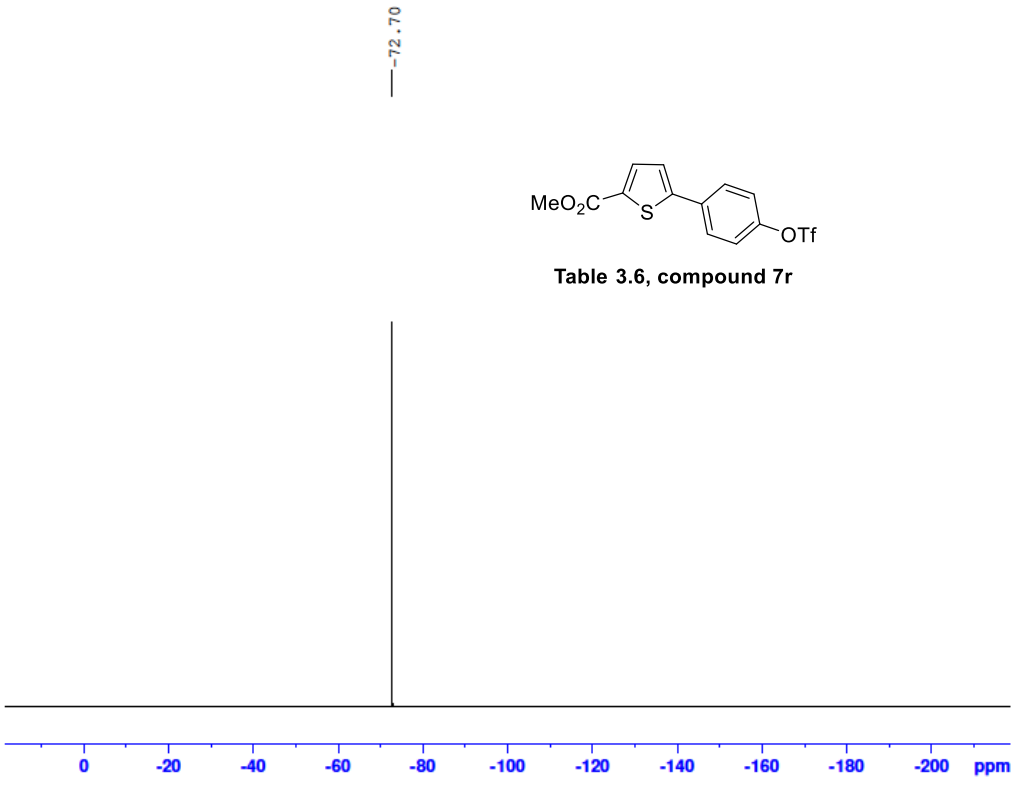

Table 3.6, compound 7r

A22-20230928-1

A22-GCX-IV-117-4-20230928-1 592 (11.726)

TOF MS EI+
709

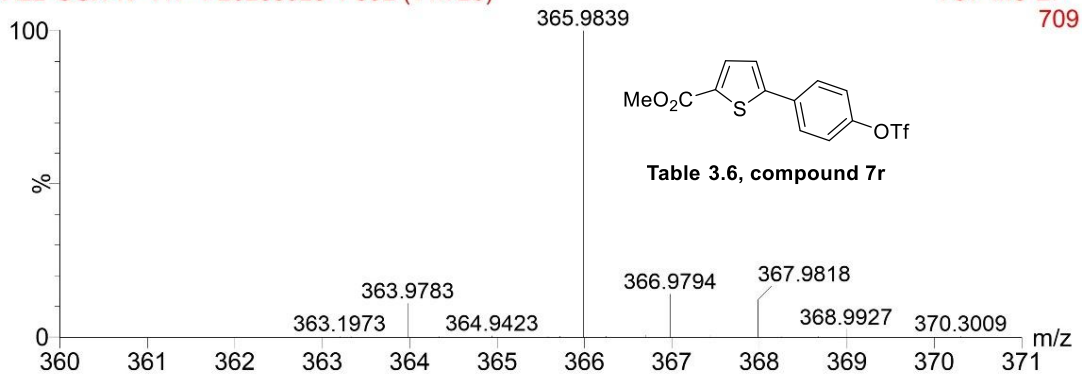

Table 3.6, compound 7r

Mass	Calc. Mass	mDa	PPM	Ion Formula
365.9839	365.9838	-0.27	-0.10	C13H9F3O5S2

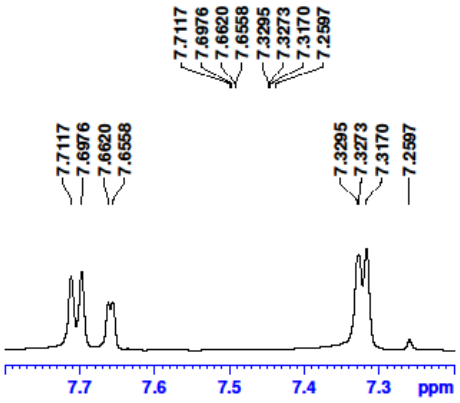

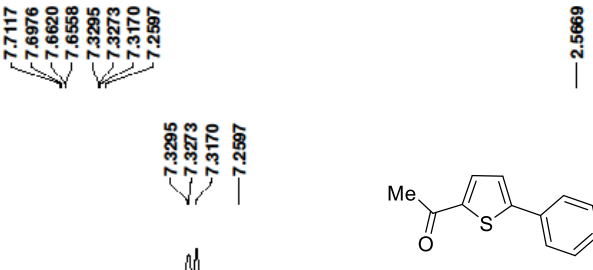

Table 3.6, compound 7s

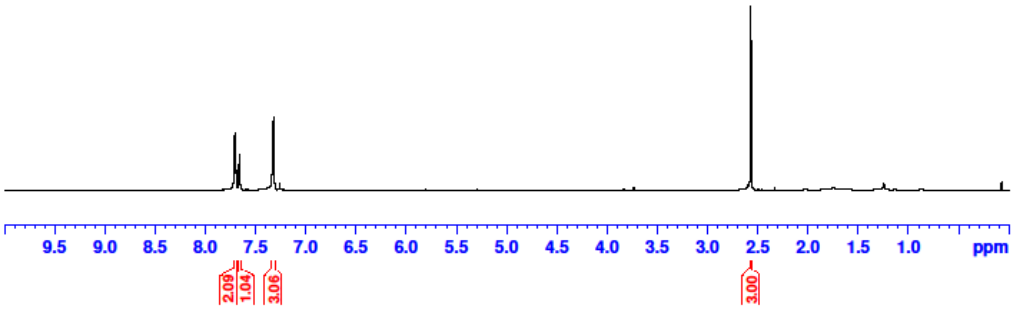

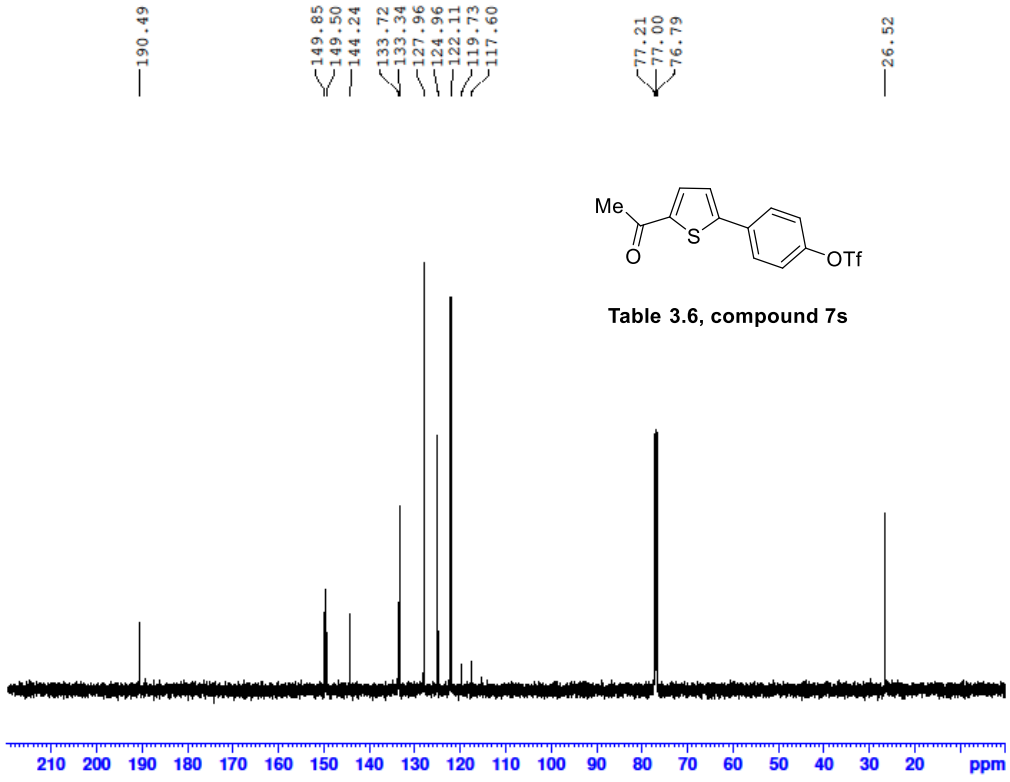

Table 3.6, compound 7s

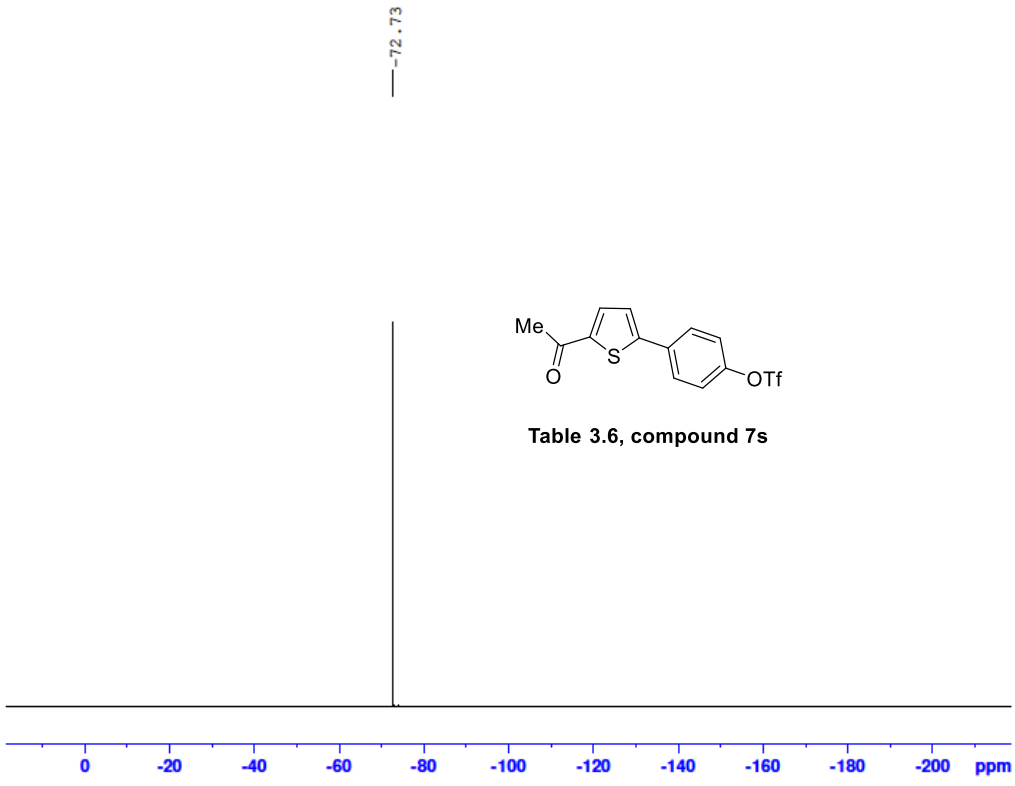

Table 3.6, compound 7s

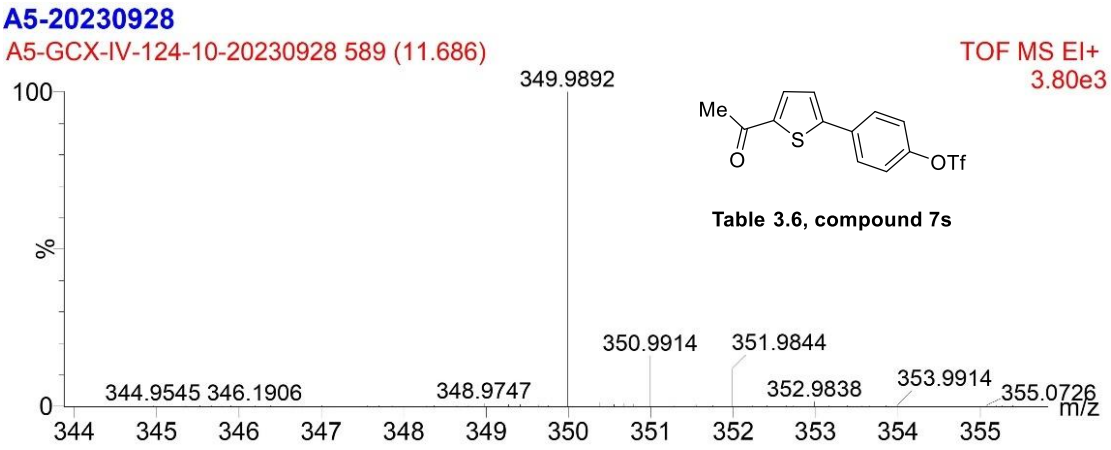

Table 3.6, compound 7s

Mass	Calc. Mass	mDa	PPM	Ion Formula
349.9892	349.9889	-0.90	-0.31	C13H9F3O4S2

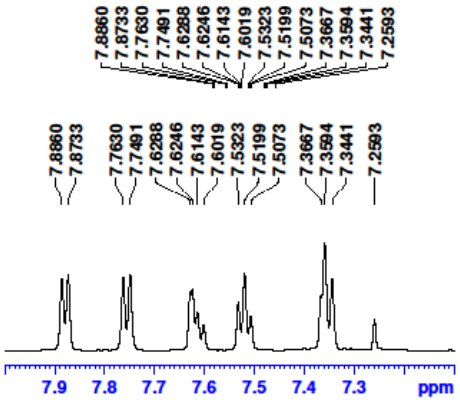

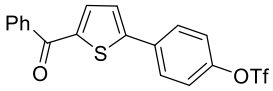

Table 3.6, compound 7t

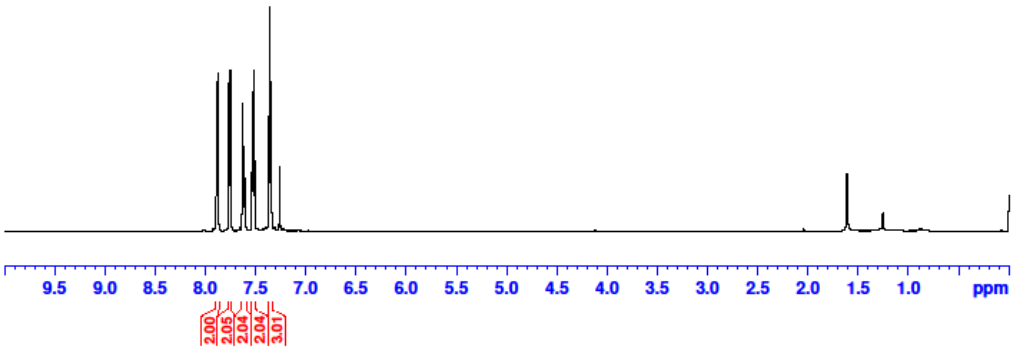

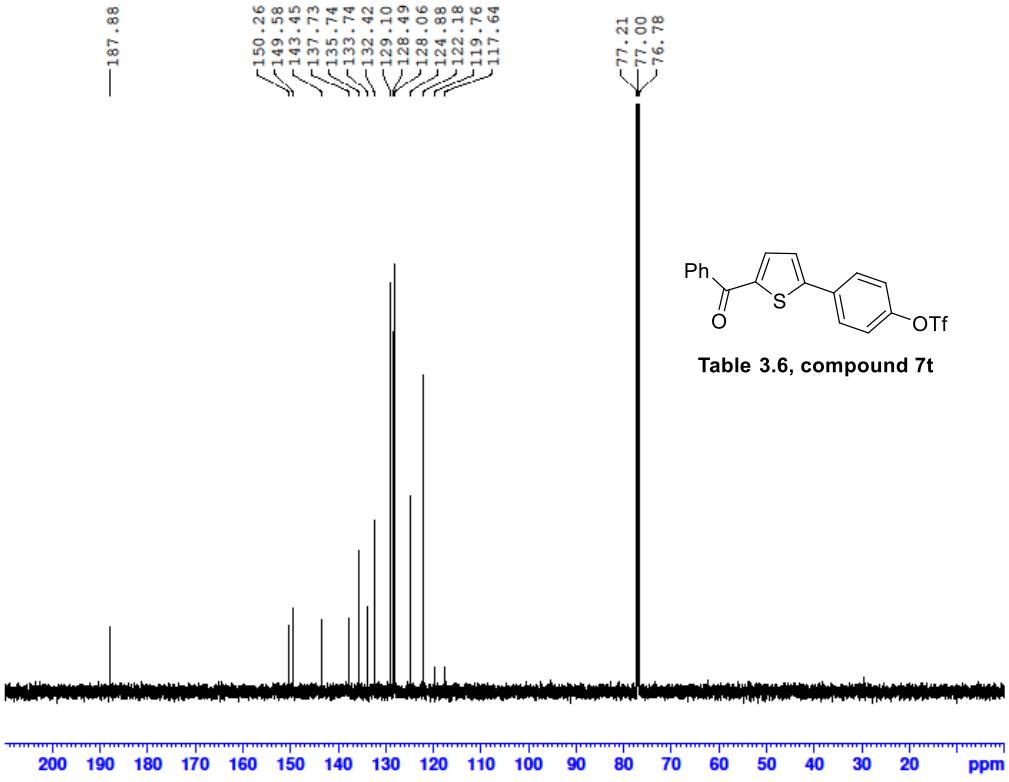

Table 3.6, compound 7t

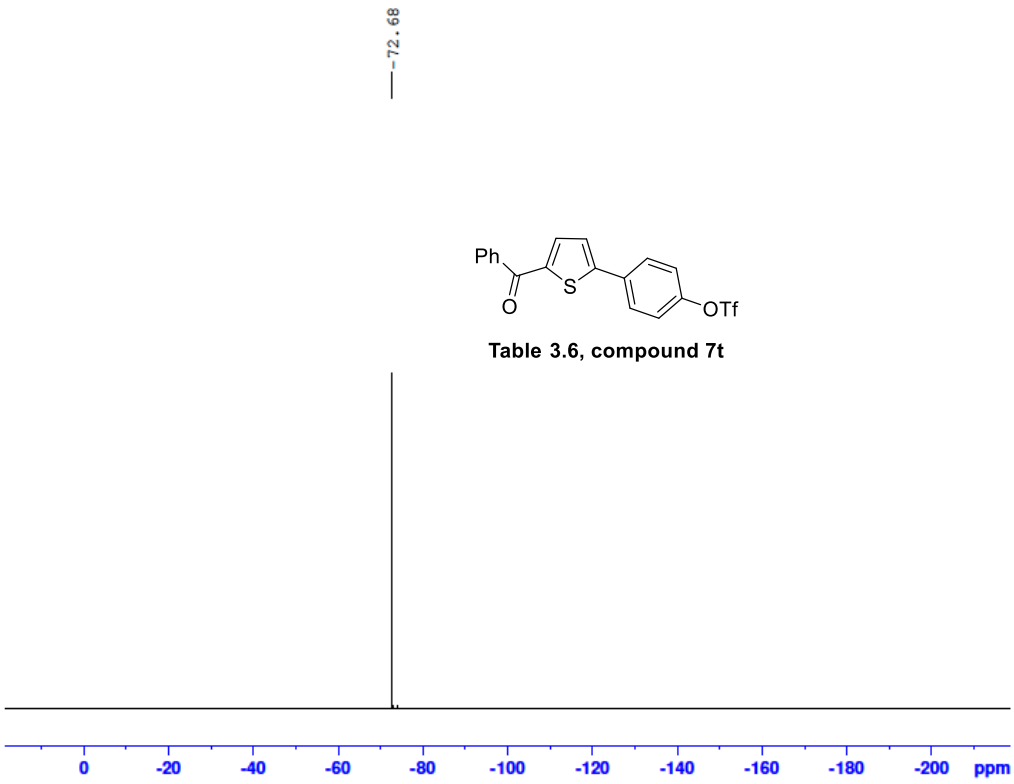

Table 3.6, compound 7t

A28-20230928-2

A28-GCX-IV-122-6-20230928-2 562 (11.333)

TOF MS EI+
5.47e3

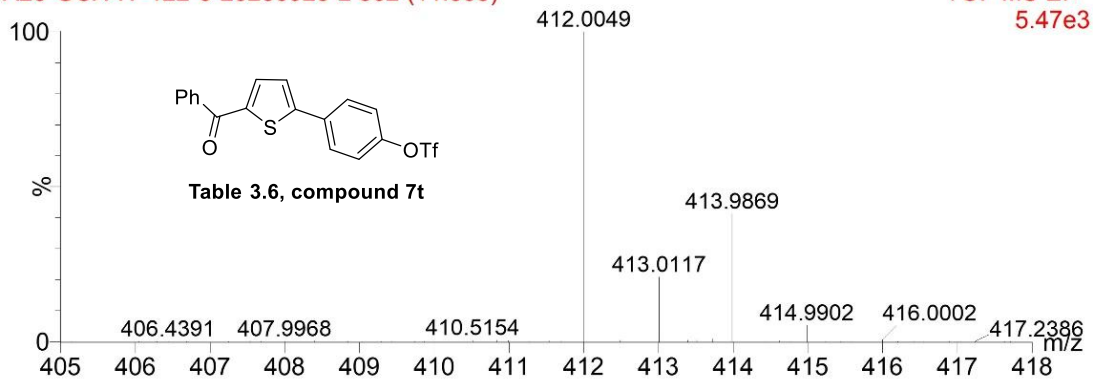

Table 3.6, compound 7t

Mass	Calc. Mass	mDa	PPM	Ion Formula
412.0049	412.0045	-0.88	-0.36	C18H11F3O4S2

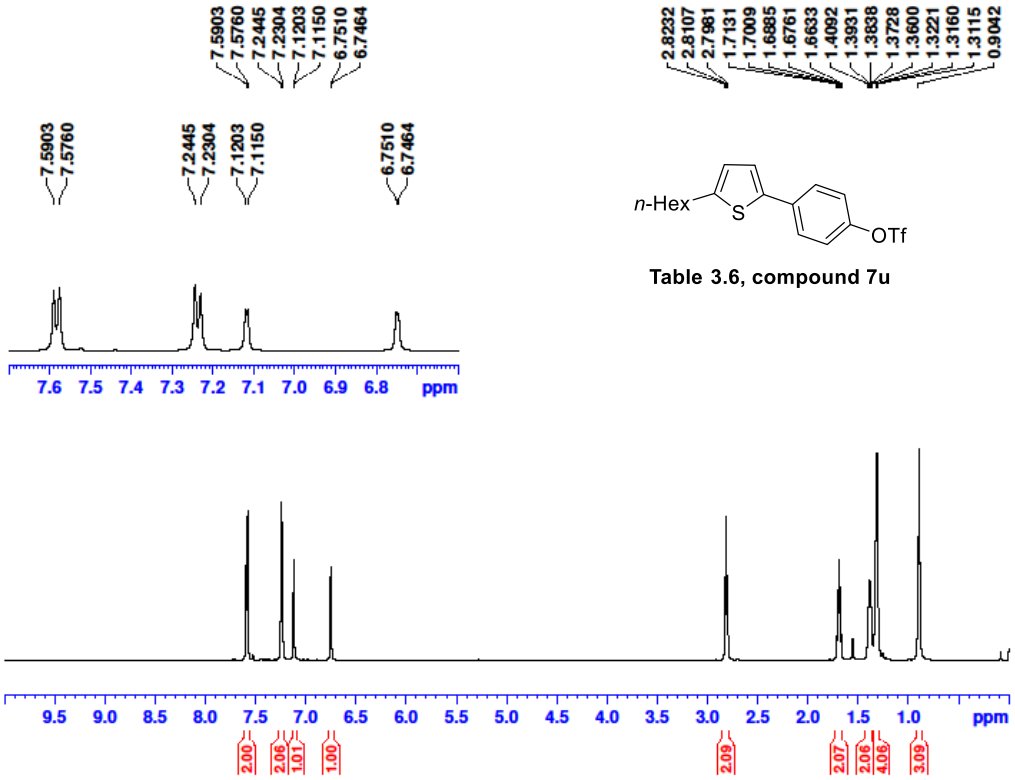

Table 3.6, compound 7u

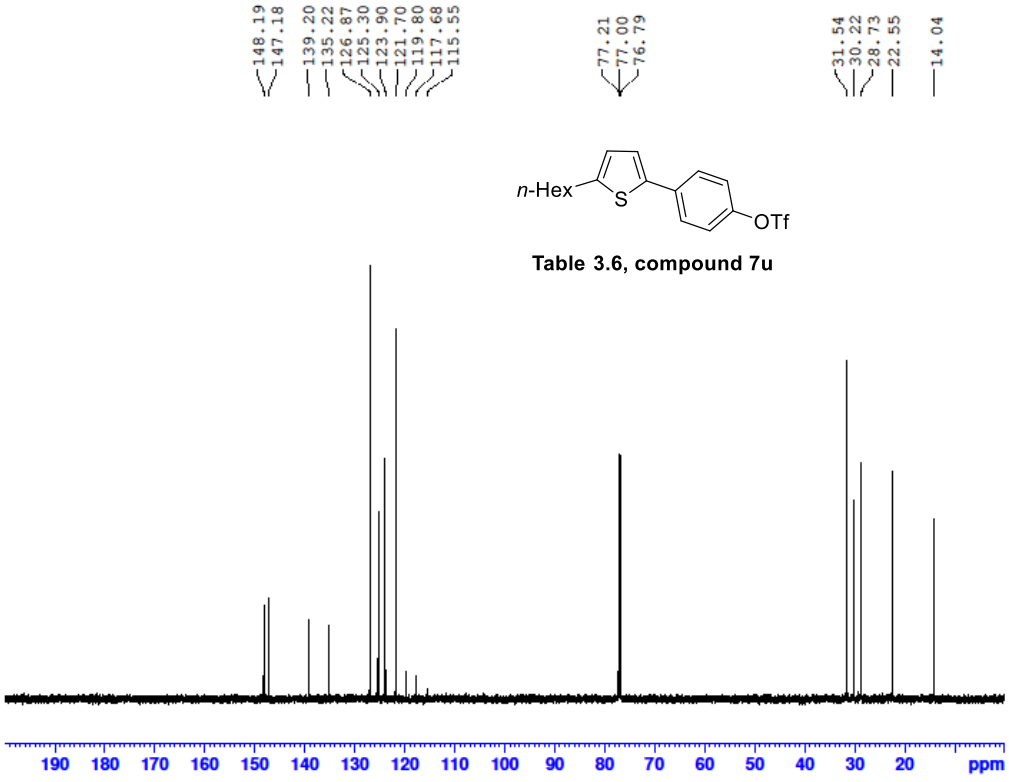

Table 3.6, compound 7u

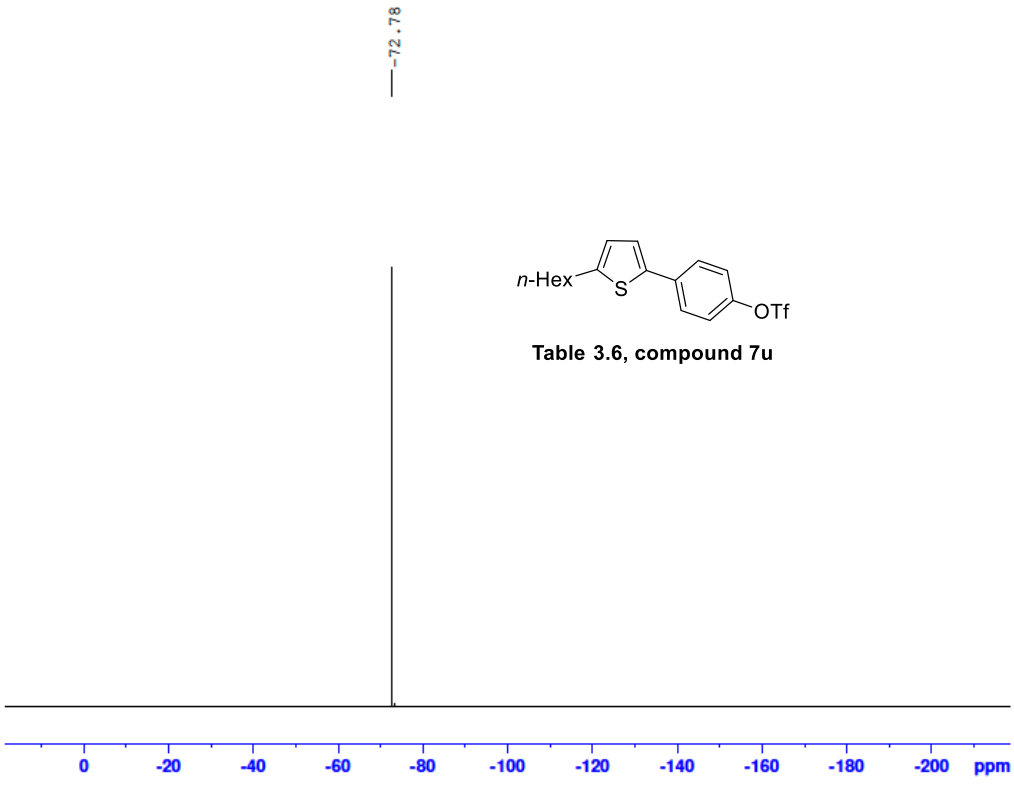

Table 3.6, compound 7u

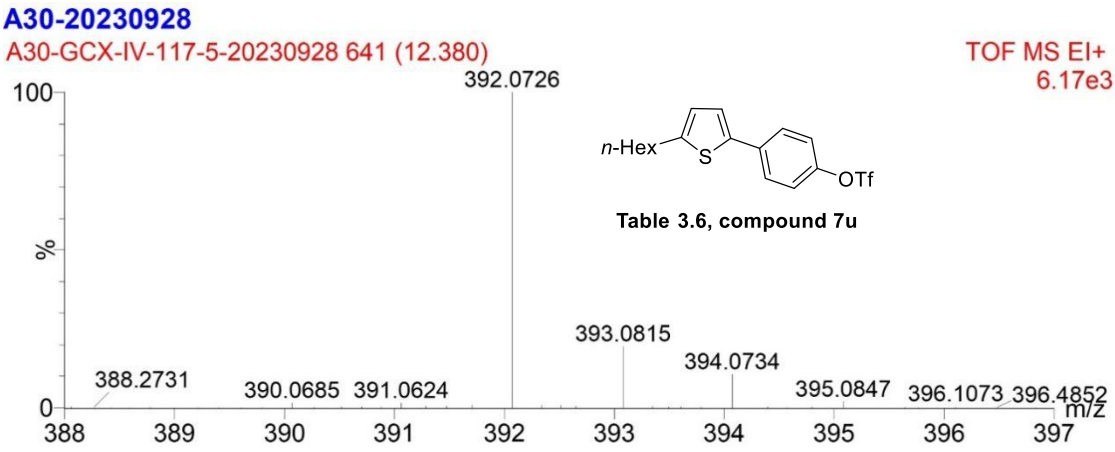

Table 3.6, compound 7u

Mass	Calc. Mass	mDa	PPM	Ion Formula
392.0726	392.0722	-0.97	-0.38	C17H19F3O3S2

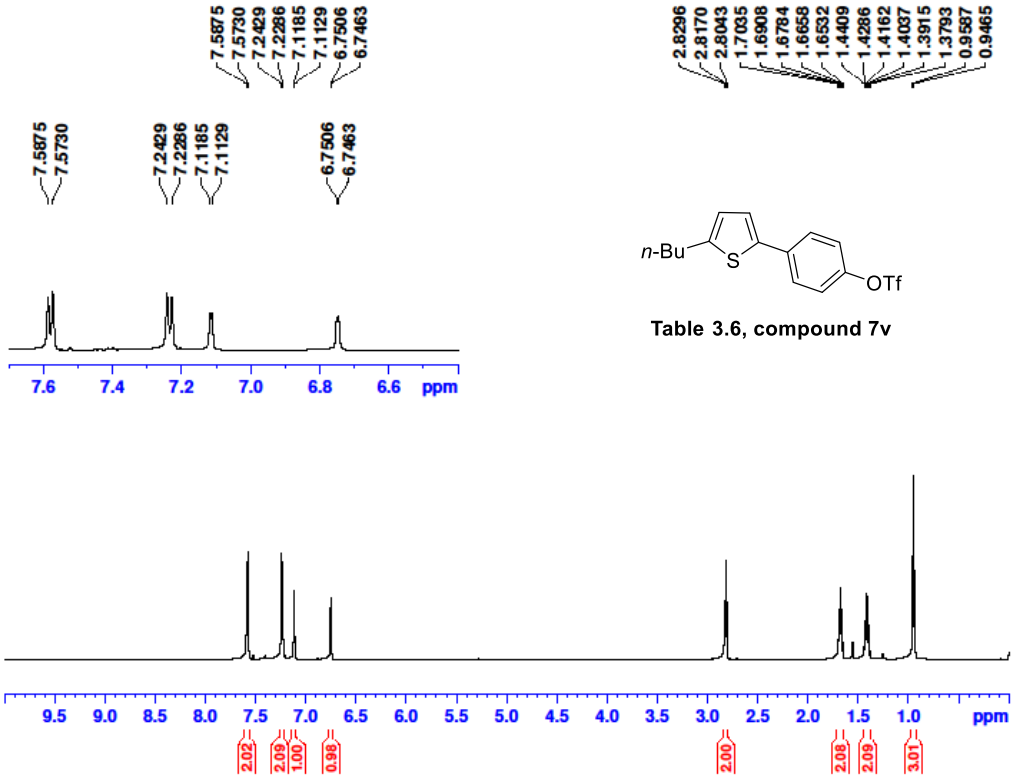

Table 3.6, compound 7v

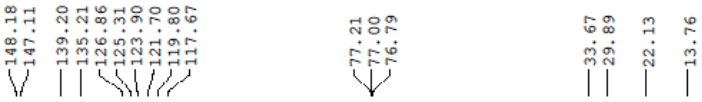

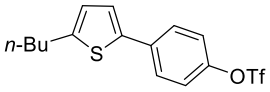

Table 3.6, compound 7v

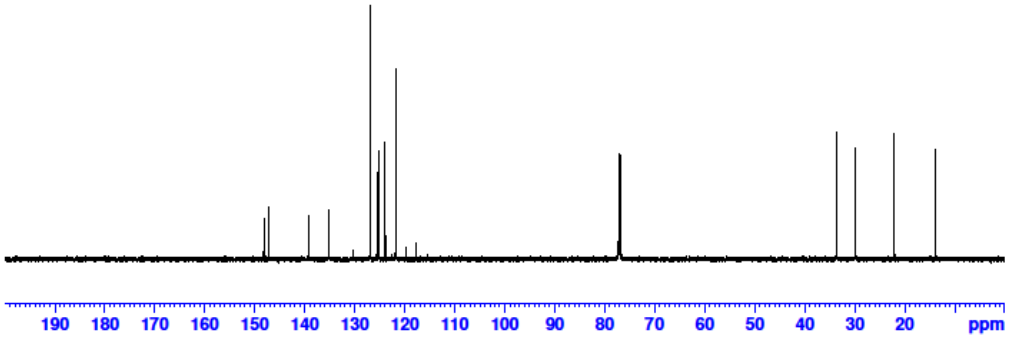

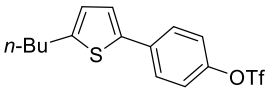

Table 3.6, compound 7v

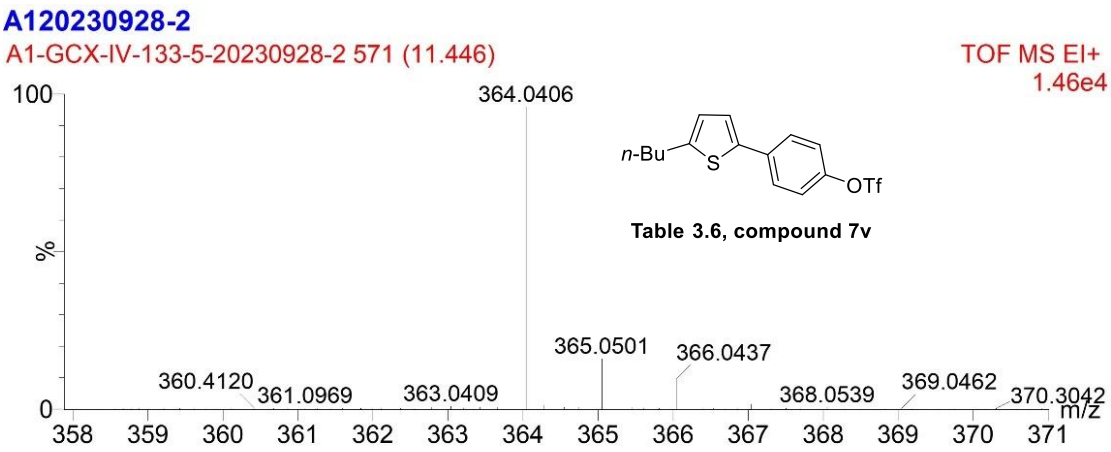

Table 3.6, compound 7v

Mass	Calc. Mass	mDa	PPM	Ion Formula
364.0409	364.0406	0.89	0.32	C15H15F3O3S2

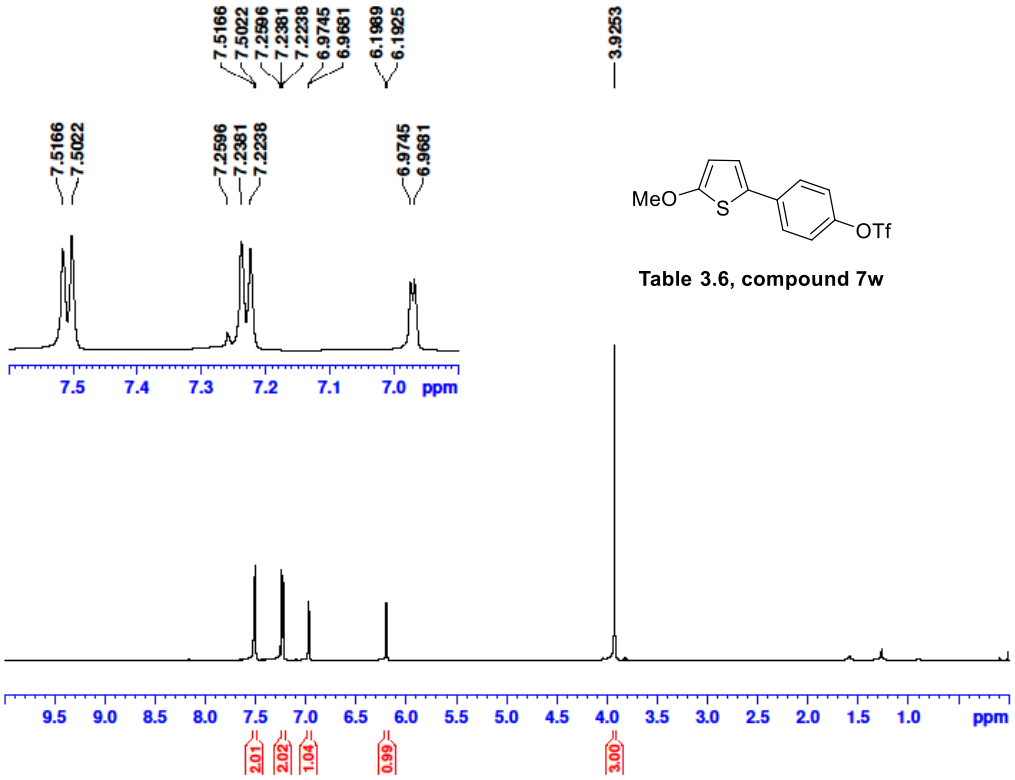

Table 3.6, compound 7w

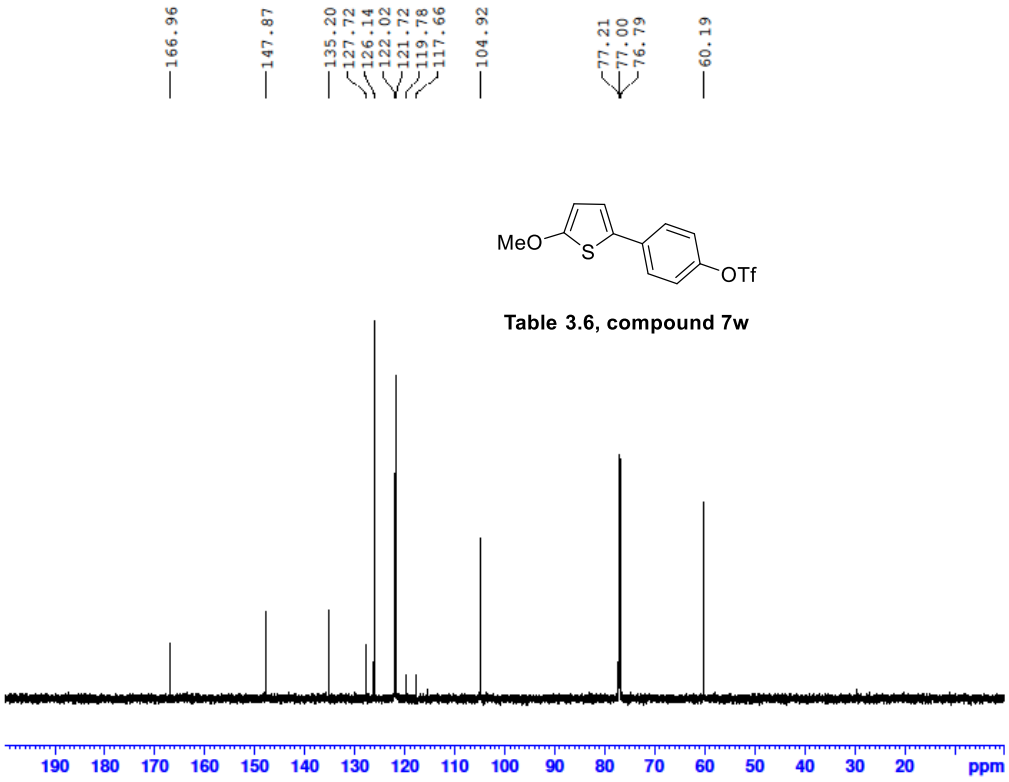

Table 3.6, compound 7w

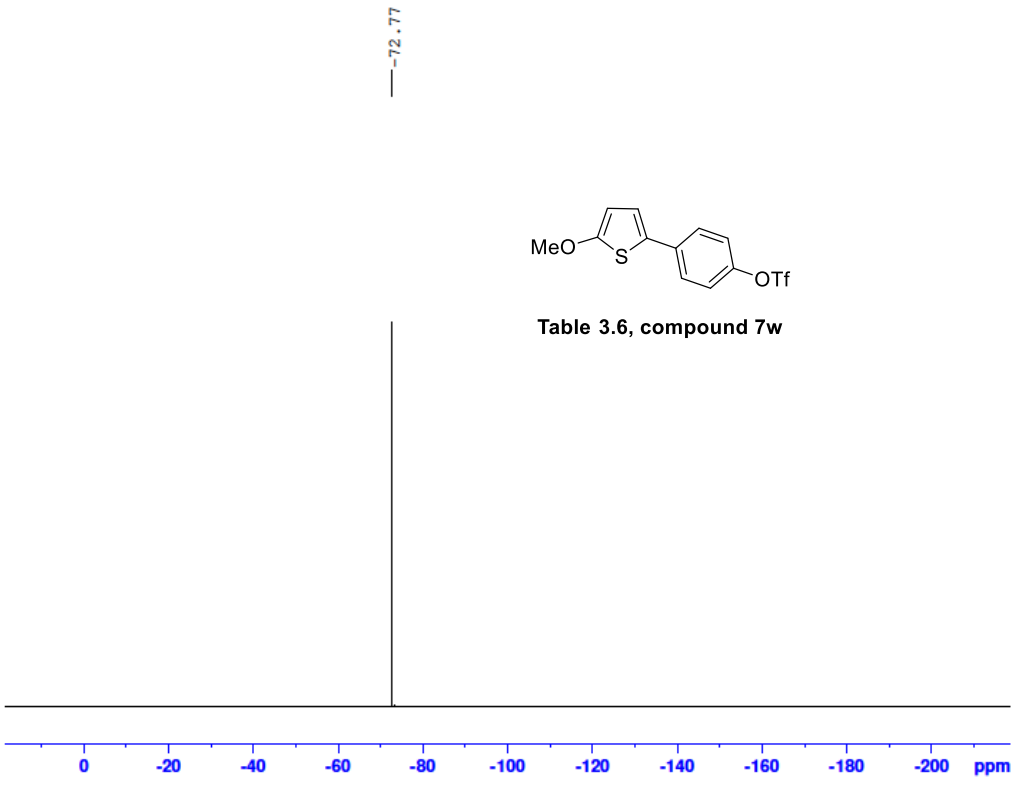

Table 3.6, compound 7w

A4-20230928

A4-GCX-IV-122-1-20230928 520 (10.766)

TOF MS EI+
1.00e3

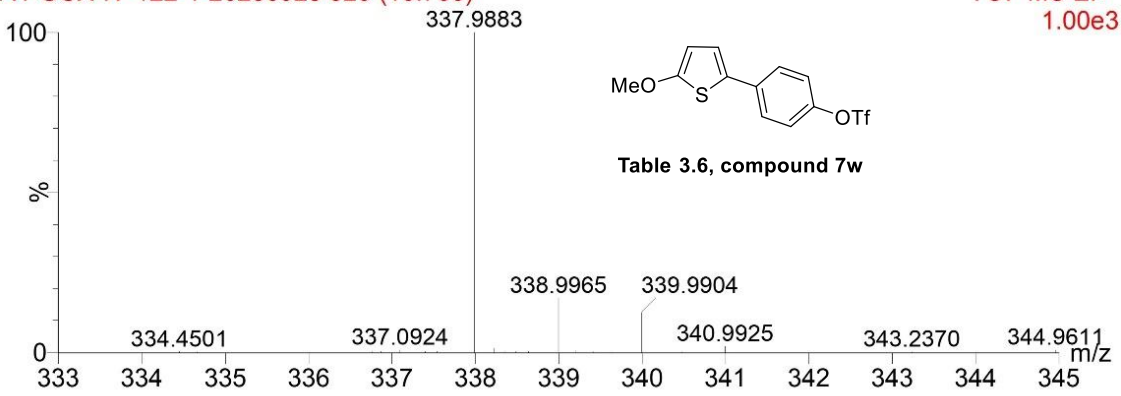

Table 3.6, compound 7w

Mass	Calc. Mass	mDa	PPM	Ion Formula
337.9883	337.9889	1.74	0.59	C12H9F3O4S2

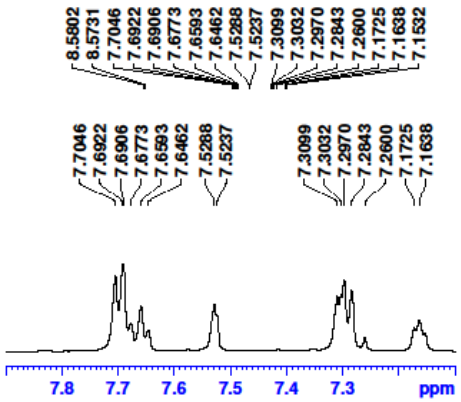

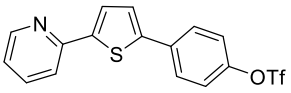

Table 3.6, compound 7x

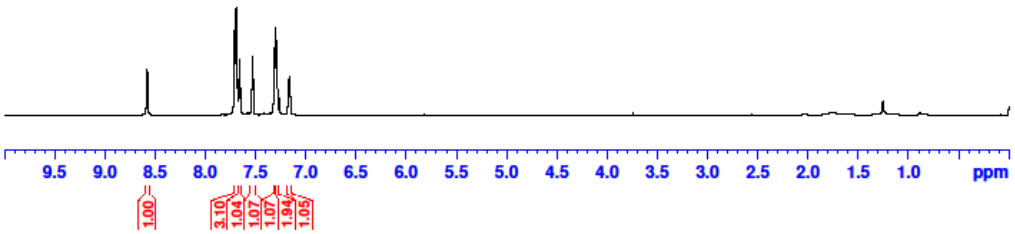

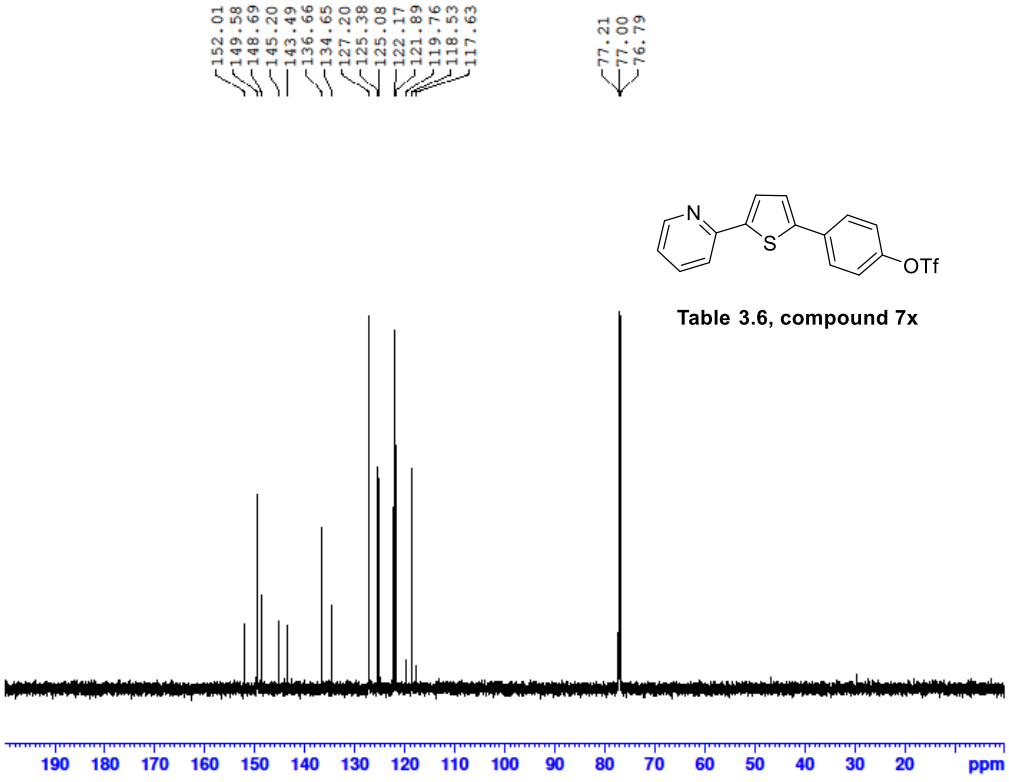

Table 3.6, compound 7x

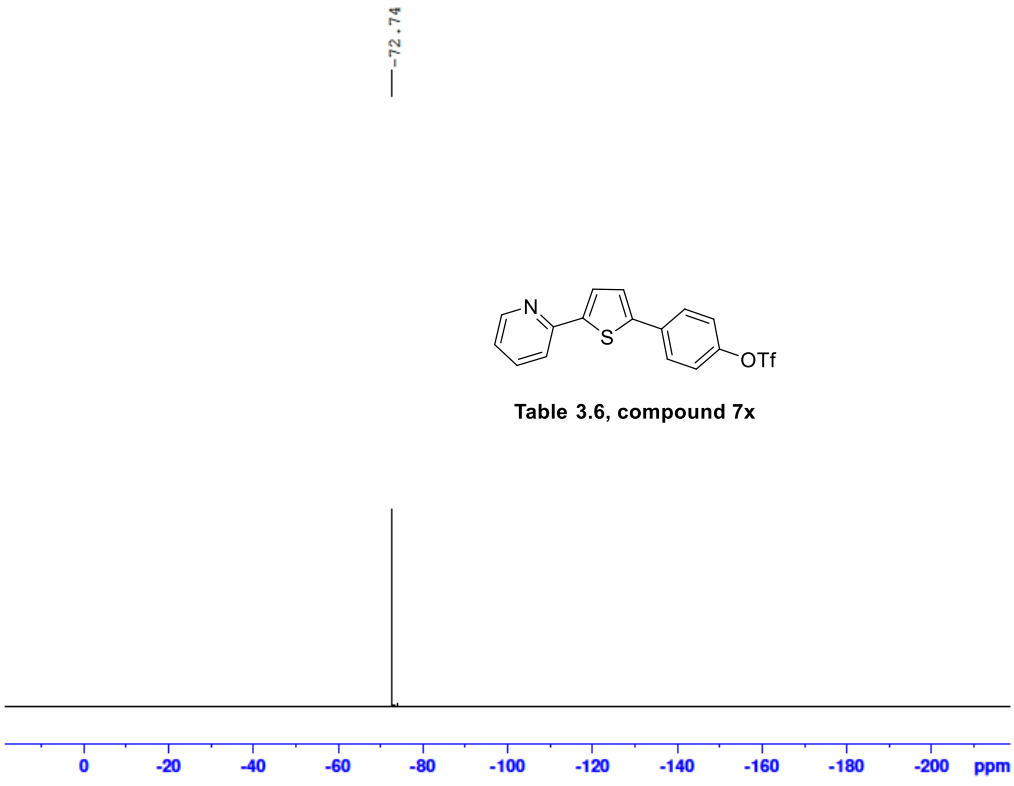

Table 3.6, compound 7x

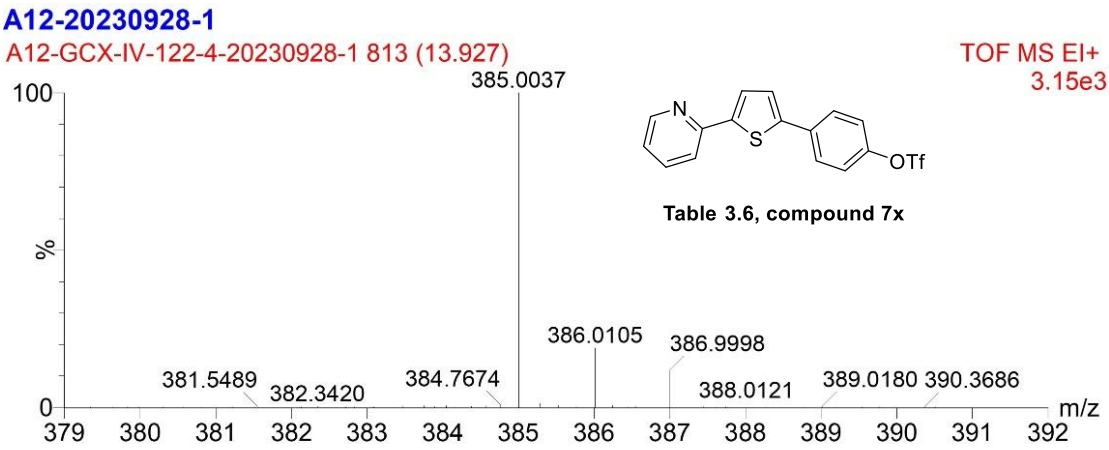

Table 3.6, compound 7x

Mass	Calc. Mass	mDa	PPM	Ion Formula
385.0037	385.0049	3.05	1.17	C16H10F3NO3S2

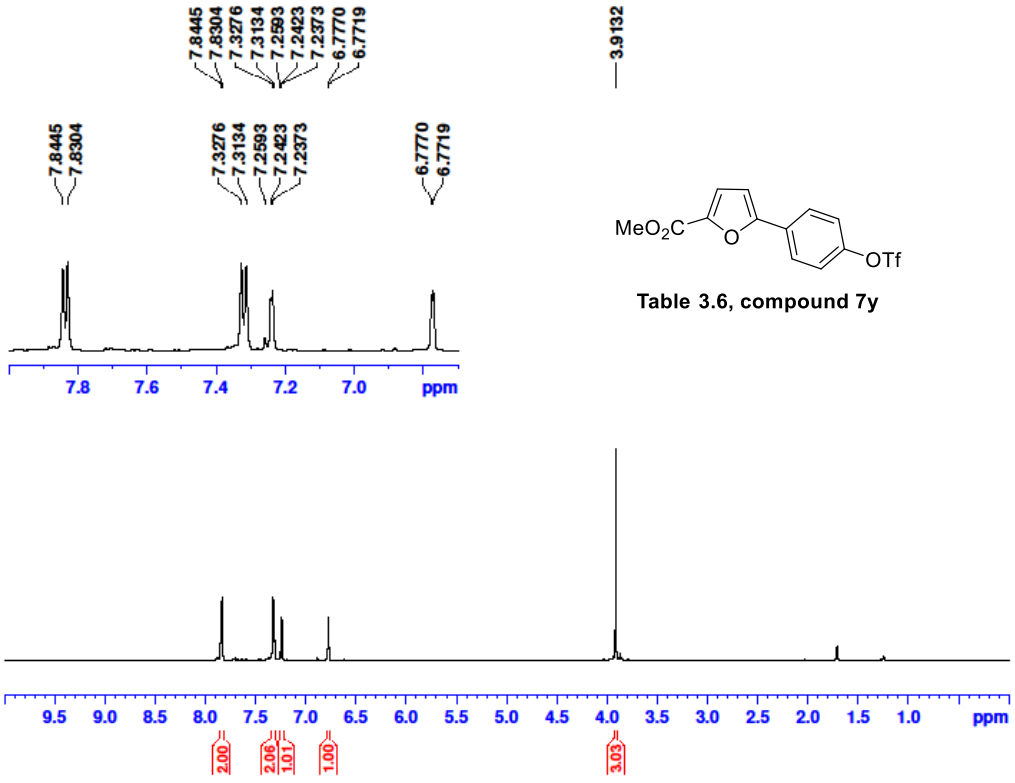

Table 3.6, compound 7y

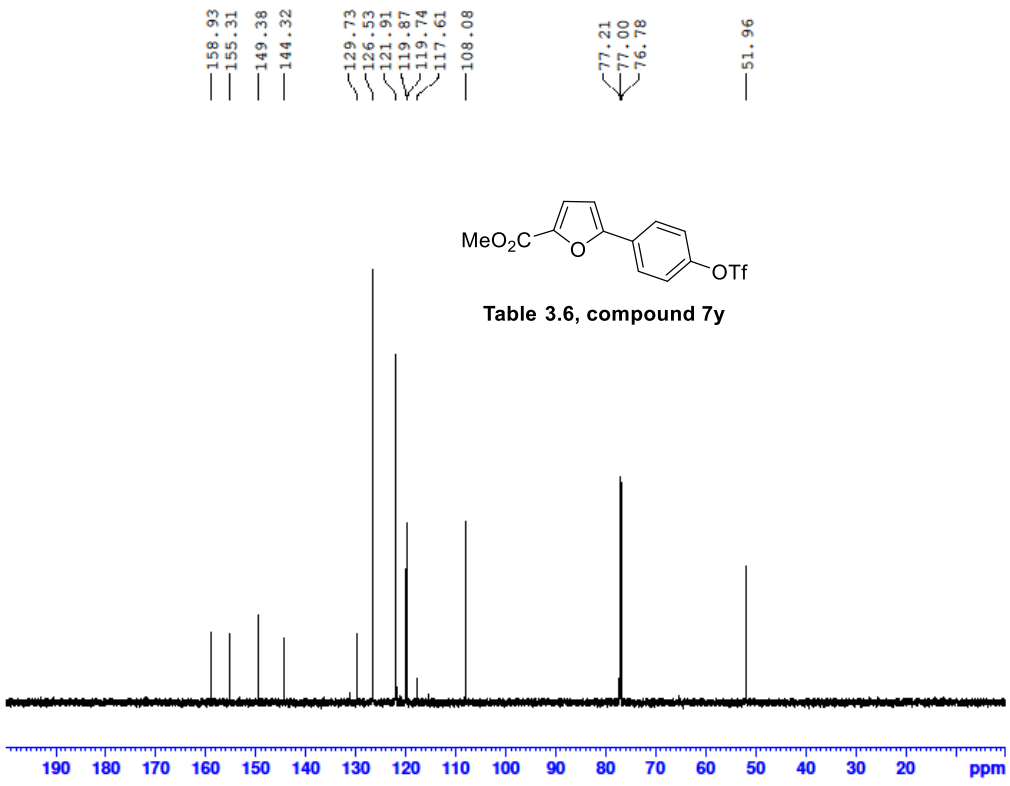

Table 3.6, compound 7y

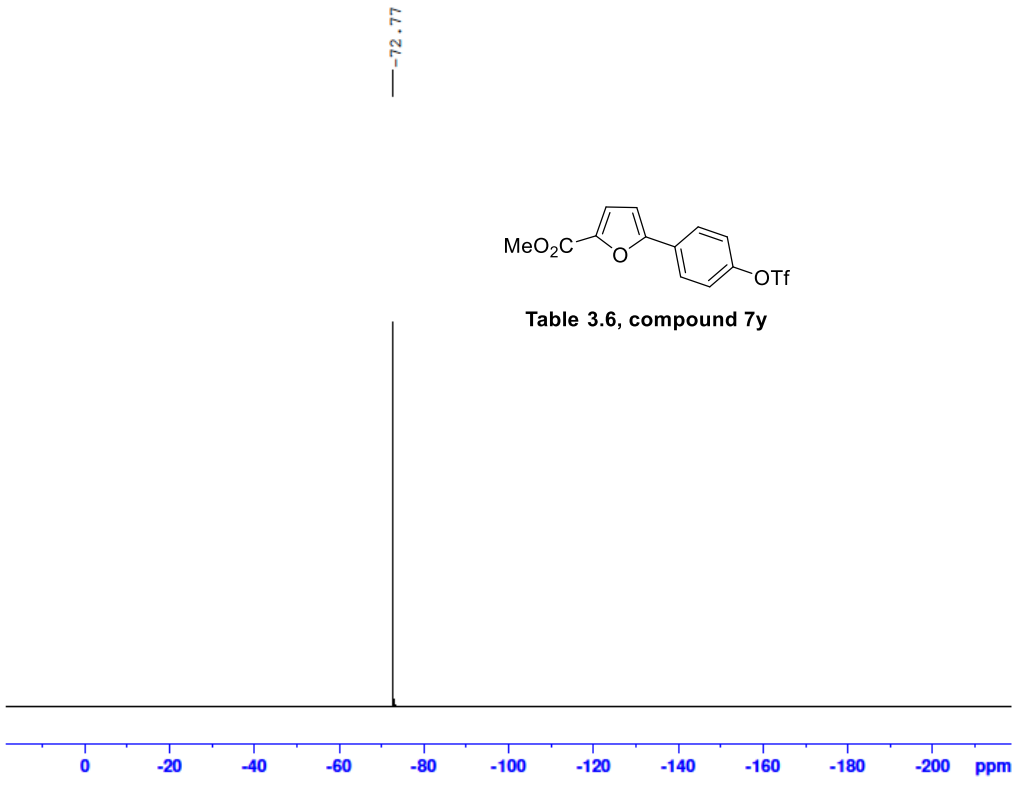

Table 3.6, compound 7y

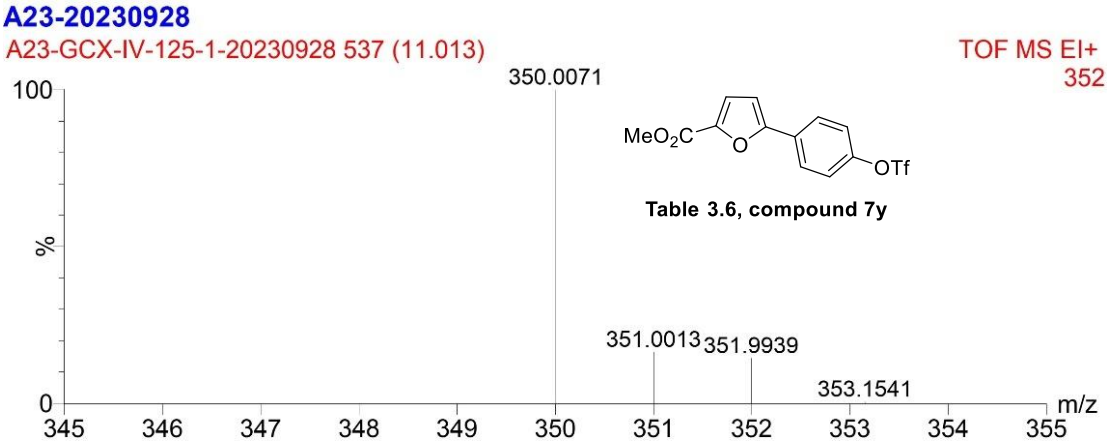

Table 3.6, compound 7y

Mass	Calc. Mass	mDa	PPM	Ion Formula
350.0071	350.0066	-1.30	-0.46	C13H9F3O6S

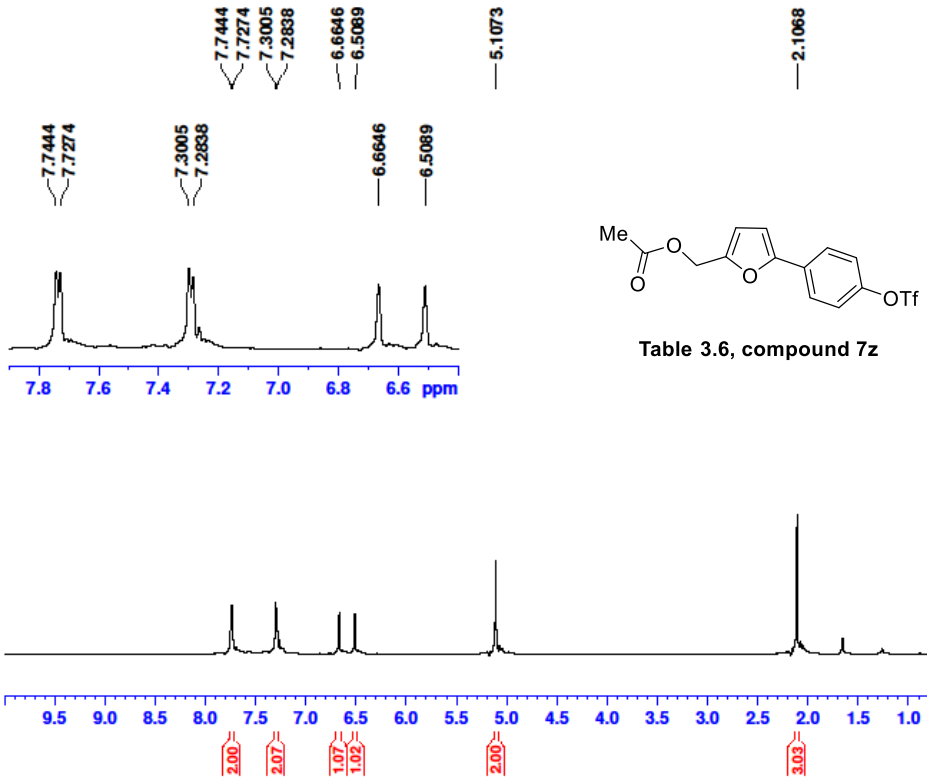

Table 3.6, compound 7z

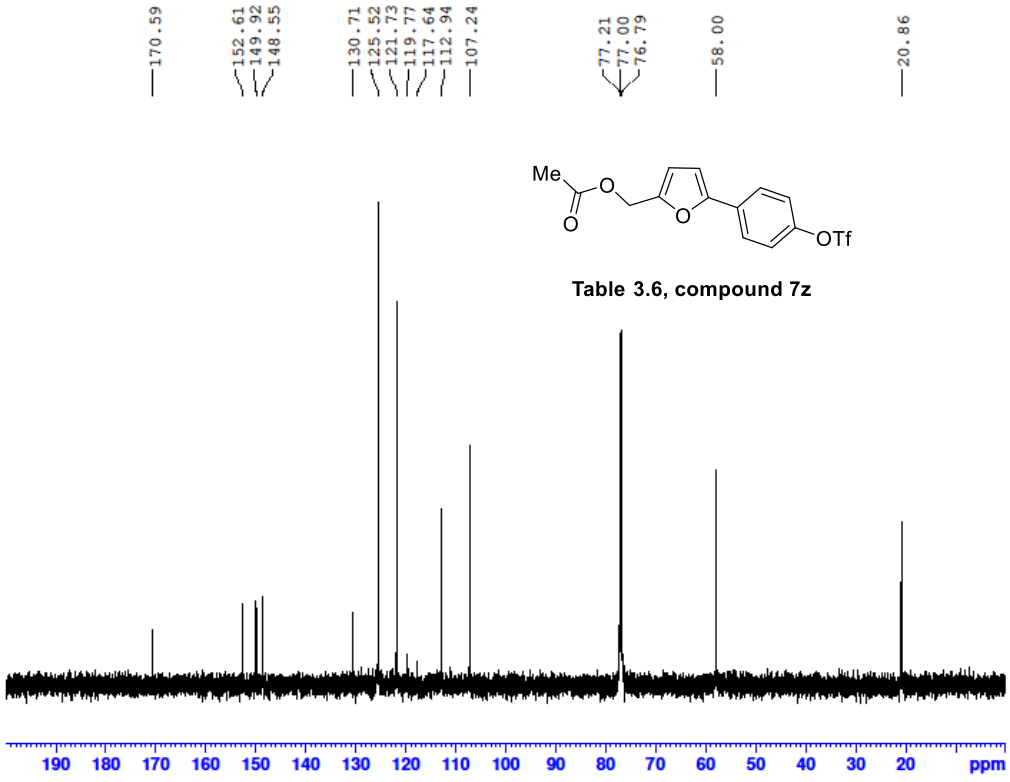

Table 3.6, compound 7z

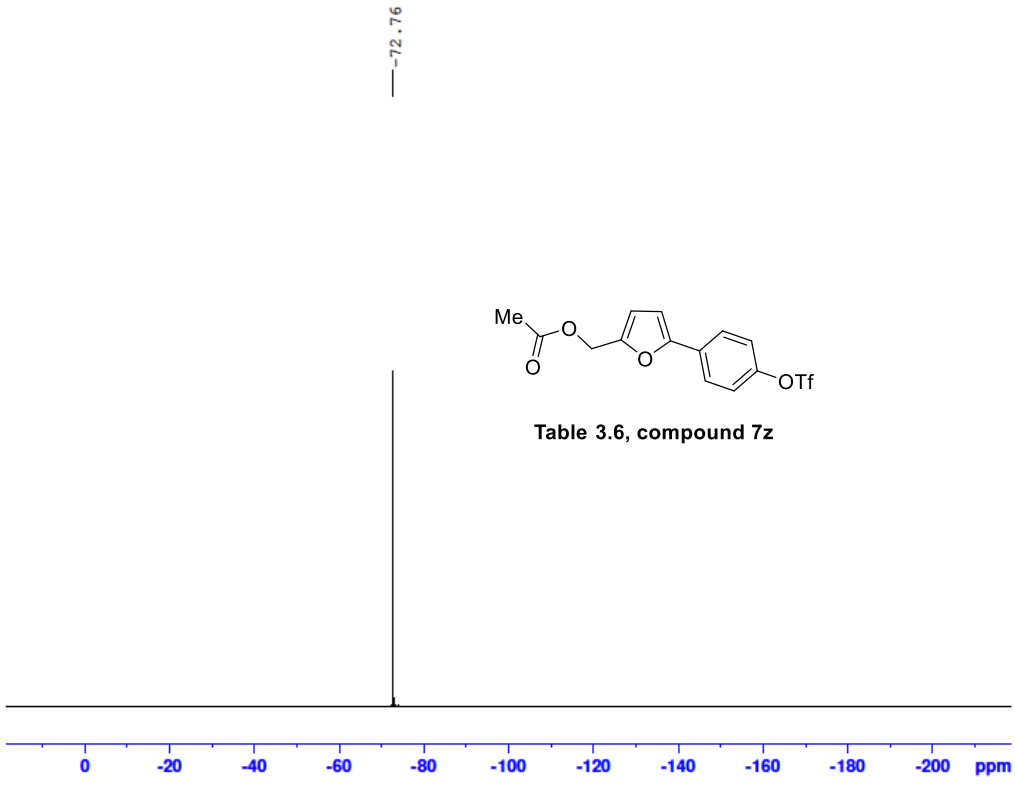

Table 3.6, compound 7z

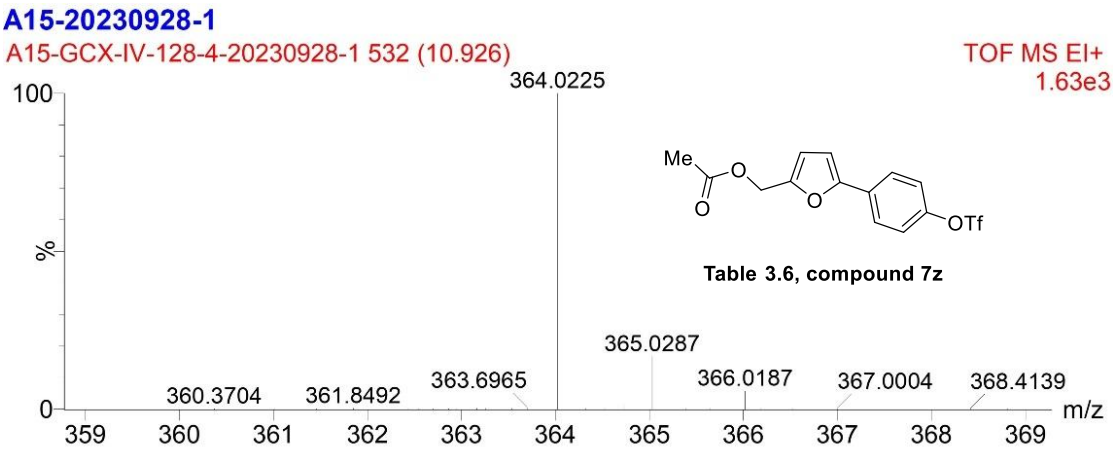

Table 3.6, compound 7z

Mass	Calc. Mass	mDa	PPM	Ion Formula
364.0225	364.0223	-0.57	-0.21	C14H11F3O6S

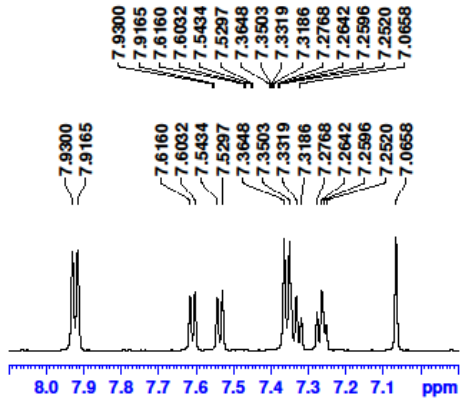

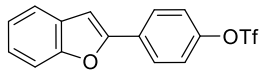

Table 3.6, compound 7aa

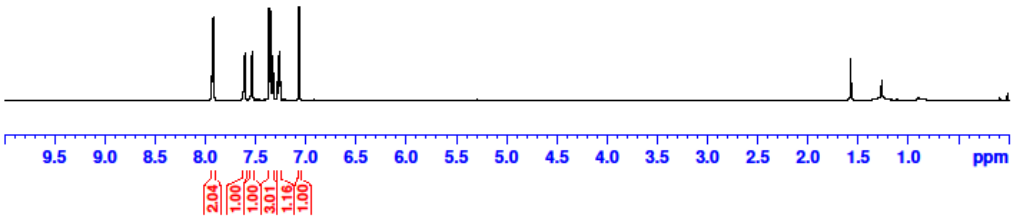

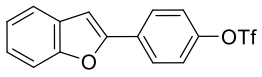

Table 3.6, compound 7aa

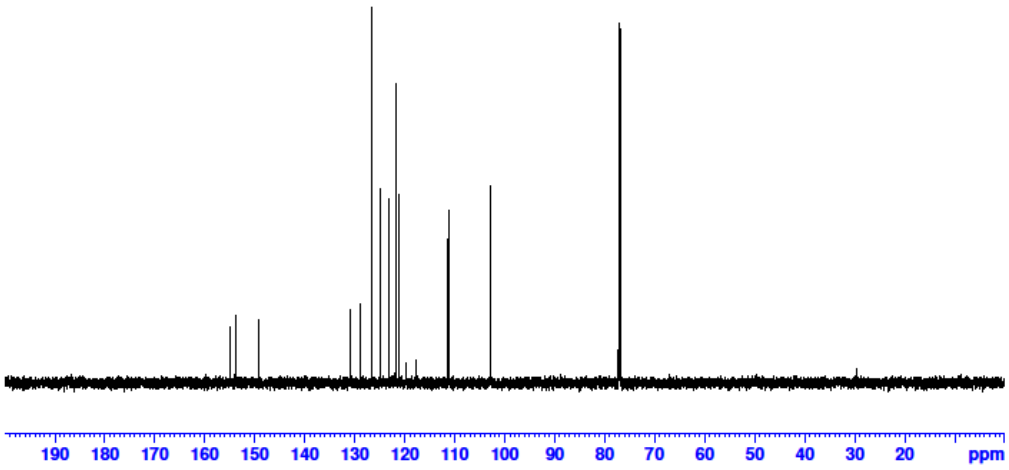

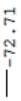

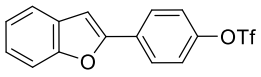

Table 3.6, compound 7aa

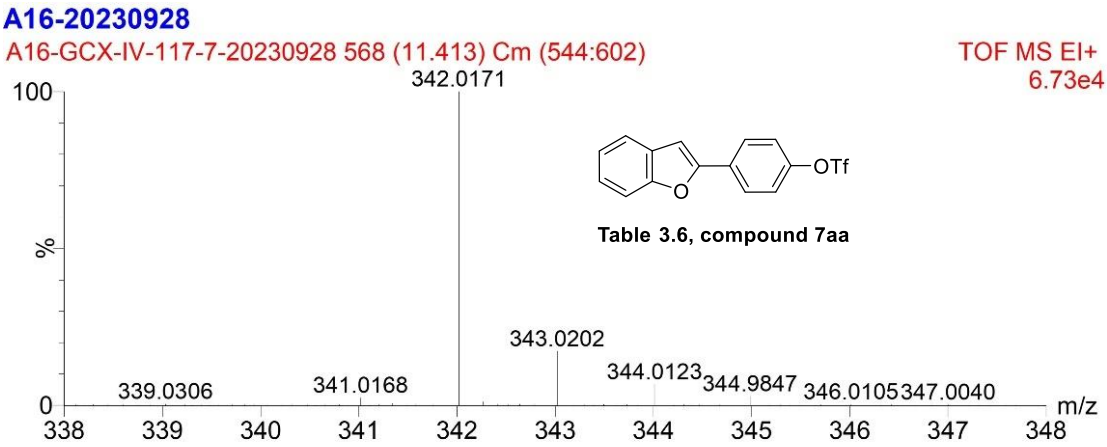

Table 3.6, compound 7aa

Mass	Calc. Mass	mDa	PPM	Ion Formula
342.0171	342.0168	-0.83	-0.28	C15H9F3O4S

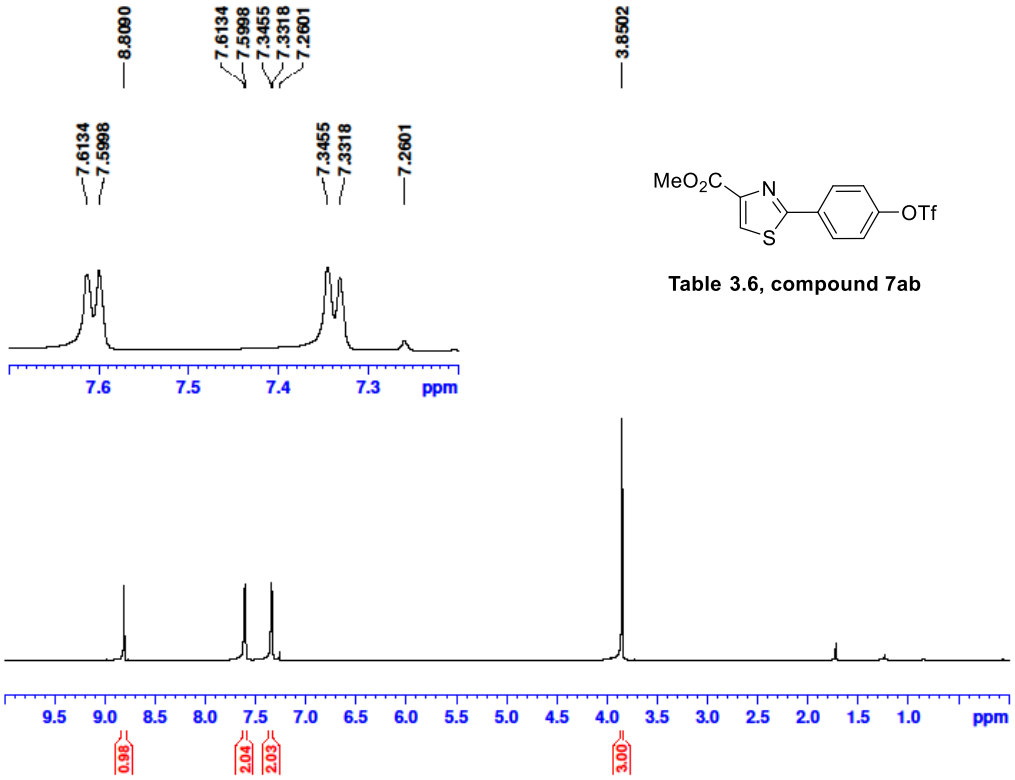

Table 3.6, compound 7ab

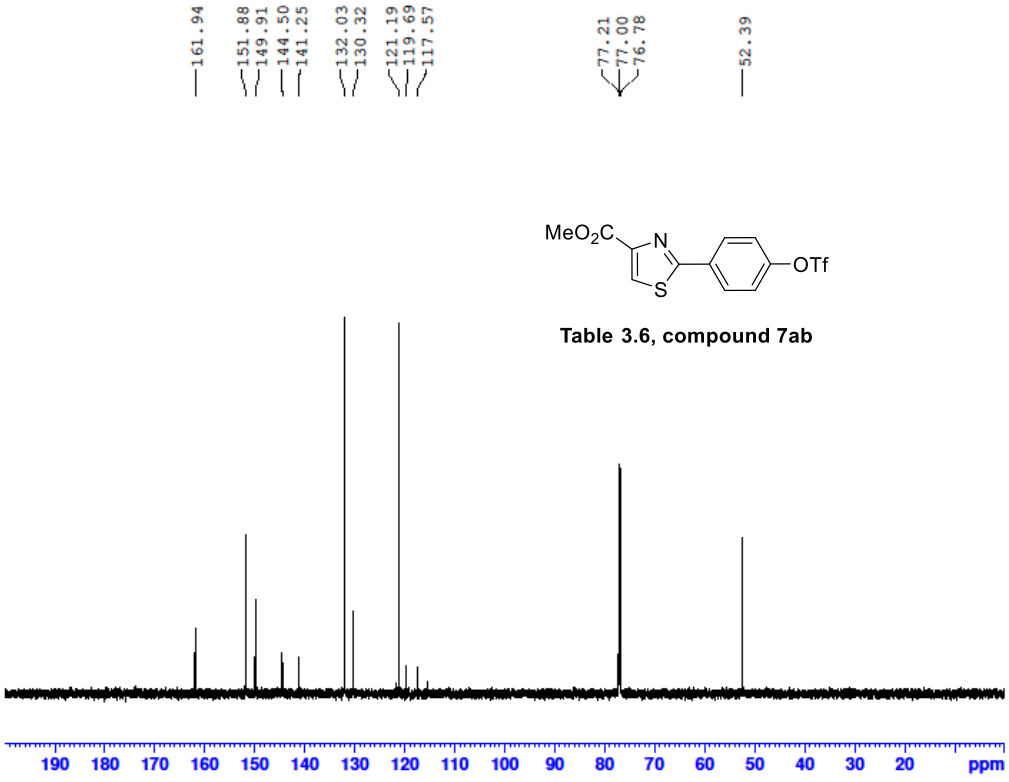

Table 3.6, compound 7ab

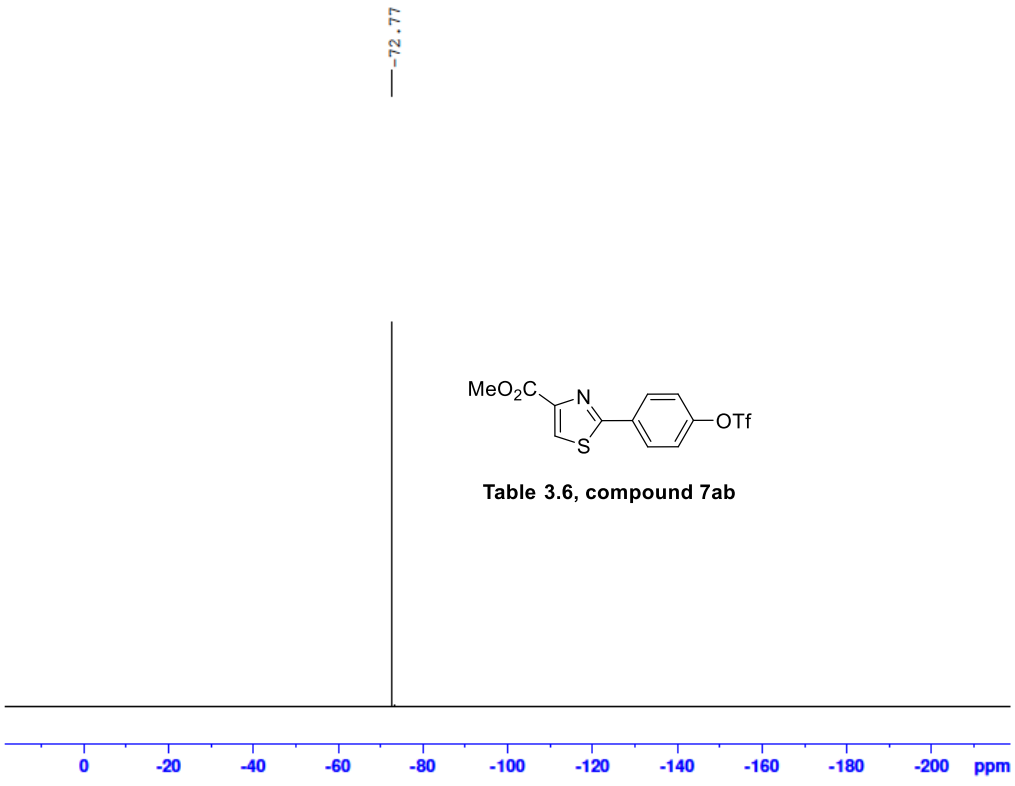

Table 3.6, compound 7ab

A6-20230928

A6-GCX-IV-128-7-20230928 554 (11.240) Cm (544:574)

TOF MS EI+
2.58e4

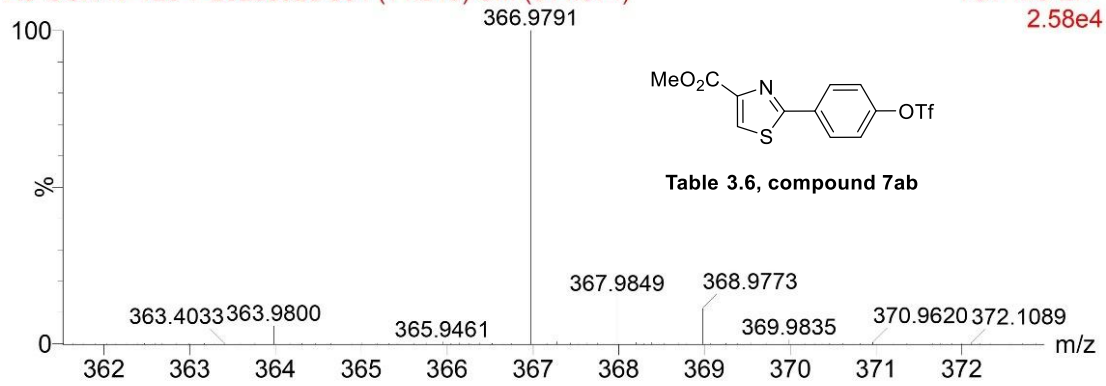

Table 3.6, compound 7ab

Mass	Calc. Mass	mDa	PPM	Ion Formula
366.9791	366.9790	-0.14	-0.05	C12H8F3NO5S2

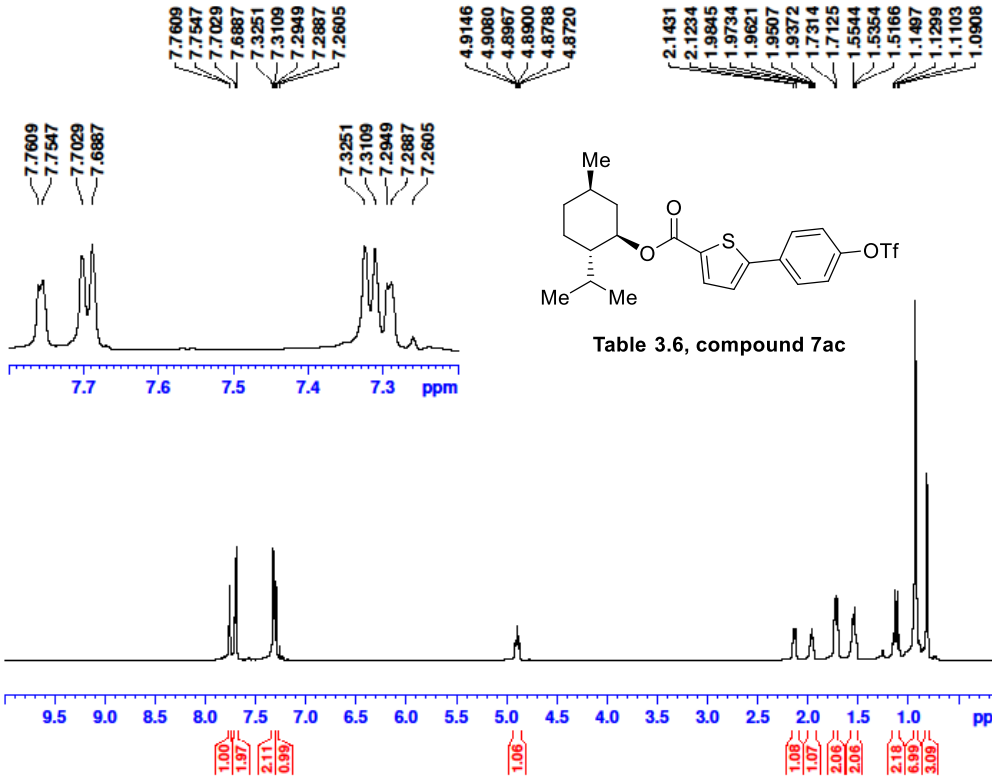

Table 3.6, compound 7ac

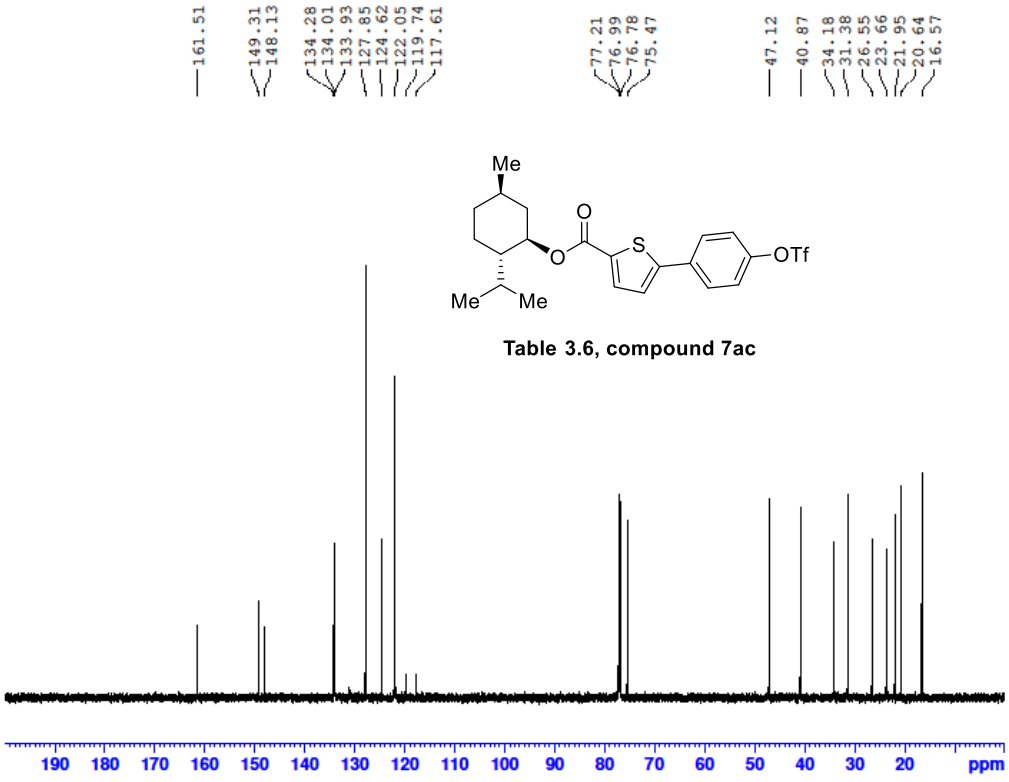

Table 3.6, compound 7ac

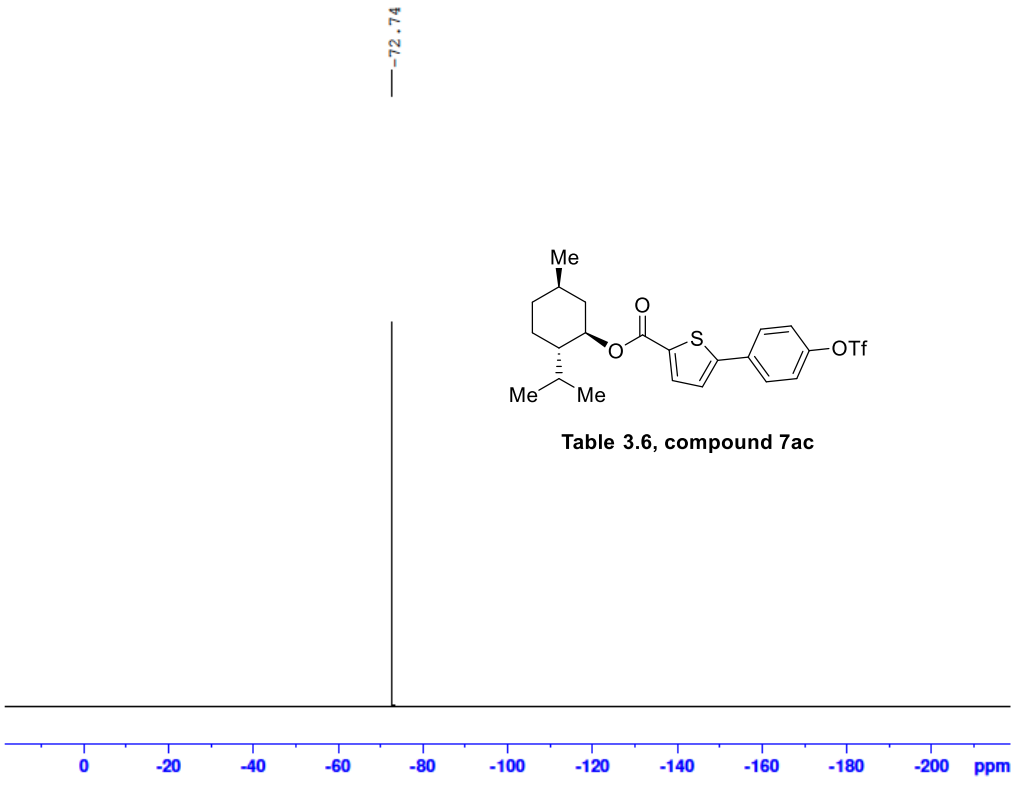

Table 3.6, compound 7ac

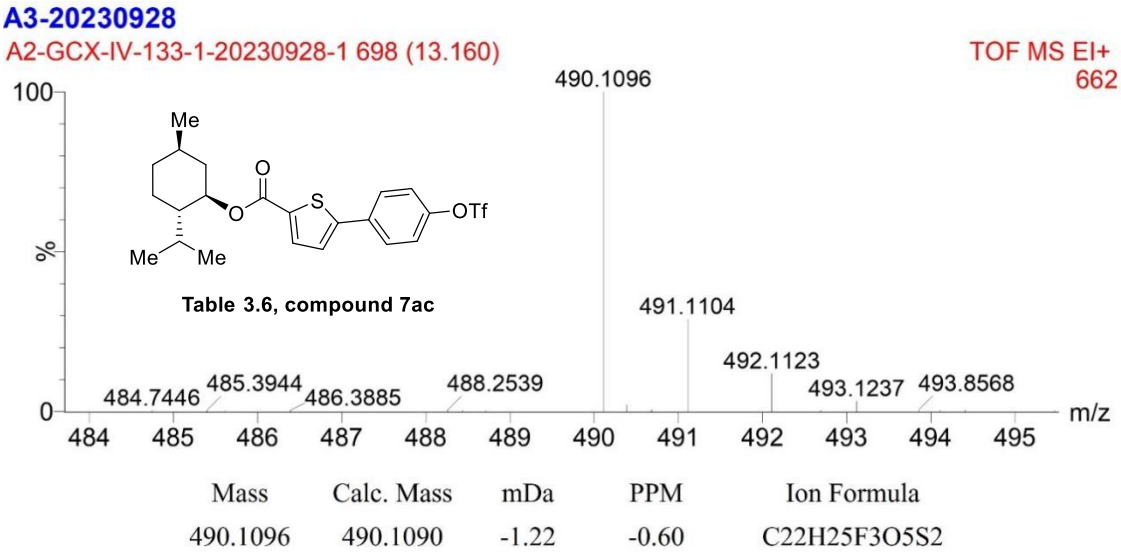

Table 3.6, compound 7ac

Mass	Calc. Mass	mDa	PPM	Ion Formula
490.1096	490.1090	-1.22	-0.60	C22H25F3O5S2

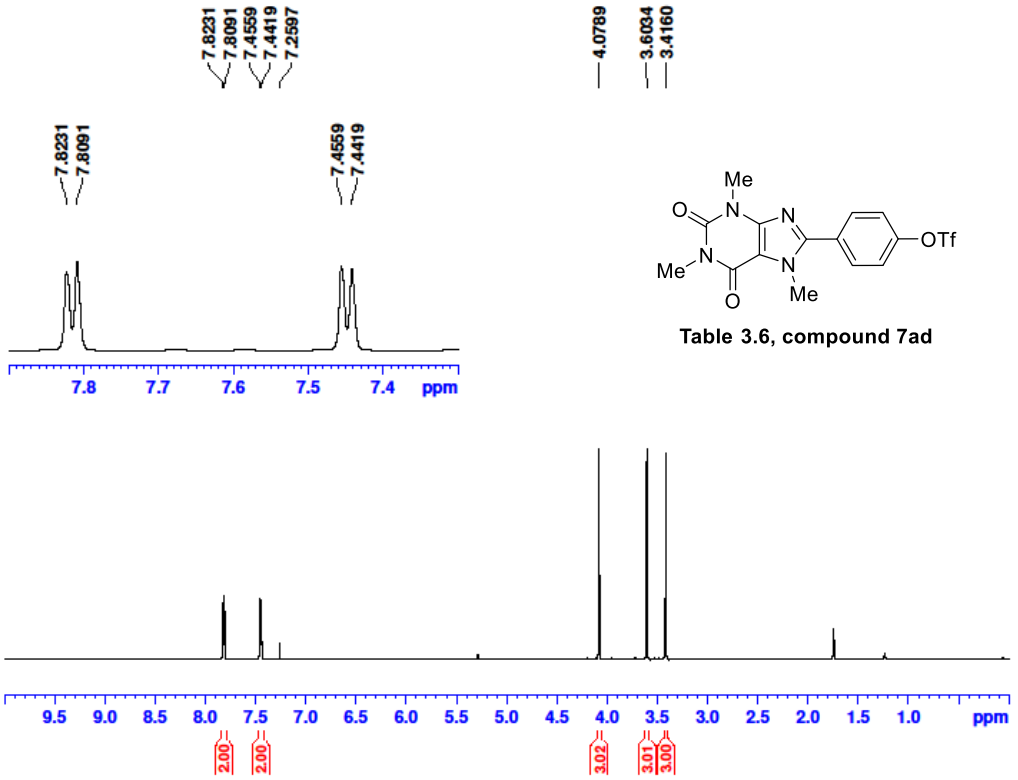

Table 3.6, compound 7ad

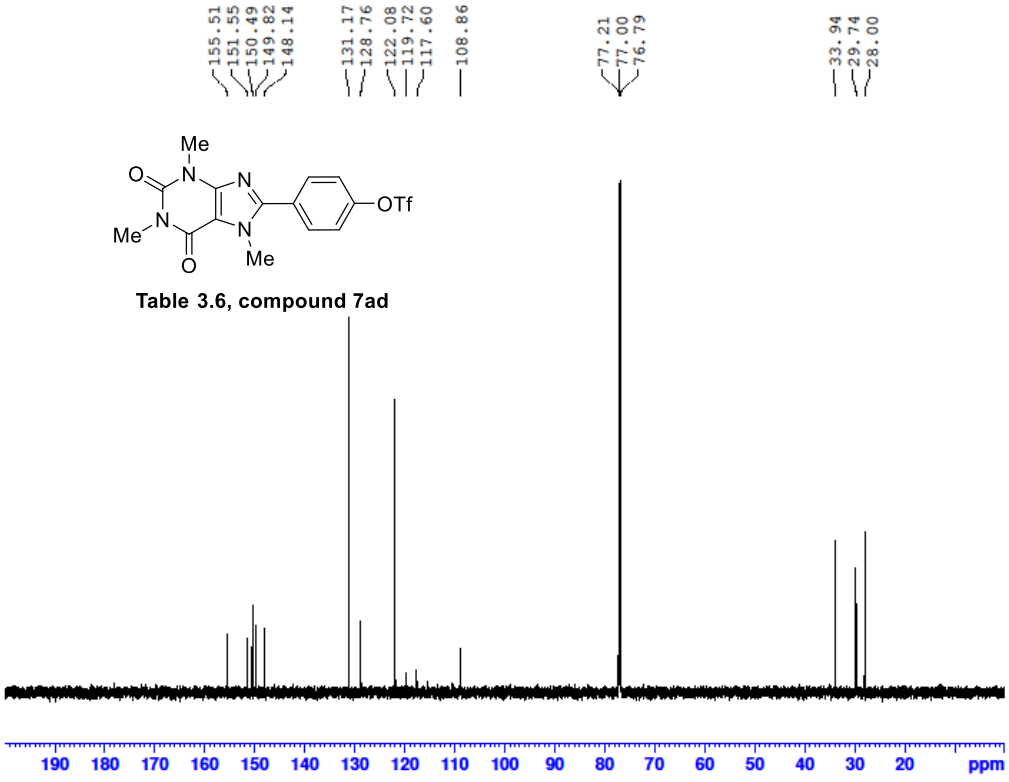

Table 3.6, compound 7ad

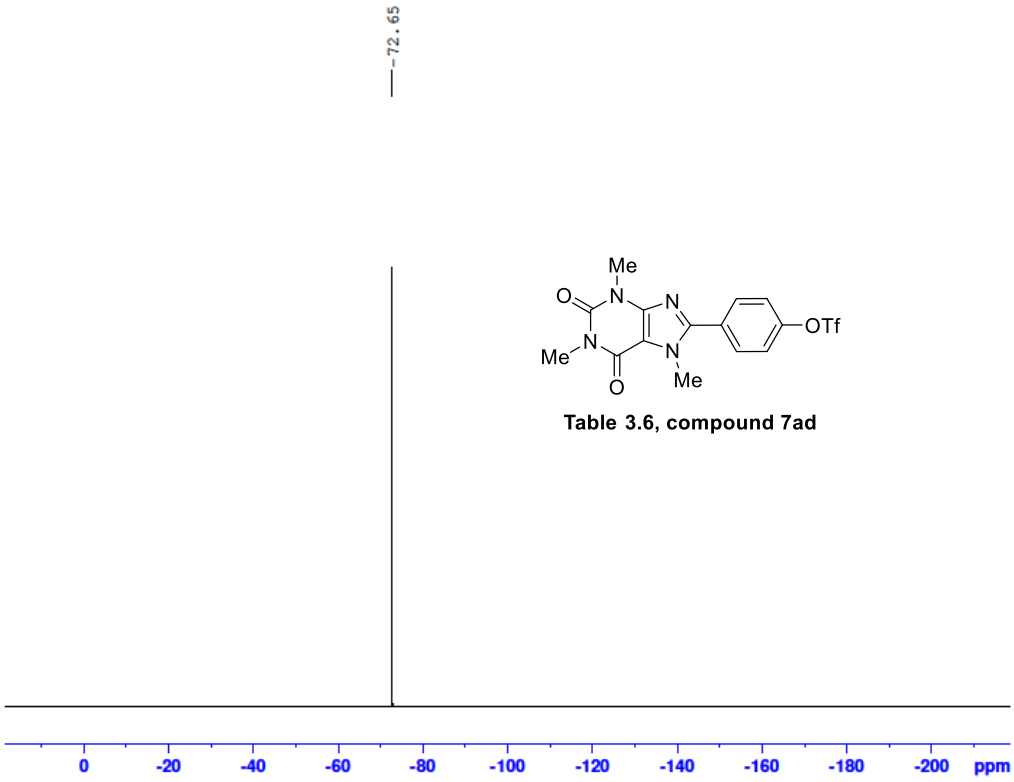

Table 3.6, compound 7ad

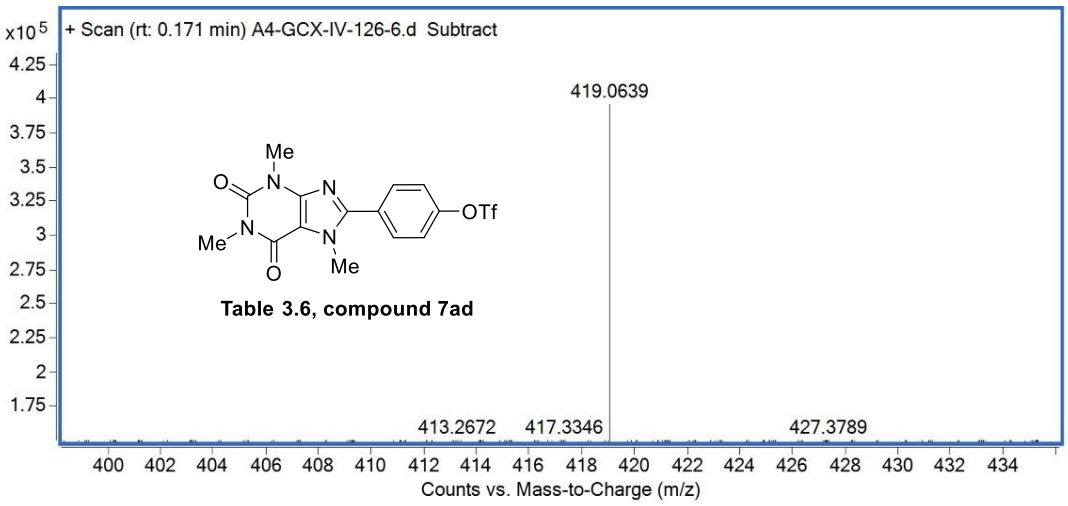

Table 3.6, compound 7ad

Mass	Calc. Mass	mDa	PPM	Ion Formula
419.0639	419.0632	-0.75	-1.79	C15H14F3O5N4S

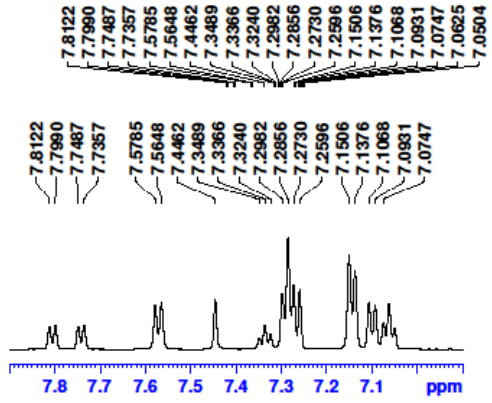

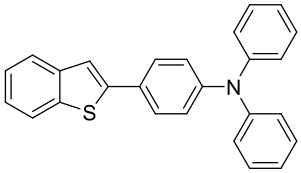

Scheme 3.4 compound 11a

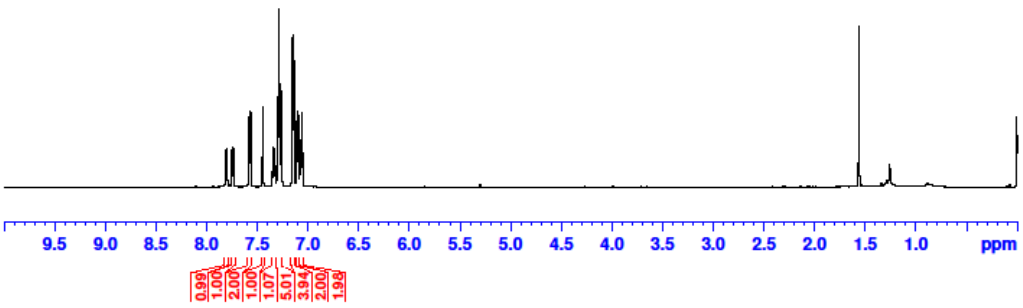

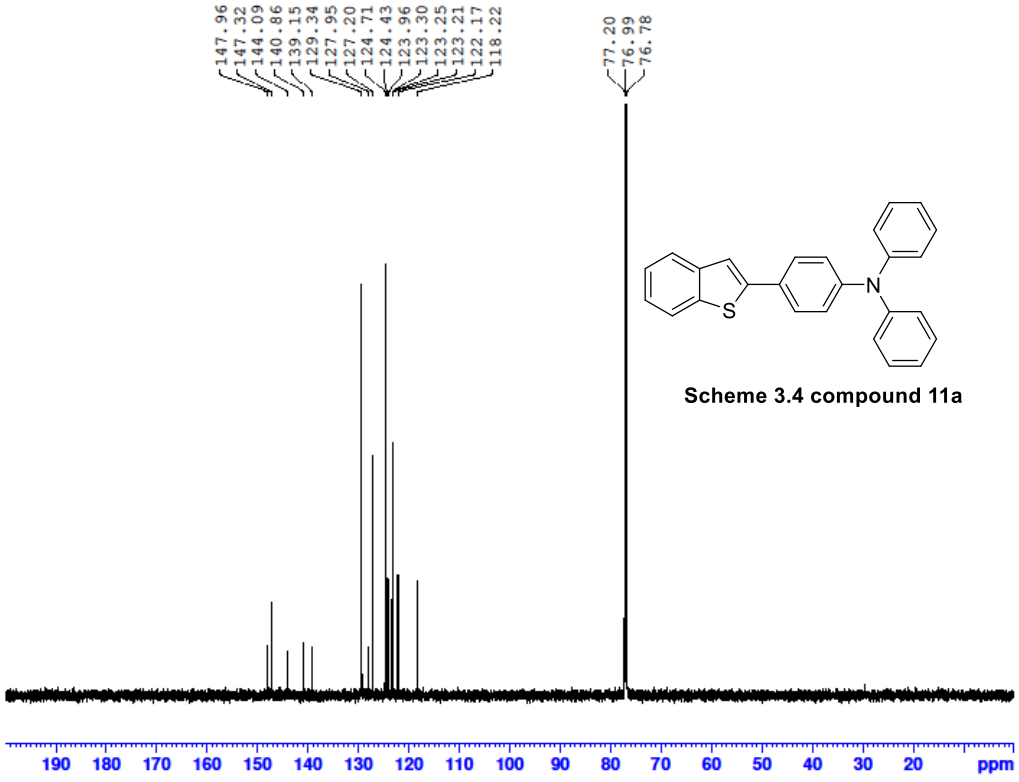

Scheme 3.4 compound 11a

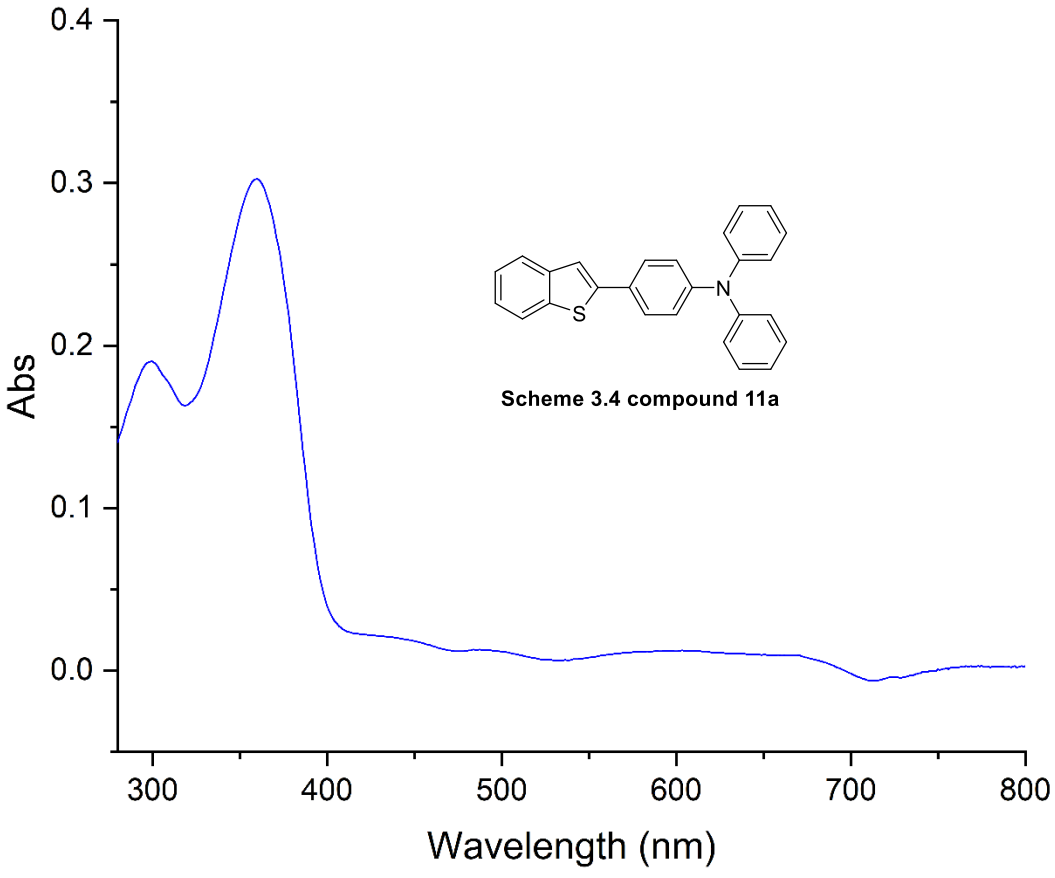

Scheme 3.4 compound 11a

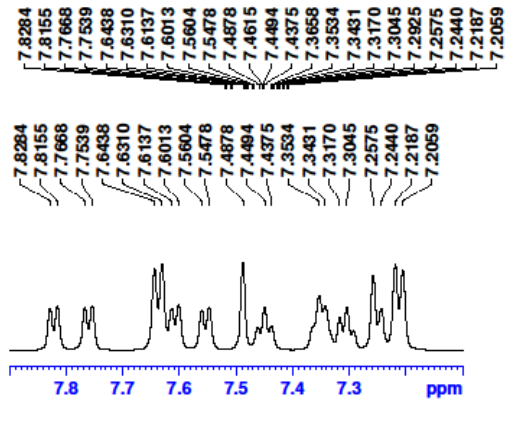

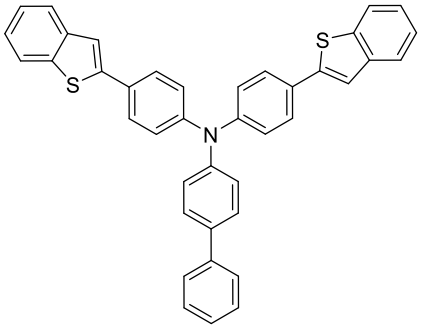

Scheme 3.4, compound 11b

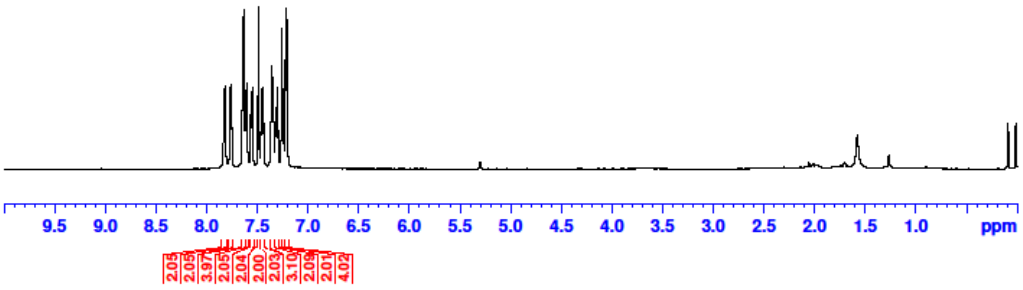

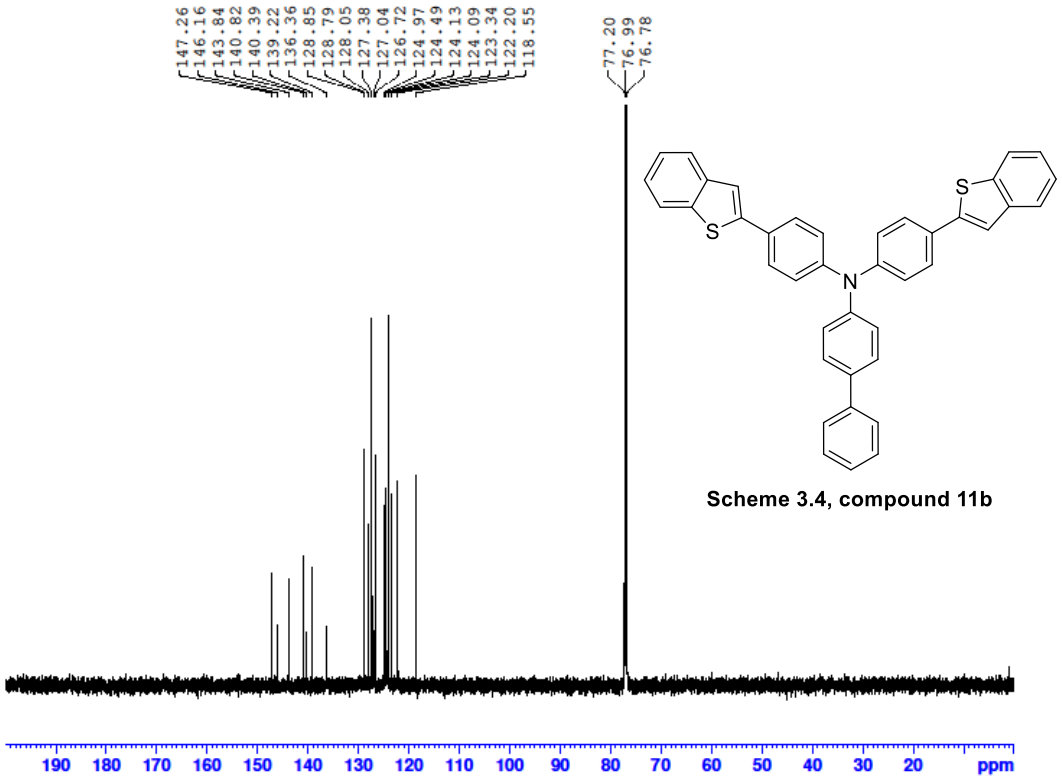

Scheme 3.4, compound 11b

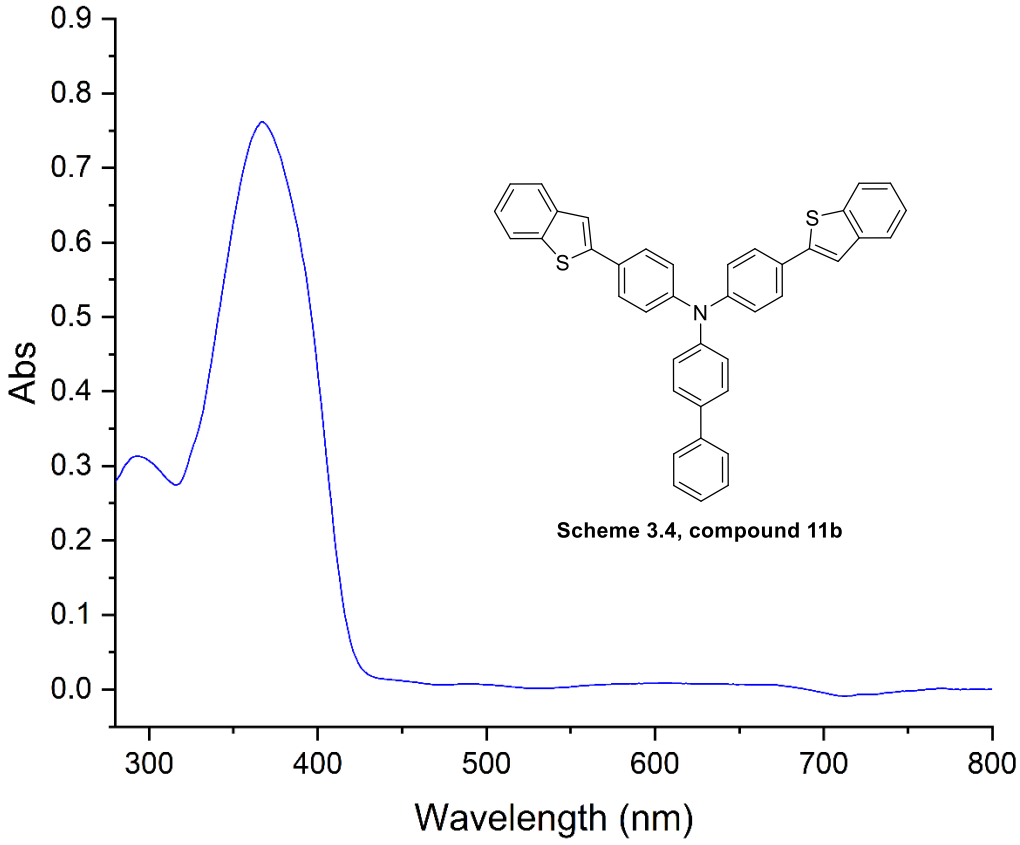

Scheme 3.4, compound 11b

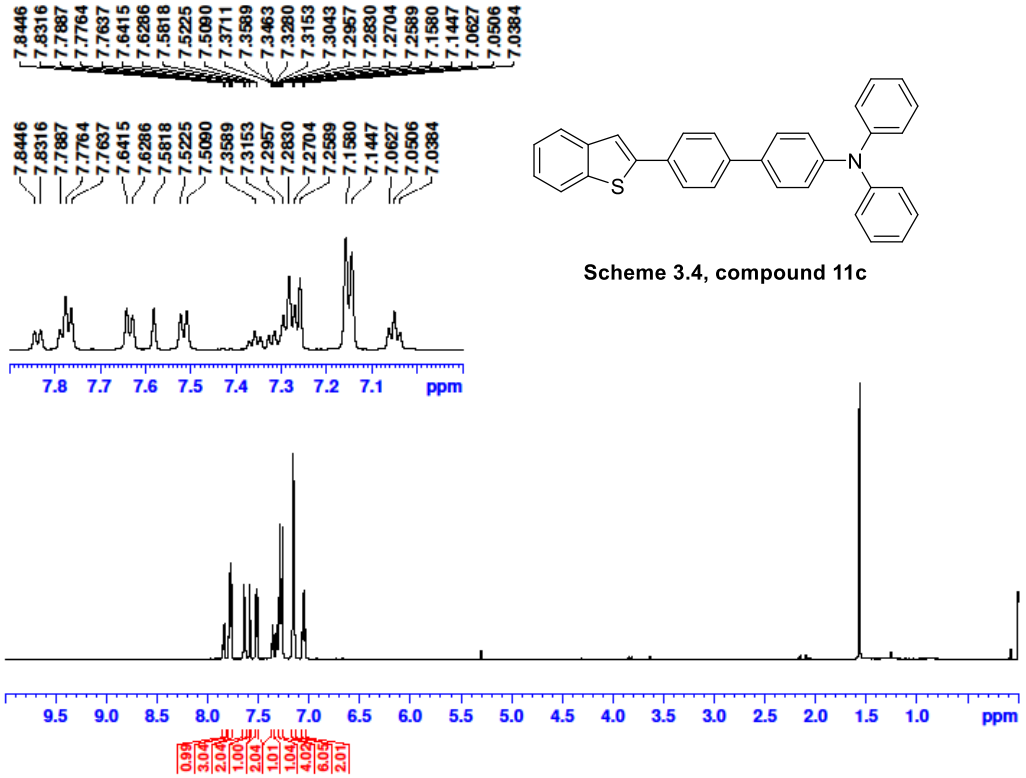

Scheme 3.4, compound 11c

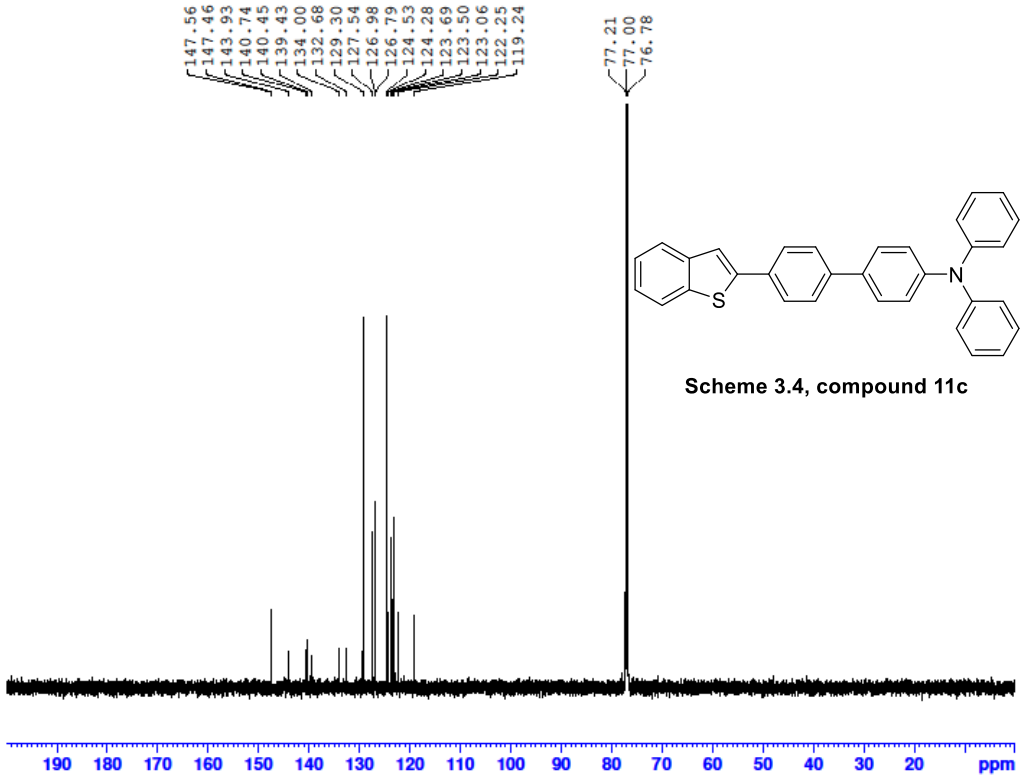

Scheme 3.4, compound 11c

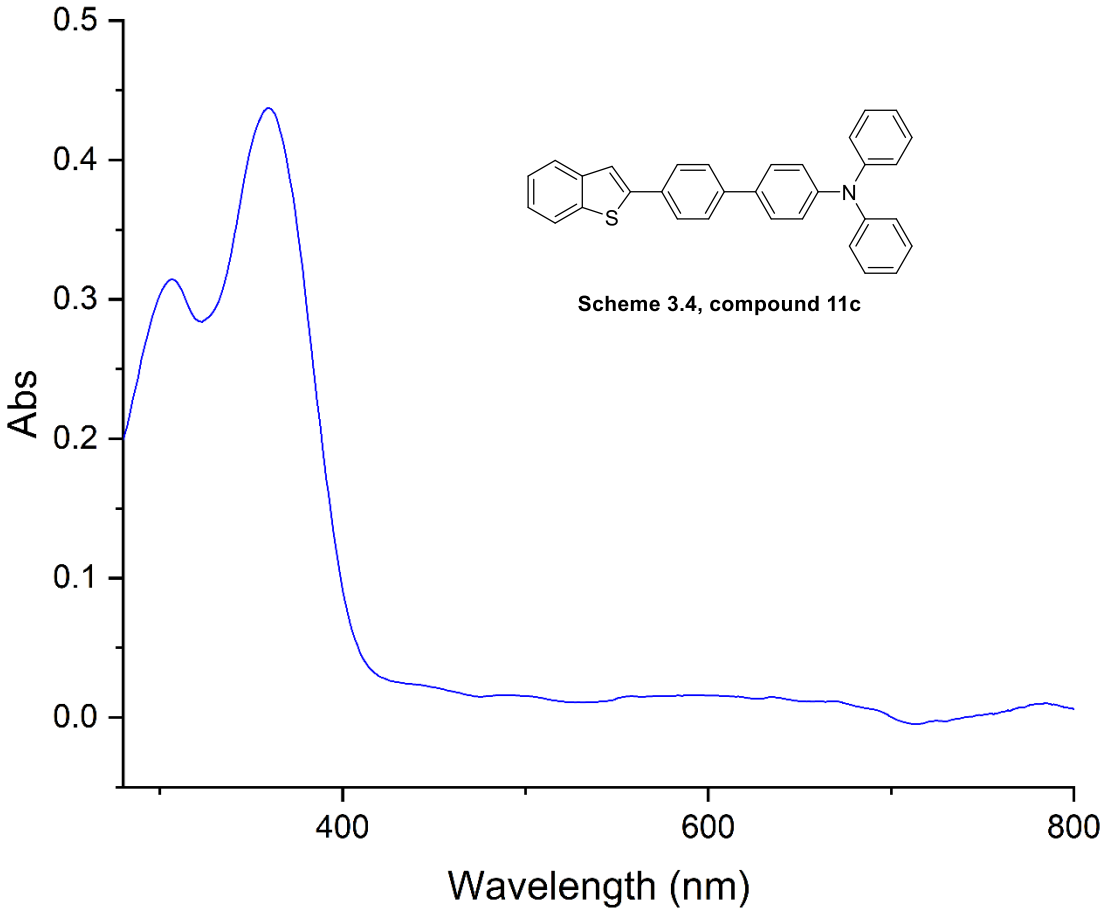

Scheme 3.4, compound 11c

NMR & HRMS Spectra of Chapter 4

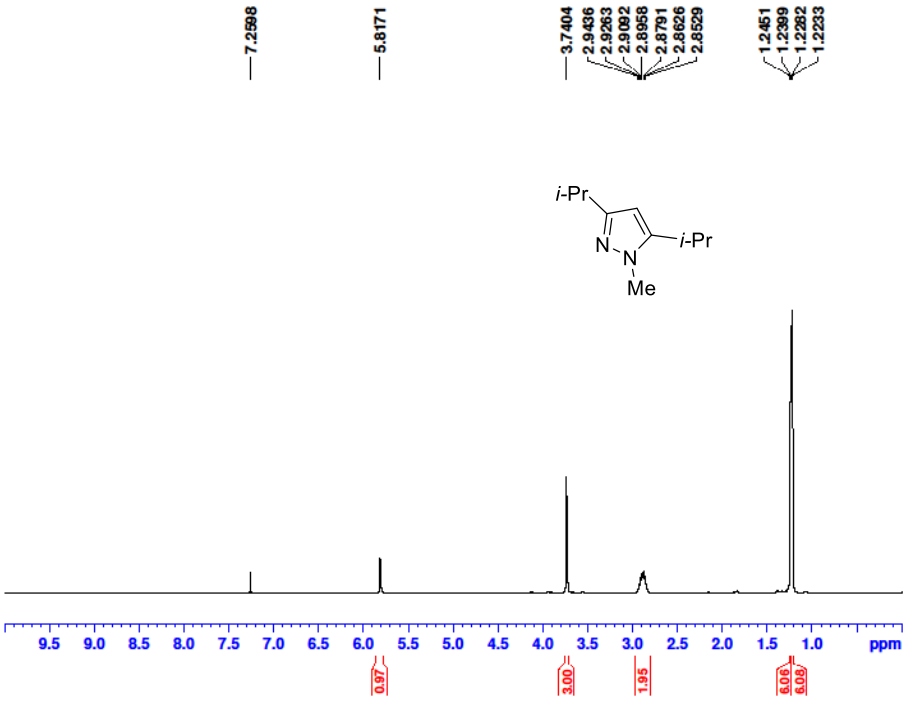

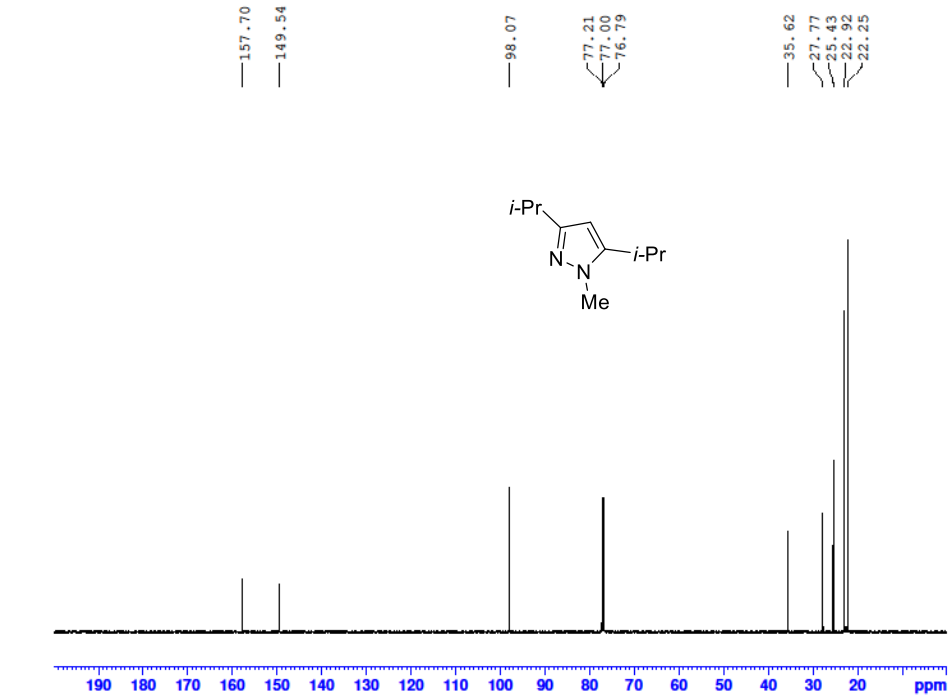

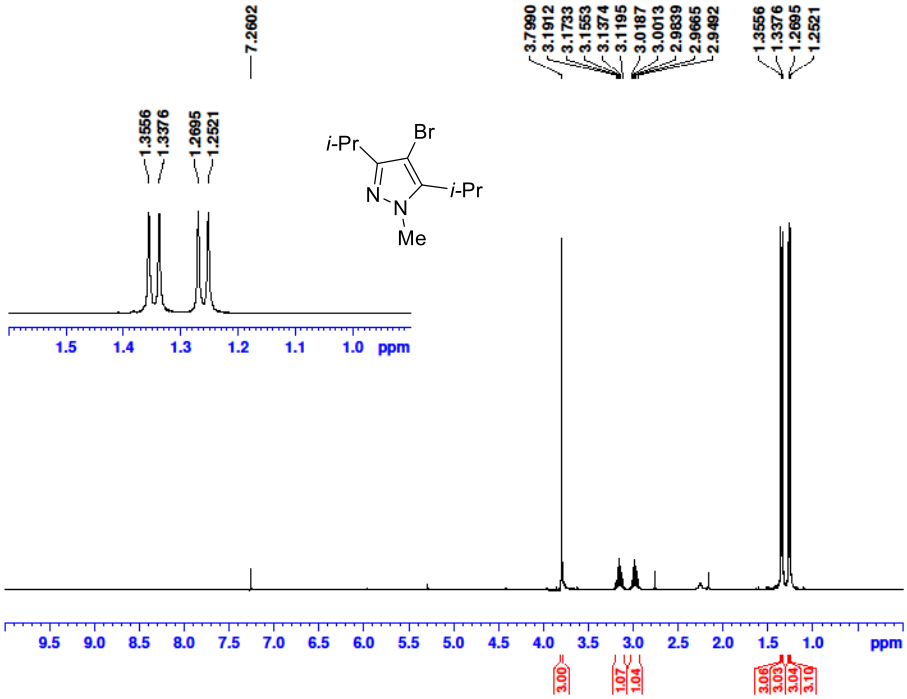
7.2602
3.7990
3.1912
3.1733
3.1553
3.1374
3.1195
3.0187
3.0013
2.9839
2.9665
2.9492
1.3556
1.3376
1.2695
1.2521
Br
i-Pr
i-Pr
N
N
Me
ppm
3.00
1.07
1.04
3.06
3.03
3.04
3.10

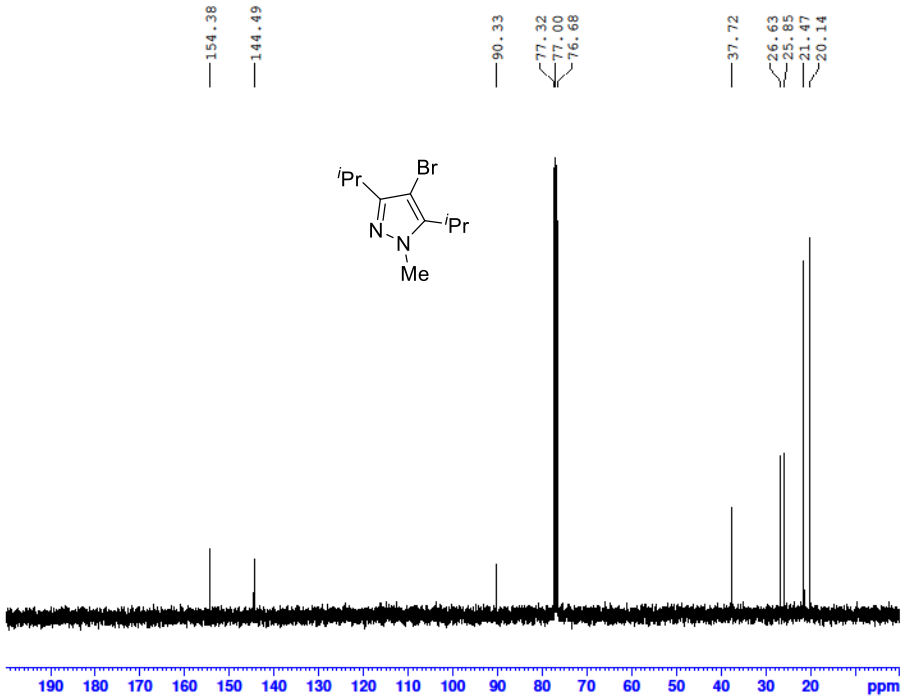
154.38
144.49
90.33
77.32
77.00
76.68
37.72
26.63
25.85
21.47
20.14
Br
iPr
iPr
N
N
Me
ppm

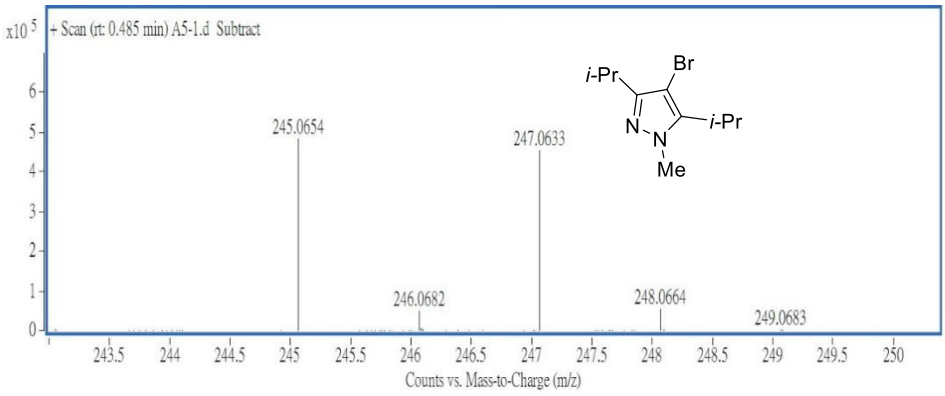

Mass	m/z (Calc)	Diff (mDa)	Diff (ppm)	Formula
245.0654	245.0848	-0.61	-2.51	C10 H18 Br N2

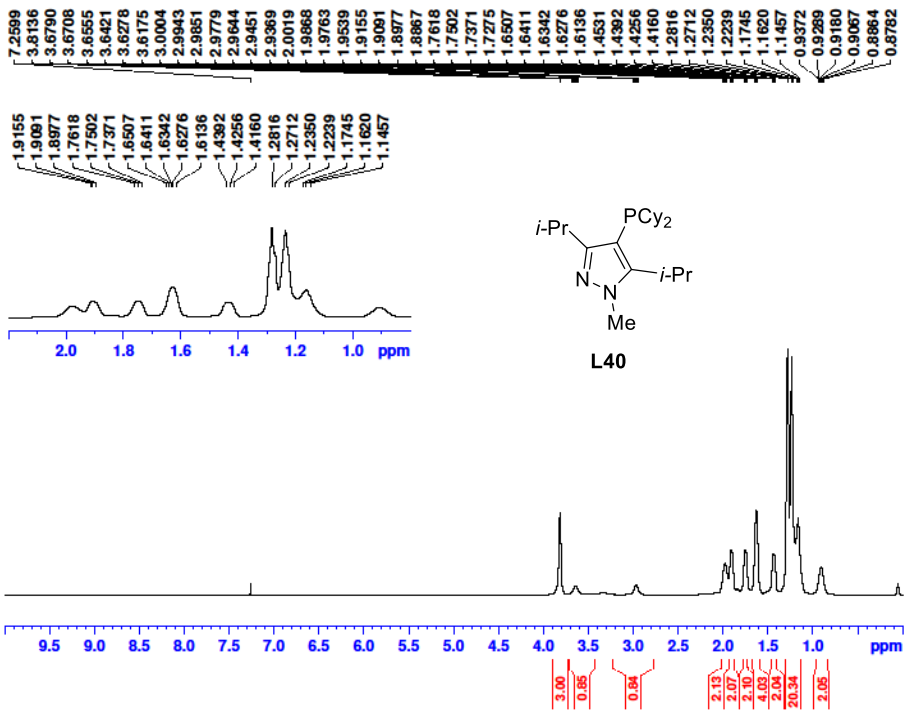

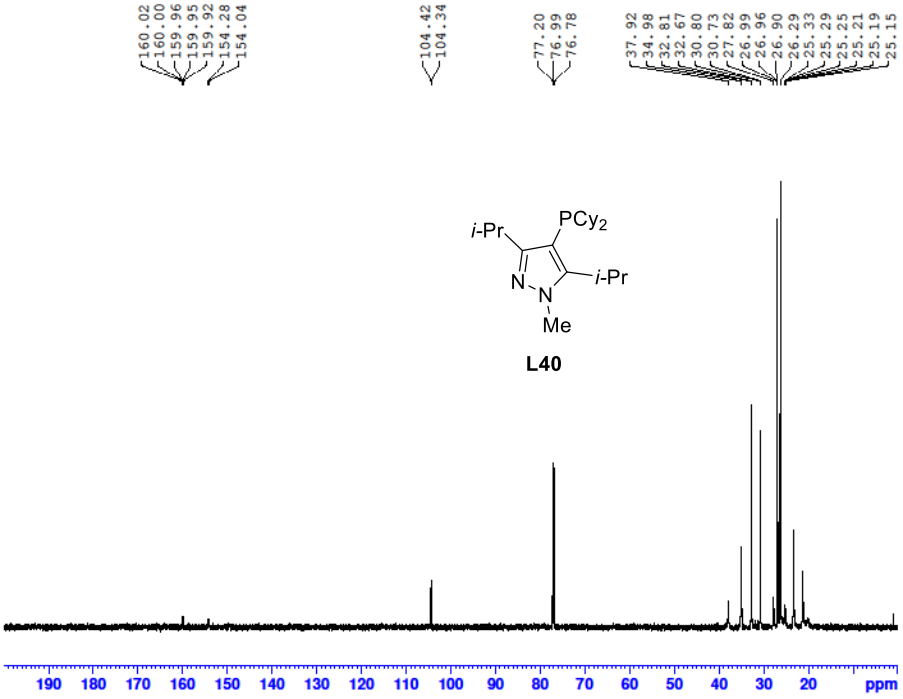
160.02
160.00
159.96
159.95
159.92
154.28
154.04
104.42
104.34
77.20
76.99
76.78
37.92
34.98
32.81
32.67
30.80
30.73
27.82
26.99
26.96
26.90
26.29
25.33
25.29
25.25
25.21
25.19
25.15
i-Pr
PCy2
i-Pr
N
N
Me
L40
190 180 170 160 150 140 130 120 110 100 90 80 70 60 50 40 30 20 ppm

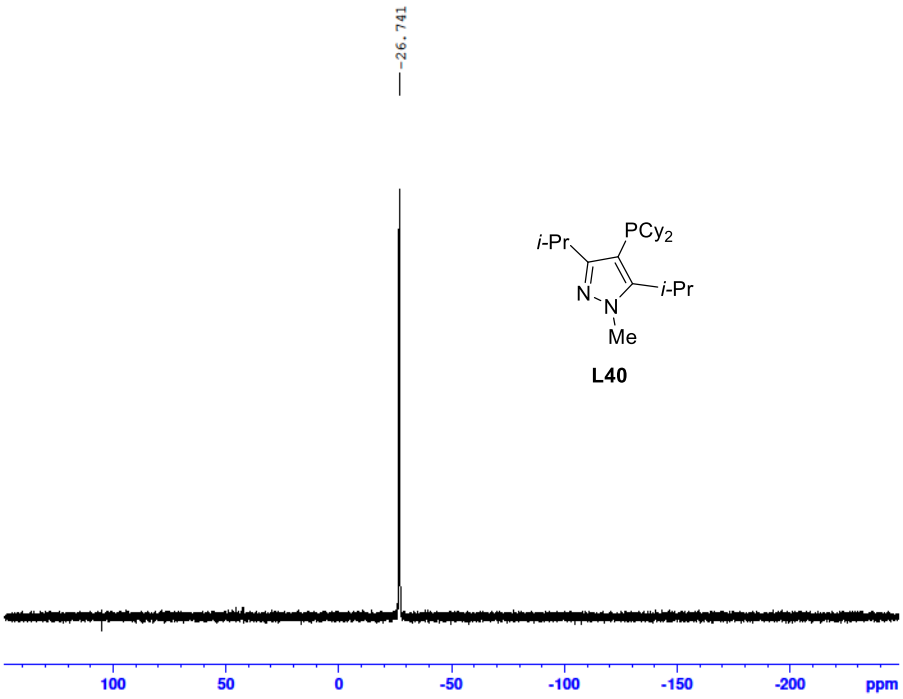
26.741
i-Pr
PCy2
i-Pr
N
N
Me
L40
100 50 0 -50 -100 -150 -200 ppm

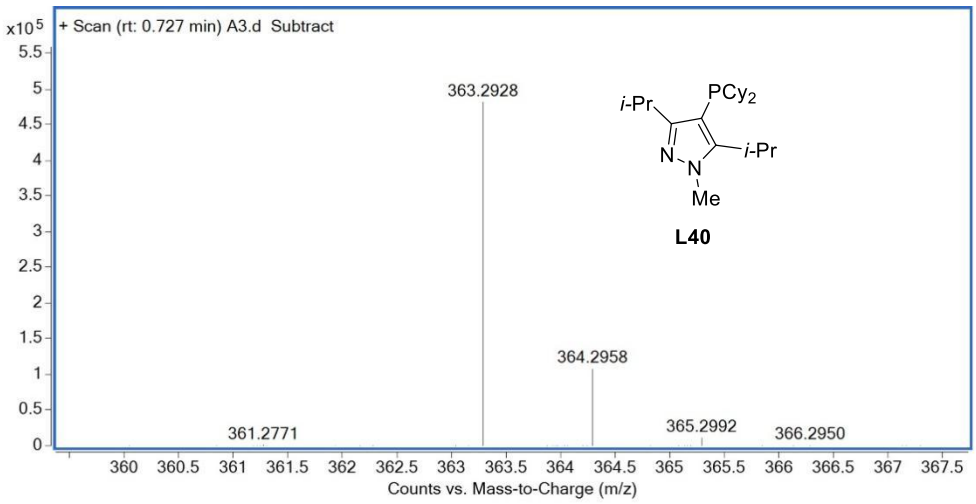

Mass	Calc. Mass	mDa	PPM	Ion Formula
363.2928	363.2924	-0.44	-1.21	C22H40N2P

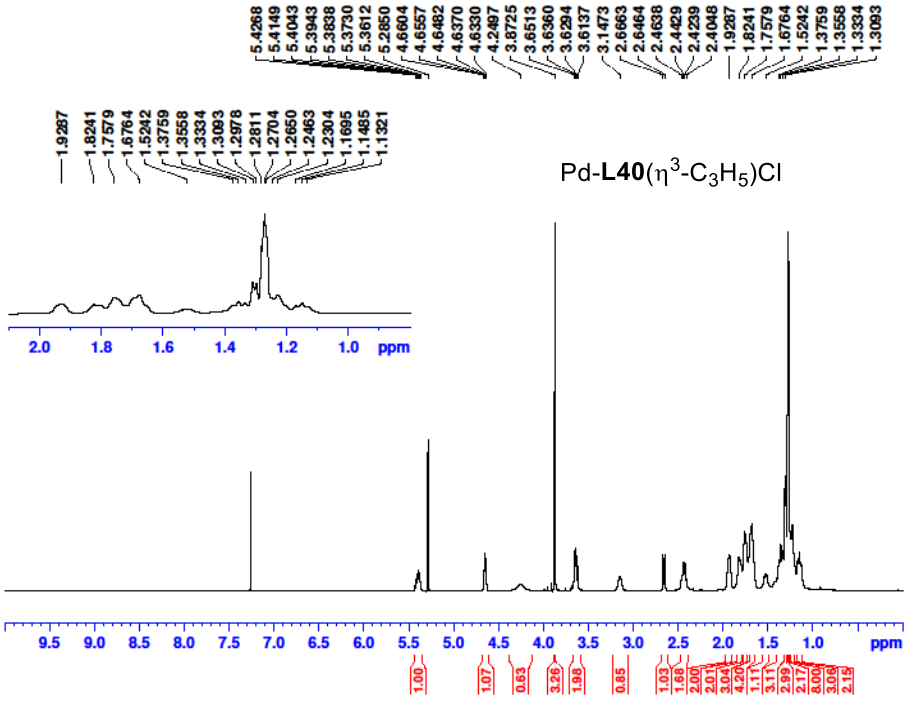

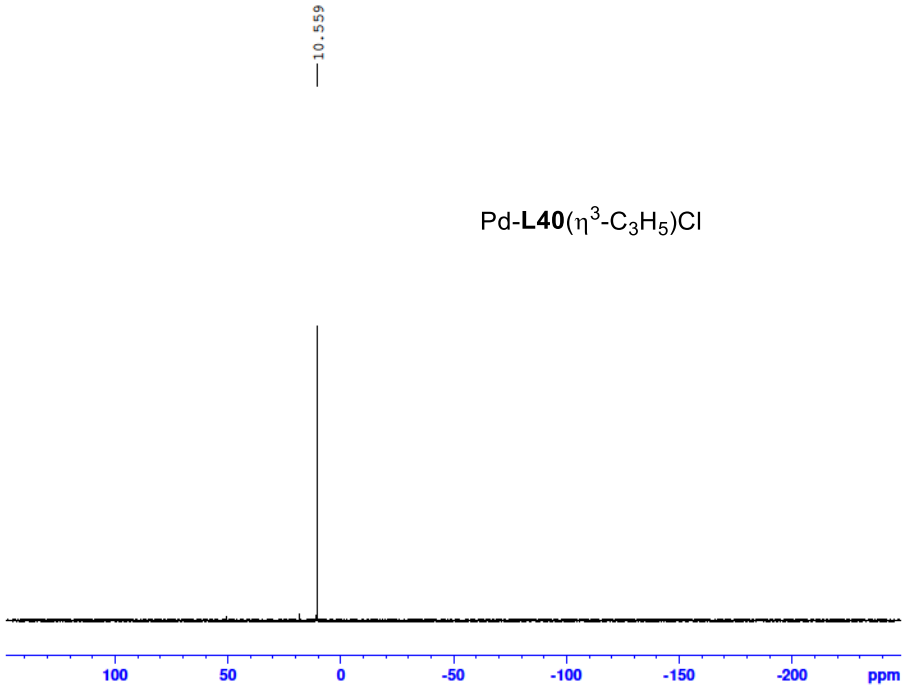

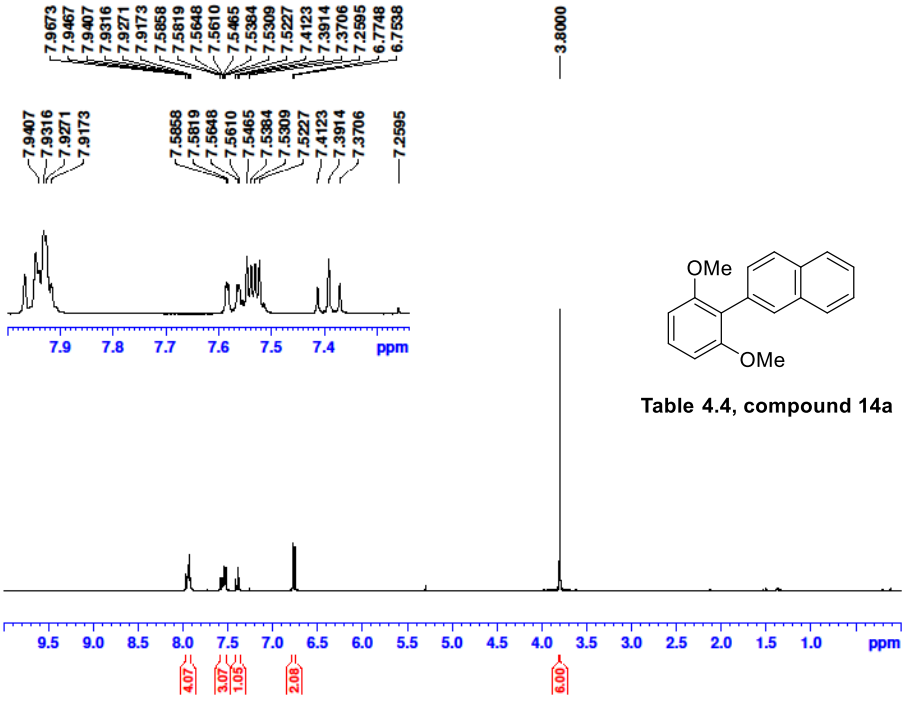

Table 4.4, compound 14a

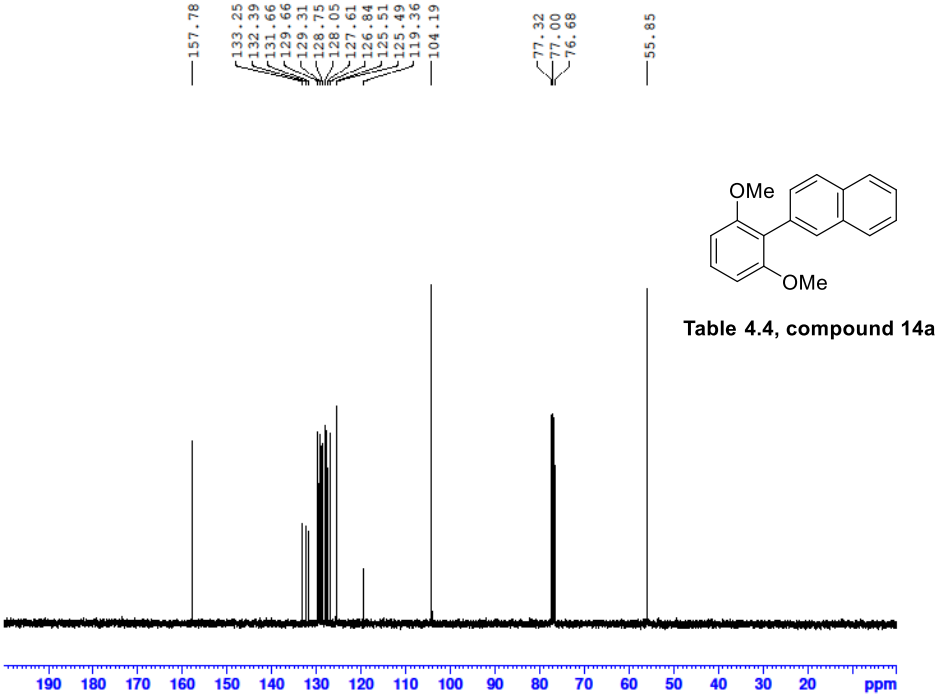

Table 4.4, compound 14a

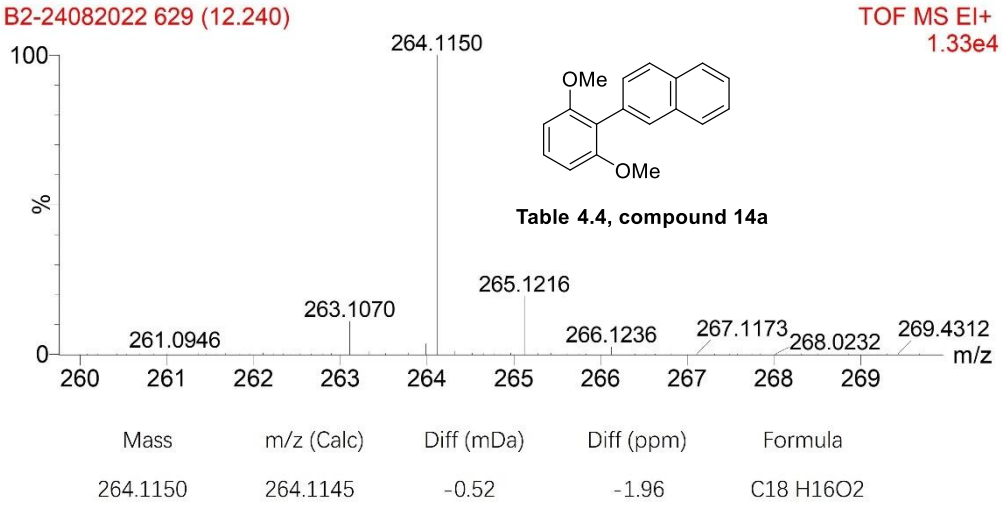

Table 4.4, compound 14a

Mass	m/z (Calc)	Diff (mDa)	Diff (ppm)	Formula
264.1150	264.1145	-0.52	-1.96	C18 H16O2

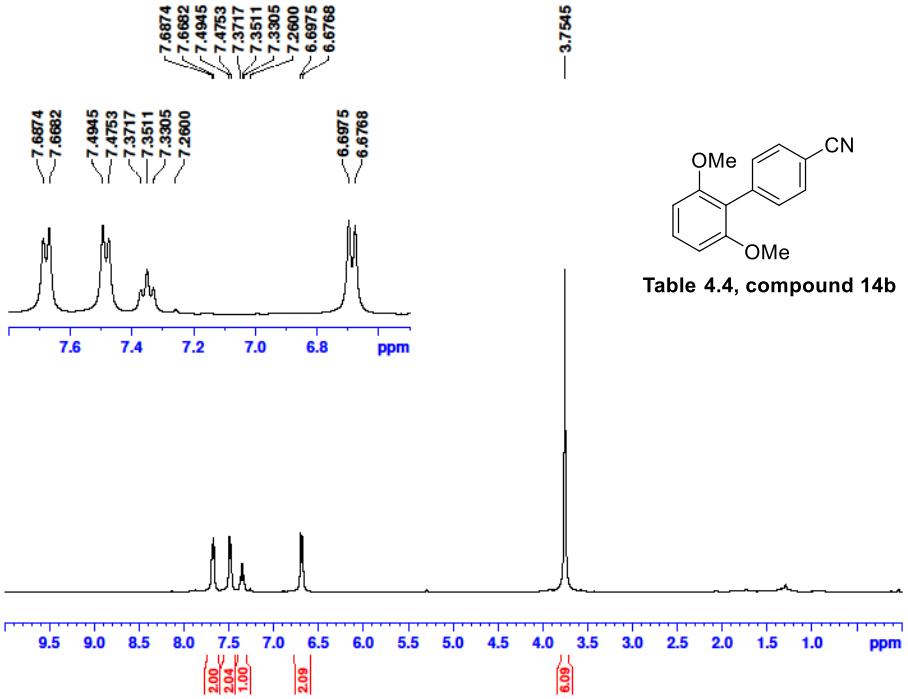

Table 4.4, compound 14b

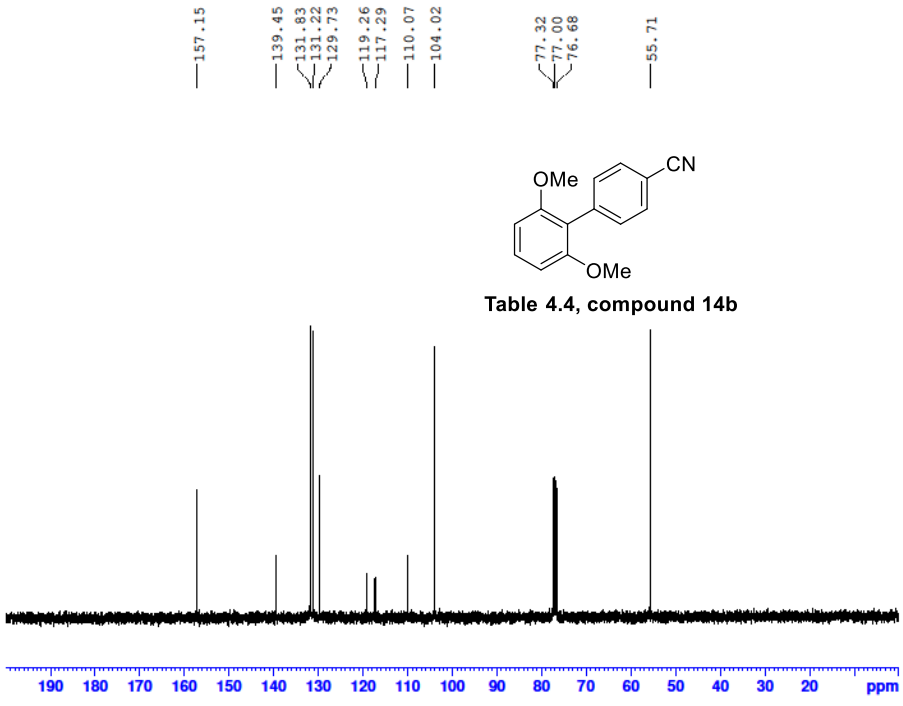

Table 4.4, compound 14b

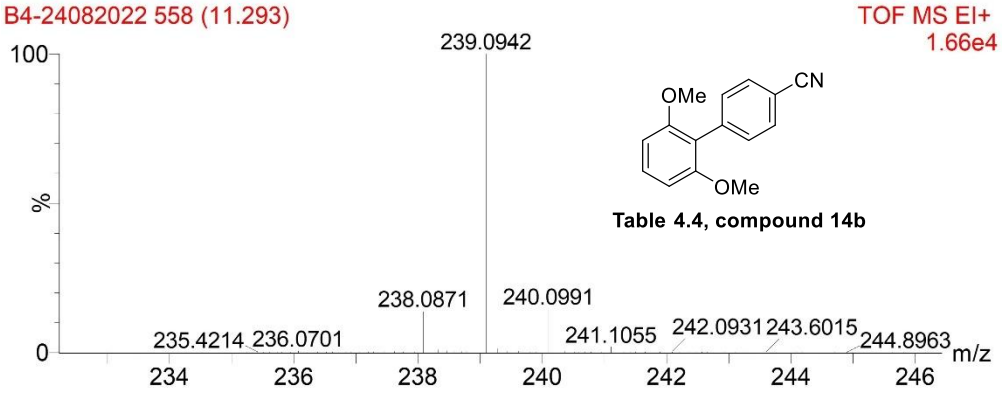

Table 4.4, compound 14b

Mass	m/z (Calc)	Diff (mDa)	Diff (ppm)	Formula
239.0942	239.0941	-0.12	-0.50	C15 H13NO2

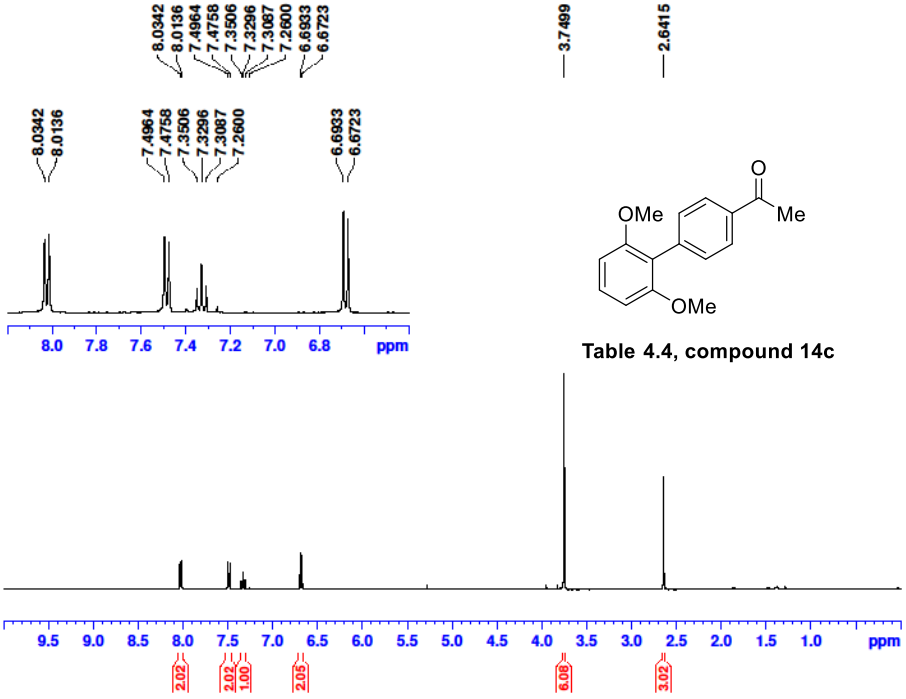

Table 4.4, compound 14c

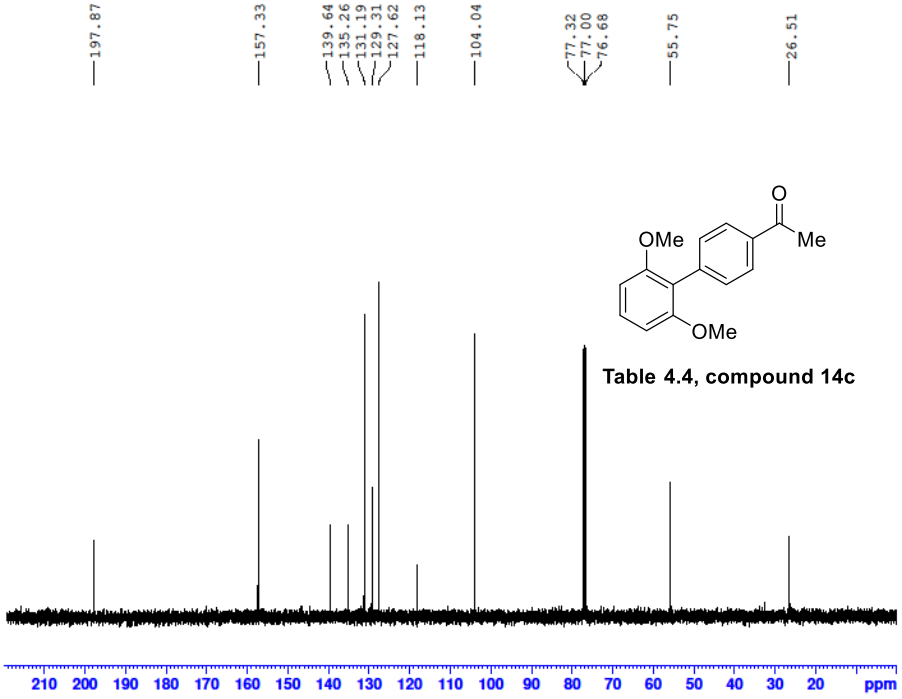

Table 4.4, compound 14c

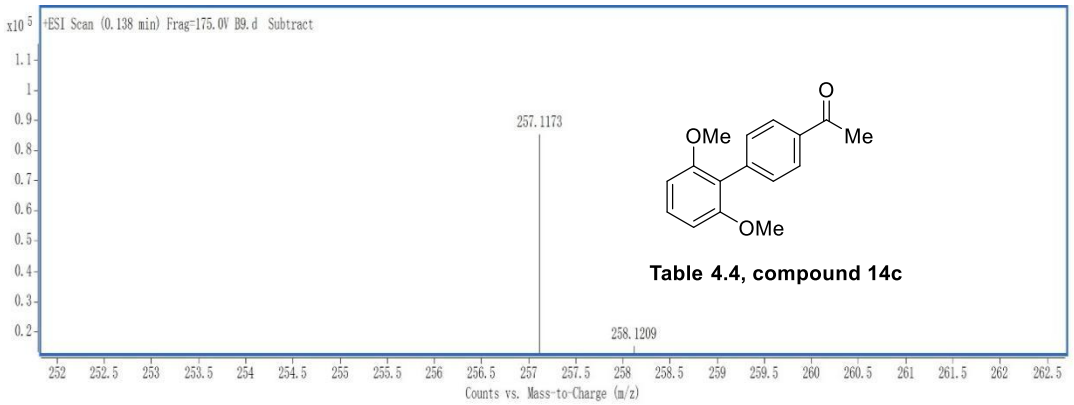

Table 4.4, compound 14c

Mass	m/z (Calc)	Diff (mDa)	Diff (ppm)	Formula
257.1173	257.1172	-0.08	-0.31	C16H17O3

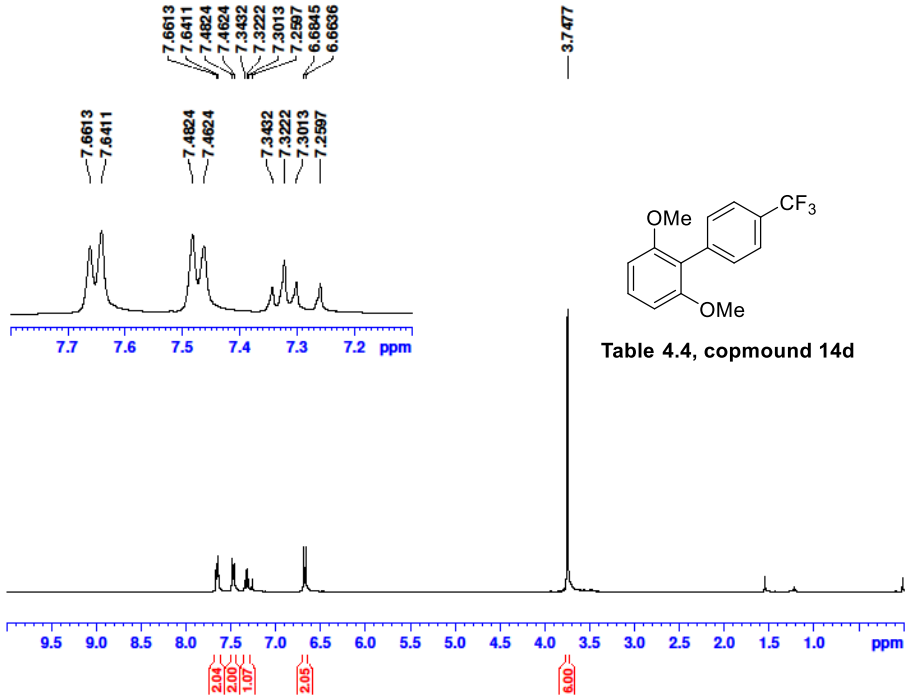

Table 4.4, copmound 14d

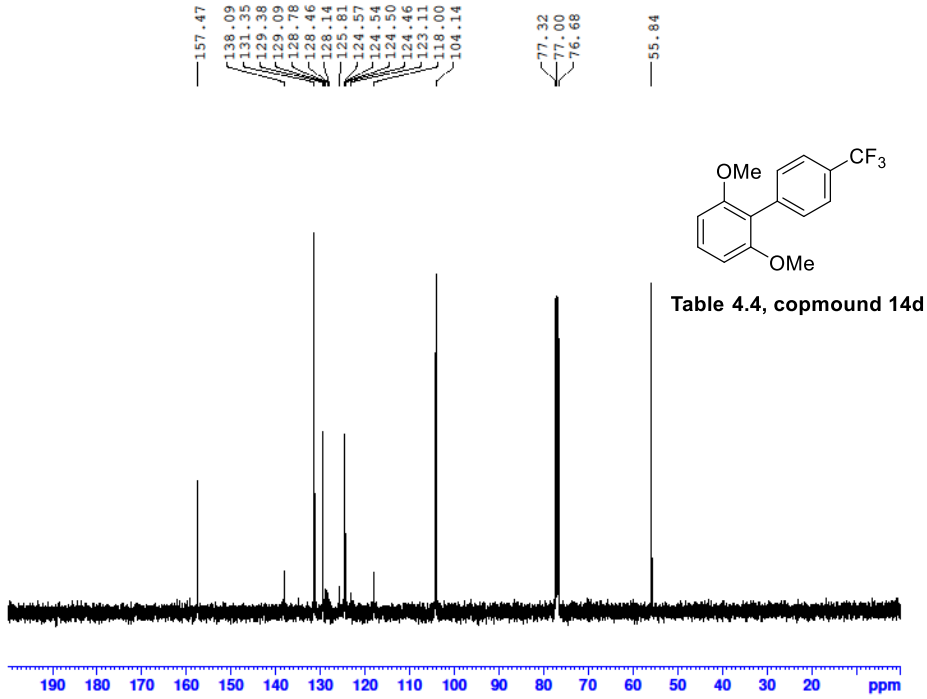

Table 4.4, copmound 14d

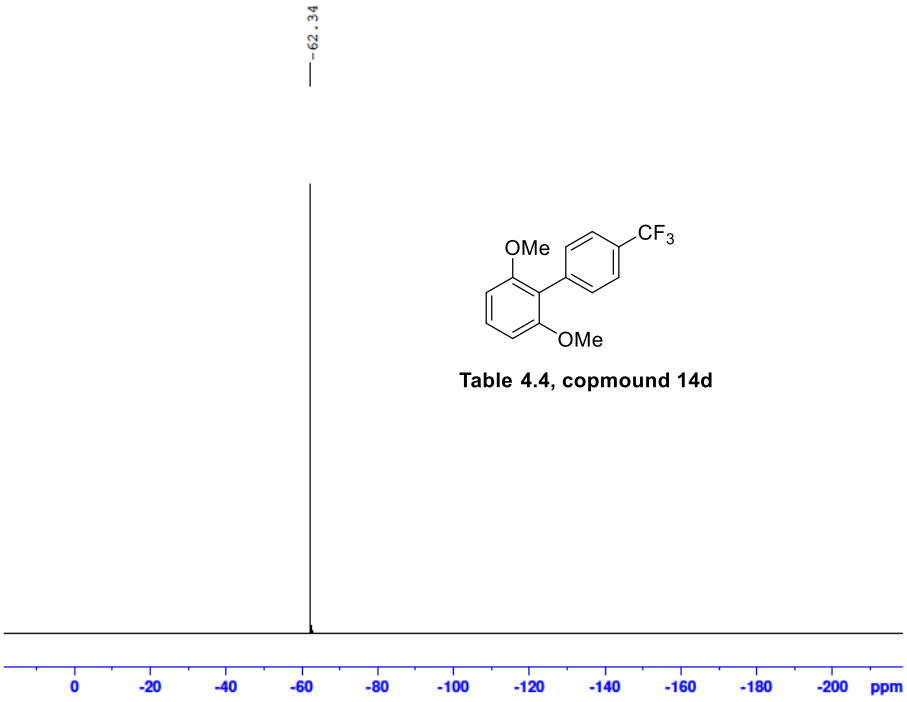

Table 4.4, copmound 14d

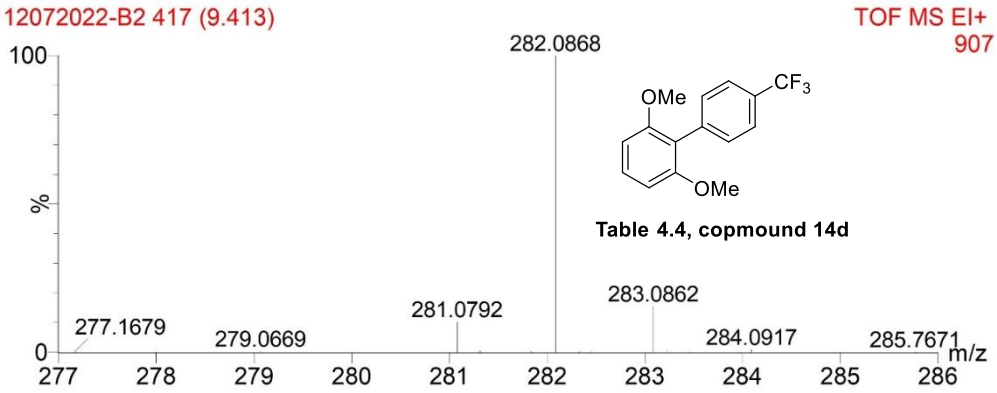

Table 4.4, copmound 14d

Mass	Calc. Mass	mDa	PPM	Ion Formula
282.0868	282.0862	-0.58	-2.07	C15H13 F3O2

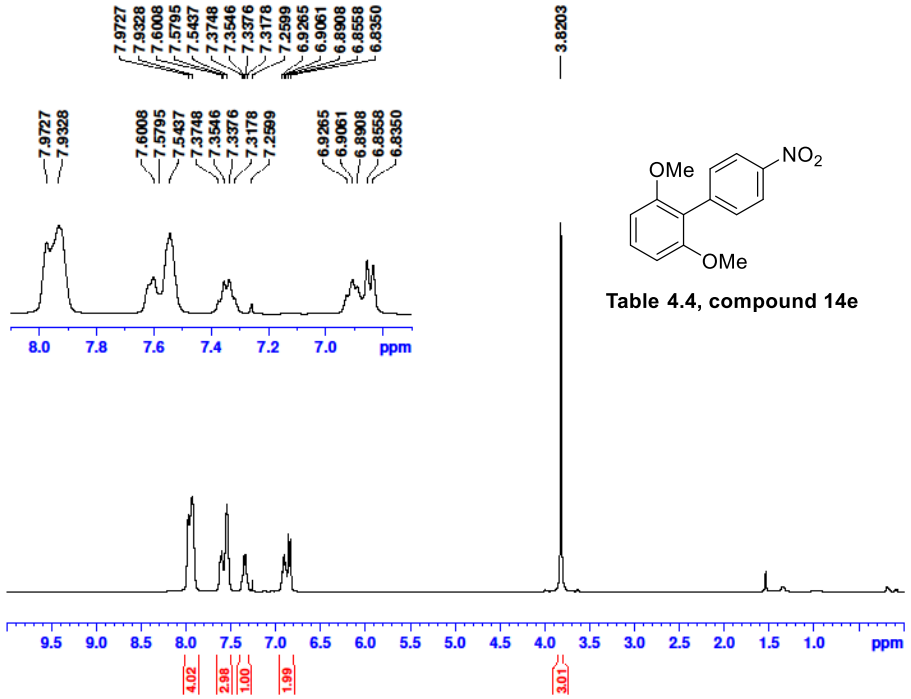

Table 4.4, compound 14e

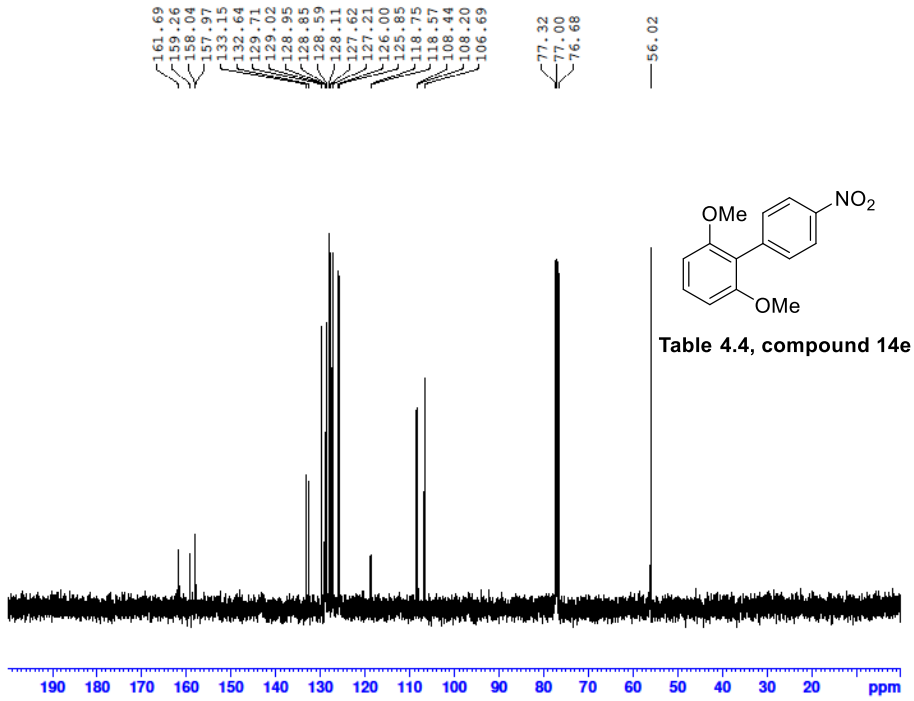

Table 4.4, compound 14e

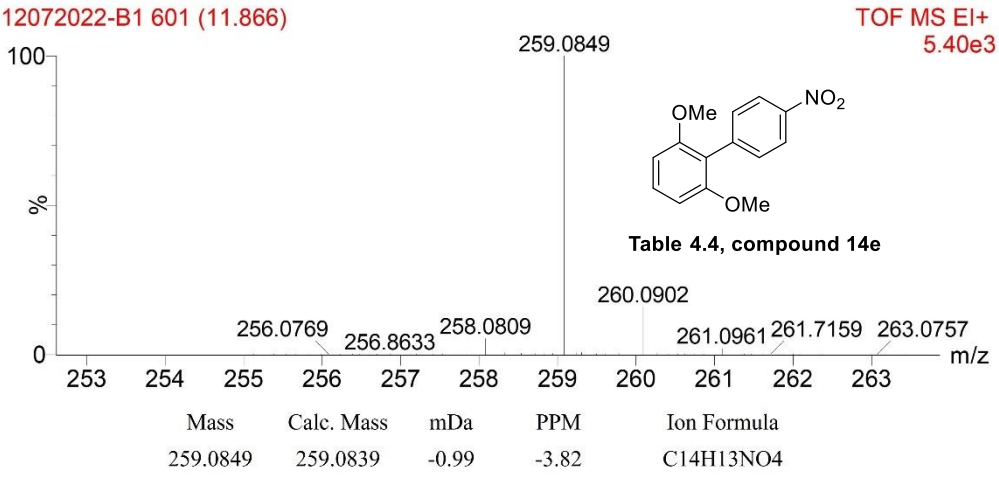

Table 4.4, compound 14e

Mass	Calc. Mass	mDa	PPM	Ion Formula
259.0849	259.0839	-0.99	-3.82	C14H13NO4

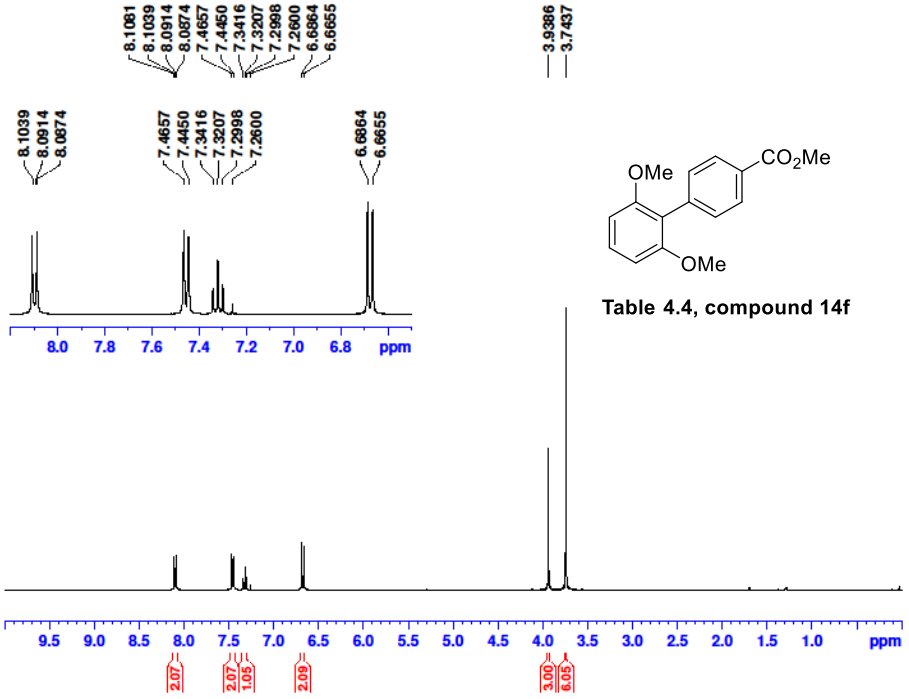

Table 4.4, compound 14f

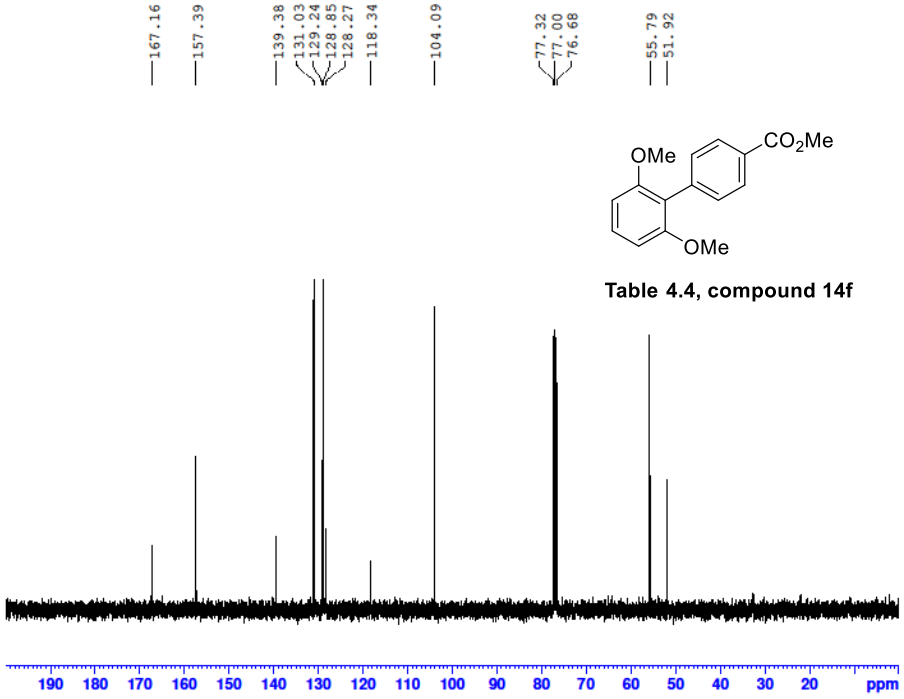

Table 4.4, compound 14f

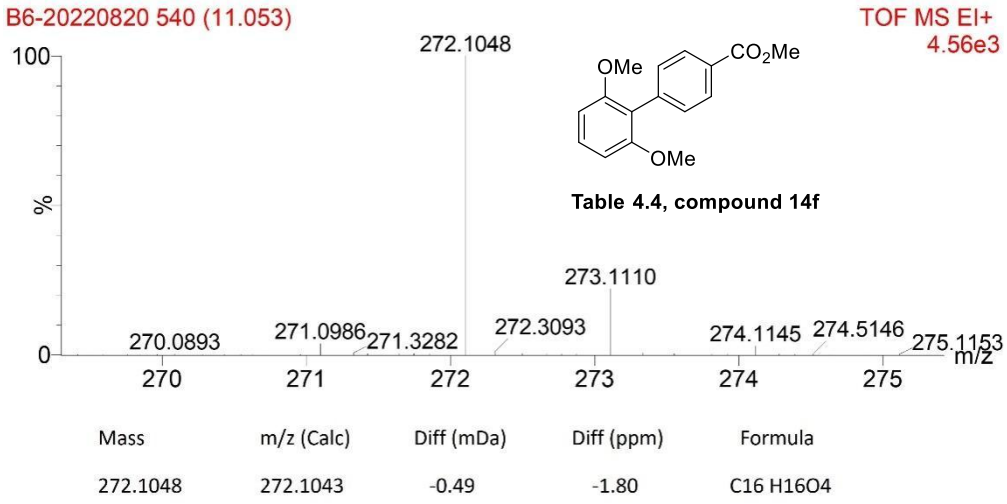

Table 4.4, compound 14f

Mass	m/z (Calc)	Diff (mDa)	Diff (ppm)	Formula
272.1048	272.1043	-0.49	-1.80	C16 H16O4

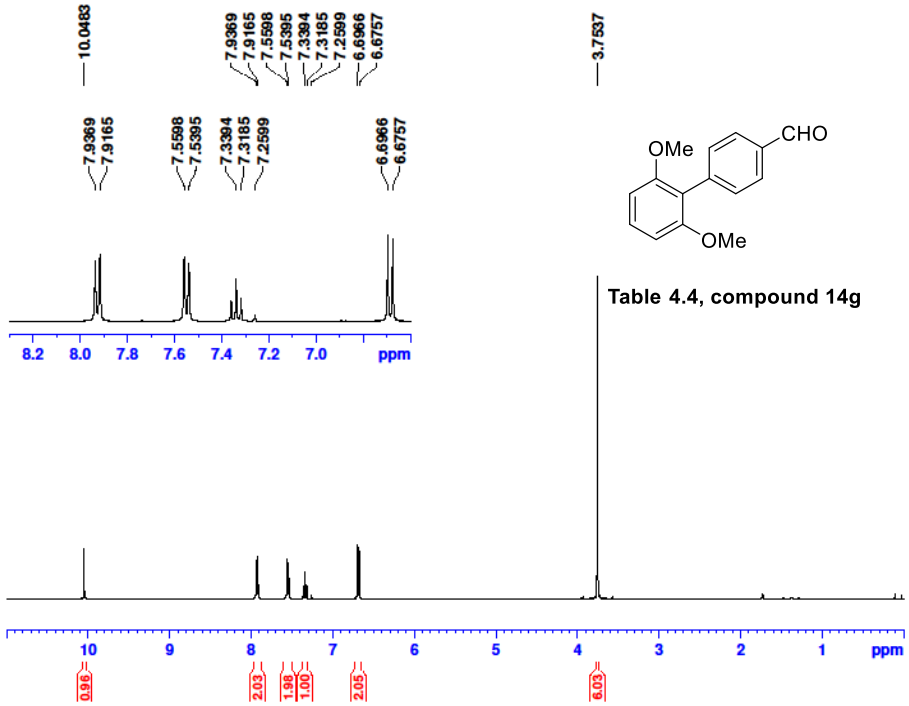

Table 4.4, compound 14g

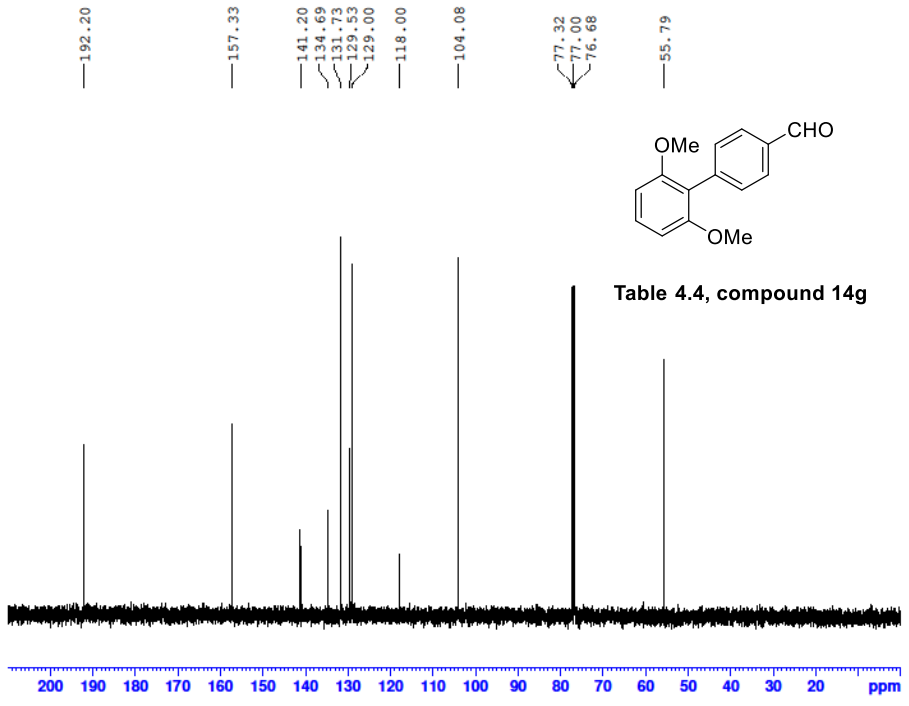

Table 4.4, compound 14g

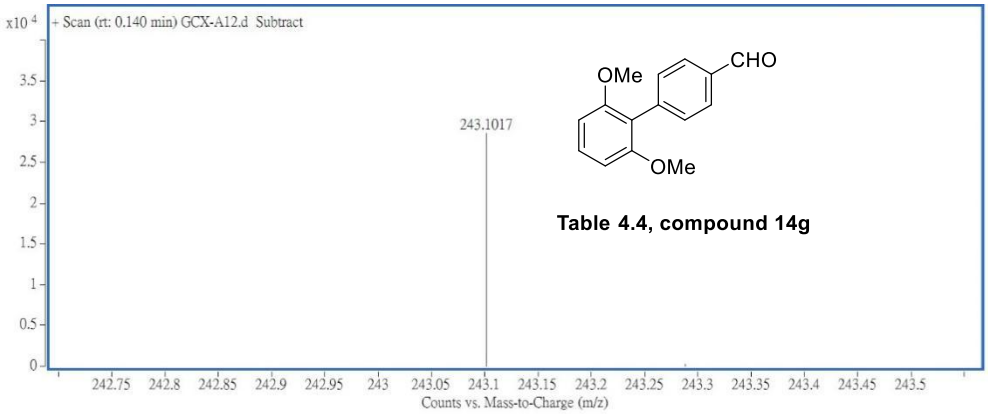

Table 4.4, compound 14g

Mass	m/z (Calc)	Diff (mDa)	Diff (ppm)	Formula
243.1017	243.1016	-0.13	-0.53	C15 H15 O3

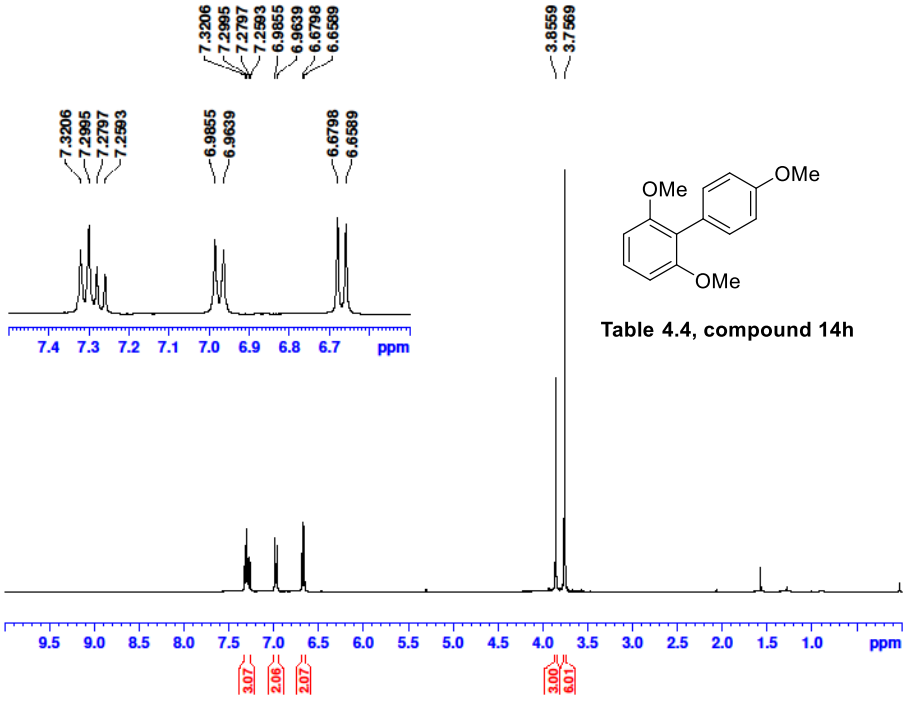

Table 4.4, compound 14h

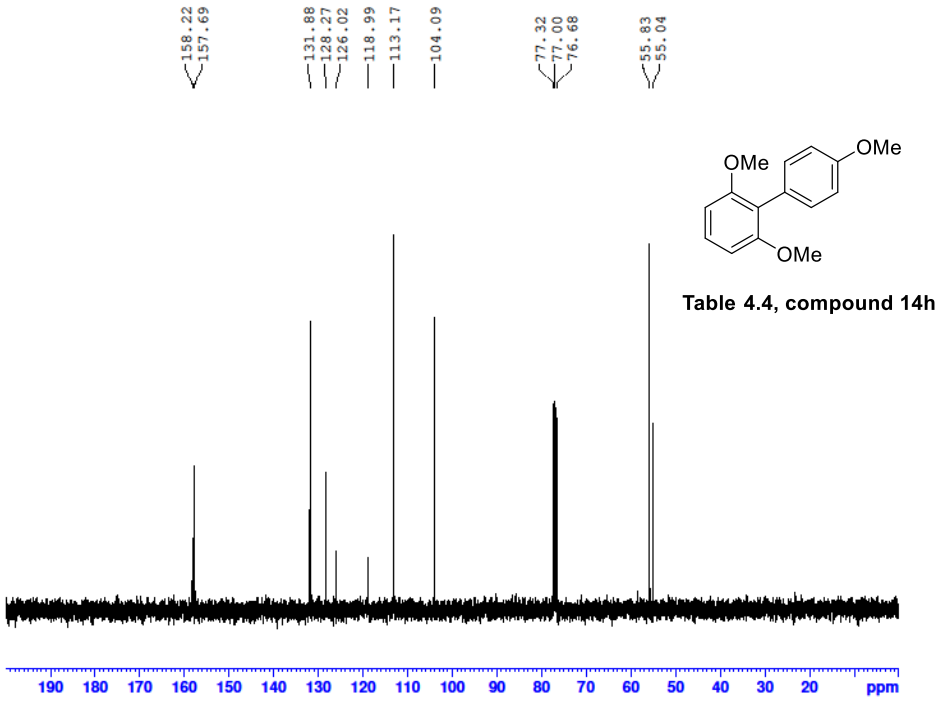

Table 4.4, compound 14h

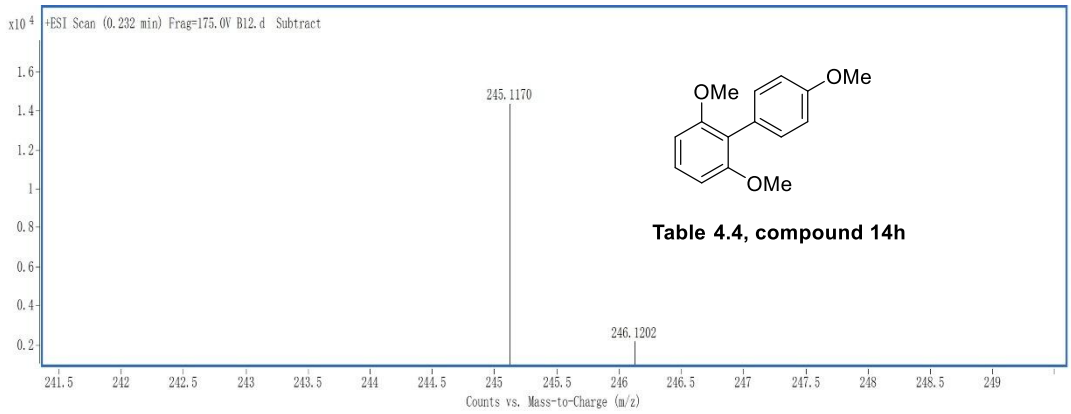

Table 4.4, compound 14h

Mass	m/z (Calc)	Diff (mDa)	Diff (ppm)	Formula
245.1170	245.1172	0.22	0.90	C15H17O3

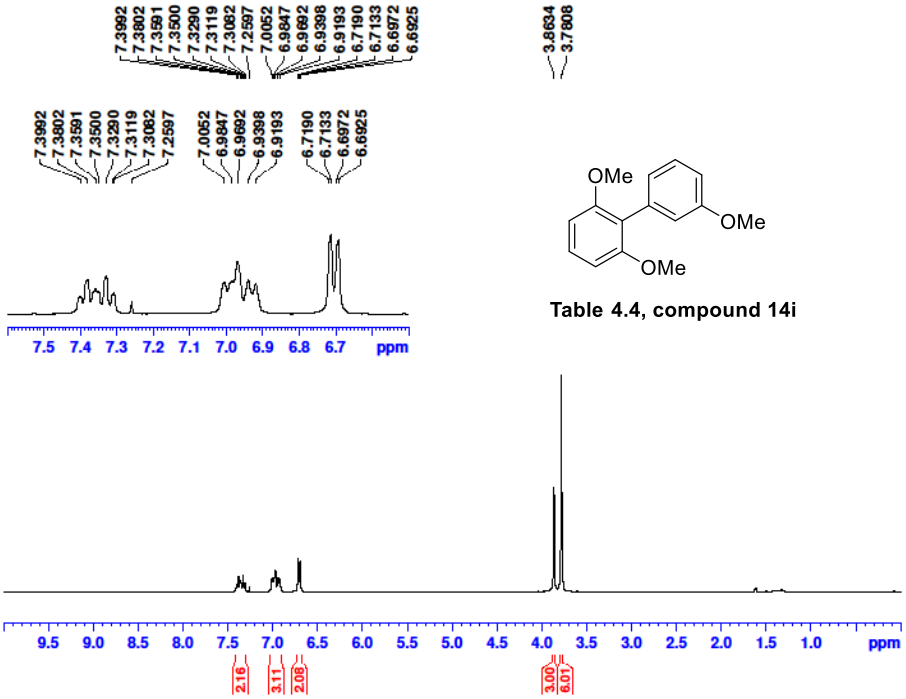

Table 4.4, compound 14i

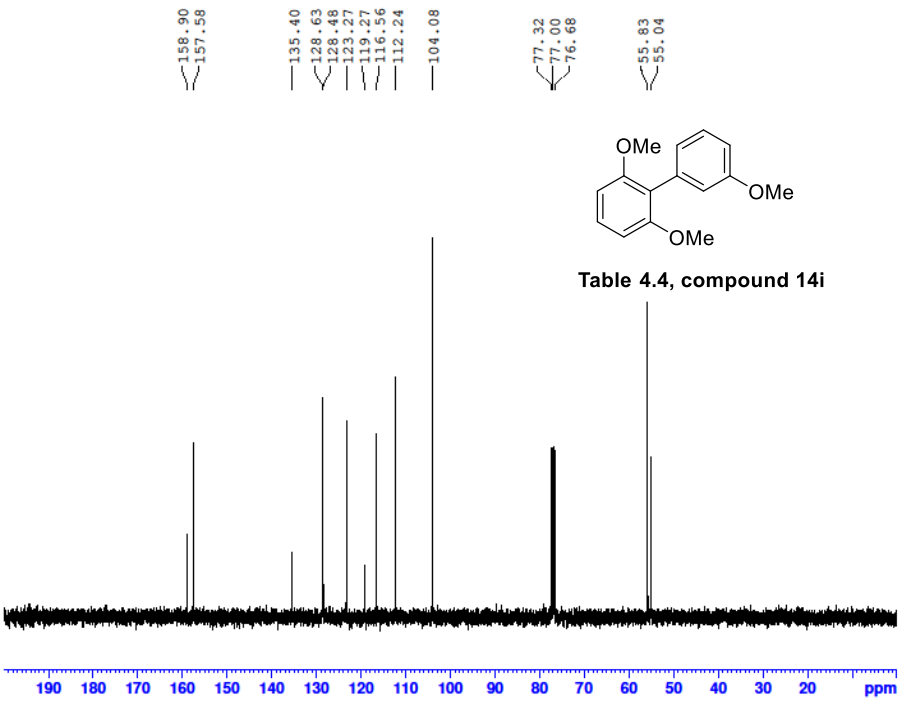

Table 4.4, compound 14i

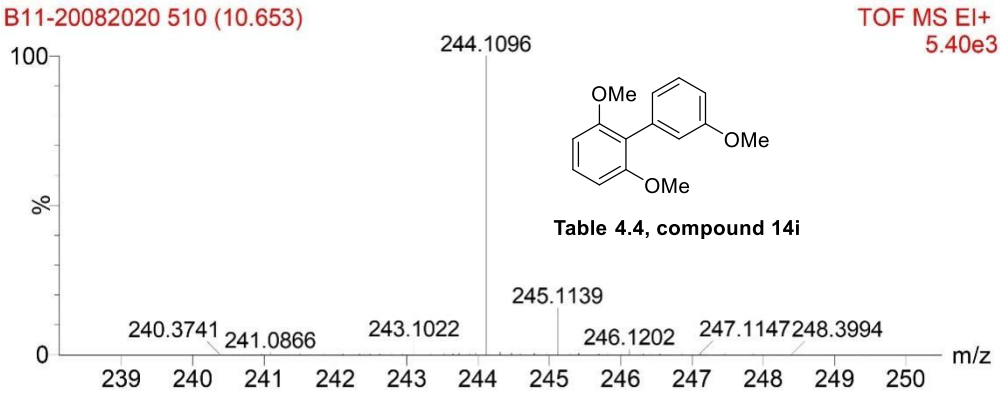

Table 4.4, compound 14i

Mass	m/z (Calc)	Diff (mDa)	Diff (ppm)	Formula
244.1096	244.1094	-0.20	-0.84	C15 H16O3

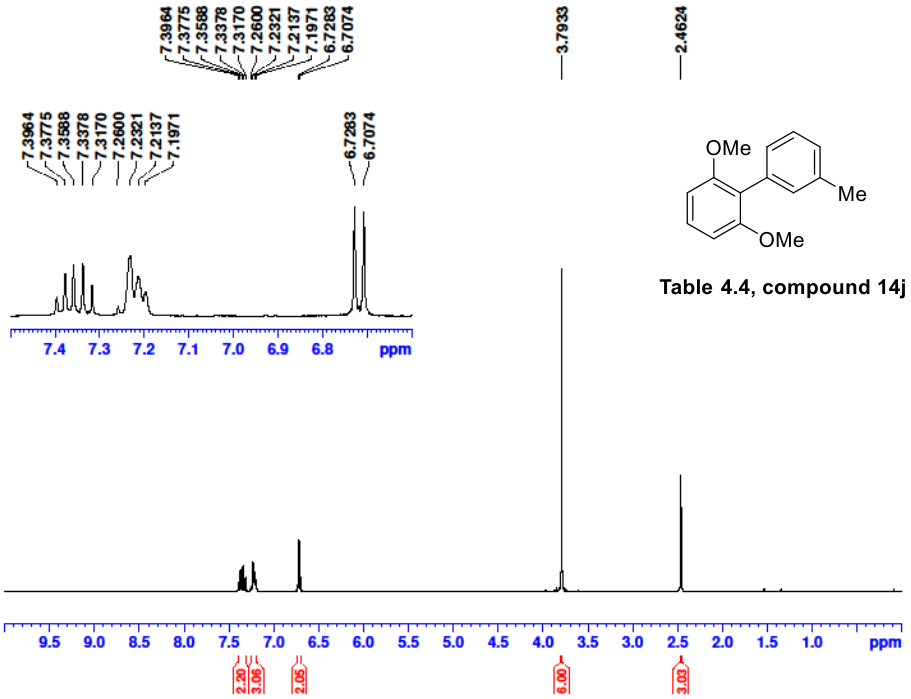

Table 4.4, compound 14j

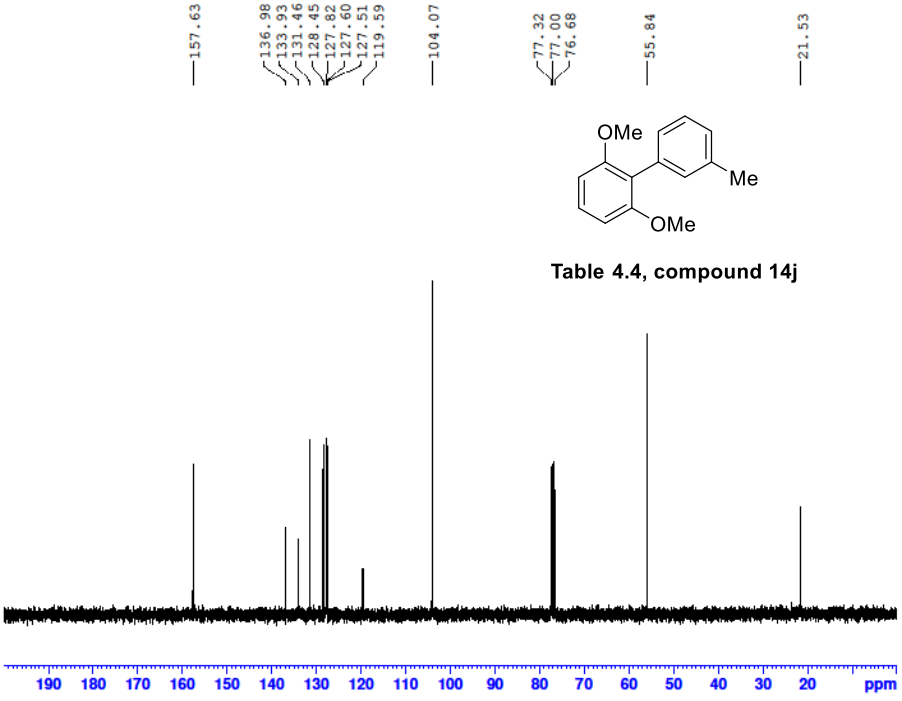

Table 4.4, compound 14j

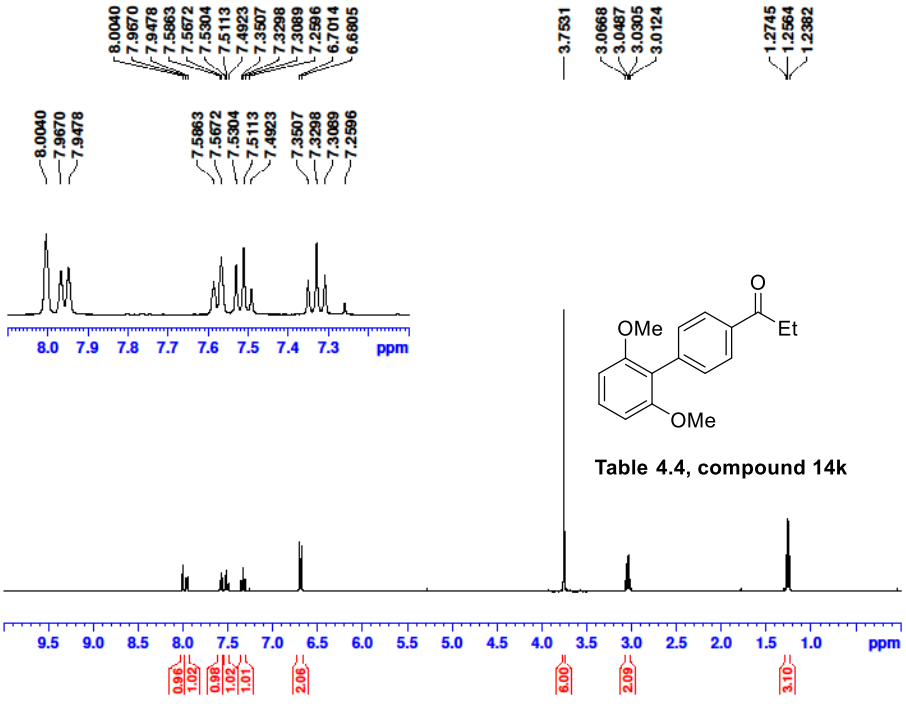

Table 4.4, compound 14k

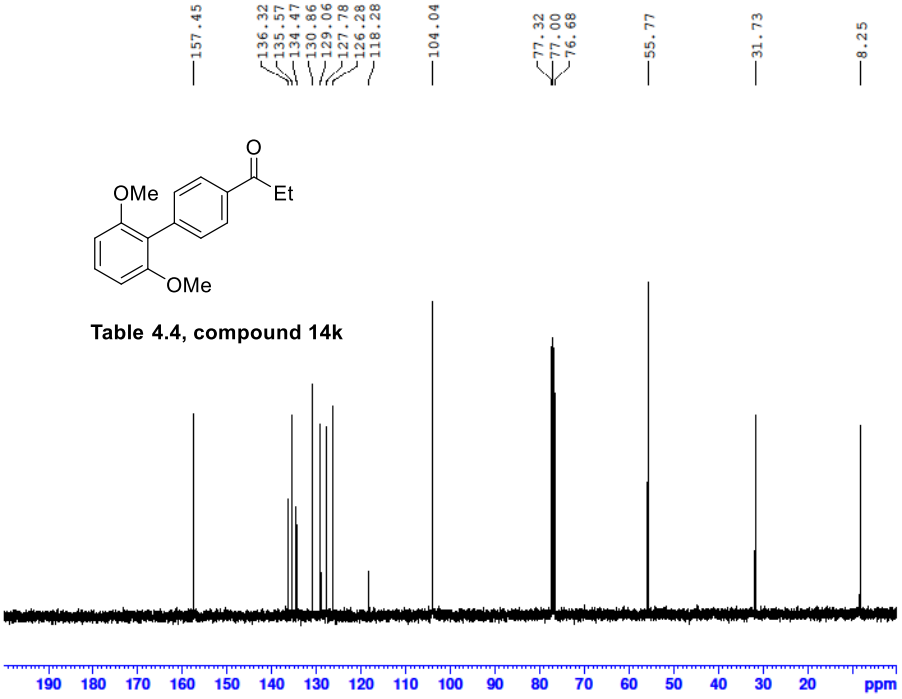

Table 4.4, compound 14k

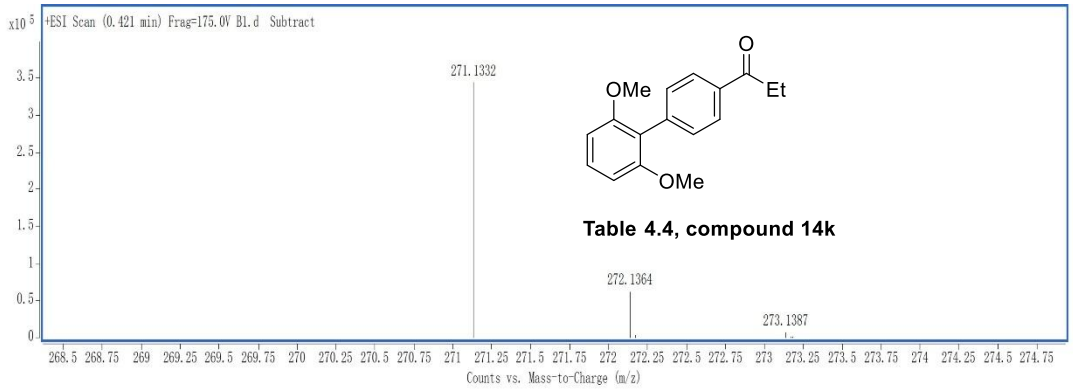

Table 4.4, compound 14k

Mass	m/z (Calc)	Diff (mDa)	Diff (ppm)	Formula
271.1332	271.1329	-0.33	-1.22	C17H19O3

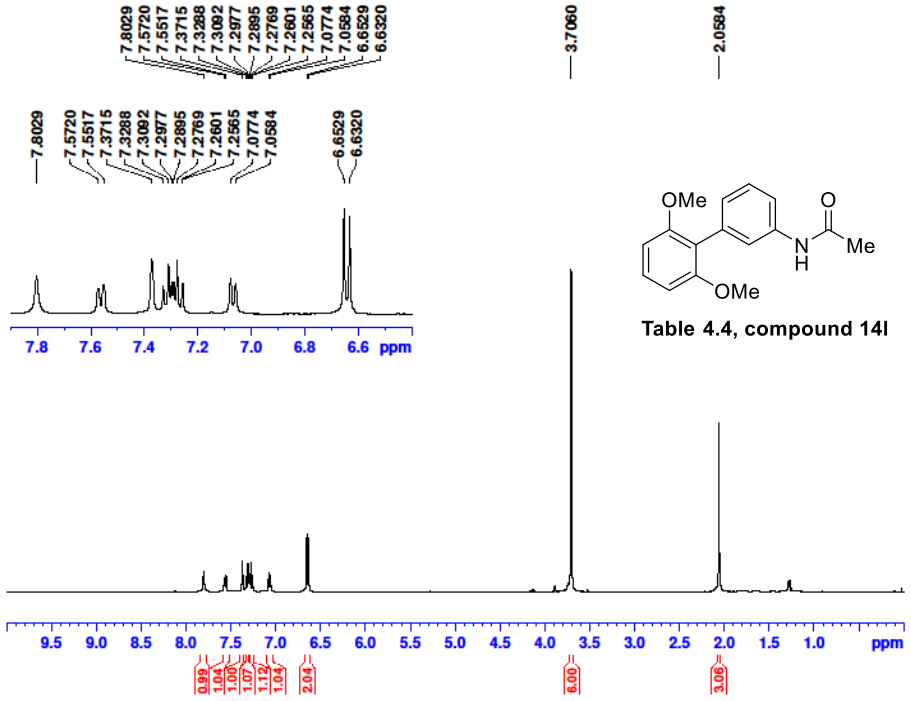

Table 4.4, compound 14l

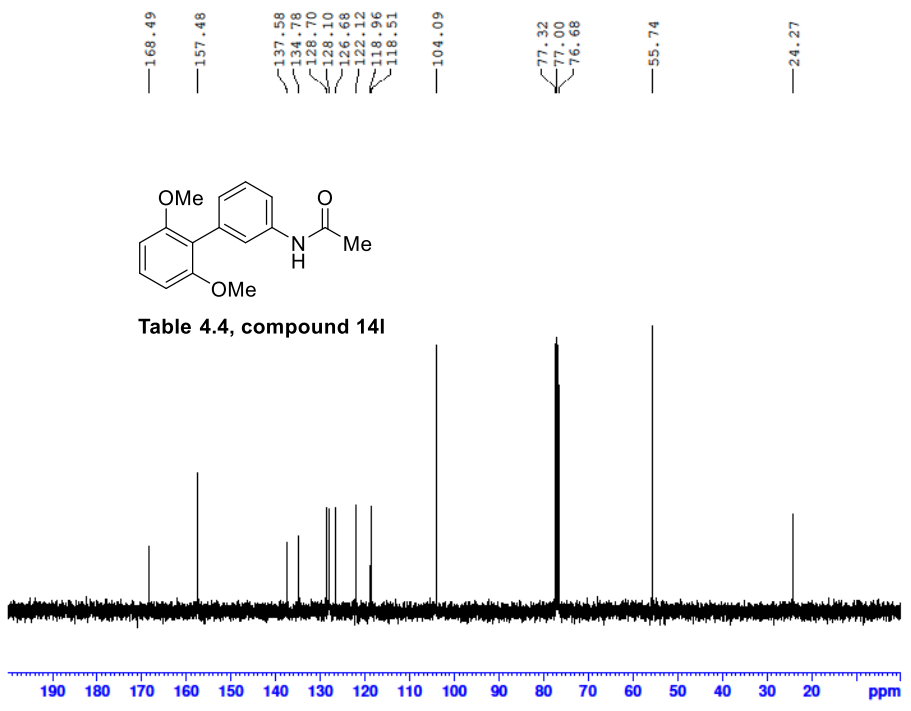

Table 4.4, compound 14l

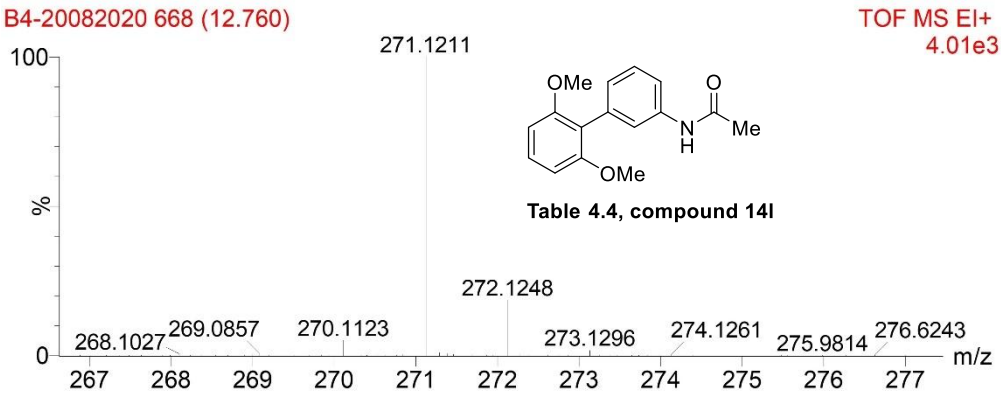

Table 4.4, compound 14l

Mass	m/z (Calc)	Diff (mDa)	Diff (ppm)	Formula
271.1211	271.1203	-0.29	-1.22	C16 H17NO3

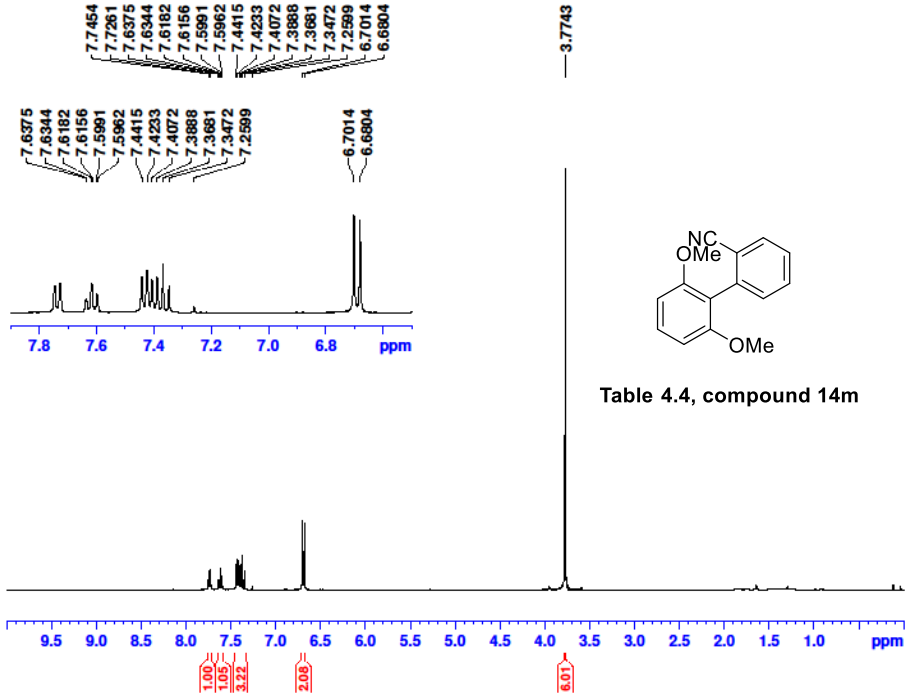

Table 4.4, compound 14m

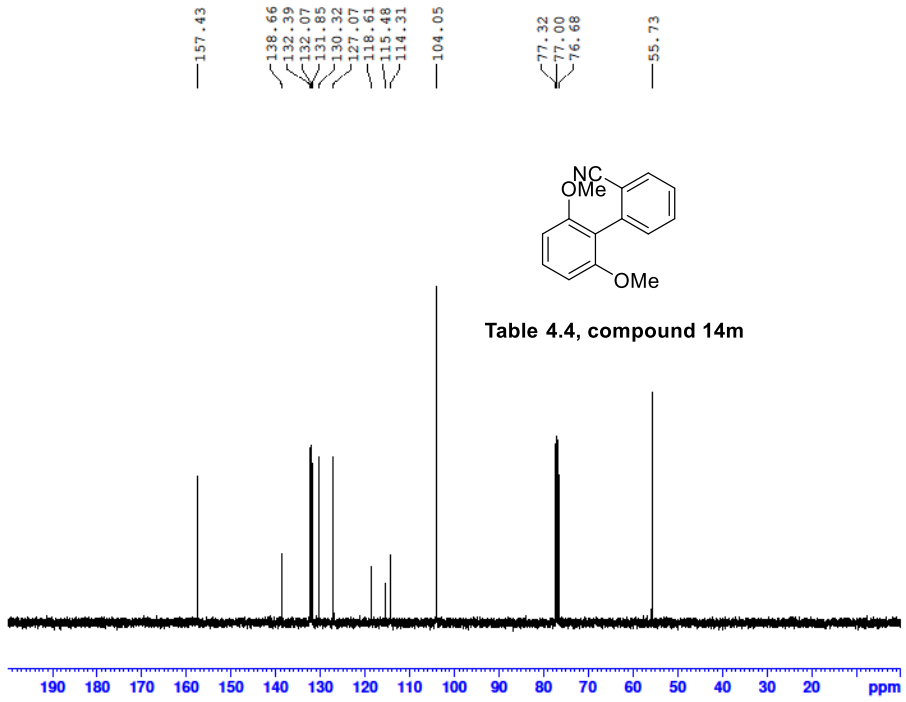

Table 4.4, compound 14m

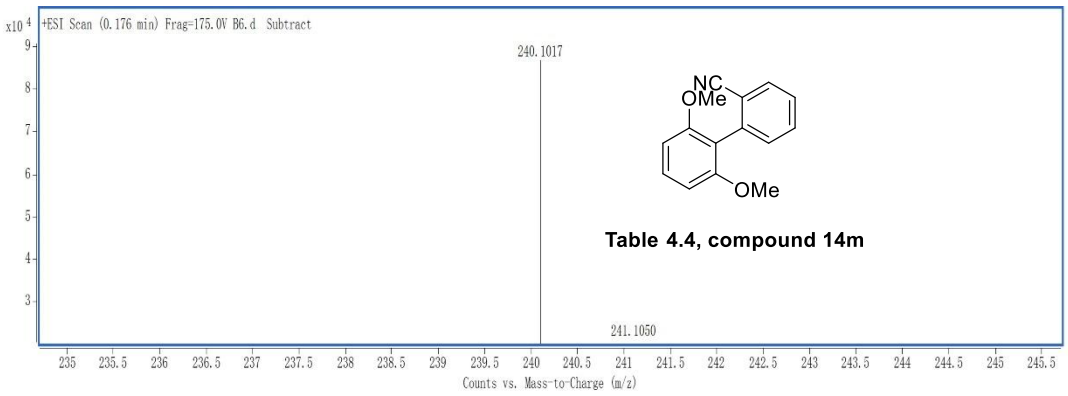

Table 4.4, compound 14m

Mass	m/z (Calc)	Diff (mDa)	Diff (ppm)	Formula
240.1017	240.1019	0.21	0.86	C15H14NO2

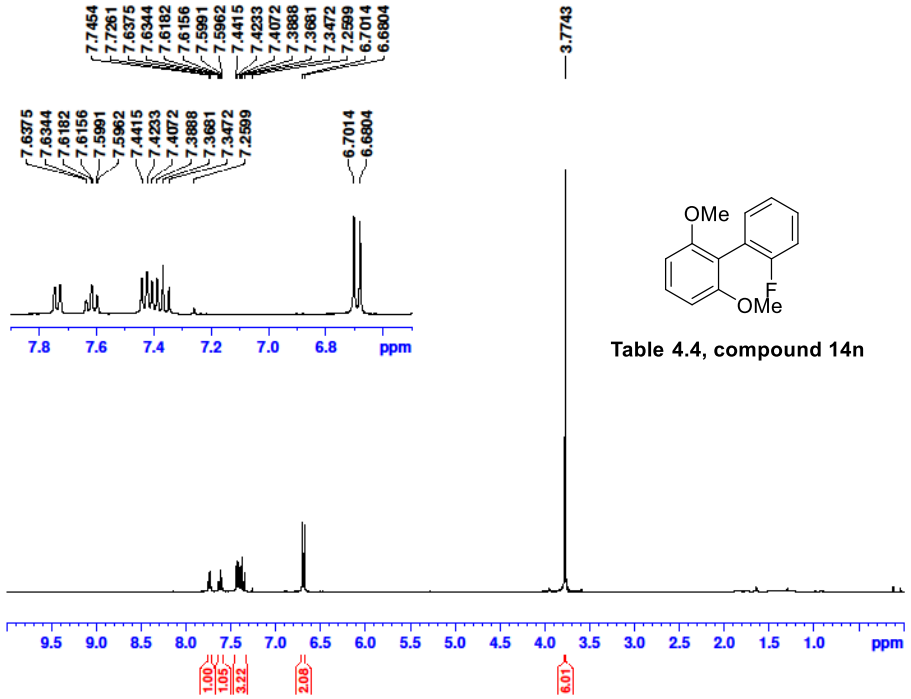

Table 4.4, compound 14n

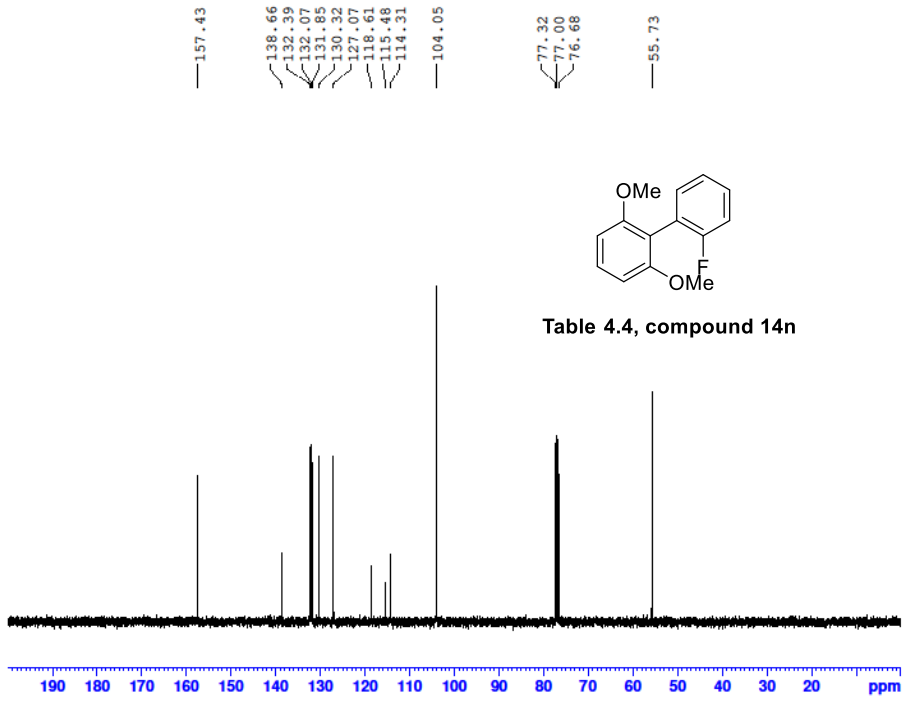

Table 4.4, compound 14n

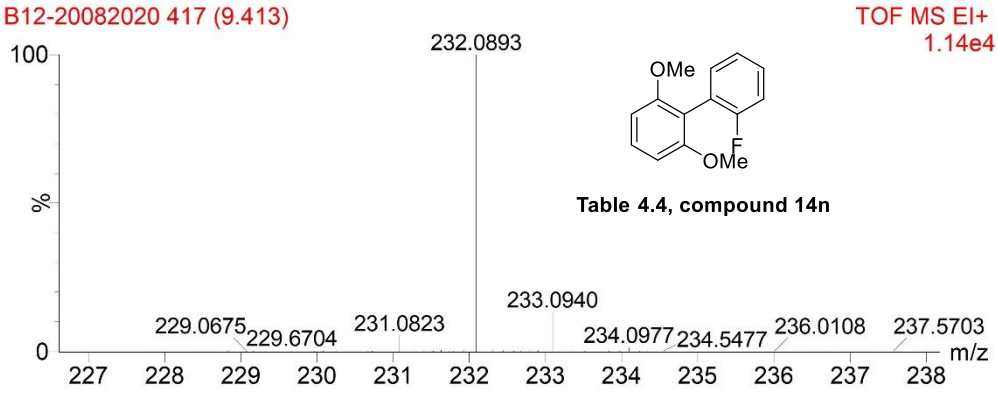

Table 4.4, compound 14n

Mass	m/z (Calc)	Diff (mDa)	Diff (ppm)	Formula
232.0893	232.0894	0.11	0.47	C14 H13FO2

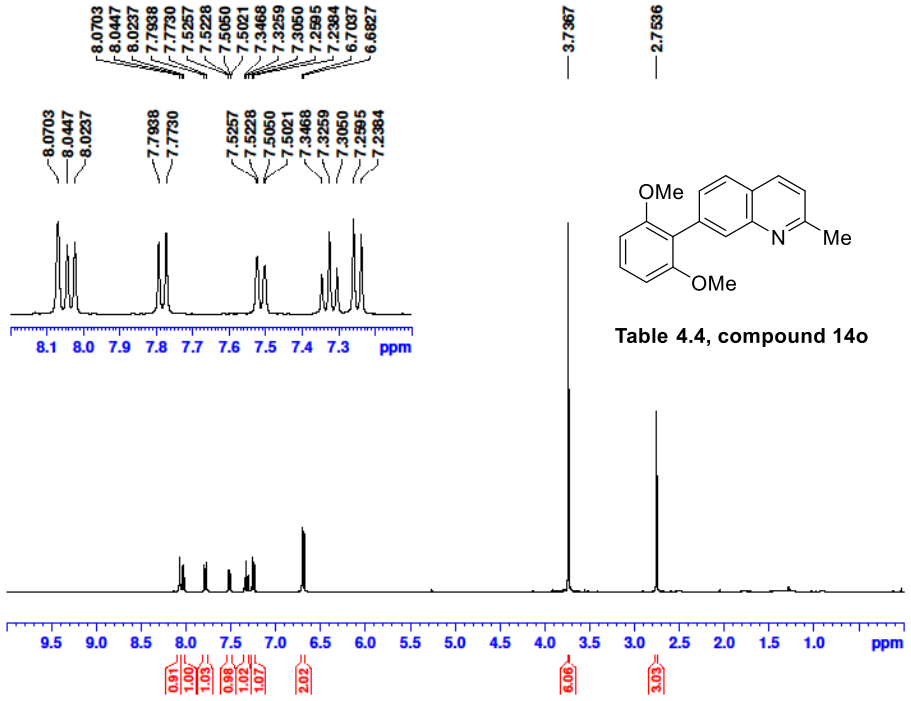

Table 4.4, compound 14o

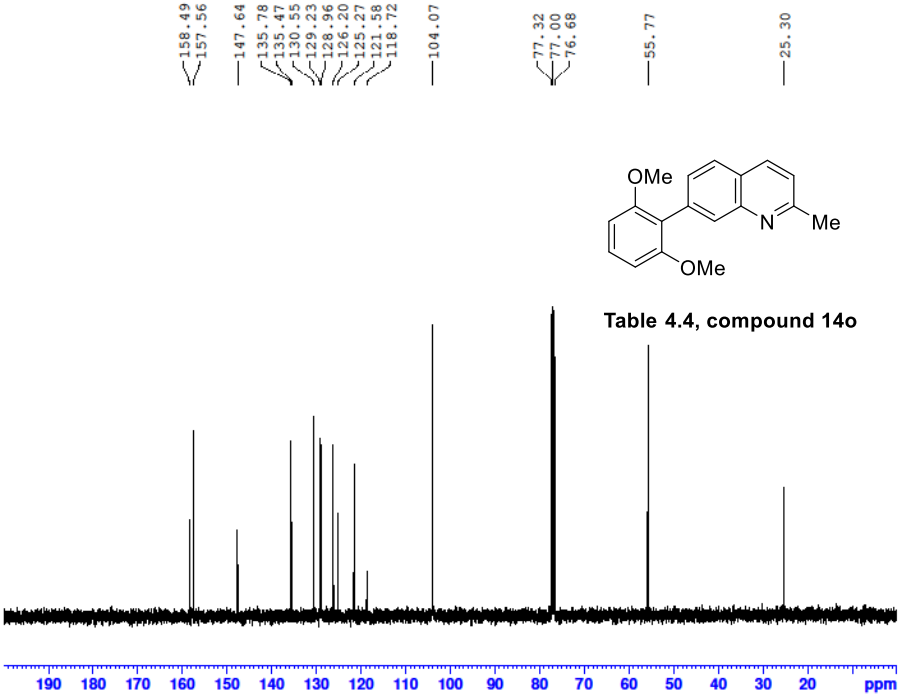

Table 4.4, compound 14o

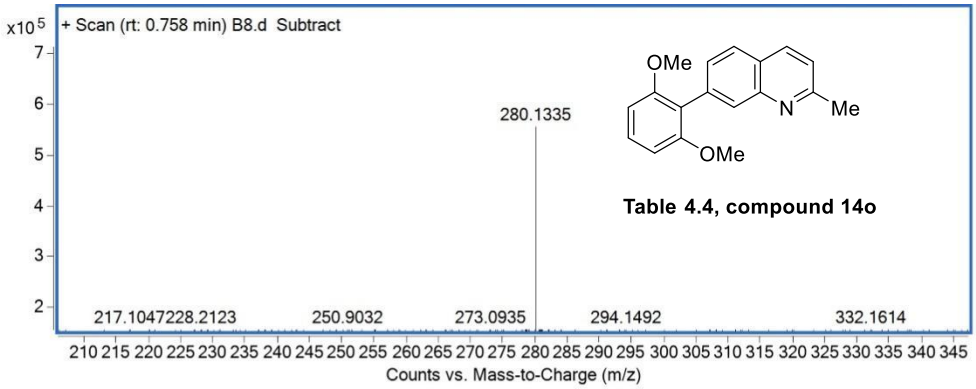

Table 4.4, compound 14o

Mass	Calc. Mass	mDa	PPM	Ion Formula
280.1335	280.1332	-0.29	-1.06	C18H18 O2N

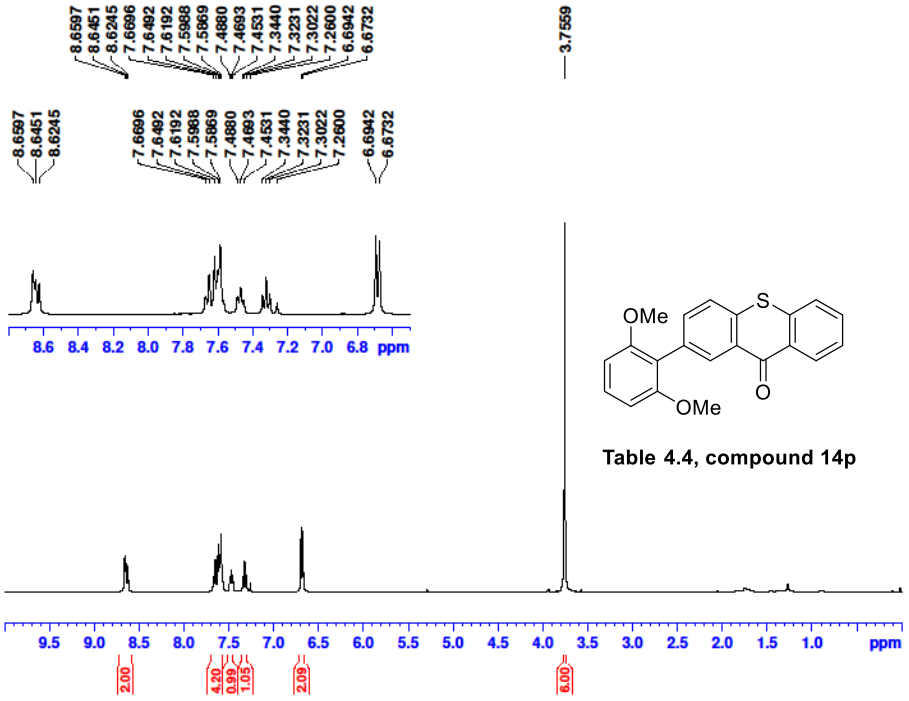

Table 4.4, compound 14p

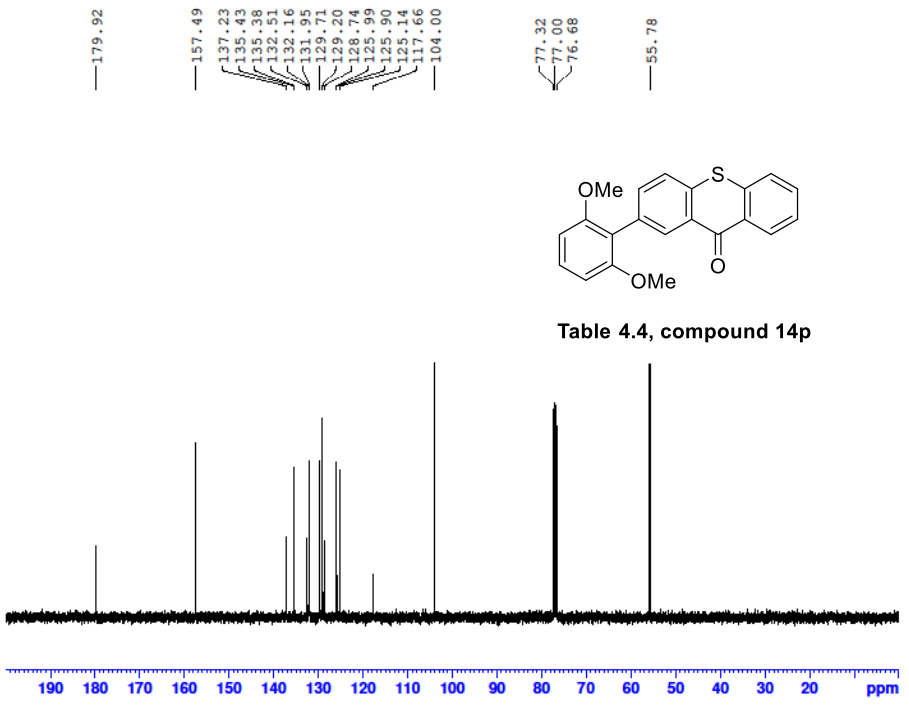

Table 4.4, compound 14p

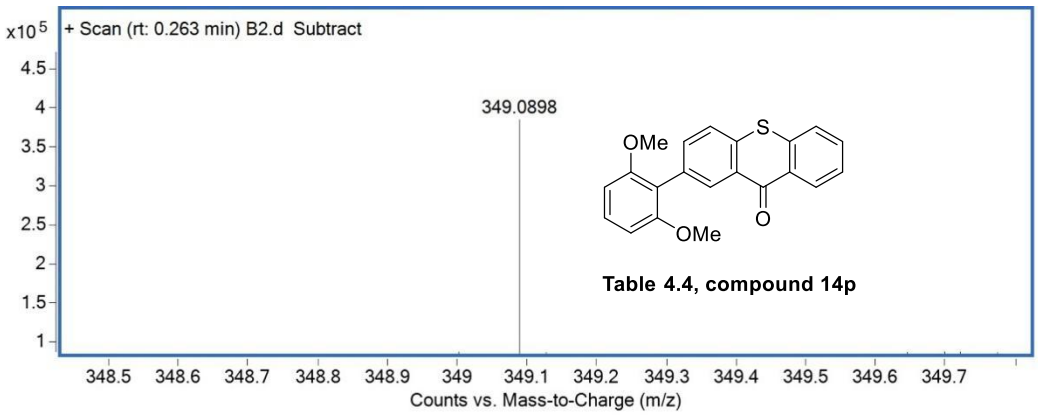

Table 4.4, compound 14p

Mass	Calc. Mass	mDa	PPM	Ion Formula
349.0898	349.0893	-0.51	-1.46	C21H17 O3 S

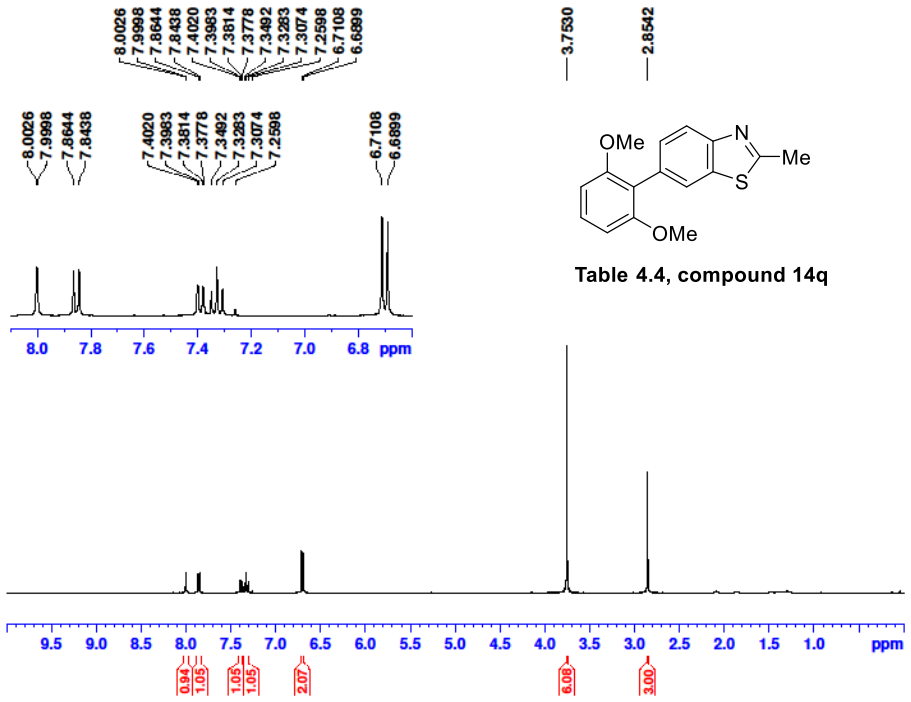

Table 4.4, compound 14q

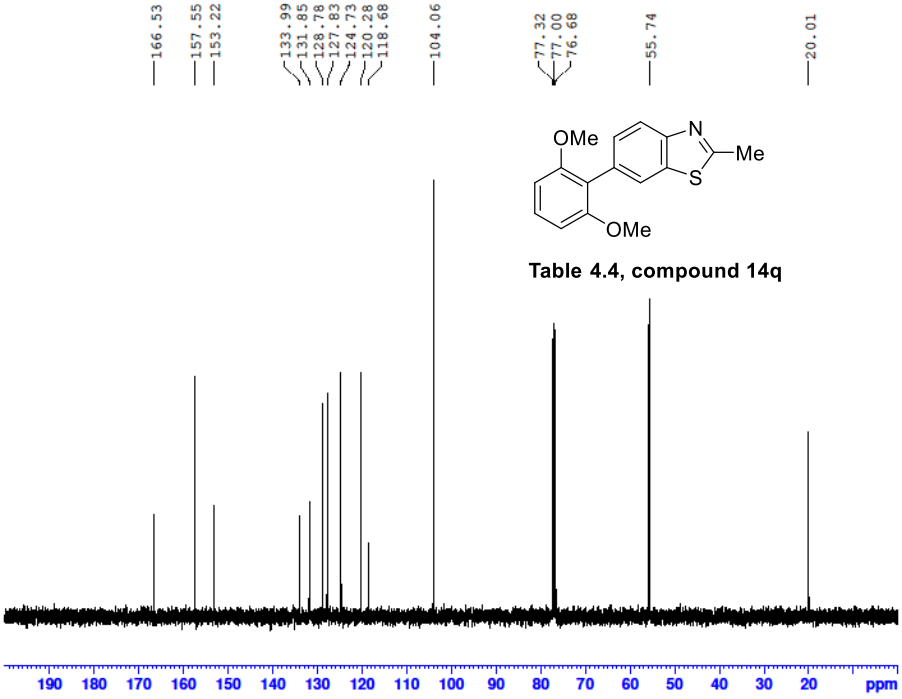

Table 4.4, compound 14q

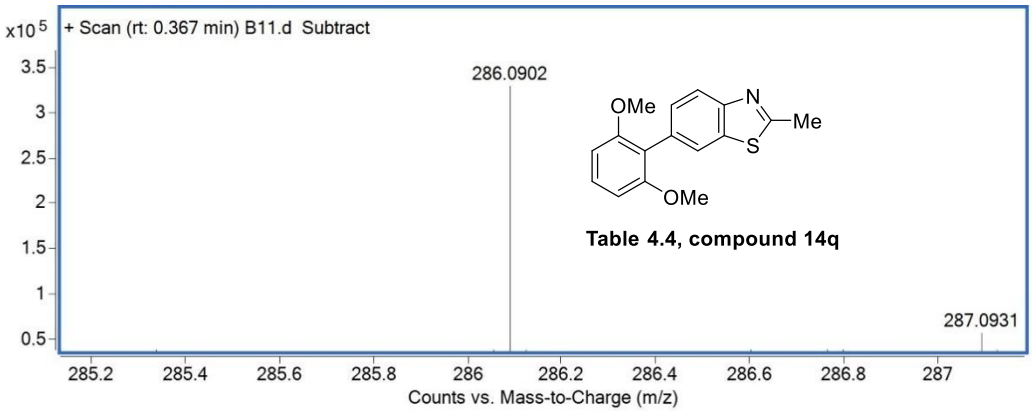

Table 4.4, compound 14q

Mass	Calc. Mass	mDa	PPM	Ion Formula
286.0902	286.0896	-0.57	-2.01	C16H16 NO2S

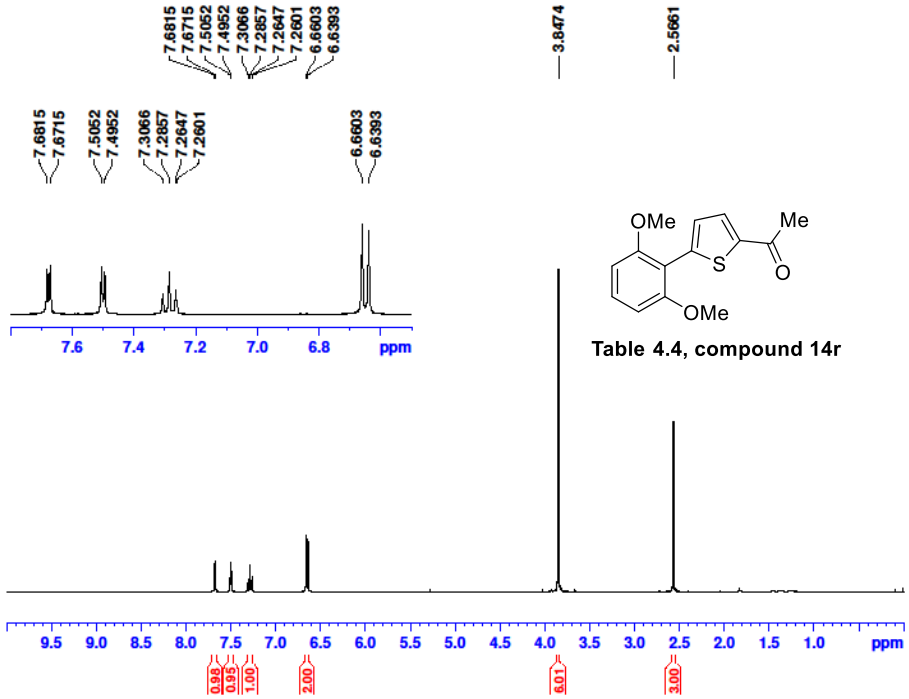

Table 4.4, compound 14r

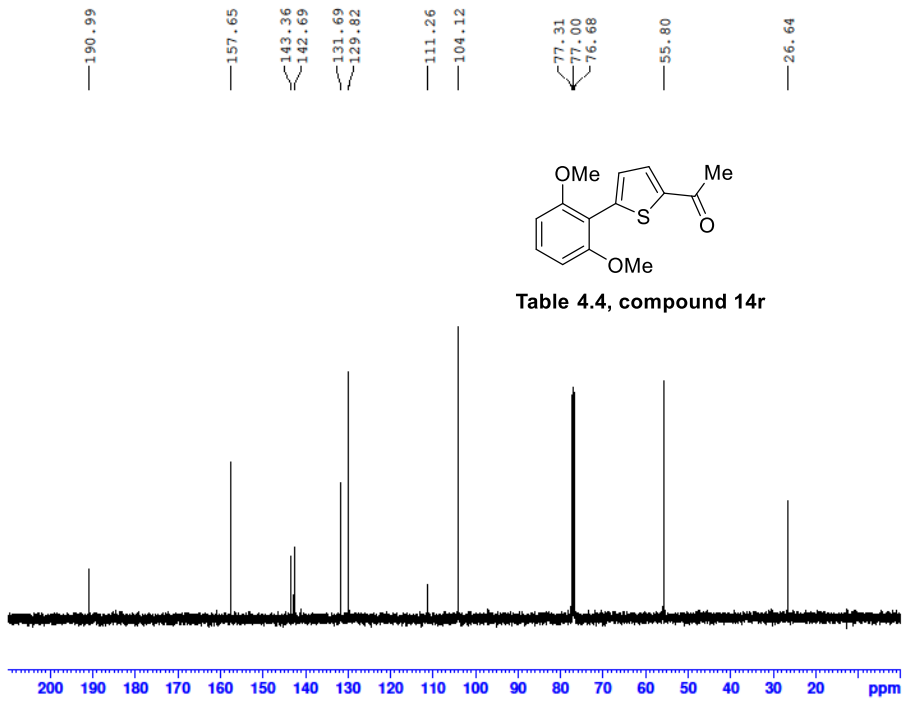

Table 4.4, compound 14r

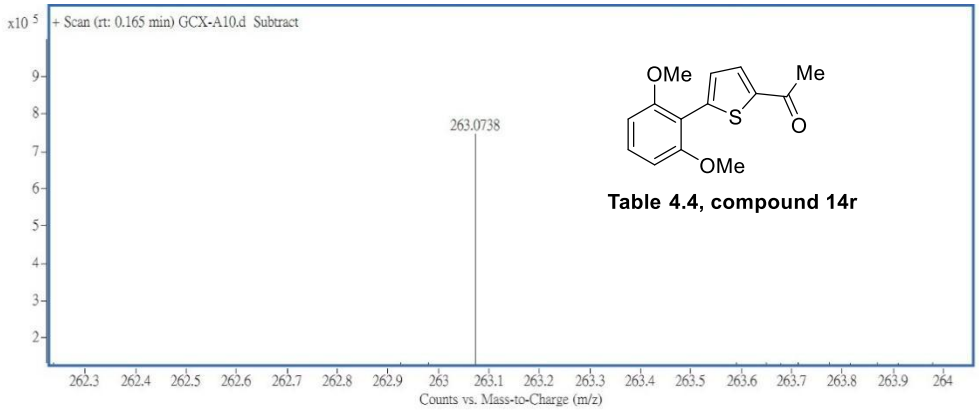

Table 4.4, compound 14r

Mass	m/z (Calc)	Diff (mDa)	Diff (ppm)	Formula
263.0738	263.0736	-0.16	-0.6	C14 H15 O3 S

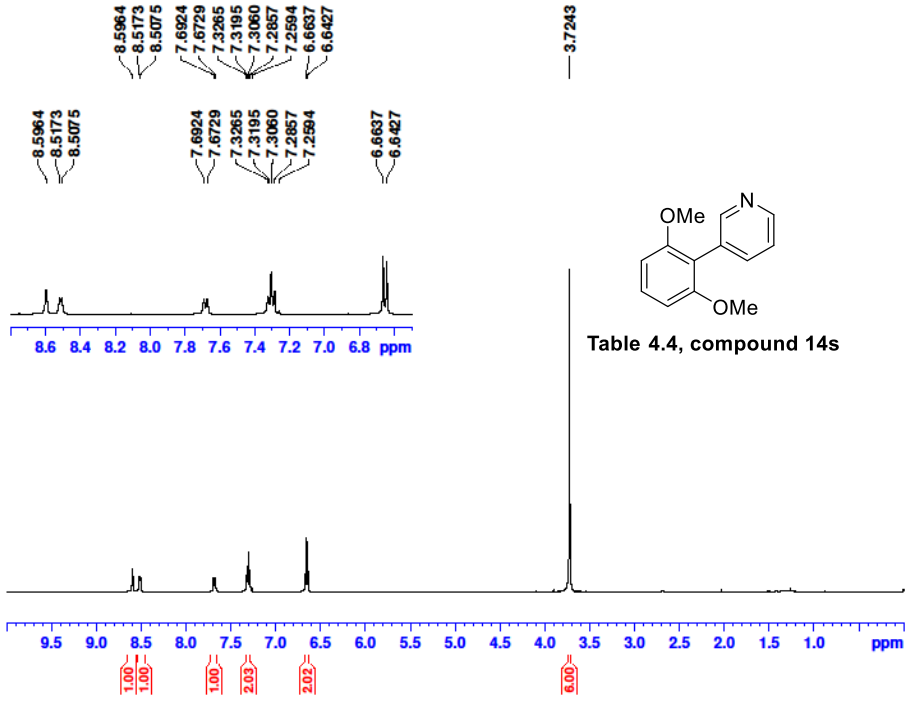

Table 4.4, compound 14s

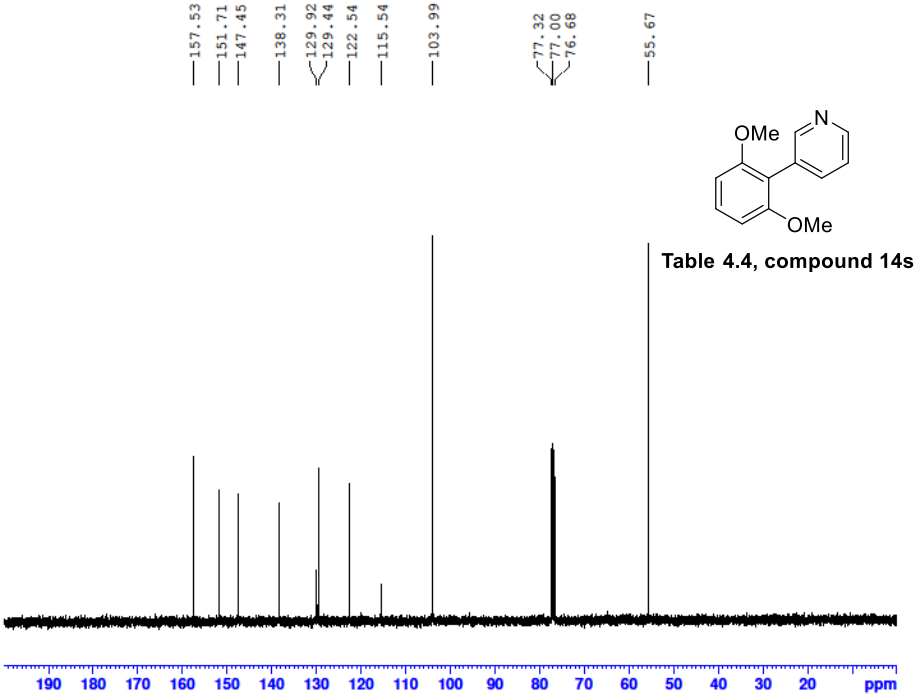

Table 4.4, compound 14s

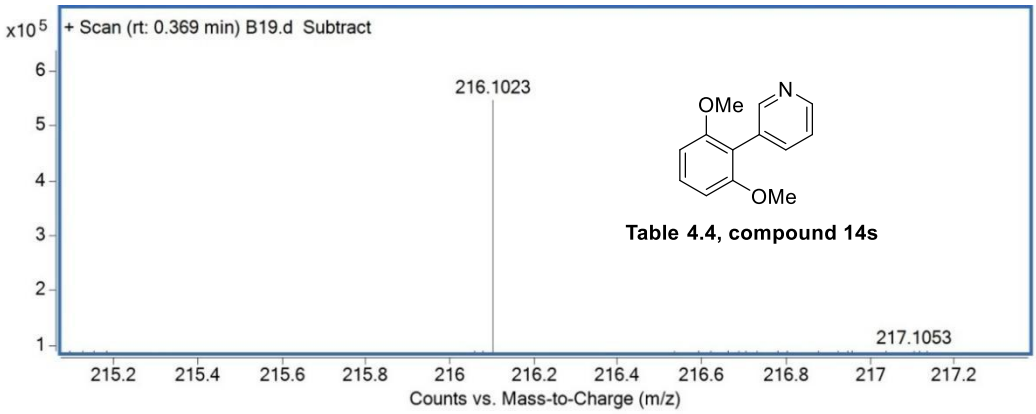

Table 4.4, compound 14s

Mass	Calc. Mass	mDa	PPM	Ion Formula
216.1023	216.1019	-0.39	-1.84	C13H14 N3O2

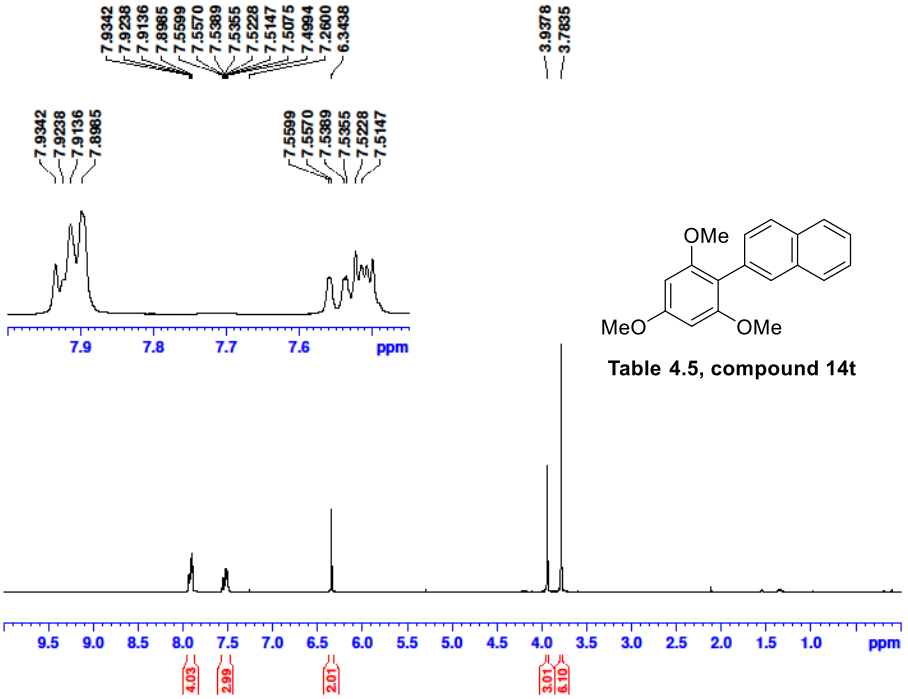
7.9342
7.9238
7.9136
7.8985
7.5599
7.5570
7.5389
7.5355
7.5228
7.5147
7.5075
7.4994
7.2600
6.3438
3.9378
3.7835
OMe
MeO
OMe
Table 4.5, compound 14t
ppm
4.03
2.99
2.01
3.01
6.10

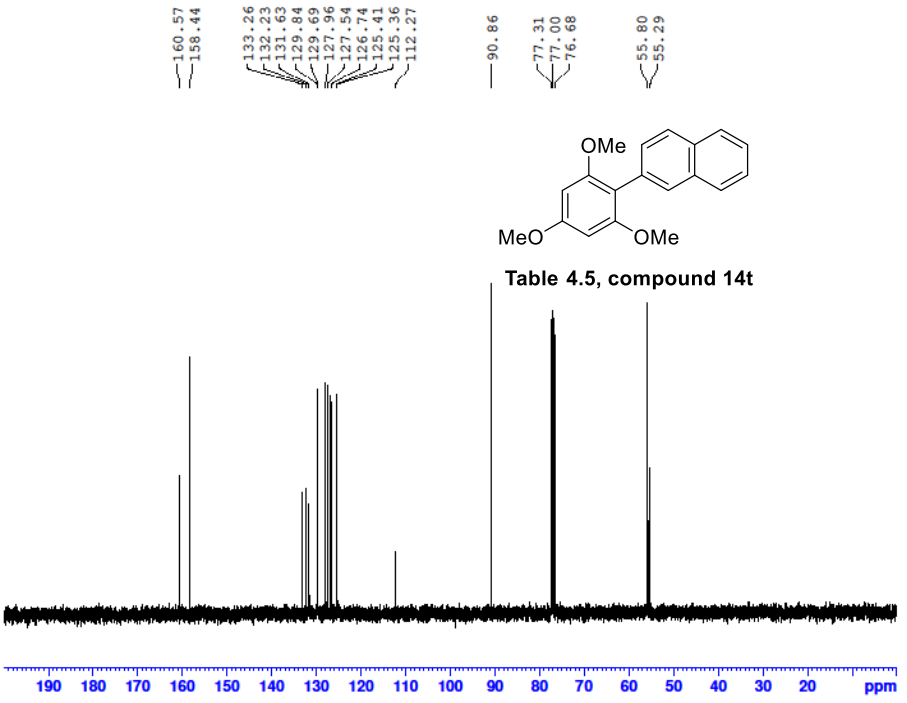
160.57
158.44
133.26
132.23
131.63
129.84
129.69
127.96
127.54
126.74
125.41
125.36
112.27
90.86
77.31
77.00
76.68
55.80
55.29
OMe
MeO
OMe
Table 4.5, compound 14t
ppm

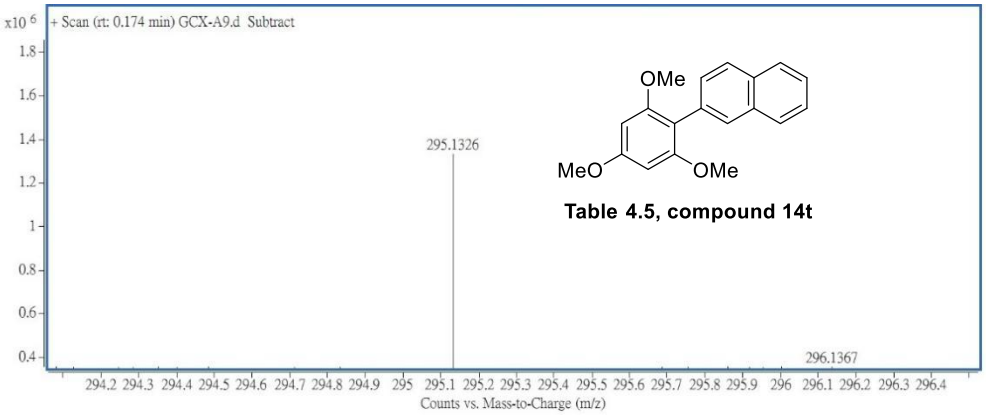

Table 4.5, compound 14t

Mass	m/z (Calc)	Diff (mDa)	Diff (ppm)	Formula
295.1326	295.1329	0.27	0.92	C19 H19 O3

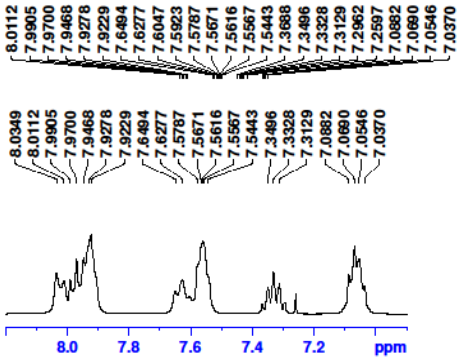

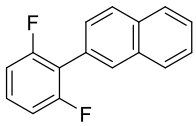

Table 4.5, compound 14u

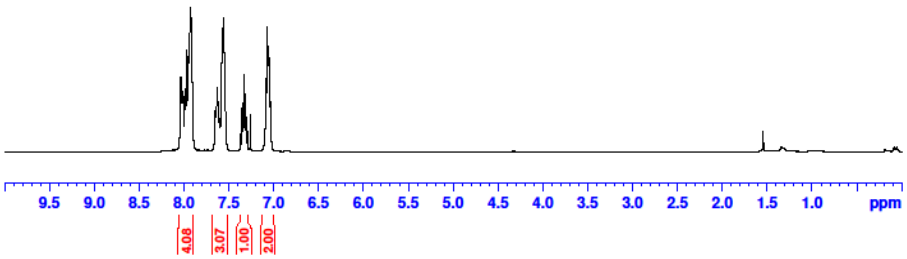

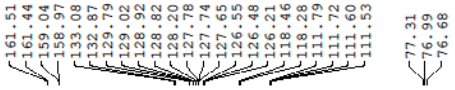

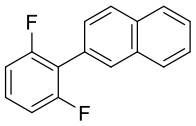

Table 4.5, compound 14u

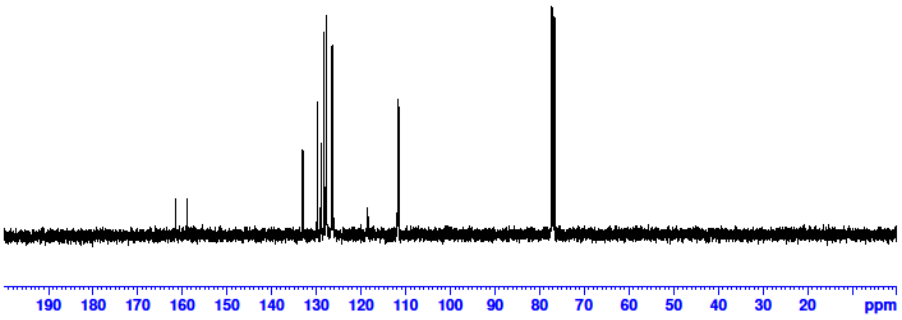

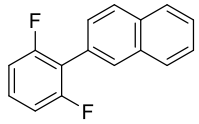

Table 4.5, compound 14u

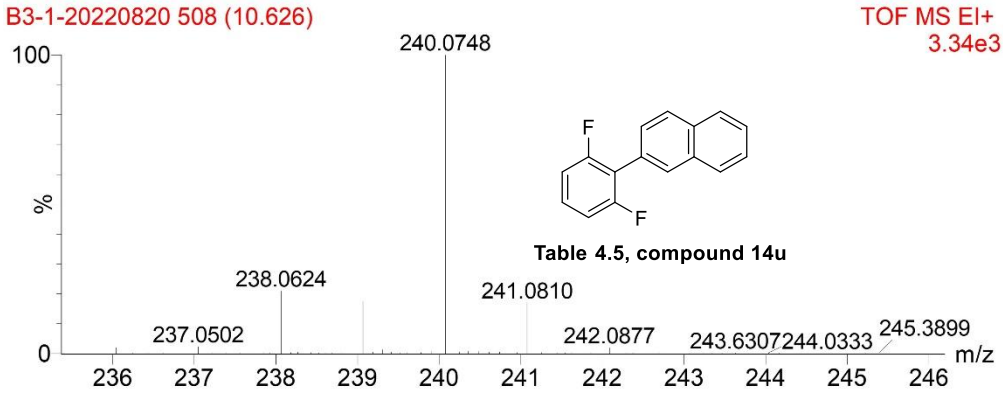

Table 4.5, compound 14u

Mass	m/z (Calc)	Diff (mDa)	Diff (ppm)	Formula
240.0748	240.0745	-0.29	-1.22	C16 H10F2

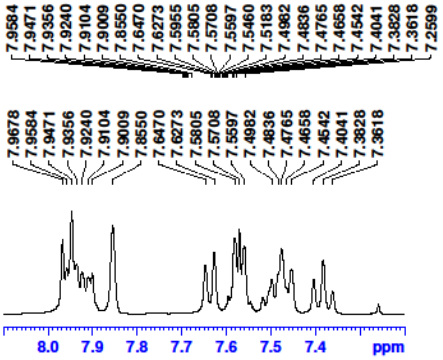

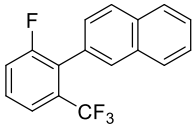

Table 4.5, compound 14v

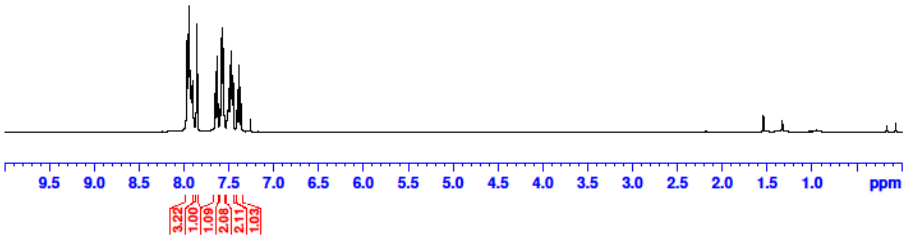

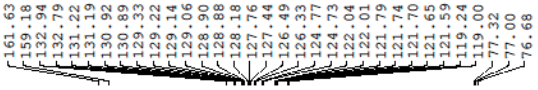

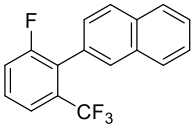

Table 4.5, compound 14v

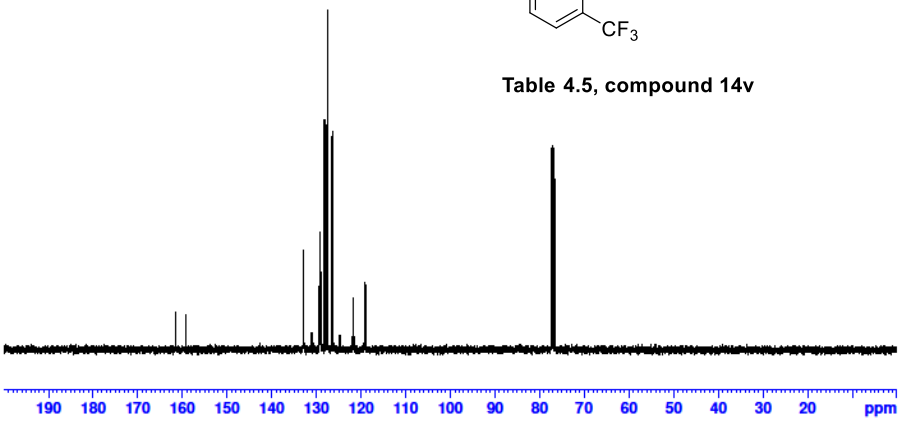

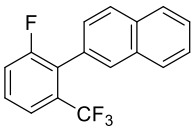

Table 4.5, compound 14v

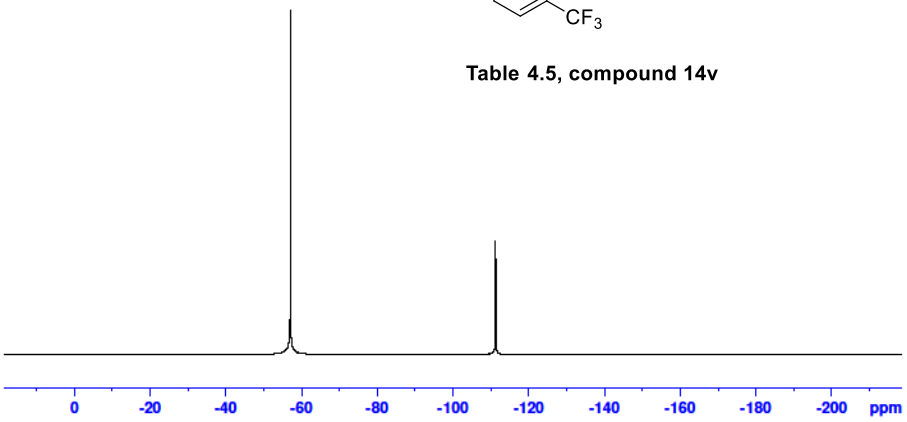

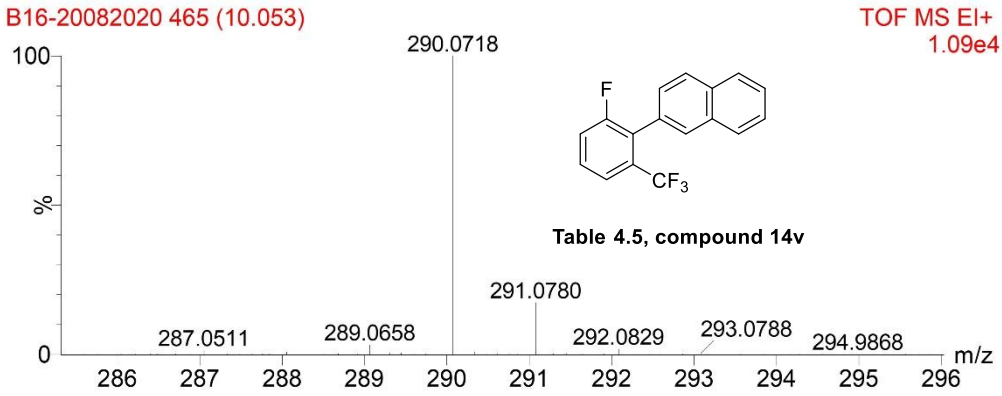

Table 4.5, compound 14v

Mass	m/z (Calc)	Diff (mDa)	Diff (ppm)	Formula
290.0718	290.0713	-0.49	-1.67	C17 H10F4

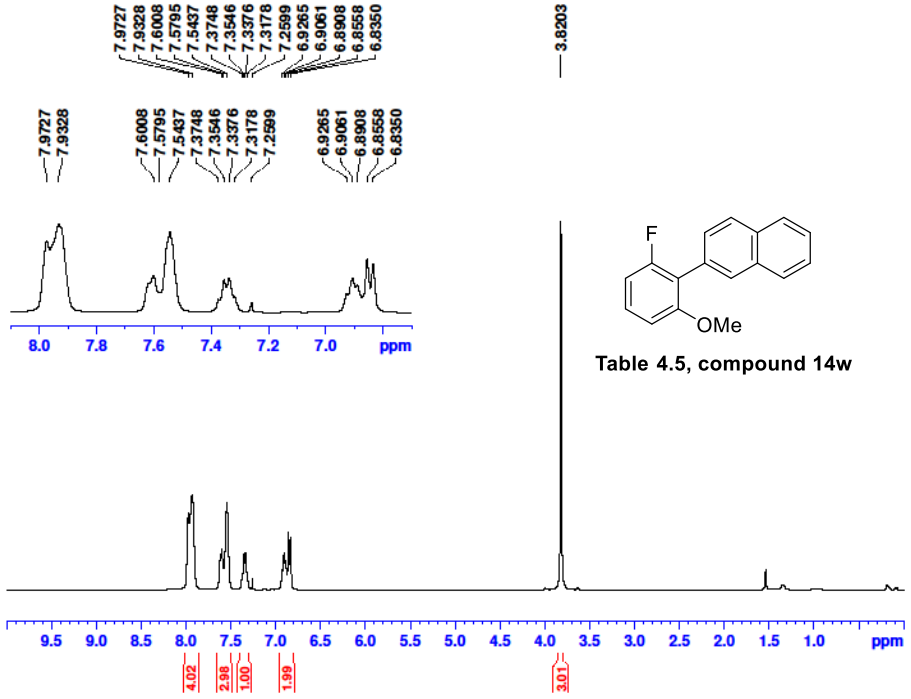

Table 4.5, compound 14w

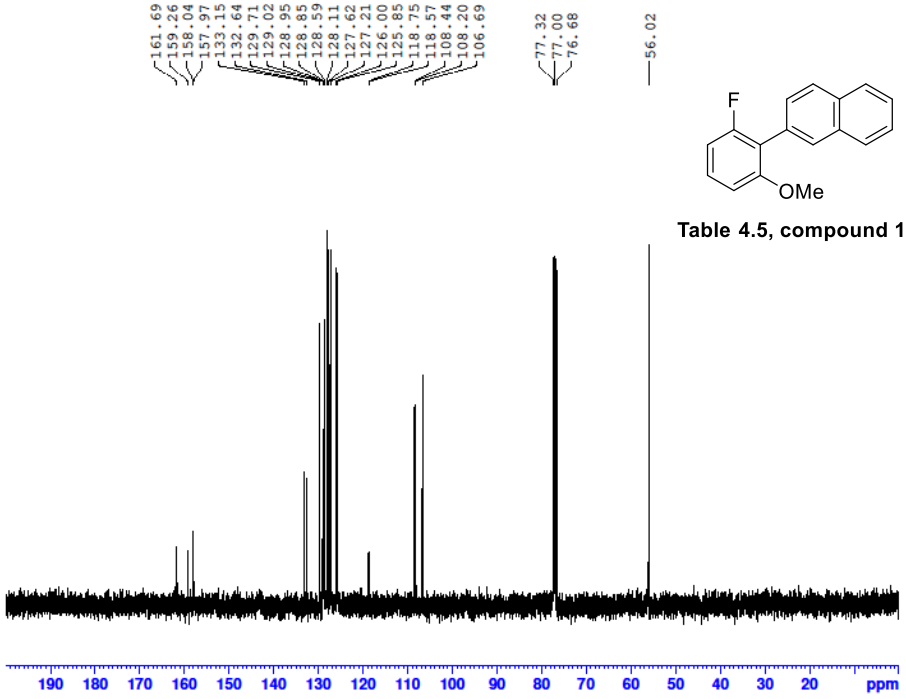

Table 4.5, compound 14w

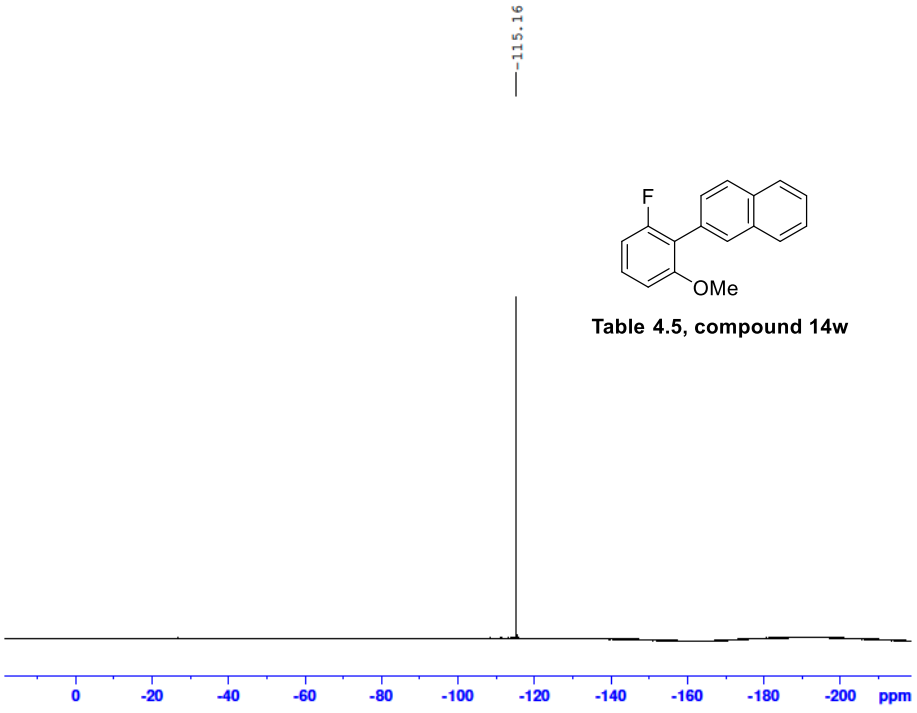

Table 4.5, compound 14w

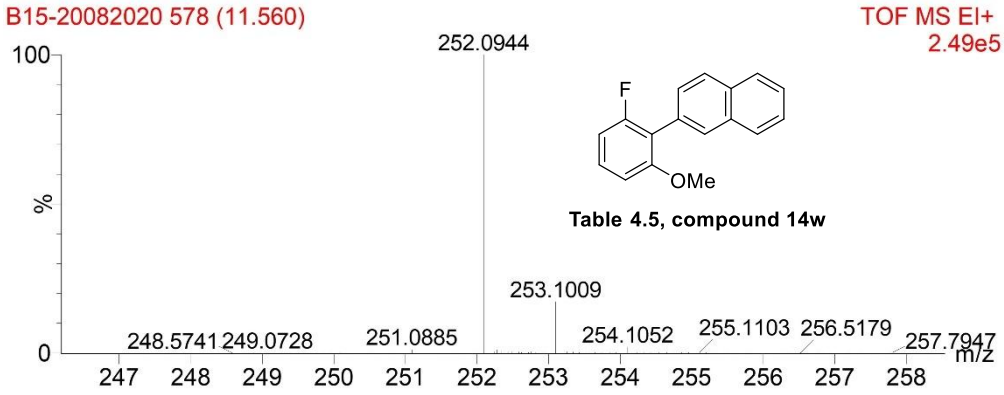

Table 4.5, compound 14w

Mass	m/z (Calc)	Diff (mDa)	Diff (ppm)	Formula
252.0944	252.0945	0.09	0.38	C17 H13FO

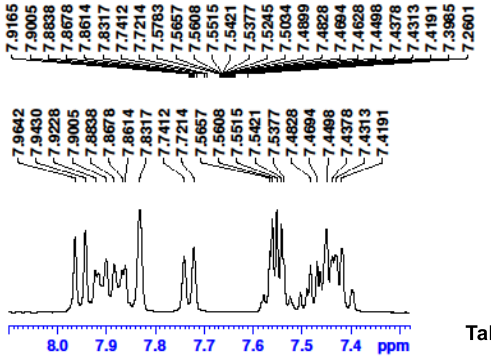

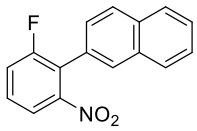

Table 4.5, compound 14x

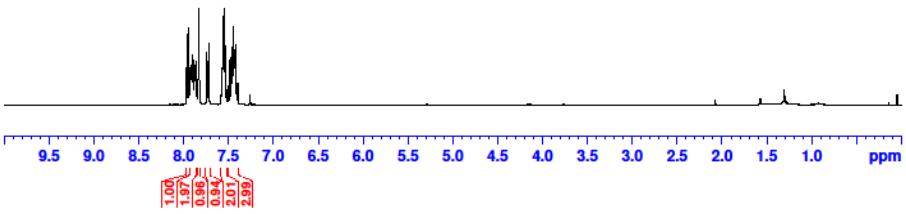

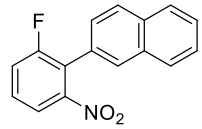

Table 4.5, compound 14x

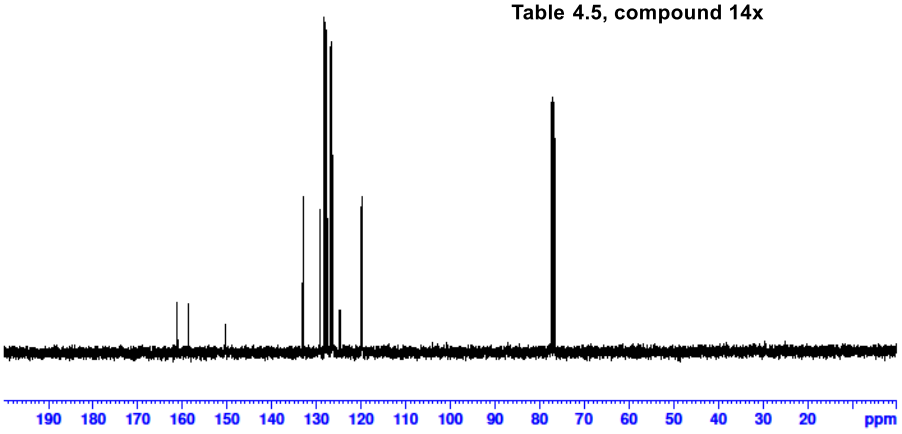

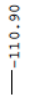

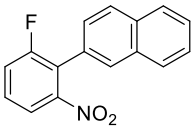

Table 4.5, compound 14x

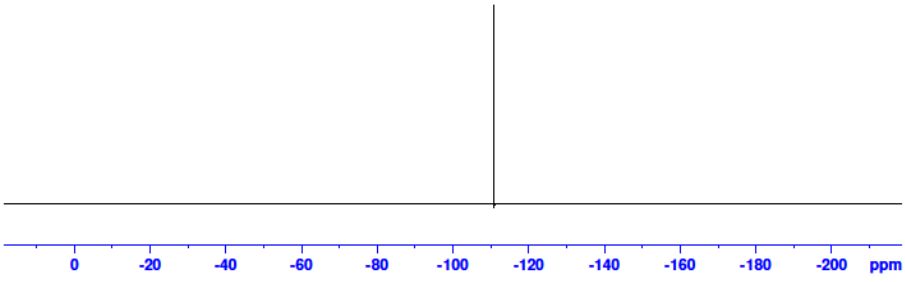

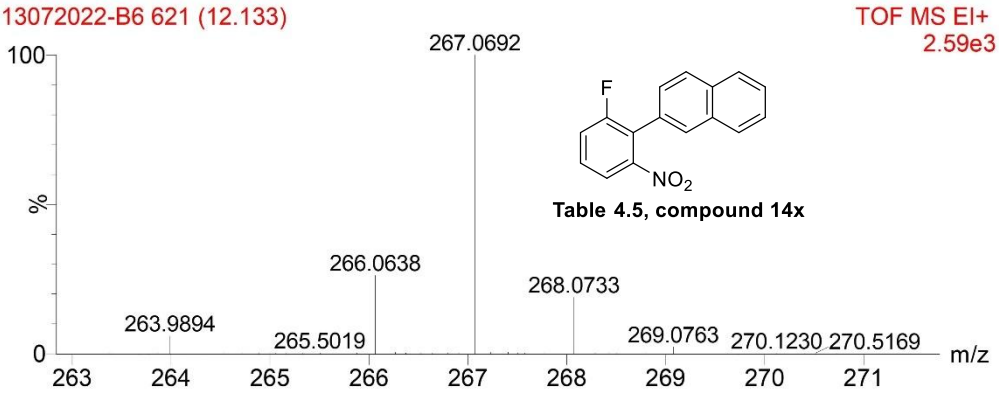

Table 4.5, compound 14x

Mass	Calc. Mass	mDa	PPM	Ion Formula
267.0692	267.0690	-0.19	-0.72	C16H10FN O2

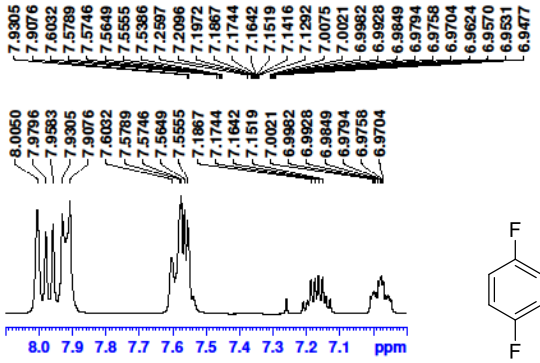

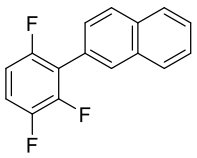

Table 4.5, compound 14y

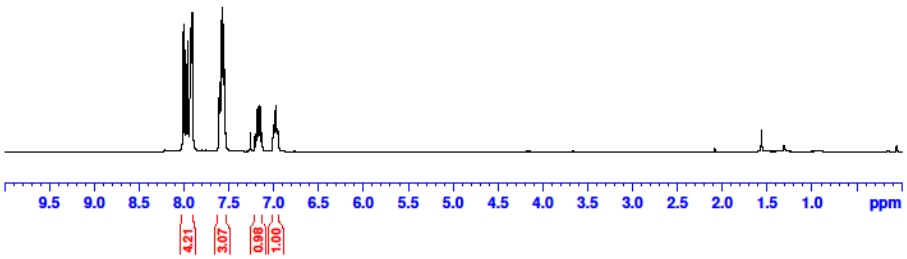

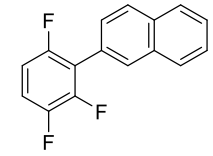

Table 4.5, compound 14y

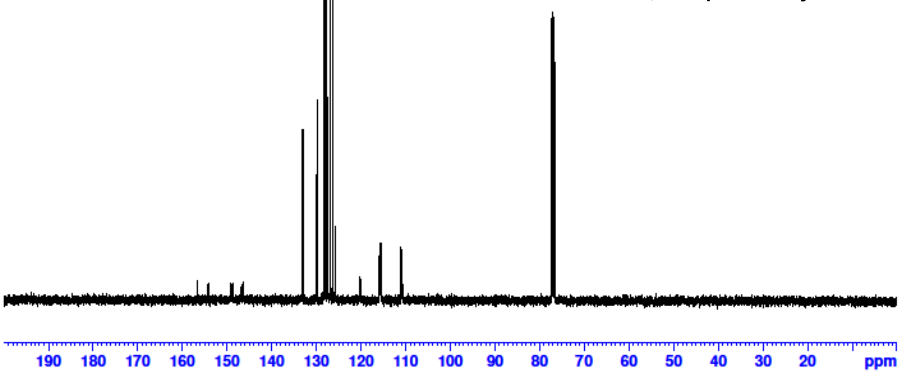

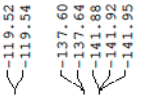

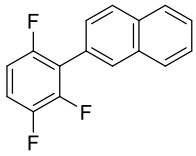

Table 4.5, compound 14y

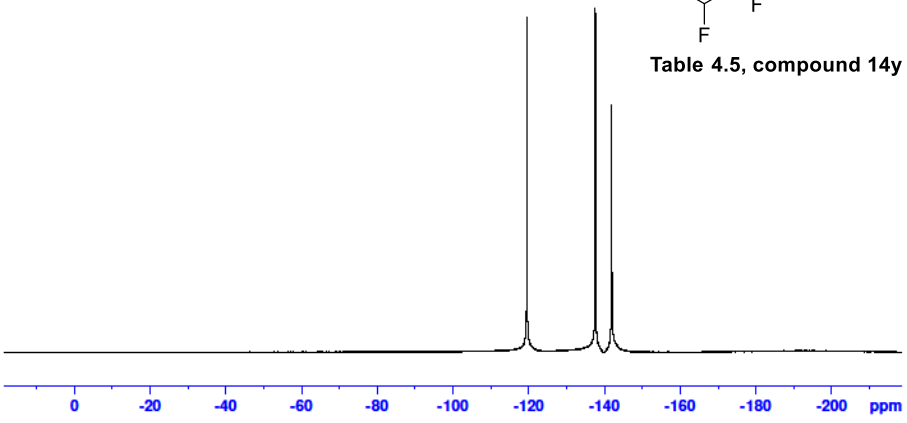

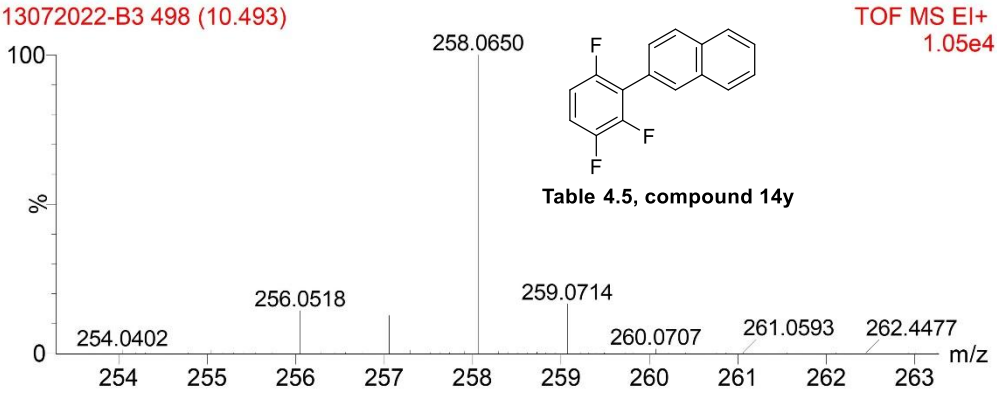

Table 4.5, compound 14y

Mass	Calc. Mass	mDa	PPM	Ion Formula
258.0650	258.0651	0.09	0.33	C16H9 F3

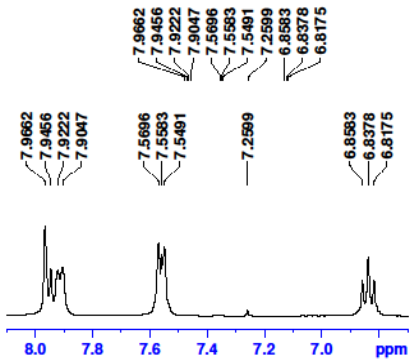

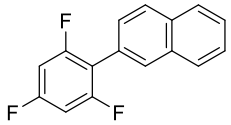

Table 4.5, compound 14z

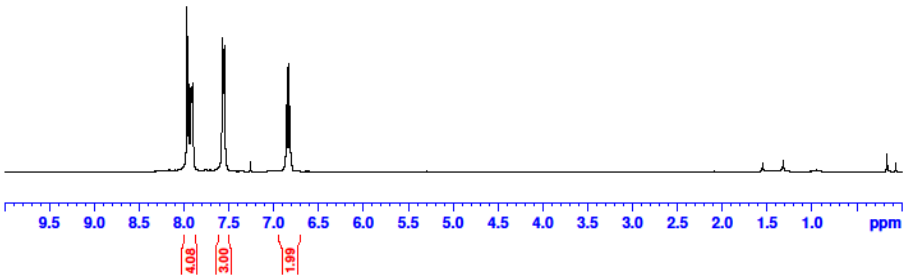

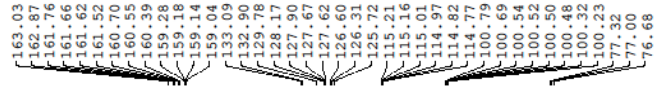

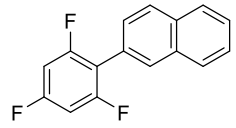

Table 4.5, compound 14z

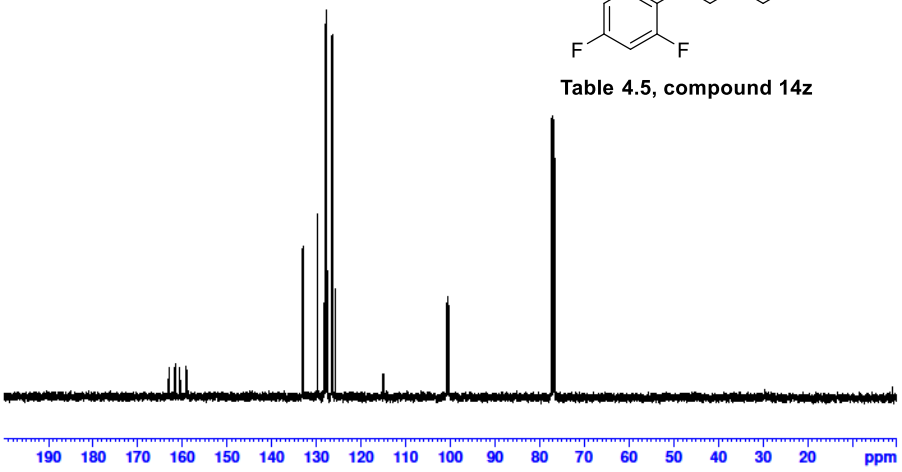

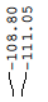

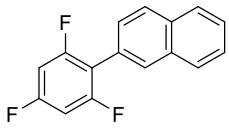

Table 4.5, compound 14z

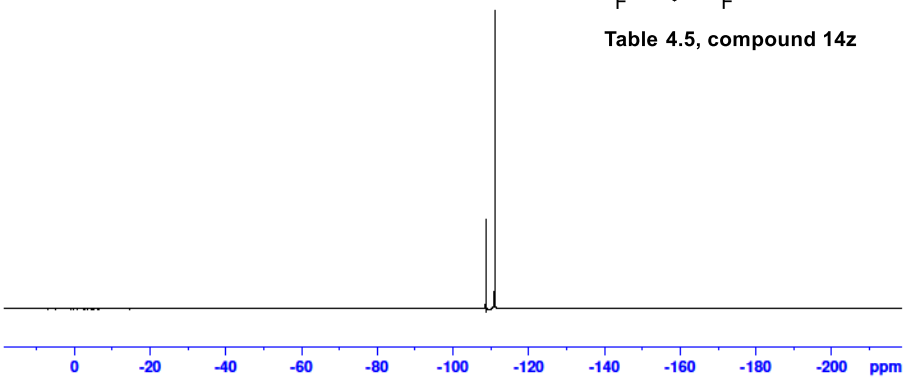

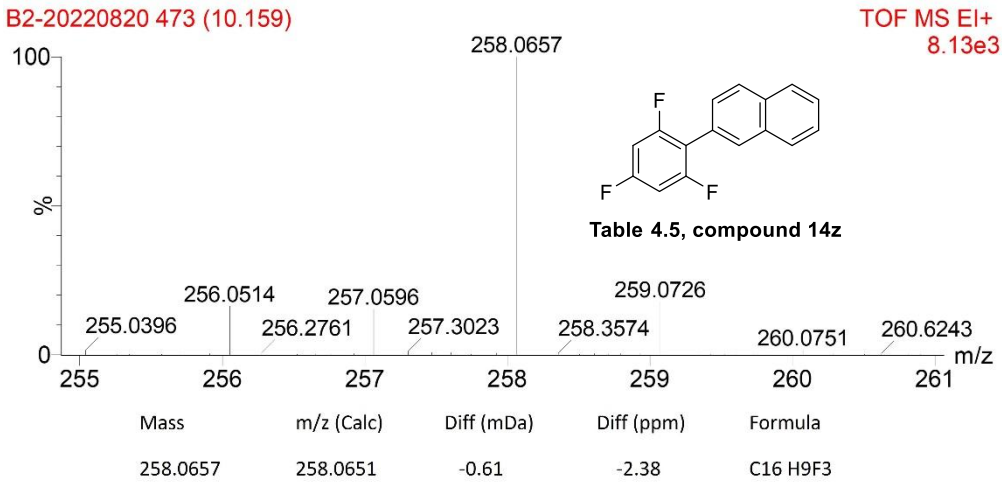

Table 4.5, compound 14z

Mass	m/z (Calc)	Diff (mDa)	Diff (ppm)	Formula
258.0657	258.0651	-0.61	-2.38	C16 H9F3

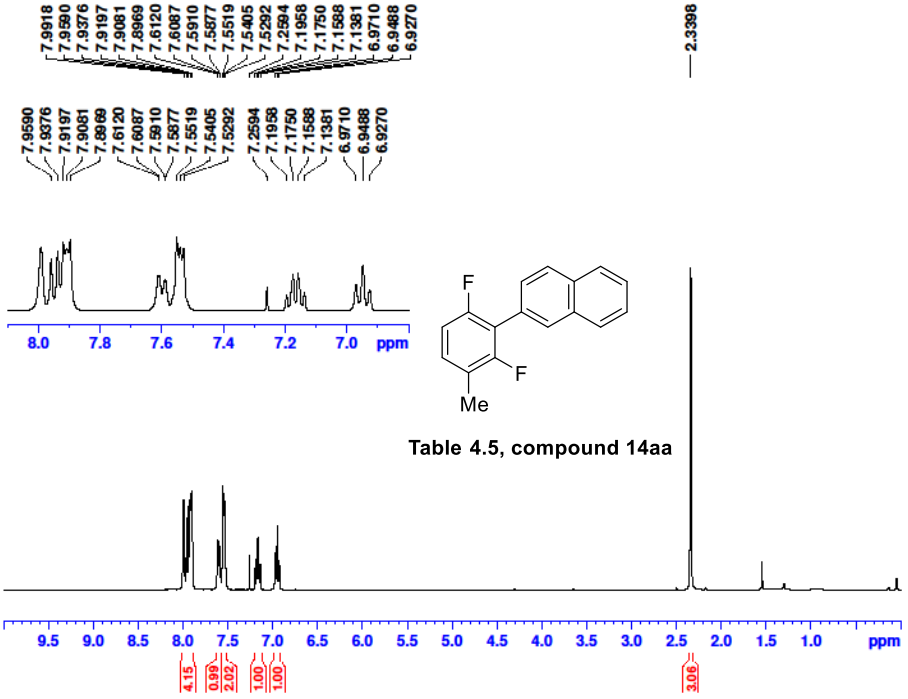

Table 4.5, compound 14aa

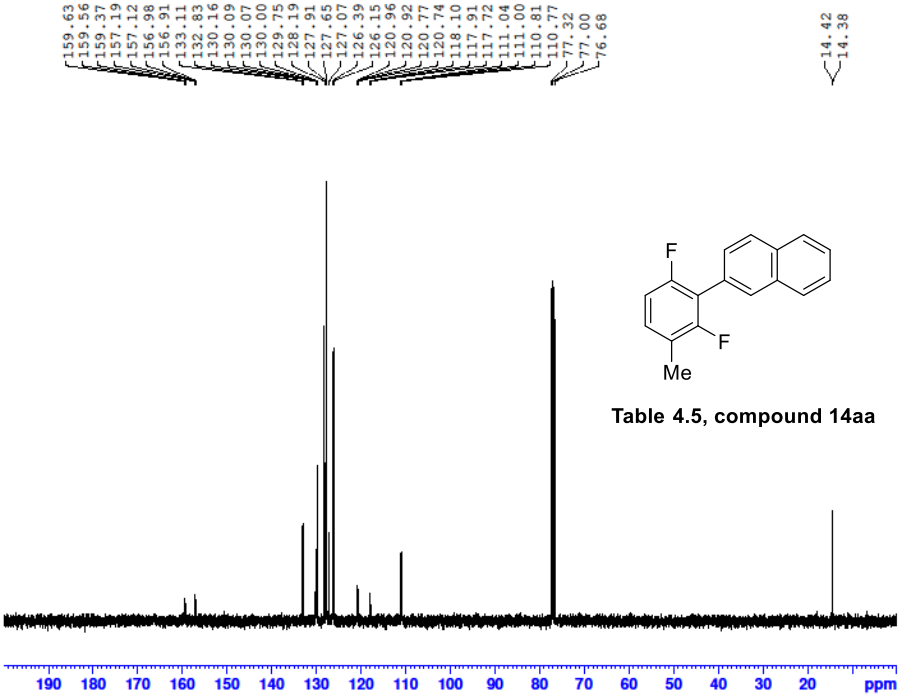

Table 4.5, compound 14aa

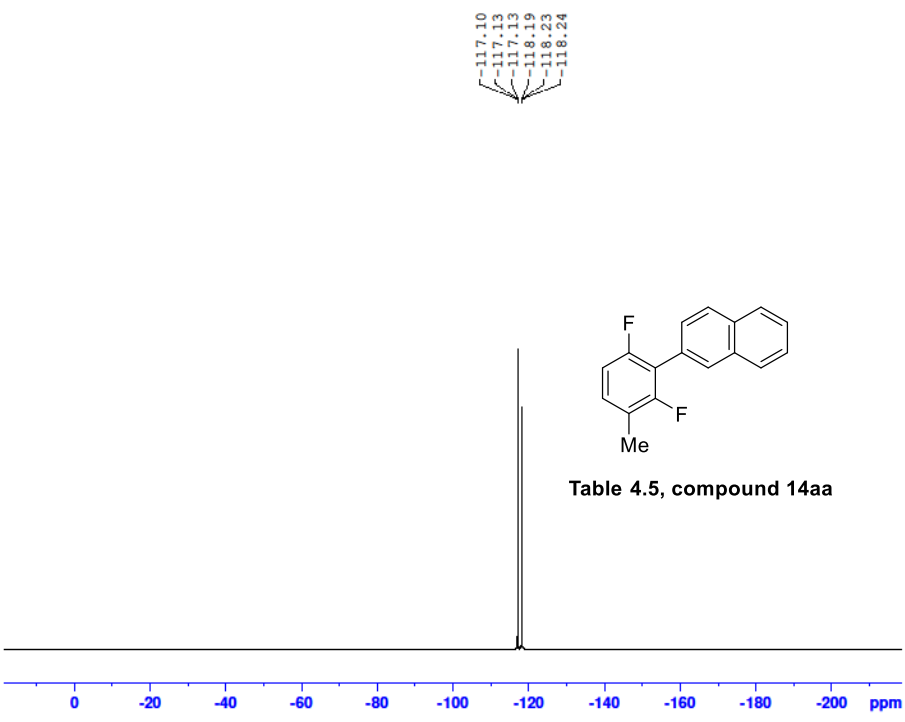

Table 4.5, compound 14aa

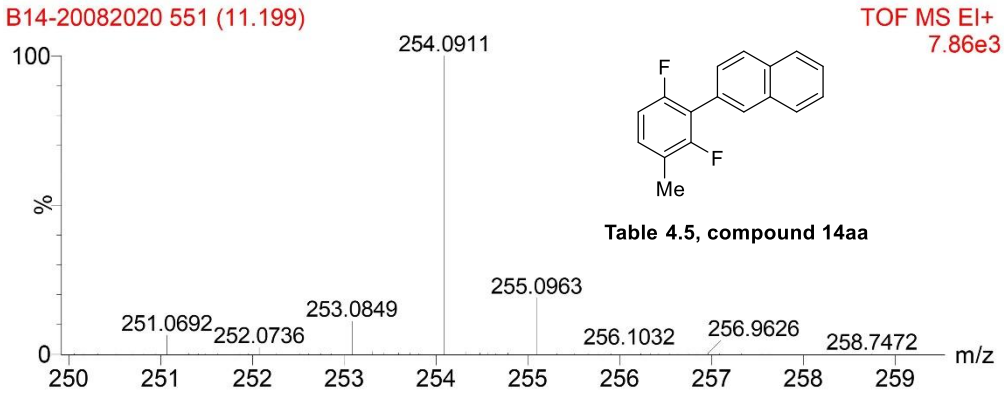

Table 4.5, compound 14aa

Mass	m/z (Calc)	Diff (mDa)	Diff (ppm)	Formula
254.0911	254.0902	-0.94	-3.71	C17 H12F2

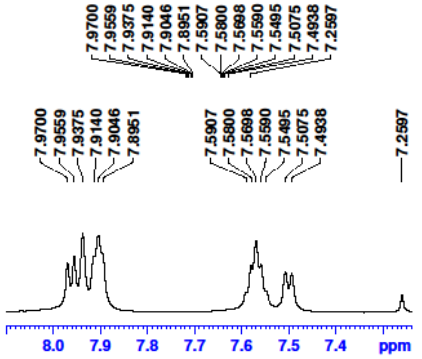

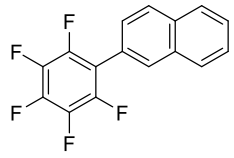

Table 4.5, compound 14ab

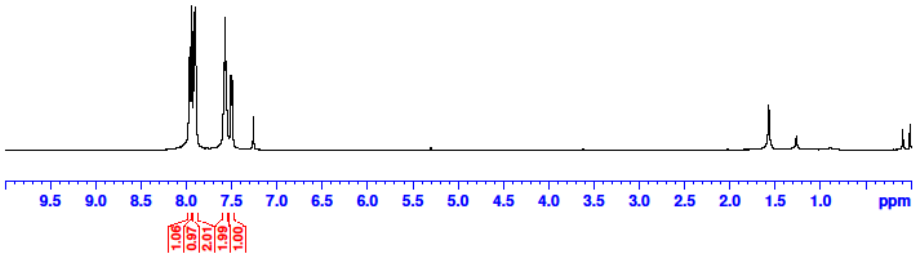

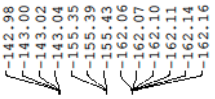

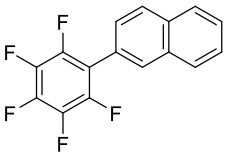

Table 4.5, compound 14ab

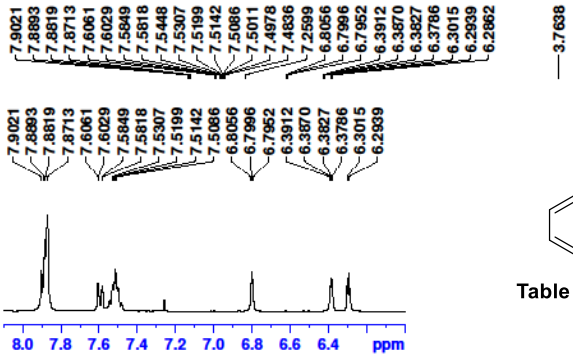

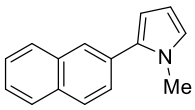

Table 4.5, compound 14ac

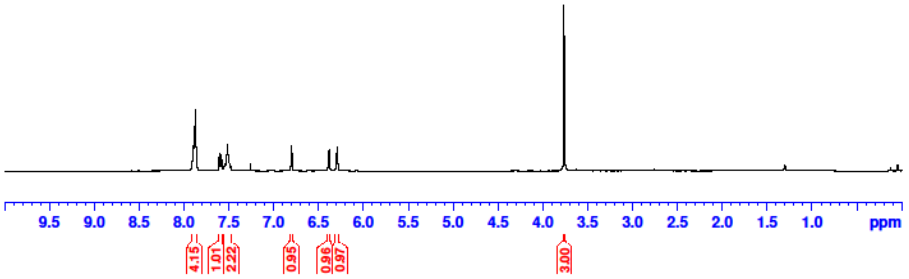

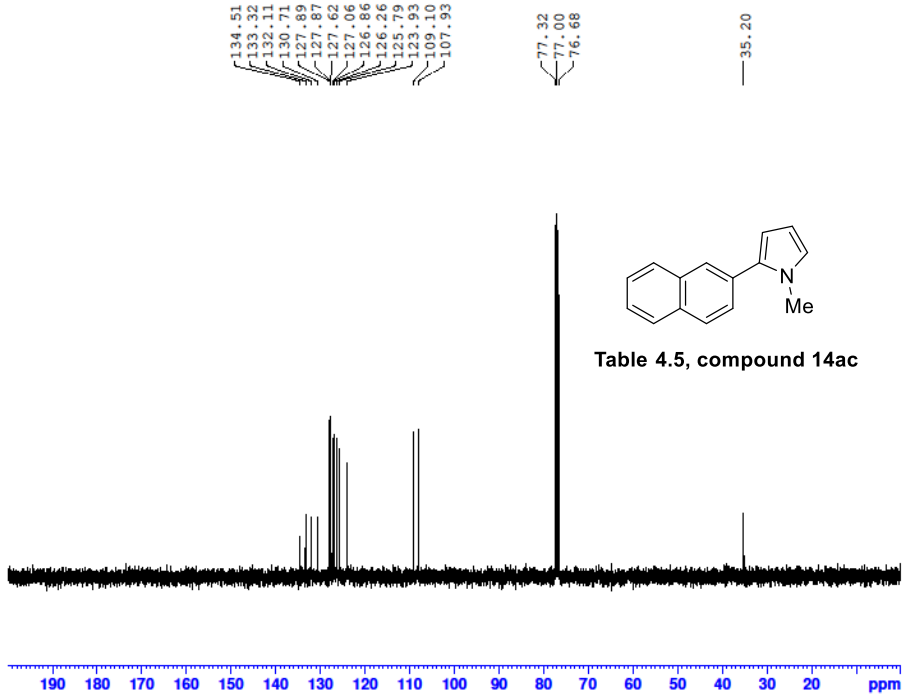

Table 4.5, compound 14ac

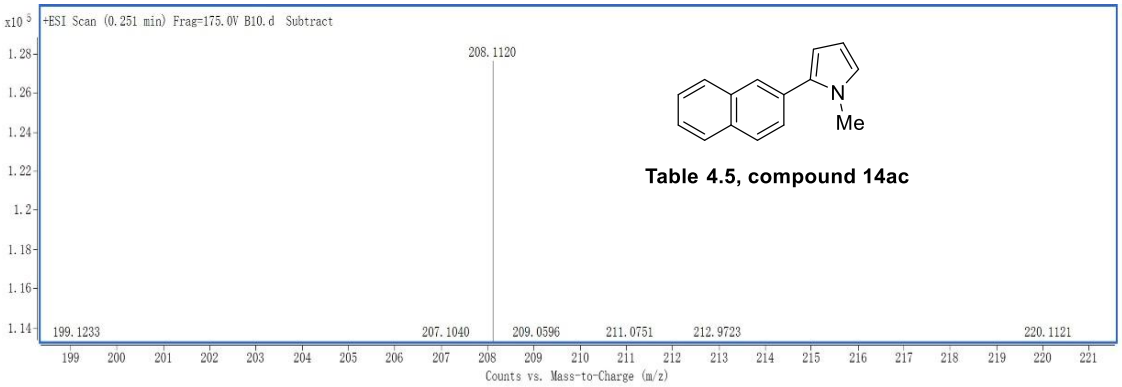

Table 4.5, compound 14ac

Mass	m/z (Calc)	Diff (mDa)	Diff (ppm)	Formula
208.1120	208.1121	0.08	0.37	C15H14N

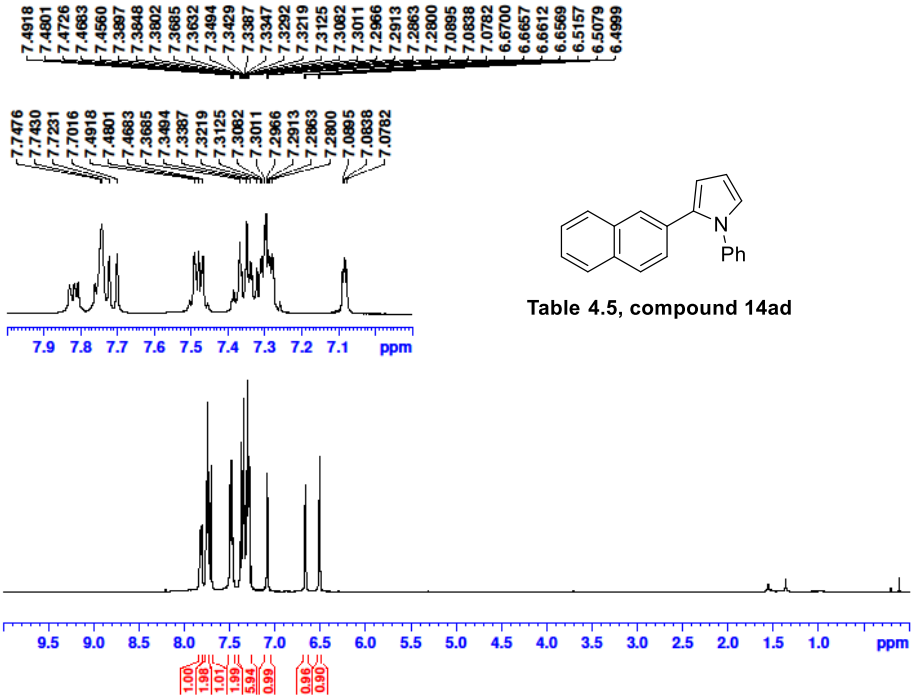

Table 4.5, compound 14ad

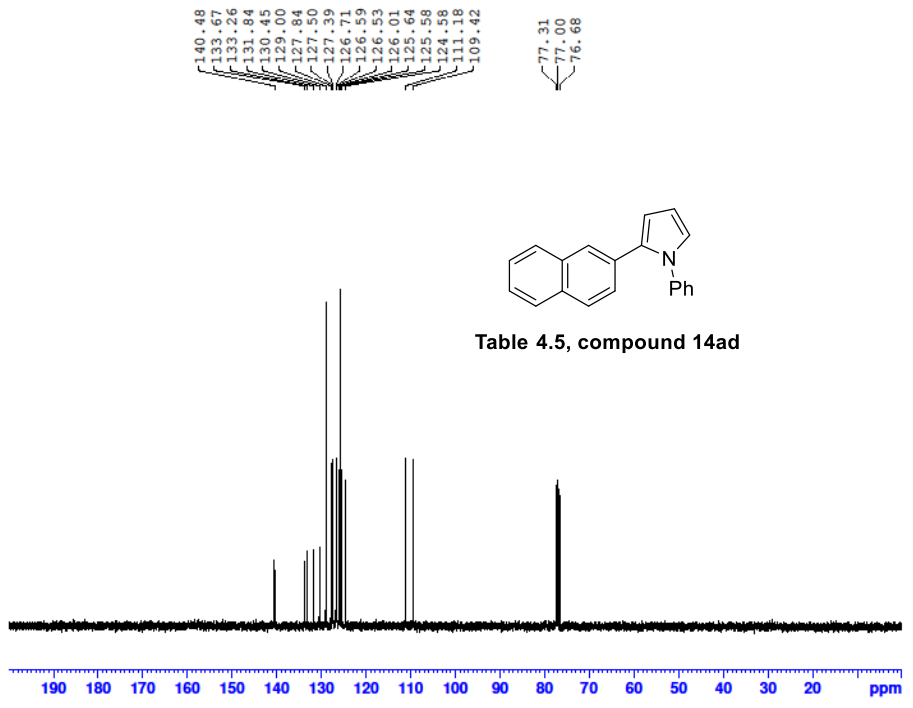

Table 4.5, compound 14ad

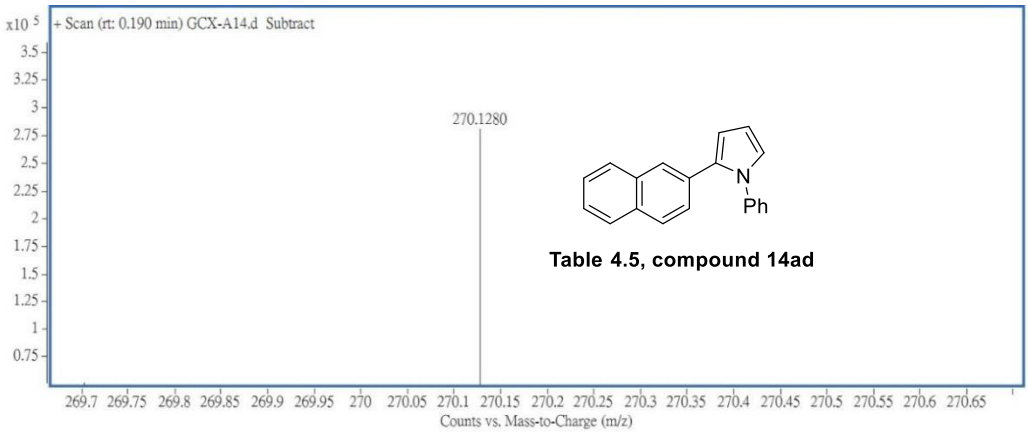

Table 4.5, compound 14ad

Mass	m/z (Calc)	Diff (mDa)	Diff (ppm)	Formula
270.1280	270.1277	-0.27	-1.02	C20 H16 N

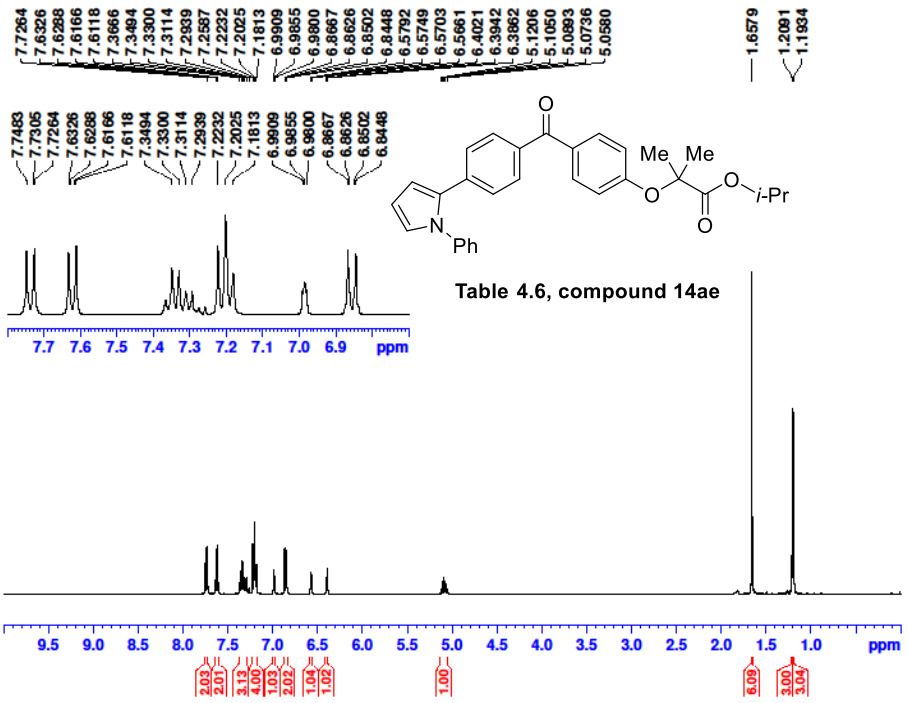

Table 4.6, compound 14ae

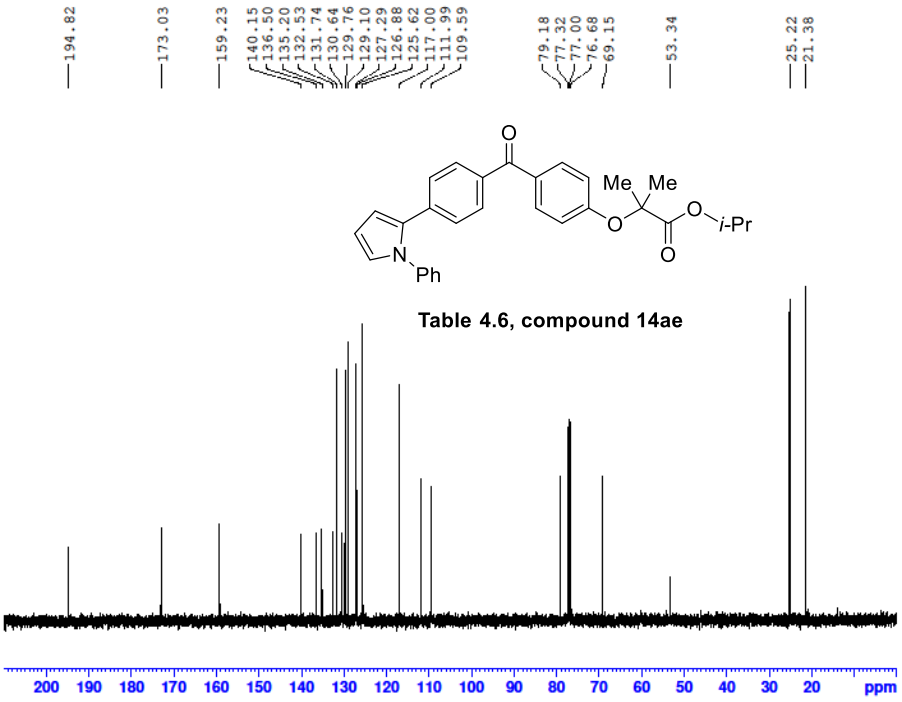

Table 4.6, compound 14ae

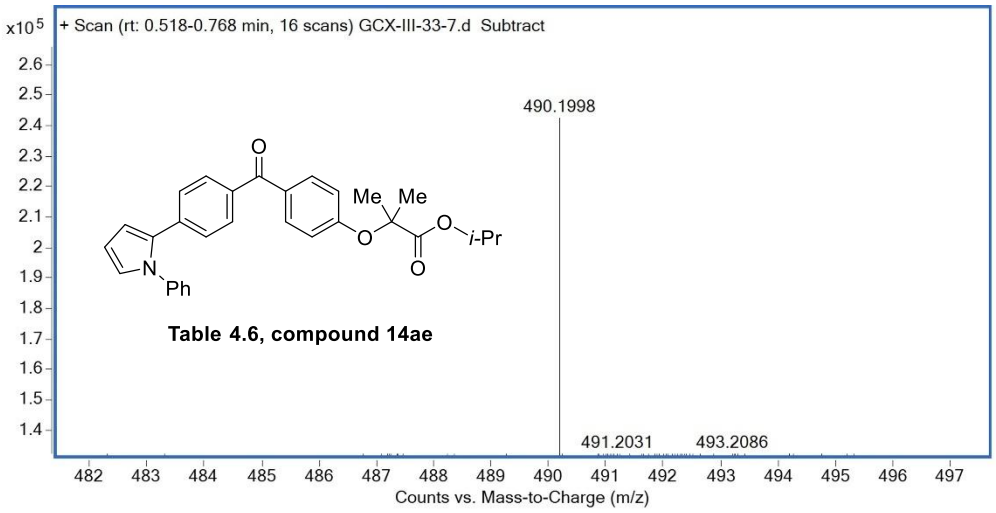

Table 4.6, compound 14ae

Mass	Calc. Mass	mDa	PPM	Ion Formula
490.1998	490.1989	-0.92	-1.97	C30H29NO4Na

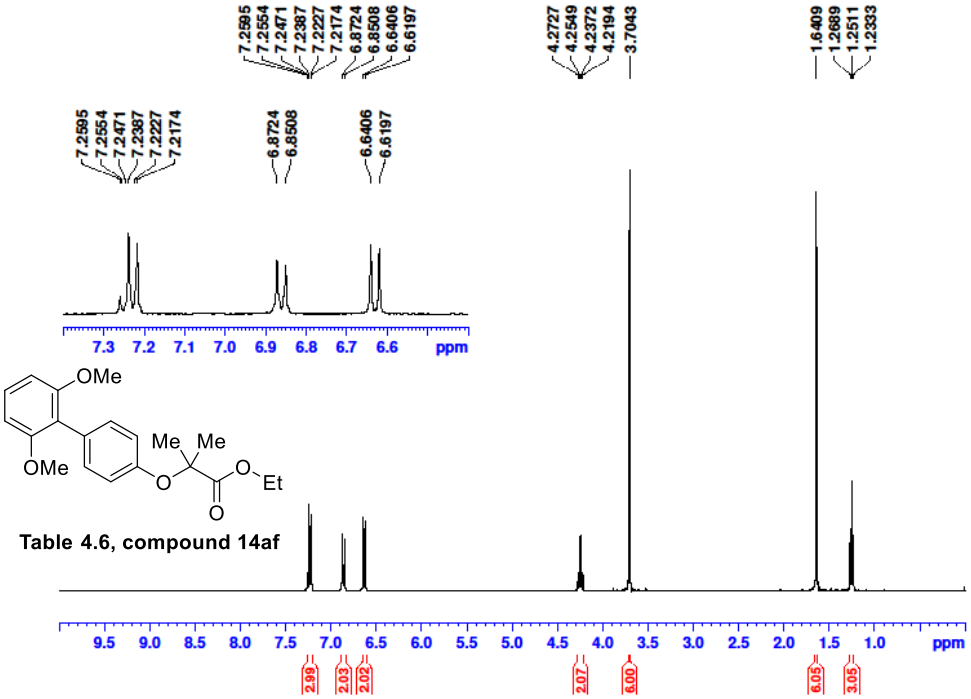
7.2595
7.2554
7.2471
7.2387
7.2227
7.2174
6.8724
6.8508
6.6406
6.6197
4.2727
4.2549
4.2372
4.2194
3.7043
1.6409
1.2669
1.2511
1.2333
7.3 7.2 7.1 7.0 6.9 6.8 6.7 6.6 ppm
OMe
OMe
Me Me
O
O
Et
O
Table 4.6, compound 14af
9.5 9.0 8.5 8.0 7.5 7.0 6.5 6.0 5.5 5.0 4.5 4.0 3.5 3.0 2.5 2.0 1.5 1.0 ppm
2.99
2.03
2.02
2.07
6.00
6.05
3.05

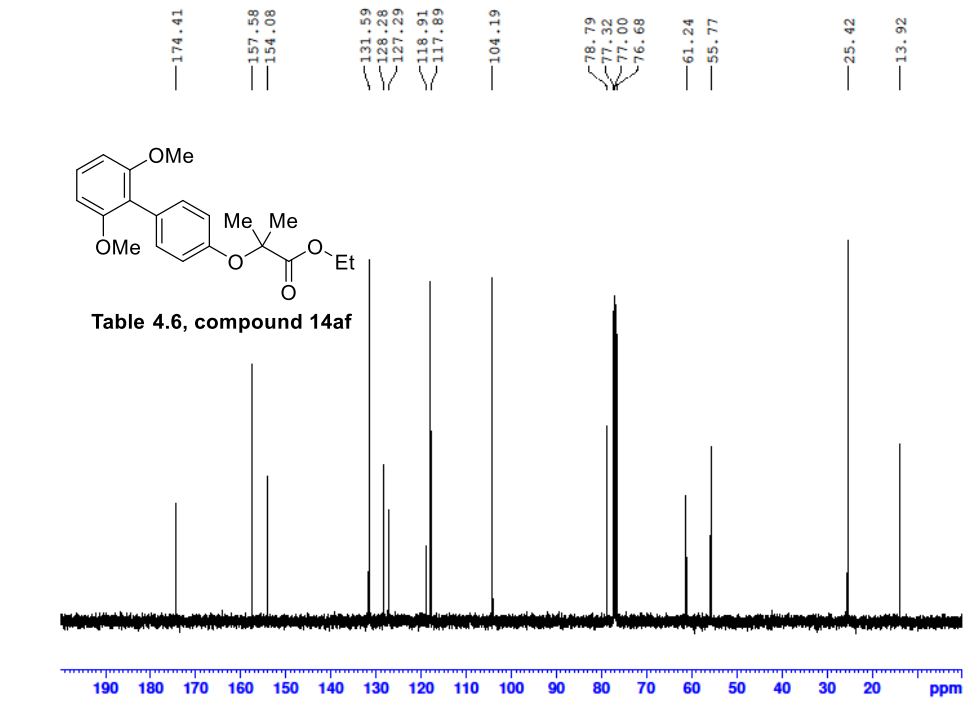
174.41
157.58
154.08
131.59
128.28
127.29
118.91
117.89
104.19
78.79
77.32
77.00
76.68
61.24
55.77
25.42
13.92
OMe
OMe
Me Me
O
O
Et
O
Table 4.6, compound 14af
190 180 170 160 150 140 130 120 110 100 90 80 70 60 50 40 30 20 ppm

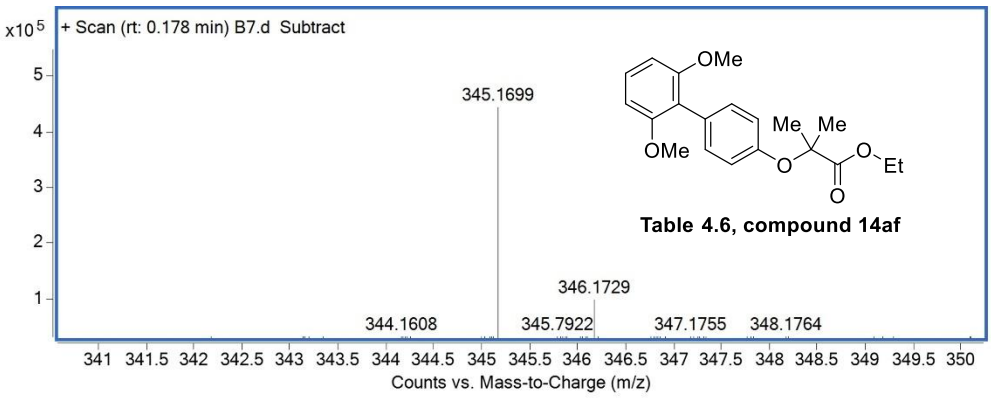

Table 4.6, compound 14af

Mass	Calc. Mass	mDa	PPM	Ion Formula
345.1699	345.1697	-0.25	-0.73	C20H25O5

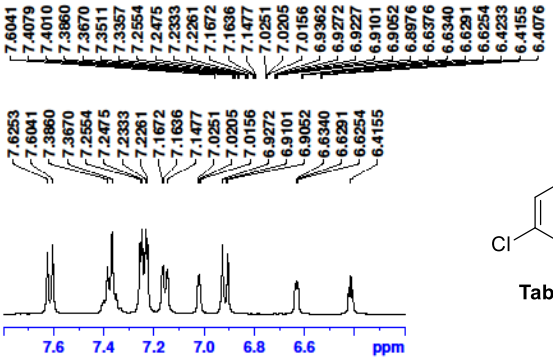

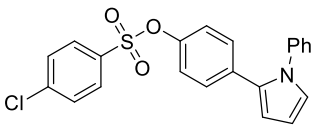

Table 4.6, compound 14ag

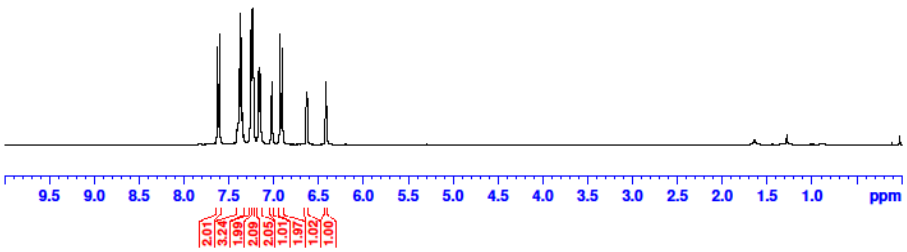

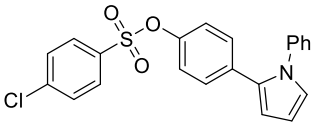

Table 4.6, compound 14ag

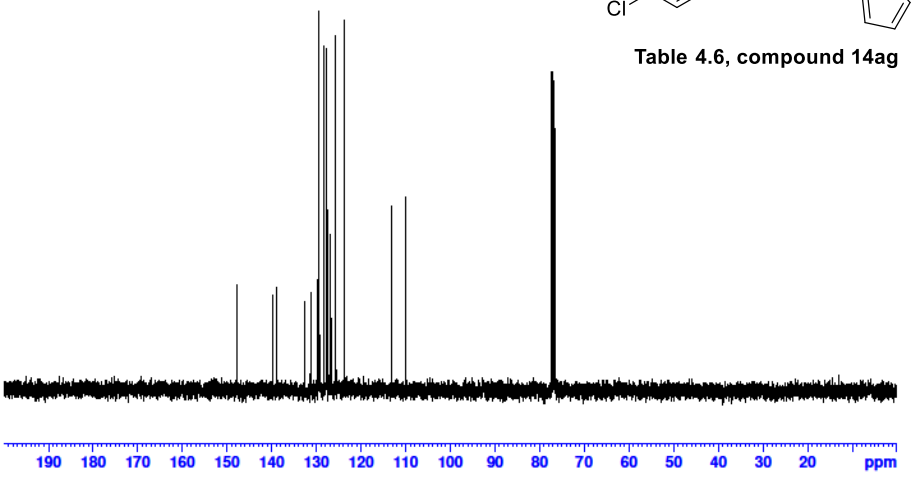

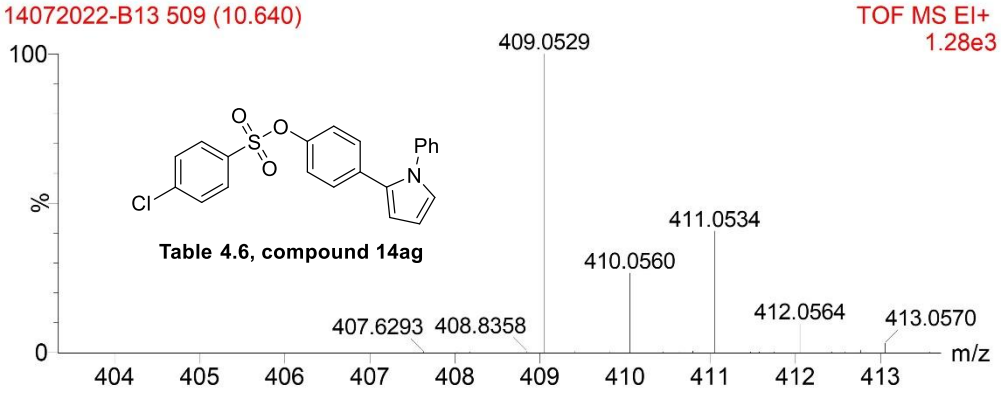

Table 4.6, compound 14ag

Mass	Calc. Mass	mDa	PPM	Ion Formula
409.0529	409.0534	0.49	1.21	C22H16ClSNO3

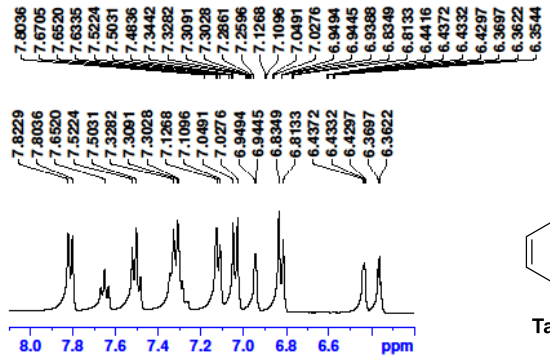

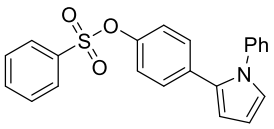

Table 4.6, compound 14ah

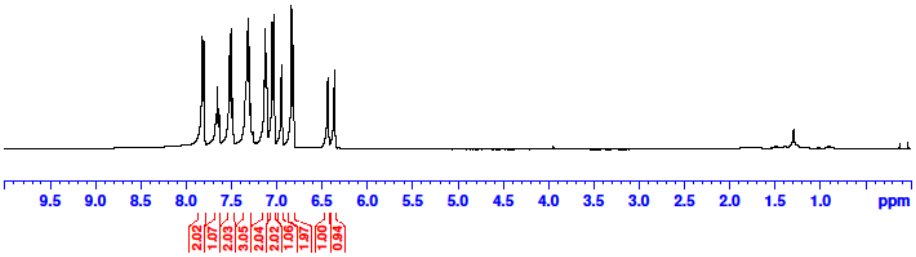

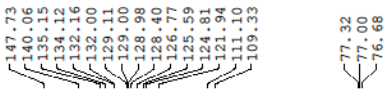

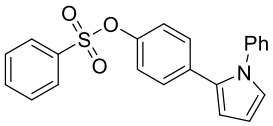

Table 4.6, compound 14ah

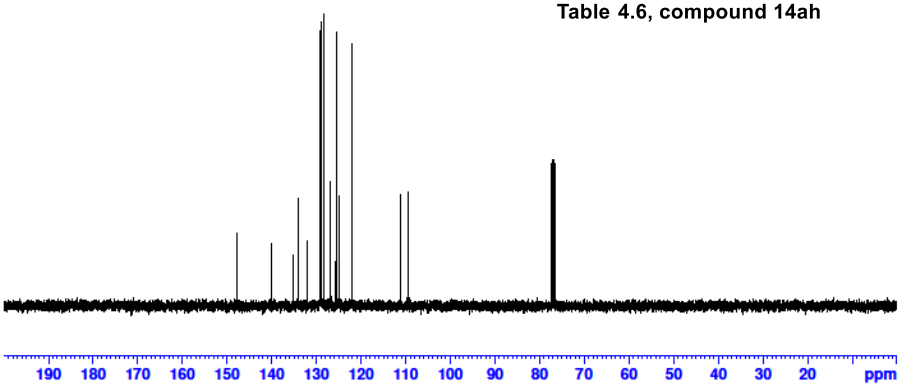

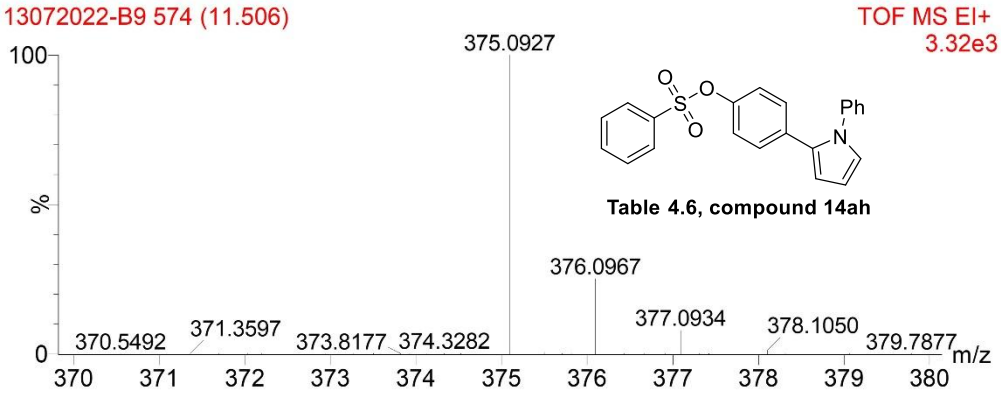

Table 4.6, compound 14ah

Mass	Calc. Mass	mDa	PPM	Ion Formula
375.0927	375.0924	-0.33	-0.89	C22H17SN O3

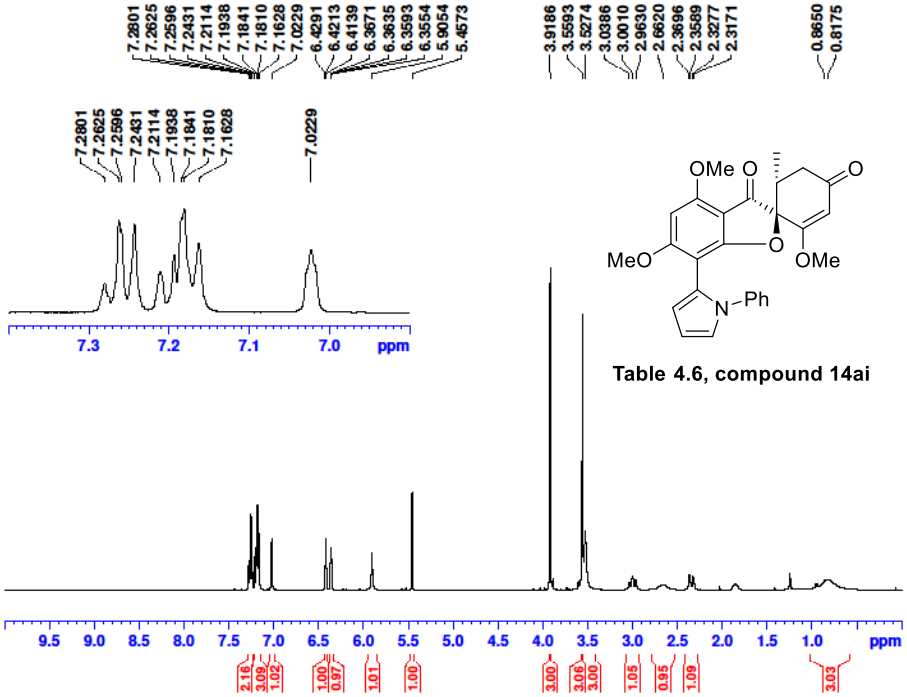

Table 4.6, compound 14ai

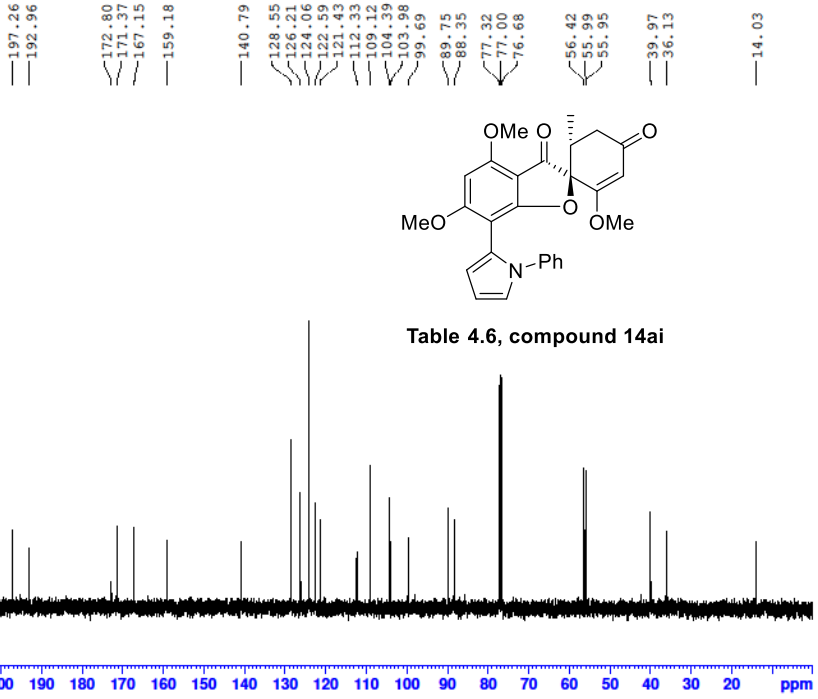

Table 4.6, compound 14ai

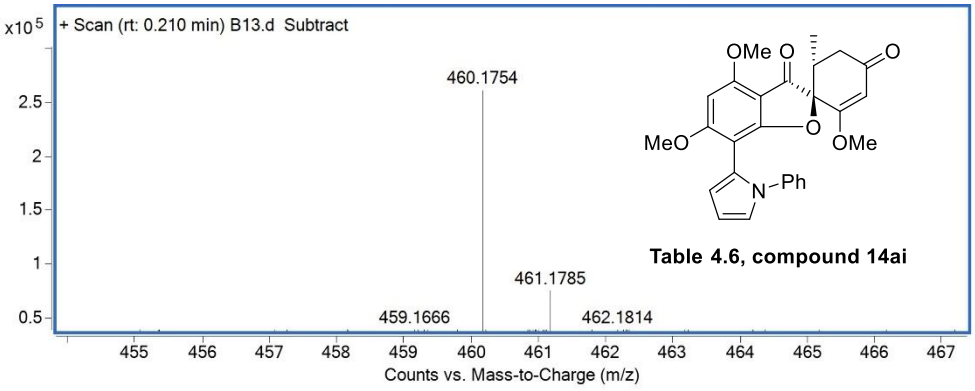

Table 4.6, compound 14ai

Mass	Calc. Mass	mDa	PPM	Ion Formula
460.1754	460.1755	0.06	0.14	C27H26 NO6

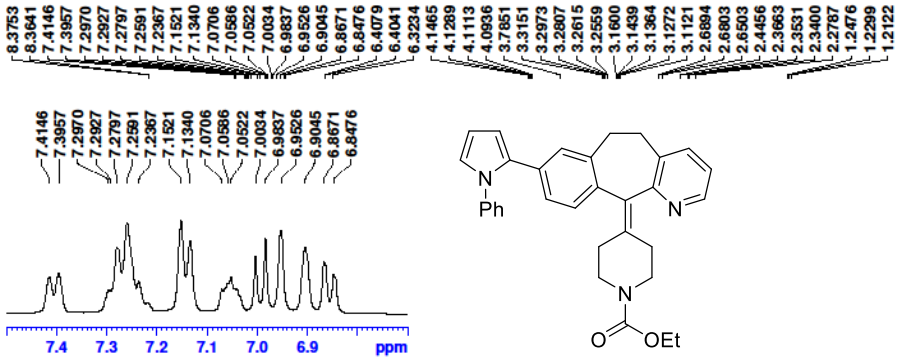

Table 4.6, compound 14aj

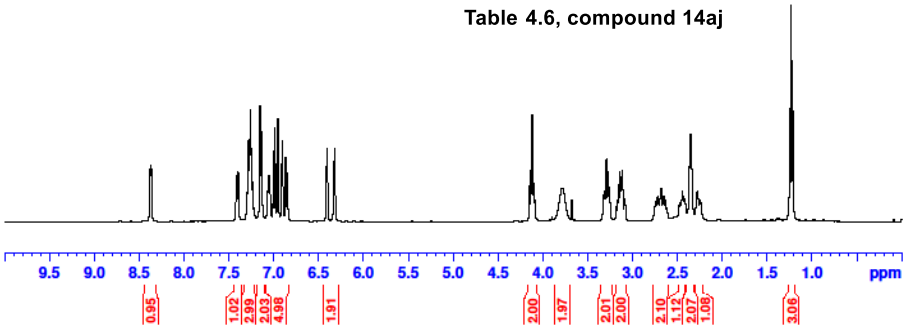

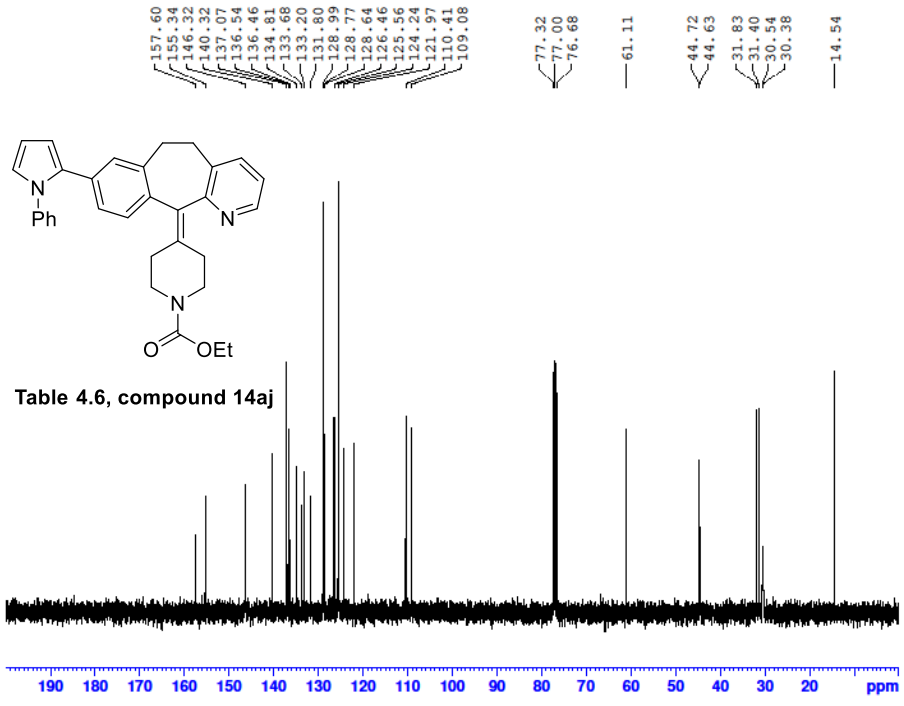

Table 4.6, compound 14aj

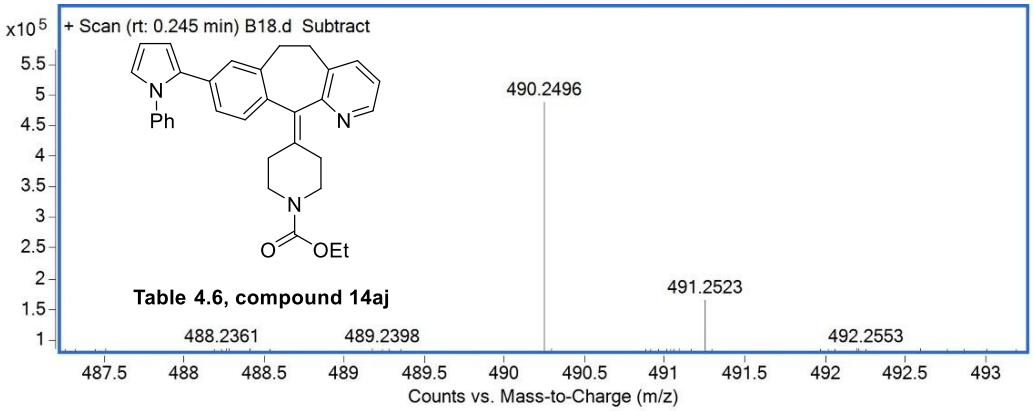

Table 4.6, compound 14aj

Mass	Calc. Mass	mDa	PPM	Ion Formula
490.2496	490.2489	-0.7	-1.42	C32H32 N3O2

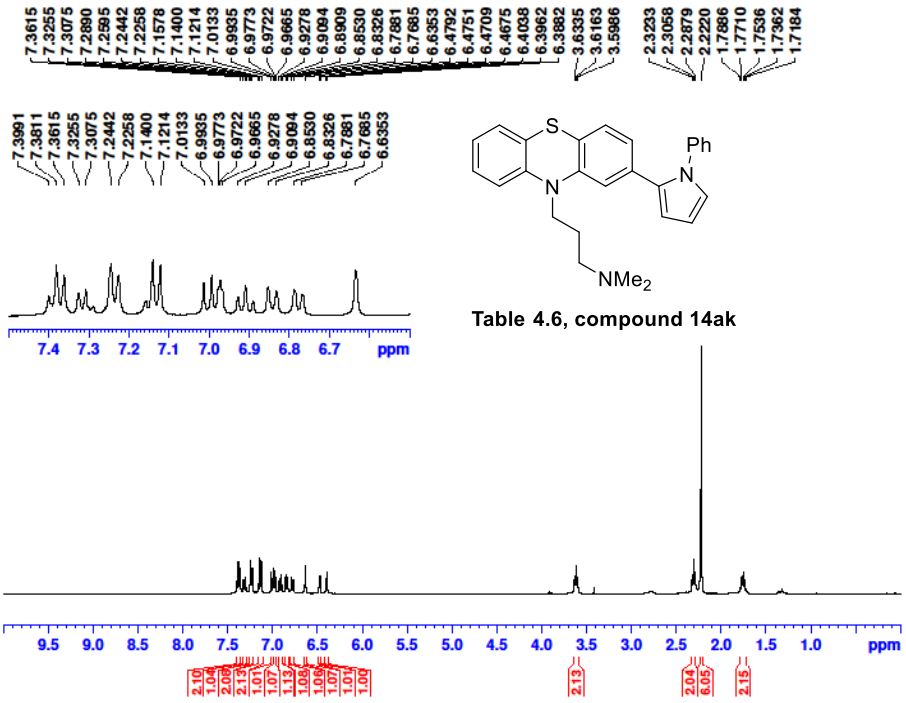

Table 4.6, compound 14ak

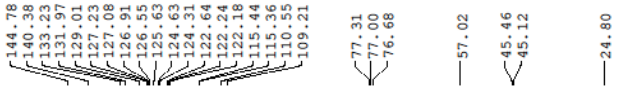

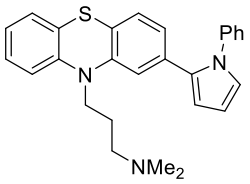

Table 4.6, compound 14ak

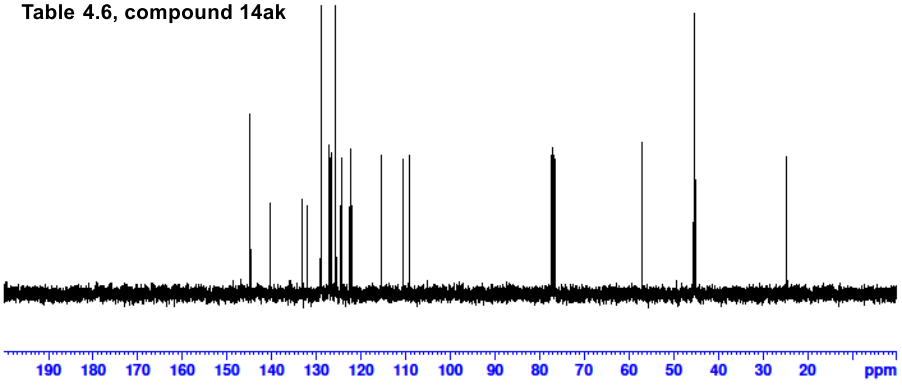

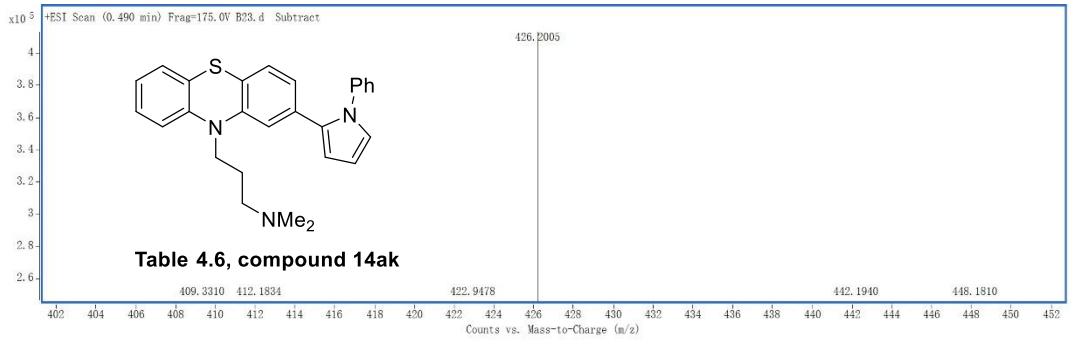

Table 4.6, compound 14ak

Mass	m/z (Calc)	Diff (mDa)	Diff (ppm)	Formula
426.2005	426.1998	-0.65	-1.54	C27H28N3S

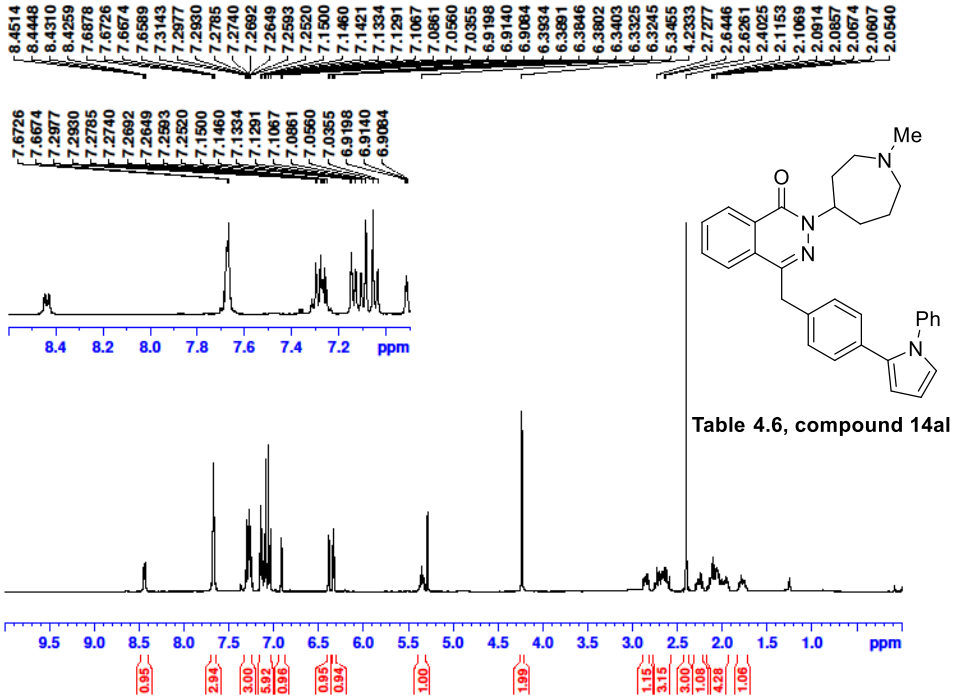

Table 4.6, compound 14al

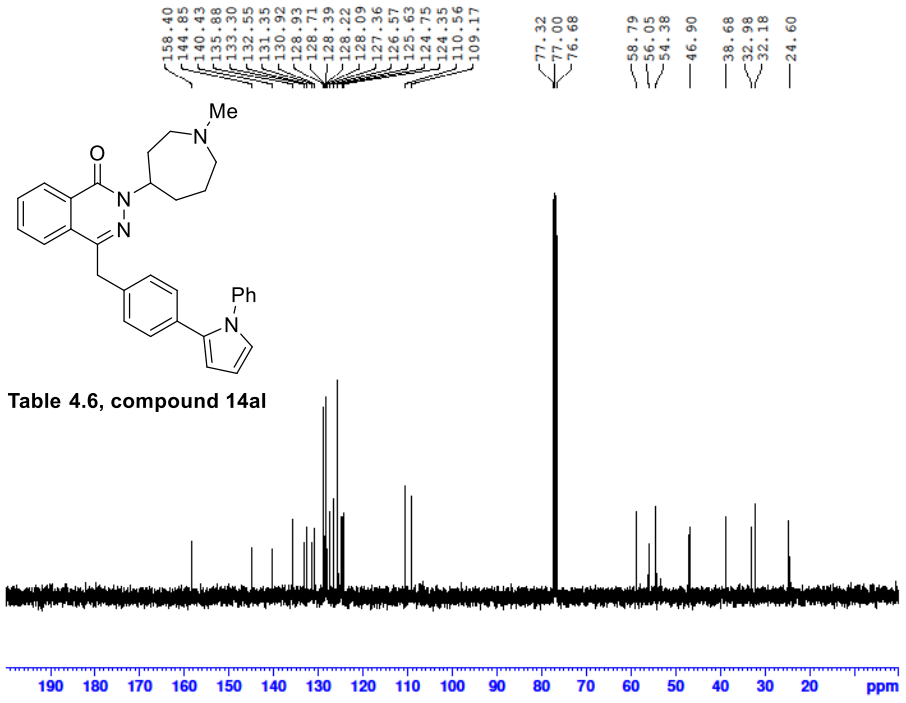

Table 4.6, compound 14al

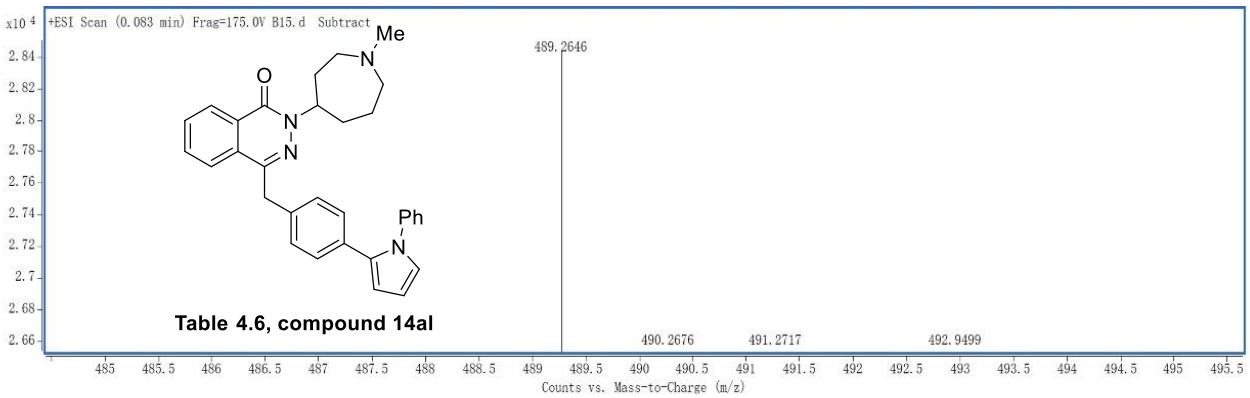

Table 4.6, compound 14al

Mass	m/z (Calc)	Diff (mDa)	Diff (ppm)	Formula
489.2646	489.2649	0.29	0.59	C32H33ON4

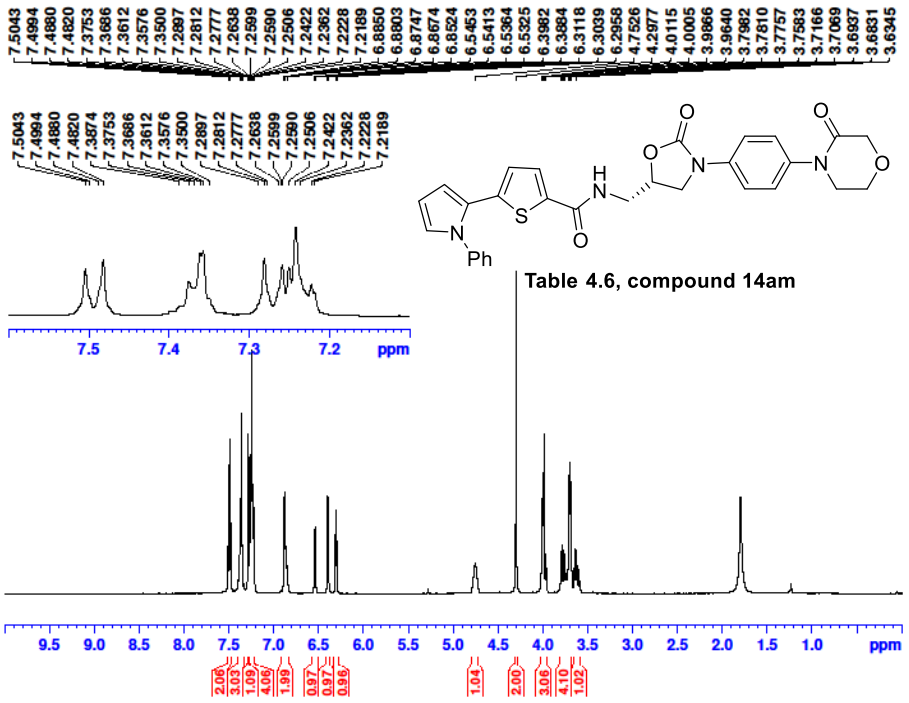

Table 4.6, compound 14am

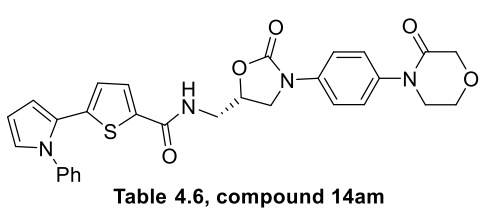

Table 4.6, compound 14am

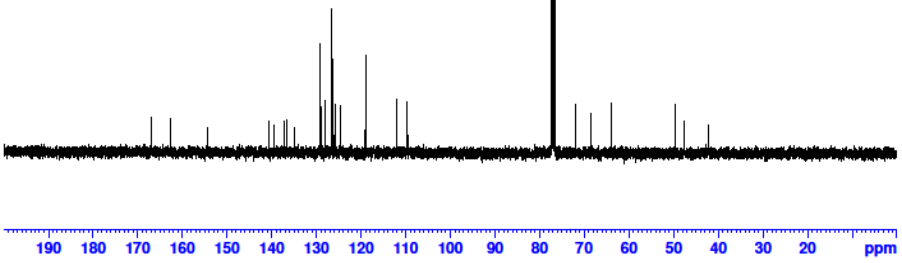

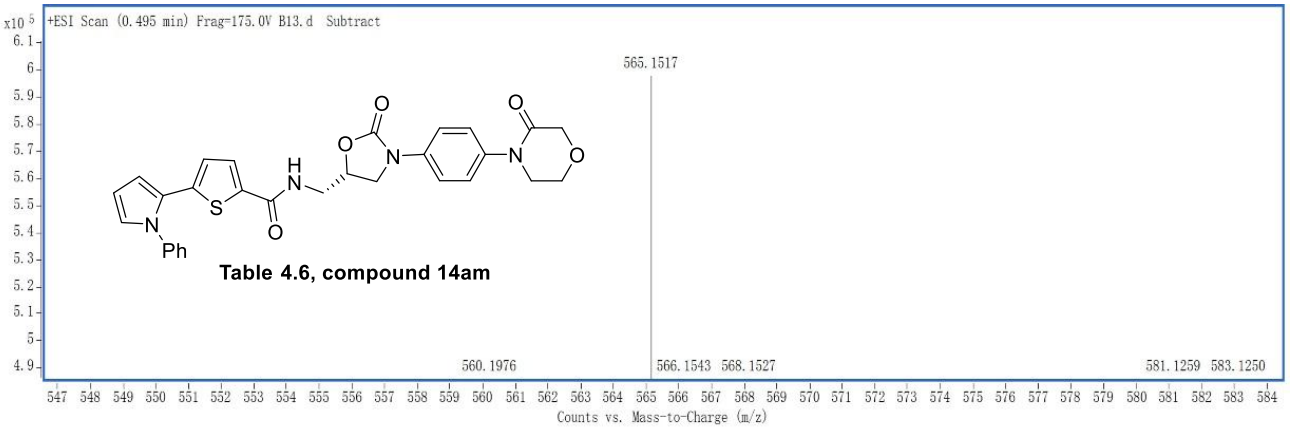

Table 4.6, compound 14am

Mass	m/z (Calc)	Diff (mDa)	Diff (ppm)	Formula
565.1517	565.1516	-0.09	-0.16	C29H26O5N4SNa

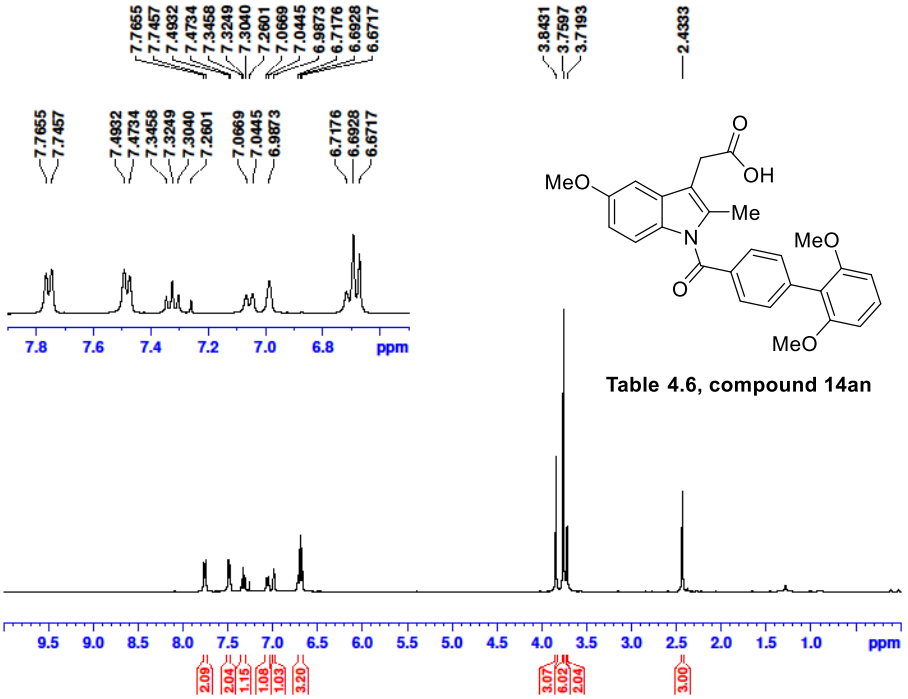

Table 4.6, compound 14an

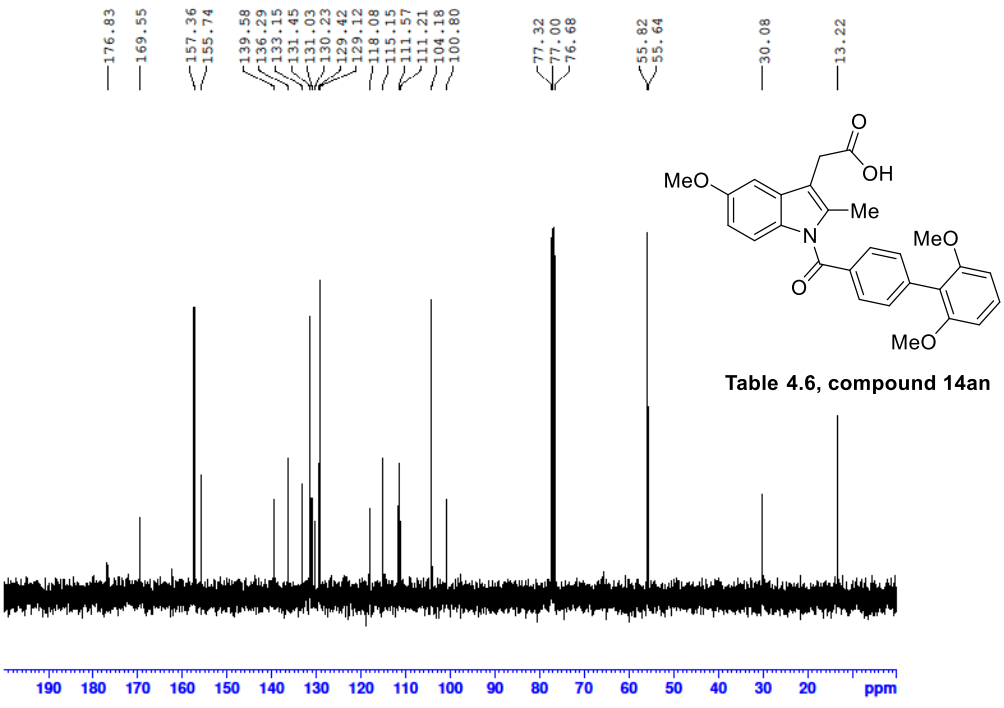

Table 4.6, compound 14an

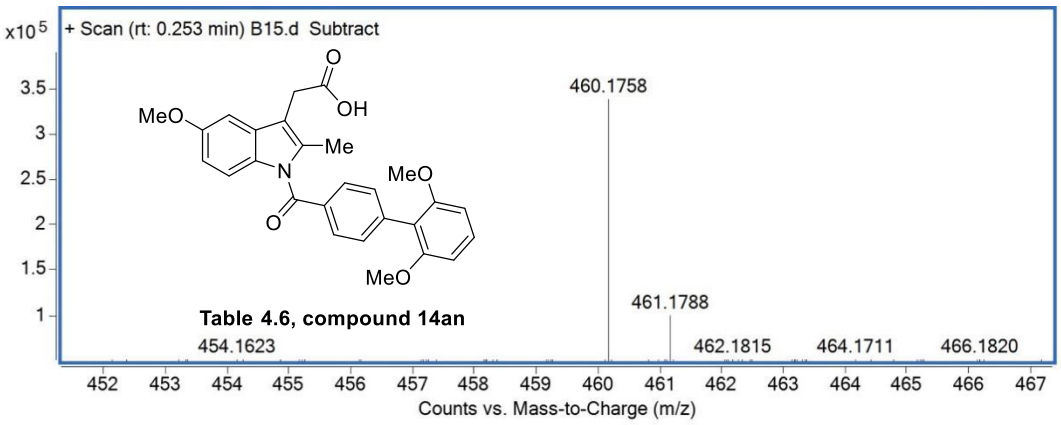

Table 4.6, compound 14an

Mass	Calc. Mass	mDa	PPM	Ion Formula
460.1758	460.1755	-0.34	-0.7	C27H26 NO6

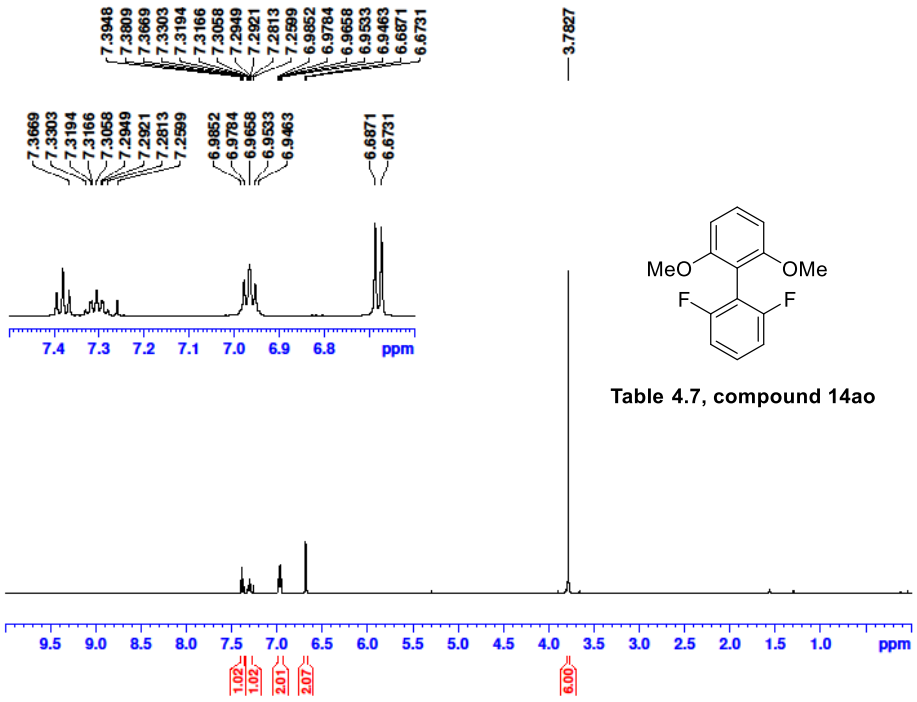

Table 4.7, compound 14ao

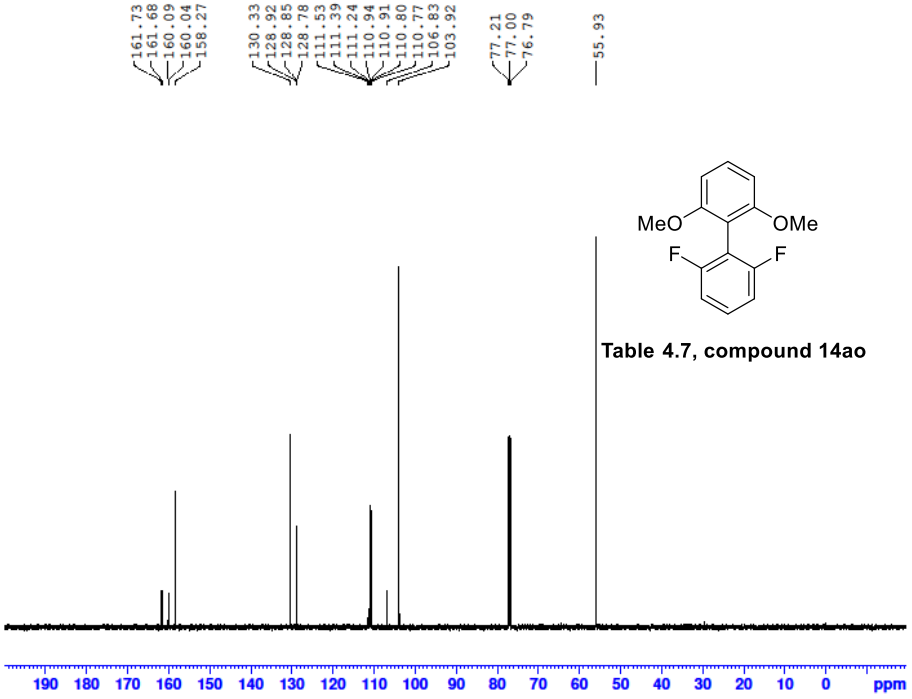

Table 4.7, compound 14ao

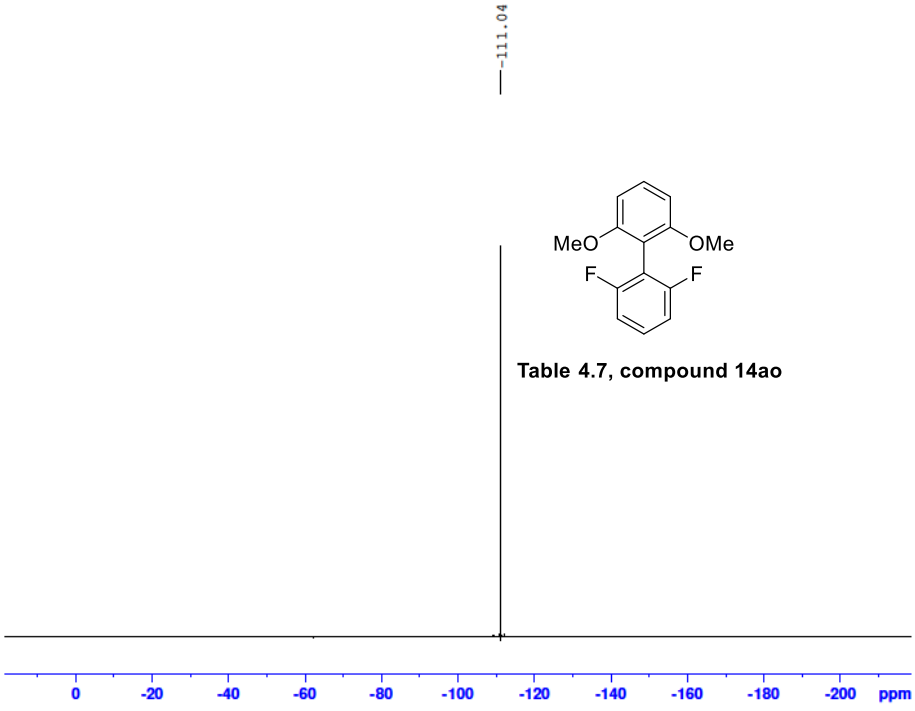

Table 4.7, compound 14ao

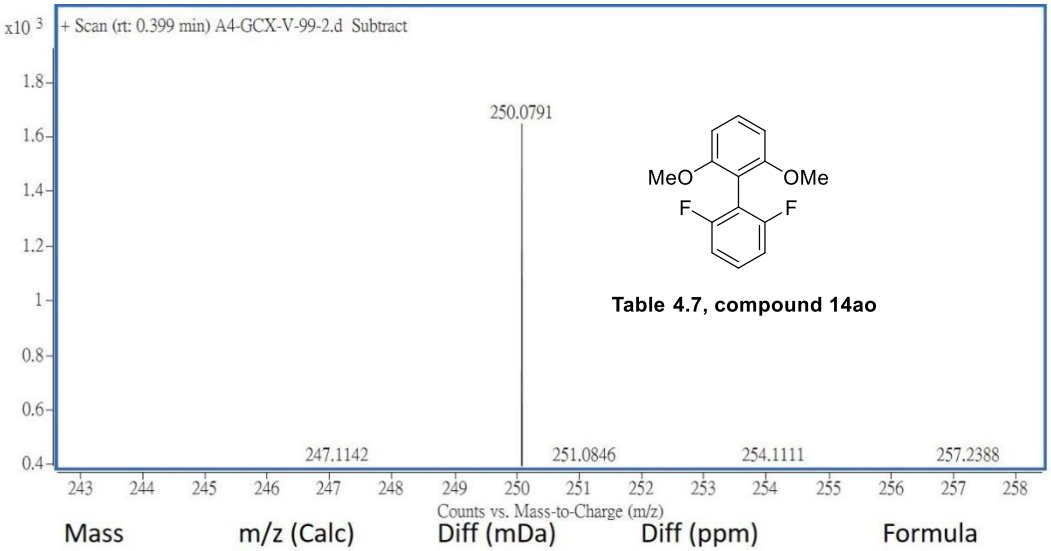

Table 4.7, compound 14ao

Mass	m/z (Calc)	Diff (mDa)	Diff (ppm)	Formula
250.0791	250.0800	0.89	3.55	C14H12F2O2

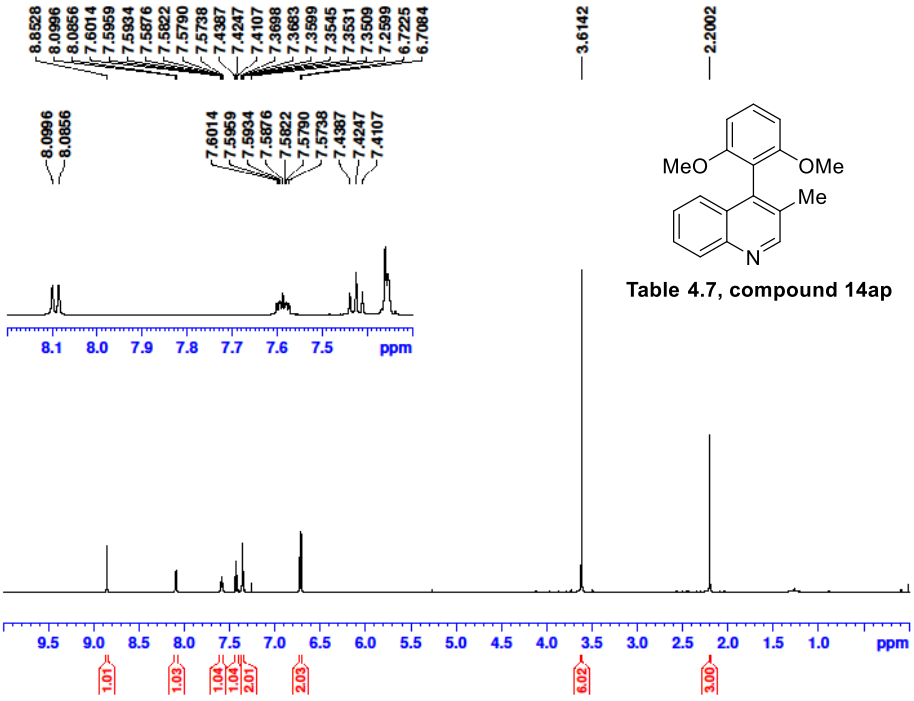

Table 4.7, compound 14ap

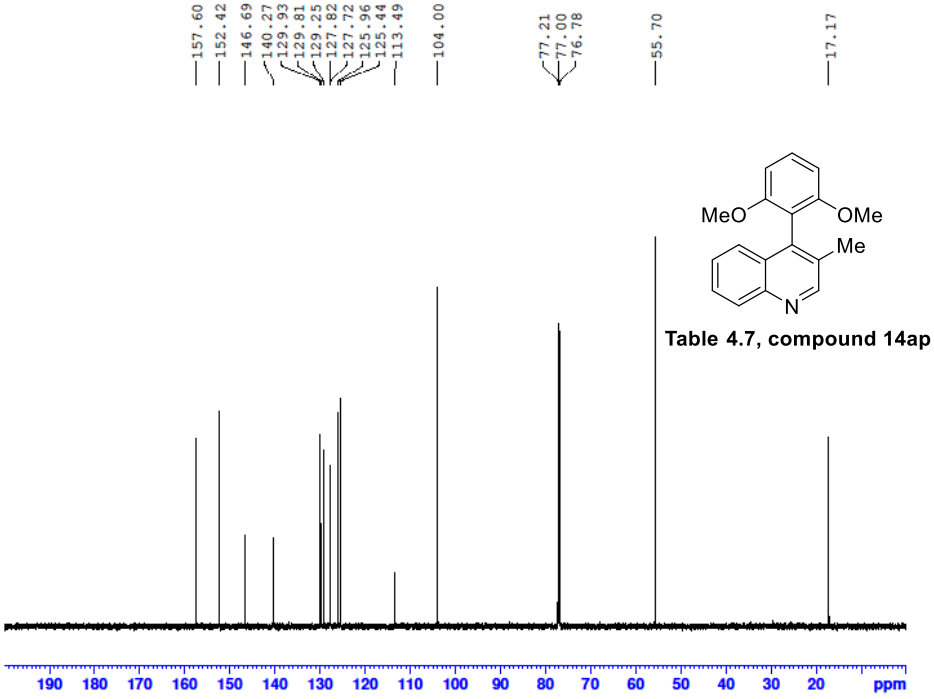

Table 4.7, compound 14ap

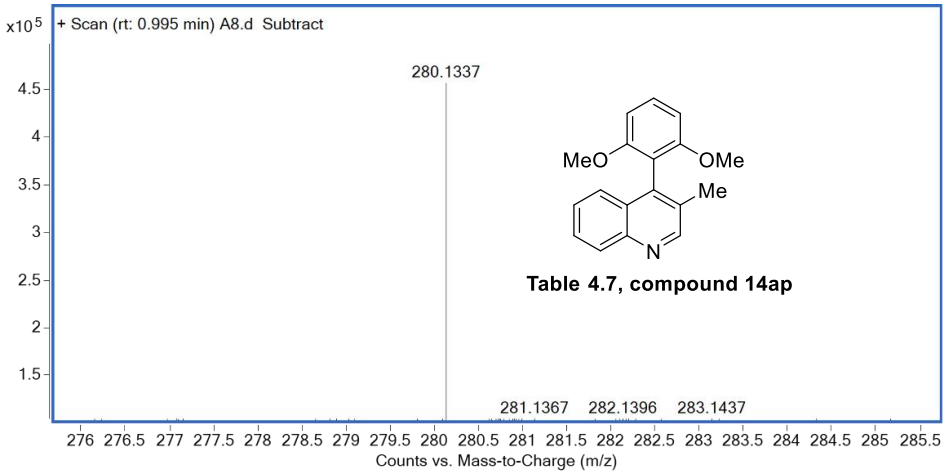

Table 4.7, compound 14ap

Mass	Calc. Mass	mDa	PPM	Ion Formula
280.1337	280.1332	-0.49	-1.77	C18H18O2N

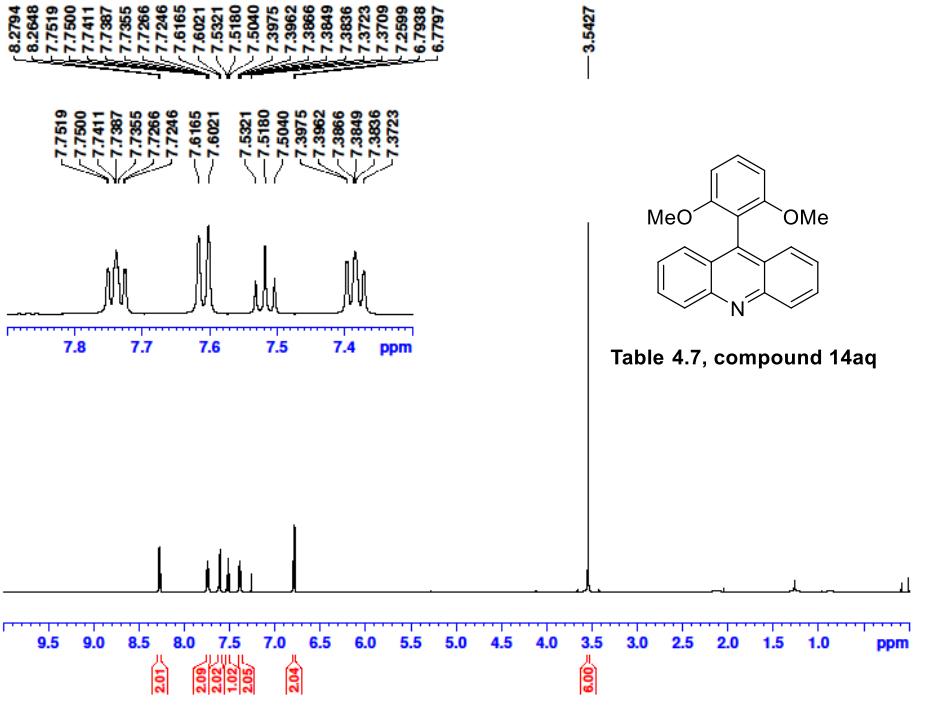

Table 4.7, compound 14aq

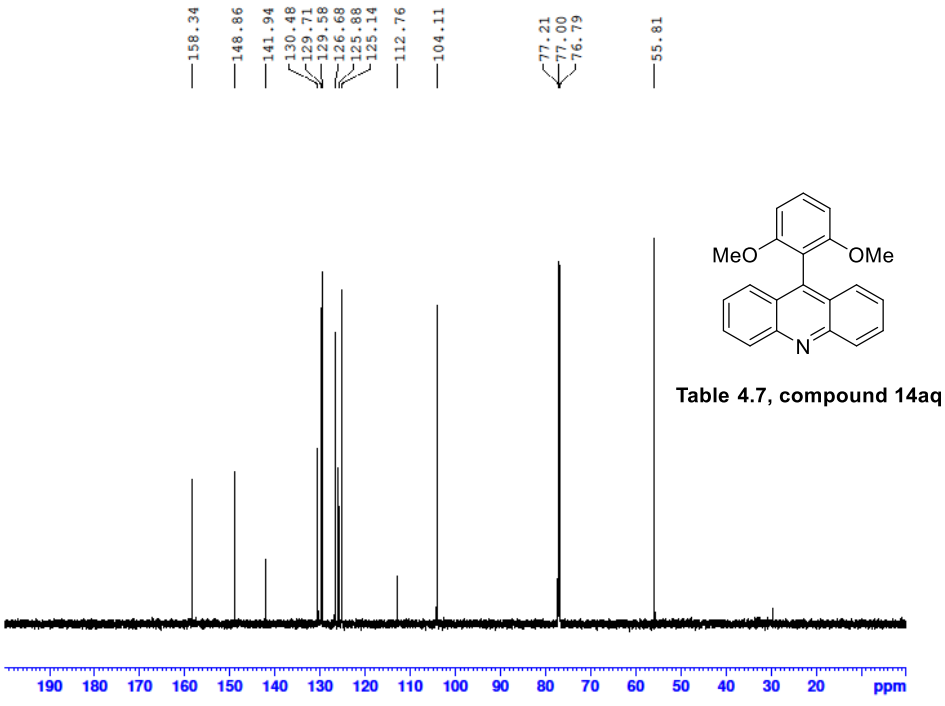

Table 4.7, compound 14aq

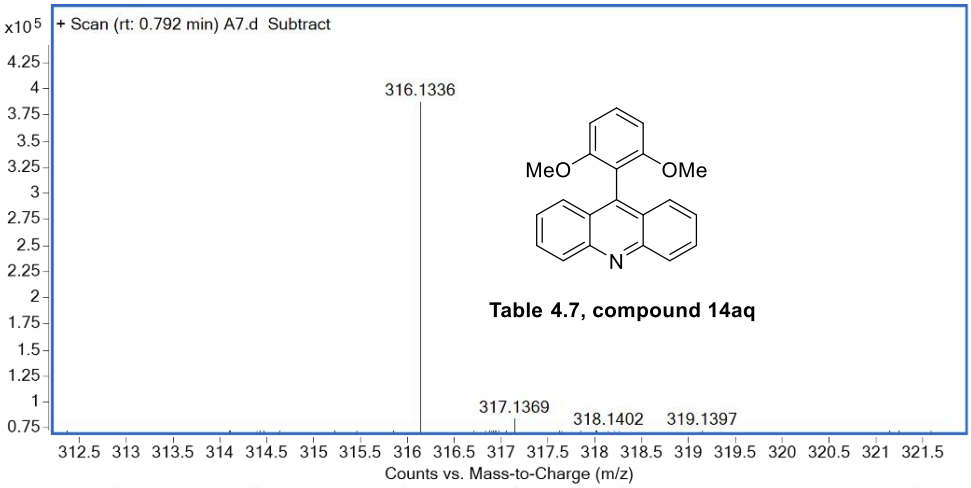

Table 4.7, compound 14aq

Mass	Calc. Mass	mDa	PPM	Ion Formula
316.1336	316.1332	-0.39	-1.25	C21H18O2N

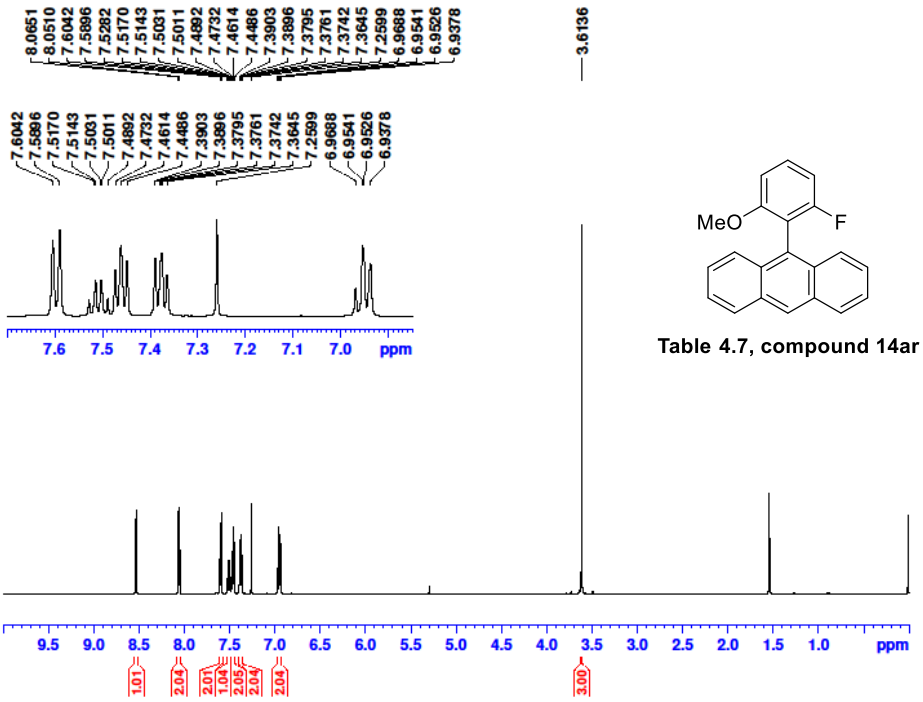

Table 4.7, compound 14ar

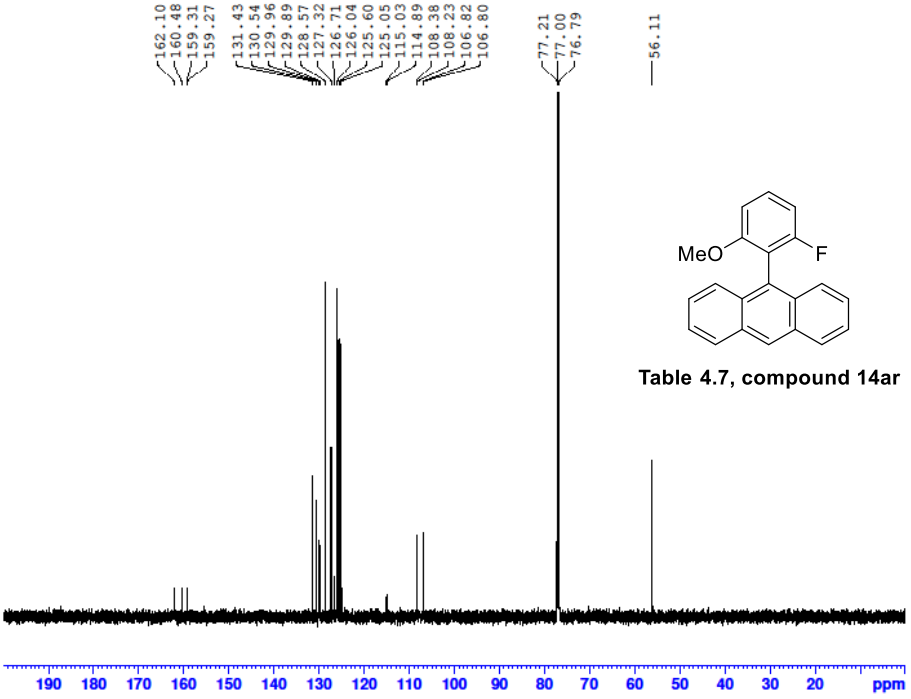

Table 4.7, compound 14ar

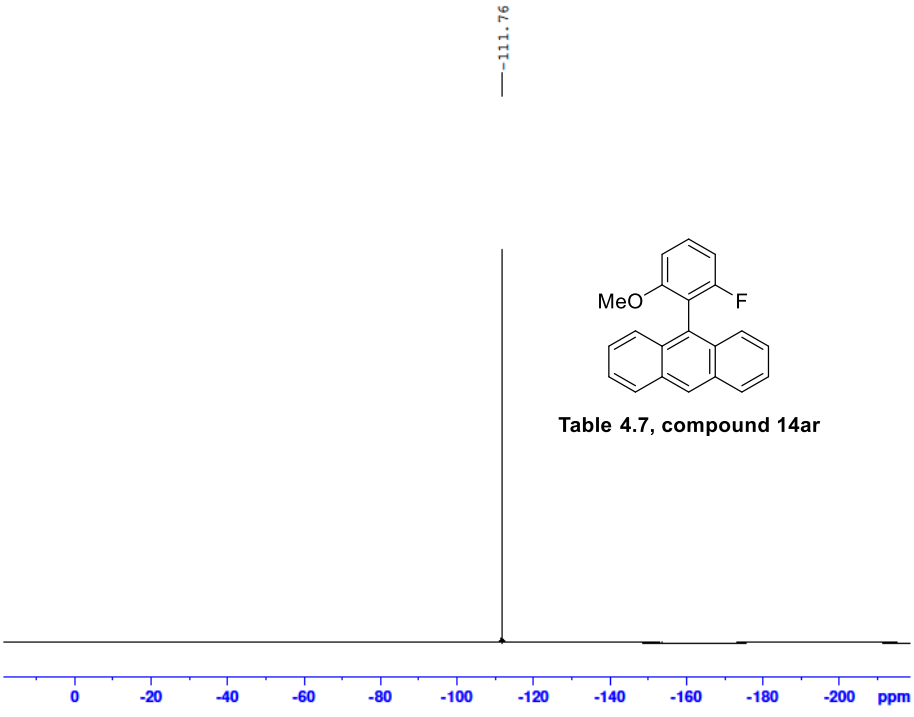

Table 4.7, compound 14ar

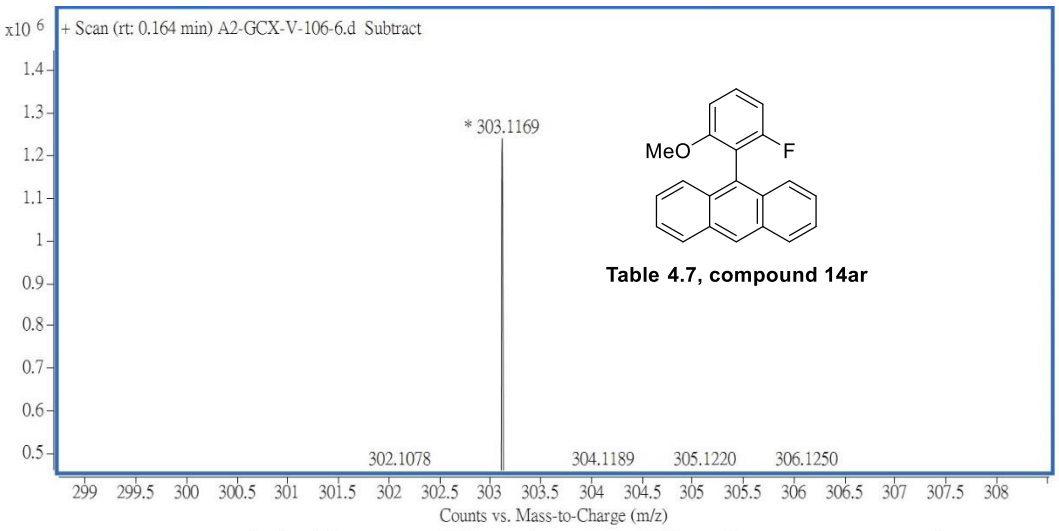

Table 4.7, compound 14ar

Mass	m/z (Calc)	Diff (mDa)	Diff (ppm)	Formula
303.1169	303.1180	1.07	3.54	C21H16FO

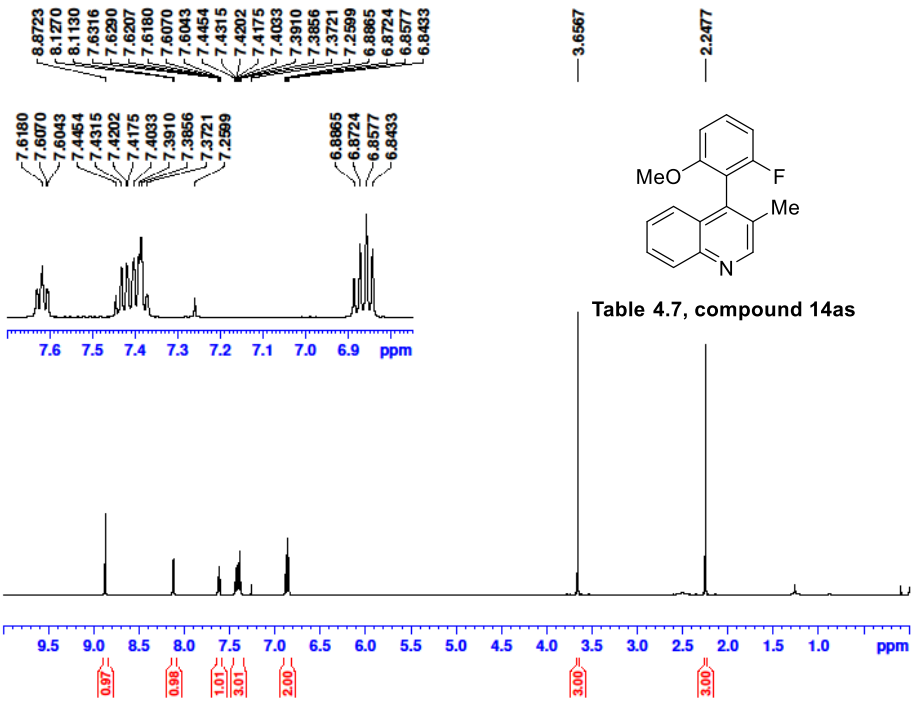

Table 4.7, compound 14as

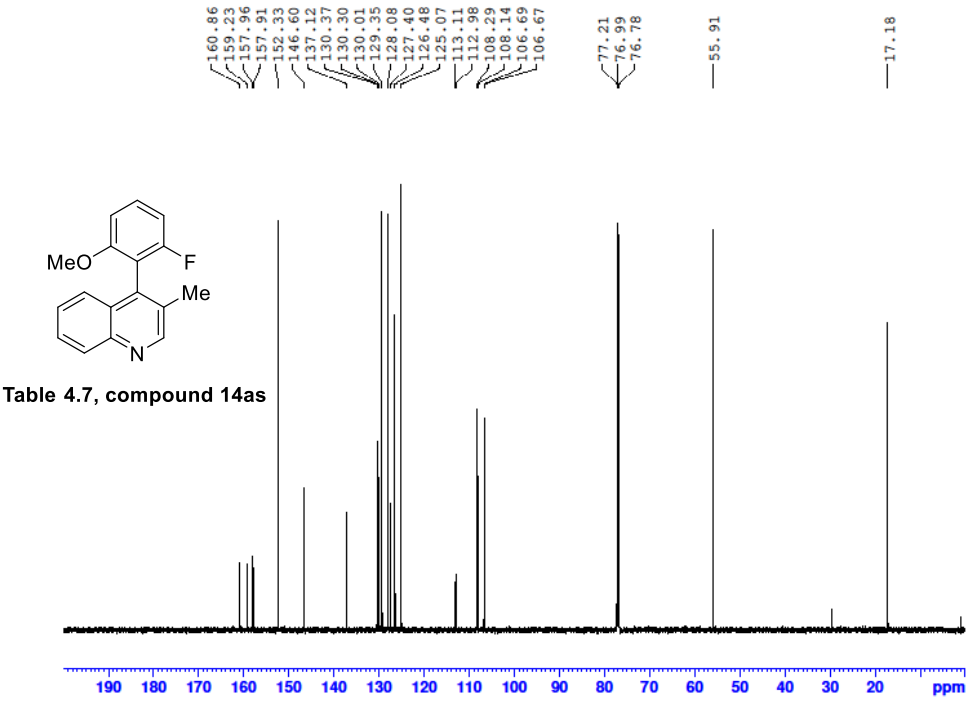

Table 4.7, compound 14as

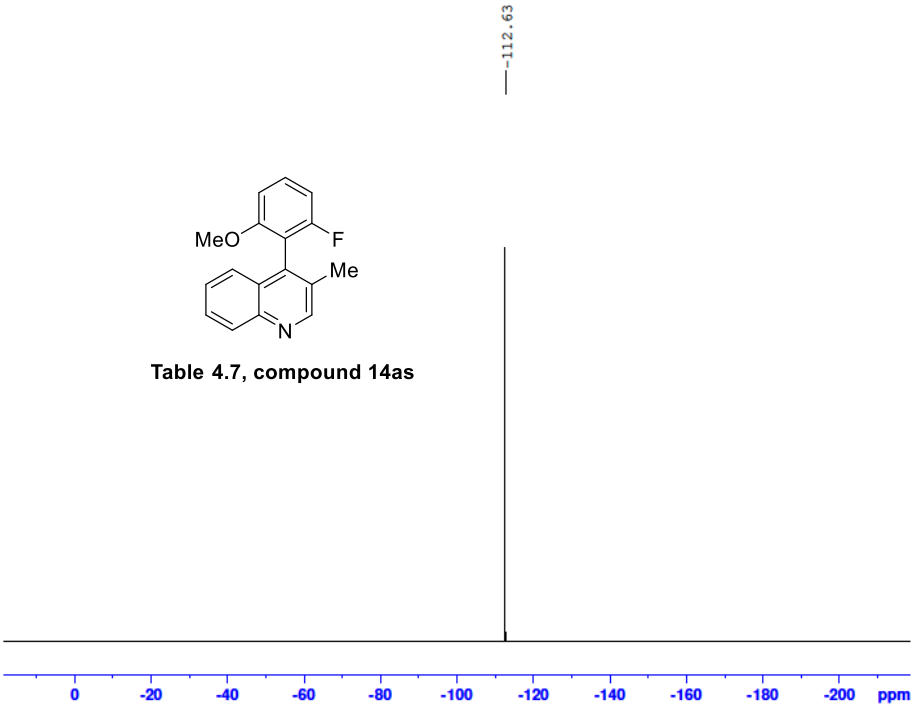

Table 4.7, compound 14as

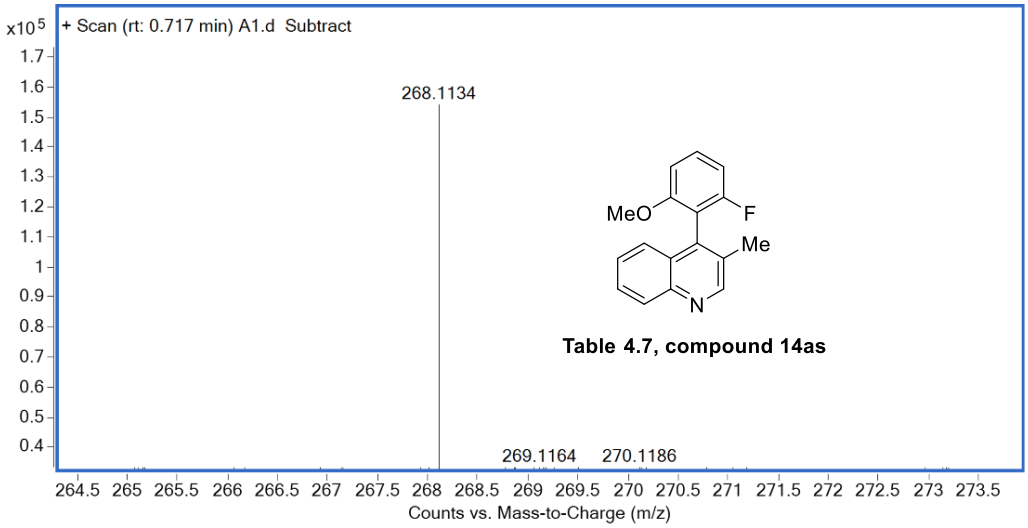

Table 4.7, compound 14as

Mass	Calc. Mass	mDa	PPM	Ion Formula
268.1134	268.1132	-0.68	-0.18	C17H15FNO

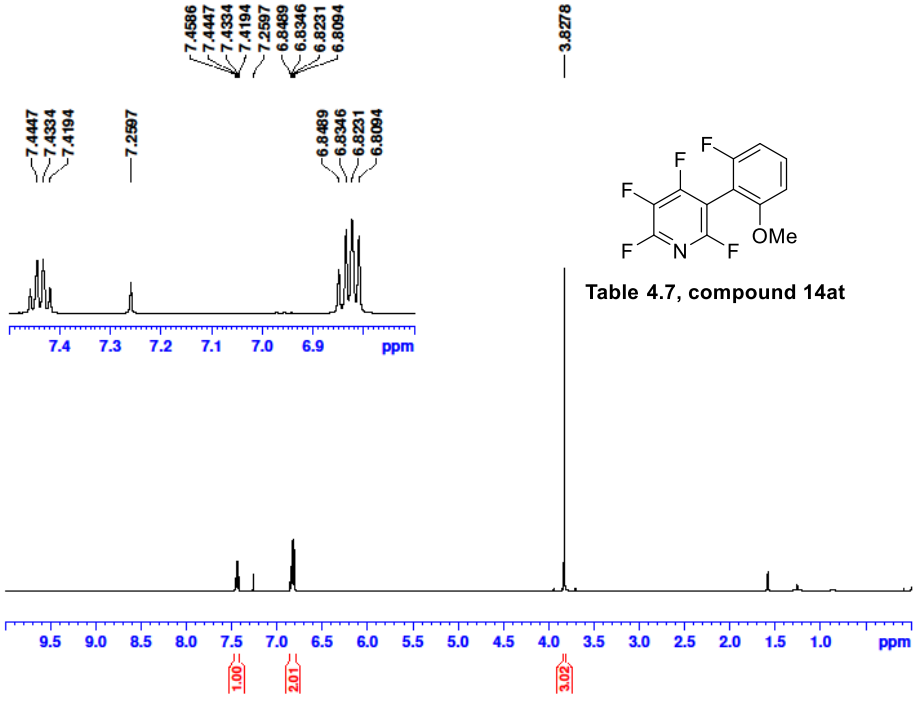

Table 4.7, compound 14at

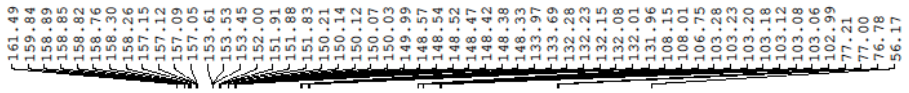

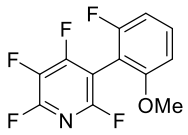

Table 4.7, compound 14at

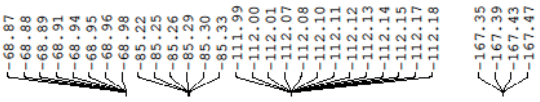

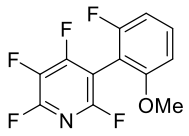

Table 4.7, compound 14at

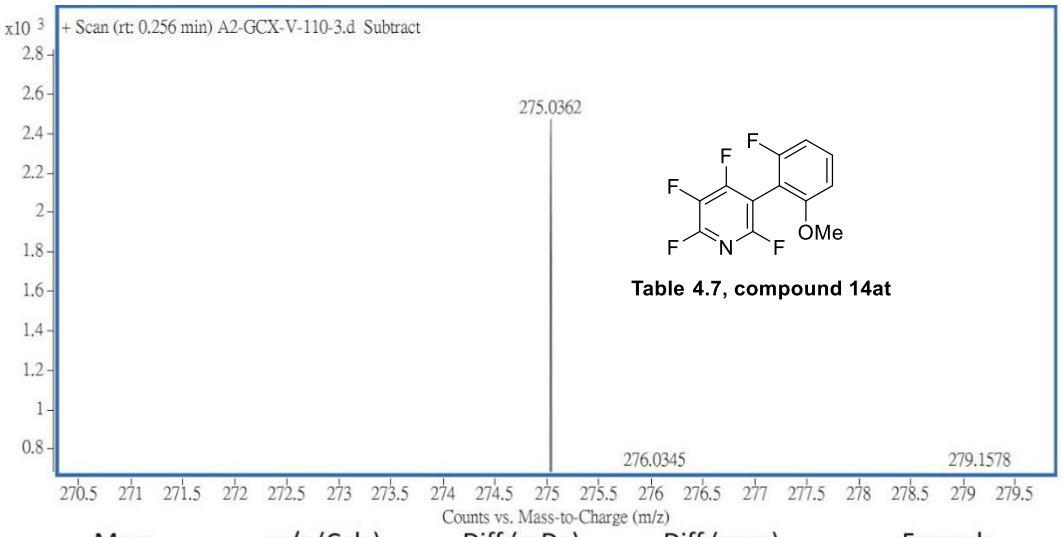

Table 4.7, compound 14at

Mass	m/z (Calc)	Diff (mDa)	Diff (ppm)	Formula
275.0362	275.0364	0.21	0.75	C12H6F5NO

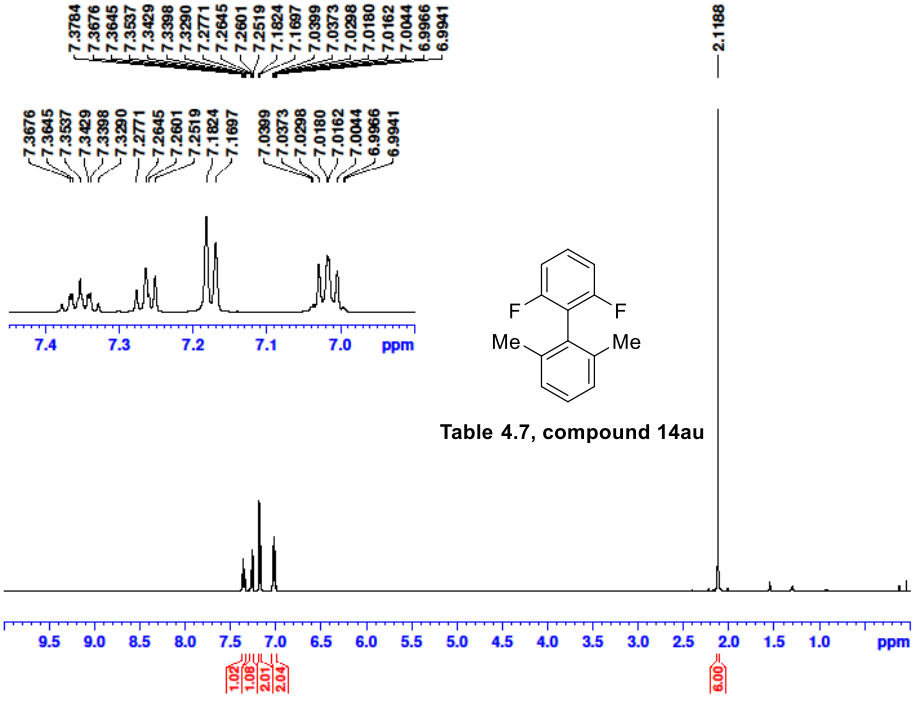

Table 4.7, compound 14au

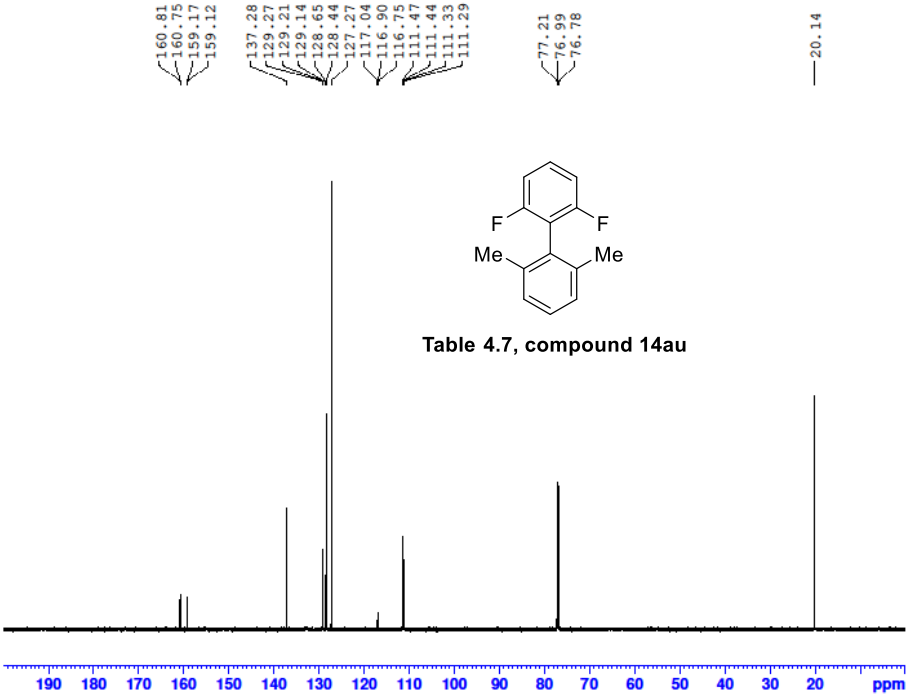

Table 4.7, compound 14au

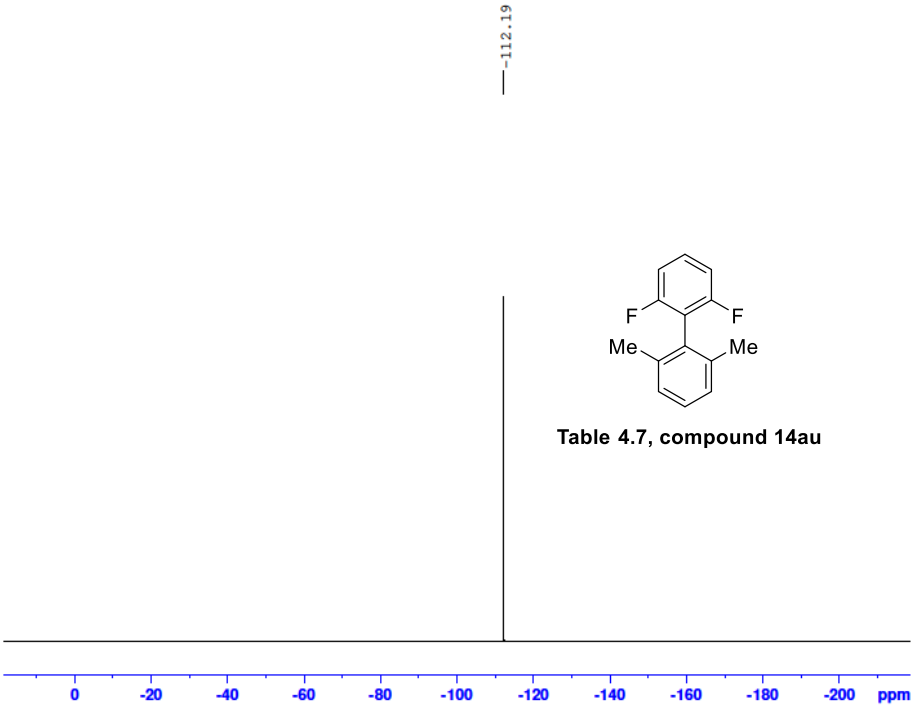

Table 4.7, compound 14au

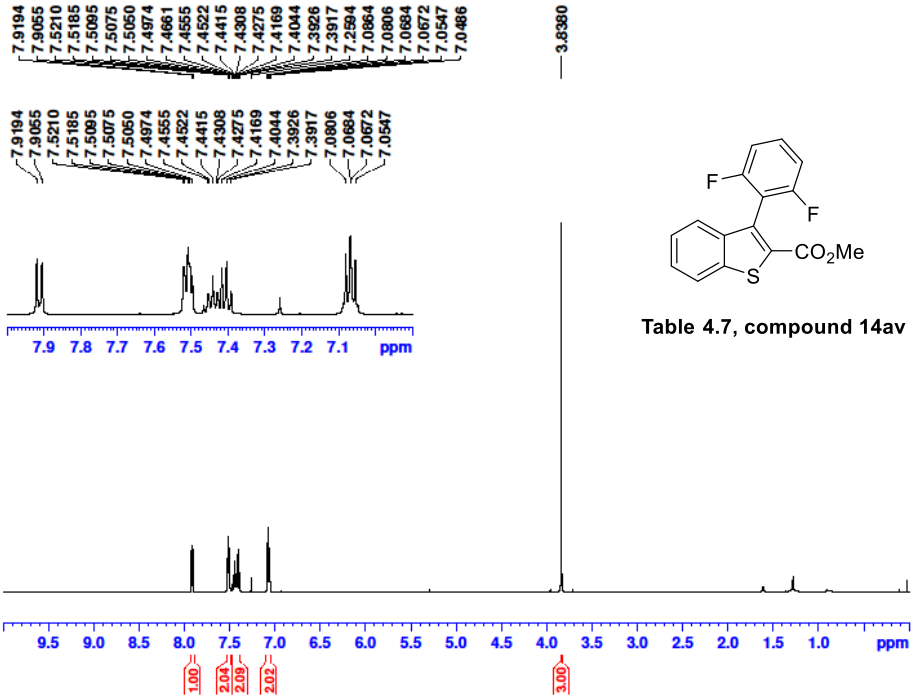

Table 4.7, compound 14av

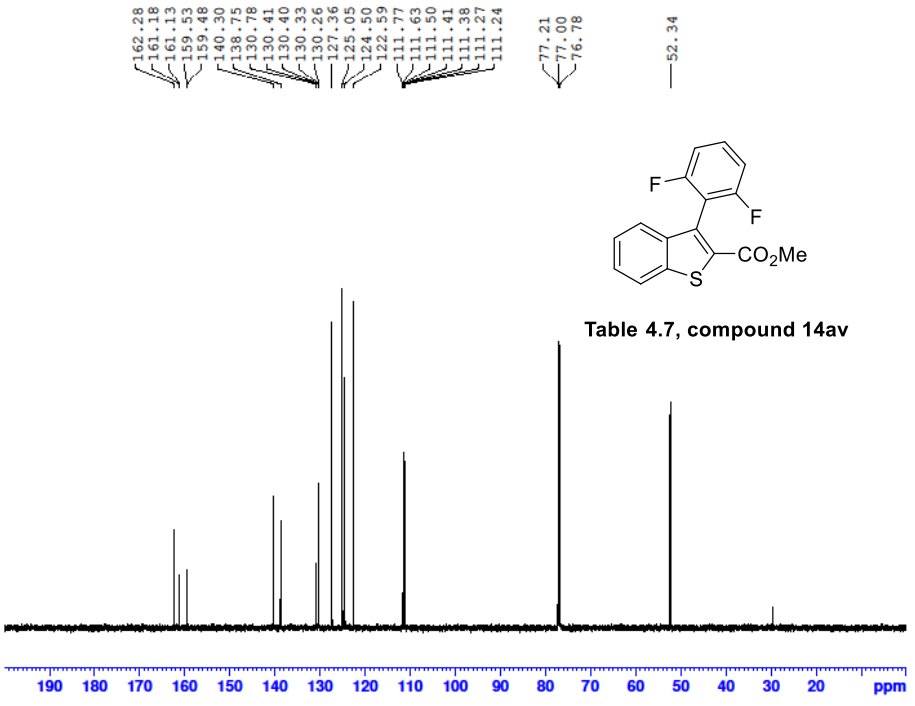

Table 4.7, compound 14av

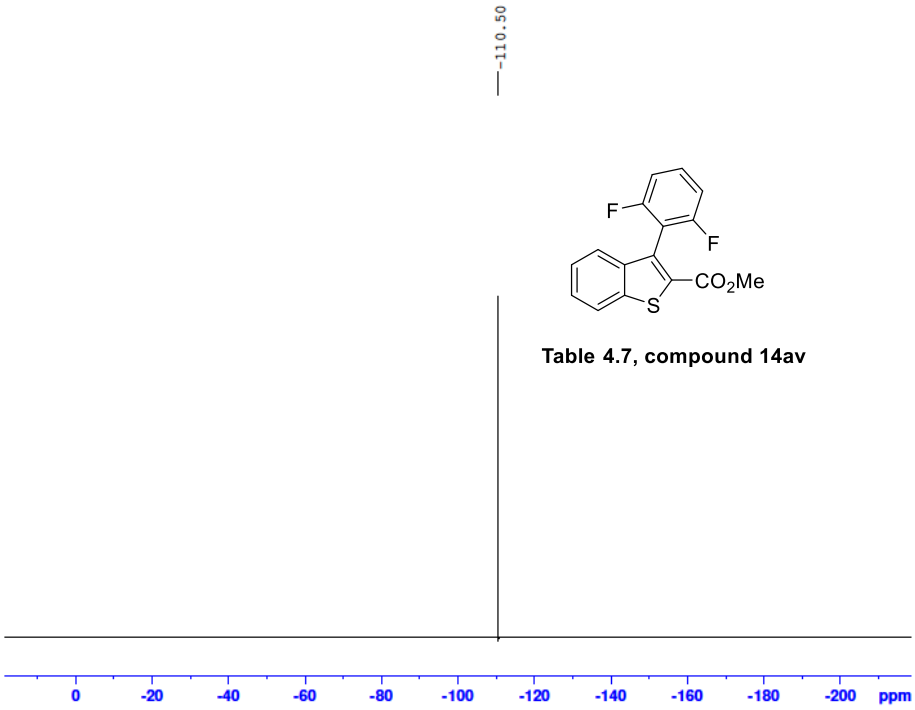

Table 4.7, compound 14av

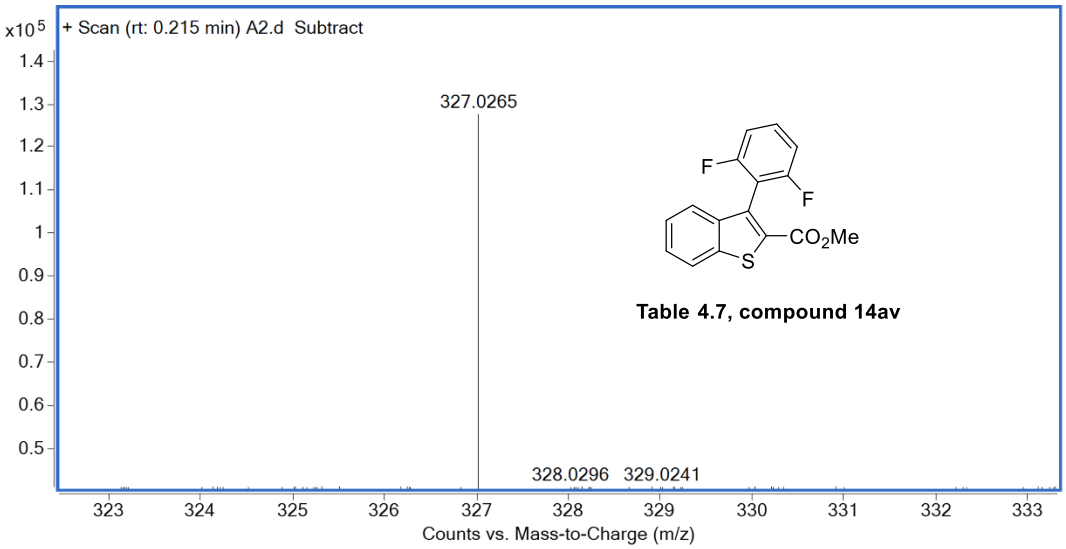

Table 4.7, compound 14av

Mass	Calc. Mass	mDa	PPM	Ion Formula
327.0265	327.0262	-0.32	-1.06	C16H10F2O2SNa

NMR & HRMS Spectra of Chapter 5

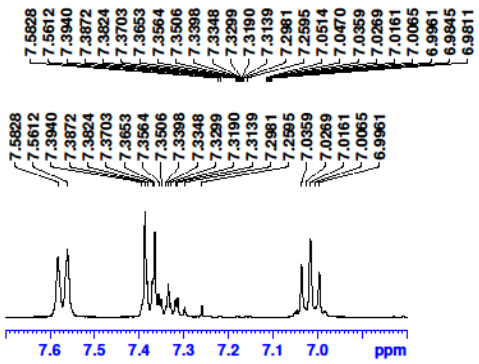

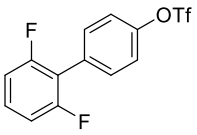

Table 5.3, compound 15a

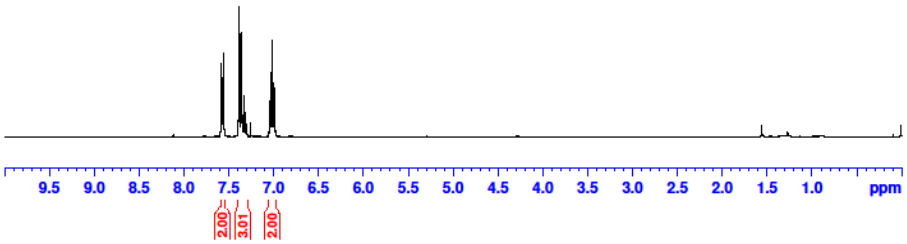

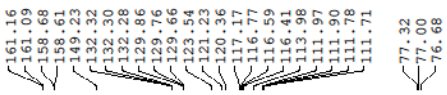

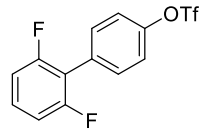

Table 5.3, compound 15a

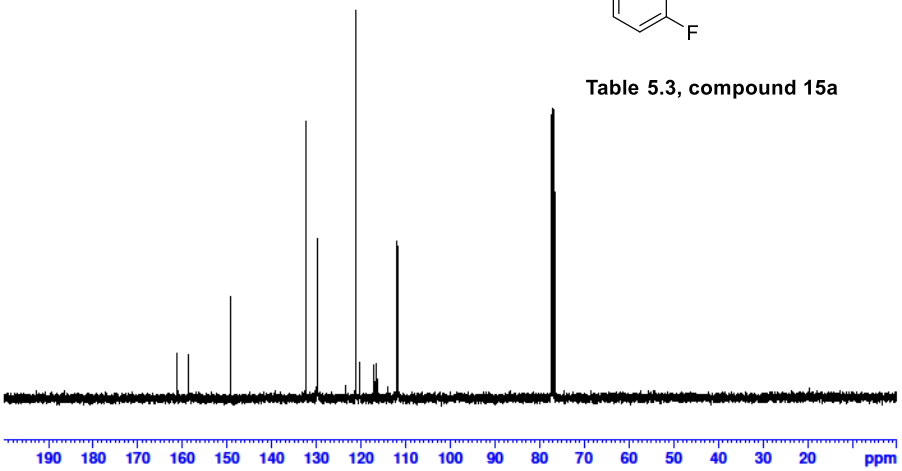

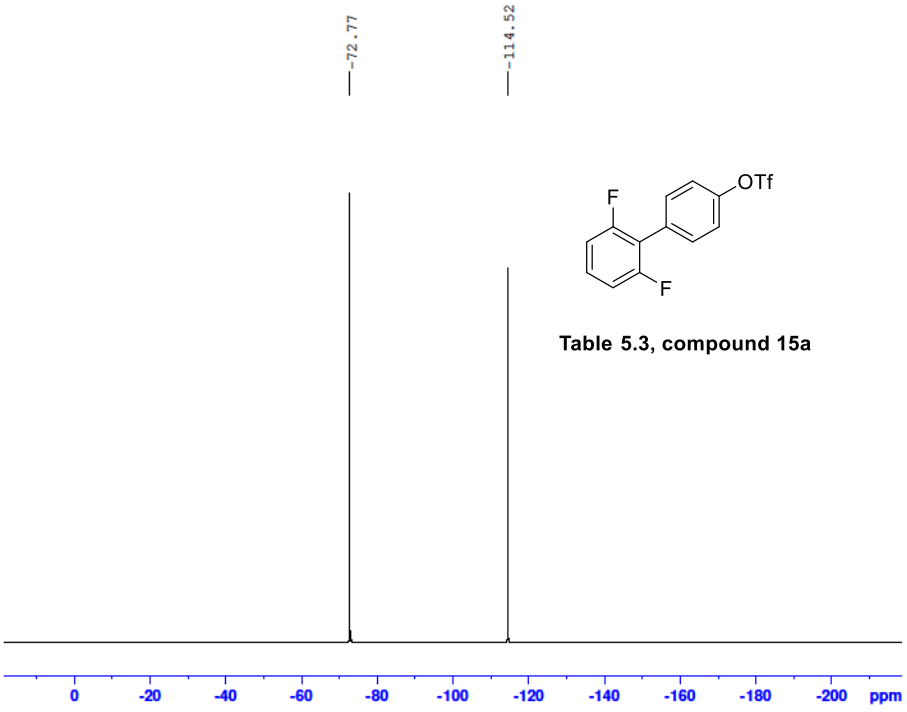

Table 5.3, compound 15a

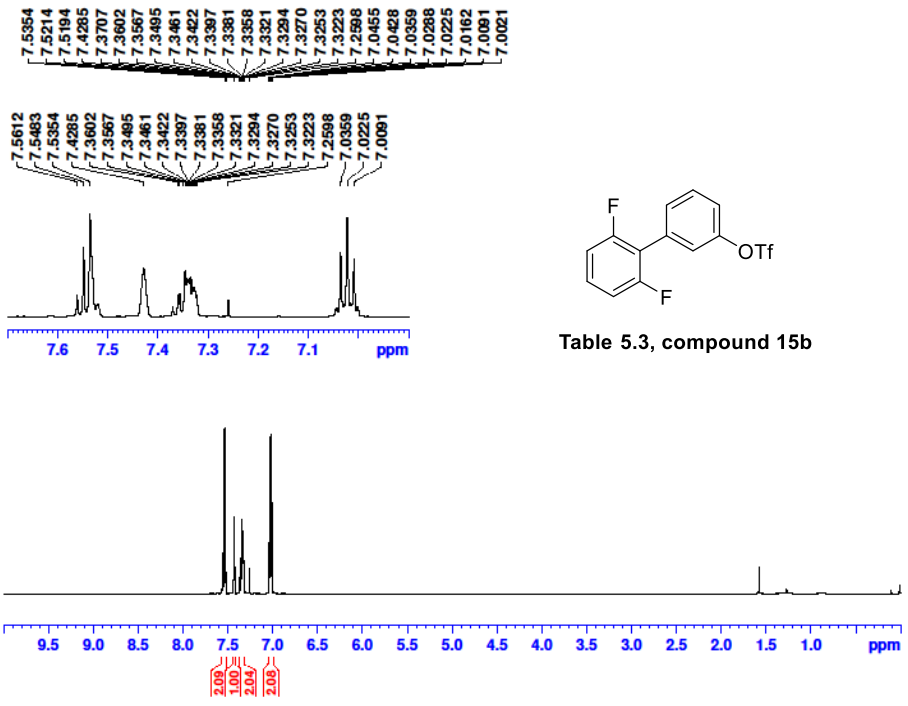

Table 5.3, compound 15b

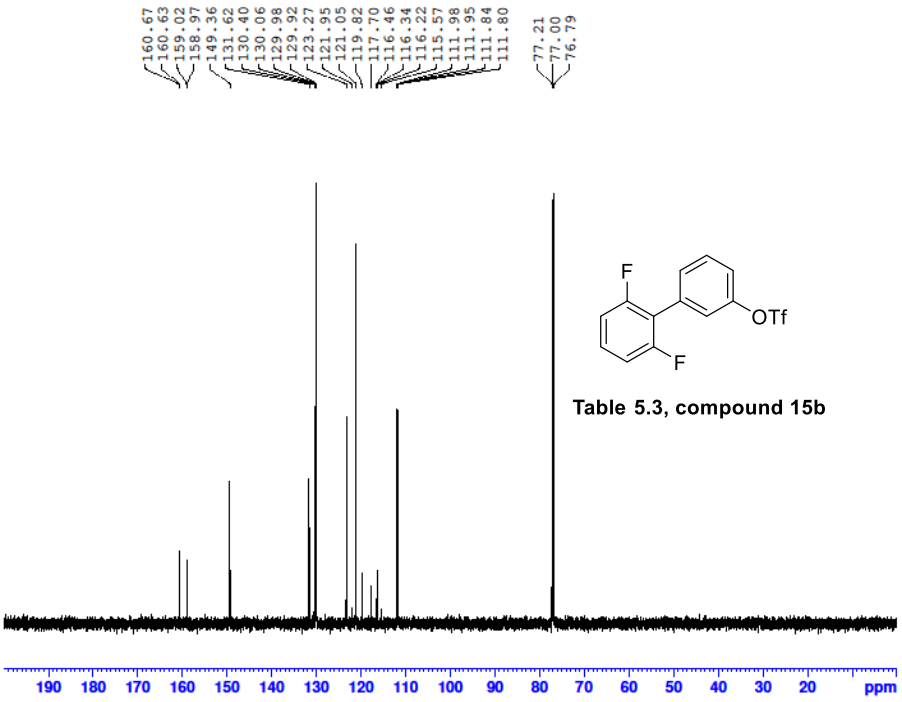

Table 5.3, compound 15b

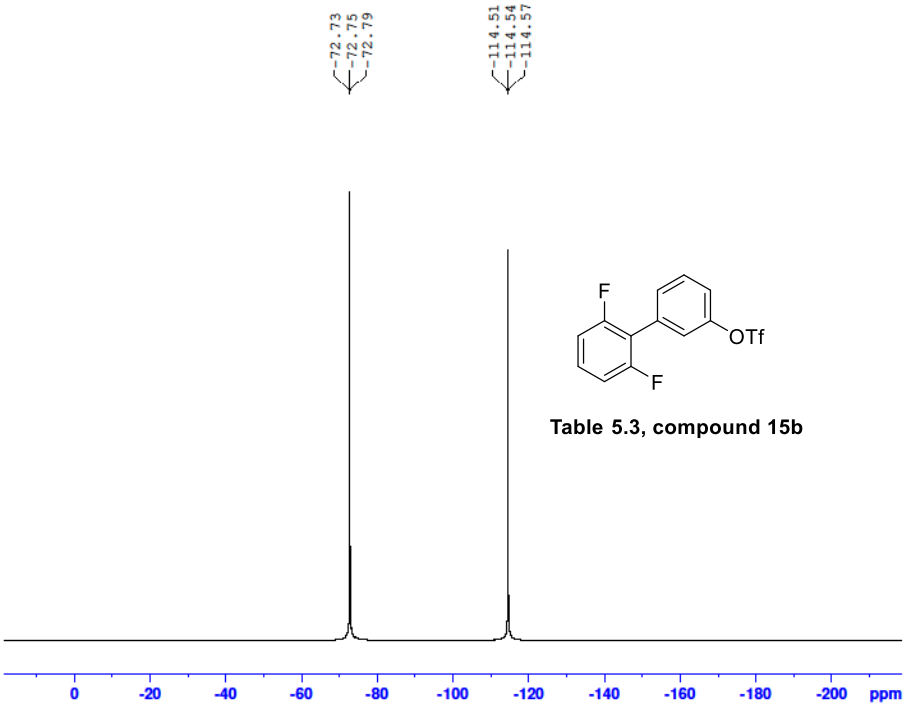

Table 5.3, compound 15b

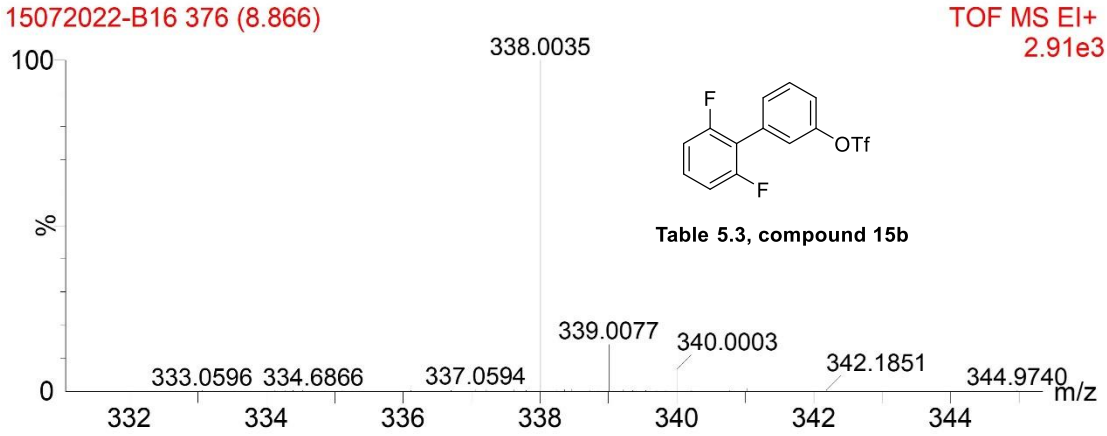

Table 5.3, compound 15b

Mass	Calc. Mass	mDa	PPM	Ion Formula
338.0035	338.0031	-0.44	-1.31	C13H7SF5O3

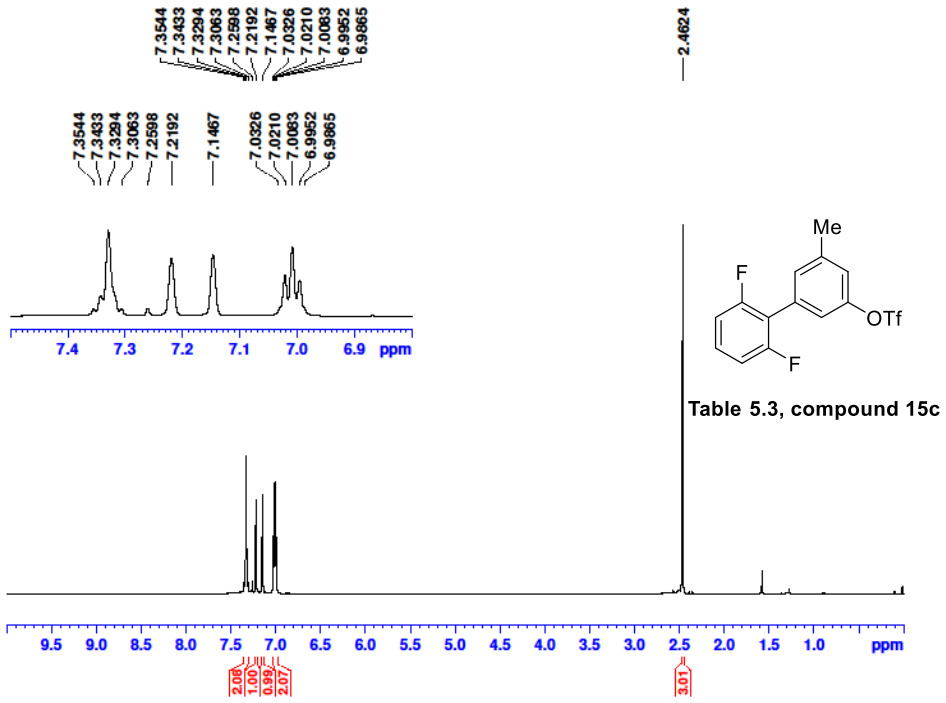

Table 5.3, compound 15c

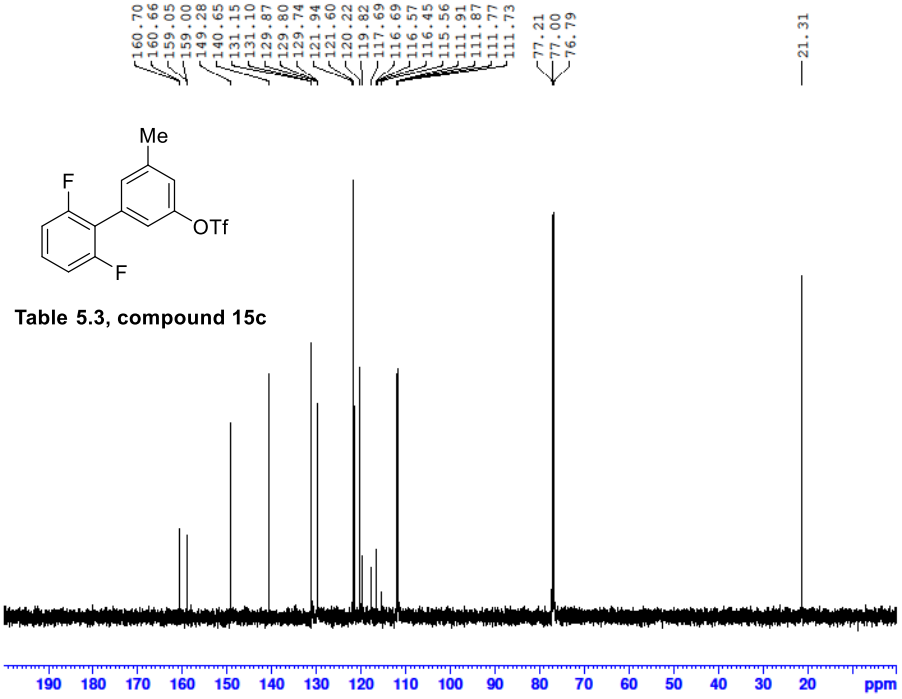

Table 5.3, compound 15c

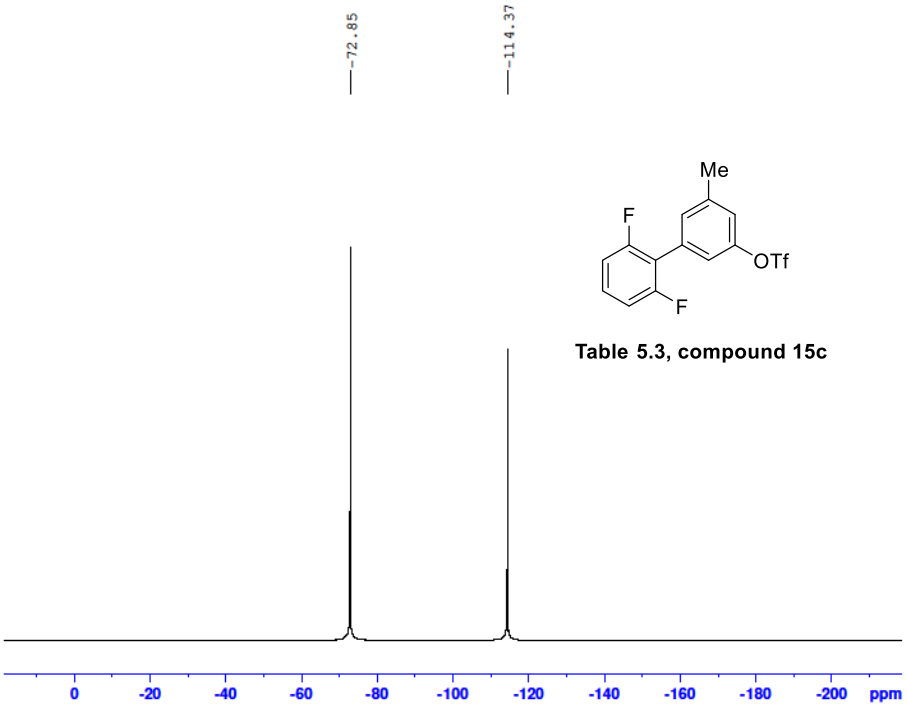

Table 5.3, compound 15c

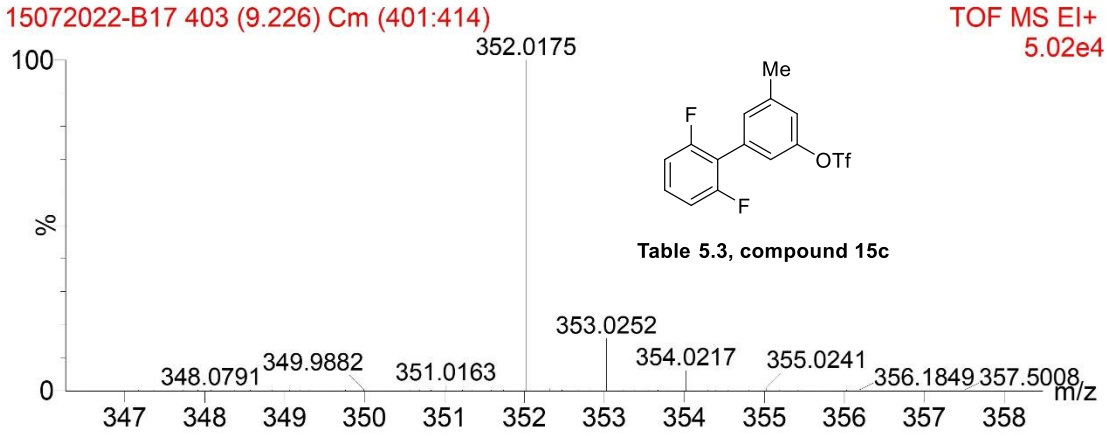

Table 5.3, compound 15c

Mass	Calc. Mass	mDa	PPM	Ion Formula
352.0175	352.0187	1.21	3.43	C14H9SF5O3

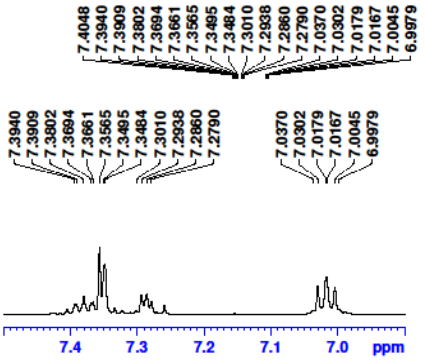

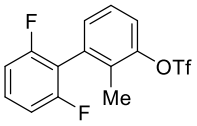

Table 5.3, compound 15d

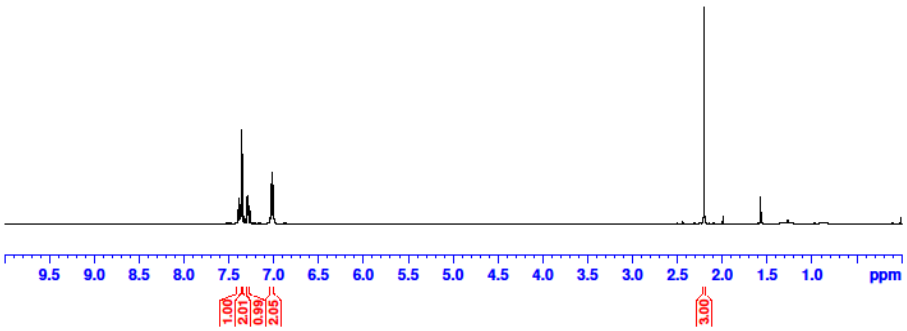

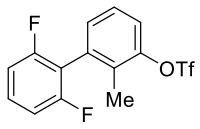

Table 5.3, compound 15d

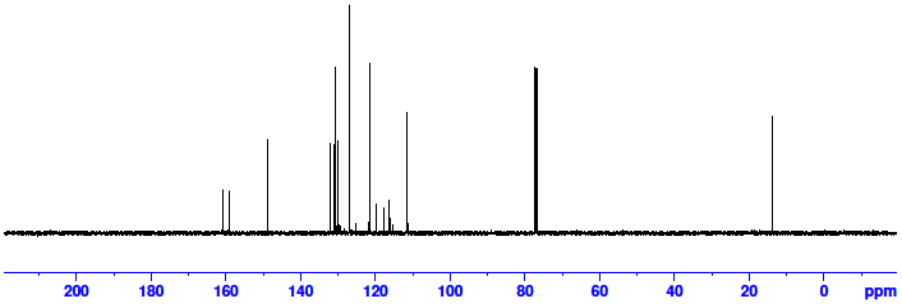

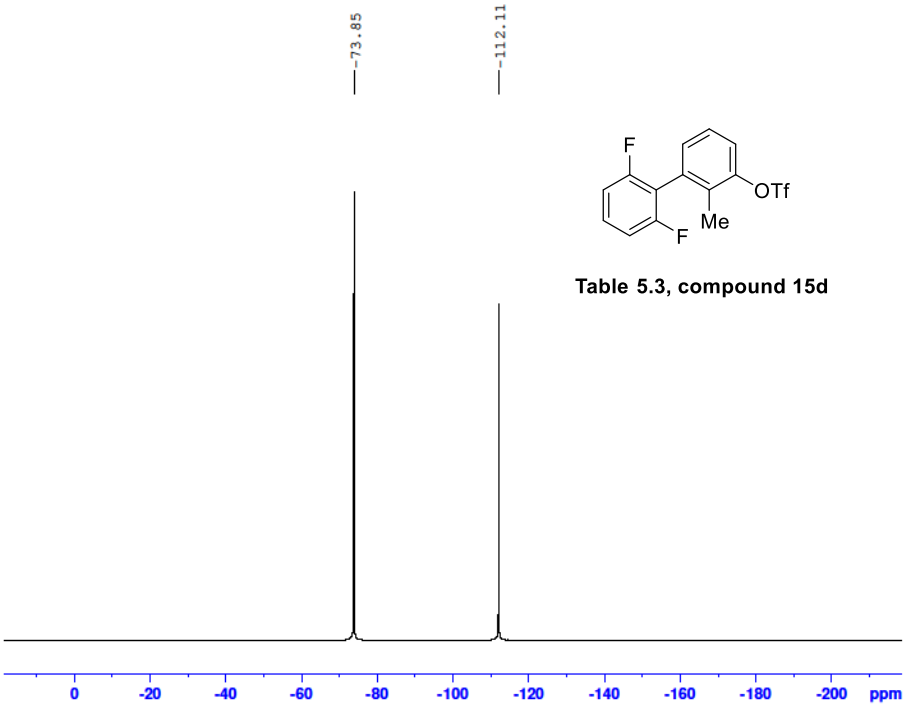

Table 5.3, compound 15d

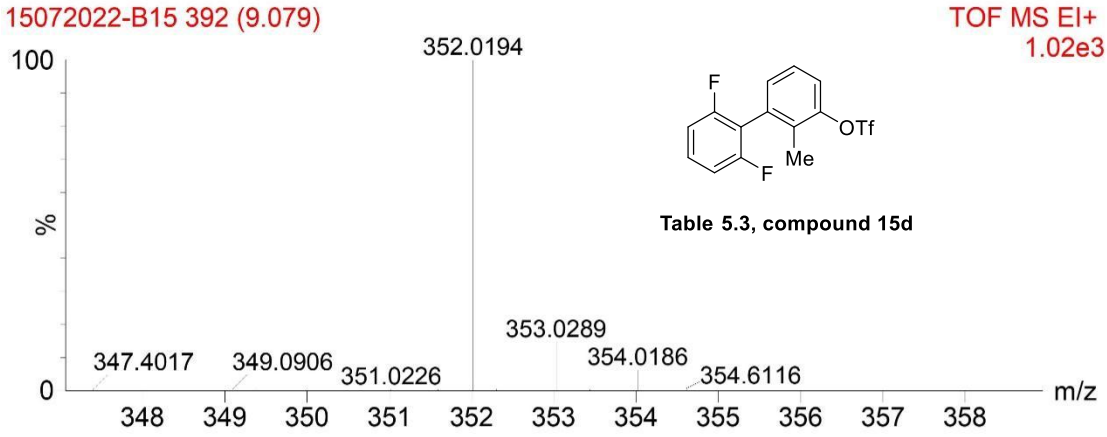

Table 5.3, compound 15d

Mass	Calc. Mass	mDa	PPM	Ion Formula
352.0194	352.0187	-0.69	-1.97	C14H9SF5O3

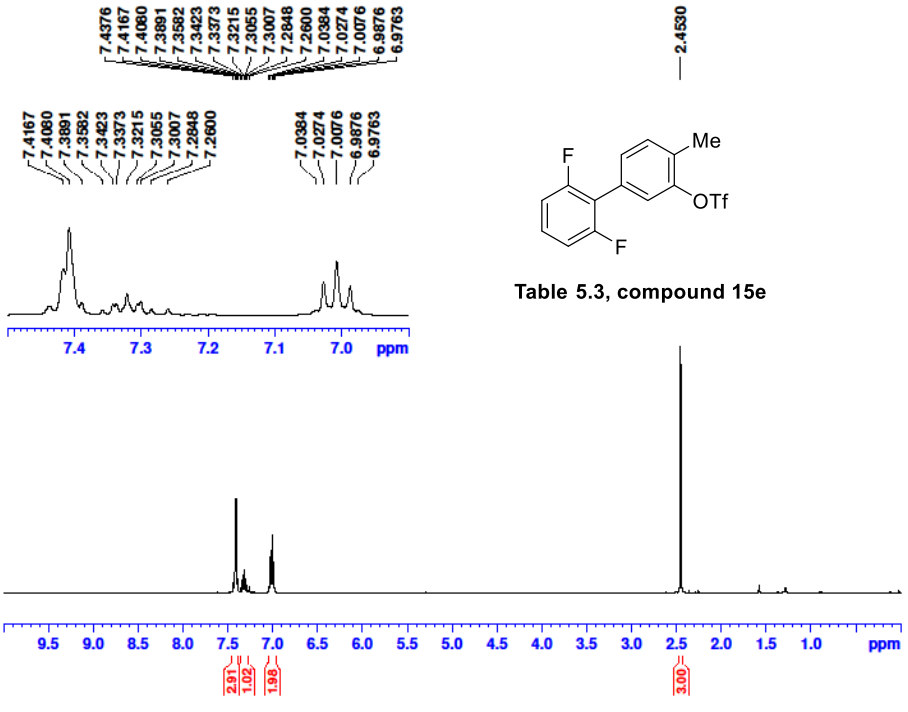

Table 5.3, compound 15e

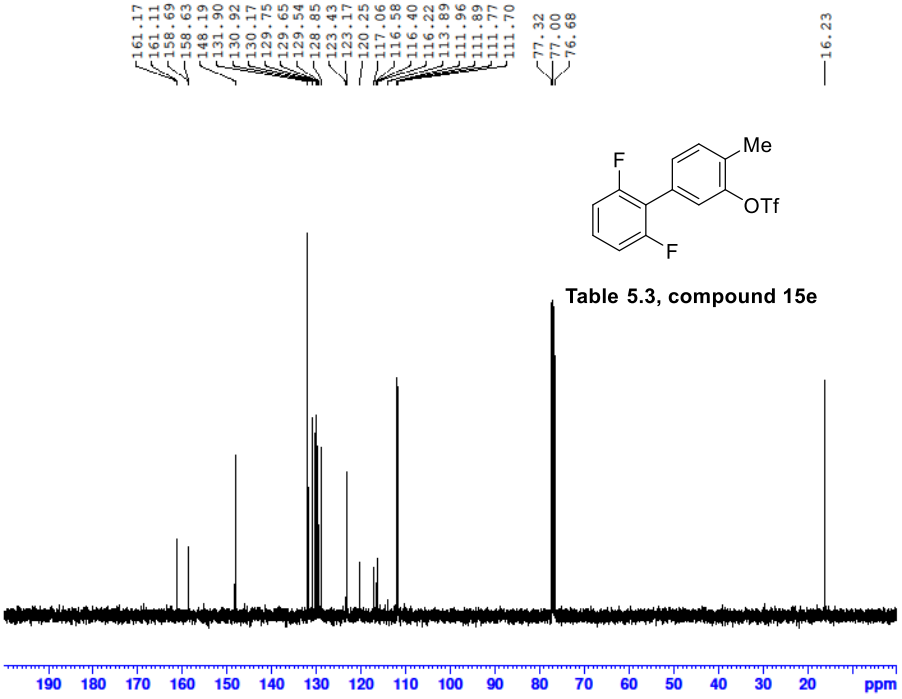

Table 5.3, compound 15e

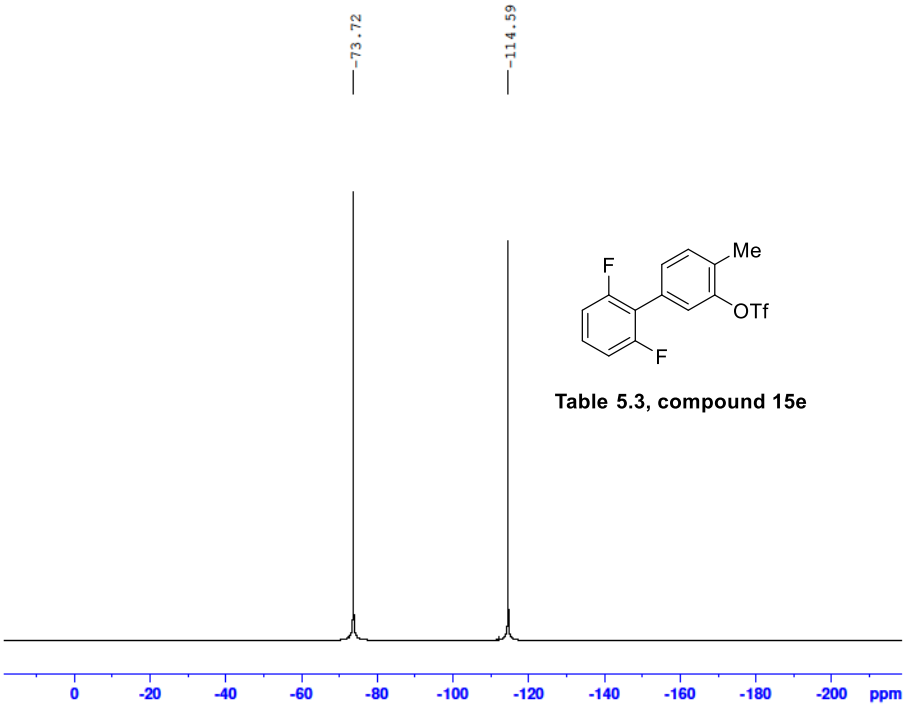

Table 5.3, compound 15e

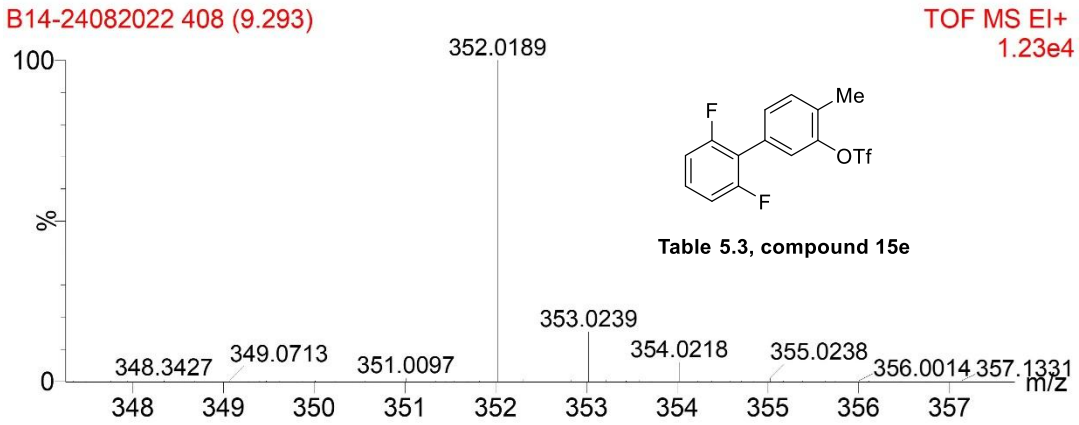

Table 5.3, compound 15e

Mass	m/z (Calc)	Diff (mDa)	Diff (ppm)	Formula
352.0189	352.0187	-0.19	-0.55	C14H9O3F5S

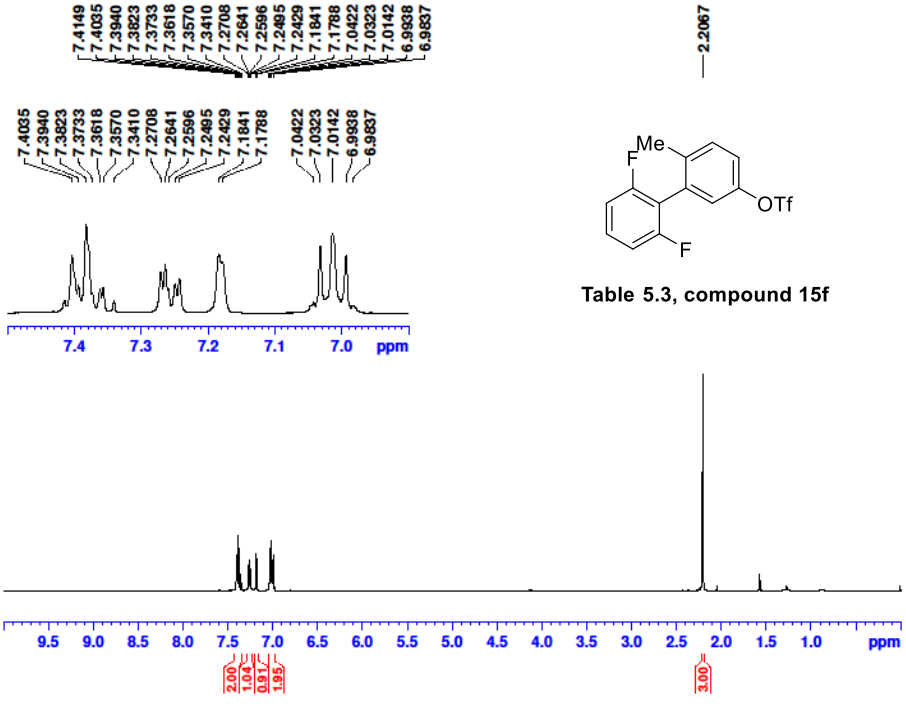

Table 5.3, compound 15f

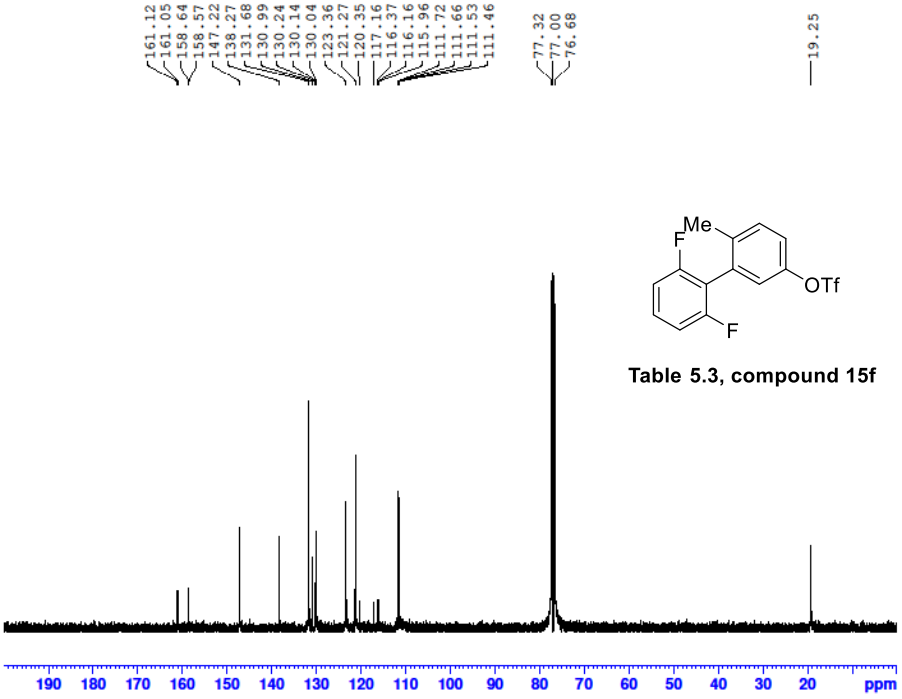

Table 5.3, compound 15f

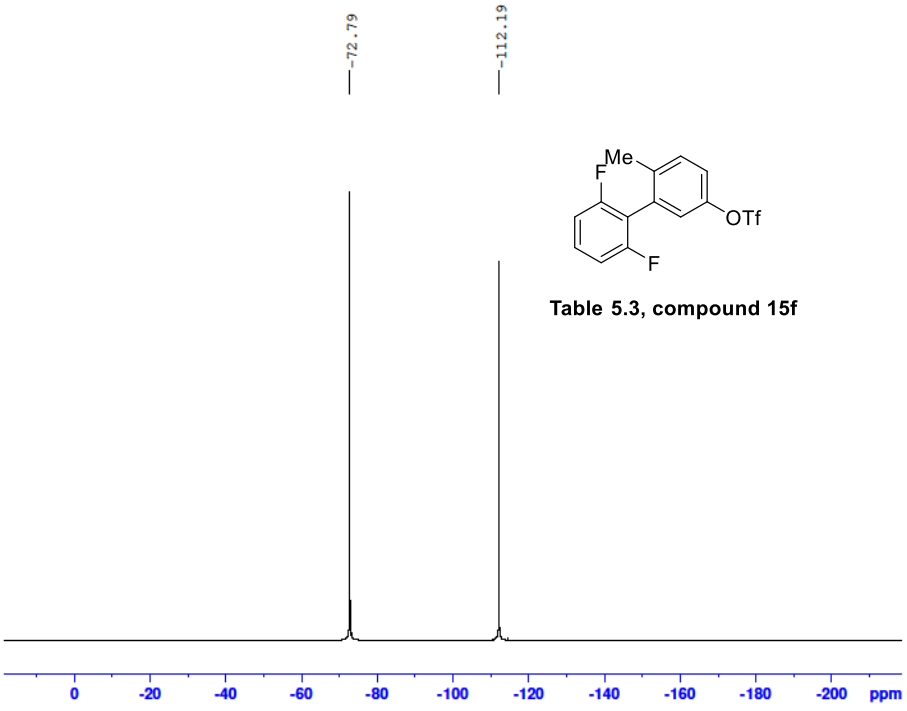

Table 5.3, compound 15f

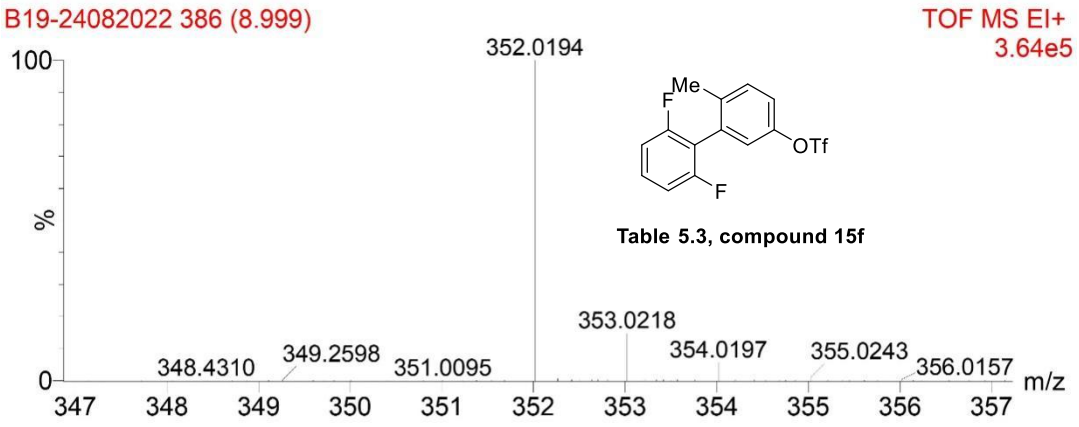

Table 5.3, compound 15f

Mass	m/z (Calc)	Diff (mDa)	Diff (ppm)	Formula
352.0194	352.0187	-0.69	-1.97	C14H9O3F5S

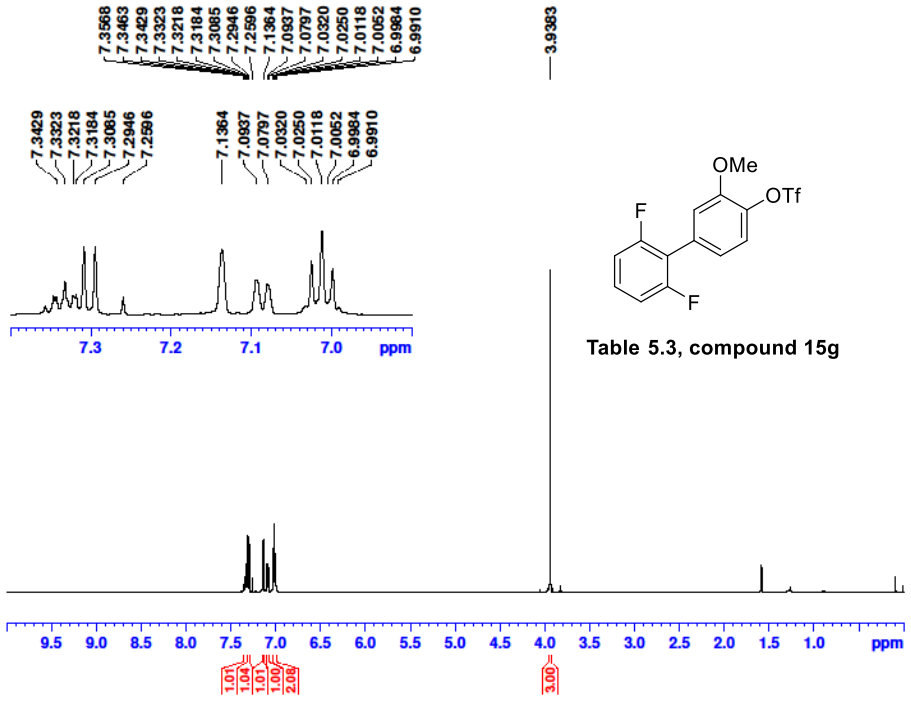

Table 5.3, compound 15g

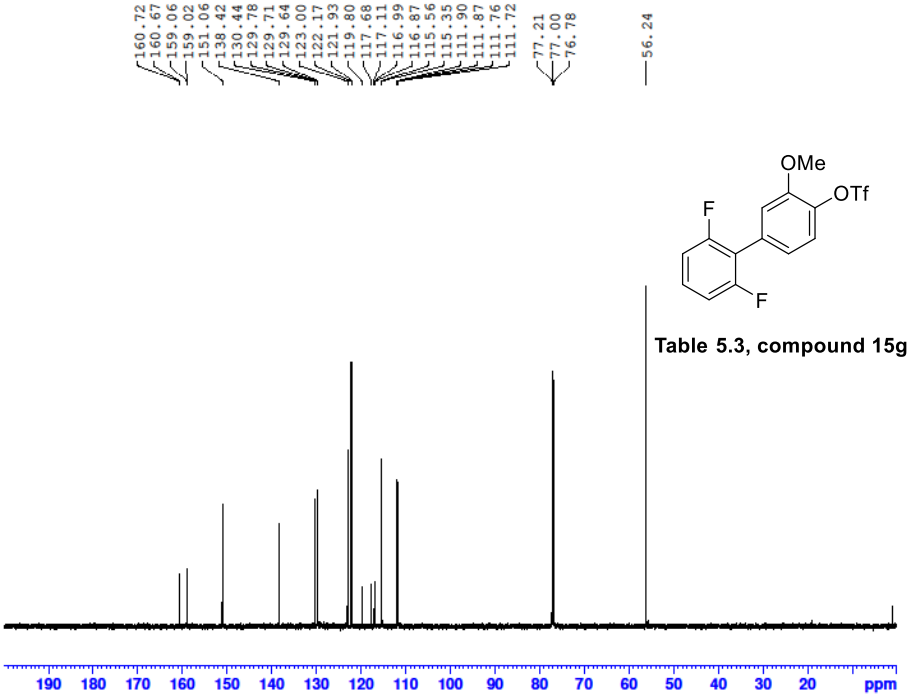
160.72
160.67
159.06
159.02
151.06
138.42
130.44
129.78
129.71
129.64
123.00
122.17
121.93
119.80
117.68
117.11
116.99
116.87
115.56
115.35
111.90
111.87
111.76
111.72
77.21
77.00
76.78
56.24
OMe
OTf
F
F
Table 5.3, compound 15g
190 180 170 160 150 140 130 120 110 100 90 80 70 60 50 40 30 20 ppm

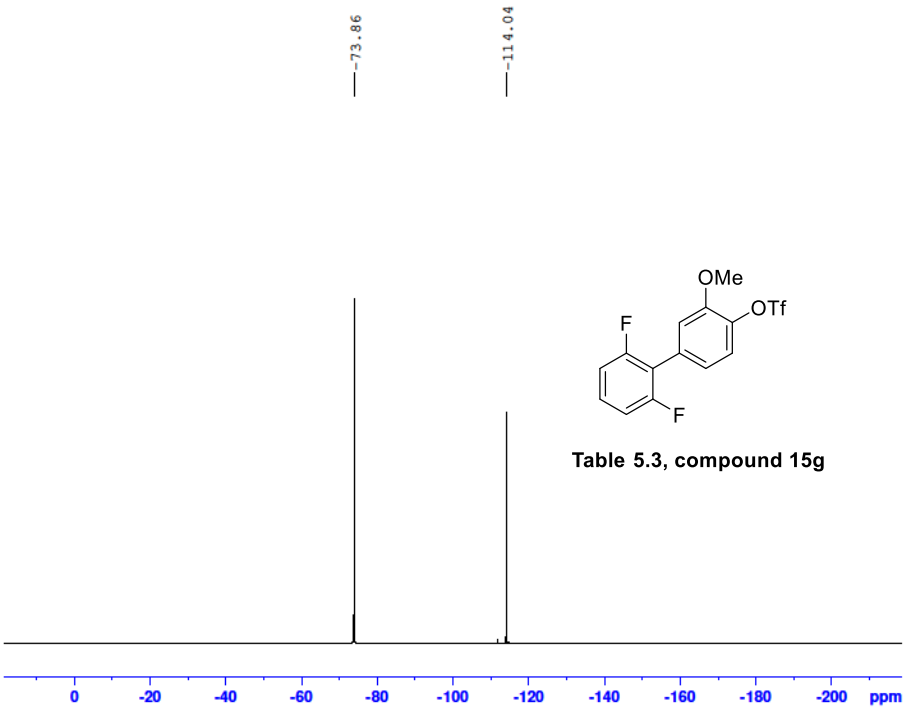
-73.86
-114.04
OMe
OTf
F
F
Table 5.3, compound 15g
0 -20 -40 -60 -80 -100 -120 -140 -160 -180 -200 ppm

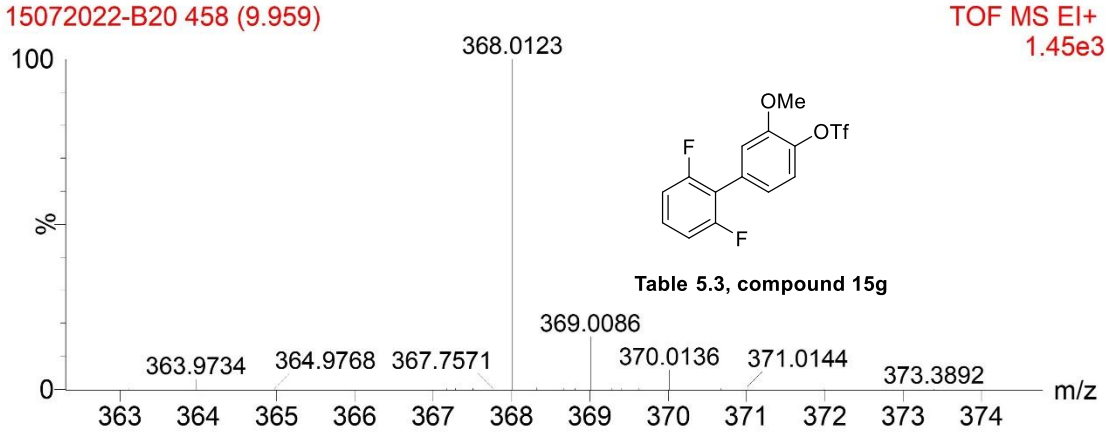

Table 5.3, compound 15g

Mass	Calc. Mass	mDa	PPM	Ion Formula
368.0123	368.0136	1.32	3.59	C14H9SF5O4

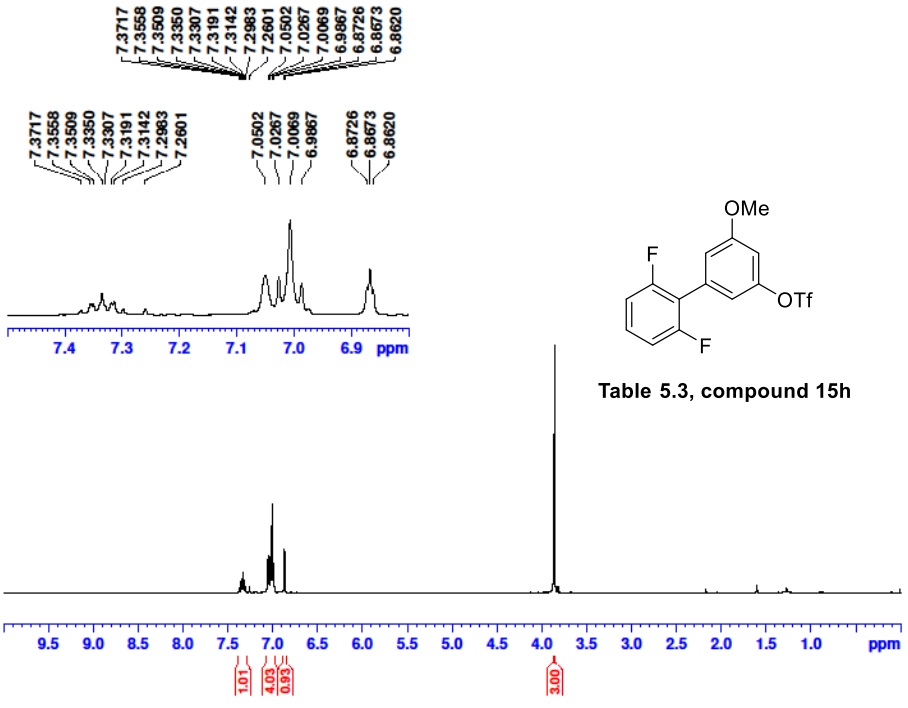

Table 5.3, compound 15h

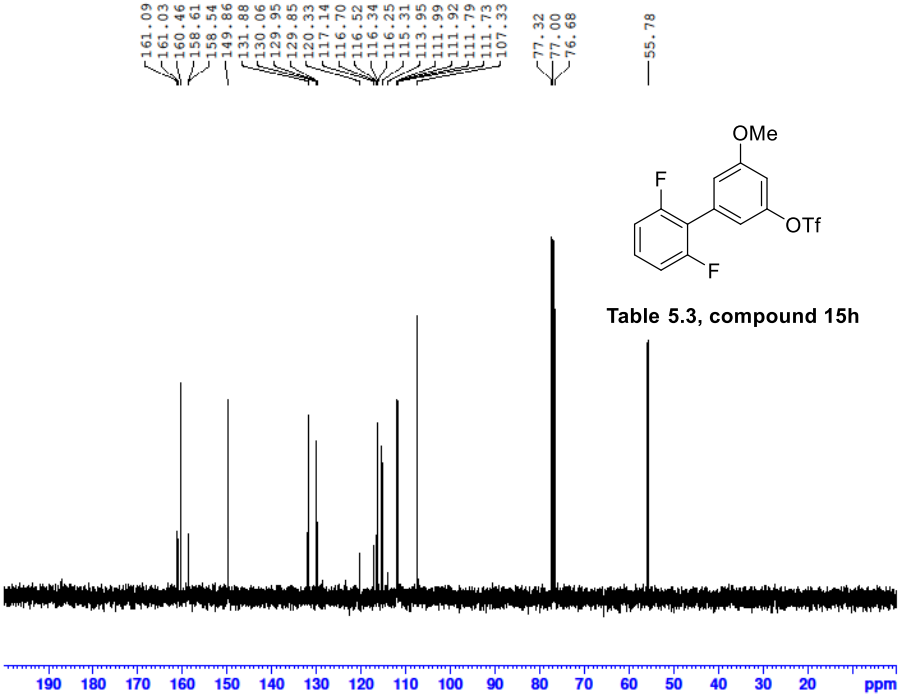

Table 5.3, compound 15h

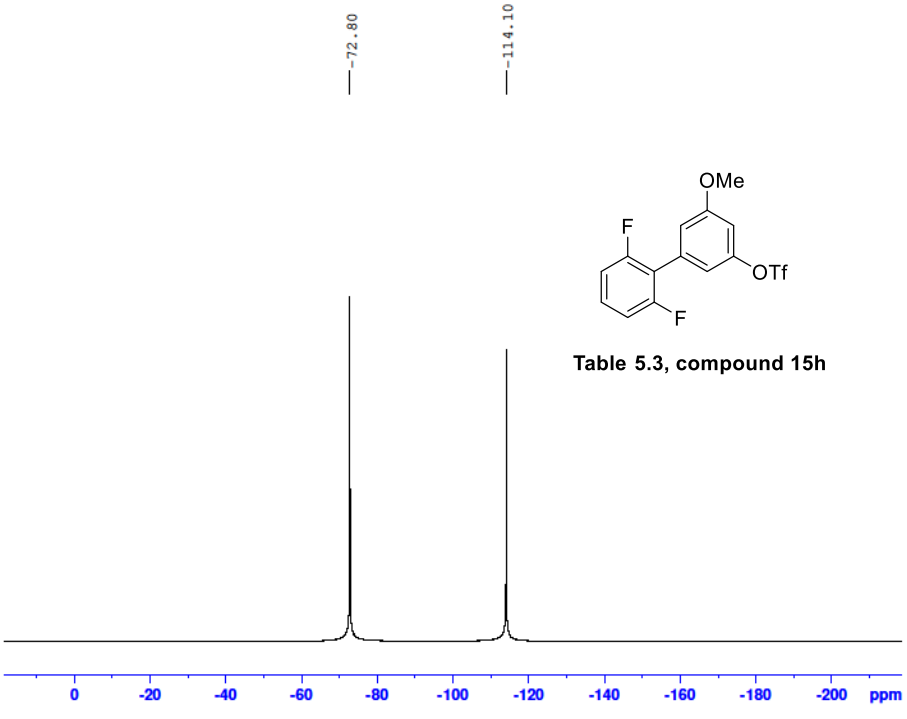

Table 5.3, compound 15h

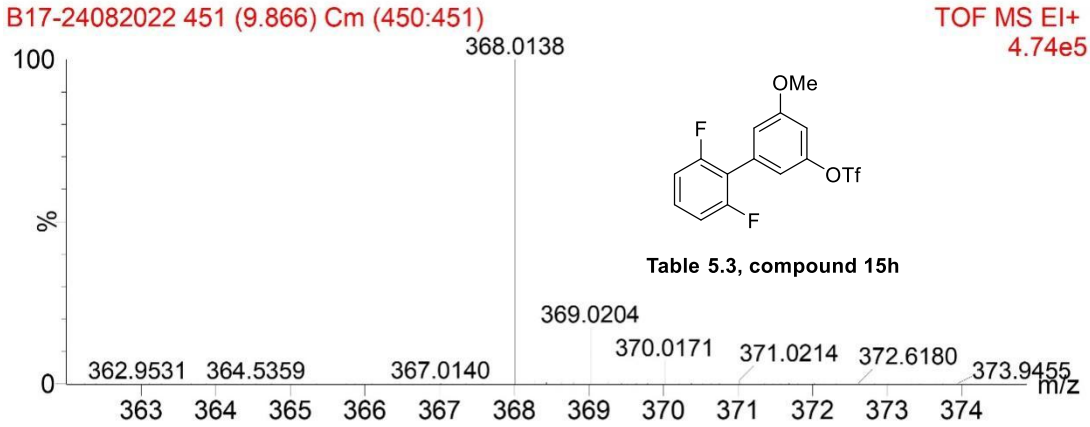

Table 5.3, compound 15h

Mass	m/z (Calc)	Diff (mDa)	Diff (ppm)	Formula
368.0138	368.0136	-0.18	-0.48	C14H9O4F5S

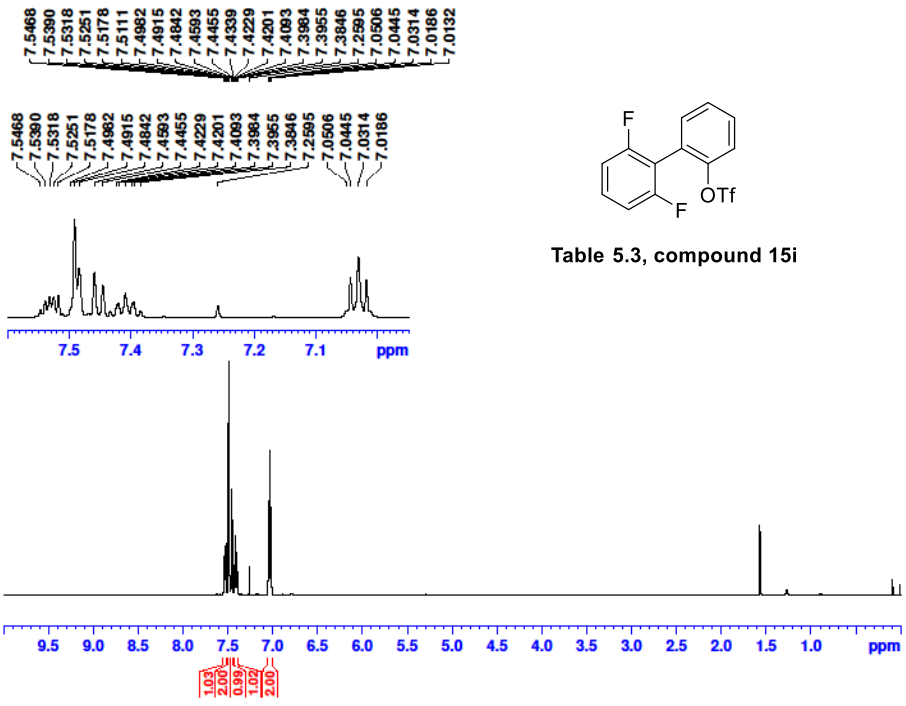

Table 5.3, compound 15i

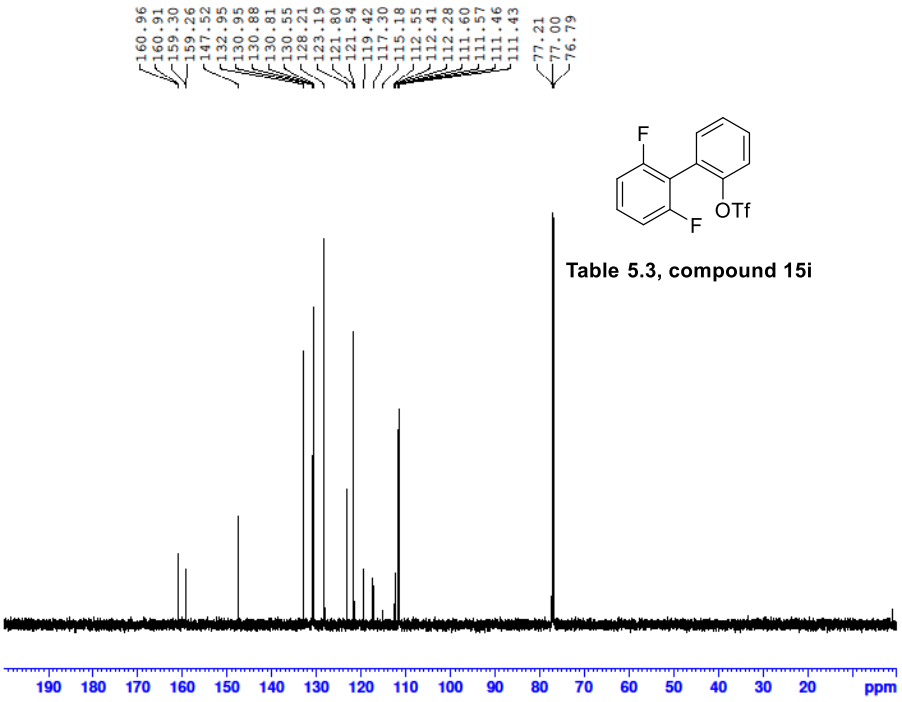

Table 5.3, compound 15i

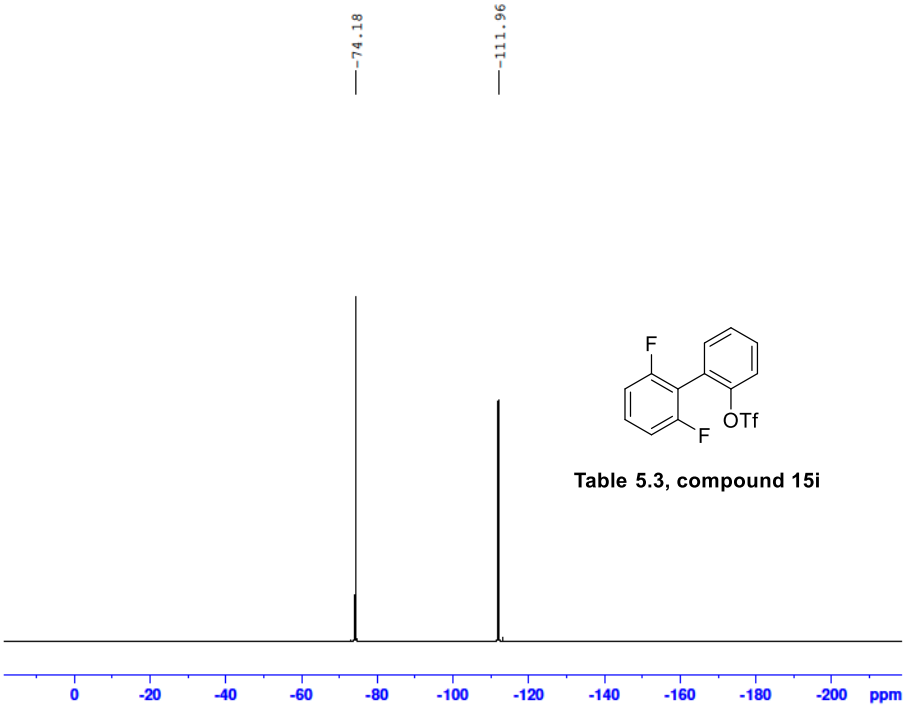

Table 5.3, compound 15i

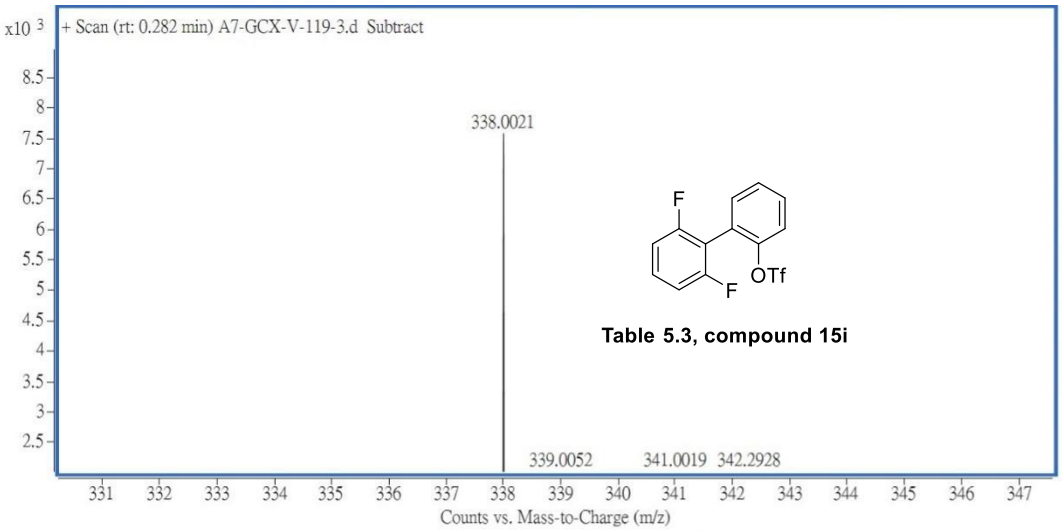

Table 5.3, compound 15i

Mass	m/z (Calc)	Diff (mDa)	Diff (ppm)	Formula
338.0021	338.0031	0.96	2.83	C13H7F5O3S

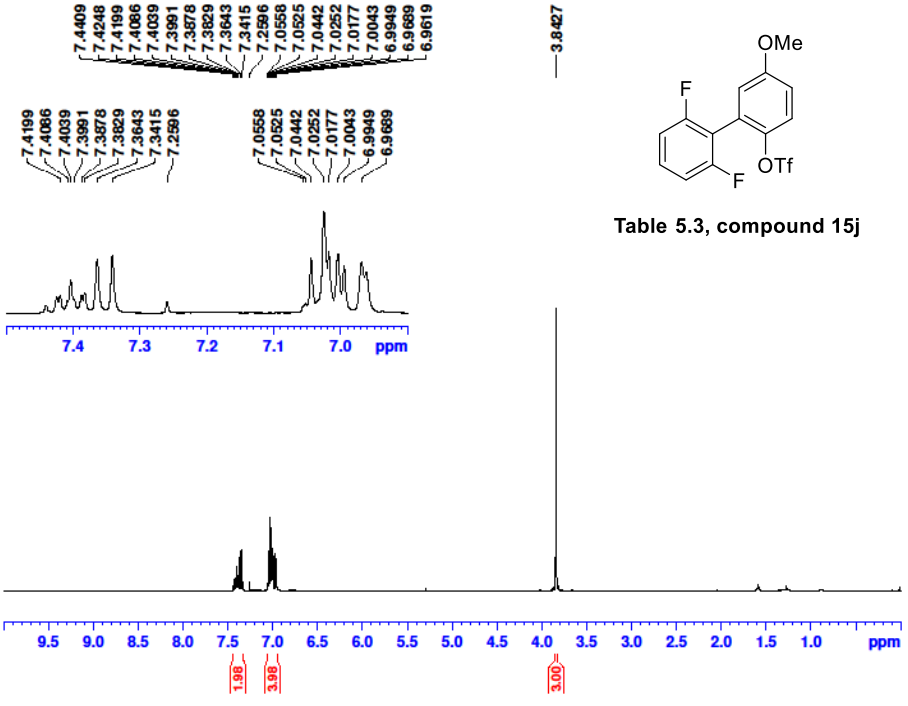

Table 5.3, compound 15j

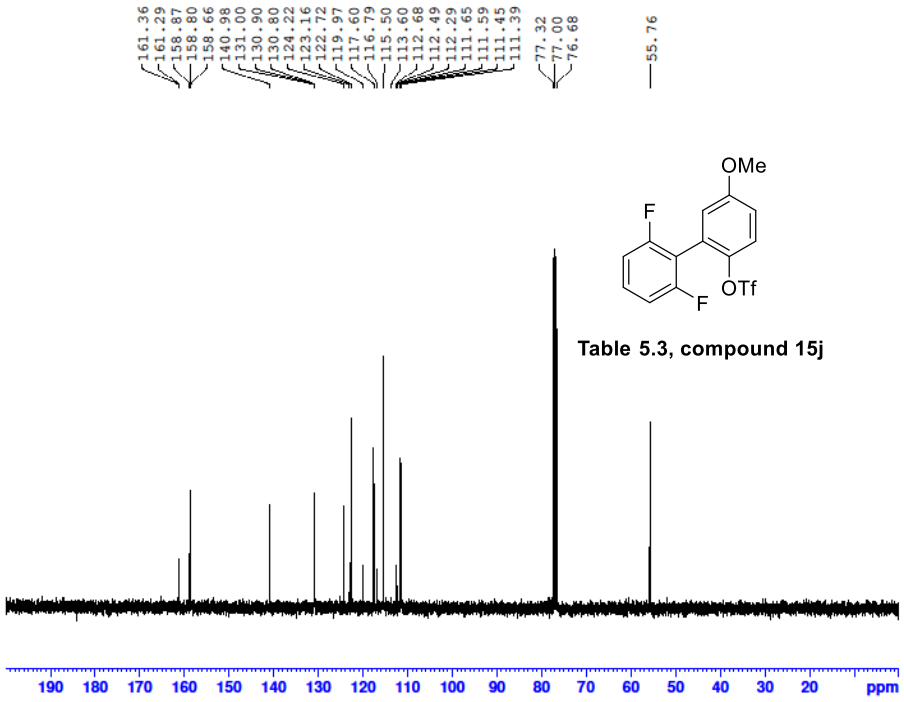

Table 5.3, compound 15j

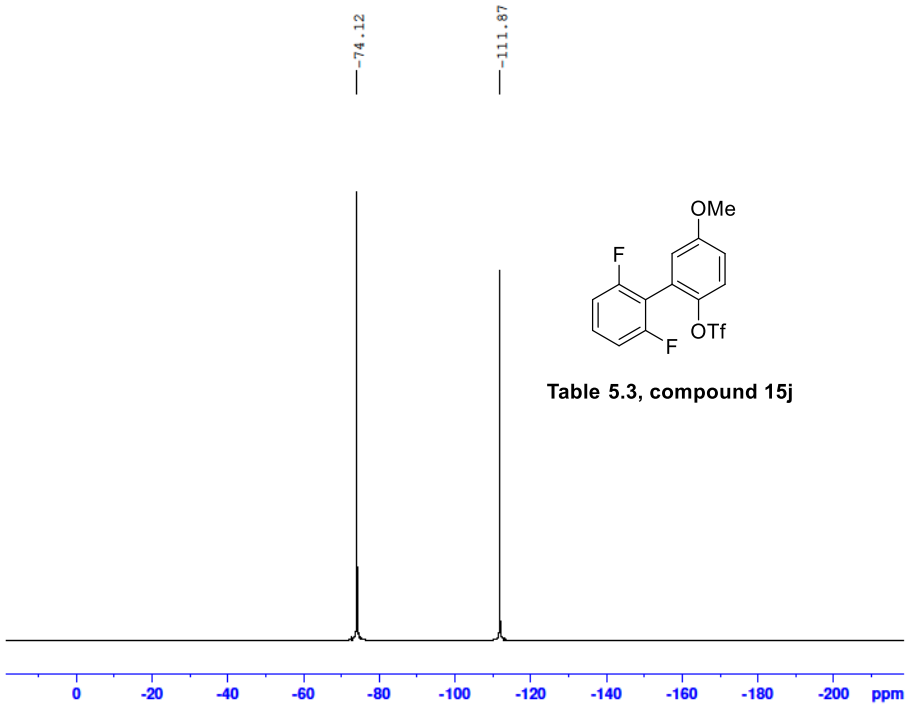

Table 5.3, compound 15j

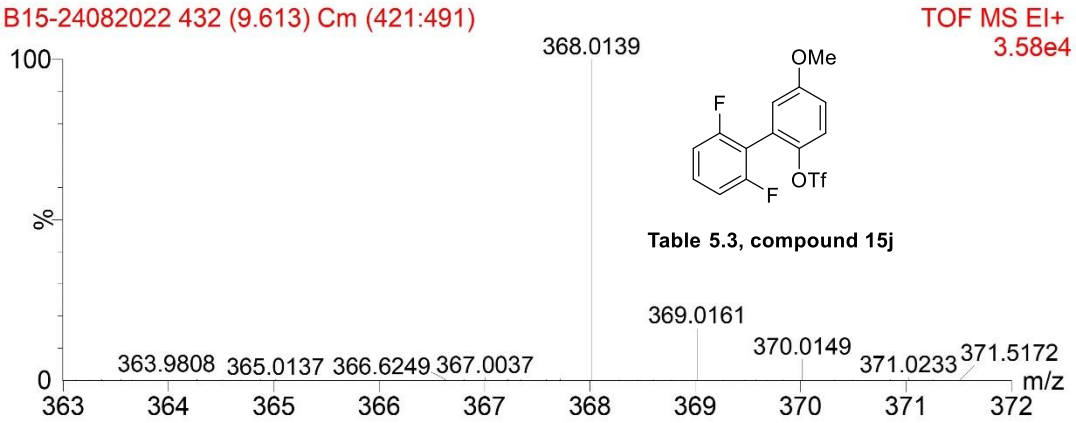

Table 5.3, compound 15j

Mass	m/z (Calc)	Diff (mDa)	Diff (ppm)	Formula
368.0139	368.0136	-0.28	-0.76	C14H9O4F5S

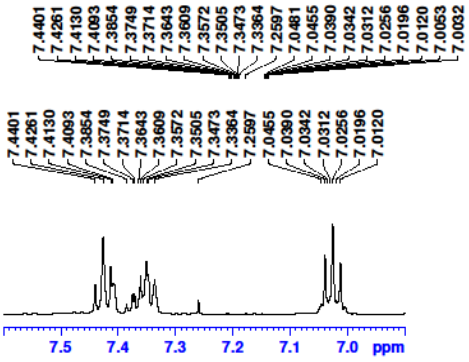

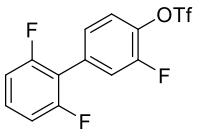

Table 5.3, compound 15k

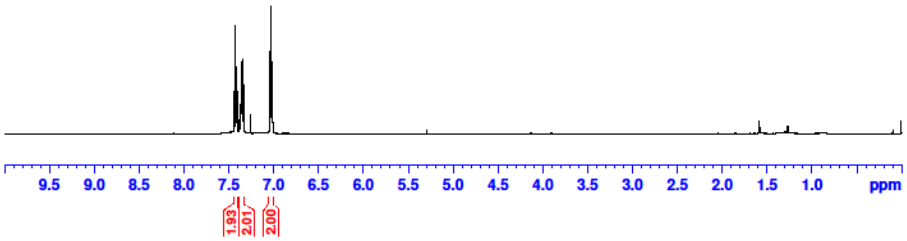

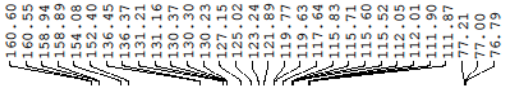

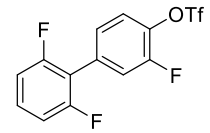

Table 5.3, compound 15k

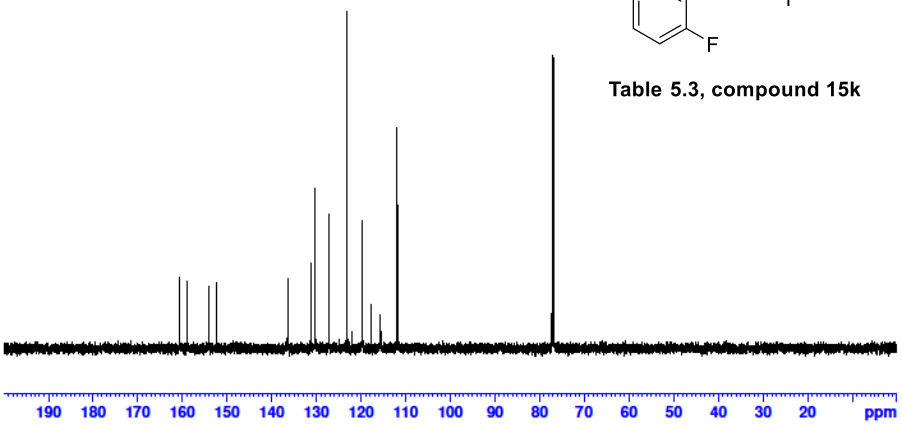

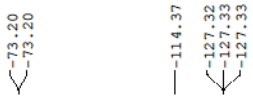

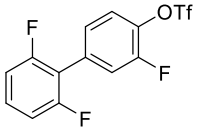

Table 5.3, compound 15k

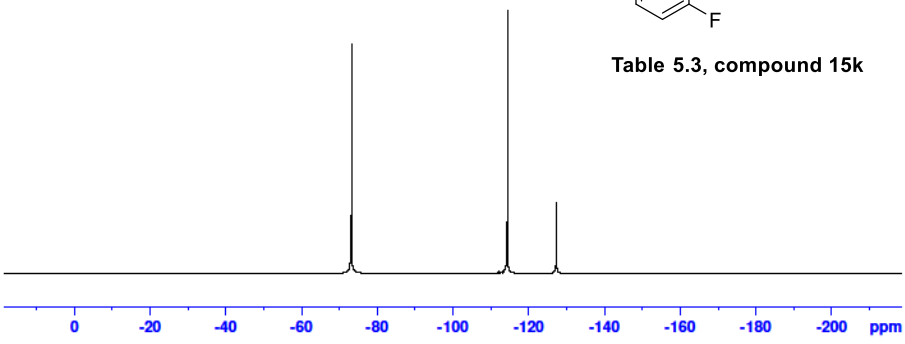

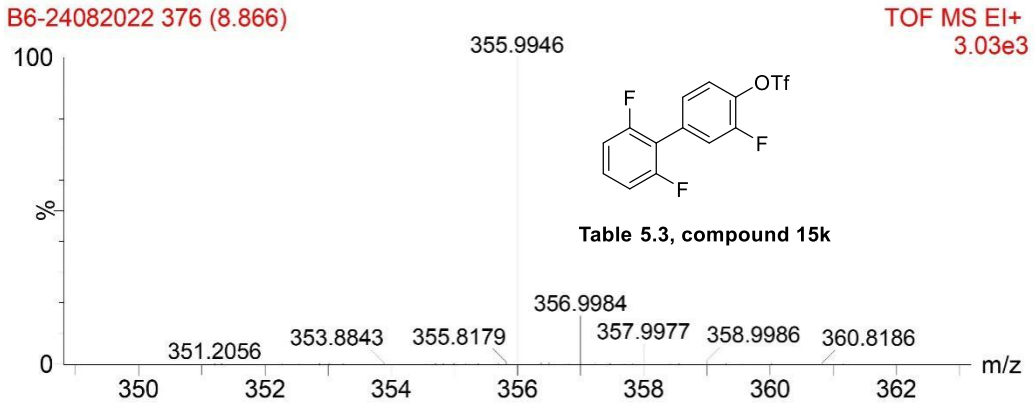

Table 5.3, compound 15k

Mass	m/z (Calc)	Diff (mDa)	Diff (ppm)	Formula
355.9946	355.9936	-0.96	-2.71	C13H6O3F6S

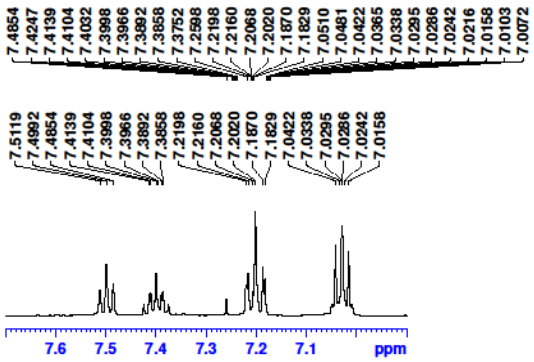

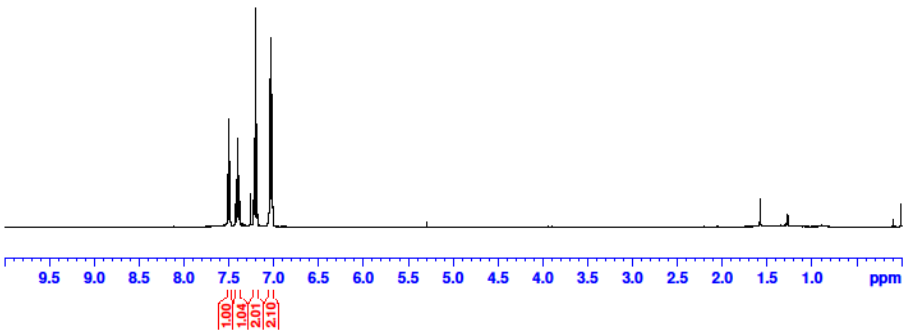

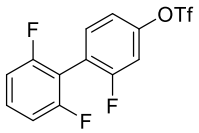

Table 5.3, compound 15l

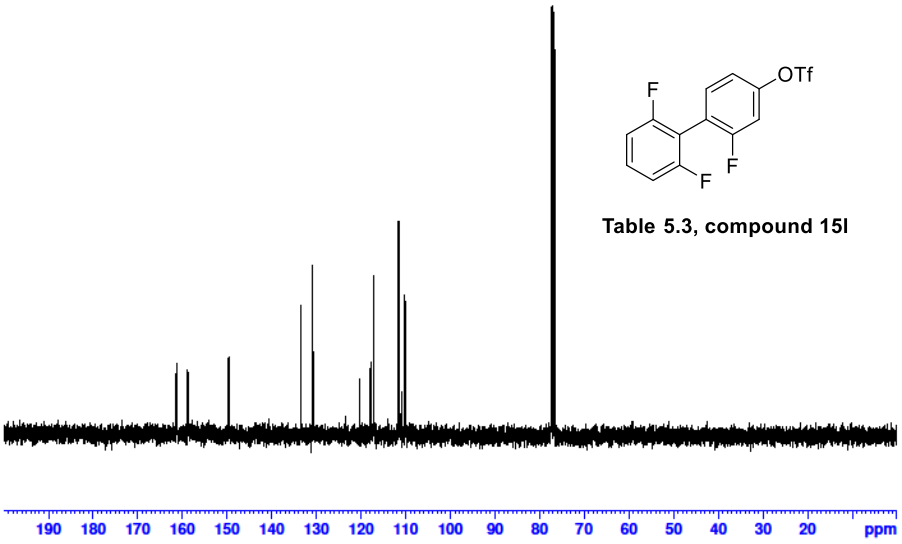

Table 5.3, compound 15l

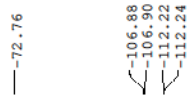

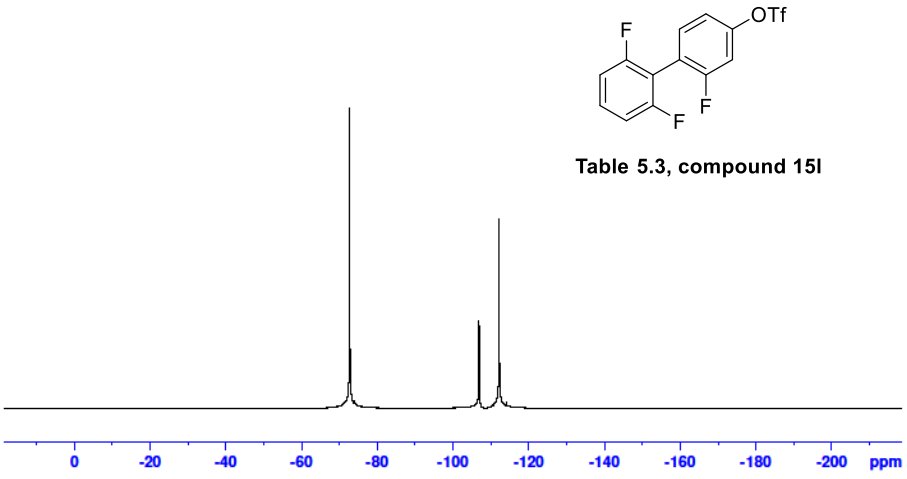

Table 5.3, compound 15l

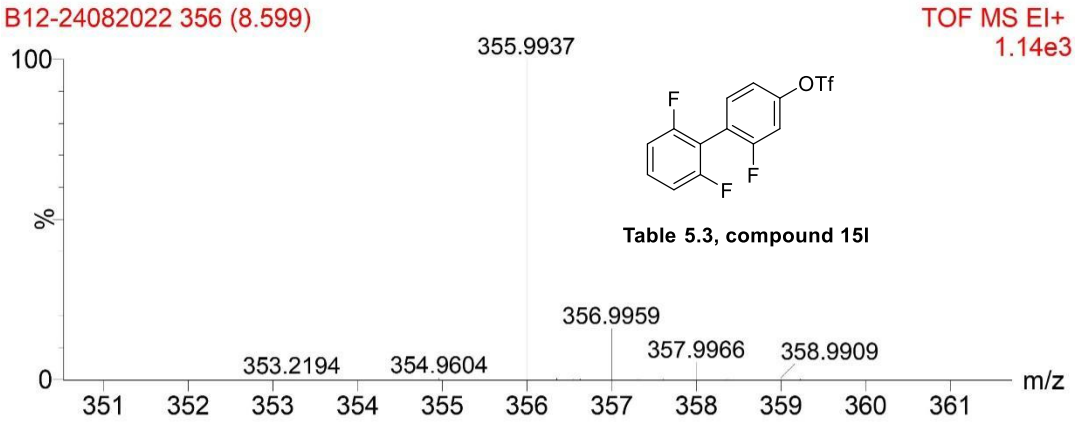

Table 5.3, compound 15l

Mass	m/z (Calc)	Diff (mDa)	Diff (ppm)	Formula
355.9937	355.9936	-0.06	-0.18	C13H6O3F6S

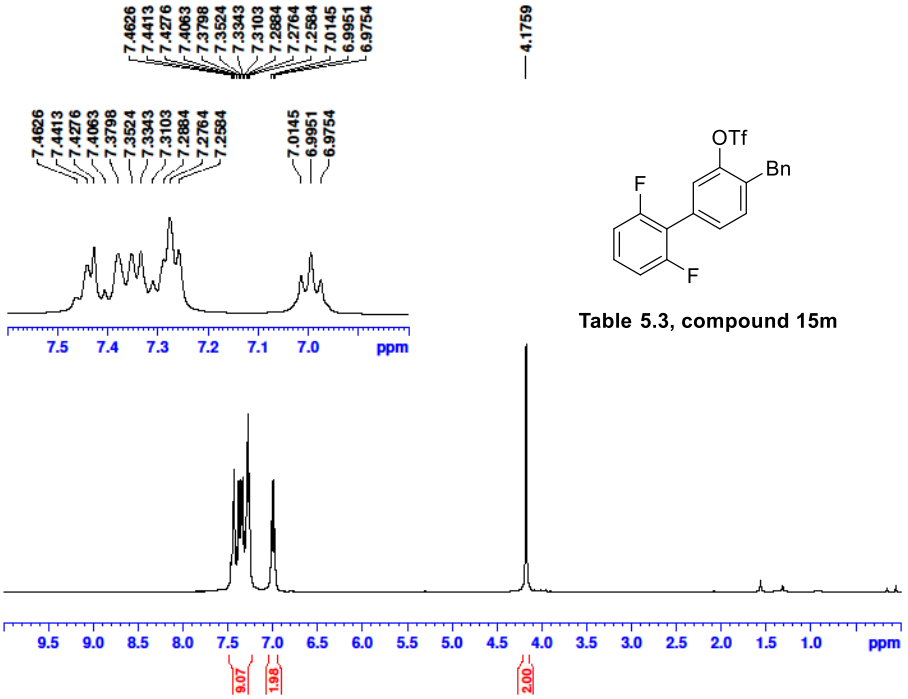

Table 5.3, compound 15m

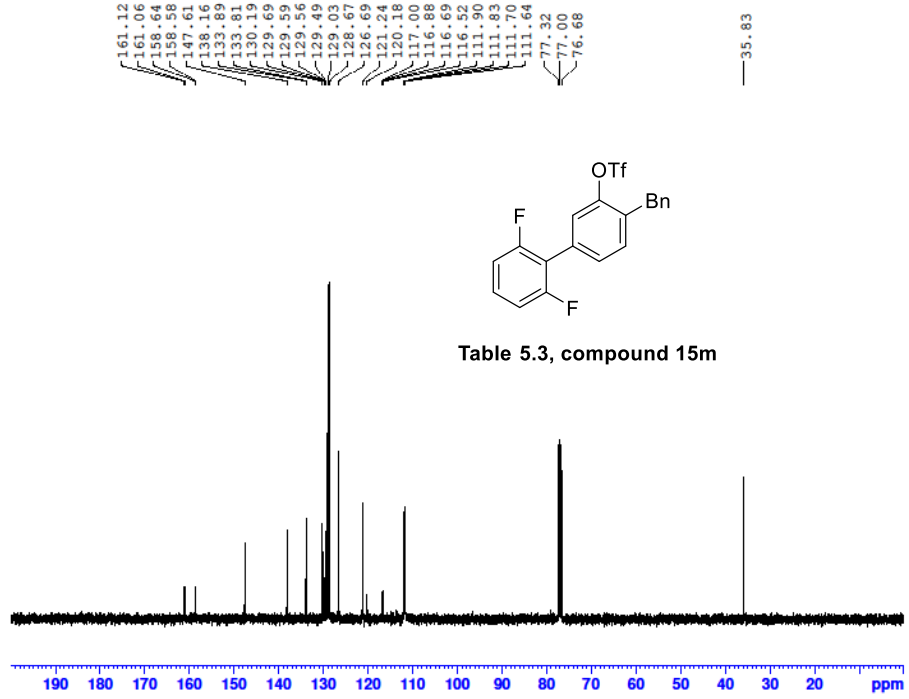

Table 5.3, compound 15m

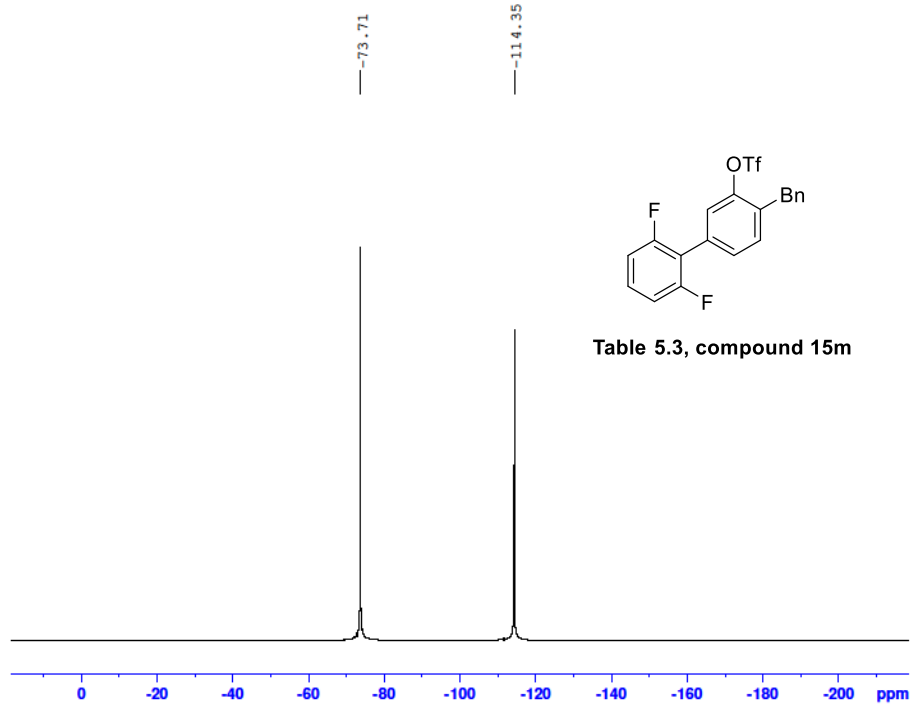

Table 5.3, compound 15m

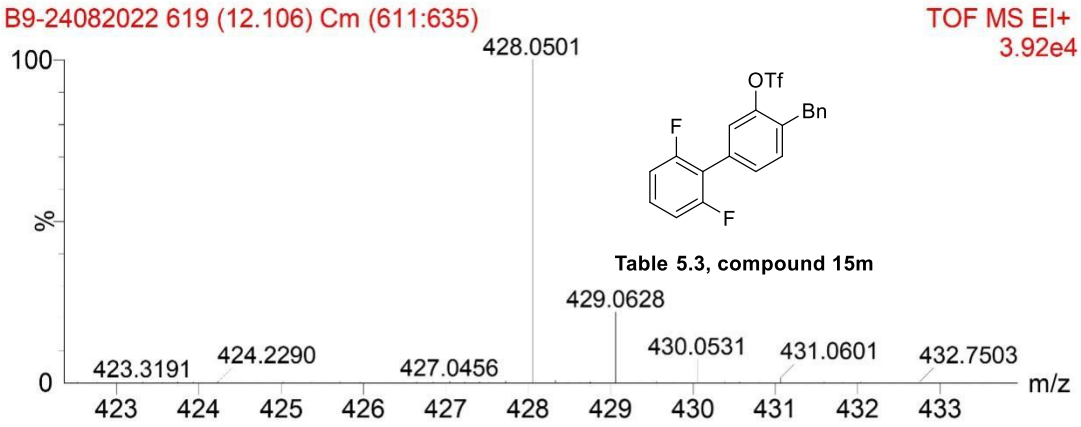

Table 5.3, compound 15m

Mass	m/z (Calc)	Diff (mDa)	Diff (ppm)	Formula
428.0501	428.0500	-0.09	-0.22	C20 H13O3F5S

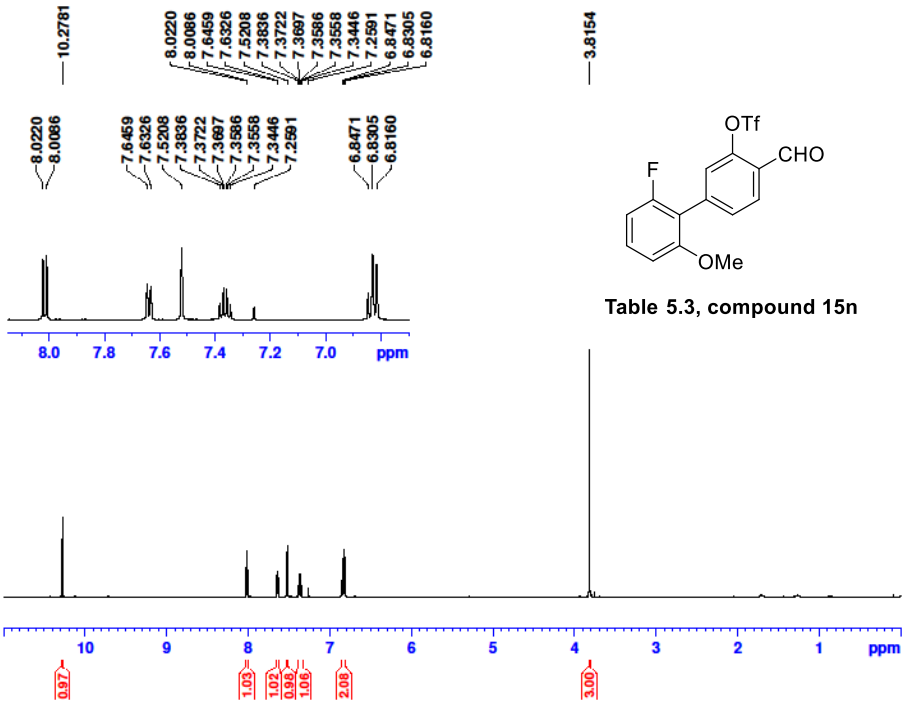

Table 5.3, compound 15n

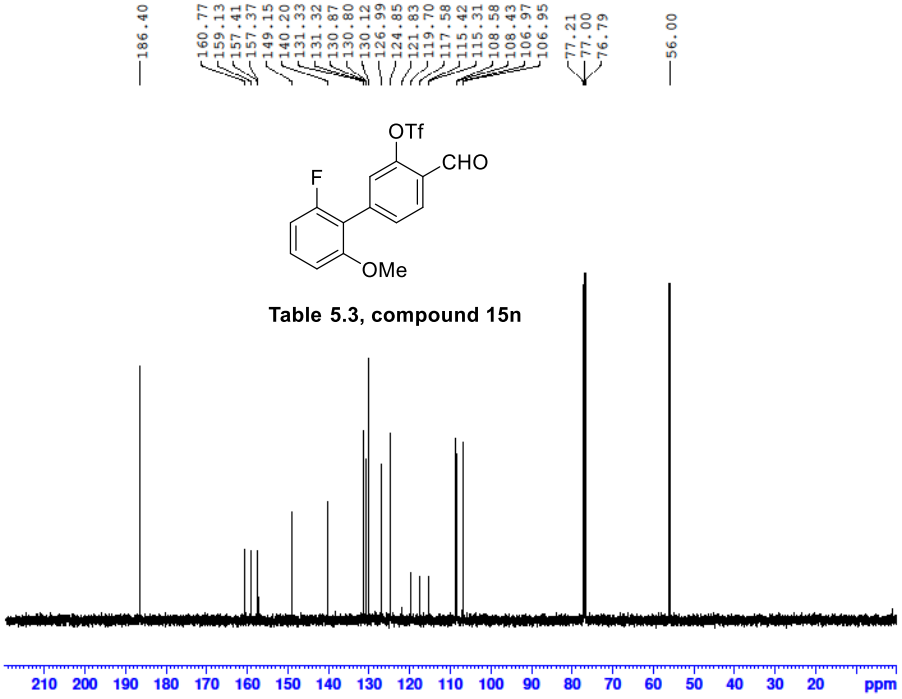

Table 5.3, compound 15n

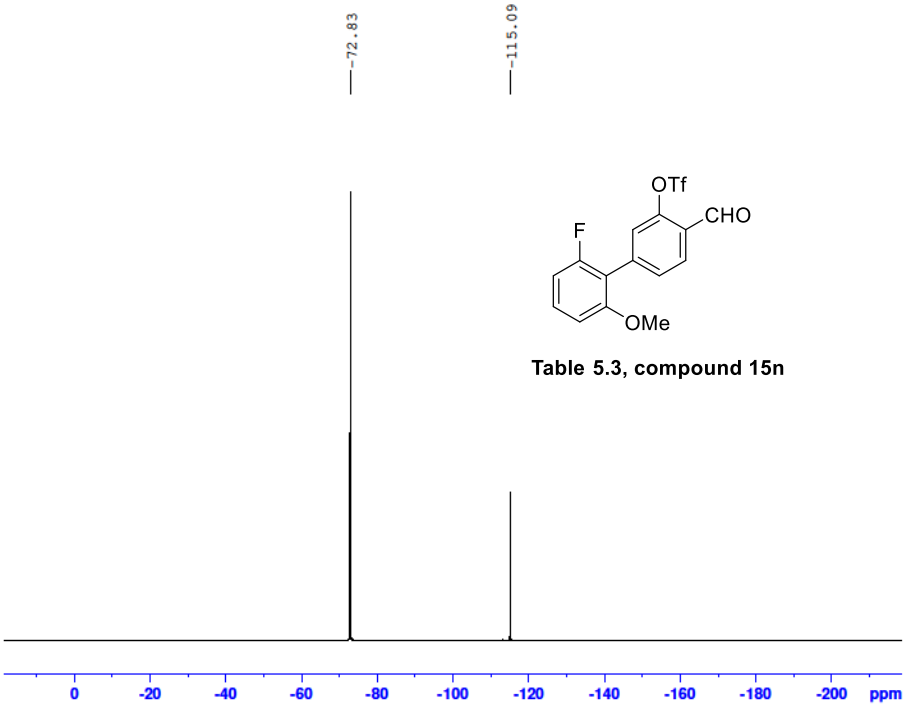

Table 5.3, compound 15n

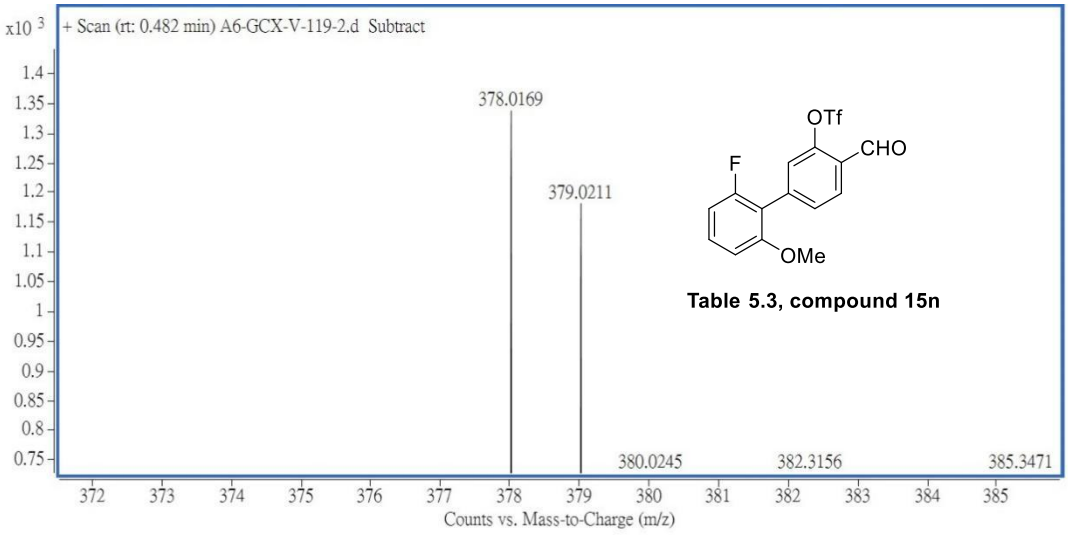

Table 5.3, compound 15n

Mass	m/z (Calc)	Diff (mDa)	Diff (ppm)	Formula
378.0169	378.0180	1.06	2.80	C15H10F4O5S

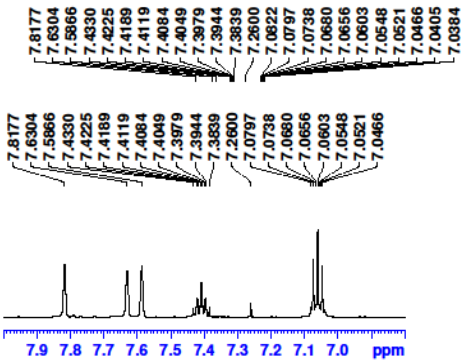

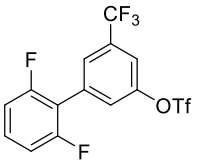

Table 5.3, compound 15o

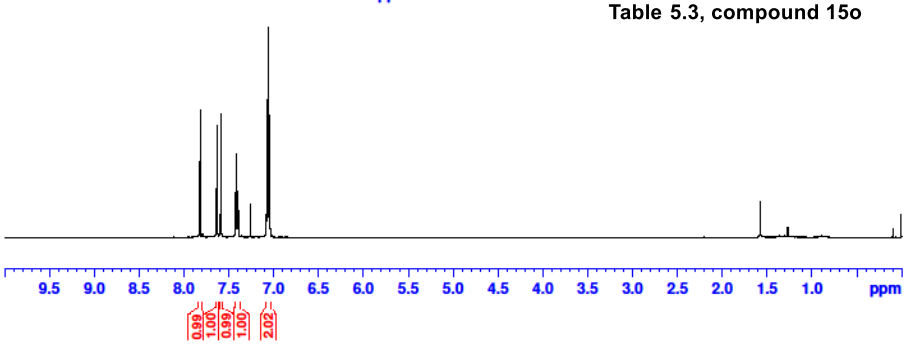

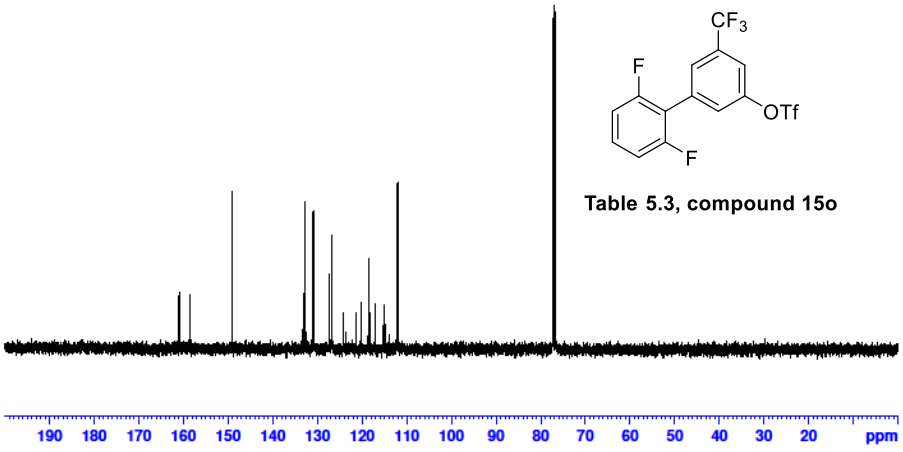

Table 5.3, compound 15o

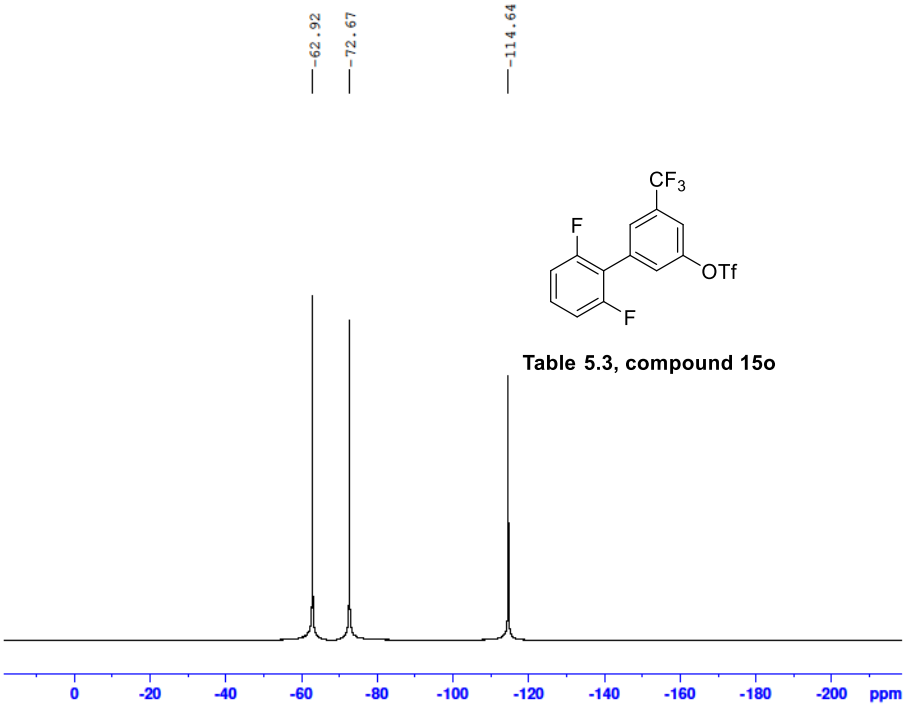

Table 5.3, compound 15o

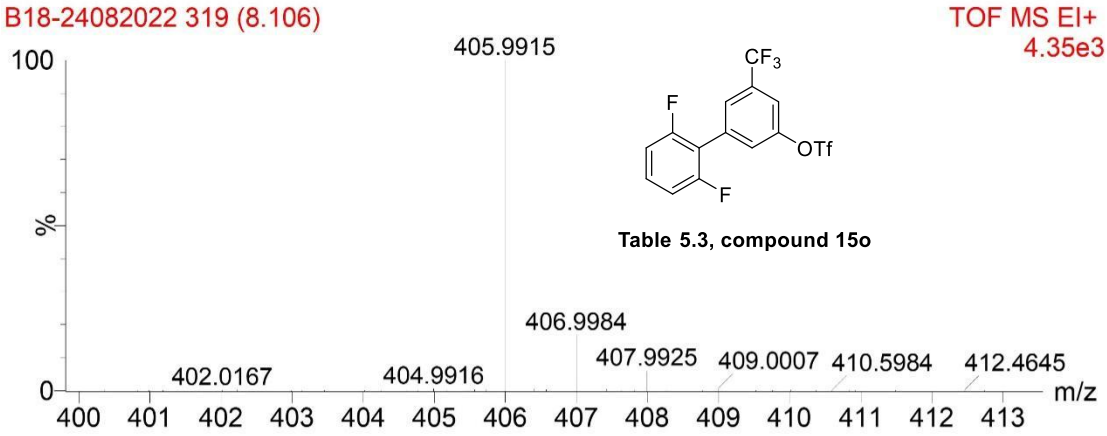

Table 5.3, compound 15o

Mass	m/z (Calc)	Diff (mDa)	Diff (ppm)	Formula
405.9915	405.9904	-1.06	-2.61	C14H6O3F8S

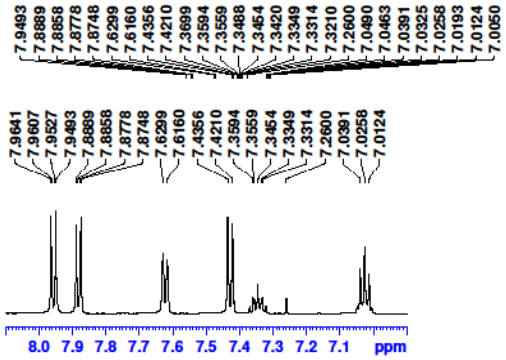

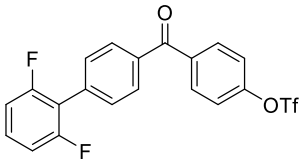

Table 5.3, compound 15p

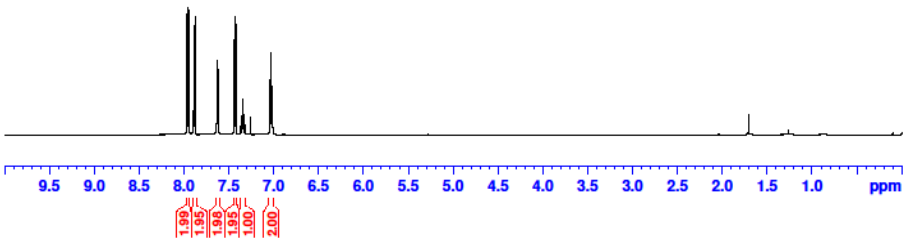

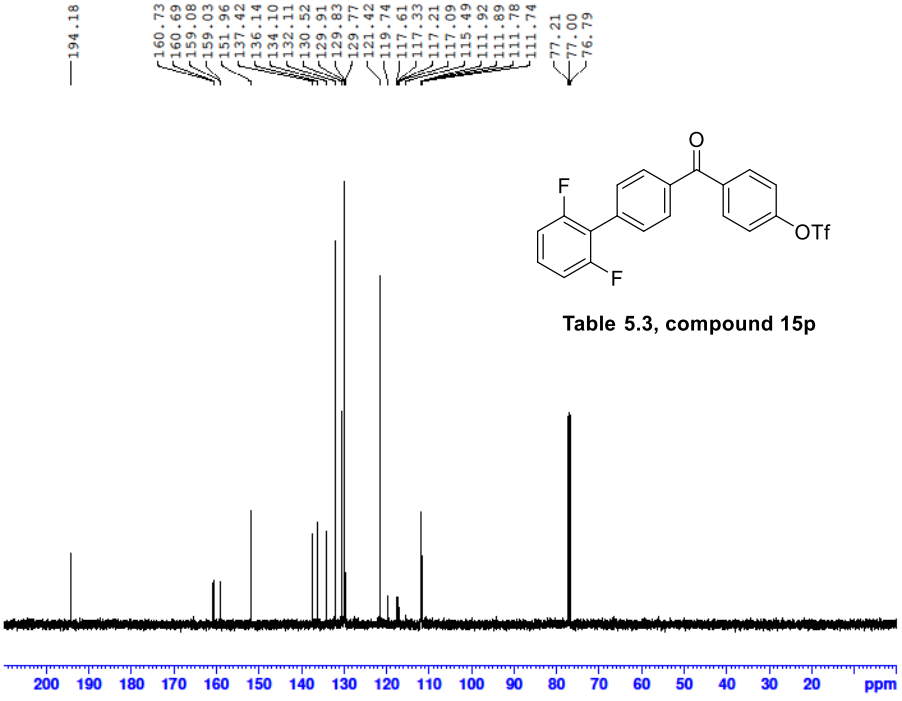

Table 5.3, compound 15p

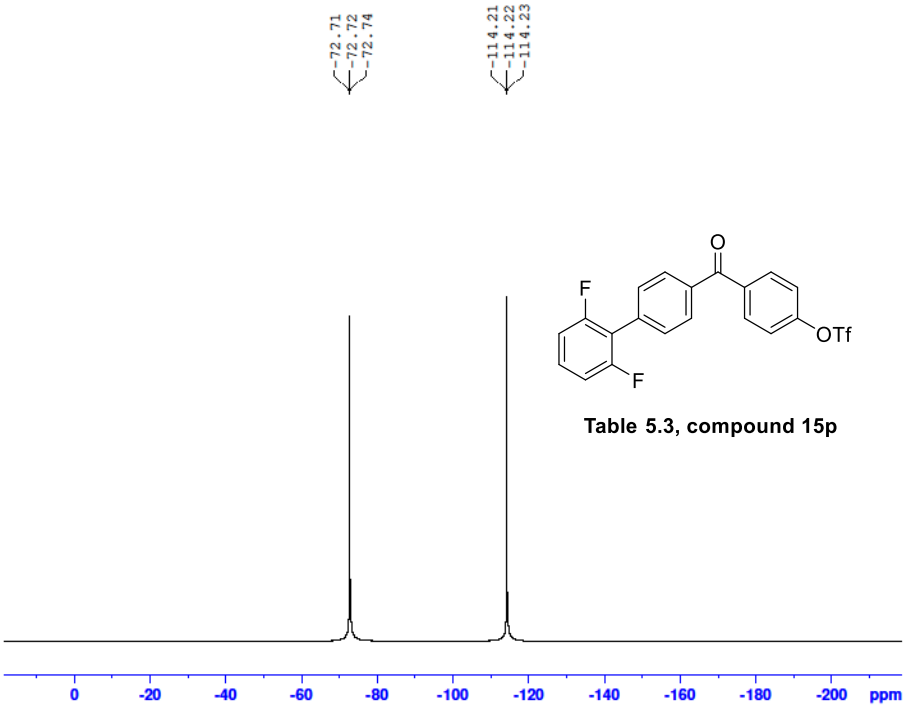

Table 5.3, compound 15p

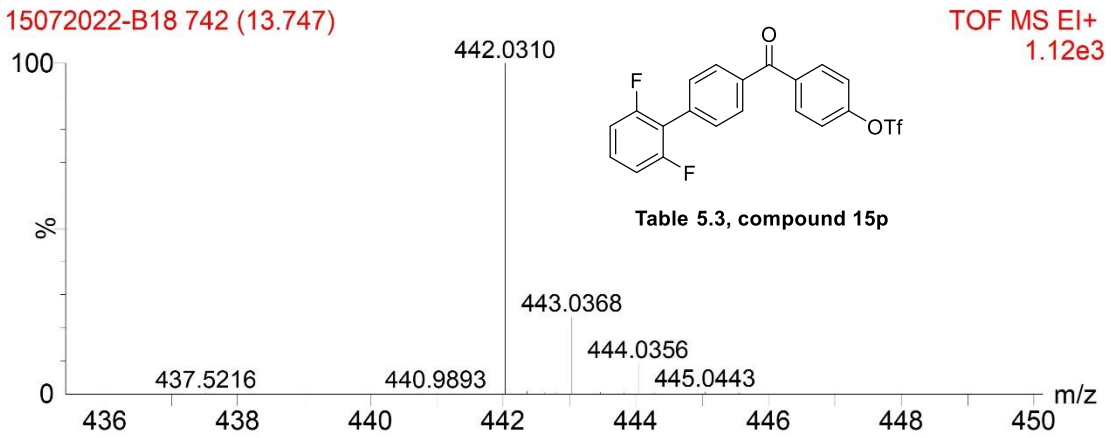

Table 5.3, compound 15p

Mass	Calc. Mass	mDa	PPM	Ion Formula
442.0310	442.0293	-1.73	-3.91	C20H11SF5O4

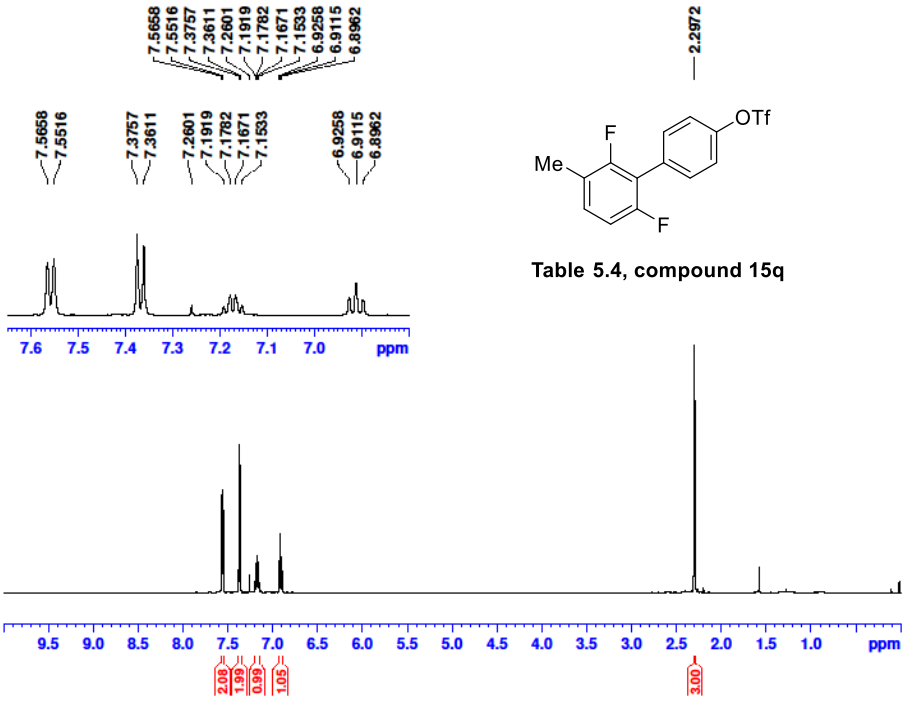

Table 5.4, compound 15q

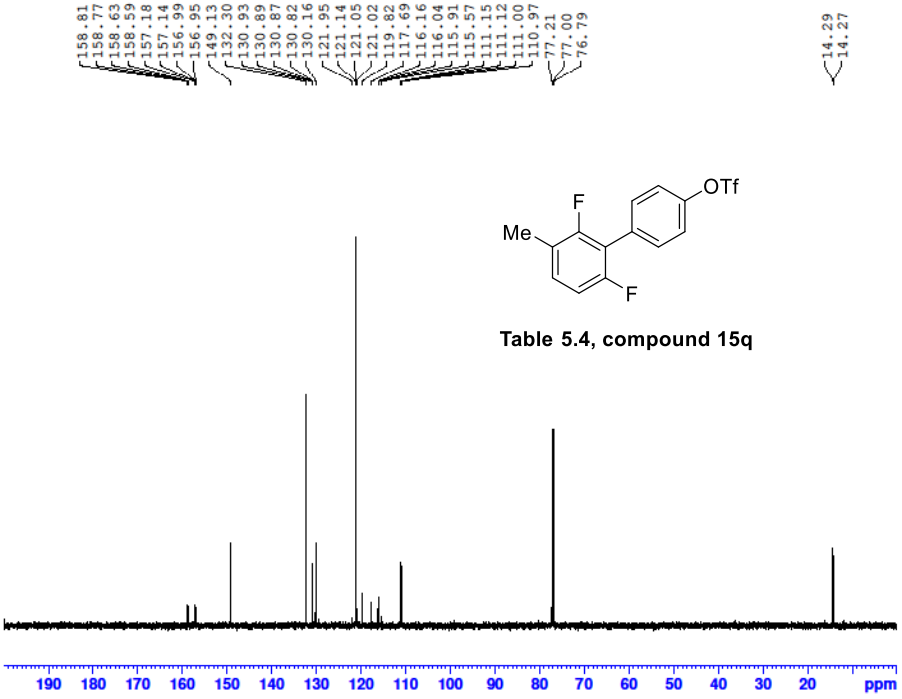

Table 5.4, compound 15q

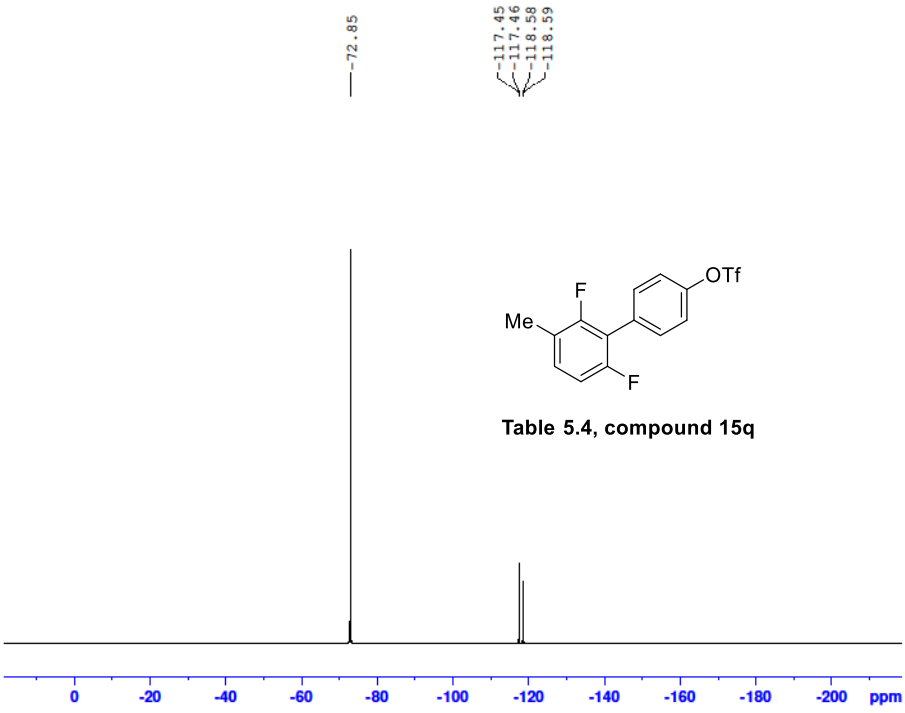

Table 5.4, compound 15q

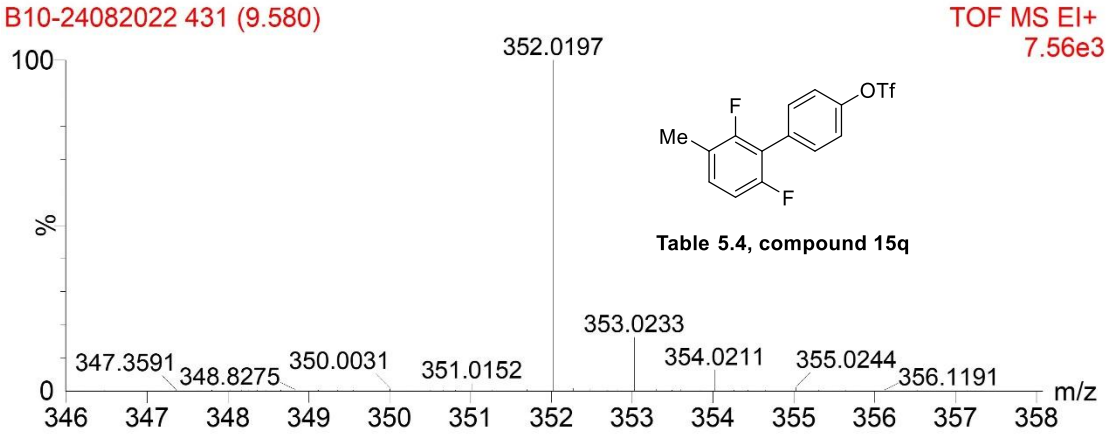

Table 5.4, compound 15q

Mass	m/z (Calc)	Diff (mDa)	Diff (ppm)	Formula
352.0197	352.0187	-0.99	-2.82	C14H9O3F5S

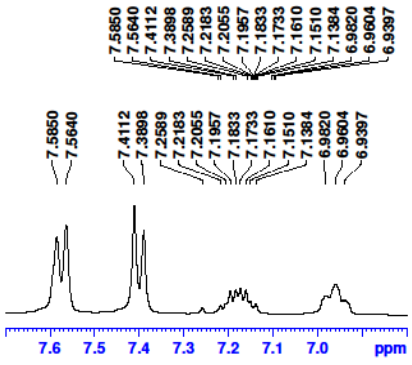

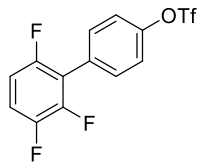

Table 5.4, compound 15r

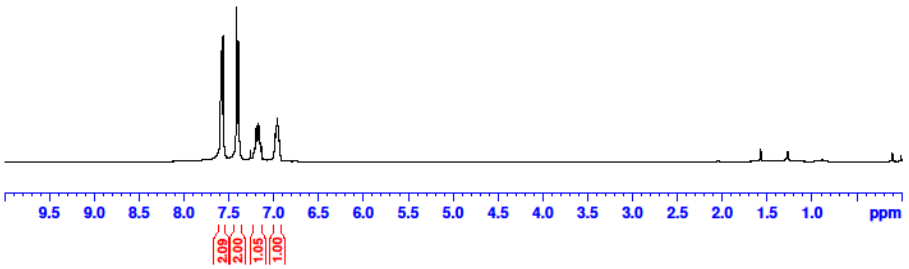

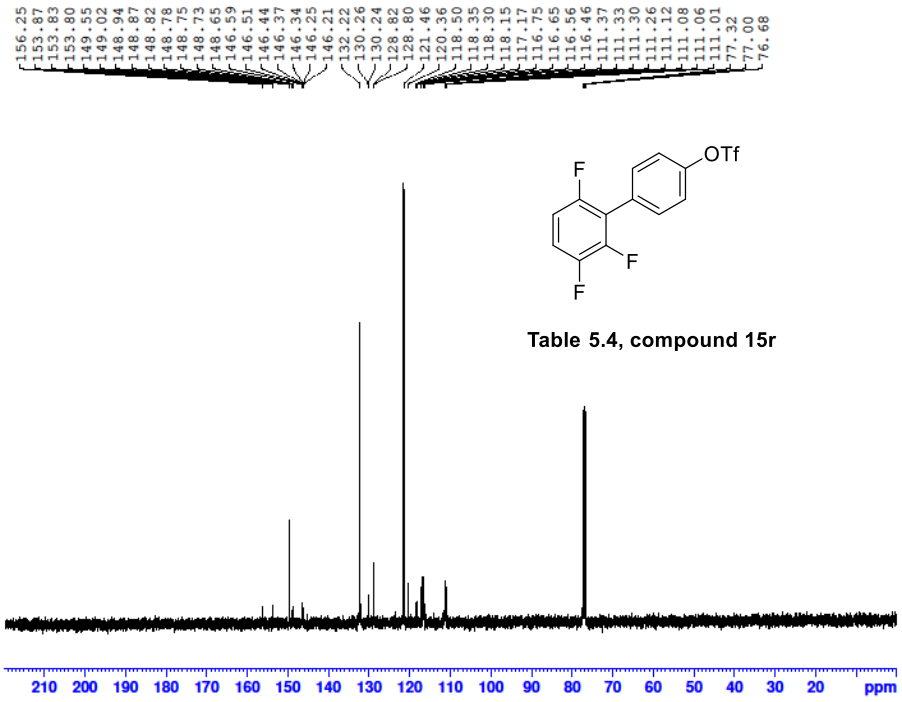

Table 5.4, compound 15r

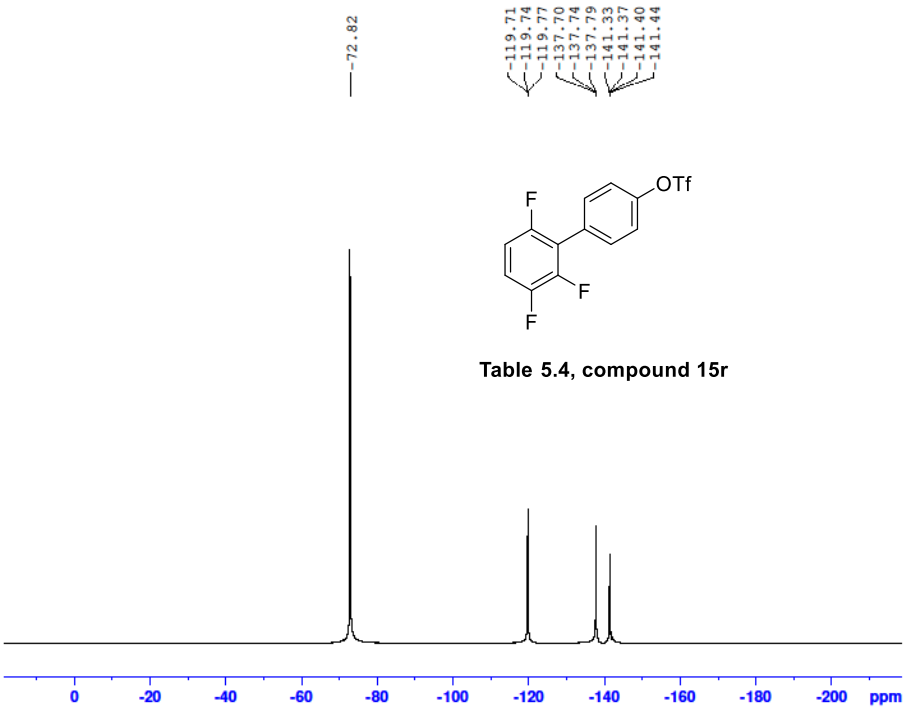

Table 5.4, compound 15r

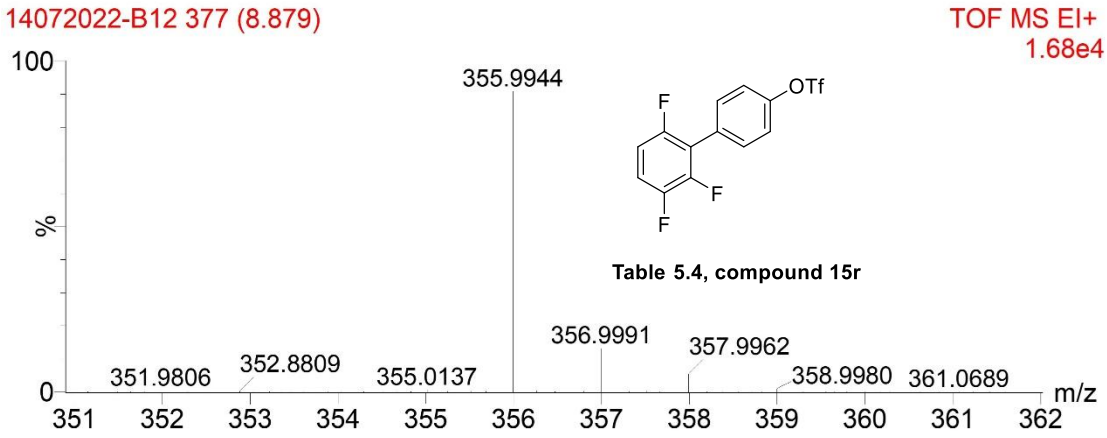

Table 5.4, compound 15r

Mass	Calc. Mass	mDa	PPM	Ion Formula
355.9944	355.9936	-0.76	-2.15	C13H7SF6O3

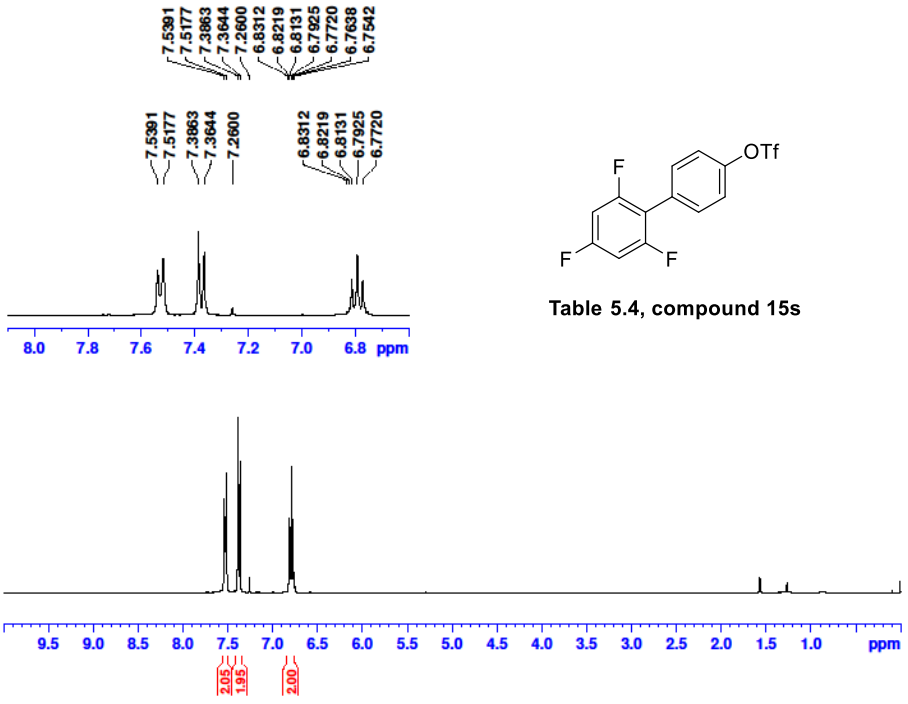

Table 5.4, compound 15s

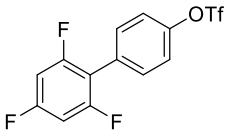

Table 5.4, compound 15s

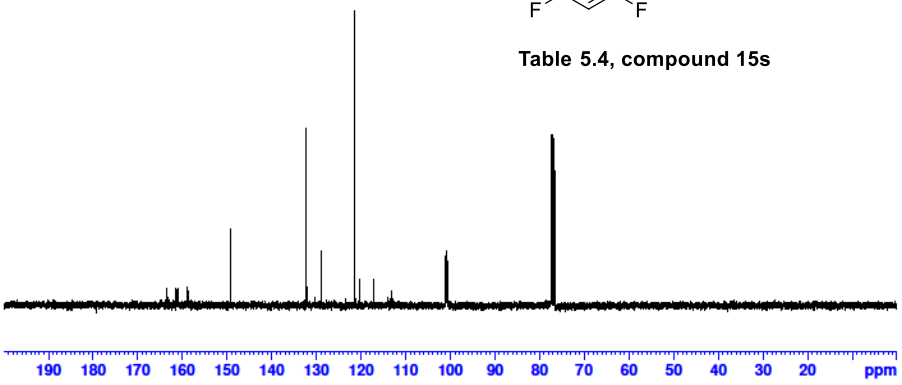

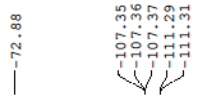

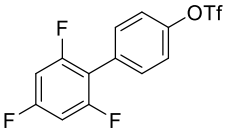

Table 5.4, compound 15s

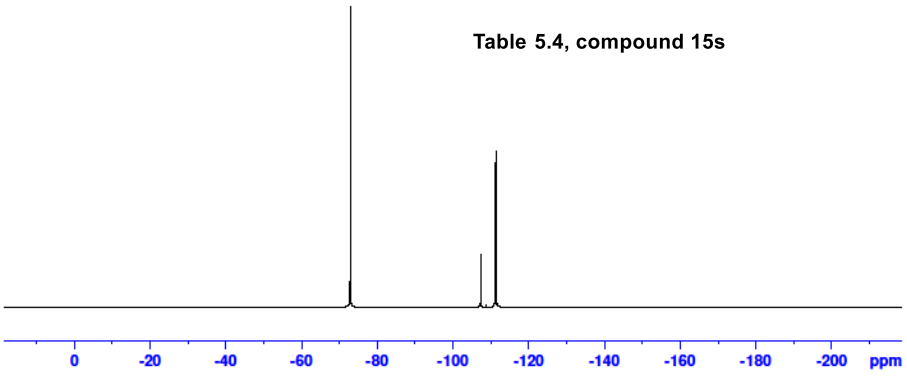

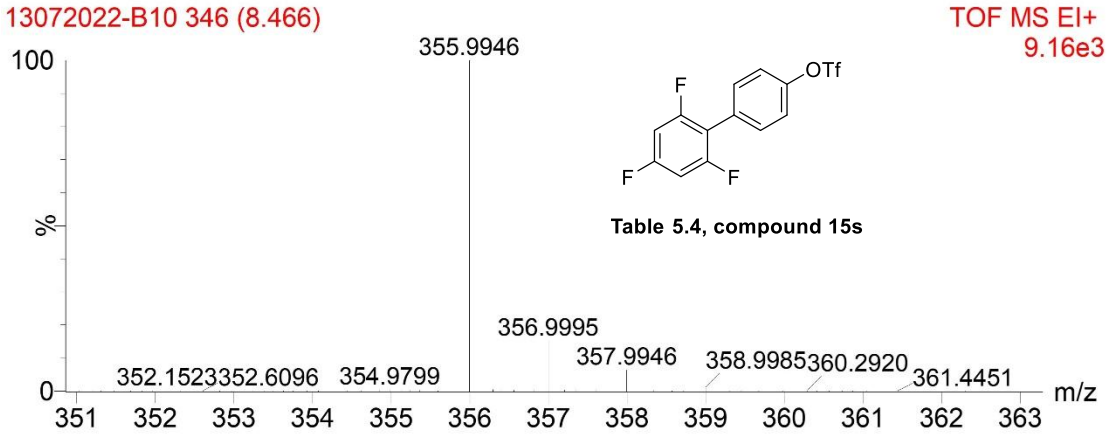

Table 5.4, compound 15s

Mass	Calc. Mass	mDa	PPM	Ion Formula
355.9946	355.9936	-0.96	-2.71	C13H7SF6O3

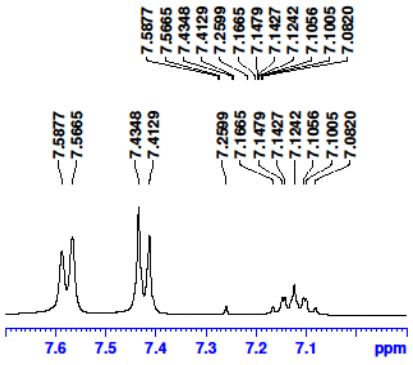

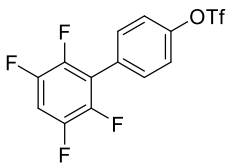

Table 5.4, compound 15t

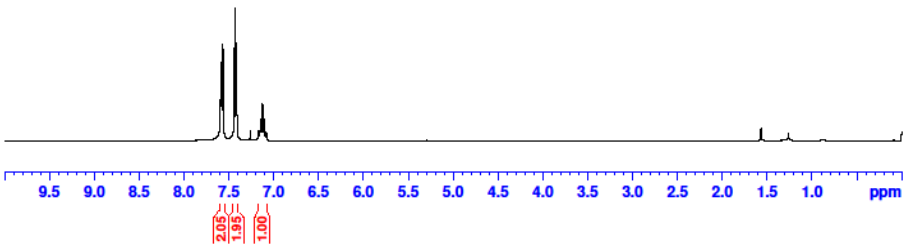

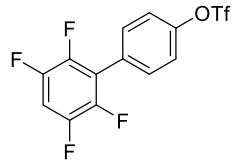

Table 5.4, compound 15t

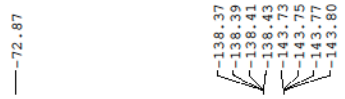

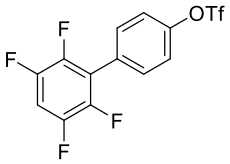

Table 5.4, compound 15t

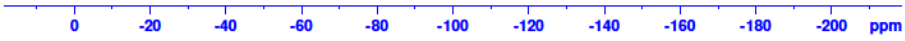

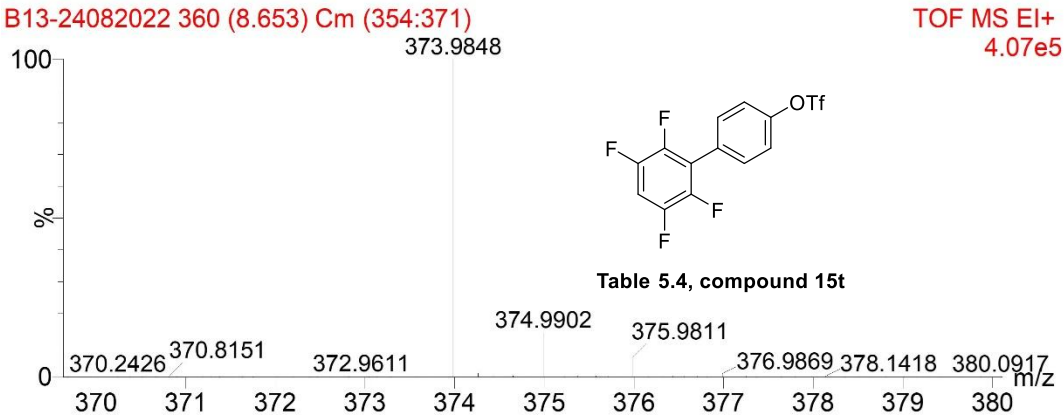

Table 5.4, compound 15t

Mass	m/z (Calc)	Diff (mDa)	Diff (ppm)	Formula
373.9848	373.9842	-0.59	-1.57	C13H5O3F7S

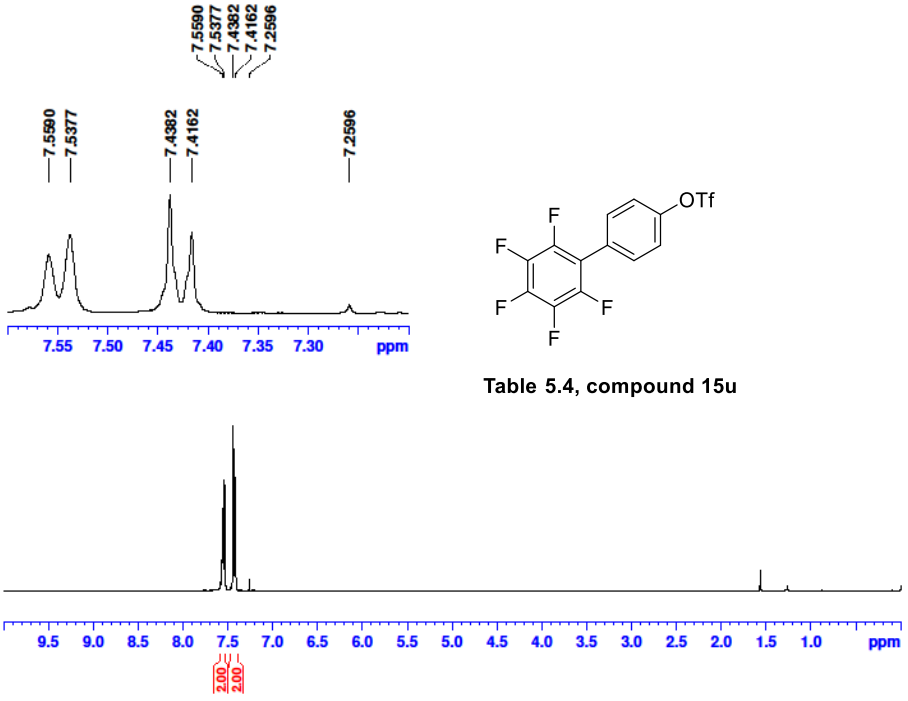

Table 5.4, compound 15u

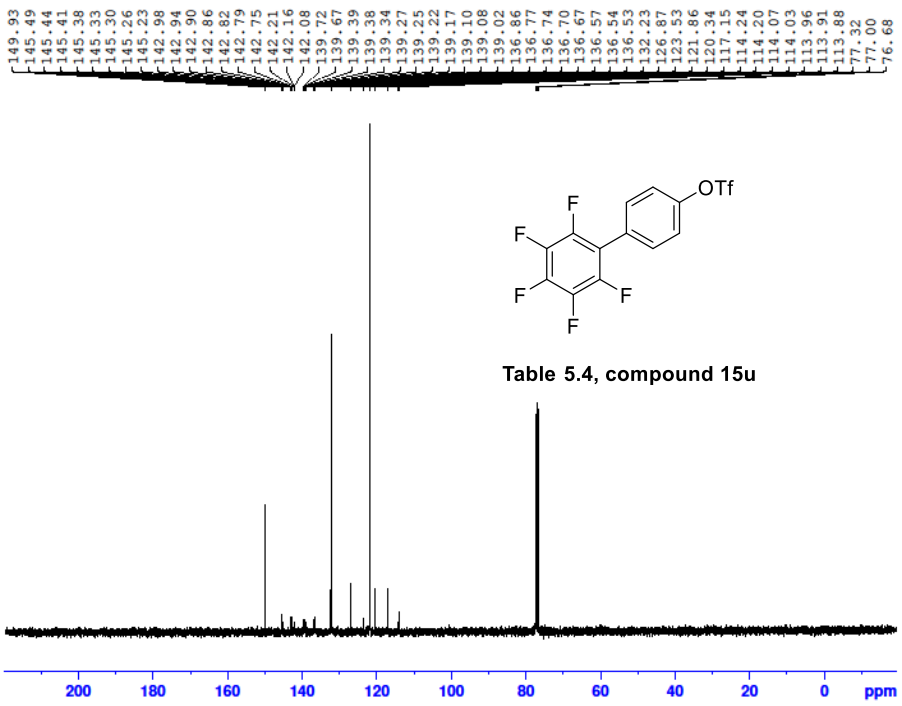

Table 5.4, compound 15u

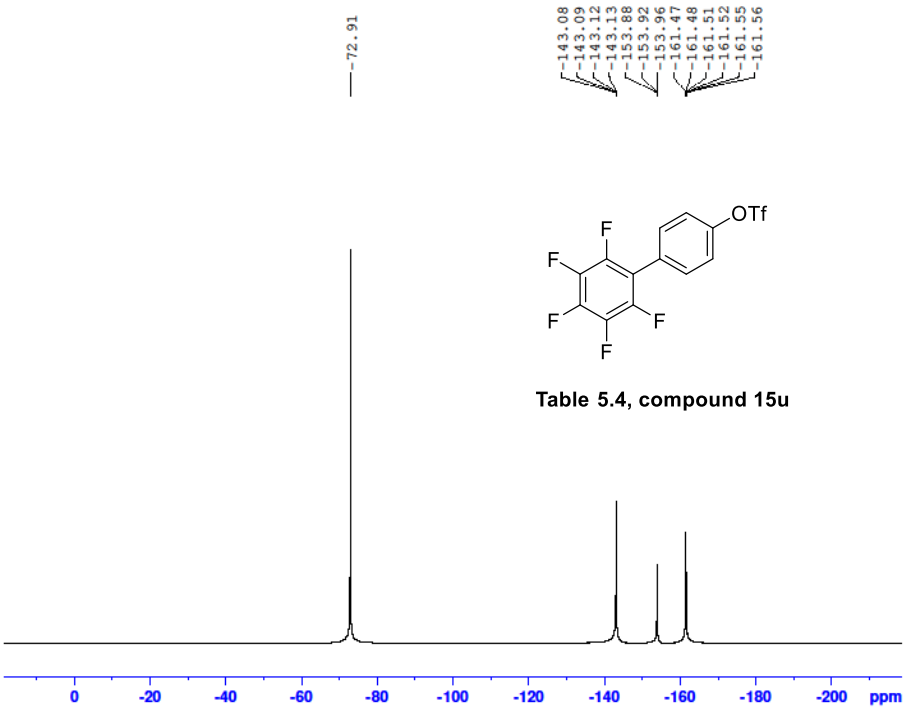

Table 5.4, compound 15u

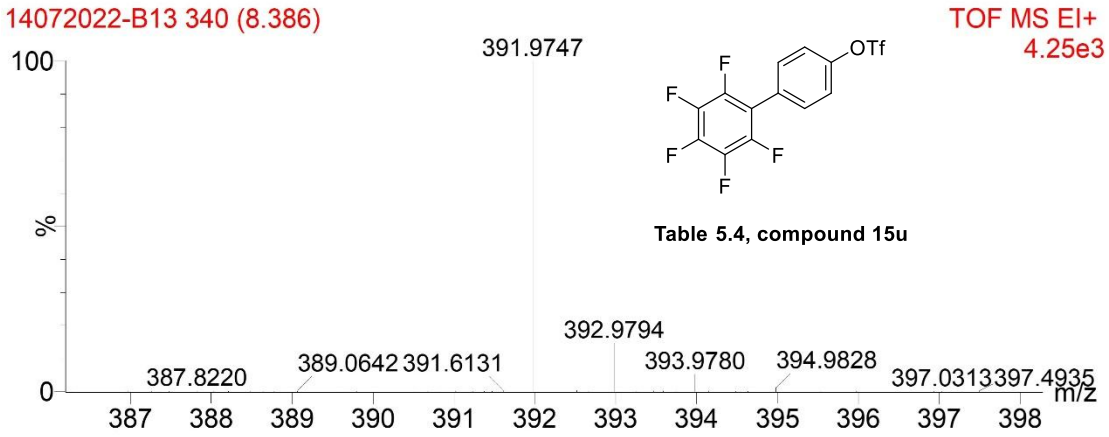

Table 5.4, compound 15u

Mass	Calc. Mass	mDa	PPM	Ion Formula
391.9747	391.9748	0.09	0.23	C13H4SF8O3

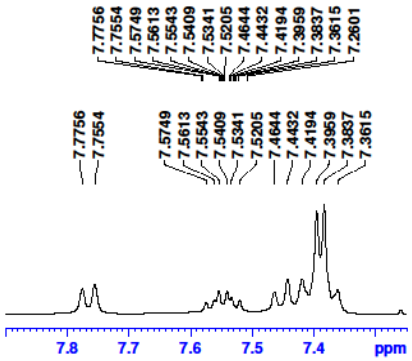

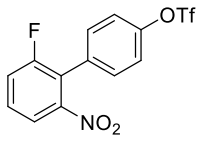

Table 5.4, compound 15v

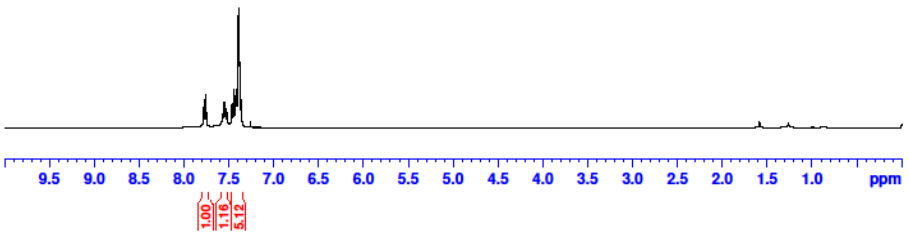

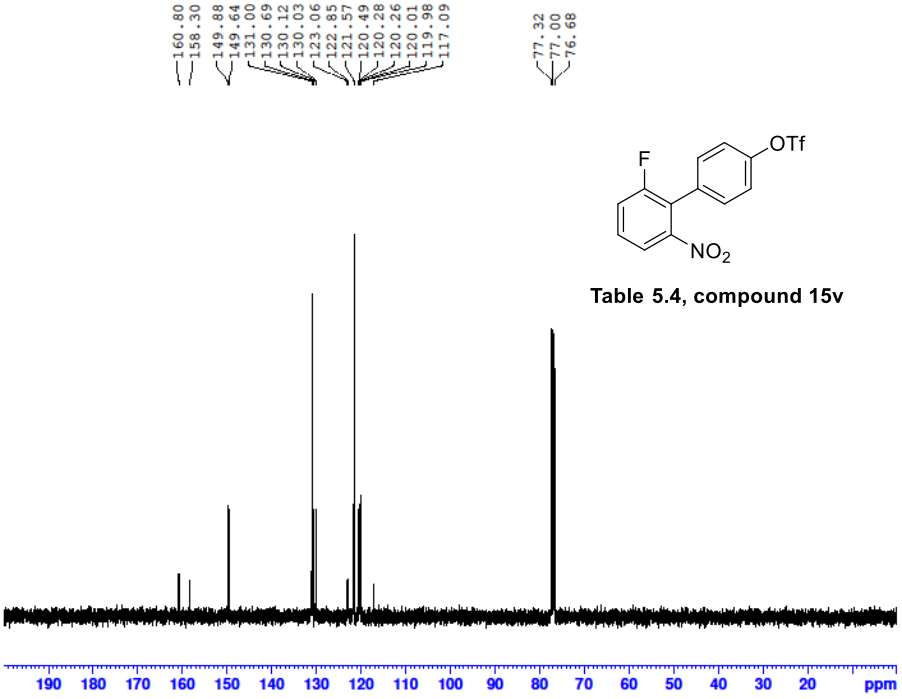

Table 5.4, compound 15v

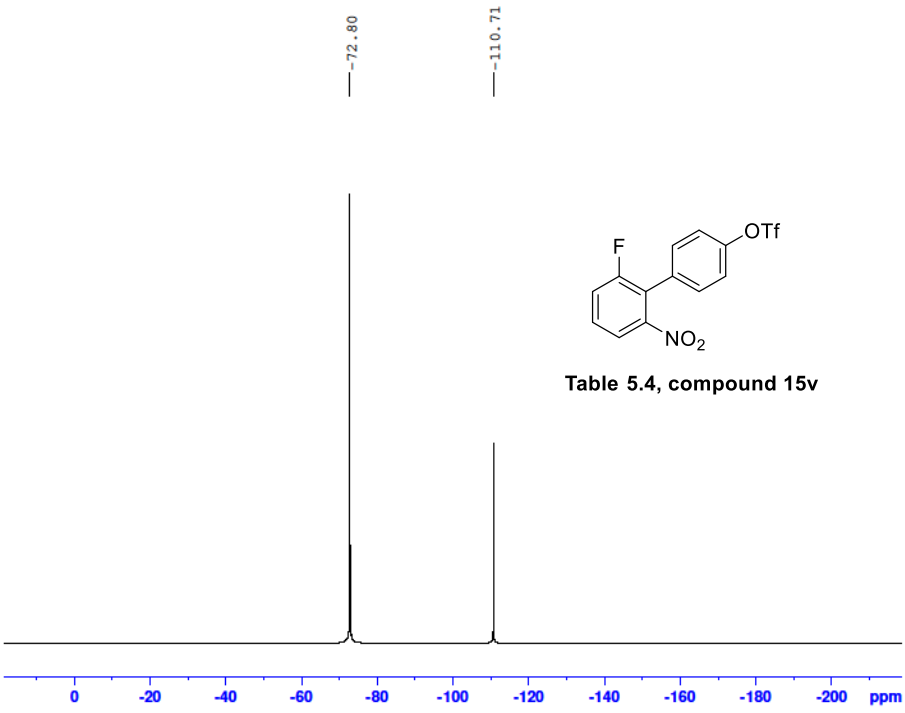

Table 5.4, compound 15v

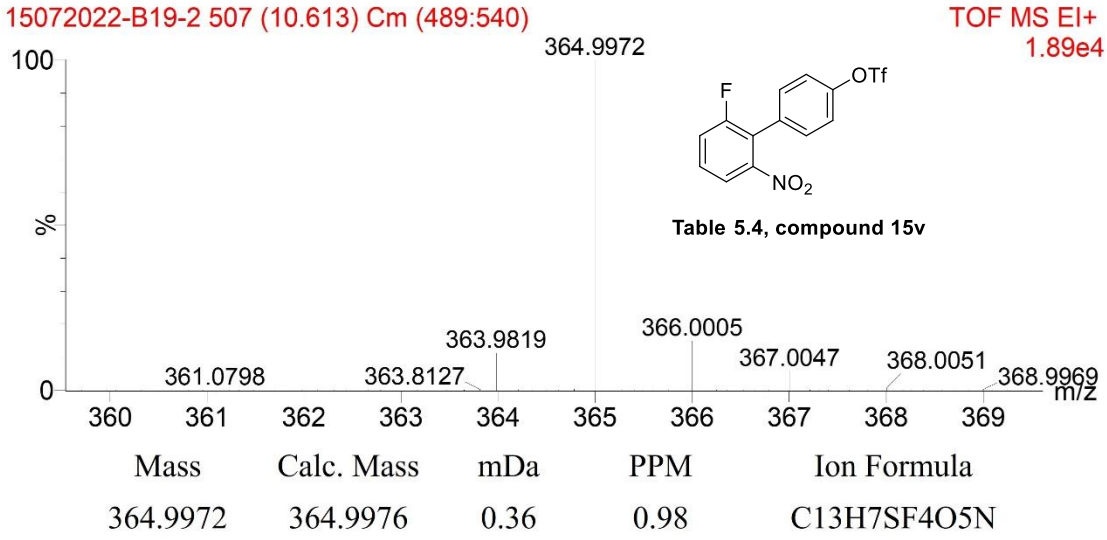

Table 5.4, compound 15v

Mass	Calc. Mass	mDa	PPM	Ion Formula
364.9972	364.9976	0.36	0.98	C13H7SF4O5N

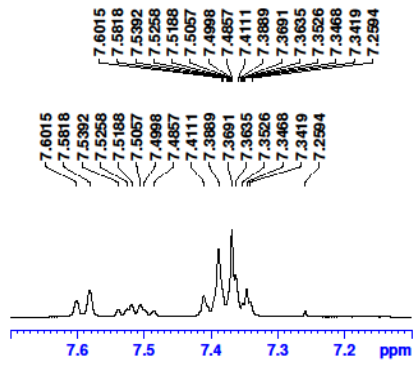

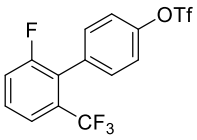

Table 5.4, compound 15w

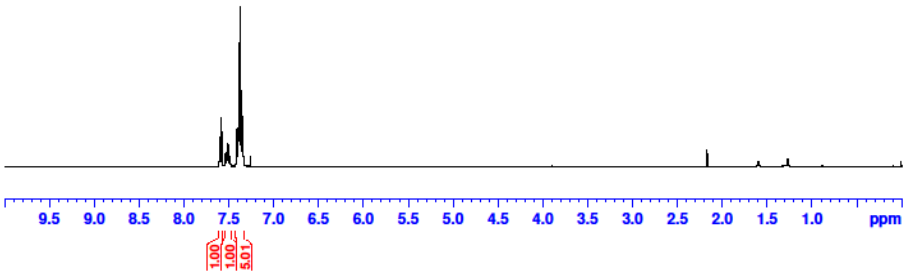

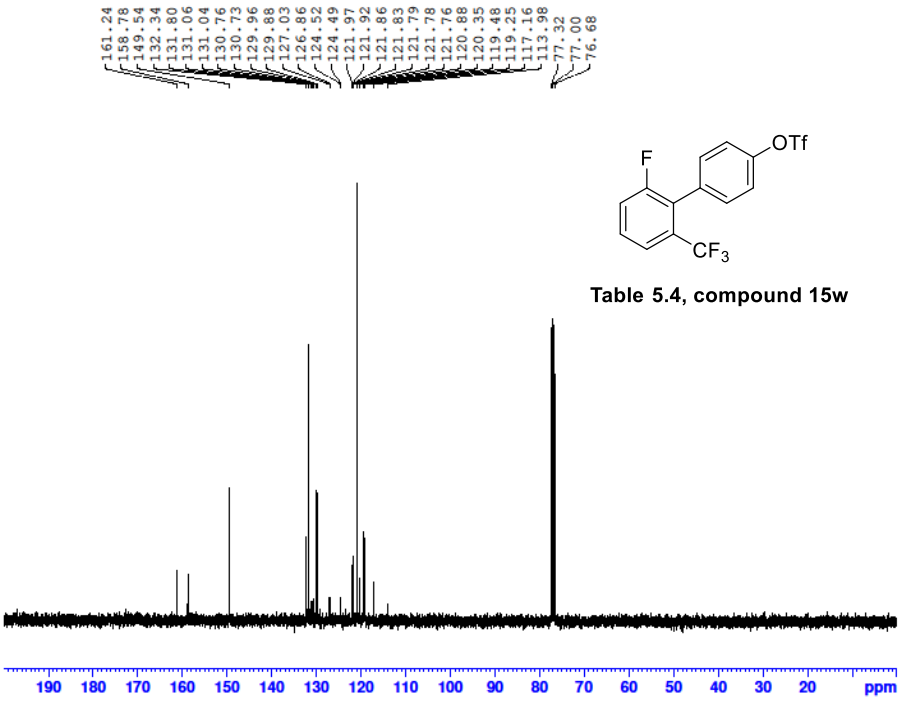

Table 5.4, compound 15w

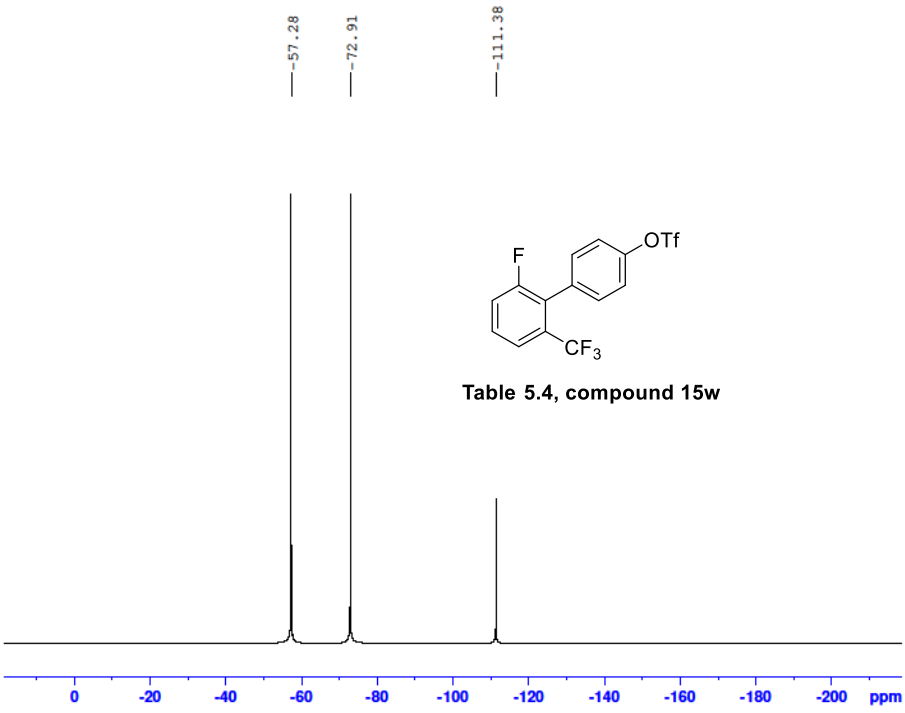

Table 5.4, compound 15w

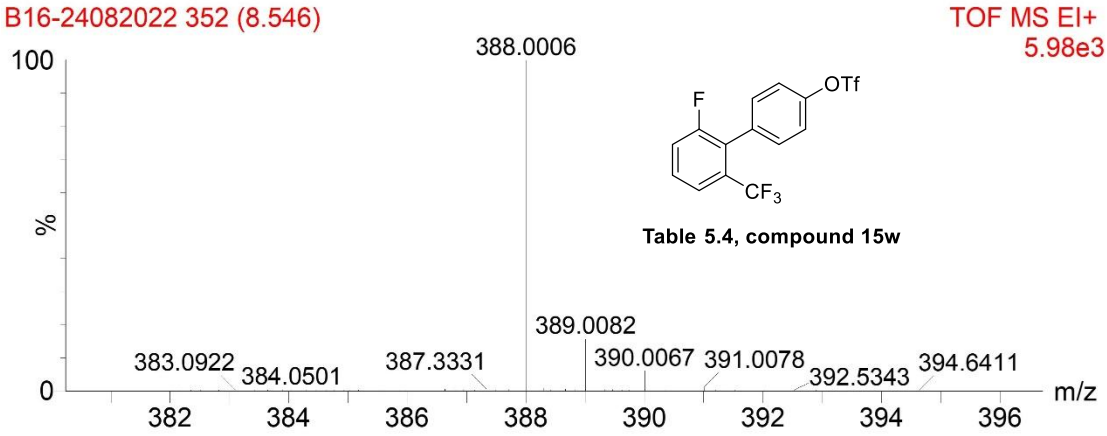

Table 5.4, compound 15w

Mass	m/z (Calc)	Diff (mDa)	Diff (ppm)	Formula
388.0006	388.0004	-0.74	-1.90	C14H7O3F7S

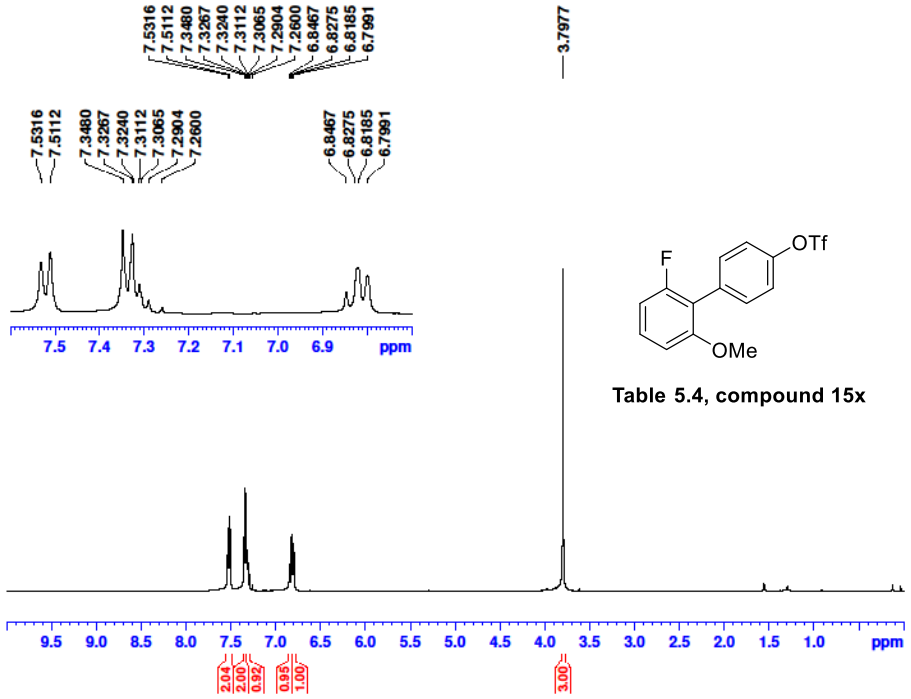

Table 5.4, compound 15x

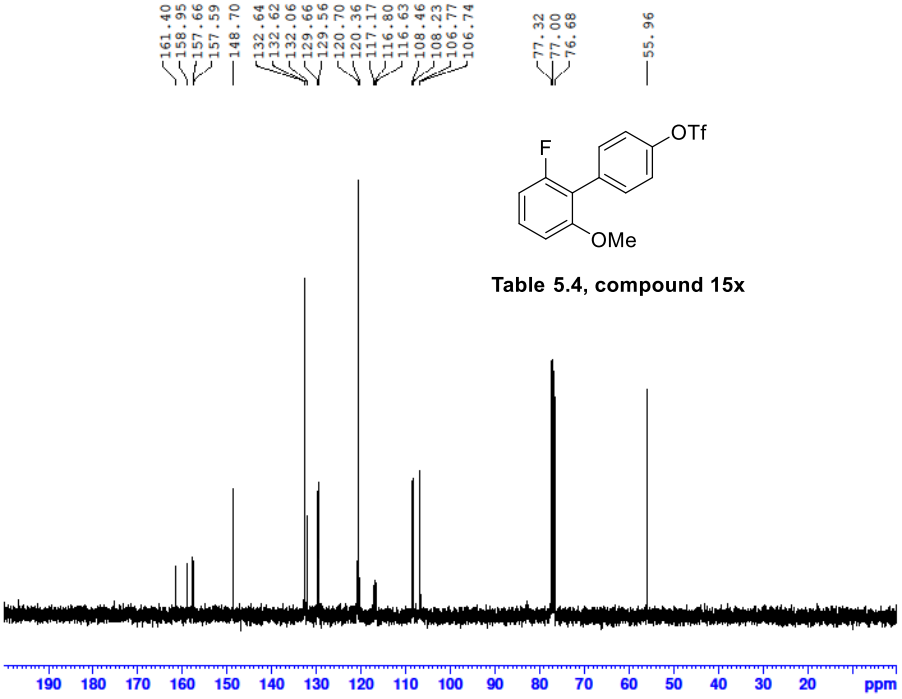

Table 5.4, compound 15x

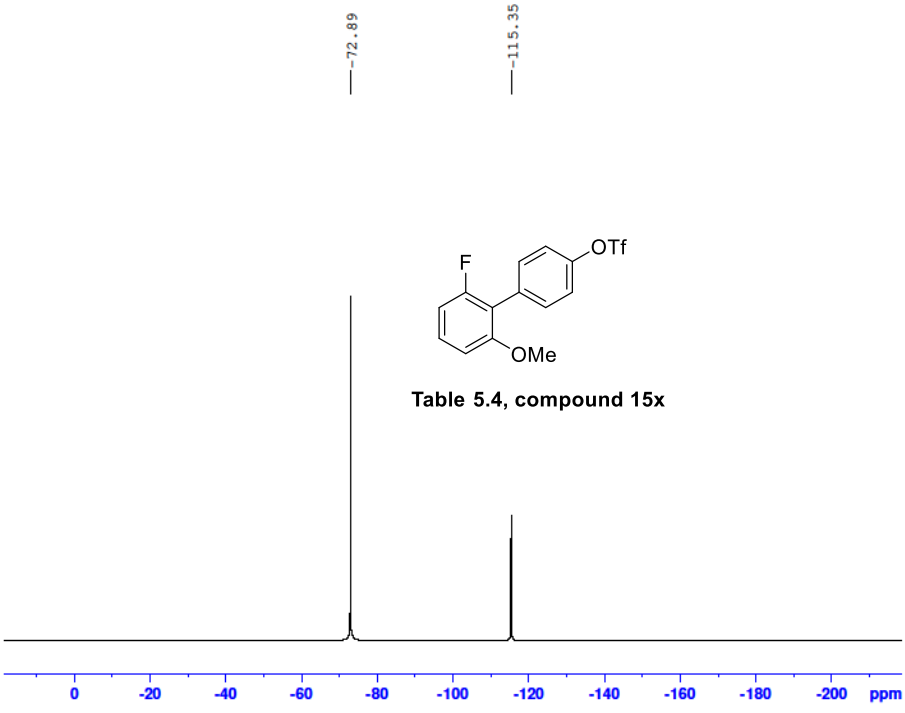

Table 5.4, compound 15x

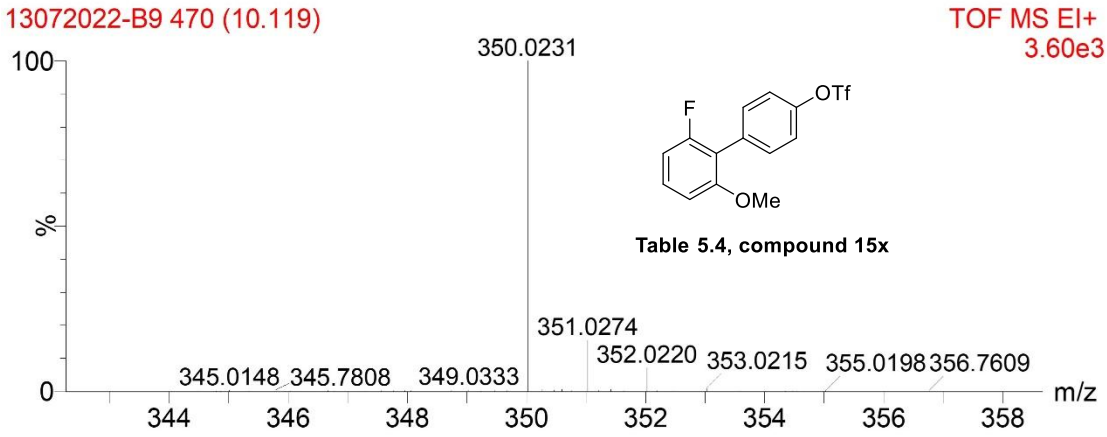

Table 5.4, compound 15x

Mass	Calc. Mass	mDa	PPM	Ion Formula
350.0231	350.0230	-0.06	-0.16	C14H10SF4O4

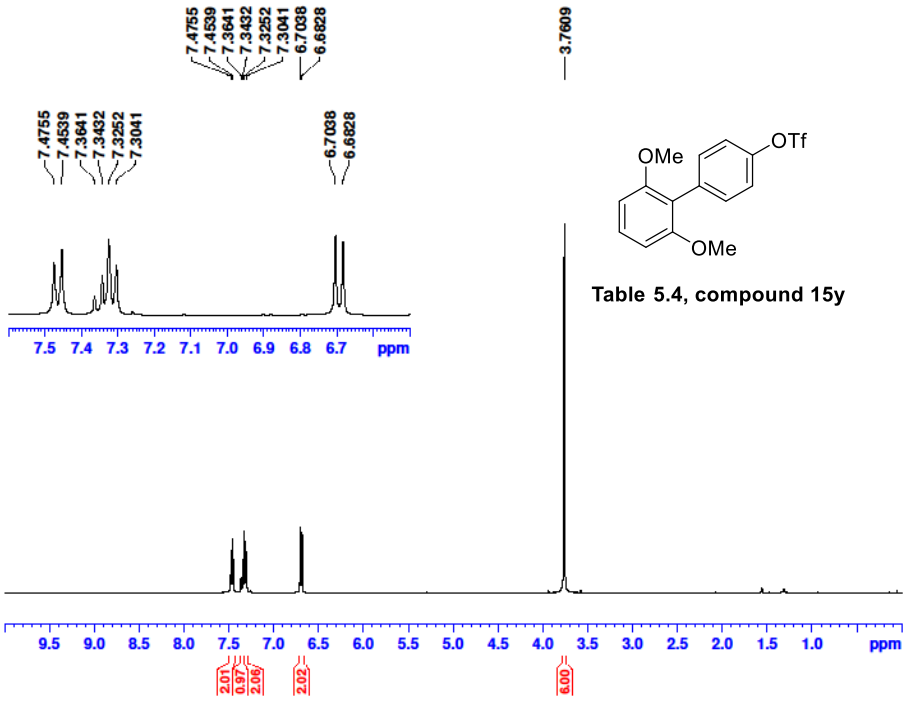

Table 5.4, compound 15y

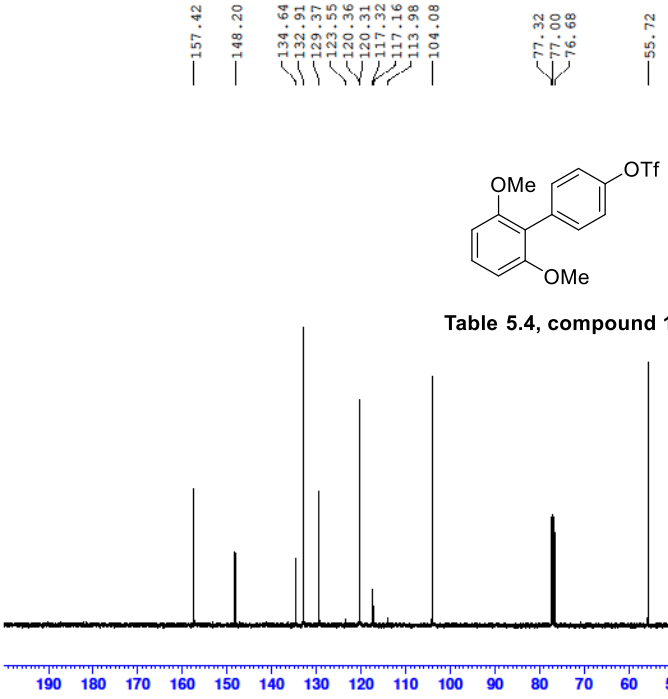

Table 5.4, compound 15y

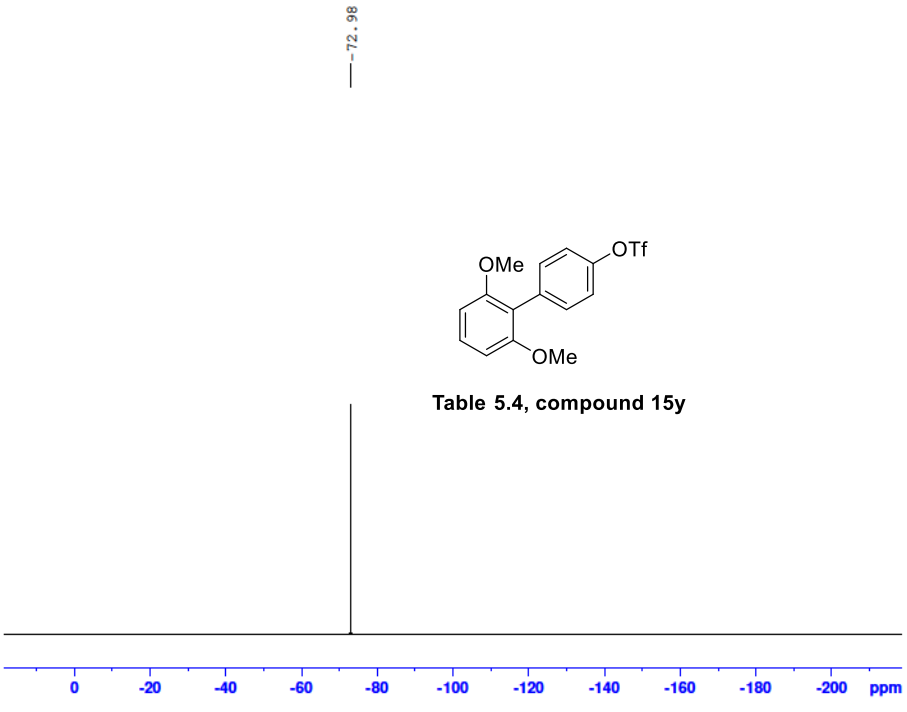

Table 5.4, compound 15y

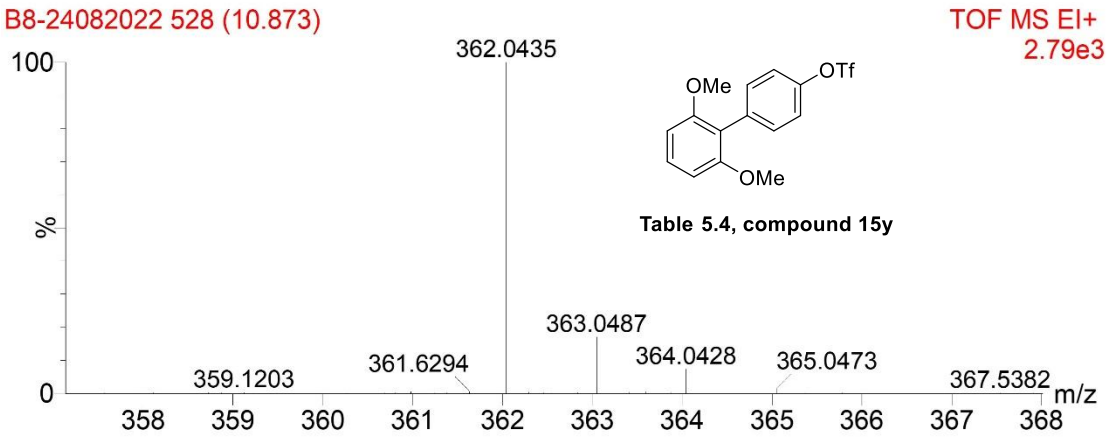

Table 5.4, compound 15y

Mass	m/z (Calc)	Diff (mDa)	Diff (ppm)	Formula
362.0435	362.0430	-0.47	-1.30	C15H13O5F3S

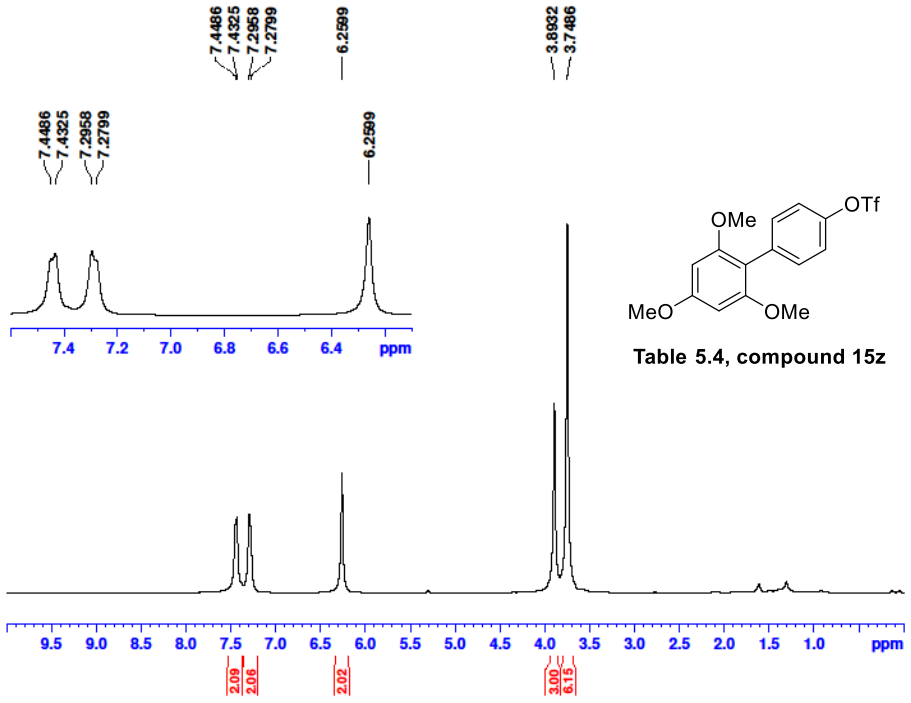

Table 5.4, compound 15z

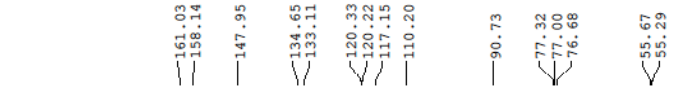

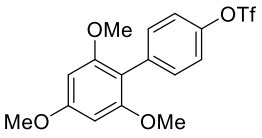

Table 5.4, compound 15z

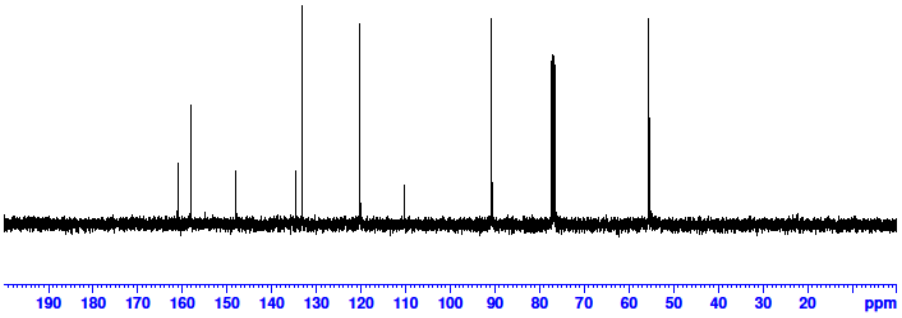

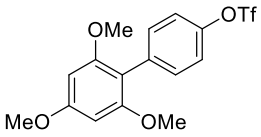

Table 5.4, compound 15z

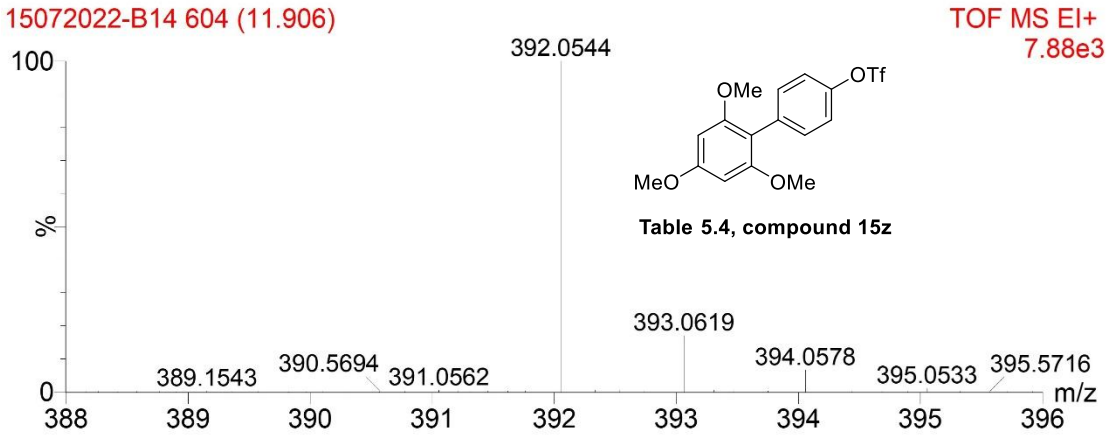

Table 5.4, compound 15z

Mass	Calc. Mass	mDa	PPM	Ion Formula
392.0544	392.0536	-0.81	-2.05	C16H15SF3O6

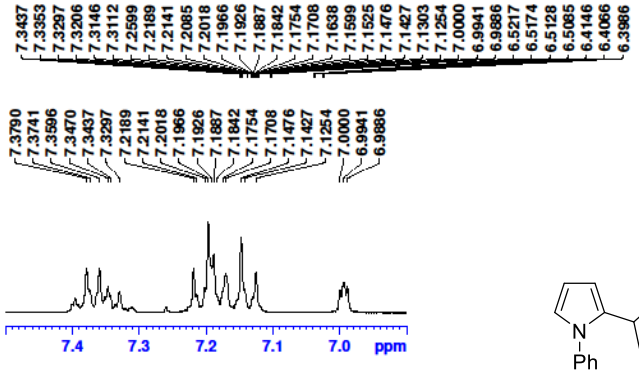

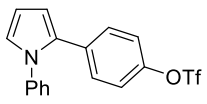

Table 5.4, compound 15aa

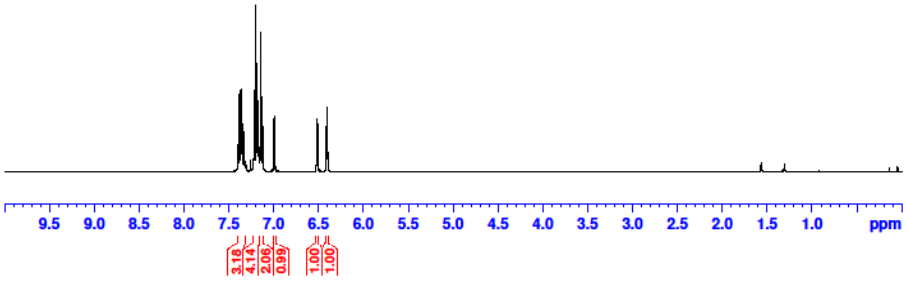

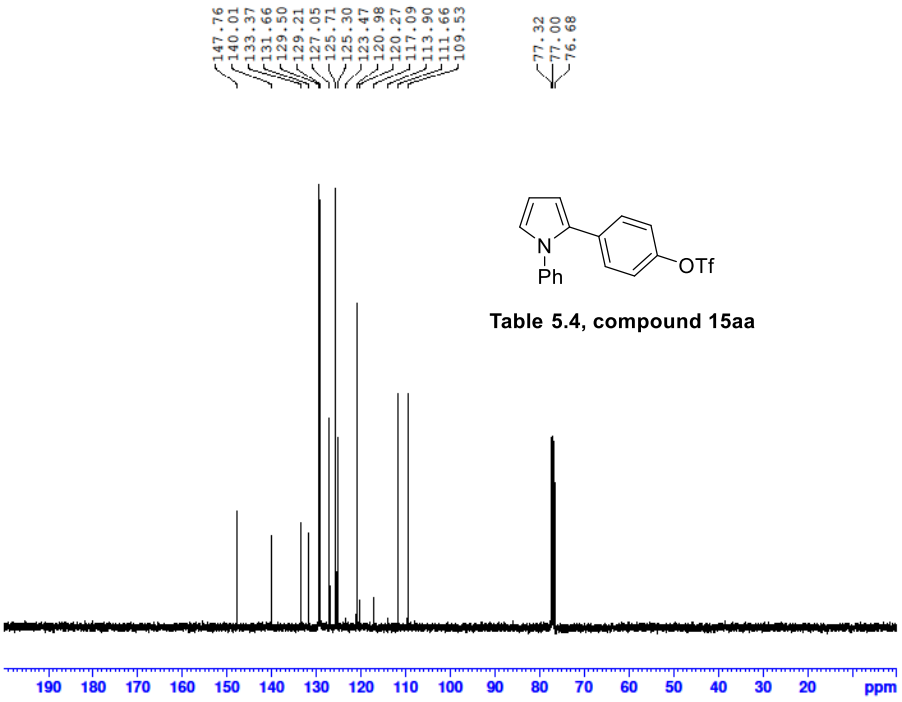

Table 5.4, compound 15aa

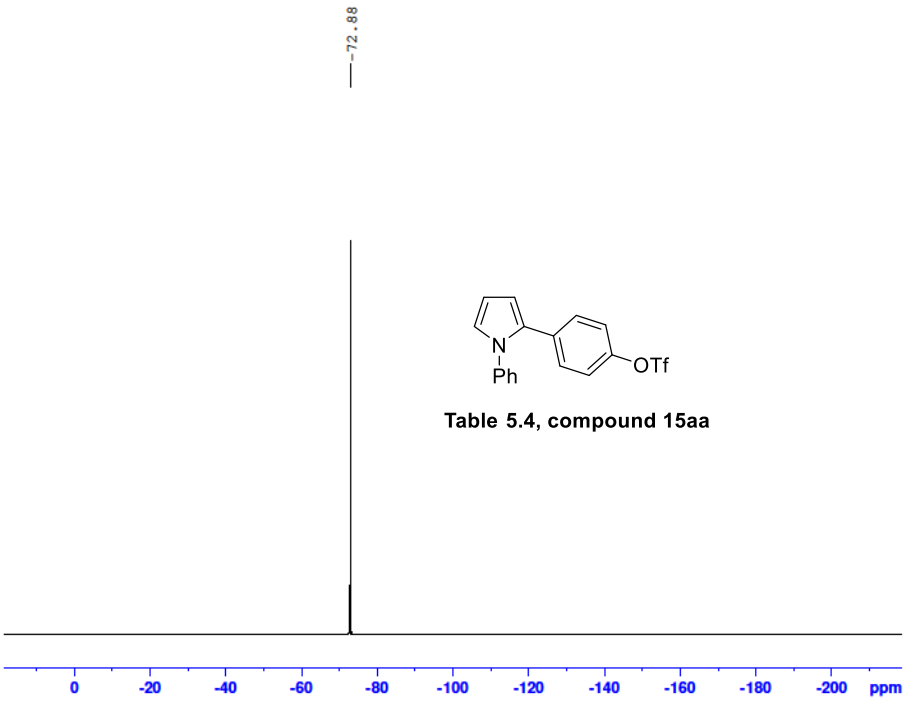

Table 5.4, compound 15aa

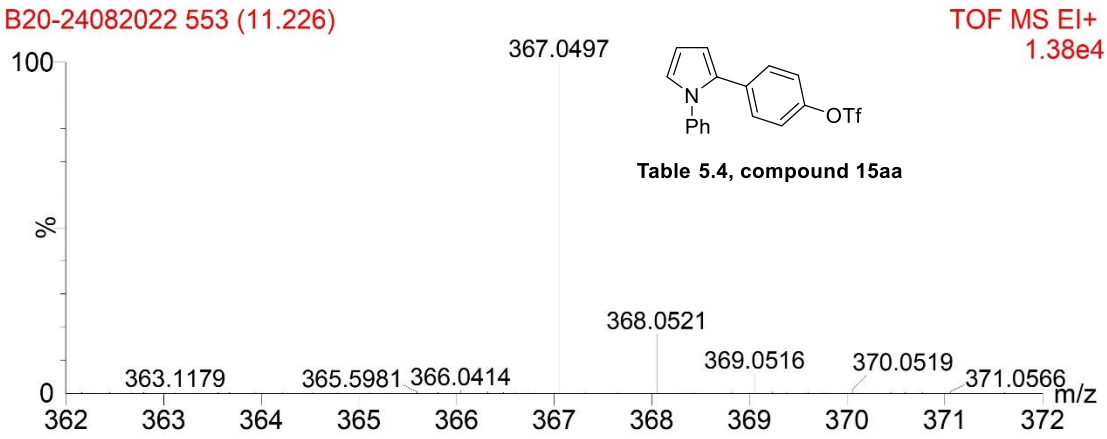

Table 5.4, compound 15aa

Mass	m/z (Calc)	Diff (mDa)	Diff (ppm)	Formula
367.0497	367.0485	-1.25	-3.41	C17H12O3F3NS

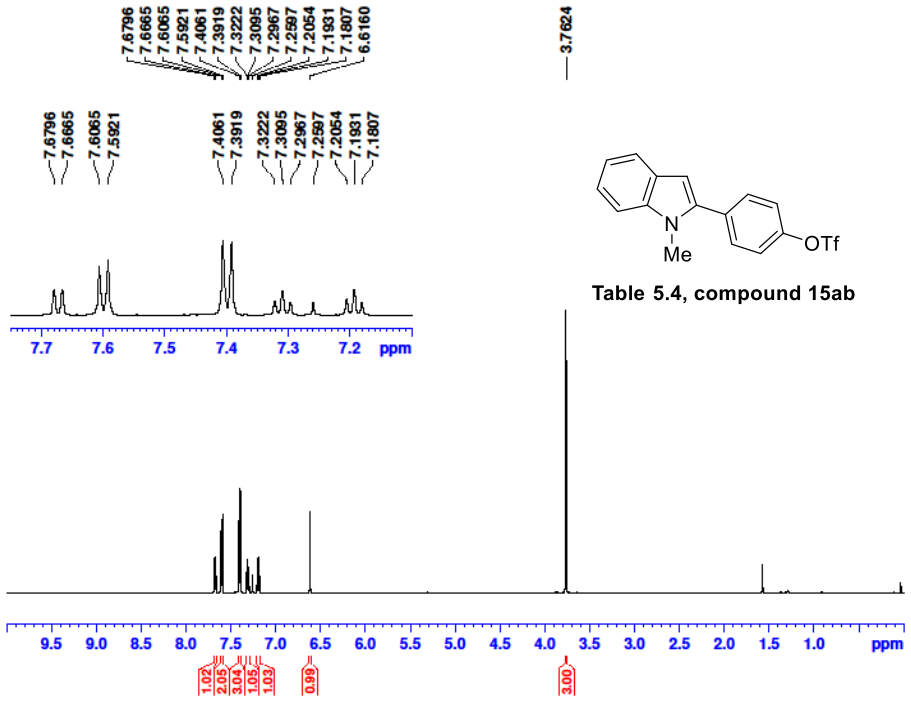

Table 5.4, compound 15ab

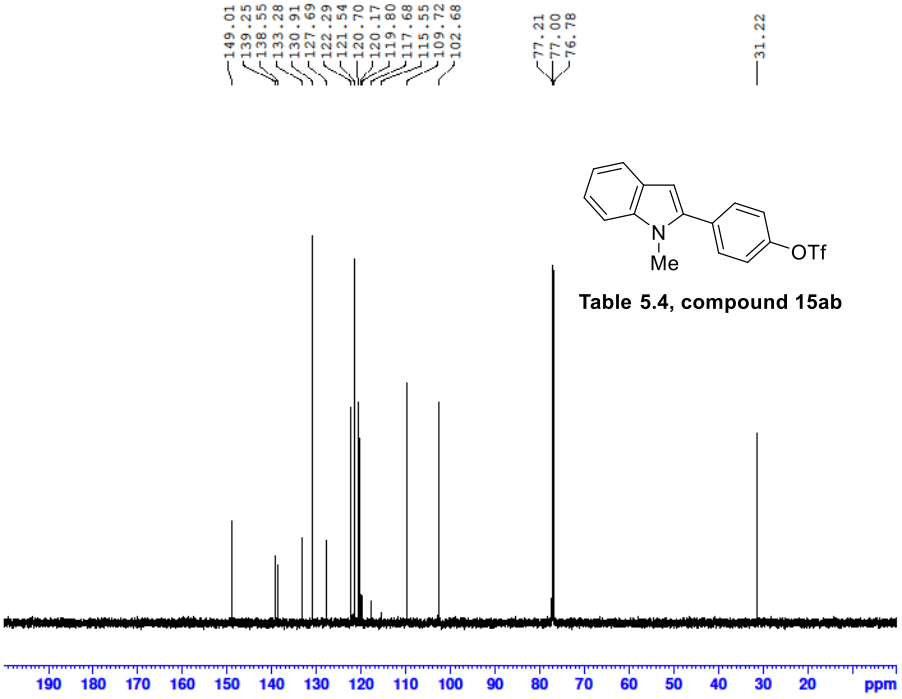

Table 5.4, compound 15ab

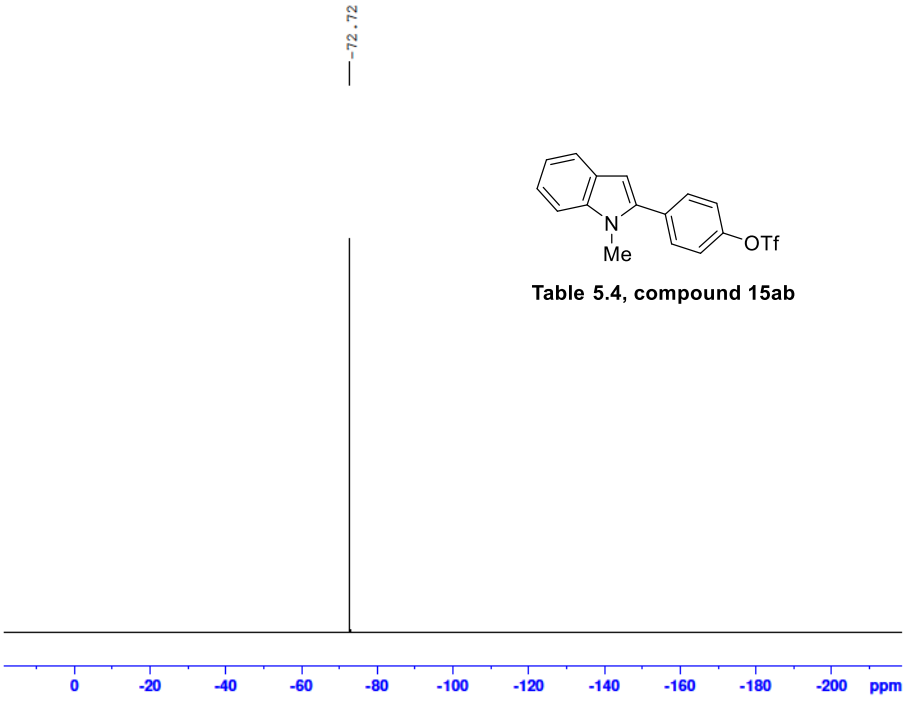

Table 5.4, compound 15ab

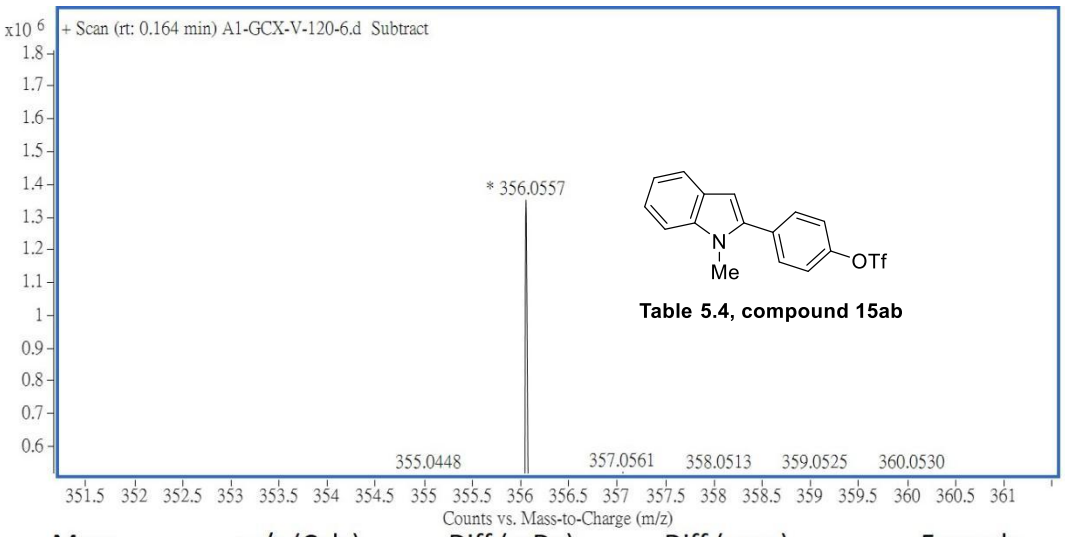

Table 5.4, compound 15ab

Mass	m/z (Calc)	Diff (mDa)	Diff (ppm)	Formula
356.0557	356.0563	0.58	1.62	C16H13F3NO3S